GEOCHEMICAL PATTERNS OF HYDROTHERMAL MINERAL DEPOSITS ASSOCIATED WITH CALC-ALKALIC AND ALKALI-CALCIC IGNEOUS ROCKS AS EVALUATED WITH NEURAL NETWORKS

by

Jan Carol Wilt

Copyright © Jan Carol Wilt 1993

A Dissertation Submitted to the Faculty of the

DEPARTMENT OF GEOSCIENCES

In Partial Fulfillment of the Requirements
For the Degree of

DOCTOR OF PHILOSOPHY

In the Graduate College

THE UNIVERSITY OF ARIZONA

1 9 9 3

THE UNIVERSITY OF ARIZONA
GRADUATE COLLEGE

As members of the Final Examination Committee, we certify that we have read the dissertation prepared by Jan Carol Wilt

entitled Geochemical patterns of hydrothermal mineral deposits associated with calc-alkalic and alkali-calcic igneous rocks as evaluated with neural networks

and recommend that it be accepted as fulfilling the dissertation requirement for the Degree of Doctor of Philosophy

John M. Guilbert	Nov 10, 1993 Date
Mary M. Poulton	11-10-93 Date
Mark D. Barton	11/10/93 Date
Charles E. Glass	11-10-93 Date
Joaquin Ruiz	11-10-93 Date

Final approval and acceptance of this dissertation is contingent upon the candidate's submission of the final copy of the dissertation to the Graduate College.

I hereby certify that I have read this dissertation prepared under my direction and recommend that it be accepted as fulfilling the dissertation requirement.

Dissertation Director John M. Guilbert / Mary M. Poulton	11/26/93 Date

STATEMENT BY AUTHOR

This dissertation has been submitted in partial fulfillment of requirements for an advanced degree at The University of Arizona and is deposited in the University Library to be made available to borrowers under rules of the Library.

Brief quotations from this dissertation are allowable without special permission, provided that accurate acknowledgement of source is made. Requests for permission for extended quotation from or reproduction of this manuscript in whole or in part may be granted by the copyright holder.

SIGNED: 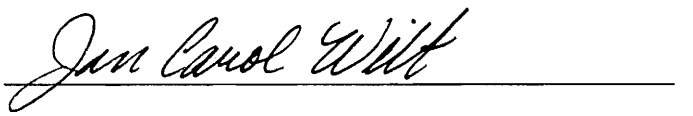

ACKNOWLEDGEMENTS

My mother, Jeannette L. Rasmussen, has my heartfelt gratitude for financially and emotionally supporting my entire doctoral program. My late father, Carol C. Rasmussen, instigated my interest in geology by his own interest in the Earth as a third generation water well driller. The encouragement of my brother, Gary S. Rasmussen, is also gratefully appreciated. My husband, G. Nelson Wilt, has earned my loving appreciation for responsibly taking care of our family. My son, Andrew, designed and built a beautiful garden for me, in which I could think, learn, grow, and write; my daughter, Janelle, helped with household duties, freeing me to work on the dissertation. My father-in-law, Grant M. Wilt, generously contributed money for computer equipment and supplies. My consulting geology clients, particularly Ted and Dan Eyde of GSA Resources and J. David Lowell, steadily supported my business and computer expenses.

Several grants during the later part of my studies were much appreciated. Half of a University of Arizona scholarship established by BHP was awarded to me for the 1991-1992 school year and the $7500 taken in a lump sum in the fall of 1991 so that computer equipment could be purchased for this study. In addition, a grant from the University of Arizona supplied $2000 in salary for data input during the first part of 1992.

This study would not have been possible without the generous support in the form of data, ideas, and enthusiastic encouragement from Stanley B. Keith of MagmaChem Exploration, Inc. Thousands of whole rock and trace element chemical analyses were supplied which would have cost hundreds of thousands of dollars. This data had been collected during 12 years of consulting for numerous MagmaChem clients. These clients are to be commended for their willingness to share geological data for the advancement of the science.

The support, encouragement, and empowerment of various guides and teachers along the path to the finished Ph.D. are greatly appreciated. Dr. John Guilbert's continuous and enthusiastic encouragement and belief in the project were major factors in its success. Dr. Karl Glass first introduced the topic of neural networks and has continually stimulated interest in exciting new ideas and topics, such as chaos theory and fractals. Dr. Mary Poulton has supplied ongoing enthusiasm and practical knowledge of neural networks, as well as grant support and advice. Dr. H. Wesley Peirce has been a valuable mentor throughout my career and has continued to open my eyes to new career paths and potentials. I also appreciate those with opposing views because their challenges forced me to be more meticulously careful and to learn and grow in more expanded ways.

DEDICATION

This work is dedicated to the Earth and to those who study it. Those who analyze its materials and processes, complex interrelationships, and causes and effects, those who exploit its resources, and those who protect its environment can coexist more compatibly with each other and with the Earth through awareness, communication, cooperation, and recognition of common benefits. We do not exist separately, but are bound together with intricate networks of interdependencies. We are connected at such a fundamental level that our simple intention to tap into the gridwork links us into open channelways of information, knowledge, and understanding. By opening our minds to new ideas, unusual concepts, and unfamiliar frequencies and energies, our viewpoint can be expanded to encompass an unlimited awareness of the world and our relationship to it. Maintaining a panoramic focus while examining minute details allows us to fit our piece of the puzzle into the broad framework. In retaining this multiple focus, we often find that the pattern in our puzzle piece duplicates that of the whole, just as a piece of a holograph transmits the same image as does the whole. Not only is the whole greater than the sum of its parts, but the interconnections and linkages between the parts are also an integral part of the whole. Perception of our bonds, mutual dependence, and co-creative interactions leads to the discovery that we are more than parts of the whole; we are all one.

TABLE OF CONTENTS

ABSTRACT 31

INTRODUCTION 33
Problem 33
Solution Potential with Petrochemical Analyses 34
Evaluation Potential with Neural Networks 35
Research Objectives 36
Six Types of Ore Deposits Studied 36
Alkali-calcic, Oxidized 37
Alkali-calcic, Weakly Oxidized 38
Alkali-calcic, Reduced 38
Calc-alkalic, Oxidized 39
Calc-alkalic, Weakly Oxidized 39
Calc-alkalic, Reduced 40
Theoretical Background 41
Magma Series Classification 41
Characteristics of Neural Networks 41
Application of Neural Network Techniques to Mineral Classification 43
Work Plan 44
Bibliographic Research 44
Data Representation 45
Whole Rock Chemical Analyses 46
Trace Element Geochemistry of Mineralized Samples 48
Statistical Analysis 48
Neural Network Analysis 49
Correlation with Geological and Geochemical Parameters 50
Benefit from this Research 51

BACKGROUND ON MAGMA SERIES CLASSIFICATION OF IGNEOUS ROCKS 52
Empirical and Logical Basis 52
Magmatic Tradition 54
History and Development of the Magma Series Classification 55
Classification Hierarchy 56
Aluminum Content 60
History and Development of Aluminum Classes 60
Description of Aluminum Classes 60
Petrotectonic Implications of Aluminum Content 61
Aluminum Classes 63
Peraluminous Mineralogic Indicators 63

TABLE OF CONTENTS -- Continued

Metaluminous Mineralogic Indicators 63
Alkalinity 64
History and Development of Alkalinity Classes 64
Description of Alkalinity 70
Alkalinity Classes 81
Ultra-Alkalic 81
Nepheline Alkalic 81
Quartz Alkalic 83
Alkali-calcic 84
Calc-alkalic 85
Calcic 86
Magnesian 87
Water content 88
History and Development of Water Content Classes 88
Water Content Classes 89
Anhydrous 90
Hydrous 90
Petrotectonic Implications of Water Content 90
Iron Content 92
Volatile Content 96
Oxygen Content 97
History and Development of Oxidation Classes 99
Oxygen Content Classes 100
Petrotectonic Implications of Oxygen Content 101
Differentiation Index 104
Alteration 105
Introduction 105
Alteration Filters 108
Loss on Ignition (LOI) Filter 108
A/CNK Versus SiO_2 Diagram 110
Alteration Index Versus SiO_2 Diagram 112
Potassium Index Versus SiO_2 Diagram 115
Sodium Index Versus SiO_2 Diagram 117
Evaluating Alteration Effects 117

VARIATION DIAGRAMS OF WHOLE ROCK DATA FOR EACH MINING DISTRICT 123
Sources of Whole Rock Data 123
Results for Each Mining District Grouped by Classes 125
Alkali-calcic, Oxidized 126

TABLE OF CONTENTS -- Continued

Tintic, UT 126
Castle, MT 135
Park City, UT 139
Tombstone, AZ 145
Alkali-calcic, Weakly Oxidized 149
Cherry Creek, NV 149
Kinsley, NV 152
Linka, NV 155
Railroad, NV 158
Santa Eulalia, MEXICO 162
Swales Mountain, NV 168
Taylor, NV 170
Tempiute, NV 170
Alkali-calcic, Reduced 180
Llallagua, Bolivia 180
Oruro, Bolivia 181
Potosi, Bolivia 182
Calc-alkalic, Oxidized 183
Christmas, AZ 183
Elk Mountain, NV 188
Eugene Mountains (Mill City), NV 193
Guichon Creek, BC, CANADA 197
Mineral Park (Ithaca Peak), AZ 202
Patagonia (Red Mountain), AZ 207
Ray, AZ 211
Sierrita, AZ 217
Calc-alkalic, Weakly Oxidized 222
Ajo, AZ 222
Copper Canyon, NV 227
Dexing, CHINA 235
Dos Pobres, AZ 239
El Salvador, CHILE 241
El Teniente, CHILE 245
Hedley, BC, CANADA 249
McCoy, NV 253
Morenci, AZ 257
Calc-alkalic, Reduced 260
Bald Mountain, NV 260
Bloody Run, NV 266
Carlin, NV 270

TABLE OF CONTENTS -- Continued

Northumberland, NV 276
Osgood Mountains, NV 25
Chimney Creek, NV 291
Getchell, NV 292
Pinson, NV 293
Preble, NV 294
Summary of Results of Classifying Each Mine 294

CHARACTERISTICS OF WHOLE ROCK DATA ARRANGED BY CLASS 297
Comparisons Among the Six Classes 297
A/CNK Versus SiO_2 Diagram 297
A/NK Versus SiO_2 Diagram 297
K_2O Versus SiO_2 Diagram 299
K_2O - CaO Versus SiO_2 Diagram 299
K_2O - MgO Versus SiO_2 Diagram 303
Nb Versus Zr Diagram 303
FeO^*/MgO Versus SiO_2 Diagram 303
Ferric/ferrous Ratio Versus SiO_2 Diagram 307
Y Versus Zr Diagram 309

PETROLOGY OF FRESH IGNEOUS ROCKS 311
Modal Mineralogy Reported from Fresh Igneous Rocks in Each Class . . 311
Whole Rock Geochemistry of Unaltered Plutonic Rocks from Each Class 317
Ternary Diagrams 323
Harker Variation Diagrams 329

CHARACTERISTICS OF MINERALIZED SYSTEMS 332
Caveats Concerning Production Data 332
Production Characteristics for Each Class 334
Production from Alkali-calcic Systems 334
Production from Alkali-calcic, Oxidized Systems 343
Production from Alkali-calcic, Weakly Oxidized Systems 343
Production from Alkali-calcic, Reduced Systems 345
Production from Calc-alkalic Systems 345
Production from Calc-alkalic, Oxidized Systems 346
Production from Calc-alkalic, Weakly Oxidized Systems 347
Production from Calc-alkalic, Reduced Systems 348
Ore Deposit Mineralogy for Each Class 348
Mineralogy in Alkali-calcic Systems 349
Mineralogy in Alkali-calcic, Oxidized Systems 349

TABLE OF CONTENTS -- Continued

Mineralogy in Alkali-calcic, Weakly Oxidized Systems 350
Mineralogy in Alkali-calcic, Reduced Systems 351
Mineralogy in Calc-alkalic Systems 352
Mineralogy in Calc-alkalic, Oxidized Systems 352
Mineralogy in Calc-alkalic, Weakly Oxidized Systems 353
Mineralogy in Calc-alkalic, Reduced Systems 354
Trace Element Geochemical Data 355
Data Set Available 355
Precious Metals 356
Toxic Metals 359
Fourth Period Transition Metals 362
Fifth Period Transition Metals 372
Lithophile Elements 376
Conclusions from Metal Distribution 383

STATISTICS ON DATA FROM SIX MAGMA SERIES CLASSES 387

BACKGROUND INFORMATION ON NEURAL NETWORKS 401
Neural Network Applications 401
Definition of Neural Networks 402
Characteristics of Neural Networks 403
Strengths of Neural Networks 405
Limitations of Neural Networks 405
Structure of Neural Networks 405
Process of Neural Network Operation 406
Types of Neural Networks 409
Back-propagation Networks 410
Competitive Filter Networks 415
Kohonen Self-Organizing Map (SOM) 415
Learning Vector Quantization (LVQ) 417

NEURAL NETWORK PROCEDURES 420
Neural Network Methodology 420
Theory of Network Design 420
Network Evaluation 424
Back-propagation Procedures 424
Learning Vector Quantization (LVQ) Procedures 425
Neural Network Procedures in this Study 426
Data Representation 426
Network Design in this Study 428

TABLE OF CONTENTS -- Continued

Evaluation in this Study 429

RESULTS OF NEURAL NETWORK TRIALS 431
Learning 431
Testing 435
Summary of Neural Network Effectiveness 438

CONCLUSIONS 440
Internal Consistency of Petrochemical Classification 443
Classification Efficiency of Neural Networks for Mineral Deposits 444
Effectiveness of Pattern Recognition by Neural Networks 444
Comparison of Neural Networks with Conventional Statistics 446
Possible Applications of Techniques in this Study 448
Alteration Filters 448
Exploration Application of Petrochemical Classification 449
Neural Networks 450

APPENDIX A: LOCATION AND DESCRIPTION OF SAMPLES COLLECTED BY MAGMACHEM EXPLORATION, INC., STAFF 452

APPENDIX B: WHOLE ROCK DATA FROM IGNEOUS ROCKS ASSOCIATED WITH MINERALIZATION 456

APPENDIX C: VARIATION DIAGRAMS WITH AND WITHOUT ALTERED AND VOLCANIC SAMPLES 500

APPENDIX D: MODAL MINERALOGY REPORTED IN LITERATURE 519

APPENDIX E: PRODUCTION REPORTED IN LITERATURE 542

APPENDIX F: MINERALOGY OF ORE SYSTEMS 547

APPENDIX G: TRACE ELEMENT DATA ON MINERALIZED SAMPLES 572

APPENDIX H: HISTOGRAMS SHOWING TRACE ELEMENTS OF MINERALIZED SAMPLES. 643

APPENDIX I: HISTOGRAMS OF STATISTICS ON MINERALIZED SAMPLES. 655

REFERENCES 688

LIST OF ILLUSTRATIONS

Figure 2-1. A/CNK versus weight percent SiO_2 variation diagram. A/CNK = molecular $Al_2O_3/(CaO + Na_2O + K_2O)$. 62
Figure 2-2. Sr (in ppm) versus weight percent CaO variation diagram showing correlation of pluton petrochemistry with tectonic settings for worldwide peraluminous granitoid series. 71
Figure 2-3. Weight percent K_2O versus weight percent SiO_2 variation diagram. $K_{57.5}$ index = weight percent K_2O at 57.5 weight percent SiO_2. Magma series classes are the alkalinity belts with positive slope. Curved lines with negative slope refer to Differentiation Index (DI) and are a function of the amount of silica in the rock. 73
Figure 2-4. Weight percent K_2O minus weight percent CaO versus weight percent SiO_2 variation diagram showing alkalinity categories in the petrochemical classification. DI= Differentiation Index. 74
Figure 2-5. Weight percent K_2O minus weight percent MgO versus weight percent SiO_2 variation diagram showing alkalinity categories in the petrochemical classification. DI= Differentiation Index. 75
Figure 2-6. Log-Log variation diagram of ppm Nb versus ppm Zr with alkalinity fields in the petrochemical classification. 76
Figure 2-7. Variation diagram illustrating technique used by Peacock (1931) to determine alkali-lime index, which is often called the Peacock index. . 78
Figure 2-8. Comparison of alkali-lime indices of Peacock (1931) with those of various alkalinity classes based on metallogenic types and correlated with the $K_{57.5}$ Index of Dickinson and Hatherton (1967). 80
Figure 2-9. Weight percent K_2O versus weight percent SiO_2 variation diagram showing rock nomenclature for each alkalinity subdivision of metaluminous rock series (from Keith, unpublished manuscript). 82
Figure 2-10. Variation diagram of Y in ppm versus Zr in ppm showing hydrous versus anhydrous fields for various alkalinities. Note x-axis and y-axis scale differ. 91
Figure 2-11. AFM ternary diagram interpreting the traditional tholeiitic/calc-alkaline distinction from the viewpoint of anhydrous (tholeiitic) versus hydrous (calc-alkaline) melting processes (from Keith and others, 1991). 93
Figure 2-12. Modified Miyashiro (1974) diagram illustrating iron enrichment. Variation diagram plots weight percent SiO_2 versus FeO^*/MgO, in which $FeO^* = 0.9(Fe_2O_3) + FeO$. 94
Figure 2-13. TiO_2 versus FeO^*/MgO variation diagram, in which $FeO^* = 0.9(Fe_2O_3) + FeO$. Low titanium fields for hydrous metaluminous series that were generated in subduction settings are distinguished from high

LIST OF ILLUSTRATIONS -- Continued

titanium fields for anhydrous metaluminous magma series that were generated in hotspot and rift geotectonic settings (from Keith and others, 1991). 95
Figure 2-14. A/NK versus weight percent SiO_2 variation diagram. A/NK = molecular $Al_2O_3/(Na_2O + K_2O)$. Peralkaline rocks have A/NK less than 1.0. 98
Figure 2-15. Ferric/ferrous variation diagram with weight percent Fe_2O_3 divided by weight percent FeO is plotted against weight percent SiO_2. Fields for the various oxidized and reduced classes are nearly horizontal with moderate rise in oxidation state at high silica values. 102
Figure 2-16. Ferric/ferrous ratio versus SiO_2 variation diagram showing indicator mineral assemblages for oxidation state in plutons compared with indicator minerals of oxidation state in associated mineral deposits (from Keith and others, 1991). 103
Figure 2-17. LOI (Loss On Ignition) histogram on a modified log scale illustrating anhydrous and hydrous categories and the cutoff for altered plutons at 2.5 percent LOI and for altered volcanics at 3.0 percent LOI. 111
Figure 2-18. A/CNK versus weight percent SiO_2 variation diagram showing altered and unaltered fields. A/CNK = molecular $Al_2O_3/(CaO + Na_2O + K_2O)$. Rock suites in the metaluminous category in the petrochemical classification that fall outside of the unaltered field are generally eliminated from the data set for further classification. 113
Figure 2-19. A.I. or Alteration index of Ishikawa and others (1976) plotted as an A.I. versus weight percent SiO_2 variation diagram. A.I. = $[(MgO + K_2O) / (Na_2O + K_2O + CaO + MgO)] * 100$. 114
Figure 2-20. K. I. or K index versus weight percent SiO_2 variation diagram. K. I. = $(Na_2O + K_2O + MgO) / (CaO + (0.9*Fe_2O_3 + FeO))$. 116
Figure 2-21. Na index variation diagram with Na I. on a log scale versus weight percent SiO_2. Na I. = (Na_2O / K_2O) + A/CNK, where A/CNK = molecular $Al_2O_3/(CaO + Na_2O + K_2O)$. 118
Figure 2-22. Flow chart for evaluating alteration in igneous rock petrochemistry. 120
Figure 3-1. Summary of isotopic ages of igneous rocks of East Tintic Mountains (# = CIMVS) (from Morris and Lovering, 1979; Keith and others, 1991). 127
Figure 3-2. Geologic map of Tintic, Utah, showing igneous stocks and volcanics with # = CIMVS (modified from Morris and Mogensen, 1978). . 128
Figure 3-3. Petrochemical variation diagrams used as alteration filters for igneous rocks at Tintic, Utah. 131
Figure 3-4. Petrochemical variation diagrams showing iron/magnesium and ferric/ferrous ratios of all samples compared to those excluding altered

LIST OF ILLUSTRATIONS -- Continued

and volcanic rocks at Tintic, Utah. 132
Figure 3-5. Magma series variation diagrams showing alkalinity of all samples compared to those excluding altered and volcanic rocks at Tintic, Utah. 133
Figure 3-6. Magma series variation diagrams using Nb and Y versus Zr to show alkalinity and hydrous nature of all samples compared to those excluding altered and volcanic rocks at Tintic, Utah. 134
Figure 3-7. Geologic map and MagmaChem sample locations for Castle stock, Montana (Ti = # = CIMVS) (adapted from McClernan, 1980). 136
Figure 3-8. Magma series variation diagrams showing A/CNK, ferric/ferrous, and alkalinity of Tertiary intrusive of Castle Mountains, Montana. 137
Figure 3-9. Petrochemical variation diagrams showing FeO^*/MgO and Nb versus Zr for Tertiary intrusive of Castle Mountains, Montana 138
Figure 3-10. Geologic map of some igneous rocks in the Park City, Utah, region (# = CIMVS = Ontario, Mayflower, Clayton Peak, and Alta stocks) (modified from Bromfield and others, 1977; John, 1989). 140
Figure 3-11. Graphical representation of radiometric dates from the Park City mining district, Utah (# = CIMVS) (from Bromfield and others, 1977). 141
Figure 3-12. Petrochemical diagrams showing A/CNK and ferric/ferrous ratio of stocks in the Park City, Utah, area with older calc-alkalic stocks on the right and younger alkali-calcic stocks (CIMVS) on the left. 143
Figure 3-13. Magma series variation diagrams showing alkalinity of stocks in the Park City, Utah, area with older calc-alkalic stocks on the right and younger alkali-calcic stocks (CIMVS) on the left. 144
Figure 3-14. Geologic map of igneous units near Tombstone, Arizona (# = CIMVS = Bronco, Uncle Sam, and Schieffelin) (modified from Gilluly, 1956). 146
Figure 3-15. Radiometric ages from Tombstone, Arizona (# = CIMVS). 147
Figure 3-16. Petrochemical variation diagrams of igneous rocks from Tombstone, Arizona, showing A/CNK, ferric/ferrous ratio, and alkalinity. 148
Figure 3-17. Petrochemical variation diagrams of igneous rocks from Tombstone, Arizona, showing FeO^*/MgO, Nb/Zr, and Y/Zr relationships. 150
Figure 3-18. Geologic map of Cherry Creek, Nevada, showing igneous rocks (Ti = Tertiary intrusive = # = CIMVS) and sample localities (modified from Hose and Blake, 1976). 151
Figure 3-19. Petrochemical variation diagrams of some Cherry Creek, Nevada, igneous rocks showing A/CNK, iron ratios, and alkalinity. 153
Figure 3-20. Map of the Kinsley mining district, Nevada, showing igneous

LIST OF ILLUSTRATIONS -- Continued

rocks (Kgr = # = CIMVS) and sample locations (modified from Coats, 1987) 154
Figure 3-21. Petrochemical variation diagrams of igneous rocks from Kinsley, Nevada, showing A/CNK, iron ratios, and alkalinity. 156
Figure 3-22. Geologic map of the Linka district, Nevada, showing igneous rocks (Jgr = # = CIMVS) and sample locations (modified from McKee, 1968). 157
Figure 3-23. Petrochemical variation diagrams of igneous rocks from Linka, Nevada, showing A/CNK, iron ratios, and alkalinity. 159
Figure 3-24. Geologic map of the Railroad district, Nevada (Tertiary granite and rhyolite porphyry = # = CIMVS) (from Lapointe and others, 1991). . 160
Figure 3-25. Petrochemical variation diagrams of igneous rocks from the Railroad mining district, Nevada, showing alteration filters. 161
Figure 3-26. Magma series variation diagrams of igneous rocks from Railroad, Nevada, showing alkalinity (left includes altered; right = unaltered only). 163
Figure 3-27. Petrochemical diagrams of igneous rocks from Railroad, Nevada, showing iron ratios (left includes altered, right = unaltered only). 164
Figure 3-28. Geologic map of Santa Eulalia, Mexico, showing igneous rocks (felsites = CIMVS) and sample locations (modified from Megaw, 1990). . 165
Figure 3-29. Petrochemical variation diagrams of igneous rocks from Santa Eulalia, Mexico, showing alteration filters. 166
Figure 3-30. Magma series variation diagrams of igneous rocks from Santa Eulalia, Mexico, showing alkalinity and iron ratios (Circle = unaltered). 167
Figure 3-31. Geologic map of the Swales Mountain area, Nevada (Ti = Tertiary intrusive = # = CIMVS) (modified from Ketner and others, 1968). 169
Figure 3-32. Petrochemical variation diagrams of igneous rocks from the Swales Mountain mining district, Nevada, showing alteration filters. . . 171
Figure 3-33. Magma series variation diagrams of igneous rocks from the Swales Mountain mining district, Nevada, showing alkalinity and iron ratios. 172
Figure 3-34. Geologic map of the Taylor district, Nevada, showing rhyolite dikes associated with mineralization (# = CIMVS) (modified from Drewes, 1969). 173
Figure 3-35. Petrochemical variation diagrams of igneous rocks from the Taylor district, Nevada, showing alteration filters. 174
Figure 3-36. Magma series variation diagrams of igneous rocks from the Taylor district, Nevada, showing alkalinity and iron ratios. 175
Figure 3-37. Geologic map of the Tempiute district, Nevada, showing

LIST OF ILLUSTRATIONS -- Continued

igneous rocks (Tg = # = CIMVS) (modified from Tschanz and Pampeyan, 1970). 177
Figure 3-38. Petrochemical variation diagrams of igneous rocks from the Tempiute mining district, Nevada, showing alteration filters. 178
Figure 3-39. Magma series variation diagrams of igneous rocks from the Tempiute mining district, Nevada, showing alkalinity and iron ratios. . . 179
Figure 3-40. Geologic map of the Potosi, Bolivia, tin-silver district (# = CIMVS) (from Wolf, 1973; Frances and others, 1981; Grant and others, 1977). 184
Figure 3-41. Petrochemical variation diagrams of Kari Kari and Kumurana rocks in the Potosi mining area, Bolivia, showing alteration filters. 185
Figure 3-42. Magma series diagrams of Kari Kari and Kumurana rocks in Potosi, Bolivia, showing alkalinity (left includes altered; right is unaltered only). 186
Figure 3-43. Petrochemical diagrams of Kari Kari and Kumurana rocks in Potosi, Bolivia, showing iron ratios (left includes altered; right = unaltered). . . 187
Figure 3-44. Geologic map of the Christmas mining district, Arizona, showing igneous rocks related to mineralization (# = CIMVS) (modified from Koski and Cook, 1982). 189
Figure 3-45. Petrochemical variation diagrams of igneous rocks of the Christmas mining district, Arizona, showing alteration filters. 190
Figure 3-46. Magma series variation diagrams of igneous rocks of the Christmas mining district, Arizona, showing alkalinity and iron ratios. . 191
Figure 3-47. Geologic map of Elk Mountain, Nevada, showing Cretaceous granodiorite to quartz monzonite (CIMVS) and prospects (from Lapointe and others, 1991; Coats, 1987). 192
Figure 3-48. Petrochemical variation diagrams of igneous rocks of the Elk Mountain mining district, Nevada, showing alteration filters. 194
Figure 3-49. Magma series variation diagrams of igneous rocks of the Elk Mountain mining district, Nevada, showing alkalinity and iron ratios. . . 195
Figure 3-50. Geologic map of the Eugene Mountains (Mill City district), Nevada, showing granodiorite (g = # = CIMVS) and sample locations (from Johnson, 1977; Johnson and Keith, 1991). 196
Figure 3-51. Petrochemical variation diagrams of igneous rocks of the Eugene Mountains (Mill City mining district), Nevada, showing alteration filters. 198
Figure 3-52. Magma series variation diagrams of igneous rocks of the Eugene Mountains (Mill City district), Nevada, showing alkalinity and iron ratios. 199
Figure 3-53. Geologic map of the Guichon Creek Batholith (Valley Copper and other districts, British Columbia) (# = intrusive rocks of the batholith =

LIST OF ILLUSTRATIONS -- Continued

CIMVS) (from McMillan, 1982). 200
Figure 3-54. Petrochemical variation diagrams of the Guichon Creek batholithic rocks, British Columbia, showing alteration filters. 203
Figure 3-55. Magma series diagrams of the Guichon Creek batholith, BC, showing alkalinity (left includes altered; right is unaltered samples only). 204
Figure 3-56. Petrochemical diagrams of the Guichon Creek batholith, BC, showing iron ratios (left includes altered; right is unaltered samples only). 205
Figure 3-57. Geologic map of the Ithaca Peak pluton (Mineral Park mine), Arizona (# = CIMVS) (modified from Wilkinson, 1981). 206
Figure 3-58. Petrochemical variation diagrams of the Ithaca Peak pluton (Mineral Park mine), Arizona showing alteration filters. 208
Figure 3-59. Magma series variation diagrams of the Ithaca Peak pluton (Mineral Park mine), Arizona, showing alkalinity and iron ratios. 209
Figure 3-60. Map of the Patagonia pluton (Red Mountain mining area), Arizona, showing igneous rocks (modified from Kistner, 1984; Dewhurst, 1976). 210
Figure 3-61. Petrochemical variation diagrams of the Patagonia pluton (Red Mountain mining area), Arizona, showing alteration filters. 212
Figure 3-62. Petrochemical variation diagrams of the Patagonia pluton (Red Mountain), Arizona (alkalinity with and without altered; Fe/Mg). 213
Figure 3-63. Geologic map of the Ray (Mineral Creek district), Arizona (# = CIMVS = Tortilla, Rattler, Tea Cup, Granite Mountain, and Teapot Mountain) (from Cornwall, 1982) 215
Figure 3-64. Petrochemical variation diagrams of igneous rocks from Ray (Mineral Creek mining district), Arizona, showing alteration filters. . . . 216
Figure 3-65. Magma series diagrams of igneous rocks from Ray, Arizona, showing alkalinity (left side includes altered; right side is unaltered samples). 218
Figure 3-66. Petrochemical variation diagrams of igneous rocks from Ray, Arizona, showing iron ratios (left side includes altered; right side is unaltered samples) and Nb/Zr and Y/Zr ratios. 219
Figure 3-67. Geologic map of the Pima district, Arizona (# = CIMVS = Ruby Star Granodiorite and quartz monzonite porphyry) (from Titley, 1982). 220
Figure 3-68. Petrochemical variation diagrams of the Ruby Star pluton (Pima mining district), Arizona, showing alteration filters. 221
Figure 3-69. Petrochemical alkalinity graphs of Cretaceous (left side) and Tertiary (right = Ruby Star Granodiorite) rocks, Pima district, Arizona. 223
Figure 3-70. Petrochemical diagrams of Cretaceous (left side) and Tertiary

LIST OF ILLUSTRATIONS -- Continued

(right = Ruby Star Granodiorite) rocks, Pima, AZ, showing iron ratios. . 224
Figure 3-71. Geologic map of the Cornelia pluton (Ajo district), Arizona (# = CIMVS) (modified from Hagstrum and others, 1987). 226
Figure 3-72. Petrochemical variation diagrams of the Cornelia pluton (Ajo mining district), Arizona showing alteration filters. 228
Figure 3-73. Magma series alkalinity diagrams of the porphyritic phase of the Cornelia pluton, Ajo, AZ (left includes altered; right is unaltered only). 229
Figure 3-74. Petrochemical iron ratio diagrams of the porphyritic phase of the Cornelia pluton, Ajo, AZ (left includes altered; right is unaltered only). 230
Figure 3-75. Geologic map of Copper Canyon area (Battle Mountain district), NV (CIMVS = # = porphyry of Copper Canyon) (Theodore and others, 1990). 232
Figure 3-76. Petrochemical variation diagrams of igneous rocks from the Copper Canyon district, Nevada, showing alteration filters. 233
Figure 3-77. Magma series variation diagrams of igneous rocks from the Copper Canyon district, Nevada, showing alkalinity and iron ratios. . . . 234
Figure 3-78. Geologic map of the Dexing mining area, China, showing mines and Granodiorite porphyry (# = CIMVS) (modified from Yan and Hu, 1980). 236
Figure 3-79. Petrochemical variation diagrams of igneous rocks from the Dexing mining area, China, showing alteration filters. 237
Figure 3-80. Magma series variation diagrams of igneous rocks from the Dexing mining area, China, showing alkalinity and iron ratios. 238
Figure 3-81. Geologic map of the Dos Pobres, AZ (# = CIMVS = Lmp = Paleocene quartz monzonite and latite porphyries) (from Langton and Williams, 1982). 240
Figure 3-82. Petrochemical variation diagrams of the Dos Pobres, Arizona, productive porphyries showing alteration filters. 242
Figure 3-83. Magma series variation diagrams of the Dos Pobres, Arizona, productive porphyries showing alkalinity and iron ratios. 243
Figure 3-84. Geologic map of the El Salvador mine, Chile (# = CIMVS = granodioritic and quartz porphyries) (Gustafson and Hunt, 1975). 244
Figure 3-85. Petrochemical variation diagrams of igneous rocks from El Salvador, Chile, showing alteration filters. 246
Figure 3-86. Magma series variation diagrams of igneous rocks from El Salvador, Chile, showing alkalinity and iron ratios. 247
Figure 3-87. Geologic map of the Braden orebody of the El Teniente mine, Chile (# = CIMVS = Quartz Diorite) (from Howell and Molloy, 1960). . . 248

LIST OF ILLUSTRATIONS -- Continued

Figure 3-88. Petrochemical variation diagrams of igneous rocks from El Teniente, Chile, showing alteration filters. 250
Figure 3-89. Magma series variation diagrams of igneous rocks from El Teniente, Chile, showing alkalinity and iron ratios. 251
Figure 3-90. Geologic map of the Hedley area, British Columbia (Hedley Intrusions = # = CIMVS) (from Ray and others, 1986). 252
Figure 3-91. Petrochemical variation diagrams of igneous rocks from the Hedley, British Columbia, showing alteration filters. 254
Figure 3-92. Magma series variation diagrams of igneous rocks from Hedley, British Columbia, showing alkalinity and iron ratios. 255
Figure 3-93. Geologic map of the McCoy mine area, Nevada (# = CIMVS = Tbs = Brown stock) (modified from Kuyper, 1988). 256
Figure 3-94. Petrochemical variation diagrams of igneous rocks from McCoy, Nevada, showing alteration filters. 258
Figure 3-95. Magma series variation diagrams of igneous rocks from McCoy, Nevada, showing alkalinity and iron ratios. 259
Figure 3-96. Geologic map of the Morenci mine area, Arizona (Lmp = Laramide quartz monzonite porphyry = CIMVS) (from Langton, 1973). . . 261
Figure 3-97. Petrochemical variation diagrams of igneous rocks from Morenci, Arizona, showing alteration filters. 262
Figure 3-98. Magma series variation diagrams of igneous rocks from Morenci, Arizona, showing alkalinity and iron ratios (+ altered, o unaltered). 263
Figure 3-99. Geologic map of the Bald Mountain area, Nevada, showing igneous rocks (Ti may = # = CIMVS), mines or prospects, and sample locations (modified from Ilchik, 1990). 265
Figure 3-100. Petrochemical variation diagrams of igneous rocks from Bald Mountain, Nevada, showing alteration filters. 267
Figure 3-101. Magma series alkalinity and iron ratio diagrams of igneous rocks from Bald Mountain, Nevada, (+ altered, o unaltered). 268
Figure 3-102. Geologic map of the Bloody Run Hills, Nevada, showing CIMVS (# = Tkg) and sample locations (modified from Willden, 1964). . 269
Figure 3-103. Petrochemical variation diagrams of igneous rocks from Bloody Run, Nevada, showing alteration filters. 271
Figure 3-104. Magma series variation diagrams of igneous rocks from Bloody Run, Nevada, showing alkalinity and iron ratios (+ altered, o unaltered). 272
Figure 3-105. Geologic map of the Carlin Trend, Nevada, showing subdistricts (from Flaherty and King, 1991). 273
Figure 3-106. Petrochemical variation diagrams of Tertiary igneous rocks from Carlin, Nevada, showing alteration filters. 278

LIST OF ILLUSTRATIONS -- Continued

Figure 3-107. Magma series variation diagrams of igneous rocks from Carlin, Nevada, showing alkalinity and iron ratios (+ altered, o unaltered). . . . 279
Figure 3-108. Geologic map of the Northumberland area, Nevada (Tertiary dikes not shown = CIMVS) (from Motter and Chapman, 1984). 280
Figure 3-109. Petrochemical variation diagrams of igneous rocks from the Northumberland area, Nevada, showing alteration filters. 283
Figure 3-110. Magma series diagrams of Tertiary dikes, Northumberland, Nevada, showing alkalinity and iron ratios (+ altered, o unaltered). . . . 284
Figure 3-111. Geologic map of the Osgood Mountains area, Nevada (Kg = Osgood Mtn. Granodiorite = # = CIMVS) (from Grauch and Bankey, 1991; Willden, 1964; Hotz and Willden, 1964). 287
Figure 3-112. Petrochemical variation diagrams of igneous rocks in the Osgood Mountains, Nevada, showing alteration filters. 289
Figure 3-113. Magma series variation diagrams of igneous rocks from the Osgood Mountains, NV, showing alkalinity and iron ratios (+ altered, o unaltered). 290
Figure 4-1. Comparison of A/CNK versus SiO_2 variation diagrams for metaluminous, alkali-calcic (left side) versus calc-alkalic (right side), oxidized (top), weakly oxidized (center), and reduced (bottom) classes. 298
Figure 4-2. Comparison of A/NK versus SiO_2 variation diagrams for metaluminous, alkali-calcic (left side) versus calc-alkalic (right side), oxidized (top), weakly oxidized (center), and reduced (bottom) classes. 300
Figure 4-3. Comparison of K_2O versus SiO_2 variation diagrams for metaluminous, alkali-calcic (left side) versus calc-alkalic (right side), oxidized (top), weakly oxidized (center), and reduced (bottom) classes. 301
Figure 4-4. Comparison of K_2O - CaO versus SiO_2 variation diagrams for metaluminous, alkali-calcic (left side) versus calc-alkalic (right side), oxidized (top), weakly oxidized (center), and reduced (bottom) classes. 302
Figure 4-5. Comparison of K_2O - MgO versus SiO_2 variation diagrams for metaluminous, alkali-calcic (left side) versus calc-alkalic (right side), oxidized (top), weakly oxidized (center), and reduced (bottom) classes. 304
Figure 4-6. Comparison of Nb versus Zr variation diagrams for metaluminous, alkali-calcic (left side) versus calc-alkalic (right side), oxidized (top), weakly oxidized (center), and reduced (bottom) classes. 305
Figure 4-7. Comparison of FeO^*/MgO versus SiO_2 variation diagrams for metaluminous, alkali-calcic (left side) versus calc-alkalic (right side), oxidized (top), weakly oxidized (center), and reduced (bottom) classes. 306
Figure 4-8. Comparison of Fe_2O_3/FeO versus SiO_2 variation diagrams for metaluminous, alkali-calcic (left side) versus calc-alkalic (right side), oxidized (top), weakly oxidized (center), and reduced (bottom) classes. 308

LIST OF ILLUSTRATIONS -- Continued

Figure 4-9. Comparison of Y versus Zr variation diagrams for metaluminous, alkali-calcic (left side) versus calc-alkalic (right side), oxidized (top), weakly oxidized (center), and reduced (bottom) classes. 310
Figure 5-1. Histograms of magnetite in percent on the x-axis (MAC=alkali-calcic, MCA=calc-alkalic, o=oxidized, ow=weakly oxidized, and r=reduced). 313
Figure 5-2. Histograms of sphene in percent on the x-axis (MAC=alkali-calcic, MCA=calc-alkalic, o=oxidized, ow=weakly oxidized, and r=reduced). 314
Figure 5-3. Modal mineralogy from magma series classes (M=Metaluminous, AC= alkali-calcic, CA= calc-alkalic, o=oxidized, ow= weakly oxidized, r=reduced) plotted on standard IUGS or Streckeisen (1976) diagrams. . 315
Figure 5-4. Comparison of data from Figure 5-3 plotted in various combinations of magma series classes showing overlap of classes (M=Metaluminous, AC= alkali-calcic, CA=calc-alkalic, o=oxidized, ow=weakly oxidized, r=reduced). 316
Figure 5-5. Peacock Index (SiO_2 where K_2O + Na_2O line and CaO line cross) of petrochemical classes (M=Metaluminous, AC=alkali-calcic, CA= calc-alkalic, o=oxidized, ow=weakly oxidized, r=reduced) (AC=51-56; CA=56-61). 318
Figure 5-6. Bar graphs of SiO_2/K_2O values from petrochemical classes (M=Metaluminous, AC= alkali-calcic, CA= calc-alkalic, o=oxidized, ow= weakly oxidized, r=reduced) showing higher values for MCA than MAC. 320
Figure 5-7. Bar graphs of Fe_2O_3/FeO values from petrochemical classes (M=Metaluminous, AC= alkali-calcic, CA= calc-alkalic, o=oxidized, ow= weakly oxidized, r=reduced) showing higher values for o than r. 321
Figure 5-8. Scatter diagrams of SiO_2/K_2O versus Fe_2O_3/FeO from petrochemical classes (M=Metaluminous, AC= alkali-calcic, CA= calc-alkalic, o=oxidized, ow= weakly oxidized, r=reduced). 322
Figure 5-9. All six magma series classes are in the calc-alkaline field on AFM diagrams (M=Metaluminous, AC=alkali-calcic, CA=calc-alkalic, o=oxidized, ow=weakly oxidized, r=reduced) (A=Na_2O+K_2O, F=FeO+0.9*Fe_2O_3, M=MgO). 324
Figure 5-10. Wide linear bands of six magma series classes on Na_2O-K_2O-CaO diagrams (M= Metaluminous, AC= alkali-calcic, CA= calc-alkalic, o= oxidized, ow= weakly oxidized, r=reduced). 325
Figure 5-11. Comparison of data from Figure 5-10 plotted on Na_2O-K_2O-CaO diagrams by combining various petrochemical classes (AC= alkali-calcic, CA=calc-alkalic, o=oxidized, ow=weakly oxidized, r=reduced). 326
Figure 5-12. Linear arrangement of six magma series classes plotted on K_2O-

LIST OF ILLUSTRATIONS -- Continued

SiO_2-Fe_2O_3/FeO diagrams (M= Metaluminous, AC= alkali-calcic, CA= calc-alkalic, o= oxidized, ow= weakly oxidized, r=reduced). 327
Figure 5-13. Comparison of data from Figure 5-12 plotted on K_2O-SiO_2-Fe_2O_3/FeO diagrams in various combinations (M= Metaluminous, AC= alkali-calcic, CA=calc-alkalic, o=oxidized, ow=weakly oxidized, r=reduced). 328
Figure 5-14. Whole-rock chemistry of petrochemical classes plotted in linear bands on K_2O vs. SiO_2 variation diagrams (M= Metaluminous, AC= alkali-calcic, CA= calc-alkalic, o= oxidized, ow= weakly oxidized, r=reduced). . 330
Figure 5-15. Comparison of data from Figure 5-14 plotted in various combinations on K_2O vs. SiO_2 variation diagrams (M= Metaluminous, AC= alkali-calcic, CA=calc-alkalic, o=oxidized, ow=weakly oxidized, r=reduced). 331
Figure 6-1. Precious metal production in each class (MAC=alkali-calcic, MCA=calc-alkalic; o=oxidized, ow=weakly oxidized, r=reduced). 335
Figure 6-2. Copper, molybdenum, and tungsten production (MAC=alkali-calcic, MCA=calc-alkalic; o=oxidized, ow=weakly oxidized, r=reduced). . 336
Figure 6-3. Lead and zinc production in magma series classes (MAC=alkali-calcic, MCA=calc-alkalic; o=oxidized, ow=weakly oxidized, r=reduced). . 337
Figure 6-4. Precious metal grade in each class (MAC=alkali-calcic, MCA=calc-alkalic; o=oxidized, ow=weakly oxidized, r=reduced). 338
Figure 6-5. Copper, molybdenum, and tungsten grades (MAC=alkali-calcic, MCA=calc-alkalic; o=oxidized, ow=weakly oxidized, r=reduced). 339
Figure 6-6. Lead and zinc grades in magma series classes (MAC=alkali-calcic, MCA=calc-alkalic; o=oxidized, ow=weakly oxidized, r=reduced). 340
Figure 6-7. Precious metal ratios in each class (MAC=alkali-calcic, MCA=calc-alkalic; o=oxidized, ow=weakly oxidized, r=reduced). 341
Figure 6-8. Base metal ratios in magma series classes (MAC=alkali-calcic, MCA=calc-alkalic; o=oxidized, ow=weakly oxidized, r=reduced). 342
Figure 6-9. Stepped histograms of silver in ppm (MAC=alkali-calcic, MCA=calc-alkalic; o=oxidized, ow=weakly oxidized, r=reduced). 357
Figure 6-10. Stepped histograms of gold in ppm (MAC=alkali-calcic, MCA=calc-alkalic; o=oxidized, ow=weakly oxidized, r=reduced). 358
Figure 6-11. Stepped histograms of arsenic in ppm (MAC=alkali-calcic, MCA=calc-alkalic; o=oxidized, ow=weakly oxidized, r=reduced). 360
Figure 6-12. Stepped histograms of antimony in ppm (MAC=alkali-calcic, MCA=calc-alkalic; o=oxidized, ow=weakly oxidized, r=reduced). 361
Figure 6-13. Stepped histograms of mercury in ppm (MAC=alkali-calcic, MCA=calc-alkalic; o=oxidized, ow=weakly oxidized, r=reduced). 363
Figure 6-14. Stepped histograms of thallium in ppm (MAC=alkali-calcic,

LIST OF ILLUSTRATIONS -- Continued

MCA=calc-alkalic; o=oxidized, ow=weakly oxidized, r=reduced). 364
Figure 6-15. Stepped histograms of copper in ppm (MAC=alkali-calcic, MCA=calc-alkalic; o=oxidized, ow=weakly oxidized, r=reduced). 366
Figure 6-16. Stepped histograms of zinc in ppm (MAC=alkali-calcic, MCA=calc-alkalic; o=oxidized, ow=weakly oxidized, r=reduced). 367
Figure 6-17. Stepped histograms of manganese in ppm (MAC=alkali-calcic, MCA=calc-alkalic; o=oxidized, ow=weakly oxidized, r=reduced). 369
Figure 6-18. Stepped histograms of vanadium in ppm (MAC=alkali-calcic, MCA=calc-alkalic; o=oxidized, ow=weakly oxidized, r=reduced). 370
Figure 6-19. Stepped histograms of titanium in ppm (MAC=alkali-calcic, MCA=calc-alkalic; o=oxidized, ow=weakly oxidized, r=reduced). 371
Figure 6-20. Stepped histograms of niobium in ppm (MAC=alkali-calcic, MCA=calc-alkalic; o=oxidized, ow=weakly oxidized, r=reduced). 373
Figure 6-21. Stepped histograms of tin in ppm (MAC=alkali-calcic, MCA=calc-alkalic; o=oxidized, ow=weakly oxidized, r=reduced). 374
Figure 6-22. Stepped histograms of yttrium in ppm (MAC=alkali-calcic, MCA=calc-alkalic; o=oxidized, ow=weakly oxidized, r=reduced). 375
Figure 6-23. Stepped histograms of zirconium in ppm (MAC=alkali-calcic, MCA=calc-alkalic; o=oxidized, ow=weakly oxidized, r=reduced). 377
Figure 6-24. Stepped histograms of lead in ppm (MAC=alkali-calcic, MCA=calc-alkalic; o=oxidized, ow=weakly oxidized, r=reduced). 378
Figure 6-25. Stepped histograms of molybdenum in ppm (MAC=alkali-calcic, MCA=calc-alkalic; o=oxidized, ow=weakly oxidized, r=reduced). 380
Figure 6-26. Stepped histograms of tungsten in ppm (MAC=alkali-calcic, MCA=calc-alkalic; o=oxidized, ow=weakly oxidized, r=reduced). 381
Figure 6-27. Stepped histograms of barium in ppm (MAC=alkali-calcic, MCA=calc-alkalic; o=oxidized, ow=weakly oxidized, r=reduced). 382
Figure 6-28. Stepped histograms of rubidium in ppm (MAC=alkali-calcic, MCA=calc-alkalic; o=oxidized, ow=weakly oxidized, r=reduced). 384
Figure 6-29. Stepped histograms of strontium in ppm (MAC=alkali-calcic, MCA=calc-alkalic; o=oxidized, ow=weakly oxidized, r=reduced). 385
Figure 7-1. Comparison of means of whole rock oxides of less than 7 percent, showing contrasts among magma series classes (MAC=alkali-calcic, MCA=calc-alkalic, o=oxidized, ow=weakly oxidized, r=reduced). . 390
Figure 7-2. Comparison of means of whole rock oxides and indices from 15 to 70 percent showing contrasts among petrochemical classes (MAC=alkali-calcic, MCA=calc-alkalic, o=oxidized, ow=weakly oxidized, r=reduced). . 391
Figure 7-3. Comparison of means of whole rock indices and ratios below 10 percent showing contrasts among petrochemical classes (MAC=alkali-calcic, MCA=calc-alkalic, o=oxidized, ow=weakly oxidized, r=reduced). . 392

LIST OF ILLUSTRATIONS -- Continued

Figure 7-4. Comparison of means of trace elements from mineralized samples (0 to 15 ppm) showing contrasts among magma series classes (MAC=alkali-calcic, MCA=calc-alkalic, o=oxidized, ow=weakly oxidized, r=reduced). 395
Figure 7-5. Comparison of means of trace elements from mineralized samples (up to 400 ppm) showing contrasts among magma series classes (MAC=alkali-calcic, MCA=calc-alkalic, o=oxidized, ow=weakly oxidized, r=reduced). 396
Figure 7-6. Comparison of means of trace elements from mineralized samples (up to 20,000 ppm) showing contrasts among magma series classes (MAC=alkali-calcic, MCA=calc-alkalic, o=oxidized, ow=weakly oxidized, r=reduced). 397
Figure 8-1. The operation of a three-layer back-propagation network. 411
Figure 8-2. The shape of a sigmoid function used to modulate the weighted sum S_j to give an activation A_j. 412
Figure 8-3. Learning vector quantization (LVQ) in which inputs X_i from the input layer of processing elements (PEs) are directed to the Kohonen layer and modified by weights W_{ij}. 416
Figure 8-4. Amplitude-distance function known as the "Mexican Hat" function that modifies neighbors around the winning processing element. 417
Figure 8-5. Kohonen layer showing that the winning PEs must be in the correct portion of the Kohonen layer to correspond to the output PE that is physically close to it. The tetrahedron below each output PE depicts the portion of the Kohonen layer that is related to that output class. 418
Figure C-1. A/CNK, A/NK, and Y/Zr diagrams of the metaluminous, alkali-calcic, oxidized class (left includes altered and volcanics; right is only unaltered). 501
Figure C-2. Alkalinity diagrams of the metaluminous, alkali-calcic, oxidized class (left side includes altered and volcanics; right is only unaltered). 502
Figure C-3. Iron and Nb/Zr diagrams of the metaluminous, alkali-calcic, oxidized class (left side includes altered and volcanics; right is only unaltered). 503
Figure C-4. A/CNK, A/NK, and Y/Zr diagrams of metaluminous, alkali-calcic, weakly oxidized (left includes altered and volcanics; right is only unaltered). 504
Figure C-5. Alkalinity diagrams of the metaluminous, alkali-calcic, weakly oxidized class (left side includes altered and volcanics; right is only unaltered). 505
Figure C-6. Iron and Nb/Zr diagrams of metaluminous, alkali-calcic, weakly

LIST OF ILLUSTRATIONS -- Continued

oxidized class (left includes altered and volcanics; right is only unaltered) 506
Figure C-7. A/CNK, A/NK, and Y/Zr diagrams of metaluminous, alkali-calcic, reduced class. 507
Figure C-8. Alkalinity variation diagrams of the metaluminous, alkali-calcic, reduced class (left includes altered and volcanics; right is only unaltered). 508
Figure C-9. Iron ratio variation diagrams of the metaluminous, alkali-calcic, reduced class (left includes altered and volcanics; right is only unaltered). 509
Figure C-10. A/CNK, A/NK, and Y/Zr diagrams of the metaluminous, calc-alkalic, oxidized class (left includes altered and volcanics; right is only unaltered). 510
Figure C-11. Alkalinity variation diagrams of the metaluminous, calc-alkalic, oxidized class (left includes altered and volcanics; right is only unaltered). 511
Figure C-12. Iron and Nb/Zr diagrams of the metaluminous, calc-alkalic, oxidized class (left includes altered and volcanics; right is only unaltered). 512
Figure C-13. A/CNK, A/NK, and Y/Zr diagrams of metaluminous, calc-alkalic, weakly oxidized (left includes altered and volcanics; right is only unaltered). 513
Figure C-14. Alkalinity variation diagrams of the metaluminous, calc-alkalic, weakly oxidized class (left includes altered and volcanics; right is only unaltered). 514
Figure C-15. Iron and Nb/Zr diagrams of the metaluminous, calc-alkalic, weakly oxidized class (left includes altered and volcanics; right is only unaltered). 515
Figure C-16. A/CNK, A/NK, and Y/Zr diagrams of the metaluminous, calc-alkalic, reduced class (left includes altered and volcanics; right is only unaltered). 516
Figure C-17. Alkalinity variation diagrams of the metaluminous, calc-alkalic, reduced class (left includes altered and volcanics; right is only unaltered). 517
Figure C-18. Iron and Nb/Zr variation diagrams of the metaluminous, calc-alkalic, reduced class (left includes altered and volcanics; right is only unaltered). 518
Figure D-1. Histograms of pyroxene in percent on the x-axis (MAC=alkali-calcic, MCA=calc-alkalic, o=oxidized, ow=weakly oxidized, and r=reduced). 524
Figure D-2. Histograms of hornblende in percent on the x-axis (MAC=alkali-

LIST OF ILLUSTRATIONS -- Continued

calcic, MCA=calc-alkalic, o=oxidized, ow=weakly oxidized, and r=reduced).525
Figure D-3. Histograms of biotite in percent on the x-axis (MAC=alkali-calcic, MCA=calc-alkalic, o=oxidized, ow=weakly oxidized, and r=reduced). 526
Figure D-4. Histograms of plagioclase in percent on the x-axis (MAC=alkali-calcic, MCA=calc-alkalic, o=oxidized, ow=weakly oxidized, and r=reduced). 527
Figure D-5. Histograms of orthoclase in percent on the x-axis (MAC=alkali-calcic, MCA=calc-alkalic, o=oxidized, ow=weakly oxidized, and r=reduced). 528
Figure D-6. Linear bands of magma series classes plotted on Al_2O_3 vs. SiO_2 variation diagrams (M= Metaluminous, AC= alkali-calcic, CA= calc-alkalic, o= oxidized, ow= weakly oxidized, r= reduced). 529
Figure D-7. Comparison of data from Figure D-6 plotted in various combinations on Al_2O_3 vs. SiO_2 variation diagrams (M= Metaluminous, AC= alkali-calcic, CA=calc-alkalic, o=oxidized, ow=weakly oxidized, r=reduced). 530
Figure D-8. Linear bands of petrochemical classes plotted on TiO_2 vs. SiO_2 variation diagrams showing no changes (M= Metaluminous, AC= alkali-calcic, CA= calc-alkalic, o= oxidized, ow= weakly oxidized, r=reduced). . 531
Figure D-9. Whole-rock chemistry of petrochemical classes plotted on Fe_2O_3 vs. SiO_2 variation diagrams (M= Metaluminous, AC= alkali-calcic, CA= calc-alkalic, o= oxidized, ow= weakly oxidized, r=reduced). 532
Figure D-10. Comparison of data from Figure D-9 plotted in various combinations on Fe_2O_3 vs. SiO_2 variation diagrams (M= Metaluminous, AC= alkali-calcic, CA=calc-alkalic, o=oxidized, ow=weakly oxidized, r=reduced). 533
Figure D-11. Whole-rock chemistry of petrochemical classes plotted on FeO vs. SiO_2 variation diagrams (M= Metaluminous, AC= alkali-calcic, CA= calc-alkalic, o= oxidized, ow= weakly oxidized, r=reduced). 534
Figure D-12. Comparison of data from Figure D-11 plotted in various combinations on FeO vs. SiO_2 variation diagrams (M= Metaluminous, AC= alkali-calcic, CA=calc-alkalic, o=oxidized, ow=weakly oxidized, r=reduced). 535
Figure D-13. Whole-rock chemistry of petrochemical classes plotted in lines on MgO vs. SiO_2 variation diagrams (M= Metaluminous, AC= alkali-calcic, CA= calc-alkalic, o= oxidized, ow= weakly oxidized, r=reduced). 536
Figure D-14. Comparison of data from Figure D-13 plotted in various combinations on MgO vs. SiO_2 variation diagrams (M= Metaluminous, AC= alkali-calcic, CA=calc-alkalic, o=oxidized, ow=weakly oxidized,

LIST OF ILLUSTRATIONS -- Continued

r=reduced). 537
Figure D-15. Whole-rock chemistry of magma series classes plotted in linear bands on CaO vs. SiO_2 variation diagrams (M= Metaluminous, AC= alkali-calcic, CA= calc-alkalic, o= oxidized, ow= weakly oxidized, r=reduced). . 538
Figure D-16. Comparison of data from Figure 5-15 plotted in various combinations on CaO vs. SiO_2 variation diagrams (M= Metaluminous, AC= alkali-calcic, CA=calc-alkalic, o=oxidized, ow=weakly oxidized, r=reduced). 539
Figure D-17. Whole-rock chemistry of magma series classes plotted in fields on Na_2O vs. SiO_2 variation diagrams (M= Metaluminous, AC= alkali-calcic, CA= calc-alkalic, o= oxidized, ow= weakly oxidized, r=reduced). . 540
Figure D-18. Comparison of data from Figure D-16 plotted in various combinations on Na_2O vs. SiO_2 variation diagrams (M= Metaluminous, AC= alkali-calcic, CA=calc-alkalic, o=oxidized, ow=weakly oxidized, r=reduced). 541
Figure H-1. Stepped histograms of beryllium in ppm (MAC=alkali-calcic, MCA=calc-alkalic; o=oxidized, ow=weakly oxidized, r=reduced). 644
Figure H-2. Stepped histograms of bismuth in ppm (MAC=alkali-calcic, MCA=calc-alkalic; o=oxidized, ow=weakly oxidized, r=reduced). 645
Figure H-3. Stepped histograms of boron in ppm (MAC=alkali-calcic, MCA=calc-alkalic; o=oxidized, ow=weakly oxidized, r=reduced). 646
Figure H-4. Stepped histograms of cadmium in ppm (MAC=alkali-calcic, MCA=calc-alkalic; o=oxidized, ow=weakly oxidized, r=reduced). 647
Figure H-5. Stepped histograms of cobalt in ppm (MAC=alkali-calcic, MCA=calc-alkalic; o=oxidized, ow=weakly oxidized, r=reduced). 648
Figure H-6. Stepped histograms of chromium in ppm (MAC=alkali-calcic, MCA=calc-alkalic; o=oxidized, ow=weakly oxidized, r=reduced). 649
Figure H-7. Stepped histograms of iron in ppm (MAC=alkali-calcic, MCA=calc-alkalic; o=oxidized, ow=weakly oxidized, r=reduced). 650
Figure H-8. Stepped histograms of fluorine in ppm (MAC=alkali-calcic, MCA=calc-alkalic; o=oxidized, ow=weakly oxidized, r=reduced). 651
Figure H-9. Stepped histograms of lithium in ppm (MAC=alkali-calcic, MCA=calc-alkalic; o=oxidized, ow=weakly oxidized, r=reduced). 652
Figure H-10. Stepped histograms of nickel in ppm (MAC=alkali-calcic, MCA=calc-alkalic; o=oxidized, ow=weakly oxidized, r=reduced). 653
Figure H-11. Stepped histograms of tellurium in ppm (MAC=alkali-calcic, MCA=calc-alkalic; o=oxidized, ow=weakly oxidized, r=reduced). 654
Figure I-1. Histograms of silver concentrations in ppm (MAC=alkali-calcic, MCA=calc-alkalic, o=oxidized, ow=weakly oxidized, r=reduced). 656
Figure I-2. Histograms of arsenic concentrations in ppm (MAC=alkali-calcic,

LIST OF ILLUSTRATIONS -- Continued

MCA=calc-alkalic, o=oxidized, ow=weakly oxidized, r=reduced). 657
Figure I-3. Histograms of gold concentrations in ppm (MAC=metaluminous alkali-calcic, MCA=calc-alkalic, o=oxidized, ow=weakly oxidized, r=reduced). 658
Figure I-4. Histograms of barium concentrations in ppm (MAC=alkali-calcic, MCA=calc-alkalic, o=oxidized, ow=weakly oxidized, r=reduced). 659
Figure I-5. Histograms of beryllium concentrations in ppm (MAC=alkali-calcic, MCA=calc-alkalic, o=oxidized, ow=weakly oxidized, r=reduced). . 660
Figure I-6. Histograms of bismuth concentrations in ppm (MAC=alkali-calcic, MCA=calc-alkalic, o=oxidized, ow=weakly oxidized, r=reduced). 661
Figure I-7. Histograms of boron concentrations in ppm (MAC=alkali-calcic, MCA=calc-alkalic, o=oxidized, ow=weakly oxidized, r=reduced). 662
Figure I-8. Histograms of cadmium concentrations in ppm (MAC=alkali-calcic, MCA=calc-alkalic, o=oxidized, ow=weakly oxidized, r=reduced). . 663
Figure I-9. Histograms of cobalt concentrations in ppm (MAC=alkali-calcic, MCA=calc-alkalic, o=oxidized, ow=weakly oxidized, r=reduced). 664
Figure I-10. Histograms of chromium concentrations in ppm (MAC=alkali-calcic, MCA=calc-alkalic, o=oxidized, ow=weakly oxidized, r=reduced). . 665
Figure I-11. Histograms of copper concentrations in ppm (MAC=alkali-calcic, MCA=calc-alkalic, o=oxidized, ow=weakly oxidized, r=reduced). 666
Figure I-12. Histograms of iron concentrations in ppm (MAC=alkali-calcic, MCA=calc-alkalic, o=oxidized, ow=weakly oxidized, r=reduced). 667
Figure I-13. Histograms of fluorine concentrations in ppm (MAC=alkali-calcic, MCA=calc-alkalic, o=oxidized, ow=weakly oxidized, r=reduced). . 668
Figure I-14. Histograms of mercury concentrations in ppm (MAC=alkali-calcic, MCA=calc-alkalic, o=oxidized, ow=weakly oxidized, r=reduced). . 669
Figure I-15. Histograms of lithium concentrations in ppm (MAC=alkali-calcic, MCA=calc-alkalic, o=oxidized, ow=weakly oxidized, r=reduced). . 670
Figure I-16. Histograms of manganese concentrations in ppm (MAC=alkali-calcic, MCA=calc-alkalic, o=oxidized, ow=weakly oxidized, r=reduced). . 671
Figure I-17. Histograms of molybdenum concentrations in ppm (MAC=alkali-calcic, MCA=calc-alkalic, o=oxidized, ow=weakly oxidized, r=reduced). . 672
Figure I-18. Histograms of niobium concentrations in ppm (MAC=alkali-calcic, MCA=calc-alkalic, o=oxidized, ow=weakly oxidized, r=reduced). . 673
Figure I-19. Histograms of nickel concentrations in ppm (MAC=alkali-calcic, MCA=calc-alkalic, o=oxidized, ow=weakly oxidized, r=reduced). 674
Figure I-20. Histograms of lead concentrations in ppm (MAC=alkali-calcic, MCA=calc-alkalic, o=oxidized, ow=weakly oxidized, r=reduced). 675
Figure I-21. Histograms of rubidium concentrations in ppm (MAC=alkali-calcic, MCA=calc-alkalic, o=oxidized, ow=weakly oxidized, r=reduced). . 676

LIST OF ILLUSTRATIONS -- Continued

Figure I-22. Histograms of antimony concentrations in ppm (MAC=alkali-calcic, MCA=calc-alkalic, o=oxidized, ow=weakly oxidized, r=reduced). . 677
Figure I-23. Histograms of tin concentrations in ppm (MAC=alkali-calcic, MCA=calc-alkalic, o=oxidized, ow=weakly oxidized, r=reduced). 678
Figure I-24. Histograms of strontium concentrations in ppm (MAC=alkali-calcic, MCA=calc-alkalic, o=oxidized, ow=weakly oxidized, r=reduced). . 679
Figure I-25. Histograms of tellurium concentrations in ppm (MAC=alkali-calcic, MCA=calc-alkalic, o=oxidized, ow=weakly oxidized, r=reduced). . 680
Figure I-26. Histograms of titanium concentrations in ppm (MAC=alkali-calcic, MCA=calc-alkalic, o=oxidized, ow=weakly oxidized, r=reduced). . 681
Figure I-27. Histograms of thallium concentrations in ppm (MAC=alkali-calcic, MCA=calc-alkalic, o=oxidized, ow=weakly oxidized, r=reduced). . 682
Figure I-28. Histograms of vanadium concentrations in ppm (MAC=alkali-calcic, MCA=calc-alkalic, o=oxidized, ow=weakly oxidized, r=reduced). . 683
Figure I-29. Histograms of tungsten concentrations in ppm (MAC=alkali-calcic, MCA=calc-alkalic, o=oxidized, ow=weakly oxidized, r=reduced). . 684
Figure I-30. Histograms of yttrium concentrations in ppm (MAC=alkali-calcic, MCA=calc-alkalic, o=oxidized, ow=weakly oxidized, r=reduced). . 685
Figure I-31. Histograms of zinc concentrations in ppm (MAC=alkali-calcic, MCA=calc-alkalic, o=oxidized, ow=weakly oxidized, r=reduced). 686
Figure I-32. Histograms of zirconium concentrations in ppm (MAC=alkali-calcic, MCA=calc-alkalic, o=oxidized, ow=weakly oxidized, r=reduced). . 687

LIST OF TABLES

Table 2-1. Logical order and criteria for petrochemical classification of igneous rock series based on whole rock chemical data (from Keith and others, 1991). 58
Table 2-2. Magma series classification showing logical subdivisions of aluminum content, alkalinity, iron and water content, volatile content, oxidation state, and selected metal specializations (from Keith and others, 1991). 59
Table 2-3. Effect of weathering and alteration on classification parameters. 109
Table 2-4. Summary of effects of alteration on variation diagrams used in the petrochemical classification. 121
Table 2-5. Synopsis of major alteration types in selected magma series of the petrochemical classification and the correlative deposit types. . . . 122
Table 3-1. List of mining districts with sufficient trace element data for possible inclusion in this study. 124
Table 7-1. Statistics on whole rock analyses of six magma series classes. . . 388
Table 7-2. Statistics on whole rock ratios of six magma series classes. . . . 389
Table 7-3. Statistics on trace elements of mineralized samples from Ag to Mn. 393
Table 7-4. Statistics on trace elements of mineralized samples from Mo to Zr. 394
Table 7-5. Classification Results of Discriminant Analysis on Whole Rock Oxides. 399
Table 7-6. Classification Results of Discriminant Analysis on Trace Elements. 399
Table 7-7. Classification Results of Discriminant Analysis on Trace Elements of Alkali-calcic Classes. 400
Table 7-8. Classification Results of Discriminant Analysis on Trace Elements of Calc-alkalic Classes. 400
Table 10-1. Results of training with LVQ (learning vector quantization) and back propagation neural networks. 432
Table 10-2. Results of testing LVQ and back propagation neural networks trained on 90, 80, 70, and 50 percent of the data. 432
Table 10-3. Results of training LVQ neural networks trained with various types of whole rock data. 432

ABSTRACT

Six alkalinity and oxidation classes of fresh igneous rocks were correlated with trace elements in rock chip samples from temporally and spatially associated ore deposits. Learning vector quantization and back-propagation artificial neural networks correctly classified 100 percent of whole rock oxides and 99 percent of mineralized samples; discriminant analysis correctly classified 96 and 83 percent, respectively. The high degree of correlation between chemistries of igneous rocks and related mineralization implies genetic links between magmatic processes or sources and the ore deposits studied.

The petrochemical classification was evaluated by assigning 43 deposits to classes defined on eight variation diagrams, training neural networks to classify analyses of 569 igneous and 887 mineralized samples, and testing the networks on their ability to classify new data. Whole rock analyses were obtained from mining districts in which trace element geochemistry was also available. Half the data was eliminated using five alteration filter graphs. The K_2O and Fe_2O_3/FeO versus SiO_2 diagrams and iron mineralogy best defined alkalinity and oxidation classes. Neural networks trained with 90, 80, 70, or 50 percent of the samples correctly classified 81 to 100 percent of randomly withheld data.

SiO_2/K_2O ratios of alkali-calcic igneous rocks are 14-20 and of calc-alkalic 20-30. Fe_2O_3/FeO ratios are >0.8 with abundant magnetite and sphene for oxidized, 0.5-1.2 with magnetite, sphene, and rare ilmenite for weakly oxidized, and <0.6 with ilmenite only in reduced subclasses. Lead-zinc-silver deposits as at

Tombstone and Tintic are related to oxidized alkali-calcic igneous rocks. Polymetallic lead-zinc-copper-tin-silver deposits, such as Santa Eulalia and Tempiute, Nevada, are associated with weakly oxidized alkali-calcic rocks. Tin-silver deposits of Llallagua and Potosi are correlated with reduced alkali-calcic intrusives. Porphyry copper deposits as at Ray and Sierrita are connected with oxidized calc-alkalic plutons. Gold-rich porphyry copper deposits, such as Copper Canyon and Morenci are linked to weakly oxidized calc-alkalic plutons. Disseminated gold deposits, such as Chimney Creek, Nevada, are temporally and chemically correlated with reduced calc-alkalic igneous rocks, although physical connections between plutons and Carlin-type deposits remain unconfirmed.

Magma series classification and neural networks have profound applications and implications to exploration, alteration and zoning studies, and metallogenesis.

INTRODUCTION

Problem

The recognition of characteristic patterns in major, minor, and trace elements in mineral deposits is of primary importance in discovering new ore deposits. It is essential in exploring for different types of deposits to know what ranges of geochemical values are significant for each type. This dissertation investigates the question, "Can mineral deposits be classified on the basis of major element oxide patterns of the associated igneous rocks into categories that correlate with classes based on the trace element characteristics of the associated ore deposits?"

Knowing which elements to include in an analysis in order to most efficiently target the desired type of deposit will reduce the expense of exploration and increase the success rate by eliminating less likely drilling targets. Large exploration expenditures are wasted because drilling is done on deposits that do not have good potential for the desired commodity. Avoiding any wastage is especially important in the current economy in which less money is available for exploration. The impact of this study could especially be felt in developing nations where local resource assessment is hindered by a lack of necessary venture capital and technical expertise.

Although a great deal of research has been done on the geochemistry of various ore deposits, much of it is unavailable, incomplete, or unevaluated. A vast geochemical data base has accumulated in the files of exploration companies

in the last twenty years, but it is scattered through the files of competing companies and is unavailable to the public. Exploration companies rarely analyze more than eight or ten elements and generally keep their conclusions about these patterns confidential. Current exploration practice commonly tests for only a few of these elements (generally Cu, Au, Ag, Pb, Zn, Mo, As, Sb, Hg, W). Analyses of varying degrees of consistency have accumulated in the geologic literature and in files of exploration companies, yet a comprehensive statistical evaluation of mineral deposit types has not previously been published. Although some deposit types have been studied in great detail for several major elements, an analysis of a broad data set to correlate geochemical patterns with geological conditions favorable for particular ore deposit types has long been overdue. This comprehensive evaluation of precise element associations, ratios, abundances, and frequencies of occurrence in six ore-deposit types is a measure of the success of one classification system that can promote greater reliability in mineral exploration.

Solution Potential with Petrochemical Analyses

The classification of ore deposits based on the petrochemistry of the associated igneous rock developed by Stanley B. Keith of MagmaChem Exploration, Inc. (Keith and others, 1991) has continued to garner interest in the exploration community as a technique to aid in mineral exploration. The magma series classification is based on empirical observations of Peacock's (1931)

alkalinity classes of plutonic rocks that are associated with porphyry copper deposits, lead-zinc-silver deposits, and other types of ore deposits. Further refinements were made to the classification based on the oxidation state as measured by ferric/ferrous or Fe_2O_3/FeO ratio and on the presence of accessory minerals, such as the magnetite/ilmenite distinction of Ishihara (1977).

In his ongoing investigations into the relationship between magma series and associated ore deposits, Keith has been collecting whole rock analyses and 30 element geochemical analyses from the literature and from exploration companies for the last ten years. However, he has not had the time, equipment, or software to rigorously evaluate this data. Although his ideas are gaining increasing acceptance in the exploration community, many will continue to be skeptical until an exacting scientific examination has been published and critiqued. Mr. Keith has demonstrated his support of this study by offering access to all of his nonconfidential files.

Evaluation Potential with Neural Networks

Recent advances in pattern recognition software and the availability of computers that can handle large amounts of information make it possible to assess part of the vast geochemical data base now available. Neural networks are a new type of computerized pattern recognition with more human-like capabilities than conventional statistics. Neural network software excels at solving problems involving patterns, such as pattern recognition or classification, pattern

completion, generalizing or determining a pattern from examples, and discovering distinguishing features.

Neural network techniques offer a powerful new tool for determining the significant elements in various mineral deposit classes. Unlike conventional classification algorithms, neural networks can accurately resolve highly complex class boundaries. Neural networks mimic biological networks by breaking problems into many parts that can be processed by simple computational units. When these simple processing elements are interconnected in sufficient numbers, they exhibit extremely complex behaviors.

Research Objectives

This study has examined and evaluated the geochemical characteristics of two classes, calc-alkalic and alkali-calcic, of mineral deposits as classified by the magma series classification (Keith and others, 1991). This research established distinctions between the classes, evaluated internal consistency within the classes of ore deposits, and evaluated the degree of correlation between the geochemical patterns in the mineralized samples of each of six classes of ore deposits and the whole rock chemistry of the igneous rocks thought to be associated with the ore deposits.

Six Types of Ore Deposits Studied

Three types of oxidation states, reduced, weakly oxidized, and oxidized,

were examined within the two classes that were studied, calc-alkalic and alkali-calcic, for a total of six types of ore deposits. The metaluminous, calc-alkalic, hydrous system includes six subclasses, but only three classes had enough samples represented in the mineralized trace element database for adequate evaluation; these were the reduced, weakly oxidized, and oxidized subclasses. The metaluminous, alkali-calcic, hydrous system contains five subclasses but only three contained sufficient samples in the data base; these were the reduced (reduced to weakly oxidized in Figure 1 of Keith and others, 1991), weakly oxidized (weakly oxidized to oxidized), and oxidized (moderately oxidized) subclasses. There were insufficient samples in the strongly oxidized and strongly reduced classes to include in this study.

Alkali-calcic, Oxidized

Alkali-calcic, oxidized igneous rocks were found to be associated with lead-zinc-silver deposits that contained no production of tin; these are similar to Tombstone AZ, Tintic and Park City UT. These types of deposits include veins, skarn and replacement deposits in which zinc production is greater in quantity than lead, and silver and manganese are frequently produced as byproducts. Lesser amounts of boron, bismuth, barium, antimony, mercury, gold, beryllium, tellurium and fluorine also occur in these districts. Epithermal and hotspring deposits are also common in this class of deposits. Examples of alkali-calcic oxidized mining districts that were researched included Apache NM, Mud Springs

NV, Park City UT, Spring City NV, Tintic UT, Tombstone AZ, Dolly Varden NV, Fireball Ridge NV, Mine Mountain NV, Castle NV, Chloride NM, and Beaverdell BC.

Alkali-calcic, Weakly Oxidized

Alkali-calcic, weakly oxidized igneous rocks were found to be associated with lead-zinc-silver deposits that contained tin, similar to Santa Eulalia, Mexico and Candelaria, Nevada. This type of deposit includes epithermal veins, skarn, and replacement deposits that have lead, zinc and silver production, with significant occurrences of tin, bismuth, manganese, boron, mercury, and arsenic. They also include epithermal hotspring deposits with greater silver production than gold and including some lead, zinc, and beryllium production and significant presence of arsenic, antimony, mercury, bismuth, scandium, and fluorine. Examples of alkali-calcic, weakly oxidized mining districts in Nevada that were researched for this study included Bull Creek, Cove, Taylor, Candelaria, Pioche, Moho, Railroad, Ackerman Canyon, Comet, Dean, Michigan Boy, White Pine, Kinsley, Oak Spring, Tempiute, Freiberg, Cherry Creek, Linka, Merrimac, Swales Mountain, Nevada, as well as Tecoma, Utah, and Tierra Blanca, New Mexico.

Alkali-calcic, Reduced

Alkali-calcic, reduced igneous rocks were found to be associated with tin-silver deposits similar to the metaluminous Bolivian tin-silver deposits. These

included epithermal veins, porphyry, skarn and replacement deposits with tin and silver production and lesser amounts of gold, copper, indium, gallium, arsenic, boron, yttrium, fluorine and phosphorous. Examples of alkali-calcic, reduced mining districts include Llallagua, Oruro, and Potosi, Bolivia.

Calc-alkalic, Oxidized

Calc-alkalic, oxidized igneous rocks were found to be associated with porphyry copper deposits similar to the Pima mining district in southern Arizona. These included porphyry, skarn, and vein deposits with major production of copper and significant production of zinc and lead, with silver production greater than gold production, some molybdenum and manganese production and lesser amounts of arsenic, boron, and tungsten. Examples of calc-alkalic, oxidized mining districts in Arizona that were researched included Mineral Park, Red Mountain, Sierrita-Esperanza, Silver Bell, Twin Buttes-Mission, Christmas, and Ray (Mineral Creek). Other examples researched included Toro Mocha, Peru, Valley Copper, BC, Bethlehem, BC, Andacollo, Chile, Dutch Miller, WA, Elk Mountain, NV, and Mill City, NV.

Calc-alkalic, Weakly Oxidized

Calc-alkalic, weakly oxidized igneous rocks were found to be associated with gold-rich porphyry copper deposits similar to Copper Canyon, Nevada, and Morenci, Arizona. These deposits included porphyry, vein, skarn, and epithermal

deposits with significant production of copper, gold, silver, zinc, molybdenum, and lead, with lesser amounts of bismuth, arsenic, antimony, vanadium, scandium, and phosphorus. Examples of calc-alkalic, oxidized mining districts in Arizona that were researched included Ajo, Dos Pobres, and Morenci; other deposits investigated were Chartam, MT, Copper Canyon, NV, El Salvador and El Teniente, Chile, Dexing, China, Hedley, BC, and McCoy, Surprize, and Empire (Copper Basin), NV.

Calc-alkalic, Reduced

Calc-alkalic, reduced igneous rocks were found to be correlated with Nevada disseminated gold deposits similar to the Carlin-type deposits. These deposits included epithermal, skarn, jasperoid, porphyry, and hot spring deposits with gold production greater than silver production. Lesser amounts of arsenic, antimony, mercury, thallium, tungsten, light rare earth elements, zinc, copper, vanadium, nickel, and barium were also characteristic, as was the low sulfur content. Examples of calc-alkalic, reduced mining districts in Nevada that were researched in this study included Pony Creek, Jerritt Canyon, Northumberland, Alligator Ridge, Carlin, Cortez, Gold Acres, Gold Strike, Horse Canyon, Illipah, Chimney Creek North, Florida Canyon, Maggie Creek, Rain, Round Mountain, Cobb, Basque, Charleston, Potosi, Getchell, Pinson, and Preble. Grassy Mountain, OR, Wenatchee, WA, and Yellow Pine, ID, were also investigated.

Theoretical Background

Magma Series Classification

The magma series classification is based on whole rock chemistry of fresh igneous rocks as shown on variation diagrams indicating aluminum content, alkalinity, iron content, volatile content, and oxidation state. The hierarchy of subclasses (Keith and others, 1991) begins with aluminum content (peraluminous or metaluminous) as shown on an A/CNK diagram, which is molecular $Al_2O_3/(CaO+Na_2O+K_2O)$. These classes are then subdivided according to alkalinity as the magnesian, calcic, calc-alkalic, alkali-calcic, and alkalic classes as shown on K_2O vs. SiO_2 and other Harker variation diagrams. Further subclasses of hydrous and anhydrous are based on water content, as shown by the presence of OH^- bearing minerals and other diagrams. Additional subclasses are based on iron content and range from strongly to weakly iron-poor to moderately to strongly iron-rich; these classes are shown on the SiO_2 versus FeO^*/MgO diagram, in which FeO^*/MgO is calculated by the formula $[0.9(Fe_2O_3) + FeO]/MgO$. Further subclasses are based on halogen content, ranging from low to high fluoride and low to high chloride, and on oxidation state, ranging from strongly reduced, reduced, weakly oxidized, oxidized, moderately oxidized, and to strongly oxidized, as shown on ferric/ferrous ratio $[Fe_2O_3/FeO]$ vs. SiO_2 diagrams.

Characteristics of Neural Networks

Neural networks are systems that have a parallel processing structure with

many simple unit processors and many interconnections between them. Because they have a structure that is similar to biological brains, artificial neural networks exhibit some of the same abilities. They can learn from experience, generalize from previous examples to new ones, and abstract essential characteristics from input data containing irrelevant information. Although neural network machines are being developed, most neural network applications are run with software simulators on traditional computers. The parallel structure and interconnections are established with software that is commercially available for the personal computer.

In contrast with traditional computer software, neural networks are not programmed; instead they learn by example. Most applications use training sets of input data paired with its output class. After each presentation of data in supervised learning, the neural network adjusts the values of its internal weights. If the neural network chose the right class for the data that was input, the connections are strengthened; if not, those connections are weakened and the weights are adjusted to minimize the error. After enough iterations, the network can produce the correct class in response to each input pattern. In unsupervised learning, only input data are supplied and the neural network modifies the connections to produce output classes where similar input patterns are grouped into the same output class.

Application of Neural Network Techniques to Mineral Classification

Neural network simulations for the personal computer allow the researcher to design a project to test a particular application. Although developed applications are primarily in other fields, such as handwritten character recognition, bomb detectors, and military vehicle recognition, neural networks have been tested on geophysical data such as seismic signals and EM ellipticity (Poulton and others, 1990). Neural networks are also being developed for well log interpretation, image processing in remotely sensed images, and geographic information systems, although they have not yet been used on geochemical data. The present study was the first to use neural network software to evaluate how well geochemical data are classified into patterns to predict the type of ore deposit.

Although the patterns displayed in the geochemical data are only one attribute in the numerous geological features that must be considered in an ore deposit model, it is easily and commonly measured and is readily quantifiable. Therefore, it offers excellent evaluation potential for determining if the various classification schemes have isolated the classes or models well enough to maintain a consistent pattern in the geochemical data. Exploration geologists use this concept intuitively when they explore for Nevada gold deposits by analyzing for Au, Ag, As, Sb, Hg, and W. Neural network analysis offers a more mathematically rigorous, faster, and potentially more accurate method of determining the important patterns in the geochemical data and of relating these patterns to the

probability that they reflect potentially economic mineralization.

Work Plan

This study was an interdisciplinary doctoral dissertation with technical support from the Department of Geosciences and the faculty of Economic Geology in the College of Arts and Sciences and from the Department of Mines and Geological Engineering in the College of Engineering and Mines. Whole rock chemistry and trace element geochemical data were supplied on disks from several industry supporters, especially MagmaChem Exploration, Inc. in Seattle, Washington, and BHP Exploration in Salt Lake City, Utah, in a demonstration of the cooperation possible between industry and academia. The data consisted of several thousand samples of 30 to 40 element analyses from several hundred mines throughout the world, and especially from the southwestern United States.

Bibliographic Research

The GEOREF bibliographic data base from the American Geological Institute on Silver Platter at the University of Arizona library was searched for references relating to each of the mines that have samples in the mineralized trace element data base. Between 0 and 300 references for each of 300 mines were obtained from a search of the GEOREF database. The ninety mining districts that were judged to have sufficient numbers of good quality trace element data on mineralized samples to be included in the study were searched

for further detail and 2600 references were downloaded to disk and printed. The articles most likely to have whole rock chemical data were examined in the library and the important references at the end of each article added to the bibliographic data base. Funds provided by a University of Arizona grant were used to purchase ProCite and BibLink, which are software programs that take downloaded bibliographic information from Silver Platter, convert them into a data base, and then print the citations in the U.S. Geological Survey format.

Names of plutons, mountain ranges, locations, and other key words were obtained from economic geology articles on each mining district in order to do another search of the GEOREF data base for information that frequently occurs in different literature from the mining district descriptions. The important articles were examined in order to obtain the detailed mineralogy, whole rock chemistry, trace element chemistry, and other details necessary for the study.

Data Representation

Because the patterns in geochemical data from different classes of ore deposits are so complex, it was necessary to do a considerable amount of preprocessing of the data. This preliminary processing included qualifying the data as fresh or altered, determining the general characteristics and separability of the classes, regulating the various types of zeroes in the data as either below the detection limit or not included in the analyses, and managing inconsistencies in the data, in which some samples were analyzed for 30 elements and some for

40 elements. It was also necessary to separate out a training set and a test set from the data.

Whole Rock Chemical Analyses

Some whole rock analyses were available from MagmaChem Exploration, Inc. on disks in the PetChem spreadsheet files but most was obtained from the literature. The data consisted of analyses of SiO_2, Al_2O_3, TiO_2, Fe_2O_3, FeO, MnO, MgO, CaO, Na_2O, K_2O, P_2O_5, and LOI for several thousand samples of igneous rocks from the southwestern United States. Additional data were obtained from the geological literature, PETROS database, and MagmaChem Exploration files in Seattle, Washington.

The PetChem database was examined in the spreadsheet computer files and about 200 samples were found from mining districts selected for the study. These samples were converted from individual Symphony spreadsheet files into individual records in six files for the subclasses in this study. The original references for these data were also examined in the geologic literature and additional information on sample locations and volatile and trace element composition added to the database file. The articles were examined to determine which phases of the plutonic rocks were related to the mineralization, which were earlier phases unrelated to mineralization and therefore excluded, and which were too altered to be used. An additional 300 samples were found in the geological literature and in the MagmaChem Exploration files and entered into

the database.

About half of the 90 mining districts that had sufficient numbers of good quality trace element analyses available on the mineralized samples were found to have whole rock analyses available on the fresh igneous rocks associated with the mining district. Out of the forty-two districts with whole rock analyses, the data from twelve districts were found to be too altered for reliable categorizing of the classes, so only 30 of the original 90 mining districts were used in the data set for statistical and neural network analysis.

The procedure for classifying mining districts into the magma series classification consisted of plotting the whole rock data from each mine separately on 13 variation diagrams. The field into which the samples fell on the variation diagrams for each mine determined the class to which the mine was assigned. After the 30 mines were assigned to a class, variation diagrams were plotted that included data from all the mines in each class. These diagrams indicated a distinctive pattern for each of the six classes.

Once the mines were assigned to the magma series classes, petrologic and mineralogical information was compiled for each mine and grouped into classes in order to determine if there were patterns present. Information on the mineralogy of the associated igneous rock for each mining district was entered in spreadsheet databases.

Trace Element Geochemistry of Mineralized Samples

Geochemical data on mineralized systems were obtained from MagmaChem Exploration, Inc. and from the geological literature. Geochemical data from the 90 mines that were classified into the six ore deposit classes of this study were extracted from the MagmaChem data base of 1000 world-wide mining districts. Analyses of 30 to 40 elements (Ag, As, Au, Ba, Be, Bi, Br, Ca, Cd, Ce, Co, Cr, Cs, Cu, Eu, F, Fe, Ga, Hf, Hg, La, Lu, Mn, Mo, Na, Nd, Ni, Pb, Rb, Sb, Sc, Se, Sm, Sr, Ta, Tb, Te, Th, Ti, Tl, U, V, W, Y, Yb, Zn, Zr) for 7,000 samples was supplied on disk from the TracElem data base in R:Base from MagmaChem Exploration. BHP Exploration of Salt Lake City supplied analyses of 116 samples from 31 mines in the economic geology sample collection at the University of Arizona. Examination of the MagmaChem TracElem file produced about 3500 samples for the 90 mining districts judged to have sufficient representative trace element data on mineralized samples. Elimination of mining districts without whole rock chemistry on associated plutonic rocks left about 1700 samples available for the study. These data were extracted from this larger data set (30 megabytes) into spreadsheet and ASCII files before the neural network analysis was done.

Statistical Analysis

Standard statistical analysis was performed on the data to ascertain the general characteristics of the data in order to more efficiently analyze the data with neural networks. These included some of the standard petrologic diagrams,

commonly used magma series plots, standard statistical histograms and other diagrams. Commercial software, such as IGPET, RockStat, and SPSS, was used to produce these comparison diagrams and categorize the classes. Discriminant analysis was also used to determine the characteristics of the six subclasses of igneous rocks and associated ore deposit types.

Neural Network Analysis

Neural networks were used to recognize patterns in two sets of data: 1) whole rock analyses of fresh igneous rocks, and 2) trace element assays of mineralized samples from ore deposits associated with those igneous rocks. In both cases, the mines in the research database were grouped according to the class determined by the magma series classification. The neural networks were then trained using the geochemical data in this study as input patterns and the ore deposit classes as the output classes. Ten, twenty, thirty, and fifty percent of the analyses in the geochemical data base were withheld at random from the data base as a test set and the remaining ninety, eighty, seventy, or fifty percent of the data were used as the training set.

This procedure was done first with the whole rock chemical analyses of the associated igneous rock as input data and the ore deposit classes as output classes; then the procedure was repeated with the trace element assays of each sample as input data and the ore deposit class as output. Each model type was analyzed for consistency and effectiveness as a class with respect to both the

trace element analyses and the whole rock analyses.

The success of various neural network techniques was evaluated by comparing different types of networks, methods of data representation, and network design and training. The results of the neural network classification methods were compared with those obtained with conventional statistical methods.

Correlation with Geological and Geochemical Parameters

Correlations were made between the classes of mineral deposits as determined from the geochemical assays of mineralized samples and various geological and geochemical factors. Some of the geological parameters investigated for correlation with the six ore deposit classes included the whole rock chemistry of the associated fresh igneous rocks, petrology, production, mineralogy, and trace element associations.

This comparison demonstrated that the six classes studied were characterized by consistent patterns of geochemical data. This criteria is of utmost importance to exploration companies that are pursuing ore deposit targets with geochemical exploration projects. Current standard procedures that only analyze two to eight elements should be modified to include those chemical elements that are most effective in defining the particular ore deposit types the company is seeking.

Benefit from this Research

This analysis with neural networks has established that certain geochemical patterns are correlated with the six types of ore deposits in this study. Exploration may more rapidly target promising areas, resulting in a savings of millions of dollars. Geochemical sampling and assaying are relatively routine and readily quantifiable and are therefore widely used throughout the mineral exploration community. With the establishment of the validity of the magma series classification indicating which observations should made in the field, this exploration technique can be easily and broadly applied throughout the world. Demonstrating the effectiveness of neural networks as applied to geochemical data could increase the efficiency of global resource assessment and promote more effective planning for worldwide resource development.

Applications of neural networks are on the cutting edge of research in many scientific fields and offer many possibilities for future research in the geosciences and geological engineering. This application of neural networks to geochemical data will be a breakthrough that can then be applied to other kinds of geological data.

BACKGROUND ON MAGMA SERIES CLASSIFICATION OF IGNEOUS ROCKS

This chapter has been summarized from a preliminary manuscript by Stanley B. Keith entitled "Magma series, mineral deposits, and geotectonics". As of 1991, this manuscript consisted of nine chapters on the philosophy, historical development, and basis for the classification, the effect of alteration, aluminum content subdivisions, alkalinity distinctions, iron and water contents, oxidation state distinctions, and differentiation effects. These chapters have been summarized in the following sections.

Empirical and Logical Basis

The petrochemical classification of igneous rocks was developed empirically (Keith and others, 1991). Boundaries between the classes were drawn between clusters on variation diagrams of whole-rock chemical data from igneous rocks associated in time and space with various types of ore deposits. The classification is based on the core concept that a suite of comagmatic igneous rocks evolves along a differentiation path and has a hydrothermal ore deposit as the final, fluid-rich phase in the crystallization sequence. Thus, the underlying concept predicts a consistent, first-order chemical link between parent magma and daughter mineral deposit. Data from 3500 samples of igneous rocks known to be associated in time and space with particular types of ore deposits align in specific bands, suggesting that the fundamental concept is reasonable. If metals in a hydrothermal ore deposit are the extremely differentiated residue of a

parent magma, then exploration predictability is intrinsic to the petrochemical classification.

The source and original composition of the magma affect first-, second-, and third-order classes of aluminum content and alkalinity; processes of melting and other processes within the crust affect fourth-, fifth-, sixth-, and seventh-order classes of iron, water, and volatile contents, oxidation state, and degree of differentiation. Melting in different layers in the mantle or crust results in different original compositions. The sequential crystallization process of Bowen's Reaction Series differs slightly in each of the classes according to which minerals are stable in the iron, water, volatile, and oxidation state conditions of each class. The composition of the volatiles in the crust are extremely important in determining the final metal content of the ore deposit because their oxidation state influences which minerals crystallize first. The ability of the earlier formed minerals to accommodate certain metals in their structure determines which metals are concentrated in the hydrothermal fluid and therefore in the ore deposit. However, this crustal influence is superimposed on fundamentally different magmas which determine the original metal availability. In a time sense, crustal processes are secondary, whereas source region is primary.

The magma series classification utilizes typical logical mechanics, such as necessary and sufficient logical linkage between higher and lower order logical levels, non-circularity, consistent use of classification criteria at a given logical level, and overall logical linkage to a single organizing parameter or paradigm,

which in this case is magma series petrochemistry. Explanatory power is the philosophical criterion used to continually evaluate critically the classification; it is evaluated by specificity, predictivity, and testability. Specificity is the ability to classify and describe a given phenomena at the most detailed logical level that is possible. Predictivity is the ability to take new data and fit it into the taxonomic structure of the classification in an organized manner. Testability refers to how well the framework provided by the classification as an overall context and perspective is able to guide subsequent hypotheses to increase the probability of successful experimentation or testing in new directions.

Magmatic Tradition

Keith's petrochemical classification follows the magmatic tradition of Hutton (1788), de Beaumont (1847), Posepny (1895), Spurr (1903), Lindgren (in Graton, 1933), and many others. In fact, Lindgren not only made the fundamental correlation between igneous rocks and mineral deposits, but also interpreted them as resulting from what we now realize was a subduction zone moving through space and time. He stated,

> "this whole process of metallization, beginning at the earliest Cretaceous, closing at the end of the Tertiary, and feebly continuing today, is actually a continuous operation of separation of the volatile constituents from magmas that in their eastward sweep gradually became more differentiated from a basic beginning

through diorites and granodiorites to monzonites and quartz monzonites and finally, near the eastern margin, into rocks of distinctly 'alkaline' facies. ...

It is held that the whole Cordilleran metallization is based on the gradual eastward movement of deep-seated magmas beginning with the original impulse from the Pacific. That impulse is no doubt caused by the reaction between the North American continent and the deep sima layers of the Pacific. ... The theory held predicates the gradual movement of molten magma, or at least a gradual eastward process of liquefaction, in a layer perhaps 60 kilometers below the surface" (Lindgren in Graton, 1933, p. 179-180).

History and Development of the Magma Series Classification

The seeds of the petrochemical classification germinated during Keith's undergraduate classes. His interest in classification systems relating ore deposits and tectonic settings began in 1973 with an essay on ore deposit classification in Spencer Titley's ore deposit class. The magma series classification has been developed by Keith during the preceding 20 years, first as a student at the University of Arizona, later as a geologist at the Arizona Bureau of Geology and Mineral Technology, and finally as a consulting geologist with MagmaChem Exploration, Inc. The inspiration of some of his professors, such as Peter Coney and William Dickinson, and his early interests in plate tectonics, mineralogy, and

ore deposits, led him to search for connections between the processes involved in each of those subjects to explain systematic variations present. When Stanley B. Keith accepted the position at the Arizona state geological survey vacated by the retirement of Stanton B. Keith, he began to systematically investigate Arizona ore deposits and plutons. Keith's process of making observations about petrochemistry, mineralogy, and tectonics, placing these observations into a framework, and developing a paradigm to explain the relationships continued on a more regional scale when he left the state survey for consulting. Each workshop participant and client contributed to the process with questions and projects that added more data and required further refinements in the classification system. In this way, the petrochemical classification grew, with Keith testing each new concept to his own satisfaction but not having the time under the urgencies of a consulting practice to rigorously test and publish his results.

Classification Hierarchy

The magma series classification uses standard, whole rock, major element oxide analyses and immobile trace element analyses to classify igneous rocks. Chemical data are plotted on x-y scatter plots or variation diagrams with only minimal calculations, such as element or oxide ratios, needed in a few cases before plotting the diagrams. Thus an appraisal of the class of a given rock suite can be made by inspection of the raw analytical data. Normative calculations and renormalization of data to volatile-free formats are avoided because they are

model dependent. Thus, the nature of the associated metallization can often be predicted by scanning the whole rock analyses.

The logical hierarchy of the petrochemical classification is subdivided primarily into source-related criteria and secondarily into process-related criteria (Table 2-1). First-, second-, and third-order classes of aluminum content and alkalinity are based on the source and original composition of the magma. Fourth-, fifth-, sixth-, and seventh-order classes are based on processes of melting and other processes within the crust. The following discussion of the full magma series classification (Table 2-2) begins with the first-order division and proceeds through seventh-order splits (from Figure 1, Keith and others, 1991).

Logical Order	Classification Level	TYPE OF CRITERIA	NOMENCLATURE FOR CRITERIA	DETERMINATION OF CRITERIA
1st	Megaseries	aluminum content	peraluminous / metaluminous (broadly equivalent to S vs I granitoid distinction)	A/CNK vs. SiO_2 variation diagram
			peralkaline / metaluminous (subaluminous)	A/NK vs. SiO2 variation diagram
			perpotassic/peralkaline	A/NK vs. SiO2 variation diagram
2nd	Superseries	potassium- calcium-magnesium-silica and Nb-Zr-Rb-Sr content	alkaline / subalkaline	For Metaluminous K20 vs. SiO,, K_2O vs. SiO_2, K_2O + Na_2O vs. SiO_2, K_2O + MgO vs. SiO_2, CaO vs. SiO_2, Nb vs. Zr, and Rb vs. Sr, Rb-Sr and Sm-Nd isotopes.
				For Peraluminous CaO vs. SiO_2. Na_2O/K_2O vs. SiO_2, Rb vs Sr, Ba vs. Sr, and CaO vs. Sr plots.
3rd	Series	potassium-calcium-magnesium-silica & Nb-Zr-Rb-Sr content	Metaluminous subalkaline= magnesian, calcic, calc-alkalic	For Metaluminous K_2O vs. SiO_2 K_2O-CaO vs. SiO_2, K_2O-MgO vs.SiO_2, K_2O + Na_2O vs. SiO_2, CaO vs. SiO_2, Nb vs. Zr, and Rb vs. Sr, Rb-Sr and Sm-Nd isotopes
			Metaluminous alkaline= alkali-calcic, quartz or hyperstene-normative alkalic, nepheline normative alkalic, ultra-alkalic	
			Peraluminous subalkaline= calcic, calc-alkalic Peraluminous alkaline= alkali-calcic, alkalic	For Peraluminous CaO vs. SiO_2, Na_2O/K_2O vs. SiO_2, Rb vs. Sr, Ba vs. Sr, and CaO vs. Sr plots
4th	Subseries	Iron content also, Ti, Y, and V contents	Fe-rich (peralkalic in the case of Fe-rich alkaline); Fe-poor	AFM ternary diagram or SiO_2 vs. FeO*/MgO variation diagram (Miyashiro plot); Y vs. Zr, FeO/Fe_2O_3
		Water content	hydrous/anhydrous	Presence of OH-bearing minerals LOI and total H_2O histograms, oxygen isotopes
5th	Mini-series	F, Cl, CO_2, CH, Volatile content	F-rich, Cl rich (peralkaline or agpaitic); F-rich, Cl poor (ongonitic);, F-poor, Cl poor (normal); moderate F, Cl poor (rapakivine)	F vs. Cl; Rb vs. Zr plots, F, Cl, C total, and CO_2 histograms
6th	Micro-series	Oxygen content sulfur content distinction	oxidized/reduced = magnetite/ilmenite series	Fe_2O_3/FeO ratio, accessory sulfide and opaque oxide mineralogy; magnetic susceptibility; volume percent of opaque oxides, Fe_2O_3/FeO vs. SiO_2, A/CNK, and FeO*/MgO plots; 5 histograms, sullur isotopes, hydrogen isotopes
7th	System	degree of differentiation	quartz diorite (andesite); granodiorite (rhyodacite), granite (rhyolite)	Differentiation Index (D.I.); Larsen Factor (LF.), A/NK (inverse Agpaitic Index); Element or element ratio on y-axis vs. D.I., LF., SiO_2, or A/NK plots; oxygen isotopes

Table 2-1. Logical order and criteria for petrochemical classification of igneous rock series based on whole rock chemical data (from Keith and others, 1991).

Alu	Alkalinity	Fe, Ti, Y	F, Cl; Ba,Rb,Sr,Zr	CO2	Oxidation	metal production	important trace elements	environment	
Per	Calcic	hydrous	low F?, Cl?	high	r	Au	As, U, Th	por, pegs	
		Fe-, Ti-poor,		mod	o	Au-Ag	As, Pb, Zn, Cu, U, Th, V	v, por, pegs	
				low	ow	Au-Ag	Pb, Zn, Cu	v, pegs	
	Calc-alkalic		F-poor	mod	r	W-Pb-Zn-Ag	Be, F, Sn, Li, Ta, P	pegs, v, repl	
				low	o	W-Be-Pb-Zn-Ag	F, Bi, B	v, repl, skarns, pegs	
	Alkali-calcic		mod-hi F, low Cl	high	r	Sn-W-Cu-U-Pb-Zn-Ag-Li-C	As, F, B, Rb, Nb, Bi, Te, P	pegs, skarns, repl	
				low	o	U-W		v, pegs	
	Alkalic		hi F, low Cl	?	r to o	U-Th	Co, Ni, As, Bi	v & por, pegs	
Met	Magnesian	anhydrous,	low F, low Cl	high	very r	Au>>Ag	As, Co, Ni, Cr	v & exhal	
		very Fe-poor,			r	Ni>>Cu, Pd, Co	As	iss, diss	
		low Ti, v low Y		?	ow	Cr (ios); Cu>Zn-Au-Ag	Co, Ni, Mn, Fe	VMS, oceanic ridges	
	Calcic	hydrous, very Fe-	low F, low Cl	mod high	very r	Au>Ag	As, CO2, Co, Ni, B, Li	v, exhal	
		poor, low Y			r	Au>Ag	As, Cu, Bi, Pb, Zn	v, exhal	
				mod	ow	Cu>Zn-Au-Ag; Cu-Zn-Ag>Au	Mo, Co; Bi, F, As, Pb	por; VMS	
		anhyd-wkly hyd.	low F, low Cl	low-mod	very r	PGE-Au	Bi-Te-FeO-As-low S	iss	
		Fe-rich, mod-hi Y			r	Cu-Co-Ni-PGE; Zn>Cu-Ag-Au	As, FeO, high S; Co-As, Mn, Fe	iss; VMS	
	Calc-alkalic	hydrous,	low F, low Cl	mod	very r	Au>Ag	As, CO2, B, Sb, Hg, W	v, exhal, por	
		Fe, Ti-poor			r	Au>Ag	As,Sb,Hg,Tl,W,LREE,Zn,Cu,V,Ni,Ba,low S	por, skarns, jasp, epi, hot	*
		low Y		to	ow	Cu-Au-Ag-Zn-Mo-Pb	Bi-As-Sb-V-Sc-P	por, v, skarns, epi	*
					o	Cu-Zn-Pb-Ag>>Au-Mo-Mn	As, B, W	skarns, por, v	*
					mod o	Cu; W-Cu-Mo; S; Pb-Zn-Ag-Au-Ba	As-Te-Bi-Se-Sn; Ag>>Ag, Bi,Pb,Zn; Bi-Sb-Hg-Tl-As	epi; skarn; volc; VMS	
				low	os	Mg	W-Cu	skarns, repl, epi	
		anhydrous,	low F, low Cl	low	very r	Au	PGE, low S, FeO, As	iss	
		Fe-rich, Ti-rich			r to ow	Zn>C-Pb-Ag	Ba	VMS oceanic ridges only	
		high Y	F,Cl-poor, peralkal.	low	r	none known			
		vy anhyd, anorth.	low F, low Cl	mod	very r to r	none known			
	Alkali-calcic	vy hyd, lamproph	mod F, low Cl	mod to h	ow to o	none known			
		hydrous	low to mod F	mod to hi	rs to r	Ag	Co, Ni, As, Bi, U	v	
		Fe, Ti-poor	low Cl		r to ow	Sn-Ag	Zn, Cu, In, Ga, As, B, Y, F, P	v, por, skarns, repl, epi	*
		low Y		mod	ow to o	Pb-Zn-Ag; Ag>>Au	Sn,Bi,Mn,B,Sb,Hg,As; Pb-Zn-Be, As,Sb,Hg,Bi,Se,F	v, skarns, repl, exhal; epi, hot	*
				low	mod o	Zn>Pb-Ag-Mn; Ag>>Au, Mn	B,Bi,Ba,Sb,Hg,As,Be,Te; Pb-Zn-Be,Ba,Hg,Sb,Bi,Te,F	v, skarns, repl; epi, exhal, hot	*
					os	?U-Th; Fe; Mn	Ag,Co,Pb,Bi,Be,F; P,Pb,Zn,Ag,F,V,Y; Be,W,Pb,Zn,Ag	v,repl; v,repl,skarns,ios; epi, exhal,hot	
		weakly hydrous	mod F, vy low Cl	mod	r to ow				
		mod Fe-rich,	Rapakivine series	to	ow to o	Mo, F	Ag, Pb, Zn, Bi, Sb	v, por	
		Ti-poor, high Y		low	os	U, Th		v, diss	
		weakly hydrous	low to mod Cl	mod	r	Sn	F, Rb	vpp	
		mod Fe-rich	high F-Rb		ow	Mo-Sn	Mn, F, Ga, In, Bi, Rb, W		
		Ti-poor, mod hi Y	F/Cl >3, low Zr	to	o	Mo	Be, Sn, Ga, Pb, Zn, Ag, Bi, F, Mn, Rb, W		
			Ongonitic series	low	os	Be; Be-F-U	F, Fe, Sn, Mn, W; Mn	skarns, repl; epi, hot	
		anhyd, wk Fe, hiY	low to mod F		r to ow	none known			
		weakly hydrous	high F, mod Cl,hi Zr	low	r to ow	HREE, Y, Hg	LREE, Zr, Mo, Sn, F, Cl, Li, U, Th, Cl	epi, diss, hot	
		wk to mod Fe-rich	F/Cl=1-3		ow ot o	Nb, Zr, U, Th, F		diss	
		Ti-poor to rich, hi Y	Peralkaline (cont.)		o to os	LREE, Be, Y, U, Th, Zr, Mo, Sn, F		v, diss	
		anhyd, mod Fe-rich	high F,low Cl,Peralk		r to ow	none known			
		anhyd, Fe-rich Anor	mod F	mod	r to ow	Ti-Fe-V	P	ios	
	Quartz Alkalic	vy hyd,Fe-poor Lam	mod F, low Cl, Sr ric	high	ow to o	none known			
		hydrous,	mod F-Cl	mod	r	PGE	Au, Cu, Ni, Co	v, iss, diss	
		Fe-poor,	Miaskitic	to	ow	Cu-Au<Ag-Pb-Zn; Au>Ag	Te, F; Be, F, Mn	v, por; epi	
		Ti-poor			o	Cu-Au-Fe-U-LREE		por	
		low Y		low	os	Fe; U-F; Cu-Ag>>Au-Pg-Zn-U-Mn; Cu,Ag,Au;	P,F,V,Y,Sc; Mo; Bi; Fe; Be,W,Fe	ios; v,epi; por; epi, diss; epi, exhal, hot	
			mod to hi F, low Cl	mod to hi	ow to om	Cu-Au<Ag, PGE,PB,Zn,Mo; PGE	Te, F, Mn, Co, Ni; Au, Ni, Cr, Co, As, Fe	v, por; iss, diss	
		anhyd, wk Fe-rich	mod F, low Cl		r to ow	none known			
			high F-Cl; Peralkaline		ow to o	Nb-Zr-U-Th-Be	F, LREE, Y	v, diss	
		anhyd, Fe rich; Anort	mod F, low Cl	mod	r to ow	Ti-Fe-V	P	ios	
	Nepheline	vy hyd,Fe-poor;Lam	mod F, low Cl, Sr-ric	high	ow to o	none known			
	Alkalic	weakly hydrous	mod F-Cl Miaskitic	mod	r	Au>Ag	Te, Fe, Co, Mo, Ba, Sr, Rb	v, epi	
		Fe-rich			ow to o	Cu-Au	Mo	por	
					os	U, Th	LREE, Pb>Zr, Ag>Ar, LREE, Ba, Sr		
		mod anhyd, Fe-rich	mod F, low Cl		r to ow	none known			
		weakly anhydrous	high F-Cl-Zr Agpaitic	mod	r to ow	Hg	F, Li, U, Zr, Cl	v, repl, diss	
		wk to mod Fe-rich			ow to o	Al	Zr, Y, Ti, F, Cl	pegs	
		high Y			o to os	LREE, Zr, U, Th, Y	Mo, Nb, F, Cl	peg, ios	
	Hyperalkalic	vy hydrous, Fe-poor	modF,lowCl,Miaskiti	high	r to ow	none known			
		Lamprophyric series	mod F-Cl, Agpaitic		ow to o	none known			
		weakly hydrous	mod F, low Cl, Sr-ric	very high	r to ow	Nb?			
		wk to mod Fe-rich	Ba-rich		ow to os	Cu, Fe, Au, P, U, Th, Zr, Sr, Ba	LREE, Nb, Ta	carb	
		Carbonatitic	Miaskitic, Shonkonitic		os	LREE	Ba-Sr-Cu	carb, v	
		hydrous, Fe-rich, hi	high f-Cl, Ba,Sr-poor	very high	r to ow	Ti>Nb, Fe	P, Pb, Zn, Ag, Ba, Zr	carb, v	
		Carbonatitic	Agpaitic, ljolitic		o	Nb>>Ti, P, Fe, Mn	LREE, Zr	carb	
		hydrous, mod Fe-ric	mod F, low Cl,Sr-ric	mod	o	Cu, Au	Ba, Sr, Ag		
		wk hydrous, wkFe-ri	modF,lowCl, Miaskit	mod	r to ow	none known			
		anhyd, mod Fe-rich	highF-Cl, ljol/Agpaiti	high	ow	none known			
	Ultra-alkalic	hyd to vy hyd, Fe-po	high F, low Cl, Perp	high	r	C	diamonds		
	kimberlite-lam	vy hydrous, Fe-poor	high F, low Cl, Perp	vy high	o	none known			
	HighK Ultra-alk	hydrous, Fe-poor	high F, low Cl, Perp	low	o to os	none known			

Abbreviations: hyd=hydrous, anhyd=anhydrous; vy=very; hi=high; r=reduced, ow=weakly oxidized, o = oxidized, os = strongly oxidized;
por=stockwork porphyries; v= mesothermal to hypothermal veins; repl=replacements; epi=epithermal veins and stockworks;
iss=immiscible sulfide segregations; ios=immiscible oxide segregations; VMS=volcanogene massive sulfides (syngenitic)
exhal=syngenietic exhalative; pegs=pegmatites; carb=carbonatites; diss=disseminations; hot=hotsprings

Table 2-2. Magma series classification showing logical subdivisions of aluminum content, alkalinity, iron and water content, volatile content, oxidation state, and selected metal specializations (from Keith and others, 1991).

Alu	Alkalinity	Fe, Ti, Y	F, Cl; Ba,Rb,Sr,Zr	CO2	Oxidation	metal production	important trace elements	environment
Per	Calcic	hydrous	low F?, Cl?	high	r	Au	As, U, Th	por, pegs
		Fe-, Ti-poor,		mod	o	Au-Ag	As, Pb, Zn, Cu, U, Th, V	v, por, pegs
				low	ow	Au-Ag	Pb, Zn, Cu	

Aluminum Content

History and Development of Aluminum Classes

A project to evaluate the uranium potential associated with various plutons of the 'metamorphic core complexes' of the western U. S. led to the recognition of two major types of plutons -- the highly aluminous muscovite- and garnet-bearing plutons and the less aluminous hornblende-bearing plutons (Keith and Reynolds, 1980; Reynolds and Keith, 1983). These two classes were somewhat similar to the 'S' and 'I' type granites of Chappell and White (1974), but enough different to require a different terminology -- the peraluminous (in the sense of Shand, 1927) and metaluminous categories. These two categories became the first-order classification split in the petrochemical classification.

Description of Aluminum Classes

The aluminum content of igneous rocks was historically the first chemical serial parameter to be investigated and characterized. In 1927 Shand classified volcanic magma series based on various ratios of aluminum versus alkali content to measure aluminum saturation within a magma series. He defined the A/CNK index, which is used in the petrochemical classification to distinguish between the two first-order classes, peraluminous and metaluminous.

The formula for the A/CNK index is:

$$\text{A/CNK} = \frac{(\text{wt\% } Al_2O_3 / 102)}{(\text{wt\% CaO} / 56) + (\text{wt\% } Na_2O / 62) + (\text{wt\% } K_2O / 94)}$$

If the A/CNK ratio for an igneous rock is greater than 1, it is classified as peraluminous; rocks with the A/CNK ratio less than 1 are classified as metaluminous (Shand, 1927). Mineralogy determines the category in the area of overlap.

In the petrochemical classification the A/CNK index is plotted versus the weight percent SiO_2 (Figure 2-1). Crustal sources are comparatively aluminum- and silica-rich and are therefore peraluminous or sialic. Mantle sources are more silica- and aluminum-poor and are therefore metaluminous or simatic.

Petrotectonic Implications of Aluminum Content

Aluminum content is believed to be related to the source material for the magma. The source and aluminum content of the magma depends upon where melting occurs. If melting occurs in the mantle above a subduction zone with melting induced by dehydration and metamorphism of the downgoing oceanic slab, then the result is metaluminous magmatism. If melting occurs in the crust as a result of continent-continent collision or very shallow subduction, then the result is peraluminous magmatism.

In a broad sense, peraluminous granitoids belong to the 'S' granite group, whereas metaluminous magmatism belongs to the 'I' granite group of Chappell and White (1974). Metaluminous magma series are thought to be produced by melting processes that initiate in simatic sources in the lower lithosphere or asthenospheric layers of the mantle. In contrast, peraluminous magmatism is

thought to be produced by fusion of sialic crustal materials in settings that involve low-angle tectonic interactions between crustal materials.

Aluminum Classes

Peraluminous Mineralogic Indicators

Peraluminous rocks are distinguished by the presence of muscovite; small red almandine-spessartine garnets are particularly diagnostic. Silica contents range between 65 percent and 78 percent SiO_2 and mineralogy commonly includes muscovite and/or cordierite and garnet in the differentiation sequence. Less common, but indicative of peraluminous affinity of igneous rocks, are the aluminum-rich minerals andalusite, sillimanite, and corundum. The presence of magmatic garnet in even trace amounts is an unequivocal guide to the peraluminous class (Keith, unpublished manuscript, 1990). Peraluminous magmatism crystallizes in the mid-crust typically below 8 km (Keith and others, 1991).

Metaluminous Mineralogic Indicators

Metaluminous rocks are generally characterized by the presence of hornblende or of pyroxene and olivine in the more mafic phases. The presence of hornblende, pyroxene, or olivine in any amount is a conclusive indication of the metaluminous category. Because of their generally less hydrous aspect, metaluminous magmatism commonly erupts on the surface as extensive volcanism.

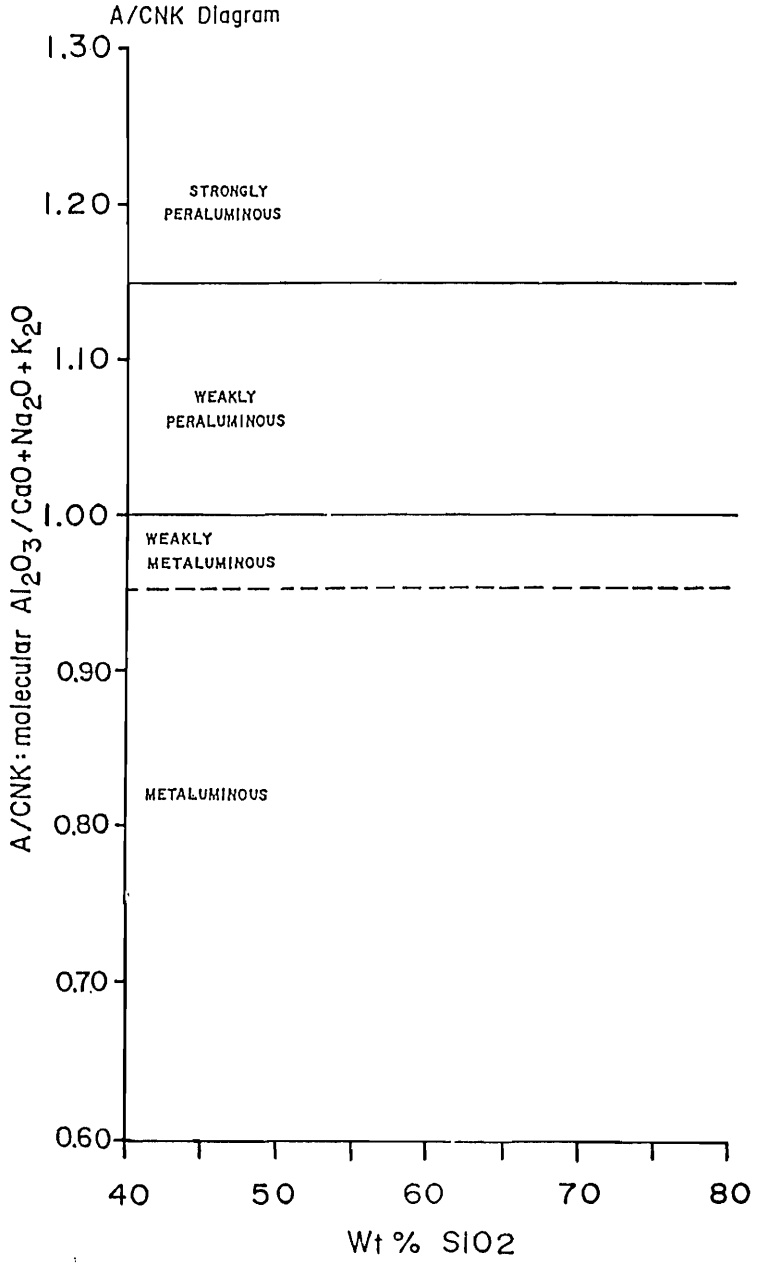

Figure 2-1. A/CNK versus weight percent SiO_2 variation diagram. A/CNK = molecular $Al_2O_3/(CaO + Na_2O + K_2O)$. Rock suites in the peraluminous category in the petrochemical classification range upward from A/CNK = 1; rock suites in the metaluminous class range downward from A/CNK = 1.15. Mineralogy determines the category in the overlap area.

There is some overlap between metaluminous rocks and peraluminous rocks between 65 percent and 78 percent SiO_2 and A/CNK values of 0.975 to 1.11. In the region of overlap, mineralogy is an important method of distinguishing the appropriate aluminum-content class. In general, the weakly peraluminous differentiates of metaluminous rocks contain only biotite as the one mica and do not contain garnet; they may commonly contain hornblende and less commonly contain pyroxene and/or olivine. Weakly peraluminous differentiates of peraluminous rocks typically contain aluminum-rich minerals such as garnet and muscovite and more rarely cordierite, corundum, and sillimanite.

Alkalinity

Alkalinity distinctions are the basis of the second- and third-order logic levels in the petrochemical classification. The second-order logic level distinguishes between alkaline and subalkaline. The third-order logic level is an expansion of the detailed distinction among the various alkalinities originally delineated by Peacock (1931) and added to by Keith. These alkalinity classes are subdivisions of both metaluminous and peraluminous categories.

History and Development of Alkalinity Classes

Keith first noticed that the Arizona porphyry copper deposits were associated with calc-alkalic igneous rocks as defined by Peacock's (1931) alkali-lime index. The Laramide lead-zinc deposits in Arizona were associated with

slightly older plutons of alkali-calcic composition than plutons associated with porphyry copper deposits that were of calc-alkalic composition (Keith, 1978a, 1979).

During his work with paleosubduction geometries in the Cretaceous and Tertiary in southwestern North America, Keith (1978b) tabulated several indices from the petrologic literature for ore deposits classified by Peacock's categories of calcic, calc-alkalic, alkali-calcic and alkalic. The $K_{57.5}$ index, which is the K_2O content of a comagmatic suite at 57.5 percent SiO_2 on a Harker variation diagram, was especially useful and was tabulated for numerous plutons in the southwestern United States. These data showed that metal character of a magma series varied as a function of the alkalinity.

Additional research into molybdenum systems led to refinements in the classification system. The correspondence of significant wulfenite specimens with oxidized alkali-calcic lead-zinc-silver districts and of molybdenite with calc-alkalic porphyry copper deposits in Arizona was noted in a study of molybdenum in Arizona (Wilt and Keith, 1981). Subsequent work showed that the chemistry of stockwork molybdenum deposits also varied with alkalinity content (Westra and Keith, 1981; 1982). Climax-type stockwork molybdenum deposits with elevated lithophile element content (F, Rb, Sn, and Nb) were clearly associated with alkali-calcic granites. Quartz Hill-type porphyry molybdenum deposits without lithophile element enrichment showed a consistent association with calc-alkalic granites.

A broader study of base and precious metal mining districts and plutons for Cretaceous through Cenozoic systems in the southwestern U. S. was done for Exxon in 1981 and 1982. The results were compiled on 15 time-slice maps which showed alkalinity and metallogenic belts transgressing and regressing across the western U. S. in a detailed chronology. One of the important contributions to the petrochemical classification from the Exxon study was the recognition of the relationship of precious metal content and alkalinity. Earlier studies emphasizing base metals had shown the correlation of copper with calc-alkalic petrochemistry and of lead-zinc with alkali-calcic petrochemistry. The Exxon study documented the association of gold with calc-alkalic and of silver with alkali-calcic systems (Keith, 1987).

Additional metallogenic, tectonic, and stratigraphic characteristics of each alkalinity class within the metaluminous and peraluminous categories were investigated during the Mojave project for Gulf Minerals in 1984. Because the Laramide and Tertiary magmatic arcs could be broken into their component alkalinity belts by the use of the petrochemical classification, it was possible to subdivide the Laramide and mid-Tertiary orogenies into much finer detail with the timing on tectonic events controlled by the timing and composition of the magmatism that the structures affected. This strato-tectonic approach plotted magmatic, stratigraphic, structural, and metallogenic information on a time column for each mountain range in southern Arizona, California, and New Mexico. These columns were then arranged approximately perpendicular to the magmatic

arc in a strato-tectonic time-distance diagram that demonstrated the sweep of these related features eastward in the Laramide and westward in the mid-Tertiary (Keith and Wilt, 1985; 1986).

Discussions with Michael Fellows of Exxon Minerals led to the inclusion of some massive sulfide deposits into the petrochemical classification. Kuroko-type Pb-Zn-Cu-Ag-barite massive sulfide deposits were found to be exhalative facies of calc-alkalic (medium-K) rhyolite magmatism erupted into submarine environments. Noranda- or Jerome-type Cu-Zn-chlorite pipe, massive sulfide deposits were recognized as exhalative products of calcic (low-K) rhyolite magmatism in submarine systems.

A 1983 study of gold metallogeny in greenstone belts of the Great Lakes region for Steve Potter of Kennecott Exploration (Keith, Swan, and Parr, 1985) extended the correlations of alkalinity and petrochemistry of associated igneous rocks from the Cretaceous into the Archean. This study integrated aspects of gold metallogeny into the petrochemical classification, which had previously been primarily focused on base metal and molybdenum metallogeny. In this study, the 2.7 Ga Hemlo deposit was found to be geochemically similar to the 35 Ma Carlin deposit in that both were associated with calc-alkalic metaluminous magmas.

In 1984, Keith and Monte M. Swan formed MagmaChem Exploration, Inc. and began a precious metal study for Steve Potter funded by Kennecott Minerals. This study showed the dramatic silver bias of the metaluminous alkali-calcic series. All metal systems with an Ag:Au ratio greater than 40:1 were associated

with igneous rocks of alkali-calcic petrochemistry. This 40:1 Ag:Au ratio was one of the first 'threshold numbers' discovered; it has subsequently been incorporated into a computerized expert system, which evaluates samples for classification into a broad array of ore deposit models.

Additional alkalinity distinctions between gold occurrences within the alkaline metaluminous class were made after discussions with Felix Mutschler in June, 1984. Data from Mutschler fell into two types of gold deposits within the alkaline category. The Te-poor gold deposits were associated with quartz-bearing (high-K) quartz-alkalic rhyolite systems; the Te-rich gold deposits were associated with nepheline-bearing syenites, monzonites, and phonolites.

To graphically display the concept of magma series and metallogeny during workshops a chart relating tectonic setting and petrochemistry was completed in September, 1984; it measured 1 m by 3 m and was therefore informally termed the 'megachart'. This chart depicted global tectonic setting, geophysical data, and possible depths to magma source, inferred crustal and mantle protoliths for magma series, and isotopic data as they each correlated to particular classes in the magma series chemical classification. The top part of the megachart was devoted to peraluminous classes resulting from crustal collisions; the middle part of the megachart depicted metaluminous classes resulting from subduction settings; and the lower part of the 'megachart' showed rift and intraplate settings responsible for the most alkalic classes.

A major upgrade on the 'megachart' was undertaken in April, 1985, to

respond to suggestions by Monte Swan and by BHP, Billiton, Kennecott, and Newmont clients to include the correlation of magma series classes with various ore deposit types. As a result the 'megachart' grew another 1.3 meters; the ore deposit types and their examples were organized according to depositional environments within aluminum and alkalinity classes.

At the request of Ray Morley of Utah Minerals the 'Geochemical Handbook' project was begun in December, 1985, to catalog the various threshold values in mineralized systems that could indicate precious metal classes in the petrochemical classification. The logic, metal content, and values of ratios that indicate significant 'switches' shunting decisions to various magma series classes have now been programmed into a MagmaChem Expert System with the cooperation of FMC Gold. This project is continuing with FMC and BHP support to extend the expert system to include base metal systems.

The publication in 1986 by the Arizona Geological Society of Keith's Laramide metallogeny and magmatism paper (Keith, 1986) marked the first peer-review publication of the diagrams used to show the fields for the various metaluminous classes in the petrochemical classification. Important variation diagrams used in this paper included those plotting SiO_2 vs. A/CNK, K_2O, K_2O-CaO, FeO^*/MgO, and ferric/ferrous ratio. The K_2O vs. SiO_2 and K_2O-CaO vs. SiO_2 variation diagrams were used to indicate the second- and third-order classes of alkalinity.

Through discussions with numerous clients, especially Nigel Grant of

Billiton and U. S. Geological Survey geologists in 1986, oxygen content, as expressed by Fe_2O_3/FeO ratio of epizonal plutons, was investigated and empirically correlated with gold:silver ratios and precious:base metal ratios of related mineral deposits. Within similar systems of alkali-calcic magma series, Sn-B-Li metal deposits were found to be associated with reduced plutons, stockwork Mo metal deposits were associated with oxidized plutons, and Be-F-U metal deposits were associated with strongly oxidized plutons. Within similar systems of calc-alkalic magma series, Au-biased precious metal deposits were associated with reduced plutons, Cu-Au metal deposits were associated with plutons of intermediate oxidation state, and Cu-biased base metal deposits were associated with oxidized plutons.

Further distinctions in the ultra-alkaline serial group were facilitated by the hiring in October, 1987, of MagmaChem employee Karl Albert, who had expertise and data on diamond and kimberlite-lamproite rock systems. The diamondiferous kimberlite-lamproite suites showed increasing reduction with increasing differentiation, whereas non-diamondiferous suites showed an oxidizing trend with increasing differentiation.

Description of Alkalinity

Alkalinity classes within the peraluminous category are shown in Figure 2-2 which plots ppm of Sr versus weight percent CaO. Numerous other classifying diagrams (Na_2O vs. SiO_2, Na_2O/K_2O vs. SiO_2, CaO vs. SiO_2, Sr vs. Ba, and Sr vs.

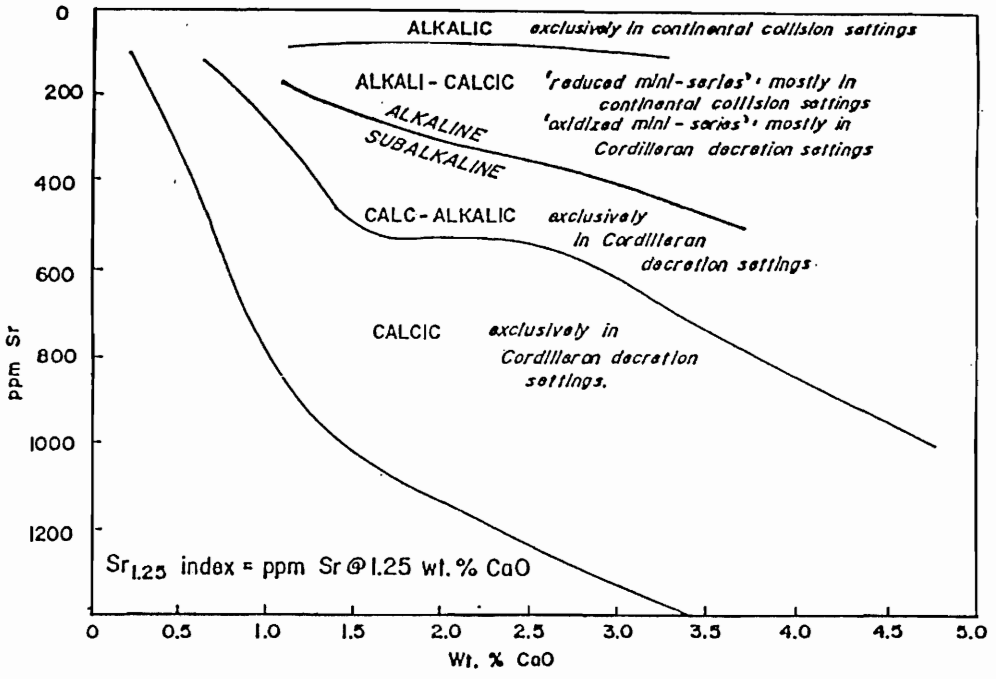

Figure 2-2. Sr (in ppm) versus weight percent CaO variation diagram showing correlation of pluton petrochemistry with tectonic settings for worldwide peraluminous granitoid series.

Rb) are used in the petrochemical classification (Keith, 1986). They are not included here because this dissertation does not examine the peraluminous class.

Alkalinity classes within the metaluminous category are shown in Figures 2-3, 2-4, 2-5, and 2-6; the fields on these diagrams were drawn between groupings of data points from ore deposits of different types in Keith's worldwide database of over 5000 mining districts. For example, the line between alkali-calcic and calc-alkalic fields was drawn between plutons associated with lead-zinc-silver deposits and plutons associated with Arizona porphyry copper deposits. The same line between alkali-calcic and calc-alkalic fields was drawn between igneous rocks associated with silver deposits and those associated with gold deposits in Nevada.

The most commonly used variation diagram is the K_2O vs. SiO_2 diagram of Figure 2-3, which shows the ultra-alkalic, nepheline-alkalic, quartz-alkalic, alkali-calcic, calc-alkalic, calcic, and magnesian fields. The same fields are shown on Figure 2-4, which is the weight percent K_2O minus CaO versus weight percent SiO_2 variation diagram, and Figure 2-5, which is the weight percent K_2O minus MgO versus weight percent SiO_2 variation diagram. A less systematic variation of alkalinity is shown by the fields in Figure 2-6, which graphs on log scale the ppm of Nb versus ppm of Zr; although these data are not commonly available, the plot is useful with samples of altered rocks and works best for subalkaline categories.

Several lines of evidence, both graphical from the whole rock data and

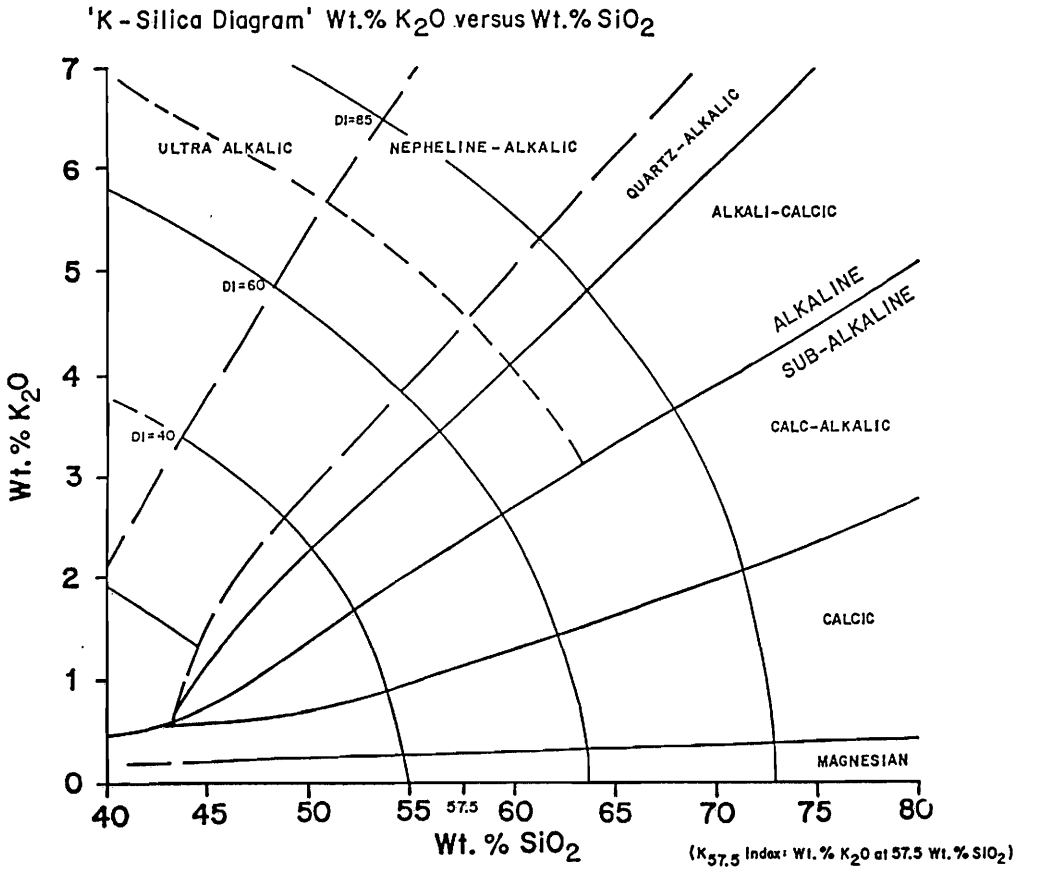

Figure 2-3. Weight percent K_2O versus weight percent SiO_2 variation diagram. $K_{57.5}$ index = weight percent K_2O at 57.5 weight percent SiO_2. Magma series classes are the alkalinity belts with positive slope. Curved lines with negative slope refer to Differentiation Index (DI) and are a function of the amount of silica in the rock.

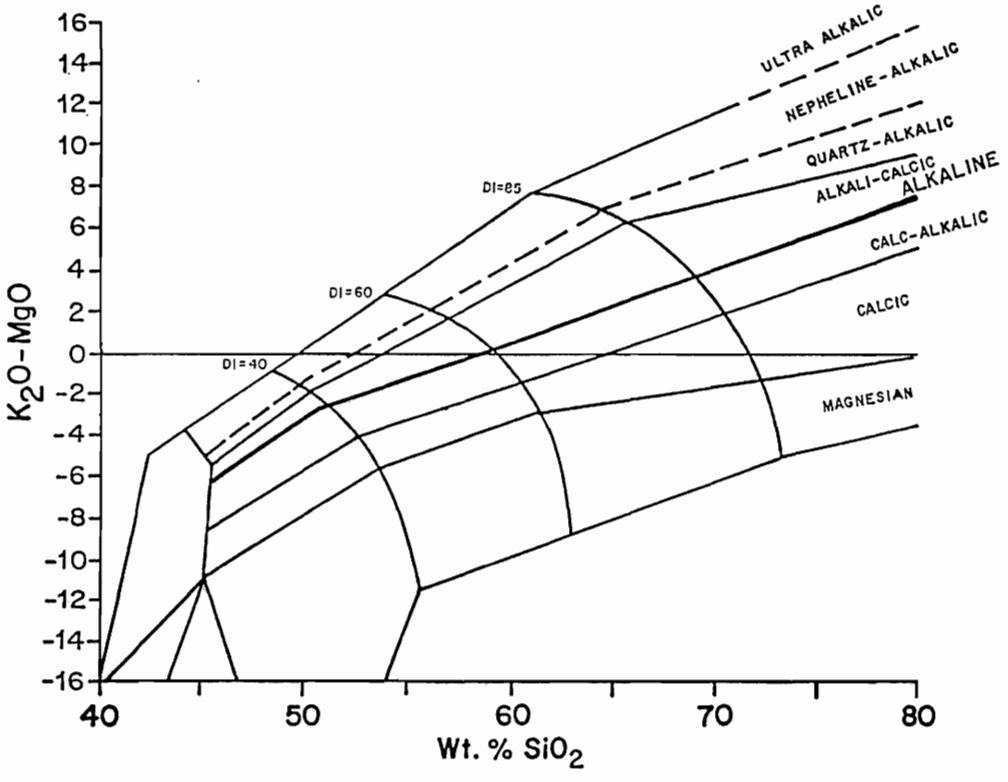

Figure 2-5. Weight percent K_2O minus weight percent MgO versus weight percent SiO_2 variation diagram showing alkalinity categories in the petrochemical classification. DI= Differentiation Index.

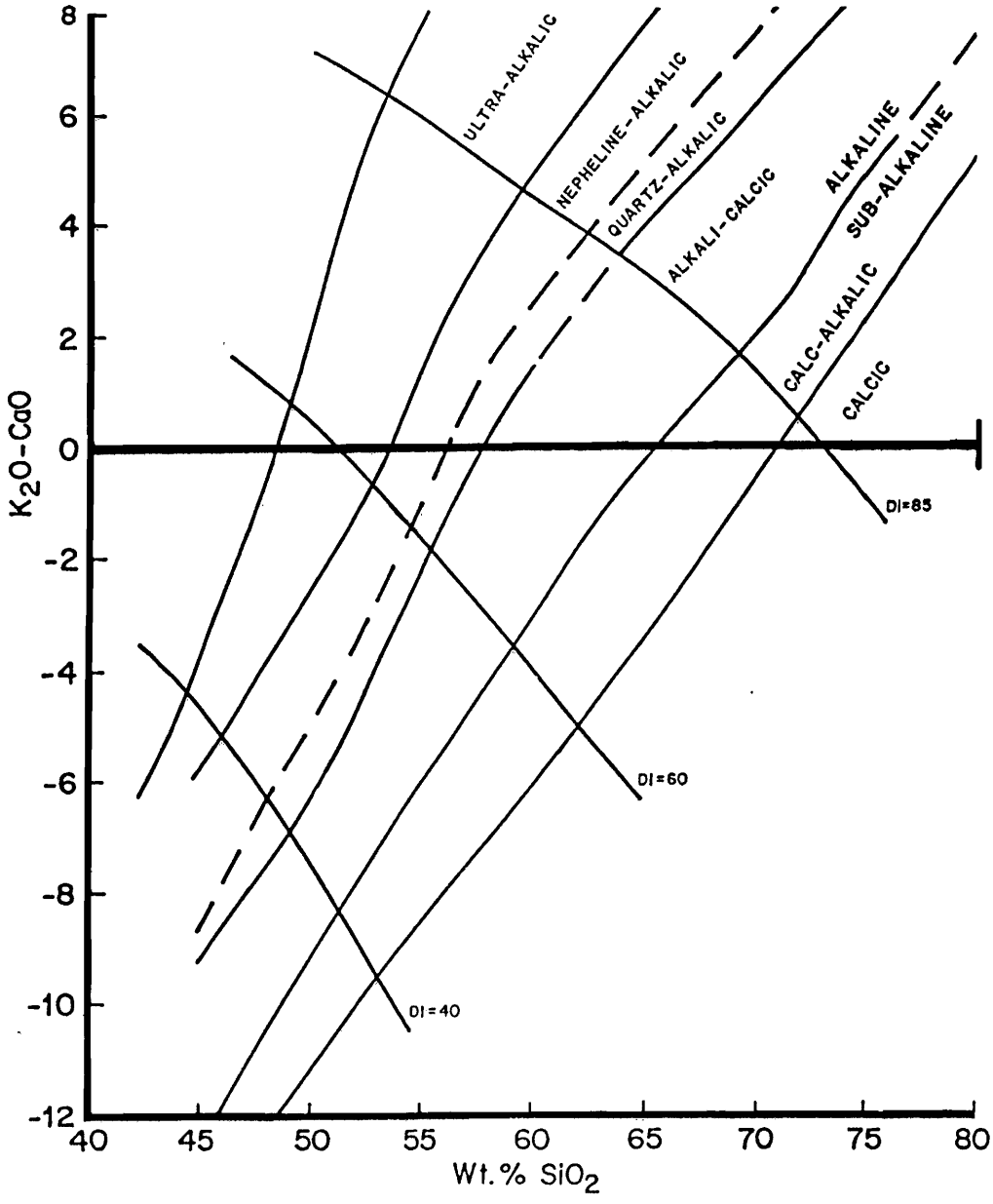

Figure 2-4. Weight percent K_2O minus weight percent CaO versus weight percent SiO_2 variation diagram showing alkalinity categories in the petrochemical classification. DI= Differentiation Index.

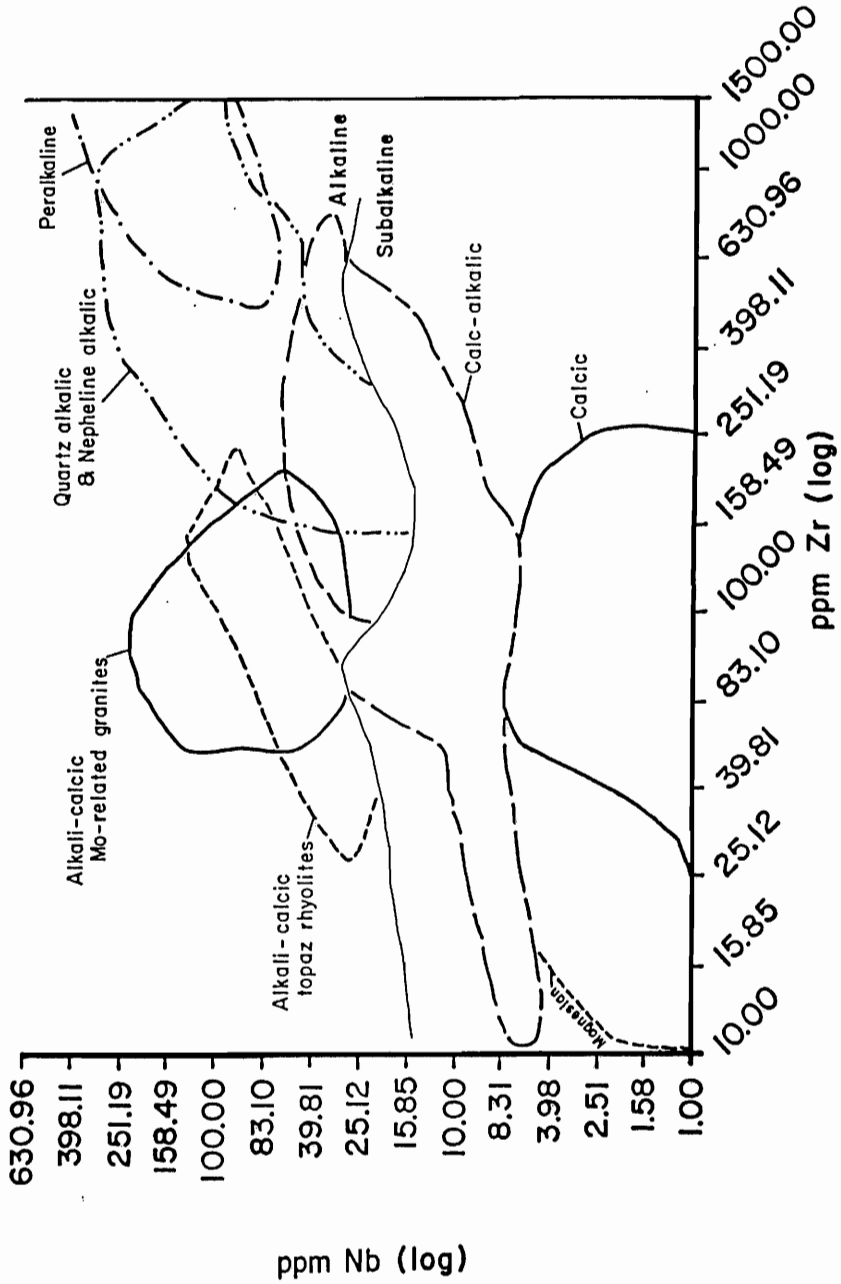

Figure 2-6. Log-Log variation diagram of ppm Nb versus ppm Zr with alkalinity fields in the petrochemical classification.

mineralogical, are used to determine the alkalinity class for a particular pluton. The data are quite well constrained within the alkalinity fields at intermediate SiO_2 values, but there is considerable overlap into other fields at high silica values, especially on the K_2O vs. SiO_2 variation diagram. Therefore, several plots are employed and the final alkalinity assignment is based on a weight of evidence argument judged from a synthesis of all the plots. At least four samples of each comagmatic suite should be taken and the alkalinity assignment made on 'weighted' patterns to eliminate ambiguities created by outlier points. Petrographic data, especially feldspar abundances, are also useful in distinguishing alkalinity series (Keith and others, 1991).

Peacock (1931) used a graphical overlay technique to obtain the alkali-lime index; a CaO versus SiO_2 curve for a comagmatic suite of igneous rocks is overlain on a total alkali ($Na_2O + K_2O$) versus SiO_2 curve. Where the two curves intersect on this diagram, a vertical line is drawn to the SiO_2 axis; this silica value is defined as the alkali-lime index (Figure 2-7). Peacock chose the boundaries of the calcic, calc-alkalic, alkali-calcic, and alkalic fields based on natural mineralogic characteristics.

Keith has modified the graphical overlay technique to be more amenable to statistical techniques by calculating Na_2O plus K_2O minus CaO and plotting it against SiO_2 content; the silica content is read where the line for the suite intersects with zero. This plot has been modified into the K_2O-CaO variation diagram (Figure 2-4) because sodium is relatively volatile in natural systems and

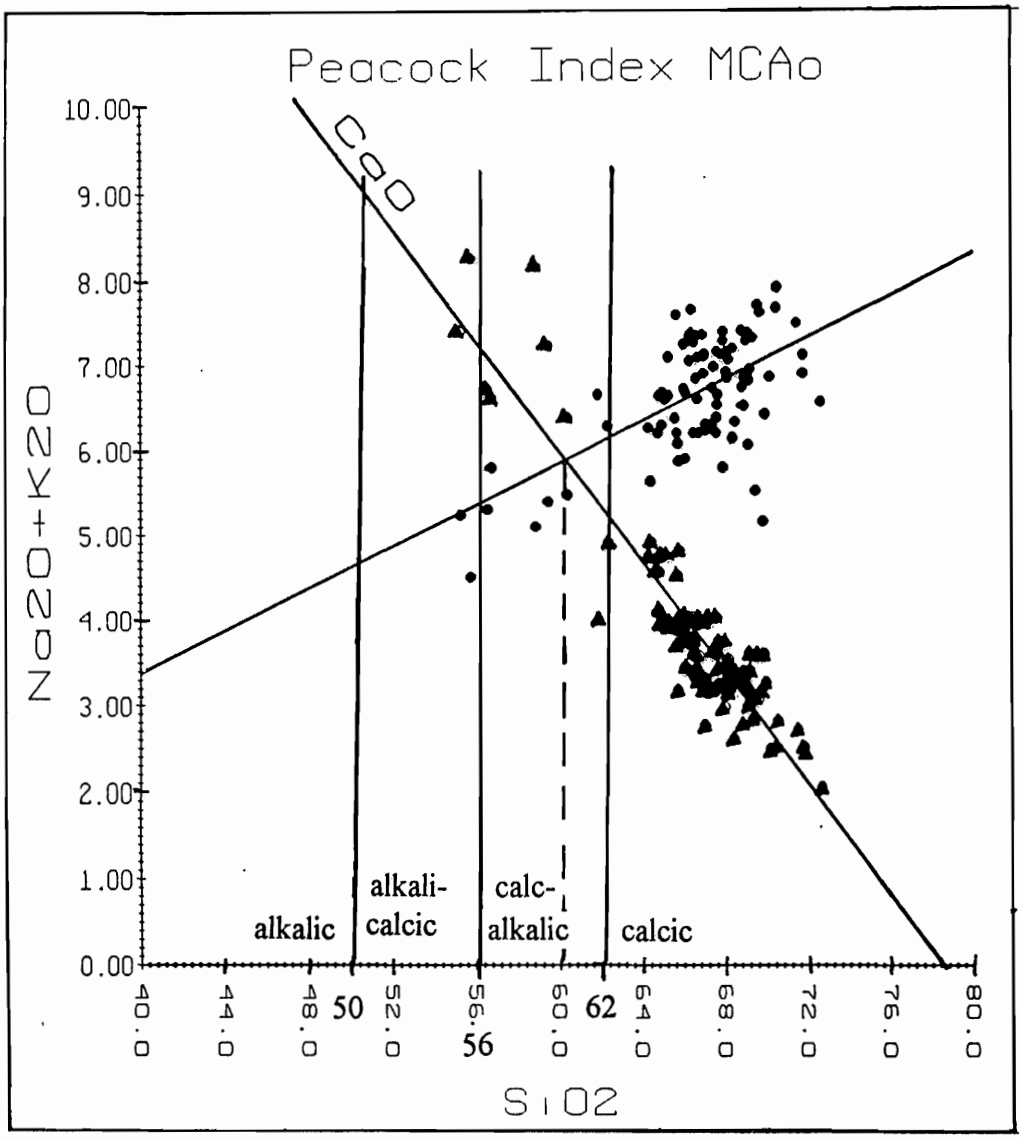

Figure 2-7. Variation diagram illustrating technique used by Peacock (1931) to determine alkali-lime index, which is often called the Peacock index.

analytic techniques. Even more importantly, sodium abundance during differentiation is highly affected by oxidation state.

To compare numerical information about alkalinity from the K_2O versus SiO_2 variation diagram, Keith uses the classic $K_{57.5}$ index diagram developed by Dickinson and Hatherton (1969); it is defined as the K_2O value of a comagmatic suite at 57.5 percent SiO_2 content. The $K_{57.5}$ index for calcic rocks is between 0.3 and 1.15; for calc-alkalic rocks is 1.15 to 2.45; for alkali-calcic rocks is 2.45 to 3.8; for quartz-alkalic rocks is 3.8 to 4; and for nepheline-alkalic rocks is 4.5 to 7.5. There is an overlap of approximately 0.15 on each side of the alkalinity classes. A comparison of Peacock index values with $K_{57.5}$ index values for the same rocks for the alkalinity classes as determined by ore deposits is shown in Figure 2-8. The boundaries indicated by the igneous rocks associated with ore deposits are similar to the boundaries determined from Peacock's samples of petrologic classes. The alkali-lime index of the calcic class in the magma series classification is above 63 instead of above 62 in Peacock's samples. The alkali-lime index of the calc-alkalic class in the petrochemical classification is between 57.25 and 63 instead of between 56 and 62 in Peacock's class; for alkali-calcic it is between 53 and 57.25 instead of between 50 and 56 in Peacock's system. Thus, Keith's alkalinity distinctions based on ore deposits validated Peacock's alkalinity distinctions based on mineralogy of igneous rocks without ore deposits.

Other indices besides the $K_{57.5}$ index that are used to define alkalinity classes in the petrochemical classification include the K_{Ca} index and the

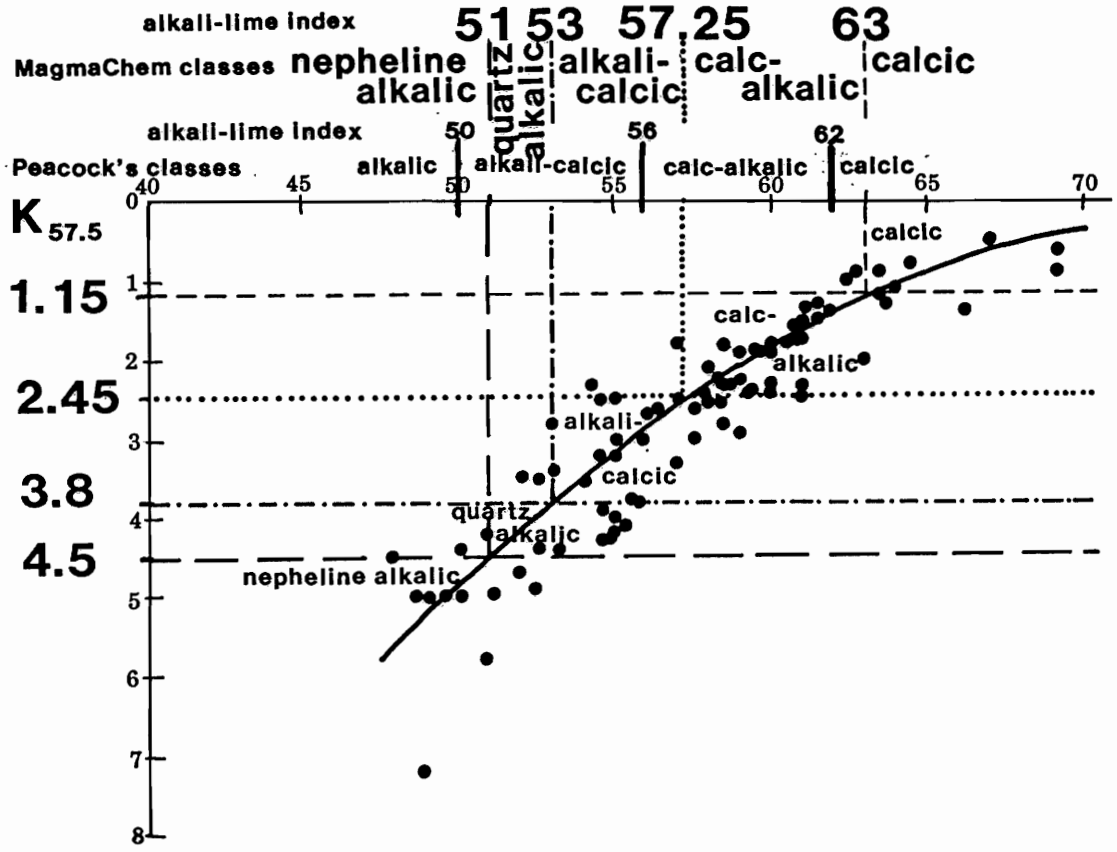

Figure 2-8. Comparison of alkali-lime indices of Peacock (1931) with those of various alkalinity classes based on metallogenic types and correlated with the $K_{57.5}$ Index of Dickinson and Hatherton (1967).

KMg index. The K_{ca} index is defined as the weight percent SiO_2 of a comagmatic suite where K_2O minus CaO is zero and is shown on the K_2O-CaO versus SiO_2 variation diagram (Figure 2-4). The K_{Mg} index is defined as the weight percent SiO_2 of a comagmatic suite where K_2O minus MgO is zero and is shown on the K_2O-MgO versus SiO_2 variation diagram (Figure 2-5).

Alkalinity Classes

Ultra-Alkalic

Indices for the metaluminous ultra-alkalic magma series include a $K_{57.5}$ index between 7.5 to more than 11.5 and a K_{Ca} index between 48.5 to 53.5 and less than 48.5 for high-K ultra-alkalic suites. Ultra-alkalic suites are undersaturated in quartz (Keith and others, 1991). Rock types in the metaluminous ultra-alkalic class include, in increasing amounts of SiO_2, kimberlite, melilite (alkali pyroxenite), nephelinite (shonkinite, ijolite), high K-phonolite (shonkinite), and high K-trachyte (high K-syenite) (Figure 2-9).

Nepheline Alkalic

Indices for the metaluminous nepheline-alkalic magma series include a $K_{57.5}$ index between 4.5 to 7.5, a K_{Ca} index between 53.5 to 56, and a K_{Mg} index between 49.5 to 52.5. Rock types in the metaluminous nepheline-alkalic suites are nepheline normative and tend to be quartz undersaturated rock types, so that

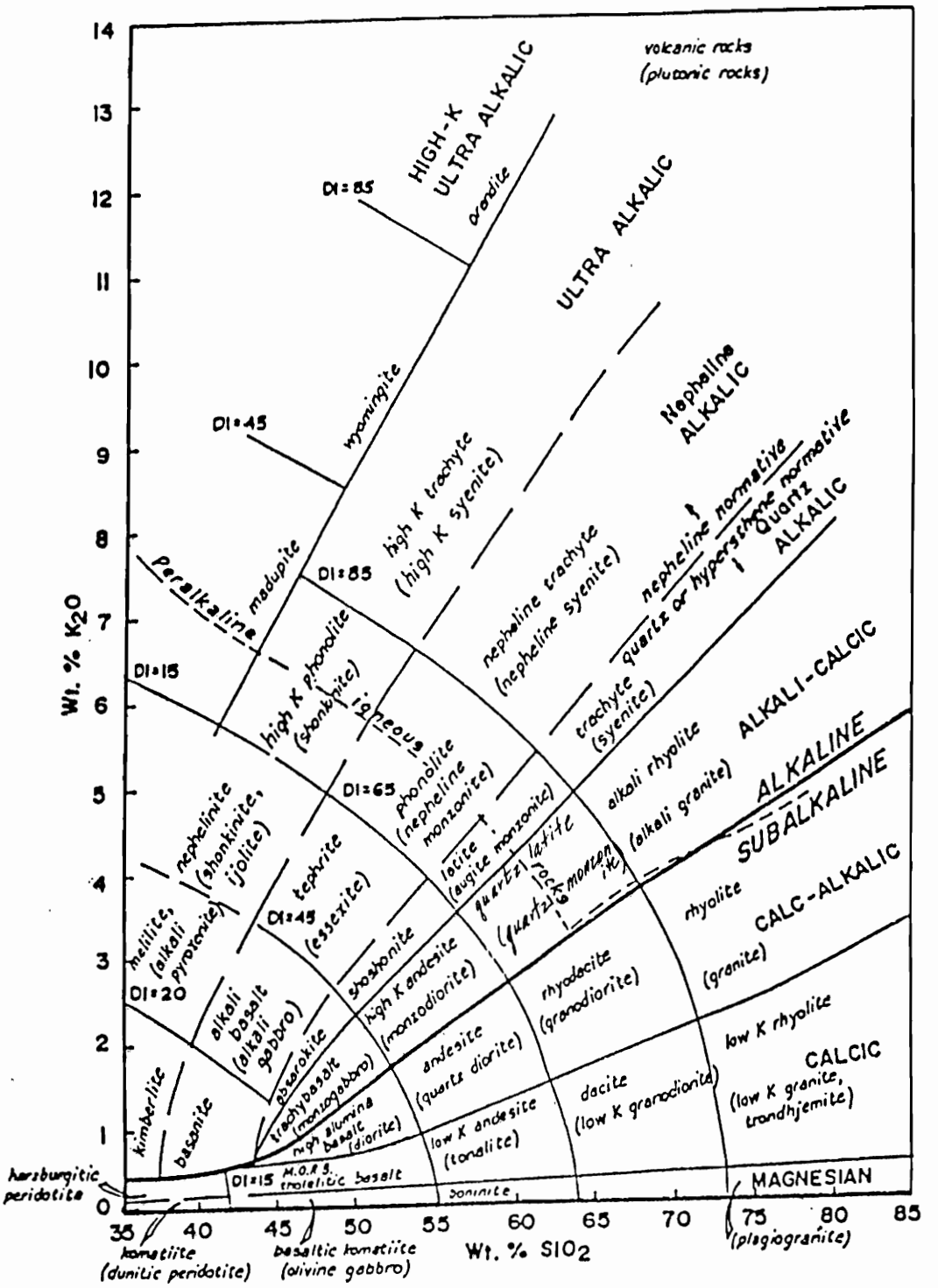

Figure 2-9. Weight percent K_2O versus weight percent SiO_2 variation diagram showing rock nomenclature for each alkalinity subdivision of metaluminous rock series (from Keith, unpublished manuscript).

nepheline is characteristic of these suites (Keith and others, 1991). Rock types include, in order of increasing Differentiation Index, basanite, alkali basalt (alkali gabbro), tephrite (essexite), phonolite (nepheline monzonite), and nepheline trachyte (nepheline syenite).

Quartz Alkalic

Distinction of metaluminous quartz-alkalic magma series depends upon several criteria. Alkalic rocks have an alkali-lime index or Peacock index of less than 50; these rocks generally contain nepheline and other feldspathoids, augite, and biotite (Peacock, 1931). The alkali-lime index of alkalic rocks in the petrochemical classification is less than 53. Other indices for the quartz-alkalic magma series include a $K_{57.5}$ index between 3.8 to 4.5, a K_{Ca} index between 56.0 to 57.5, and a K_{Mg} index between 52.5 to 53.75.

Rock types characteristic of the metaluminous quartz-alkalic suites tend to be quartz saturated rock types, so that latite or monzonite are characteristic of these suites (Keith and others, 1991). Rock types are quartz or hypersthene normative and include, in order of increasing Differentiation Index, absarokite, shoshonite, latite (augite monzonite), and trachyte (syenite) (Figure 2-19).

Production characteristics of mineral deposits associated with quartz-alkalic rocks are slightly different for peraluminous and metaluminous rock suites. Peraluminous alkalic suites are characterized by production of U and Th and by trace amounts of Co, Ni, As, and Bi. Metaluminous quartz-alkalic suites are

characterized by production of Cu, Au, U, LREE, and Fe, as well as by the presence of significant amounts of Pb, Zn, Ag, Ti, and Mo, and by trace amounts of V, P, Ge, Th, PGE, Be, and F (Keith and others, 1991).

Alkali-calcic

Determination that a magmatic suite belongs in the metaluminous alkali-calcic magma series is made on the basis of variation diagrams and several indices. Alkali-calcic rocks have an alkali-lime index or Peacock index between 50 and 56; these rocks generally contain biotite, hornblende, minor pyroxene in hydrous magma, and diopside in anhydrous magma (Peacock, 1931). The alkali-lime index for metaluminous alkali-calcic suites in the magma series classification is between 53 and 57.25 instead of between 50 and 56. Other indices for the alkali-calcic magma series include a $K_{57.5}$ index between 2.45 to 3.8, a K_{Ca} index between 57.5 to 65.5, and a K_{Mg} index between 53.75 to 58.5.

Rock types typical of metaluminous alkali-calcic suites generally contain quartz. Metaluminous alkali-calcic suites tend to be quartz oversaturated rock types, so quartz latite or quartz monzonite lithologies are characteristic of these suites. Alkali-calcic magma series have more K-feldspar developed earlier in the crystallization sequence than calc-alkalic suites, so have quartz monzonite lithologies (Keith and others, 1991). Rock types, in order of increasing differentiation, include trachybasalt (monzogabbro), high K-andesite and trachyandesite (monzodiorite), quartz latite (quartz monzonite), and alkali

rhyolite (alkali granite) (Figure 2-9).

An outstanding production characteristic of metaluminous alkali-calcic ore deposits is the elevated Ag content and Ag:Au ratios of more than 40:1. Higher total base metal contents, higher Mn contents, and higher Pb-Zn ratios are also characteristic of alkali-calcic ore deposits (Keith and others, 1991). Metaluminous alkali-calcic suites are characterized by significant production of Ag, Pb, Zn, Sn, B, Mo, and Be, as well as by significant byproduct production of In, F, Li, Mn, and W, and by significant trace amounts of Au, Cu, Ga, Fe, U, Th, P, Se, Hg, Sb, Br, As, Ba, and Mg (Keith and others, 1991).

Peraluminous alkali-calcic suites are characterized by production of Sn and W, by some production of Li, Th, and C, and by trace amounts of Cu, Ag, Au, and U (Keith and others, 1991).

Calc-alkalic

Determination that a magmatic suite belongs in the metaluminous calc-alkalic magma series is made on the basis of variation diagrams and several indices. Calc-alkalic rocks have an alkali-lime index (or Peacock index) between 56 and 62; these rocks contain biotite, hornblende, and hypersthenic pyroxene and are the hypersthenic series (Peacock, 1931). The Peacock index of the calc-alkalic class in the magma series classification is between 57.25 and 63 instead of between 56 and 62. Other indices for the metaluminous calc-alkalic magma series include a $K_{57.5}$ index between 1.15 to 2.45, a K_{Ca} index between 65.5 to 71.0, and a

K_{Mg} index between 58.5 to 65.0.

Rock types typical of the metaluminous calc-alkalic class are quartz saturated. Metaluminous calc-alkalic magma series have less K-feldspar developed early in the crystallization sequence than alkali-calcic suites, so typically have granodiorite lithologies rather than quartz monzonite rock types (Keith and others, 1991). Rock types, in order of increasing SiO_2 content, include high alumina basalt (diorite), andesite (quartz diorite), rhyodacite (granodiorite), and rhyolite (granite) (Figure 2-9).

Production characteristics of peraluminous and metaluminous calc-alkalic suites are somewhat different. Peraluminous calc-alkalic suites are characterized by Ag and W production, as well as by significant amounts of Au, Be, Pb, Zn, and Cu. Metaluminous calc-alkalic suites are characterized by significant production of Cu, Au, W, and Mg, by production of Ag, Zn, Pb, Mo, Sb, Hg, and S as byproducts, and by significant trace amounts of Ba, As, Tl, Fe, and Se (Keith and others, 1991).

Calcic

Determination that a magmatic suite belongs in the metaluminous calcic magma series is made on the basis of variation diagrams and several indices. Calcic rocks have an alkali-lime index or Peacock index above 62; these rocks contain pyroxenes, particularly pigeonite and are the pigeonitic series (Peacock, 1931). The Peacock index of the calcic class in the petrochemical classification

is greater than 63 instead of above 62. Other indices for the metaluminous calcic magma series include a $K_{57.5}$ index between 0.2 to 1.15, a K_{Ca} index greater than 71.0, and a K_{Mg} index greater than 65.0.

Rock types typical of metaluminous calcic suites, in order of increasing differentiation, include harzburgitic peridotite, M.O.R.B. and tholeitic basalt, low K-andesite (tonalite), dacite (low K-granodiorite), and low K-rhyolite (low K-granite, and trondhjemite) (Figure 2-9).

Production characteristics of peraluminous and metaluminous calcic suites differ slightly. Peraluminous calcic suites are characterized by Au production and by significant amounts of Ag, as well as by various trace elements depending upon the oxidation state. Metaluminous calcic suites are characterized by significant production of Au, Cu, Zn, Ni, and PGE, by significant amounts of Co, and by trace amounts of Ag, Pb, Cr, Fe, As, and S (Keith and others, 1991).

Magnesian

Although the magnesian magma series was not included in Peacock's original classification, the category was added to the magma series classification to accommodate certain massive sulfide deposit types. Magnesian series contain very high magnesium contents that are generally greater than 18 percent MgO (Arndt and Nisbet, 1982). In addition, magnesian series are characterized by the absence of potassium, which clearly distinguishes it from other metaluminous magma series.

Rock types typical of metaluminous magnesian suites, in order of increasing differentiation, include komatiite (dunitic peridotite), basaltic komatiite (olivine gabbro), boninite, and (plagiogranite) (Figure 2-9). Metaluminous magnesian suites are characterized by significant production of Au, Cr, and Ni, by production of Mg and Cu as byproducts, and by significant amounts of Ag, Zn, Pb, and PGE (Keith and others, 1991).

Water content

History and Development of Water Content Classes

Keith's discussions with Richard Nishimori at a workshop for Mobil Minerals in March, 1983, about alkalinity versus water content of a magma as a controlling factor of the quantity of expressed metallogeny led to a major breakthrough in the predictivity of the petrochemical classification by adding additional logic levels. Nishimori had established a clear empirical relationship between hydrous metaluminous gabbros and calcic gold veins in the coastal batholith, whereas anhydrous pyroxenites and pyroxene-rich norites were not associated with gold metallogeny. He correlated this difference with the amount of iron enrichment; hydrous, iron-poor magmas series were associated with metallogenic deposits, whereas anhydrous, iron-rich magma series lacked an epigenetic metallogenic expression.

Research by Keith and the MagmaChem staff documented the significance

of water and iron content. Hydrous, iron-poor magma series that plot calc-alkaline on an AFM ternary diagram are associated with mineral deposits containing possible commercial quantities of metals. Anhydrous, iron-rich magma series that plot tholeiitic on an AFM ternary diagram are not associated with commercial ore deposits; these generally include basalts in ocean basins, some oceanic islands, and continental basaltic plateaus.

A project for Billiton Exploration was begun in the summer of 1984 to update the MagmaChem metallogenic data base for the Pacific Northwest. During this project the insights on water and iron content mentioned above were documented and incorporated into the petrochemical classification as the fourth-order classification category.

Water Content Classes

Iron and water content are fourth-order distinctions that subdivide the alkalinity categories in the petrochemical classification. They reflect conditions under which melting of source material occurred. Hydrous melting conditions are reflected by their iron-poor nature whereas anhydrous conditions are characterized by an iron-rich character. Water content, as defined by anhydrous versus hydrous character, is chiefly evaluated by the presence of OH^--bearing minerals, by loss on ignition (LOI) histograms, by total H_2O histograms, or by oxygen isotopes (Keith and others, 1991). Major and minor element concentrations also differ between the classes.

Anhydrous

Anhydrous metaluminous magmatism of rift or hot spot origin has higher amounts of high field strength elements (Y, Nb, Zr, Ta, Lu, Yb, V, Ti, and Sc, as well as Fe) than hydrous magmatism (Figure 2-10).

Hydrous

Hydrous metaluminous magmatism of subduction origin is distinguished from anhydrous magmatism by lower amounts of the high field strength elements. Hydrous magmas are HFSE-poor, more silica-rich, less complete melts (Keith and others, 1991). These differences can be accounted for by the type of melting.

Petrotectonic Implications of Water Content

In tectonic settings for 'dry' or anhydrous magmatism, such as hotspots, oceanic rifts, and mature continental rifts, melting occurs under anhydrous conditions at a "hot" mantle geotherm. This style of melting allows a more complete breakdown of relatively refractory Fe-Ti-oxide compounds that are major reservoirs of high field strength elements. The result is a high field strength element-enriched, low-silica, relatively complete partial melt of the mantle protolith (Keith and others, 1991).

Melting in subduction zones is triggered by dehydration in the down-going slab and by volatile- or water-induced melting of various sources -- in a layered, submoho, mantle lithosphere or asthenosphere, or in the mantle hanging wall

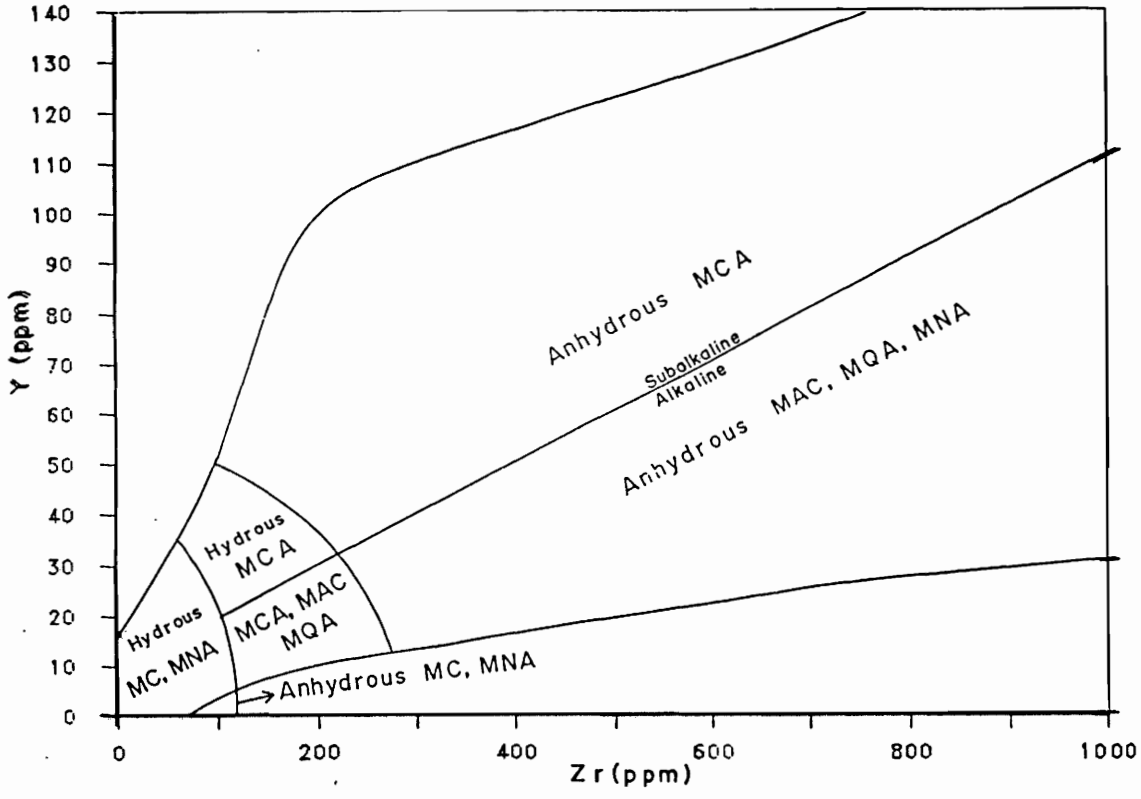

Figure 2-10. Variation diagram of Y in ppm versus Zr in ppm showing hydrous versus anhydrous fields for various alkalinities. Note x-axis and y-axis scale differ.

above the descending slab. Hydrous melting of these mantle sources occurs under much lower temperature conditions where the refractory Fe-Ti compounds in the mantle protoliths are not as effectively broken down. As a result the high field strength element component is mostly retained in mantle resistate phases. The result is a HFSE-poor, more silica-rich, less complete hydrous melt (Keith and others, 1991).

Iron Content

Iron content can be evaluated with a variety of variation diagrams. Varying degrees of iron-rich versus iron-poor character are depicted on AFM ternary diagrams (Figure 2-11), FeO^*/MgO vs. SiO_2 variation diagrams or Miyashiro plots (Miyashiro, 1974) (Figure 2-12), Y vs. Zr plots (Figure 2-10), and FeO^*/TiO_2 plots (Figure 2-13) (Keith and others, 1991). The iron content reflects conditions under which melting of source material occurred.

Hydrous metaluminous magmas of subduction origin are chemically distinguished by magnesium enrichment on a Miyashiro plot (Figure 2-11), which plots FeO^*/MgO vs. SiO_2, where $FeO^* = 0.9(Fe_2O_3) + FeO$. The magnesium enrichment is the result of continuous removal of iron by hydrous ferromagnesian minerals such as early hornblende and late biotite during crystallization. This iron removal is combined with the relative lack of minerals, such as clinopyroxene, that would have preferentially removed magnesium (Keith and others, 1991). The categories of iron content on this diagram include strongly

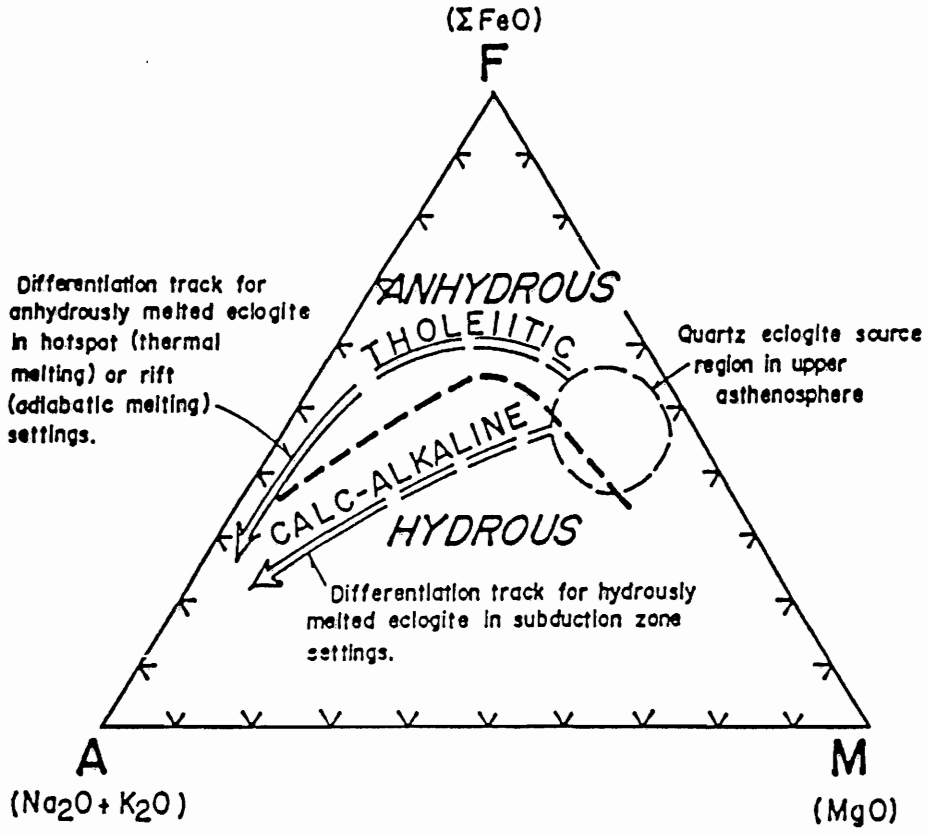

Figure 2-11. AFM ternary diagram interpreting the traditional tholeiitic/calc-alkaline distinction from the viewpoint of anhydrous (tholeiitic) versus hydrous (calc-alkaline) melting processes (from Keith and others, 1991).

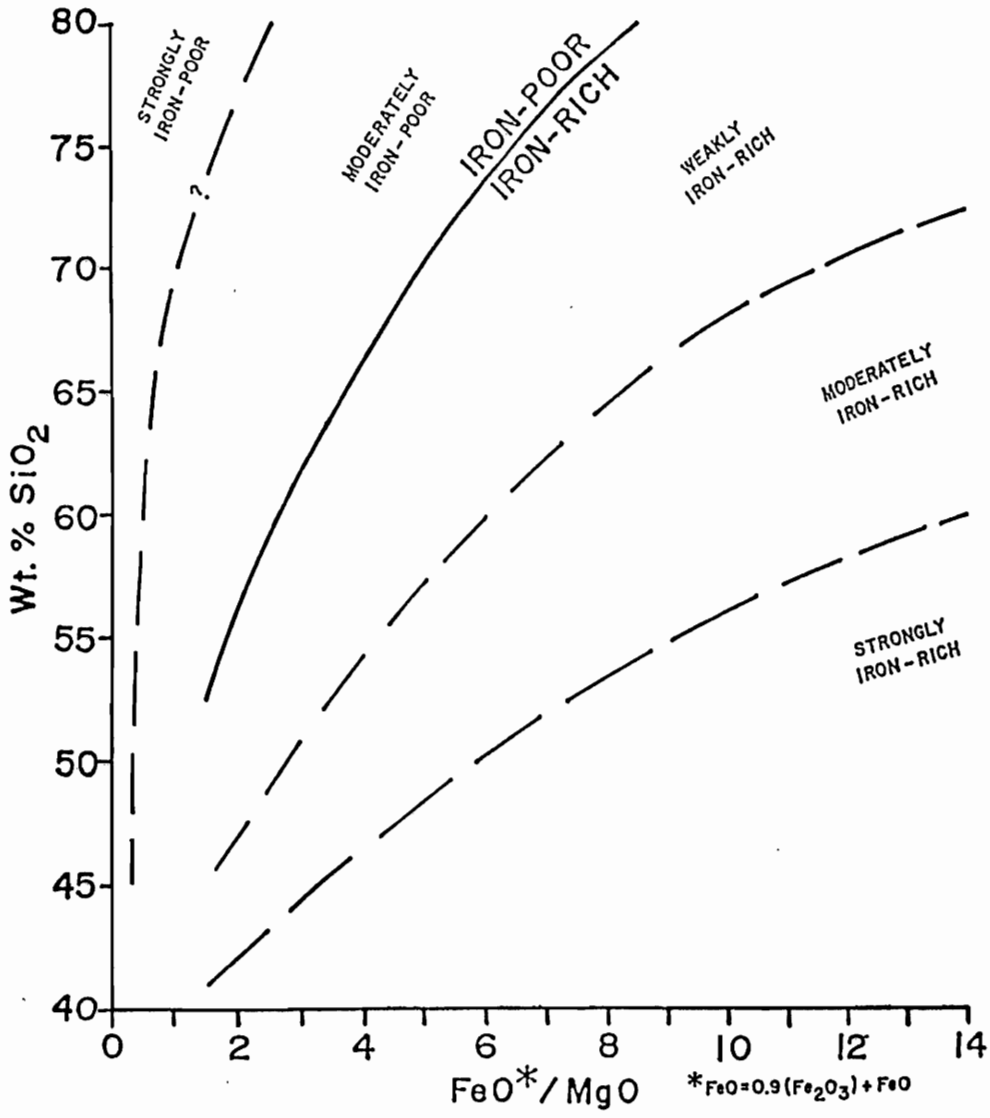

Figure 2-12. Modified Miyashiro (1974) diagram illustrating iron enrichment. Variation diagram plots weight percent SiO_2 versus FeO^*/MgO, in which $FeO^* = 0.9(Fe_2O_3) + FeO$.

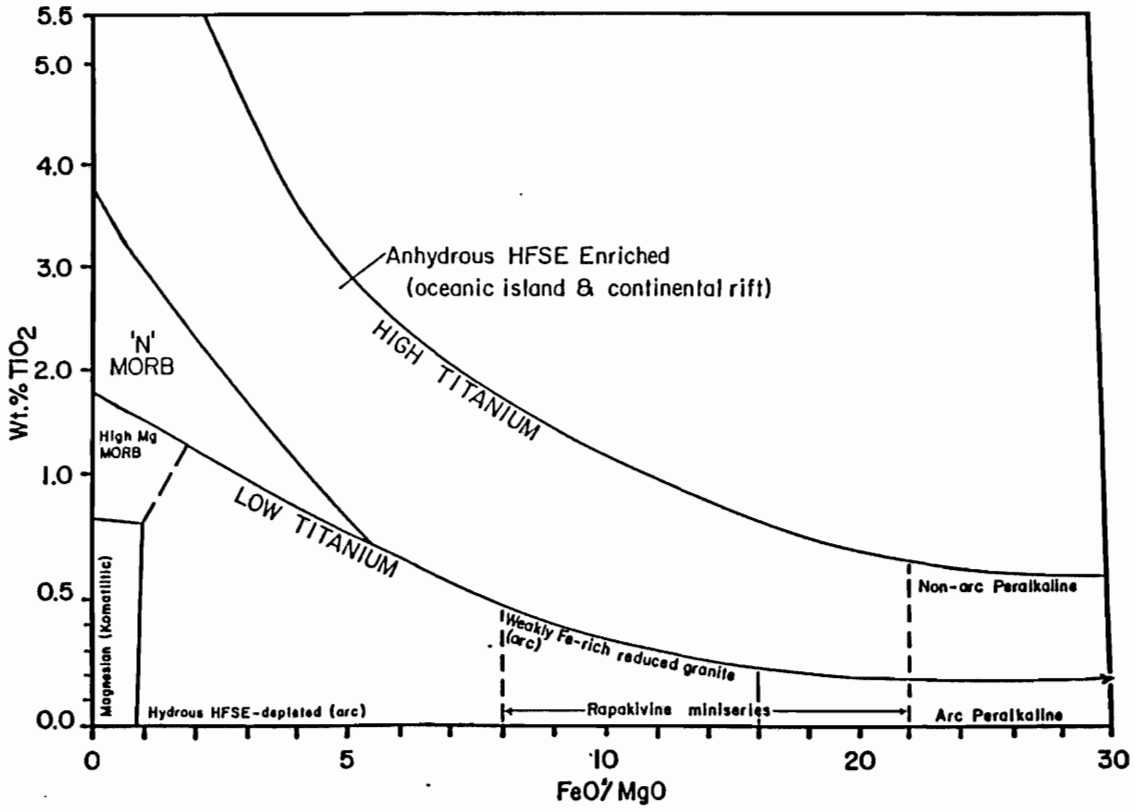

Figure 2-13. TiO_2 versus FeO^*/MgO variation diagram, in which $FeO^* = 0.9(Fe_2O_3) + FeO$. Low titanium fields for hydrous metaluminous series that were generated in subduction settings are distinguished from high titanium fields for anhydrous metaluminous magma series that were generated in hotspot and rift geotectonic settings (from Keith and others, 1991).

iron-poor, moderately iron-poor, weakly iron-rich, moderately iron-rich, and strongly iron-rich.

The split between tholeiitic and calc-alkaline trends on an AFM diagram (Wager and Brown, 1939; Nockolds and Allen, 1954) also can be interpreted as indicating the difference between anhydrous iron-rich suites and hydrous iron-poor suites. The AFM diagram (Figure 2-11) plots M or mafic minerals as MgO, A or alkalis as Na_2O+K_2O, and F or iron as total Fe (Fe_{total}= $0.9(Fe_2O_3)$ + FeO). The AFM diagram emphasizes the iron-enrichment of anhydrous suites (tholeiitic field) versus the more iron-poor hydrous suites (called calc-alkaline on the AFM diagram). This use of the term calc-alkaline in this diagram has a very different meaning than the calc-alkalic category of Peacock (1931).

The yttrium versus zirconium variation diagram (Figure 2-10) was an outgrowth of petrological observations by Thompson and others (1984). The Y vs. Zr diagram is also useful because they are 'immobile' elements and show less variation with alteration than most rock components.

Volatile Content

The relative amounts of various volatile components of magmas, especially fluorine and chlorine, as well as carbon dioxide and methane, comprise the fifth-order level in the petrochemical classification. These are not yet completely constrained by variation diagrams because so few modern analyses determine these volatile constituent. However, where available, F vs. Cl, Rb vs. Zr plots,

and histograms of F, Cl, total C, and CO2 are useful (Keith and others, 1991).

Shand (1927) defined several indices based on aluminum versus alkali content; the A/NK ratio is useful in determining peralkalinity.

The formula for the A/NK index is:

$$A/NK = \frac{(wt\%\ Al_2O_3 / 102)}{(wt\%\ Na_2O / 62) + (wt\%\ K_2O / 94)}.$$

When the agpaitic index or A/NK ratio of an igneous rock is less than 1.0, the rock is defined as peralkaline. Figure 2-14 shows the peralkaline field on an A/NK vs. SiO_2 variation diagram. Peralkalinity in igneous rocks is commonly accompanied by the presence of alkali ferro-magnesian minerals such as aegirine and riebeckite.

Oxygen Content

The sixth-order level of the petrochemical classification is oxidation state. The oxidized/reduced distinction is similar to the magnetite/ilmenite series distinction of Ishihara (1977, 1981) and Takahasi and others (1980). Classification criteria include Fe_2O_3/FeO ratios, mineralogy of accessory sulfides and opaque oxides, magnetic susceptibility, volume percent and mineralogy of opaque sulfides, oxides, and other accessory minerals (especially sphene), Fe_2O_3/FeO vs. SiO_2 variation diagrams, and others (Keith and others, 1991).

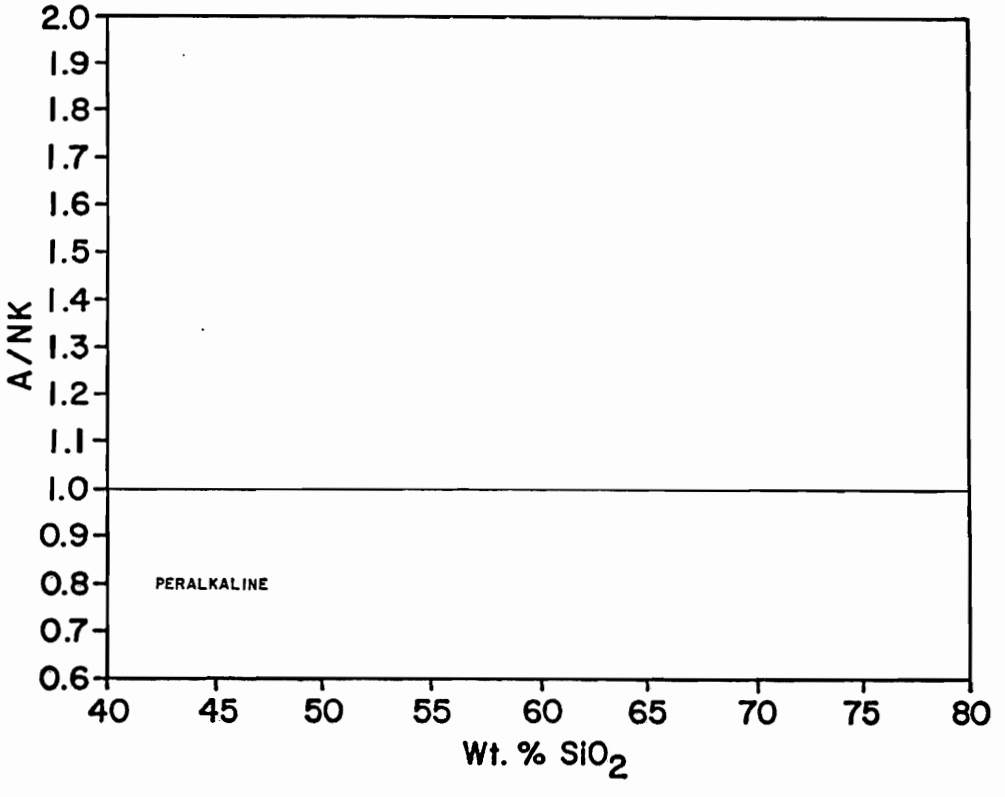

Figure 2-14. A/NK versus weight percent SiO_2 variation diagram. A/NK = molecular $Al_2O_3/(Na_2O + K_2O)$. Peralkaline rocks have A/NK less than 1.0.

History and Development of Oxidation Classes

In mid-1983 the concept of oxidation state, based on the ilmenite-magnetite series distinction of Ishihara (1977), was added to the petrochemical classification and correlated with the production and mineralogical expression of metal deposits.

To the degree that a correlation between the metal content of hydrothermal ore deposits and the petrochemistry of associated igneous rocks exists, it should be possible to predict specific chemistry within certain minerals of the associated igneous rocks. The availability in mid-1988 of mineral chemistry on biotite and hornblende from more than 400 samples in the California coastal batholith (Ague and Brimhall, 1988) encouraged Keith and Karen Schwab of the MagmaChem Exploration staff to obtain 120 of these samples from George Brimhall at Berkeley for whole rock chemical analysis. The data demonstrated that samples from the reduced or ilmenite only petrochemical classes had different amphibole and biotite compositions than samples from the oxidized classes with magnetite and visible sphene (Schwab, 1990).

When market conditions favored platinum group elements late in 1986, Keith and MagmaChem employee, George Smith, observed correlations between petrochemistry and precipitation of immiscible sulfide segregations. Stillwater-type plutons were metaluminous, calcic, anhydrous and very reduced in oxidation state; Sudbury-type intrusions with Cu-Ni immiscible sulfide segregates had a less reduced oxidation state.

Production of the oxidation state map of the southwestern U. S. by MagmaChem Exploration in mid-1988 generated enough client interest to expand the compilation throughout the western U. S. by the end of 1988. Field sampling by Stan Keith, Jed Maughan, Monte Swan, and Steve Ruff added enough data to that in the literature to delineate crustal oxidation state terranes that elicit some provocative correlations with previously defined lithotectonic terranes (Keith and Swan, 1987).

The correspondence between oxidized terranes and base metal deposits and between reduced terranes and precious metal deposits is very important to exploration companies. An example of the use of metal chemistry and petrochemistry was the screening of epithermal Hg-Sb-As occurrences for gold metallization (Keith and others, 1988).

A comprehensive paper (Keith and others, 1991) published by the Geological Society of Nevada itemizes the 75 classes within the magma series classification, explains the logical levels, and documents numerous Nevada examples of the various classes. During the writing of this paper, Keith realized the importance of crustal volatiles on processes that affect the ultimate metal expression. F, Cl, and CO_2 are particularly important in determining some of the less common ore deposit classes.

Oxygen Content Classes

The principal plot used to distinguish oxidation state in the petrochemical

classification is the Fe_2O_3/FeO vs. SiO_2 variation diagram (Figure 2-15). Categories on this diagram include strongly oxidized, moderately oxidized, weakly oxidized, weakly reduced, and strongly reduced classes. The reduced or ilmenite-only class is characterized by ferric/ferrous ratios of less than 0.6; the weakly oxidized or ilmenite + magnetite class has ferric/ferrous ratios between 0.4 and 0.9; whereas the oxidized or magnetite-sphene class has ferric/ferrous ratios between 0.9 and 2.0. Selected indicator minerals in associated mineral deposits that are correlated with various oxidation states are shown in Figure 2-16 (Keith and others, 1991).

Petrotectonic Implications of Oxygen Content

The oxidation state is partly dependent on oxygen content of the source region, but it mainly reflects modification of the magma after its generation. Factors affecting oxidation state of a magma include: the amount of water added, the kind of crust it interacts with, the degree to which it differentiates, and the degree to which it interacts with atmospheric oxygen in shallow subaerial volcanic environments.

The clear correlation between oxidation state of the plutons and lithotectonic terranes pointed to a very important crustal influence on magmatism and their associated ore deposits. Keith's crustal fluids paper (Keith, 1991) addressed the influence of mid-crustal fluids in altering the original oxidation state of magmatic materials from the mantle. If the magma were originally

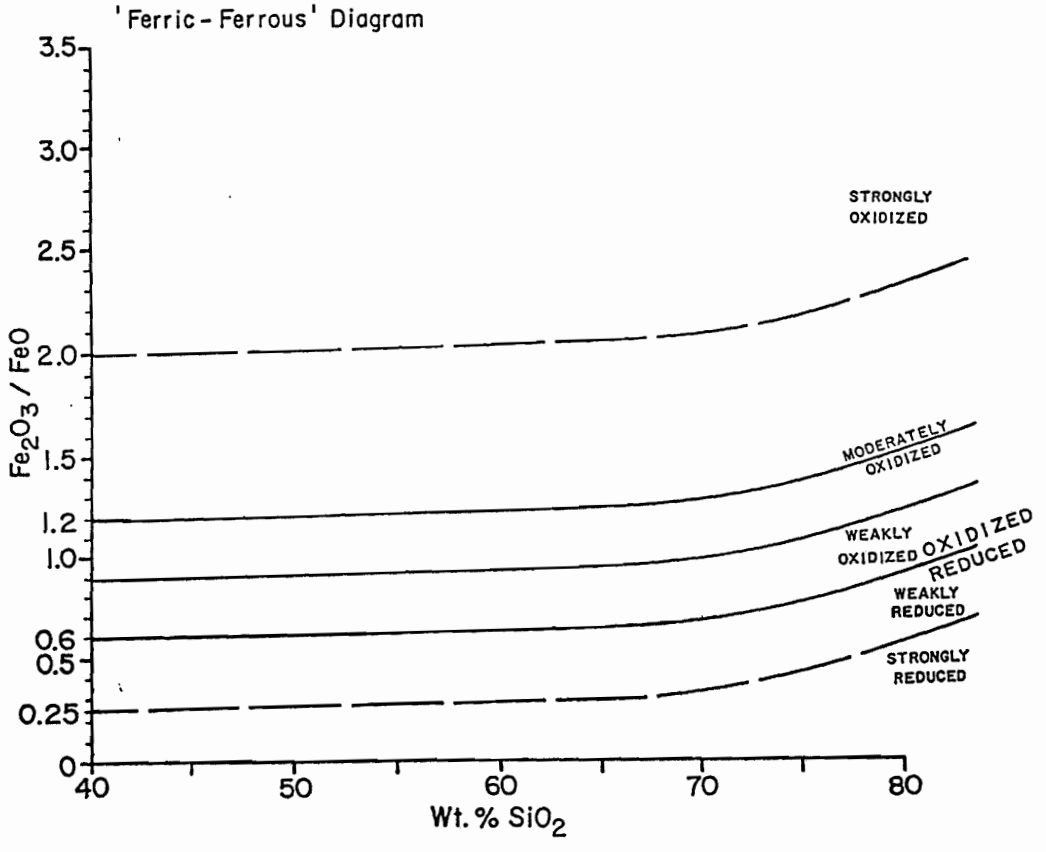

Figure 2-15. Ferric/ferrous variation diagram with weight percent Fe_2O_3 divided by weight percent FeO is plotted against weight percent SiO_2. Fields for the various oxidized and reduced classes are nearly horizontal with moderate rise in oxidation state at high silica values.

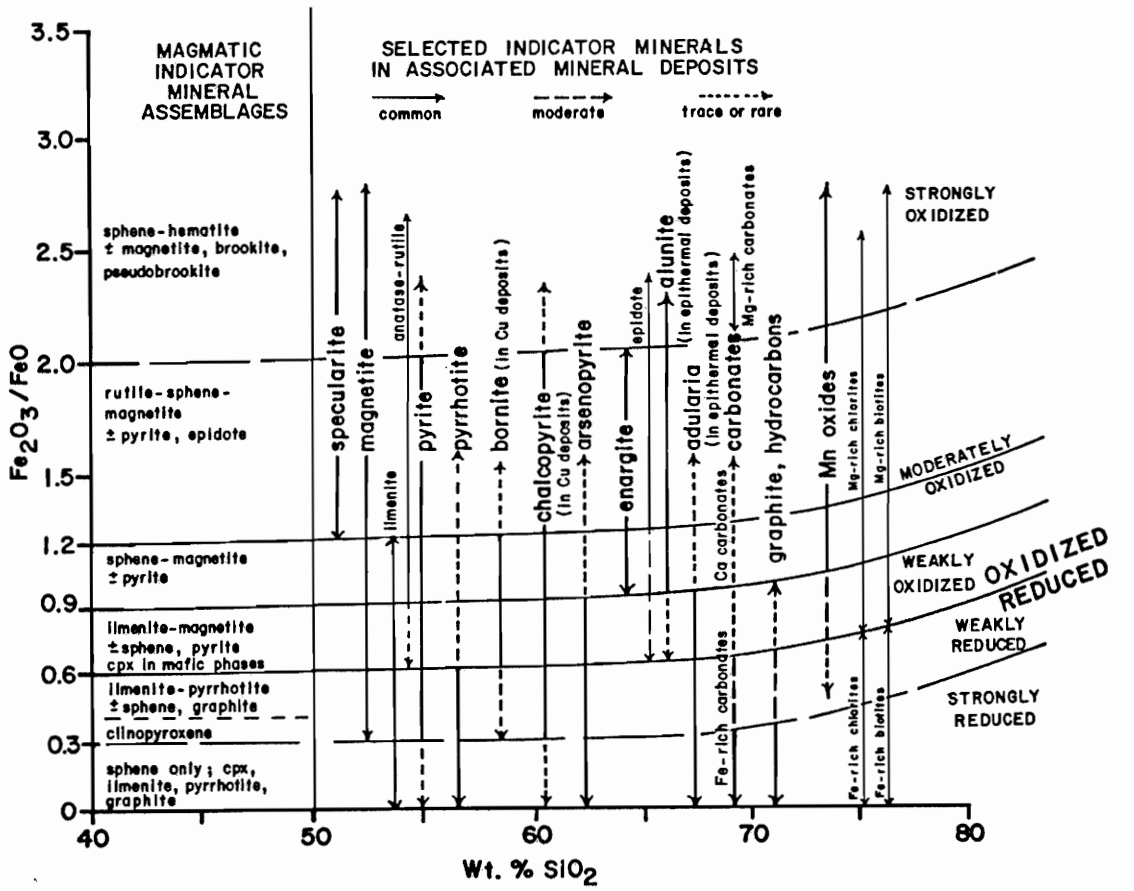

Figure 2-16. Ferric/ferrous ratio versus SiO_2 variation diagram showing indicator mineral assemblages for oxidation state in plutons compared with indicator minerals of oxidation state in associated mineral deposits (from Keith and others, 1991).

reduced and traveled through reduced crust, it remained reduced and produced precious metal deposits. If the magma were originally reduced and traveled through oxidized crust, it became oxidized and produced base metal deposits. It was Keith's assertion that these changes were accomplished by incorporation of mid-crustal formation fluids into the parent magma, not by melting and assimilating the crust or by mixing of solid state rock and metal material in the crust. The amount of contamination by the volatiles or deeper crustal fluids varies with the mass number of the isotope of Sr, Nd, and Pb, thus explaining the varying amounts of 'crustal mixing' documented by different isotopes.

Differentiation Index

Degree of differentiation forms the basis for the seventh-order level of the petrochemical classification. Various criteria indicating degree of differentiation include the Differentiation Index (D.I.) and Larsen Factor (L.F.). Various diagrams indicating degree of differentiation include plots with the element or element ratio on the y-axis vs. D. I., L. F., or SiO_2 (Keith and others, 1991). Differentiation index is a petrologic classification technique developed by Thornton and Tuttle (1960) that quantifies the tendency of magmatic differentiation processes to enrich residual liquids in certain felsic minerals. Differentiation Index (D. I.) is calculated by summing the following sialic anhydrous normative minerals from the C.I.P.W. norms: quartz, orthoclase, albite, nepheline, potassium metasilicate, and leucite (D.I.= Q + Or + Ab + Ne + Ks + Lc).

Alteration

Introduction

Naive use of petrochemical data can be risky; bad petrochemical data can lead to serious errors in class assignment of rock suites. Assuming proper analytical procedures were followed, significant error can be introduced by poor sample selection in the field by collecting igneous rocks that have been affected by physical and chemical weathering or by hydrothermal alteration processes. These alteration processes can induce compositional changes by changing rock volume and/or rock chemistry.

In the field, five to ten igneous rock samples from a given comagmatic igneous suite should be collected ranging from mafic to felsic in composition with as wide a range of differentiation as possible. If a specific igneous phase appears to be closely related to mineralization, three to six samples of that phase are desirable. Size of the sample depends on grain size. Fine-grained intrusions and aphanitic volcanics require about two pounds of petrographically fresh material; medium-grained materials require four to six pounds; coarse-grained material requires 10-15 pounds of material; and pegmatitic materials require 25-45 pounds of sample.

Freshness of hand samples is best evaluated by checking the color and luster of the ferromagnesian minerals and plagioclase. Ferromagnesian minerals such as amphibole, biotite, and pyroxene should be as black and lustrous as possible. Any green tints may indicate chloritization or serpentinization.

Plagioclase should be clear and glassy with twinning striae visible. Any cloudiness or chalkiness reveals the presence of clays indicative of argillic alteration or sericite indicative of phyllic alteration. Thin-section control is desirable but the practiced eye is also very effective. If alteration is unavoidable, propylitic alteration seems to affect the whole-rock oxide data the least, although oxidation state data are affected. Argillic, phyllic, and spilitic alteration induce major chemical changes that are mainly alkali depletions and should be strictly avoided.

Certain reporting procedures for major-element chemical data in the literature adopt misleading standardization practices that can interfere with the proper assignment to petrochemical categories. Recalculating the major element oxide date to a value of 100 minus the volatile component is particularly precarious, especially because renormalized anhydrous rock suites will plot more alkaline than the correct value. Such procedures forget the fundamental definition of a magma, which is a mixture of silicate liquid and dissolved volatiles.

Another confusing practice is the reporting of iron as total ferrous iron (FeO_T) or as total ferric iron (Fe_2O_{3T}). The newer major element analytical techniques can more cheaply and quickly analyze total iron than could older wet chemical techniques. This practice eliminates one of the most important criteria for determining oxidation state, which is used to distinguish between precious metal and base metal mining districts. Even worse is the practice of converting

total iron into ferric and ferrous components using a standard conversion factor from the literature that is highly model dependent, such as the titanium correction of Irvine and Barragar (1971), rather than from the rock suite sampled. It is even more irresponsible when the conversion factors are not mentioned in the data set.

Although detailed comparisons of different laboratories show differences depending on the laboratory used and their various procedures, it has been MagmaChem Exploration's experience that the natural variation of the geologic systems being sampled far exceed the laboratory errors introduced by machine drift, analytical standards, or instrumental or procedural differences between laboratories. An exception to this statement is oxidation state, because ferrous iron (FeO) is very susceptible to procedures such as time between grinding and analyzing, cigarette smoking, changes in humidity and temperature during titration, and other factors. It takes very little to make a sample give a more oxidized value than it really has.

The effects of regional metamorphism on original igneous rock petrochemistry were of obvious concern, especially possible effects on the ferric/ferrous ratio, so various suites were examined to evaluate these effects. Regional prograde metamorphism which featured dehydration reactions, such as the relatively anhydrous metamorphism of protolith, was found to induce little chemical change on the whole rock chemistry, even of the ferric/ferrous ratio. However, retrograde metamorphism which featured extensive water/rock

interactions significantly altered the whole rock ferric/ferrous ratio, as well as other major, minor, and trace element chemistry. The effects of retrograde metamorphism associated with hydrothermal alteration also produced major changes in whole rock ferric/ferrous ratios as well as in other chemical components. Table 2-3 documents the changes in the various parameters used in the petrochemical classification with alteration.

Alteration Filters

To remove the effects of the alteration types described in Table 2-3, Keith has developed several alteration filters which screen out altered samples. In order to develop these filters he plotted known altered and unaltered samples from the literature and from the MagmaChem Exploration database using standard diagrams from the literature as well as diagrams modified from them. Chemical gains and losses for the various alteration phenomena were noted and major element oxide ratios were devised that were sensitive to these changes. When these ratios were plotted against weight percent SiO_2, fields were drawn between fresh and altered samples.

Loss on Ignition (LOI) Filter

Effects of hydrothermal alteration and weathering and accompanying volume losses are efficiently detected by examination of the loss on ignition (LOI) parameter in a major element whole-rock analysis. LOI is the loss of all

Table 2-3. Effect of weathering and alteration on classification parameters.

Chemical Distinction	Graphs	Affected by	How affected
Aluminum	A/CNK	Feldspar destructive alteration (spilitization, phyllic, and argillic alteration and lateritic weathering)	Increases A/CNK values, resulting in more peraluminous character than in original chemistry. Feldspar destructiv alteration is much more effective than weathering in raising A/CNK ratios.
Alkalinity	K57.5 Sr70 K-Ca K-Mg Nb-Zr	Feldspar destructive alteration (spilitization, phyllic, and argillic alteration and lateritic weathering)	Introduces "scatter" on alkalinity plots, increases alkalinity on K-Ca plots, lowers alkalinity on Peacock plots. Immobile elements (Nb, Zr, Tl, Ta, REE are little affected unless high LOI (>6%
		Feldspar-stable alteration (potassic, sodic, and carbonate alteration	Increases alkalinity and scatters data on alkalinity plots. Drastically changes Na2O/K2O ratios.
		Volume change (typically volume loss)	Immobile elements may experience some depletion, elevate Zr and Nb values due to volume loss.
Iron and Water Content	FeO*/MgO	Strong propylitization and chloritization, potassic alteration	Commonly lowers Fe, resulting in a more magnesian character on SiO2 vs. FeO*/MgO graphs
	LOI	Carbonatization and most kinds of alteration	Very commonly increases total rock LOI parameter
Oxidation State	Fe2O3/FeO	All types of extreme weathering (complete grusification) where oxidation state buffers (sphene, opaque oxides & sulfides) are destroyed by oxidation	Greatly oxidizes rocks except for Na-carbonate stable alteration, which reduces oxidation state
Rock System	Differentiation Index (D.I.)	Silicification, feldspar destructive alteration, lateritic weathering	Generally increases D.I. producing a more differentiated aspect

volatiles during ignition or completion of fusion of the rock material being analyzed, typically at approximately 1100°C. In many chemical analyses where the volatile component is analyzed directly, it is expressed as H_2O_{total}, H_2O^+ (which is H_2O driven off above 250° C.), H_2O^- (which is H_2O driven off below 250° C.), CO_2, Cl, F, S, and O. Generally only the first few are analyzed, with H_2O and CO_2 having the highest values. Figure 2-17 illustrates the use of the LOI filter, but simple inspection of the whole rock chemical data can eliminate altered volcanics as those with more than 3.0 percent LOI and altered plutonics as those with more than 2.5 percent LOI.

A/CNK Versus SiO_2 Diagram

A principal effect of spilitic, argillic, and phyllic alteration is to reduce calcium, sodium, and potassium levels in the igneous rock; aluminum content remains relatively isochemical through the alteration process. Typically in mafic igneous rocks, sodium and calcium, and to a lesser extent, potassium, are removed relative to aluminum content. In felsic igneous rocks, sodium, and to a lesser extent, calcium and potassium, are removed relative to aluminum content. Thus, the ratio of aluminum to calcium plus sodium plus potassium is typically increased by spilitic, phyllic, or argillic alteration. This ratio is expressed by the A/CNK index, where A/CNK is the molecular ratio of $Al_2O_3/(CaO + Na_2O + K_2O)$.

$$\text{A/CNK} = \frac{(\text{wt\% } Al_2O_3 \,/\, 102)}{(\text{wt\% CaO} \,/\, 56) + (\text{wt\% } Na_2O \,/\, 62) + (\text{wt\% } K_2O \,/\, 94)}.$$

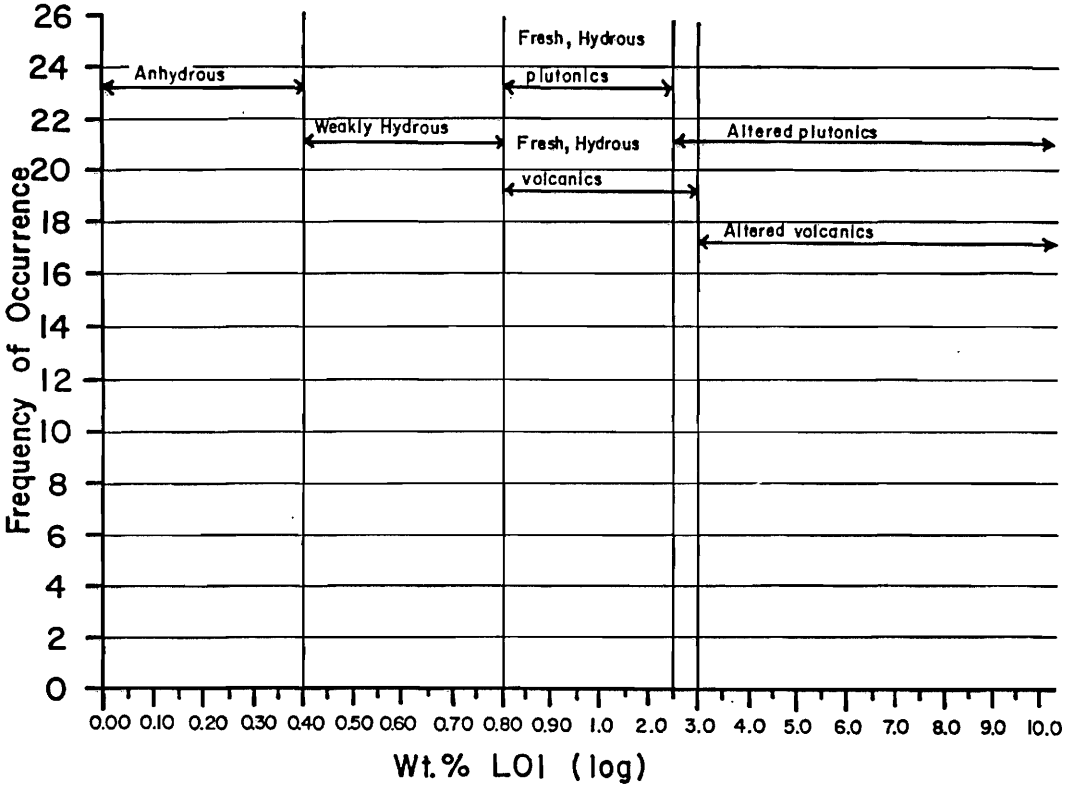

Figure 2-17. LOI (Loss On Ignition) histogram on a modified log scale illustrating anhydrous and hydrous categories and the cutoff for altered plutons at 2.5 percent LOI and for altered volcanics at 3.0 percent LOI.

Figure 2-18 illustrates the use of the A/CNK filter. A/CNK is plotted on the y-axis versus weight percent SiO_2 on the x-axis. Samples in the altered area on this variation diagram are rejected and not considered useful for determining categories within the metaluminous part of the petrochemical classification. The A/CNK filter is not designed to work on naturally peraluminous magma series.

The A/CNK filter has worked well on regionally spilitized and chloritized Precambrian greenstone metavolcanics and on phyllic and argillic alteration of Cenozoic volcanics. The A/CNK filter does not effectively eliminate feldspar-stable alteration, such as the potassic alteration in porphyry copper and molybdenum systems or the albitization in gold deposits associated with carbonate metasomatism. However, these types of alteration increase LOI values because of increased secondary hydrous biotite and increased CO_2, so they generally 'fail' the LOI filter.

Alteration Index Versus SiO_2 Diagram

The Alteration index (A.I.) of Ishikawa and others (1976) and Date and others (1983) was found to be a useful discriminator for several types of alteration. The Alteration index was effective at detecting various kinds of feldspar-stable alteration, especially potassic alteration in base metal systems, as well as phyllic and illite-stable argillic and alunitic alteration types. The Alteration Index diagram has A.I. plotted versus weight percent SiO_2 (Figure 2-19).

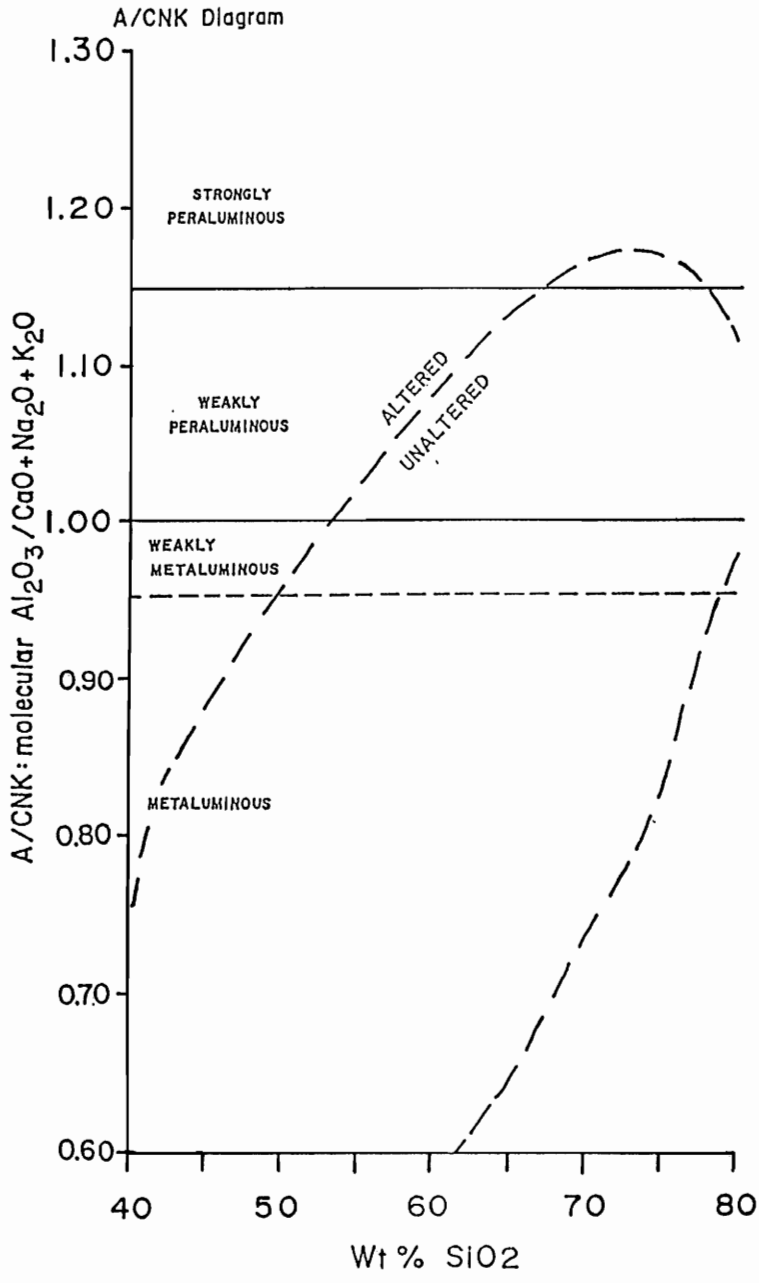

Figure 2-18. A/CNK versus weight percent SiO_2 variation diagram showing altered and unaltered fields. A/CNK = molecular $Al_2O_3/(CaO + Na_2O + K_2O)$. Rock suites in the metaluminous category in the petrochemical classification that fall outside of the unaltered field are generally eliminated from the data set for further classification.

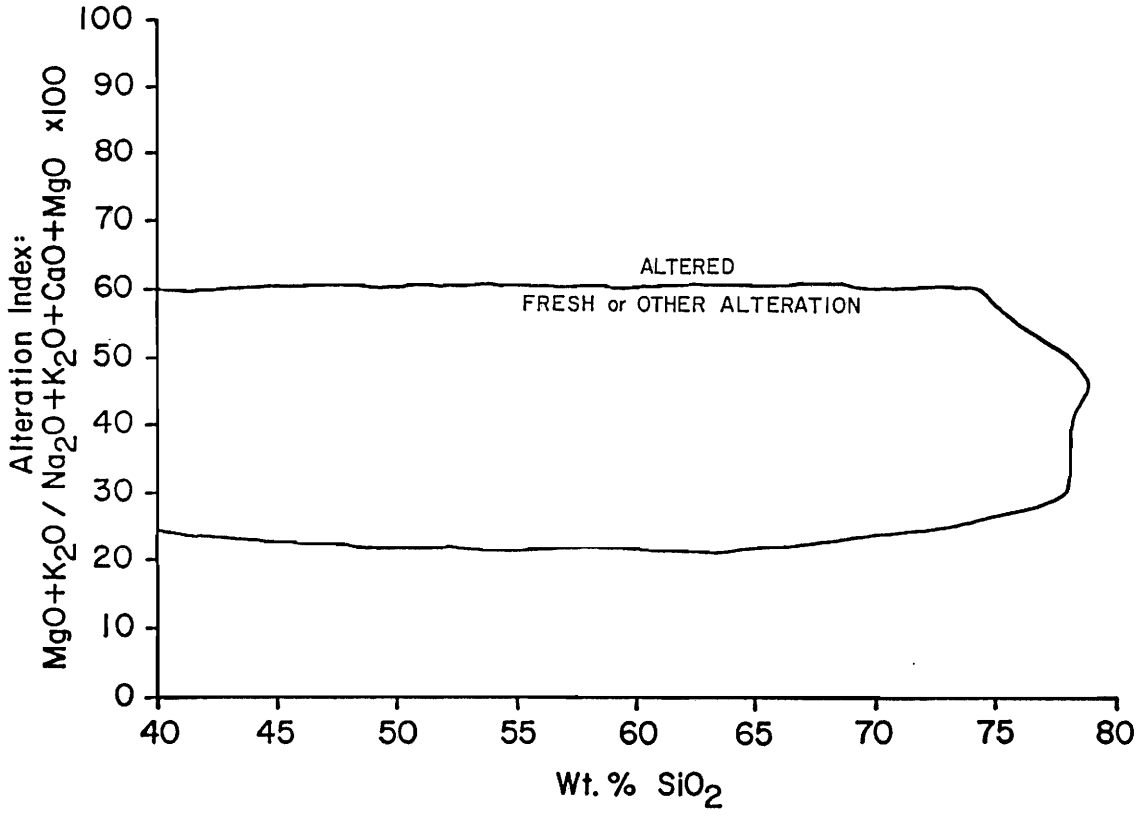

Figure 2-19. A.I. or Alteration index of Ishikawa and others (1976) plotted as an A.I. versus weight percent SiO_2 variation diagram. A.I. = [($MgO + K_2O$) / ($Na_2O + K_2O + CaO + MgO$)] * 100.

The A.I. is defined by the following equation:

$$\text{Alteration index or A. I.} = \frac{K_2O + MgO}{K_2O + MgO + Na_2O + CaO} \times 100.$$

Potassic, illitic-argillic, alunitic, chloritic, and phyllic alteration consistently have A.I. values greater than 60.0. Most fresh rocks have A.I. values of less than 60.0, although propylitic, non-illite-argillic, and carbonate alteration also have A.I. less than 60. Some albitic alteration samples are displaced downward and to the right in the A.I. diagram away from the fresh field. Although the A.I. filter is less efficient at removing samples affected by feldspar-destructive alteration, it is very effective at removing samples affected by potassic alteration.

Potassium Index Versus SiO_2 Diagram

Examination of chemical gains and losses that occur with potassic alteration reveal dramatic potassium addition, slight to no sodium loss, and consistent gain in magnesium. These gains contrast with distinct calcium and iron depletions during potassic alteration. Hence, the K.I. or potassium index was developed to detect potassic alteration. The equation for K.I. is:

$$\text{K index or K.I.} = \frac{K2O + Na2O + MgO}{CaO + (0.9*Fe_2O_3 + FeO)}.$$

In the K index variation diagram (Figure 2-20), K.I. is plotted along the y-axis versus weight percent SiO_2 on the x-axis. The K.I. variation diagram also

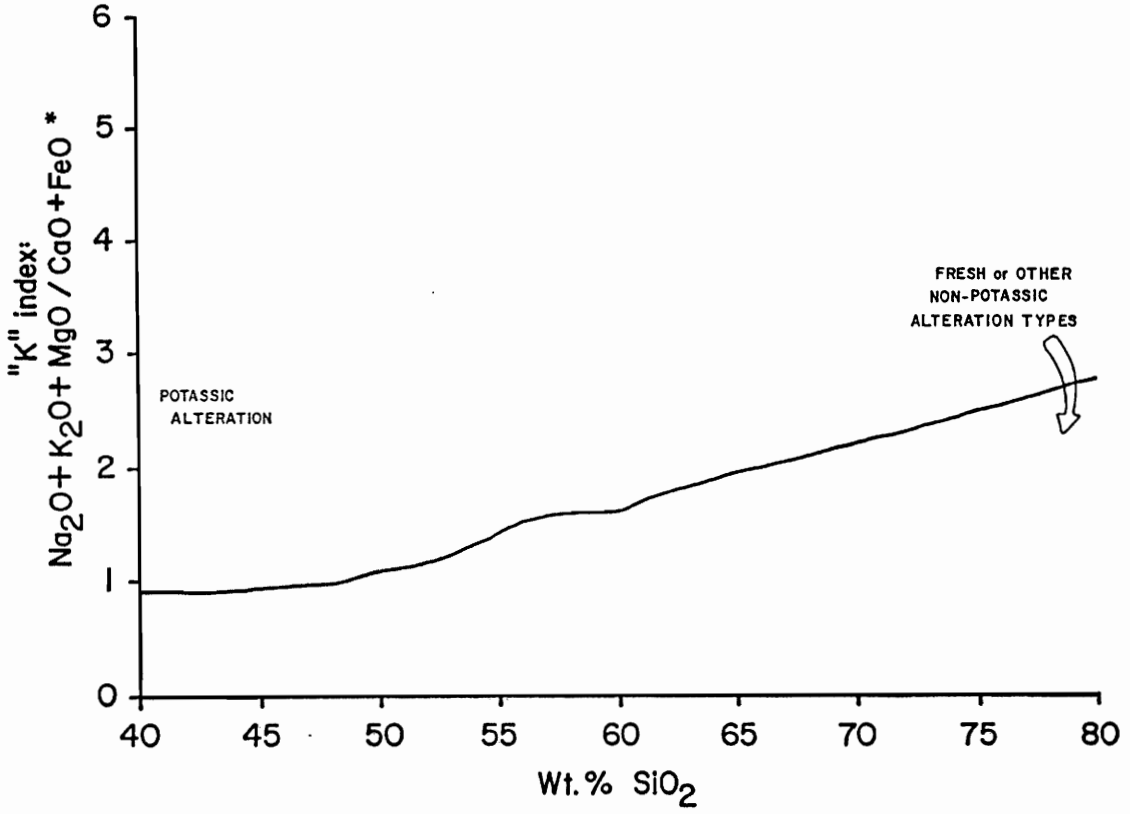

Figure 2-20. K. I. or K index versus weight percent SiO_2 variation diagram. K. I. = $(Na_2O + K_2O + MgO) / (CaO + (0.9*Fe_2O_3 + FeO))$.

detects phyllic and alunitic alteration types and also screens for illite-stable argillic alteration.

Sodium Index Versus SiO_2 Diagram

The A/CNK, A.I., and K.I. filters fail to remove samples affected by sodium metasomatism. Examination of several suites of sodically altered rocks revealed that the main chemical changes that accompany sodic alteration are a dramatic increase in the Na:K ratio and a moderate to strong increase in the A/CNK ratio. These phenomena are expressed by the equation: Na Index or Na I. = $(Na_2O / K_2O) + A/CNK$.

In the Na index variation diagram (Figure 2-21) Na I. is plotted along the y-axis as a log scale versus weight percent SiO_2 on the x-axis. Sodic alteration appears in the upper right portion of the diagram and strong potassic alteration appears in the lower right. Unaltered metaluminous samples or samples of other alteration types appear in the central part of the diagram.

Evaluating Alteration Effects

In practice, the bewildering array of alteration types can be identified using the flow chart sequence shown in Figure 2-22. Some types of alteration prohibit using samples which fail the various alteration filters; however, other types of alteration permit the sample to be used for certain classification splits such as alkalinity. Ferric/ferrous ratios are generally sensitive to any type of

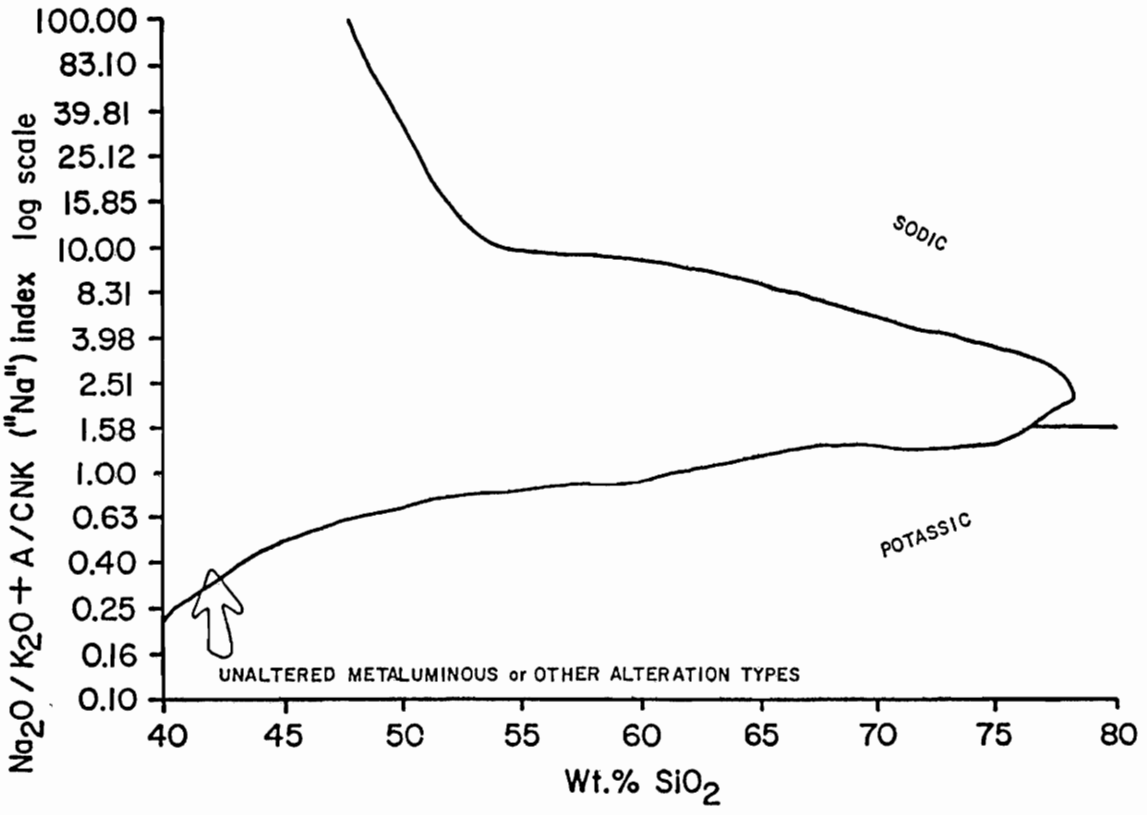

Figure 2-21. Na index variation diagram with Na I. on a log scale versus weight percent SiO_2. Na I. = (Na_2O / K_2O) + A/CNK, where A/CNK = molecular $Al_2O_3/(CaO + Na_2O + K_2O)$.

alteration and altered samples cannot be used to determine oxidation state.

Even though a suite of samples fails the alteration filters, useful information can be gained by understanding the type of alteration. Each alteration type on Table 2-4 is characterized by a unique combination of positive and negative tests according to the alteration filters and scattering or shifting of data on alkalinity and oxidation variation diagrams. In addition, these alteration indexes have potential value in a mapping exercise as a way of focusing on the center of alteration and the potentially highest ore grade depending on the type of ore deposit.

Once the specific type of alteration is identified, certain broad geologic characteristics become apparent (Table 2-5). For example, carbonate alteration strongly indicates precious metal systems and Mg-type potassic alteration characterizes base metal porphyry systems. Phyllic, argillic, and alunitic alteration are characteristic of oxidizing alteration in subaerial tectonic settings, whereas spilitic alteration is characteristic of oxidizing alteration in submarine environment. The spilitic alteration is induced by initial submarine weathering or smectization and by conversion to an epidote-chlorite stable suite during regional prograde metamorphism to greenschist facies.

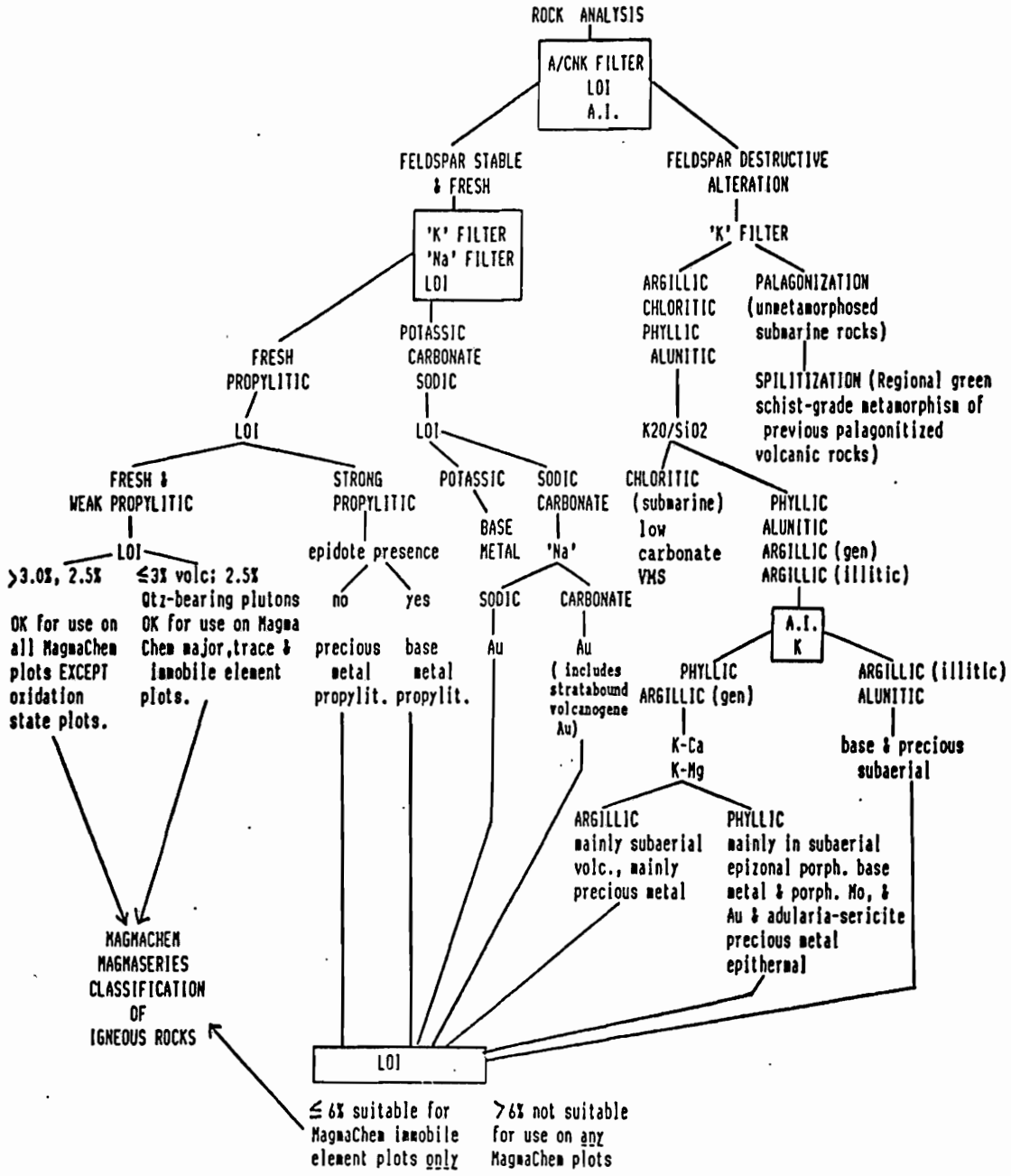

Figure 2-22. Flow chart for evaluating alteration in igneous rock petrochemistry.

	Alteration Filters					Alkalinity Plots			Oxidation
Alteration Type	A/CNK	A.I.	K	Na	LOI	K_2O	K-Ca	K-Mg	Plots
Spilitic	X	-,O	X,O	-	X	-	+		+
Chloritic	X	O	X	-	X,O	O	+		+
Strong	X	O	-,O	-	X	+	+,O	+,O	+
(illite-stable)	X	X	X	-	X	+	+		+
Phyllic	X	O	O	-	X	+	+	+	+
Alunitization	X	X	XX		X	+	+	O,+	+
Oxidizing: Potassic	-	X	X	O	-	+	+		+,-?
Propylitic and actinolitic	_	_	_	_	X	O	+	O	O
Sodic	O,-	O	-	X	X	-	-	-	+,-
Reducing Carbonate	_	_	_	_	XX	O	+	O	O

KEY

Alteration Filters

X mostly removed
O moderately removed
- not removed
XX strongly removed

Alkalinity + Oxidation

+ more alkaline or oxidized
O no change or scatter
- less alkaline and scattered

Table 2-4. Summary of effects of alteration on variation diagrams used in the petrochemical classification.

Magma series	Alteration type	Deposit Type - Rock Type
PCrowh	carbonatization and albitization	Na episyenite (hongorock) mariposite-ankerite rocks
PCroh	potassic and deep phyllic (sericite-pyrophyllite-quartz kyanite assemblage) +/- dumortierite	Cargo Muchacho-Gold Basin type peraluminous Au deposits
PCAoh	(sericite-pyrophyllite--andalusite +/- rutile, tourmaline assemblage	Rochester type Ag deposit Oreana-McCullough Butte type W +/- Be deposit
PACoh		
PACrh	albitization and phyllic (sericite [zinnwaldite in Li-rich systems] - quartz + or - tourmaline, siderite, and 'chlorite)	Panasquieria (Sn-W) - Kourgarok (Sn) type deposits
PAoh	carbonatization-silification (sideroplesite-quartz)	Homestake type Au deposits
MCrh	carbonatization-phyllic-albitization (sericite - [mariposite in Cr-rich systems] - quartz + tourmaline, and ankerite subaerial)	Timmins-Grass Valley type gold deposits
MCowh	propylitic and alkali-silica submarine chloritization (major chlorite, minor biotite-phlogopite)	Panguna type porphyry Cu-Au deposits Noranda type Cu-Zn massive sulfide deposits
MCAow	SUBAERIAL propylitic, potassic, always; phyllic commonly argillic occasionally	Freida River-Ajo type Cu-Mo-Au porphyry deposits
	SUBMARINE chloritization, phyllic, moderate argillic (chlorite-sericite-montmorillonite). Alteration may be encased in more regional spillitically altered submarine volcanic piles of oceanic island arcs	Kuroko type Pb-Zn-Cu-Ag barite massive sulfide deposits

key: P=peraluminous, M=metaluminous; C=calcic, CA=calc-alkalic, AC=alkali-calc A=alkalic; o=oxidized, ow=weakly oxidized; r=reduced; h=hydrous.

Table 2-5. Synopsis of major alteration types in selected magma series of the petrochemical classification and the correlative deposit types.

VARIATION DIAGRAMS OF WHOLE ROCK DATA FOR EACH MINING DISTRICT

In this chapter connections are established between hydrothermal mineralization in the districts involved in the study and igneous rocks of the same age. Thus, a specific igneous rock is identified that is part of the Cogenetic Igneous-Metal-Volatile Suite (CIMVS), which represents three products from a progenitor magma. Mining districts were selected for this study based on the availability of abundant 20 to 40 element geochemical data on mineralized systems in the Trace Element Data Base of MagmaChem Exploration Inc. Districts fitting those criteria and estimated to be associated with classes in this study are listed in Table 3-1. The literature on each of these districts was searched for whole rock geochemical data on associated igneous rocks. About half of the districts that had adequate trace element data on the mineralization also had whole rock data available on the associated igneous rock. These districts are described in this chapter along with results of plots using the magma series classification.

Sources of Whole Rock Data

Whole rock data on the igneous suites associated with mineralization in space and time came largely from the literature. Some of this data was available in MagmaChem Exploration Inc.'s PetChem database on Symphony or Lotus 1-2-3 spreadsheets, but the original references were consulted for additional information and accuracy. Sample locations and rock descriptions are

Table 3-1. List of mining districts with sufficient trace element data for possible inclusion in this study. Dot● indicates those which were used.

mining district	ST	County
Calc-alkalic reduced		
Pony Creek (JAK)	NV	Elko
●Alligator Ridge	NV	White Pine
Gold Acres (Bullion)	NV	Lander
Horse Canyon (Cortez, Mill Canyon	NV	Eureka
Cortez	NV	Lander
●Goldstrike (Lynn, Gold Strike)	NV	Elko-Eureka
●Northumberland	NV	Nye
Jerritt Canyon (Burns Basin, Bell	NV	Elko
●Carlin (Lynn)	NV	Eureka
Illipah	NV	White Pine
●Rain (Carlin)	NV	Eureka-Elko
Cobb	NV	Elko
Shale Pit (Round Mountain)	NV	Nye
Grassy Mountain	OR	Mahlhuer
●Chimney Creek North (Potosi, Getc	NV	Humboldt
Maggie Creek (Schroeder, Gold Qua	NV	Elko-Eureka
Florida Canyon (Imlay)	NV	Pershing
Wenatchee	WA	Chelan
Charleston	NV	Elko
●Basque (Shon, Sherman, Bloody Run	NV	Humboldt
●Potosi (Getchell)	NV	Humboldt
●Getchell (Potosi)	NV	Humboldt
Yellow Pine	ID	Valley
●Preble (Golconda)	NV	Humboldt
●Pinson (Potosi)	NV	Humboldt
Calc-alkalic weakly oxidized		
Chartam	MT	?
●Copper Canyon (Galena Can.) (Batt	NV	Lander
●Dexing	?	Jiangxi
●Dos Pobres	AZ	Graham
●Morenci	AZ	Greenlee
●El Salvador	?	?
●El Teniente	?	?
●Ajo	AZ	Pima
●McCoy gold skarn	NV	Lander
Surprise (Copper Basin, Battle Mt	NV	Lander
●Hedley (Nickel Plate Mine)	BC	?
Empire Mine (Copper Basin) (Battl	NV	Lander
Calc-alkalic oxidized		
Silver Bell	AZ	Pima
●Valley Copper	BC	?
●Twin Buttes-Mission (Pima m.d.)	AZ	Pima
●Mineral Park (Wallapai m.d.)	AZ	Mohave
Toro Mocha	?	Peru
●Red Mountain	AZ	Santa Cruz
●Christmas	AZ	Gila-Pinal
●Bethlehem	BC	?
●Mineral Creek (Ray)	AZ	Pinal
●Sierrita-Esperanza	AZ	Pima
Andacollo	?	Chile
Dutch Miller	WA	King
79 Mine	AZ	Pinal
●Elk Mountain	NV	Elko
●Mill City (Tungsten, Central)	NV	Pershing
Alkali-calcic reduced		
Llallagua	?	Bolivia
Oruro		Bolivia
Colquiri		Bolivia
●Potosi		Bolivia
Alkali-calcic weakly oxidized		
Tecoma	UT-NV	Box Elder-Elk
Cove (McCoy)	NV	Lander
Bull Creek	NV	White Pine
Tierra Blanca	NM	Sierra
Candelaria (Columbus)	NV	Mineral
●Taylor	NV	White Pine
●Railroad (Bullion)	NV	Elko
Pioche (Highland)	NV	Lincoln
Michigan Boy (Oak Spring)	NV	Nye
Ackerman Canyon	NV	Lander
Moho (Marietta)	NV	Mineral
Comet	NV	Lincoln
Dean Mine (Lewis)	NV	Lander
●Santa Eulalia	?	Chihuahua
Freiberg (Worthington)	NV	Lincoln
●Tempiute	NV	Lincoln
●Cherry Creek (Egan Canyon, Gold C	NV	White Pine
Oak Spring	NV	Nye
●Kinsley (Kingsley)	NV	Elko-White Pi
White Pine (Mt. Hamilton, Treasur	NV	White Pine
●Linka	NV	Lander
Merrimac (Lone Mountain)	NV	Elko
●Swales Mountain	NV	Elko
Alkali-calcic oxidized		
●Tintic	UT	Juab-Utah
Dolly Varden (Mizpah, Granite)	NV	Elko
●Tombstone	AZ	Cochise
●Castle	MT	Meagher
●Park City	UT	Summit
Chloride (St. Cloud)	NM	Sierra
Mine Mountain	NV	Nye
Beaverdell	BC	?
Spring City (Paradise Valley)	NV	Humboldt
Fireball Ridge (Truckee)	NV	Churchill
Mud Springs (Medicine Springs, De	NV	Elko
Apache No. 2	NM	Hidalgo

listed in Appendix A; whole rock analyses are listed in Appendix B.

Results for Each Mining District Grouped by Classes

The procedure used to classify each district into a particular petrochemical class involved plotting whole rock oxide values on variation diagrams, excluding data that did not pass alteration filters and data from volcanic rocks, and classifying the district based on plots of unaltered plutonic rocks and mineralogic criteria. Alteration filters used in this study include diagrams with SiO_2 plotted against A/CNK, Alteration index, Na index, K index, and LOI. Variation diagrams used to classify each district include SiO_2 versus K_2O, K_2O-MgO, K_2O-CaO, $(FeO+0.9*Fe_2O_3)/MgO$, and Fe_2O_3/FeO. In many cases, excluding altered and volcanic samples eliminated from half to all of the data. Comparison of alkalinity charts with and without data from volcanics and altered rocks shows a dramatic tightening of points into specific fields when altered samples are excluded.

In several United States districts the Cretaceous-Cenozoic eastward, then westward sweep of magmatism resulted in overprinted magmatism and mineralization, such that magmatism as little as 5 million years older or younger than the deposit of interest plotted in different alkalinity fields. This result required careful examination of the literature in order to exclude irrelevant rocks, such as some in Park City, Tombstone, and Sierrita described below.

The following descriptions and results for each mining district are

arranged in the six classes studied in order to notice similarities within the classes and differences among the classes. The first mining district is described in more detail and two sets of variation diagrams are shown to illustrate the methodology, first with all the data, including altered and volcanic samples, and second with only unaltered samples.

Alkali-calcic, Oxidized

Tintic, UT

The East, North, and Main Tintic mining districts in Juab and Utah counties, Utah, have produced silver and base-metals from limestone-replacement ore bodies in Paleozoic rocks affected by early Oligocene magmatism (Morris, 1964; Morris and Lovering, 1979; Morris and Mogensen, 1978). The major polymetallic replacement deposits of the Main and East Tintic districts are spatially related to the Silver City stock, which is the Cogenetic Igneous-Metal-Volatile Suite (CIMVS) (Figure 3.1, 3.2). Carbonate rocks in these districts host polymetallic vein and replacement deposits that display a lateral and vertical zonation from lead- and silver-rich zones to zinc- and manganese-rich zones with increasing distance from the Silver City stock (Hannah and others, 1991).

The oldest Oligocene volcanic group is the Packard Quartz Latite at 32.75 Ma (Laughlin and others, 1969). Overlying the Packard is a sequence of dark-gray latite tuffs, flows, welded tuff, and agglomerates of the Tintic Mountain Volcanic group (Copperopolis Latite, Latite Ridge Latite, Big Canyon Latite).

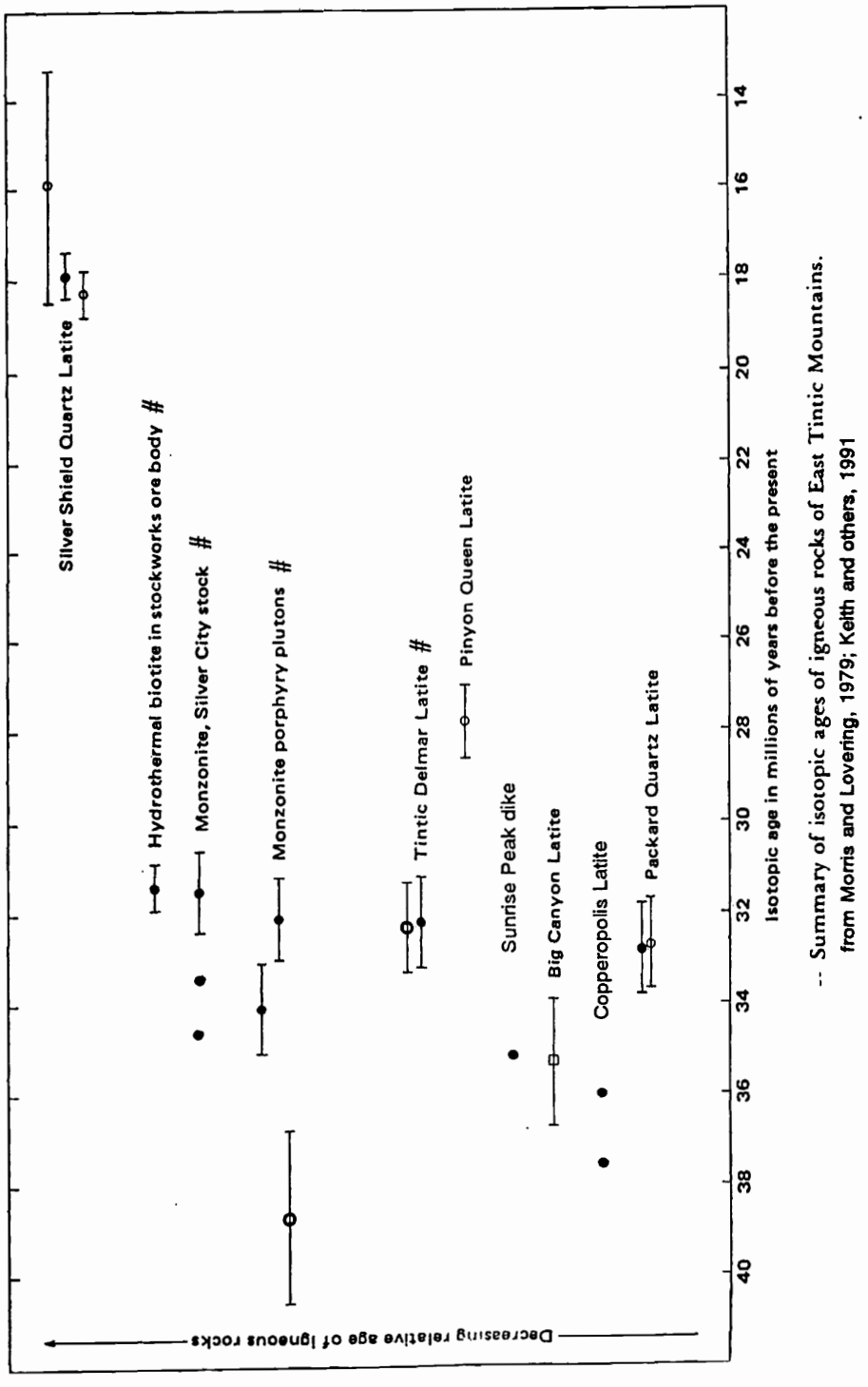

Figure 3-1. Summary of isotopic ages of igneous rocks of East Tintic Mountains (# = CIMVS) (from Morris and Lovering, 1979; Keith and others, 1991).

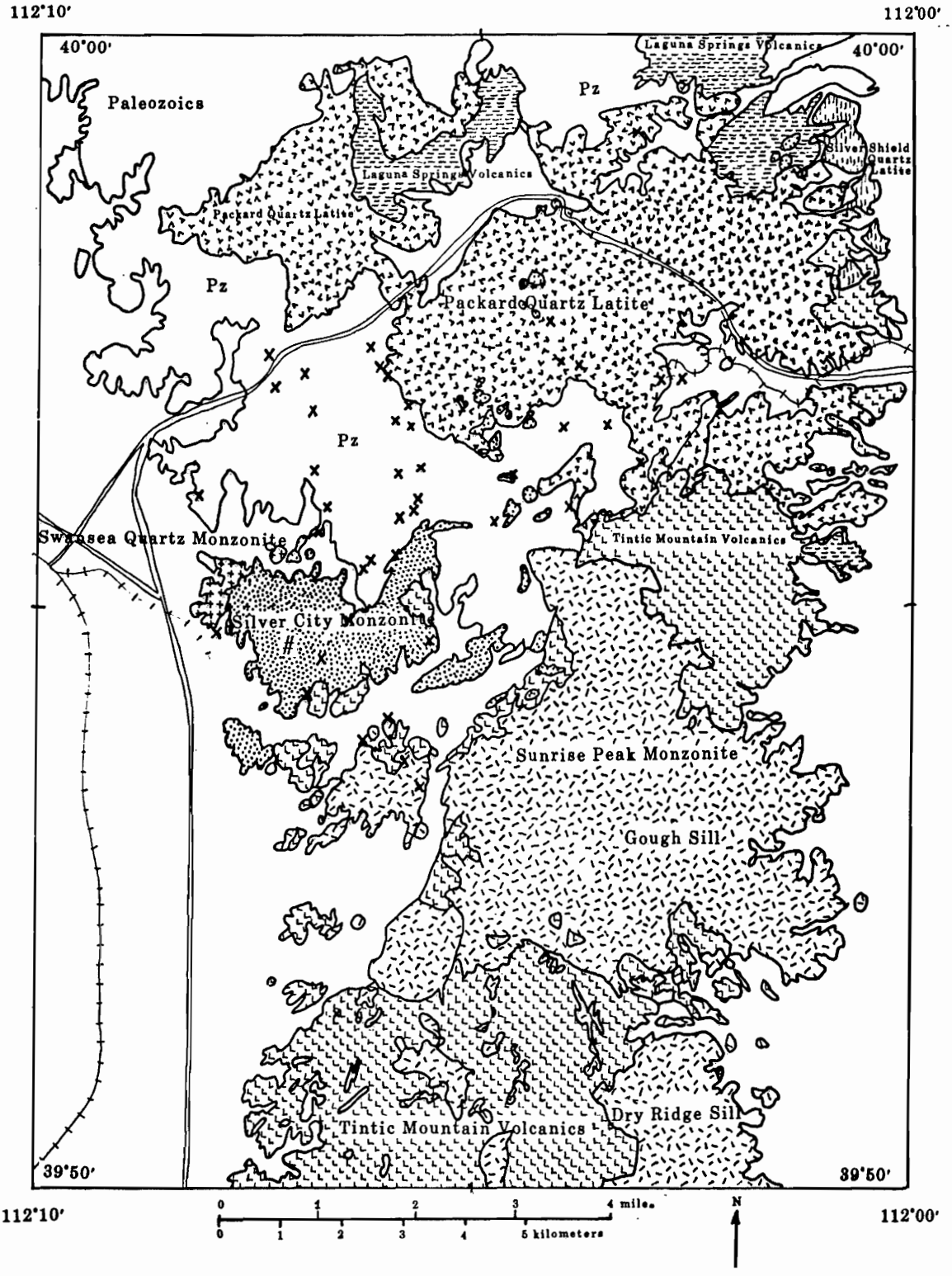

Figure 3-2. Geologic map of Tintic, Utah, showing igneous stocks and volcanics with # = CIMVS (modified from Morris and Mogensen, 1978).

This sequence terminated in the intrusion of many stocks and sills such as the Sunrise Peak Monzonite of the Gough and Dry Ridge sills. Argon 40/argon 39 ages on biotite from a Sunrise Peak dike yielded a date of 35.3 $\pm$ 0.1 Ma (Keith and others, 1991).

The youngest of the Oligocene volcanics is the Laguna Springs Volcanic Group (North Standard Latite, Pinyon Queen Latite, Tintic Delmar Latite), which has an average potassium-argon isotopic age of 31.5 Ma; this sequence was terminated by the intrusion of the ore-related Silver City Monzonite Porphyry (CIMVS) and numerous plugs and dikes and intrusion breccia (Morris and Mogensen, 1978). Ages of hydrothermal biotite and numerous potassium-argon isotopic dates on these magmatic sequences related to caldera development cluster around 32 Ma, indicating a close temporal relationship between magmatism and mineralization (Hannah and others, 1991). Fission-track ages and argon 40-argon 39 ages on the Silver City stock and related intrusions cluster around 33.6 Ma (Keith and others, 1991).

The youngest igneous rock in the Tintic district is the Silver Shield Quartz Latite with a K-Ar age of about 17 Ma (Laughlin and others, 1969). These Miocene igneous rocks were excluded from the whole rock data set because they were younger than the mineralization event and are not related to it.

Whole rock analyses on these volcanics and stocks in the Tintic district were found in Morris and Lovering (1979), Lindgren and Loughlin (1919), Tower and Smith (1899), and Clarke (1915); these are listed in Appendix B. Additional

analyses in Keith and others (1991) did not include FeO, so were not used.

Variation diagrams of the Tintic whole rock analyses that were used as alteration filters include SiO_2 versus A/CNK, Alteration Index (AI), Na Index (NAI), and K index (KI) (Figure 3-3). Samples that fell in the altered fields and volcanic samples were eliminated from the data set.

The next diagrams are iron/magnesium versus SiO_2 and ferric/ferrous versus SiO_2 (Figure 3-4). The charts on the left side of Figure 3-4 use all the data, including that from altered, unaltered, plutonic, and volcanic samples; those on the right side exclude altered and volcanic samples. The scatter on graphs that include altered and volcanic samples is eliminated on the graphs for the unaltered plutonic samples. Tintic district samples fall in the moderately iron-poor part of the FeO^*/MgO or modified Miyashiro plot and in the oxidized part of the ferric/ferrous diagram.

Alkalinity is categorized on diagrams with SiO_2 versus K_2O, K_2O - CaO, and K_2O - MgO (Figure 3-5) and with Zr versus Nb and Zr versus Y (Figure 3-6). Again, the charts on the left side of the figures (including data from all samples) show more scatter than those on the right side (excluding altered and volcanic samples). In both cases, samples from Tintic fall in the alkali-calcic field. Samples on the K_2O - MgO versus SiO_2 variation diagram tend to fall lower on the diagram and overlap into the calc-alkalic field. Only a few samples included niobium, zirconium, and yttrium values, so the data are not well constrained. The samples generally fall in the alkali-calcic field, though the altered and volcanic

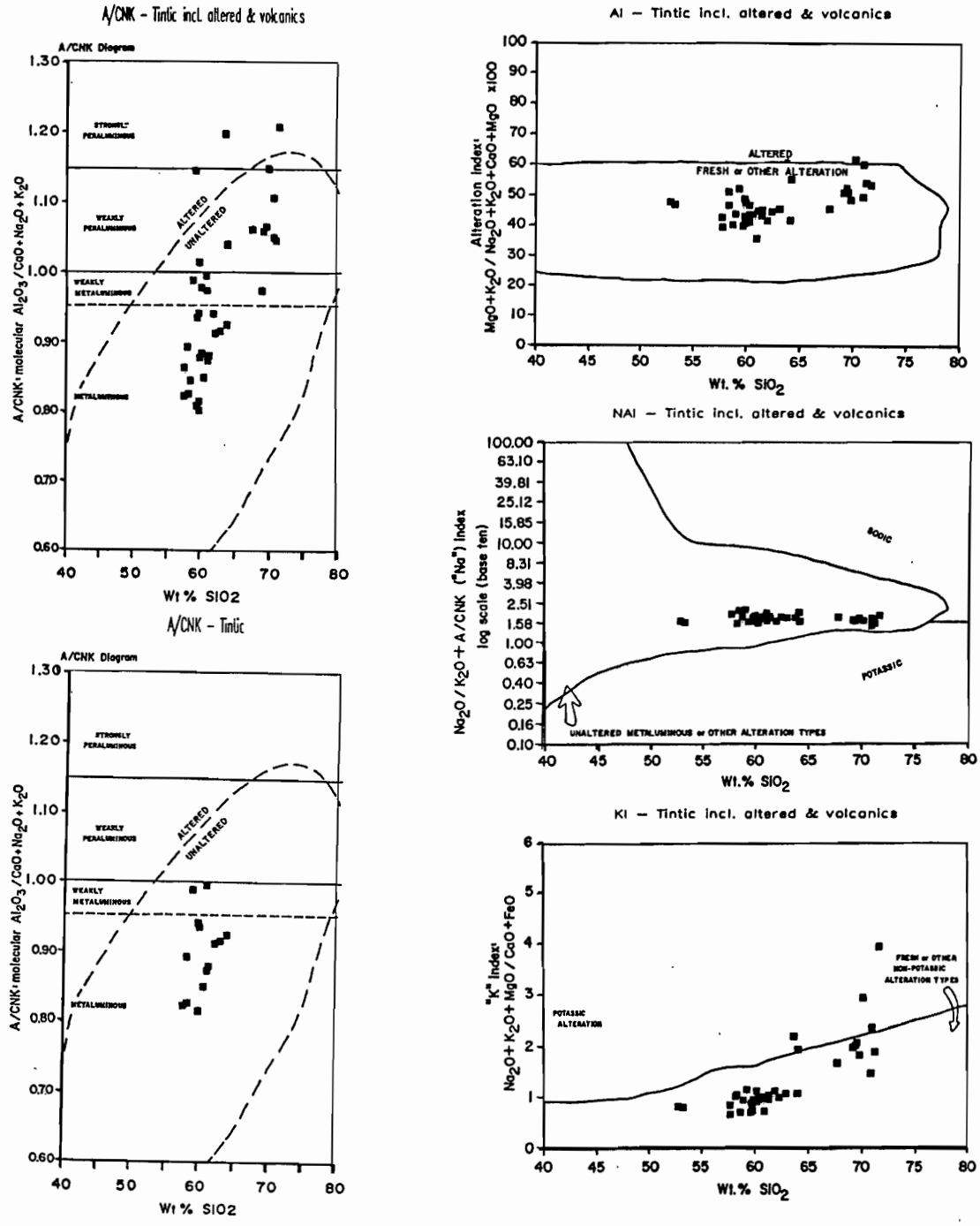

Figure 3-3. Petrochemical variation diagrams used as alteration filters for igneous rocks at Tintic, Utah.

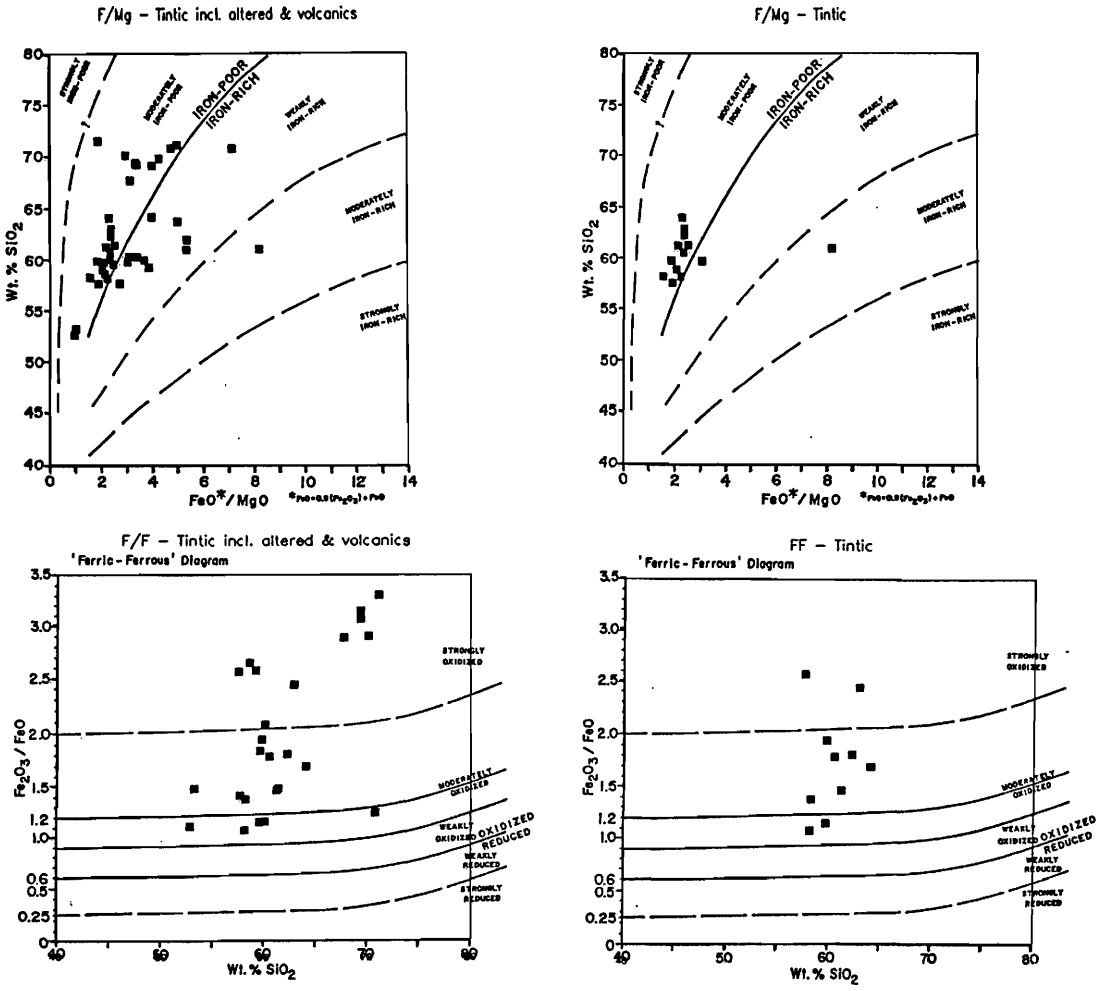

Figure 3-4. Petrochemical variation diagrams showing iron/magnesium and ferric/ferrous ratios of all samples compared to those excluding altered and volcanic rocks at Tintic, Utah.

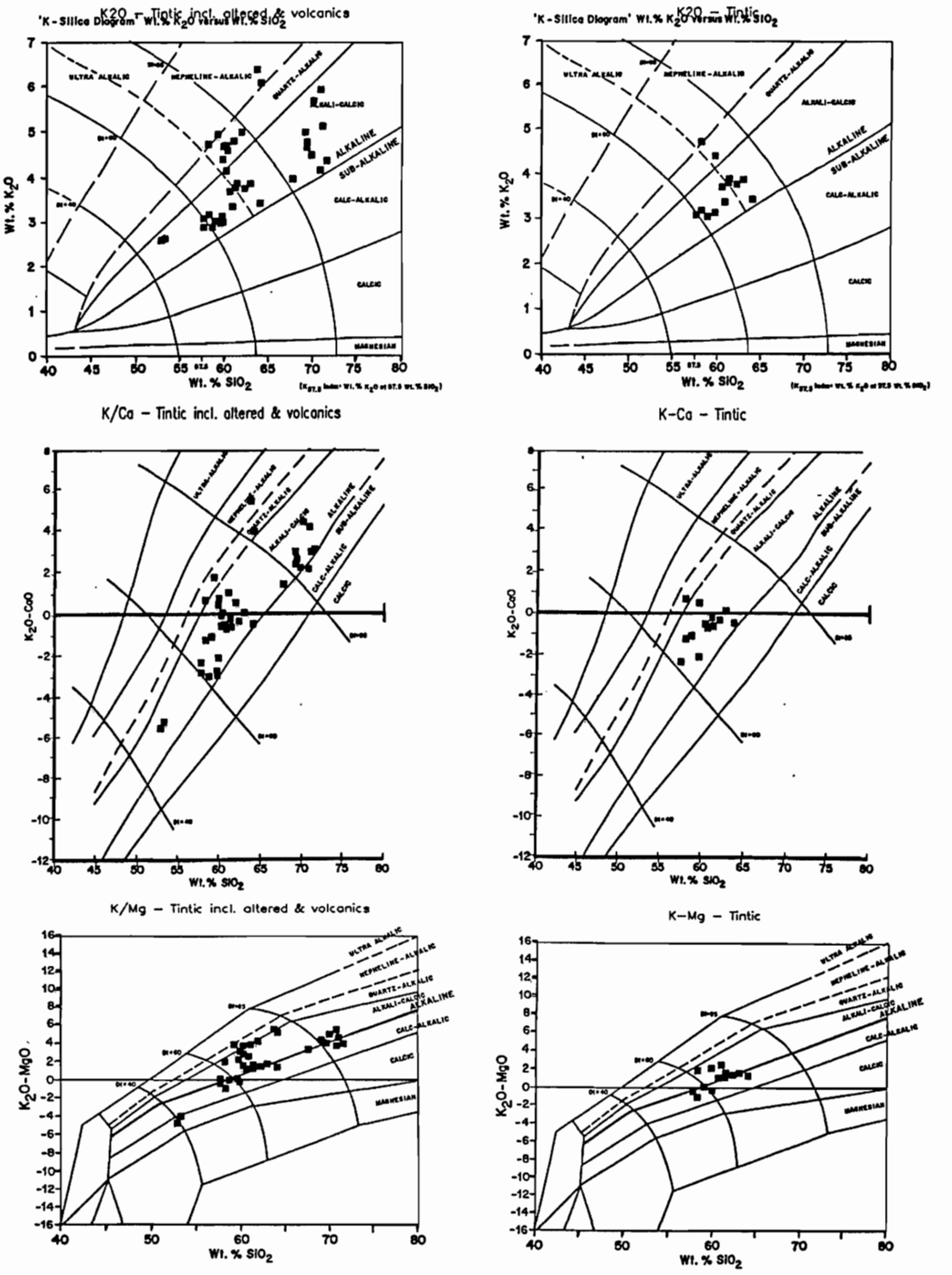

Figure 3-5. Magma series variation diagrams showing alkalinity of all samples compared to those excluding altered and volcanic rocks at Tintic, Utah.

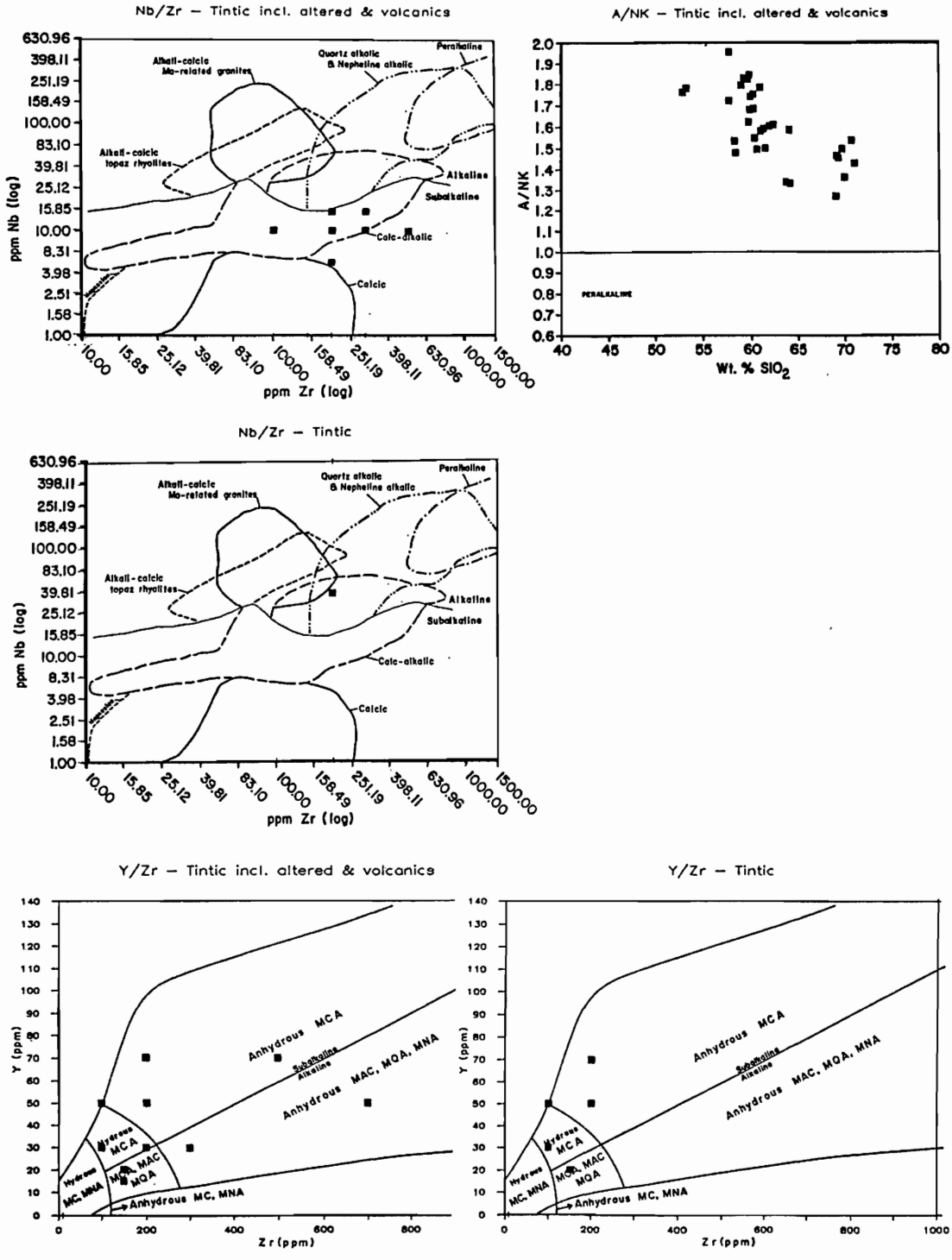

Figure 3-6. Magma series variation diagrams using Nb and Y versus Zr to show alkalinity and hydrous nature of all samples compared to those excluding altered and volcanic rocks at Tintic, Utah.

samples are in the calc-alkalic fields. The A/NK versus SiO_2 variation diagram indicates the samples are not peralkaline.

Castle, MT

The Castle Mountain district is in Meagher County southeast of White Sulphur Springs, Montana (Figure 3-7). The lead-zinc-silver ore deposits on the southeastern flank of the Castle stock were formed through hydrothermal processes associated with the Blackhawk diorite stock and Castle granite stock and associated dacite porphyry (quartz porphyry) and rhyolite (Smith, 1983; Winters, 1968). These represent the Cogenetic Igneous-Metal-Volatile Suite (CIMVS).

Whole rock analyses from the Castle Mountains were obtained from the literature (Weed and Pirsson, 1896) and from MagmaChem Exploration files. Samples collected by MagmaChem are located in Figure 3-7 and are described in Appendix A. The Castle Mountains granite and Blackhawk diorite (CIMVS) are shown as Tertiary intrusives (Ti) on the geologic map. The rhyolite feldspar porphyry in the dikes (Ti) was dated at 47.6 $\pm$ 1.8 Ma on biotite and at 47.6 $\pm$ 2.1 on feldspar (Chadwick, 1980).

The four samples of Tertiary intrusives (Ti) were not altered and are in the metaluminous, alkali-calcic, oxidized fields (Figure 3-8). The samples fall in the moderately iron-poor field on the FeO*/MgO versus SiO2 graph (Figure 3-9) and in the alkali-calcic field on the niobium versus zirconium plot.

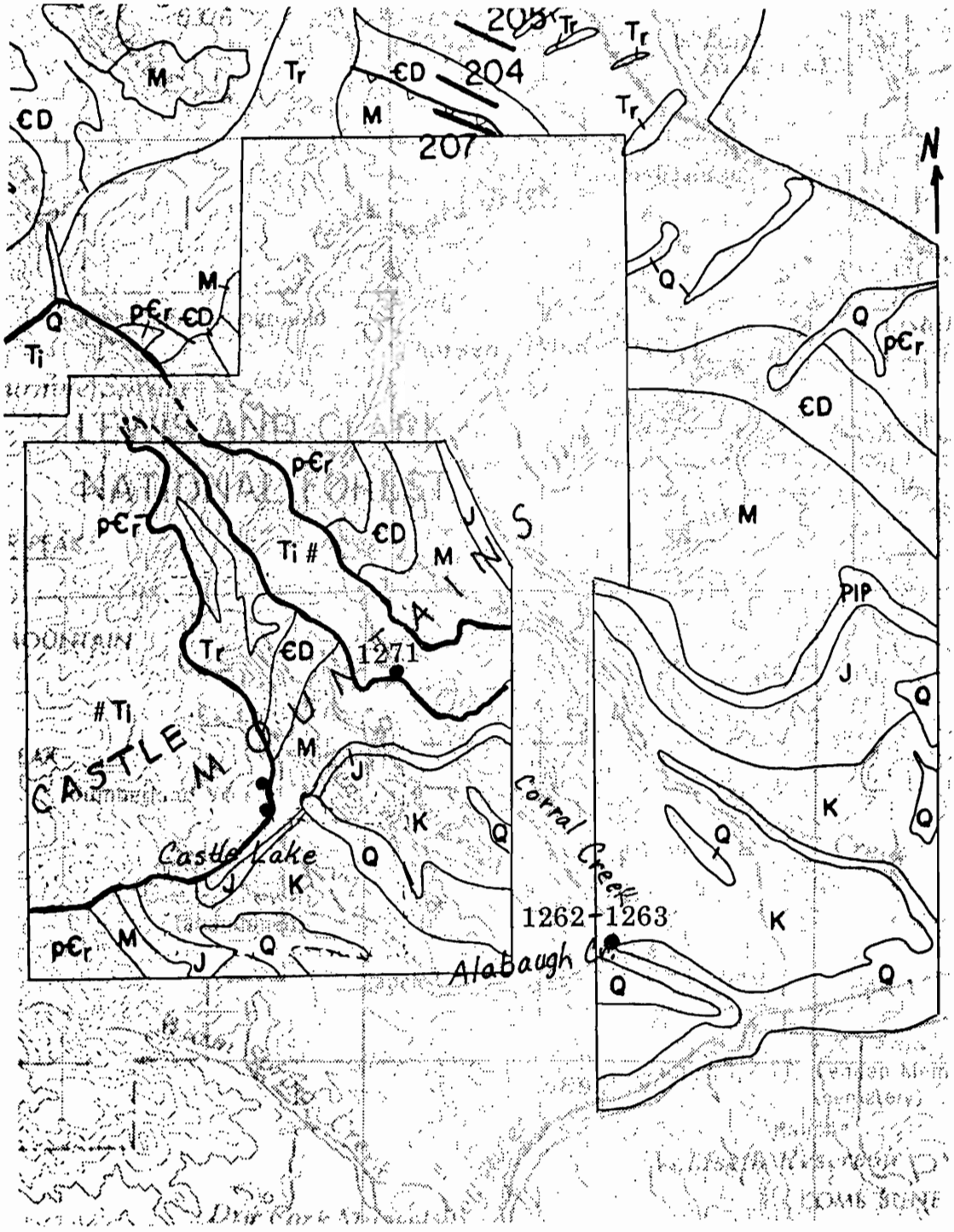

Figure 3-7. Geologic map and MagmaChem sample locations for Castle stock, Montana (Ti = # = CIMVS) (adapted from McClernan, 1980).

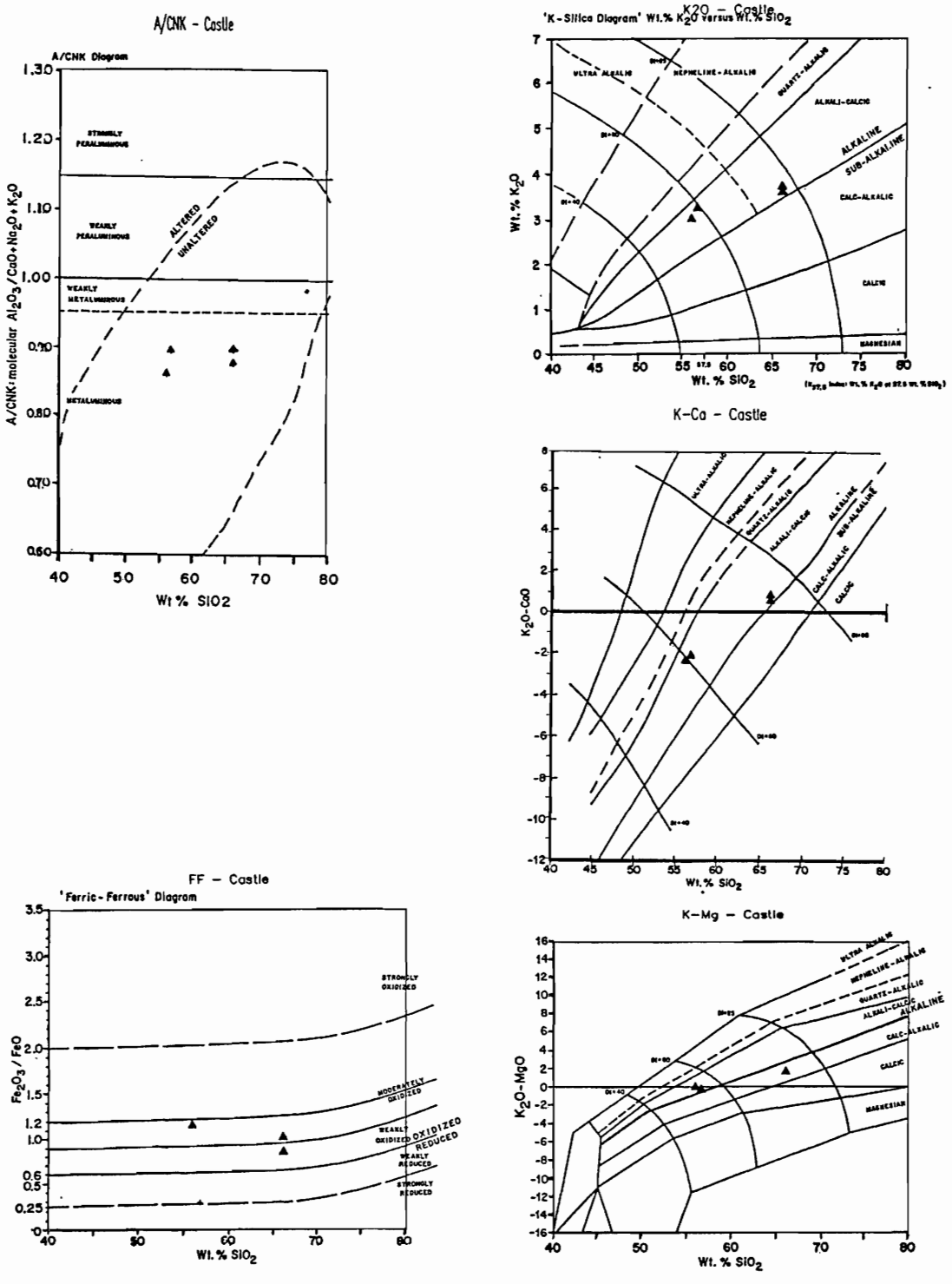

Figure 3-8. Magma series variation diagrams showing A/CNK, ferric/ferrous, and alkalinity of Tertiary intrusive of Castle Mountains, Montana.

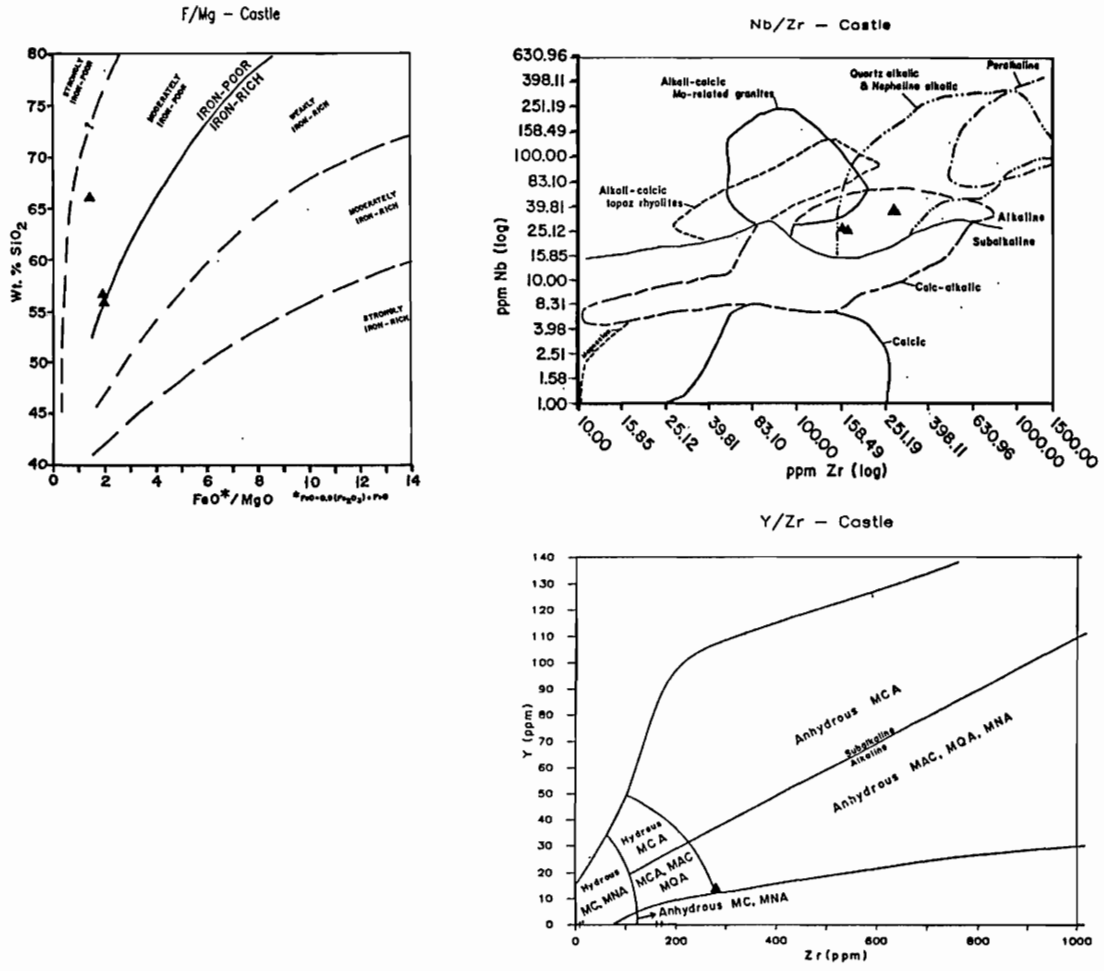

Figure 3-9. Petrochemical variation diagrams showing FeO^*/MgO and Nb versus Zr for Tertiary intrusive of Castle Mountains, Montana.

Park City, UT

Park City is in the Wasatch Range southeast of Salt Lake City, Utah (Figure 3-10). The ore deposits occur as lode and bedded replacement deposits in Carboniferous to Triassic sedimentary rocks and are spatially and temporally associated with a composite porphyry pluton (the Ontario and Mayflower stocks), the Clayton Peak stock, and the east lobe of the Alta stock (Bromfield and others, 1977; Barnes and Simos, 1968). These stocks represent the Cogenetic Igneous-Metal-Volatile Suite (CIMVS).

Whole rock analyses of igneous rocks from Park City appear in Bromfield and others (1977), Villas and Norton (1977), John (1991), Calkins and Butler (1943), Wilson (1961), and Villas (1975); these are listed in Appendix B. Because the data for the entire region were evenly spread between the alkali-calcic and calc-alkalic fields, data from each stock were replotted separately.

The Pine Creek, Valeo, and Flagstaff stocks are clearly calc-alkalic; these stocks and the Mayflower stock have slightly older potassium-argon isotopic dates (40 to 35 Ma) (Figure 3-11). The Pine Creek stock gave ages of 36.8 Ma (Crittenden and others, 1973) and 35.2 on biotite (Bromfield and others, 1977); the Valeo stock gave hornblende ages of 40.3 and 39.8 Ma (paired with a biotite age of 34.6 Ma); hornblende form the Flagstaff stock gave an age of 39.7 Ma (Bromfield and others, 1977). Hornblende from the Mayflower stock gave an age of 41.2 Ma, but the stock intrudes the Keetley Volcanics, which is dated at 34 to 37 Ma; this relationship suggests the Mayflower stock is younger (Bromfield and

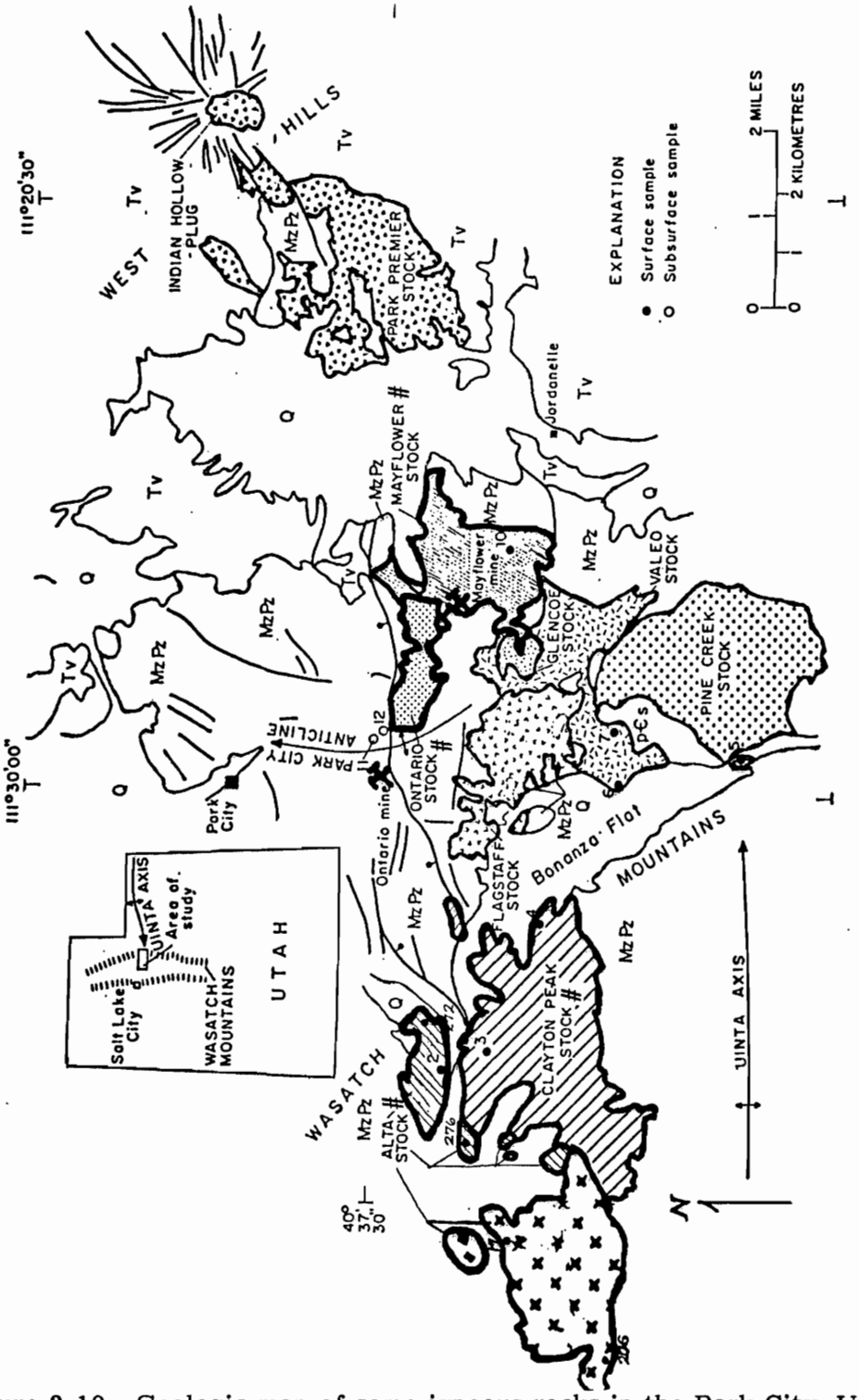

Figure 3-10. Geologic map of some igneous rocks in the Park City, Utah, region (# = CIMVS = Ontario, Mayflower, Clayton Peak, and Alta stocks) (modified from Bromfield and others, 1977; John, 1989).

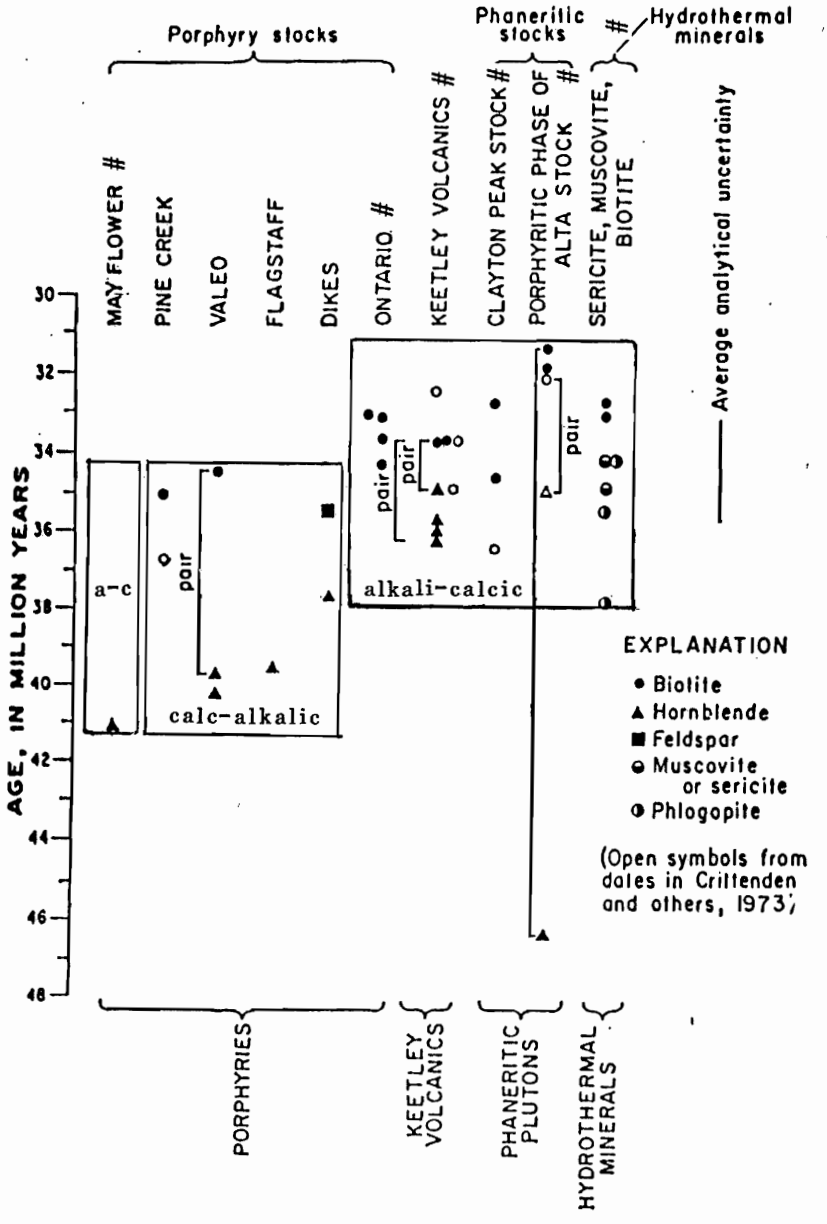

Figure 3-11. Graphical representation of radiometric dates from the Park City mining district, Utah (# = CIMVS) (from Bromfield and others, 1977).

others, 1977). Its alkali-calcic alkalinity fits better with the younger age.

The Ontario stock, Clayton Peak stock, Alta stock, Keetley volcanics, and Mayflower stock are clearly alkali-calcic; these rocks are slightly younger (36 to 31 Ma) than the calc-alkalic stocks (40 to 35 Ma) (Figure 3-11). Biotite from the Clayton Peak stock gave ages of 32.9 and 34.7 Ma; biotite from the porphyritic phase of the Alta stock yielded ages of 31.7, 31.6, and 32.1 Ma (Bromfield and others, 1977); a biotite-hornblende pair from the Alta stock was dated at 32.4 and 35.1 Ma (Crittenden and others, 1973). Biotite samples from the Ontario porphyry stock gave consistent ages of 33.4, 33.9, 34.5, and 33.3 Ma (Bromfield and others, 1977).

Ages of hydrothermal minerals include dates of 33.1 and 33.3 Ma on biotite from the Mayflower mine, of 34.4 on coarse muscovite from the Ontario mine, and of 35.1 Ma on sericite from the Ontario mine (Bromfield and others, 1977). Thus, a clear temporal relationship exists between the alkali-calcic igneous rocks (the Ontario, Clayton Peak, Mayflower, and Alta stocks) and the mineralization; together they form a Cogenetic Igneous-Metal-Volatile Suite (CIMVS).

Comparisons are made between the older calc-alkalic stocks on the right sides and the younger alkali-calcic stocks on the left sides of Figures 3-12 and 3-13. Both sets of stocks are in the metaluminous and oxidized fields; however, the younger and older groups are in different alkalinity fields (Figure 3-13).

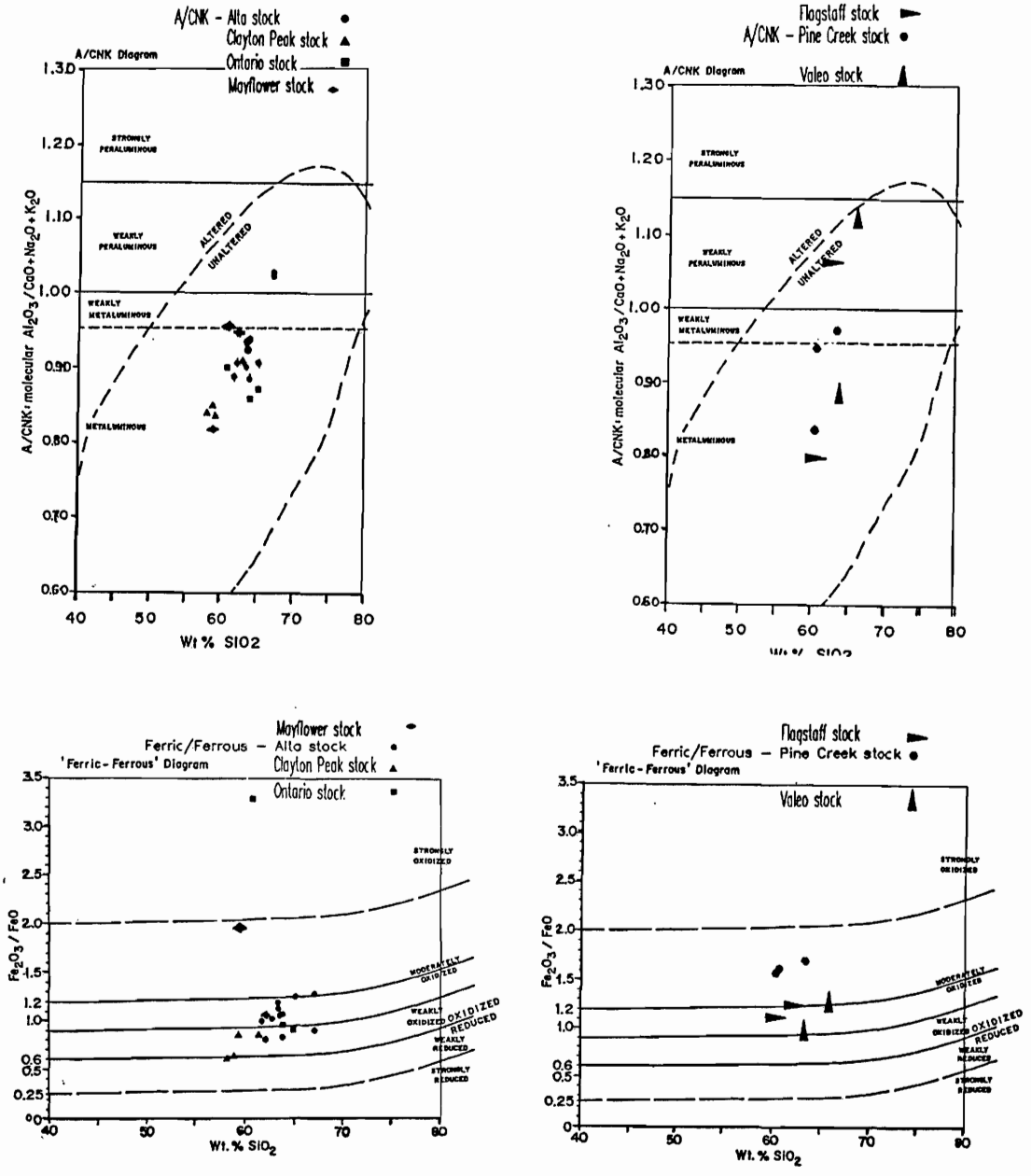

Figure 3-12. Petrochemical diagrams showing A/CNK and ferric/ferrous ratio of stocks in the Park City, Utah, area with older calc-alkalic stocks on the right and younger alkali-calcic stocks (CIMVS) on the left.

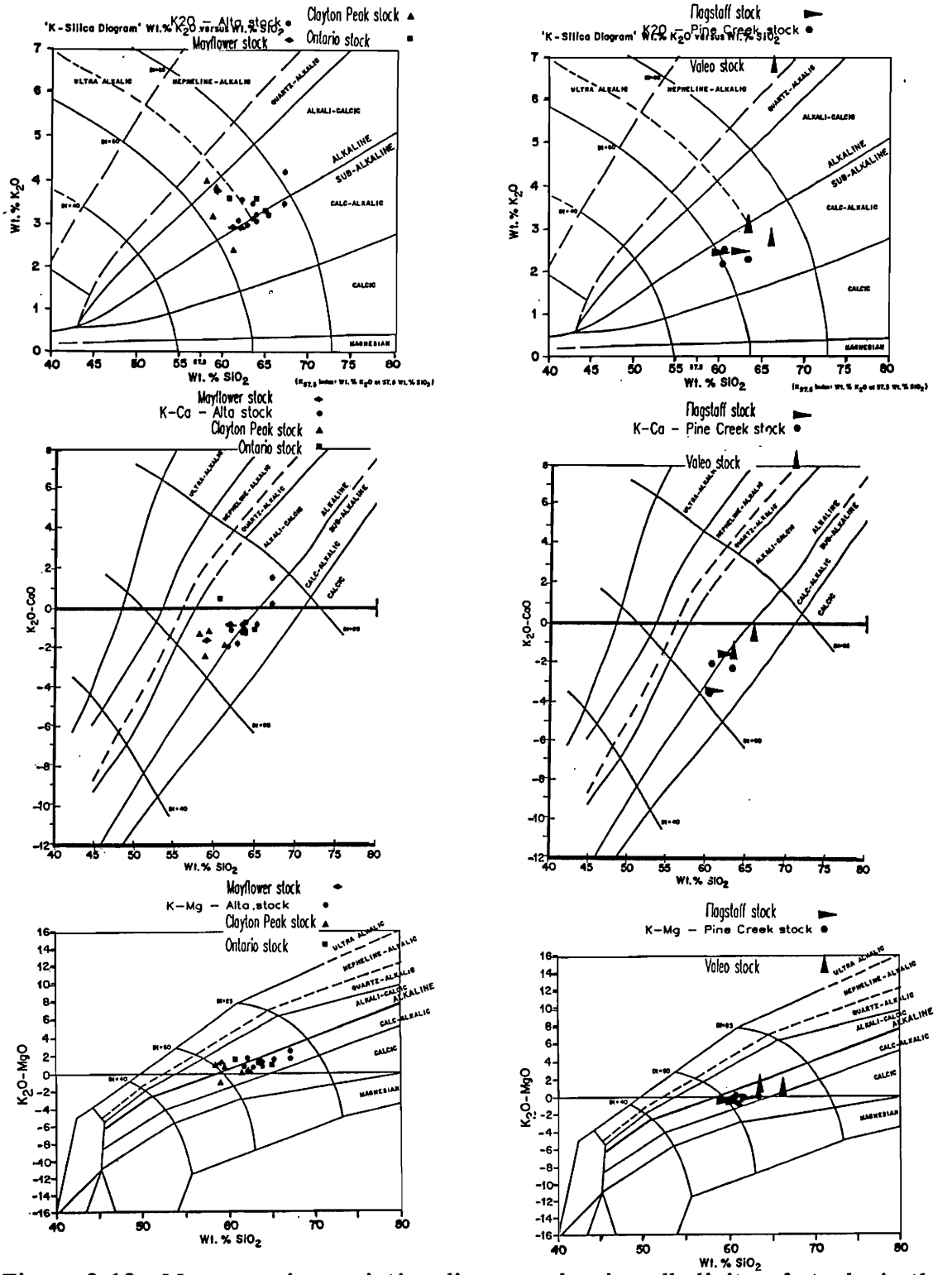

Figure 3-13. Magma series variation diagrams showing alkalinity of stocks in the Park City, Utah, area with older calc-alkalic stocks on the right and younger alkali-calcic stocks (CIMVS) on the left.

Tombstone, AZ

Tombstone is in Cochise County in southeastern Arizona (Figure 3-14). The silver-lead-zinc ore deposits are concentrated in veins and replacement deposits that are spatially associated with hornblende andesite dikes; metal zoning patterns are consistent with stock-associated mineralization at depth (Newell, 1974).

Whole rock analyses of igneous rocks in the Tombstone area were obtained from Clarke (1915), Gilluly (1956), Dewhurst (1976), and Lang (1991) (Appendix B). The mineralization and most of the volcanic and plutonic units are between 77 to 73 Ma (CIMVS) (Figure 3-15). The sequence of igneous events in the Tombstone area included extrusion of the Bronco Volcanics before 76 Ma, emplacement of the Schieffelin Granodiorite and venting of the equivalent Uncle Sam Porphyry Tuff, and emplacement of quartz latite porphyry dikes, hornblende andesite dikes, and rhyodacite stocks, and hydrothermal mineralization (CIMVS). However, the Tombstone Rhyolite east of the mineralized part of the district is between 67 and 65 Ma (Marvin and Cole, 1978); because it is about ten million years younger than the mineralization, it is excluded from this study.

After excluding samples that are altered or volcanics, the data are in the metaluminous field in the A/CNK and in the oxidized field in the ferric/ferrous charts (Figure 3-16). The data are in the alkali-calcic fields on the K_2O and K_2O - CaO variation diagrams, with some overlap into the calc-alkalic fields. The field boundaries are transitional and a 15 percent overlap into the next category

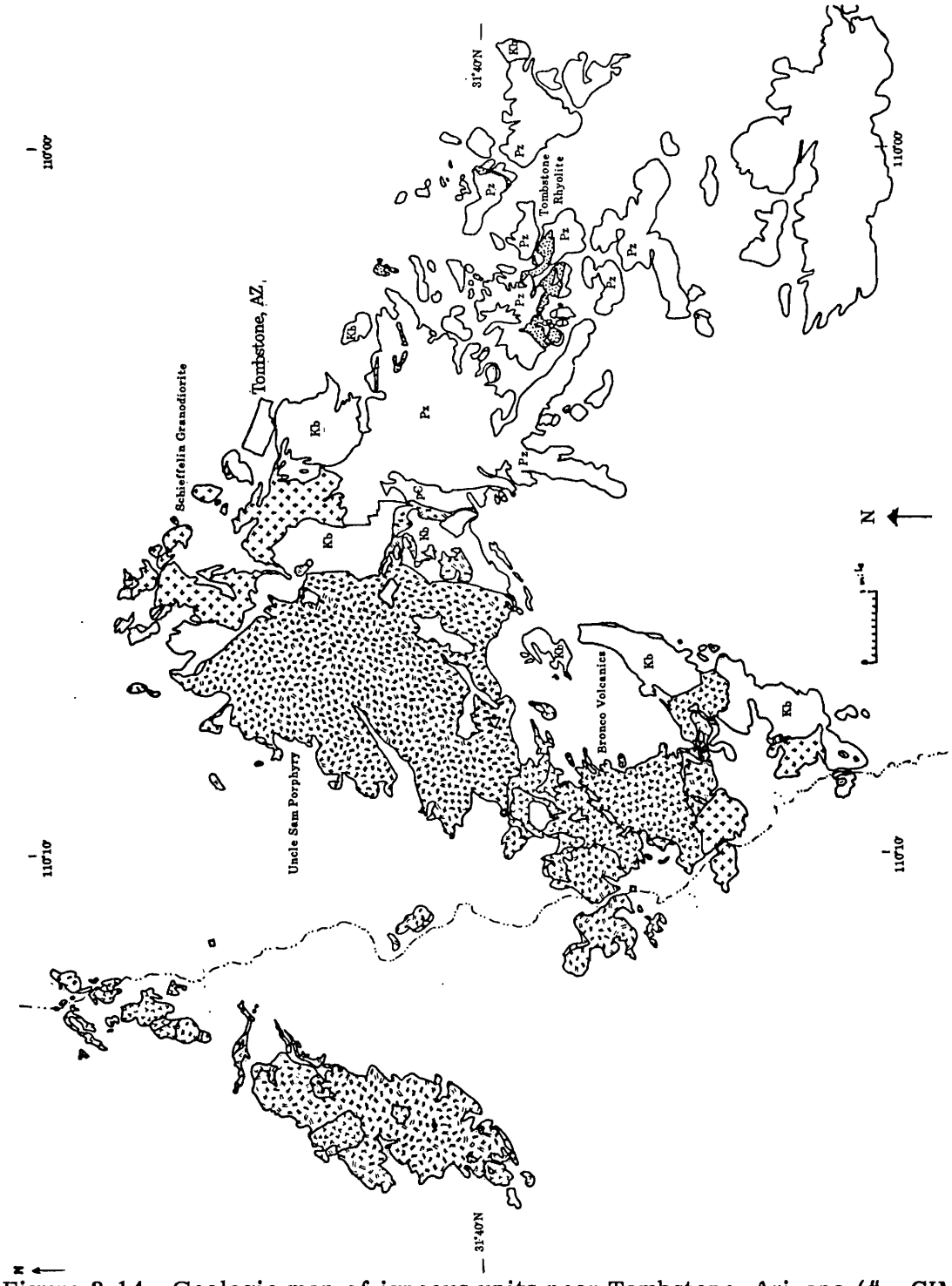

Figure 3-14. Geologic map of igneous units near Tombstone, Arizona (# = CIMVS = Bronco, Uncle Sam, and Schieffelin) (modified from Gilluly, 1956).

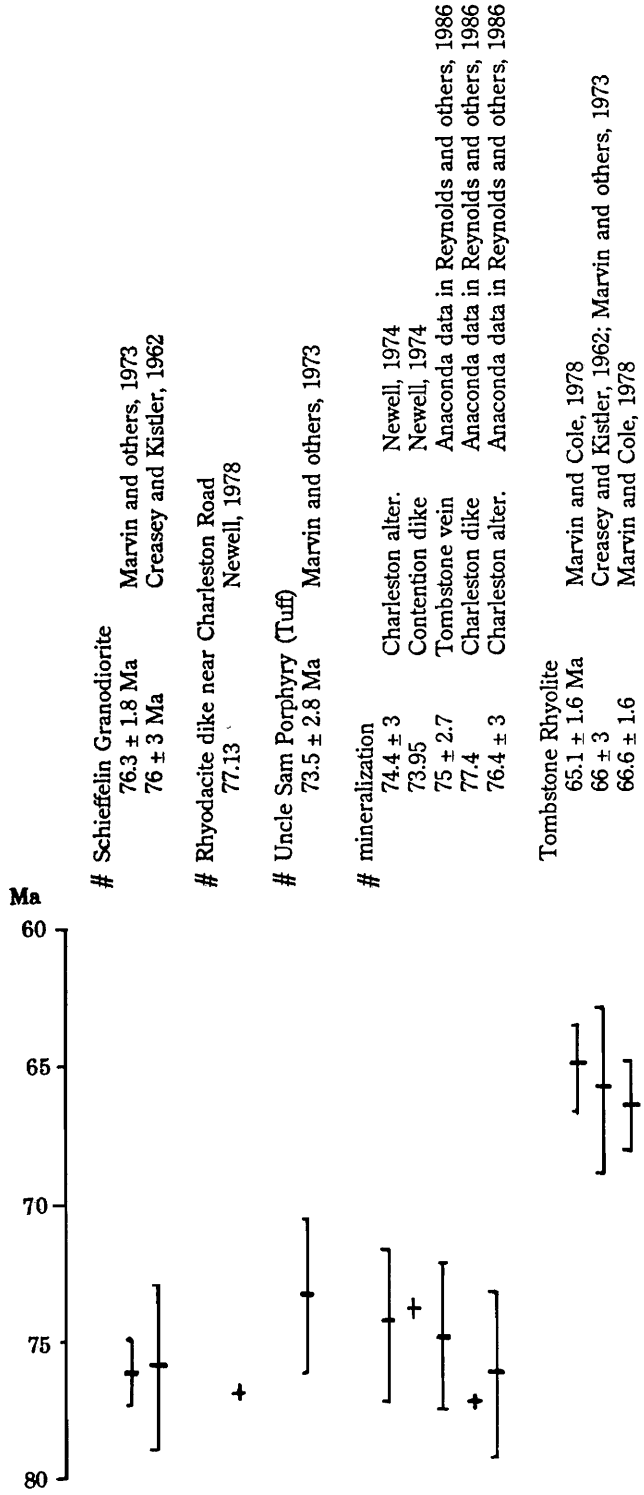

Figure 3-15. Radiometric ages from Tombstone, Arizona (# = CIMVS).

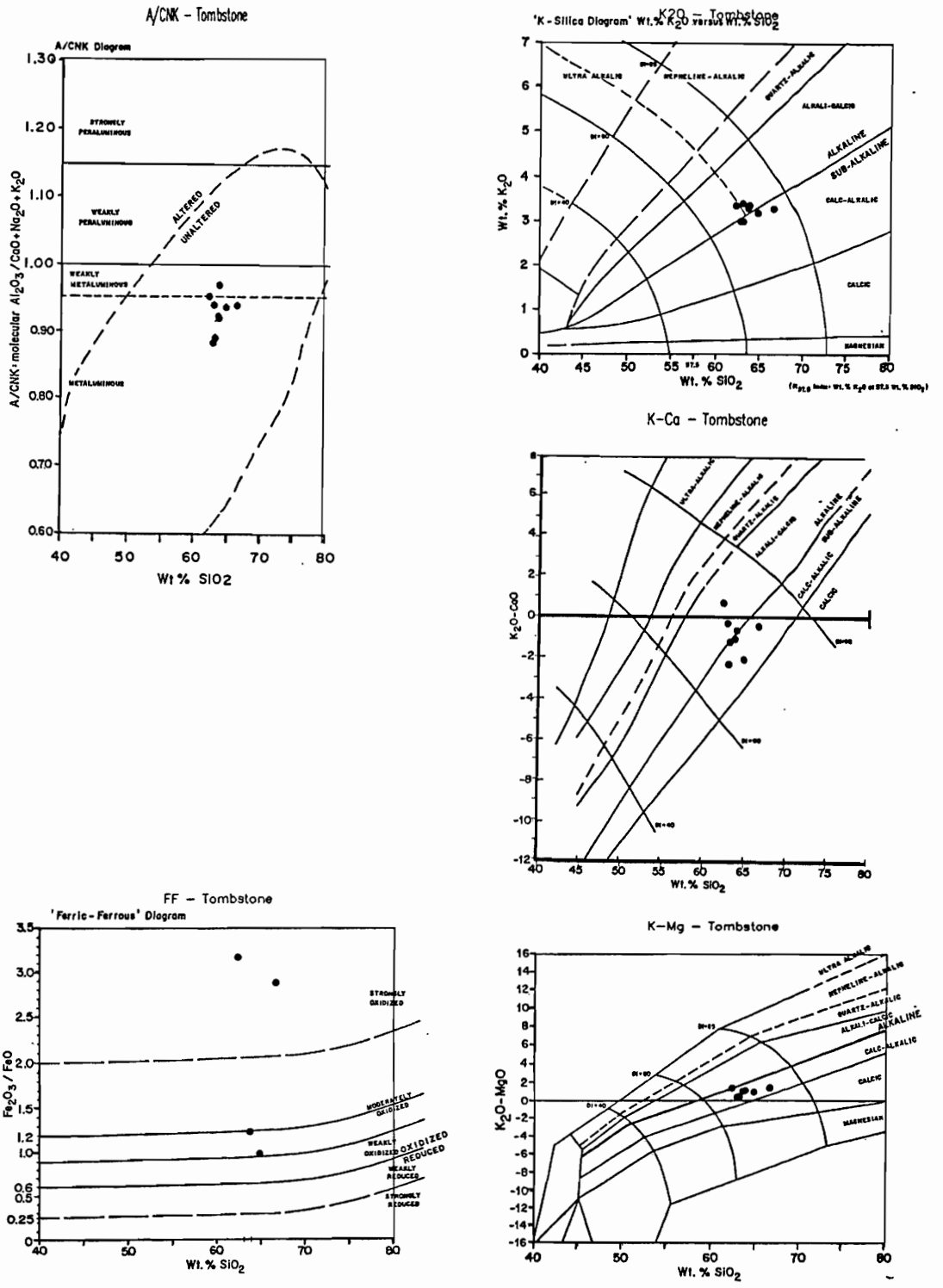

Figure 3-16. Petrochemical variation diagrams of igneous rocks from Tombstone, Arizona, showing A/CNK, ferric/ferrous ratio, and alkalinity.

is not uncommon. The K_2O - MgO variation diagram indicates calc-alkalic alkalinity, but the district is assigned to the alkali-calcic class because the K_2O versus SiO_2 graph is more significant and because two of the three diagrams indicated alkali-calcic. The data are in the moderately iron-poor field of the FeO^*/MgO versus SiO_2 graph (Figure 3-17), in the calc-alkalic field on the Nb versus Zr graph, and in the hydrous field on the Y versus Zr graph.

Alkali-calcic, Weakly Oxidized

Cherry Creek, NV

The Cherry Creek area is in White Pine County, Nevada, on the east side near the conjunction of the northern Egan Range and southern Cherry Creek Range about 80 km (50 miles) north of Ely. The Cherry Creek mining district produced silver and lead, with lesser amounts of zinc and gold (Smith, 1976). The lead-silver ore bodies occur in Cambrian quartzites and limestones as veins or replacement bodies along faults. The ore deposits are clearly associated with intrusions of gray, medium-grained quartz monzonite noted as Ti (CIMVS) on Figure 3-18 (Schrader, 1931; Hose and Blake, 1976; Smith, 1976).

Whole rock analyses from plutonic rocks in the Cherry Creek area used in this study include a sample from Clarke (1915, I, p. 164) and samples of Tertiary intrusives (Ti) collected by MagmaChem Exploration staff (Appendix A). The age of the quartz monzonite (porphyritic biotite adamellite dike) that is 5 miles south of the town of Cherry Creek was dated at 32.1 $\pm$ 0.6 Ma (Armstrong, 1970b).

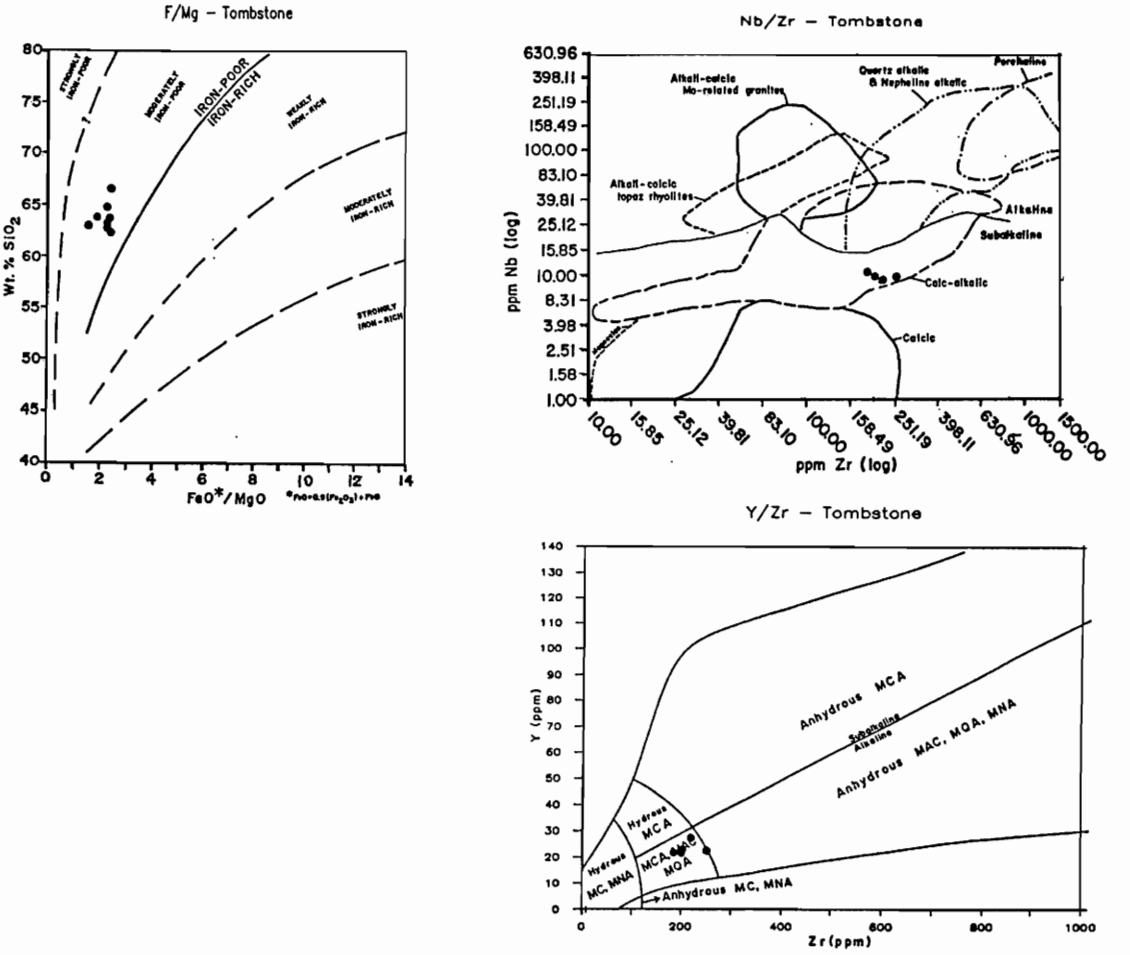

Figure 3-17. Petrochemical variation diagrams of igneous rocks from Tombstone, Arizona, showing FeO*/MgO, Nb/Zr, and Y/Zr relationships.

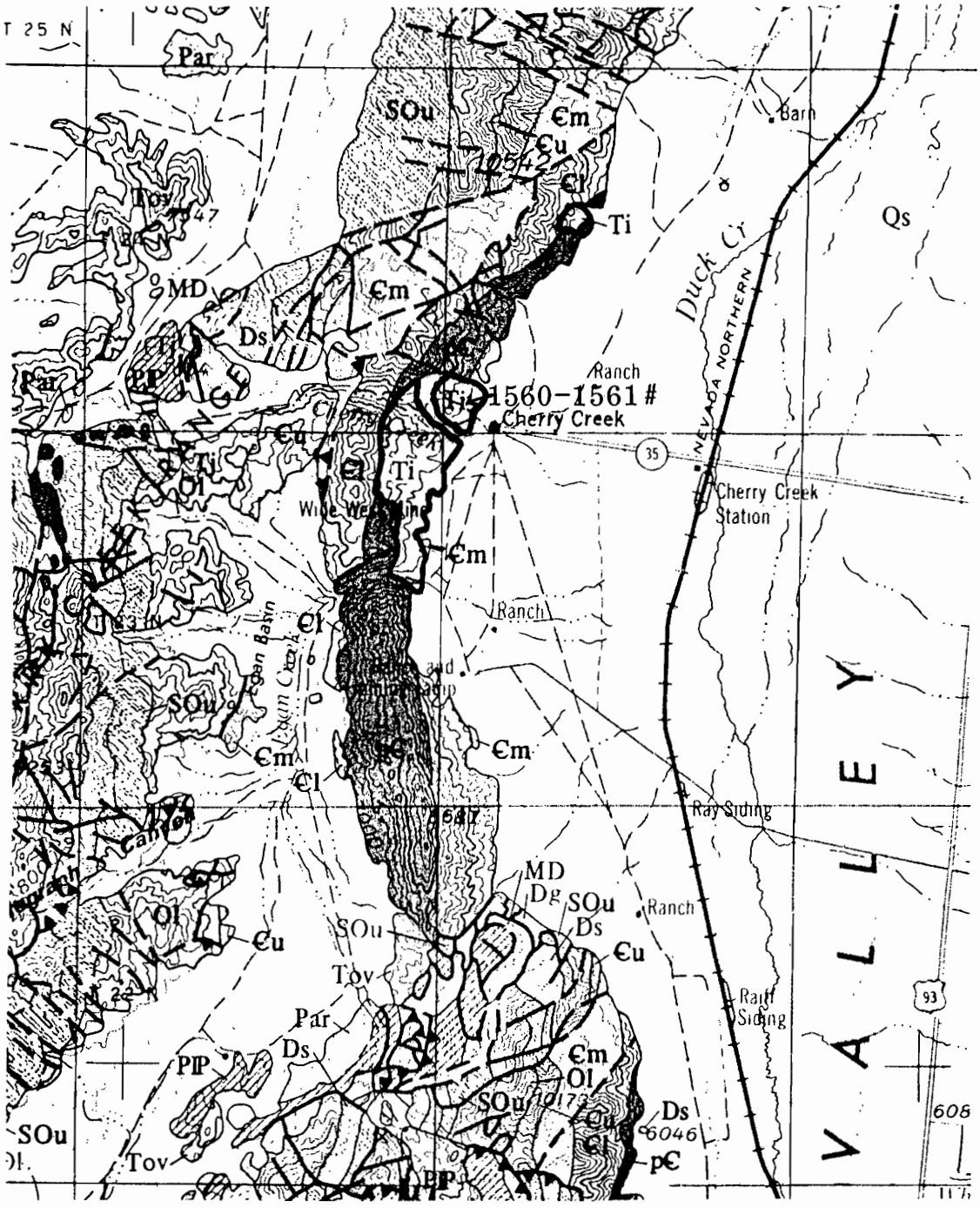

Figure 3-18. Geologic map of Cherry Creek, Nevada, showing igneous rocks (Ti = Tertiary intrusive = # = CIMVS) and sample localities (modified from Hose and Blake, 1976).

Fission track ages of the biotite quartz monzonite from nearby Egan Creek Canyon averaged 40.3 Ma (Naeser, in Hose and Blake, 1976).

The three whole rock analyses (Figure 3-19) passed the alteration filters and are in the metaluminous, alkali-calcic, weakly oxidized, moderately iron-poor fields. The K_2O versus SiO_2 chart is given more importance than the K_2O - CaO and K_2O - MgO charts, especially because the samples are in the upper half of the calc-alkalic field in the K_2O - MgO graph and in the portion of the alkali-calcic field that overlaps 15 percent into the calc-alkalic field on the K_2O - CaO graph.

Kinsley, NV

The Kinsley (Kingsley) district is in southeastern Elko County, Nevada, in the southern end of the Kingsley Mountains about 80 km (50 miles) southwest of Wendover. Silver-bearing lead-copper deposits occur as small lenses and pods along faults; they are contact metamorphic deposits in veins and replacement deposits near the stock (CIMVS) in steeply dipping faults and in adjacent gently dipping limestones (Stager and Tingley, 1988; Smith, 1976).

Lower Paleozoic sedimentary rocks, particularly dolomitic Cambrian limestones, are intruded in the southern part of the range by a quartz monzonite stock (Kgr on Figure 3-20 = CIMVS), that generated an aureole of contact metamorphism and mineralization (Steininger, 1966; Hill, 1916). The stock mapped as Kgr has been dated at 35 $\pm$ 3 Ma by K-Ar and 41 Ma by lead-alpha (Armstrong, 1963) and at 40 $\pm$ 2 Ma using lead-alpha and Rb-Sr (Sayyah, 1978).

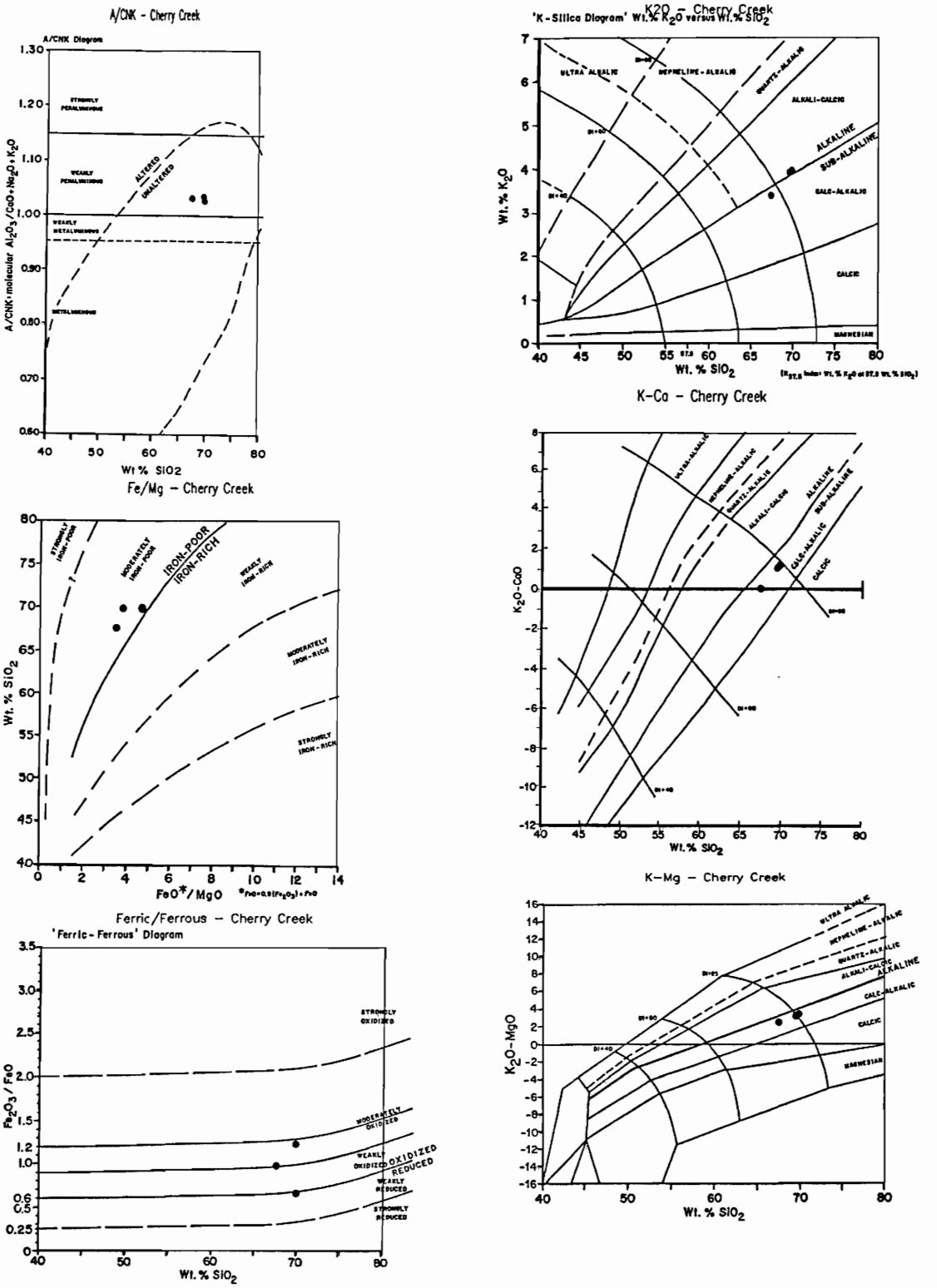

Figure 3-19. Petrochemical variation diagrams of some Cherry Creek, Nevada, igneous rocks showing A/CNK, iron ratios, and alkalinity.

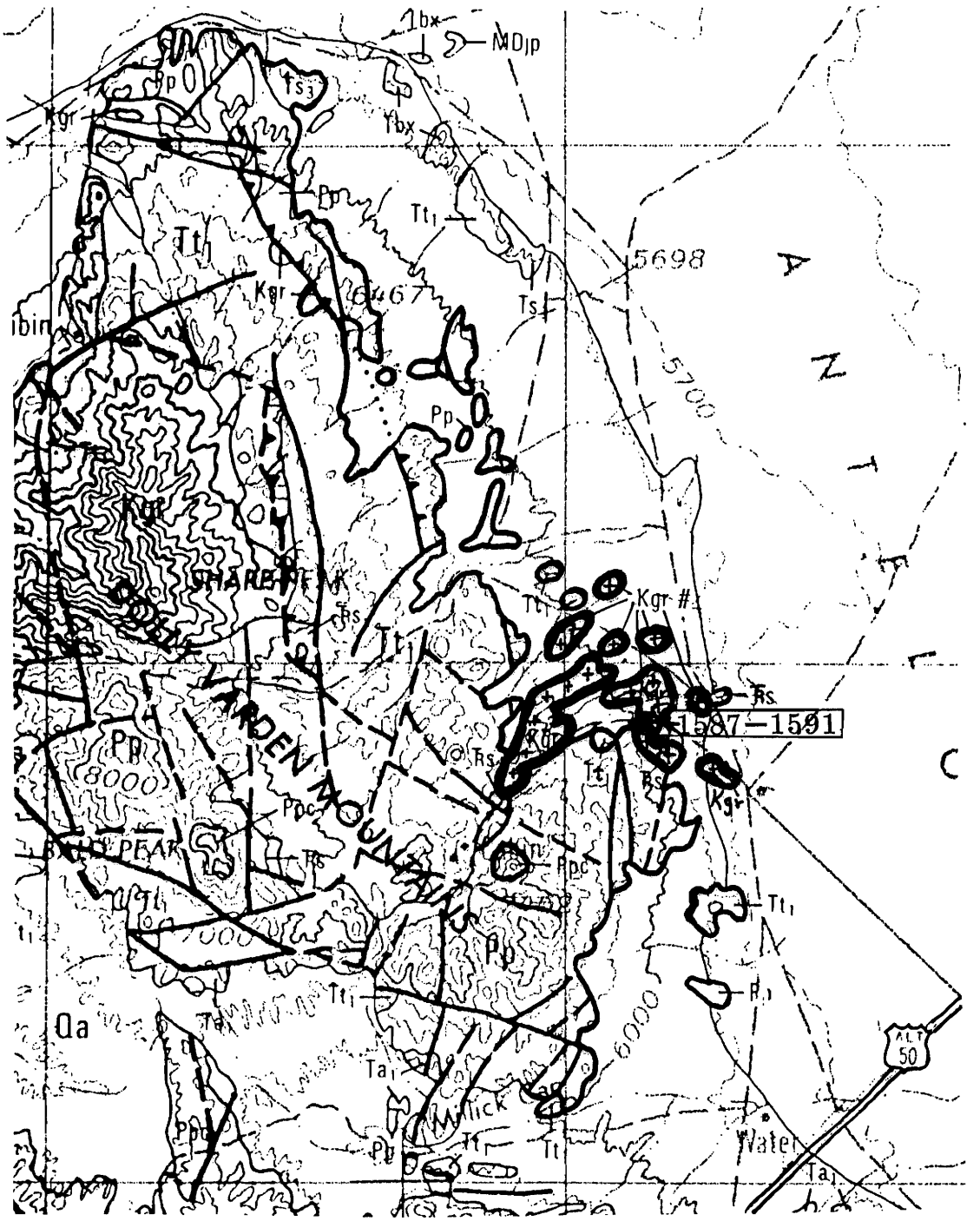

Figure 3-20. Map of the Kinsley mining district, Nevada, showing igneous rocks (Kgr = # = CIMVS) and sample locations (modified from Coats, 1987).

Whole rock analyses from samples collected by MagmaChem Exploration (Appendix A) are plotted in Figure 3-21. One of the samples did not pass the alteration filters, but the two remaining samples categorize the district as metaluminous, alkali-calcic, and weakly oxidized.

Linka, NV

The Linka district or Spencer Hot Springs area is in the northeast end of Big Smoky Valley about 32 km (20 miles) southeast of Austin, Lander County, Nevada; it was primarily known for its tungsten production, though silver, copper and molybdenum were also present (Stewart and others, 1977). The mine is also known by alternate names Garnetite, Spruce Mountain, and Toiyabe claims; it is a replacement or shear zone type of deposit caused by contact metasomatism and hydrothermal activity (Lowe and others, 1985). On the geologic map (Figure 3-22) Jurassic granitic rocks (Jg), more specifically biotite quartz monzonite to granodiorite, occur adjacent to the Linka mine and are probably the CIMVS. Similar Jurassic rocks 16 km (10 miles) north of the quadrangle were dated at 168 Ma by K-Ar (McKee, 1968). An age date of 161 Ma is associated with the Linka mine (Stewart and McKee, 1977, p. 31).

Whole rock analyses used for this study were from MagmaChem Exploration samples (Figure 3-22 and Appendix A). Two of the samples were altered and didn't pass the LOI (loss on ignition) alteration filter; the other two samples are

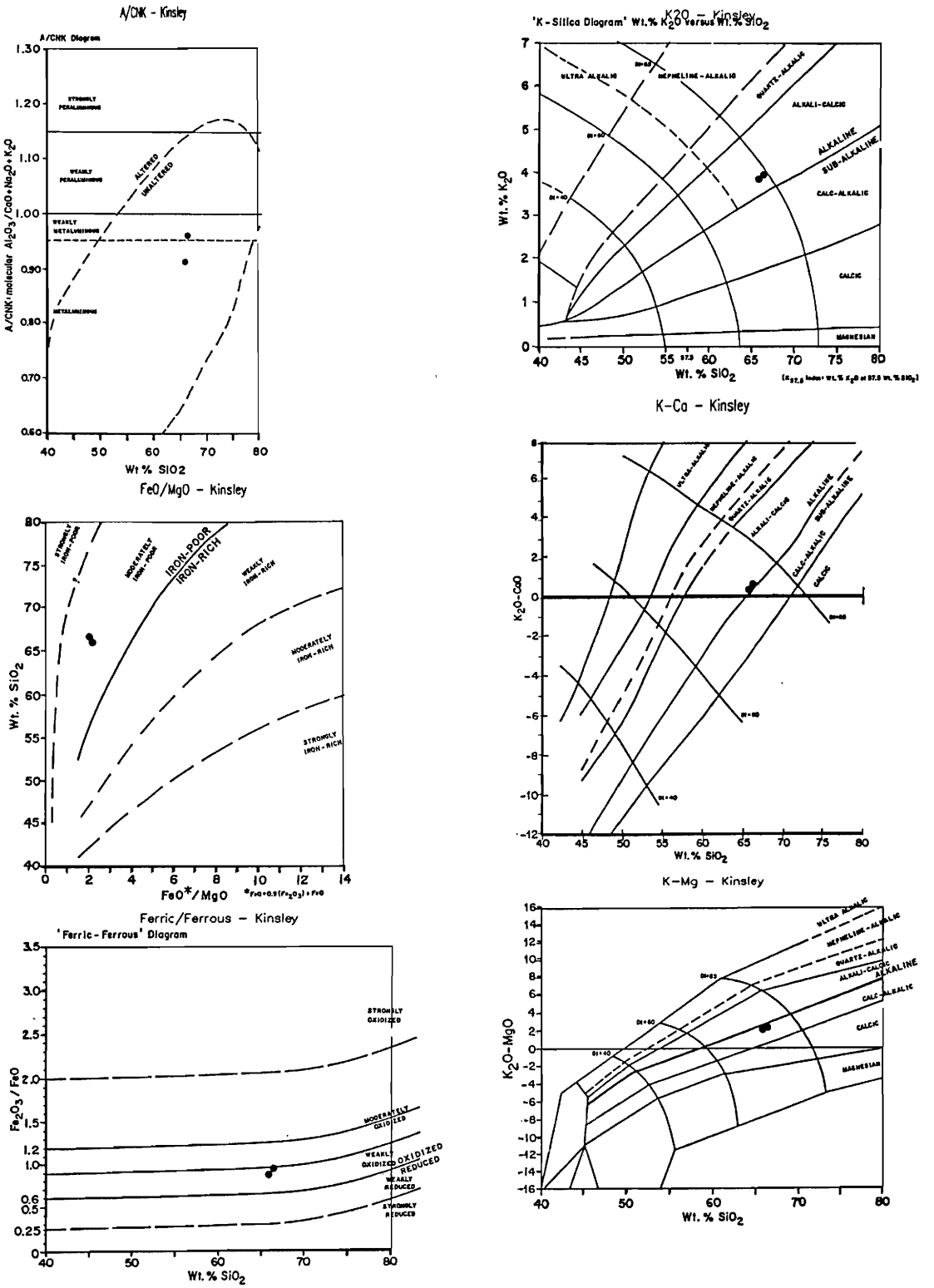

Figure 3-21. Petrochemical variation diagrams of igneous rocks from Kinsley, Nevada, showing A/CNK, iron ratios, and alkalinity.

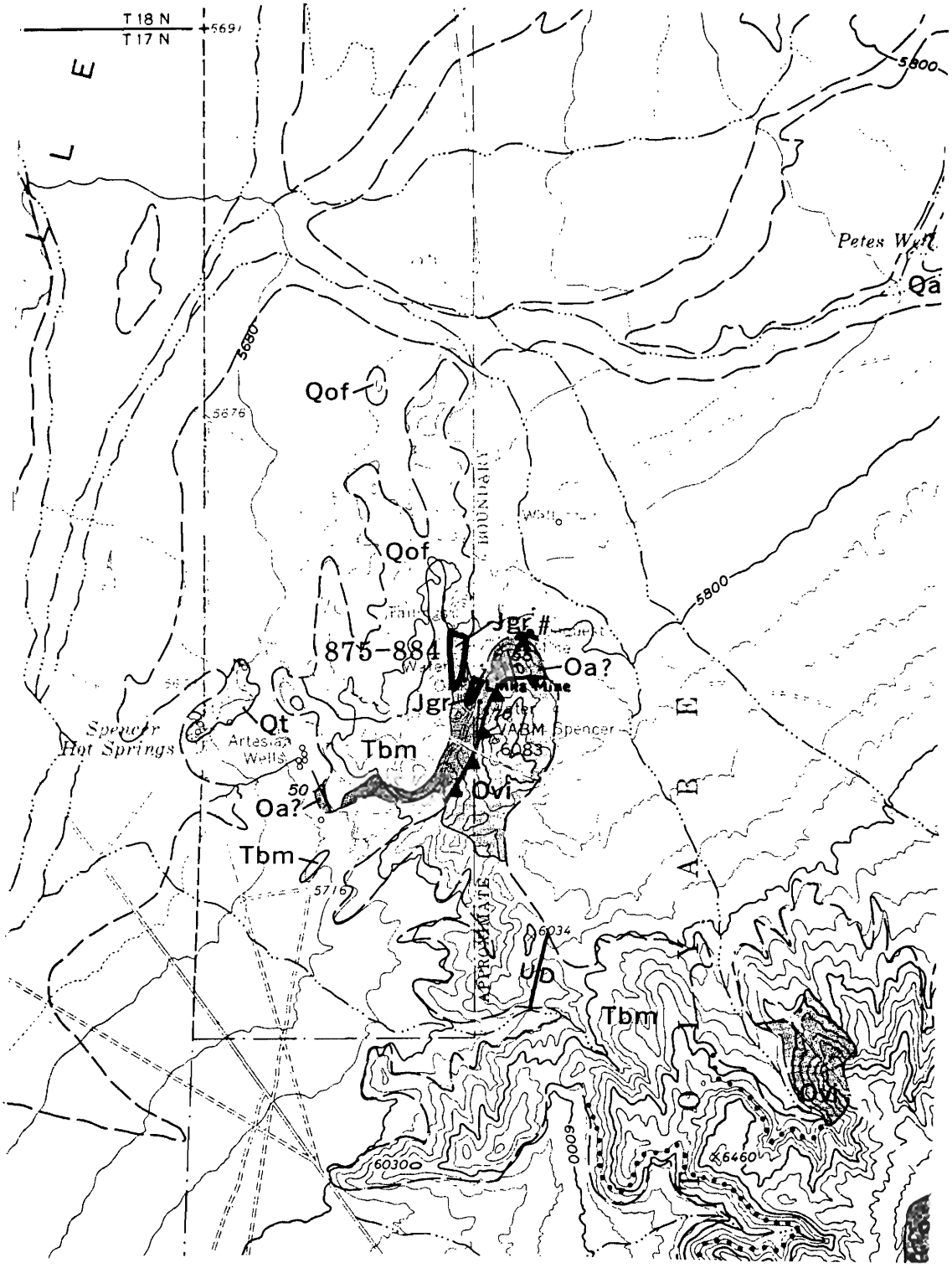

Figure 3-22. Geologic map of the Linka district, Nevada, showing igneous rocks (Jgr = # = CIMVS) and sample locations (modified from McKee, 1968).

in the metaluminous, alkali-calcic, weakly oxidized, and moderately iron-poor fields (Figure 3-23).

Railroad, NV

The Railroad mines are at Bullion on Bunker Hill in the Inskip or Pinyon Range in southwestern Elko County about 40 km (25 miles) southwest of Elko, Nevada. The lead-silver-copper orebodies are replacement deposits in Ordovician limestone where it has been intruded by granodiorite and quartz porphyry (Lincoln, 1923).

The intrusive stock (CIMVS) in the Railroad mining district (Gr and Qtz P in Figure 3-24) has an outer shell of medium-grained granite, quartz monzonite, monzonite, and quartz diorite; the core is essentially rhyolite porphyry (Smith and Ketner, 1976). Age dates from this stock include K-Ar ages of 35.4 $\pm$ 1.1 Ma on feldspar and 36.8 $\pm$1.1 Ma on biotite from the granitic outer shell (Marvin and others, in Coats, 1987), 35.5 $\pm$ 0.7 Ma on biotite from the biotite adamellite, 36 $\pm$ 1.4 Ma on the whole-rock rhyolite porphyry (Armstrong, in Coats, 1987), and 33 $\pm$ 3 Ma on biotite from the Railroad district quartz monzonite stock (Armstrong, 1964, p. 164). Granodiorite from the district yields a date of 37-41 Ma (Gillerman, 1984); ash flow tuffs in the nearby Indian Well Formation also range from 33.2 to 37.6 Ma (McKee and others, 1971; Smith and Ketner, 1976).

Whole rock analyses used in this study (Appendix B) come from Ketner and Smith (1976). Several of the samples failed the alteration filters (Figure 3-25)

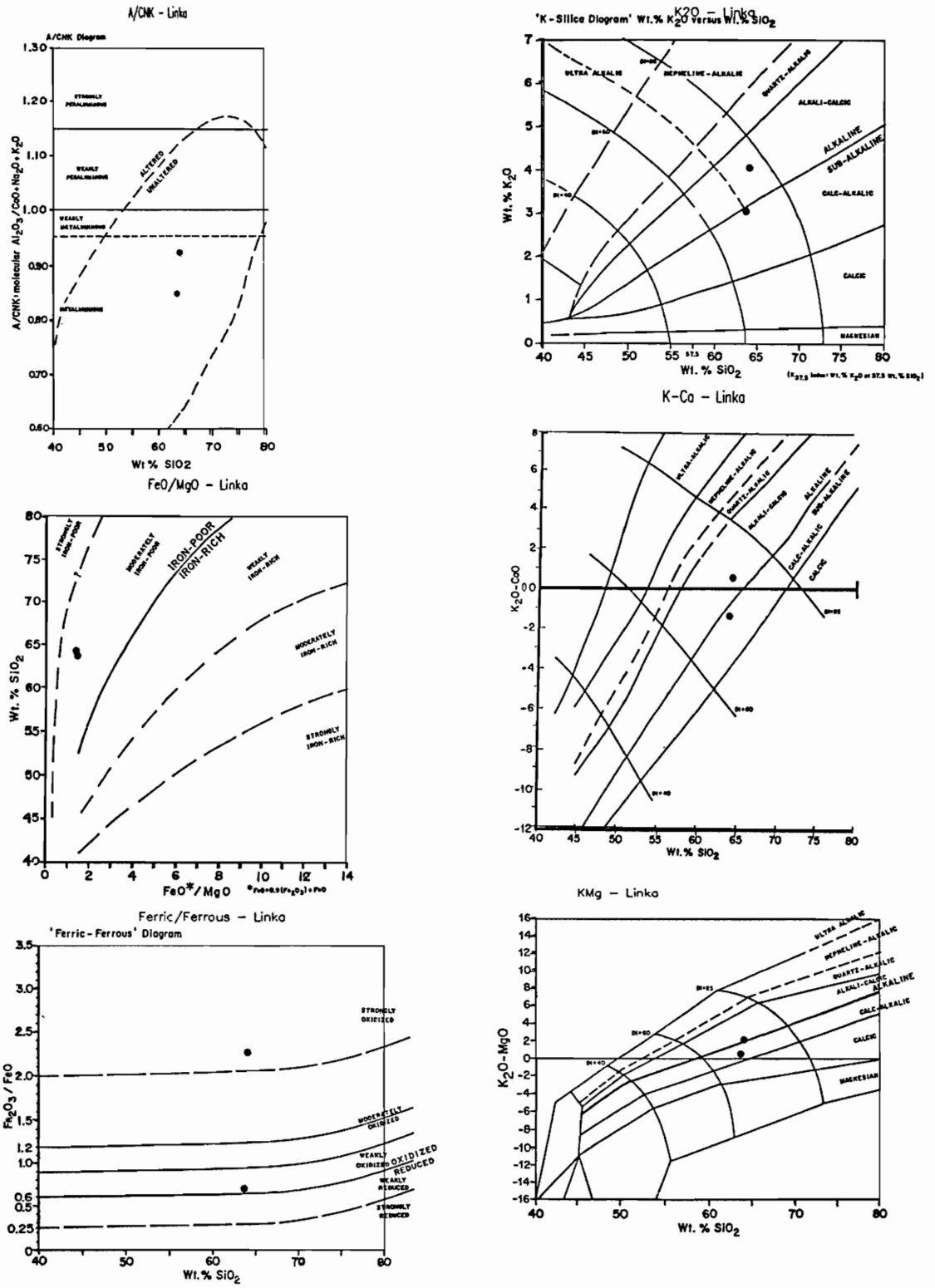

Figure 3-23. Petrochemical variation diagrams of igneous rocks from Linka, Nevada, showing A/CNK, iron ratios, and alkalinity.

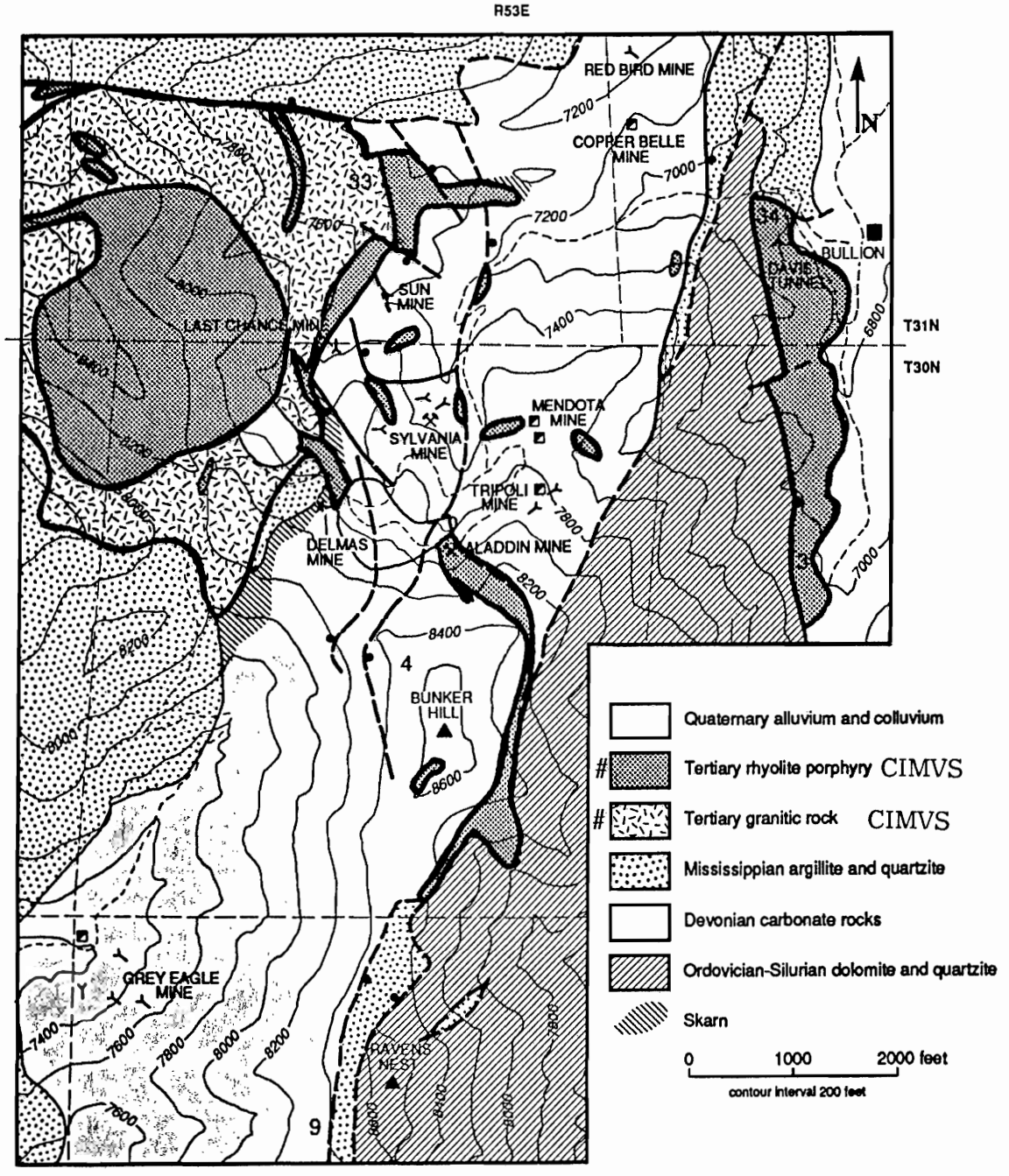

Figure 3-24. Geologic map of the Railroad district, Nevada (Tertiary granite and rhyolite porphyry = # = CIMVS) (from Lapointe and others, 1991).

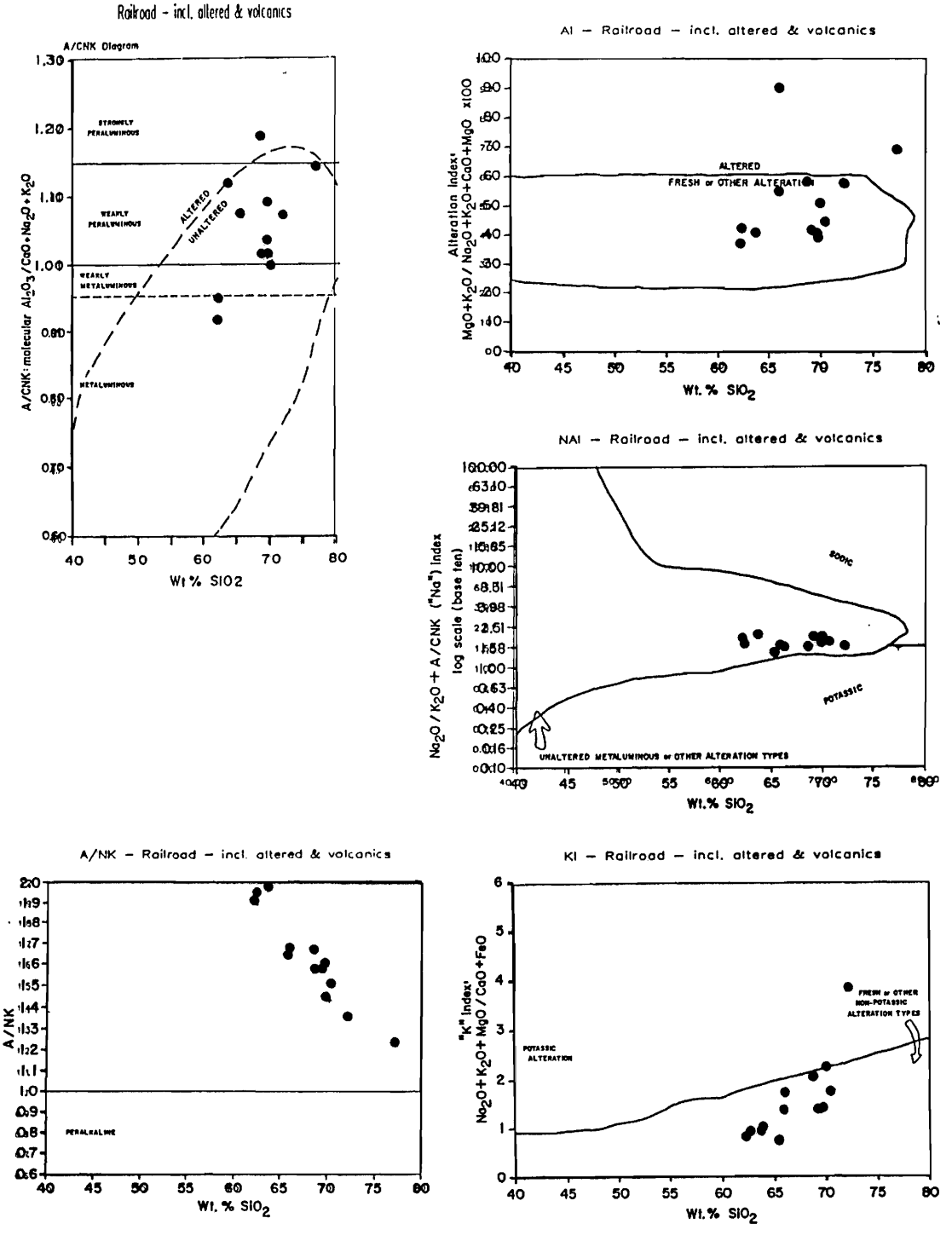

Figure 3-25. Petrochemical variation diagrams of igneous rocks from the Railroad mining district, Nevada, showing alteration filters.

and were excluded, as were the volcanics. However, most of the altered samples also fall in the metaluminous, alkali-calcic fields (Figure 3-26) and are moderately iron-poor and weakly oxidized (Figure 3-27).

Santa Eulalia, MEXICO

Santa Eulalia is in central Chihuahua, Mexico, about 25 km (15 miles) southeast of Chihuahua City. The principal production was lead-silver with tin, vanadium, and zinc, as well as by-product copper and gold (Hewitt,1943). The limestone replacement (mantos and chimneys) mineralization is temporally and spatially related to felsite dikes and sills (Figure 3-28) and the metals probably came from the felsite parent magma (CIMVS) (Megaw, 1990). The felsite was dated at 26.6 $\pm$ 0.6 and 37.5 $\pm$ 0.2 (Clark and others, 1979) and the quartz monzonite intrusion encountered in deep drill holes was dated at 37.8 $\pm$ 0.9 (Megaw, 1990).

Whole rock data on the felsites and quartz monzonite were obtained by Megaw (1990) for MagmaChem Exploration (Appendix B). Most of the data failed the alteration filters (Figure 3-29), although they are still clearly in the metaluminous, alkali-calcic, and moderately iron-poor fields on the petrochemical variation diagrams (Figure 3-30). The encircled dot indicates the one sample that passed the alteration filters.

The felsites are clearly associated with major sulfide mineralization that is typical of magnetite-series granitoids, yet they contain associated cassiterite and

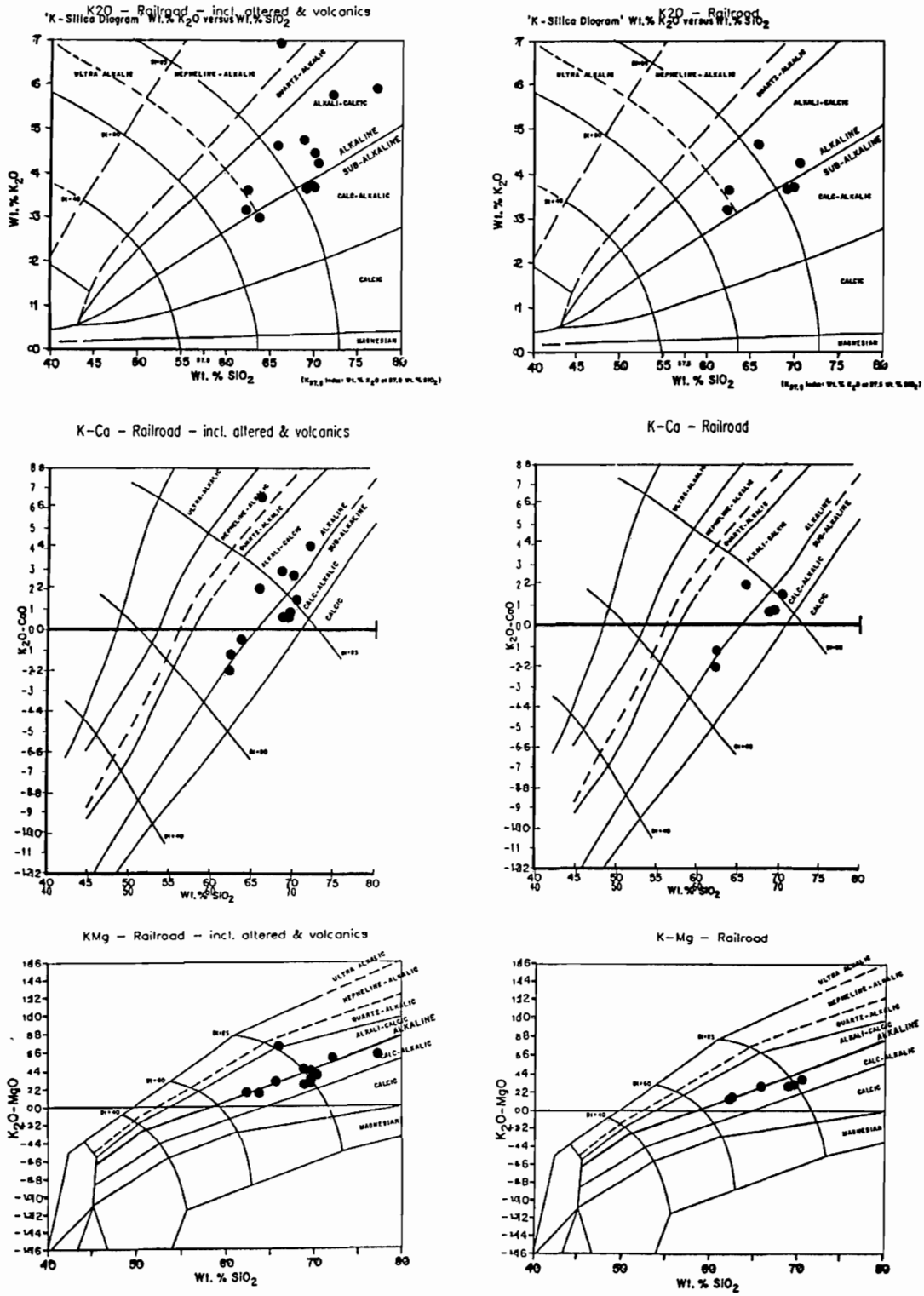
K2O – Railroad – incl. altered & volcanics
'K-Silica Diagram' Wt.% K2O versus Wt.% SiO2
K2O – Railroad
'K-Silica Diagram' Wt.% K2O versus Wt.% SiO2
ULTRA ALKALIC
PERALKALIC
PERALK.
PERALK
PERALK
PERALK

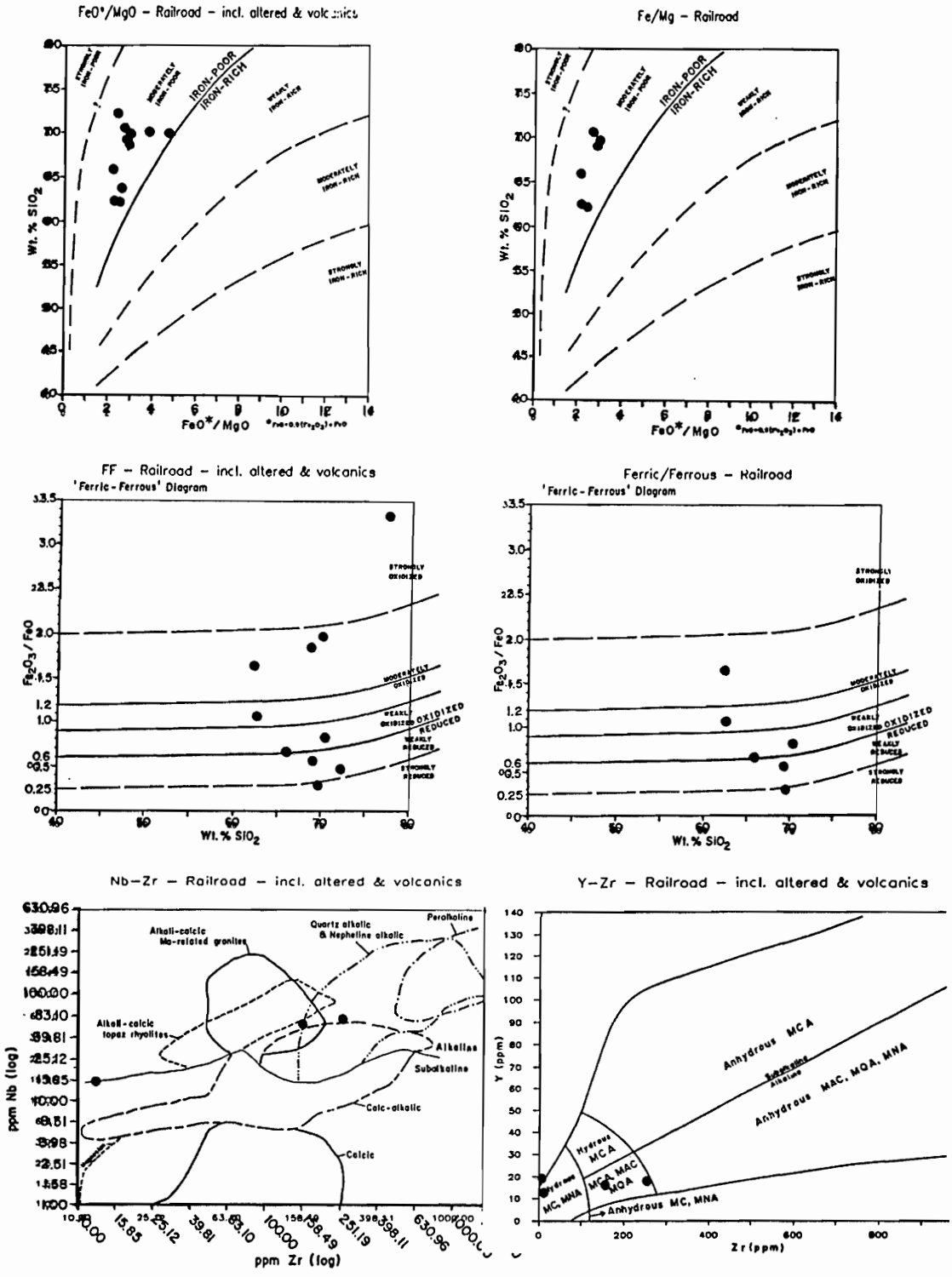

Figure 3-27. Petrochemical diagrams of igneous rocks from Railroad, Nevada, showing iron ratios (left includes altered, right = unaltered only).

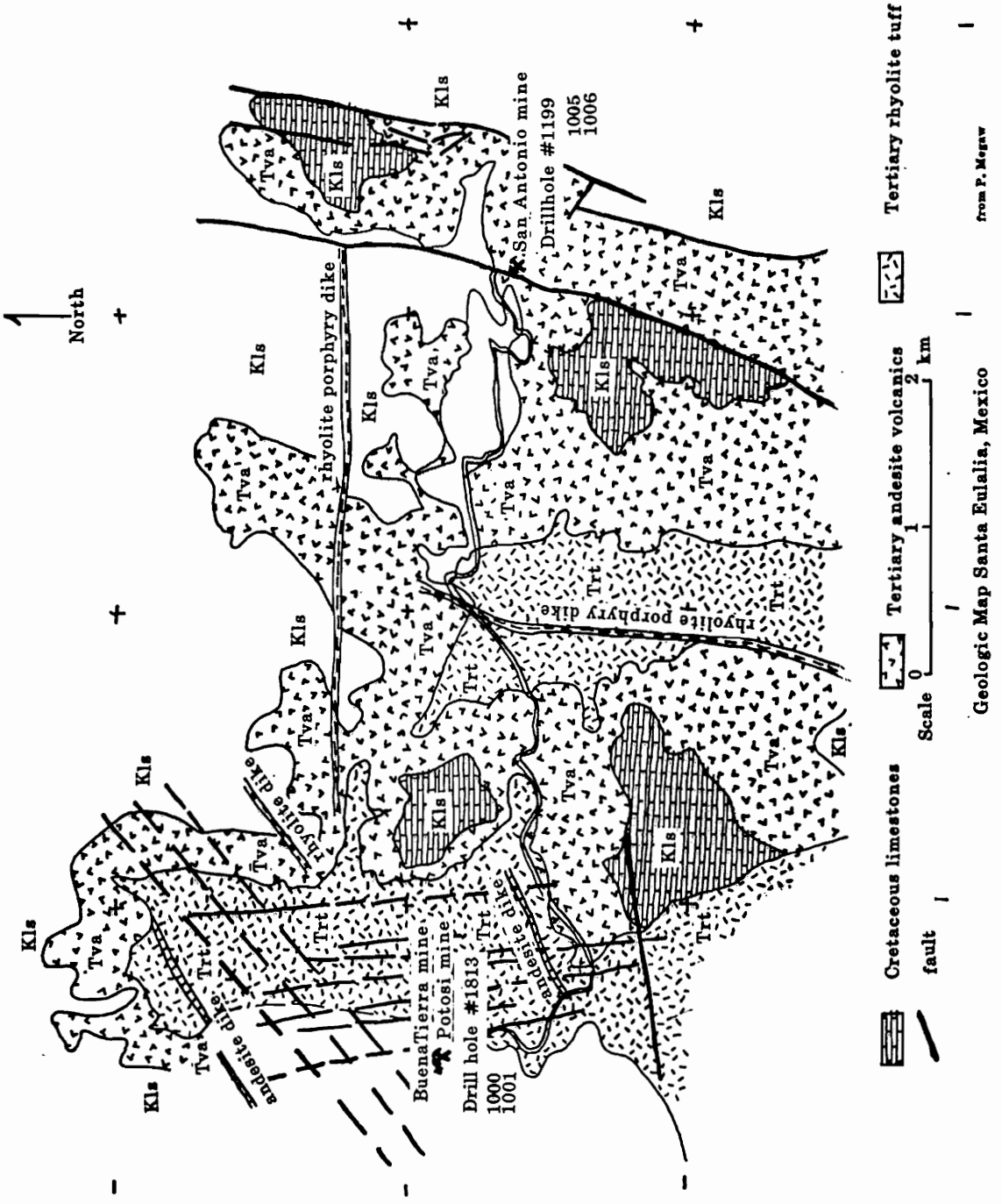

Figure 3-28. Geologic map of Santa Eulalia, Mexico, showing igneous rocks (felsites = CIMVS) and sample locations (modified from Megaw, 1990).

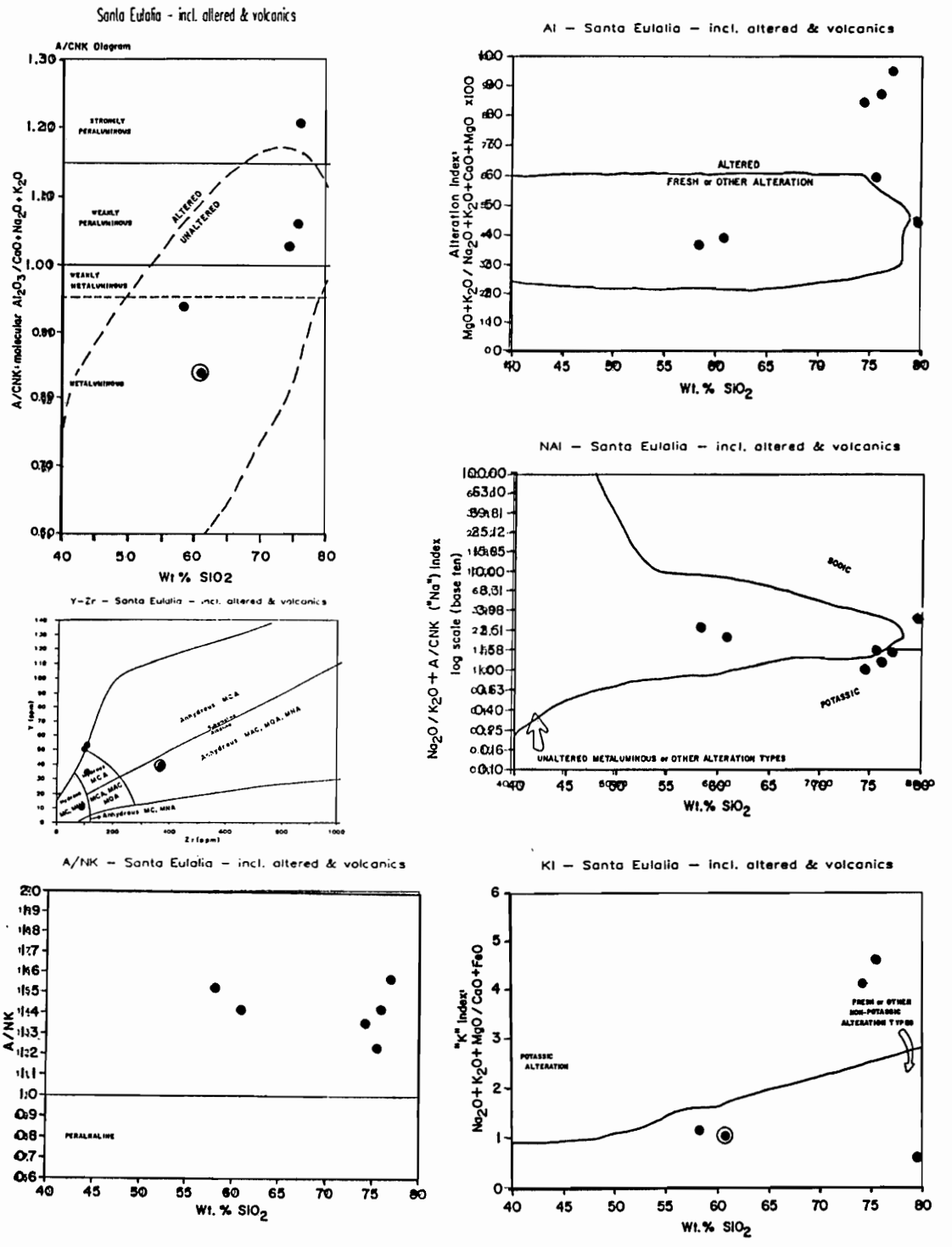

Figure 3-29. Petrochemical variation diagrams of igneous rocks from Santa Eulalia, Mexico, showing alteration filters.

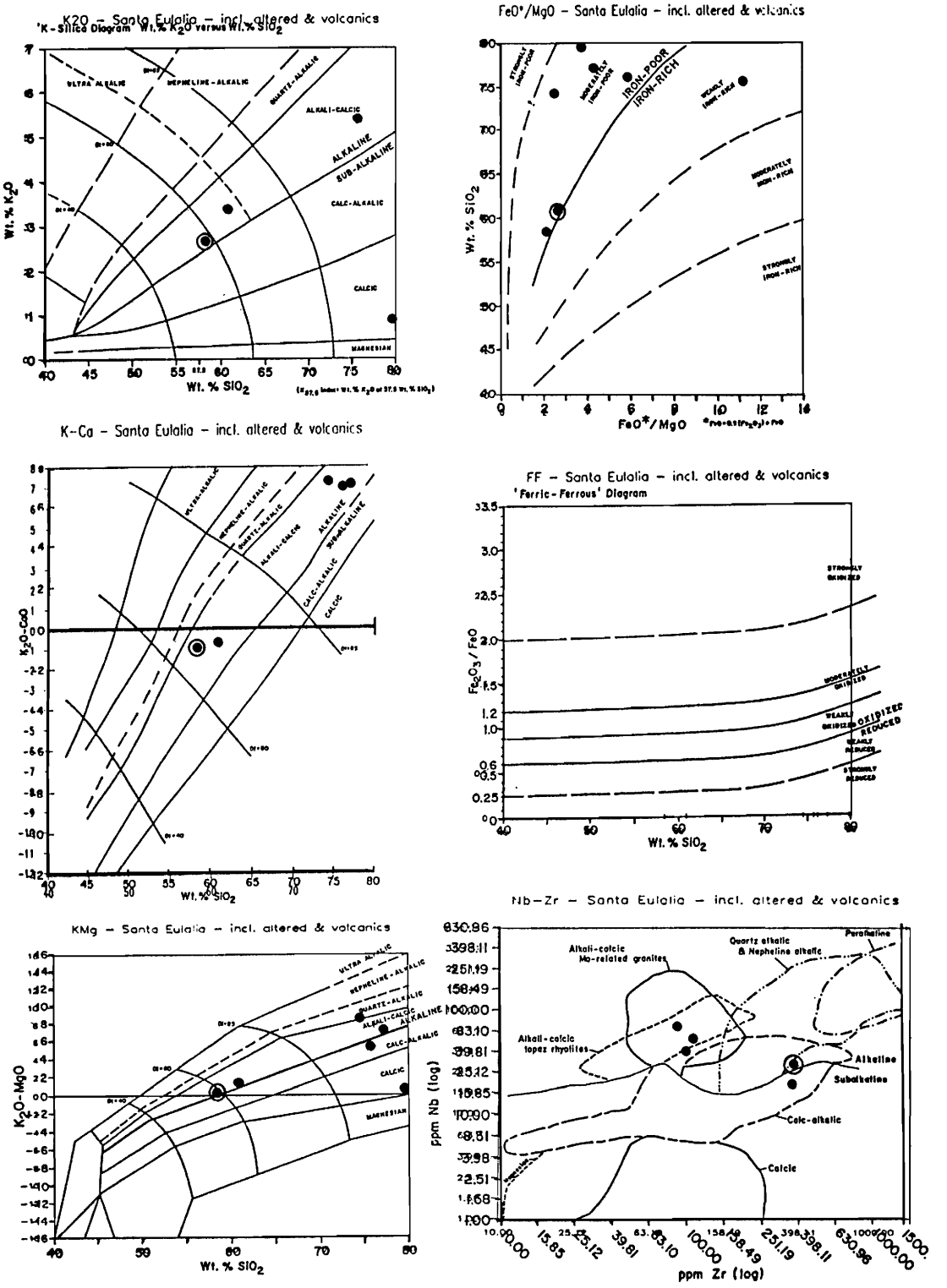

Figure 3-30. Magma series variation diagrams of igneous rocks from Santa Eulalia, Mexico, showing alkalinity and iron ratios (Circle = unaltered).

wolframite typical of ilmenite-series; thus the composition of the felsite is intermediate between ilmenite- and magnetite-series (Megaw, 1990). This is equivalent to the weakly oxidized class as determined by the ferric/ferrous ratio.

Swales Mountain, NV

Most of the mines are on the east slope of Swales Mountain, the southern peak of the Independence Mountains, about 25 km (15 miles) north of Carlin, Nevada. Mines and prospects are in limestone adjacent to the eastern and southern margin of a north-south trending monzonite porphyry stock (Stager and Tingley, 1988). The mineralization is generally concentrated at the contact of the porphyry (Ti on Figure 3-31 = CIMVS) with upper plate chert. A stock of monzonite porphyry forms the south end of Swales Mountain and a thick dike of monzonite extends northward; quartz porphyry also occurs in the district (Ketner and others, 1968).

The Swales Mountain pluton, which includes phases of biotite-quartz monzonite porphyry and biotite-hornblende monzonite porphyry, ranges in composition from quartz monzonite to diorite (Evans and Ketner, 1971). The biotite granodiorite porphyry from the east face of Swales Mountain gave a lead-alpha age on zircon of 40 $\pm$ 10 Ma (Coats and others, 1965) and a K-Ar age on potassium feldspar of 38.7 $\pm$ 1.3 Ma and on biotite of 38 $\pm$ 1.3 Ma (Marvin in Evans and Ketner, 1971).

Two whole rock analyses were obtained on samples collected from Swales

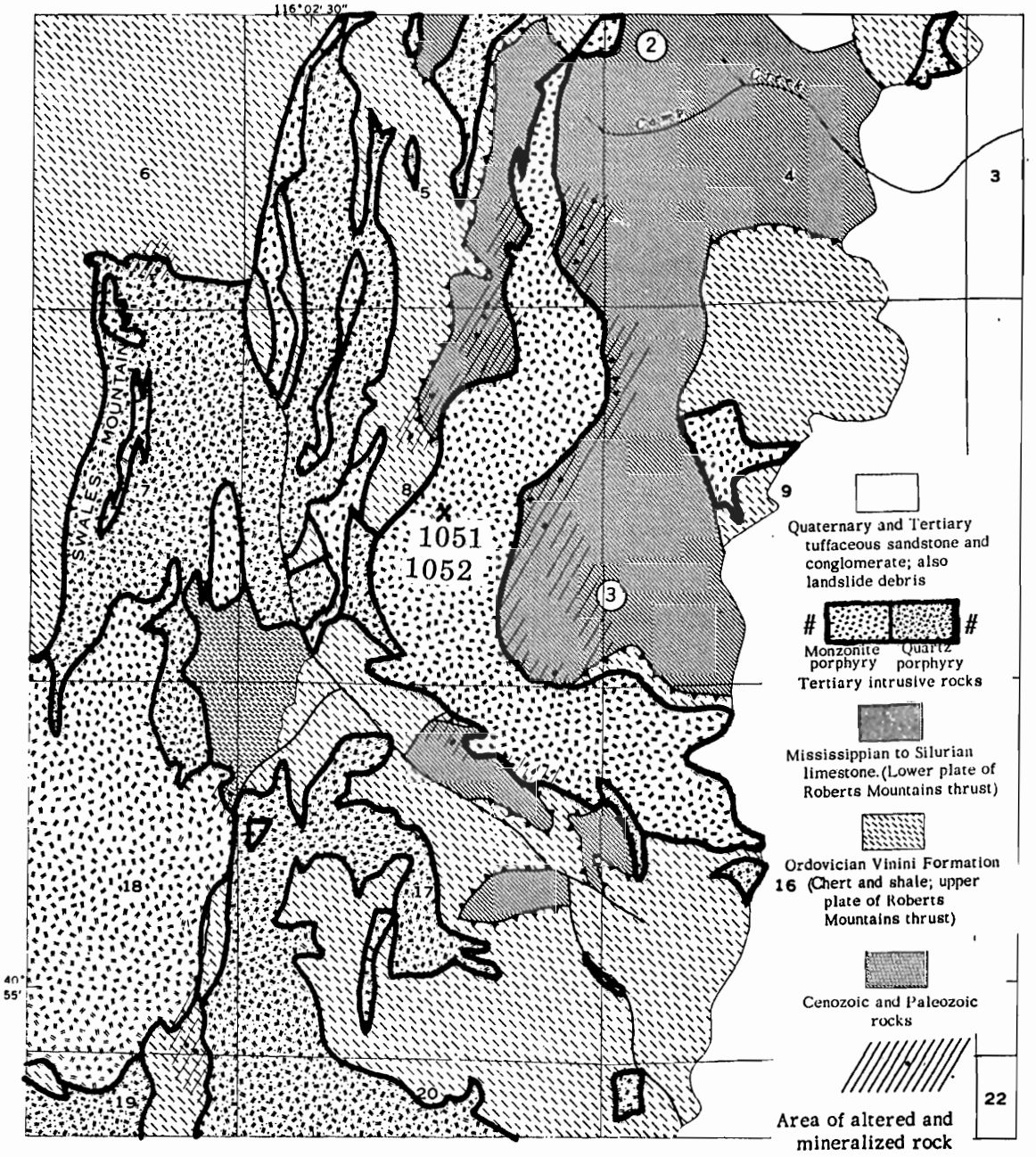

Geologic map of part of the Swales Mountain quadrangle, T. 35 N., R. 53 E., Nevada.

Figure 3-31. Geologic map of the Swales Mountain area, Nevada (Ti = Tertiary intrusive = # = CIMVS) (modified from Ketner and others, 1968).

Mountain (Appendix A). Both samples passed the petrochemical alteration filters (Figure 3-32); they are in the metaluminous, alkali-calcic, moderately iron-poor, and weakly oxidized fields (Figure 3-33).

Taylor, NV

The Taylor district is on the west slope of the Schell Creek Range about 25 km (15 miles) south of Ely in White Pine County, Nevada. Silver has been produced since 1875, along with considerable lead and minor copper, zinc, and gold; some antimony has also been produced from south of Taylor (Hose and others, 1976). The silver-lead ore bodies are localized in silicified limestone along the bedding in brecciated zones in jasperized Guilmette Limestone.

Many granophyric rhyolite porphyry dikes and sills (black lines on Figure 3-34 = CIMVS) of probable Tertiary age intrude the sedimentary rocks and are probably related to a granitic stock buried beneath the Taylor district (Lovering and Heyl, 1974). Samples of these dikes were collected by MagmaChem Exploration (Appendix A, B). All three samples failed the alteration filters (Figure 3-35), but the altered samples are in the alkali-calcic field (Figure 3-36) although the iron and A/CNK values are significantly affected. These samples were not included in the neural network study.

Tempiute, NV

The Tempiute (also called Tem Piute) district is near the north end of the

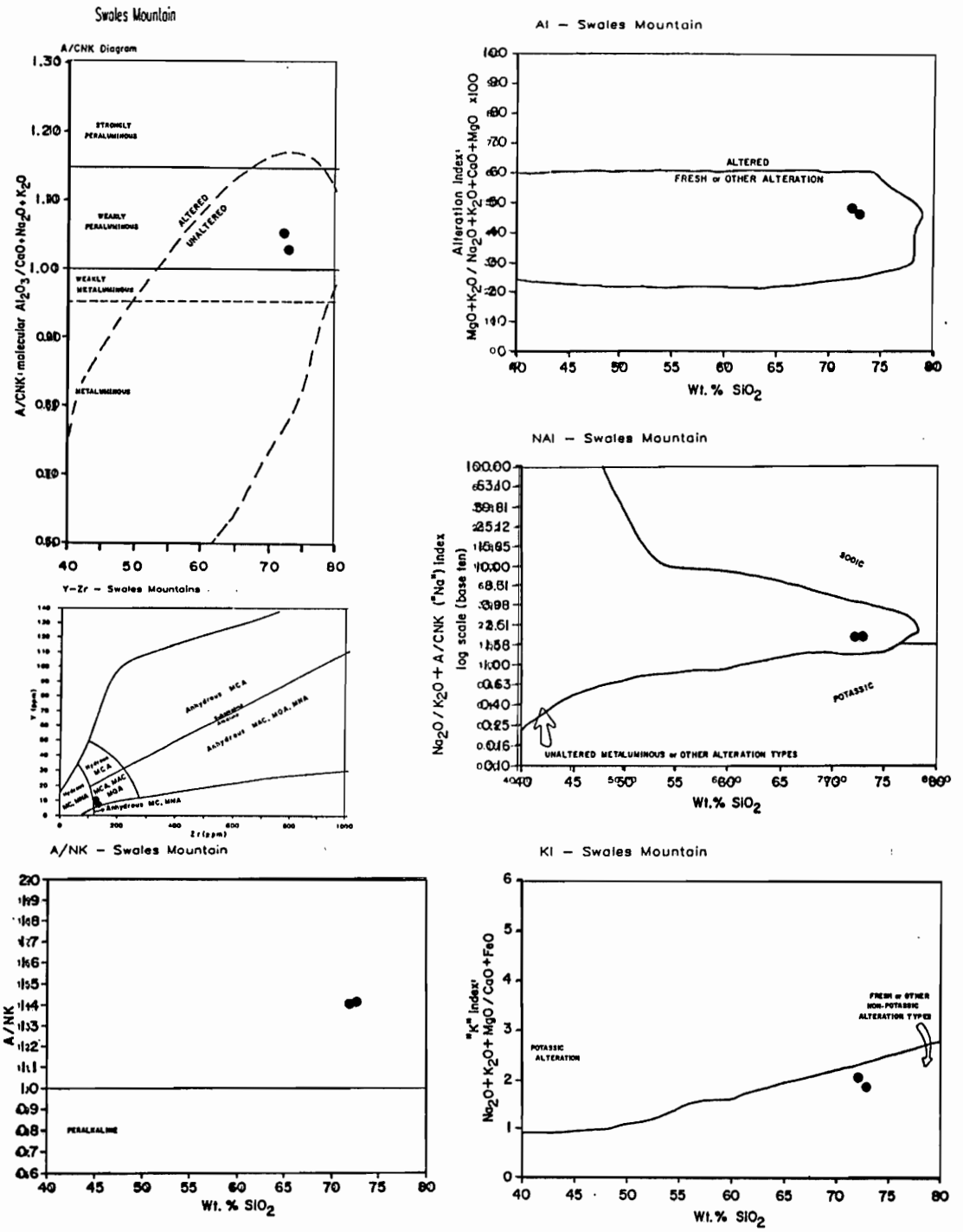

Figure 3-32. Petrochemical variation diagrams of igneous rocks from the Swales Mountain mining district, Nevada, showing alteration filters.

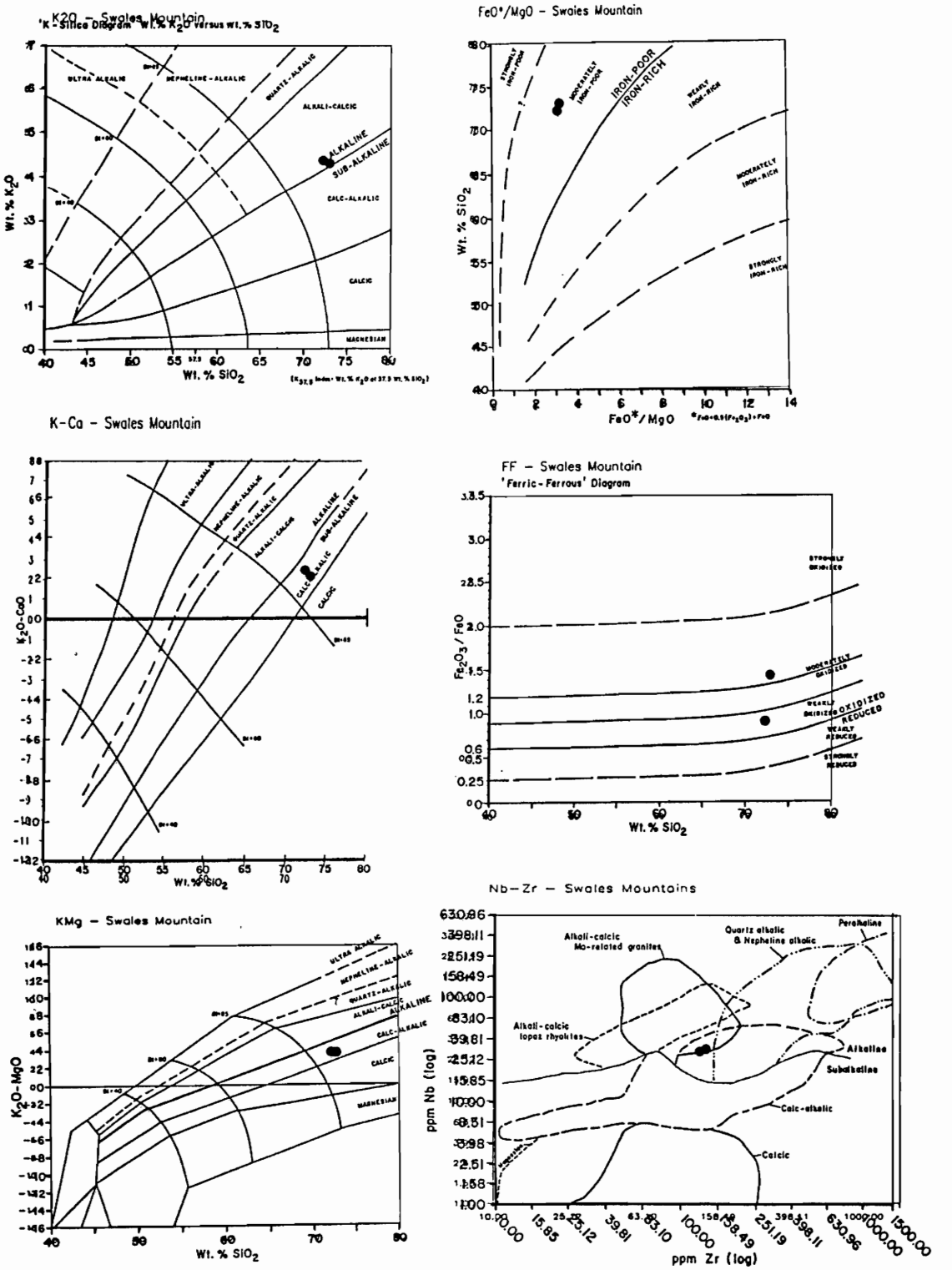

Figure 3-33. Magma series variation diagrams of igneous rocks from the Swales Mountain mining district, Nevada, showing alkalinity and iron ratios.

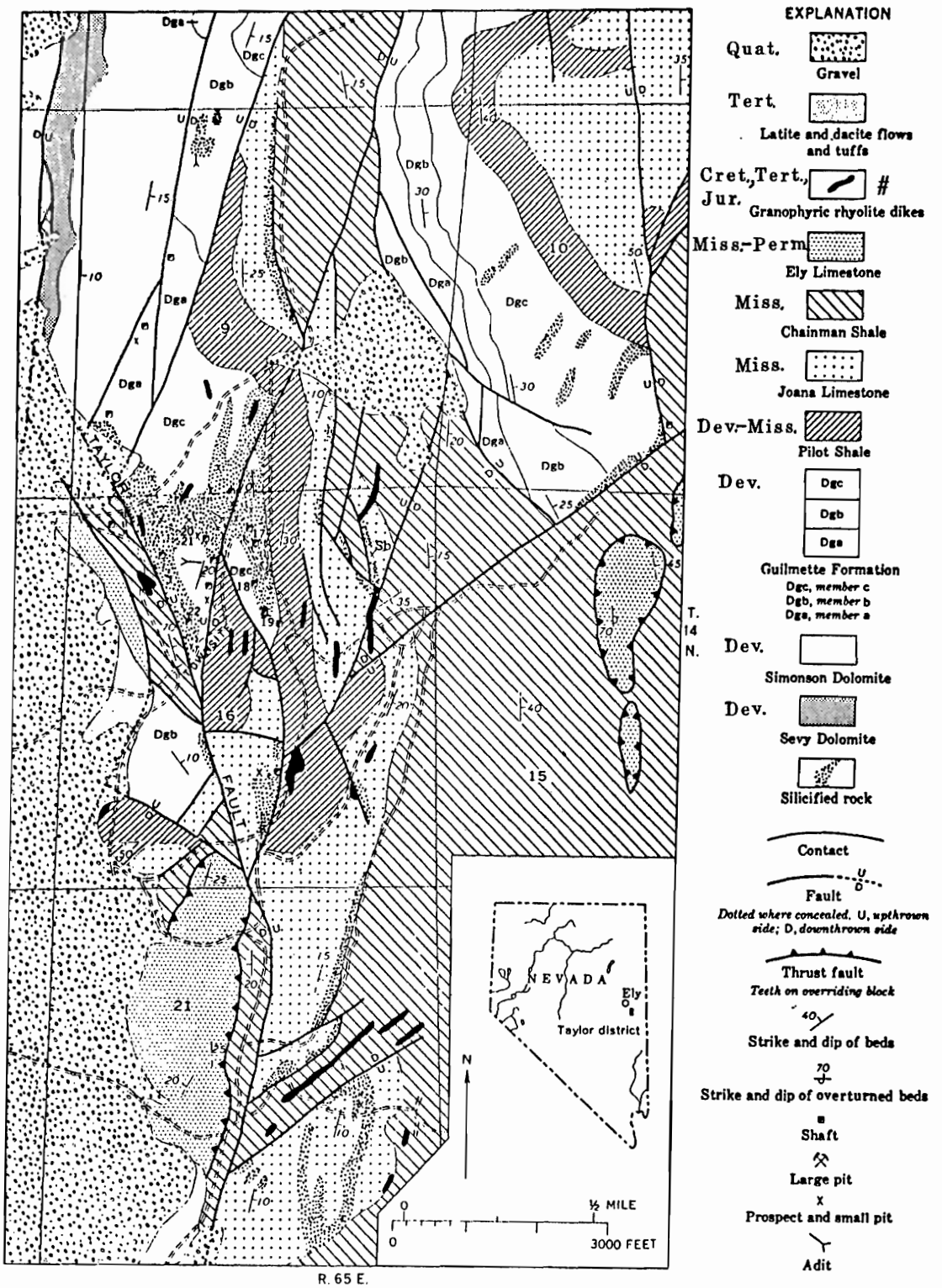

Figure 3-34. Geologic map of the Taylor district, Nevada, showing rhyolite dikes associated with mineralization (# = CIMVS) (modified from Drewes, 1969).

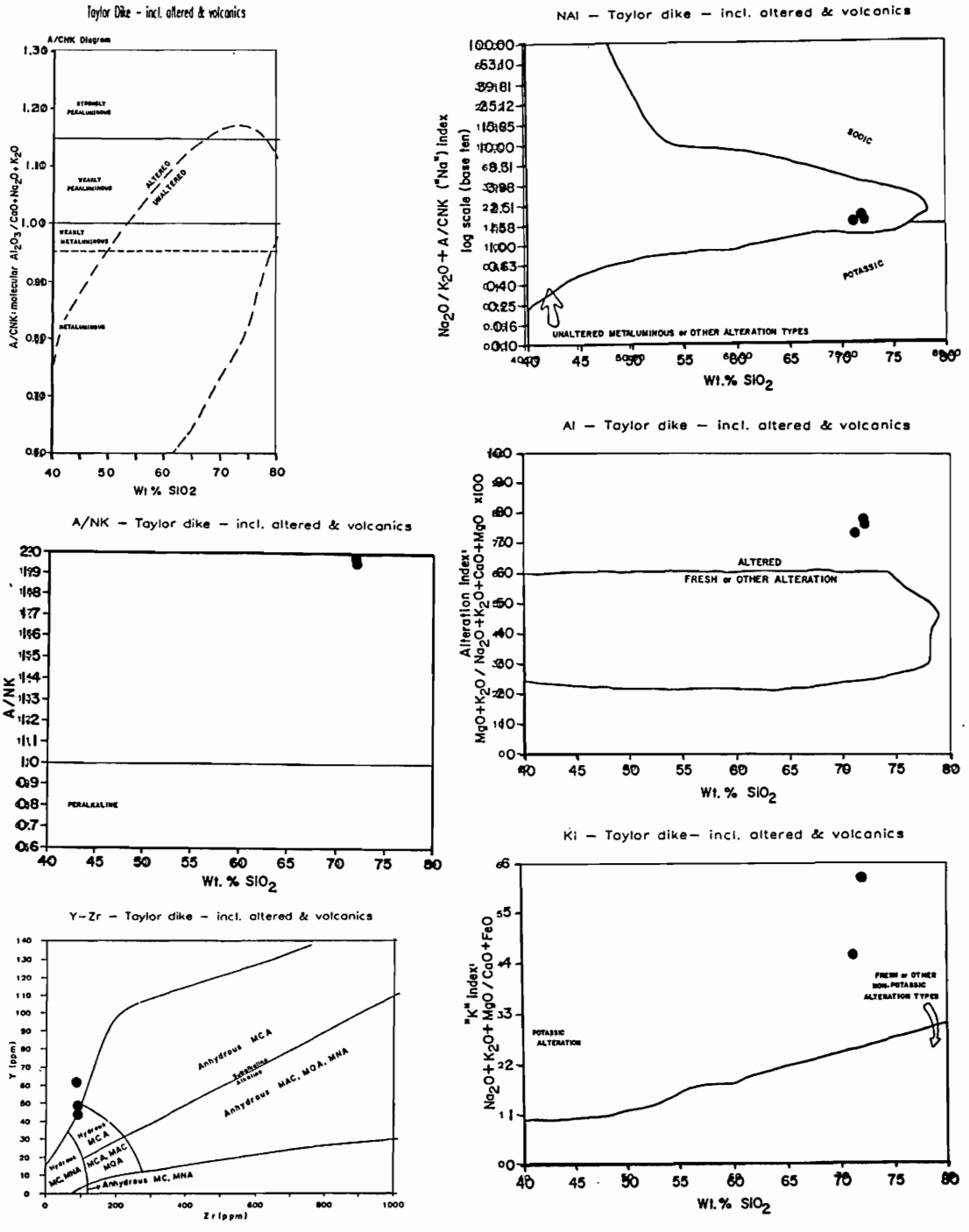

Figure 3-35. Petrochemical variation diagrams of igneous rocks from the Taylor district, Nevada, showing alteration filters.

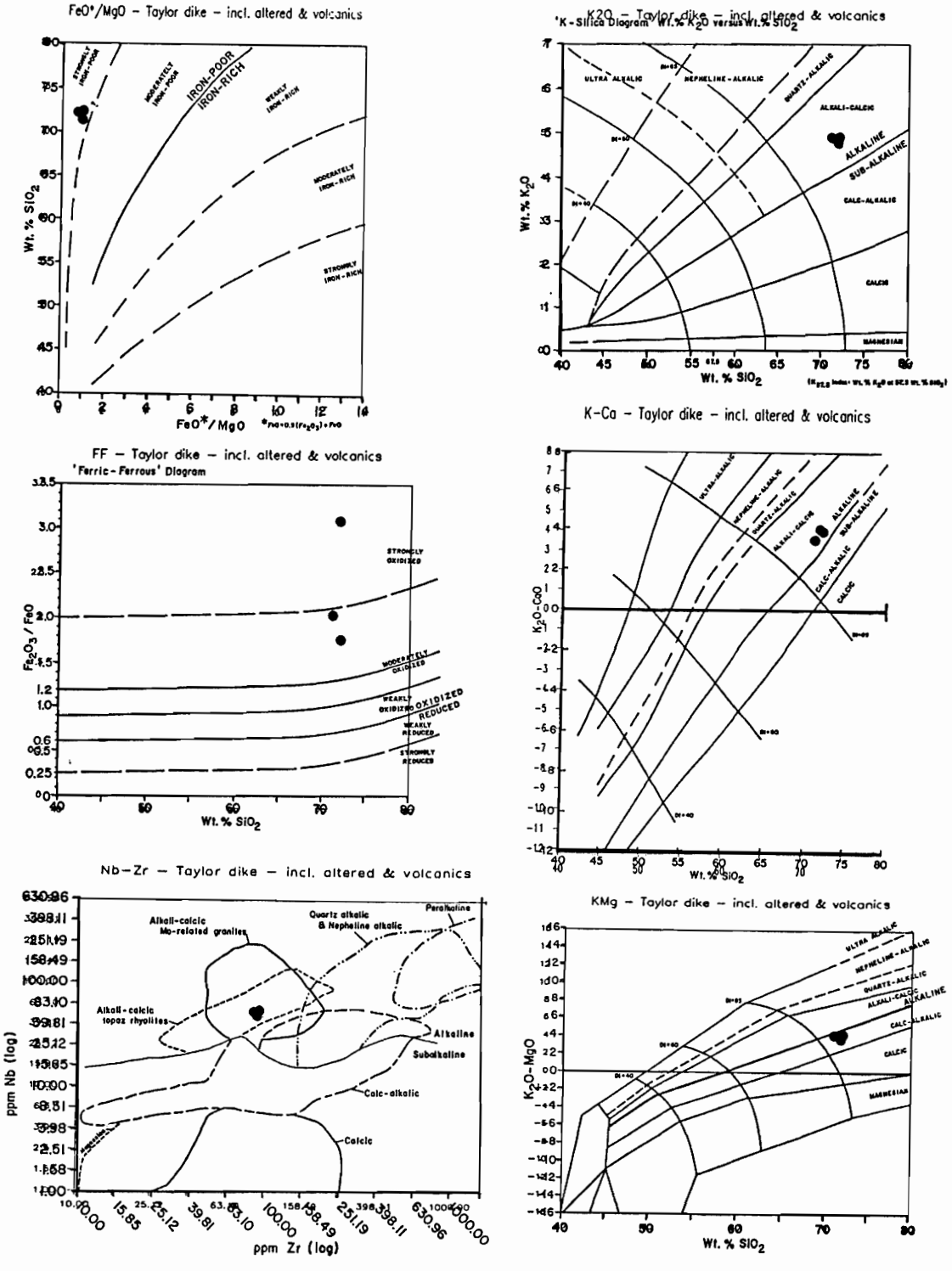

Figure 3-36. Magma series variation diagrams of igneous rocks from the Taylor district, Nevada, showing alkalinity and iron ratios.

Timpahute Mountains about 250 km (160 miles) north of Las Vegas in Lincoln County, Nevada. The silver-bearing brecciated quartz veins follow bedding plane faults in limestone and dolomite in the southwestern part of the district. The tungsten-bearing skarn zones formed in the contact zones of the intrusives in the north end of the range (Tingley, 1984). The silver deposits mined at old Tem Piute contained 13 to 81 ounces of silver per ton. These ores came from siliceous veins and replacement deposits along breccia zones in lower Paleozoic dolomites and in the Guilmette Formation (Tschanz and Pampeyan, 1970). Tungsten ores at Tem Piute occur in a zoned contact-metasomatic garnet-pyroxene skarn separating limestone and hornfels from quartz monzonite (Tg on Figure 3-37 is the CIMVS). Pyrrhotite, marcasite, magnetite and molybdenite and ilvaite occur close to the quartz monzonite; sphalerite, galena, and bismuth minerals occur closer to the limestone (Buseck, 1967).

Whole rock analyses from Tem Piute intrusives were obtained from Lee (1984). The Tem Piute quartz monzonite stocks have been dated at 88 to 95 Ma by the K-Ar method on biotite. The samples are in the metaluminous field and pass all the alteration filters (Figure 3-38); they are in the alkali-calcic field on the alkalinity variation diagrams (Figure 3-39). The samples appear to be more oxidized on the ferric/ferrous diagram (Figure 3-39) than would be expected from the presence of pyrrhotite, which is an indicator of more reduced conditions. Because of this combination of oxidized and reduced features, the district is placed in the weakly oxidized category.

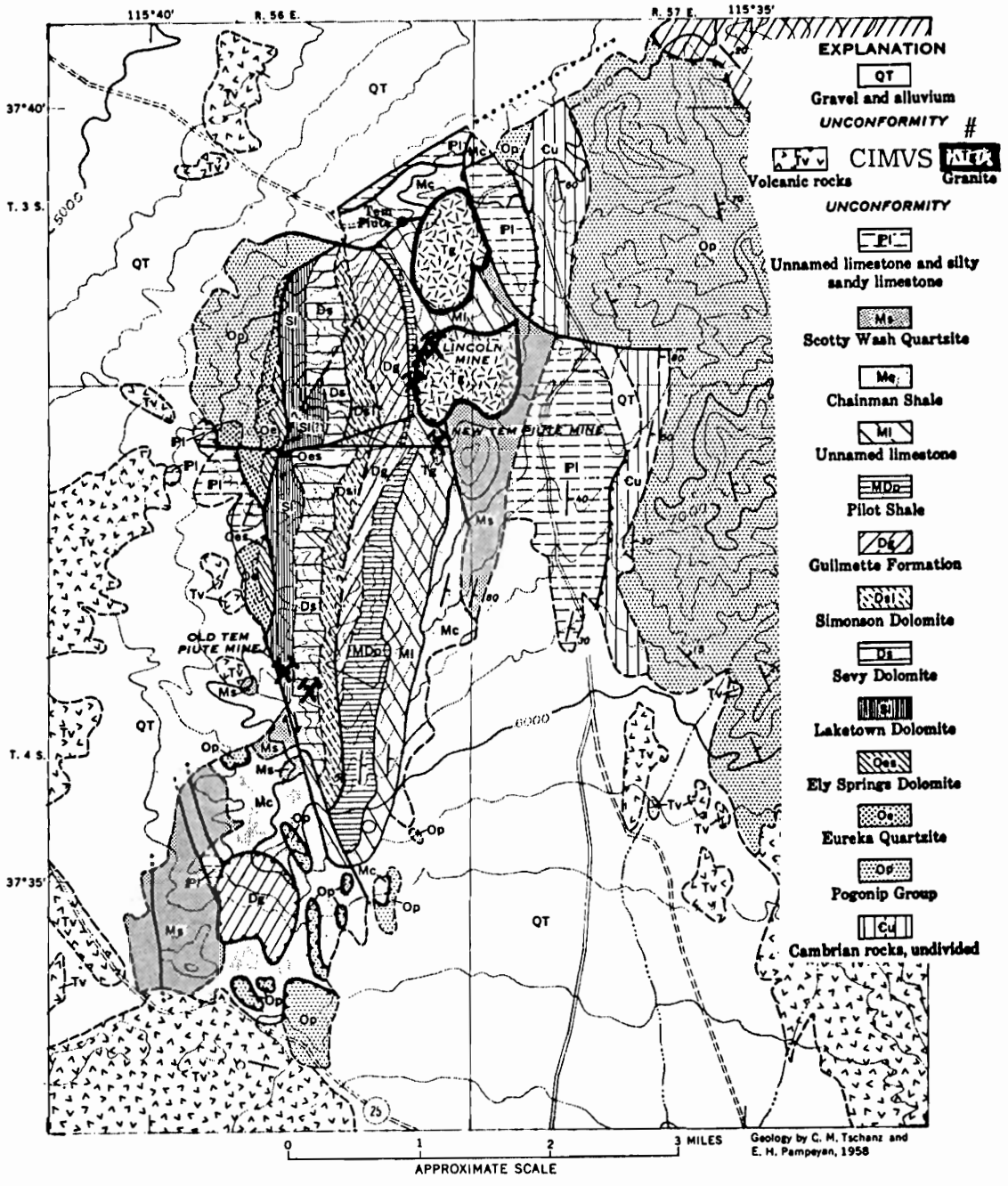

Figure 3-37. Geologic map of the Tempiute district, Nevada, showing igneous rocks (Tg = # = CIMVS) (modified from Tschanz and Pampeyan, 1970).

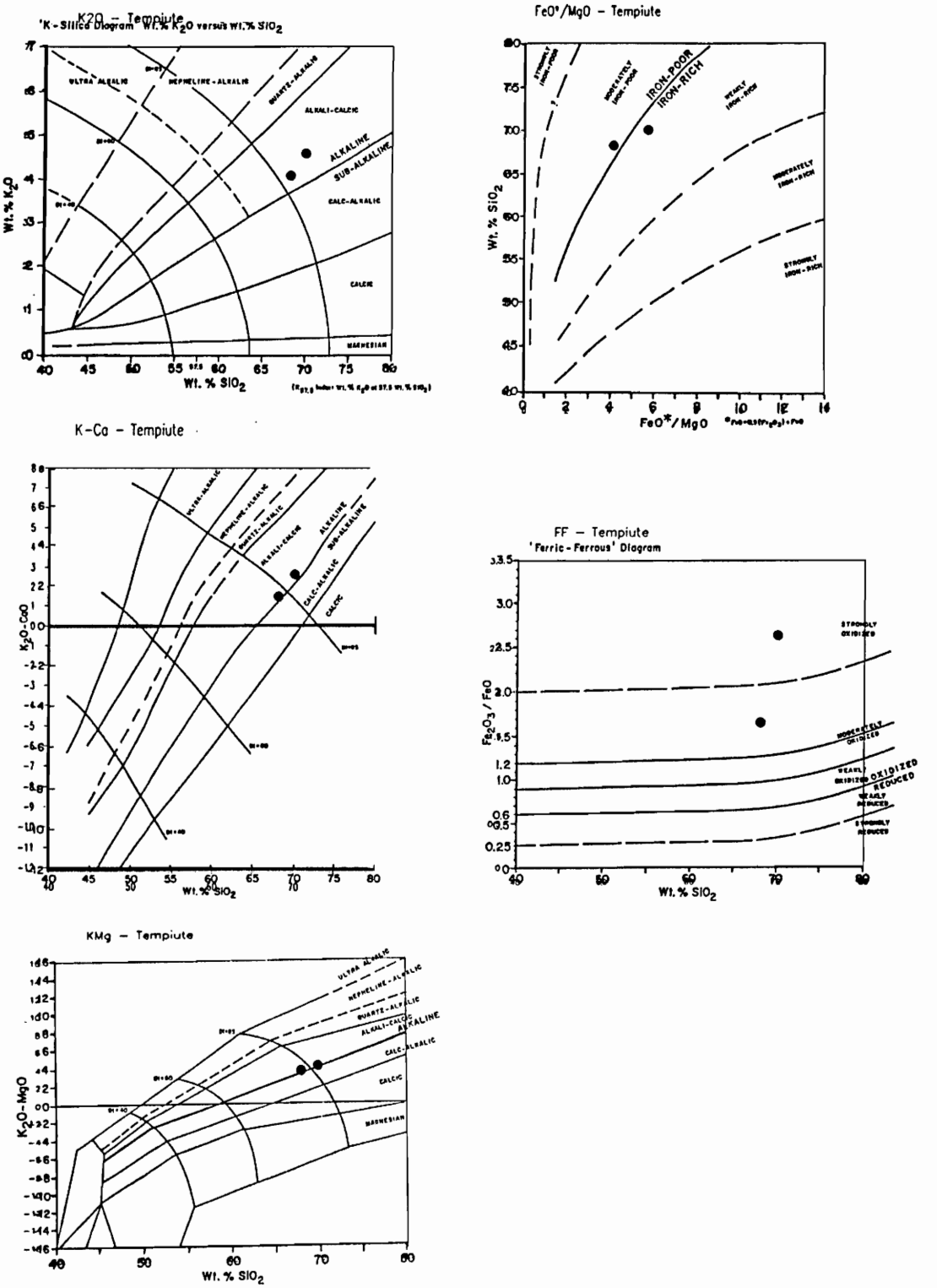

Figure 3-39. Magma series variation diagrams of igneous rocks from the Tempiute mining district, Nevada, showing alkalinity and iron ratios.

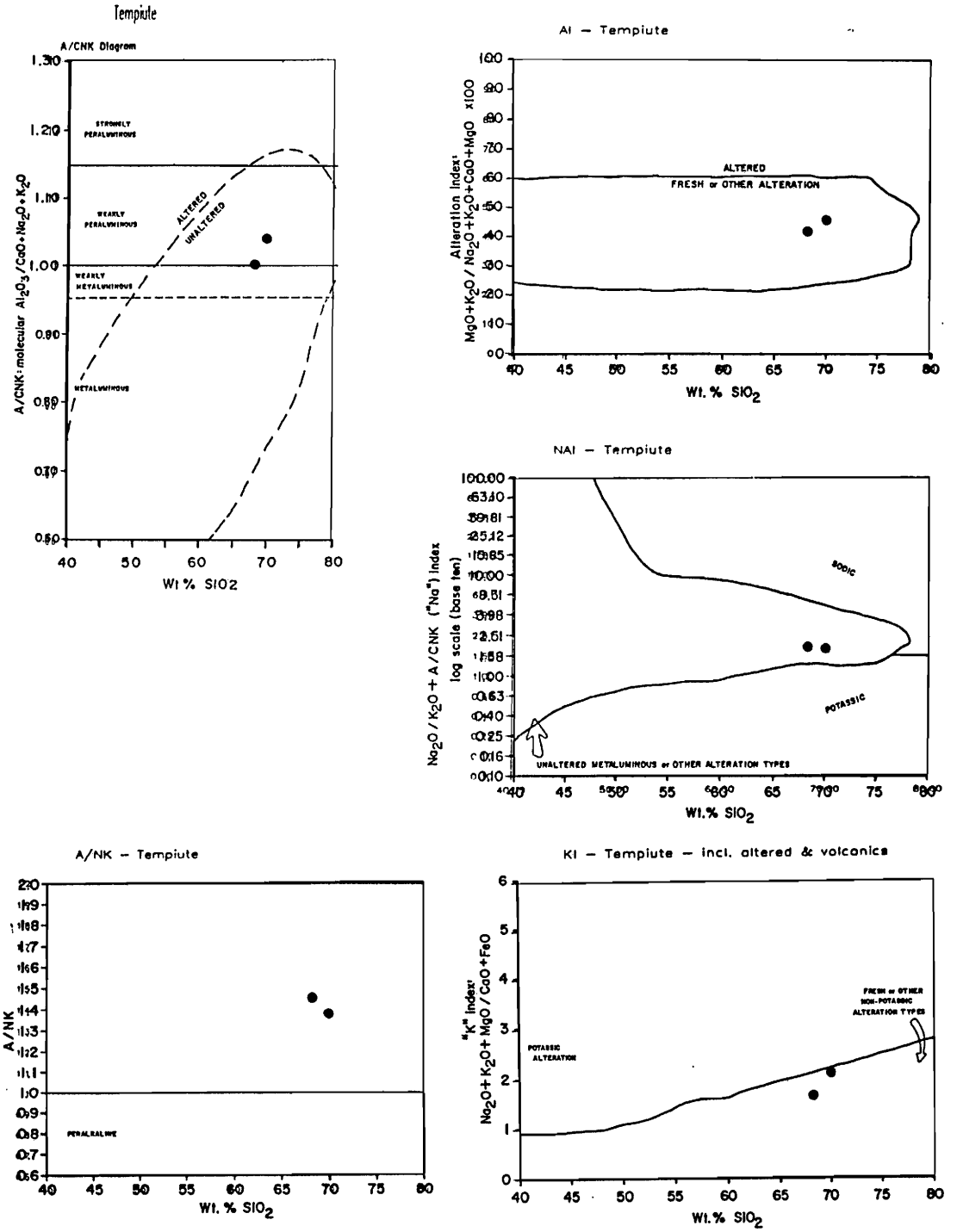

Figure 3-38. Petrochemical variation diagrams of igneous rocks from the Tempiute mining district, Nevada, showing alteration filters.

Alkali-calcic, Reduced

The porphyry tin deposits of the Eastern Cordillera in Bolivia are characterized by subvolcanic tin mineralization in silicic stocks and associated volcanics and breccias of Miocene age (Sillitoe and others, 1975; Francis and others, 1983). In central and southern Bolivia the tin deposits are complex vein systems carrying tin, tin-silver, or tin with base metals and silver and are mostly associated with acid eruptive complexes (Grant and others, 1977). The mineralization is centered on small (one to 2 km^2) porphyry stocks of intermediate to silicic composition that were emplaced at shallow levels (<2 km) beneath or within the vent of a volcanic edifice (Grant and others, 1980). Hydrothermal breccias are very common and the stocks and adjacent wallrocks have undergone intense pervasive hydrothermal alteration (Grant and others, 1980). This alteration makes it very difficult to obtain fresh igneous rocks for whole rock oxide analysis; most of the samples obtained in this study failed the alteration filters and nearby, apparently coeval rock samples were used.

Llallagua, Bolivia

The Llallagua deposit (Catavi mine) is about 80 km southeast of Oruro, Bolivia. The deposit is a complex system of veins, mineralized breccia and disseminated mineralization located within a small isolated stock of porphyry, the Salvadora stock (CIMVS) (Turneaure, 1935). The Salvadora stock at Llallagua, Bolivia, was emplaced in late Miocene time (average of 21.4 Ma) into Silurian-

Devonian graywackes, sandstones, and shales (Grant and others, 1979). The Salvadora stock is so severely altered that the original rock is difficult to determine, but textural evidence indicates that it was a quartz latite porphyry (Francis and others, 1983). The stock is 1700 m by 1050 m wide at the surface and tapers downwards; hydrothermal breccias are abundant. A whole rock analysis (Appendix B) was reported in Ahlfeld (1931), but the sample was too altered to include in the neural network study.

Oruro, Bolivia

The San Jose de Oruro mine, Bolivia, is a silver-tin-base metal mine in veins that cut Tertiary intrusive rhyolite porphyry, quartz monzonite porphyry, and Silurian shale (U. S. Geological Survey and Servicio Geologico de Bolivia, 1992). Mineralization occurs in the smaller San Jose and Isos stocks and in the San Pedro stock, which are quartz porphyry and quartz monzonite porphyry intrusions of Miocene age (Sugaki and others, 1981). The quartz latite porphyry stocks have volcanic affinities and were intruded at relatively shallow depths into folded Paleozoic sedimentary rocks and were accompanied or followed by extrusive lava flows (Chace, 1948). The complex of quartz latitic domes and dacite flows (CIMVS) have an average radiometric age of 16.4 Ma; the main alteration zone in the center of the Oruro hills has a sericite age of 15.1 $\pm$ 0.7 Ma. These ages are statistically identical and give a mean age of 16.1 Ma for intrusion, alteration, and mineralization (CIMVS) at Oruro (Redwood and

Macintyre, 1989). Analyses used in this study were obtained from Ahlfeld (1931) and U. S. Geological Survey and Servicio Geologico de Bolivia (1992), but all samples failed the alteration filters (Appendix B).

Potosi, Bolivia

The Cerro Rico stock, Potosi, Bolivia, is an example of caldera-related tin-silver mineralization. The stock is a dacite or quartz-latite porphyry, which is pervasively altered throughout and which is located on the margins of the prominent Kari Kari caldera (Francis and others, 1981). The stock has an oval shape approximately 1700 by 1200 m at the surface and tapers downwards to a 100 m wide dike at depth (Francis and others, 1983). The upper part of Cerro Rico is a silicified rhyolitic porphyry; at deeper levels it is clearly intrusive into Paleozoic sediments and into the intracaldera, lacustrine Caracoles formation (Francis and others, 1981). The Cerro Rico stock represents the eroded root of a rhyodacitic dome which was extruded along caldera ring fractures; thus the Cerro Rico stock is distinctly younger than the main Kari Kari massif, but is genetically related to it (Francis and others, 1981), suggesting the Kari Kari rocks are part of the Cogenetic Igneous-Metal-Volatile Suite (CIMVS).

Rocks from the resurgent center, outflow ignimbrites, and moat deposits of the nearby Kari Kari massif have yielded radiometric ages averaging 21.7 Ma (Grant and others, 1979). Evernden and others (1977) suggested that the Cerro Rico stock is penecontemporaneous with the Kari-Kari pluton; Francis and others

(1981) suggested that the Cerro Rico stock may be a late intrusion along the caldera ring fractures of the Kari Kari resurgent caldera. The intensely sericitized porphyry of the Cerro Rico stock gave an average age of 13.8 Ma (Grant and others, 1979), although the extreme alteration of the stock makes the young age suspect (Francis and others, 1981).

The Kumurana mine is 30 km south of Potosi city at the southern end of the Kari Kari caldera. High grade tin ore (about 2 percent Sn) is found at the intersections of veins in intrusive granite (Sugaki and others, 1983).

Samples for this study (Figure 3-40) were obtained from Wolf (1973); the samples from Cerro Rico were too altered and did not pass the alteration filters, so samples from the nearby Kari Kari massif and Kumurana granodiorite were used as the closest related plutonic rock (Appendix B). Although a number of the samples did not pass the alteration filters (Figure 3-41), most samples clustered in the alkali-calcic field on two of the three alkalinity graphs (Figure 3-42). The unaltered samples are very reduced, with many of the samples plotting in the strongly reduced field on the ferric/ferrous variation diagram (Figure 3-43).

Calc-alkalic, Oxidized

Christmas, AZ

The Christmas porphyry copper mine is in the southeastern Dripping Spring Mountains in southern Gila County approximately 27 km southeast of the Ray mine. Upper Paleozoic Naco Limestone and Cretaceous Williamson Canyon

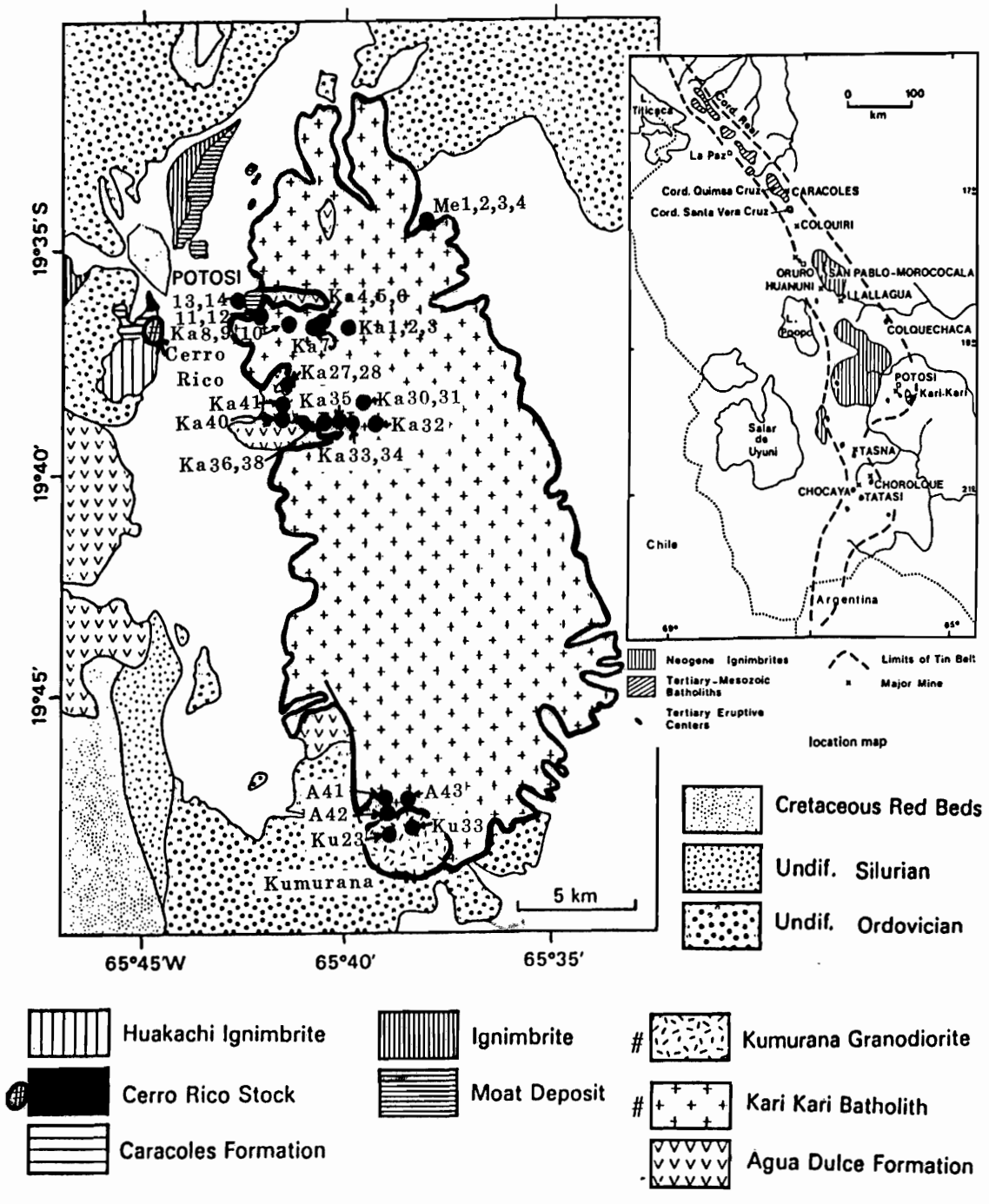

Figure 3-40. Geologic map of the Potosi, Bolivia, tin-silver district (# = CIMVS) (from Wolf, 1973; Frances and others, 1981; Grant and others, 1977).

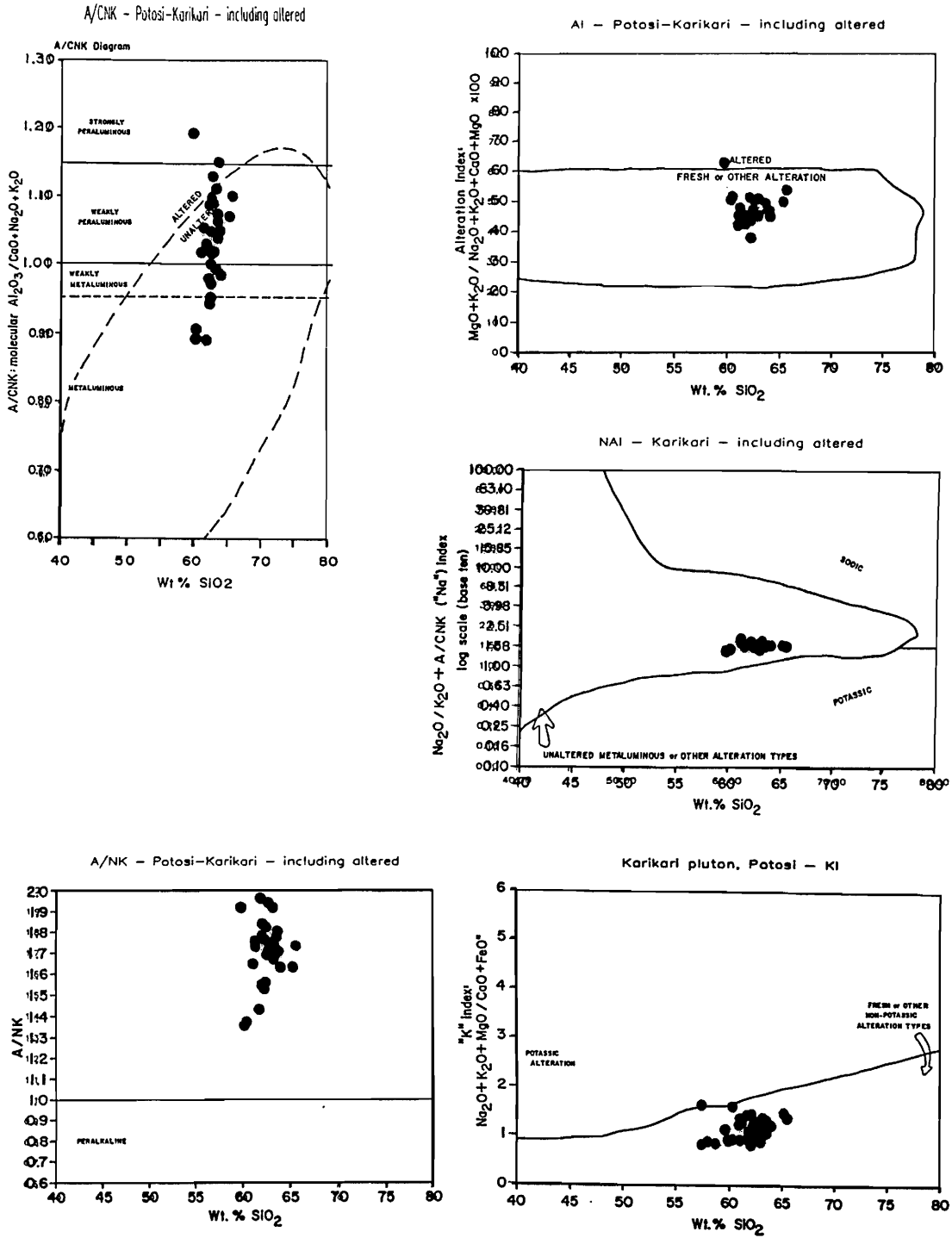

Figure 3-41. Petrochemical variation diagrams of Kari Kari and Kumurana rocks in the Potosi mining area, Bolivia, showing alteration filters.

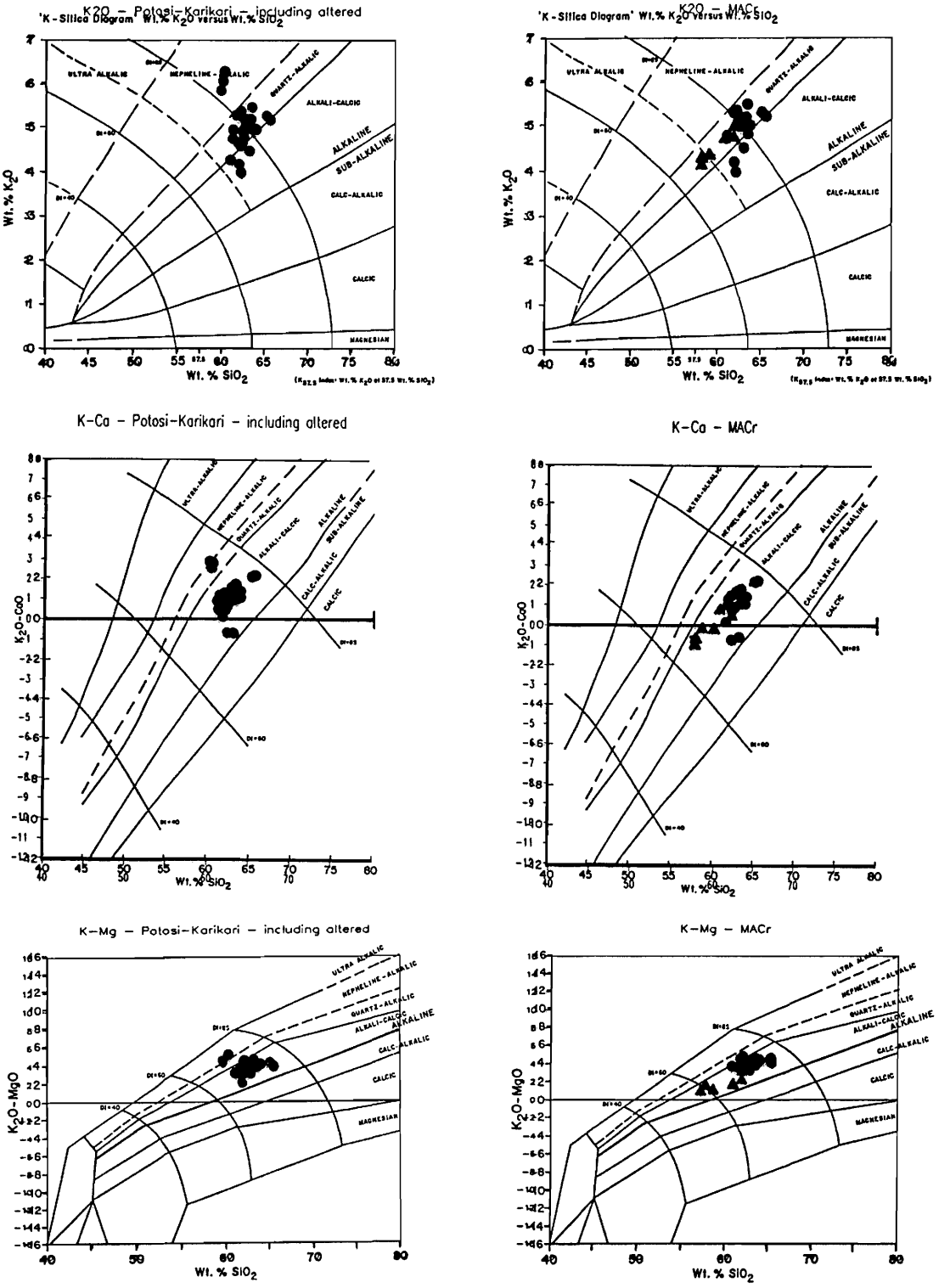

Figure 3-42. Magma series diagrams of Kari Kari and Kumurana rocks in Potosi, Bolivia, showing alkalinity (left includes altered; right is unaltered only).

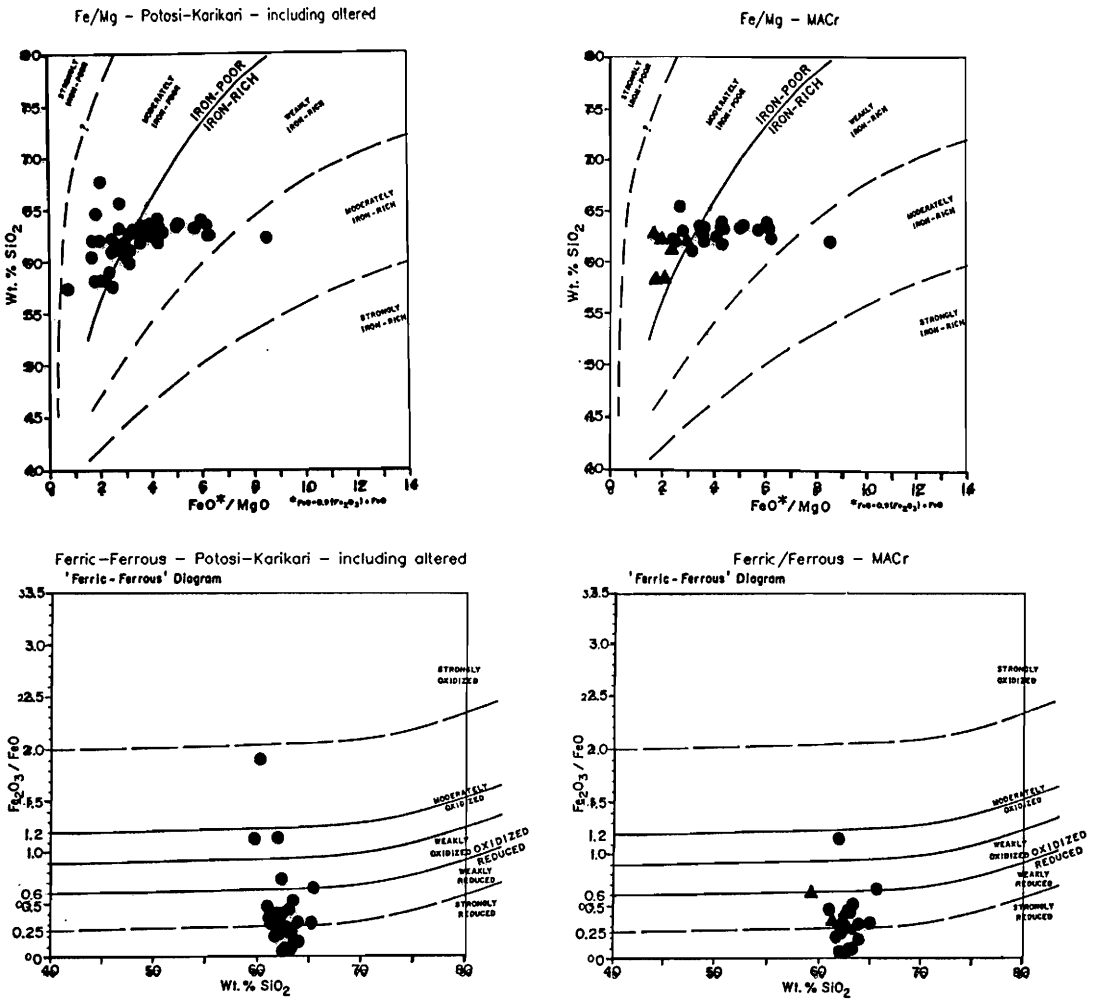

Figure 3-43. Petrochemical diagrams of Kari Kari and Kumurana rocks in Potosi, Bolivia, showing iron ratios (left includes altered; right = unaltered).

Volcanics are intruded by numerous Laramide stocks, sills, and dikes (Figure 3-44). These intrusive rocks range in composition from the earlier hornblende andesite porphyry, to hornblende rhyodacite porphyry, and to the later facies of the granodioritic Christmas intrusive complex (CIMVS) (Koski and Cook, 1982). The most differentiated phases of the Christmas stock are emplaced along an east-west fracture zone and are spatially related to copper mineralization (Koski and Cook, 1982). The Christmas intrusive complex has been dated at 62 Ma (Creasey and Kistler, 1962); this date coincides with the K-Ar ages of biotite and sericite from veins in the Christmas stock (McKee and Koski, 1981).

Whole rock analyses used in this study (Appendix B) were obtained from Koski (1978), Koski and Cook (1982), and Lang (1991). All of the samples passed the alteration filters (Figure 3-45) and are in the calc-alkalic field on the alkalinity variation diagrams (Figure 3-46), in the moderately iron-poor field on the FeO^*/MgO graph, and in the oxidized field on the ferric/ferrous graph.

Elk Mountain, NV

The Elk Mountain district is on the south end of Elk Mountain in northern Elko County, just south of the Idaho state line; mines and prospects are in the vicinity of White Elephant Butte and Red Elephant Butte. The copper and tungsten skarn deposits and veins are associated with faults or dikes and are related to the contact zone surrounding the granodiorite intrusive (Kg on Figure 3-47 = CIMVS) (Lapointe and others, 1991). Quartzite, shale, and limestone of

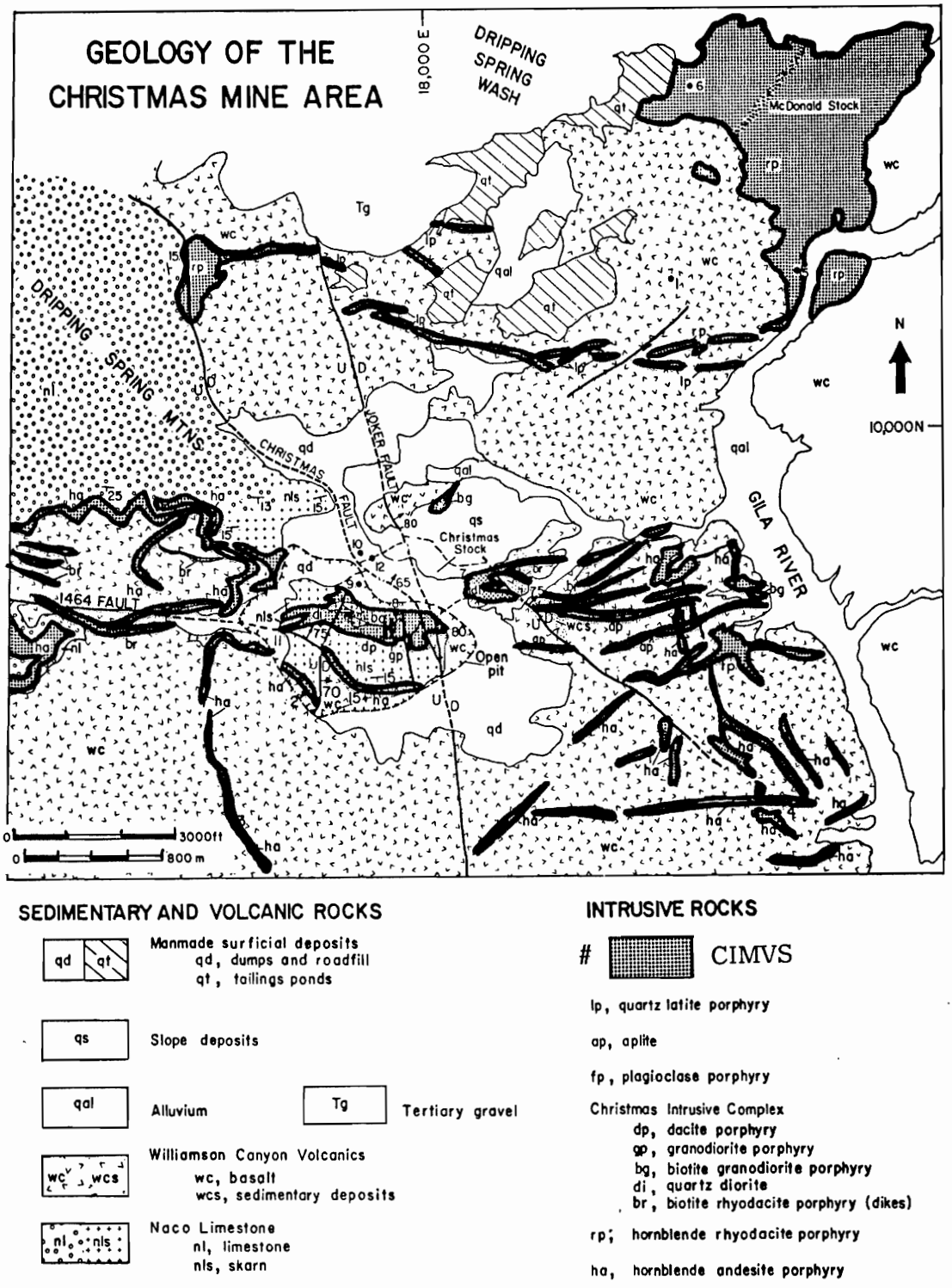

Figure 3-44. Geologic map of the Christmas mining district, Arizona, showing igneous rocks related to mineralization (# = CIMVS) (modified from Koski and Cook, 1982).

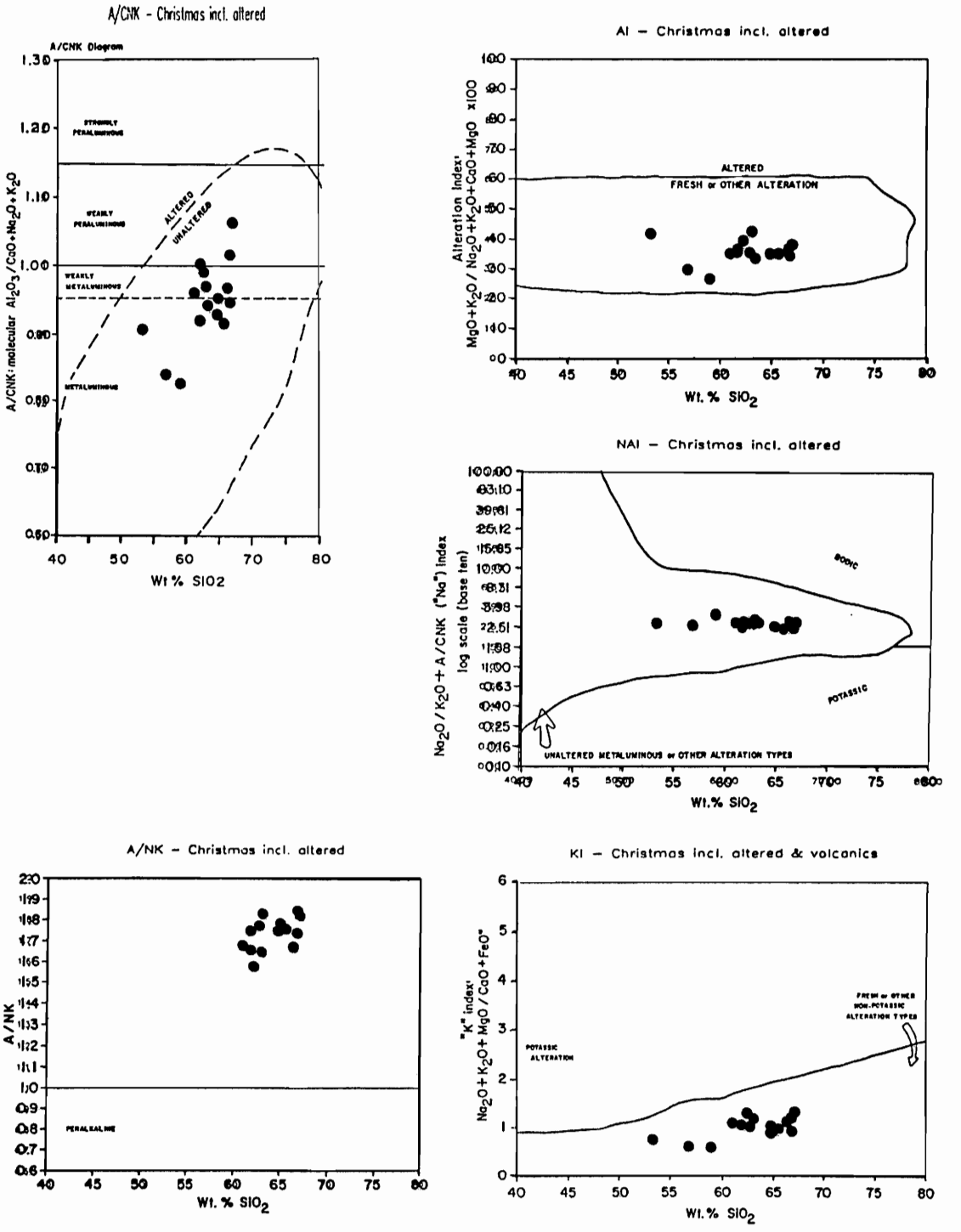

Figure 3-45. Petrochemical variation diagrams of igneous rocks of the Christmas mining district, Arizona, showing alteration filters.

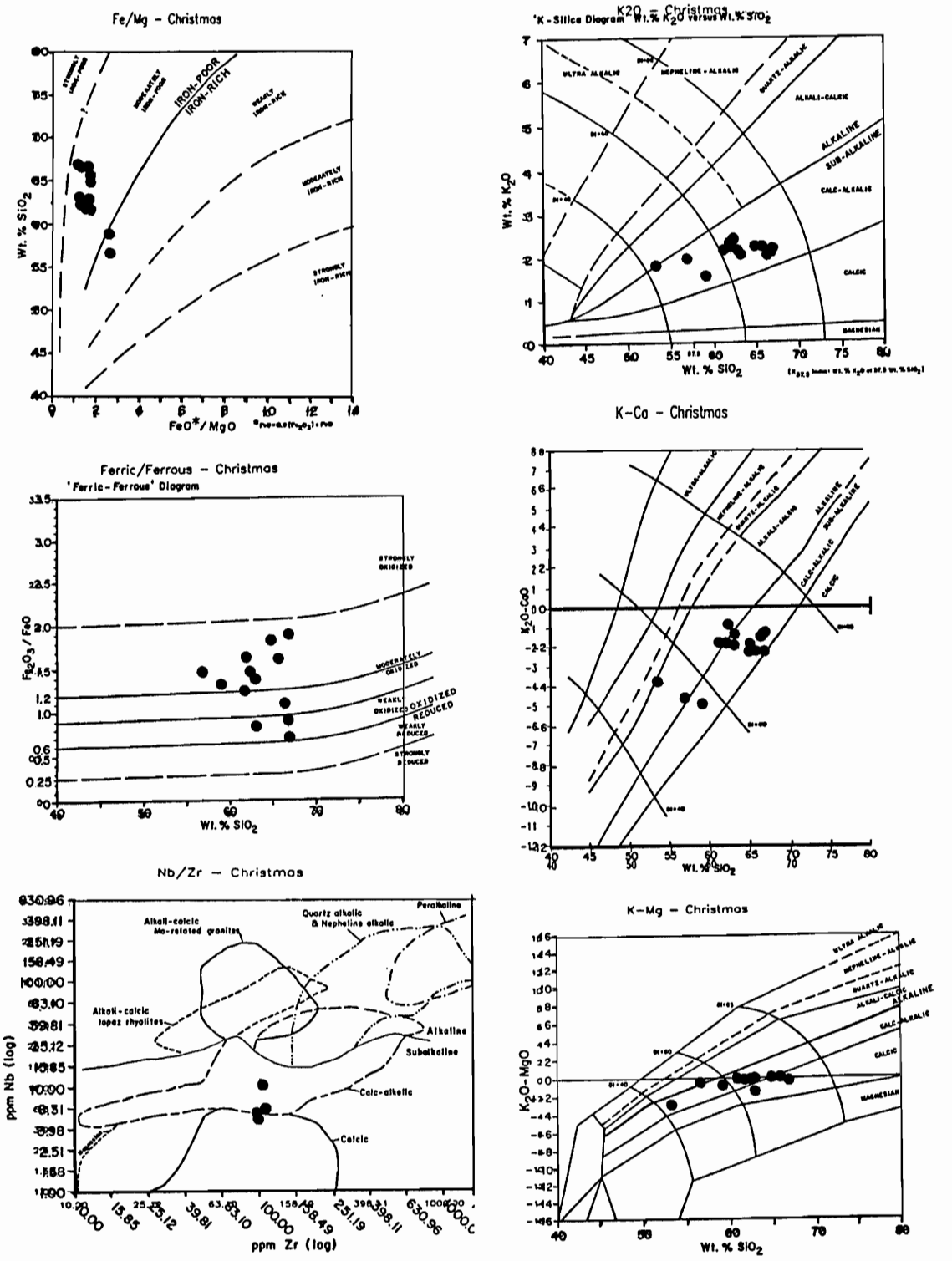

Figure 3-46. Magma series variation diagrams of igneous rocks of the Christmas mining district, Arizona, showing alkalinity and iron ratios.

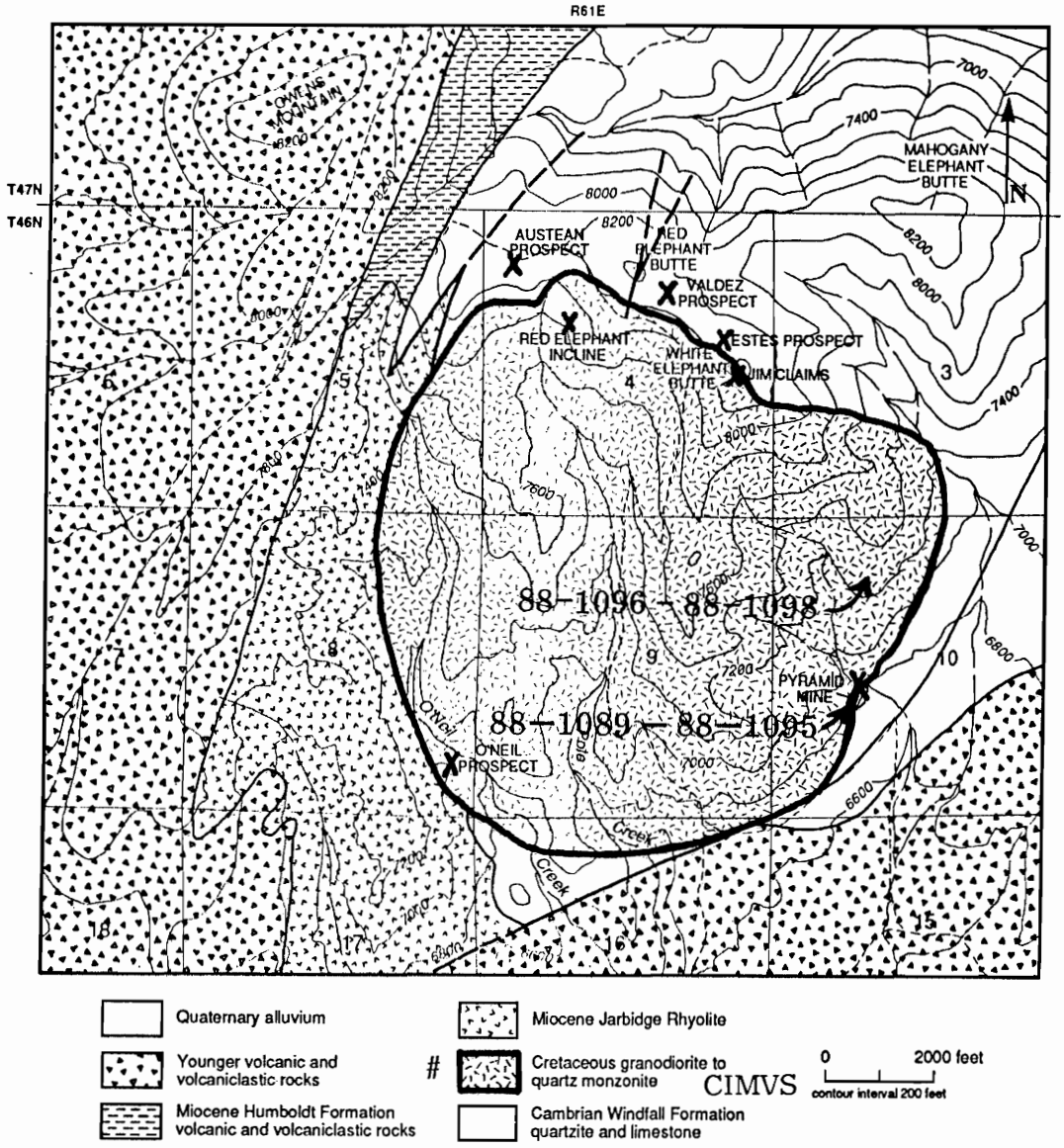

Figure 3-47. Geologic map of Elk Mountain, Nevada, showing Cretaceous granodiorite to quartz monzonite (CIMVS) and prospects (from Lapointe and others, 1991; Coats, 1987).

the Cambrian Windfall Formation have been domed and intruded by a stock of granodiorite to quartz monzonite that is approximately 100 ± 10 Ma (U-Pb on zircon by Stern in Coats, 1987).

Approximately 15 of the 60 samples collected by MagmaChem Exploration staff (Appendix A) failed the alteration filters (Figure 3-48); the remaining samples are in the calc-alkalic field on the alkalinity variation diagrams and in the moderately iron-poor field on the FeO^*/Mg versus SiO_2 graph (Figure 3-49). Most of the unaltered samples are in the oxidized field on the ferric/ferrous graph. Although many of the samples are in the weakly oxidized subfield, the mining district is placed in the oxidized class because the iron minerals are magnetite, sphene, and pyrite and not ilmenite or pyrrhotite, which are characteristic of more reduced classes.

Eugene Mountains (Mill City), NV

The Mill City (Tungsten or Central) district is in the southeastern Eugene Mountains about 13 km (8 miles) west of Mill City, Nevada, in northern Pershing County on the Humboldt County border (Lemmon in Johnson, 1977). Although originally a copper district, the major production has been tungsten, with 3 million tons of ore produced averaging 0.70 percent WO_3 (Johnson and Keith, 1991). The high-grade scheelite skarn deposits were formed by intrusion of the Springer granodiorite stock (g on Figure 3-50 = CIMVS) into lower carbonate beds of the Upper Triassic Raspberry Formation (Johnson and Keith, 1991). The

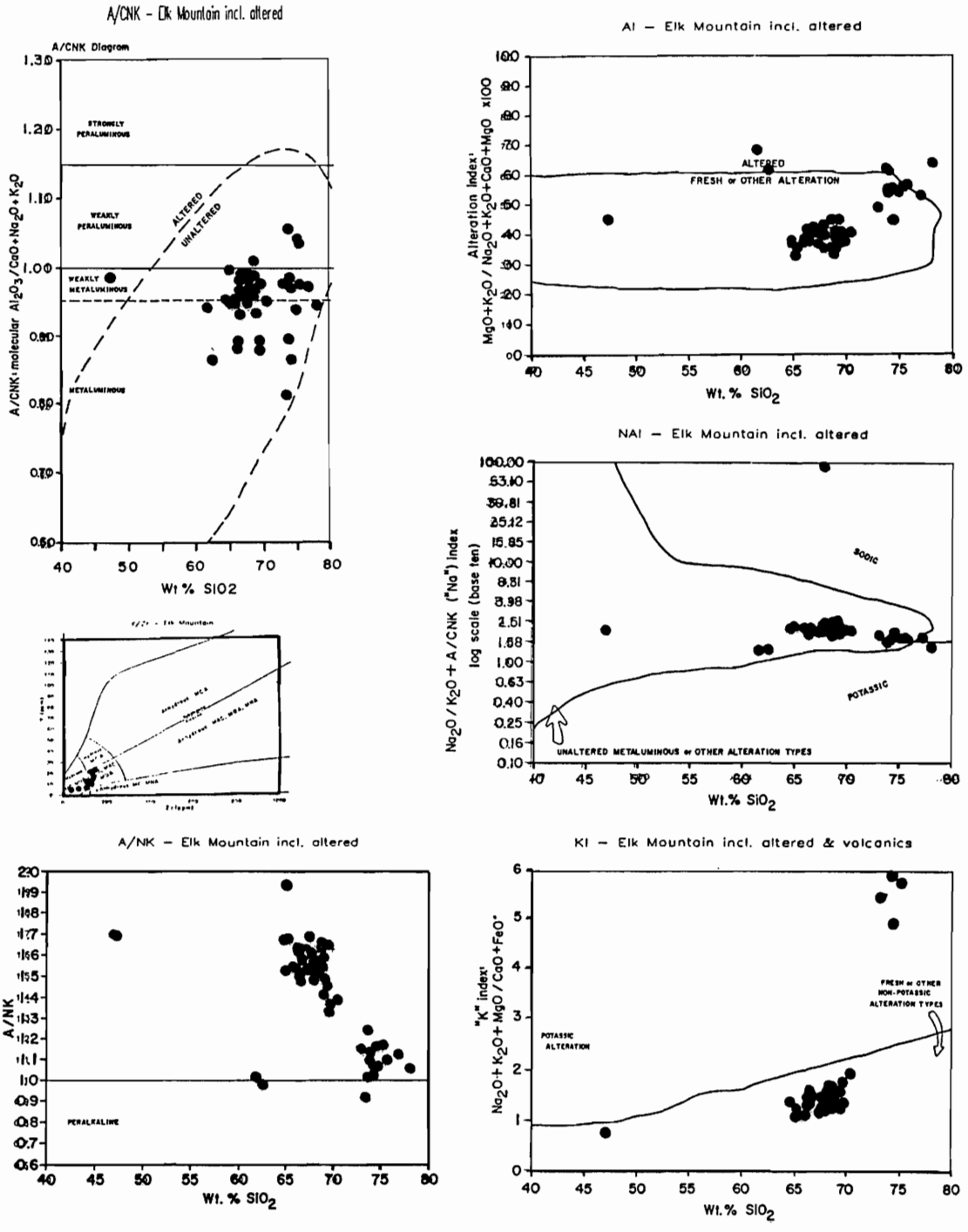

Figure 3-48. Petrochemical variation diagrams of igneous rocks of the Elk Mountain mining district, Nevada, showing alteration filters.

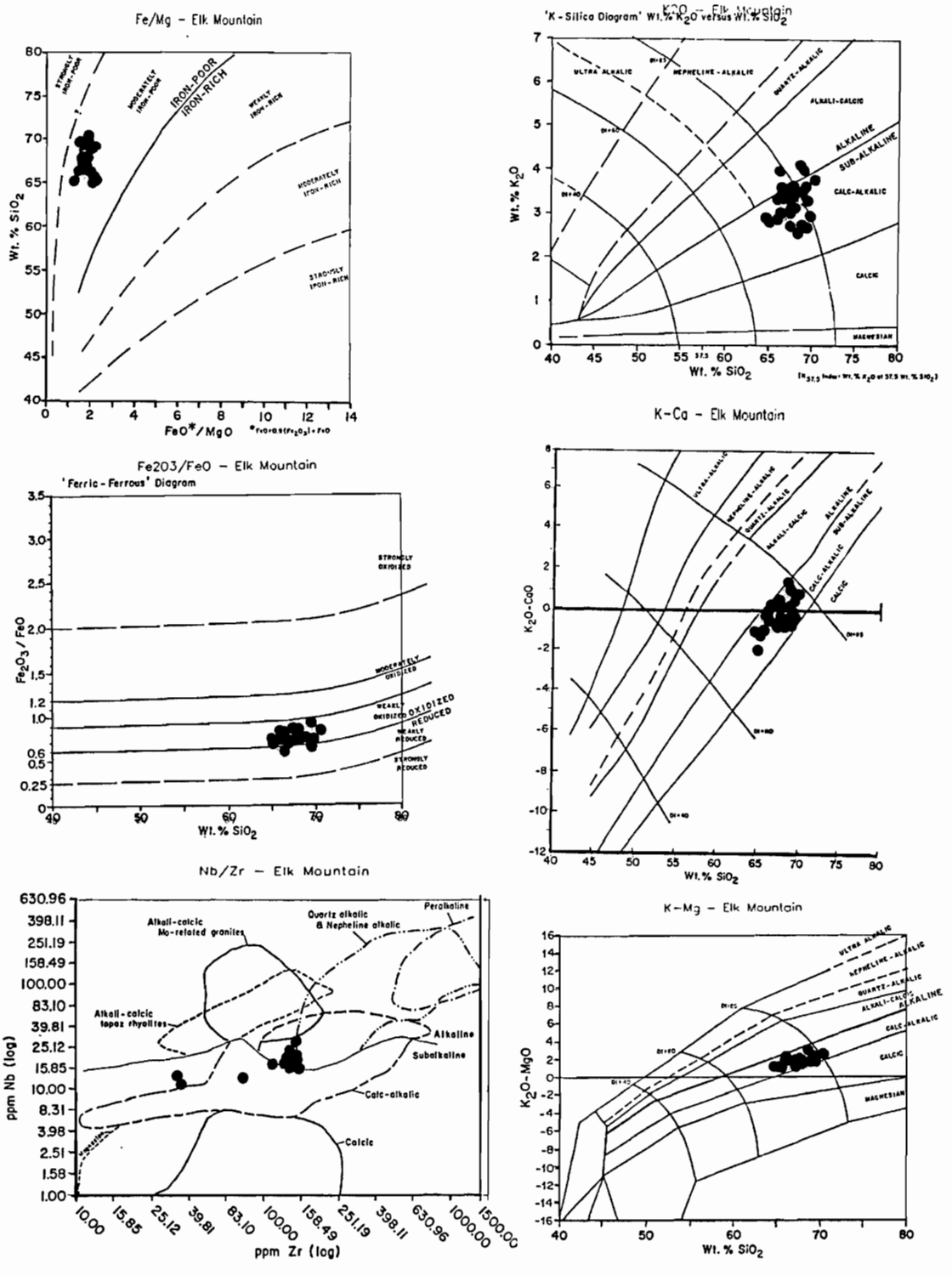

Figure 3-49. Magma series variation diagrams of igneous rocks of the Elk Mountain mining district, Nevada, showing alkalinity and iron ratios.

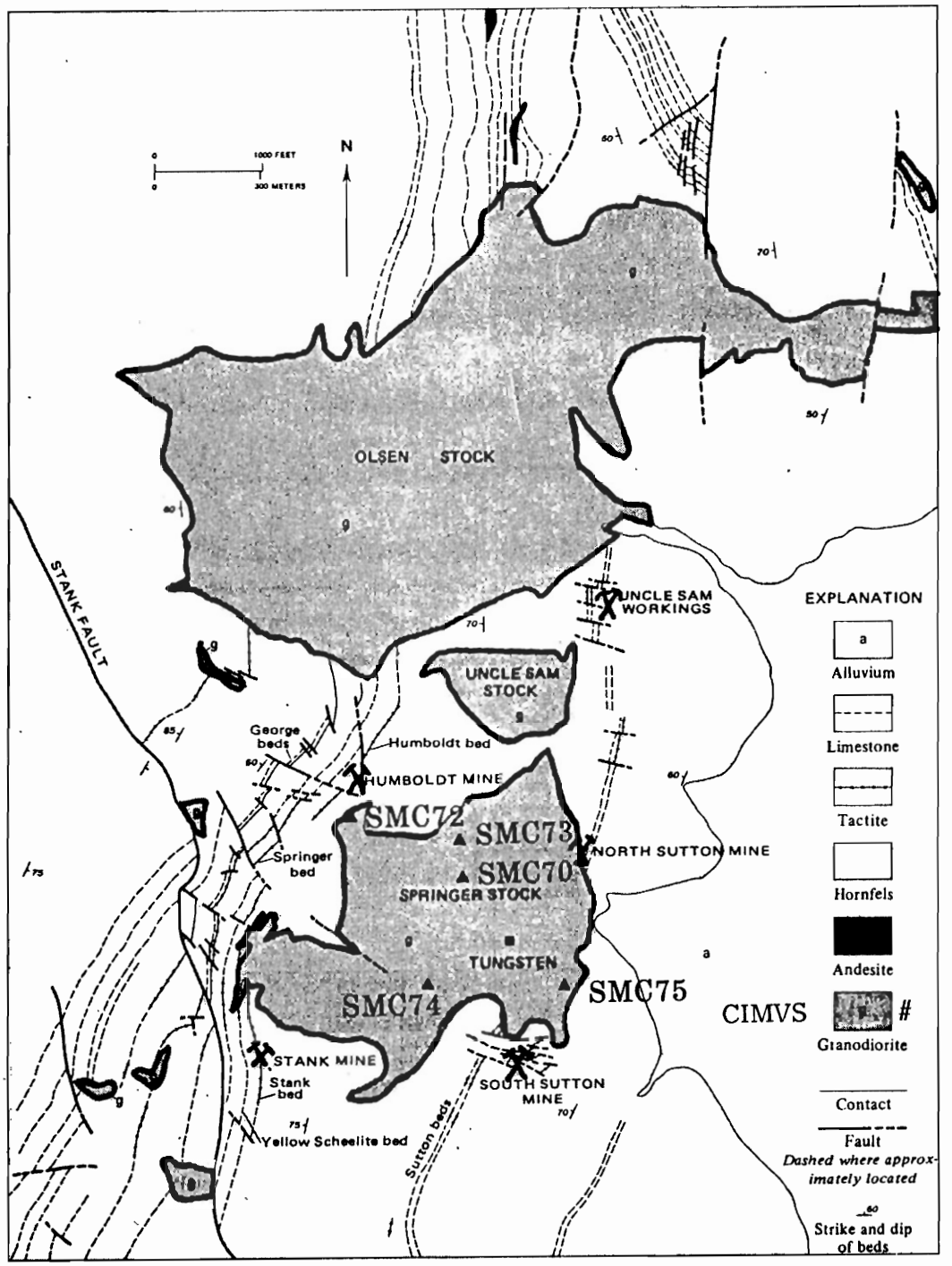

Figure 3-50. Geologic map of the Eugene Mountains (Mill City district), Nevada, showing granodiorite (g = # = CIMVS) and sample locations (from Johnson, 1977; Johnson and Keith, 1991).

age of the Springer stock (CIMVS) (K-Ar date of 78.4 ± 2.9 Ma) is close to that of pegmatitic adularia from the Springer stock (76.0 ± 2.7 Ma) and to adularia from a scheelite-bearing quartz vein cutting tactite at the southern margin of the Springer stock (72.0 ± 2.6 Ma) (Tingley, 1975; Johnson and Keith, 1991).

Samples used in this study were obtained from Lee (1984) and Johnson and Keith (1991). Most of the samples passed the alteration filters (Figure 3-51) and are in the metaluminous, calc-alkalic fields on the magma series alkalinity variation diagrams (Figure 3-52) and in the weakly oxidized and moderately iron-poor fields of the iron graphs (Figure 3-52). The lack of ilmenite in the magmatic phases of the granodiorite (Johnson and Keith, 1991) and the presence of abundant magnetite and titanite (sphene) place the stock in the oxidized class.

Guichon Creek, BC, CANADA

The Guichon Creek batholith is in south-central British Columbia on the north side of the Highland Valley approximately 50 km southwest of Kamloops and 350 km northeast of Vancouver (CIMVS = intrusive rocks of the batholith in Figure 3-53). Associated with the batholith are numerous porphyry copper deposits, including the Lornex, Highmont, Valley Copper, Bethlehem Copper, J.A., Krain, and South Seas deposits (McMillan, 1976; 1985). The Guichon Creek batholith intrudes and metamorphoses Late Triassic (Karnian and Norian) volcanic and sedimentary rocks and is dated at 202 ± 8 Ma by K-Ar and 205 ± 10 Ma by Rb-Sr (McMillan, 1985) and at 198 ± 8 Ma (Northcote, 1969). Hydrothermal

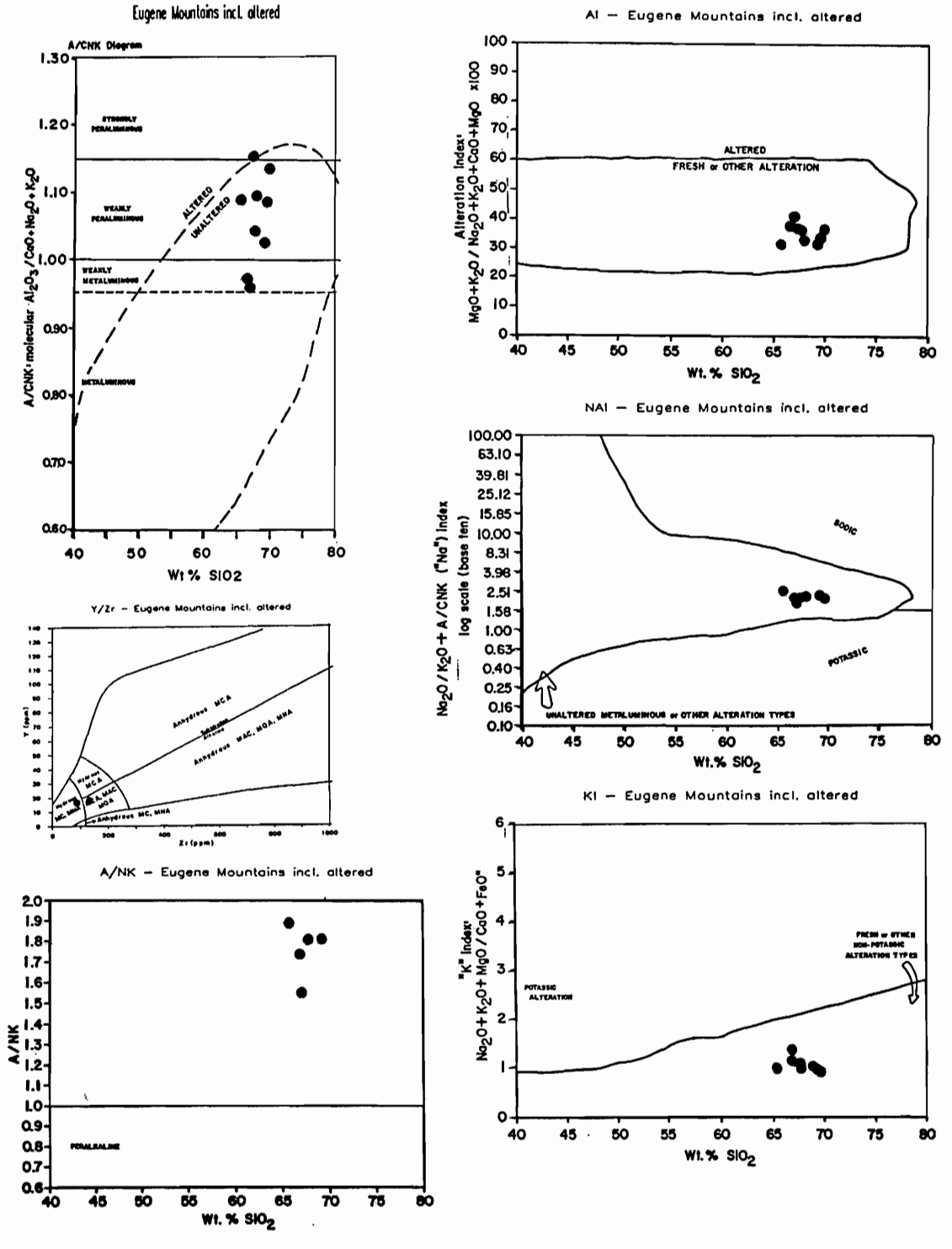

Figure 3-51. Petrochemical variation diagrams of igneous rocks of the Eugene Mountains (Mill City mining district), Nevada, showing alteration filters.

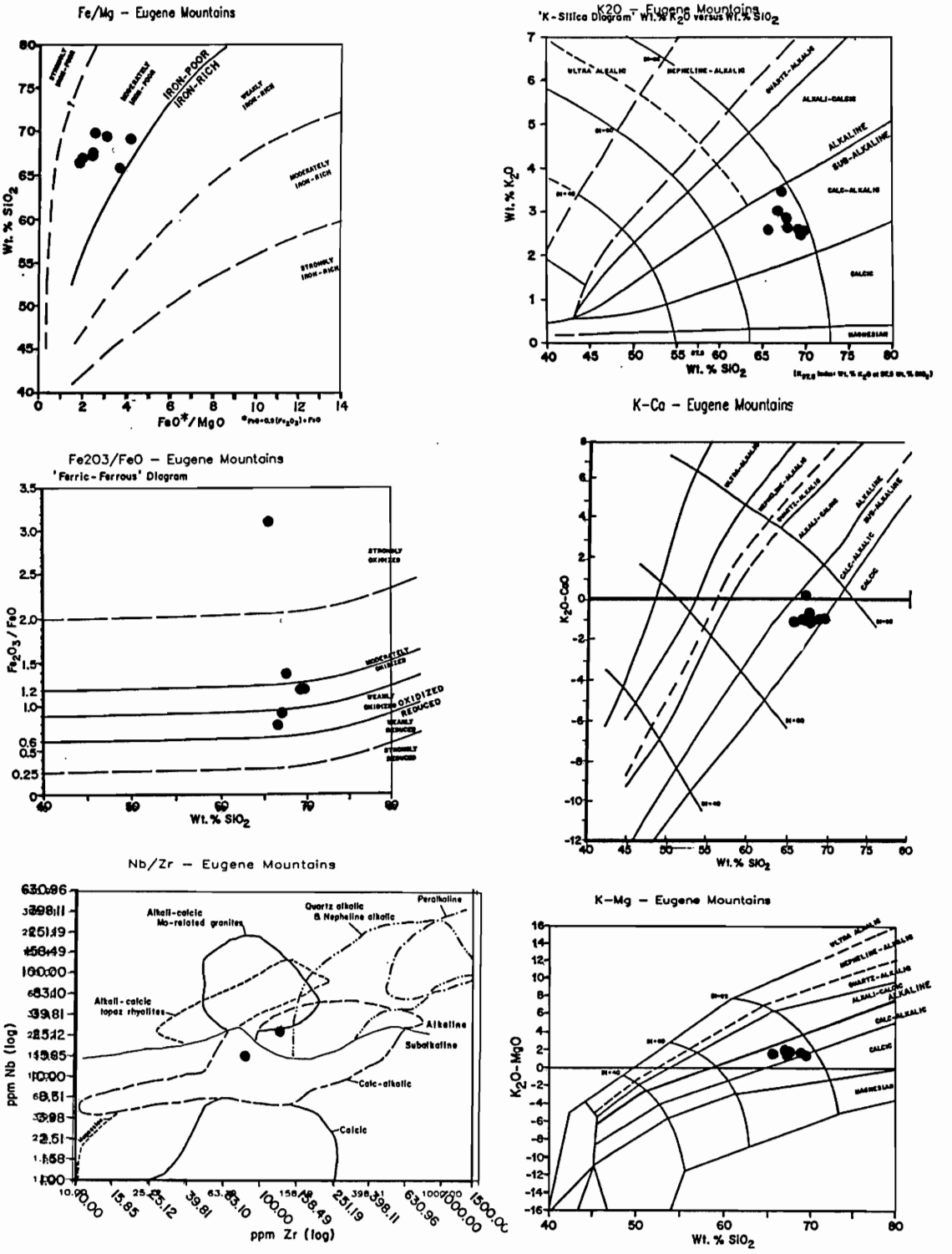

Figure 3-52. Magma series variation diagrams of igneous rocks of the Eugene Mountains (Mill City district), Nevada, showing alkalinity and iron ratios.

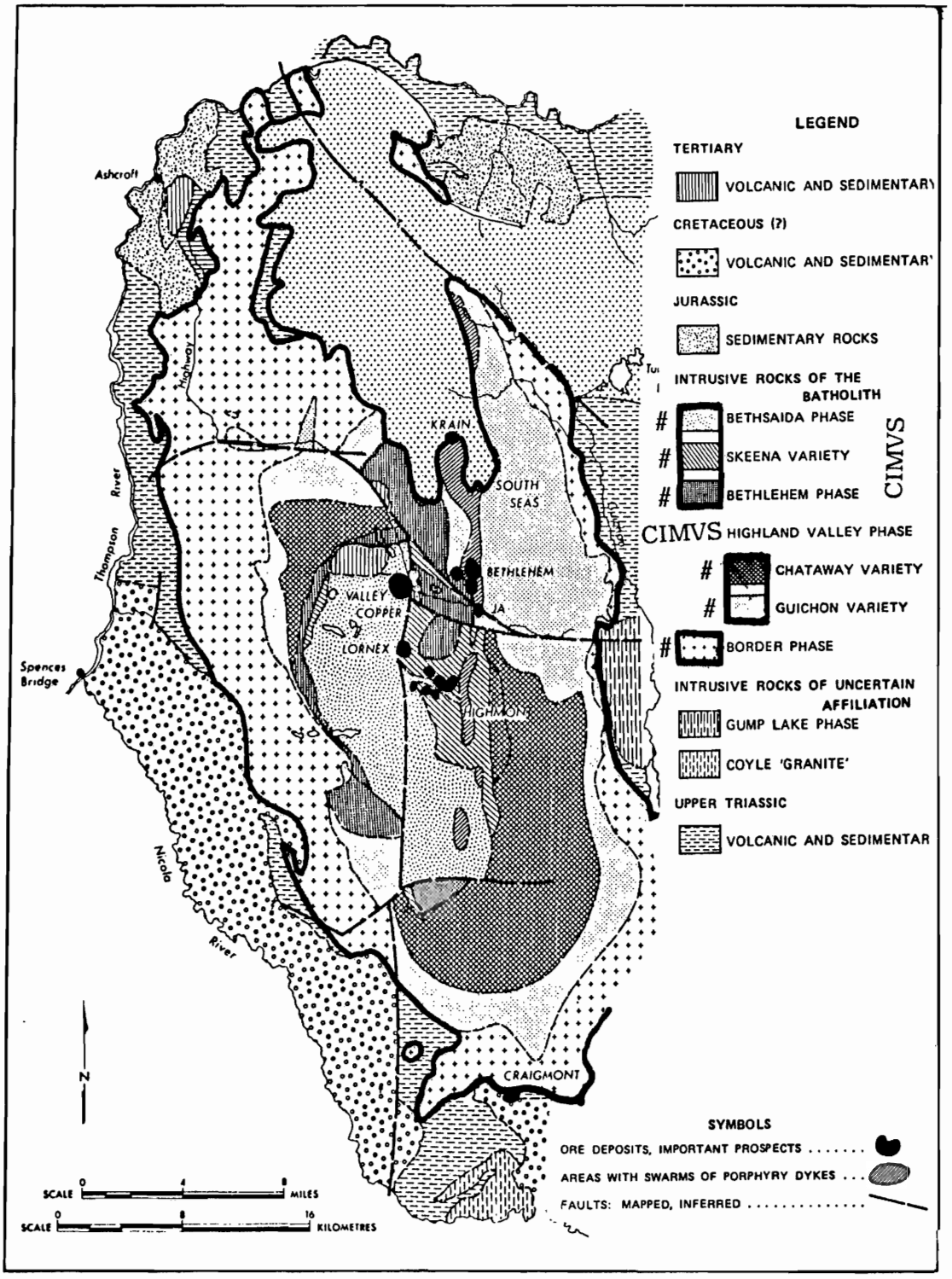

Figure 3-53. Geologic map of the Guichon Creek Batholith (Valley Copper and other districts, British Columbia) (# = intrusive rocks of the batholith = CIMVS) (from McMillan, 1982).

alteration products from the Lornex orebody were dated at 190 $\pm$ 4 Ma (Jones and others, 1972; Waldner and others, 1976)

The Guichon Creek batholith is characterized by a concentric pattern of phases that become younger toward the center. The Hybrid phase (a mafic-rich diorite or quartz diorite) is the oldest and is marginal to the batholith; it is succeeded inward by the Highland Valley phase (quartz diorite to granodiorite), the Bethlehem phase (also granodiorite), and the Bethsaida phase (quartz monzonite to granodiorite) as the innermost and youngest phase. Phases of more restricted extent transect this concentric pattern as irregular masses and swarms of porphyritic dikes (Brabec and White, 1971).

All the large deposits are either associated with the dike swarm north of Highland Valley or occur in or near the contact of the Bethsaida phase and related dikes; deposits in and south of Highland Valley appear to be younger than the Bethsaida phase (Brabec and White, 1971). Intrusive breccias, dacite and rhyodacite porphyry dikes, plugs of granite, granodiorite and porphyritic quartz latite, faults and fractures, and hydrothermal mineralization and alteration have been localized along the contact between the older Guichon Granodiorite and younger Bethlehem Granodiorite phases of the batholith. Late-stage concentration of mineralizers in the dacite porphyry melts were probably the source of hypogene metallization, which post-dates all intrusive rocks and breccias at Bethlehem (Briskey and Bellamy, 1976).

Whole rock oxide analyses for this study were obtained from Briskey and

Bellamy (1976), Jones (1974), Briskey (1980), and Olade (1976). Although many samples did not pass the alteration filters (Figure 3-54), most of the samples plotted in the calc-alkalic field on the alkalinity variation diagrams (Figure 3-55). Excluding altered samples removed much of the scatter that fell into the calcic fields. Most samples are in the moderately iron-poor field on the FeO^*/Mg diagram and in the oxidized class on the ferric/ferrous graph (Figure 3-56).

Mineral Park (Ithaca Peak), AZ

The Mineral Park porphyry copper deposit is approximately 26 km north of Kingman, Arizona in Mohave County in the Cerbat Mountains in the central part of the Wallapai (or Chloride) mining district (Wilkinson and others, 1982). Folded Precambrian schist, quartz-feldspar gneiss, and amphibolite were intruded by Laramide quartz monzonite, fractured into a stockwork of northwest and northeast-trending fractures, and mineralized (Eidel and others, 1968).

The Ithaca Peak intrusive complex (# = CIMVS on Figure 3-57) includes biotite quartz monzonite porphyry, biotite quartz diorite porphyry, and rhyolite dikes centered at the Mineral Park mine (Wilkinson and others, 1982). A K-Ar age of 71.5 $\pm$ 2.6 Ma (recalculated to 73.1 $\pm$ 2.6 Ma, Reynolds and others, 1986) on vein biotite from Ithaca Peak establishes the Laramide age for early stages of alteration (Damon and Mauger, 1966). Although the exposed Ithaca Peak stock is not directly related to the mineralization, it represents an apophysis from a deeper co-magmatic batholith whose extent is outlined by the lateral extent of

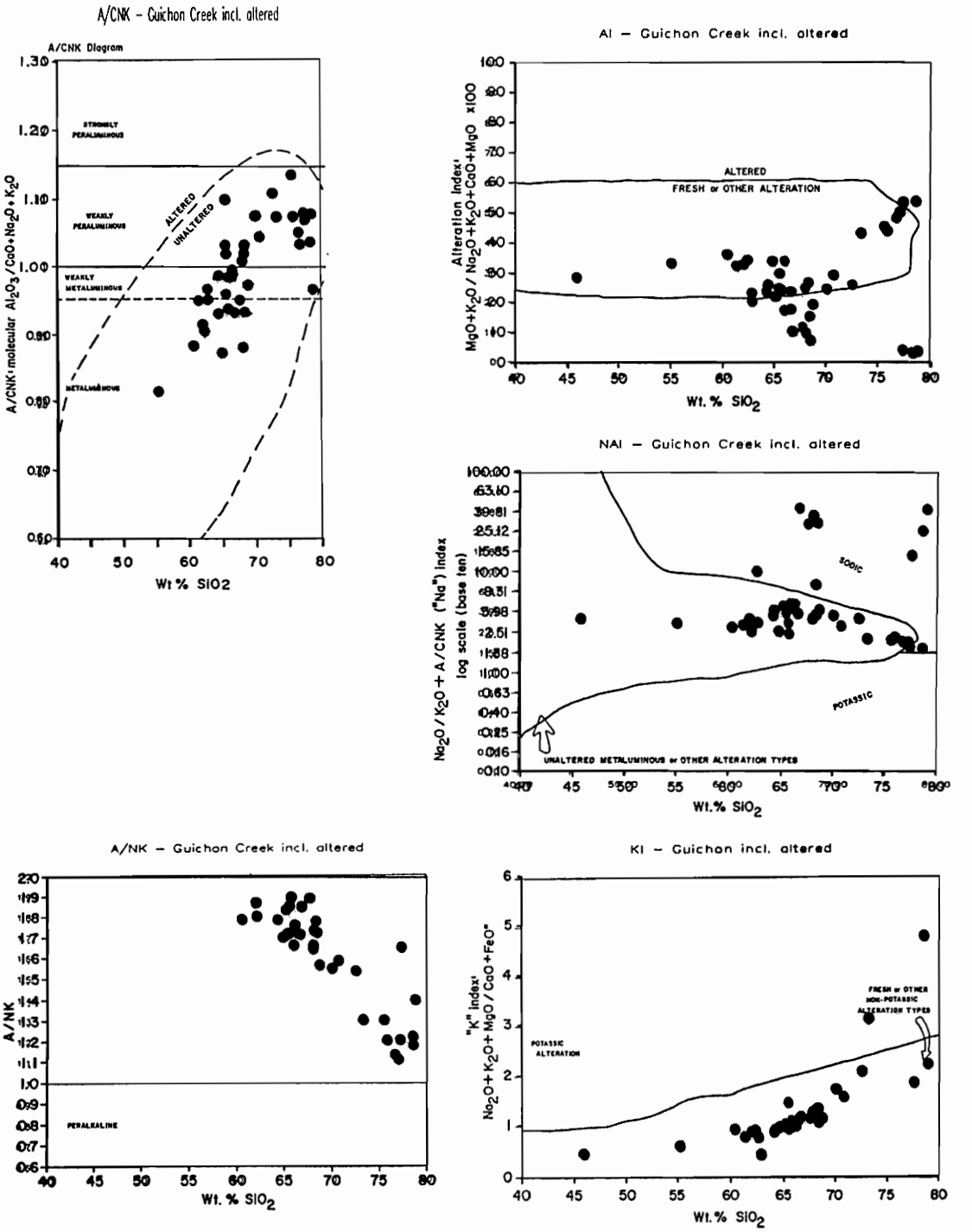

Figure 3-54. Petrochemical variation diagrams of the Guichon Creek batholithic rocks, British Columbia, showing alteration filters.

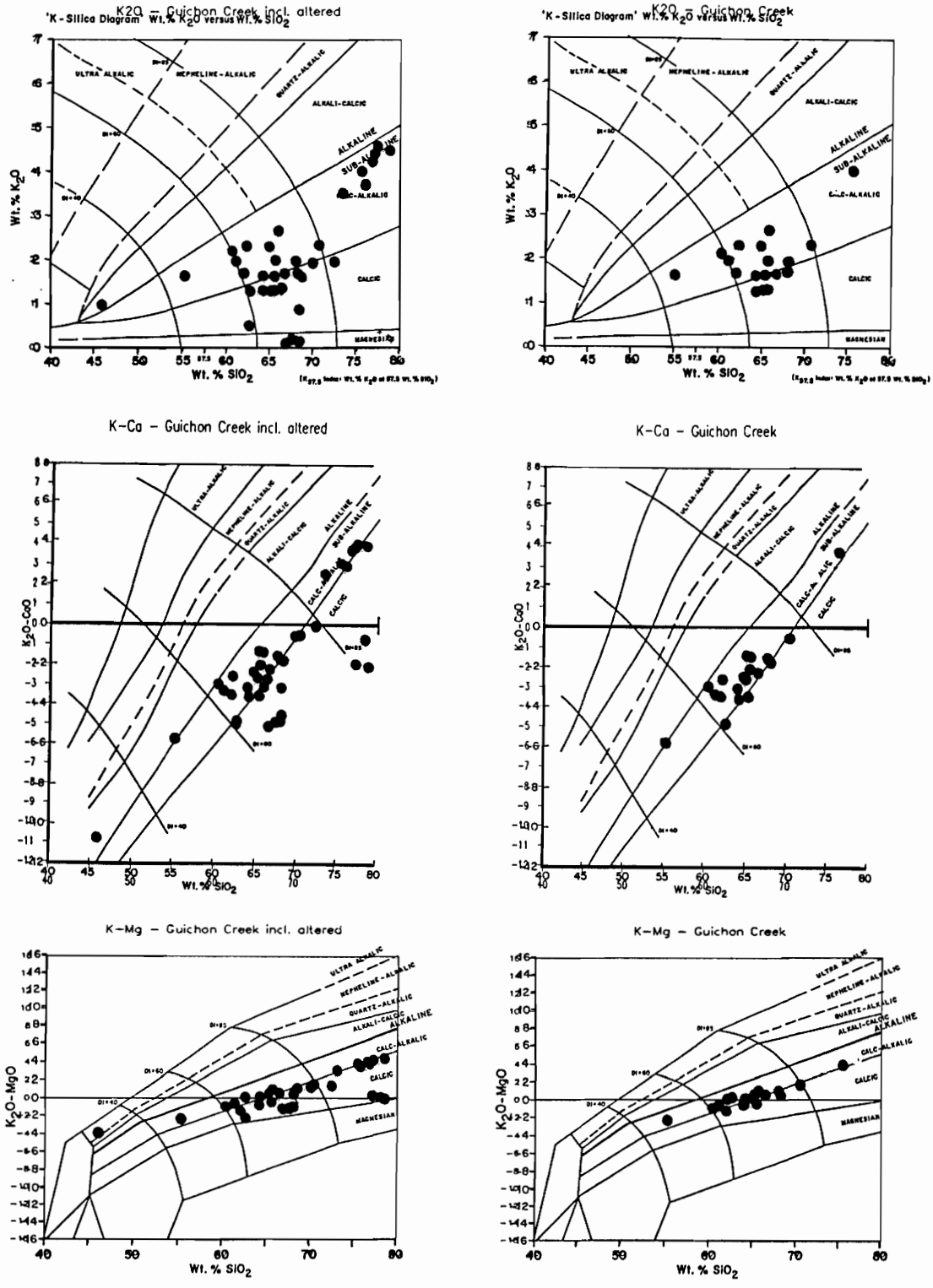

Figure 3-55. Magma series diagrams of the Guichon Creek batholith, BC, showing alkalinity (left includes altered; right is unaltered samples only).

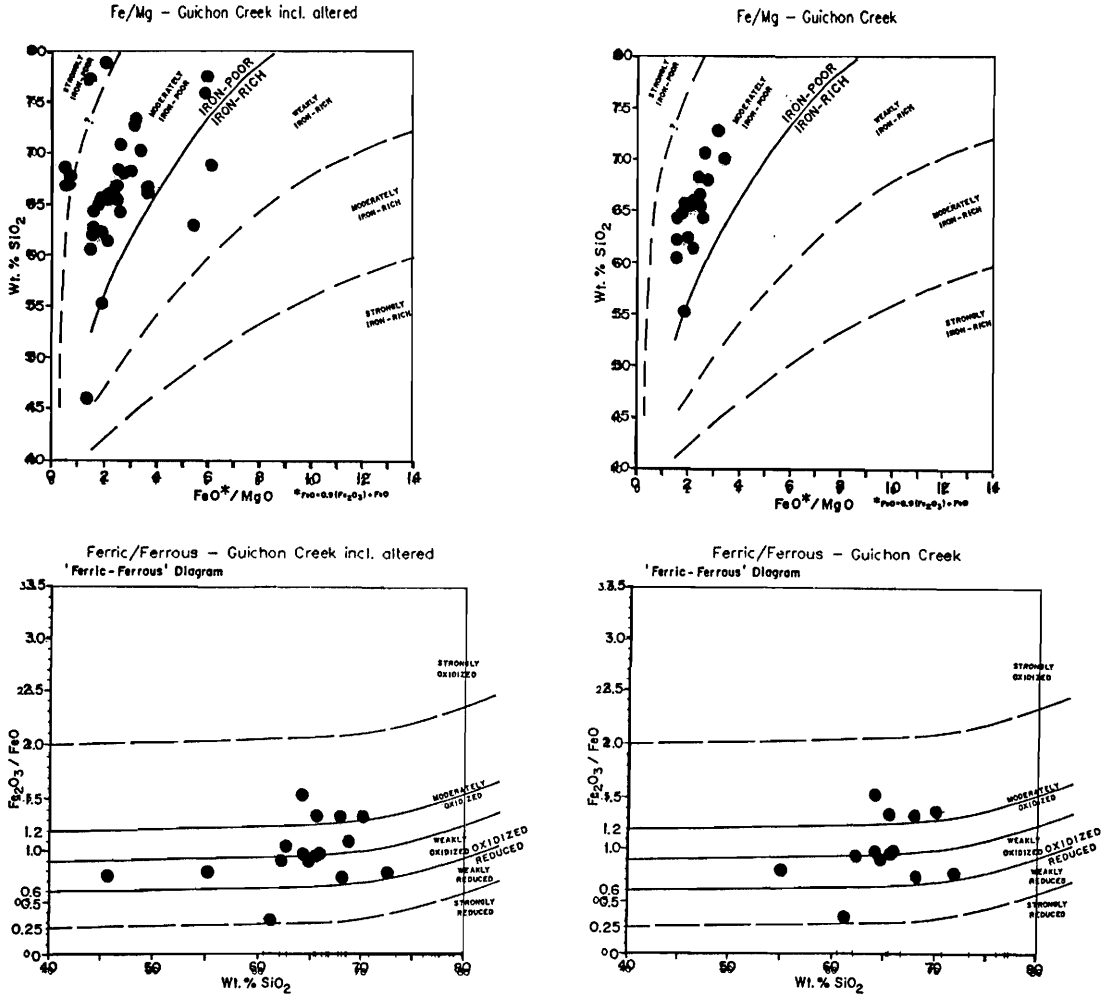

Figure 3-56. Petrochemical diagrams of the Guichon Creek batholith, BC, showing iron ratios (left includes altered; right is unaltered samples only).

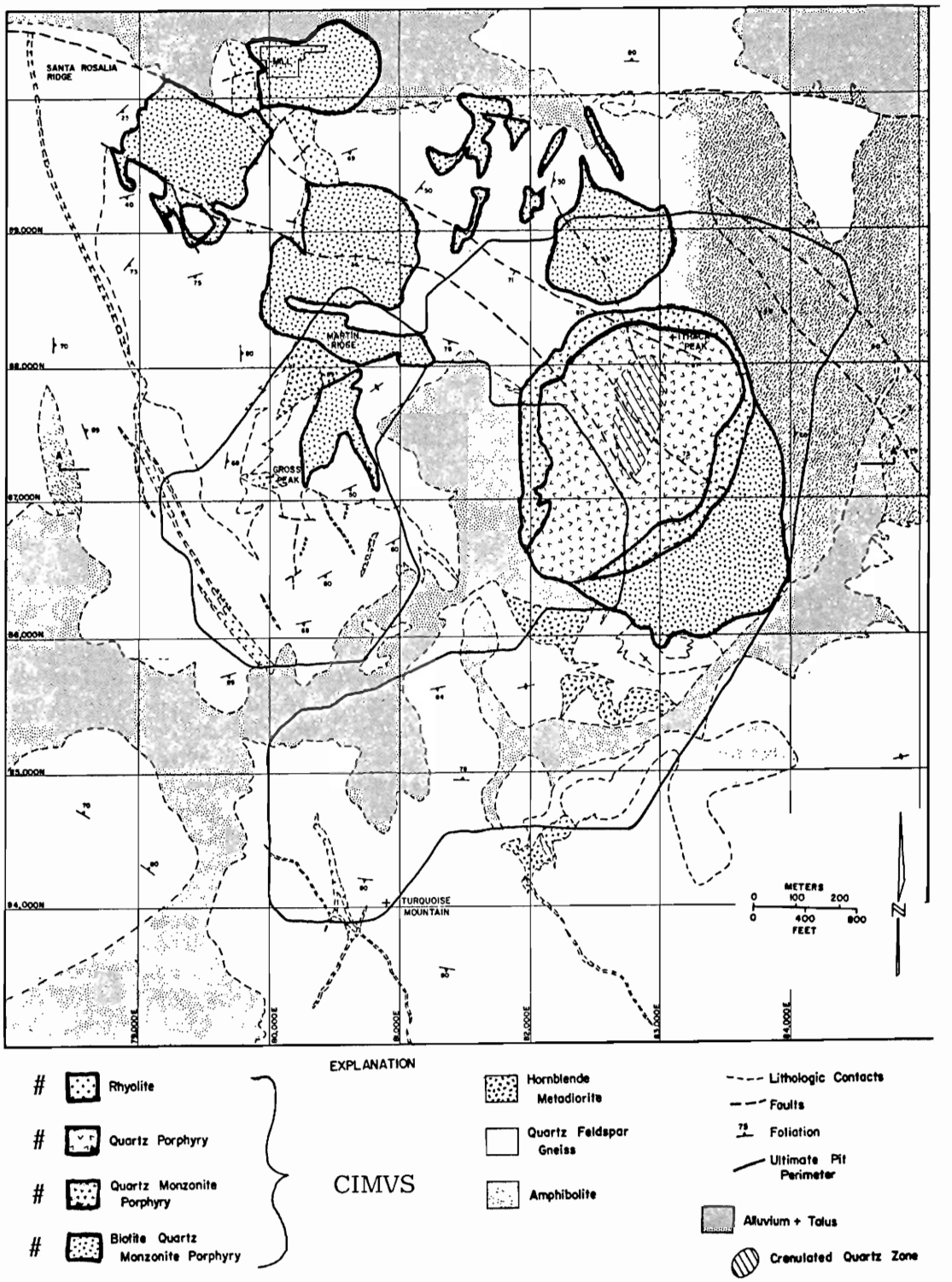

Figure 3-57. Geologic map of the Ithaca Peak pluton (Mineral Park mine), Arizona (# = CIMVS) (modified from Wilkinson, 1981).

dikes and veins (Wilkinson and others, 1982). Fluid inclusion and geologic data indicate that the early mineralizing fluids were magmatic in origin (Lang and Eastoe, 1988).

The whole rock analyses in the literature (Wilkinson and others, 1982) were from mineralized samples and therefore failed the alteration filters (Figure 3-58). However, even though altered, they are in the calc-alkalic fields in the petrochemical alkalinity variation diagrams (Figure 3-59).

Patagonia (Red Mountain), AZ

The Red Mountain porphyry copper deposit is in the northern Patagonia Mountains near the Mexican border approximately 80 km south of Tucson, Arizona. The core of the Patagonia Mountains is composed of Patagonia granodiorite (T on Figure 3-60), which is a northwesterly elongated intrusion covering 80 km^2 (30 square miles); the granodiorite becomes more porphyritic along its eastern margin (Graybeal, 1973). The quartz monzonite and granodiorite facies of the Patagonia pluton were dated by the K-Ar method on biotite and hornblende at 59.5 $\pm$ 3 Ma (Marvin and others, 1973; Reynolds and others, 1986); the earlier quartz diorite phase was dated at 65.4 $\pm$ 2 Ma (Damon and others, 1964; Reynolds and others, 1986).

Alteration, lithologic characteristics, and deep exploratory drilling indicate that Red Mountain, Arizona, represents the upper level lithocap region of a porphyry copper system (Bodnar and Beane, 1980; Quinlan, 1986). The

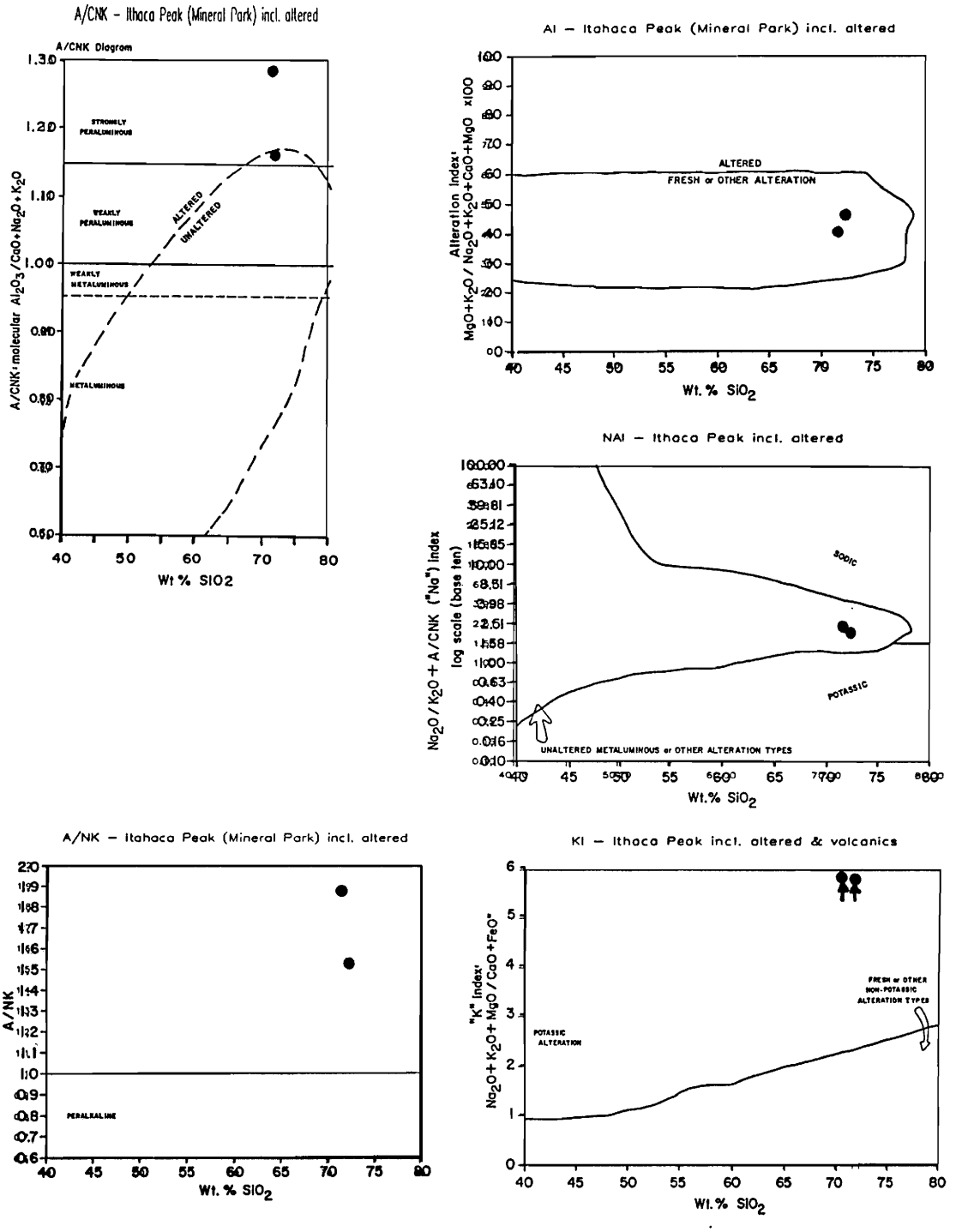

Figure 3-58. Petrochemical variation diagrams of the Ithaca Peak pluton (Mineral Park mine), Arizona showing alteration filters.

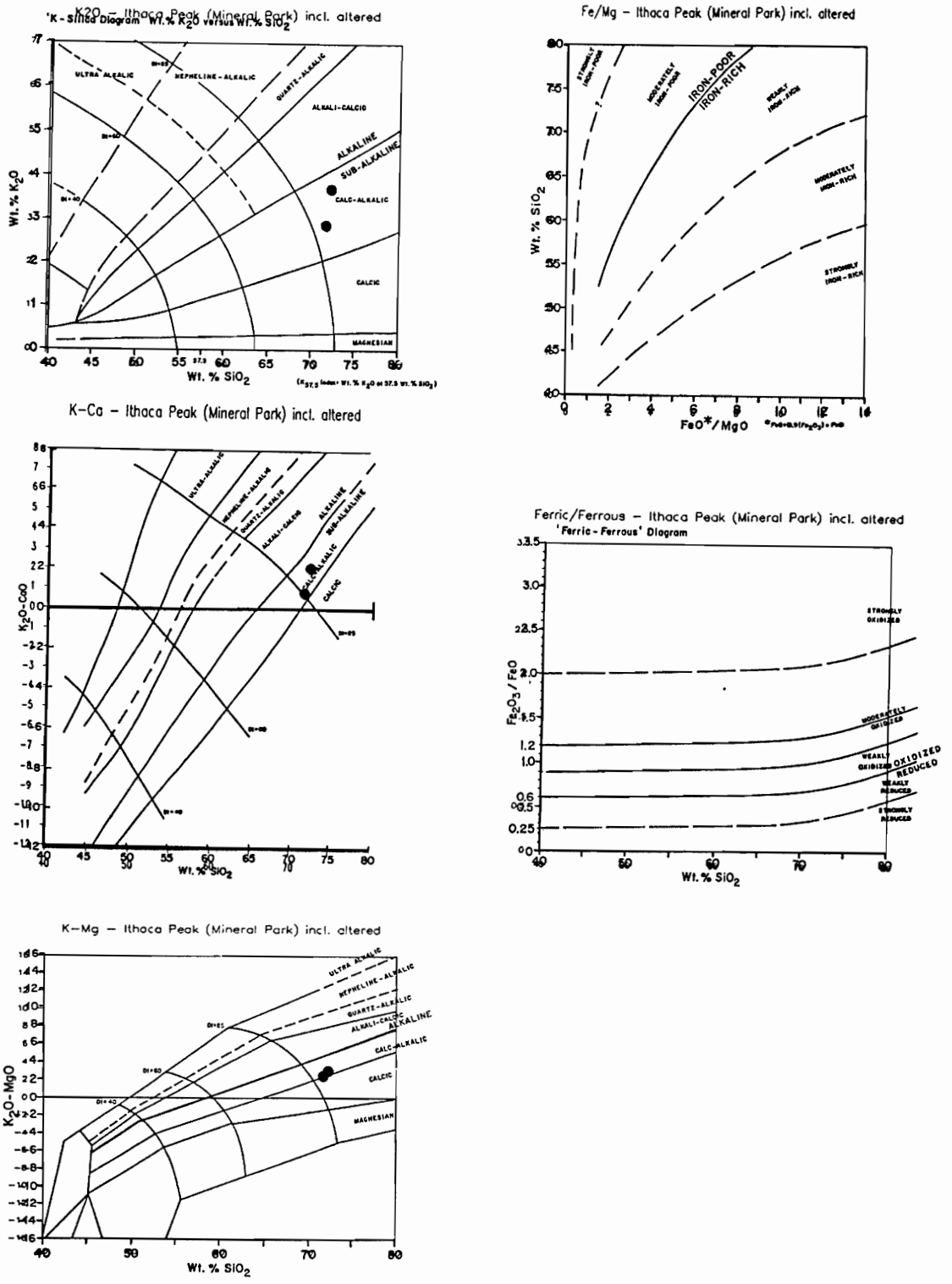

Figure 3-59. Magma series variation diagrams of the Ithaca Peak pluton (Mineral Park mine), Arizona, showing alkalinity and iron ratios.

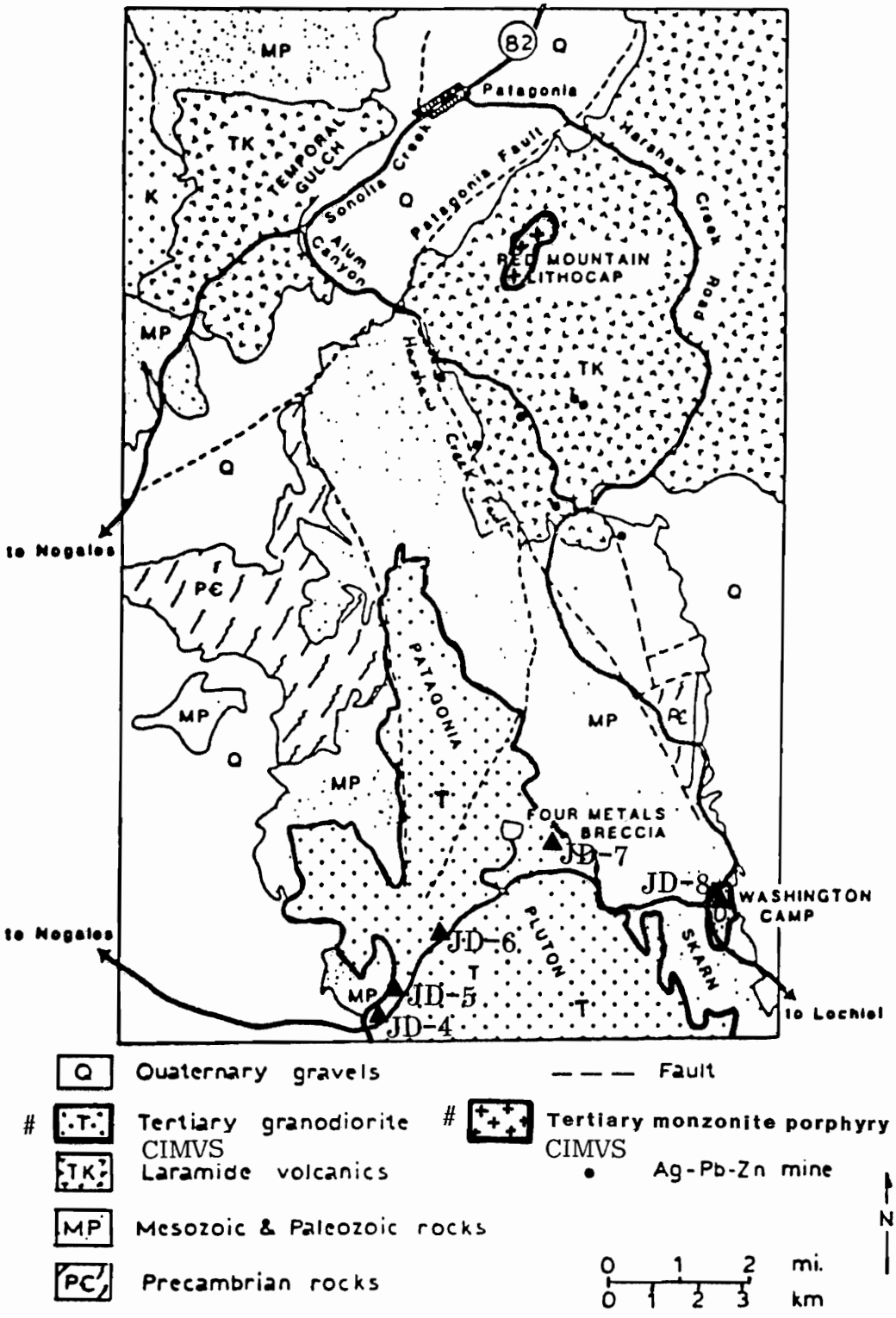

Figure 3-60. Map of the Patagonia pluton (Red Mountain mining area), Arizona, showing igneous rocks (modified from Kistner, 1984; Dewhurst, 1976).

alteration and lithologic characteristics suggest the presence of a cupola beneath Red Mountain which may interconnect with the copper-bearing Patagonia pluton that lies 3 km to the south (Kistner, 1984). Metallization and hydrothermal alteration at Red Mountain exhibit concentric zoning patterns centered on the area of monzonite porphyry and quartz monzonite porphyry intrusions and indicate that they are interdependent (Corn, 1975) (+++ = Tertiary monzonite porphyry in Figure 3-60 = CIMVS). These porphyry intrusions and the mineralization are younger than approximately 60 Ma (Corn, 1975), because they crosscut a sequence of highly altered latitic to trachytic tuffaceous rocks which Drewes (1972) correlated with the Gringo Gulch volcanics dated at approximately 61.3 $\pm$ 4.3 and 62 $\pm$ 3 Ma (Marvin and others, 1973; Reynolds and others, 1986).

Samples used in this study were obtained from Dewhurst (1976) and Graybeal (1973). Although several samples were potassically altered and were excluded from the data set (Figure 3-61), most samples are in the calc-alkalic alkalinity field in the magma series variation diagrams (Figure 3-62). Ferric/ ferrous ratios were not available for these samples because only total iron was obtained; however, the presence of abundant magnetite and sphene and the absence of ilmenite (Graybeal, 1973; Dewhurst, 1976) indicates that the samples belong in the oxidized to strongly oxidized category.

Ray, AZ

The Ray porphyry copper deposit of the Mineral Creek mining district is in

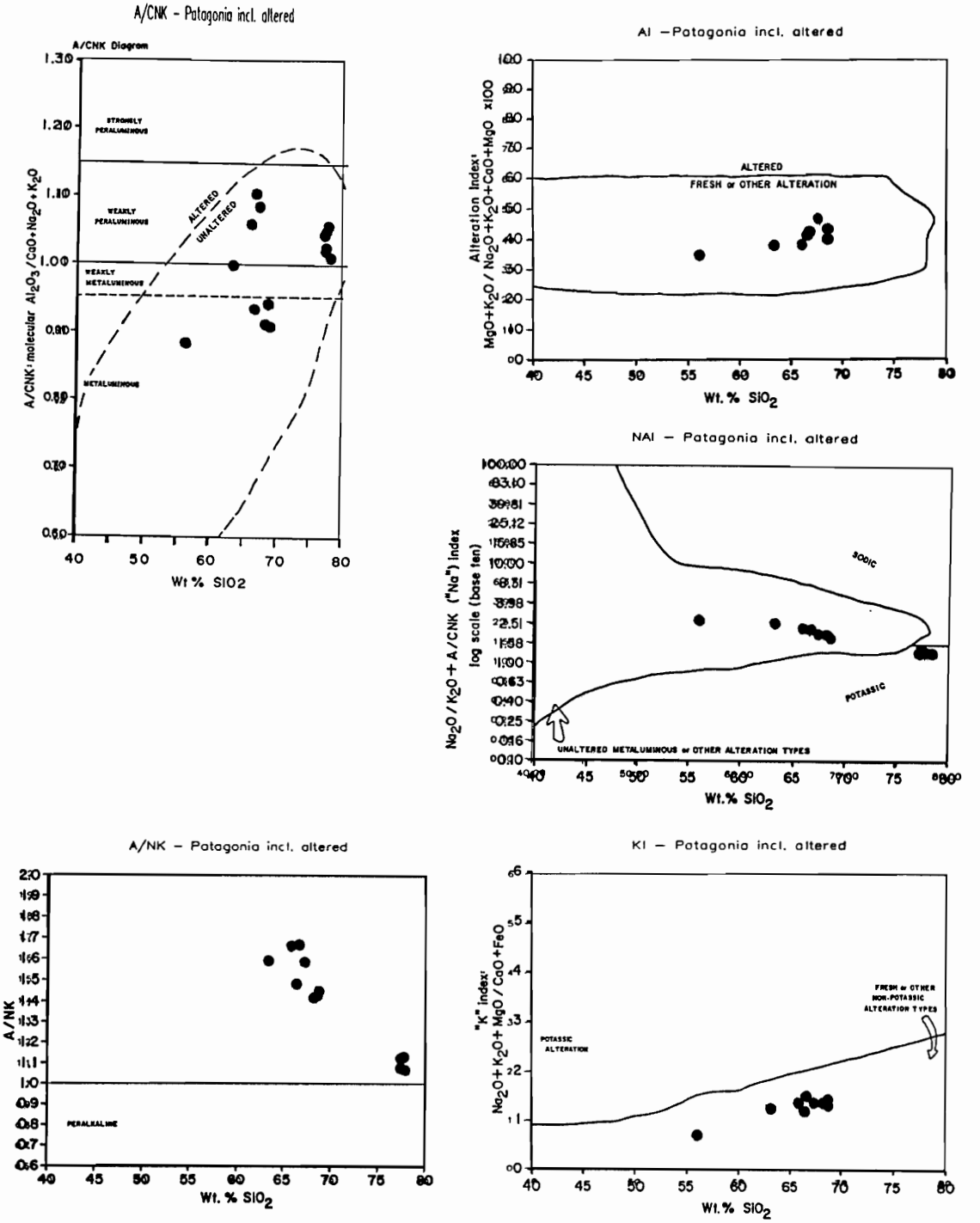

Figure 3-61. Petrochemical variation diagrams of the Patagonia pluton (Red Mountain mining area), Arizona, showing alteration filters.

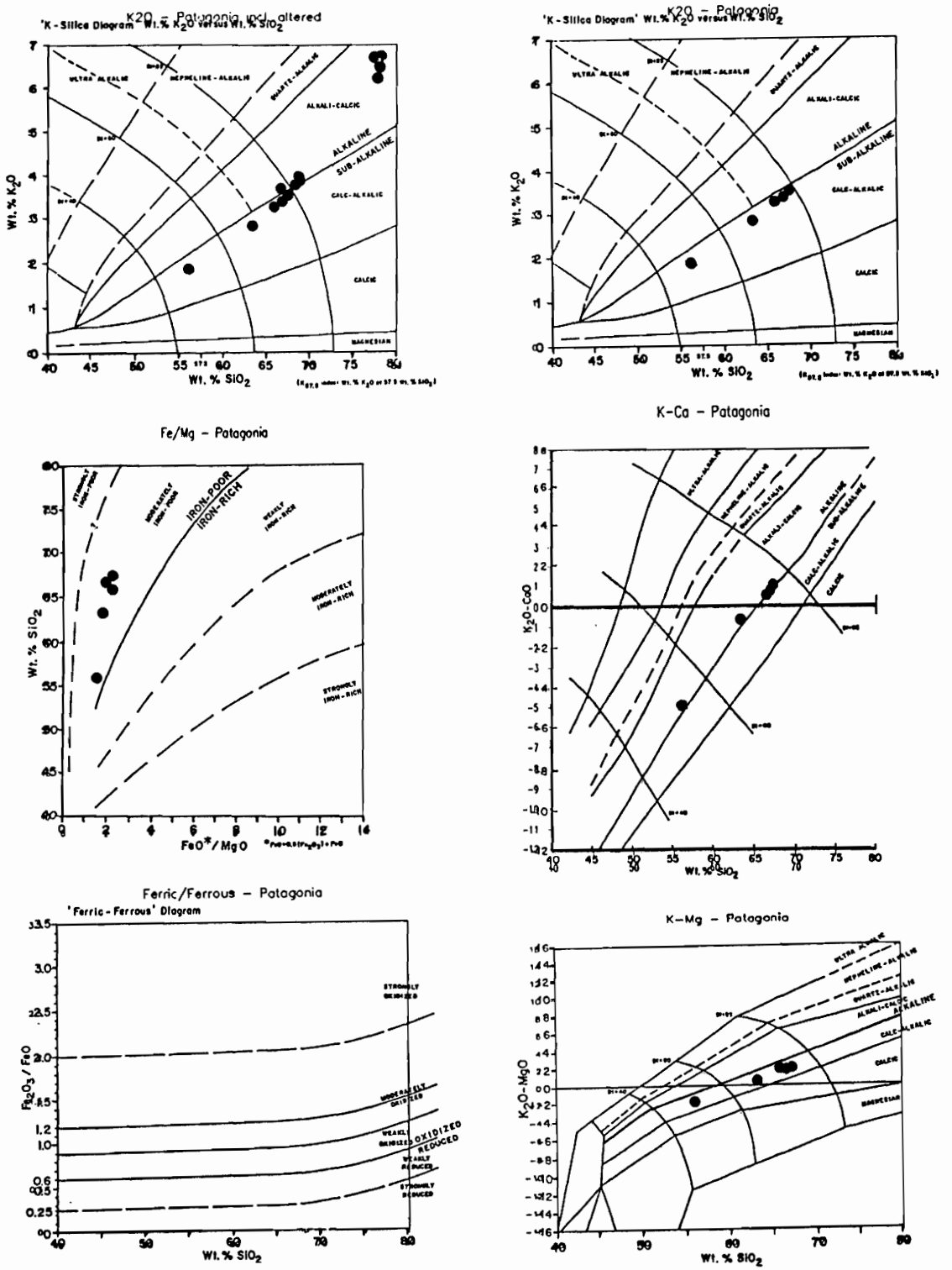

Figure 3-62. Petrochemical variation diagrams of the Patagonia pluton (Red Mountain), Arizona (alkalinity with and without altered; Fe/Mg).

Pinal County in east-central Arizona approximately 110 km (70 miles) north of Tucson. Most of the ore occurs in Precambrian diabase intruded into the Apache Group and in small intrusive bodies of a Laramide granodiorite, the Granite Mountain Porphyry (Cornwall, 1982) (Tgm on Figure 3-63 = CIMVS).

Laramide intrusive bodies were emplaced from 70 to 60 Ma and include the Tortilla Quartz Diorite (Kt) (average age of 70.4 Ma) and Rattler Granodiorite (Kr) (average age of 69.2 Ma), Tea Cup Granodiorite (Ttc) (average age of 62.1 Ma), Granite Mountain Porphyry (Tgm) (average of 60.9 Ma), Teapot Mountain Porphyry (Ttm) (younger than 63 Ma), and andesitic to quartz latitic dikes. These plutons are progressively more felsic, increasing in differentiation index with decreasing age (Cornwall, 1982) and are part of a comagmatic suite. Age relationships were determined by geologic relations (Cornwall and others, 1971) and by K-Ar and fission-track ages (Creasey and Kistler, 1962; Damon and Mauger, 1966; Damon, 1970; Banks and others, 1972; Banks and Stuckless, 1973; Creasey, 1983; Reynolds and others, 1986). Although mineralization occurred after emplacement of the Granite Mountain Porphyry, hydrothermal biotite intergrown with ore yielded anomalously old K-Ar apparent ages of 65 Ma (Banks and others, 1972).

Data for this study were obtained from Ransome (1919), Banks and others (1972), Creasey (1984), and Lang (1991). About half of the more than 30 samples did not pass the alteration filters (Figure 3-64). A comparison of the alkalinity diagrams for samples including and omitting altered sample data clearly indicate

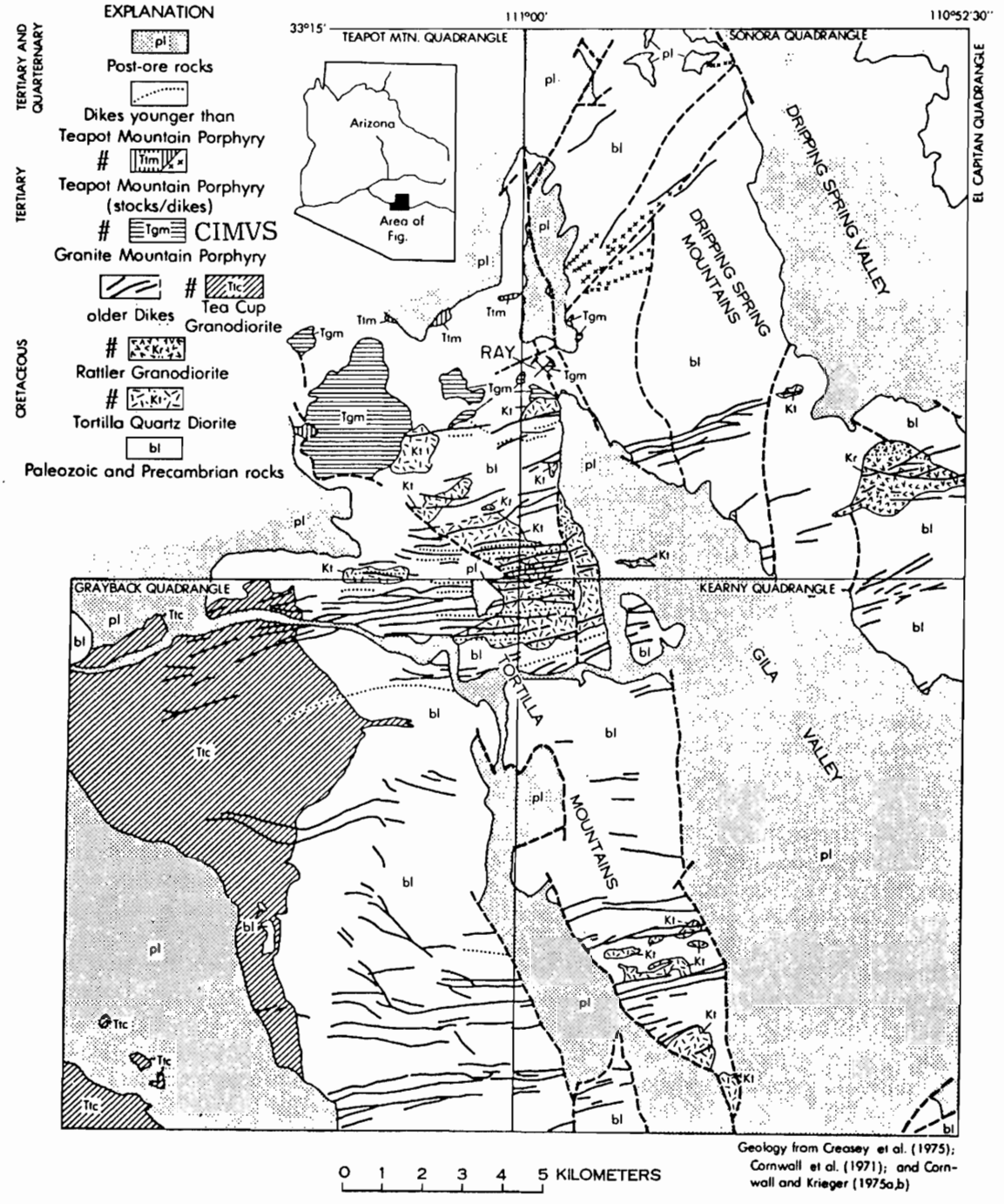

Figure 3-63. Geologic map of the Ray (Mineral Creek district), Arizona (# = CIMVS = Tortilla, Rattler, Tea Cup, Granite Mountain, and Teapot Mountain) (from Cornwall, 1982).

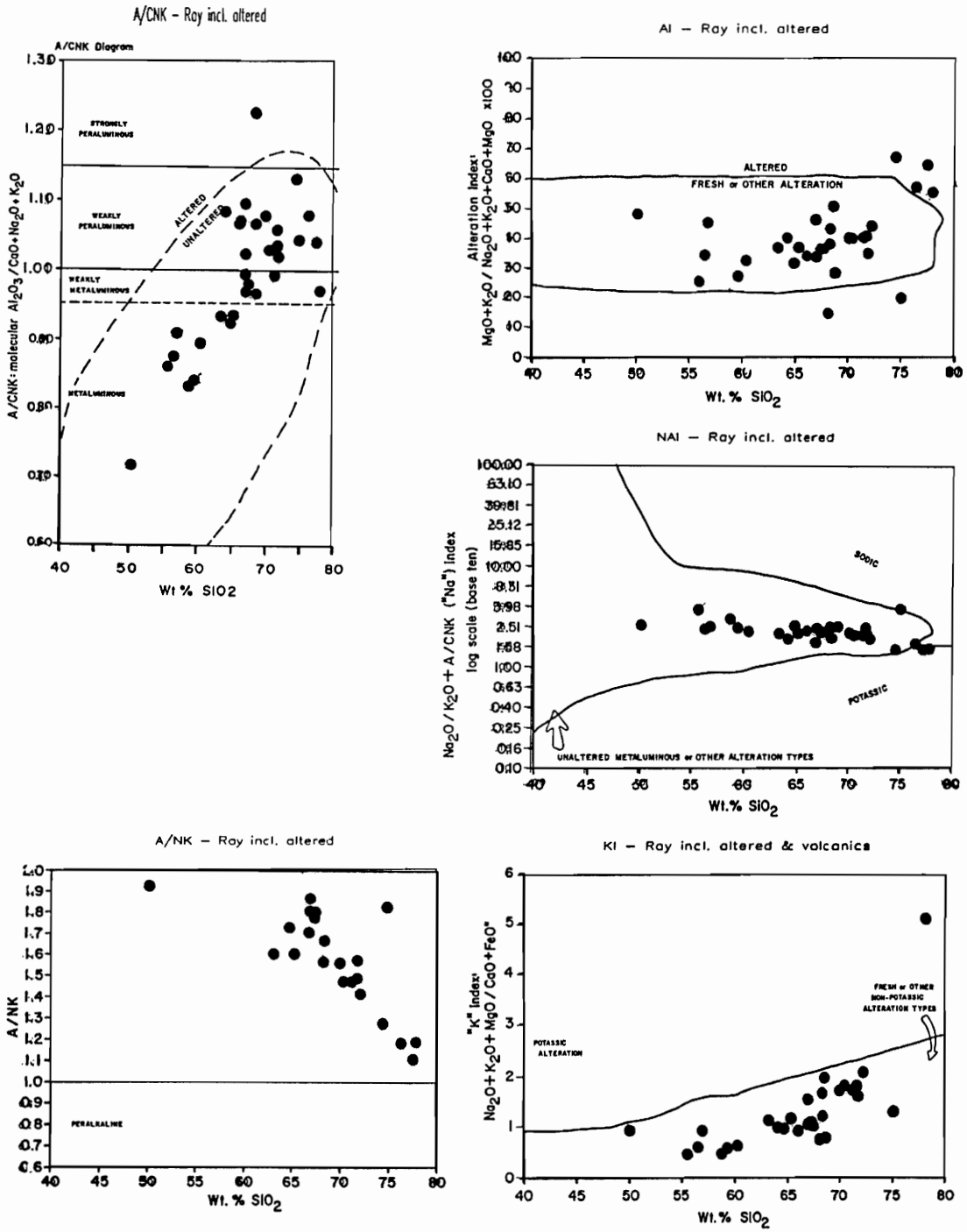

Figure 3-64. Petrochemical variation diagrams of igneous rocks from Ray (Mineral Creek mining district), Arizona, showing alteration filters.

calc-alkalic alkalinity for the Ray plutonic suite (Figure 3-65). The samples are moderately iron-poor on the FeO^*/MgO graphs and oxidized on the ferric/ferrous graphs (Figure 3-66).

Sierrita, AZ

The Pima district is on the east flank of the Sierrita Mountains approximately 30 km (20 miles) south of Tucson, Arizona; it is one of the premier porphyry copper districts in the world and includes the San Xavier North, Mission, Pima, Twin Buttes, Sierrita, and Esperanza porphyry copper mines (Figure 3-67) (Titley, 1982). The porphyritic phase of the Ruby Star granodiorite (CIMVS) (60-63 Ma) and its associated younger porphyries (55-58 Ma) are genetically related to mineralization at Sierrita, Esperanza, and Twin Buttes (Titley, 1982). Mineralization ages determined from alteration products are also about 58-60 Ma (Shafiqullah and Langlois, 1978). The quartz monzonite porphyry differentiate of the batholithic Ruby Star Granodiorite is intimately associated with mineralization and alteration in the Sierrita-Esperanza system, and is considered to be the source of metal-bearing hydrothermal solutions (West and Aiken, 1982).

Whole rock chemical data for samples included in this study were obtained from Anthony (1986), Hess (1986), Laine (1974), Mauger (1966), Hillman (1972), and Smith (1975). About half of the samples did not pass the alteration filters (Figure 3-68) and were not used in the neural network study. The older

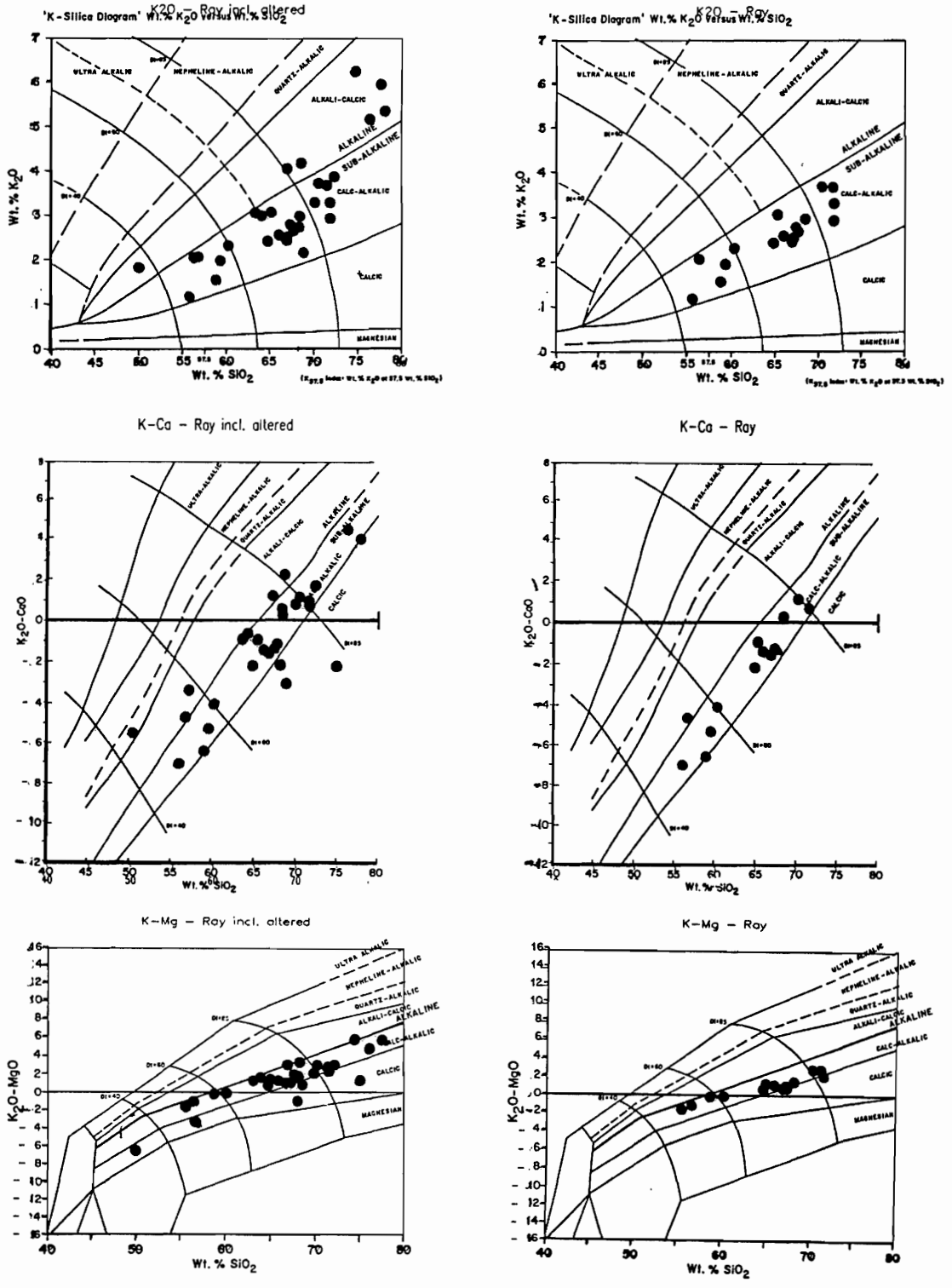

Figure 3-65. Magma series diagrams of igneous rocks from Ray, Arizona, showing alkalinity (left side includes altered; right side is unaltered samples).

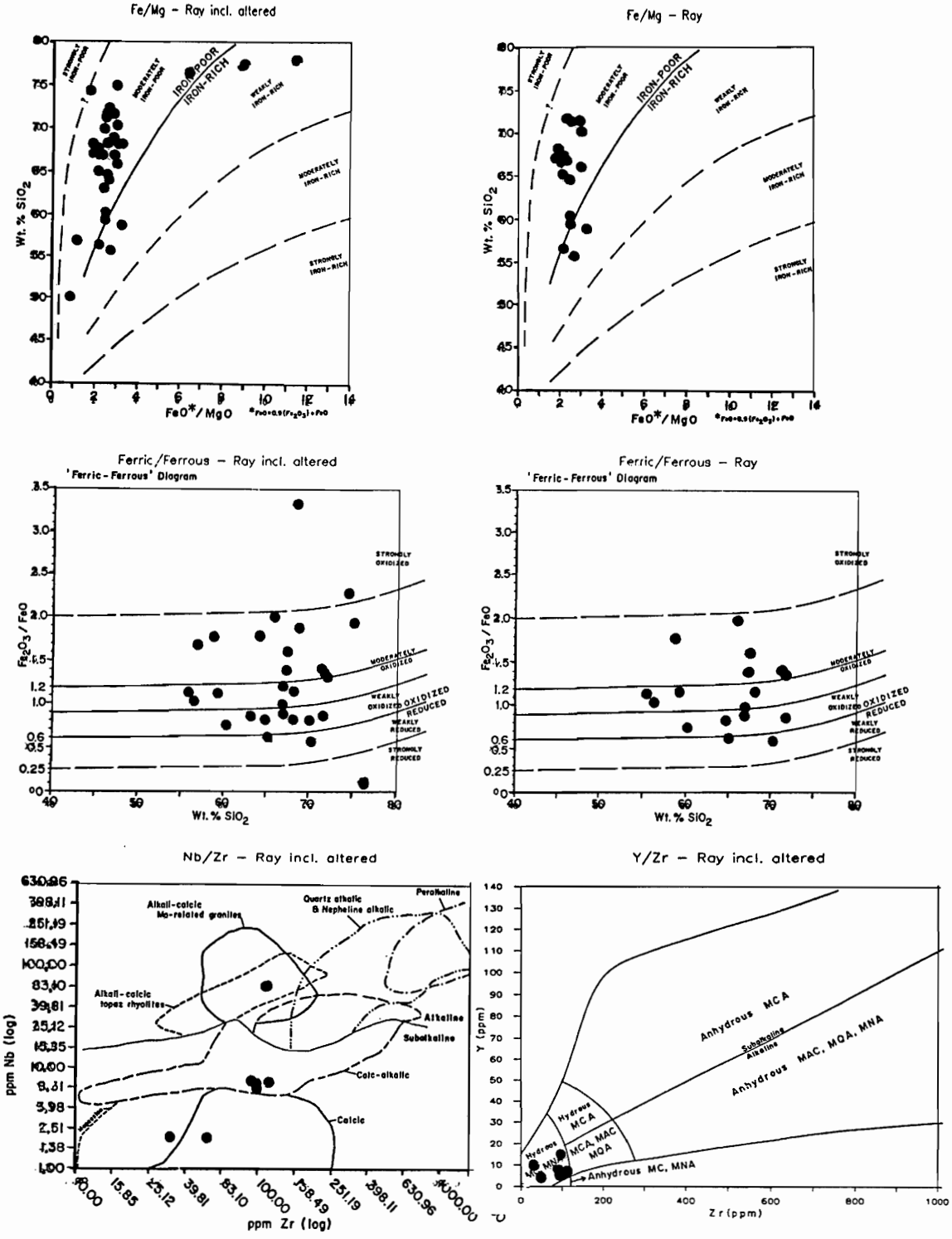

Figure 3-66. Petrochemical variation diagrams of igneous rocks from Ray, Arizona, showing iron ratios (left side includes altered; right side is unaltered samples) and Nb/Zr and Y/Zr ratios.

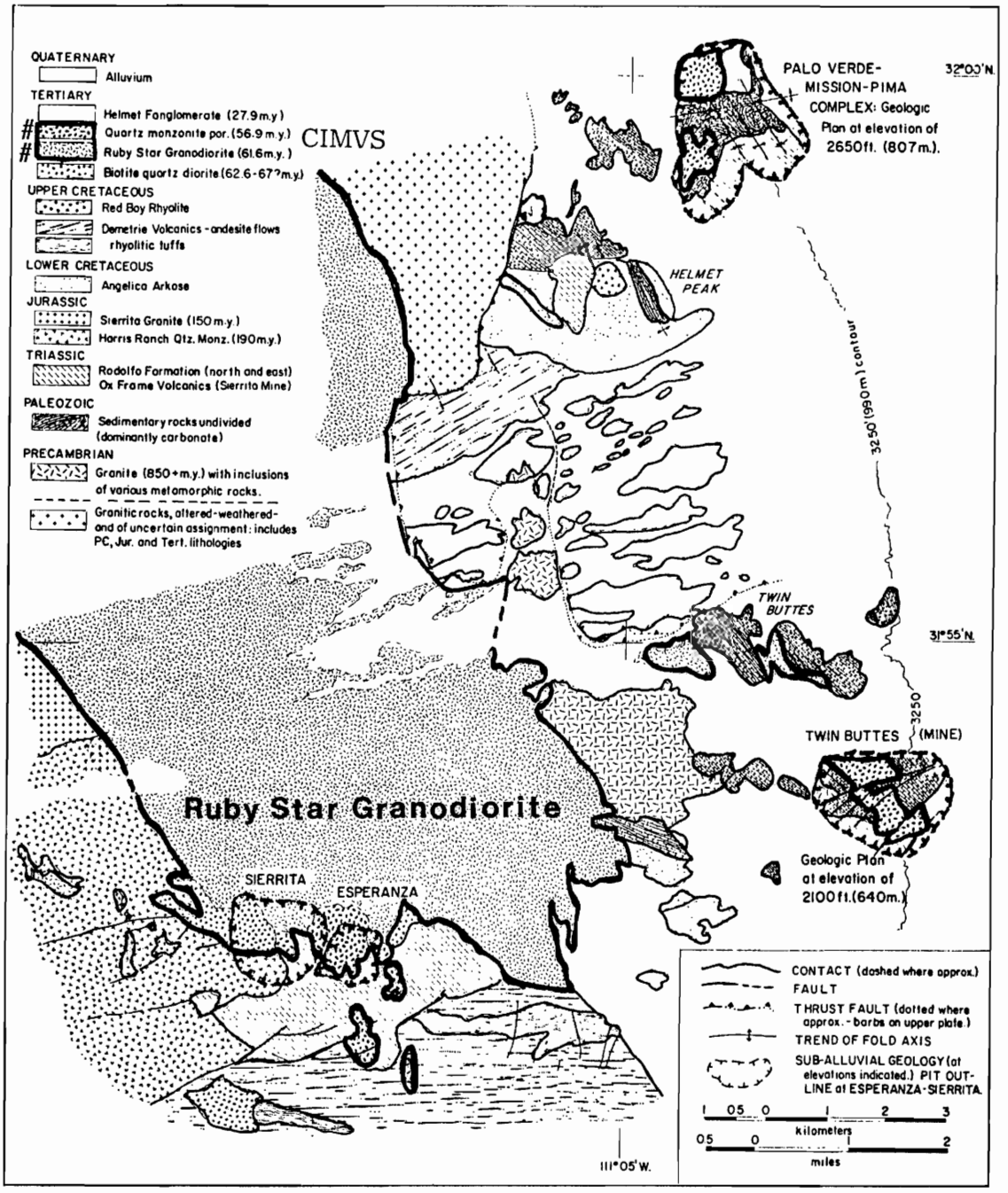

Figure 3-67. Geologic map of the Pima district, Arizona (# = CIMVS = Ruby Star Granodiorite and quartz monzonite porphyry) (from Titley, 1982).

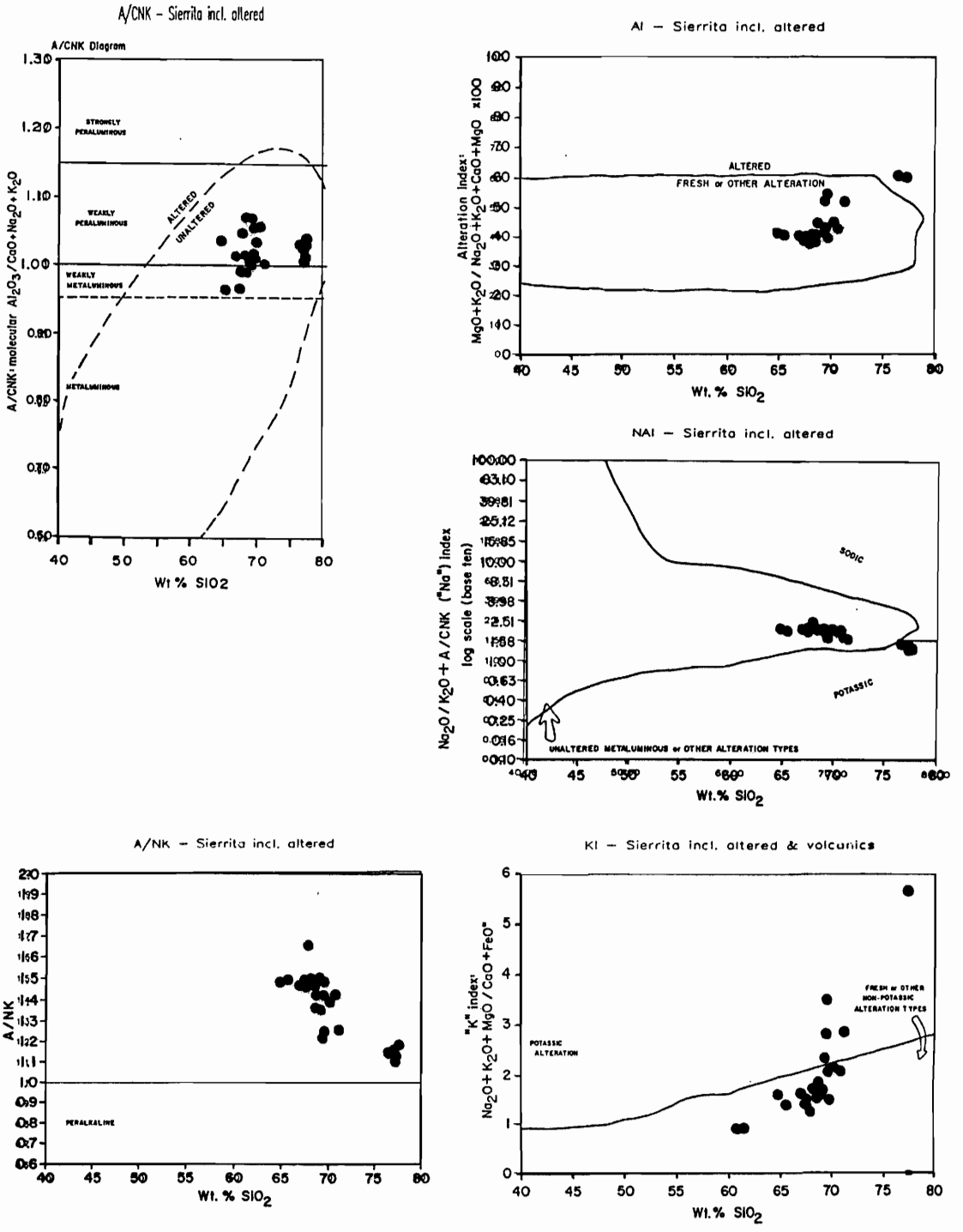

Figure 3-68. Petrochemical variation diagrams of the Ruby Star pluton (Pima mining district), Arizona, showing alteration filters.

(Cretaceous) igneous rocks [Demetrie Volcanics (67 Ma, Titley and Beane, 1981), Red Boy Rhyolite, and biotite quartz diorite (67 Ma, Cooper, 1973)] were plotted separately from the younger Ruby Star granodiorite and associated quartz monzonite porphyries (58.7, 59.0, 61.6, 63.1 Ma, Damon, 1966; Damon, 1965; Cooper, 1973; Marvin and others, 1973). The Cretaceous igneous rocks are in the alkali-calcic field on the alkalinity variation diagrams, whereas the Tertiary plutons are in the calc-alkalic fields (Figure 3-69). The younger intrusions related to porphyry copper mineralization are in the moderately iron-poor field, whereas the earlier barren quartz diorite and related volcanics are in the weakly iron-rich field of the FeO^*/MgO graph (Figure 3-70). Most of the chemical analyses did not analyze for both Fe_2O_3 and FeO, so do not appear on the ferric/ferrous diagram (Figure 3-70). However, Anthony (1986) recorded ferrous/total iron ratios by wet chemical analysis of 0.5 and 0.48, which gives a ferric/ferrous ratio of 1.0; this ratio is in the oxidized field, which is consistent with reported magnetite and sphene and the absence of ilmenite.

Calc-alkalic, Weakly Oxidized

Ajo, AZ

The Ajo porphyry copper mine is in the Little Ajo Mountains in western Pima County approximately 200 km (130 miles) west of Tucson, Arizona, along State Highway 86 (Dixon, 1966). It is a porphyry copper-gold type of deposit similar to the Lone Star mining district in Graham County, Arizona (Hagstrum and

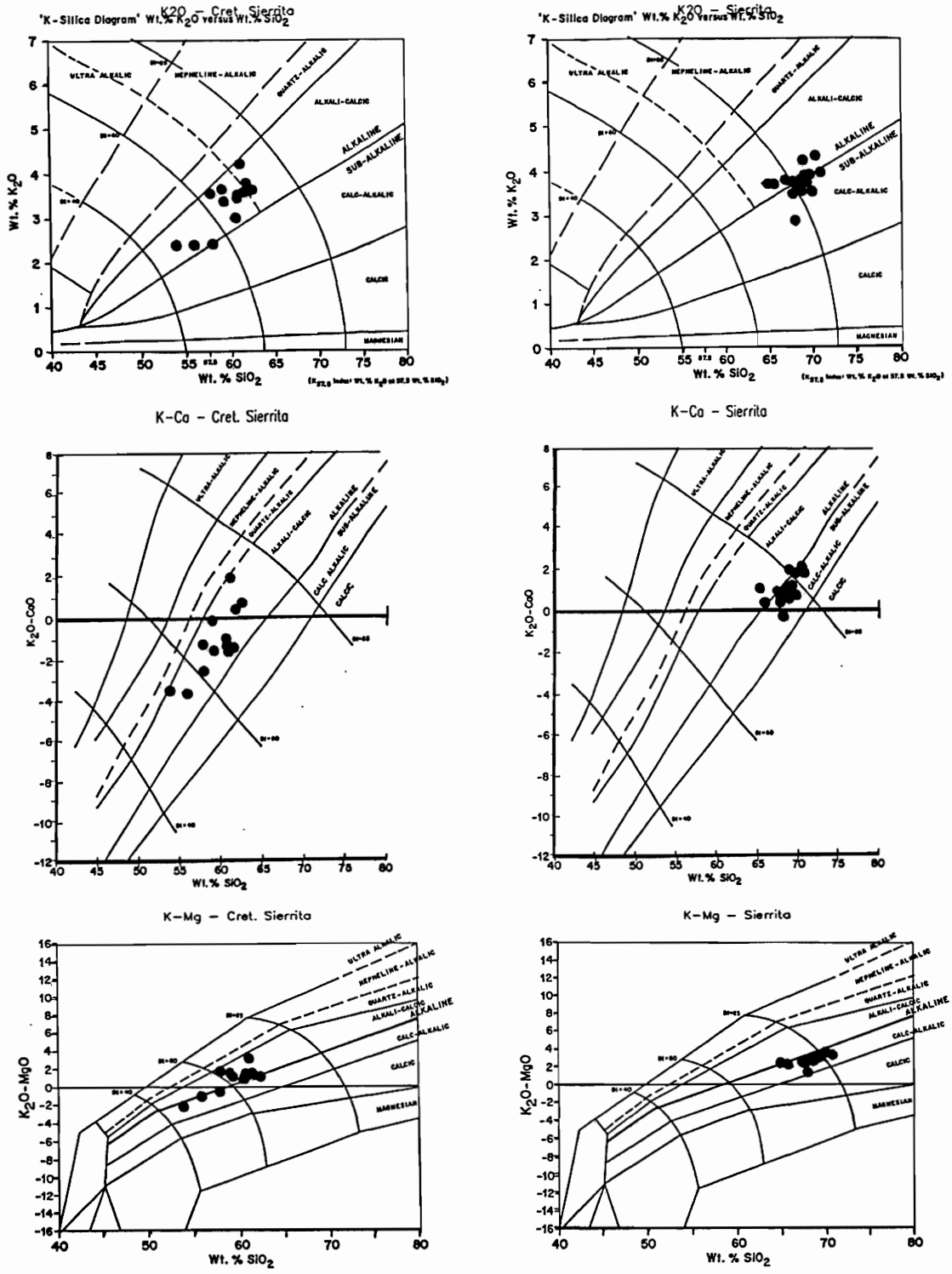

Figure 3-69. Petrochemical alkalinity graphs of Cretaceous (left side) and Tertiary (right = Ruby Star Granodiorite) rocks, Pima district, Arizona.

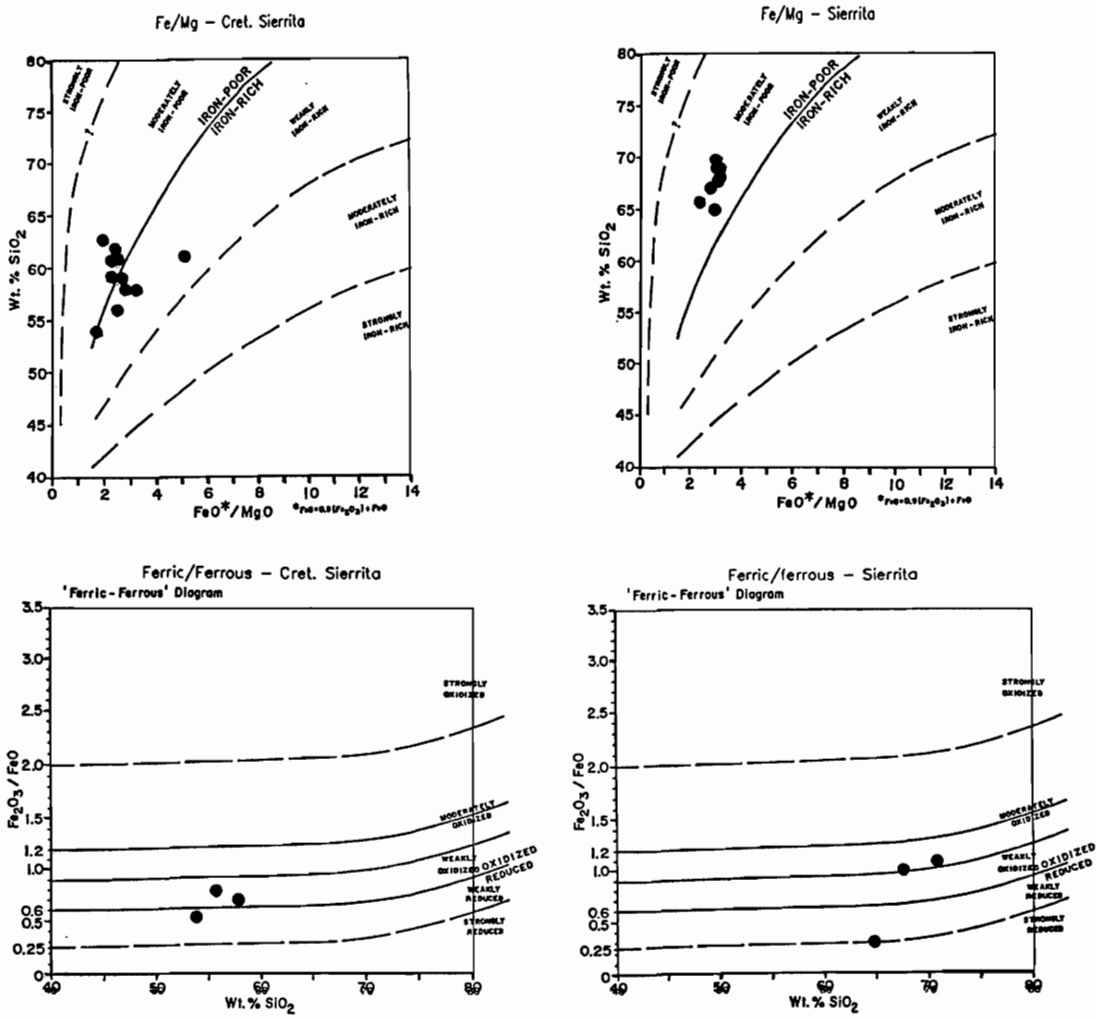

Figure 3-70. Petrochemical diagrams of Cretaceous (left side) and Tertiary (right = Ruby Star Granodiorite) rocks, Pima, AZ, showing iron ratios.

others, 1987). Earlier workers in the Ajo mining district concluded that the orebody is associated with the porphyritic phase of the Cornelia quartz monzonite in the displaced apex of a large pluton (the equigranular phase of the Cornelia quartz monzonite) that is exposed west of the mine area (Gilluly, 1946; Wadsworth, 1968). The Cogenetic Igneous-Metal-Volatile Suite (CIMVS) is represented on Figure 3-71 by Granodiorite porphyry, Granodiorite, and Fine-grained diorite at Camelback Mountain and at the New Cornelia Mine). The granodiorite and granodiorite porphyry of the Camelback Mountain block that is associated with the New Cornelia mine (Gilluly's porphyritic phase of the Cornelia quartz monzonite) yield K-Ar ages on biotite of 62.9 to 64.2 $\pm$ 1.9 Ma (McDowell, 1971, recalculated in Hagstrum and others, 1987).

Although fluid inclusions (Cox and others, 1981) and alteration assemblages (Cox and Ohta, 1984) indicated the presence of mineralization and suggested a cogenetic relationship between the western pluton and the orebody, recent age dates confirm a mid-Tertiary age for the western pluton (Fine-grained granite, monzogranite, and monzodiorite in Figure 3-71). Recalculated K-Ar ages on biotite and hornblende from the monzogranite and monzodiorite of the Cardigan Peak block west of the mine range from 19.6 $\pm$ 1.3 to 23.0 $\pm$ 0.7 Ma (McDowell, 1971; Hagstrum and others, 1987); these mid-Tertiary ages are supported by unpublished U-Pb data (Hagstrum and others, 1987).

Whole rock analyses for this study were obtained from Gilluly (1937; 1946), Dewhurst (1976), and Laine (1974) (Appendix B). Most of the samples did

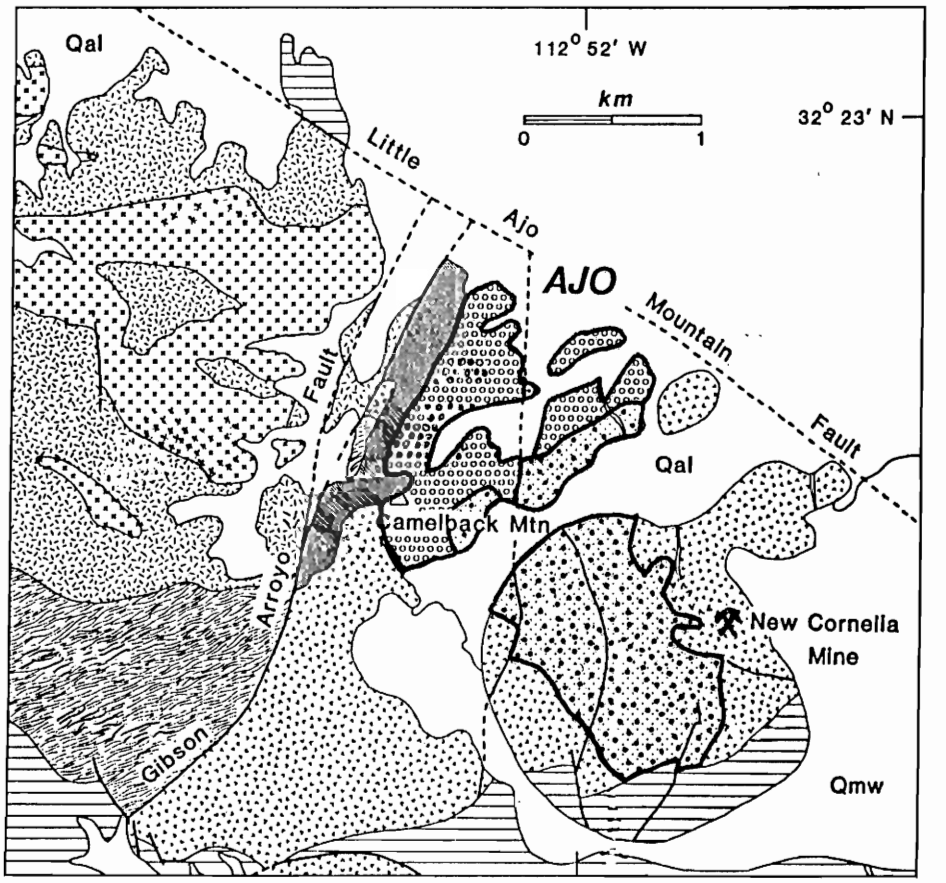

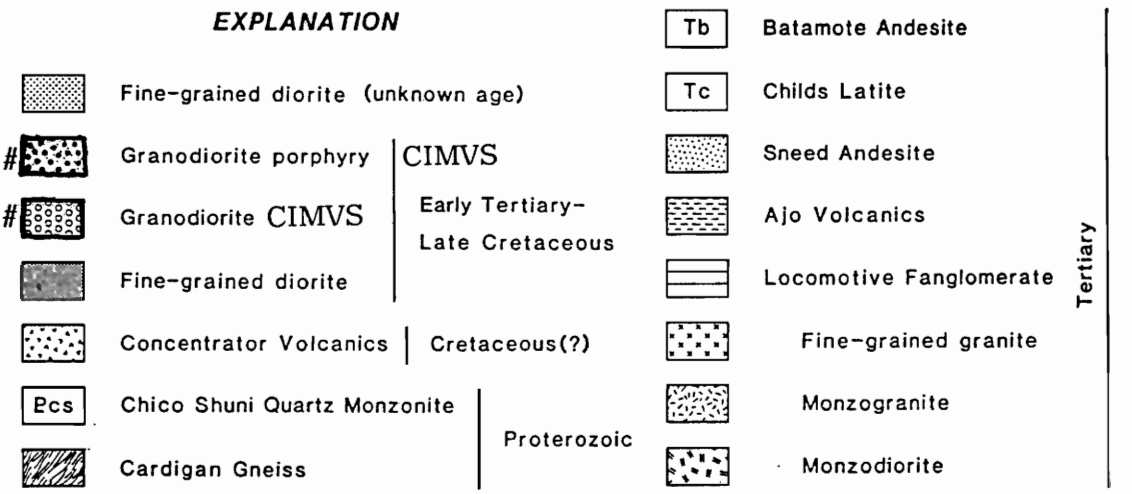

Figure 3-71. Geologic map of the Cornelia pluton (Ajo district), Arizona (# = CIMVS) (modified from Hagstrum and others, 1987).

not pass the alteration filters (Figure 3-72) and were not used for the neural network study. The unaltered samples from the western equigranular phase (the mid-Tertiary pluton), such as numbers 3 and JD-25, are in the alkali-calcic field, whereas the unaltered samples from the eastern porphyritic phase (the Laramide pluton), such as numbers 4, A-19, and A-41, are in the calc-alkalic field or just over the boundary within the 15 percent overlap (Figure 3-73). Gilluly also noted that samples from the porphyritic phase had about 2 percent less 'potassa' than those from the equigranular phase (Gilluly, 1937, p. 38). This difference in alkalinity is additional evidence that the two plutons are of different ages.

Iron ratios of the Laramide samples of the Cornelia pluton are in the weakly iron-poor field in the FeO^*/MgO graph (Figure 3-74). The graph of ferric/ferrous ratios including altered samples range from reduced to oxidized; that there are any reduced samples at all suggests that the oxidation state is more reduced than is indicated on the graph of unaltered samples, which are in the oxidized field. The presence of ilmenite (Thomas and Gibbs, 1983) and the relative rarity of magnetite as an accessory also suggests a weakly oxidized category for the porphyritic phase of the Cornelia pluton.

Copper Canyon, NV

The Copper Canyon 'wallrock' porphyry copper-gold deposit is in north-central Nevada approximately 20 km (12 miles) southwest of Battle Mountain, Lander County, Nevada (Theodore and Blake, 1975). Thrust plates of lower to

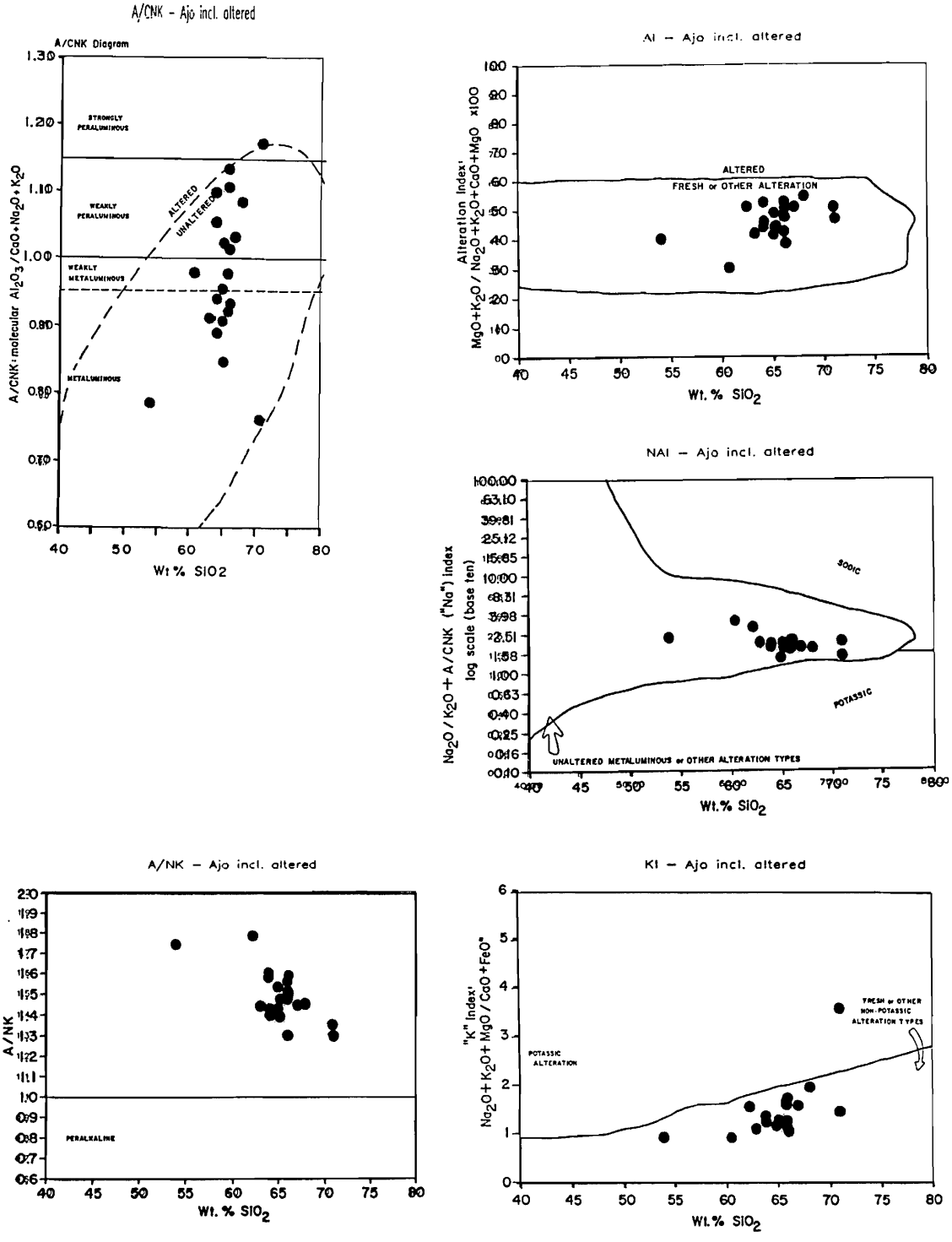

Figure 3-72. Petrochemical variation diagrams of the Cornelia pluton (Ajo mining district), Arizona showing alteration filters.

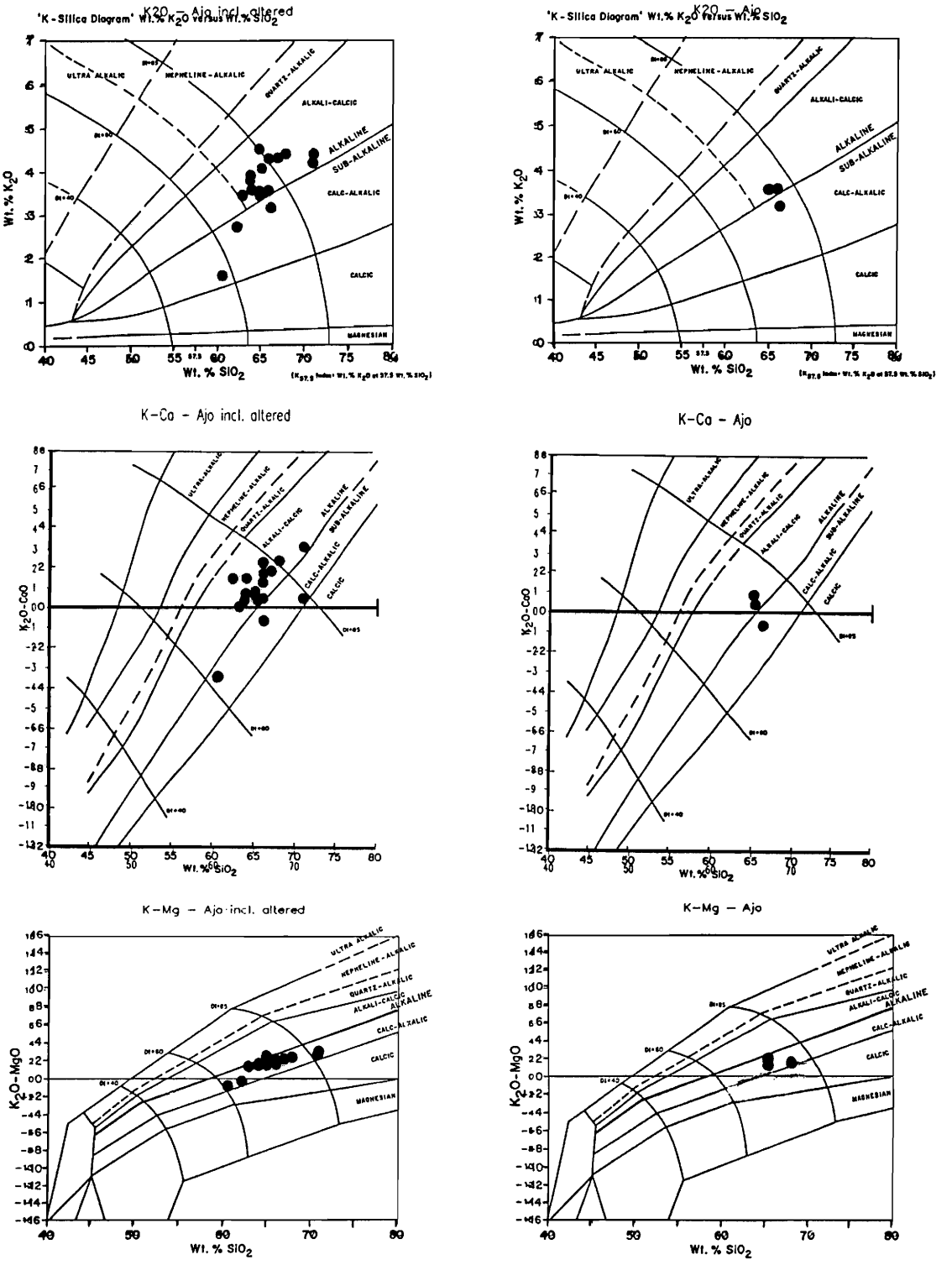

Figure 3-73. Magma series alkalinity diagrams of the porphyritic phase of the Cornelia pluton, Ajo, AZ (left includes altered; right is unaltered only).

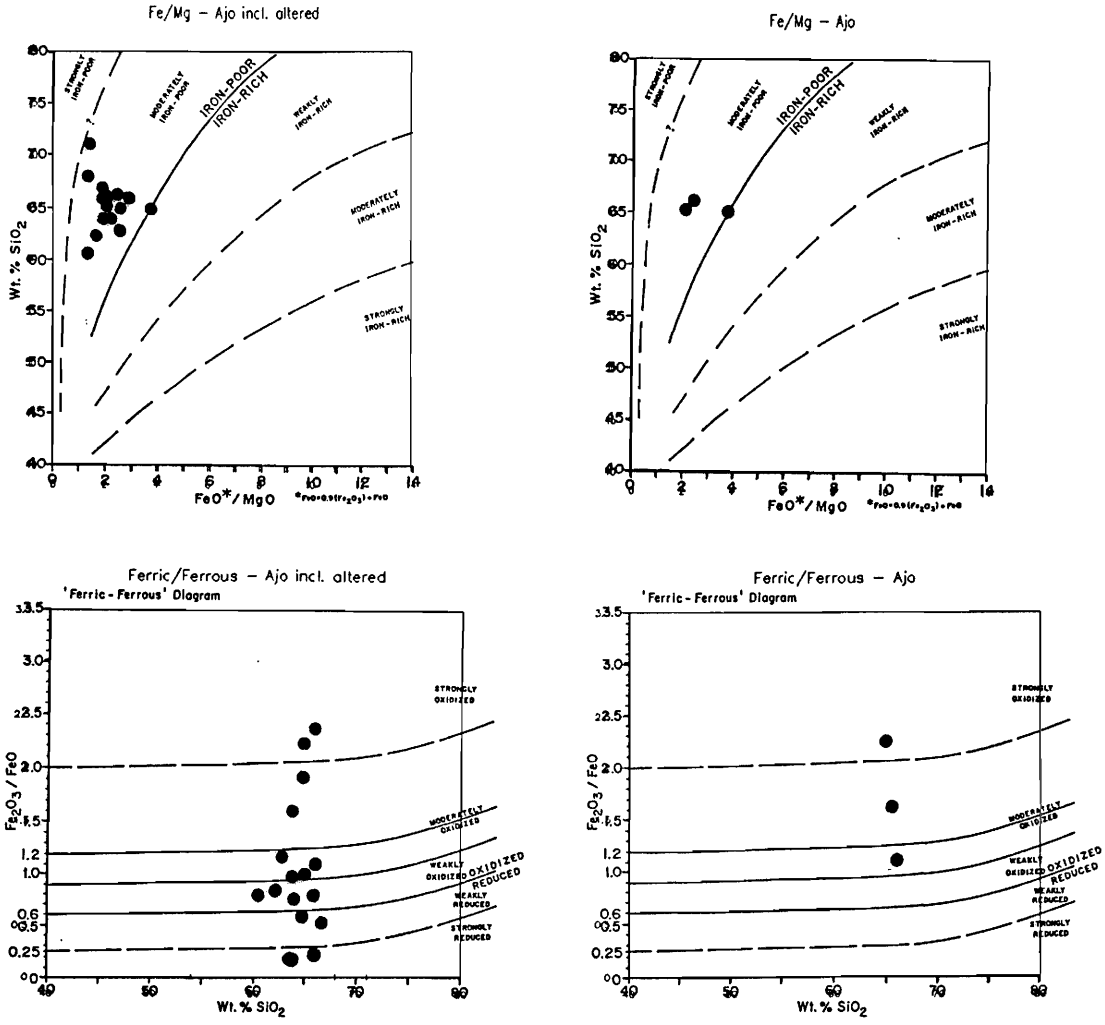

Figure 3-74. Petrochemical iron ratio diagrams of the porphyritic phase of the Cornelia pluton, Ajo, AZ (left includes altered; right is unaltered only).

upper Paleozoic sedimentary rocks were intruded by Tertiary granodiorite stocks and dikes from 41 to 38 Ma. The former calcareous sedimentary rocks were altered into calc-silicate assemblages containing mineralization as disseminations and massive sulfide replacements and veins and veinlets in wallrocks (Wotruba and others, 1986). The CIMVS is represented by the Quartz diorite and Altered granodiorite porphyry of Copper Canyon in Figure 3-75. K-Ar ages of the altered granodiorite associated with the nearby porphyry copper deposit averages 38.2 Ma and the age of metallization in the deposit averages 37.2 Ma (Theodore and others, 1973).

Base- and precious-metal deposits are arranged in zones around the Tertiary granodiorite. The Copper Canyon porphyry copper-gold deposit (the Copper Canyon Underground, East, and West ore bodies) is in a central copper-gold-silver zone, the Tomboy-Minnie and Fortitude gold skarn deposits are in the adjacent gold-silver zone, and minor galena-silver occurrences are in the outermost lead-zinc-silver zone (Roberts and Arnold, 1965; Blake and others, 1984; Myers, 1990).

Whole rock analyses of samples from the Copper Canyon granodiorite were obtained from Theodore and others (1973) and from Roberts (1964). Although most of the rocks in the mine area are altered, these samples passed the alteration filters (Figure 3-76) and are in the calc-alkalic, moderately iron-poor, and weakly reduced fields on the magma series diagrams (Figure 3-77). The Copper Canyon stock is reduced relative to most other porphyry copper-related

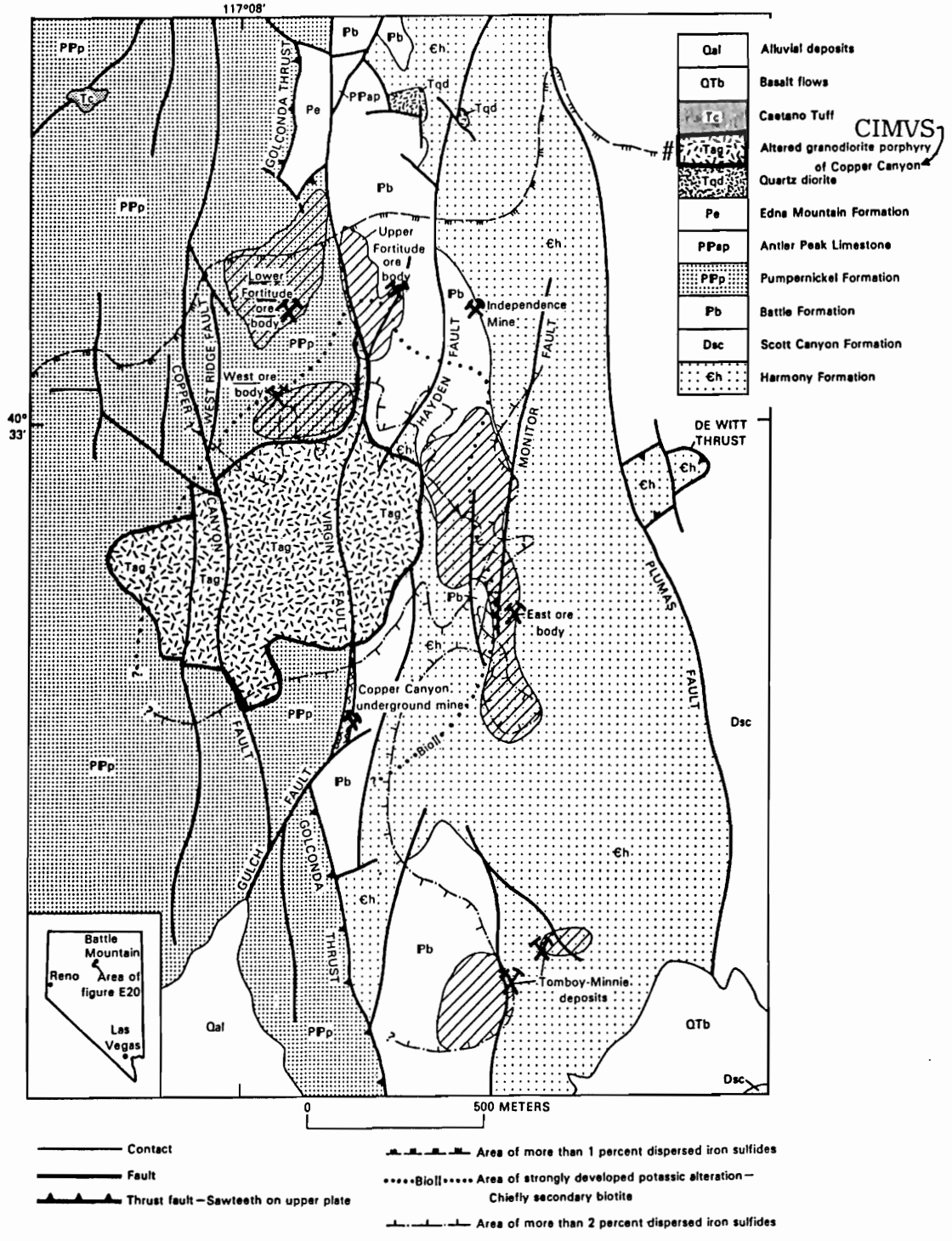

Figure 3-75. Geologic map of Copper Canyon area (Battle Mountain district), NV (CIMVS = # = porphyry of Copper Canyon) (Theodore and others, 1990).

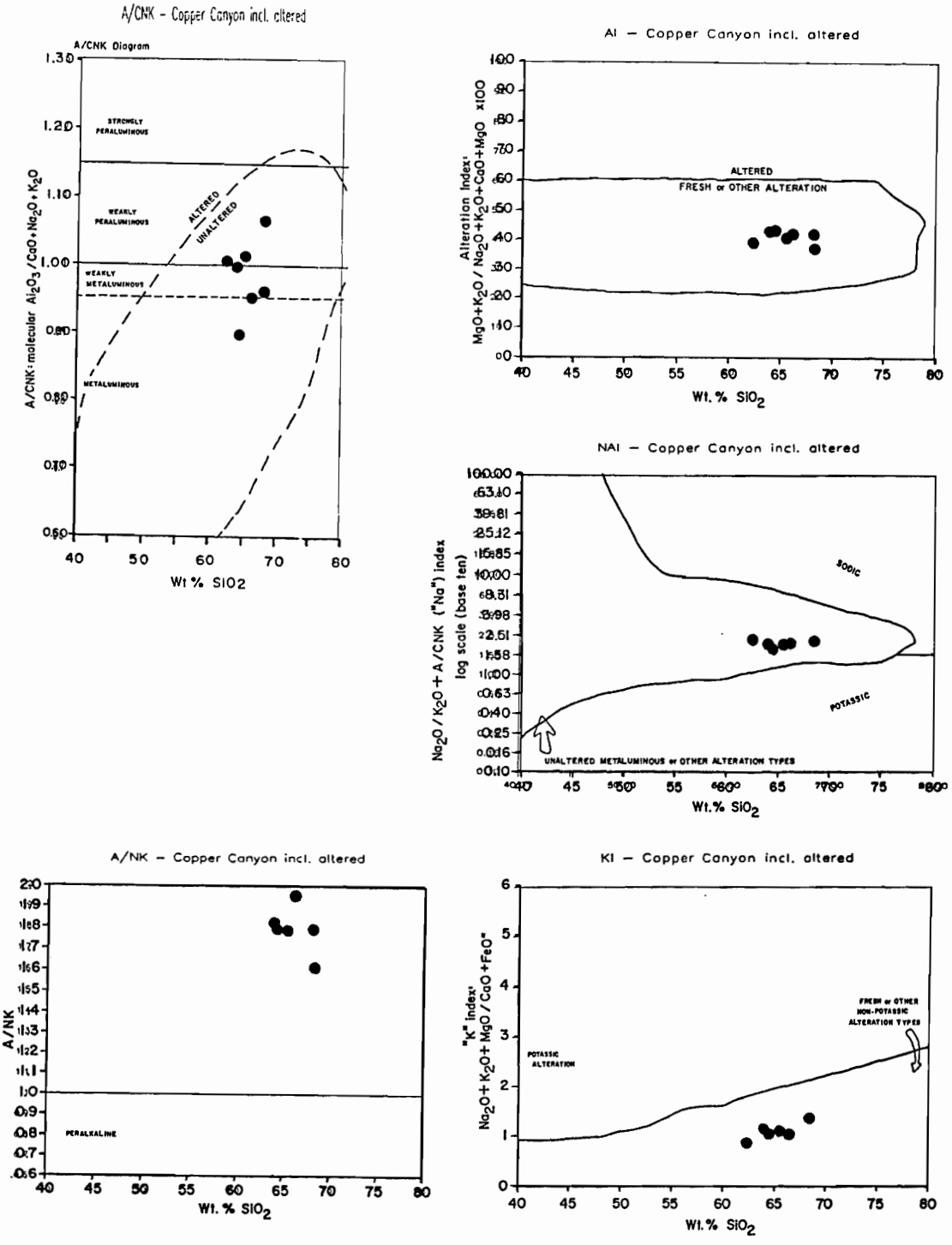

Figure 3-76. Petrochemical variation diagrams of igneous rocks from the Copper Canyon district, Nevada, showing alteration filters.

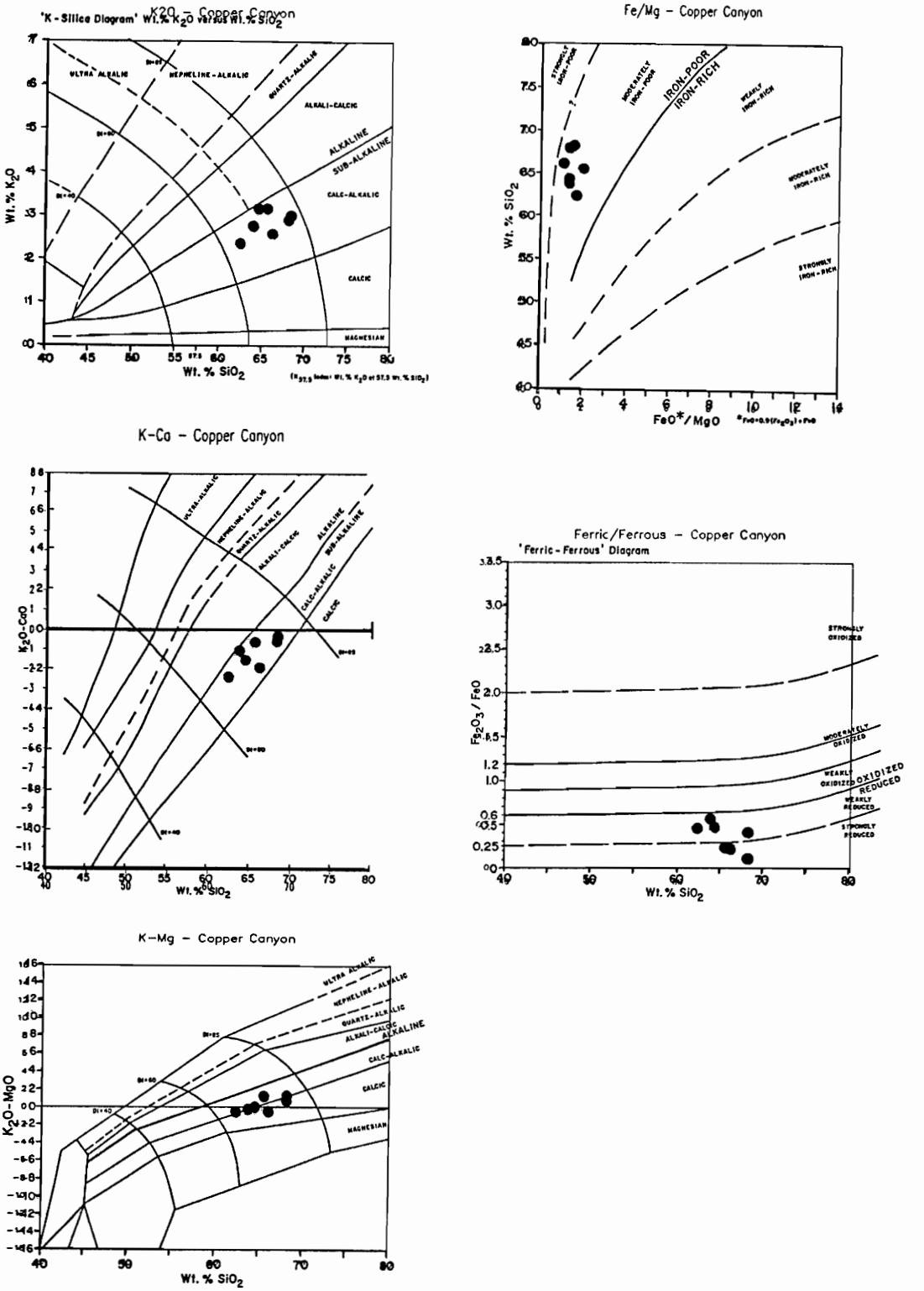

Figure 3-77. Magma series variation diagrams of igneous rocks from the Copper Canyon district, Nevada, showing alkalinity and iron ratios.

plutons in that whole rock ratios of Fe_2O_3/FeO are less than 0.5 (Myers and Meinert, 1991).

Dexing, CHINA

The Dexing porphyry copper deposit in Jiangxi province of China consists of three large-scale deposits, the Tongchang, Fujiawu, and Zhushahong deposits, which have reserves of 8.53 million tons of copper (Yan and Hu, 1980). The deposits show a close genetic connection to granodiorite porphyry of middle Jurassic age [161-170 Ma by the K-Ar method on biotite (Yan and Hu, 1980)]. Granodiorite porphyry stocks on Figure 3-78 are marked with small pluses and represent the CIMVS). The stocks intrude alternating beds of sericite phyllite and meta-tuff of the Sinian subgroup dated at 1400 Ma by the Rb-Sr method. The intrusions occur in a northwest-trending zone at fault and fold intersections (Yan and Hu, 1980; Chung-Wen, 1981). Ore bodies are localized at the contact zone of the porphyry stocks and show zoning symmetrical about the intrusions from the center outwards of molybdenite-chalcopyrite-specularite-sphalerite and galena (Chung-Wen, 1981).

Whole rock analyses used in this study were obtained from Yan and Hu (1980) and Chung-Wen (1981). Most of the samples passed the alteration filters (Figure 3-79) and are in the calc-alkalic field or in the 15 percent overlap zone (Figure 3-80). The iron ratios are in the moderately iron-poor field on the FeO^*/MgO diagram and the weakly oxidized field in the ferric/ferrous diagram.

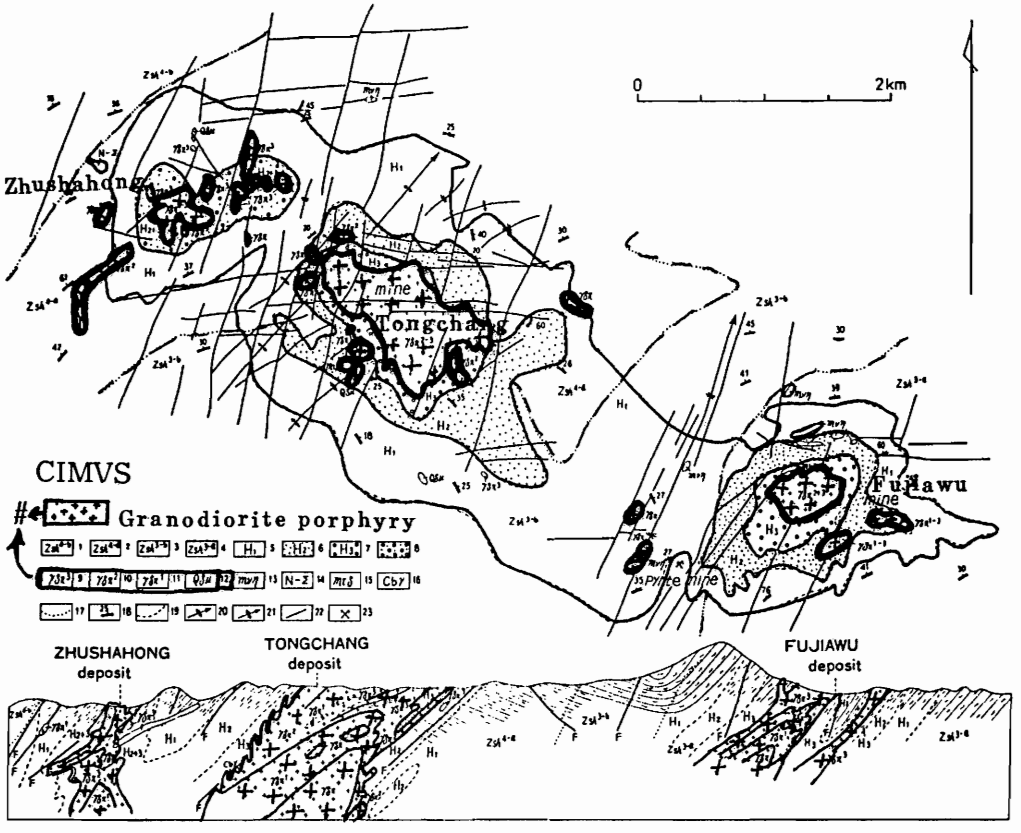

Geological sketch map of Dexing porphyry copper (-molybdenum) district.

1. Upper portion of the 4th member of Shuangqiaoshan group of Sinian suberathem; 2. Lower portion of the 4th member of Shuangqiaoshan group of Sinian suberathem; 3. Upper portion of the 3rd member of Shuangqiaoshan group of Sinian suberathem; 4. Lower portion of the 3rd member of Shuangqiaoshan group of Sinian suberathem; 5. Weakly altered phyllite (meta-tuff); 6. Moderately altered phyllite (meta-tuff); 7. Strongly altered phyllite (meta-tuff); 8. Moderately and strongly altered phyllite (meta-sedimentary-tuff); (9) Strongly altered granodiorite porphyry; (10) Moderately altered granodiorite porphyry; (11) Weakly altered granodiorite porphyry; (12) Quartz diorite porphyry; 13. Meta-diabase (diabase porphyry); 14. Gabbro-pyroxenite; 15. Fine-grained metadiorite; 16. Contact breccia; 17. Boundary of rock formation; 18. Schistosity occurrence; 19. Boundary of alteration zone; 20. Anticline and its pitch direction; 21. Syncline and its pitch direction; 22. Fault; 23. Pyrite ore pits.

Figure 3-78. Geologic map of the Dexing mining area, China, showing mines and Granodiorite porphyry (# = CIMVS) (modified from Yan and Hu, 1980).

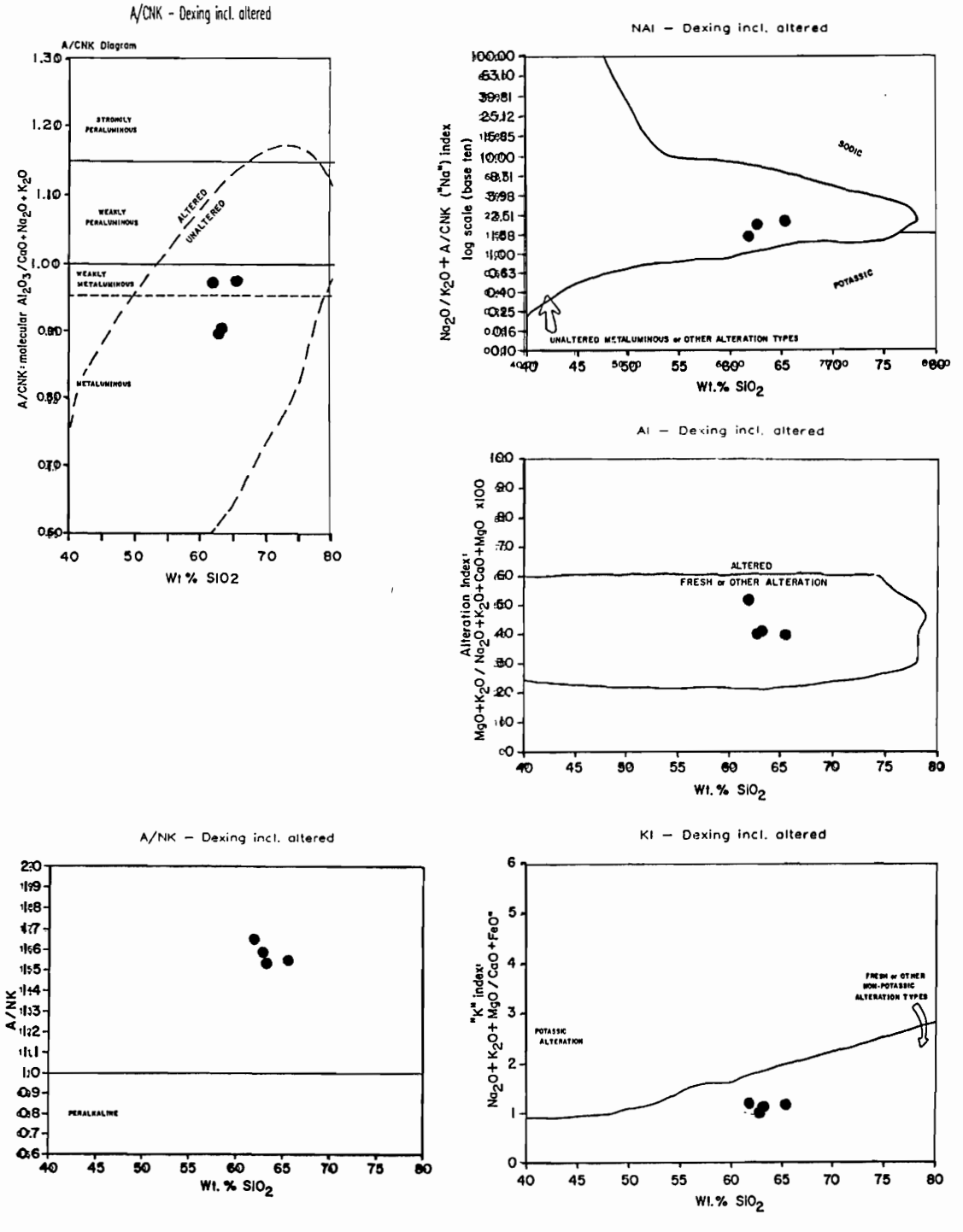

Figure 3-79. Petrochemical variation diagrams of igneous rocks from the Dexing mining area, China, showing alteration filters.

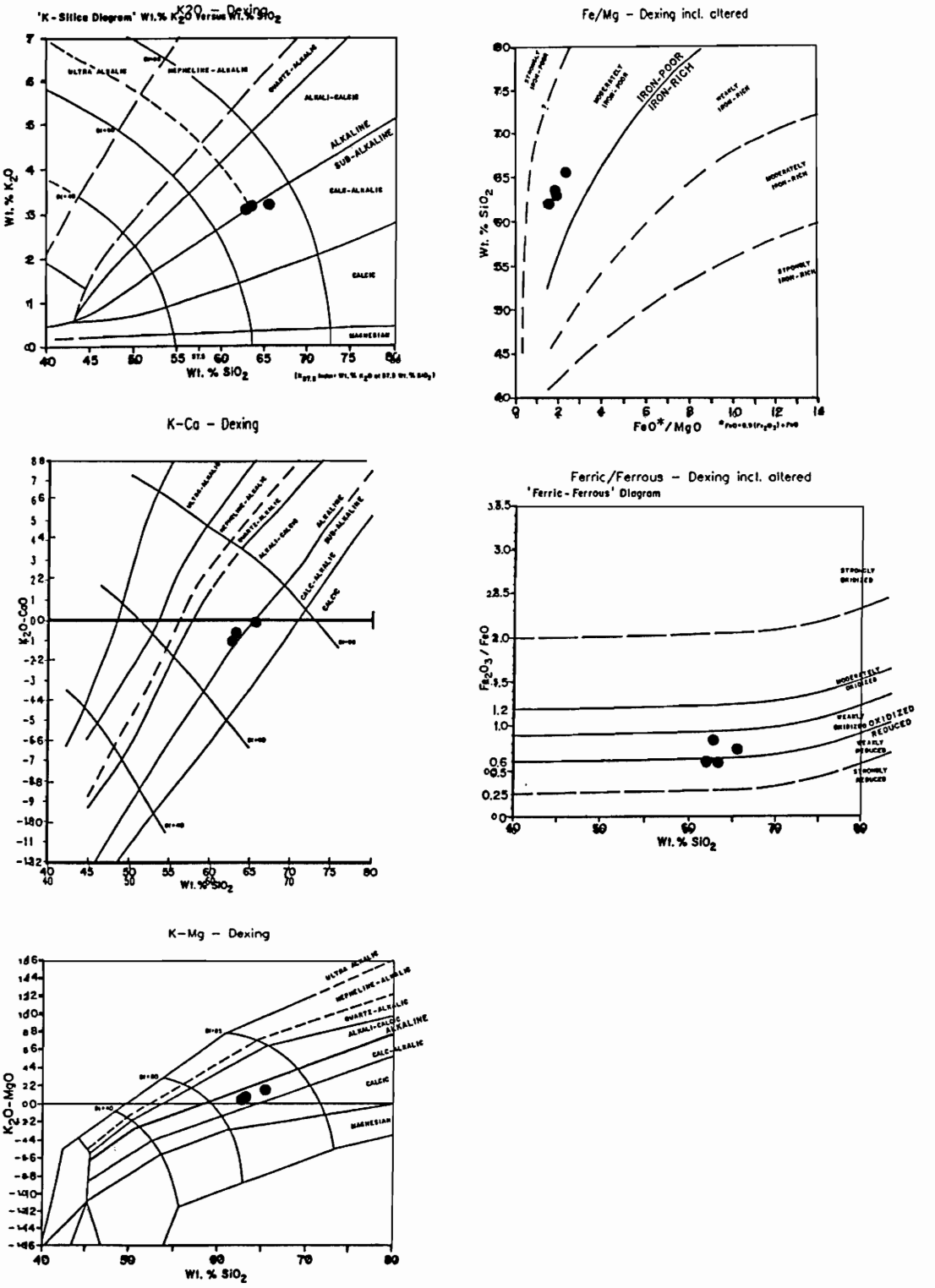

Figure 3-80. Magma series variation diagrams of igneous rocks from the Dexing mining area, China, showing alkalinity and iron ratios.

Dos Pobres, AZ

The Dos Pobres porphyry copper deposit is in the Lone Star mining district on the southwest slope of the Gila Mountains in Graham County, eastern Arizona. The Dos Pobres orebody occurs in folded Safford metavolcanics consisting of hornblende and pyroxene andesite flows and agglomerates, latites and dacites. Contact metamorphism by granodiorite has been dated at 69.8 $\pm$ 2.7 Ma (Langton and Williams, 1982). The principal productive porphyry in the Dos Pobres orebody is quartz monzonite, ranging to tonalite or granodiorite and appearing as dikes or fragments of dikes in the center of the orebody. Paleocene quartz monzonite and latite porphyries are labeled Lmp on Figure 3-81 and represent the CIMVS. The dikes were dated at 52.5 $\pm$ 2.0 Ma and the larger mass of the porphyry at depth in the northwest part of the deposit was dated at 47.8 $\pm$ 1.8 Ma (Langton and Williams, 1982). Late- and post-mineral hornblende andesite dikes and sills were intruded into east-northeast shear zones away from the ore body and are related to the overlying Baboon volcanics and are estimated to be 47-36 Ma in age (Langton and Williams, 1982).

The gap of nearly 20 million years between the older Cretaceous volcanics and possibly related intrusions and the younger Eocene productive quartz monzonite porphyries are similar to the ten million year gap between Cretaceous and Laramide magmatic activity in Tombstone and Sierrita. These two magmatic episodes have different alkalinities and different types of mineralization - 'barren' or lead-zinc-silver in the Cretaceous and porphyry copper in the Eocene

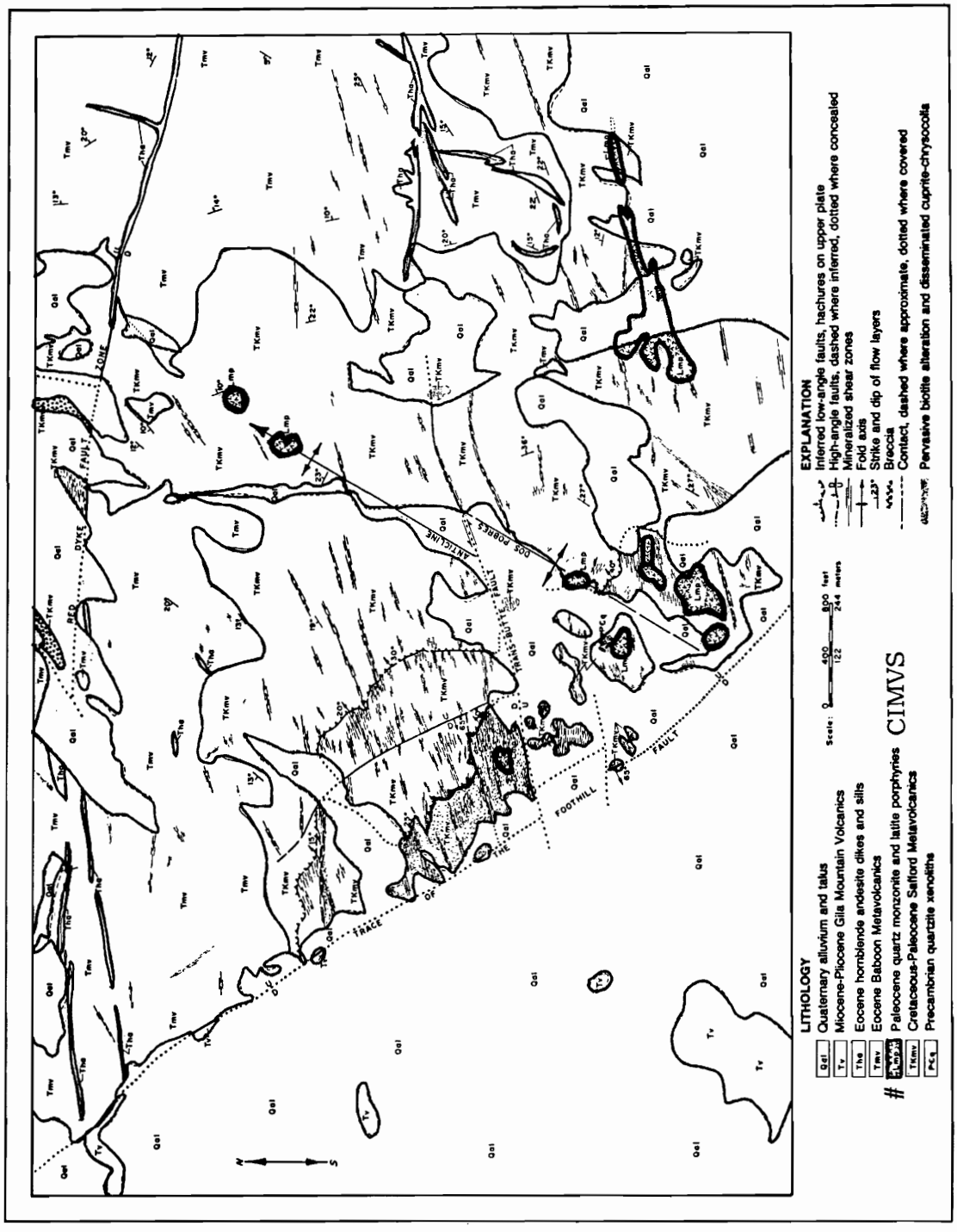

Figure 3-81. Geologic map of the Dos Pobres, AZ (# = CIMVS = Lmp = Paleocene quartz monzonite and latite porphyries) (from Langton and Williams, 1982).

(Keith and Wilt, 1986). Therefore, this study excluded the older volcanics and used only samples from the productive porphyries at Dos Pobres.

Whole rock analyses for this study were obtained from Langton and Williams (1982) and Lang (1991). Although the sample from Langton and Williams failed the Loss on Ignition (LOI) filter, the other samples passed the filters (Figure 3-82) and are in the calc-alkalic, moderately iron-poor, and weakly oxidized fields on the magma series variation diagrams (Figure 3-83).

El Salvador, CHILE

The El Salvador porphyry copper deposit is in the Indio Muerto mining district in the Atacama Desert of northern Chile, approximately 800 km north of Santiago and 25 km (15 miles) north of Potrerillos (Swayne and Trask, 1960). Early Tertiary rhyolite domes formed about 50 Ma contemporaneous with rhyolitic and andesitic volcanics; these volcanics were intruded by quartz rhyolite and quartz porphyry and accompanying minor copper-molybdenum mineralization about 46 Ma. A granodioritic porphyry complex was intruded about 41 Ma and was accompanied by the main copper mineralization and alteration (Figure 3-84). These productive porphyries (CIMVS) were named the "X Porphyry" for the earlier intrusion and the "L Porphyry" for the later, less mineralized feldspar porphyry. These were followed by post-mineral latite dikes and clastic pebble dikes (Gustafson and Hunt, 1975).

The gap of nine million years between the rhyolite domes and the feldspar

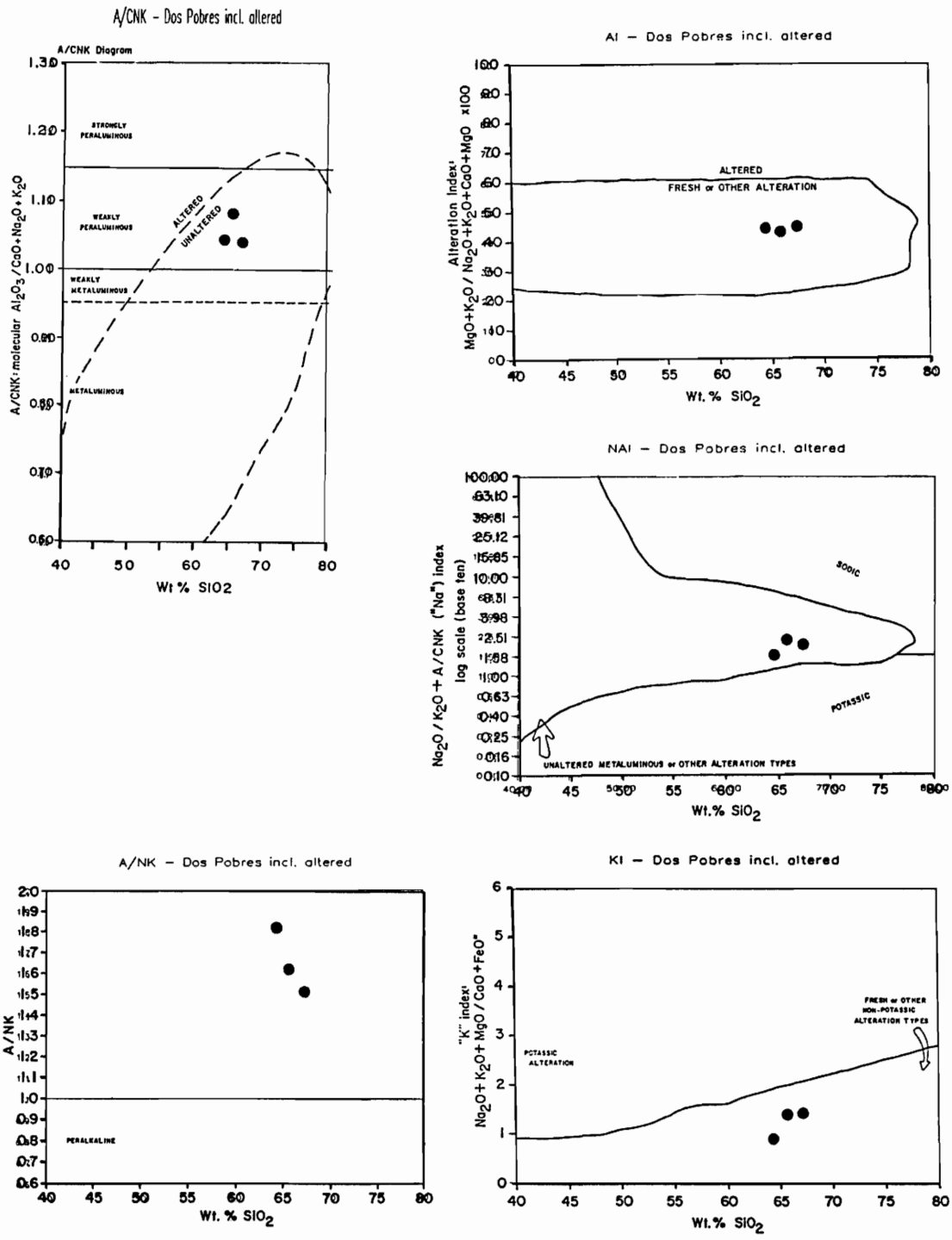

Figure 3-82. Petrochemical variation diagrams of the Dos Pobres, Arizona, productive porphyries showing alteration filters.

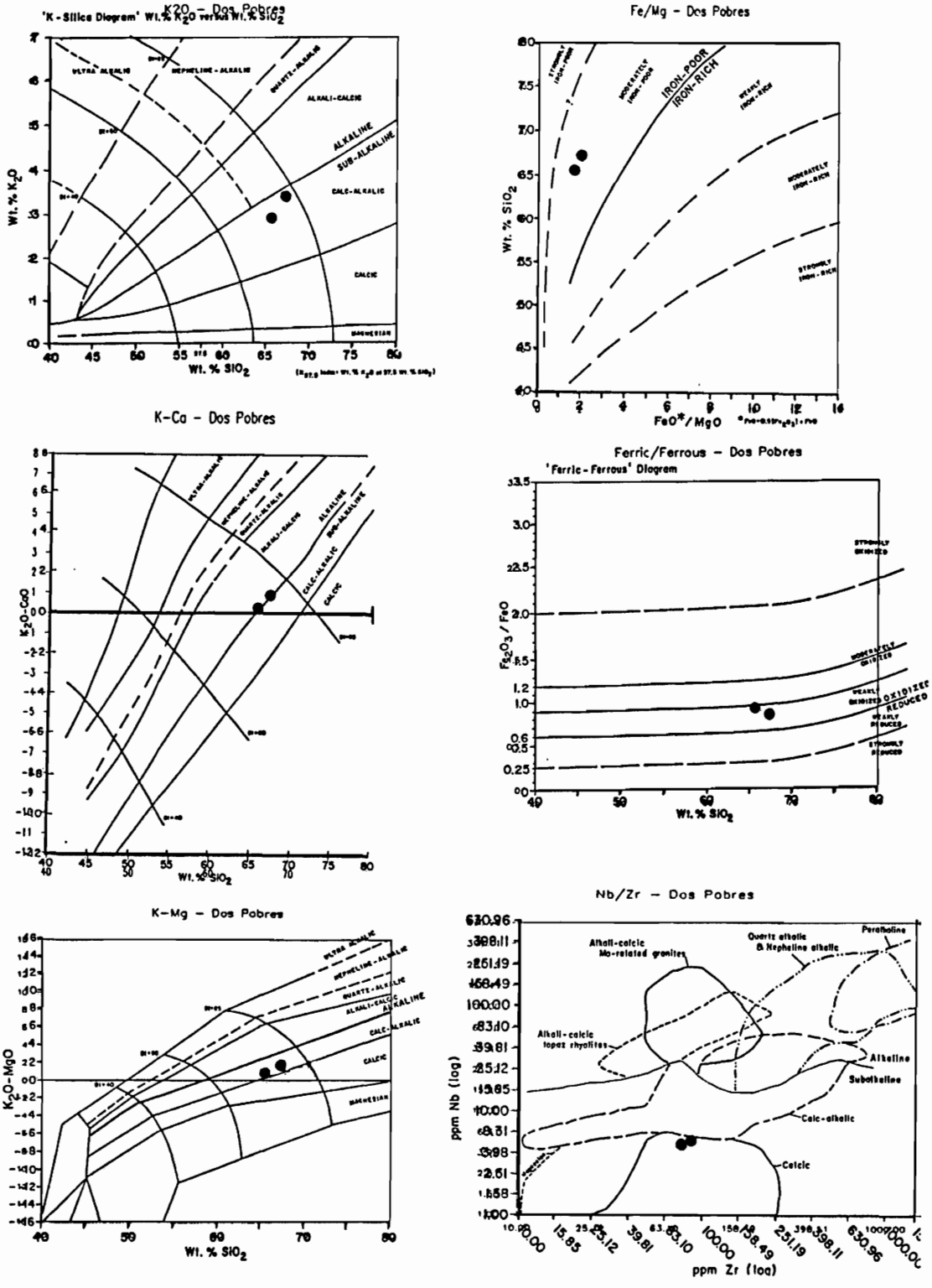

Figure 3-83. Magma series variation diagrams of the Dos Pobres, Arizona, productive porphyries showing alkalinity and iron ratios.

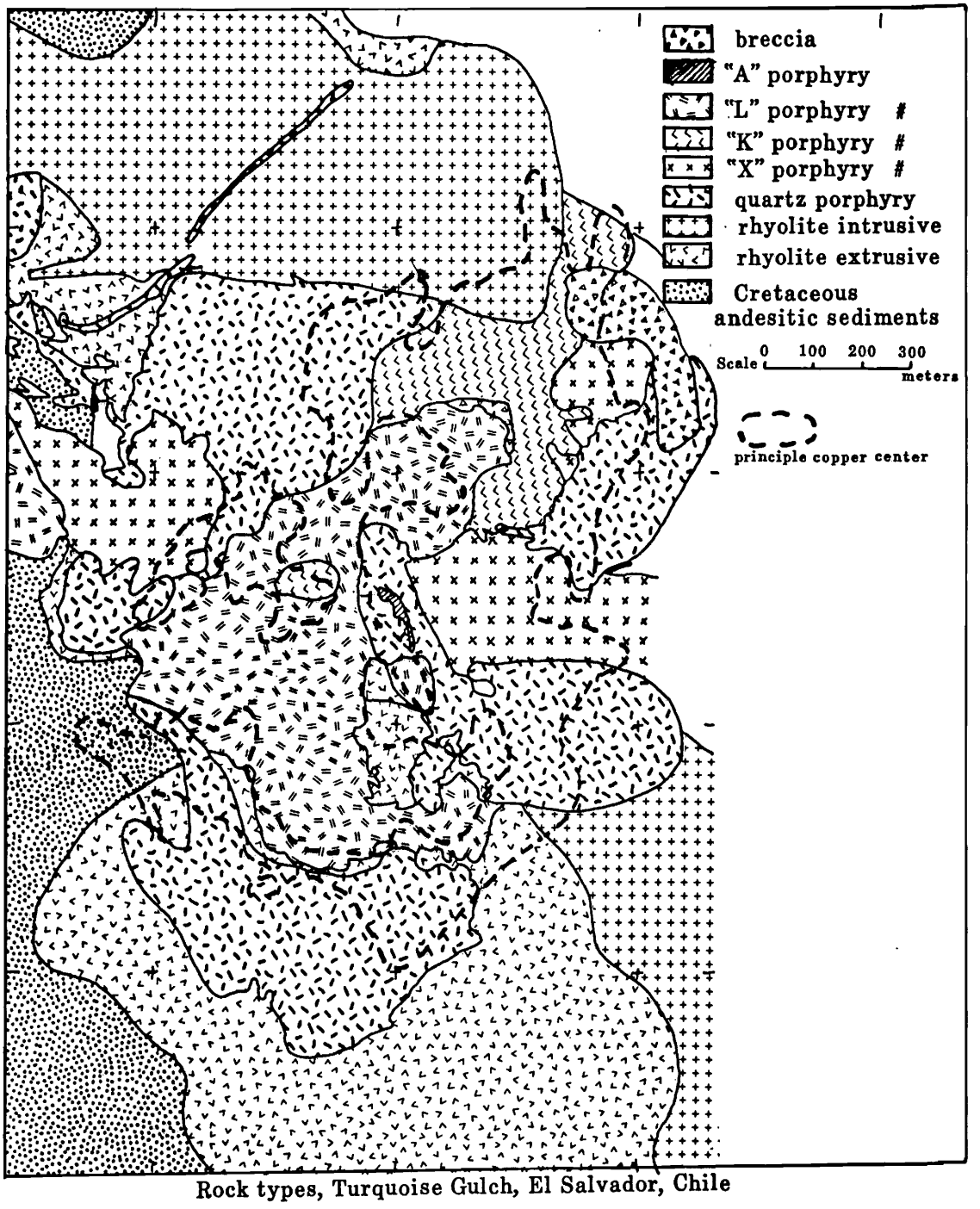

Figure 3-84. Geologic map of the El Salvador mine, Chile (# = CIMVS = granodioritic and quartz porphyries) (Gustafson and Hunt, 1975).

porphyries associated with porphyry copper mineralization is similar to preceding examples. The early rhyolites are more siliceous and have higher K_2O/Na_2O ratios than the granodiorite porphyries associated with the main period of mineralization (Gustafson and Hunt, 1975); their sample (1) is alkali-calcic.

Whole rock analyses for this study were obtained from Gustafson and Hunt (1975) and from Baldwin and Pearce (1982). Most of the samples passed the alteration filters (Figure 3-85) and are in the calc-alkalic, weakly iron-poor, and weakly oxidized to oxidized fields in the variation diagrams (Figure 3-86).

El Teniente, CHILE

The El Teniente porphyry copper deposit (formerly known as the Braden orebody) is 67 km east of the town of Rancagua and 55 km southeast of Santiago in the province of O'Higgins, Chile, on the west flank of the Andes (Howell and Molloy, 1960; Camus, 1975). A quartz diorite to dacite porphyry intrusive complex is related to the alteration-mineralization of the area (Quartz Diorite = CIMVS on Figure 3-87) (Camus, 1975). This Pliocene (Quirt and others, 1971) igneous complex intrudes Upper Cretaceous volcanics and lower Tertiary andesitic and basaltic flows of the overlying Farellones formation, which is the main host rock to the deposit (Camus, 1975). A hornblende lamprophyre dike is the youngest intrusive rock and is clearly post-ore and is later than the Braden formation, which is a pipe-filling breccia (Howell and Molloy, 1960).

Whole rock analyses used in this study were obtained from Camus (1975).

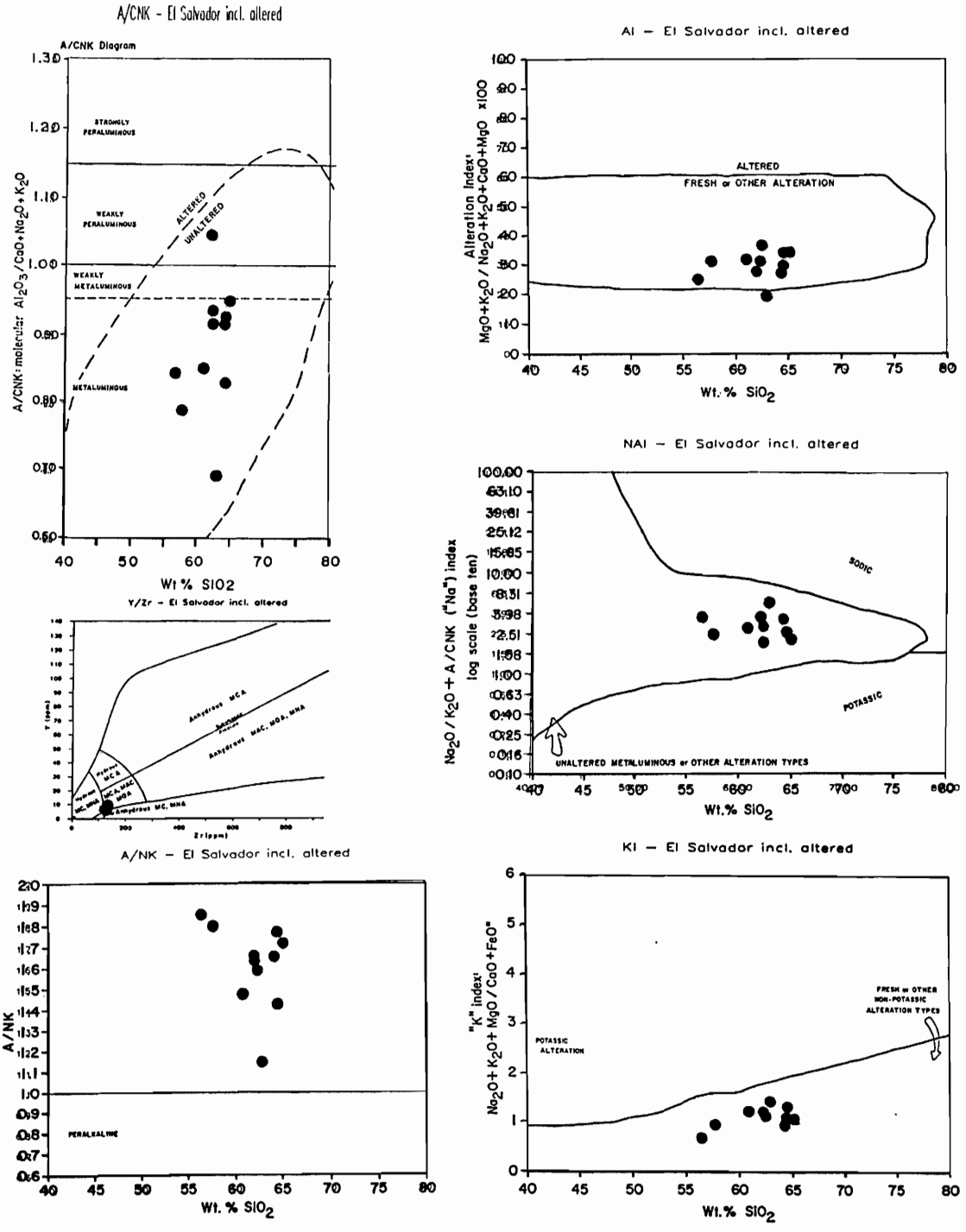

Figure 3-85. Petrochemical variation diagrams of igneous rocks from El Salvador, Chile, showing alteration filters.

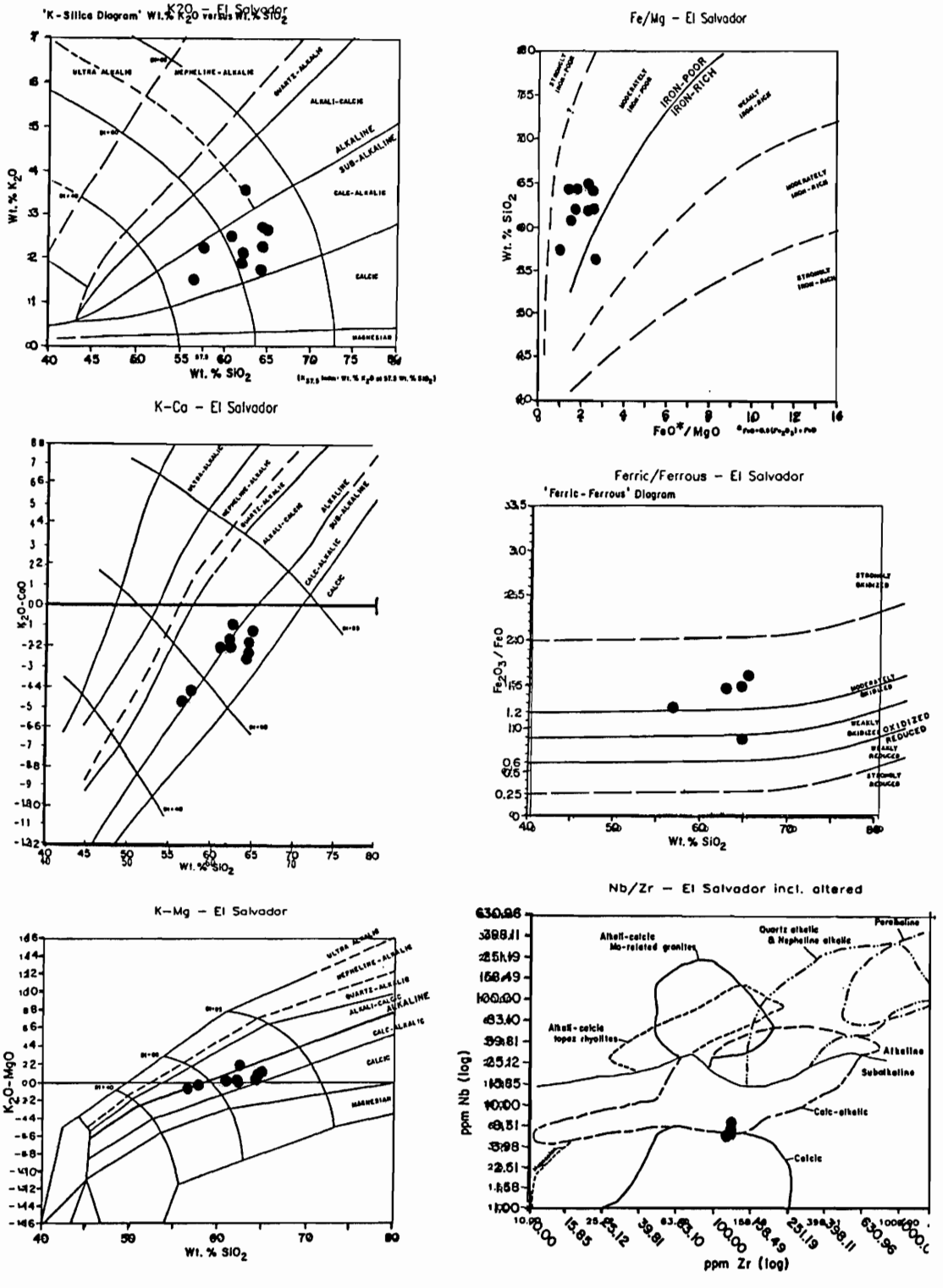

Figure 3-86. Magma series variation diagrams of igneous rocks from El Salvador, Chile, showing alkalinity and iron ratios.

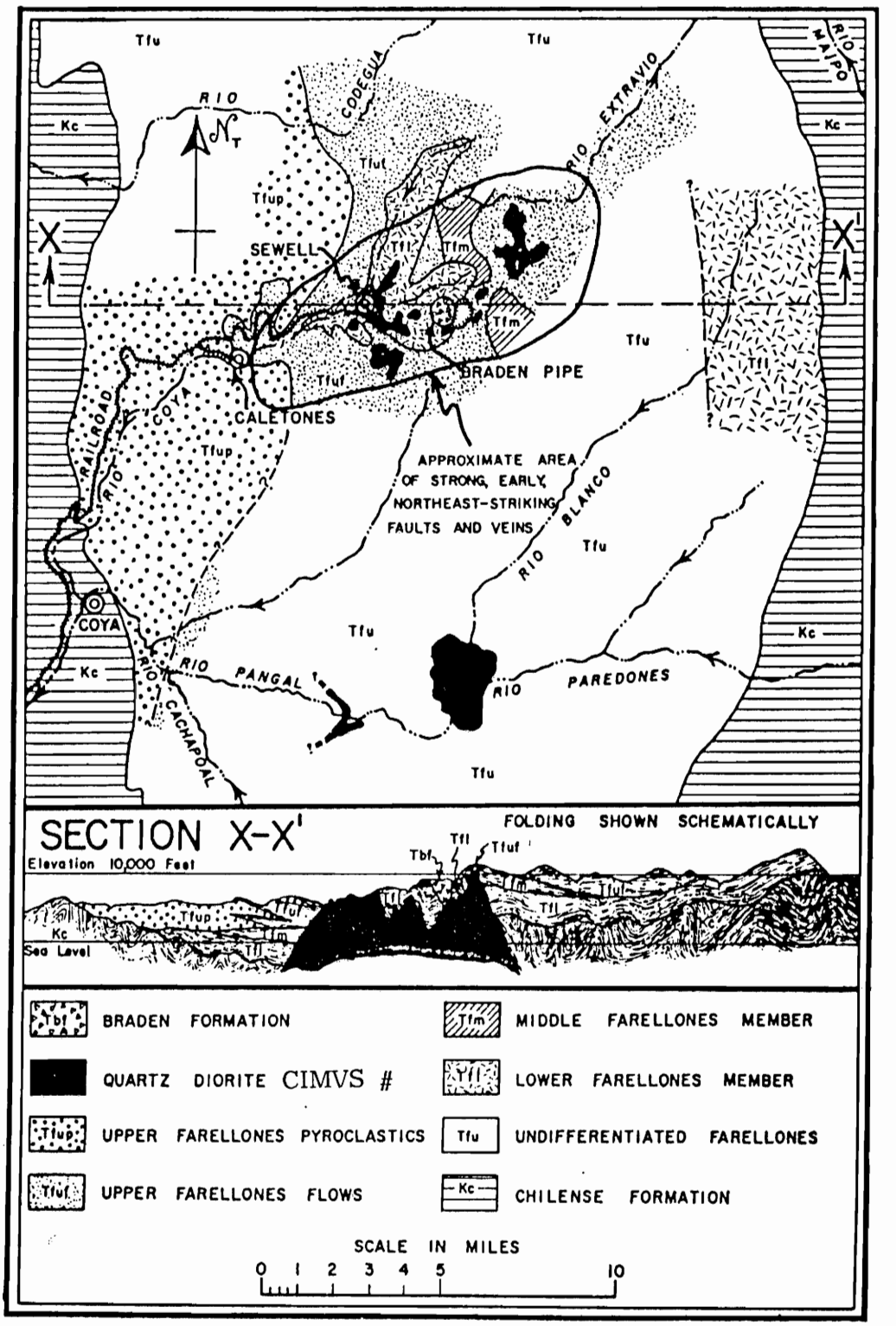

Figure 3-87. Geologic map of the Braden orebody of the El Teniente mine, Chile (# = CIMVS = Quartz Diorite) (from Howell and Molloy, 1960).

All of the rocks in the mine area are altered; however, one of the samples (number 6) passed the alteration filters (Figure 3-88). It is calc-alkalic, weakly iron-poor, and weakly reduced on the magma series diagrams (Figure 3-89).

Hedley, BC, CANADA

The Hedley gold district is in southern British Columbia, Canada, approximately 40 km east-southeast of Princeton, 250 km east of Vancouver, and 30 km north of the U.S.-Canada international boundary (Ray and others, 1986). The Hedley area has a long history of gold mining from several gold-copper skarn orebodies; more than 95 percent of the gold production came from the Nickel Plate and Hedley Mascot mines (Ray and others, 1987). The gold-skarn mineralization is hosted in Upper Triassic Nicola Group limy argillites, limestones, and volcaniclastic rocks and is genetically related to a suite of dioritic intrusions of middle Jurassic age (Rice, 1947). The Hedley intrusions on Figure 3-90 represent the Cogenetic Igneous-Metal-Volatile Suite (CIMVS). The Hedley intrusions vary in composition from diorite to quartz diorite, gabbro and biotite and hornblende granodiorite. K-Ar age dates on amphibole from the Hedley intrusions range between 170 and 190 Ma (Roddick and others, 1972).

All of the gold occurrences and deposits are spatially associated with dioritic bodies of the Hedley intrusions. These intrusions vary in size from the relatively narrow sills and dikes at the Nickel Plate and Hedley Mascot mines to the larger stocks at the Banbury and Peggy mines (Ray and others, 1986). It is

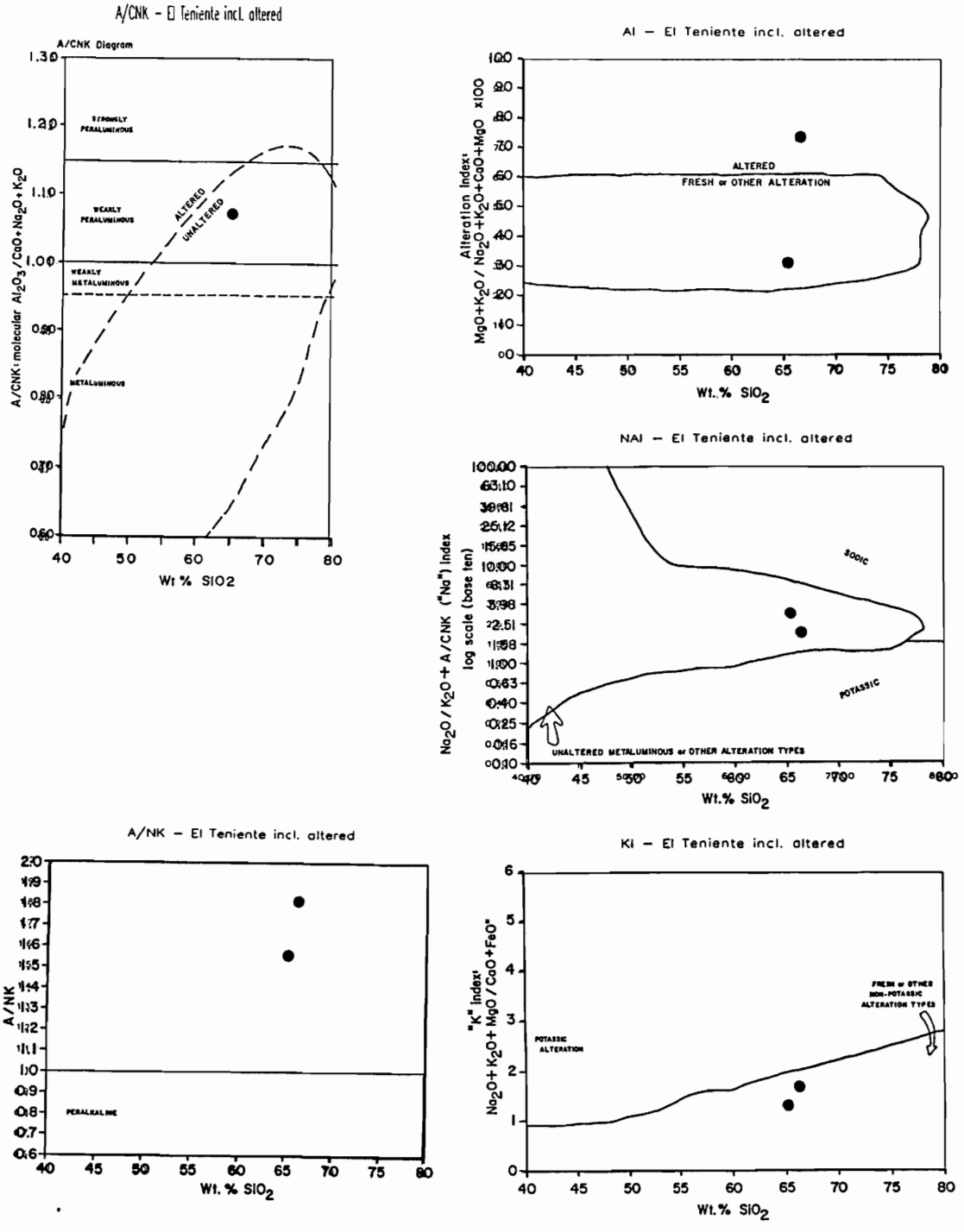

Figure 3-88. Petrochemical variation diagrams of igneous rocks from El Teniente, Chile, showing alteration filters.

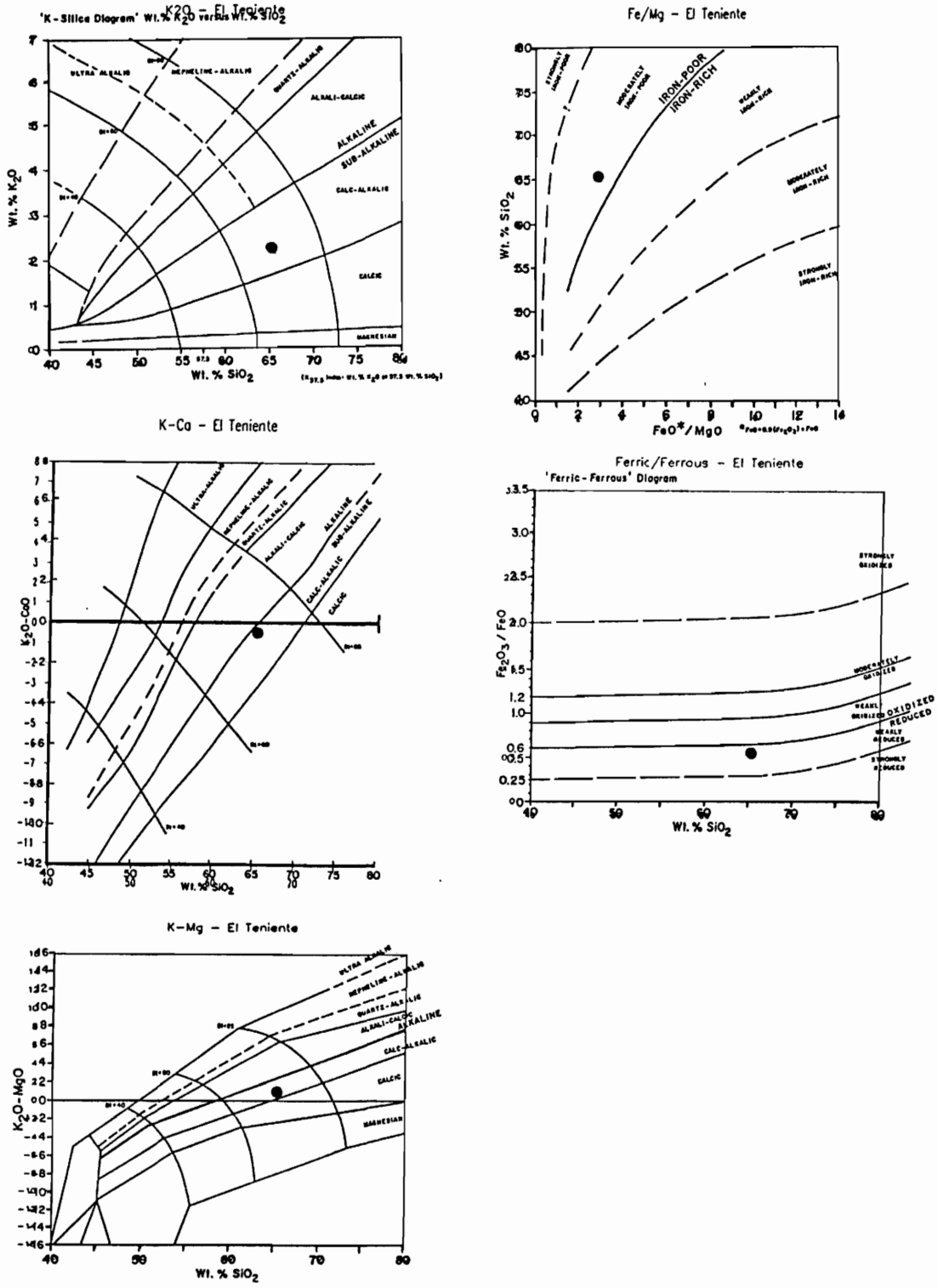

Figure 3-89. Magma series variation diagrams of igneous rocks from El Teniente, Chile, showing alkalinity and iron ratios.

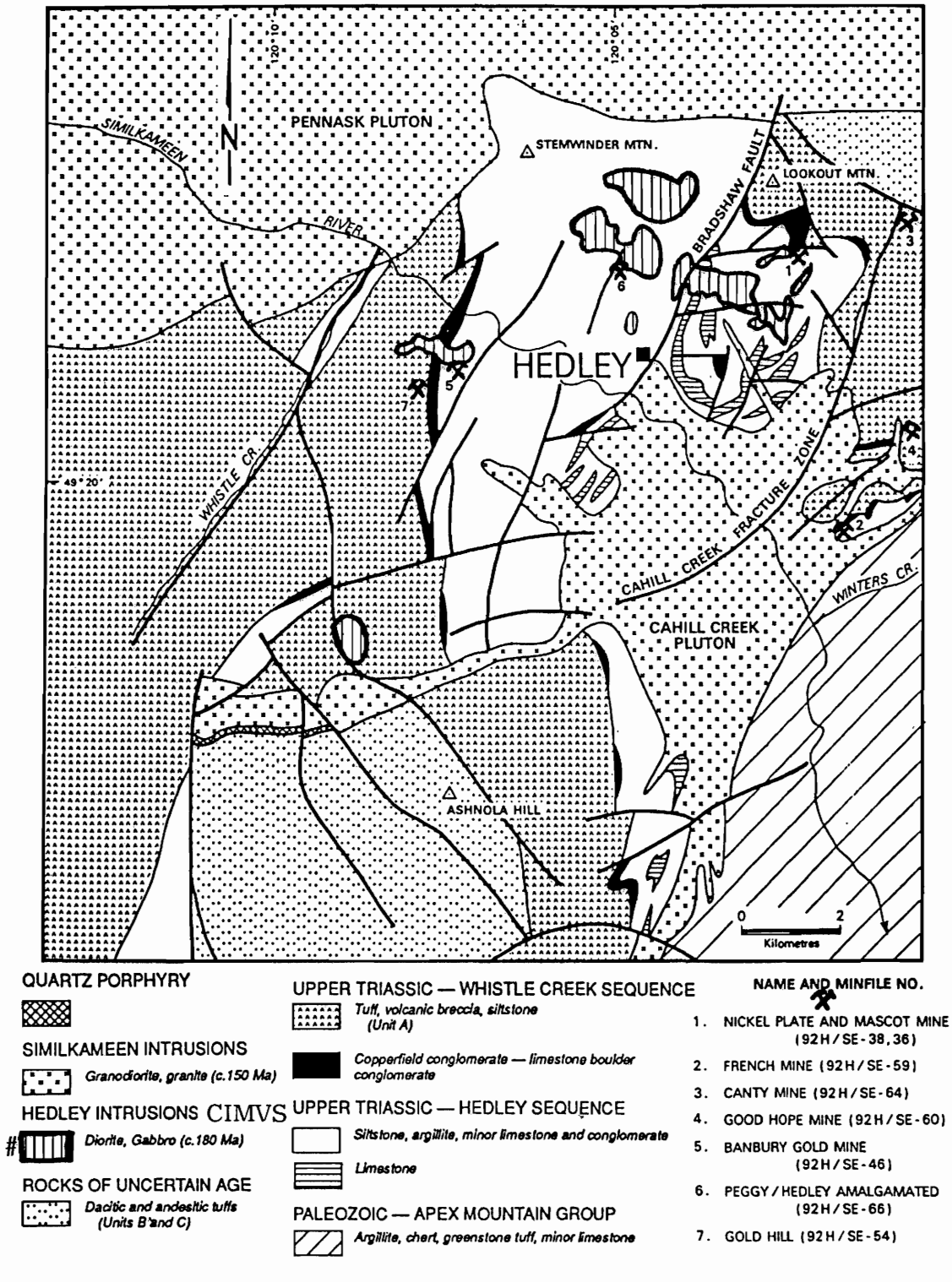

Figure 3-90. Geologic map of the Hedley area, British Columbia (Hedley Intrusions = # = CIMVS) (from Ray and others, 1986).

believed that the dikes and sills responsible for the Nickel Plate gold deposit emanated from the nearby Toronto stock of the Hedley intrusive complex (Billingsley and Hume, 1941; Dolmage and Brown, 1945; Ray and others, 1986). Both the Hedley intrusions and the Cahill Creek pluton are in the subalkaline field on alkalis (K_2O + Na_2O) versus silica diagrams (Ray and others, 1987).

Whole rock chemical analyses used in this study were obtained from Ray and others (1987) and Camsell (1910). Nearly all the samples passed the alteration filters (Figure 3-91) and are in the calc-alkalic, moderately iron-poor, weakly reduced to weakly oxidized fields on magma series diagrams (Figure 3-92).

McCoy, NV

The McCoy gold skarn deposit is in the McCoy mining district in the north-central part of the Fish Creek Mountains approximately 48 km (30 miles) southwest of Battle Mountain, Lander County, Nevada (Kuyper, 1988). The gold skarn mineralization occurs in limestones and siltstones of the Triassic Augusta Mountain Formation at the contact with the quartz monzonitic to granodioritic Brown stock (Brooks and others, 1991). The Brown stock is mapped as Tbs on Figure 3-93 and represents the CIMVS.

An older plutonic episode and associated magnesian iron skarns (magnetite-pyrrhotite) is represented by the McCoy pluton located approximately 1.6 km (1 mile) southwest of the McCoy mine (Kuyper, 1988). The McCoy pluton consists of biotite granodiorite and quartz monzonite with peripheral hornblende diorite

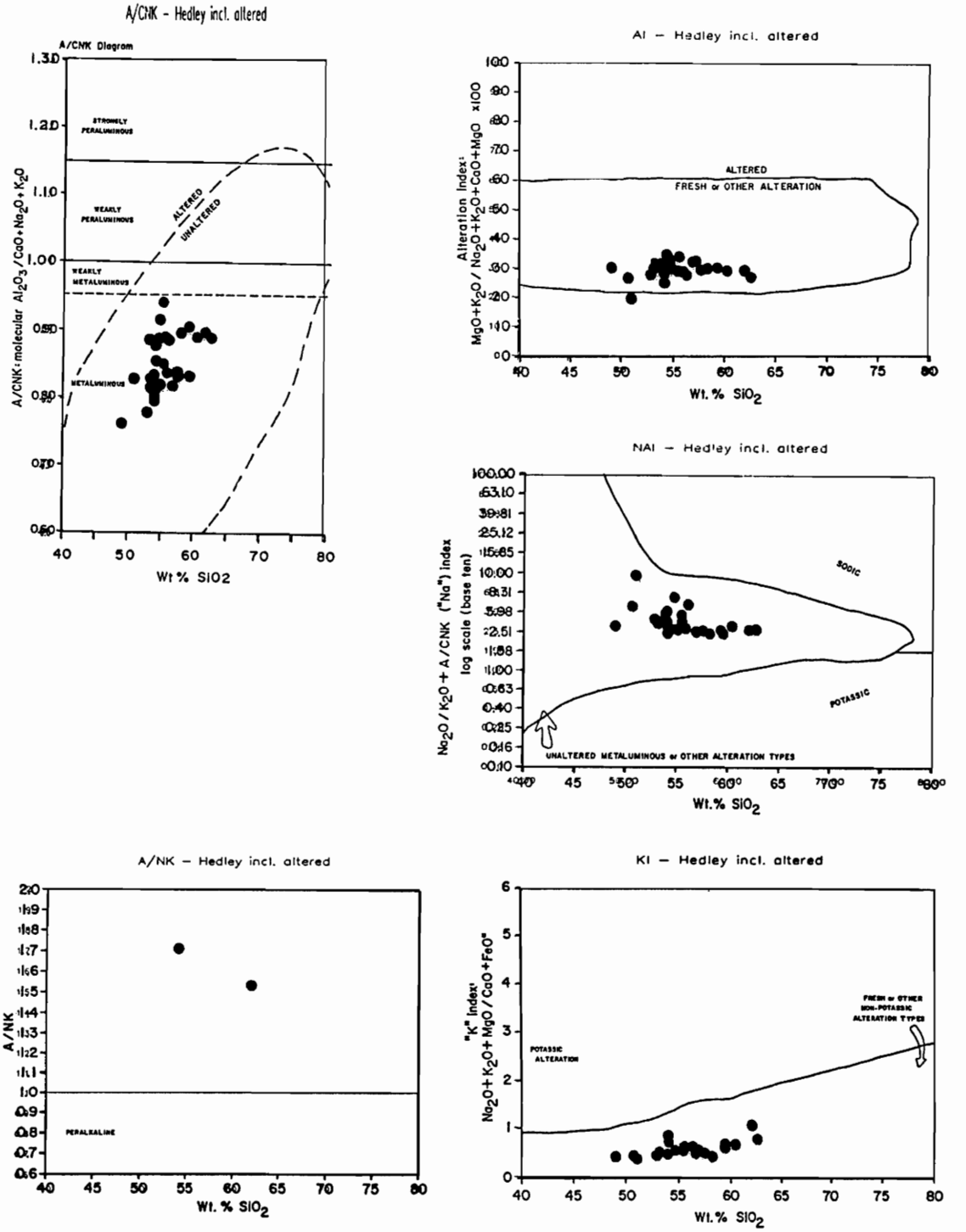

Figure 3-91. Petrochemical variation diagrams of igneous rocks from the Hedley, British Columbia, showing alteration filters.

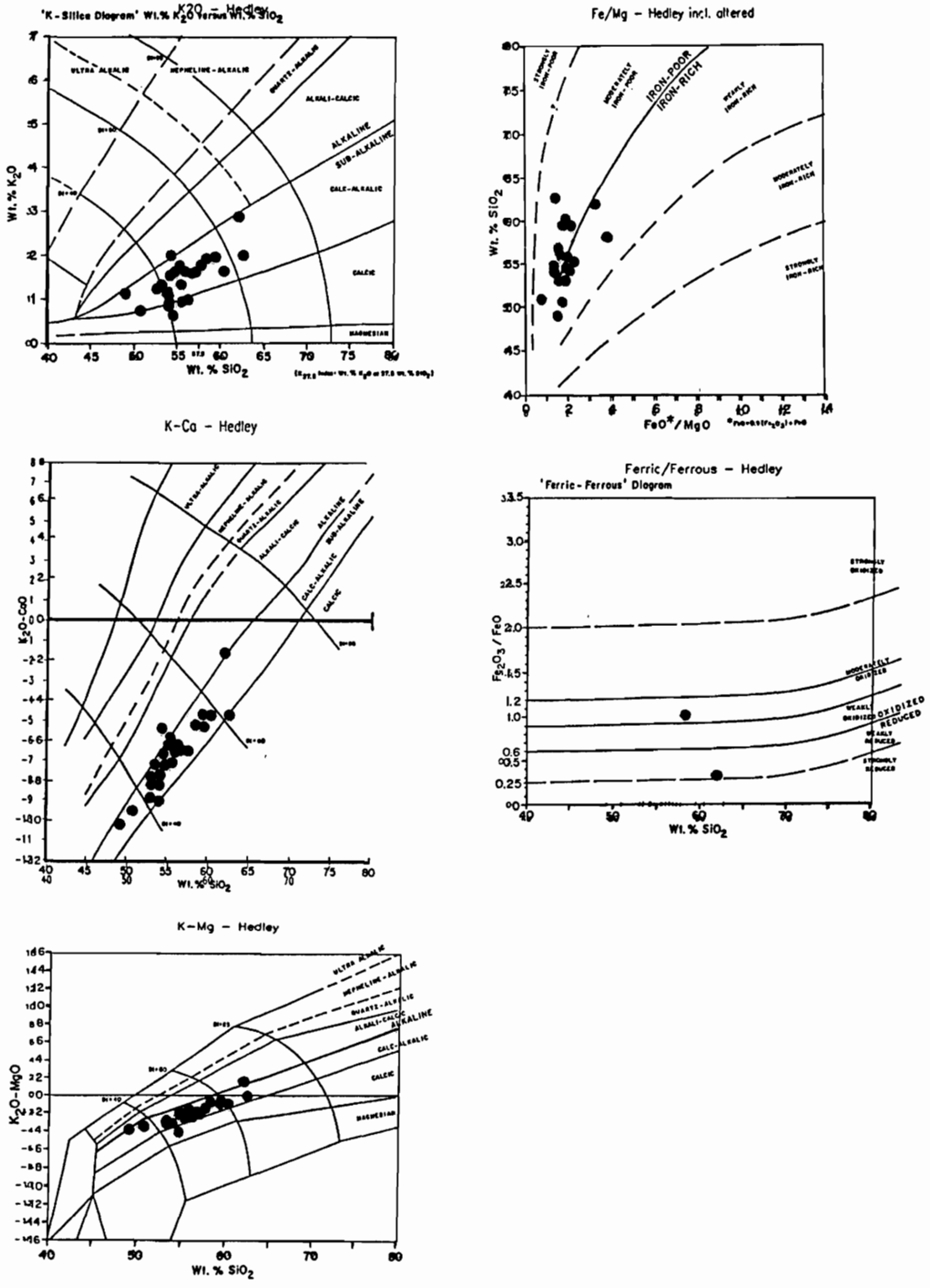

Figure 3-92. Magma series variation diagrams of igneous rocks from Hedley, British Columbia, showing alkalinity and iron ratios.

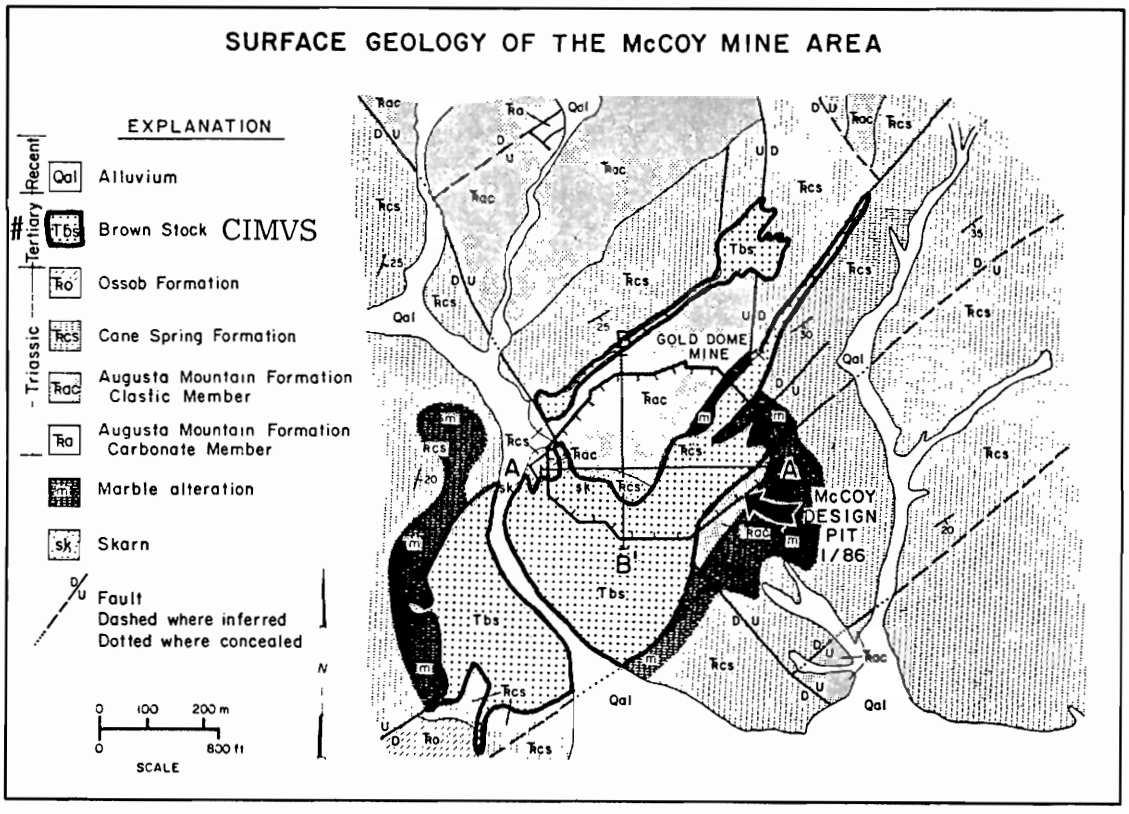

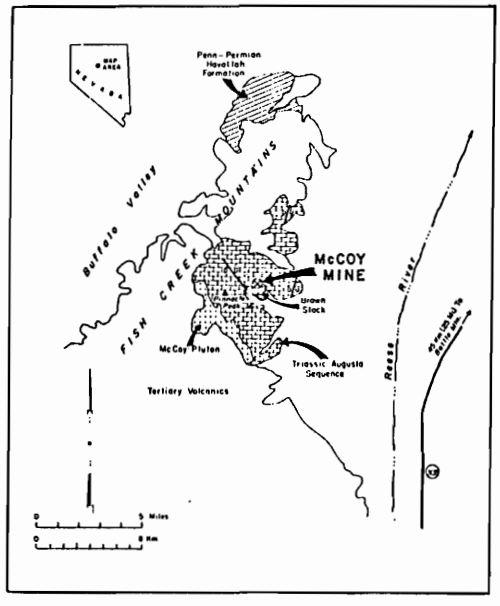

Figure 3-93. Geologic map of the McCoy mine area, Nevada (# = CIMVS = Tbs = Brown stock) (modified from Kuyper, 1988).

(Stewart and McKee, 1977); the McCoy pluton has been dated at 151 Ma by the K-Ar method on biotite (Silberman and McKee, 1971).

The Brown granodioritic stocks and dikes are the intrusive rocks most closely associated with the gold skarn alteration and mineralization (Brooks and others, 1991). K-Ar age determinations on fresh biotite from biotite-hornblende granodiorite of the Brown stock and on adularia and sericite from alteration in the Brown stock range from 38 to 41 Ma (Stewart and McKee, 1977; Brooks and others, 1991).

Whole rock analyses for this study were obtained from Brooks and others (1991); most of the samples passed the alteration filters (Figure 3-94). The samples are in the calc-alkalic, moderately iron-poor fields (Figure 3-95). Although the analyses were for total iron, Fe^{+3}/Fe^{+2} ratios were supplied which are moderately oxidized. However, the presence of magnetite with rare ilmenite (Brooks and others, 1991, p. 425) suggests that the oxidation state of unaltered rocks is weakly oxidized or weakly reduced. The presence of ilmenite, rather than magnetite, as the dominant iron oxide in the hornblende-biotite granodiorite also indicates the somewhat reducing nature of the pluton.

Morenci, AZ

The Morenci porphyry copper deposit is on the southern slope of the White Mountains in Greenlee County, Arizona, approximately 8 km (5 miles) northwest of Clifton. Laramide intrusive rocks in the district include an early diorite

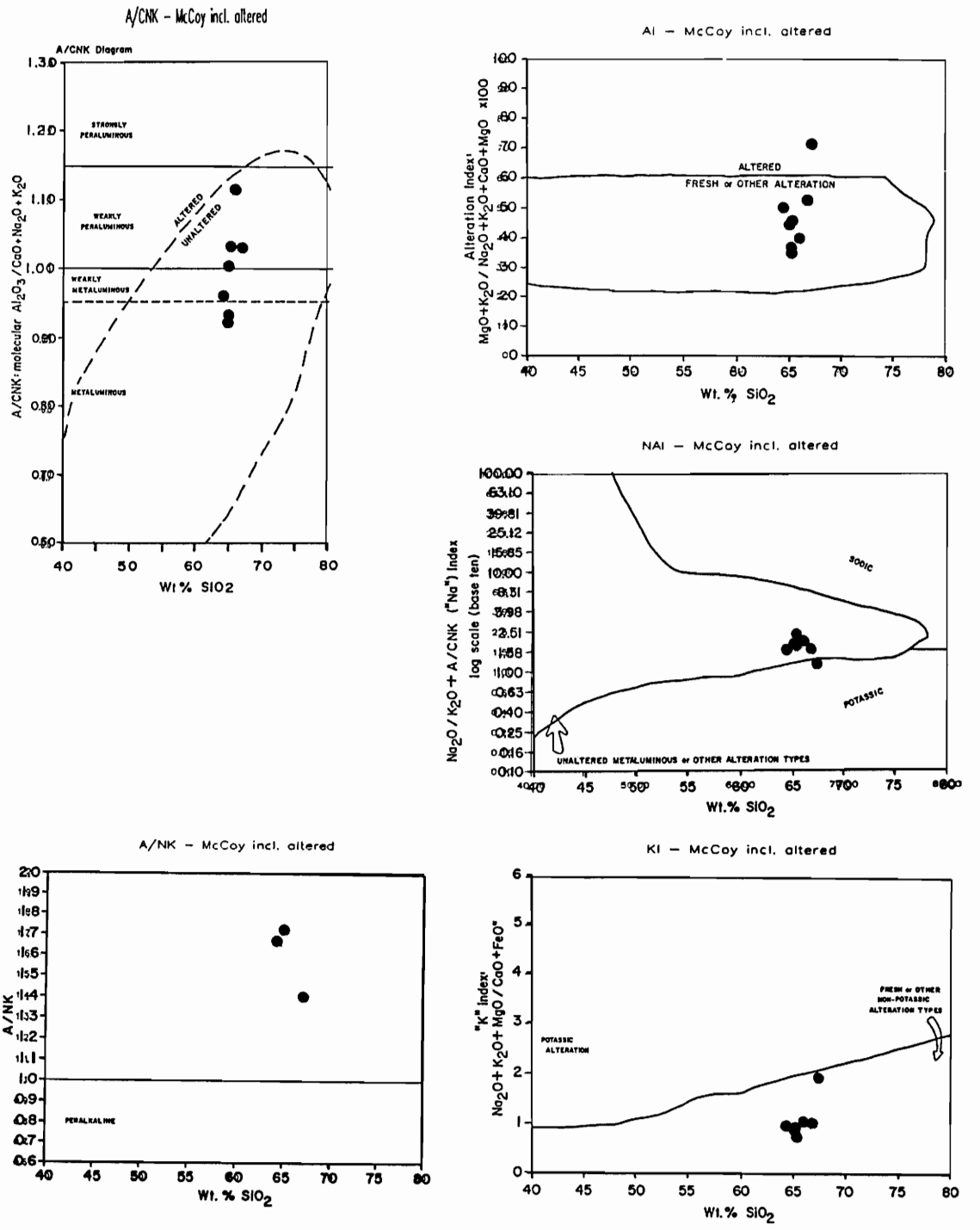

Figure 3-94. Petrochemical variation diagrams of igneous rocks from McCoy, Nevada, showing alteration filters.

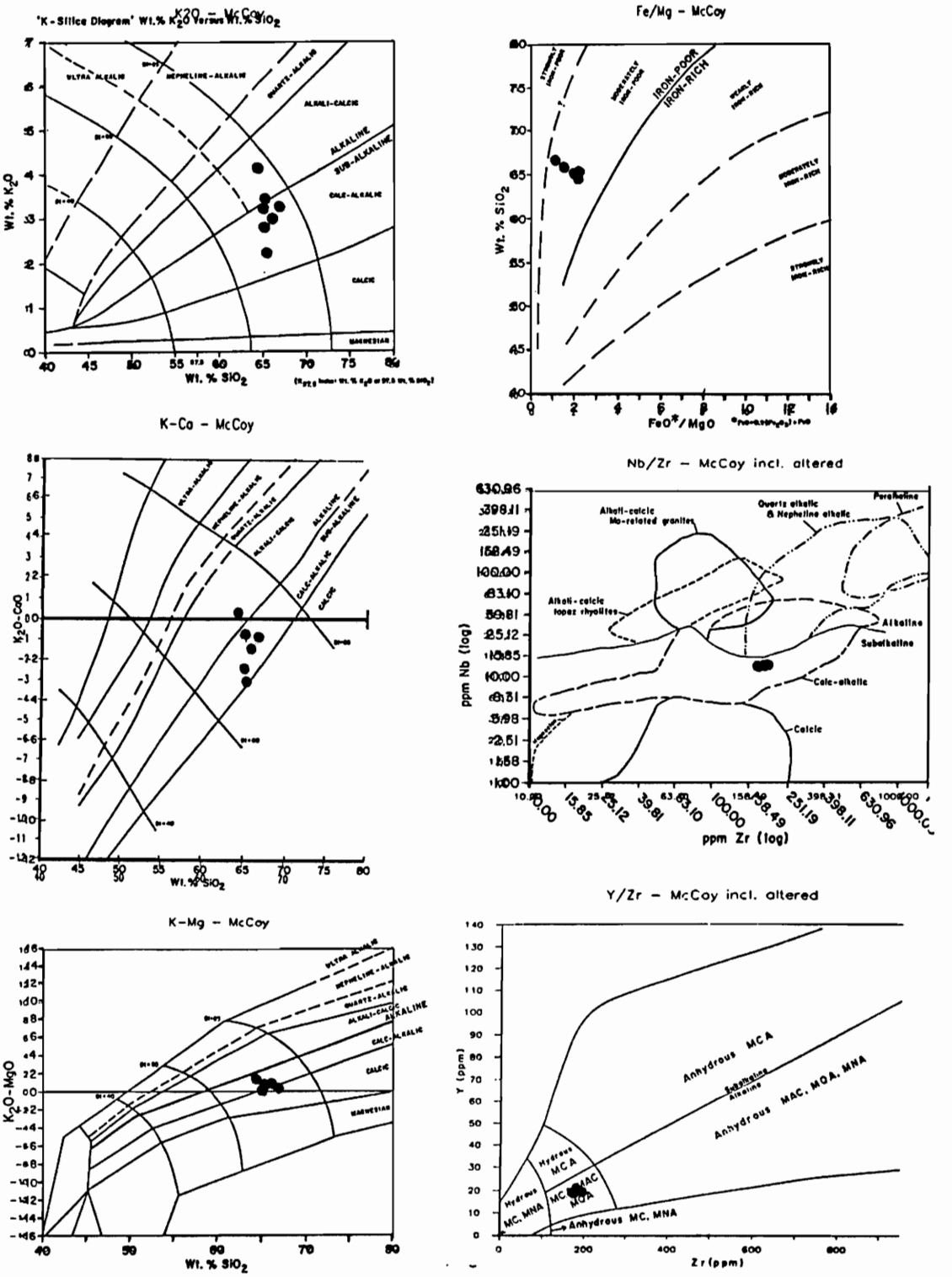

Figure 3-95. Magma series variation diagrams of igneous rocks from McCoy, Nevada, showing alkalinity and iron ratios.

porphyry or tonalite porphyry (Ltp in Figure 3-96) in dikes and thick sills dated at 62 Ma on hornblende (McDowell, 1966), quartz monzonite porphyry (Lmp) in an extensive laccolith dated at 55 Ma on biotite (McDowell, 1966), diabase (Ldb) dikes, and a granite porphyry complex (Lgp) (Langton, 1973). The quartz monzonite porphyry is the principal ore-bearing rock and is believed to be most closely related to the mineralization (CIMVS) (Moolick and Durek, 1966).

Whole rock analyses for this study were obtained from Clarke (1915), Lindgren (1905), and Dewhurst (1976). Although the samples in the mine area are altered, several passed the alteration filters (Figure 3-97). The samples are in the calc-alkalic, moderately iron-poor, and weakly reduced fields on magma series variation diagrams (Figure 3-98).

Calc-alkalic, Reduced

The link between a plutonic source and the disseminated gold deposits of the calc-alkalic reduced class is generally much more tenuous than in the calc-alkalic weakly oxidized and oxidized classes. However, in the interests of experimentation, the nearest plutonic rock of the same age as the ore deposit was used as a possible representative of the Cogenetic Igneous-Metal-Volatile Suite (CIMVS) and whole rock chemistry was obtained for it.

Bald Mountain, NV

The Alligator Ridge-Bald Mountain mining district is near the southern end

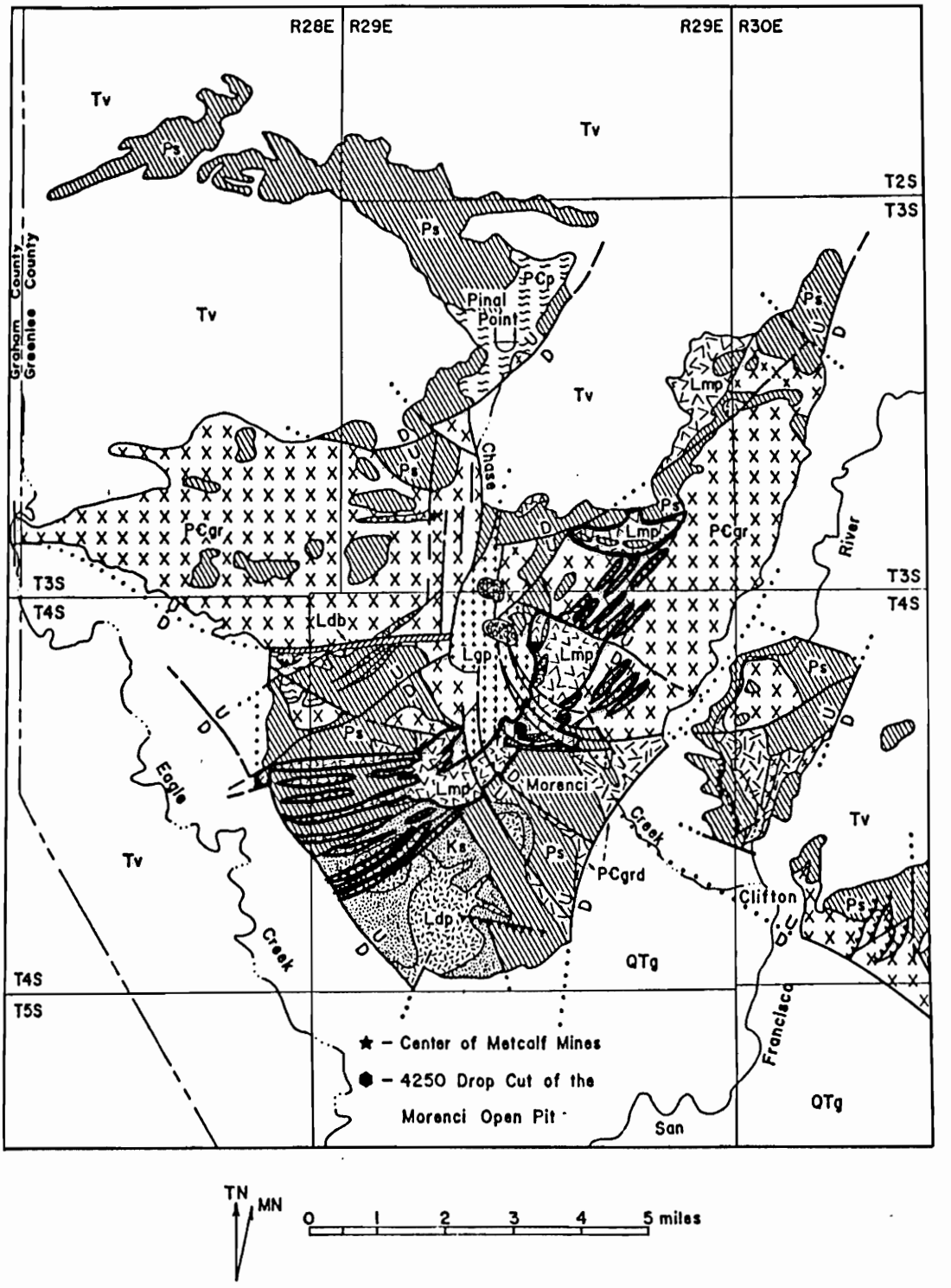

Figure 3-96. Geologic map of the Morenci mine area, Arizona (Lmp = Laramide quartz monzonite porphyry = CIMVS) (from Langton, 1973).

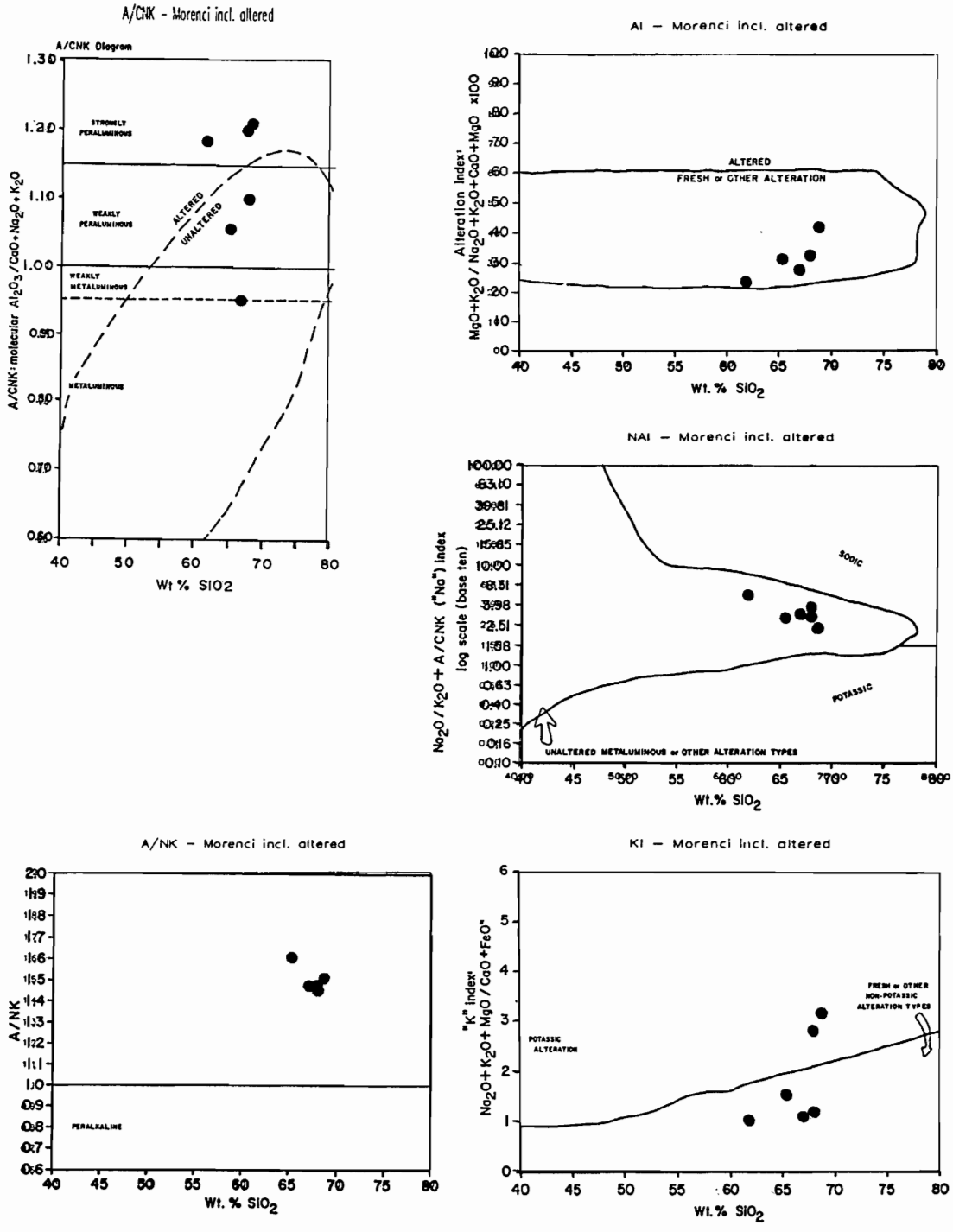

Figure 3-97. Petrochemical variation diagrams of igneous rocks from Morenci, Arizona, showing alteration filters.

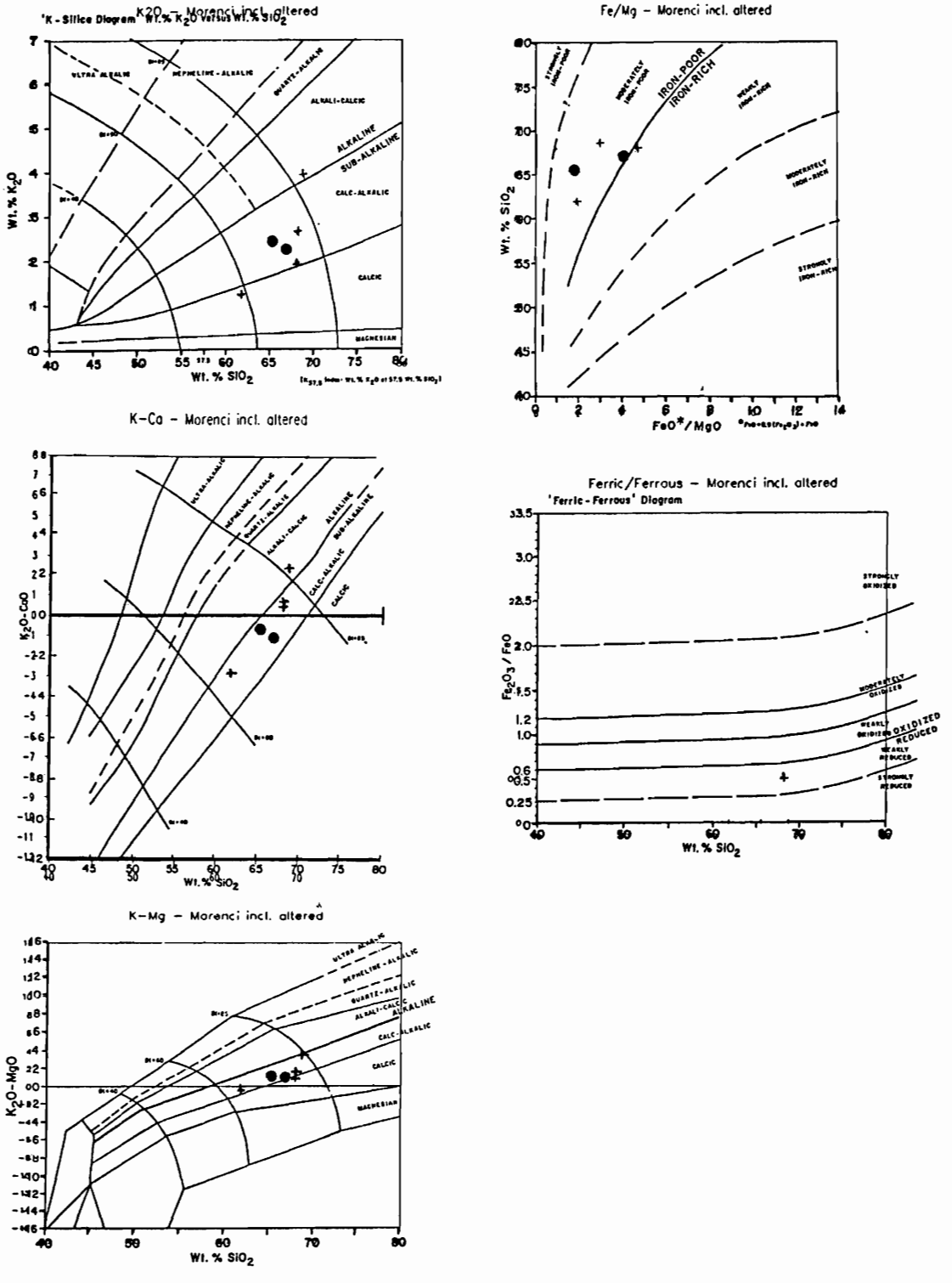

Figure 3-98. Magma series variation diagrams of igneous rocks from Morenci, Arizona, showing alkalinity and iron ratios (+ altered, ● unaltered).

of the Ruby Mountains in northwestern White Pine County, about 80 km northwest of the town of Ely (Figure 3-99) (Ilchik, 1990). Mines of the Bald Mountain area are on the slopes of Little Bald Mountain and in the saddle between it and Big Bald Mountain (Smith, 1976). Mines of the Alligator Ridge area include the Vantage disseminated gold deposits; they are in the Vantage Basin between the southern Ruby Mountains on the west and Alligator Ridge, a part of the Maverick Springs Range, on the east (Tapper, 1986). The district contains 18 gold deposits and prospects, two of which are found along the contact of a granitic intrusion located between Big and Little Bald Mountains (Ilchik, 1990). The Vantage disseminated gold deposits are hosted primarily by the lower 300 feet of the Pilot Shale, a sequence of thin-bedded calcareous, carbonaceous siltstones and claystones of Devonian-Mississippian age (Klessig, 1984).

Quartz-feldspar porphyry dikes are quite abundant near the southeastern margin of the quartz monzonite stock and a similar, small leucocratic dike occurs between the Bald Mountain stock and the Vantage deposits (Ilchik, 1990). The age of the stock is unknown but it petrographically resembles other Tertiary granodiorite stocks in White Pine County (Blake, 1964; Hose and Blake, 1976). Similar rocks in the region range in age from 39 to 24 Ma (Gans and others, 1989; Ilchik, 1991). The age of the mineralization at Alligator Ridge is bracketed by the movement of the Vantage fault after Oligocene volcanism and before 11.5 $\pm$ 0.7 Ma, which is the age of alunite from the oxidation assemblage (Ilchik, 1991). Thus, the quartz monzonite stock (Ti on Figure 3-99) may represent the CIMVS.

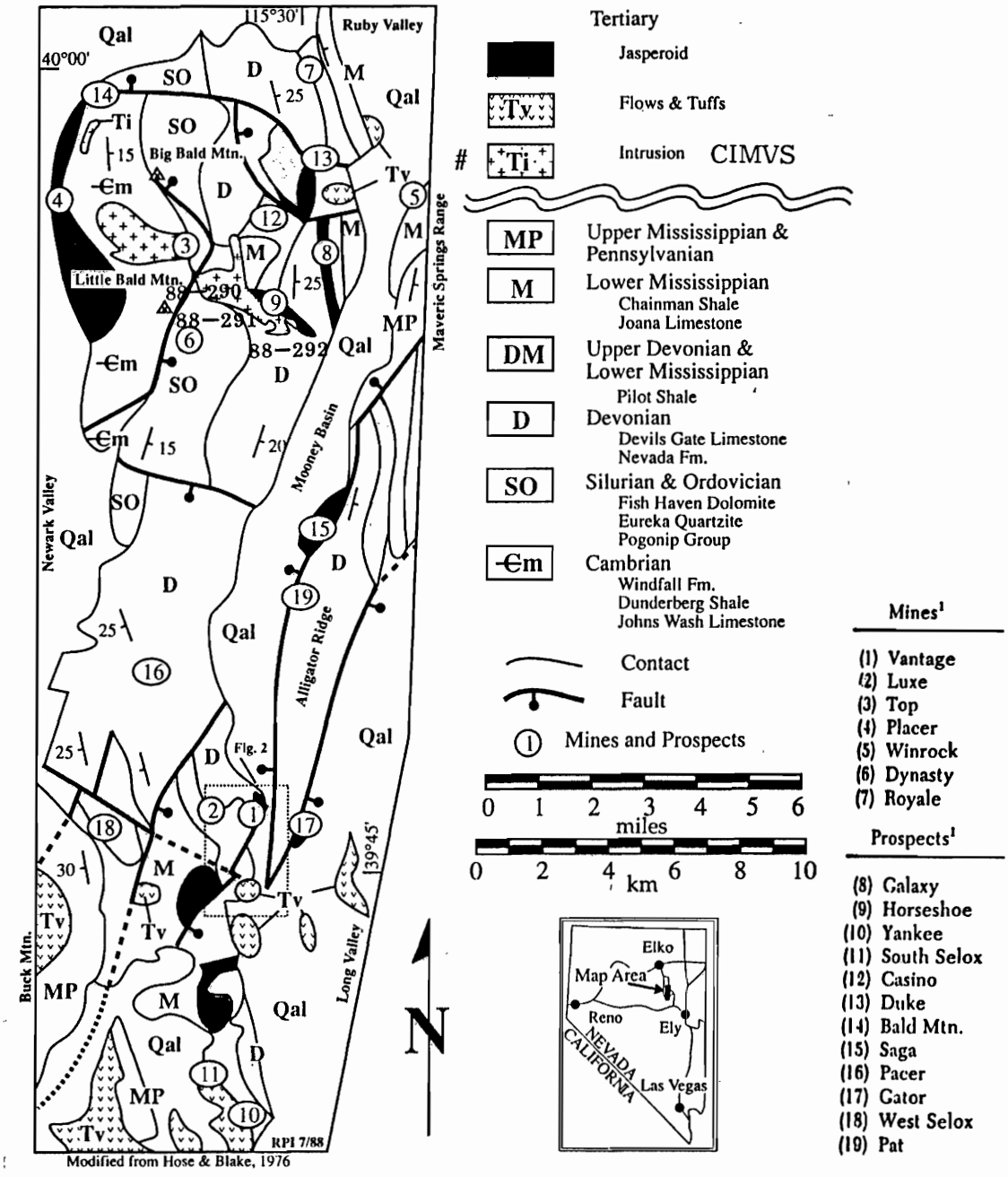

Figure 3-99. Geologic map of the Bald Mountain area, Nevada, showing igneous rocks (Ti may = # = CIMVS), mines or prospects, and sample locations (modified from Ilchik, 1990).

Whole rock analyses were obtained from MagmaChem files (Appendix A). One of the plutonic samples failed the alteration filters (Figure 3-100). The plutonic samples (excluding the dikes) are in the calc-alkalic, moderately iron-poor, and weakly reduced fields in the petrochemical variation diagrams (Figure 3-101). The deposit was classified as reduced because the preservation of organic matter and sulfides during gold deposition indicated that the ore fluid was reduced (H_2S > sum SO_4) (Ilchik, 1990).

Bloody Run, NV

The Bloody Run Hills are in the southern part of the Santa Rosa Range in southern Humboldt County, approximately 30 km (18 miles) north of Winnemucca, Nevada. Two Cretaceous-Tertiary granodioritic plutons are associated with mineralization (labeled Tkg on Figure 3-102 = CIMVS); One pluton is in the central part of the hills in Asa Moore Canyon associated with gold-quartz veins in the Basque mine and the other is in the southern part of the hills near Bloody Run Peak associated with scheelite- and molybdenite-bearing quartz veins of the Jupiter group (Wilden, 1964). The Late Cretaceous-early Tertiary plutons are dominantly sodic hornblende-biotite granodiorite which locally grades into tonalite (Willden, 1964). The southernmost stock on the east side of Bloody Run Peak yielded a lead-alpha age date of 55 $\pm$ 10 Ma by H. W. Jaffe (Willden, 1964).

Whole rock analyses for this study were obtained from MagmaChem Exploration (Appendix A), Willden (1964), Smith and others (1971), and Lee

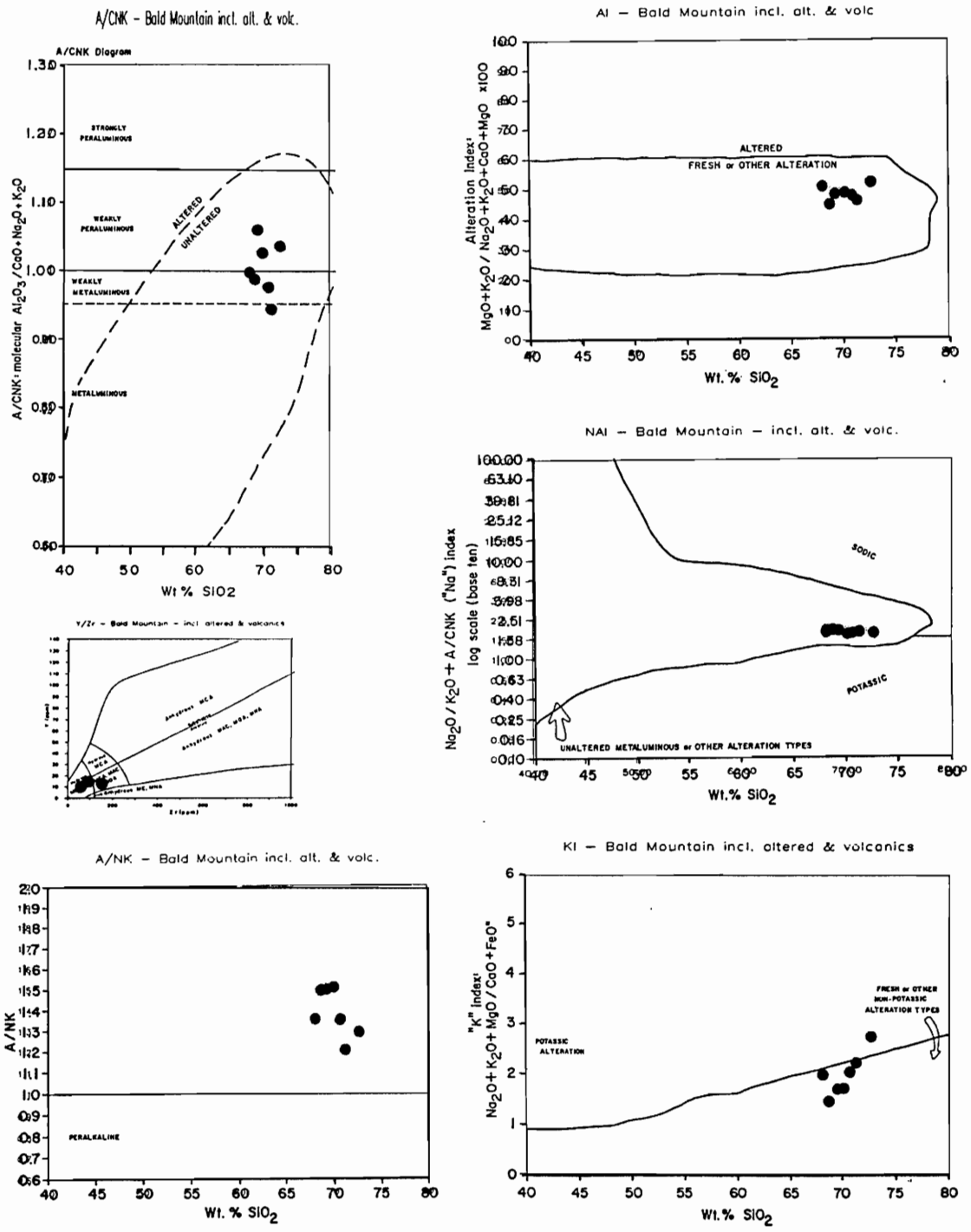

Figure 3-100. Petrochemical variation diagrams of igneous rocks from Bald Mountain, Nevada, showing alteration filters.

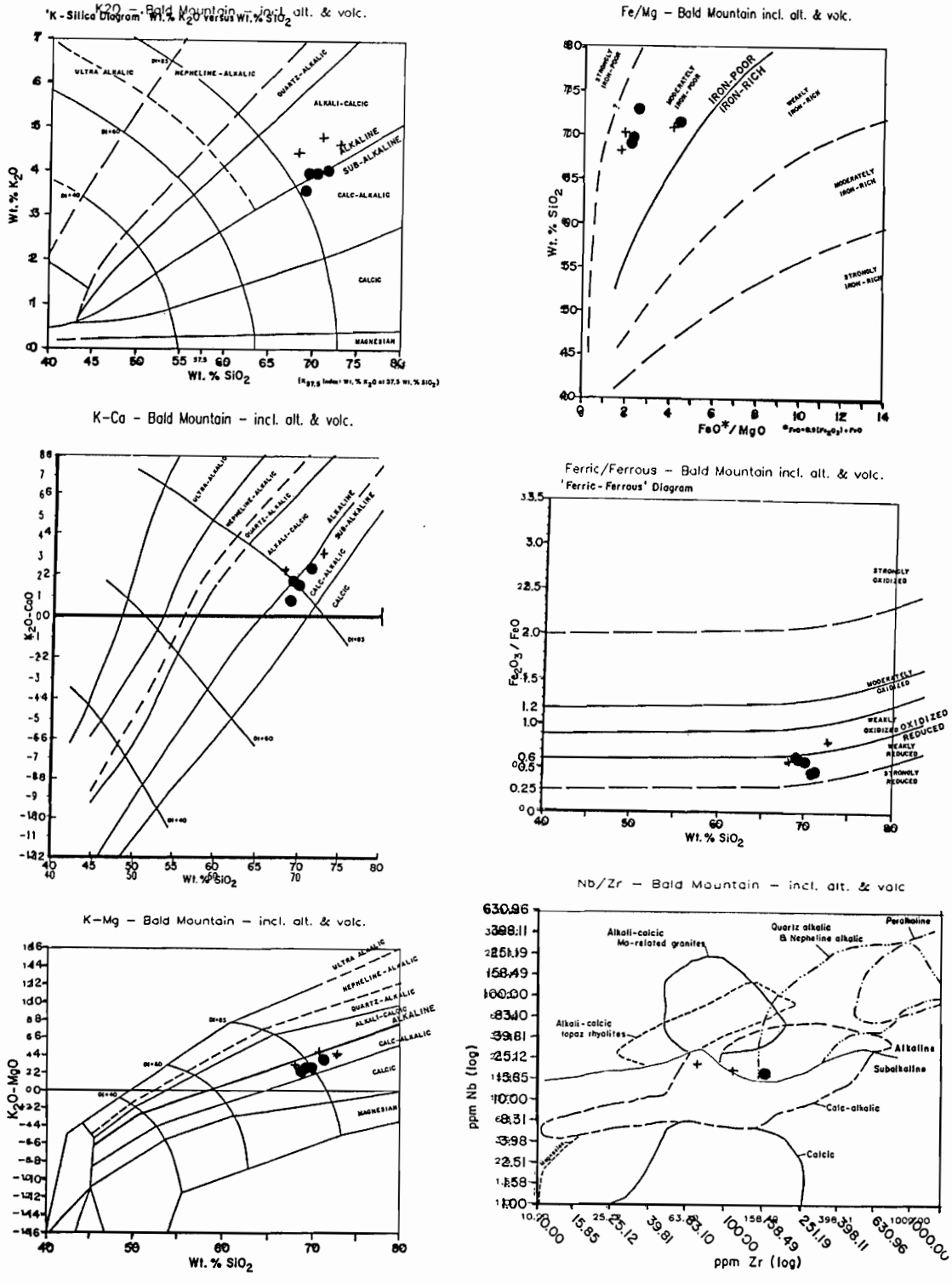

Figure 3-101. Magma series alkalinity and iron ratio diagrams of igneous rocks from Bald Mountain, Nevada, (+ altered, ● unaltered).

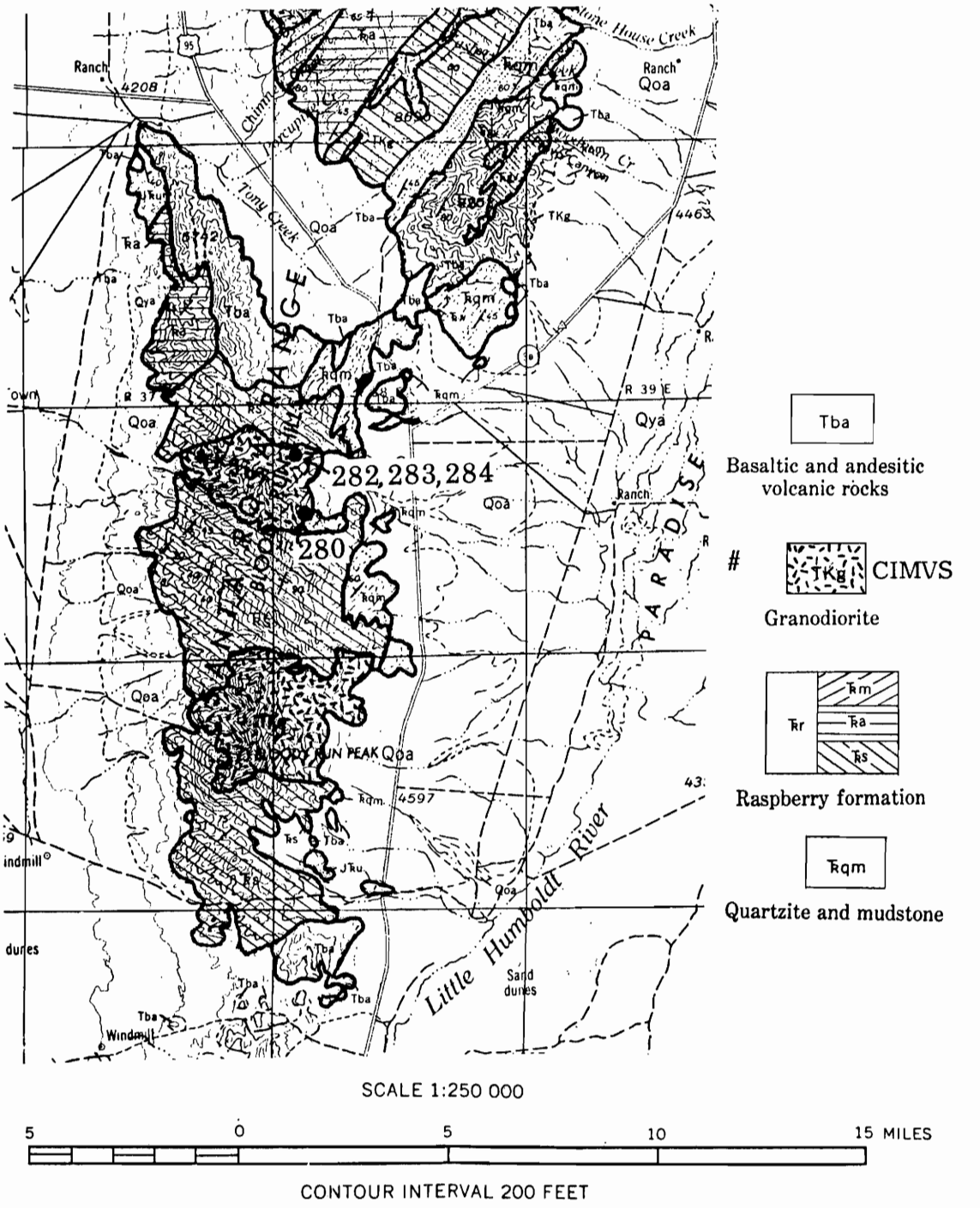

Figure 3-102. Geologic map of the Bloody Run Hills, Nevada, showing CIMVS (# Tkg) and sample locations (modified from Willden, 1964).

(1984). Most of the samples passed the alteration filters (Figure 3-103). The samples are in the calc-alkalic, moderately iron-poor, weakly oxidized fields on petrochemical variation diagrams (Figure 3-104). The presence of very graphitic phyllitic material on the dump of the Basque mine (Keith field notes, sample 88-0280, 1988) suggests that the mine belongs in the reduced class. Because of the uncertainty as to whether the Bloody Run belongs in the calc-alkalic reduced or weakly oxidized class, it was not used in the neural network analysis.

Carlin, NV

The Carlin Trend of disseminated, sediment-hosted gold deposits is a 40-mile long, northwesterly alignment of 21 gold deposits containing presently announced resources of over 53 million ounces of gold (Harvey, 1991). The central Carlin Trend is in the Tuscarora Mountains, approximately 35 km northwest of the town of Carlin in northeastern Eureka County, Nevada (Figure 3-105) (Lewis, 1991). Subdistricts of the Carlin Trend include the Carlin/Lynn, Maggie Creek/Gold Quarry, Blue Star/Goldstrike, Bootstrap, and Rain subdistricts (Flaherty and King, 1991).

Gold mineralization is associated with decalcification, silicification, argillization, and oxidation in these districts and is controlled by structure and stratigraphy (Flaherty and King, 1991). Mineralization at Carlin resulted from the migration of hydrothermal fluids up steep normal faults, commonly filled by dikes, and spread into permeable thin-bedded carbonaceous, arenaceous limy

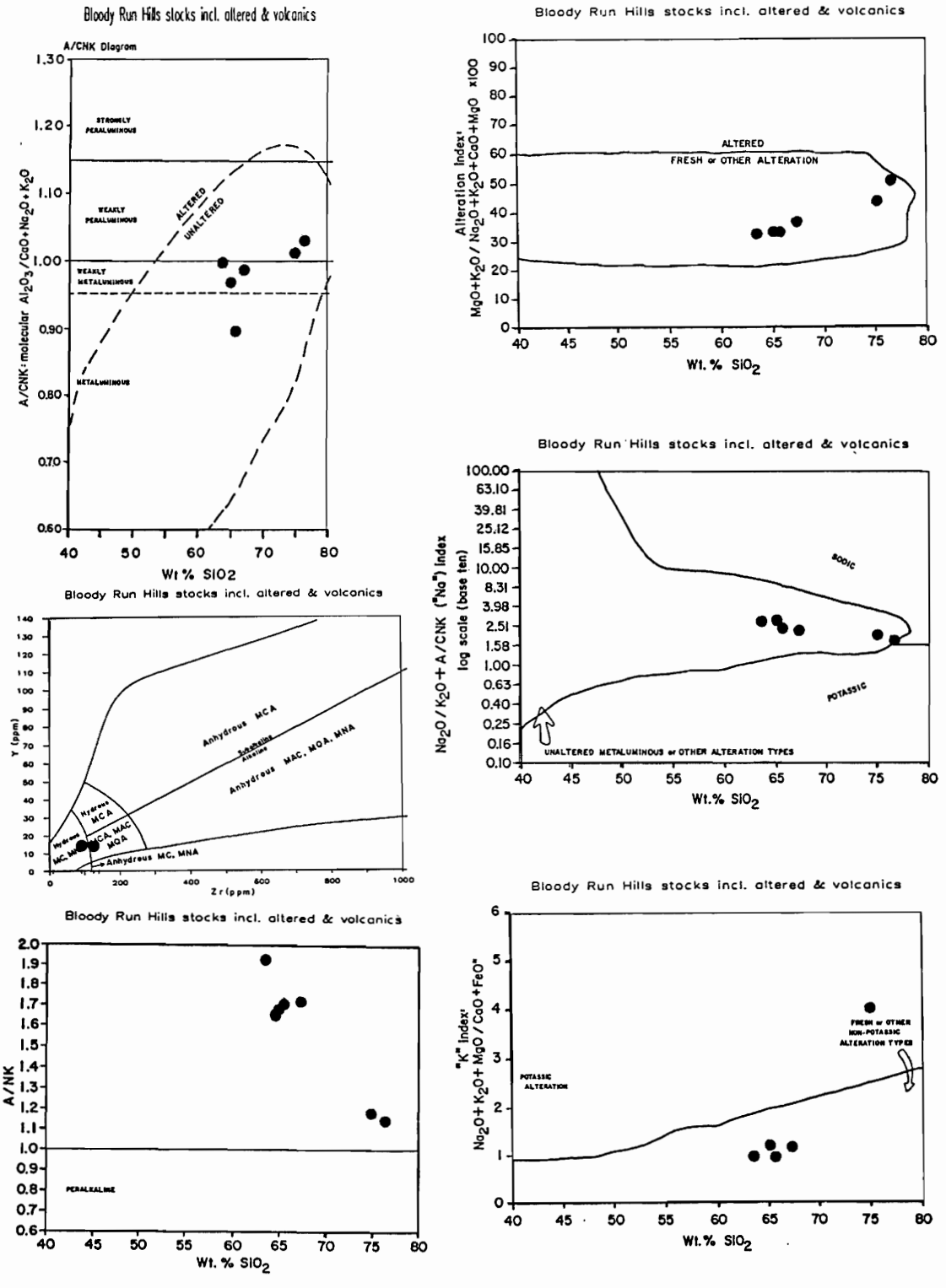

Figure 3-103. Petrochemical variation diagrams of igneous rocks from Bloody Run, Nevada, showing alteration filters.

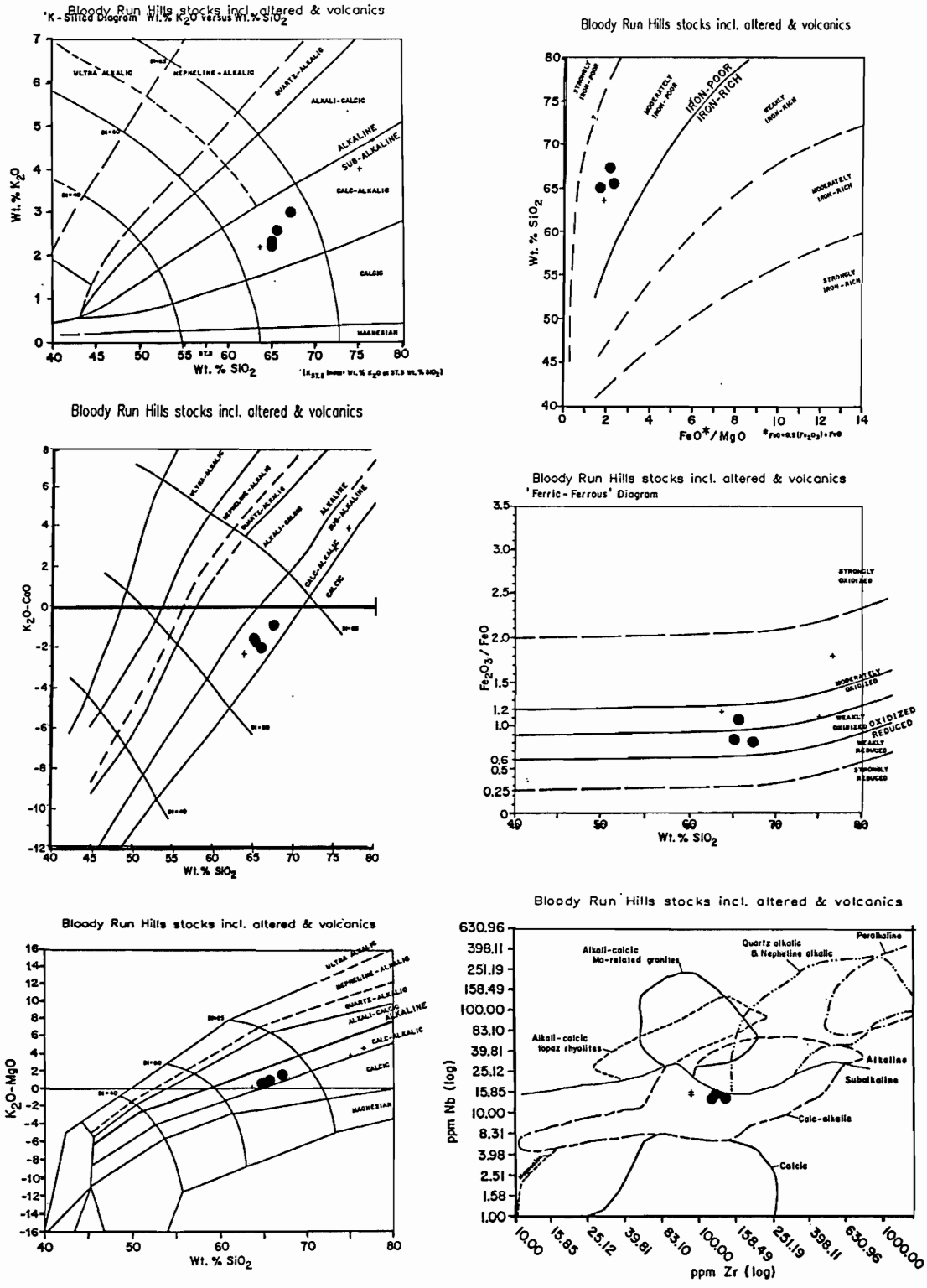

Figure 3-104. Magma series variation diagrams of igneous rocks from Bloody Run, Nevada, showing alkalinity and iron ratios (+ altered, ● unaltered).

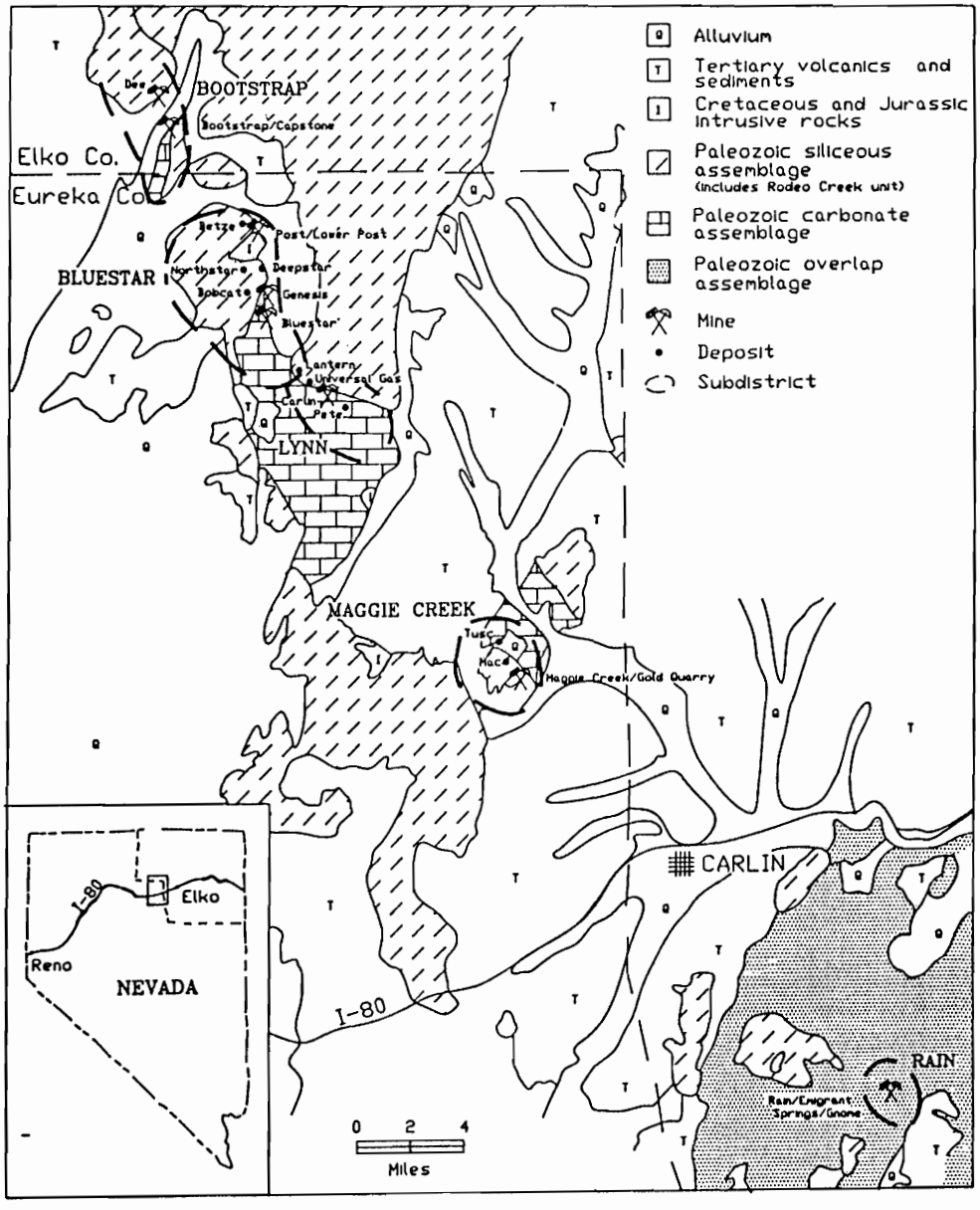

Figure 3-105. Geologic map of the Carlin Trend, Nevada, showing subdistricts (from Flaherty and King, 1991).

dolomite (Dickson and Rytuba, 1988). These fluids could have originated from low- to moderate-grade metamorphic fluids at depth, from magmatic fluids from underlying intrusives (CIMVS), or from very deep circulating meteoric water (Kuehn, 1989). The north-northwest-striking faults focused the flow of hydrothermal fluids into the Siluro-Devonian Roberts Mountains Formation (Bakken and Einaudi, 1986).

The apparent close association of mineralization to the structures suggests a mid-Tertiary age for the gold mineralization (Lewis, 1991; Lowe and others, 1985; Radtke, 1985). Displacement on the high-angle normal faults chiefly occurred during and after Oligocene time, although a few of the faults are invaded by dikes of Late Jurassic to Early Cretaceous age (Radtke, 1985). The most probable age of the Carlin mineralization is sometime between the Early Cretaceous and late Eocene/early Oligocene (Kuehn, 1989). Lines of evidence supporting a Tertiary age for the Carlin deposit are ore control by mid-Tertiary faults, ore bodies crosscutting Jurassic and Cretaceous igneous dikes, correspondence of alteration zones to the present topography, and K-Ar age data (Radtke, 1985). Sericite from the contact between dolomite and an altered dike in the main pit at Carlin yielded a composite K-Ar age of 57.6 $\pm$ 2.5 Ma, which is excessively old because the sample contained original illite from the carbonate rock (Radtke and others, 1980; Radtke, 1985). Because the north-northwest-striking faults of probable Mesozoic age predate mineralization and the north-northeast-striking faults of probable late-Tertiary age cut mineralization, a pre-

late Tertiary age is preferred for the Carlin deposit (Bakken, 1991). An Oligocene age for the mainstage Gold Quarry mineralization is likely, based on gold-bearing clasts within the 6 million year old Carlin Formation (Ekburg and others, 1991).

Several large dioritic intrusive masses are found along the Carlin trend and range in age from Tertiary (Evans, 1980) to Jurassic-Cretaceous (Radtke, 1985). A granodiorite dike in the southwest corner of the Carlin main pit was dated at 128 Ma (Radtke and others, 1980). The Goldstrike stock gave a radiometric K-Ar age determination on biotite of 121 $\pm$ 5 Ma (Hausen and Kerr, 1968). An earlier base metal-barite assembage is related to this intrusive and thus the whole rock chemistry from this pluton was not used in the neural network analysis in this study. A later low temperature Au-As-Hg-Sb assemblage was emplaced nearer the surface (Hausen and Kerr, 1968). Narrow dikes of feldspar porphyry (CIMVS) are believed to be of early Tertiary age (Hardie, 1966).

Magmatism of Oligocene age is widespread in this part of Nevada (Smith and Ketner, 1976, 1977). A granodiorite dike from Welches Canyon south of the Lynn Window yielded a K-Ar age date of 37 $\pm$ 0.8 Ma (Evans, 1980). Many other small intrusions in north central Nevada, as at Battle Mountain, the northern Shoshone Range, the Cortez Mountains, and the southern Independence Mountains, range in age from 34 to 39 Ma (Evans, 1980; Roberts and others, 1971). Tuff in the upper part of the Elko Formation yields a K-Ar age date of 38.6 $\pm$ 0.8 Ma on biotite (McKee and others, 1971). Ash flow tuff in the Indian

Well Formation yields K-Ar age dates of 33.3 ± 0.7 on sanidine and 34.9 ± 0.7 Ma on biotite; a sample from another area yielded a K-Ar age date of 36.2 ± 0.7 Ma on biotite (McKee and others, 1971). The lapilli tuff of the Indian Well Formation yielded a date of 37.6 ± 1.3 Ma from biotite (Smith and Ketner, 1976).

Whole rock analyses for mines of the Carlin Trend were obtained from Evans (1980) and Smith and Ketner (1977); most of these analyses were from dikes that did not pass the alteration filters (Figure 3-106). The two samples that passed the alteration filters are in the calc-alkalic, moderately iron-poor, moderately oxidized fields on the petrochemical variation diagrams (Figure 3-107). The presence of carbon in the ore deposits (Radtke and Scheiner, 1970) indicates reducing conditions, so the deposits are placed in the calc-alkalic reduced class.

Northumberland, NV

The Northumberland district is in the northern Toquima Range of Nye County, Nevada, where East and West Northumberland Canyons meet at the crest of the range. The district is approximately 130 km (80 miles) northeast of Tonopah and about 80 km (50 miles) south of Austin, Nevada (Figure 3-108) (Kokinos and Prenn, 1985). Gold mineralization at the Northumberland mine is primarily located in silicified, argillaceous and carbonaceous limestones of the Ordovician Pogonip group (Goldstein, 1973). The gold at Northumberland is chiefly in a carbonaceous shale above a limestone (Kral, 1951); submicroscopic gold mineralization is disseminated through a nearly horizontal jasperoid horizon

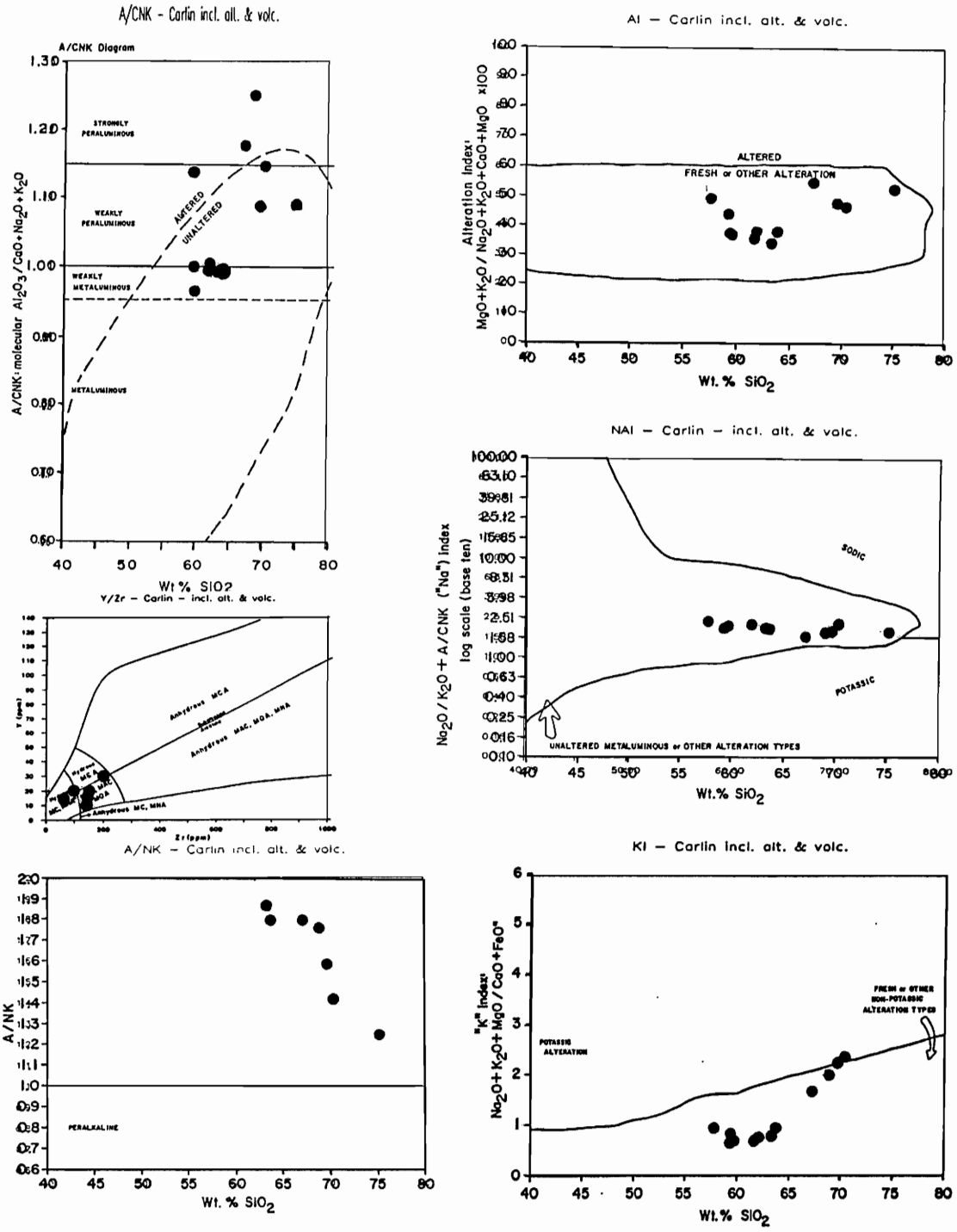

Figure 3-106. Petrochemical variation diagrams of Tertiary igneous rocks from Carlin, Nevada, showing alteration filters.

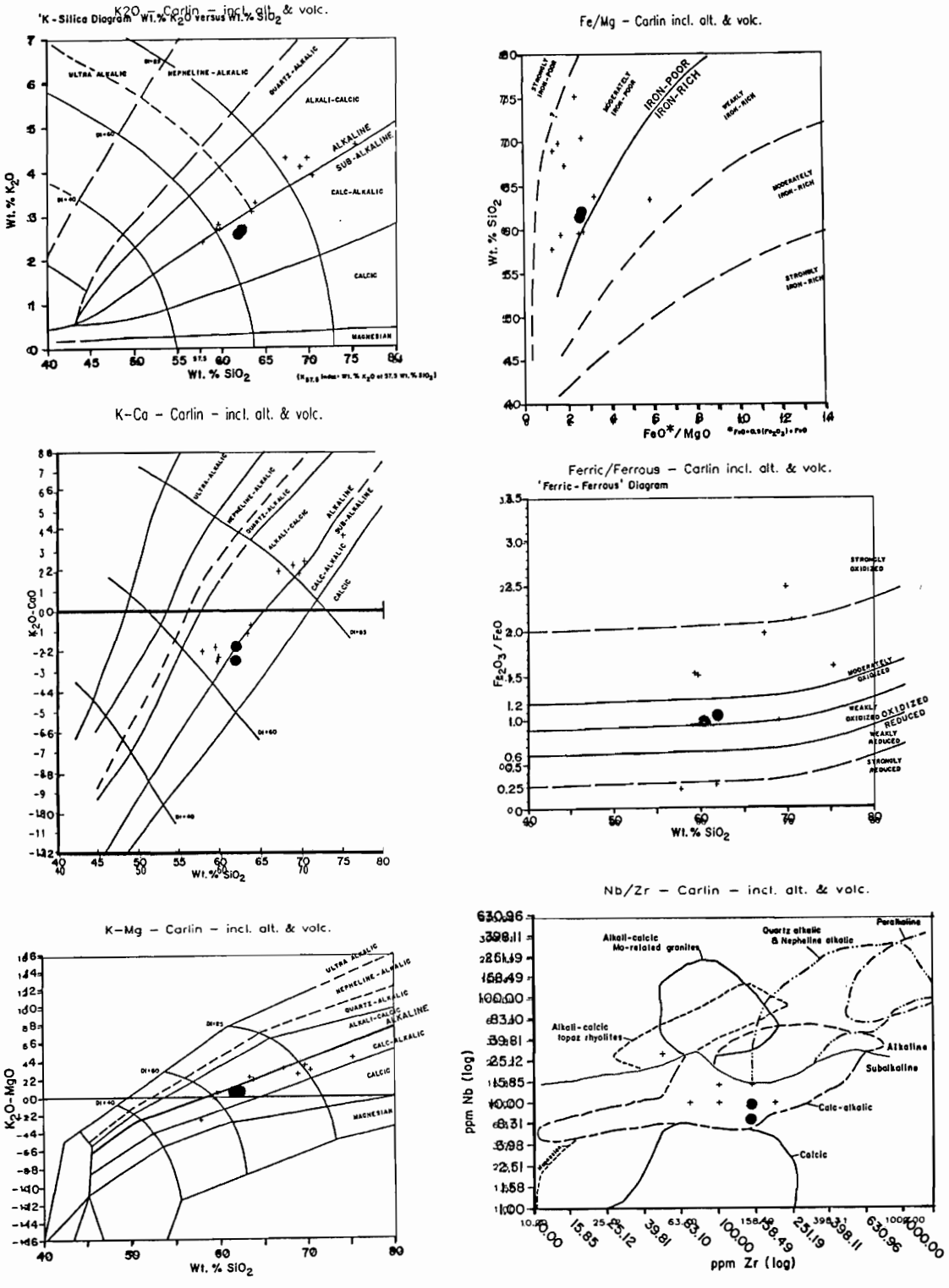

Figure 3-107. Magma series variation diagrams of igneous rocks from Carlin, Nevada, showing alkalinity and iron ratios (+ altered, • unaltered).

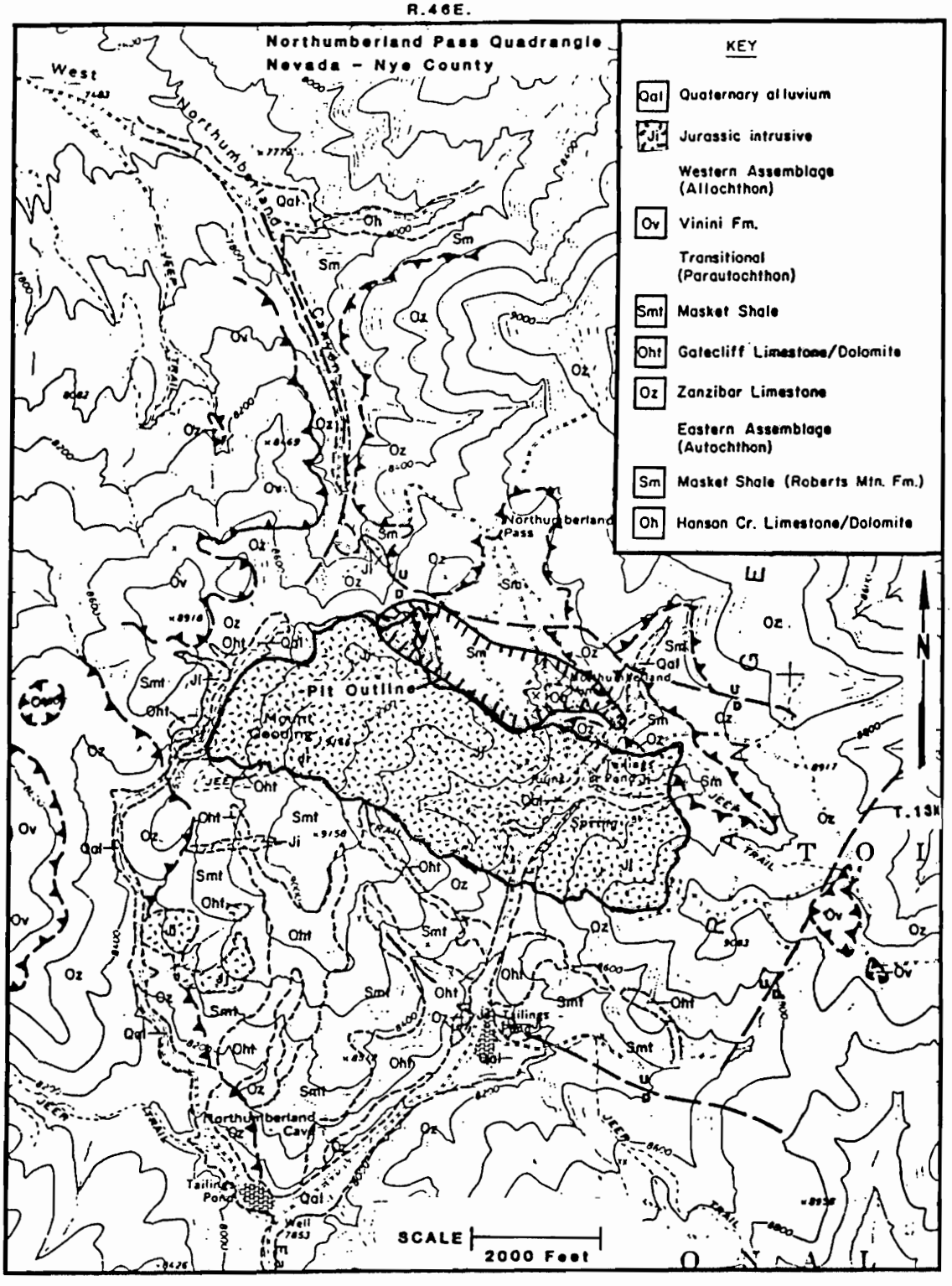

Figure 3-108. Geologic map of the Northumberland area, Nevada (Tertiary dikes not shown = CIMVS) (from Motter and Chapman, 1984).

and in silty carbonate horizons immediately below a Cretaceous(?) tonalite sill (Ott, 1983).

The granodiorite stock may be related to the emplacement of quartz-silver veins and silicification of the sediments (Kokinos and Prenn, 1985). A Jurassic plutonic complex crops out as several small bodies in the Northumberland district. The Northumberland intrusive (Kay and Crawford, 1964) is about 154 $\pm$ 3 Ma (McKee, 1976; Kleinhampl and Ziony, 1984); it ranges in composition from granite to the more abundant quartz diorite (Kay and Crawford, 1964). A large plutonic body approximately 16 km (10 miles) to the south of Northumberland Canyon is another Middle Jurassic granodiorite named the Clipper Gap pluton; it was dated by K-Ar method at 151 $\pm$ 3 Ma (McKee, 1972; 1976; Kleinhampl and Ziony, 1984).

Dikes and sills of a younger tonalite (quartz porphyry) intrude the sediments in the mine area (Kokinos and Prenn, 1985). These dikes are of diorite to felsite composition and were originally believed to be Cretaceous in age (McKee, 1972). The felsite dikes cut the Jurassic Clipper Gap pluton and are overlain by Oligocene volcanic rocks; apatite from an unaltered dike of biotite granodiorite porphyry yielded a fission track age of 93 Ma (McKee, 1976). The altered portion of the tonalite was dated by the U. S. Geological Survey at 84.6 $\pm$ 1.7 Ma (Motter and Chapman, 1984).

Argillically altered, rhyolitic to dacite dikes (CIMVS), also called felsitic (rhyolite?) porphyry dikes, are probably of Tertiary age and may be related to the stage of hydrothermal activity associated with gold metallization (Ott, 1983;

Kleinhampl and Ziony, 1984; Motter and Chapman, 1984). The disseminated gold mineralization and an associated late stage of broad alteration is superimposed over the high-grade silver veins and silicified zones (Kokinos and Prenn, 1985). The felsite dikes are not known to cut the overlying Tertiary volcanic rocks (Kay and Crawford, 1964).

Oligocene and Miocene welded tuffs and lesser amounts of tuffaceous lacustrine deposits lie discordantly on the older rocks and partly formed after emplacement of the precious-metal deposits (Kleinhampl and Ziony, 1984). These Tertiary ash flow tuffs and shallow rhyolitic intrusive bodies are related to the Northumberland volcanic center and caldera 6 km west of the mine area. The Northumberland Tuff is Oligocene based on a K-Ar determination of 32.3 $\pm$ 1 Ma on sanidine from tuff collected along Northumberland Canyon road (McKee, 1974). Some dikes of more intermediate composition than the felsite dikes cut Tertiary welded tuffs as well as the Jurassic Clipper Gap pluton and its bordering metamorphic belt (Kleinhampl and Ziony, 1984). A rhyolite dome about 28 Ma at Mt. Ziggurat intrudes part of the Tertiary tuff section about 8 km (5 miles) southwest of Northumberland (Kleinhampl and Ziony, 1984).

Whole rock analyses used for this study were obtained from Lee (1984) and McKee (1976) for the Cretaceous(?) dike, which is the felsitic rhyolite porphyry dike of probable Tertiary age (CIMVS). The samples passed the alteration filters (Figure 3-109) and are in the calc-alkalic, moderately iron-poor, reduced fields in the petrochemical variation diagrams (Figure 3-110).

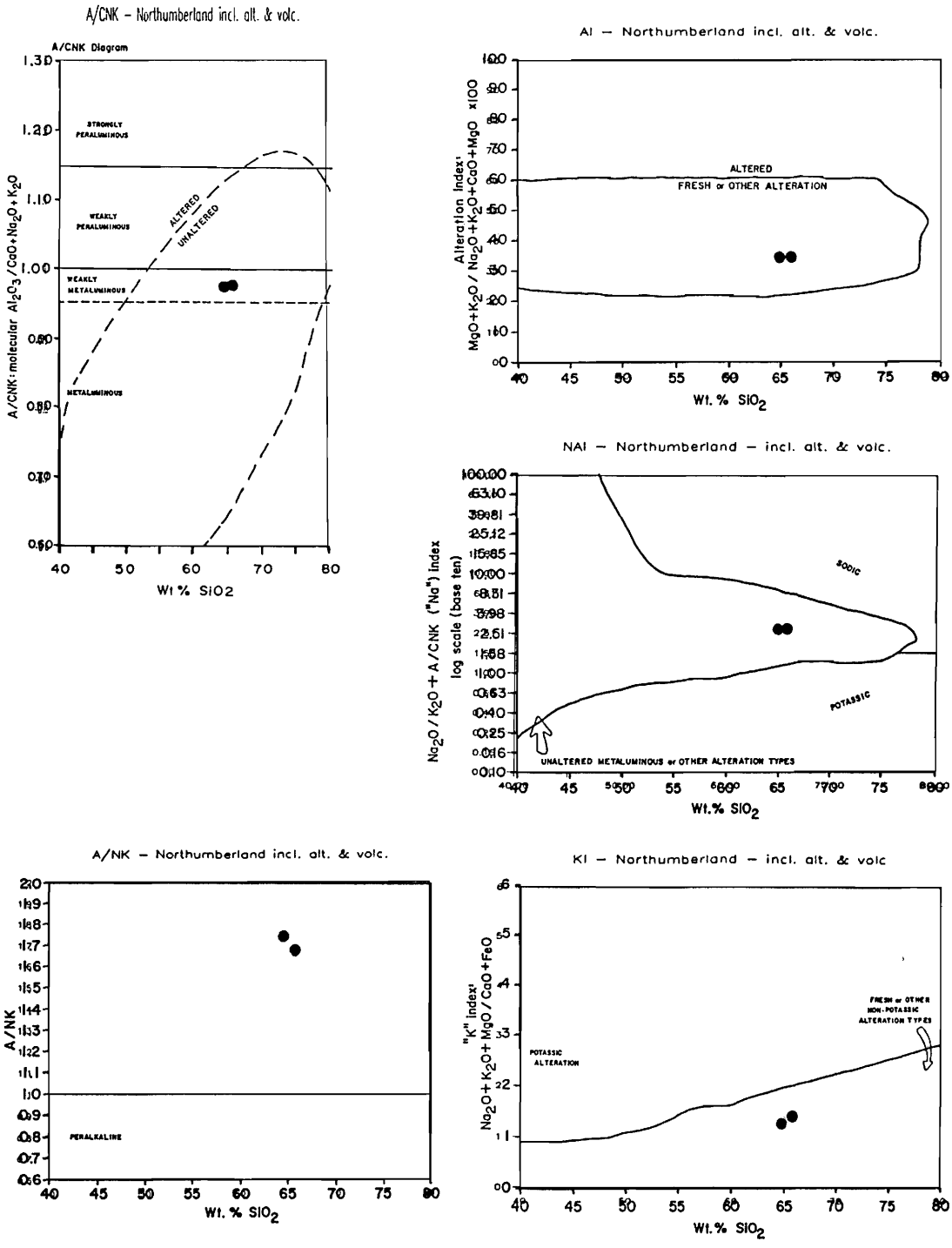

Figure 3-109. Petrochemical variation diagrams of igneous rocks from the Northumberland area, Nevada, showing alteration filters.

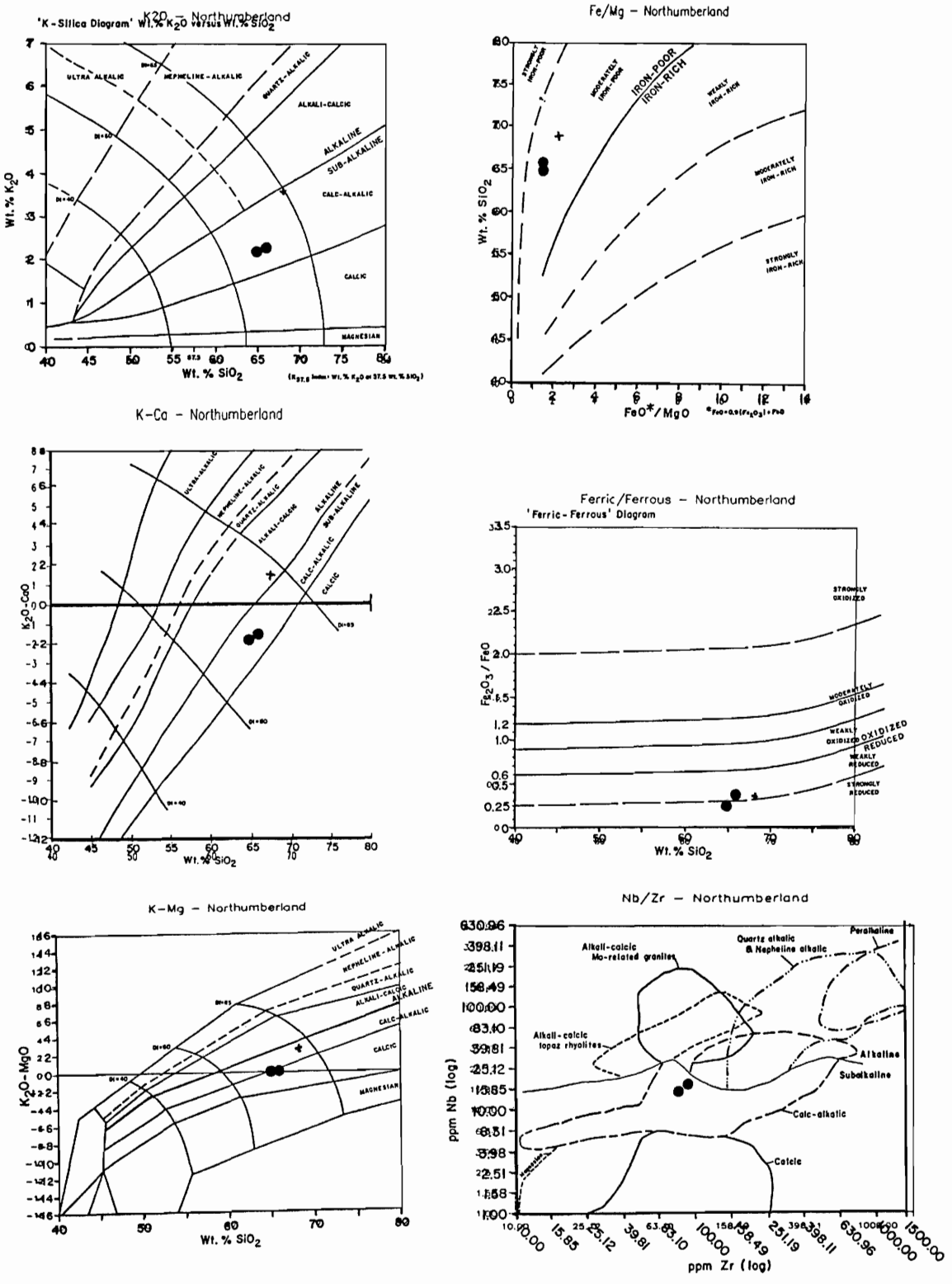

Figure 3-110. Magma series diagrams of Tertiary dikes, Northumberland, Nevada, showing alkalinity and iron ratios (+ altered, ● unaltered).

Osgood Mountains, NV

The Osgood Mountains are in eastern Humboldt County, Nevada, northeast of the town of Golconda (Figure 3-111). Numerous tungsten and disseminated gold deposits are on the northern, eastern, and southern sides of the Osgood Mountains granodiorite stock (CIMVS), which is surrounded by a metamorphic aureole as much as two miles wide (Silberman and others, 1974). From north to south the disseminated gold deposits include Chimney Creek, Rabbit Creek, Getchell, Mag, Pinson, and Preble. These deposits are included in the Potosi mining district, which is in the northern part of the Osgood Mountains, approximately 50 km (30 miles) northeast of Winnemucca (Stager and Tingley, 1988). Altered igneous rocks occur within the ore zones of all the disseminated gold deposits (Silberman and others, 1974).

A Cretaceous granodiorite stock intrudes complexly folded and thrust-faulted Paleozoic sedimentary rocks in the northern Osgood Mountains (Willden, 1964; Hotz and Wilden, 1964). The north lobe of the Osgood Mountains stock yielded a K-Ar date of 89.9 $\pm$ 1.8 Ma on biotite and the south lobe yielded a K-Ar date of 92.2 $\pm$ 1.8 Ma on biotite and 88.3 $\pm$ 1.8 Ma on hornblende (Silberman and McKee, 1971).

Dacite porphyry dikes cut the Paleozoic sedimentary rocks and are probably related genetically to the stock. Andesite porphyry dikes cut both sedimentary rocks and the granodiorite in the northern part of the Osgood Mountains (Silberman and others, 1974). These dikes are cut by gold-bearing

DESCRIPTION OF MAP UNITS

Qal - Quaternary alluvium

Qoa - Older Quaternary alluvium

Qg - Quaternary gravel

Tb - Pliocene basalt

Tr - Miocene rhyolite flows and tuffs

Ts - Miocene clastic rocks and tuffs

Tba - Miocene basalt and basaltic andesite

CIMVS # Kg - Cretaceous granodiorite (about 90 Ma) Osgood Mountains granodiorite

JTRu - Jurassic and Triassic metaclastic rocks, undivided

PPu - Permian and Pennsylvanian clastic and carbonate rocks, undivided. Includes Edna Mountain Formation (Permian), Antler Peak Limestone (Pennsylvanian and Permian), Highway Limestone (Pennsylvanian), and Battle Formation (Pennsylvanian). In the Osgood Mountains, includes the Etchart Limestone (Pennsylvanian and Permian) and the Adam Peak Formation (Pennsylvanian and Permian).

PPp - Pumpernickel Formation (Pennsylvanian and Permian)--siliceous sedimentary and volcanic rocks

PPh - Pennsylvanian and Permian siliceous sedimentary and volcanic rocks, undivided. Includes the Havallah Formation (Pennsylvanian and Permian), rocks similar to the Havallah and Pumpernickel Formations in the Hot Springs range, and the Farrel Canyon Formation (Pennsylvanian and Permian) in the Osgood Mountains.

Msv - Mississippian siliceous sedimentary and volcanic rocks. In the Osgood Mountains includes the Goughs Canyon Formation.

Ov - Valmy Formation (Ordovician)--Chert and greenstone

Oc - Comus Formation (Ordovician)--Carbonate rocks and sandstone

Ch - Harmony Formation (Cambrian)--Sandstone and shale. Includes small exposures of Paradise Valley Chert (Cambrian) on the west side of the Hot Springs Range.

Cp - Preble Formation (Cambrian)--Shale and limestone

Com - Osgood Mountain Quartzite (Cambrian)

Contact

Fault, dashed where approximately located, dotted where concealed

Thrust fault, sawteeth on upper plate

MAG Gold deposit; names indicate operational or developing mines

Tungsten deposit

Barite deposit

Silver deposit

Manganese deposit

Explanation for Figure 3-111. Rock units on geologic map of the Osgood Mountains area, Nevada (from Grauch and Bankey, 1991).

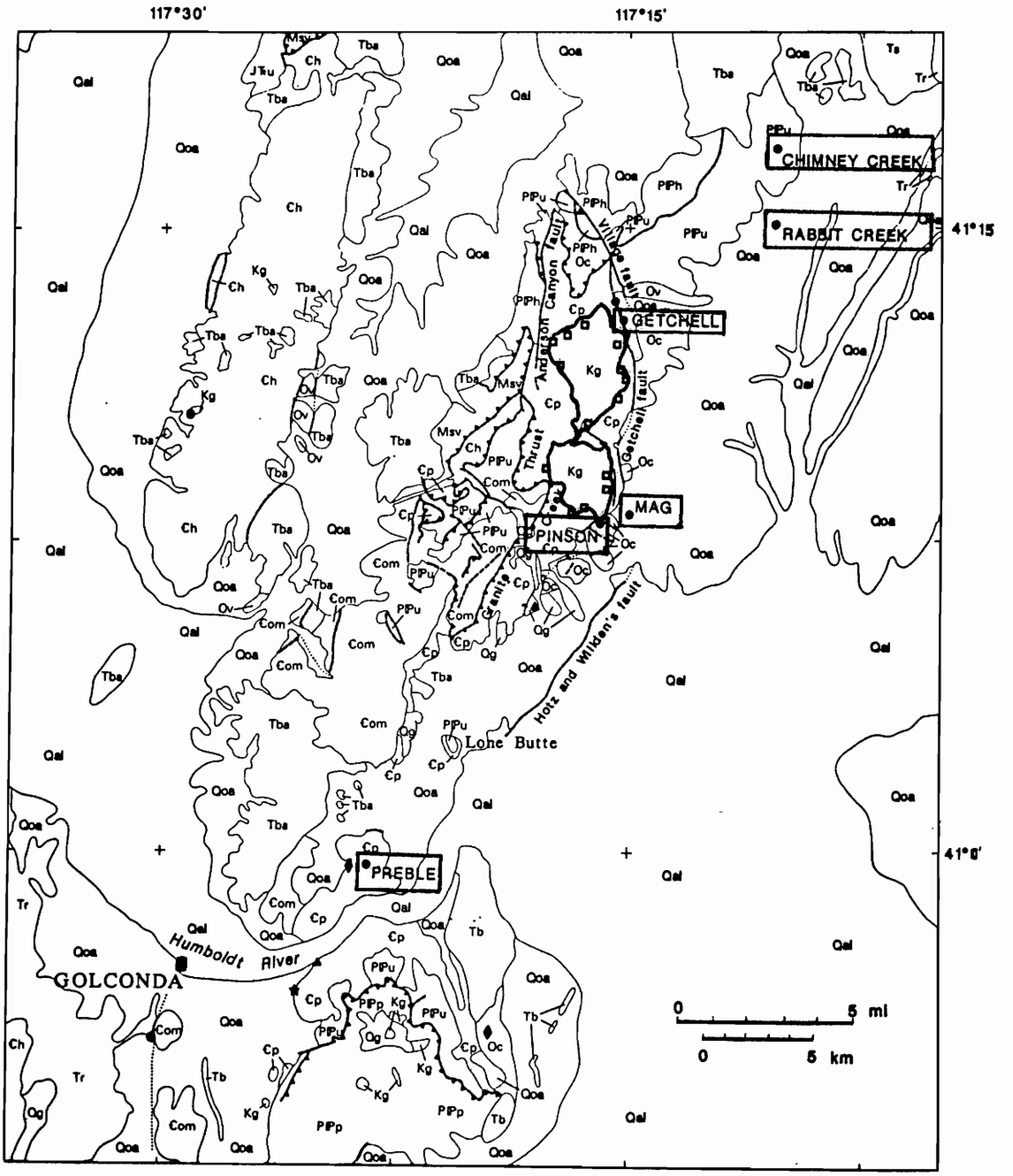

Figure 3-111. Geologic map of the Osgood Mountains area, Nevada (Kg = Osgood Mtn. Granodiorite = # = CIMVS) (from Grauch and Bankey, 1991; Willden, 1964; Hotz and Willden, 1964).

mineralization at the Getchell mine; they are a later phase of the granodiorite stock and are cogenetic with it (Hobbs, 1948; Hotz and Willden, 1964). An andesite porphyry dike from the north pit at Getchell yielded a K-Ar age on biotite of 89.9 $\pm$ 3.4 Ma (Silberman and others, 1974).

Scheelite was deposited during the final stages of silicification by solutions sweated out of the granodiorite after emplacement (Silberman and others, 1974). Sericitized blocks of granodiorite that were mineralized in the Kirby, Marcus, and Mountain King tungsten mines yielded K-Ar ages of 87.6 $\pm$ 3.4 Ma, 88.4 $\pm$ 3.3 Ma, and 92.6 $\pm$ 2.8 Ma (Silberman and others, 1974).

Whole rock analyses of the Osgood Mountains Granodiorite and associated dikes were obtained from Silberman and others (1974) and Hotz and Willden (1964). Although only two of the samples were plutonic and were included in the data set for the neural network study, all the andesite porphyry dike samples passed the alteration filters (Figure 3-112). The unaltered samples are in the calc-alkalic field on the magma series variation diagrams (Figure 3-113); the dike samples also are in the calc-alkalic field on the K_2O-MgO versus SiO_2 diagram. The plutonic samples are in the moderately iron-poor and weakly reduced fields on the iron diagrams (Figure 3-113). The presence of ilmenite in a ten-meter wide zone inboard from the country rock-granodiorite contact (Osterberg, 1990) indicates the pluton belongs in the reduced category. This conclusion is also supported by relatively low Fe_2O_3/FeO ratios (average of 18 samples = 0.67) reported by Taylor (1976), and by the presence of pyrrhotite (Osterberg, 1990).

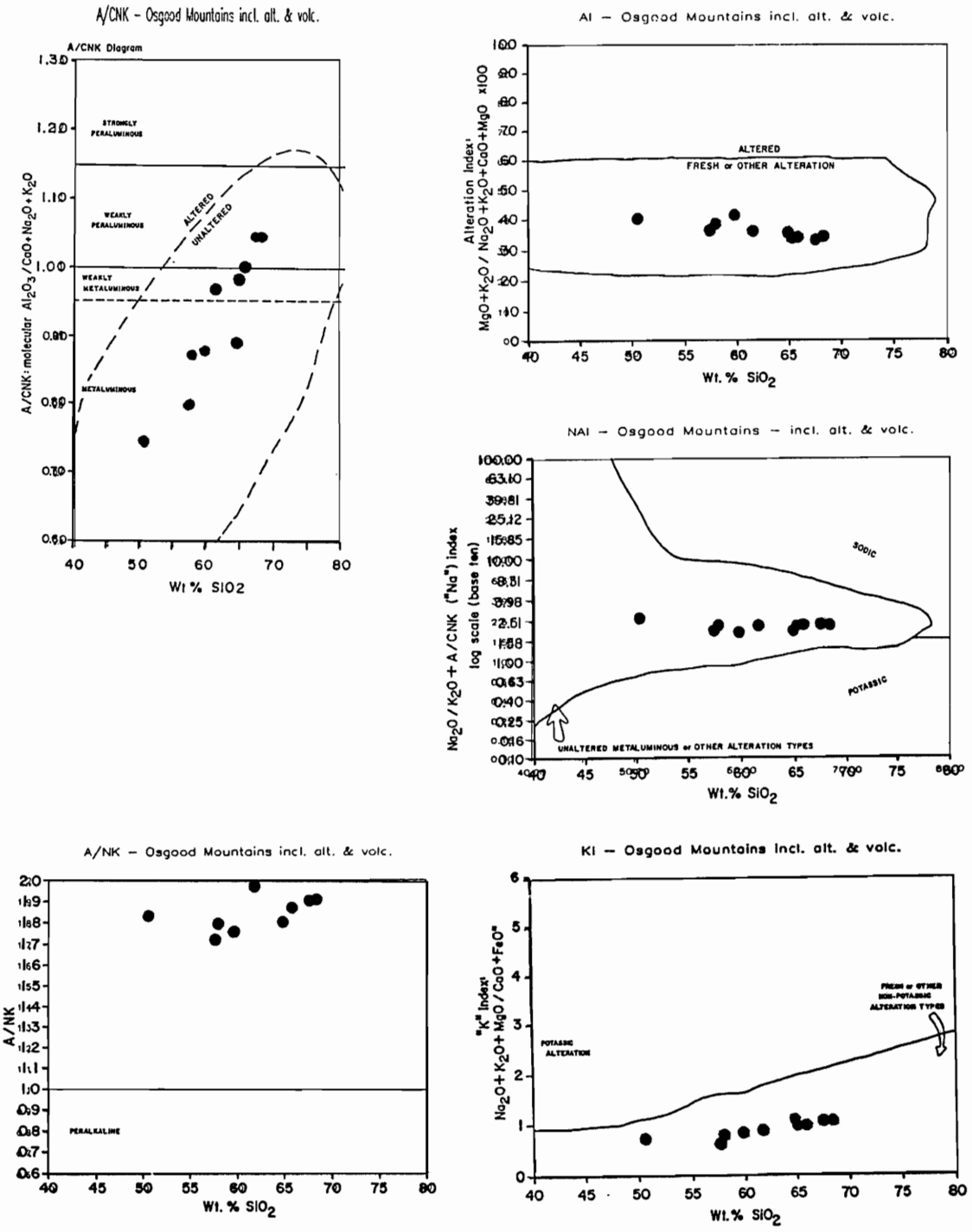

Figure 3-112. Petrochemical variation diagrams of igneous rocks in the Osgood Mountains, Nevada, showing alteration filters.

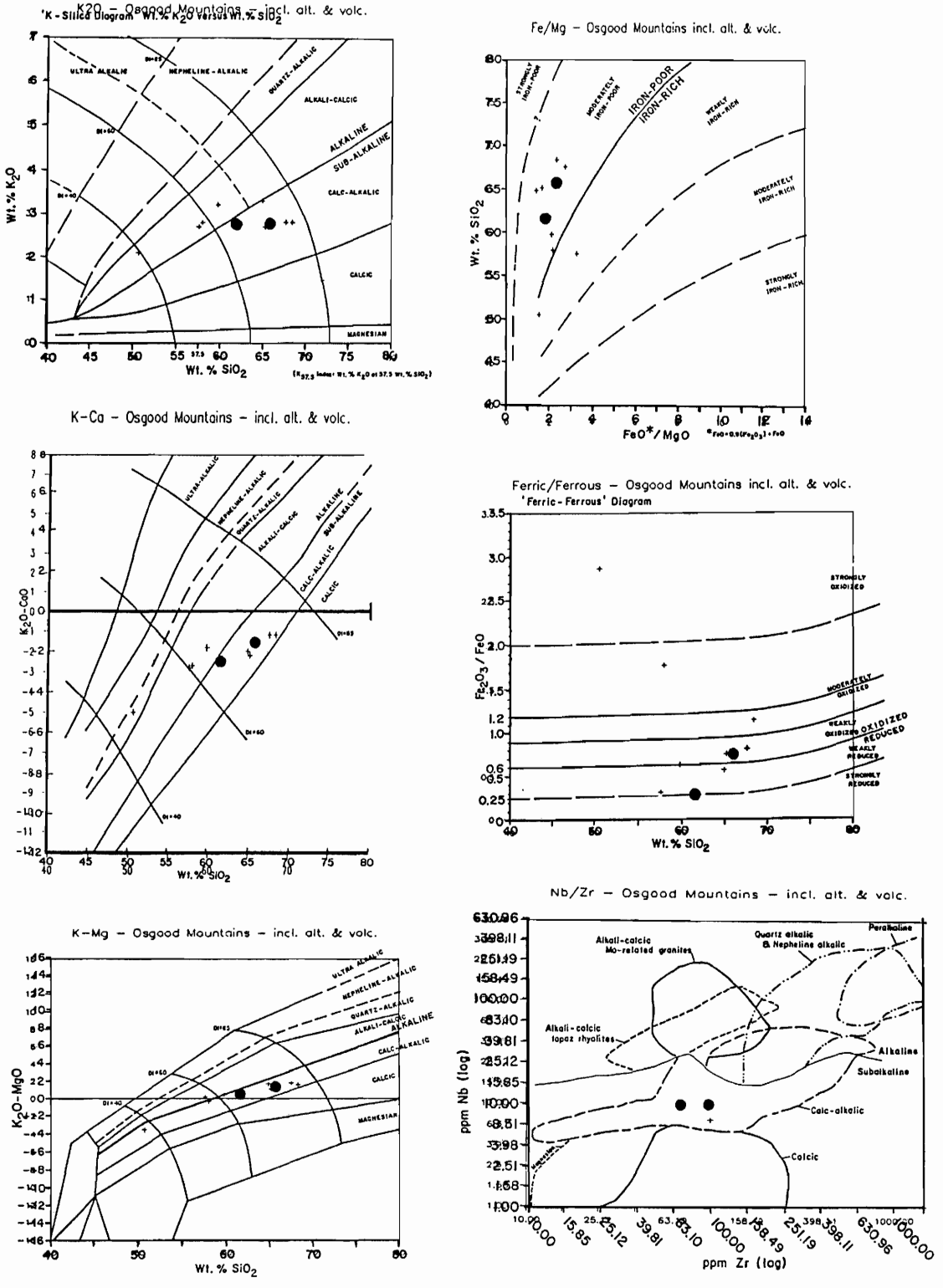

Figure 3-113. Magma series variation diagrams of igneous rocks from the Osgood Mountains, NV, showing alkalinity and iron ratios (+ altered, ● unaltered).

Chimney Creek, NV

The Chimney Creek disseminated gold deposit is at the north end of the Osgood Mountains approximately 10 km (6 miles) northeast of the Getchell deposit. Most of the orebody is hosted in silici-clastics and carbonates of the Etchart Limestone of Pennsylvanian-Permian age and some of the ore is hosted in the underlying propylitic basalts of the Mississippian Goughs Canyon Formation (Osterberg and Guilbert, 1991). These sediments and volcanics are bounded by the Roberts Mountain and Golconda thrust faults and are intruded by the mid-Cretaceous Osgood Mountains Granodiorite. Trachyandesitic dikes related to the Osgood Mountains Granodiorite cut the orebody (Osterberg and Guilbert, 1991). The Chimney Creek deposit occurs along a northeasterly range-front lineament that is probably an extension of the Getchell fault.

Gold deposition occurred without the presence of carbonaceous matter in the host rock and was related to a district-wide system of the late Cretaceous Osgood Mountains Granodiorite (Osterberg, 1990). Cross-cutting relationships between the Paul's Hill felsic dike (dated at 92.4 $\pm$ 2.2 Ma) and wall rock alteration prove that the dike is contemporaneous with or younger than the orebody (Osterberg, 1990). Sericites from altered basalt and sediments and from the Paul's Hill dike gave K-Ar ages ranging from 92.1 $\pm$ 2.1 Ma to 98.6 $\pm$ 3.5 Ma (Osterberg, 1990). Recalculated published dates on the Osgood Mountains granodiorite and mineralized and altered stocks and dacites also cluster around an age of 92.4 $\pm$ 2.2 Ma for the Osgood Mountains Granodiorite (Osterberg, 1990).

Getchell, NV

The Getchell gold deposit, 65 km (42 miles) by road northeast of Winnemucca, is localized along approximately 5 km (3 miles) of the strike-length of the Getchell fault, a major north-trending structural feature extending along the eastern margin of the Osgood Mountains (Joralemon, 1951; Nanna and others, 1987). Another major control on mineralization at Getchell is the host rock lithology, which was originally carbonaceous shales, thin-bedded limestones and siltstones (Nanna and others, 1987).

Gold ore deposition at Getchell could have occurred any time after the emplacement of the andesite porphyry dikes (Silberman and others, 1974). Erickson and others (1964) demonstrated the occurrence of small amounts of tungsten in and over the gold-bearing ore at Getchell and the enrichment of arsenic over both the tungsten tactite and gold ores. They concluded that both the tungsten and gold deposits are genetically related to each other and to the granodiorite intrusive mass and that they formed as successive and overlapping stages of one period of complex mineralization. Two sericitized blocks of granodiorite that were mineralized in the Getchell fault zone at the Getchell gold mine yielded K-Ar ages of 92.2 $\pm$ 2.8 Ma and 80.9 $\pm$ 3.3 Ma (Silberman and others, 1974). The presence of sericitized cordierite crystals in gold-bearing hornfels indicate that sericitic alteration accompanied the gold mineralization; only one episode of sericite formation was found (Silberman and others, 1974). Further support of a Cretaceous age for the Getchell gold deposit comes from

fluid inclusions which indicate confining pressures during or subsequent to gold precipitation were greater than those generally associated with epithermal mineralization (Bagby and Cline, 1991).

Pinson, NV

The Pinson deposit is 60 km (38 miles) northeast of Winnemucca on the east flank of the Osgood Mountains in the Potosi mining district. It lies within the contact metamorphic aureole of the Osgood Mountains granodiorite and occurs along the Getchell fault system (Kretschmer, 1984). The Ordovician Comus Formation is the host rock for the Pinson deposits (Foster and Kretschmer, 1991). Dacite dikes in the mine area are probably related to the Osgood Mountains granodiorite stock (Hotz and Willden, 1964; Foster and Kretschmer, 1991). Aplite, pegmatite, and porphyritic dikes and sills of intermediate composition are associated with the Osgood Mountains stock (Kretschmer, 1986). A prominent northeast-trending normal fault has controlled the gold mineralization (Kretschmer, 1986); this fault system is believed to be of late Cretaceous age (Berger and Taylor, 1980).

The Mag deposit is a few miles northeast of the Pinson pit; it is hosted by carbonate-bearing argillite and shale within the Late Ordovician upper Comus Formation. Minor dikes in the Mag deposit are completely sericitized and/or argillized, though textures indicate a dacitic composition (Foster and Kretschmer, 1991). Disseminated sub-micron gold is localized along north-northwest and

northeast striking normal faults in favorable host rocks (Foster and Kretschmer, 1991).

Preble, NV

The Preble deposit is 50 km (30 miles) northeast of Winnemucca approximately 16 km (10 miles) south of the Pinson deposit. The Preble deposit is within carbonaceous shales and silty limestones of the middle member of the Cambrian Preble Formation along a broad shear zone (Kretschmer, 1984).

Summary of Results of Classifying Each Mine

Qualifying the data is an extremely important and time-consuming part of this research. Obtaining isotopic age dates and cross-cutting geologic relationships to establish links between the mineralizing event and a particular igneous rock is crucial to the classification process. Applying alteration filters to exclude data from altered rocks and eliminating volcanic rocks are also important in order to be rigorously uniform in comparing data from the various magma series classes. Mineralogy, especially of iron, is significant in determining oxidation class; it is more effective than the ferric/ferrous ratio, which is highly susceptible to alteration, weathering, analytical errors, and careless handling. These rigorous screens eliminate more than half of the whole rock data.

The complexity of overprinted igneous systems that are typical of most mineralized areas make it especially important that geologic relationships be

worked out in as much detail as possible. Absolute ages of mineralization and of each of the plutonic and volcanic rocks and crosscutting relationships should be established by mapping and geologic observations. In nearly every mining district documented in this chapter, there are plutonic or volcanic rocks that were eliminated from the data set because they were older or younger than the mineralizing event. In several cases, such as Tombstone, Sierrita, and Park City, the alkalinity was different in rocks that were 5 to 10 million years older or younger than the principal mineralization event. Because of changes in alkalinity in areas that have experienced transgressing or regressing subduction-zone magmatism, combining all igneous rocks in a mining district blurs correlations between mineralization and whole rock geochemistry of associated plutons. Each individual igneous pluton, dike, or volcanic flow must be plotted separately to show changes in alkalinity with time.

The application of alteration filters was a rigorous step that eliminated more than half of the data encountered in this study, but that tightened sample point clusters into particular fields in the variation diagrams of each district. Although a general idea of the alkalinity of a mining district can be obtained from variation diagrams that include altered sample data, this practice is risky if there are few sample points and if many of the altered samples are outside of the fresh-rock field.

The elimination of altered samples from the data base is especially important in determining the oxidation state of the class; altered samples

contribute much of the scatter to the ferric/ferrous ratio versus SiO_2 variation diagrams. In many cases, especially for the reduced and weakly oxidized classes, it is necessary to know the mineralogy of the igneous rock and the mineralogy of the mineralized system in order to assign the district to an oxidation-reduction class. In many of the mining districts, the presence of ilmenite in the igneous rocks and of pyrrhotite or carbon in the mineralized system is an indication of reduced status. The presence of magnetite and sphene in the igneous rock and of pyrite in the primary sulfides is an indication of oxidized status, especially in the absence of ilmenite and pyrrhotite. If there are indications of both reduced and oxidized mineralogies in the fresh igneous rocks and primary mineralization, the district is probably weakly oxidized.

CHARACTERISTICS OF WHOLE ROCK DATA ARRANGED BY CLASS

Whole rock geochemical data from the mining districts described in the previous chapter were combined into their respective classes and plotted on petrochemical variation diagrams. Figures comparing graphs with altered and volcanic samples and graphs with only unaltered plutonic data demonstrate a dramatic tightening into specific fields when ambiguous data are eliminated (Appendix C). Figures comparing the different classes arranged by type of diagram are analyzed below.

Comparisons Among the Six Classes

A/CNK Versus SiO_2 Diagram

Although no fields are drawn on the A/CNK diagram, several differences are apparent between the classes (Figure 4-1). This graph is used to distinguish between metaluminous and peraluminous categories; as all the districts in this study are metaluminous because of the presence of hornblende and other petrologic indicators, samples from all classes are in approximately the same position. Most of the points define a zone with a steep positive slope, although the alkali-calcic reduced (MACr) class has a slope that is nearly vertical.

A/NK Versus SiO_2 Diagram

None of the samples in this study were peralkaline, so samples from all the classes are in the same portion of the A/NK versus SiO_2 variation diagram (Figure

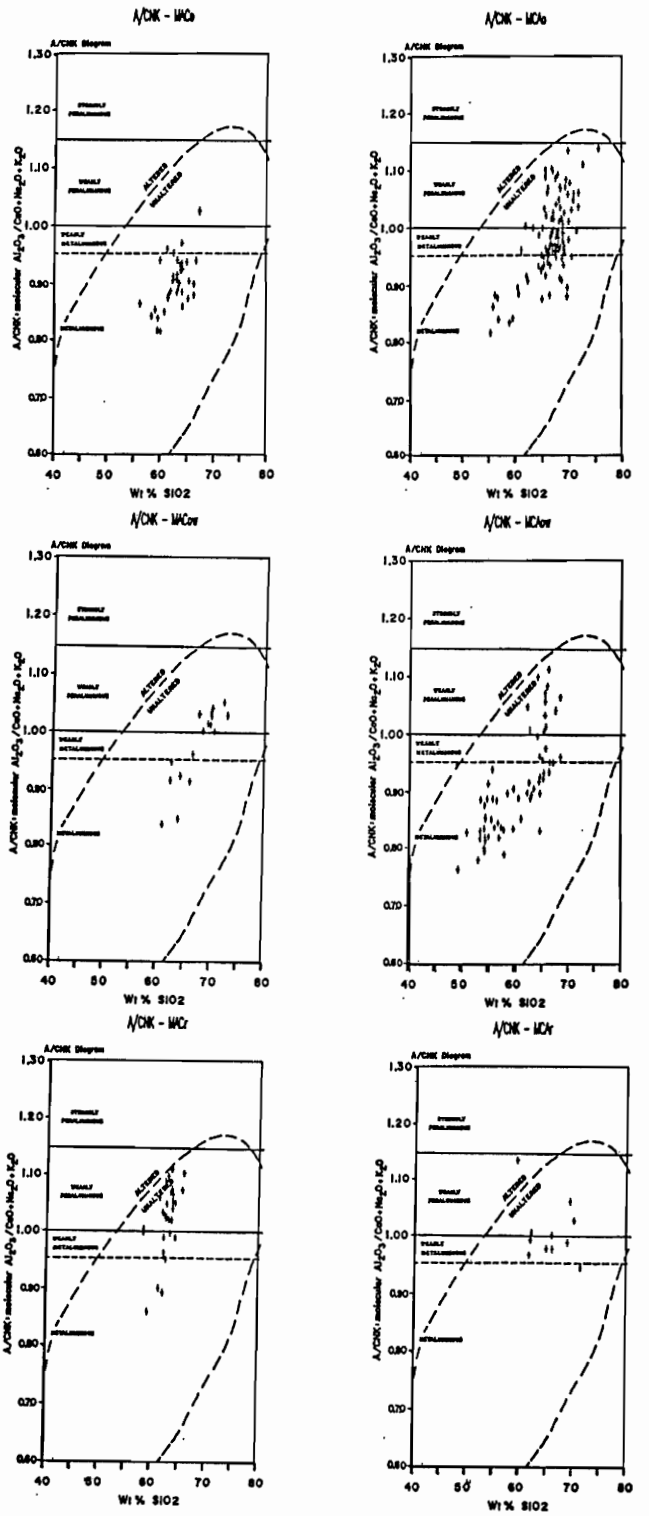

Figure 4-1. Comparison of A/CNK versus SiO_2 variation diagrams for metaluminous, alkali-calcic (left side) versus calc-alkalic (right side), oxidized (top), weakly oxidized (center), and reduced (bottom) classes.

4-2). A strong negative slope is obvious in the calc-alkalic oxidized (MCAo) and calc-alkalic reduced (MCAr) classes. Several of the other classes do not show a clear trend, although the alkali-calcic reduced (MACr) set of points has a vertical slope.

K_2O Versus SiO_2 Diagram

The K_2O versus SiO_2 variation diagram clearly separates alkali-calcic (on the left side of the Figure 4-3) from calc-alkalic (on the right). There is a slight 15 percent overlap into adjacent fields, especially at higher SiO_2 values above D.I. = 85. There is no difference between the oxidized at the top of the figure, weakly oxidized in the middle, and reduced at the bottom classes on this diagram. Samples from the alkali-calcic reduced class extend into the quartz-alkalic field; this may result from including samples of the Kari Kari 'batholith', which has recently been shown to be a caldera complex and not plutonic.

K_2O - CaO Versus SiO_2 Diagram

The K_2O - CaO versus SiO_2 graph clearly separates alkali calcic (on the left side of Figure 4-4) from calc-alkalic (on the right). There is a fairly large amount of overlap into the adjacent fields in the alkali-calcic oxidized (MACo) class, but only minor overlap in the alkali-calcic weakly oxidized (MACow) and calc-alkalic weakly oxidized (MCAow) classes.

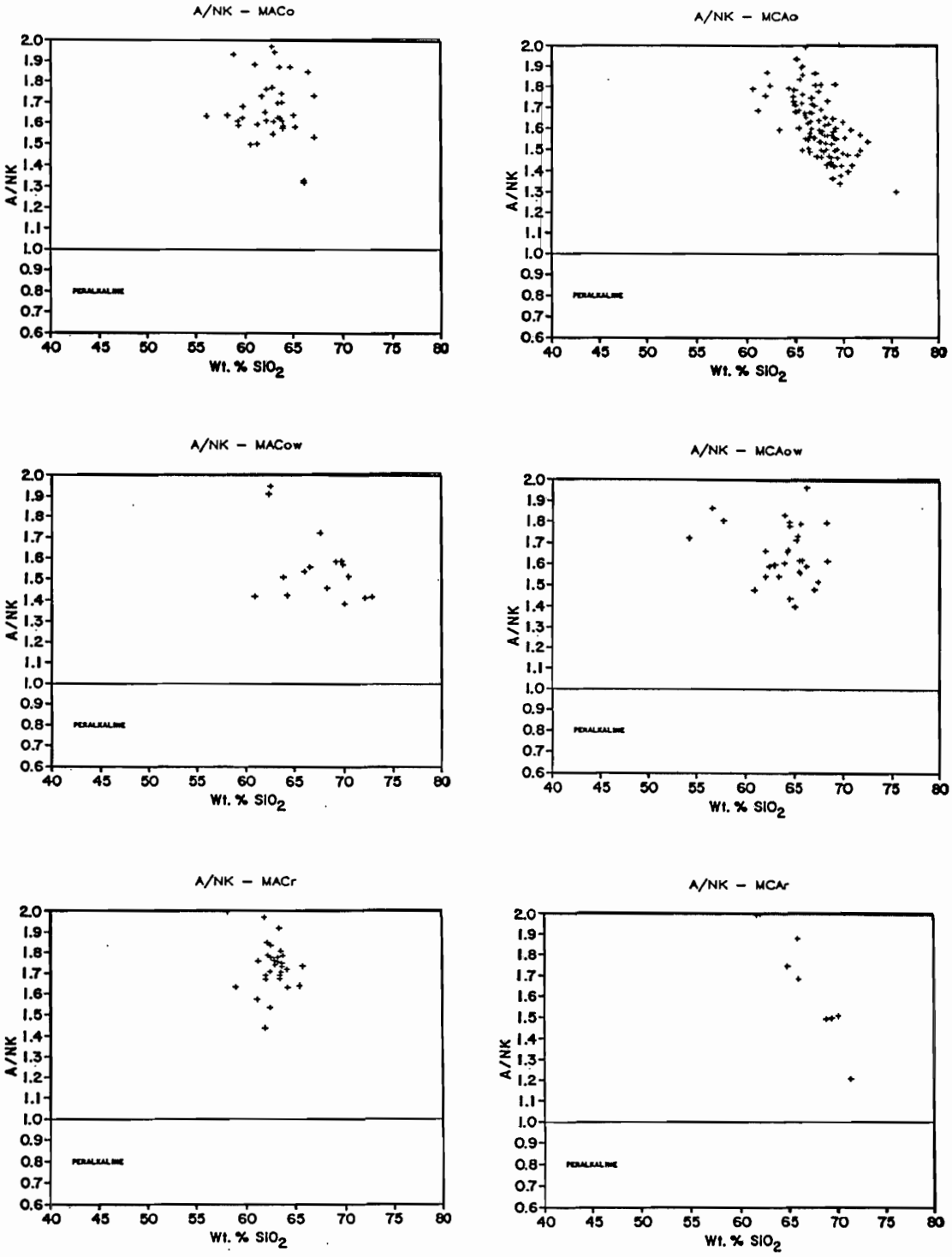

Figure 4-2. Comparison of A/NK versus SiO_2 variation diagrams for metaluminous, alkali-calcic (left side) versus calc-alkalic (right side), oxidized (top), weakly oxidized (center), and reduced (bottom) classes.

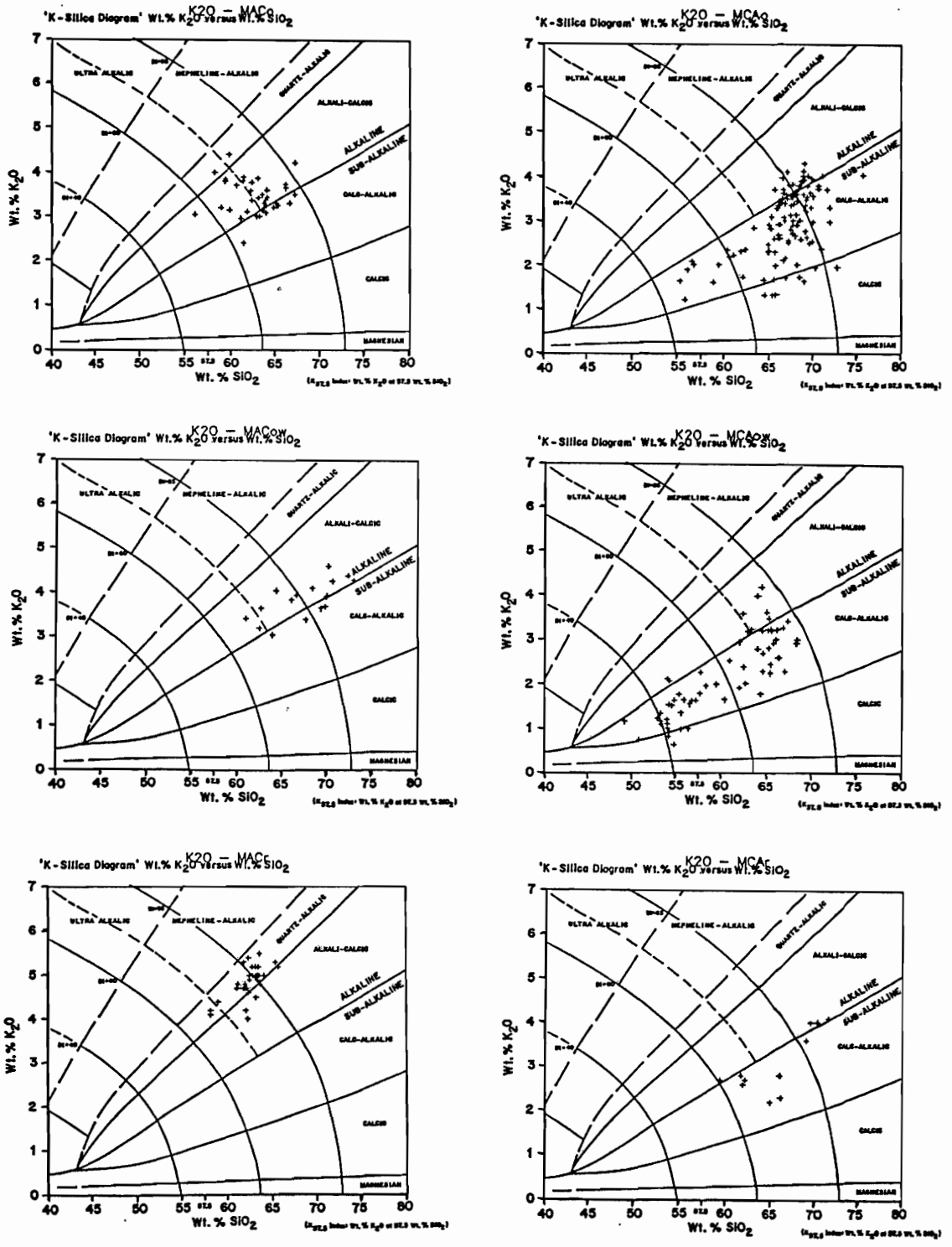

Figure 4-3. Comparison of K_2O versus SiO_2 variation diagrams for metaluminous, alkali-calcic (left side) versus calc-alkalic (right side), oxidized (top), weakly oxidized (center), and reduced (bottom) classes.

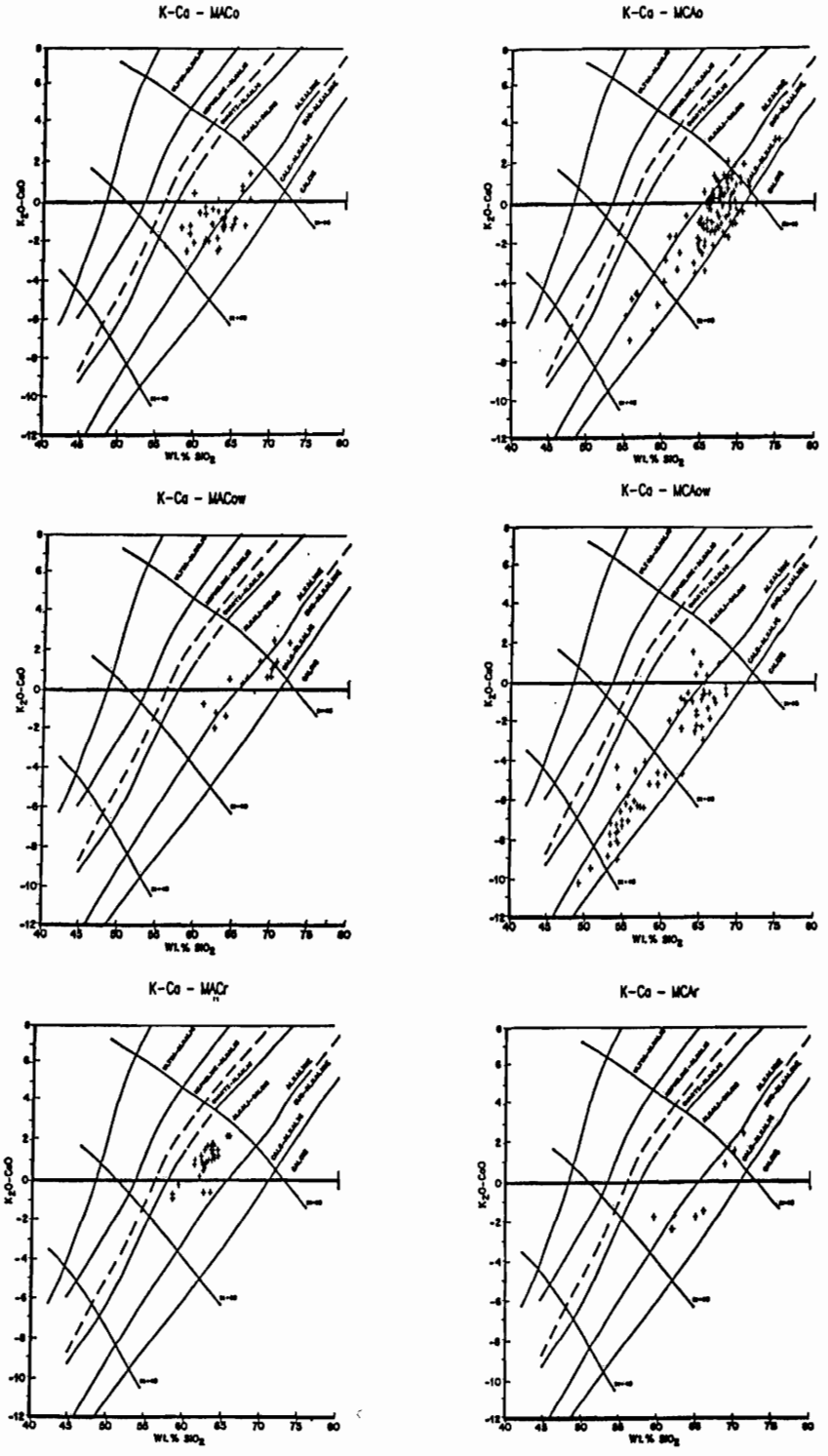

Figure 4-4. Comparison of K_2O - CaO versus SiO_2 variation diagrams for metaluminous, alkali-calcic (left side) versus calc-alkalic (right side), oxidized (top), weakly oxidized (center), and reduced (bottom) classes.

K_2O - MgO Versus SiO_2 Diagram

The K_2O - MgO versus SiO_2 variation diagram clearly separates alkali-calcic (on the left side of Figure 4-5) from calc-alkalic (on the right). There is only minor overlap (15-20 percent) into the adjacent fields in most of the classes, although the alkali-calcic oxidized (MACo) and alkali-calcic weakly oxidized (MACow) classes have more overlap into the calc-alkalic class.

Nb Versus Zr Diagram

The Nb versus Zr variation diagram does not appear to separate the classes in all cases (Figure 4-6). The alkali-calcic weakly oxidized (MACow) is clearly in the alkaline field, although the alkali-calcic oxidized (MACo) has samples in both the alkaline (alkali-calcic) and subalkaline (calc-alkalic) fields. The calc-alkalic weakly oxidized (MCAow) and calc-alkalic reduced (MCAr) are isolated into the calc-alkalic field, but the calc-alkalic oxidized (MCAo) has samples in both alkaline and subalkaline fields. This diagram is not a good discriminator between alkalinity classes, although it is useful for altered samples.

FeO^*/MgO Versus SiO_2 Diagram

All of the samples in this study were related to mineralized systems and all are in the moderately iron-poor fields in the FeO^*/MgO versus SiO_2 variation diagram (Figure 4-7). An exception is the barren Cretaceous alkali-calcic diorites in the Sierrita district and the older, barren calc-alkalic stocks in the

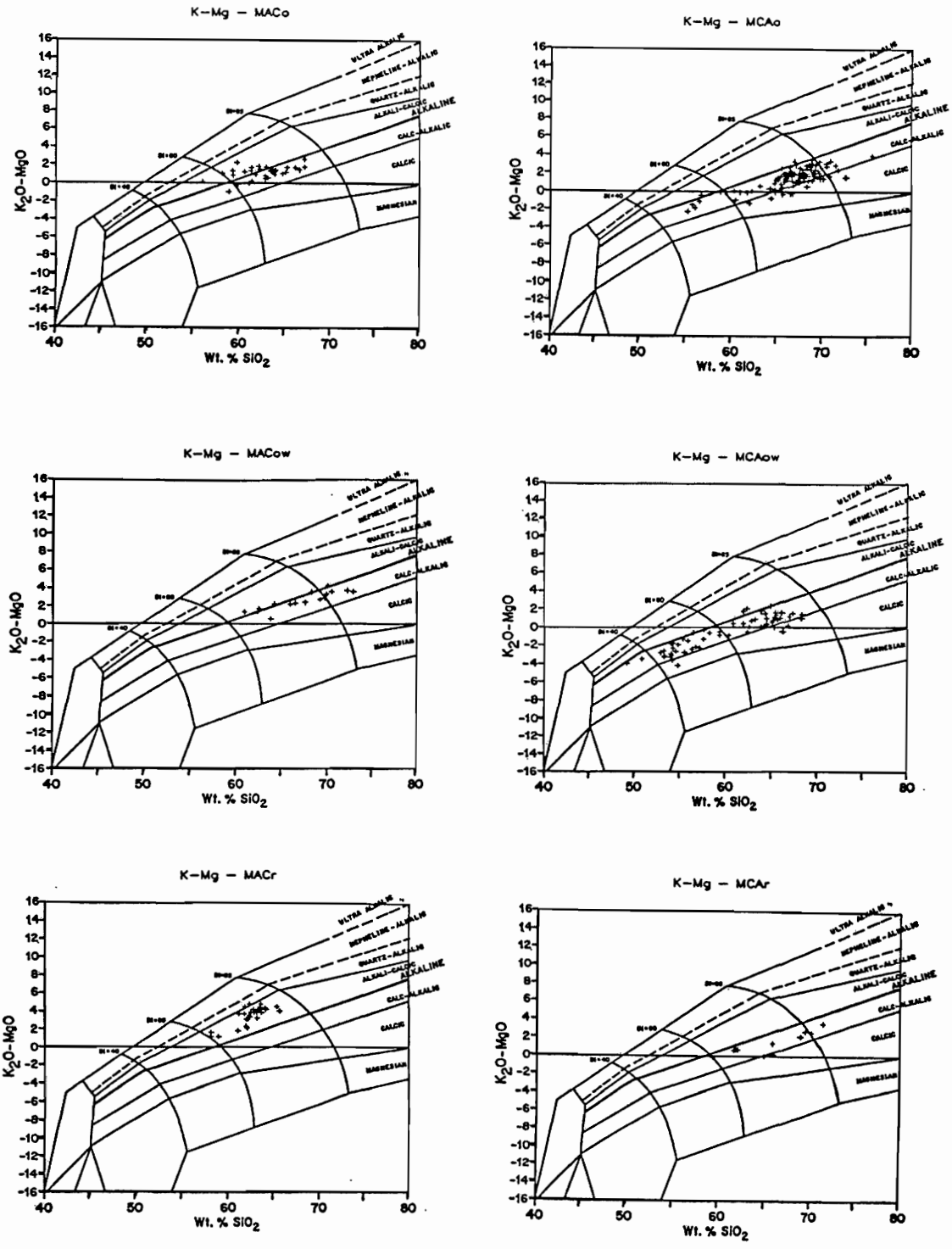

Figure 4-5. Comparison of K_2O - MgO versus SiO_2 variation diagrams for metaluminous, alkali-calcic (left side) versus calc-alkalic (right side), oxidized (top), weakly oxidized (center), and reduced (bottom) classes.

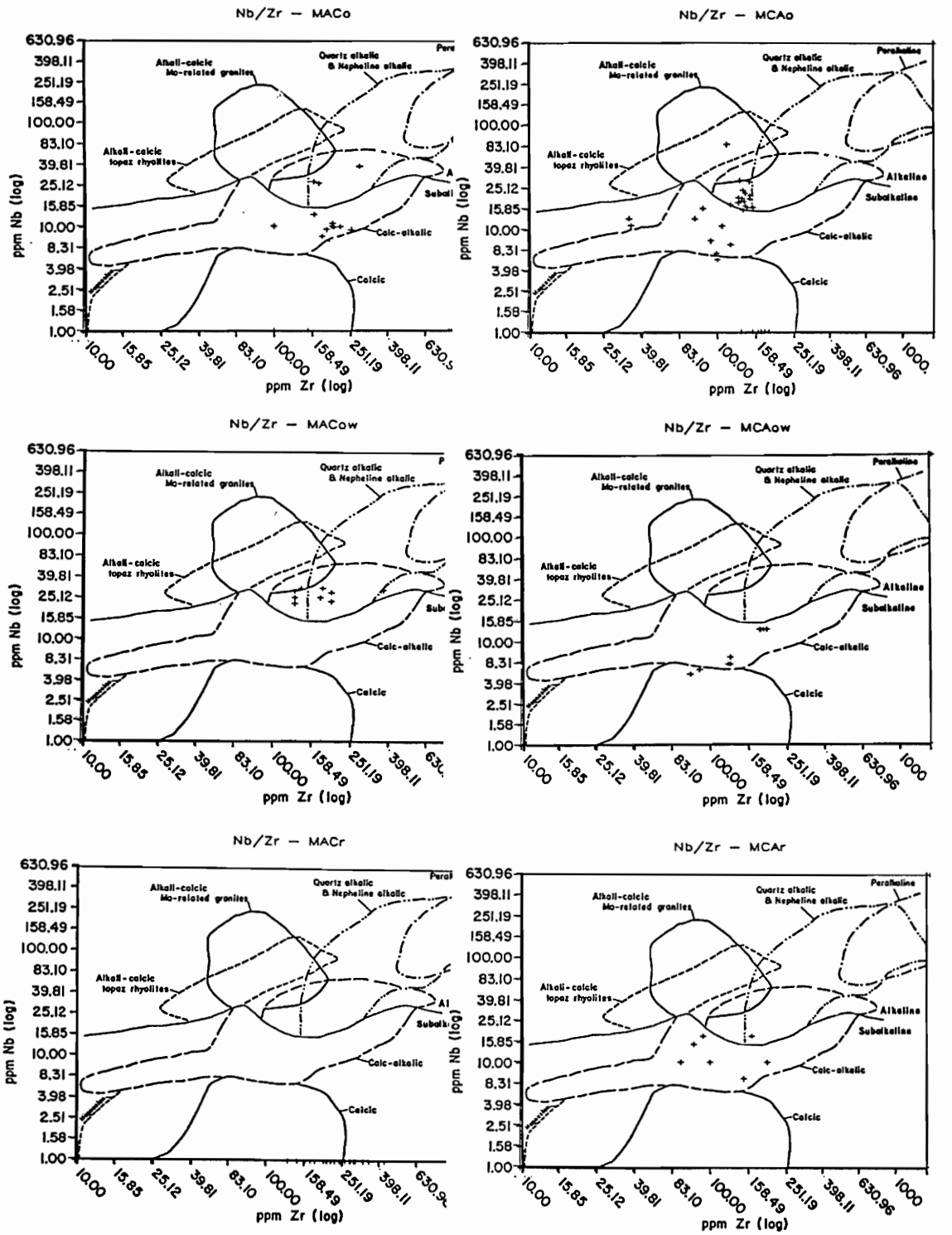

Figure 4-6. Comparison of Nb versus Zr variation diagrams for metaluminous, alkali-calcic (left side) versus calc-alkalic (right side), oxidized (top), weakly oxidized (center), and reduced (bottom) classes.

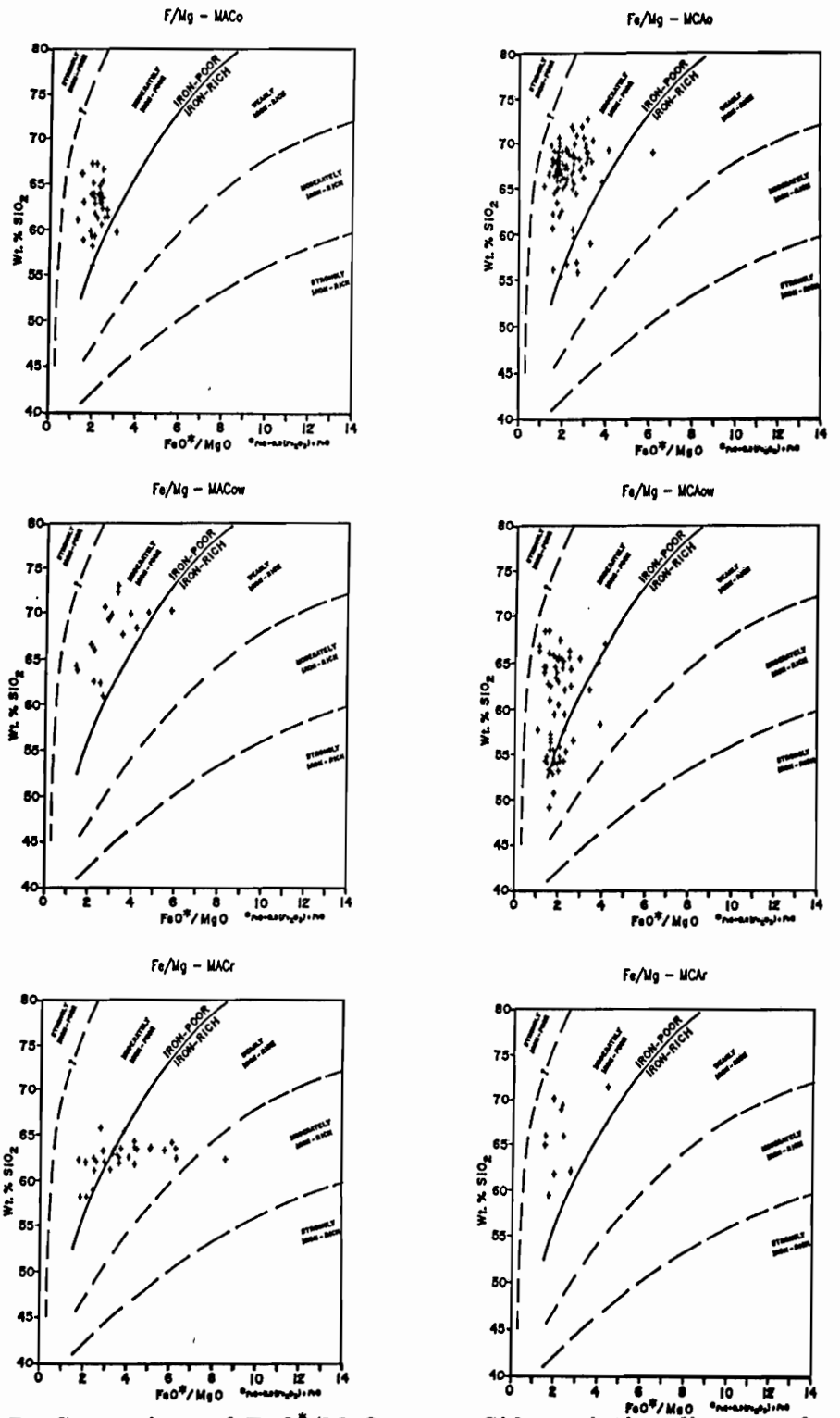

Figure 4-7. Comparison of FeO^*/MgO versus SiO_2 variation diagrams for metaluminous, alkali-calcic (left side) versus calc-alkalic (right side), oxidized (top), weakly oxidized (center), and reduced (bottom) classes.

Park City district. Another possible exception is the Kari Kari 'pluton' at Potosi, Bolivia, which is not directly associated with mineralization. This exception may explain the portion of the alkali-calcic reduced (MACr) group of points that extends into the weakly iron-rich field in the lower left graph in Figure 4-7.

Ferric/ferrous Ratio Versus SiO_2 Diagram

The ferric/ferrous ratio versus SiO_2 variation diagrams show a clear difference between oxidation classes at the top, middle, and bottom in Figure 4-8, but show no difference between alkalinity classes on the left versus right sides. All the sample points in the oxidized subclasses from both alkali-calcic (MACo) and calc-alkalic (MCAo) classes are above the $Fe_2O_3/FeO = 0.6$ line, which is the subdivision between oxidized (above the line) and reduced (below) classes. In the weakly oxidized subclasses in the middle of Figure 4-8, some sample points in both alkali-calcic (MACow) and calc-alkalic (MCAow) classes extend down into the weakly reduced fields between the $Fe_2O_3/FeO = 0.6$ and 0.25 lines. For the reduced subclasses at the bottom of Figure 4-8, some sample points extend below the $Fe_2O_3/FeO = 0.25$ line.

Because the ferric/ferrous ratio is so sensitive to alteration, weathering, analytical errors, and careless handling, samples can easily become oxidized. Therefore, many samples fall into more oxidized portions of the graph than they would have if tested immediately after emplacement. For this reason, mineralogic criteria are more reliable in assigning oxidation class.

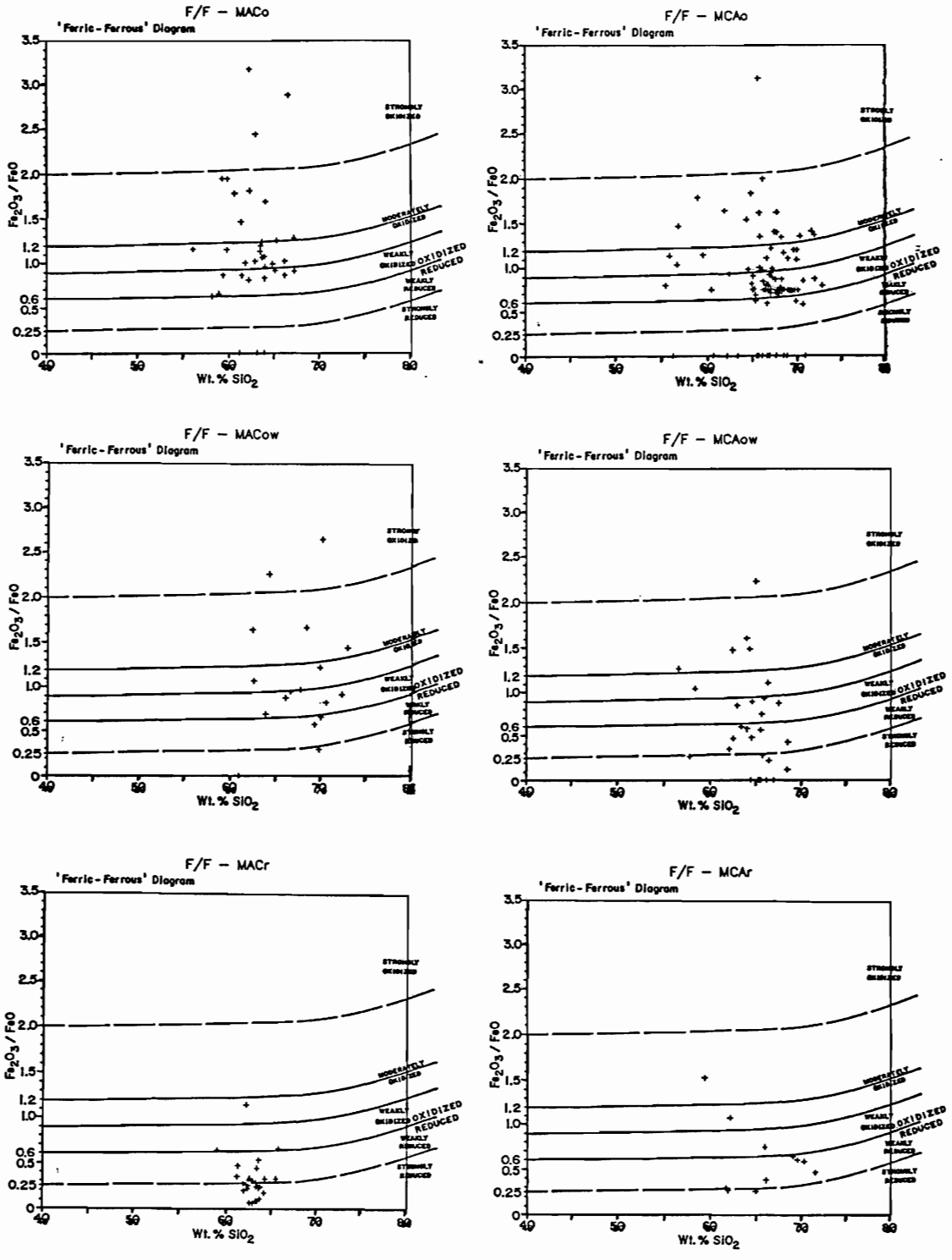

Figure 4-8. Comparison of Fe_2O_3/FeO versus SiO_2 variation diagrams for metaluminous, alkali-calcic (left side) versus calc-alkalic (right side), oxidized (top), weakly oxidized (center), and reduced (bottom) classes.

The presence of ilmenite, pyrrhotite, carbon, or graphite suggest the reduced or weakly oxidized subclasses; the presence of magnetite, titanite (sphene), or pyrite as primary minerals indicate oxidized subclasses.

Y Versus Zr Diagram

All the samples in this study were associated with hydrous magmatism and therefore plot in the lower left portion of the Y versus Zr variation diagram (Figure 4-9). There does not appear to be any distinction between the alkalinity or oxidation state classes.

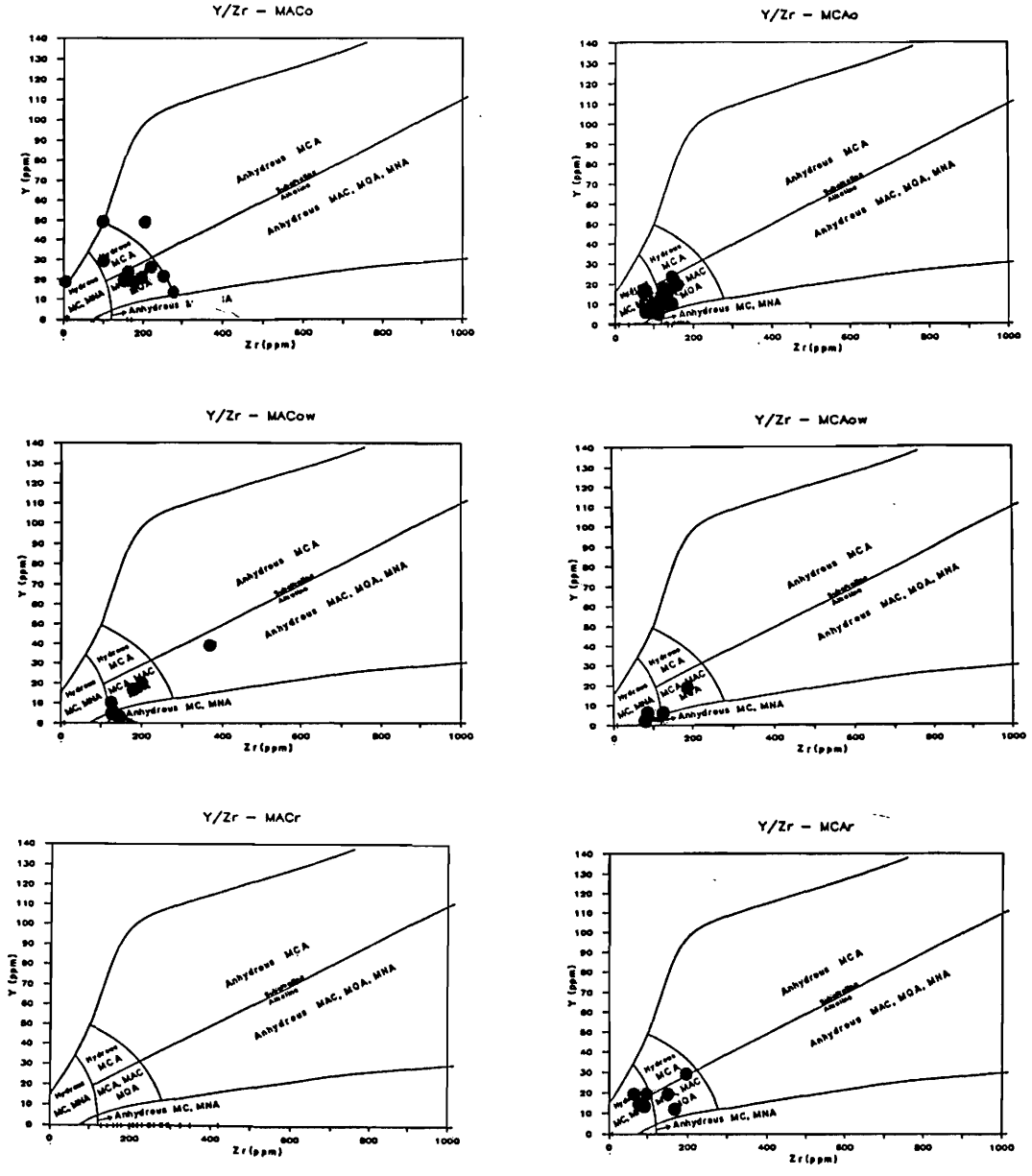

Figure 4-9. Comparison of Y versus Zr variation diagrams for metaluminous, alkali-calcic (left side) versus calc-alkalic (right side), oxidized (top), weakly oxidized (center), and reduced (bottom) classes.

PETROLOGY OF FRESH IGNEOUS ROCKS

If the fresh igneous rocks and the related ore deposit are parts of a cogenetic igneous-metal-volatile suite that represents the end products of differentiation from a more primitive magma, then the igneous rocks and their petrologic details contain clues to that process. The modal mineralogy and whole rock chemistry of igneous rocks from the six petrochemical classes in this study are compared on standard petrologic diagrams in this chapter. This information provides important evidence concerning differences in the crystallization process that could explain the metal distribution in the six classes of ore deposits.

Modal Mineralogy Reported from Fresh Igneous Rocks in Each Class

Modal mineralogy from plutonic rocks in each mining district was obtained from the literature (Appendix D), compiled into the six petrochemical classes, and plotted on standard petrologic diagrams using RockStat software from RockWare and on histograms using spreadsheet programs, such as Excel and Lotus 1-2-3. In spite of the paucity of modal mineralogic information in the literature for the districts in this study, significant differences are obvious in some of the minerals described in this chapter; other minerals are shown in histograms in Appendix D. Additional information can be obtained by examining the amounts of minerals, such as hornblende and biotite, in early versus late phases of an igneous complex in districts such as Ray (Figure 3-63 and Appendix D).

The amounts of iron minerals, such as magnetite, ilmenite, and sphene,

differ significantly with oxidation state of the class. Magnetite is abundant, ranging from 0.6 to 5.5 percent, in the oxidized classes of both alkali-calcic and calc-alkalic districts (Figure 5-1). Magnetite is less abundant, ranging from 0.05 to 2.1 percent, in the weakly oxidized classes; it has not been reported from the reduced classes. Ilmenite has not been reported from oxidized or weakly oxidized districts, but occurs in trace amounts in reduced classes (Appendix D). Sphene occurs in larger amounts in oxidized districts ranging from 0.05 to 2.3 percent, in lesser amounts in weakly oxidized districts ranging from 0.05 to 0.3 percent, and in only trace amounts or not at all in reduced districts (Figure 5-2). Thus, the oxidized classes are characterized by abundant magnetite and sphene, the weakly oxidized classes by moderate amounts of magnetite and very minor sphene, and the reduced classes by the absence of magnetite, no sphene, and traces of ilmenite.

The Streckeisen (1976) ternary diagram (Figure 5-3) is not useful in discriminating between petrochemical classes as the fields for alkalinity and oxidation state classes overlap, especially when all oxidized classes are compared to all reduced classes (bottom right in Figure 5-4). The fields for alkalinity differ slightly (bottom left in Figure 5-4), in that none of the calc-alkalic samples are in the K-feldspar corner of the diagram. When the samples are isolated by oxidation state (top and middle right of Figure 5-4), alkalinity fields are clearly distinct.

Various other combinations of minerals were used at the apices of ternary

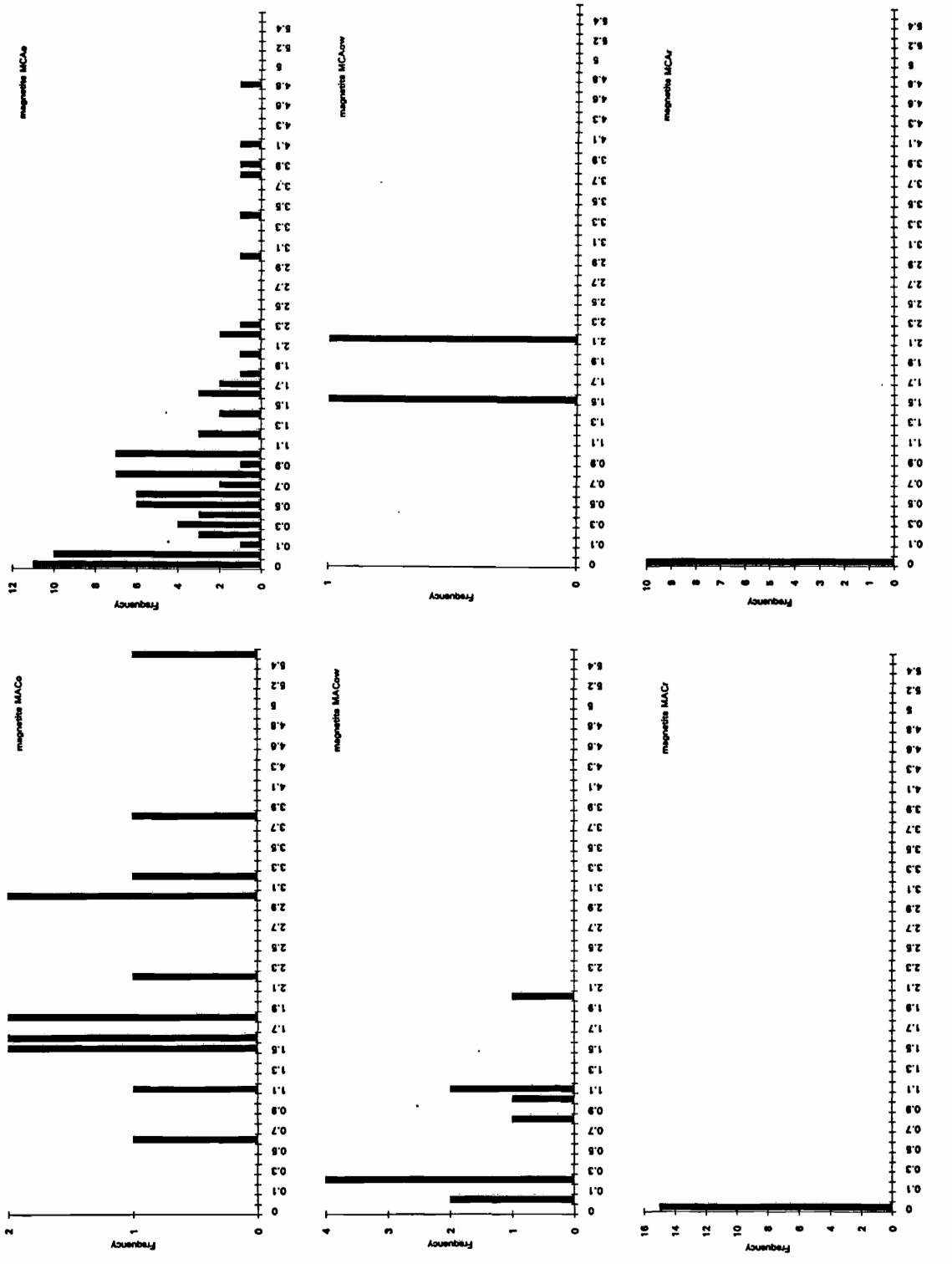

Figure 5-1. Histograms of magnetite in percent on the x-axis (MAC=alkali-calcic, MCA=calc-alkalic, o=oxidized, ow=weakly oxidized, and r=reduced).

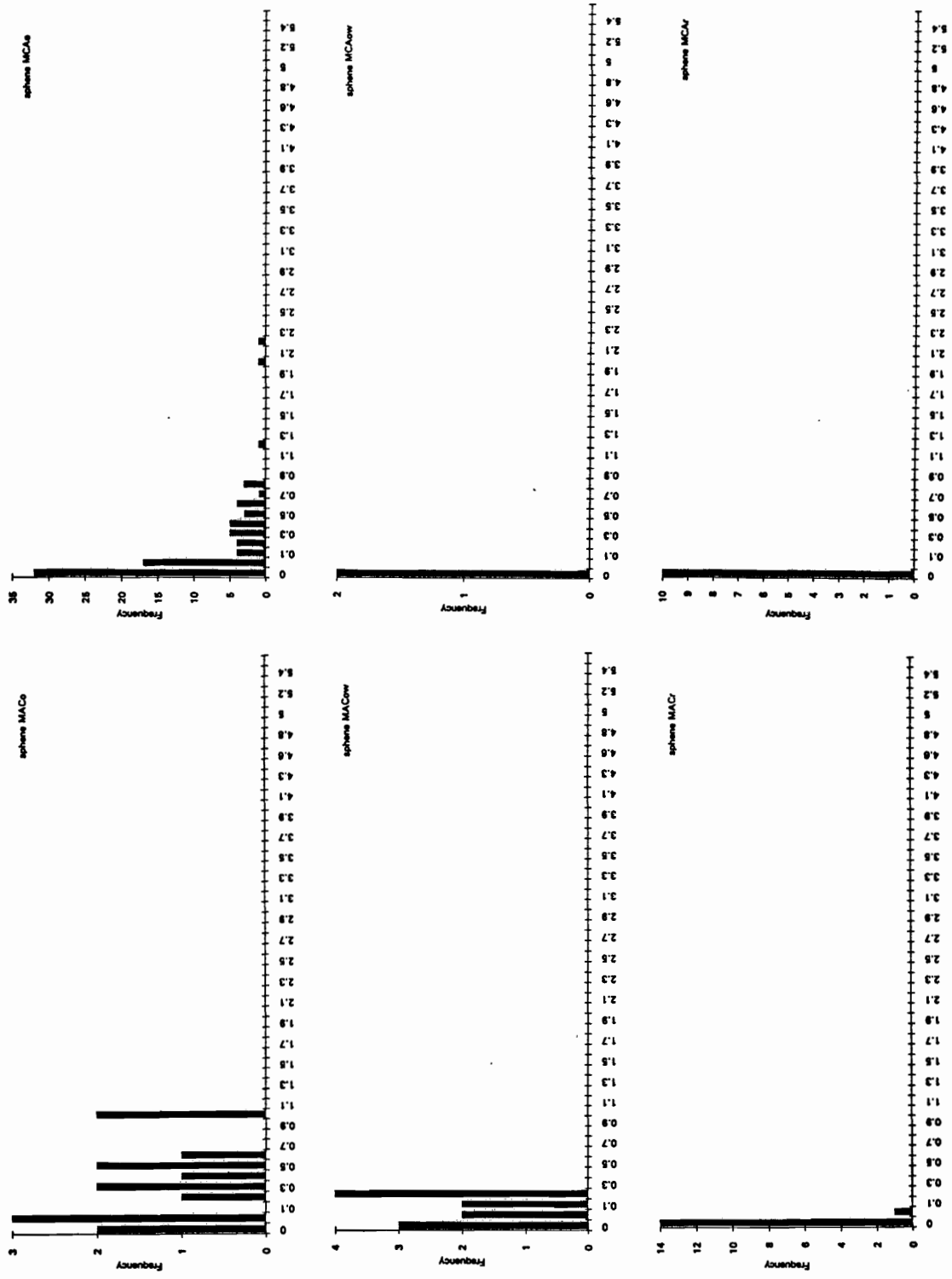

Figure 5-2. Histograms of sphene in percent on the x-axis (MAC=alkali-calcic, MCA=calc-alkalic, o=oxidized, ow=weakly oxidized, and r=reduced).

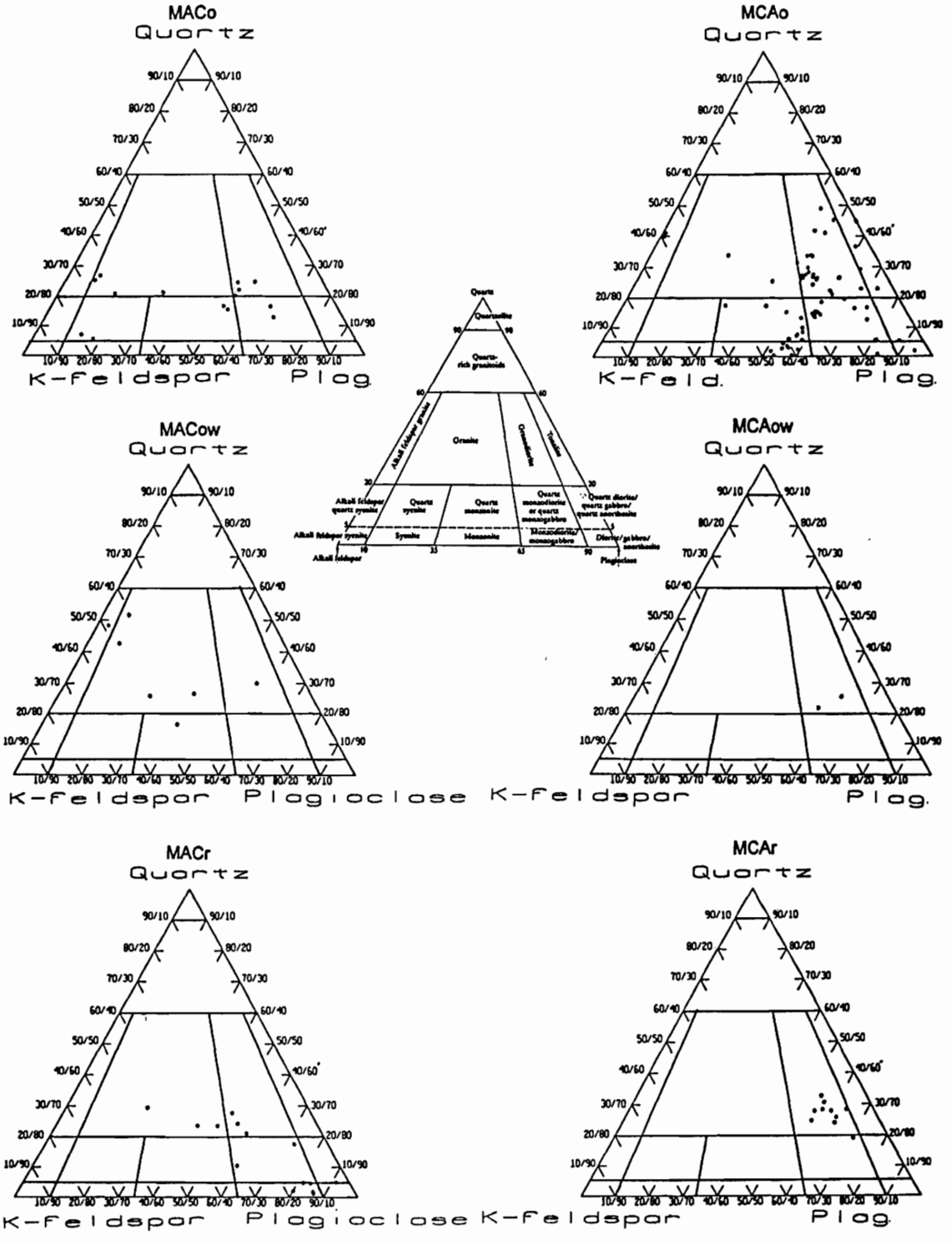

Figure 5-3. Modal mineralogy from magma series classes (M=Metaluminous, AC= alkali-calcic, CA= calc-alkalic, o=oxidized, ow= weakly oxidized, r=reduced) plotted on standard IUGS or Streckeisen (1976) diagrams.

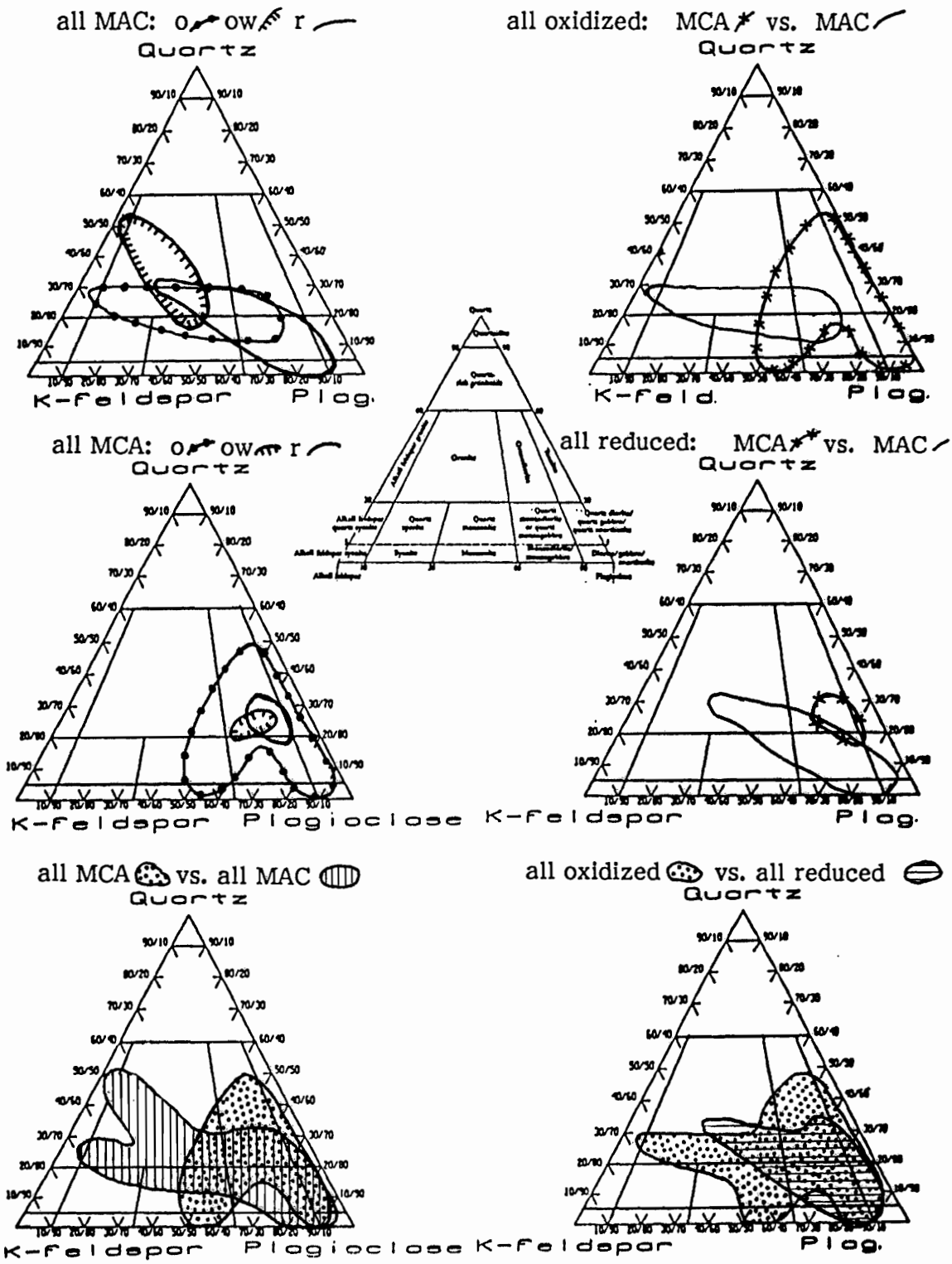

Figure 5-4. Comparison of data from Figure 5-3 plotted in various combinations of magma series classes showing overlap of classes (M=Metaluminous, AC= alkali-calcic, CA=calc-alkalic, o=oxidized, ow=weakly oxidized, r=reduced).

diagrams, but these diagrams did not show any clear patterns, possibly because the data was not uniformly detailed in each deposit. Careful examination of modal mineralogy in the evolving comagmatic suite at Ray (Lang, 1991) indicated that later phases associated with mineralization (Granite Mountain porphyry and Teacup granodiorite) contained very little or no hornblende or sphene (Figure 3-63 and Appendix D). This distribution was qualitatively recognized in other districts, although petrography and microprobe analyses should be done to substantiate the general impression. The observation raises the question, "Does the lack of hornblende indicate a major shift from water dissolved in the magma to water excluded from the magma and expelled into a hydrothermal fracturing event with accompanying escape of mineralizing fluids into veins and fractures?" This research is beyond the scope of this dissertation, but is suggested for further investigation.

Whole Rock Geochemistry of Unaltered Plutonic Rocks from Each Class

The alkali-lime index of Peacock (1931) was originally defined to subdivide alkaline and sub-alkaline rock series into the more detailed classes of alkalic, alkali-calcic, calc-alkalic, and calcic groups. This classification was based on mineralogic and chemical characteristics of certain rock suites that had no relationship to ore deposits. The Peacock index is graphically determined by finding the intersection of the $K_2O + Na_2O$ line and the CaO line on a variation diagram with SiO_2 on the x-axis (Figure 5-5); a line is drawn vertically to

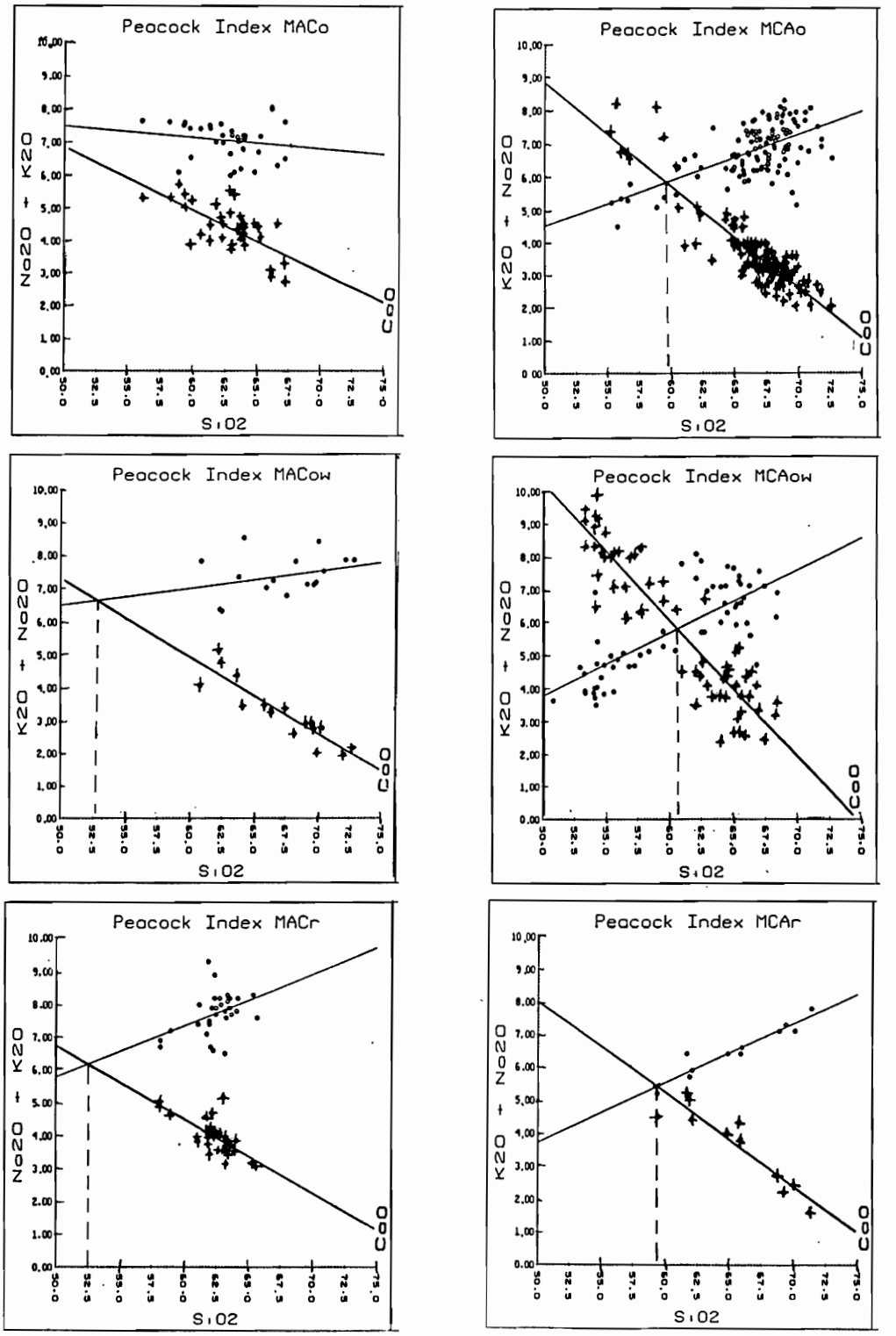

Figure 5-5. Peacock Index (SiO_2 where K_2O + Na_2O line and CaO line cross) of MagmaChem classes (M=Metaluminous, AC=alkali-calcic, CA= calc-alkalic, o=oxidized, ow=weakly oxidized, r=reduced) (AC=51-56; CA=56-61).

determine the percent SiO_2. Categories of Peacock's alkali-lime index are: calcic = more than 61 percent, calc-alkalic = 56-61 percent, alkali-calcic = 51-56 percent, and alkalic = less than 51 percent (Peacock, 1931). Classes in this study fell within the expected categories; metaluminous alkali-calcic weakly oxidized and reduced was 52.5 and metaluminous calc-alkalic oxidized was 59.5, calc-alkalic weakly oxidized was 61, and calc-alkalic reduced was 59.

Bar graphs were made of whole rock oxides from unaltered plutonic samples in each class in order to determine general characteristics of each class for the neural network analysis and to detect samples which fell outside the normal limits of the class. Because oxides in igneous rocks vary with SiO_2 or Differentiation Index, values within classes were not uniform for each oxide; instead, various oxide ratios were found to be characteristic. The SiO_2/K_2O ratio was the best discriminator between alkalinity classes with values for calc-alkalic classes on the right side of Figure 5-6 consistently higher at 20 than values for alkali-calcic classes at 18 to 12 on left side of the figure. The Fe_2O_3/FeO ratio was the best discriminator between oxidation classes with values for oxidized classes at the top of Figure 5-7 consistently higher at 0.8 to 1.0 than values for weakly oxidized classes at 0.5-0.8 in the middle of the figure or for reduced classes at 0.3-0.5 at bottom of the figure. The two discriminating ratios were used on scatter plots with SiO_2/K_2O on the x-axis and Fe_2O_3/FeO on the y-axis to demonstrate all six classes on one variation diagram (Figure 5-8).

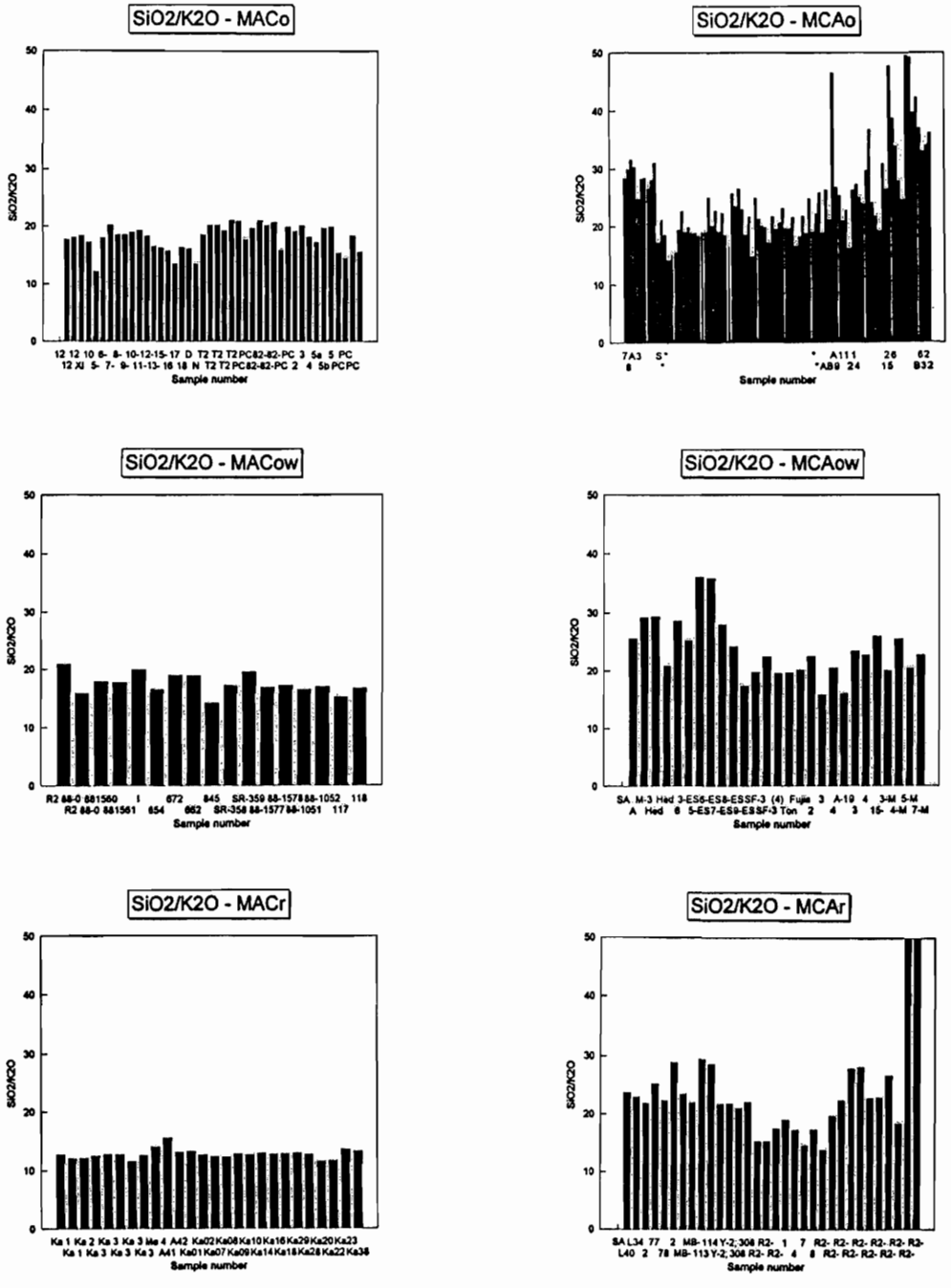

Figure 5-6. Bar graphs of SiO_2/K_2O values from petrochemical classes (M=Metaluminous, AC= alkali-calcic, CA= calc-alkalic, o=oxidized, ow= weakly oxidized, r=reduced) showing higher values for MCA than MAC.

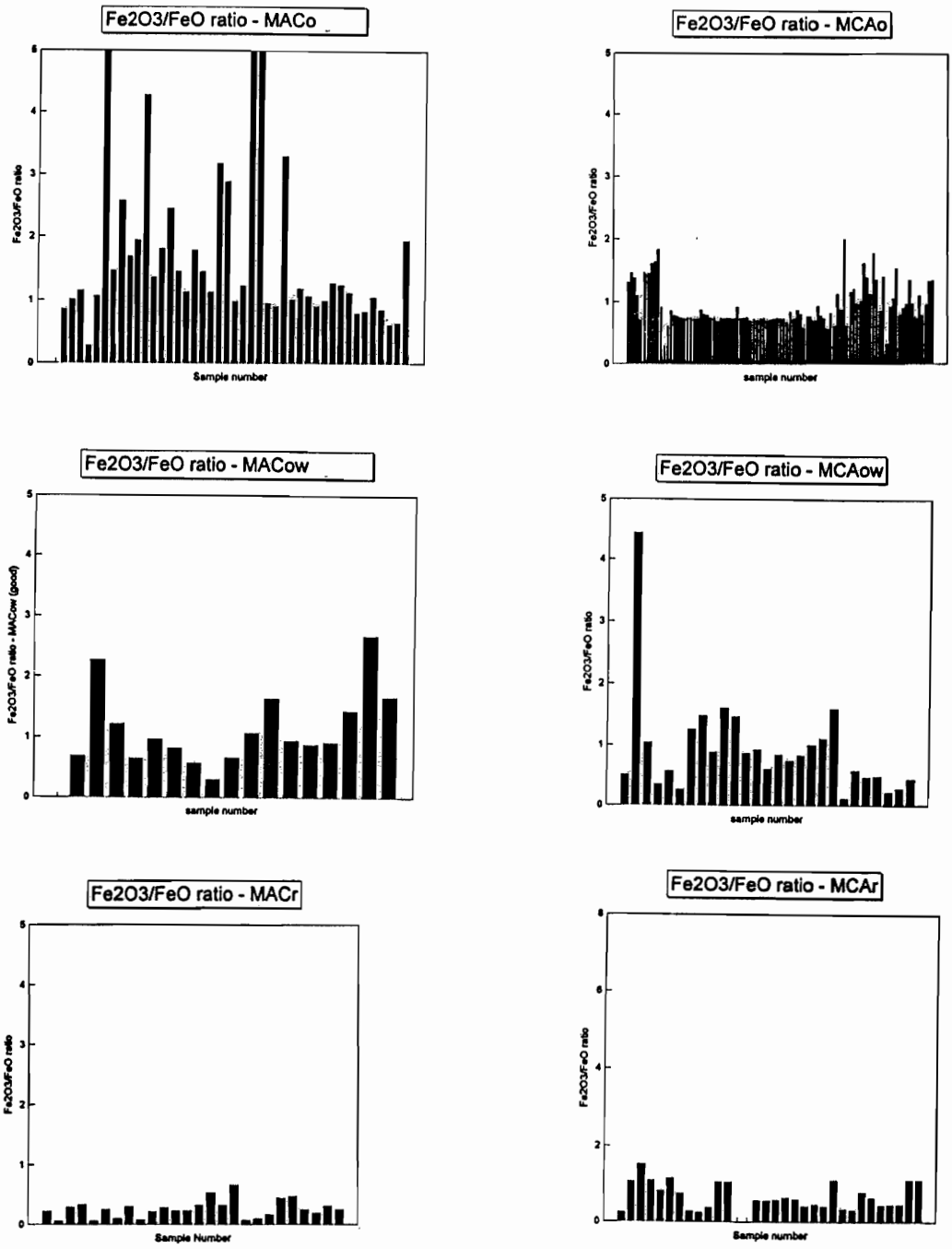

Figure 5-7. Bar graphs of Fe_2O_3/FeO values from petrochemical classes (M=Metaluminous, AC= alkali-calcic, CA= calc-alkalic, o=oxidized, ow= weakly oxidized, r=reduced) showing higher values for o than r.

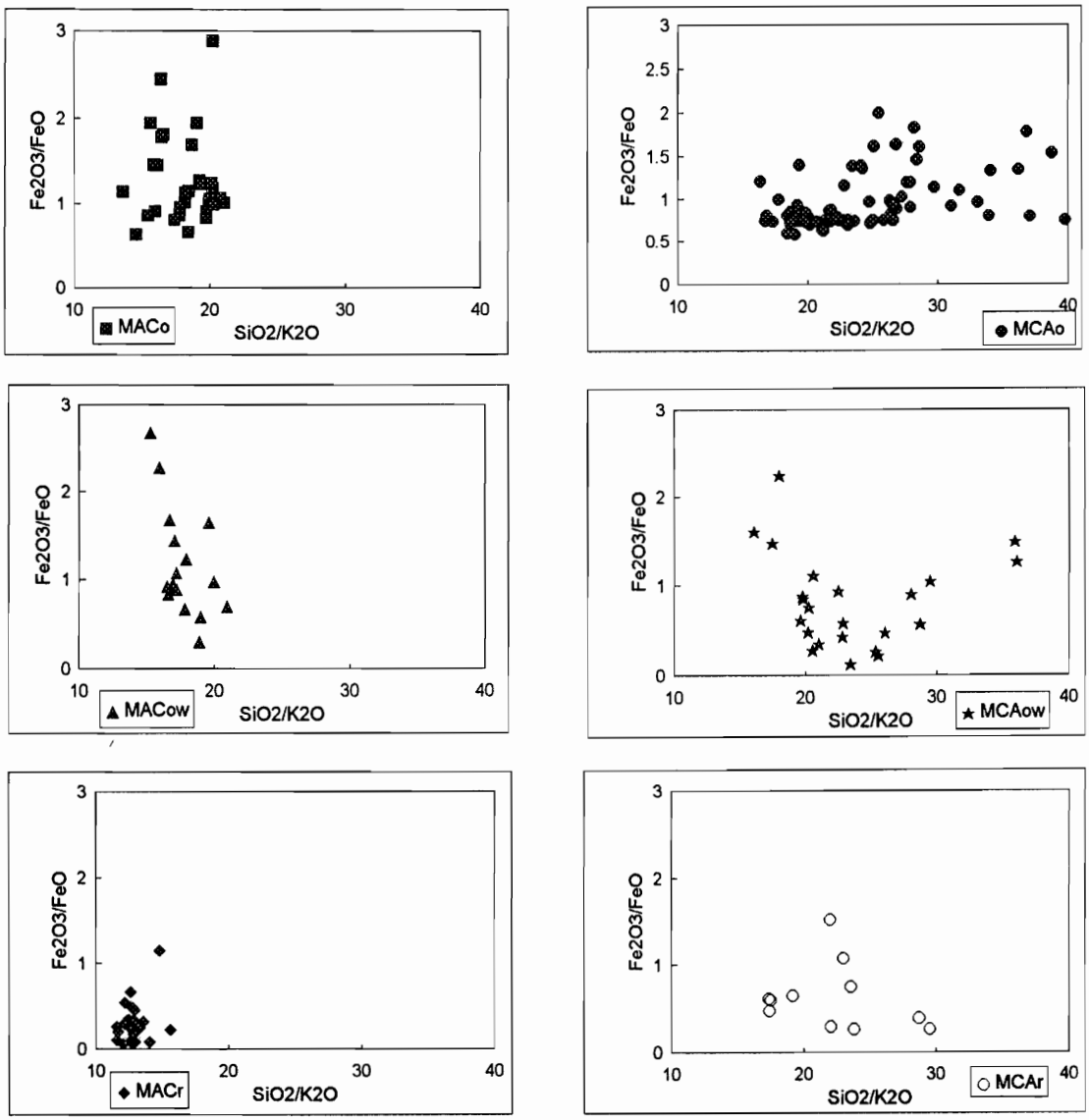

Figure 5-8. Scatter diagrams of SiO_2/K_2O versus Fe_2O_3/FeO from petrochemical classes (M=Metaluminous, AC= alkali-calcic, CA= calc-alkalic, o=oxidized, ow= weakly oxidized, r=reduced).

Ternary Diagrams

Samples from all petrochemical classes are in the calc-alkaline field on the AFM ternary diagram (Figure 5-9), where A = Na_2O + K_2O, F = FeO + 0.9*Fe_2O_3, and M = MgO. The term calc-alkaline on the AFM diagram is misleading as it does not correspond with the meaning defined by Peacock (1931). Samples from both alkaline (alkali-calcic) and subalkaline (calc-alkalic) classes are in the calc-alkaline field on the AFM diagram. For more observational terminology, the term tholeiitic should be replaced with iron-enriched and calc-alkaline should be replaced with alkali-magnesium-enriched.

Ternary diagrams were made with various combinations of whole rock oxide data, but were not as effective as other types of graphs in discriminating between the petrochemical classes. Samples from each petrochemical class fall in negatively sloped linear bands near the center of Na_2O-K_2O-CaO ternary diagrams (Figure 5-10). Although the bands overlap, alkali-calcic classes are more enriched in K_2O than calc-alkalic (bottom left side of Figure 5-11) and reduced classes are also more K-enriched (bottom right side of Figure 5-11). Ternary diagrams based on the best class discriminators (K_2O, SiO_2, and Fe_2O_3/FeO) showed the clearest separation into linear fields (Figure 5-12) when scaling factors were included (dividing SiO_2 by 10 and multiplying Fe_2O_3/FeO by 10). Alkalinity distinctions had very little overlap (bottom left of Figure 5-13) with alkali-calcic consistently more K-enriched; oxidation distinctions were not well distinguished.

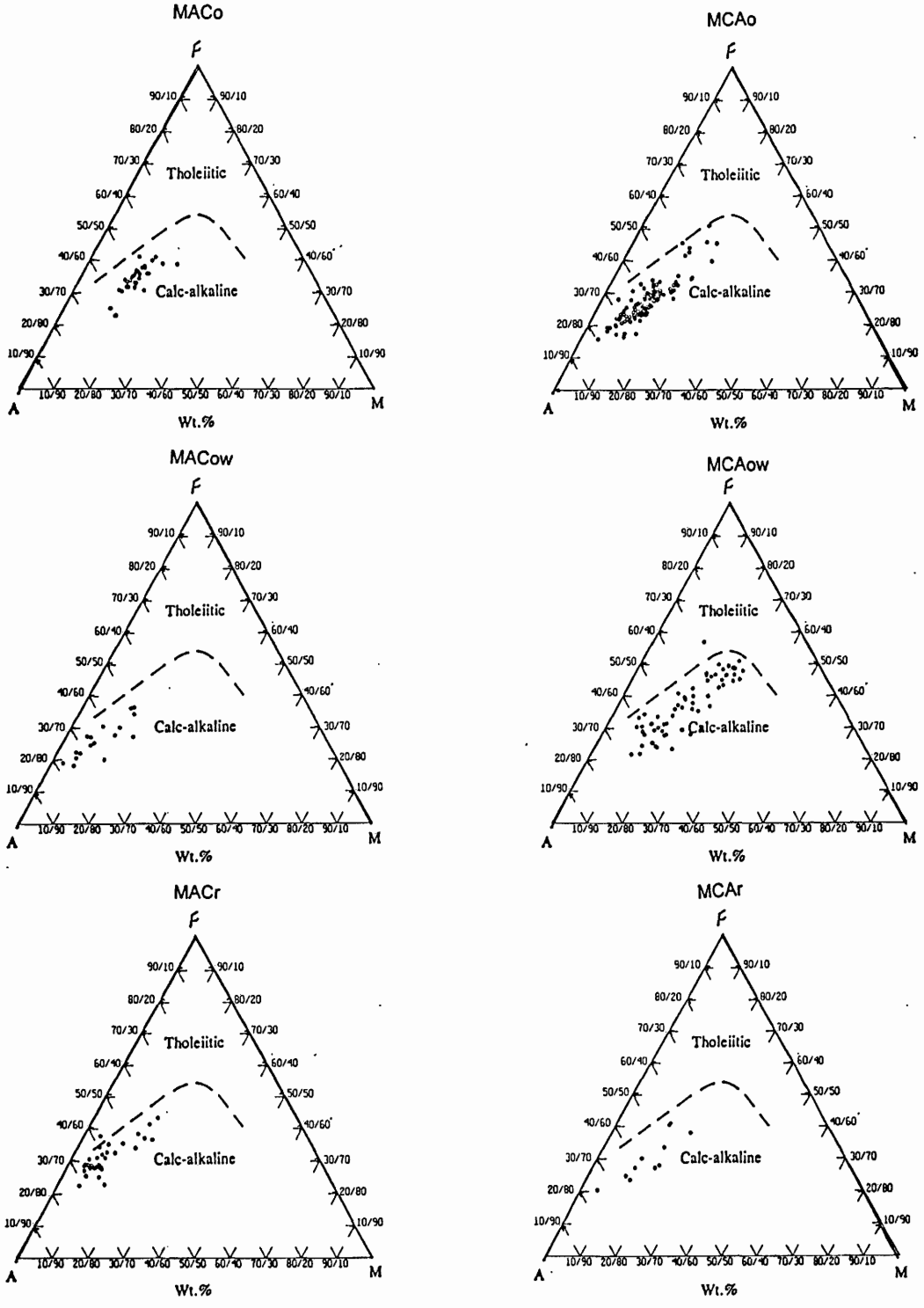

Figure 5-9. All six magma series classes are in the calc-alkaline field on AFM diagrams (M=Metaluminous, AC=alkali-calcic, CA=calc-alkalic, o=oxidized, ow=weakly oxidized, r=reduced) (A=Na_2O+K_2O, F=$FeO+0.9*Fe_2O_3$, M=MgO).

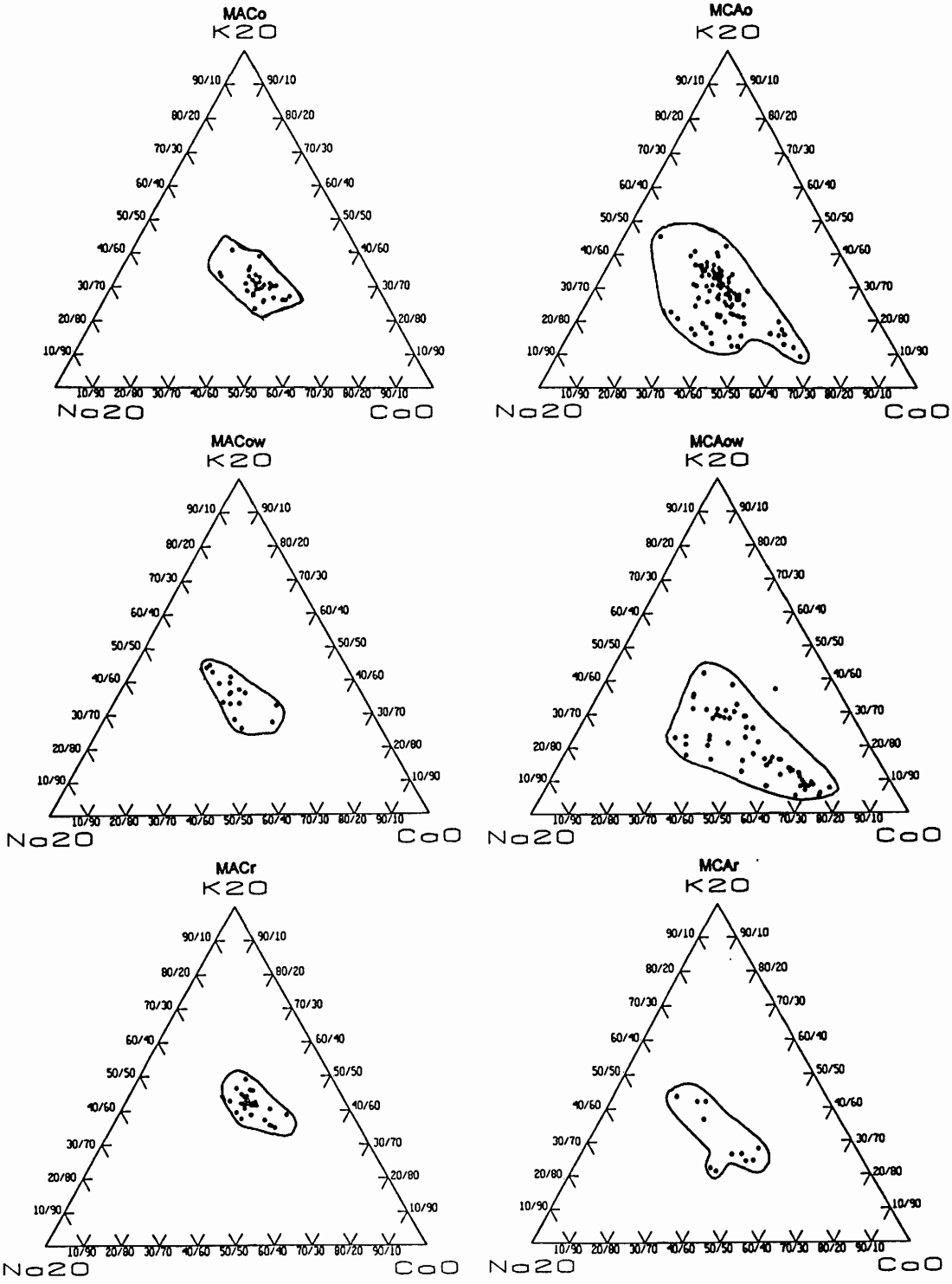

Figure 5-10. Wide linear bands of six magma series classes on Na_2O-K_2O-CaO diagrams (M= Metaluminous, AC= alkali-calcic, CA= calc-alkalic, o= oxidized, ow= weakly oxidized, r=reduced).

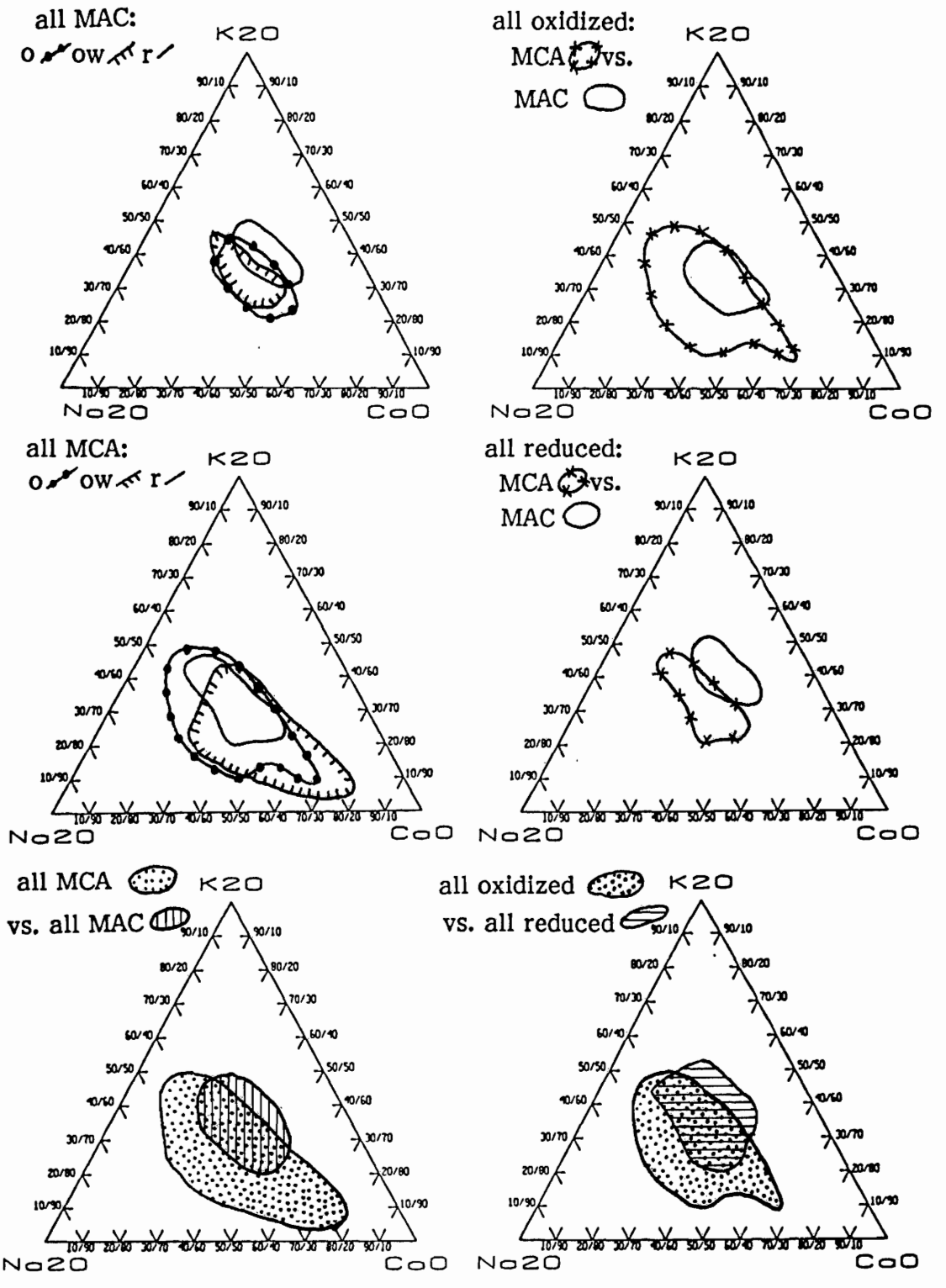

Figure 5-11. Comparison of data from Figure 5-10 plotted on Na_2O-K_2O-CaO diagrams by combining various petrochemical classes (AC= alkali-calcic, CA=calc-alkalic, o=oxidized, ow=weakly oxidized, r=reduced).

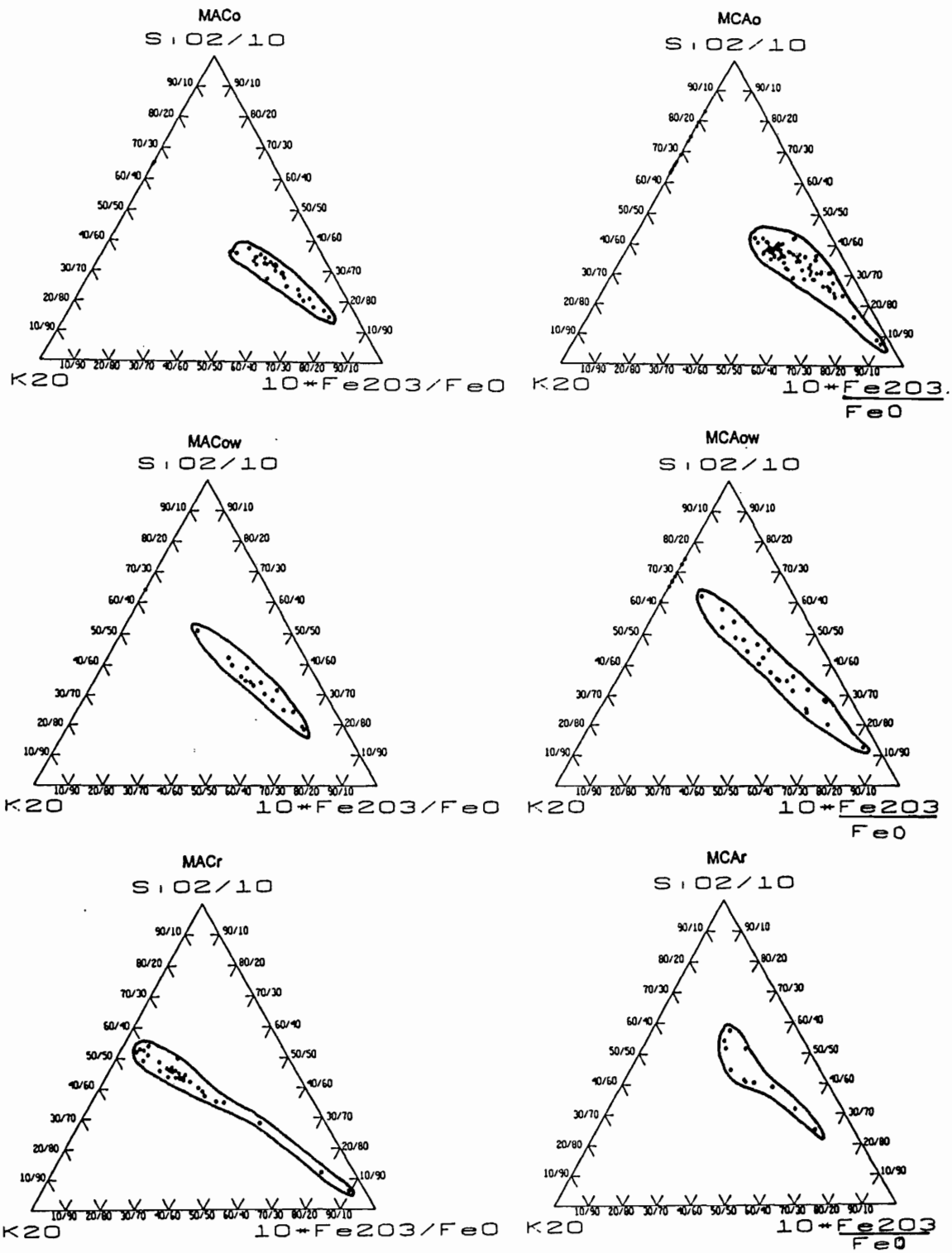

Figure 5-12. Linear arrangement of six magma series classes plotted on K_2O-SiO_2-Fe_2O_3/FeO diagrams (M= Metaluminous, AC= alkali-calcic, CA= calc-alkalic, o= oxidized, ow= weakly oxidized, r=reduced).

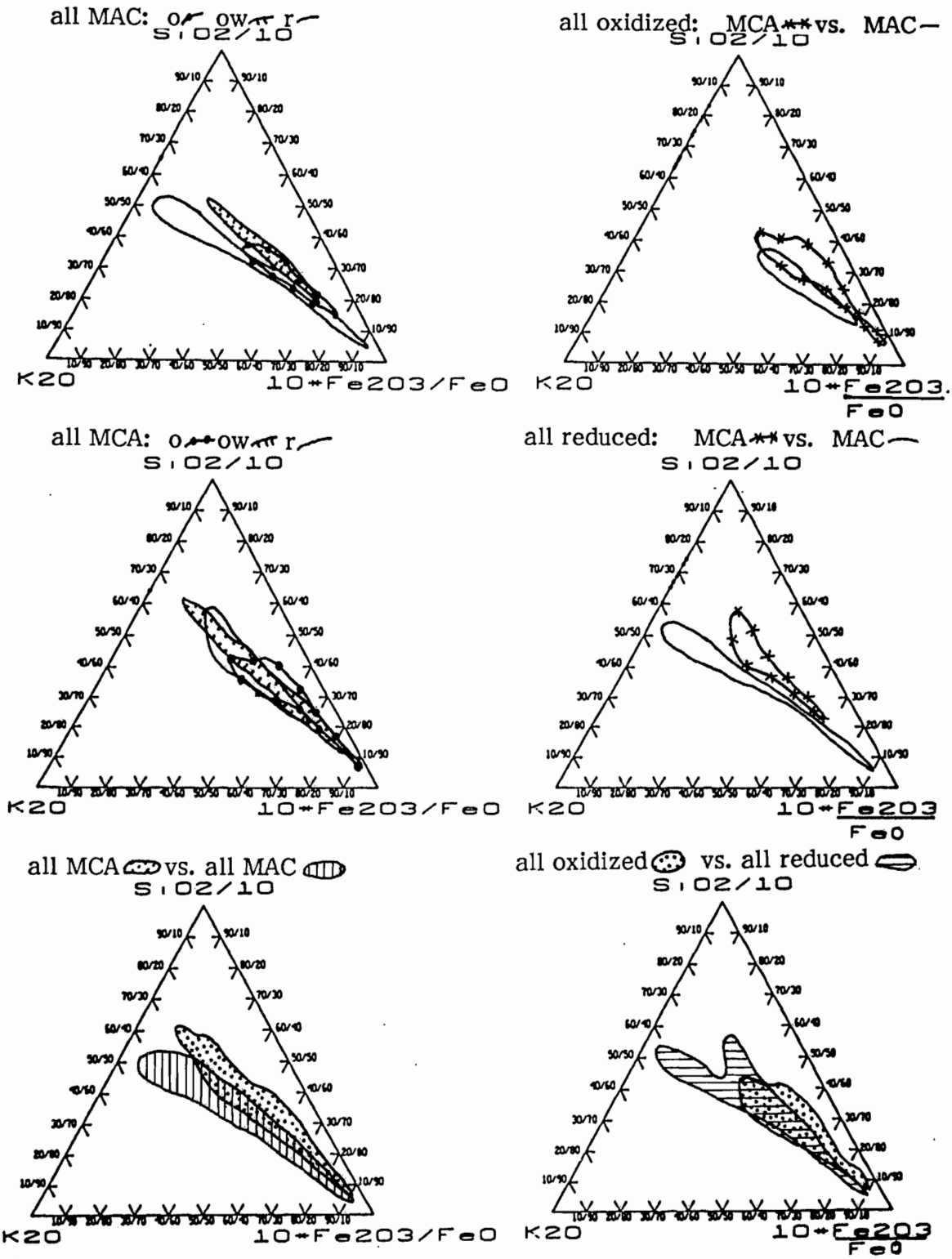

Figure 5-13. Comparison of data from Figure 5-12 plotted on K_2O-SiO_2-Fe_2O_3/FeO diagrams in various combinations (M= Metaluminous, AC= alkali-calcic, CA=calc-alkalic, o=oxidized, ow=weakly oxidized, r=reduced).

Harker Variation Diagrams

Because whole rock oxides in igneous rocks vary with SiO_2, Harker variation diagrams best illustrate trends in the data; these were plotted using RockStat software, which draws lines and calculates equations and statistical parameters. The K_2O versus SiO_2 diagrams that clearly discriminated between the petrochemical classes are included here; others are included in Appendix D.

The best Harker variation diagram for discriminating petrochemical alkalinity classes is the K_2O versus SiO_2 graph (Figure 5-14). The narrow linear bands of sample points have moderately steep positive slopes with fair correlation coefficients (0.5-0.8), except for alkali-calcic oxidized. The slopes of the lines are nearly identical (Figure 5-15), but values for alkali-calcic are considerably higher than for calc-alkalic, with only minor 20 percent overlap as shown in the lower left part of Figure 5-15. The contrast between calc-alkalic and alkali-calcic is particularly noticeable when the classes are isolated by oxidation state as shown in the upper right and middle right parts of Figure 5-15. Oxidized and reduced fields overlap in the bottom right graph, so the diagram is not useful to discriminate oxidation state.

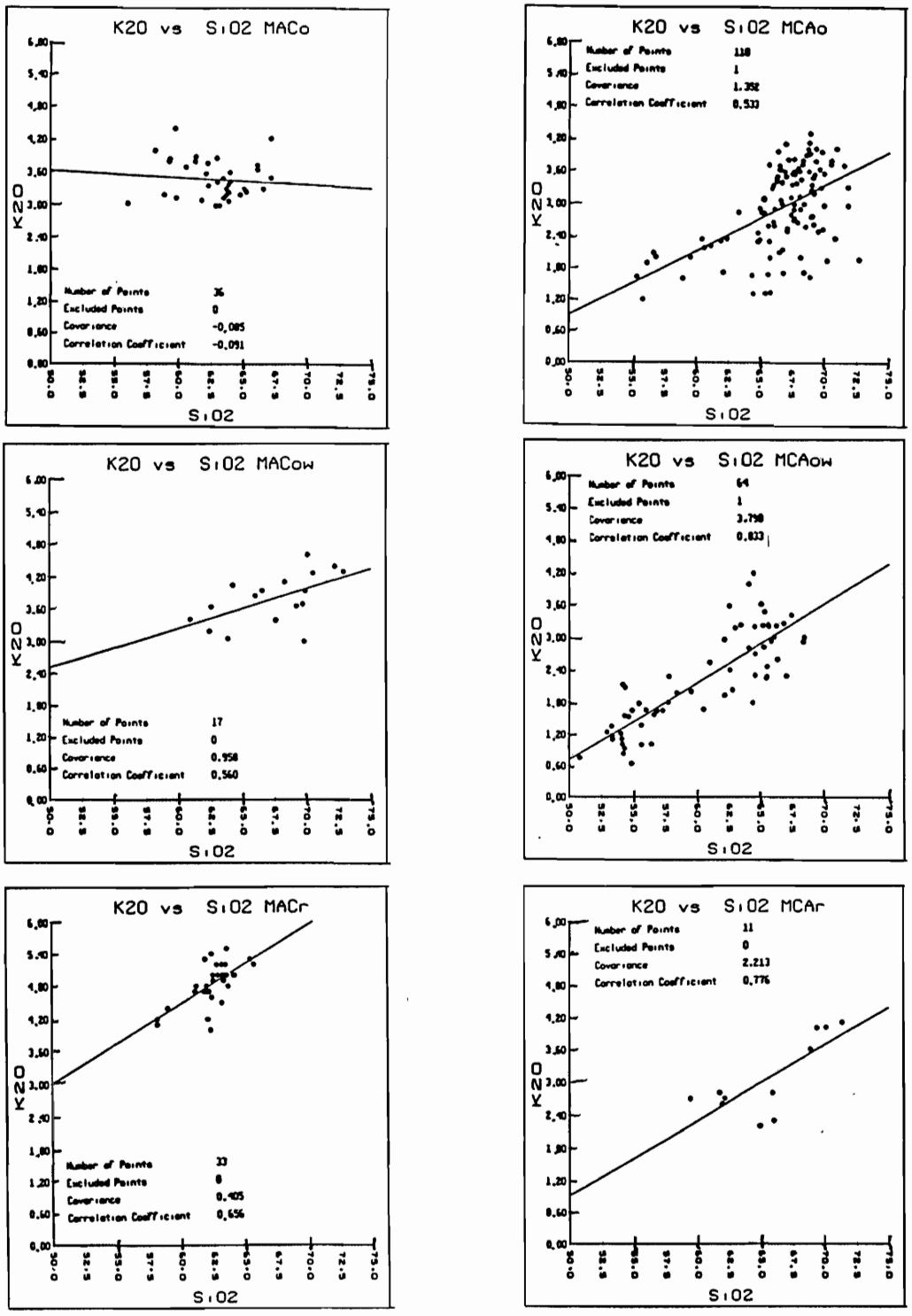

Figure 5-14. Whole-rock chemistry of petrochemical classes plotted in linear bands on K_2O vs. SiO_2 variation diagrams (M= Metaluminous, AC= alkali-calcic, CA= calc-alkalic, o= oxidized, ow= weakly oxidized, r=reduced).

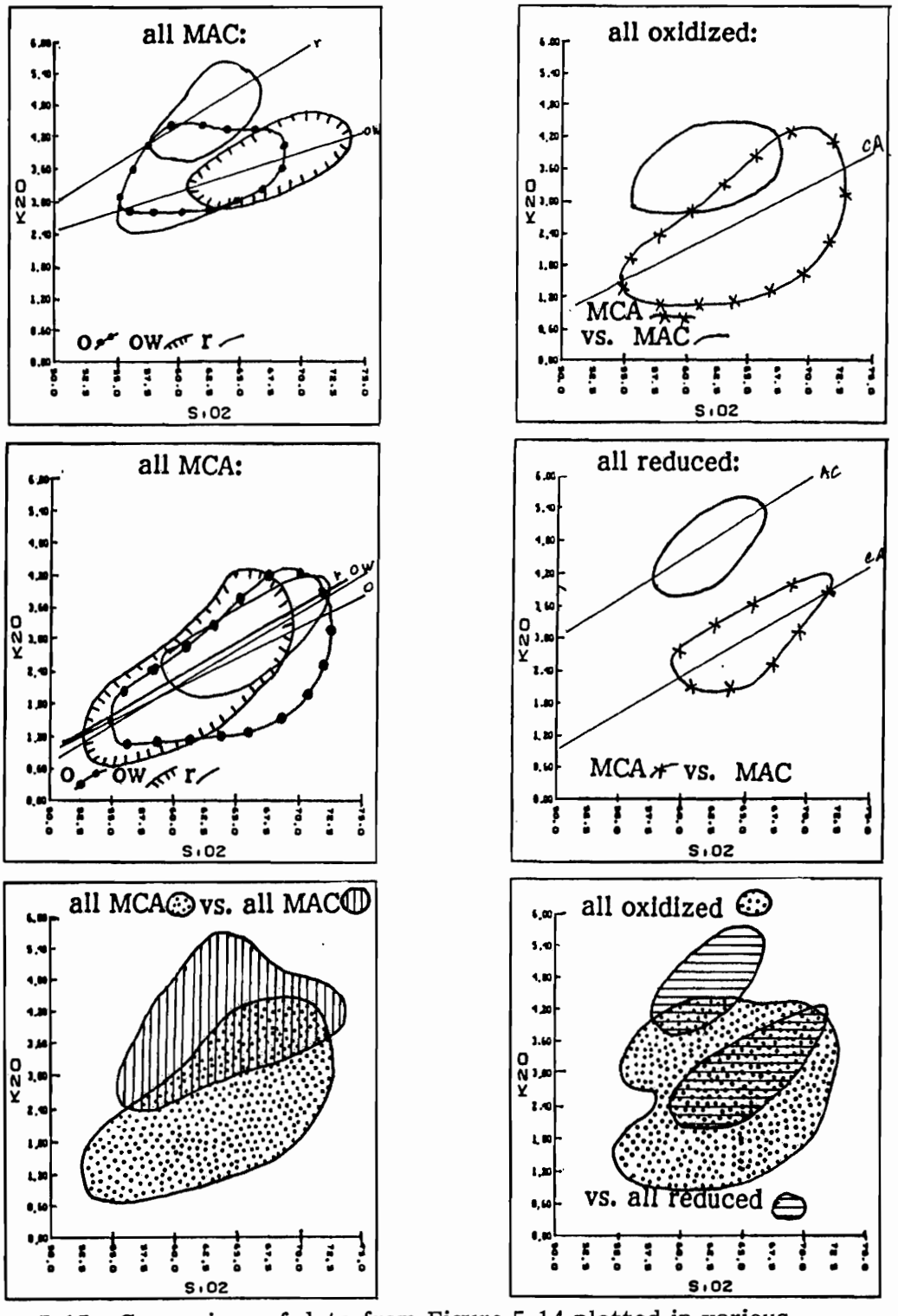

Figure 5-15. Comparison of data from Figure 5-14 plotted in various combinations on K_2O vs. SiO_2 variation diagrams (M= Metaluminous, AC= alkali-calcic, CA=calc-alkalic, o=oxidized, ow=weakly oxidized, r=reduced).

CHARACTERISTICS OF MINERALIZED SYSTEMS

If the anions and cations in an ore deposit associated with an igneous complex are the products of differentiation of a cogenetic igneous-metal-volatile suite, then the distribution of metals should be separable into the same classes as the igneous suites. Characteristics of the mineralized systems can be measured by the quantity and grades of metals produced, types and relative amounts of ore minerals, and concentrations of elements in rock chip samples.

Caveats Concerning Production Data

Production information in the literature is subject to numerous caveats because of inconsistent reporting, dependence on temporary economic conditions, lack of precise and accurate information, different recovery efficiencies, and the combination of data from different ore deposit subtypes into one geographic district.

There are various types of inconsistencies in production reports. In some references, only the most important commodity is reported and coproduct metals are ignored. In others, only grades and total ore tonnage are recorded; in a few districts, such as those with production before accurate records were kept, only approximate tonnage of ore and metal are known. There is also little consistency in units used; most U.S. production is listed as short tons of ore and pounds or troy ounces of metal, whereas production in other countries is reported as metric tons of ore and grams or kilograms of metal. In some cases the type of ton is not

specified and is assigned based on the country of origin or publication.

Production figures commonly are affected by economic conditions at the time of mining, particularly for base metals such as zinc produced as byproducts of other metals. For example, this dependence on economics rather than geology prevented gold and silver production from base metal districts when their prices were regulated at artificially low prices before 1968.

Production information from recently active districts, such as the Carlin gold deposits, is difficult to document, although reserve information is generally available. Some production data is available in annual reports to company stockholders, which are not easily accessible. Specific production data from mines and districts held by a single company are withheld by the U. S. Bureau of Mines to protect confidentiality.

In some cases, production from several types or ages of deposits in a region are combined, resulting in misleading ratios and totals. The Arizona production information (Keith and others, 1983) was compiled from U.S. Bureau of Mines records according to geologic parameters rather than geographic proximity. Information similar to that in the Arizona bulletin is needed to accurately compare mining districts in a geologically meaningful way. As production data are used to supplement evidence for the type of ore deposit, potential ambiguities are negligible in class assignment. Most of the districts in this study, except Tintic and Park City, contained only one type of deposit.

Production Characteristics for Each Class

There are major differences among magma series classes in production (Figures 6-1 through 6-3), grade (Figures 6-4 through 6-6), and metal ratios (Figures 6-7 through 6-8). Values listed in Appendix E differ by one or two orders of magnitude among the six classes in this study. Alkali-calcic districts are shown in the top half of each figure and calc-alkalic are in the bottom half; in each alkalinity type the topmost graph is oxidized and succeeding lower plots are more reduced.

Production from Alkali-calcic Systems

Alkali-calcic ore deposits are characterized by the dominance of silver over gold and of lead over copper. Silver production is at least 100 times gold production (Figure 6-1). Copper and molybdenum or tungsten production (Figure 6-2) is ten times less than lead and zinc production (Figure 6-3) in the alkali-calcic classes. Silver grades are ten times higher than gold grades in alkali-calcic ore deposits (Figure 6-4). Copper grades in alkali-calcic districts (Figure 6-5), while of similar orders of magnitude between all classes, are ten times less than lead and zinc grades (Figure 6-6). Precious metal ratios for the oxidized and weakly oxidized classes are strongly silver-rich (Figure 6-7); reduced classes are not shown as they generally only had production of silver or tin without the standard base metals. Base metal/precious metal ratios for the alkali-calcic oxidized and weakly oxidized classes are ten times higher than for calc-alkalic

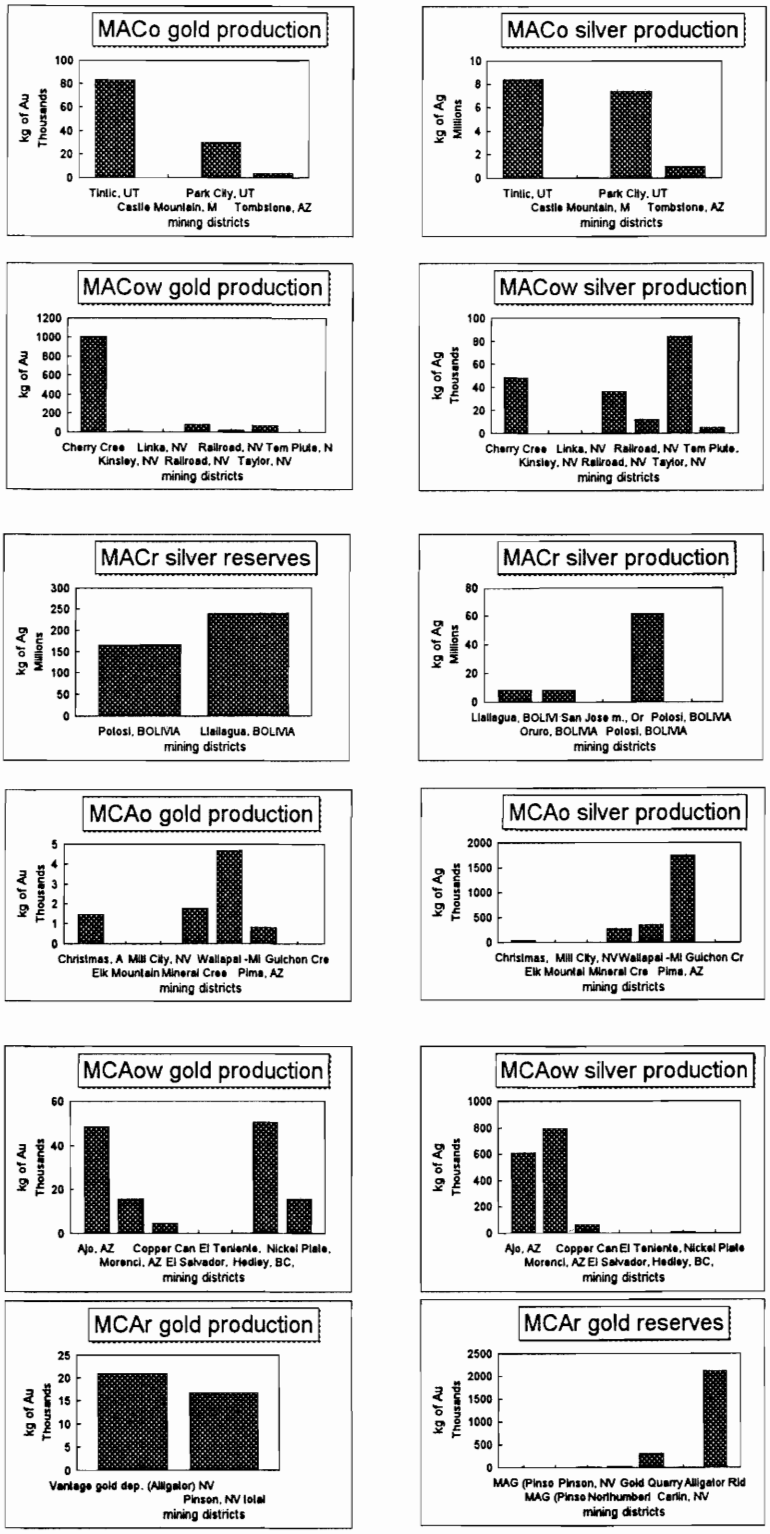

Figure 6-1. Precious metal production in each class (MAC=alkali-calcic, MCA=calc-alkalic; o=oxidized, ow=weakly oxidized, r=reduced).

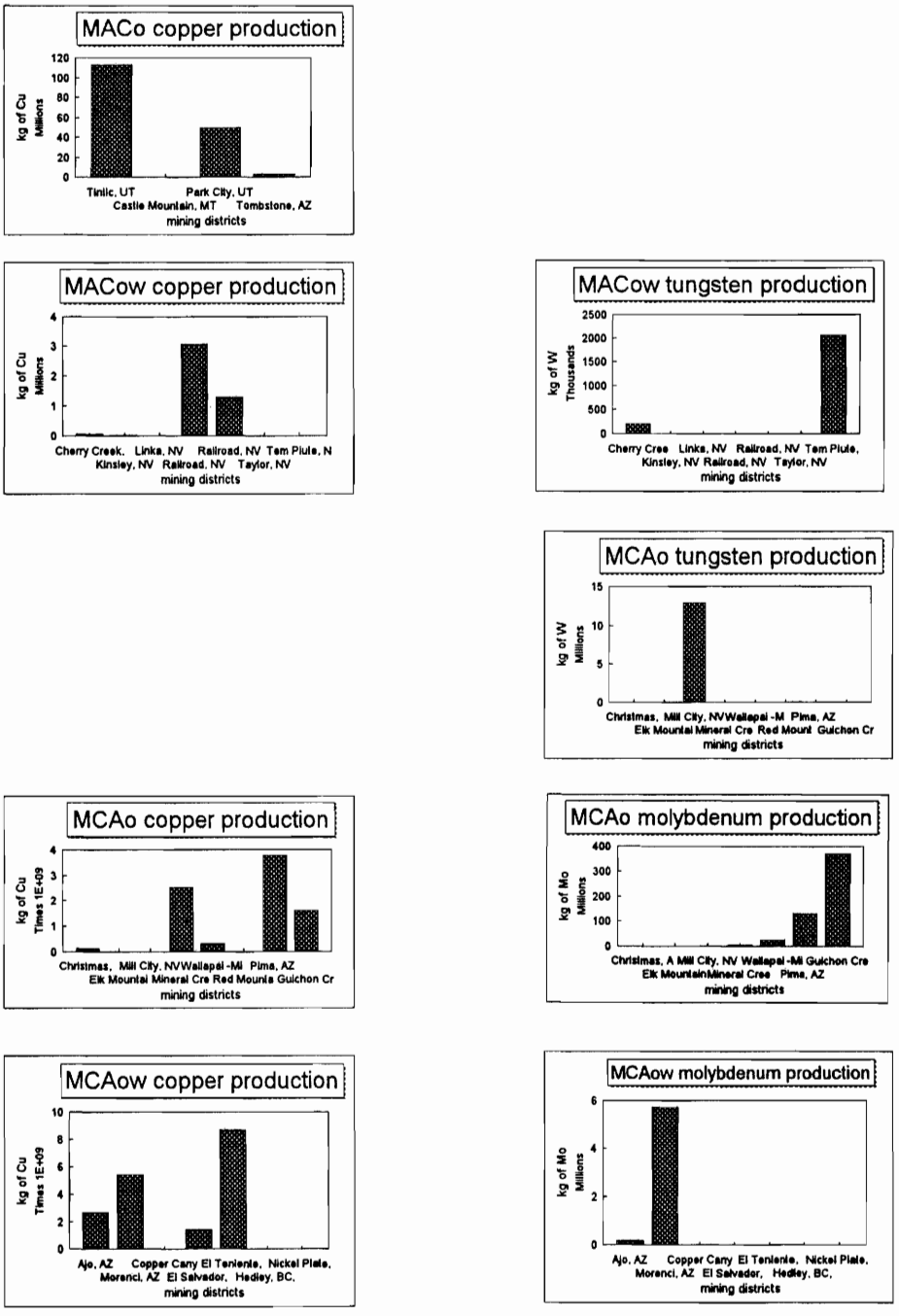

Figure 6-2. Copper, molybdenum, and tungsten production (MAC=alkali-calcic, MCA=calc-alkalic; o=oxidized, ow=weakly oxidized, r=reduced).

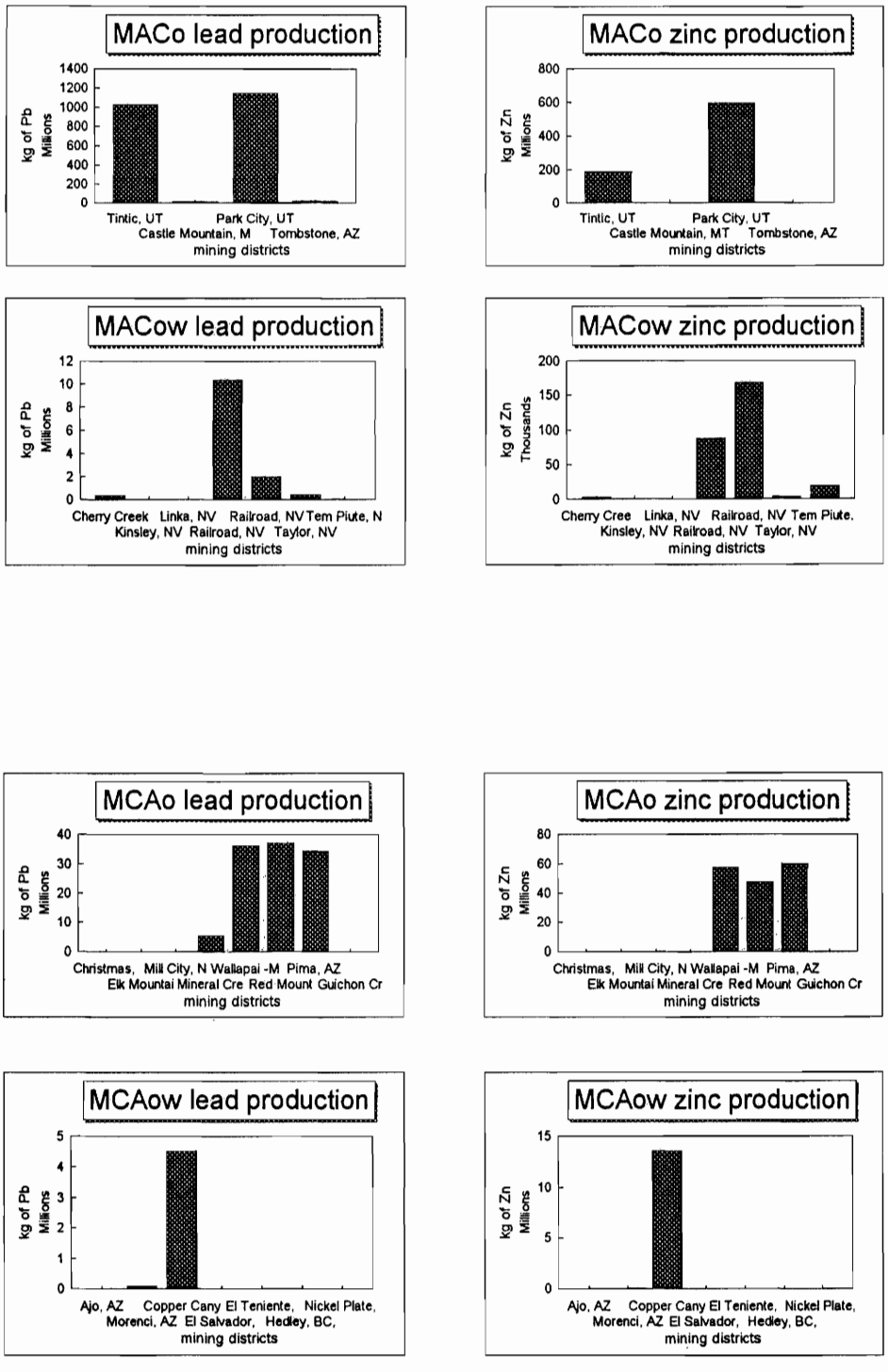

Figure 6-3. Lead and zinc production in magma series classes (MAC=alkali-calcic, MCA=calc-alkalic; o=oxidized, ow=weakly oxidized, r=reduced).

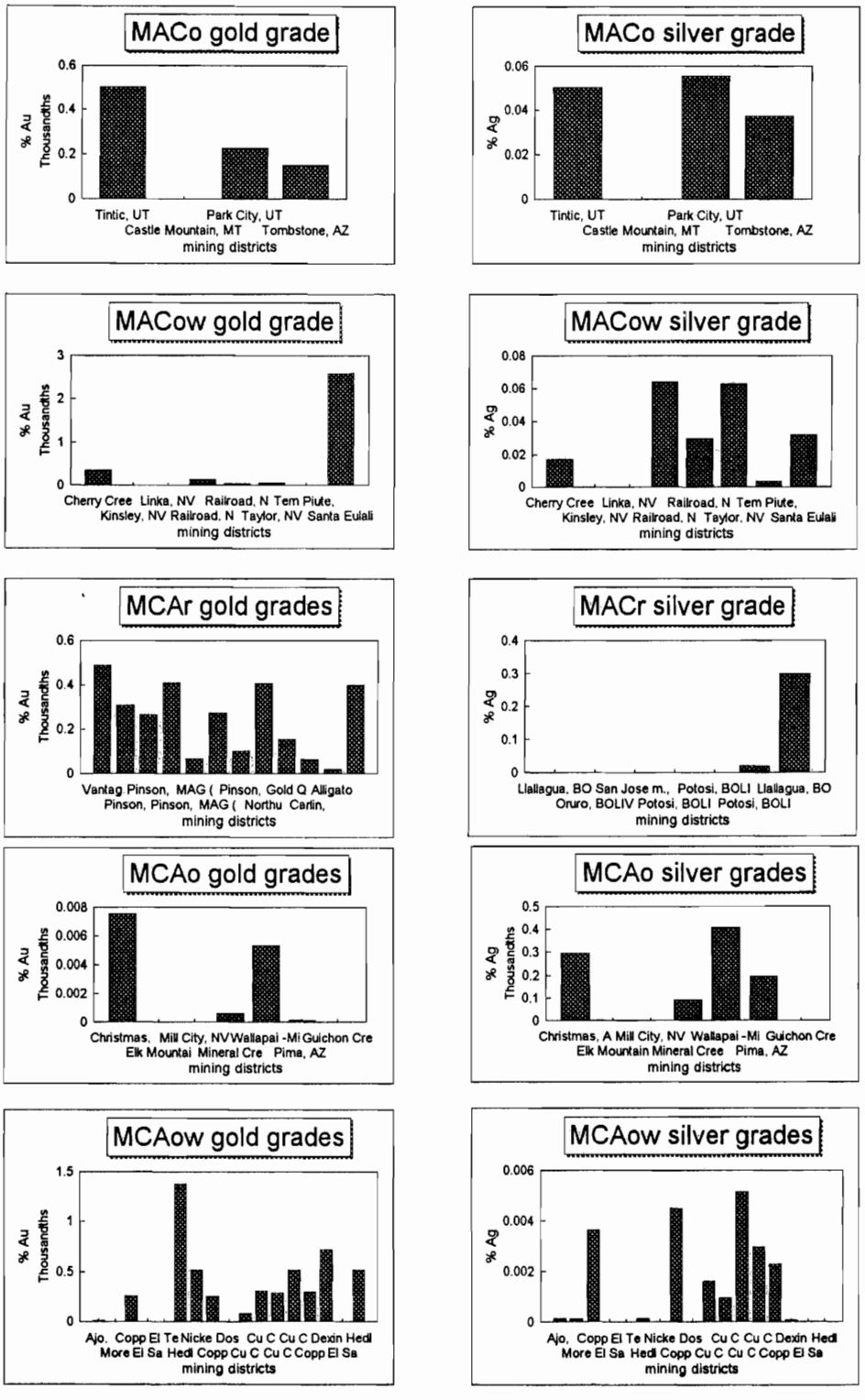

Figure 6-4. Precious metal grade in each class (MAC=alkali-calcic, MCA=calc-alkalic; o=oxidized, ow=weakly oxidized, r=reduced).

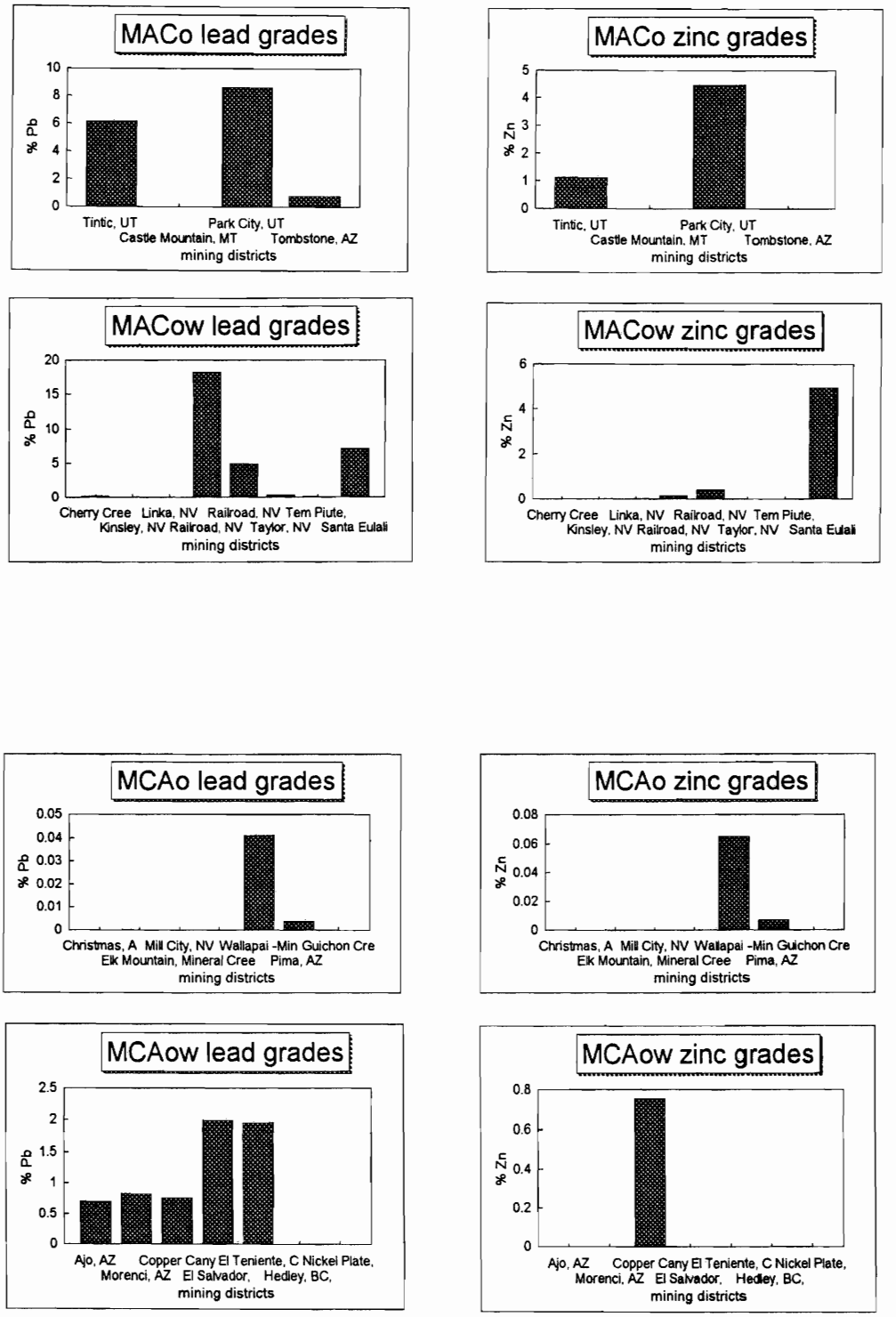

Figure 6-5. Lead and zinc grades in MagmaChem classes (MAC=alkali-calcic, MCA=calc-alkalic; o=oxidized, ow=weakly oxidized, r=reduced).

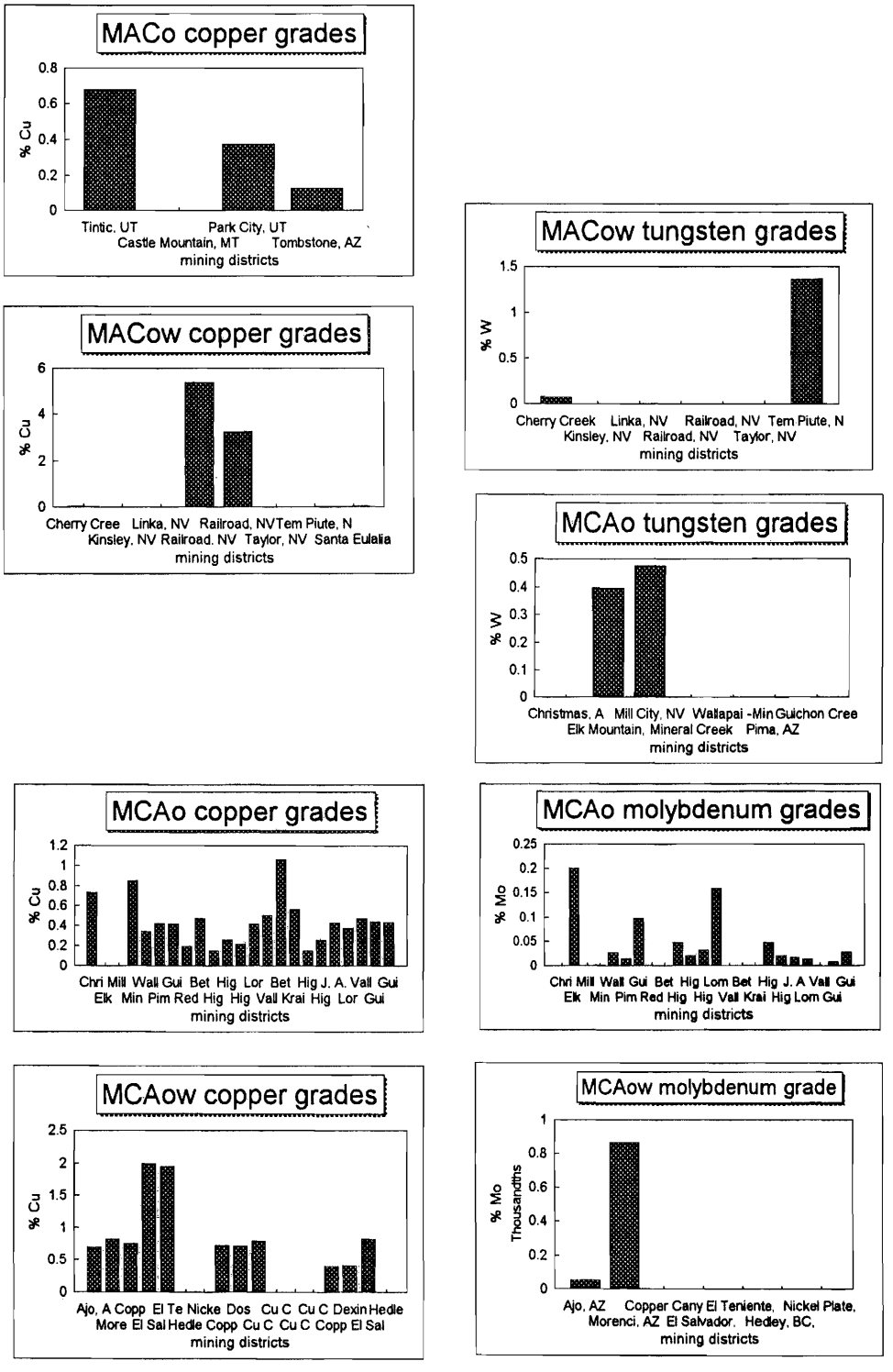

Figure 6-6. Lead and zinc grades in magma series classes (MAC=alkali-calcic, MCA=calc-alkalic; o=oxidized, ow=weakly oxidized, r=reduced).

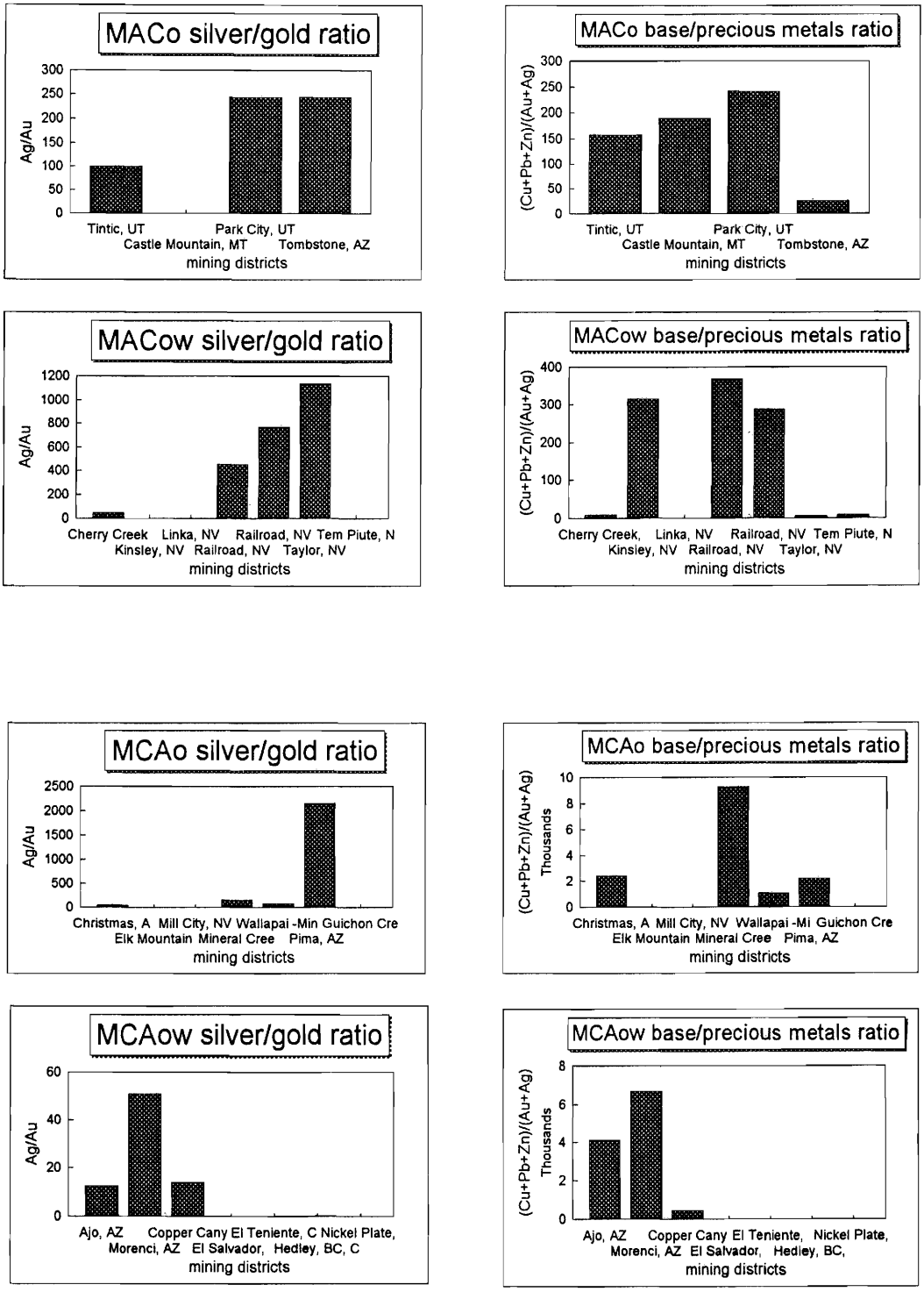

Figure 6-7. Precious metal ratios in each class (MAC=alkali-calcic, MCA=calc-alkalic; o=oxidized, ow=weakly oxidized, r=reduced).

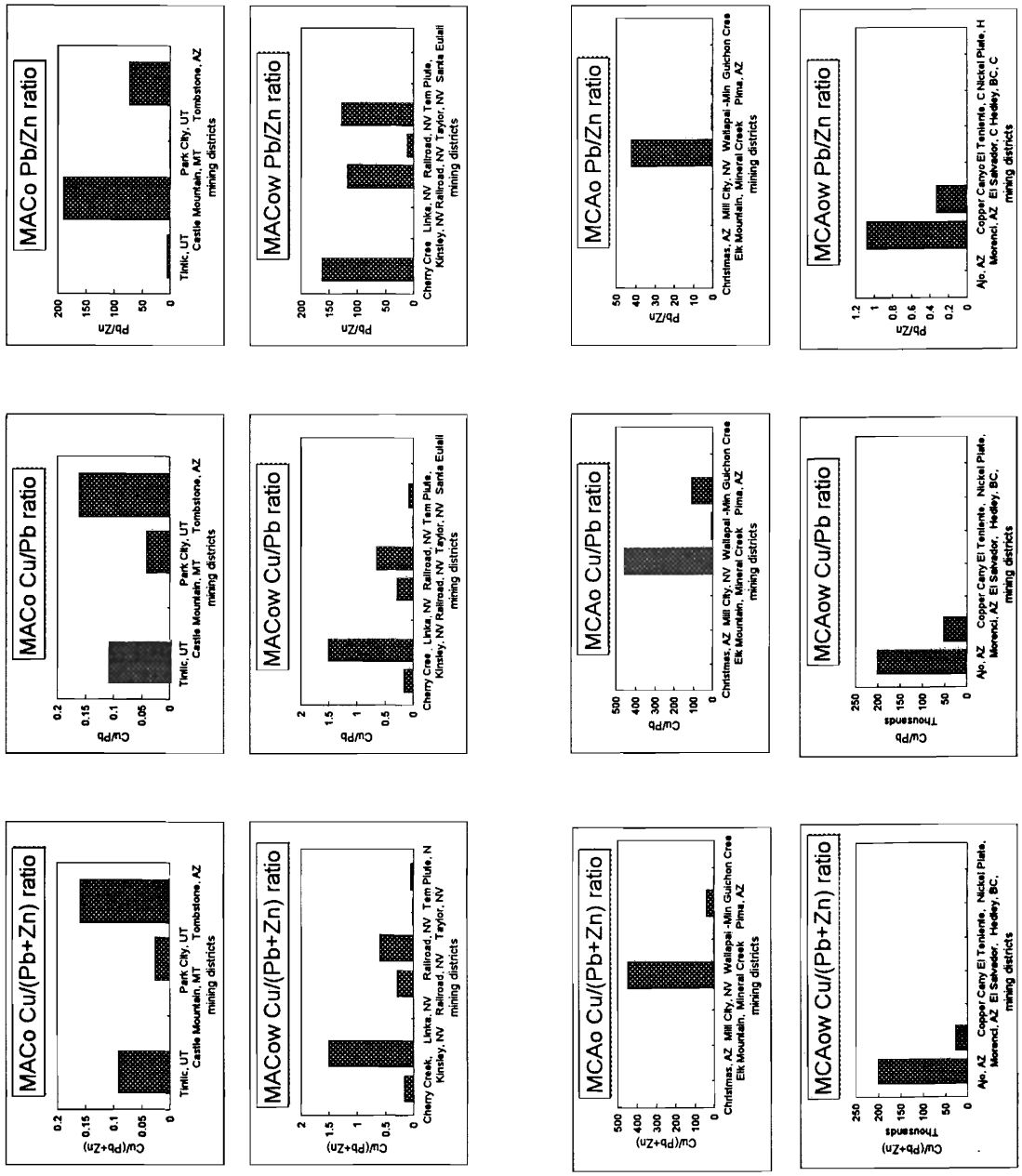

Figure 6-8. Base metal ratios in magma series classes (MAC=alkali-calcic, MCA=calc-alkalic; o=oxidized, ow=weakly oxidized, r=reduced).

classes (Figure 6-7). The alkali-calcic classes have grades that are 10 times less copper rich, have 200 times less copper than lead, and have 10 times more lead than silver (Figure 6-8). In summary, silver dominates gold at a ratios higher than 40:1 Ag:Au and lead exceeds copper at ratios of 100:1 to 2:1 Pb:Cu.

Production from Alkali-calcic, Oxidized Systems

The alkali-calcic oxidized districts are clearly silver-rich lead deposits with byproduct zinc and copper. These mining districts, such as Tintic, Tombstone, and Park City, each had production of several million kg of silver, one billion kg of lead, several hundred million kg of zinc and copper, and tens of thousands kg of gold. Silver grades range from 0.04 to 0.06%, lead grades from 0.8 to 9%, zinc grades from 0.01% (reflecting historical economic limitations) to 5%, copper grades from 0.1 to 0.7%, and gold grades from 0.0002 to 0.0005%. Metal ratios show a heavy silver bias (244:1 to 100:1 Ag:Au), a strong lead-zinc bias (Cu/[Pb+Zn] from 0.03 to 0.2), and a base/precious metal ratio from 30 to 250.

Production from Alkali-calcic, Weakly Oxidized Systems

The alkali-calcic weakly oxidized districts are silver-rich lead deposits with byproduct zinc and copper; they are not large volume systems and are more even in base metal distribution than the alkali-calcic oxidized deposits. Weakly oxidized alkali-calcic mining districts, such as Cherry Creek, Railroad, Taylor,

and Tempiute, each had production of several tens of thousands kg of silver, up to ten million kg of lead, several tens of thousands kg of zinc, as much as several million kg of copper, and only a few kg of gold. Silver grades range from 0.003 to 0.06%, lead grades from 0.1 to 20%, zinc grades from 0.002 to 0.4%, copper grades from 0.001 to 5%, and gold grades from 0.00006 to 0.0004%. Metal ratios show a heavy silver bias (1000:1 to 5:1 Ag:Au), a strong lead-zinc bias (Cu/[Pb+Zn] from 0.008 to 0.6), and a base/precious metal ratio from 10 to 400.

Comparing alkali-calcic weakly oxidized districts with oxidized ones generally shows 100 times less volume, but similar grades. The weakly oxidized deposits have a higher Ag/Au ratio and a higher proportion of base metals with higher amounts of copper and zinc compared to lead. Production of the alkali-calcic weakly oxidized districts was 100 times less silver than from the oxidized class, 200 times less gold, 30 times less copper, 100 times less lead, and 200 times less zinc. Gold and silver grades were similar between the two alkali-calcic subclasses, but their silver grades were 10 to 100 times higher than those of the calc-alkalic classes. Copper, lead, and zinc grades for both weakly oxidized and oxidized alkali-calcic classes were similar; however, the lead and zinc grades in the calc-alkalic classes are considerably smaller. Zinc grades in the weakly oxidized class were generally less than in the oxidized class. The silver/gold ratio was three times higher in the weakly oxidized class and the base/precious metals ratio was also slightly higher than in the oxidized districts. The copper/lead and copper/(lead + zinc) ratios were generally 2 to 10 times higher

in the alkali-calcic weakly oxidized districts than in oxidized ones; these ratios were 100 to 200 times higher in calc-alkalic districts.

Production from Alkali-calcic, Reduced Systems

The alkali-calcic reduced districts are silver-rich tin deposits with no byproduct gold or base metals; they are very large volume systems. These mining districts (Llallagua, Oruro, and Potosi, Bolivia) each had production of several hundred million kg of tin, several tens of millions kg of silver, and no lead, zinc, copper, or gold. Because production began in the 1500's in these districts, accurate production records do not exist. Some data on current reserves establish the silver grade at from 0.02 to 0.3%; tin grades from one year's production may be as high as 50%. These districts contrast strongly with gold-rich calc-alkalic reduced districts, which generally lack silver production.

Production from Calc-alkalic Systems

Calc-alkalic ore deposits are characterized by the dominance of copper over lead and zinc (shown in the bottom two or three graphs of each figure) and silver production is only 10 times more than gold production or was not present (Figure 6-1). Copper production (Figure 6-2) in calc-alkalic classes is 150 times more than lead and zinc production (Figure 6-3). Silver grades are ten to fifty times higher than gold grades in calc-alkalic ore deposits (Figure 6-4). Copper grades in calc-alkalic districts (Figure 6-5), while of similar orders of magnitude

between all classes, are ten times higher than lead and zinc grades (Figure 6-6). Precious metal ratios for the oxidized and weakly oxidized classes are more silver-rich than the reduced classes (Figure 6-7); reduced classes are not shown as they have only gold production. The calc-alkalic districts include the classic Arizona porphyry copper deposits and the Carlin-type disseminated gold deposits of Nevada.

Calc-alkalic ore deposits differ from alkali-calcic systems by lower silver to gold ratios and higher copper to lead ratios. Although silver production is at least 10 times gold production, the Ag:Au ratio is lower than 40:1 in weakly oxidized and reduced calc-alkalic districts. Copper and molybdenum or tungsten production is one thousand times higher than in alkali-calcic districts. Cu:Pb ratios are 100:1 or 100,000:1 in calc-alkalic systems in contrast to 0.01:1 to 1:1 in alkali-calcic deposits.

Production from Calc-alkalic, Oxidized Systems

The calc-alkalic oxidized districts are porphyry copper deposits with byproduct molybdenum, zinc, lead, silver, and gold. The large mining districts, such as Pima, Mineral Creek (Ray), and Valley Copper and other districts associated with the Guichon Creek batholith, each produced several billion kg of copper. These districts produced several tens of millions of kg of lead and zinc, several hundred thousand kg of silver, and a few thousand kg of gold. Copper grades range from 0.2 to 0.9%, molybdenum grades from 0.01 to 0.1%, lead grades

from 0.004 to 0.04%, zinc grades from 0.0004 to 0.07%, silver grades from 0.0001 to 0.0004%, and gold grades from 0.000001 to 0.00008%. Metal ratios show a strong copper bias (Cu/[Pb+Zn] from 4 to 450), a silver bias (40:1 to 2000:1 Ag:Au), and a base/precious metal ratio from 1000 to 9000.

Production from Calc-alkalic, Weakly Oxidized Systems

The calc-alkalic weakly oxidized districts are gold-rich porphyry copper deposits with byproduct molybdenum, zinc, lead, silver, and gold. These mining districts, such as Ajo, Morenci, Copper Canyon, and El Salvador, each produced several billion kg of copper. These districts produced several million of kg of lead and zinc, several hundred thousand kg of silver, and tens of thousands kg of gold; some districts produced molybdenum. Copper grades range from 0.4 to 2%, molybdenum grades from 0.00005 to 0.0009%, lead grades from 0.00002 to 0.02%, zinc grades from 0.0001 to 0.8%, silver grades from 0.0001 to 0.005%, and gold grades from 0.00001 to 0.001%. Metal ratios show a strong copper bias (Cu/[Pb+Zn] from 7 to 200,000), a gold bias (50:1 to 3:1 Ag:Au), and a base/precious metal ratio from 200 to 7000.

The weakly oxidized calc-alkalic districts contrast with the oxidized ones in that they are more gold-rich and have lesser amounts of silver, lead, and zinc. The weakly oxidized districts have about ten times as much gold production, half as much silver, similar amounts of copper, less molybdenum, and one tenth the lead and zinc. The weakly oxidized deposits have higher gold grades, higher

silver grades, similar copper grades, and higher lead and zinc grades than the oxidized calc-alkalic districts. The silver/gold ratios are considerably lower in the weakly oxidized class commensurate with the gold-rich character of the deposits, but have similar base/precious metal ratios. Base metal ratios are similar between oxidized and weakly oxidized calc-alkalic districts, except for lead/zinc ratios, which are more zinc rich in the weakly oxidized systems.

Production from Calc-alkalic, Reduced Systems

The calc-alkalic reduced districts are disseminated gold deposits with no byproduct production, although some districts such as Getchell had tungsten production from skarns adjacent to plutons. These mining districts, such as Carlin, Getchell, and Northumberland, produced or have reserves of several million kg of gold. These districts have not produced copper, lead, zinc, silver, or molybdenum. Gold grades range from 0.00007 to 0.04%.

The gold production of the calc-alkalic reduced districts contrasts strongly with the silver and tin production of the alkali-calcic reduced districts. Both reduced alkalinity classes were precious metal producers with no lead, zinc, or copper base metal production; this contrasts with the large amounts of base metal production from the oxidized and weakly oxidized classes.

Ore Deposit Mineralogy for Each Class

The compilation of mineralogical information from each ore deposit

(Appendix F) also demonstrates clear differences between petrochemical classes. Detailed information on mineralogy is generally found in journals devoted to mineral collecting and in classic U. S. Geological Survey studies of mining districts. Using diverse sources, it is not possible to be precise about abundances of particular minerals, as one person's designation of 'common' is another person's 'rare'. Also, many researchers simply record the presence of a mineral without commenting on its relative abundance. The lack of mention of a mineral does not mean that it is not present or common in the ore deposit because different authors emphasize various aspects of an ore deposit. In spite of this diversity of detail, obvious patterns emerge upon examination of the data.

Mineralogy in Alkali-calcic Systems

Alkali-calcic ore deposits contain a rich assortment of silver minerals, abundant lead minerals, and common manganese minerals; they lack molybdenum, cobalt, nickel, thallium, and mercury minerals. Sulfosalts of most metals are present or abundant and tellurides, particularly silver tellurides, are present in the oxidized alkali-calcic districts, although they are rare.

Mineralogy in Alkali-calcic, Oxidized Systems

Because the mineralogy of the Tintic, Tombstone, and Park City districts were so well-described, more detail is available for the alkali-calcic oxidized deposits than for other classes. The common sulfides of pyrite, chalcopyrite,

galena, and sphalerite are ubiquitous and abundant; sometimes bornite is listed as being present. Native silver and gold are generally reported. Copper minerals frequently occur, but not in large amounts; these include copper sulfides, sulfosalts, oxides, carbonates, sulfates, and arsenates. Lead minerals are abundant, particularly anglesite and cerussite; a wide variety of lead sulfosalts, oxides, sulfates, arsenates, phosphates, vanadates, and molybdates are recorded as present or rare. Zinc minerals include zinc carbonates, oxides, sulfates, and others. A rich assortment of silver minerals is documented and includes silver sulfides, sulfosalts, halides and tellurides; argentite and chlorargyrite frequently occur. The common iron minerals, magnetite, hematite, limonite, and arsenopyrite are generally present or abundant and some of the more unusual iron sulfates and arsenates are found at Tintic. Bismuth minerals also occur at Tintic, but are atypical at Tombstone. Arsenic minerals are mentioned, although antimony and tin minerals are absent; manganese oxides are customary. Cobalt, cadmium, nickel, thallium, and mercury minerals are conspicuously missing. A large variety of rare and unusual tellurium minerals has been described from Tombstone (Williams, 1980).

Mineralogy in Alkali-calcic, Weakly Oxidized Systems

A smaller variety of minerals is described from weakly oxidized alkali-calcic ore deposits, such as Cherry Creek, Kinsley, Railroad, and Taylor, Nevada. The common sulfides, pyrite, chalcopyrite, galena, sphalerite, and bornite, are

abundant. Precious metals as native silver or gold are sporadically noted as present or infrequent. Fewer copper minerals are cataloged from these districts, although copper carbonates are routine; copper sulfates, arsenates, and phosphates are not mentioned. Very few lead or zinc minerals are recorded, although cerussite, bindheimite, and duftite are common. Lead and zinc oxides, sulfates, phosphates, vanadates, molybdates are absent. Very few silver minerals are documented, although argentite, a few sulfosalts, and halides are present; silver tellurides are not recorded. The common iron minerals, manganese oxides, and a few tungsten (scheelite) and antimony (stibnite and cervantite) minerals occur in these districts. Molybdenum, bismuth, arsenic, tin, cobalt, cadmium, nickel, thallium, mercury, and tellurium minerals are lacking.

Mineralogy in Alkali-calcic, Reduced Systems

Even fewer minerals are described as abundant in the reduced alkali-calcic ore deposits of Potosi, Llallagua, and Oruro, Bolivia. The common sulfides (pyrite, chalcopyrite, galena, and sphalerite) occur frequently, but precious metals as native silver or gold are not mentioned. Copper and zinc minerals are conspicuous by their absence, although tetrahedrite is recurrent and enargite is present. The common secondary lead minerals of anglesite and cerussite generally are reported, but lead oxides, sulfates, arsenates, phosphates, vanadates, and molybdates are lacking. Some of the more unusual lead sulfosalts, such as andorite, boulangerite, frankeite, and zinkenite, are numerous. Silver

sulfosalts and halides occur and pyrargyrite (ruby silver) is reported as abundant. Common iron oxides and sulfides are present, but not iron sulfates and arsenates. The tungsten minerals huebnerite and wolframite are minor occurrences; bismuth minerals occur in these deposits frequently as bismuthinite. Antimony minerals are present and tin minerals, particularly cassiterite and stannite, are ubiquitous. Molybdenum, arsenic, manganese, cobalt, cadmium, nickel, thallium, mercury, and tellurium minerals are not mentioned.

Mineralogy in Calc-alkalic Systems

Calc-alkalic ore deposits generally contain abundant copper minerals, locally important molybdenite and scheelite, and some antimony minerals; silver, lead, and zinc minerals are unusual, except for galena and sphalerite. Antimony, arsenic, cobalt, nickel, thallium, and mercury minerals occur in all calc-alkalic classes and are common in the reduced class, but tellurium minerals are lacking.

Mineralogy in Calc-alkalic, Oxidized Systems

Very few minerals are listed from the porphyry copper deposits in this study, although this may result from a lack of detailed mineralogical studies in the literature on these particular districts. The common sulfides (pyrite, chalcopyrite, galena, sphalerite, and bornite) are abundant, as is the secondary copper sulfide, chalcocite. Other copper minerals, including copper sulfides, sulfosalts, oxides, carbonates, and phosphates (turquoise), occur frequently, but

copper sulfates and arsenates are missing. Molybdenite is abundant and powellite and ferrimolybdite are generally present; scheelite is also recurrent and wolframite is unusual. Lead and zinc minerals are not described, nor are the silver sulfosalts, halides, or tellurides. Native silver and gold occur in minor amounts, as does argentite. Magnetite, hematite, and limonite are normal and arsenopyrite and pyrrhotite are reported. Antimony minerals are sometimes present, bismuthinite is rare or not mentioned, and manganese oxides are locally abundant at Valley Copper. Arsenic, tin, cobalt, cadmium, nickel, thallium, mercury, and tellurium minerals are lacking.

Mineralogy in Calc-alkalic, Weakly Oxidized Systems

There are generally one or two minerals of each Dana class in the weakly oxidized calc-alkalic ore deposits. Of the common sulfides, pyrite, chalcopyrite, and bornite are abundant and galena and sphalerite are rare, minor, or present. Precious metals (native silver, gold, and electrum) are scattered, but a wide variety of copper minerals are standard. Secondary copper minerals (chalcocite, azurite, malachite, and chrysocolla) are abundant and copper sulfosalts (enargite and tennantite) are locally important; copper oxides, carbonates, sulfates, arsenates, and phosphates are reported. Lead and zinc minerals are not mentioned, except cerussite, willemite, and smithsonite. Silver minerals are rarely listed, except for an occasional silver sulfosalt, halide, or telluride. Of the common iron minerals, pyrrhotite and arsenopyrite are abundant, magnetite is

sparse, hematite and marcasite are customary, and limonite is sometimes present. Molybdenite is abundant or locally important and some bismuth minerals (hedleyite, joseite, and native bismuth) are frequently recorded. Arsenic minerals (realgar and orpiment) are listed from McCoy and Morenci and antimony minerals (stibnite and stibiconite) are present in a few deposits. Manganese oxides, cobalt minerals (erythrite and cobaltite), and nickel minerals (millerite and gersdorffite) occur in Morenci, McCoy, Nickel Plate, and El Teniente. No mention is made of tin, cadmium, thallium, mercury, or tellurium minerals.

Mineralogy in Calc-alkalic, Reduced Systems

In contrast with earlier ore deposits, reduced calc-alkalic districts frequently contain arsenic, mercury, and thallium minerals. Of the common sulfides, pyrite is abundant and chalcopyrite, galena, and sphalerite are sometimes present. Native gold is common or present in nearly all the districts and native silver is rare or not mentioned. Copper minerals, generally chalcocite, azurite, or malachite, are reported from a few of the districts, and occasionally the copper sulfosalts, tetrahedrite-tennantite and famatinite are recorded. Copper or lead oxides, sulfates, arsenates, and phosphates are not mentioned, nor are zinc minerals. A few lead sulfosalts (jordanite, geocronite, bournonite, and jamesonite) are listed. Silver sulfosalts (proustite, freibergite, laffittite, and jalpaite) occur at Getchell and Northumberland. Of the common iron minerals, pyrrhotite is minor, magnetite is rare, and marcasite and arsenopyrite are present

in half the districts. Molybdenite and its oxidation products occur in some of the districts and scheelite and stibnite are common in most deposits. Arsenic minerals, particularly realgar and orpiment, are generally present, along with more exotic arsenic minerals and elemental arsenic. The tin mineral, teallite, and cobalt mineral, linnaeite, are present at Getchell. Manganese, cadmium, nickel, and tellurium minerals are absent, mercury minerals are present, and cinnabar is generally abundant. A wide variety of thallium minerals is recorded from Carlin and Getchell.

Trace Element Geochemical Data

Data Set Available

Trace element geochemical data obtained from the TracElem data base of MagmaChem Exploration Inc. consisted of 30 or 40 element geochemical analyses of 12,600 samples from 266 mines in 74 magma series classes. This data base was searched in R:Base for those mining districts included in this study, which were sorted into a separate file (Appendix G).

Rock chips or drill cuttings were generally analyzed by Inductively Coupled Plasma (ICP) emission spectroscopy for Ag, As, Au, Bi, Cd, Co, Cu, Fe, Ga, Hg, Mn, Mo, Ni, Pb, Sb, Se, Te, Tl, V and Zn with Graphite Furnace Atomic Absorption finish for very low levels of Au. Some rock chip or drill cutting samples were analyzed for 22 elements by Neutron Activation (NA). The 22 elements generally analyzed by NA include Ba, Br, Ca, Ce, Cr, Cs, Eu, Hf, La, Lu,

Na, Nd, Rb, Sc, Sr, Sm, Ta, Th, Tb, U, W, and Yb. For Ba, Be, Cr, F, Sr, Ti, Y, and Zr.

Values for many of these elements extend over such a broad range, in some cases from 0.1 ppm to 100,000 ppm, that standard histograms compress the data too much on the lower part of the scale to show useful patterns. In order to spread out the data, stepped histograms were constructed by designating equal size bins within each order of magnitude. Thus, there are ten equal divisions between 0 and 1, nine equally spaced bins between 1 and 10, another set between 10 and 100, another between 100 and 1000, and continuing to 100,000 (Figure 6-9). Each histogram, therefore, consists of six order of magnitude steps; the data are expanded close to zero and compressed at high values. Differences of a few parts per million are significant at low concentrations, but are insignificant at high concentrations.

Precious Metals

Alkali-calcic classes are more silver-rich than calc-alkalic classes; most samples in the alkali-calcic classes contain between 100 and 2000 ppm Ag and samples in calc-alkalic classes contain less than 100 ppm and generally less than 10 ppm (Figure 6-9). Gold is the opposite; alkali-calcic classes generally contain less than 6 ppm Au and calc-alkalic classes commonly have between 1 and 40 ppm Au (Figure 6-10).

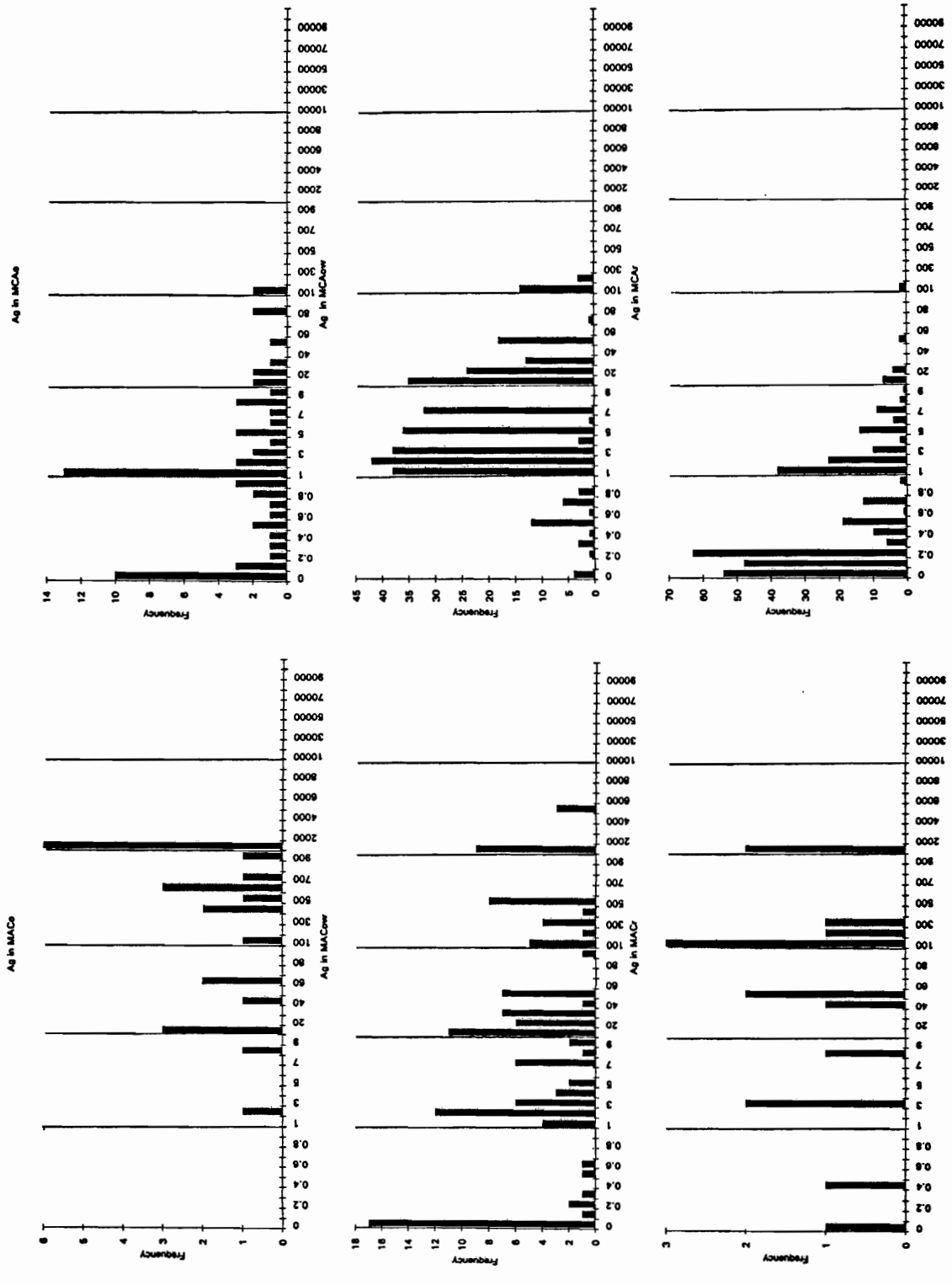

Figure 6-9. Stepped histograms of silver in ppm (MAC=alkali-calcic, MCA=calc-alkalic; o=oxidized, ow=weakly oxidized, r=reduced).

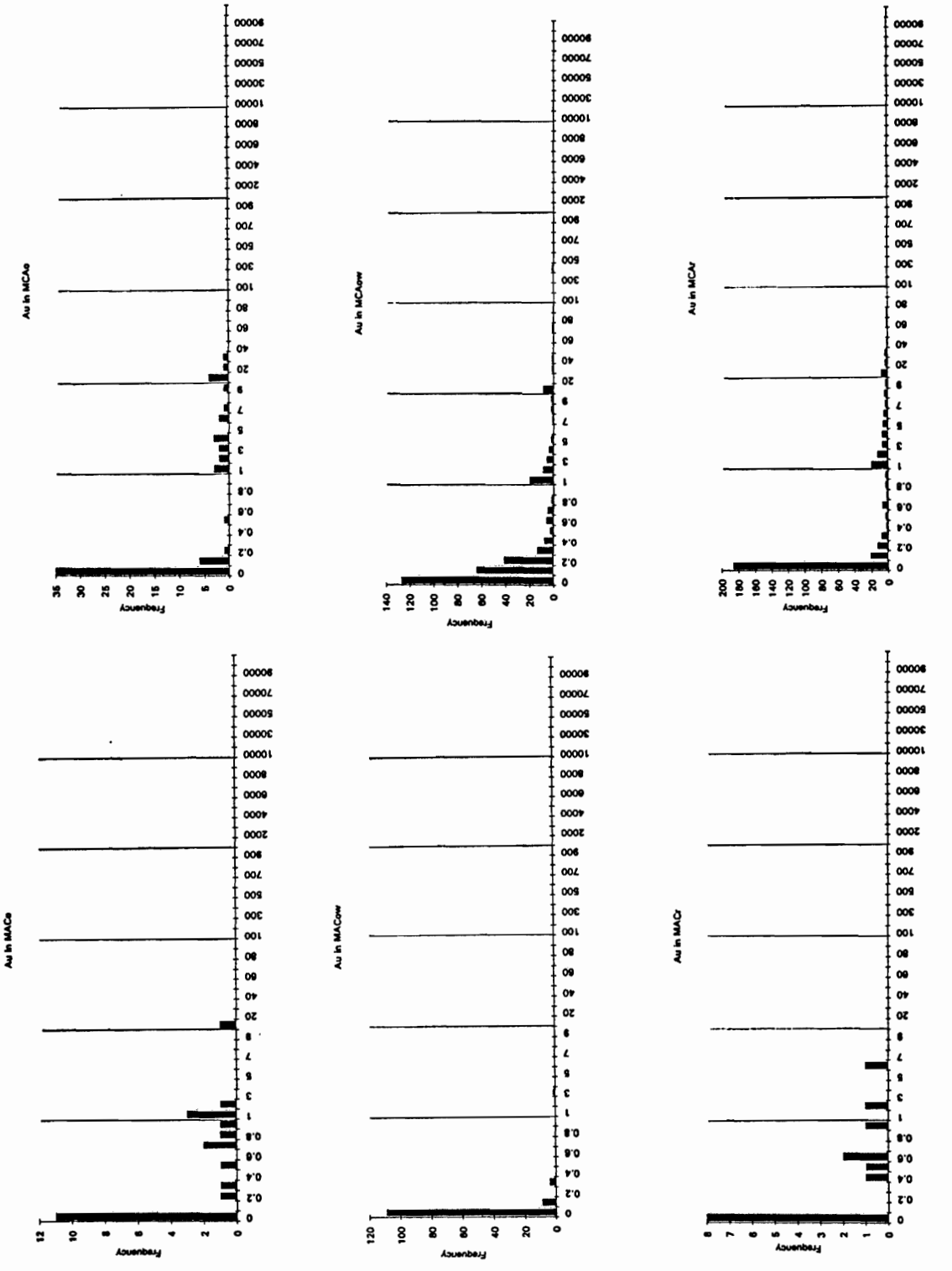

Figure 6-10. Stepped histograms of gold in ppm (MAC=alkali-calcic, MCA=calc-alkalic; o=oxidized, ow=weakly oxidized, r=reduced).

Toxic Metals

Some of the toxic metals that typically have different concentrations for some of the petrochemical classes include arsenic, antimony, mercury, and thallium. Tellurium and other elements that show little difference among magma series classes are depicted in Appendix H.

Arsenic concentrations range from 1 ppm to 100,000 ppm, with the majority of samples falling between 100 and 10,000 ppm in the calc-alkalic weakly oxidized and reduced classes and between 10 and 100 in the calc-alkalic oxidized (Figure 6-11). Arsenic concentrations in the alkali-calcic class have similar maxima and minima, but most samples are between 100 and 4000 ppm in the alkali-calcic oxidized class and between 10 and 2000 ppm in the alkali-calcic weakly oxidized class. The large numbers of samples cluster at 1 ppm resulted from using 10 percent of the detection limit for samples that were below the detection limit of 10 ppm; some other analyses had lower detection limits.

Antimony concentrations range up to 20,000 ppm in alkali-calcic classes, but only up to 5000 ppm in calc-alkalic reduced classes (Figure 6-12). Calc-alkalic oxidized samples are generally between 1 ppm and 40 ppm, whereas most calc-alkalic weakly oxidized samples are between 10 and 800 ppm. Calc-alkalic reduced samples most commonly cluster around 100 ppm, but range up to 5000 ppm. The majority of samples in the alkali-calcic classes are higher by one order of magnitude than those in comparable calc-alkalic classes. Most alkali-calcic oxidized samples are 900 to 5000 ppm, alkali-calcic weakly oxidized

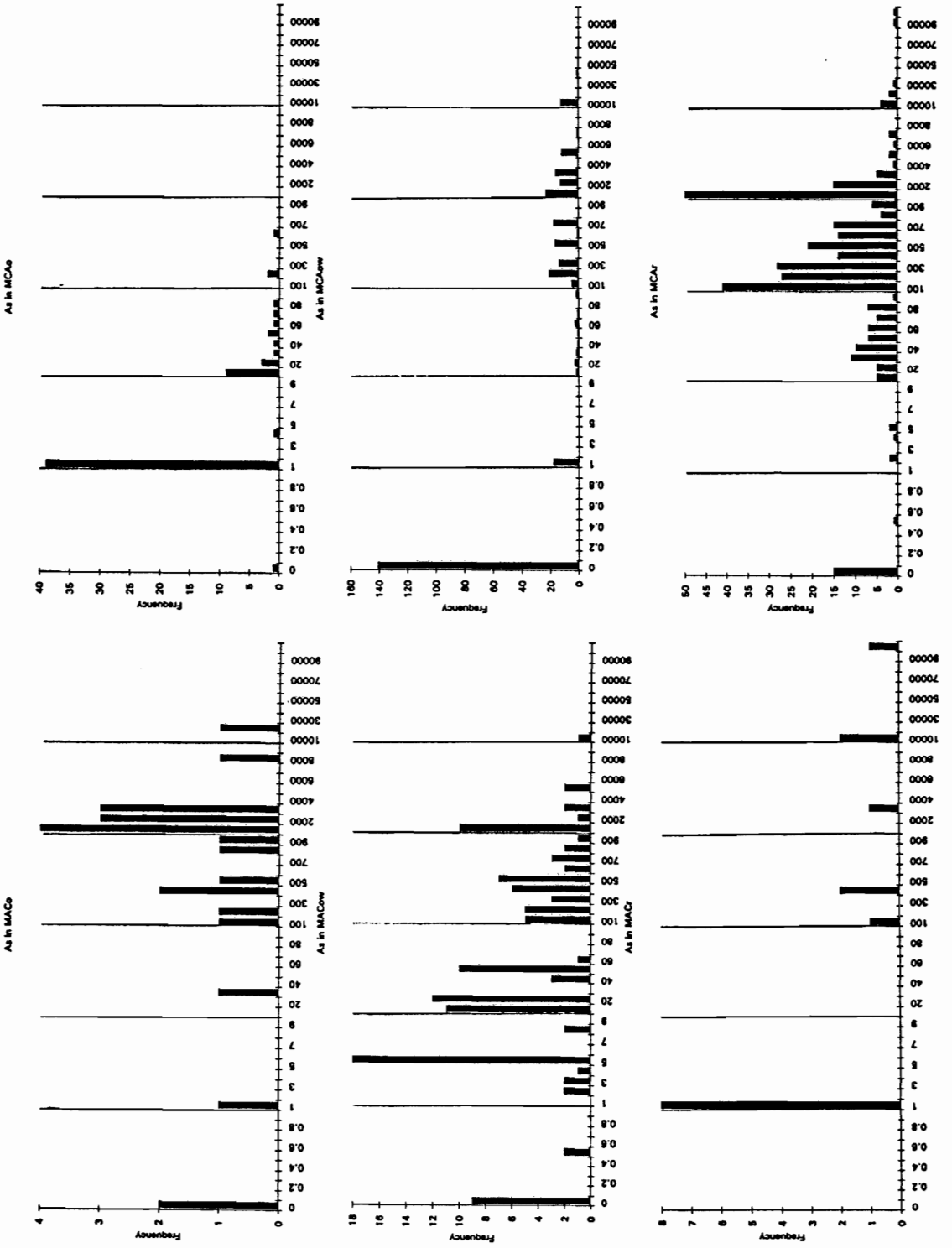

Figure 6-11. Stepped histograms of arsenic in ppm (MAC=alkali-calcic, MCA=calc-alkalic; o=oxidized, ow=weakly oxidized, r=reduced).

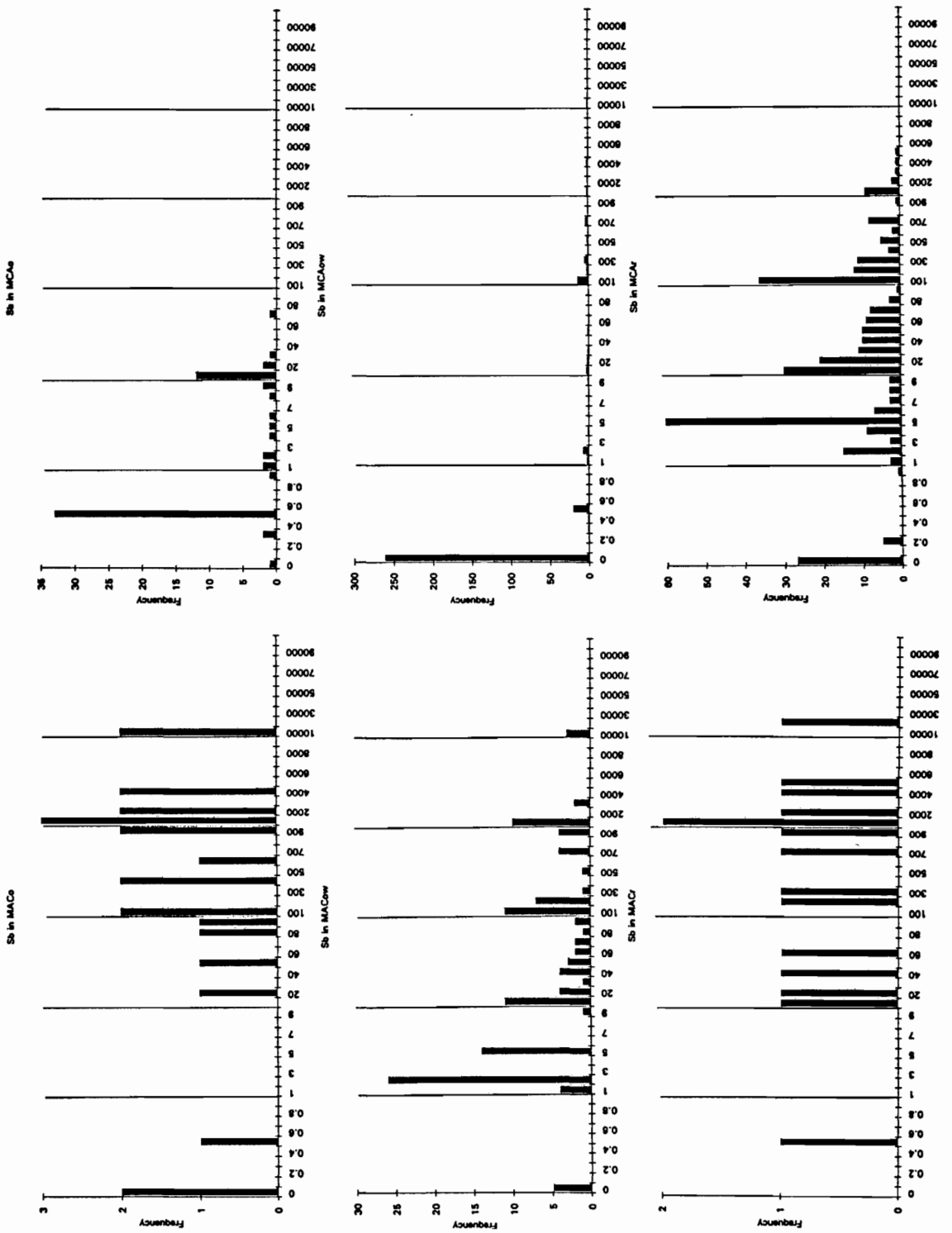

Figure 6-12. Stepped histograms of antimony in ppm (MAC=alkali-calcic, MCA=calc-alkalic; o=oxidized, ow=weakly oxidized, r=reduced).

samples are 100 to 1000 ppm, and alkali-calcic reduced ones are 100 to 5000 ppm. In both alkalinity cases the reduced samples are richer in antimony than the oxidized ones. The large spike at 5 ppm in the reduced calc-alkalic class resulted from using 10 percent of the detection limit of 50 ppm for samples below the detection limit; many of the antimony analyses had detection limits of 2 ppm.

Mercury concentrations are much higher in the calc-alkalic reduced samples than in the other classes, although mercury was not measured in alkali-calcic oxidized and reduced systems in this study (Figure 6-13). Mercury concentrations are generally between 1 and 9 ppm in calc-alkalic oxidized, between 0.2 and 3 ppm in calc-alkalic weakly oxidized, between 0.2 and 30 ppm in alkali-calcic weakly oxidized, and between 0.3 and 500 ppm in calc-alkalic reduced classes. Detection limits for mercury on most analyses were quite low, generally less than 2 ppm, and sometimes less than 0.09 ppm.

Thallium concentrations are also much higher in reduced classes than in oxidized and weakly oxidized classes (Figure 6-14). In oxidized classes, thallium concentrations range from 4 to 50 ppm in alkali-calcic and from 2 to 7 ppm in calc-alkalic samples. In reduced classes, thallium values range from 2 to 400 ppm in alkali-calcic samples and from 0.2 to 200 ppm in calc-alkalic ones. Detection limits for thallium generally were 2, 5, or 10 ppm.

Fourth Period Transition Metals

Metals from the fourth line on the periodic table of elements include

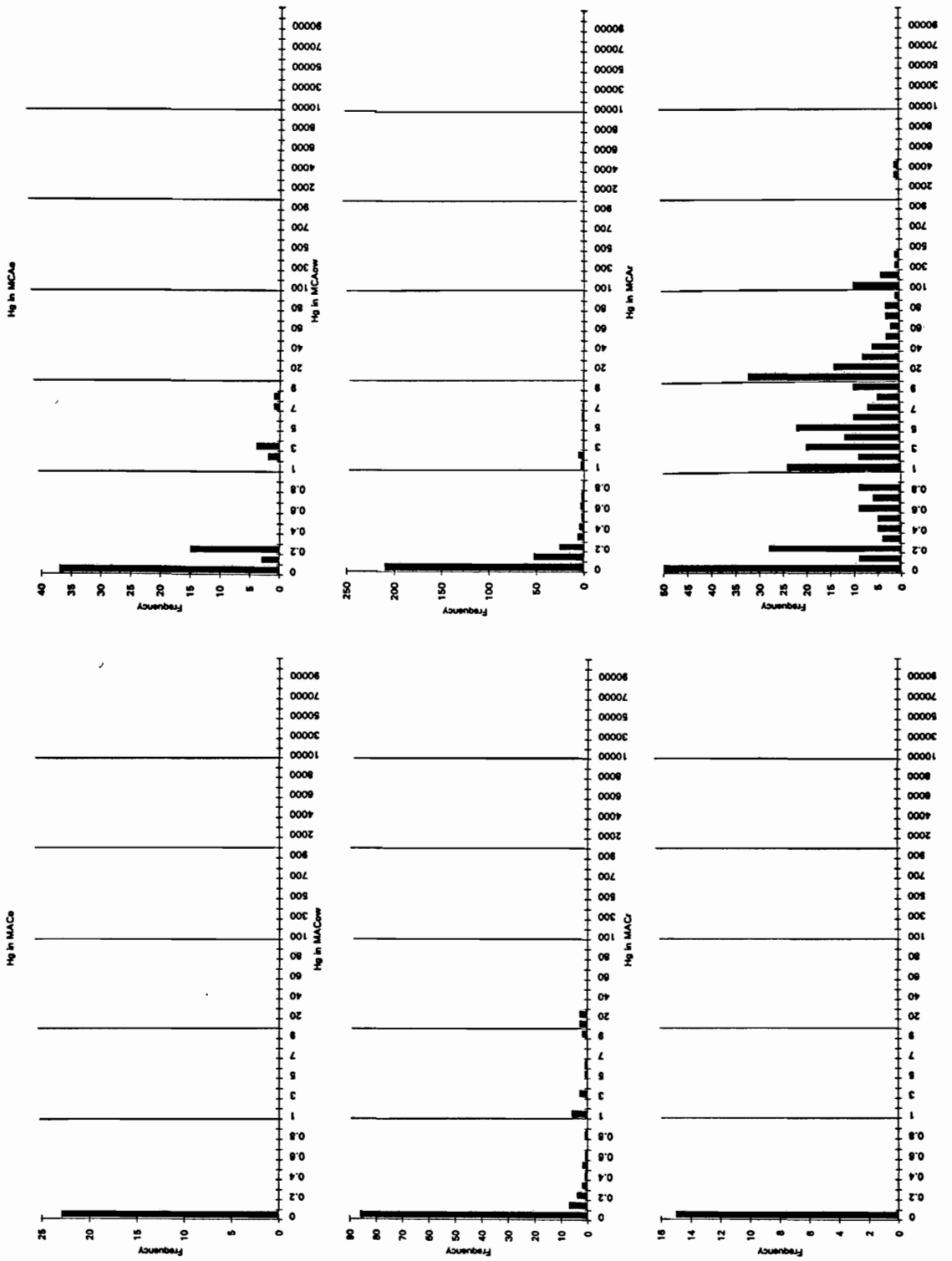

Figure 6-13. Stepped histograms of mercury in ppm (MAC=alkali-calcic, MCA=calc-alkalic; o=oxidized, ow=weakly oxidized, r=reduced).

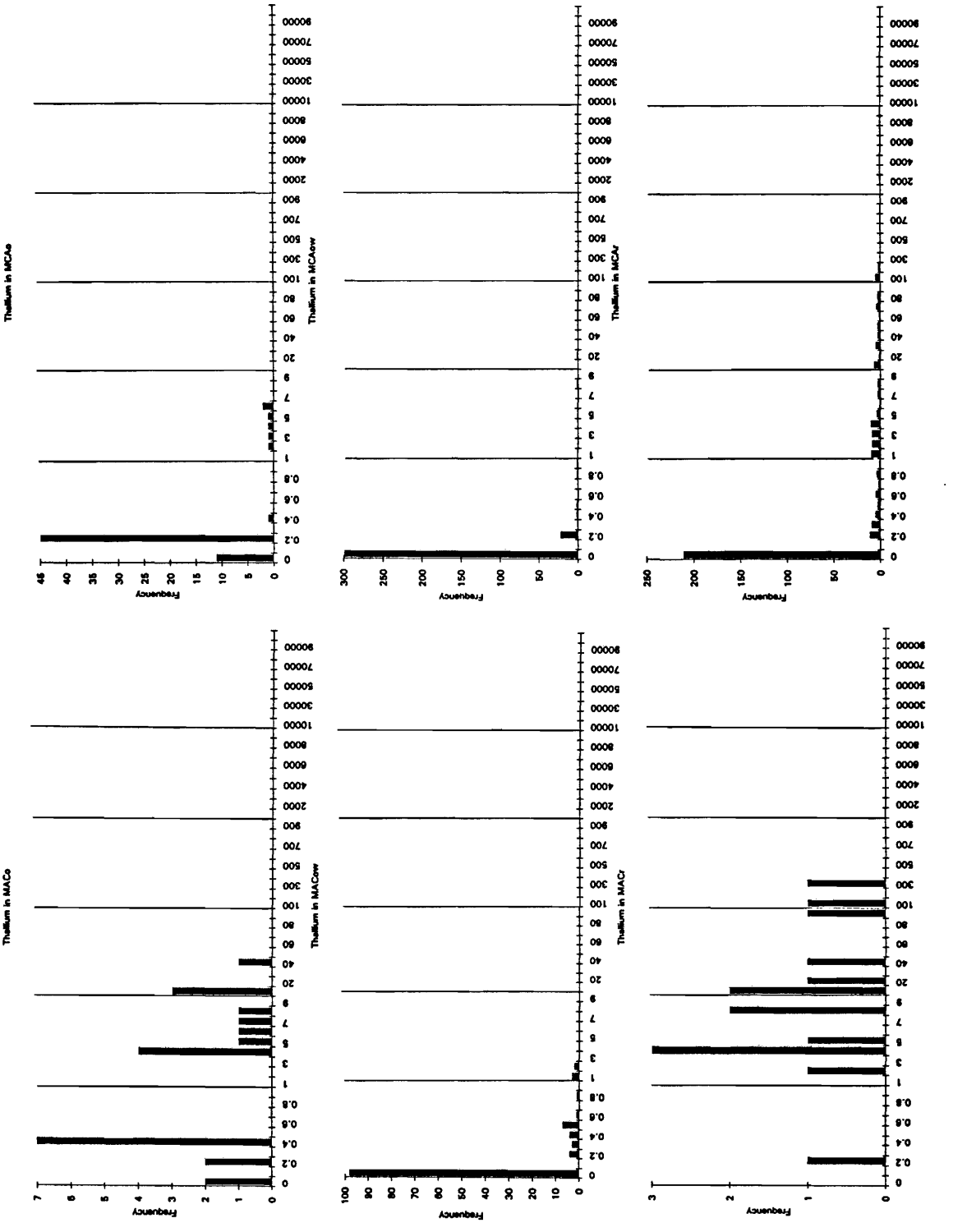

Figure 6-14. Stepped histograms of thallium in ppm (MAC=alkali-calcic, MCA=calc-alkalic; o=oxidized, ow=weakly oxidized, r=reduced).

copper, zinc, cobalt, iron, chromium, nickel, manganese, vanadium, and titanium. Elements which did not show obvious differences among the petrochemical classes in this study include cobalt, chromium, iron, and nickel (Appendix H).

Copper concentrations are higher in the oxidized classes than in the weakly oxidized and reduced classes; the maximum copper values are also higher in the calc-alkalic oxidized classes than in the alkali-calcic classes (Figure 6-15). Most calc-alkalic oxidized and weakly oxidized samples are between 1000 and 10,000 ppm, whereas most calc-alkalic reduced samples are between 10 and 200 ppm. Most alkali-calcic oxidized and weakly oxidized samples are between 100 and 6000 ppm, whereas most alkali-calcic reduced samples are between 10 and 1000 ppm. Nearly all the samples were above the detection limit of 5 ppm.

Zinc concentrations are generally one order of magnitude higher for alkali-calcic classes than for calc-alkalic classes (Figure 6-16). Zinc values in alkali-calcic oxidized samples range from 80 to 100,000 ppm with most samples having between 1000 and 30,000 ppm; the minimum for alkali-calcic weakly oxidized samples is lower and most samples are between 100 and 10,000 ppm. Most samples in the calc-alkalic oxidized class are between 20 and 200 ppm, although the maximum zinc value extended to 40,000 ppm. Zinc concentrations in the calc-alkalic weakly oxidized class generally cluster between 200 and 1000 ppm; they are usually between 10 and 300 ppm in the calc-alkalic reduced class. In some cases the detection limit for zinc was 5 ppm and in others it was 200 ppm.

Manganese concentrations are much higher in the oxidized classes than in

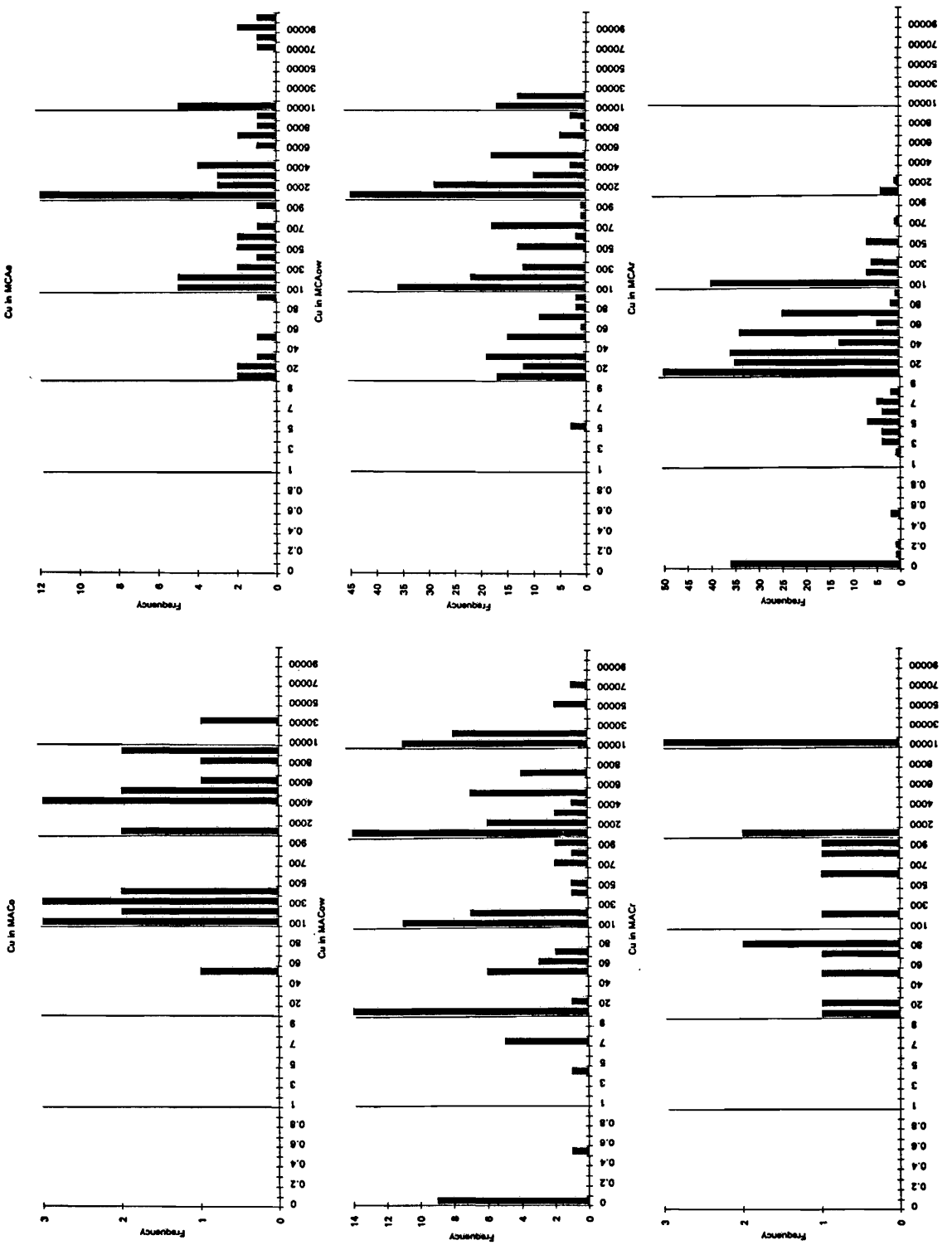

Figure 6-15. Stepped histograms of copper in ppm (MAC=alkali-calcic, MCA=calc-alkalic; o=oxidized, ow=weakly oxidized, r=reduced).

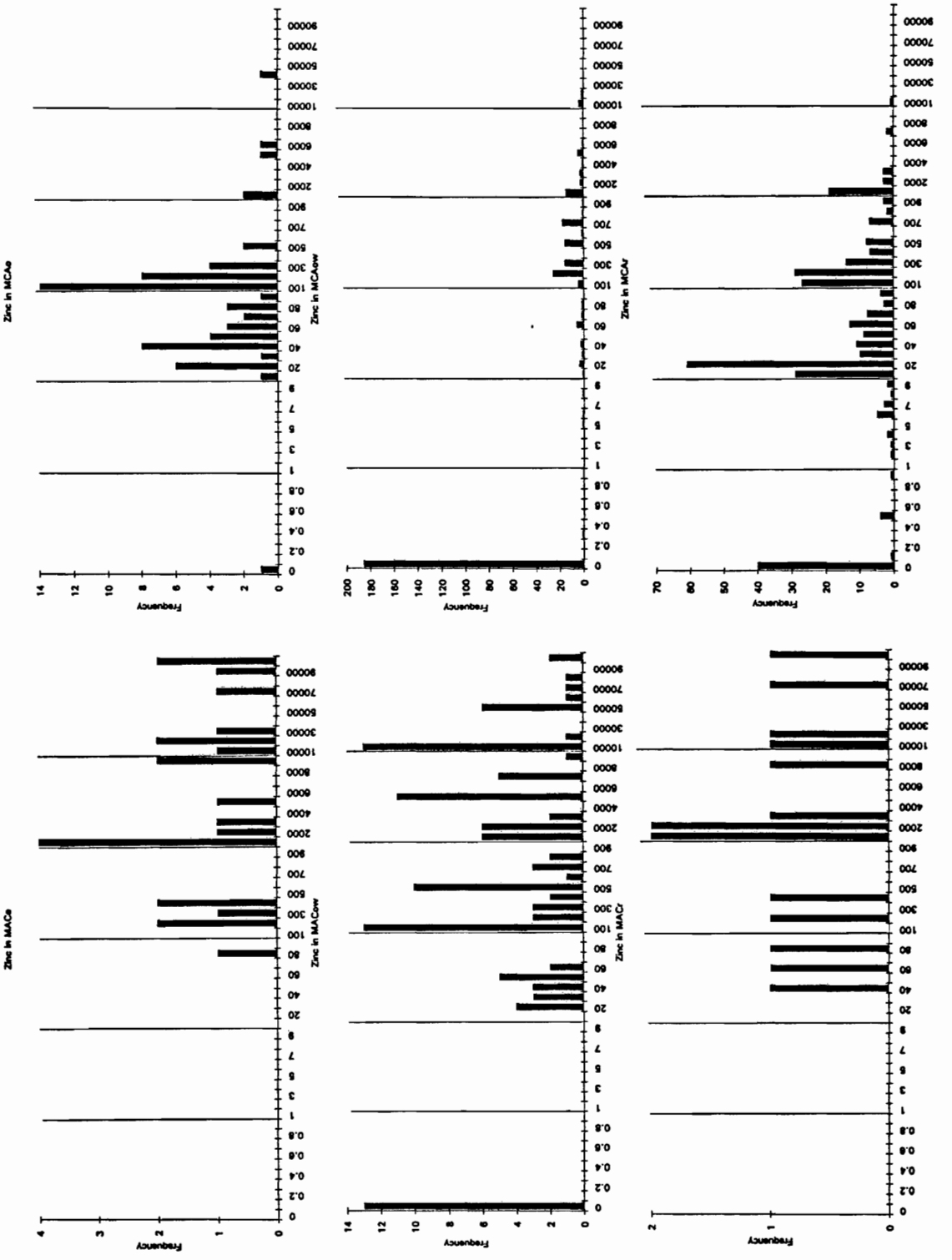

Figure 6-16. Stepped histograms of zinc in ppm (MAC=alkali-calcic, MCA=calc-alkalic; o=oxidized, ow=weakly oxidized, r=reduced).

the weakly oxidized or reduced classes (Figure 6-17). Most samples in the alkali-calcic oxidized class have zinc values between 1000 and 10,000 ppm, whereas those in the alkali-calcic reduced class are between 100 and 1000 ppm zinc. Most samples in the calc-alkalic oxidized class have zinc concentrations between 200 and 2000 ppm, whereas those in the calc-alkalic weakly oxidized and reduced classes are close to 100 ppm. Nearly all samples were above the detection limit for zinc of 5 ppm.

Vanadium concentrations are higher in the calc-alkalic classes than in the alkali-calcic classes (Figure 6-18). Most samples in the calc-alkalic classes are clustered near 100 ppm; those in alkali-calcic classes cluster near 10 ppm. There was little difference in zinc values between the different oxidation state classes. Very few samples were below the detection limits of 1, 2, 3, or 10 ppm.

Titanium concentrations are generally one order of magnitude higher in calc-alkalic classes than in alkali-calcic ones (Figure 6-19). Titanium values in calc-alkalic oxidized, weakly oxidized, and reduced classes cluster near 1000 ppm and range up to 20,000 ppm. Titanium concentrations in the alkali-calcic oxidized class range from 20 to 1000 ppm, with most near 20 ppm; titanium in the alkali-calcic weakly oxidized class cluster between 100 and 700 ppm; Ti values in the alkali-calcic reduced class are mostly near 10 ppm, with some values near 100 ppm. Detection limits for titanium were generally either 10 ppm or 100 ppm.

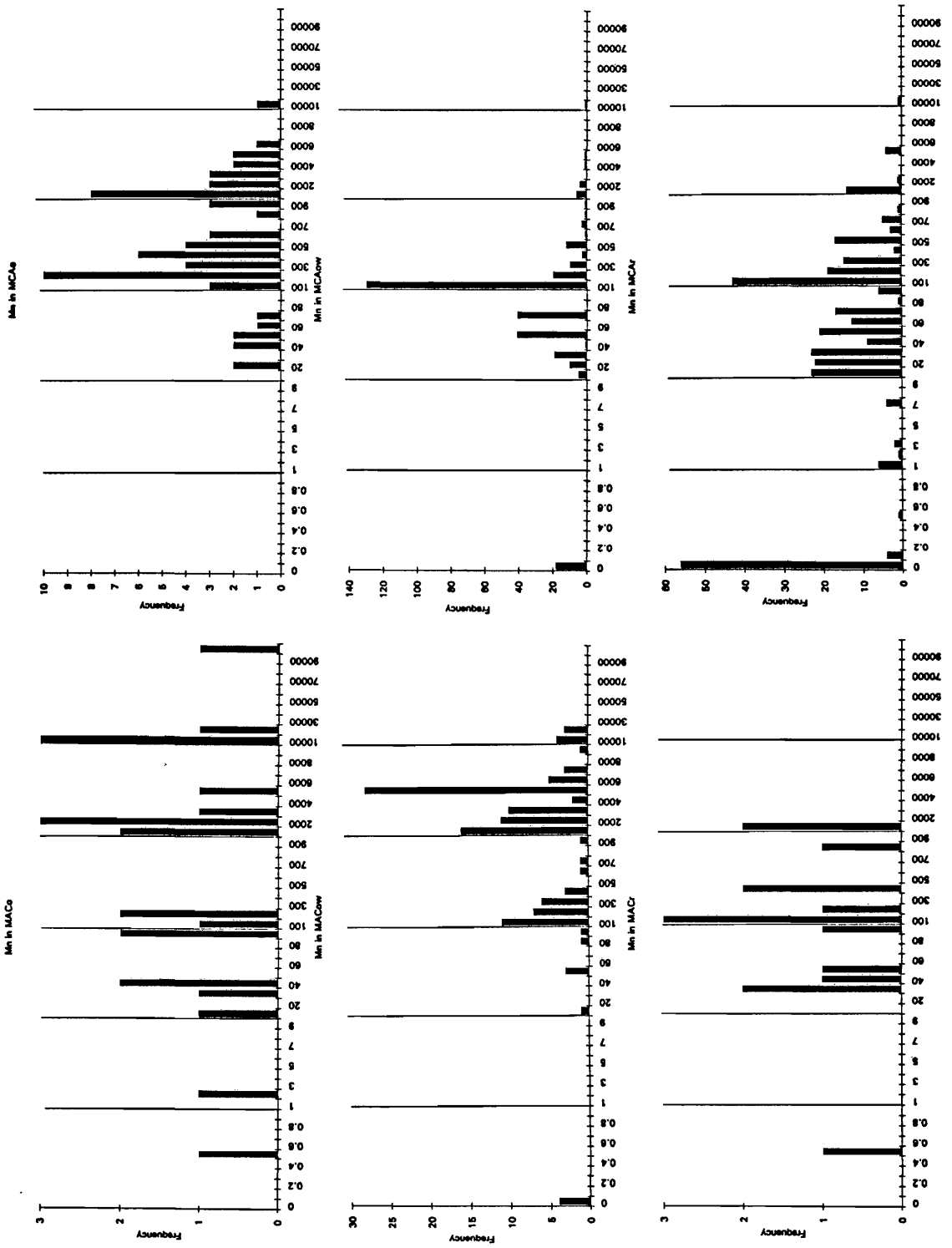

Figure 6-17. Stepped histograms of manganese in ppm (MAC=alkali-calcic, MCA=calc-alkalic; o=oxidized, ow=weakly oxidized, r=reduced).

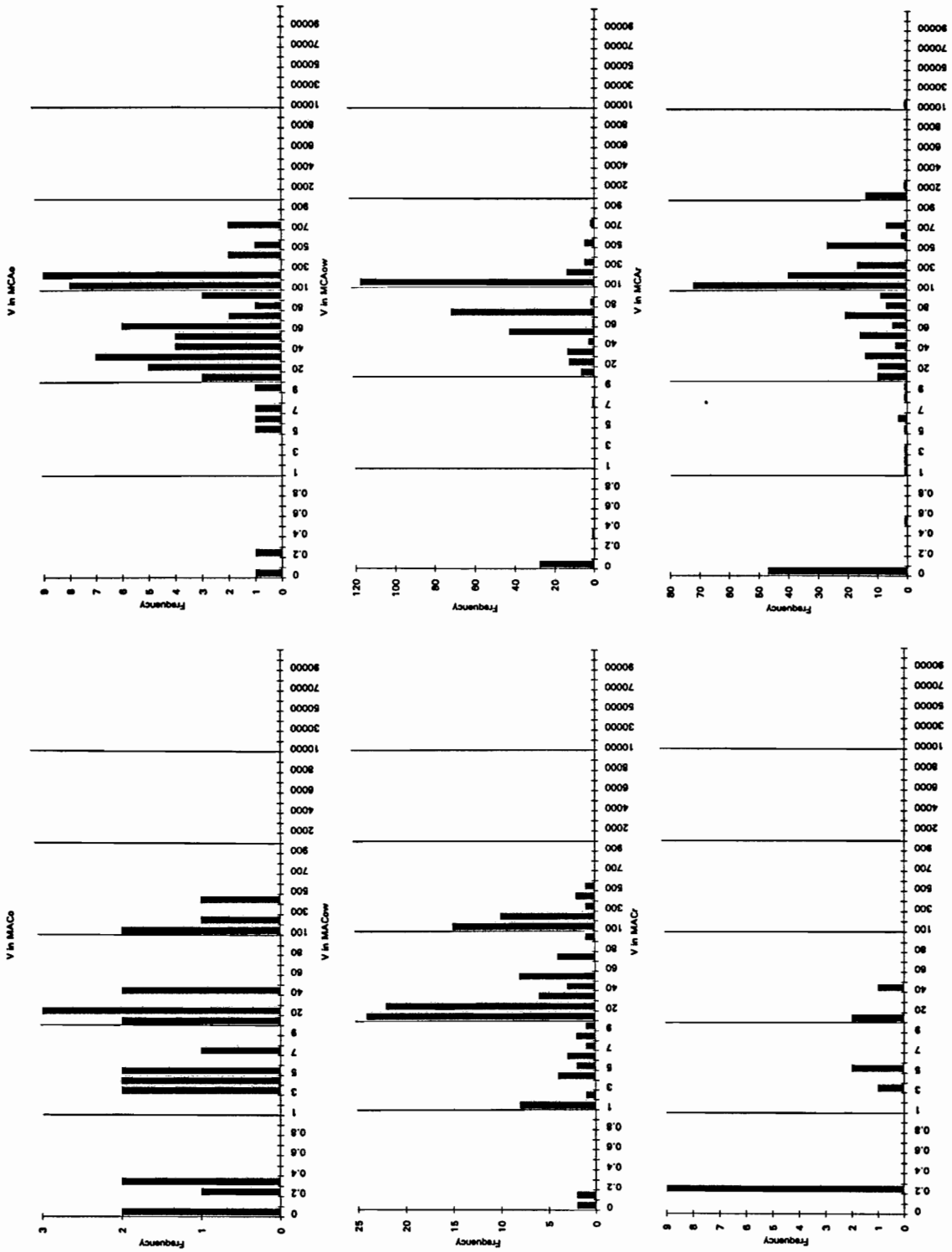

Figure 6-18. Stepped histograms of vanadium in ppm (MAC=alkali-calcic, MCA=calc-alkalic; o=oxidized, ow=weakly oxidized, r=reduced).

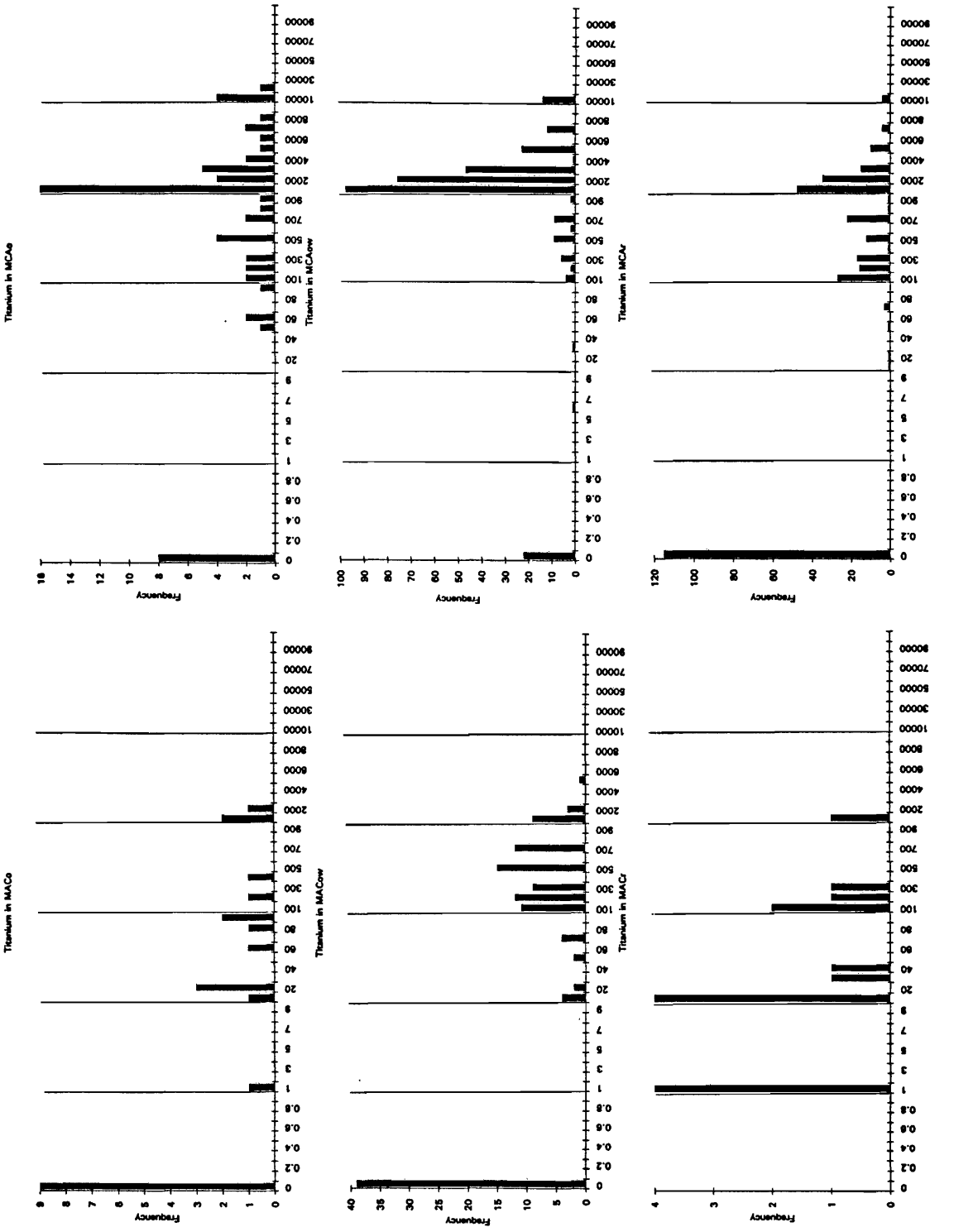

Figure 6-19. Stepped histograms of titanium in ppm (MAC=alkali-calcic, MCA=calc-alkalic; o=oxidized, ow=weakly oxidized, r=reduced).

Fifth Period Transition Metals

Metals from the fifth line on the periodic table of elements include niobium, tin, cadmium, yttrium, and zirconium. Cadmium did not show obvious differences among the magma series classes in this study (Appendix H).

Niobium values cluster near 20 ppm for samples in the calc-alkalic oxidized and weakly oxidized classes, but are lower for the alkali-calcic oxidized and reduced classes, in which niobium values cluster near 4 ppm (Figure 6-20). Niobium was not analyzed in most of the reduced and weakly oxidized samples of both alkalinity types. Detection limits were 1, 2, 5, or 20 ppm.

Tin concentrations are two or three orders of magnitude higher in the alkali-calcic reduced class than the other classes (Figure 6-21). Tin values are generally one order of magnitude higher in alkali-calcic classes than in calc-alkalic classes. Most samples in calc-alkalic classes cluster near 10 ppm tin, whereas most samples in alkali-calcic classes are higher than 20 ppm. Tin concentrations in the alkali-calcic weakly oxidized class cluster near 100 ppm and tin values in the alkali-calcic reduced class cluster near 1000 ppm, with values ranging to 30,000 ppm. Detection limits were 0.5, 1, 5, or 10 ppm tin.

Yttrium concentrations are generally higher for calc-alkalic classes than for alkali-calcic ones, although yttrium values for weakly oxidized classes of both alkalinities are similar (Figure 6-22). Yttrium quantities cluster near 20 ppm in calc-alkalic samples and in alkali-calcic weakly oxidized ones, while ranging from 1 to 80 ppm; yttrium values are usually between 1 to 20 ppm for alkali-calcic

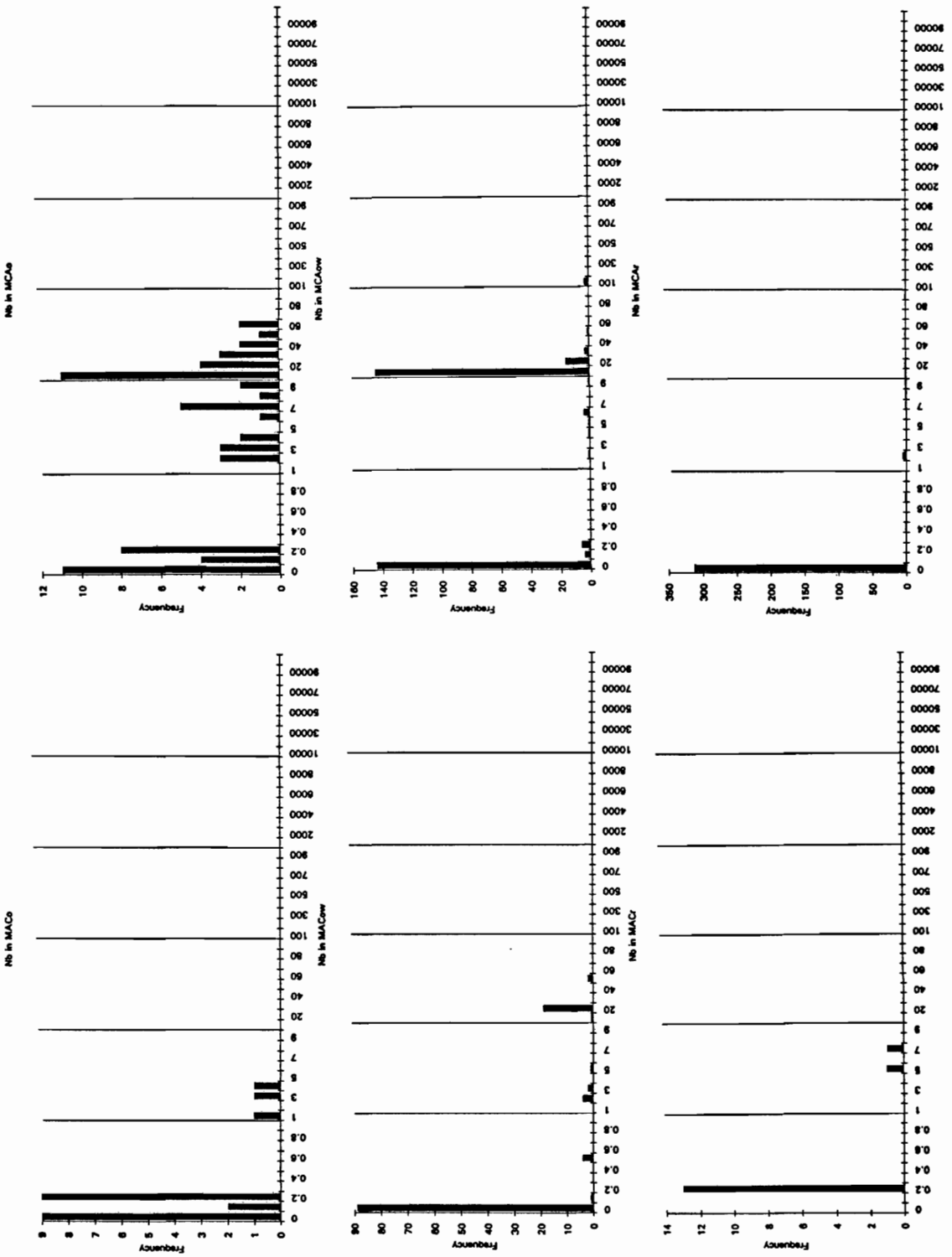

Figure 6-20. Stepped histograms of niobium in ppm (MAC=alkali-calcic, MCA=calc-alkalic; o=oxidized, ow=weakly oxidized, r=reduced).

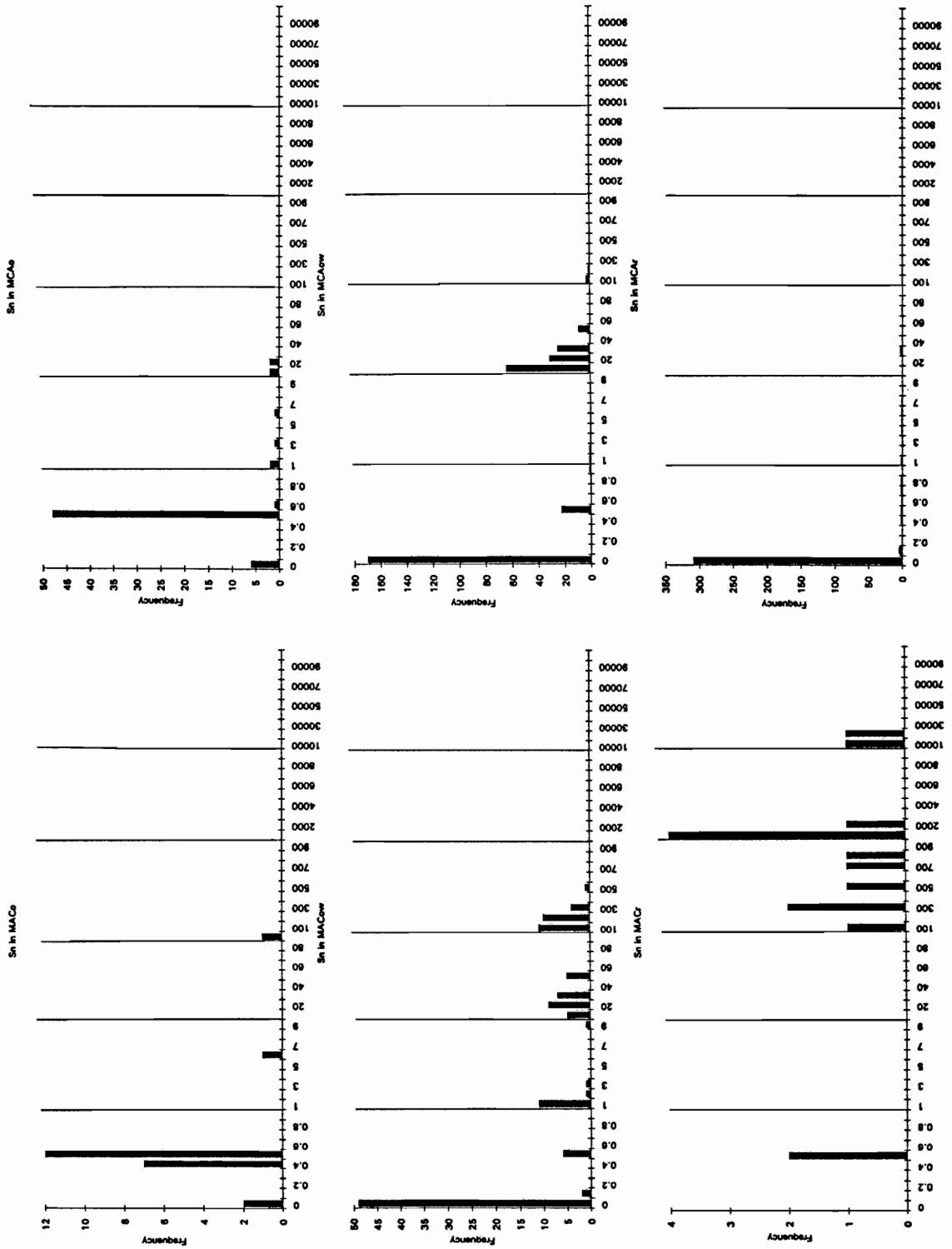

Figure 6-21. Stepped histograms of tin in ppm (MAC=alkali-calcic, MCA=calc-alkalic; o=oxidized, ow=weakly oxidized, r=reduced).

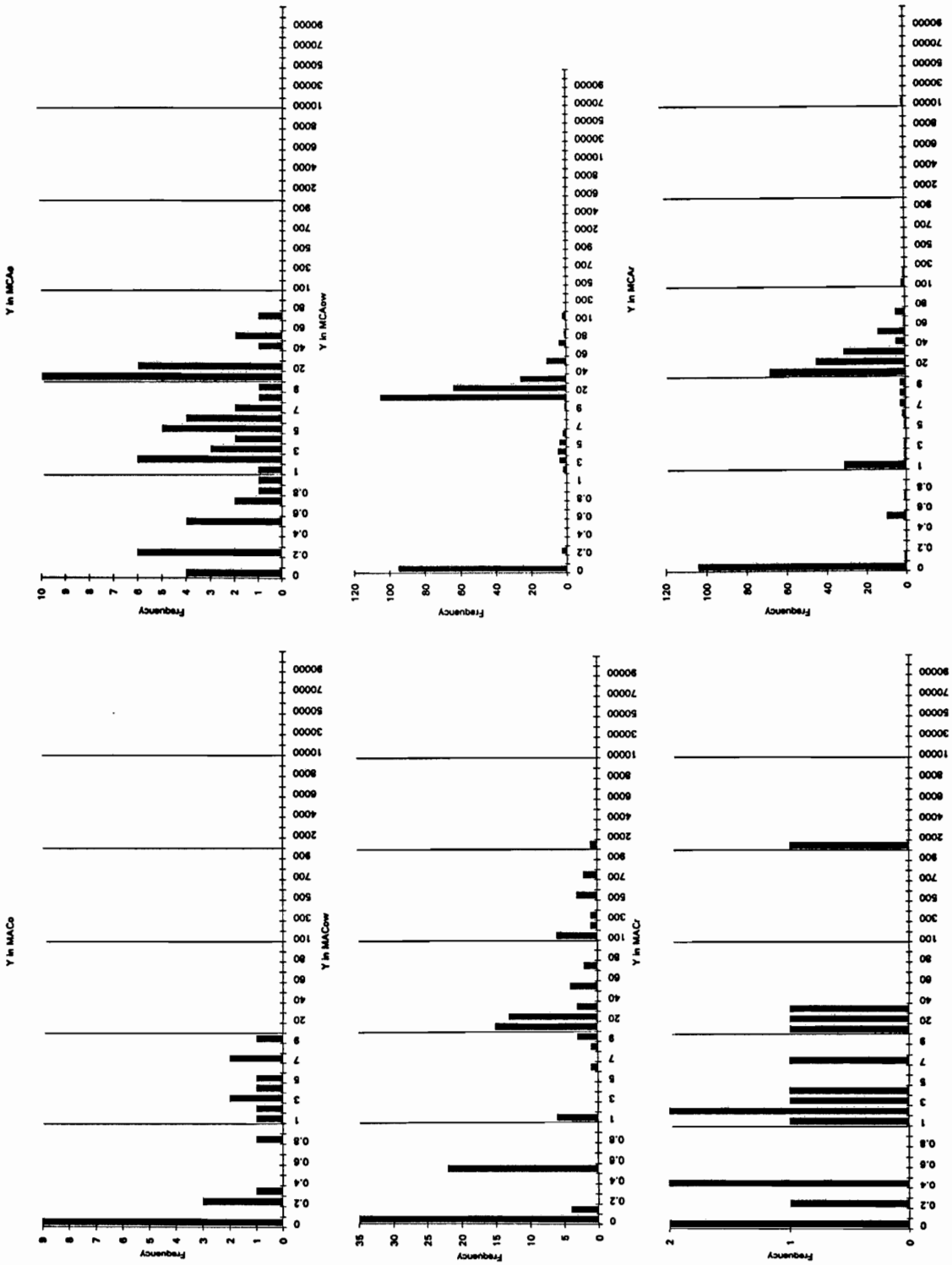

Figure 6-22. Stepped histograms of yttrium in ppm (MAC=alkali-calcic, MCA=calc-alkalic; o=oxidized, ow=weakly oxidized, r=reduced).

samples. Detection limits for yttrium were 1, 2, 5, or 10 ppm.

Zirconium concentrations are generally higher in calc-alkalic samples than in alkali-calcic ones (Figure 6-23). Most alkali-calcic samples do not range above 10 ppm Zr, whereas calc-alkalic oxidized samples cluster at 10 ppm and range to 100 ppm and calc-alkalic weakly oxidized and reduced samples cluster at 50 ppm Zr. Detection limits for zirconium are 2, 5, or 10 ppm.

Lithophile Elements

Lithophile elements used in this study include lead, molybdenum, lithium, boron, tungsten, barium, rubidium, strontium, fluorine, and beryllium. Lithium, boron, fluorine, and beryllium did not show obvious differences among the magma series classes in this study (Appendix H).

Lead concentrations are two to three orders of magnitude higher for alkali-calcic classes than for calc-alkalic ones (Figure 6-24). Lead values in the alkali-calcic oxidized class cluster near 60,000 ppm, which is higher than any other classes. Lead amounts in the alkali-calcic weakly oxidized class range from 10 to 10,000 ppm with most samples near 100 ppm Pb. Most lead quantities in the alkali-calcic reduced class range from 100 to 10,000 ppm, with more samples from 100 to 700 ppm. Although a few samples in the calc-alkalic weakly oxidized and reduced classes range up to 20,000 ppm, most samples in the calc-alkalic classes cluster near 20 ppm or near 100 ppm. Nearly all samples were above the detection limit of 2 or 10 ppm lead.

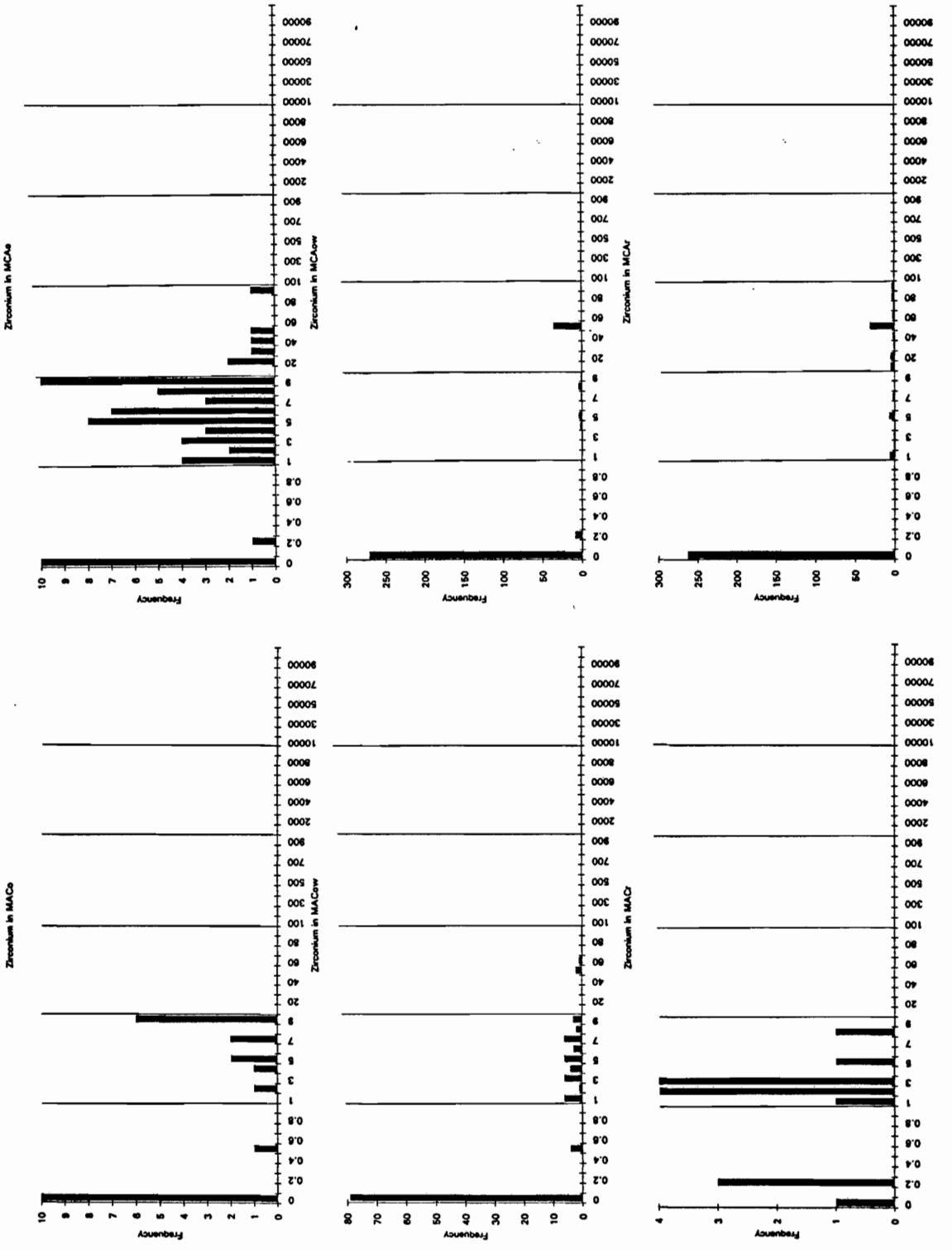

Figure 6-23. Stepped histograms of zirconium in ppm (MAC=alkali-calcic, MCA=calc-alkalic; o=oxidized, ow=weakly oxidized, r=reduced).

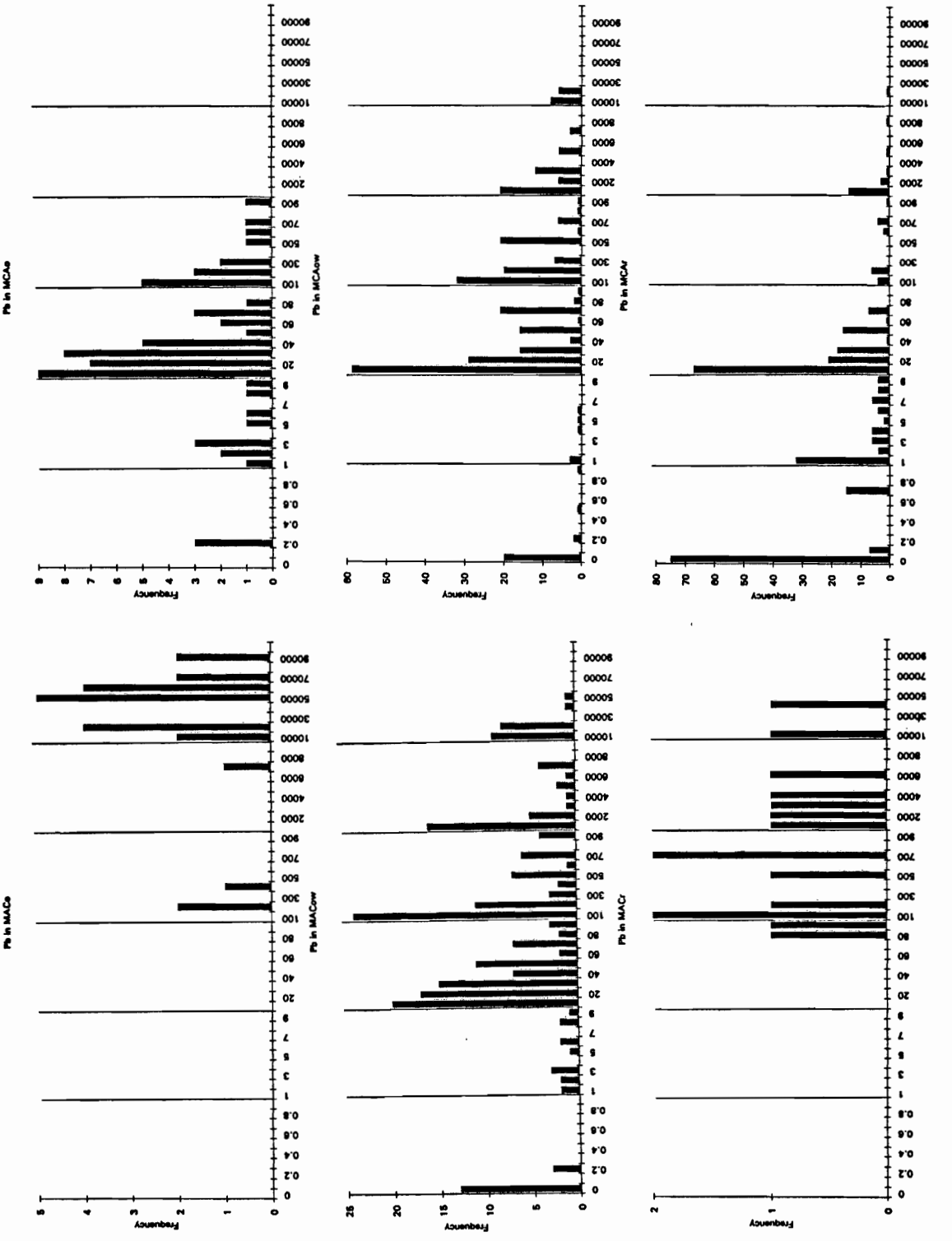

Figure 6-24. Stepped histograms of lead in ppm (MAC=alkali-calcic, MCA=calc-alkalic; o=oxidized, ow=weakly oxidized, r=reduced).

Molybdenum concentrations are one to two orders of magnitude higher for calc-alkalic samples than for alkali-calcic samples (Figure 6-25). Whereas molybdenum values center near 20 ppm in all classes, the range extends up to 4000 ppm in calc-alkalic oxidized, up to 10,000 ppm in calc-alkalic weakly oxidized, and up to 2000 ppm in calc-alkalic reduced and alkali-calcic weakly oxidized classes. Molybdenum is usually less than 200 ppm in alkali-calcic oxidized samples and less than 90 ppm in alkali-calcic reduced ones. Detection limits were 1, 2, or 5 ppm.

Tungsten concentrations are low in alkali-calcic oxidized samples, but higher in the other classes, except the calc-alkalic weakly oxidized class (Figure 6-26). Tungsten values range from 5 to 5000 ppm and cluster near 20 ppm in calc-alkalic oxidized samples, range from 1 to 100 ppm and cluster near 50 ppm in calc-alkalic weakly oxidized ones, and range from 1 to 7000 and cluster near 100 ppm in calc-alkalic reduced samples. Tungsten quantities range from 6 to 70 ppm and cluster near 20 ppm in alkali-calcic oxidized samples, range from 1 to 10,000 ppm and cluster near 100 ppm in alkali-calcic weakly oxidized samples, and range from 8 to 8000 ppm and cluster near 100 ppm in alkali-calcic reduced samples. Detection limits for tungsten were 2, 5, 10, or 20 ppm.

Barium concentrations are generally one order of magnitude higher for calc-alkalic classes than alkali-calcic ones (Figure 6-27). Most barium values range between 100 and 2000 ppm in calc-alkalic samples; they are centered at 1000 ppm in all three oxidation subclasses. Barium quantities range between 10

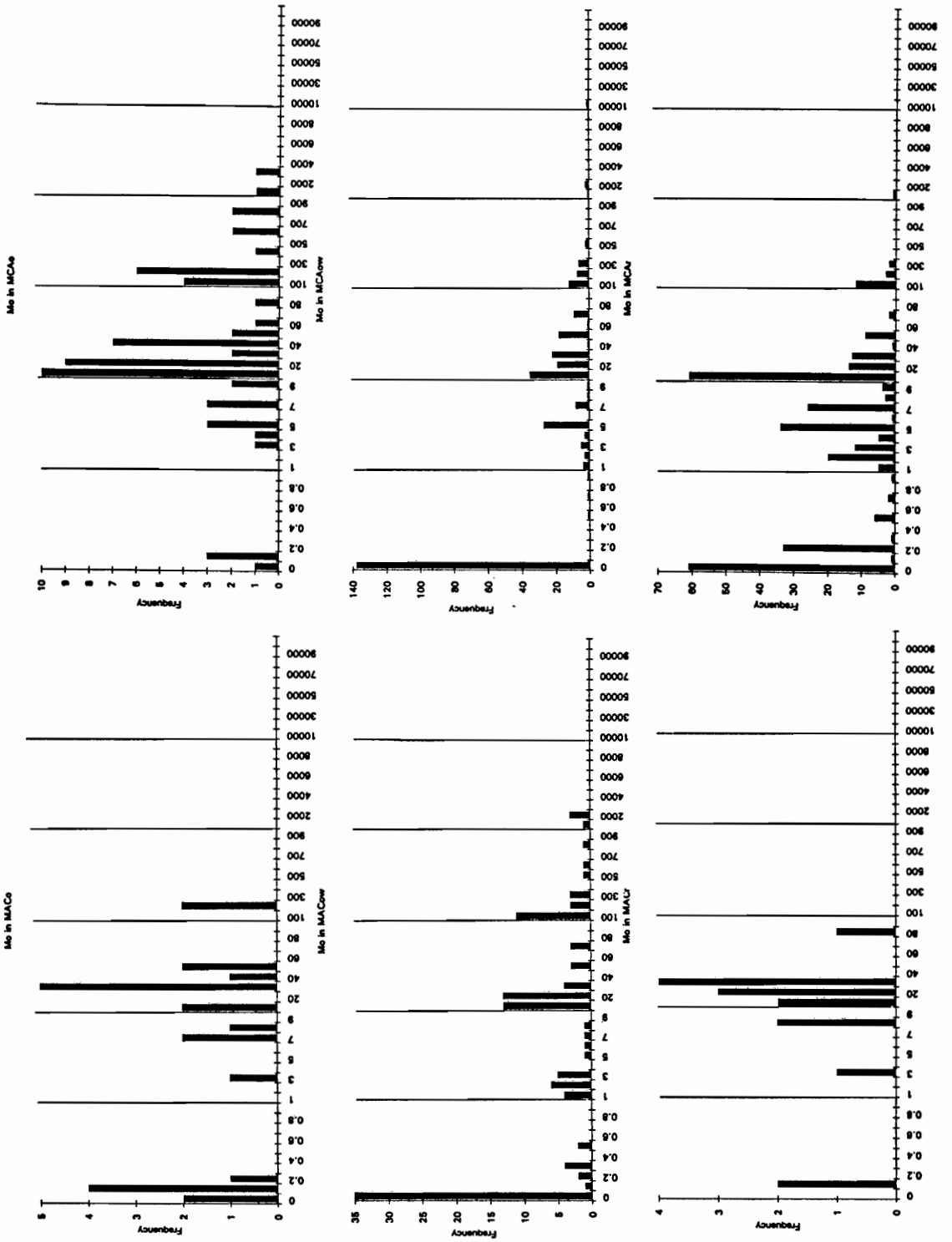

Figure 6-25. Stepped histograms of molybdenum in ppm (MAC=alkali-calcic, MCA=calc-alkalic; o=oxidized, ow=weakly oxidized, r=reduced).

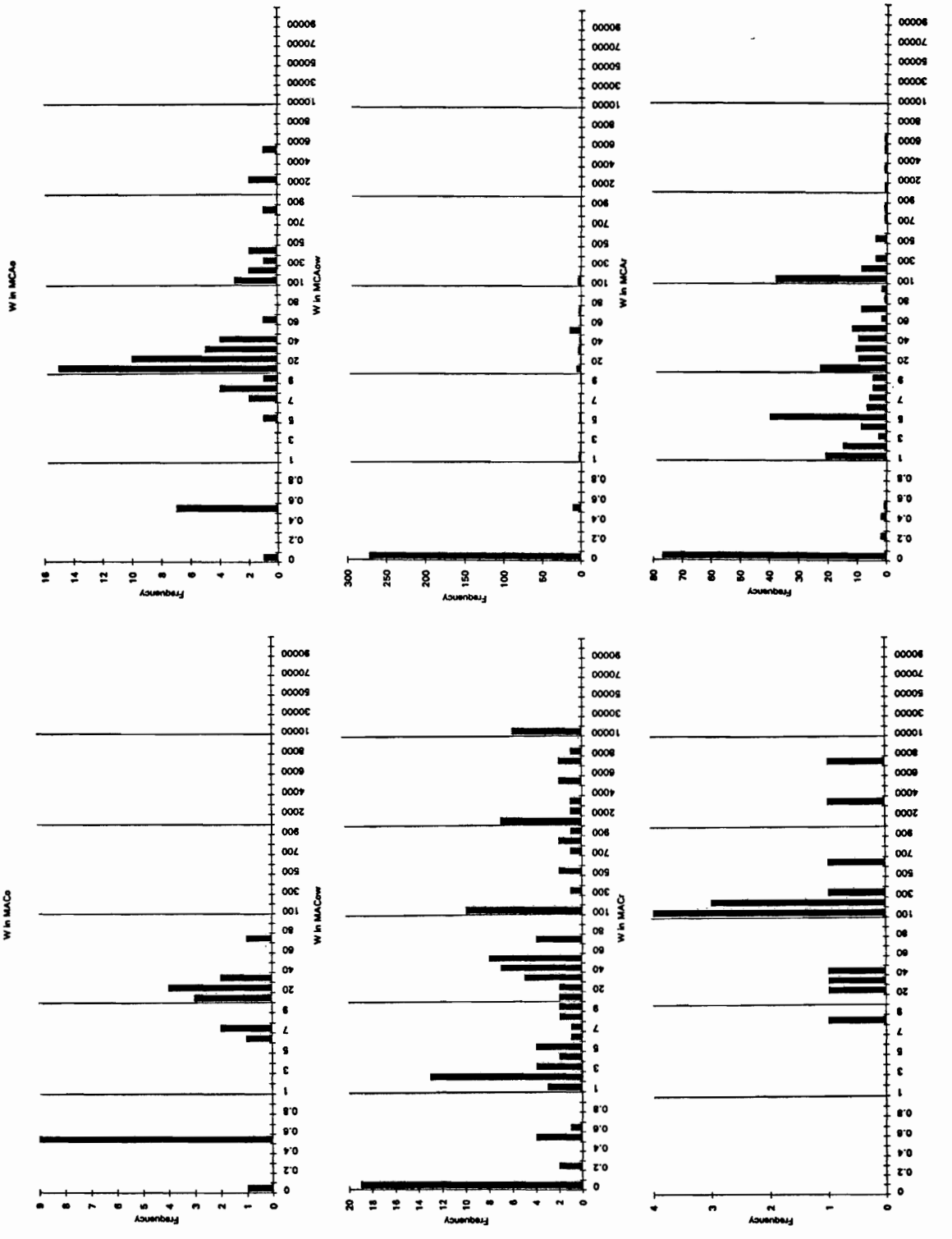

Figure 6-26. Stepped histograms of tungsten in ppm (MAC=alkali-calcic, MCA=calc-alkalic; o=oxidized, ow=weakly oxidized, r=reduced).

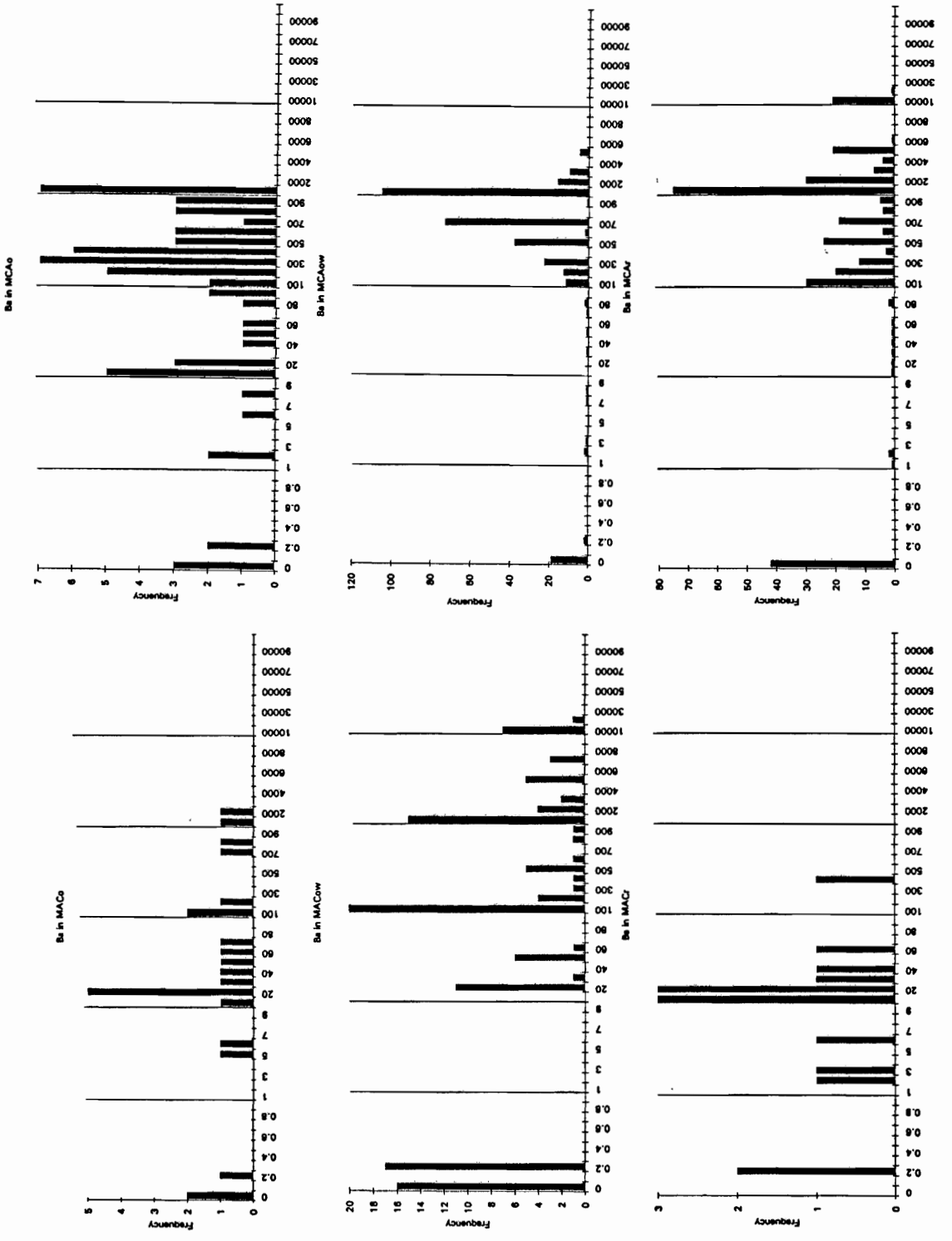

Figure 6-27. Stepped histograms of barium in ppm (MAC=alkali-calcic, MCA=calc-alkalic; o=oxidized, ow=weakly oxidized, r=reduced).

and 100 ppm in alkali-calcic oxidized and reduced samples; barium values range between 20 and 10,000 ppm in alkali-calcic weakly oxidized samples, with most samples near 100 ppm. Detection limits for barium were 2 or 20 ppm.

Rubidium concentrations are generally one order of magnitude higher for calc-alkalic oxidized samples than for alkali-calcic oxidized samples (Figure 6-28). Most samples in the calc-alkalic weakly oxidized and reduced classes were not analyzed for rubidium; the ones that were analyzed ranged between 10 and 100 ppm. Rubidium values in the alkali-calcic classes range from 5 to 50 ppm and cluster near 10 ppm in the oxidized samples, range from 7 to 1000 ppm and center near 20 ppm in the weakly oxidized ones, and range from 2 to 100 ppm in the reduced samples. Rubidium quantities in the calc-alkalic oxidized samples range from 4 to 700 ppm and cluster near 100 ppm. Detection limits for rubidium were 1, 2, or 5 ppm.

Strontium concentrations generally range between 10 and 700 ppm in each of the classes except the alkali-calcic reduced class, in which Sr ranges between 5 and 60 ppm (Figure 6-29). The strontium values usually cluster near 100 ppm in each of the six classes, although maximum values are generally higher in the calc-alkalic classes. Detection limits for strontium were 2, 5, or 100 ppm.

Conclusions from Metal Distribution

The data in this chapter on production, mineralogy, and trace element geochemistry clearly indicate that the mineralized systems in this study cluster

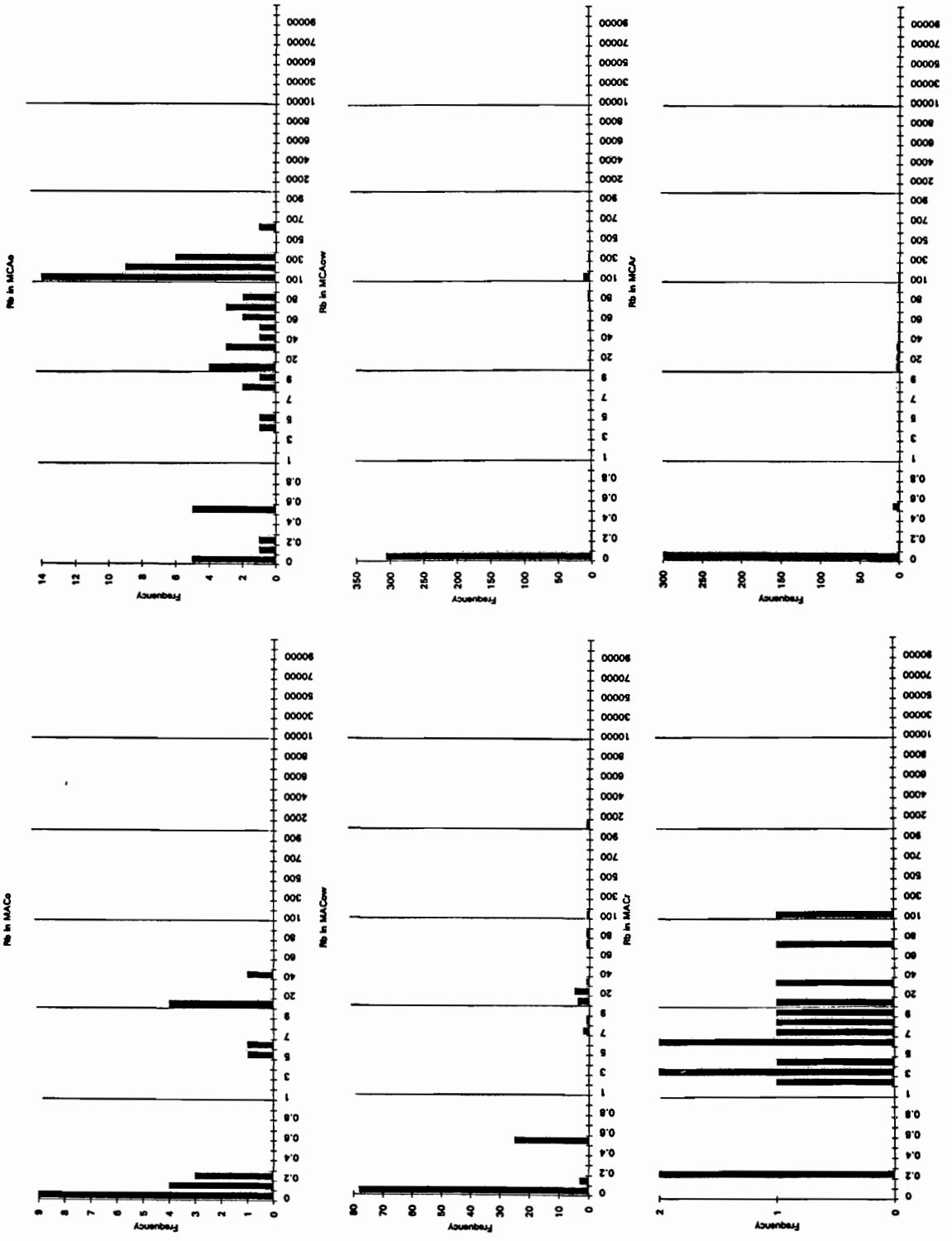

Figure 6-28. Stepped histograms of rubidium in ppm (MAC=alkali-calcic, MCA=calc-alkalic; o=oxidized, ow=weakly oxidized, r=reduced).

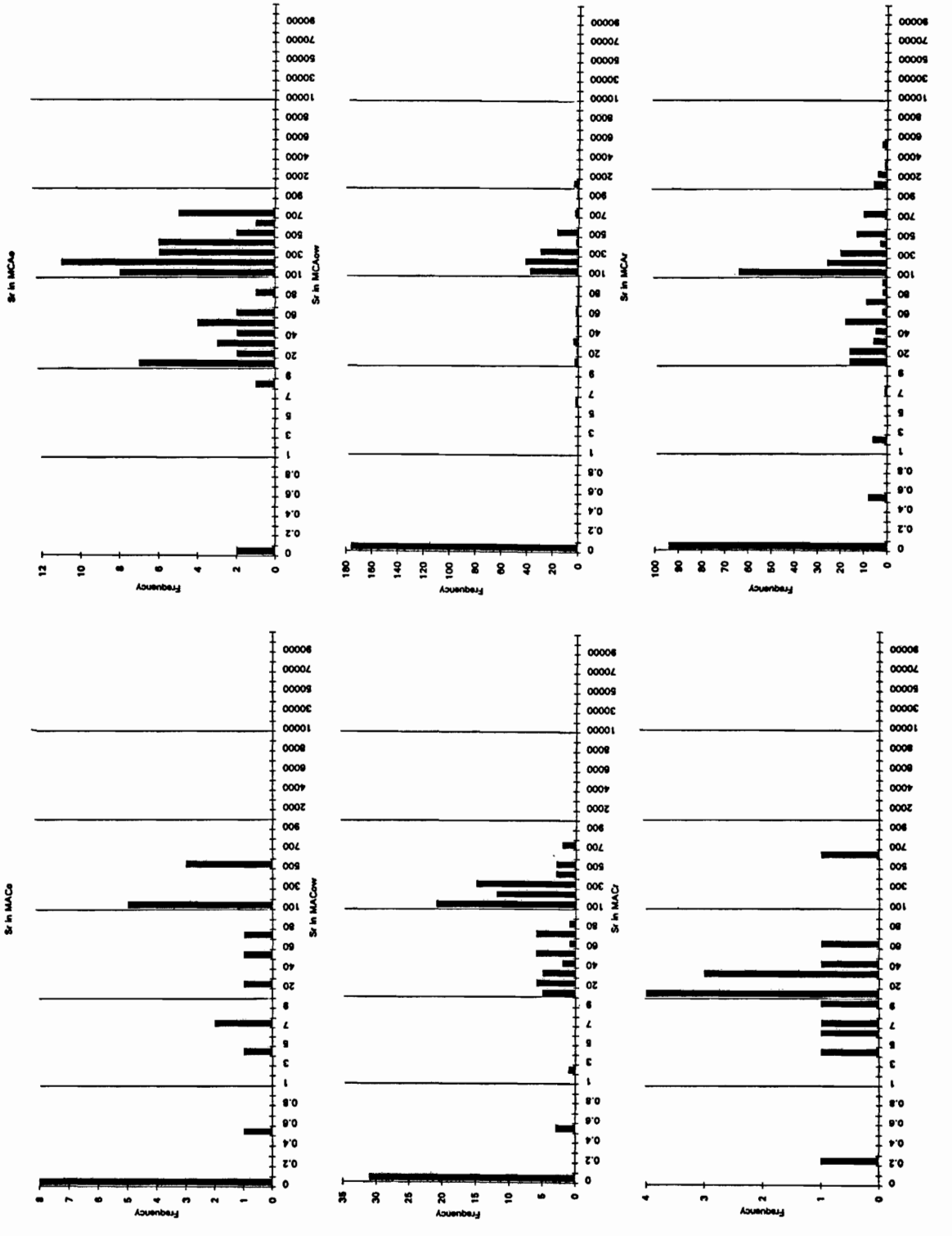

Figure 6-29. Stepped histograms of strontium in ppm (MAC=alkali-calcic, MCA=calc-alkalic; o=oxidized, ow=weakly oxidized, r=reduced).

into classes that correlate with magma series igneous classes.

In spite of meager production information in the literature, alkali-calcic classes clearly have high silver and lead production or grades, whereas calc-alkalic classes have high gold or copper production or grades. Oxidized classes have high amounts but low grades of base metal production and byproduct precious metal production, whereas reduced classes have high amounts of precious metals and little or no base metals.

Although it is not possible to quantify the mineralogy of the various magma series classes, a qualitative examination of the data shows clear differences between the classes. The rich assortment of silver and lead minerals, tin, and manganese in the alkali-calcic classes and their lack of molybdenum, thallium, and mercury minerals strongly contrasts with the abundant copper minerals, molybdenite, scheelite, and various arsenic, antimony, mercury, and thallium minerals of the calc-alkalic classes.

STATISTICS ON DATA FROM SIX MAGMA SERIES CLASSES

Statistics on the six classes of whole rock and mineralized trace element data in this study indicate that the data vary widely within each class, yet they exhibit clear differences among the classes. The means, standard deviations, and variances of the whole rock analyses (Table 7-1, 7-2, Figures 7-1, 7-2, 7-3) deviate less than those of the mineralized trace elements (Tables 7-3, 7-4, Figures 7-4, 7-5, 7-6). Because most of the whole rock oxides vary with SiO_2, their means do not signify class differences; however, ratios such as SiO_2/K_2O and Fe_2O_3/FeO clearly differentiate the six classes as discussed in the petrology chapter.

Each trace element from the mineralized rock chip samples has an extremely wide variance within each class, yet the means differ enough among the classes to allow the classes to be distinguished. (See histograms in Appendix I, Figures I-1 through I-32). For example, alkali-calcic classes have 10 to 100 times as much silver as the calc-alkalic classes (Figure I-1). Most elements do not have a normal distribution. This asymmetrical distribution is partly because the distribution is so wide that, in order to display 21 equal classes, most of the samples fell in the bin closest to zero. The large number of zeros for each element also occurs because most samples were only analyzed for half the elements.

In spite of the diversity in the data, discriminant analysis was able to properly classify the whole rock data in 88% of the cases (Table 7-5) and the

Table 7-1. Statistics on whole rock analyses of six magma series classes.

parameter	MACo	MACow	MACr	MCAo	MCAow	MCAr
AC=Alkali-calcic, CA=Calc-alkalic, o=oxidized, ow=weakly oxidized, r=reduced						
SiO2 mean	62.787	67.86	62.561	66.629	59.451	65.613
std.dev.	2.589	3.307	1.662	3.326	5.203	3.999
variance	6.703	10.937	2.761	11.065	27.076	15.991
TiO2 mean	0.665	0.443	0.7	0.439	0.587	0.572
std.dev.	0.237	0.222	0.227	0.158	0.14	0.232
variance	0.056	0.049	0.051	0.025	0.02	0.054
Al2O3 mean	15.889	15.04	17.591	15.792	17.423	15.756
std.dev.	0.694	0.656	0.946	0.859	1.543	1.564
variance	0.482	0.431	0.895	0.738	2.38	2.445
Fe2O3 mean	3.054	1.602	1.45	1.672	2.544	1.414
std.dev.	1.077	0.6	1.503	0.764	1.036	0.866
variance	1.16	0.36	2.26	0.583	1.074	0.75
FeO mean	2.153	1.561	2.867	1.66	3.383	2.418
std.dev.	0.795	0.54	1.025	0.625	1.327	0.81
variance	0.632	0.292	1.052	0.391	1.761	0.656
MgO mean	2.31	1.167	1.291	1.489	2.871	1.741
std.dev.	0.526	0.653	0.756	0.62	1.103	0.651
variance	0.276	0.426	0.571	0.384	1.217	0.424
MnO mean	0.073	0.046	0.057	0.08	0.1	0.061
std.dev.	0.036	0.036	0.014	0.044	0.059	0.025
variance	0.001	0.001	0	0.002	0.004	0.001
CaO mean	4.393	3.179	3.894	3.742	6.278	3.647
std.dev.	0.728	0.939	0.524	1.169	2.472	1.216
variance	0.53	0.882	0.275	1.367	6.111	1.48
Na2O mean	3.574	3.476	2.888	3.862	3.594	3.464
std.dev.	0.417	0.435	0.382	0.441	0.757	0.512
variance	0.174	0.189	0.146	0.194	0.573	0.263
K2O mean	3.469	3.869	4.885	2.845	2.075	3.074
std.dev.	0.358	0.426	0.372	0.753	0.86	0.713
variance	0.128	0.182	0.138	0.567	0.739	0.508
P2O5 mean	0.265	0.175	0.329	0.136	0.097	0.19
std.dev.	0.156	0.093	0.087	0.091	0.152	0.127
variance	0.024	0.009	0.008	0.008	0.023	0.016
LOI mean	0.793	0.747	1.467	0.943	0.449	0.081
std.dev.	0.524	0.475	0.4	0.558	0.913	0.268
variance	0.275	0.226	0.16	0.311	0.834	0.072
SiO2/K2O mean	18.287	17.686	12.948	25.584	33.776	22.181
std.dev.	1.971	1.568	0.855	8.5	14.271	4.225
variance	3.887	2.459	0.731	72.244	203.672	17.855
Fe2O3/FeO mean	2.415	1.173	1.031	1.143	0.848	0.624
std.dev.	4.458	0.63	2.124	1.009	0.605	0.384
variance	19.873	0.397	4.511	1.018	0.366	0.147
magnetite mean	2.075	0.172	0	1.627	1.511	0.5
std.dev.	0.413	0.06	0	0.709	0.08	0
variance	0.171	0.004	0	0.502	0.006	0
ilmenite mean	0	0	0.05	0	0	0.05
std.dev.	0	0	0	0	0	0
variance	0	0	0	0	0	0

Table 7-2. Statistics on whole rock ratios of six magma series classes.

parameter	MACo	MACow	MACr	MCAo	MCAow	MCAr
Total mean	99.529	99.548	99.982	98.438	99.243	99.05
std.dev.	1.125	1.15	0.219	8.913	1.179	1.283
variance	1.265	1.323	0.048	79.436	1.39	1.646
A/CNK mean	0.903	0.984	1.03	0.977	0.901	1.008
std.dev.	0.048	0.059	0.063	0.062	0.082	0.054
variance	0.002	0.003	0.004	0.004	0.007	0.003
A/NK mean	1.658	1.565	1.766	1.693	2.278	1.777
std.dev.	0.15	0.165	0.157	0.243	0.685	0.356
variance	0.022	0.027	0.025	0.059	0.469	0.126
Na2O+K2O mean	7.043	7.344	7.742	6.707	5.669	6.537
std.dev.	0.545	0.623	0.627	0.717	1.355	0.76
variance	0.297	0.388	0.393	0.515	1.837	0.578
Na2O/K2O mean	1.041	0.911	0.595	1.502	2.012	1.195
std.dev.	0.161	0.165	0.074	0.617	0.83	0.388
variance	0.026	0.027	0.005	0.381	0.689	0.151
Na2O+K2O-CaO mea	2.651	4.166	3.848	2.966	-0.61	2.89
std.dev.	1.088	1.435	1.007	1.78	3.73	1.913
variance	1.184	2.06	1.013	3.168	13.913	3.661
K2O-CaO mean	-0.923	0.69	0.961	-0.897	-4.204	-0.574
std.dev.	0.945	0.328	0.812	1.736	3.245	1.86
variance	0.893	1.723	0.659	3.015	10.531	3.46
K2O-MgO mean	1.159	2.702	3.564	1.357	-0.796	1.333
std.dev.	0.664	0.997	1.021	1.15	1.844	1.288
variance	0.441	0.993	1.043	1.322	3.399	1.66
FeO*/MgO mean	2.153	3.092	3.854	2.278	2.016	2.322
std.dev.	0.338	1.186	1.534	0.71	0.651	0.829
variance	0.115	1.406	2.354	0.504	0.423	0.688
Larsen factor mean	17.701	22.144	20.524	19.824	12.743	19.556
std.dev.	1.964	2.938	1.879	3.214	5.896	3.694
variance	3.856	8.631	3.529	10.328	34.76	13.644
Alkali index mean	-0.319	-1.9	0.47	-2.078	-0.447	-1.87
std.dev.	1.184	1.108	0.674	0.995	1.156	0.799
variance	1.401	1.227	0.454	0.989	1.335	0.639
Alteration index mean	42.059	43.23	47.515	36.375	33.889	40.762
std.dev.	3.174	2.953	3.205	5.943	6.031	5.912
variance	10.074	8.723	10.271	35.321	36.375	34.953
K index mean	1.176	1.468	1.148	1.286	0.843	1.254
std.dev.	0.295	0.384	0.181	0.341	0.338	0.463
variance	0.087	0.147	0.033	0.116	0.114	0.215
Na index mean	1.943	1.895	1.626	2.48	2.913	2.2
std.dev.	0.157	0.136	0.083	0.615	0.802	0.37
variance	0.025	0.019	0.007	0.378	0.643	0.137
Al2O3/Na2O mean	4.5	4.49	6.18	4.14	5.076	4.656
std.dev.	0.516	0.566	0.78	0.524	1.23	0.967
variance	0.266	0.32	0.609	0.275	1.513	0.936
SiO2/Al2O3 mean	3.963	4.418	3.566	4.239	3.464	4.225
std.dev.	0.291	0.363	0.207	0.394	0.6	0.698
variance	0.084	0.132	0.043	0.156	0.36	0.488

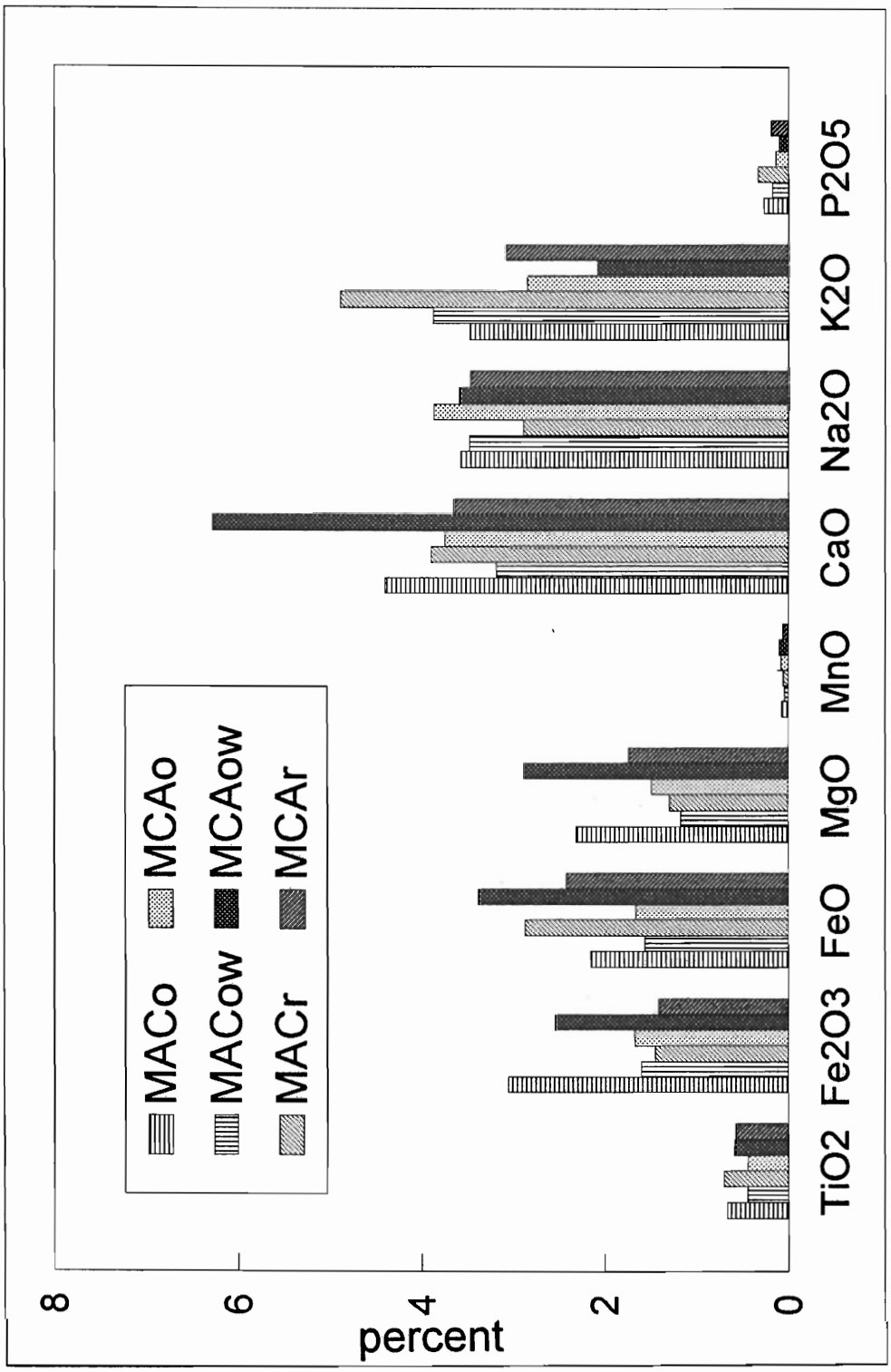

Figure 7-1. Comparison of means of whole rock oxides of less than 7 percent, showing contrasts among magma series classes (MAC=alkali-calcic, MCA=calc-alkalic, o=oxidized, ow=weakly oxidized, r=reduced).

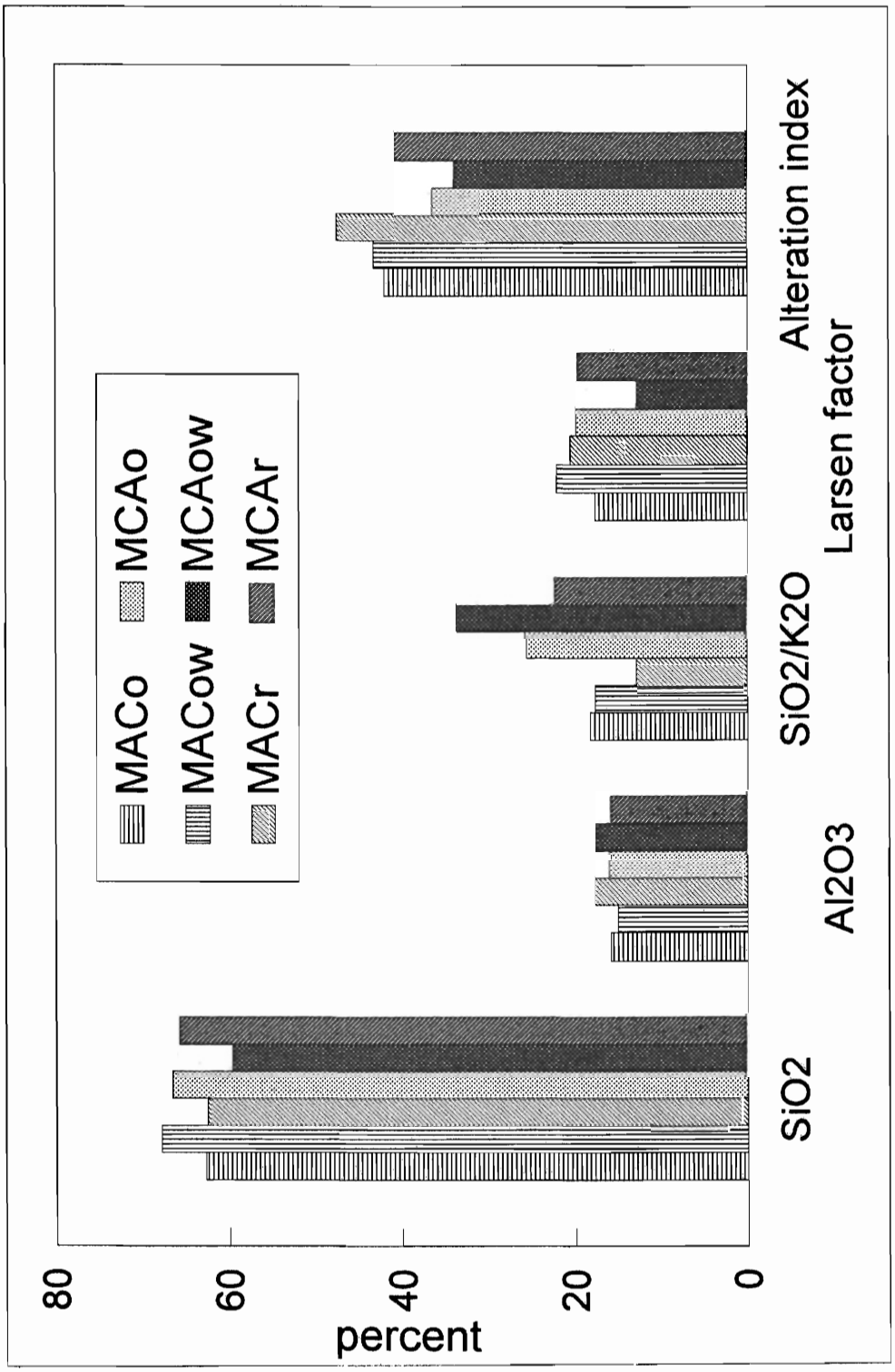

Figure 7-2. Comparison of means of whole rock oxides and indices from 15 to 70 percent showing contrasts among petrochemical classes (MAC=alkali-calcic, MCA=calc-alkalic, o=oxidized, ow=weakly oxidized, r=reduced).

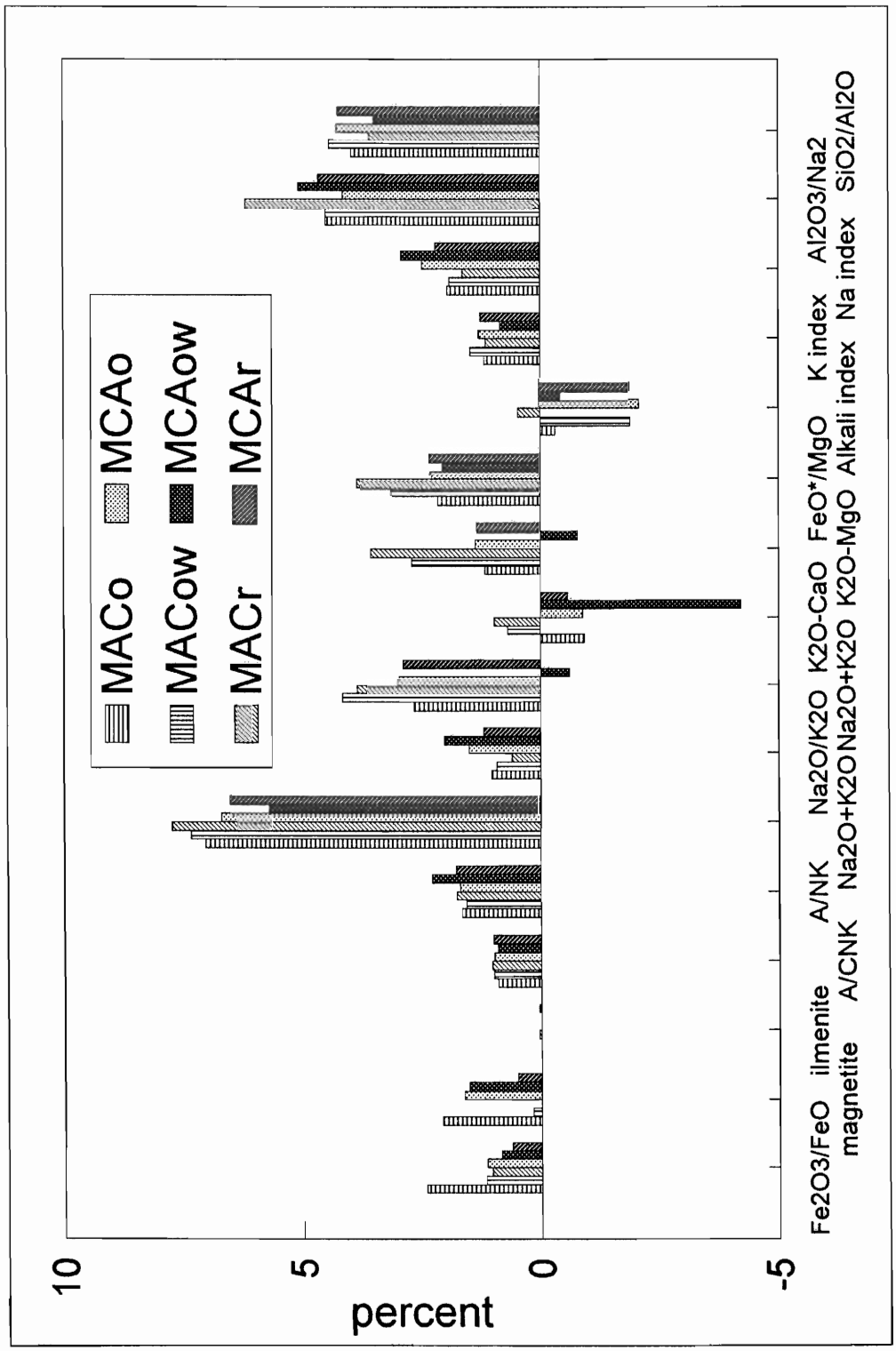

Figure 7-3. Comparison of means of whole rock indices and ratios below 10 percent showing contrasts among petrochemical classes (MAC=alkali-calcic, MCA=calc-alkalic, o=oxidized, ow=weakly oxidized, r=reduced).

Table 7-3. Statistics on trace elements of mineralized samples from Ag to Mn.

parameter	MACo	MACow	MACr	MCAo	MCAow	MCAr
Mo mean	35.626	109.880	22.413	175.420	88.609	18.192
std.dev.	59.872	353.672	21.127	460.442	843.318	64.707
variance	3,584.656	125,084.228	446.333	212,006.525	711,185.976	4,187.009
Nb mean	0.435	4.261	0.973	11.127	7.175	0.876
std.dev.	1.001	9.501	2.076	15.540	11.469	6.554
variance	1.001	90.261	4.308	241.506	131.530	42.956
Ni mean	13.013	28.272	219.160	19.311	18.307	38.149
std.dev.	11.250	62.324	590.562	18.795	36.181	73.957
variance	126.558	3,884.252	348,763.464	353.262	1,309.049	5,469.593
Pb mean	44,895.522	3,222.260	5,272.600	99.180	1,167.657	236.758
std.dev.	30,008.006	7,348.751	11,595.812	180.695	3,509.293	1,514.836
variance	900,480,431.000	54,004,142.800	134,462,858.000	32,650.712	12,315,138.700	2,294,729.320
Rb mean	4.562	14.462	23.960	123.378	7.299	3.478
std.dev.	9.654	113.556	50.646	125.147	32.605	15.231
variance	93.199	12,894.964	2,564.990	15,661.686	1,063.069	231.983
Sb mean	2,038.822	494.237	2,582.300	6.183	85.301	175.219
std.dev.	3,476.546	1,709.042	5,279.100	11.391	946.486	521.941
variance	12,086,369.500	2,920,825.520	27,868,898.300	129.751	895,836.257	272,422.876
Sn mean	4.840	48.257	3,839.667	1.688	9.303	1.028
std.dev.	19.906	88.345	8,121.483	4.282	18.101	9.488
variance	396.260	7,804.828	65,958,487.500	18.339	327.636	90.019
Sr mean	110.022	126.492	63.613	233.190	122.046	199.764
std.dev.	187.905	155.142	167.269	222.349	198.288	507.139
variance	35,308.193	24,068.918	27,978.871	49,439.028	39,318.068	257,190.288
Te mean	0.145	0.885	0.000	0.005	0.291	0.629
std.dev.	0.224	5.363	0.000	0.015	3.118	3.739
variance	0.050	28.762	0.000	0.000	9.722	13.981
Ti mean	263.217	359.024	150.267	2,724.778	2,424.544	990.997
std.dev.	570.813	607.172	311.662	4,314.021	2,360.861	1,643.584
variance	325,827.269	368,658.057	97,132.924	18,610,776.900	5,573,662.570	2,701,369.360
Tl mean	5.945	0.140	51.947	0.568	12.565	7.327
std.dev.	10.072	0.346	99.849	1.318	225.762	26.045
variance	101.449	0.119	9,969.871	1.738	50,968.372	678.354
V mean	55.078	62.546	5.787	125.289	93.186	227.203
std.dev.	108.233	93.915	11.866	155.995	90.099	607.907
variance	11,714.413	8,820.012	140.791	24,334.432	8,117.896	369,551.262
W mean	13.283	917.325	843.600	213.230	6.160	90.172
std.dev.	18.220	2,459.529	1,910.950	743.927	21.073	469.342
variance	331.973	6,049,283.750	3,651,728.540	553,426.684	444.077	220,281.968
Y mean	2.026	53.670	76.943	10.012	13.866	59.148
std.dev.	3.012	178.437	272.143	14.316	15.288	823.139
variance	9.072	31,839.877	74,061.906	204.961	233.708	677,558.340
Zn mean	26,587.522	9,503.780	15,593.200	1,031.411	611.853	301.893
std.dev.	46,323.718	27,197.274	30,356.649	5,487.133	2,492.033	962.903
variance	2,145,886,814.000	739,691,706.000	921,526,123.000	30,108,630.400	6,210,227.280	927,182.306
Zr mean	3.674	2.740	2.307	8.368	5.711	7.892
std.dev.	3.953	8.459	2.110	13.987	15.597	19.380
variance	15.627	71.547	4.451	195.634	243.263	375.579

MACo = Alkali-calcic oxidized
MACow = Alkali-calcic weakly oxidized
MACr = Alkali-calcic reduced
MCAo = Calc-alkalic oxidized
MCAow = Calc-alkalic weakly oxidized
MCAr = Calc-alkalic reduced

Table 7-4. Statistics on trace elements of mineralized samples from Mo to Zr.

parameter	MACo	MACow	MACr	MCAo	MCAow	MCAr
Ag mean	591.479	280.490	233.961	10.910	16.068	2.522
std.dev.	554.119	851.678	398.794	27.468	32.946	9.098
variance	307,048.330	725,354.620	159,036.557	754.467	1,085.433	82.774
As mean	2,652.652	471.860	14,343.867	28.015	1,138.200	1,769.329
std.dev.	5,254.574	1,249.157	46,931.430	90.528	3,064.951	9,916.123
variance	27,610,547.100	1,560,393.990	2,202,559,089.000	8,195.356	9,393,923.660	98,329,504.000
Au mean	1.033	0.067	0.823	2.722	2.670	2.638
std.dev.	2.594	0.309	1.683	6.564	24.026	10.298
variance	6.727	0.095	2.832	43.086	577.251	106.041
Ba mean	271.487	1,524.857	47.360	416.276	899.564	1,801.987
std.dev.	595.325	3,382.889	108.797	435.387	814.580	2,787.696
variance	354,412.054	11,443,935.200	11,836.681	189,561.766	663,540.840	7,771,250.430
Be mean	1.372	8.015	1.685	1.665	0.754	1.959
std.dev.	2.198	13.367	3.261	1.345	1.411	13.790
variance	4.829	178.687	10.637	1.808	1.991	190.164
Bi mean	32.401	228.164	12,302.667	16.523	21.227	1.844
std.dev.	110.700	1,464.643	25,519.267	41.788	64.685	16.946
variance	12,254.470	2,145,179.850	651,233,007.000	1,746.231	4,184.086	287.172
B mean	22.848	80.062	0.000	27.346	110.318	75.202
std.dev.	38.320	331.262	0.000	52.704	869.776	186.860
variance	1,468.396	109,734.612	0.000	2,777.700	756,509.839	34,916.554
Cd mean	250.443	61.529	345.360	7.353	9.914	2.482
std.dev.	436.750	163.235	740.077	19.384	48.753	17.341
variance	190,750.504	26,645.512	547,714.076	375.748	2,376.863	300.706
Co mean	4.226	15.618	312.720	28.106	6.509	7.583
std.dev.	6.228	29.377	1,144.747	36.621	13.870	16.437
variance	38.792	862.995	1,310,446.080	1,341.120	192.380	270.172
Cr mean	138.174	30.463	127.400	114.492	91.468	83.331
std.dev.	175.289	46.607	57.913	73.097	82.131	117.463
variance	30,726.150	2,172.247	3,353.971	5,343.157	6,745.451	13,797.593
Cu mean	4,339.857	4,687.069	3,283.800	9,899.468	2,478.294	76.954
std.dev.	7,520.905	10,330.649	5,811.155	24,491.807	4,595.366	174.827
variance	56,564,016.300	106,722,310.000	33,769,527.200	599,848,630.000	21,117,389.400	30,564.632
Fe mean	37,630.435	41,624.390	143,353.333	79,280.952	63,952.280	18,559.757
std.dev.	63,045.340	72,636.330	137,292.778	86,192.691	68,224.060	33,538.061
variance	3,974,714,941.000	5,276,036,449.000	18,850,000,000.000	7,429,179,954.000	4,654,522,380.000	1,124,801,553.000
F mean	203.478	681.870	0.000	1,124.127	18.255	327.618
std.dev.	254.426	2,752.394	0.000	5,434.524	102.458	684.654
variance	64,732.806	7,575,673.930	0.000	29,534,053.700	10,497.733	468,751.442
Hg mean	0.029	1.363	0.000	0.549	0.284	41.007
std.dev.	0.045	4.315	0.000	1.496	0.977	319.982
variance	0.002	18.616	0.000	2.238	0.955	102,388.345
Li mean	7.174	7.439	0.000	4.032	1.137	2.021
std.dev.	17.567	13.252	0.000	9.395	7.232	6.716
variance	308.605	175.609	0.000	88.257	52.307	45.111
Mn mean	10,473.978	3,290.000	348.500	1,260.460	228.164	257.165
std.dev.	32,698.004	3,927.396	434.503	1,864.181	710.713	817.710
variance	1,069,159,450.000	15,424,440.300	188,793.250	3,475,171.190	505,112.717	668,650.151

MACo = Alkali-calcic oxidized
MACow = Alkali-calcic weakly oxidized
MACr = Alkali-calcic reduced
MCAo = Calc-alkalic oxidized
MCAow = Calc-alkalic weakly oxidized
MCAr = Calc-alkalic reduced

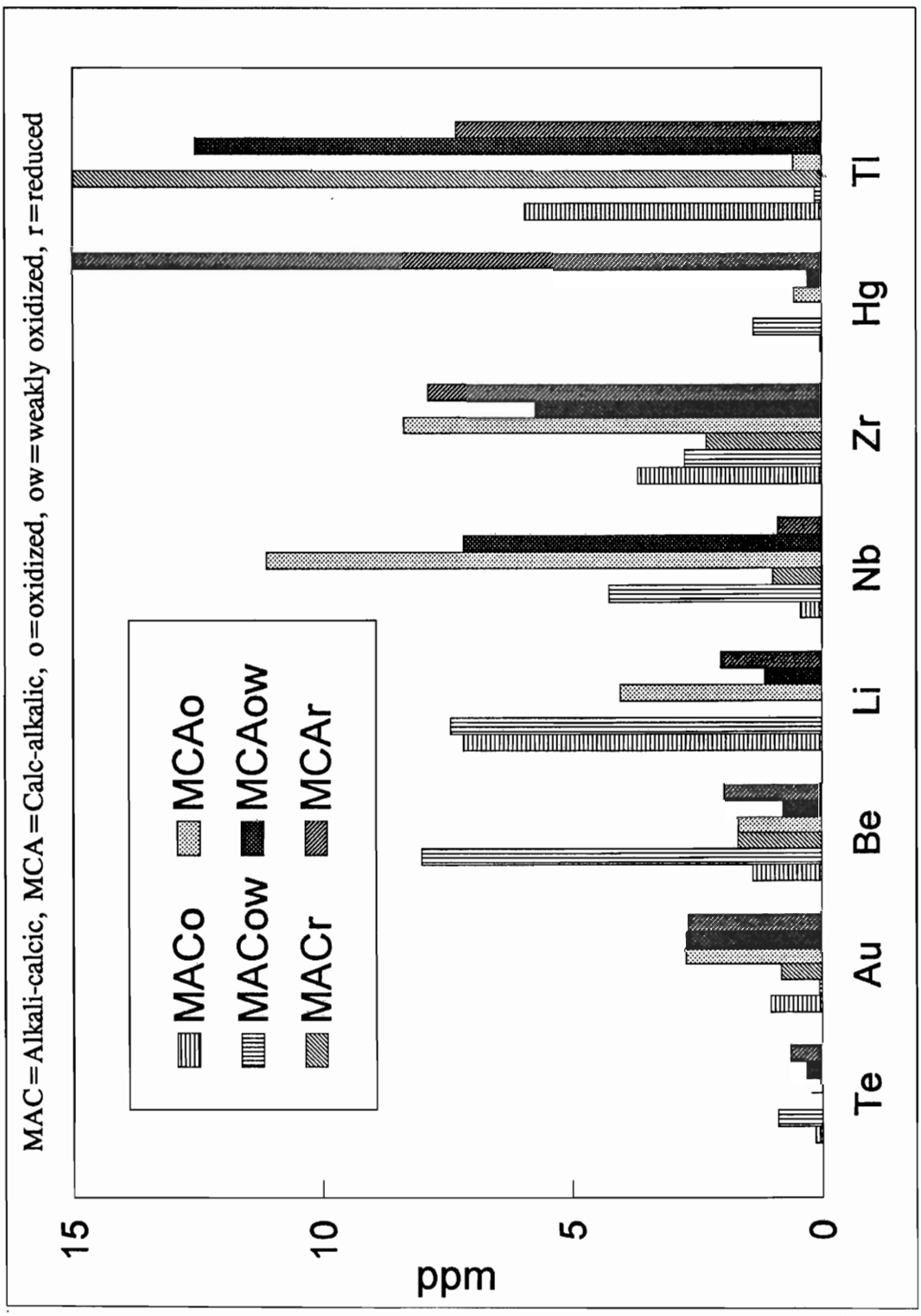

Figure 7-4. Comparison of means of trace elements from mineralized samples (0 to 15 ppm) showing contrasts among magma series classes (MAC=alkali-calcic, MCA=calc-alkalic, o=oxidized, ow=weakly oxidized, r=reduced).

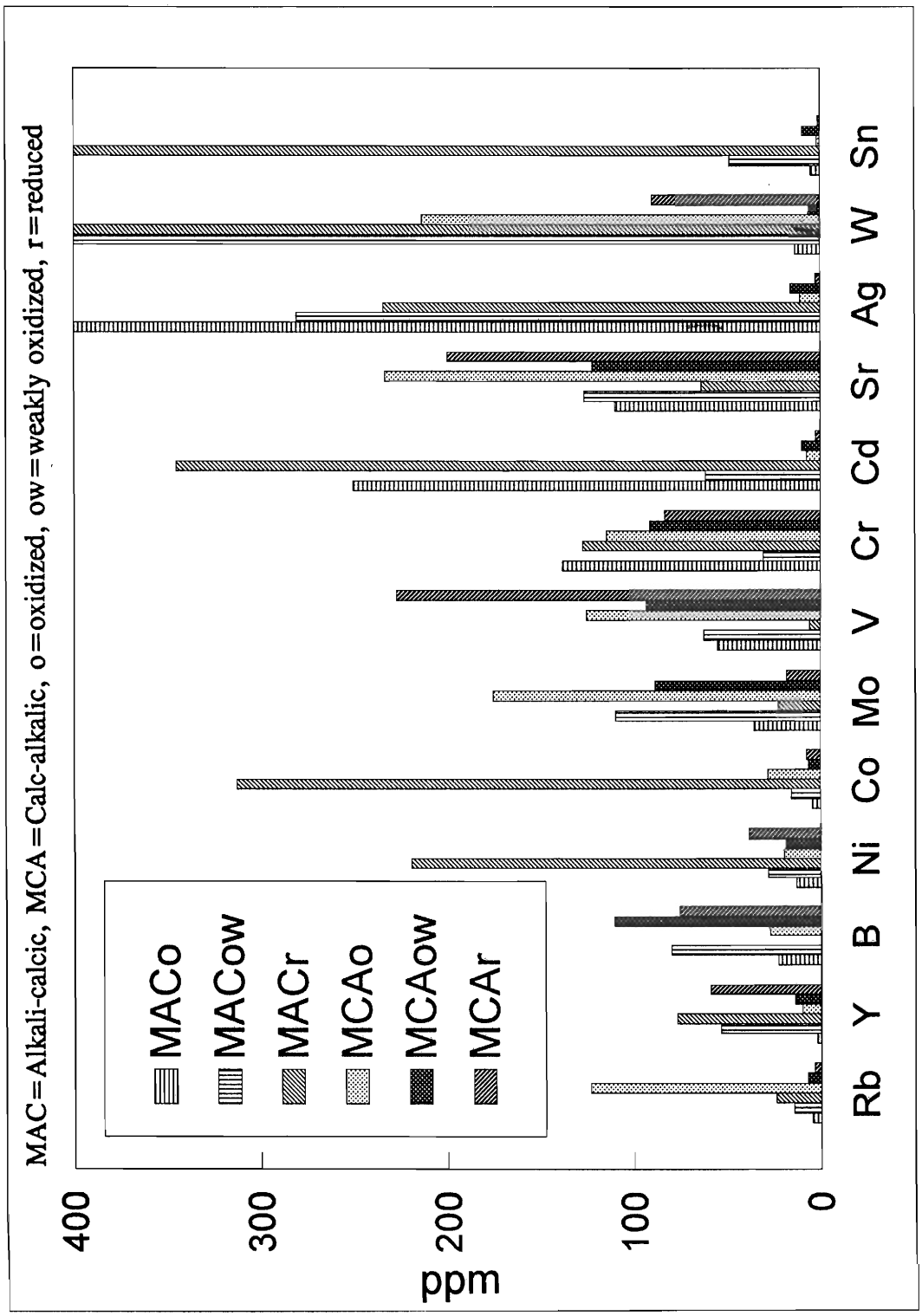

Figure 7-5. Comparison of means of trace elements from mineralized samples (up to 400 ppm) showing contrasts among magma series classes (MAC=alkali-calcic, MCA=calc-alkalic, o=oxidized, ow=weakly oxidized, r=reduced).

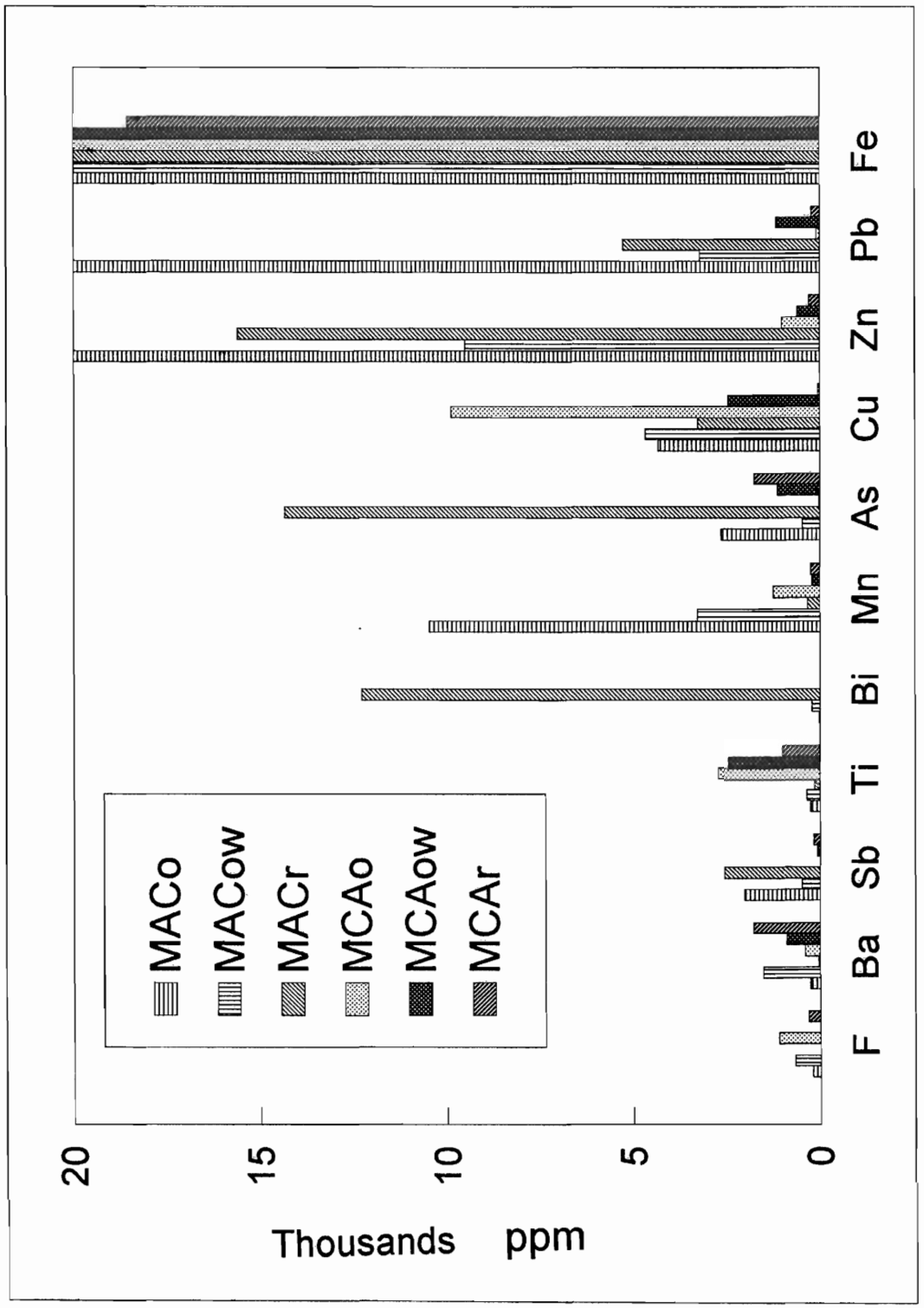

Figure 7-6. Comparison of means of trace elements from mineralized samples (up to 20,000 ppm) showing contrasts among magma series classes (MAC=alkali-calcic, MCA=calc-alkalic, o=oxidized, ow=weakly oxidized, r=reduced).

trace element data in 76% of the samples (Table 7-6). When the mineralized samples were first classified into alkali-calcic or calc-alkalic and then subdivided into oxidation classes, discriminant analysis correctly classified 96% of the alkali-calcic samples (Table 7-7) and 83% of the calc-alkalic samples (Table 7-8). Thus, despite the variety in the data, the six magma series classes are clearly distinguished.

Table 7-5. Classification Results of Discriminant Analysis on Whole Rock Oxides.

		NO. OF	PREDICTED GROUP MEMBERSHIP				
Class	Cases	1	2	3	4	5	6
MACo	36	36	0	0	0	0	0
		100.0%	0.0%	0.0%	0.0%	0.0%	0.0%
MACow	16	0	16	0	0	0	0
		0.0%	**100.0%**	0.0%	0.0%	0.0%	0.0%
MACr	33	0	0	33	0	0	0
		0.0%	0.0%	**100.0%**	0.0%	0.0%	0.0%
MCAo	101	1	6	0	87	7	0
		1.0%	5.9%	0.0%	**86.1%**	6.9%	0.0%
MCAow	56	3	0	0	10	40	3
		5.4%	0.0%	0.0%	17.9%	**71.4%**	5.4%
MCAr	11	0	0	0	0	0	11
		0.0%	0.0%	0.0%	0.0%	0.0%	**100.0%**

PERCENT OF "GROUPED" CASES CORRECTLY CLASSIFIED: **88.14%**

Table 7-6. Classification Results of Discriminant Analysis on Trace Elements.

		NO. OF	PREDICTED GROUP MEMBERSHIP				
Class	CASE	1	2	3	4	5	6
MACo	23	18	2	0	0	1	2
		78.3%	8.7%	0.0%	0.0%	4.3%	8.7%
MACow	123	1	75	0	6	8	33
		0.8%	**61.0%**	0.0%	4.9%	6.5%	26.8%
MACr	15	1	2	8	1	1	2
		6.7%	13.3%	**53.3%**	6.7%	6.7%	13.3%
MCAo	63	0	7	0	40	12	4
		0.0%	11.1%	0.0%	**63.5%**	19.0%	6.3%
MCAow	329	0	2	0	15	234	78
		0.0%	0.6%	0.0%	4.6%	**71.1%**	23.7%
MCAr	333	0	9	0	1	22	301
		0.0%	2.7%	0.0%	0.3%	6.6%	**90.4%**

PERCENT OF "GROUPED" CASES CORRECTLY CLASSIFIED: **76.30%**

Table 7-7. Classification Results of Discriminant Analysis on Trace Elements of Alkali-calcic Classes.

		NO. OF	PREDICTED GROUP MEMBERSHIP	
Class	CASES	1	2	3
MACo	23	20	3	0
		87.0%	13.0%	0.0%
MACow	123	0	123	0
		0.0%	**100.0%**	0.0%
MACr	15	0	3	12
		0.0%	20.0%	**80.0%**

PERCENT OF "GROUPED" CASES CORRECTLY CLASSIFIED: **96.27%**

Table 7-8. Classification Results of Discriminant Analysis on Trace Elements of Calc-alkalic Classes.

		NO. OF	PREDICTED GROUP MEMBERSHIP	
Class	CASES	4	5	6
MCAo	63	53	8	2
		84.1%	12.7%	3.2%
MCAow	329	15	242	72
		4.6%	**73.6%**	21.9%
MCAr	333	4	21	308
		1.2%	6.3%	**92.5%**

PERCENT OF "GROUPED" CASES CORRECTLY CLASSIFIED: **83.17%**

BACKGROUND INFORMATION ON NEURAL NETWORKS

This chapter introduces neural networks with a short explanation of what they are, how they have been used, and how they work. As there are numerous texts on neural networks, only the types of networks used in this study are discussed. The following material is summarized from several texts: 'Naturally Intelligent Systems' (Caudill and Butler, 1990), 'Neural Network Architectures, An Introduction' (Dayhoff, 1990), 'Neural Computing, Theory and Practice' (Wasserman, 1989), and 'Neural Networks, Algorithms, Applications, and Programming Techniques' (Freeman and Skapura, 1992). Instruction manuals from Neural Ware (1991) on the NeuralWorks Professional II/Plus software used in this study also explain neural networks.

Neural Network Applications

Neural networks have been applied to problems of prediction, data association, pattern recognition, classification, data conceptualization, data filtering, and optimization. Applications range from converting text to speech, image compression and reconstruction, optical character recognition from handwriting and Japanese characters, military target classification, industrial inspection, signal processing, and financial and economic modeling.

In earth science applications, neural networks have been used to classify seismic signals (Dysart and Pulli, 1990), estimate first break picks in seismic data (McCormack, 1990), interpret well logs (Wiener and others, 1991; Baldwin and

others, 1989, 1990), locate buried targets in subsurface images (Poulton and others, 1992), classify satellite images (Benediktsson and others, 1990), compress images (Naillon and Theeton, 1989), and stratigraphic correlation and identification of minerals (Petersen and Haileab, 1993).

Definition of Neural Networks

Neural networks are patterned on natural biological neural systems and both consist of three basic components: processing elements (biological neurons), interconnects (axons, dendrites, or paths between neurons), and junctions where interconnects meet processing elements (synapses). Neural networks are massively parallel systems that rely on dense arrangements of interconnections between uncomplicated processors. A network is composed of many very simple processing elements that communicate through a rich set of interconnections that have variable weights or strengths. Memories are stored or represented in a neural network in the pattern of alterable interconnection weights among the processing elements (PEs). When hundreds or millions of simple Pes are interconnected, they resemble a complicated web or net, which is the source of the term 'network'. The great power of both artificial and biological systems lies in their massive and complex connectivity.

Characteristics of Neural Networks

Neural networks are not programmed, they learn by example. A neural

network learns through supervised training or through trial and error in unsupervised learning where the network is self-organizing. Typically, a neural network is presented with a 'training set', a set of bits of data that are known to constitute certain patterns. During supervised learning, a network is presented with an input pattern coupled with the target output, which usually is the 'correct answer' or 'proper classification' for each sample. The neural network iteratively adjusts the values of its internal weights to the point where the network produces the correct output in response to each similar input pattern. During supervised training, the training set is presented many thousand times to allow the network to gradually adjust its internal parameters. During unsupervised training, the network is presented with input patterns and it groups similar patterns together.

Neural networks are able to generalize from previous examples to new ones. A neural network can learn the characteristics of a general category of objects based on a series of specific examples from that category. To develop a neural network that can generalize, the training set must include examples that demonstrate the boundaries and general characteristics of the class. The training session must limit iterations to prevent "overlearning", in which the network memorizes specific examples instead of generalizing effective classification criteria. Once trained, a network is insensitive to minor variations in its input. This ability to see through noise and distortion to the inherent pattern is vital to pattern recognition in the real world.

Artificial neural networks can abstract the essence of a set of inputs, discover the distinguishing features needed to classify a pattern, and complete patterns. A network can be trained on a set of variously distorted versions of the pattern; after adequate training, it can produce or generalize complete patterns that it had never experienced. A network can discover distinguishing features between the different categories in the "feature-detection" layer of processing elements. Neural networks can also be used for pattern completion to fill in pieces missing from a pattern because of noise or partial concealment. In a pattern-completion experiment, the neural network is trained to output the same pattern that is input (homoassociative training). The internal layers of the network develop a distributed encoding of each pattern during training. After training, a partial pattern is presented as input and the network recalls the full pattern.

Neural networks encode information by distributing it among many processing units. This distributed encoding contrasts with memory storage in conventional computers where information is stored in specific locations. In neural networks, numerous processing units are used simultaneously to identify a pattern. This internal representation is thus distributed across all or part of the network. Distributed memory schemes provide many advantages, chief of which is the redundancy of information representation. A neural network can be partially destroyed yet still function correctly. Thus, neural networks tolerate errors and omissions in the data and system operation.

Strengths of Neural Networks

Neural networks are highly fault tolerant or "fail soft", a characteristic also called "graceful degradation." A neural network keeps working even after a significant fraction of its neurodes and interconnections have become defective. Performance degrades slowly and smoothly as neurodes and interconnections fail.

Limitations of Neural Networks

Another difficulty results from the inability of traditional artificial neural networks to "explain" how they solve problems. The internal representations that result from training are often so complex as to defy analysis. This is understandable given our inability to explain how humans recognize visual patterns despite differences in distance, angle, illumination, and the passage of time. Recent research on this accountability problem holds promise for the future.

Structure of Neural Networks

Artificial neural networks consist of processing elements (PEs), layers, and synaptic connections. The numbers of PEs and layers in a network are specified by the user according to the type of problem. The minimum structure involves three layers, an input layer, one internal or hidden layer, and an output layer. Simple processing elements communicate through a complex gridwork of interconnections that store memories as variable weights or strengths. Each link

between processing units acts as a communication route. Numeric values are passed along these interconnections from one processing unit to another. These values are weighted by a connection's strength when they are used computationally by the target processing unit. Connection strengths associated with each interconnection are adjusted during training to produce the final neural network. Synaptic connections start with positive and negative random values; training proceeds by iteratively finding a set of weights that either minimizes an error function or minimizes a distance between specified vectors. During training, network weights gradually converge to values such that each input vector produces the desired output vector. A learning rule is used to specify how the weights are adjusted during training.

Process of Neural Network Operation

The learning procedure begins by presenting data to processing elements in the input layer, which are connected to other processing elements in the next hidden layer. Each interconnection has an associated connection strength, given as w_1, w_2, ..., w_n. The processing element performs a weighted sum on the inputs and uses a nonlinear threshold function, f, to compute its output. The calculated result is sent along the output connections to the target processing elements.

In supervised training, input patterns are presented to the network, resulting outputs are compared with the desired outputs, and network weights are adjusted to reduce the difference. Supervised training requires the pairing of

each input vector with a target vector representing the desired output; together these are called a training pair. Usually a network is trained over many such training pairs. An input vector is applied, the output of the network is calculated and compared to the corresponding target vector, the difference or error is fed back through the network, and weights are changed according to an algorithm that tends to minimize the error. The vectors of the training set are applied sequentially, and errors are calculated and weights adjusted for each vector until the error for the entire training set is acceptably low.

In unsupervised training, input patterns are applied and the network self-organizes by adjusting its weights according to a predefined algorithm. Because no desired output is specified during the training process, the results are unpredictable. The network organizes itself to develop congruent properties of the training set. The training algorithm modifies network weights to produce output vectors that are consistent, so that application of a training vector or a similar one produces the same output. For example, input patterns may be classified according to their degree of similarity, such that comparable patterns activate the same output processing element. The training process extracts statistical properties of the training set and groups similar vectors into the same classes. Prior to training there is no way to predict which output class will be produced by a given input.

Operation of a neural network is controlled by the transfer function of the processing elements (PEs), the details of the structure of the connections among

the PEs, and the learning law followed by the network. Important factors in designing and implementing a neural network application are the choice of network, data representation, selection of training and test examples, and the number of hidden layers and PEs.

A processing element accepts input from a large number of other PEs, processes these inputs, and sends copies of its single output to yet other PEs over a network of interconnects. Each such output interconnect ends at the input of the recipient PE in an unidirectional junction similar to a synapse. The artificial synapses may be plastic or fixed and can have varying weights or strengths; they can be either excitatory (positive) or inhibitory (negative).

Each PE receives a large number of individual input signals that together constitute an input pattern. This input pattern causes the PE to reach some level of activity. If the activity is strong enough, the PE generates a single output signal that is transmitted over the PE's interconnects to other PEs. The PE computes a function that associates a given level of input stimulus to a particular level of output activity. This overall mapping is called the transfer function for the PE.

Computation of the transfer function is a three-step process. First, the processing element (PE) calculates the total incoming stimulation from all sources and correlates that to a particular level of activity. The PE generates the appropriate output signal for that level of activity and transmits it along its output interconnect to PEs in the next layer. The output signal is generally the

activation level, although it is often modified by a threshold value, which does not allow the PE's output to rise until the activation exceeds some minimum value. The same output value is transmitted along all output interconnects to all receiving PEs. The output value is not split or apportioned among all possible receivers; every receiving processing element sees the same signal from this transmitting PE. The basic procedure computes input-activation-output.

The value of the synapse weights is the critical factor determining the activity patterns that a given input pattern generates at each layer. Learning in a neural network consists of changing the values of these weights. The method of altering synapse weights is governed by learning rules that dictate by how much and in which direction connection weights will be changed.

Types of Neural Networks

Neural networks can be divided into several categories based on the method of learning, structure, and control. The most fundamental difference among networks is the direction that information flows. In feed-forward networks, processing elements receive input only from the previous layer and send output only to the next layer. Feed-back networks can send a PE's output back to its own input or to a previous layer's input.

The type of network chosen depends upon the problem. There are several types of neural networks that are best for classification problems. These include the probabilistic neural net (Specht, 1990), functional link network (Pao, 1989),

learning vector quantization (Kohonen and others, 1988), counterpropagation (Hecht-Nielsen, 1990), adaptive resonance (Carpenter and Grossberg, 1987), and self-organizing map (Kohonen, 1988).

Based on a comparison of algorithms by Poulton and Zaverton (1992), the learning vector quantization (LVQ) network was selected for this study. As numerous papers contain detailed explanations of the mathematical foundation of the back-propagation and the Kohonen layers that are used in LVQ, only a short summary of the methods is presented here.

Back-propagation Networks

Back-propagation is a form of non-linear regression. The method seeks a function that maps the set of input patterns to the set of output patterns with minimum error. The technique was derived independently by Werbos (1974) and Parker (1982, 1985) and was popularized by Rumelhart and others (1986). Although it is not comparable to biological systems, back-propagation is the most popular and best understood neural paradigm.

The back-propagation learning algorithm involves a forward-propagating step followed by a backward-propagating step. There are three layers of processing elements in a typical back-error propagation network. The first layer consists of input processing elements (PEs). These PEs adopt the values of an input pattern, represented as a vector. Each of the inputs is multiplied by a weight and the products are summed. The middle or "hidden" layer of this

network consists of "feature detectors"; these are processing elements that respond to particular features that may appear in the input pattern. Back-propagation networks usually have each layer fully connected to the layers below and above. Although there can be more than one hidden layer, in most cases one hidden layer is sufficient. The last layer is the output layer.

The operation of a three-layer back-propagation network is shown in Figure 8-1. The input data X_{ip} is multiplied by the connection weights W_{ij} that lead to the hidden layer to obtain a weighted sum S_{jp}.

$$S_{jp} = \sum_i X_{ip} W_{ij} + \theta_j \qquad (1)$$

θ_j is a bias unit connected to each PE in the hidden and output layers. It has a constant value of 1.0 but the connection weights are trainable.

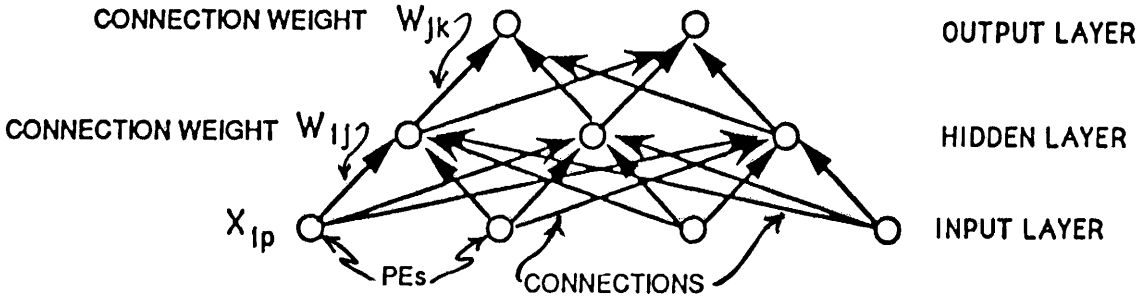

Figure 8-1. The operation of a three-layer back-propagation network.

The weighted sum S_{jp} is modulated by a threshold or activation function f_j that is usually sigmoidal in shape (Figure 8-2); sigmoidal functions are similar to thresholding performed by biological neurons. The function used in this study is a

hyperbolic tangent described by equation (2).

$$f(x) = \frac{e^{Sp} - e^{-Sp}}{e^{Sp} + e^{-Sp}} \qquad (2)$$

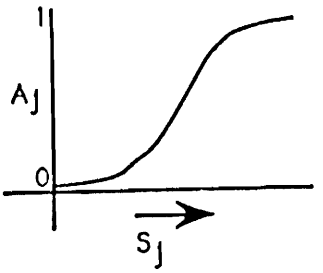

Figure 8-2. The shape of a sigmoid function used to modulate the weighted sum S_j to give an activation A_j.

The activation A_{jp} of a PE is a function f_j of the weighted sum S_{jp}.

$$A_{jp} = f_j(S_{jp}) = \frac{1}{1 + e^{-Sjp}} \qquad (3)$$

A gain term can also be applied to change the slope of the threshold. The activation of the hidden PE becomes the input to the next layer of PEs (the output layer in Figure 8-1).

$$X_{jp} = A_{jp} \qquad (4)$$

$$S_{kp} = \sum_j X_{jp} W_{jk} + \theta_k \qquad (5)$$

$$A_{kp} = f_k(S_{kp}) = \frac{1}{1 + e^{-Skp}} \qquad (6)$$

The activation A_{kp} is compared to the desired output pattern D_{kp} to obtain an

error E_{kp}.

$$E_{kp} = (D_{kp} - A_{kp}) \tag{7}$$

This error must be apportioned to all the connection weights in the network through the back-error propagation cycle. The change in weights or the delta weights δ^{o}_{kp} between the layers are computed as

$$\text{OUTPUT - HIDDEN}$$
$$\delta^{o}_{kp} = (D_{kp} - A_{kp})\ f'_{k}\ (A_{kp}) \tag{8}$$

where f'_{k} is the derivative of the threshold function. In this study

$$f'_{k} = (1 + f_{k}(A_{p}))\ (1 - f_{k}(A_{p})) \tag{9}$$

$$\text{HIDDEN - INPUT}$$
$$\delta^{H}_{jp} = f'_{j}(A_{jp})\ \Sigma\ \delta^{o}_{kp} W_{jk} \tag{10}$$

Since the error for the hidden PEs is unknown we must use the sum of the delta weight, δ^{H}_{jp}, times connection weight from the output layer as the error. Weights are updated as

$$W_{jk}(t + 1) = W_{jk}(t) + \eta\ \delta^{o}_{kp}\ A_{jp} + \alpha\ \Delta_{p} W^{o}_{jk}\ (t - 1) \tag{11}$$

$$W_{ij}(t + 1) = W_{ij}(t) + \eta\ \delta^{H}_{jp}\ A_{jp} + \alpha\ \Delta_{p} W^{H}_{ij}\ (t - 1) \tag{12}$$

where t is an iteration number and η is a step size. α is a momentum term and $\Delta_{p} W^{o}_{jk}$ is the weight change made at the previous iteration. After the weights are updated, one iteration is complete and the entire process is repeated until an acceptable error, E_{p}, is achieved for each pattern.

$$E_{p} = \tfrac{1}{2} \sum_{k=1}^{m} \delta o^{2}_{kp} \tag{13}$$

Weight updates can be made after each pattern is presented or accumulated over

the entire training set or over some subset thereof.

The role of the hidden PEs is to abstract the input data. Too few PEs in the hidden layer will overgeneralize the mapping function, which results in a high bias component of the total error. Too many PEs will fit the training data too closely, which results in a high variance component of the total error (Geman and others, 1992). The error is often a quadratic function of the number of hidden Pes, which can vary over a broad range of acceptable values.

The principal strength of back-error propagation is its capability in general pattern-mapping; it can learn a great variety of pattern-mapping relationships. It does not require any knowledge of a mathematical function that maps input patterns to output patterns; back-propagation merely needs examples of the mapping to be learned. The flexibility of the paradigm is enhanced by the large number of available design choices, such as number of layers, interconnections, processing units, learning constants, and data representations.

The largest drawback with back-error propagation is the excessive convergence time. Training sessions can require thousands or millions of iterations for relatively simple problems. Realistic applications may have thousands of examples in a training set, and it may take days of computing time to complete training. Another limitation is that back-error propagation is susceptible to training failures, in which the network never converges to a point where it has learned the training set.

Competitive Filter Networks

Competitive learning and lateral inhibition are neural networks in which processing elements oppose each other; this competition generates networks that excel at pattern classification. Kohonen layers and LVQ networks are examples of competitive networks. Lateral inhibition uses a layer in which each processing element inhibits other nearby units. The resulting network is useful for preprocessing sensory data and for edge and contrast enhancement.

A competitive learning network consists of two layers -- an input layer and a competitive layer. In the competitive layer, processing units compete to respond to the input pattern. The winner is the classification category for the input pattern. Competition is accomplished through an algorithm that selects the winning unit or through inhibition among the processing elements in the competitive layer until only the winning unit is active.

Kohonen Self-Organizing Map (SOM)

Kohonen's self-organizing feature map is a two-layered network that preserves topological relationships among the patterns that are given to the network. Similarities among input patterns are mapped into closeness relationships on the competitive layer. After training is complete, pattern associations are observed from the competitive layer. The network combines an input layer with a competitive layer of processing units (Figure 8-3).

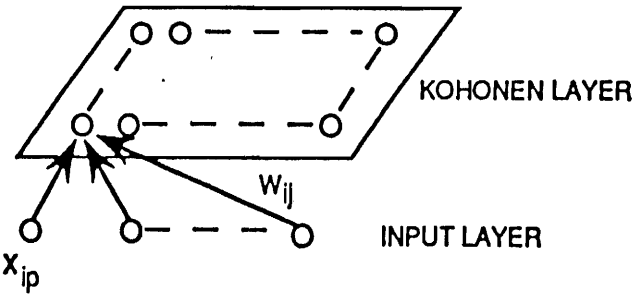

Figure 8-3. Learning vector quantization (LVQ) in which inputs X_i from the input layer of processing elements (PEs) are directed to the Kohonen layer and modified by weights W_{ij}.

The goal of each PE in an Kohonen layer is to arrange its incoming input pattern. Each PE in the input layer is one element of the input pattern vector. The input layer is fully connected to the Kohonen layer so each PE in the Kohonen layer represents a vector of the same dimensionality as the input pattern vector. The connection weights start with uniformly distributed random values. The distance between the input pattern vector and the weight vector at each Kohonen PE is calculated as the Euclidean distance between the two vectors:

$$\partial_i = \| W_j - X_i \| = \sqrt{\sum_{i=1}^{n} (w_{ij} - x_i)^2} \qquad (14)$$

Since the Kohonen layer uses competitive learning, the Kohonen PE with the smallest distance ∂_i wins the competition. Neighbors around the winning PE are identified and allowed to remain active by an amplitude-distance function known as a "Mexican Hat" function (Figure 8-4).

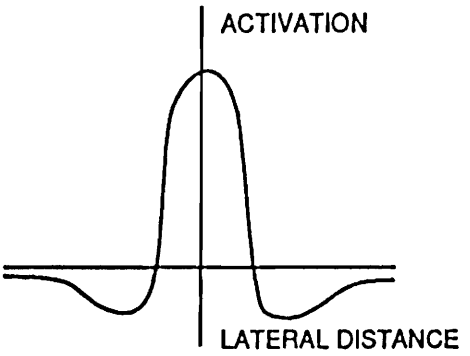

Figure 8-4. Amplitude-distance function known as the "Mexican Hat" function that modifies neighbors around the winning processing element.

The weights of the winning PE are adjusted so that they more closely match the input vector, thus ensuring that they will win the competition the next time the pattern is presented. Input patterns that are close to each other in the n-dimensional input space should map to PEs that are spatially close in the Kohonen layer.

Learning Vector Quantization (LVQ)

The LVQ network (Kohonen, 1988) is a variant of the Kohonen Self Organizing Map (SOM) that uses supervised learning. One of the key differences between SOM and LVQ is that the LVQ network subdivides the Kohonen layer for each output PE. The PE that wins the competition must be in the correct portion of the Kohonen layer in order for the classification to be correct (Figure 8-5).

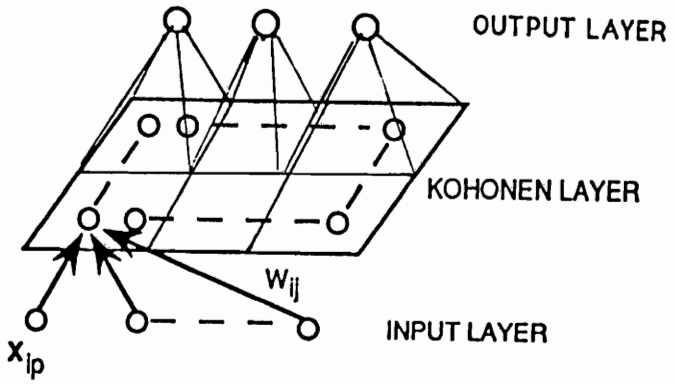

Figure 8-5. Kohonen layer showing that the winning PEs must be in the correct portion of the Kohonen layer to correspond to the output PE that is physically close to it. The tetrahedron below each output PE depicts the portion of the Kohonen layer that is related to that output class.

If the winning PE in the Kohonen layer is in the correct vicinity, then its weights are adjusted to move it closer to the correct region:

$$w_{ij}(t + 1) = w_{ij}(t) + \eta_1(x_{ij} - w_{ij}(t)) \qquad (15)$$

If the winning PE is not in the correct class, its weights are adjusted to move it further away from that region:

$$w_{ij}(t + 1) = w_{ij}(t) - \eta_2(x_{ij} - w_{ij}(t)) \qquad (16)$$

The constants η_1 and η_2 determine how much right solutions are rewarded and wrong solutions are punished.

Some PEs may have a tendency to dominate the competition by winning when many different input patterns are presented. A "conscience" mechanism (DiSieno, 1988) can be added to ensure a PE does not win too often. Several modifications to LVQ exist that refine the solution if the second-best PE is in the

correct class.

LVQ is a very fast algorithm but has the disadvantage of only outputting 0s and 1s, so that only yes or no answers are available for the class assignment of each sample. The advantage of floating point outputs of a back propagation network is the ability to assign a "confidence" in the result based on nearness to 0 or 1.

NEURAL NETWORK PROCEDURES

Procedures used by neural networks in general, by the paradigms of back-propagation and learning vector quantization (LVQ), and by this study are described in this chapter. In each case, details are provided on network design, parameters, and evaluation.

Neural Network Methodology

Even when using commercial software that requires no programming skills, there are many choices. Most alternatives relate to network design, such as type of network and parameters, but some pertain to evaluation.

Theory of Network Design

Design choices in developing a neural network include choosing an application, selecting a network paradigm, assigning types of inputs and outputs, designing the internal structure, determining the number and sizes of each layer, deciding upon the number and type of hidden layers and hidden processing elements (PEs), and experimenting with various training schedules to find the best one.

First, a network paradigm is selected that is most likely to solve the application problem. A variety of neural net paradigms are available; they differ in the processing done at each element and in the method of updating internal parameters. Each paradigm dictates how the readjustment of parameters takes

place; this readjustment results in "learning" by the network. Examples of neural net paradigms include back propagation and LVQ.

The problem must be defined precisely so that inputs and outputs can be selected. These choices identify the patterns that go into the network and their target output. In some applications, preprocessing is necessary before the data can be presented to the network.

Careful selection of training data is crucial to the success of a neural network. After data are assembled for training and testing, a representation is designed for the input and output to the network. The quality of training data presented to the neural network influences whether or not the network "learns" a particular task. The set of training examples must reflect the variability in input patterns that the network will encounter after training.

Next, internal structure of the network is designed, including the topology and size of the network. Internal parameters are then "tuned" to optimize the neural net design. These parameters influence the rate of learning by the network and its success. Typically, network parameters are tuned experimentally according to previous experience with the type of application.

The number and sizes of each layer are then chosen and processing elements are interconnected in layers or individually. Next, the number of processing units are specified, along with specific interconnections in the network. Processing units are usually organized into distinct layers, which are either fully or partially interconnected. Then, the network's internal

computations are chosen.

Several researchers have studied the optimum size of a training set that is required for good generalization. Baum and Haussler (1988) show that for a desired accuracy level ($1 - \epsilon$), the number of training examples should be ω/ϵ, where ω is the number of connection weights in the network. Thus, for an accuracy on test data of 90 percent one would need ten times as many examples as connection weights. Soulie and others (1988) observed the variation in accuracy with size of the training set and found that generalization capability was best when at least 60 percent of the available data were used for training. Because of assumptions in the above studies, equations or heuristics for number of training examples should not be applied to a problem without understanding the conditions under which the assumptions are valid. In general, larger networks and more complicated input patterns require more training examples to produce good generalization.

The number of hidden layers and hidden PEs in a network are generally found by trial and error. Lippmann (1987) researched decision regions formed by hidden layers of a network that used a hard-limited threshold function and had one output PE. Such networks required no more than two hidden layers to form complex decision regions (Lippmann, 1987). Cybenko (1989) found that one hidden layer was sufficient to compute arbitrary decision functions of outputs. Given a fixed size for the input and output patterns and a fixed training set size, Baum and Haussler's (1988) approach could be used to select the number of

hidden PEs. Kung and Hwang (1988) used algebraic projection to predict the optimal number of hidden units. Hecht-Nielsen (1987) used a neural network adaption of Kolmogorov's Theorem to show that for a network with one hidden layer, the hidden layer requires n+1 PEs, where n is the number of input PEs. Many other researchers have studied the problem of how many hidden PEs are required; their work is summarized by Maren and others (1990). For back propagation networks more PEs are required in the hidden layer when the relationship between input data and desired output is more complex. The upper bounds for the number of PEs in the hidden layer, h, can be calculated by:

$$h = \frac{\text{cases}}{10 * (m + n)} \qquad (17)$$

where cases is the number of rows of training data, m is the number of PEs in the output layer and n is the number of PEs in the input layer (NeuralWare, 1991).

Training the network successfully involves many choices and training experiments. The training schedule specifies the number of training iterations to be done and any changes that are made during training to the learning rate parameters. While a network is being trained, an error learning curve can be observed. If training experiments are done, the training data and network parameters are varied; the paradigm, network size, and interconnection topology may also be modified. These experiments establish which configurations train the network most successfully for the application.

The design of the training experiments must minimize global error.

Experiments should be done to the point of minimizing error while ignoring noise, yet not done to the point of memorizing the input data. The purpose is to generalize the characteristics of the classes, not to memorize each of the input data points.

Network Evaluation

Performance evaluation is designed to measure the effectiveness of the neural network. Sensitivity analysis determines which components are most significant. Making changes to the input data in increments and calculating the percent change at output is known as 'dithering' and is a way of determining the sensitivity of the neural network. Performance evaluation also includes testing the plasticity of network, which determines the effect of corrupted data. The test with artificially altered or obscured data examines the ability of these neural network pattern recognition paradigms to work effectively in spite of 'fuzzy' data, noisy data, typographical errors in the data, or poorly analyzed data.

In the ideal case, a neural network's answers would be traceable so that the network is "accountable" for its decisions. Although traceability in large neural networks appears difficult or incomprehensible, several possibilities exist.

Back-propagation Procedures

Creating a back-propagation network requires choosing parameters for the

hidden and output layers. The numbers of processing elements in the input, hidden, and output layers are specified. The connection scheme between layers, such as fully interconnected, and the range of values for randomization are designated. Finally, the learning rule and a learning schedule are specified. Once all parameters have been specified, the network is trained for a specific number of passes through the training set or until the desired error level is achieved.

Learning Vector Quantization (LVQ) Procedures

Creating a learning vector quantization (LVQ) network also requires setting the number of processing elements (PEs) and coefficients in the learn/recall schedule. LVQ is selected as the control strategy, learn/recall schedule, and various Kohonen layer parameters; these parameters are automatically set by the software when LVQ is chosen. The number of input processing elements is set to equal the number of measurements on each sample. The number of hidden PEs is set to equal the number of processing elements per class; this parameter is varied as experimentation progresses. The number of output PEs is set to equal the number of output classes. A minimum/maximum table is generated to survey the data limits of each type of measurement in the input numbers. In the learn/recall schedule, various parameters and coefficients are set according to recommendations of the software designers; these parameters can be varied according to the results of experimentation. Then, the

program is run to learn for a specified number of iterations. Finally, the results of the learning are tested and parameters are readjusted in the preceding procedure to achieve the best correlation with the target outputs.

Neural Network Procedures in this Study

Neural network paradigms that are good at classification, learning vector quantization (LVQ) and back-propagation, were chosen for this study. Both sets of data (whole rock geochemistry of fresh igneous rocks and trace element geochemistry of the related mineralized systems) were submitted to both types of neural networks. Various combinations of network design and parameters were attempted until the network converged, achieving 100 percent learning, or until it nearly converged, achieving more than 95 percent learning. Then, some of the data was randomly withheld during retraining the network while using the previously successful network configuration. The network was then tested with the withheld data to evaluate how well the network learned the classes based on the limited training set.

Data Representation

Data representation involved selecting data, presenting it in the proper format, and assigning a target output class. Whole rock data (Appendix B) were obtained from the literature as documented in Chapter 3 and trace element data (Appendix G) were supplied by MagmaChem Exploration Inc. as reported in

Chapter 6. Geochemical data in this study were extracted as numbers in ASCII files from a spreadsheet (Lotus 1-2-3) or a data base manager (R:Base). Within the six classes of this study there were 1700 samples with trace element data on as many as 59 elements; samples analyzed for less than 10 elements were culled. In addition, elements which were not analyzed in the majority of specimens were excluded, leaving approximately 900 samples analyzed for as many as 32 chemical elements. The numbers were then edited in a DOS editor to conform with the format required by the neural network software. Data were presented to the network in rows of numbers in which each consecutive number represented a different chemical element, oxide, or mineral for a particular sample. Consecutive samples were listed in successive rows. The network format consisted of exclamation points before comment lines for the mining district name and sample number, rows of numbers that represented the concentration of various chemical elements for each sample, and a final row for each sample that consisted of 0s and 1s indicating the target output class. For example, the metaluminous alkali-calcic oxidized (MACo) class was designated as 0 0 0 0 0 1, the MACow class as 0 0 0 0 1 0, and so forth to the MCAr class as 1 0 0 0 0 0.

Potential problems included various meanings for zeros in the data, differences in the types of samples, and diversity in sample locations. Some zeros in the data indicated the concentrations were below the detection limits for a particular element and some zeros indicated the element was not analyzed. In this study, the values for elements below the detection limit were set at ten

percent of the detection limit; they could also have been set at zero without much change in the results. The trace element data had been analyzed by many different laboratories. There were also substantial differences in which and how many chemical elements were included in each analysis. A considerably more significant problem was whether the sample was located in the central versus peripheral part of the ore deposit. Although it is possible to quantify the distance from the central ore zone with various ratios or numbers, that process would take more time than was available in this study. Once that number was quantified, it could be used as another input in the row of elements and the neural network would consider that value in its classification. Neural networks that could be used to classify map or spatial data and the areal distribution of geochemical samples would be a profitable direction for further research.

Network Design in this Study

Once the paradigm selections were made, numerous design choices were possible within each type of network. The number of input processing elements was set as the number of chemical elements, oxides, or minerals for each sample. For the whole rock data, the number of input processing elements was generally 32; the data included SiO_2, TiO_2, Al_2O_3, Fe_2O_3, FeO, MgO, MnO, CaO, Na_2O, K_2O, P_2O_5, LOI, Total, A/CNK, A/NK, Na_2O+K_2O, Na_2O/K_2O, Na_2O+K_2O-CaO, K_2O-CaO, K_2O-MgO, $(FeO+0.9*Fe_2O_3)/MgO$, Fe_2O_3/FeO, Larsen Factor, alkali index, alteration index, K-index, Na Index, Al_2O_3/Na_2O, SiO_2/Al_2O_3, SiO_2/K_2O,

magnetite, and ilmenite. Various combinations of these data were used in the neural network experiments. For the trace element data, the number of input processing elements was also 32; chemical elements included Ag, As, Au, Ba, Be, Bi, B, Cd, Co, Cr, Cu, Fe, F, Hg, Li, Mn, Mo, Nb, Ni, Pb, Rb, Sb, Sn, Sr, Te, Ti, Tl, V, W, Y, Zn, and Zr. The number of output classes, six, remained the same for all trials, except when trials were run in an hierarchy that first classified into alkali-calcic or calc-alkalic (two output classes) and subsequently into oxidized, weakly oxidized, and reduced (three output classes).

Although the number of input processing elements and number of output classes generally remained the same during most of the trials, internal design choices varied widely. The options mostly included experimenting with different numbers of processing elements in the hidden layer, with various combinations in the learn/recall schedule, and with different iterations. With the larger sample set of the trace elements, the learn/recall schedule was changed from the default amounts to larger numbers. This extended the range of iterations broadly enough so that the network could run all the way through the training set enough times to learn the correct output class. Details of the internal design selections are documented in the next chapter on results of the neural network experiments.

Evaluation in this Study

After the neural network achieved 98 percent or 100 percent learning with the full training set of data, the successful network configuration was evaluated.

Assessment consisted of learning the classification with a reduced set of data and then testing that classification with the full data set. The random sampler in Excel was used to select the samples to be excluded: first, all the samples were numbered; then, the numbers were entered in rows in the Excel spreadsheet; then, the random sampler chose 10 percent, 20 percent, or 30 percent of the numbers in each class to be excluded. Exclamation points were put in front of these samples in the ASCII file to turn them into comment lines, and the number of samples was reduced accordingly. The previously successful neural network configuration was then used with the reduced set of data as the training set. Then, the network was tested with the full data set to discover if the network classified the missing or unknown samples correctly. Details of the results of these tests are given in the next chapter on results.

RESULTS OF NEURAL NETWORK TRIALS

Neural networks performed very well in classifying the data from both whole rock and trace element samples into the correct magma series classes. The neural networks classified all of the mines into the same classes as those obtained with petrochemical variation diagrams. The results of learning with the LVQ (Learning Vector Quantization) were 100 percent for the whole rock data and 99 percent for the trace element data, while the results with back propagation were 99.2 percent for igneous rocks and 93.3 percent for mineralized samples (Table 10-1). The outcomes of testing with LVQ were 90 percent, 90 percent, 94 percent, and 85.2 percent for withholding 10 percent, 20 percent, 30 percent, and 50 percent of the whole rock samples (Table 10-2). The results of testing with back propagation were 100 percent, 81.1 percent, 89.6 percent, and 85.2 percent for withholding 10 percent, 20 percent, 30 percent, and 50 percent of the igneous rock samples. The success of the neural networks in classifying the data is promising, especially considering the enormous variability, particularly in the trace elements.

Learning

Various combinations of data from the fresh igneous rocks were used to train numerous LVQ networks constructed with different design parameters (Table 10-3). The structure of the LVQ network was changed by the number of input PEs (processing elements), number of PEs in the hidden layer, transition

Table 10-1. Results of training with LVQ and back propagation neural networks.

data type	LVQ	back-prop	MAC LVQ	MCA LVQ
training with 100% of whole rock data	100%	99.2%		
training with 90% of whole rock data	100%	94.4%		
training with 80% of whole rock data	100%	98.9%		
training with 70% of whole rock data	100%	98.1%		
training with 50% of whole rock data	100%	100.0%		
training with 100% of mineralized data	99.6%	93.3%	100%	95.7%
training with 90% of mineralized data	94.4%		99.3%	93.1%
training with 80% of mineralized data	98.9%		100%	96.1%
training with 70% of mineralized data	98.1%		99.2%	98.7%
training with 50% of mineralized data	94.0%	93.8%		

Table 10-2. Results of testing successful LVQ and back propagation networks.

training set	90%	80%	70%	50%
LVQ whole rock results on test cases	90.0%	90%	94.0%	85.2%
LVQ trace elem. results on test cases	87.2%	90.2%	92.1%	80.2%
back prop. wh. rock results, test cases	100.0%	81.1%	89.6%	85.2%
back prop. trace elem. results test cases				83.9%

Table 10-3. Results of training with various type of whole rock data.

type of whole rock data	input PEs	idden PEs	iterations	results
SiO2/K2O and Fe2O3/FeO	2	6	10,000	56%
ratios only, no oxides or minerals	14	6	10,000	80%
whole rock oxides, Si/K and Fe ratios	16	6	10,000	92%
all oxide, indices, and ratios, no minerals	37	6	10,000	96%
all oxides, ratios, import. indices, minerals	32	10	20,000	99%
all data avobe with incorrect Fe oxides	32	14	15,000	99.2%
all data above with recalculated Fe oxides	32	14	10,560	100%
data above, no samples with 0 in Fe oxides	32	14	9,000	100%

points and coefficients in the learn/recall schedule, and number of iterations. The type of data was modified by omitting oxides or ratios, by calculating Fe_2O_3 or FeO from Fe_2O_3/FeO ratios from the same pluton, and by adding magnetite and ilmenite. The LVQ network consistently classified more than 90 percent of the samples properly in all the trials except the one using only SiO_2/K_2O ratio and Fe_2O_3/FeO ratio as the input. The networks performed best when they had more types of input processing elements (32 PEs) representing different kinds of data.

Changing the types of data presented to the networks demonstrated the ability of the network to obtain information about the classes even from ratios and indices derived from the whole rock oxides. When the two main classification tools, SiO_2/K_2O and Fe_2O_3/FeO, were used as the only two input PEs, the network performed poorly with less than 60 percent accuracy. When only ratios were used as the 14 input PEs without whole rock oxides or alteration indexes, the network correctly classified 80 percent of the samples. When only whole rock oxides were used as the 16 input PEs without ratios, alteration indexes, LOI, total, or minerals, the network correctly classified 92 percent of the samples. When all of the oxide, index, and ratio data were used as the 37 input PEs, the network correctly classified 96 percent of the cases within 10,000 iterations. When mineralogic information about the concentration of magnetite and ilmenite was added to each sample based on the modal mineralogy of the sample or ones from the same pluton, the network performed much better with 99 percent accuracy, even with less types of input, using only 32 PEs. The network using 32 PEs was

able to correctly classify 99.2 percent of the samples even when erroneous Fe_2O_3 or FeO data was used from samples where total Fe was assigned to one and the other was zero. When the Fe_2O_3 and FeO data was recalculated according to the average of the Fe_2O_3/FeO ratio on the same pluton, the network was quickly able to converge to 0 percent error. Even faster results were obtained by omitting samples that contained zeros in either Fe_2O_3 or FeO.

The LVQ type of neural network correctly classified 94 percent of the trace element samples, after considerable experimentation with the number of PEs in the hidden layer, changes in the learn/recall schedule, and increases in the iterations. The most successful network that achieved 94.5 percent accuracy used 16 hidden PEs per output class, a learn/recall schedule graduated in steps of 17,744, and 110,000 iterations. Even better success was achieved at 98 percent by classifying in two steps: first into the two alkalinity classes, alkali-calcic and calc-alkalic, and second into the three oxidation subclasses. The network converged by successfully classifying the three subclasses of the alkali-calcic group and achieved 95.7 percent accuracy within the calc-alkalic group. Considering the enormous variety within the mineralized trace element data, the classification success of the neural networks is remarkable. Using trace element data on mineralized samples, all the mines were correctly classified into the same magma series classes as obtained using the whole rock igneous data. The two to six percent of the samples that were erroneously classified were a small minority of the samples from each mine.

percent of the calc-alkalic mineralized data, and different iterations (100,000, 55,000, and 60,000); they were then tested with the full data set of 726 samples. Training success was 98.7 percent for the first network, 97.8 percent for the second and 98.2 percent for the third. Testing success was approximately 85 percent for all three networks, with 27 of the 179 test cases generally missed; each of the three networks generally missed different sample numbers. That each network misclassified different test cases suggests that each network learned slightly different ways of classifying the data. This is an important method to get more accurate results when only a few samples are available. By retraining the same data on the same network design to construct several different networks, it is possible to increase the certainty of classification of test cases.

The back-propagation network trained on the whole rock data was very successful; it obtained 77.6 percent accuracy after 20,000 iterations and 99.5 percent after 70,000 iterations. This successful structure of 32 input PEs, 10 hidden PEs, and 6 output PEs was used to retrain 90 percent, 80 percent, 70 percent, and 50 percent of the data. Testing with the full data set resulted in 100 percent, 81.1 percent, 89.6 percent, and 85.2 percent accuracy, respectively on the withheld samples. The percentage of test cases missed apparently depends more on which samples were removed rather than on the amount removed.

The best classification success occurred when each class was well represented in the training set by large numbers of samples and by samples that included the largest number of chemical elements in the analyses. The 205 whole

was retrained on 70 percent of the data converged after 9000 iterations; it properly classified 94 percent of the test cases. The network that was retrained on 50 percent of the data correctly classified 85.2 percent of the test cases. Thus, accuracy remains at over 85 to 90 percent after removal of various amounts of samples; only ten to fifteen percent of the test samples were missed in any of the trials. Because there were sufficient examples of each pluton, even when a test sample was misclassified, the majority of samples from that rock suite were correctly classified.

The structure of the LVQ network that successfully classified 98 percent of the mineralized data into the two alkalinity classes had 32 input PEs, 14 hidden PEs, 2 output PEs; it was retrained with 90 percent, 80 percent, and 70 percent of the data. When tested with the full data sets, they correctly classified 87.2 percent, 90.2 percent, and 92.1 percent of the test samples. When the networks were retrained on the three oxidation subclasses of the alkali-calcic group using the same structure and 3 output PEs, the results for 90 percent, 80 percent, and 70 percent of the data were correct for 86.7 percent, 71 percent, and 92 percent of the withheld samples. When retrained on the oxidation subclasses of the calc-alkalic group, the results for 90 percent, 80 percent, and 70 percent were accurate for 82 percent, 90.2 percent, and 85.5 percent of the omitted cases.

Three different LVQ networks were trained with the same structure of 32 input PEs, 10 hidden PEs, 3 output PEs, with the same 547 input samples of 70

The whole rock oxide data were accurately classified with 99.2 percent of the samples correctly identified by a back propagation network. The most successful back propagation network used 10 PEs in the hidden layer, delta rule for a learning rule, hyperbolic tangent transfer function, and 85,000 iterations. Back propagation correctly classified 93.3 percent of the mineralized trace elements, although it needed large numbers of hidden PEs (20), small increments (0.01 and 0.02) in the hyperbolic tangent transfer function, a very large number of iterations (2,000,000), and a long training time (eight hours).

Testing

Each of the successful networks was tested by withholding data from the input used for learning and then testing with the data set that included the omitted samples. Withheld samples were randomly selected using the random sampling procedure from Excel described in the previous chapter. Success was evaluated by test case performance.

The structure of the LVQ network that successfully learned 100 percent of the whole rock data had 32 input PEs and 14 hidden PEs; when it was retrained with 90 percent of the samples, it achieved convergence after 9500 iterations. When tested with the full data set, it correctly classified 90 percent of the omitted or test cases. The network was retrained using 80 percent of the data; it converged after 7000 iterations. When tested with all of the data, it was accurate on 90 percent of the originally withheld test samples. The network that

rock samples were distributed as 35 alkali-calcic oxidized samples, 15 alkali-calcic weakly oxidized, 33 alkali-calcic reduced, 97 calc-alkalic oxidized samples, 25 calc-alkalic weakly oxidized, and 10 calc-alkalic reduced analyses. The 887 mineralized samples were represented by 23 alkali-calcic oxidized samples, 123 alkali-calcic weakly oxidized, 15 alkali-calcic reduced, 64 calc-alkalic oxidized samples, 329 calc-alkalic weakly oxidized, and 334 calc-alkalic reduced analyses.

In the whole rock samples, LVQ training success was 100 percent in all classes. Testing was more often erroneous in the MCAow class, although in some cases one test case was also missed in the MACow or MCAo classes. In the mineralized samples, LVQ training successes per class were MACo = 95.7 percent, MACow = 93.5 percent, MACr = 100 percent, MCAo = 90.5 percent, MCAow = 93 percent, and MCAr = 95.5 percent. The best results for the alkali-calcic reduced probably occurred because only one mine was represented in the data set; the next best results for calc-alkalic weakly oxidized and reduced probably occurred because there so many samples in the training set.

Summary of Neural Network Effectiveness

The LVQ (Learning Vector Quantization) type of neural network is excellent in its ability to easily classify geochemical data into the six petrochemical classes in this study. It required very few iterations to converge on correct classes for the whole rock data and easily classified the mineralized trace element data. The back-propagation type of neural network took more

iterations to correctly classify the whole rock data, but was useful because it gave a percentage of certainty for each decision per sample rather than a simple yes or no (1 or 0) as in LVQ. Back propagation was also successful on the mineralized data, although the time required for learning was great. Neural networks, particularly LVQ, are a very effective means of classifying igneous whole rock data and mineralized trace element data from mining districts into petrochemical classes.

Once a network is trained on data from either fresh igneous rocks or mineralized trace elements from mining districts whose magma series class is known, the network can be tested on similar types of data from districts whose class is unknown. Thus, it will not be necessary to obtain whole rock data on fresh igneous rocks related to mineralization in order to correctly assign a magma series class to a mining district. Using neural networks, trace element data on the mineralized rock chips can be used to classify the district equally well.

CONCLUSIONS

The origin of metals in ore deposits has always been controversial, especially in debates concerning the importance of magmatic versus wall rock influences. Because the formation of an ore deposit cannot be witnessed directly, circumstantial evidence must be used to understand the process. Since the circulation of meteoric water is the most recent process, it overprints and obscures any earlier orthomagmatic processes or the possible contribution from a source region. As with most issues that have a great deal of irrefutable truth on both sides, the whole picture is probably a combination of both, either at different times in the sequence of events or at slightly different places.

Resolving these issues was beyond the scope of a doctoral dissertation, but a small piece of the challenge was an appropriate study. The magma series classification developed and used in the exploration industry by Stanley Keith (Keith and others, 1991) was judged to be a testable theory. This petrochemical classification predicted that certain types of ore deposits would be associated with particular categories of aluminum content, alkalinity, and oxidation state in fresh igneous rocks that were spatially and temporally related to mineralization. As the classification contained 75 classes, most of which were not well documented by analyses in the geologic literature, only six of the most common classes were selected for study.

Oxidized, weakly oxidized, and reduced subclasses in both alkali-calcic and calc-alkalic classes were tested. SiO_2/K_2O ratios of alkali-calcic igneous rocks

are 14-20 and of calc-alkalic 20-30. Fe_2O_3/FeO ratios are >0.8 with abundant magnetite and sphene for oxidized, 0.5-1.2 with magnetite, sphene, and rare ilmenite for weakly oxidized, and <0.6 with ilmenite only in reduced subclasses.

The petrochemical classification was evaluated by assigning 43 deposits to classes defined on eight variation diagrams, training neural networks to classify analyses of 569 igneous and 887 mineralized samples, and testing the networks on their ability to classify new data. Whole rock analyses were obtained from mining districts in which trace element geochemistry was also available, but half the data was eliminated using five alteration filter graphs. The K_2O and Fe_2O_3/FeO versus SiO_2 diagrams and iron mineralogy best defined alkalinity and oxidation classes. Neural networks trained with 90, 80, 70, or 50 percent of the samples correctly classified 81 to 100 percent of randomly withheld data.

This study established that the six alkalinity and oxidation classes of fresh igneous rocks correlate with trace elements in rock chip samples from temporally and spatially associated ore deposits. Learning vector quantization and back-propagation artificial neural networks correctly classified 100 percent of whole rock oxides and 99 percent of mineralized samples; discriminant analysis correctly classified 96 and 83 percent, respectively. The success of both computer classification methods was remarkable considering the high degree of variability in the data. Production and mineralogy from mines in those classes also demonstrated distinctions between the classes.

Lead-zinc-silver deposits as at Tombstone and Tintic are related to

oxidized alkali-calcic igneous rocks. Polymetallic lead-zinc-copper-tin-silver deposits, such as Santa Eulalia and Tempiute, Nevada, are associated with weakly oxidized alkali-calcic rocks. Tin-silver deposits of Llallagua and Potosi, Bolivia, are correlated with reduced alkali-calcic intrusives. Porphyry copper deposits as at Ray and Sierrita are connected with oxidized calc-alkalic plutons. Gold-rich porphyry copper deposits, such as Copper Canyon, Nevada, and Morenci and Ajo are linked to weakly oxidized calc-alkalic plutons. Disseminated gold deposits, such as Chimney Creek, Carlin, and Getchell, Nevada, are temporally and chemically correlated with reduced calc-alkalic igneous rocks, although physical connections between plutons and Carlin-type deposits are yet to be confirmed.

The six petrochemical classes investigated in this study are internally consistent through all types and scales of chemical information from microscopic trace elements to whole rock oxides and petrology of fresh igneous rocks to ore mineralogy to district-wide metal production. Thus, any type of compositional information can identify the magma series class, just as a broken fragment of a holograph transmits the same image as the whole.

For a classification to be meaningful and predictive it must be based on a fundamental truth, organizing principle, or causative process. Because the magma series classification was empirically developed by grouping similar ore deposits together and investigating the geochemistry of fresh igneous rocks related to them, correlation is built into the classification. If the metals in an ore deposit are one of the end products of differentiation of a Cogenetic Igneous-

Metal-Volatile suite, then one would expect that the ore characteristics would be divisible into the same classes as the igneous suites. The high degree of correlation between chemistries of igneous rocks and related mineralization demonstrated in this study implies genetic links between magmatic processes or sources and the ore deposits studied.

Internal Consistency of Petrochemical Classification

Both conventional statistics and neural networks correctly classified analyses of fresh igneous rocks and mineralized rock chips into the six magma series classes in this study. Two types of neural networks, back propagation and learning vector quantization (LVQ), accurately classified all the whole rock samples and 99 percent of the mineralized samples. The missed samples were ones that had been analyzed for fewer elements than most of the samples that had been used to train the network. Discriminant analysis correctly classified 88 percent of the whole rock samples and 76 percent of the mineralized samples.

These excellent results using computer methods are quite remarkable considering the amount of overlap into incorrect fields of some igneous samples and the high degree of variance in the mineralized samples. Many of the samples from each district fell outside of the correct field on the variation diagrams occupied by the majority of samples (Figures 3-16, 3-26). The neural networks were able to correctly classify even these outlying samples. The neural networks were also able to accurately classify the trace element samples in spite of

extremely high variances (Table 7-3, 7-4). Because there were sufficient numbers of samples from each mining district, the misclassified samples could be corrected based on the class that the neural network assigned to the majority of samples from that mine.

The care used in selecting whole rock analyses that determined the class assignment of each mining district contributed to the success of the study. Using only districts that were clear examples of each class, the neural networks were able to find recognizable differences in the trace element data. Confining the whole rock data to plutonic or porphyritic rocks and eliminating volcanics was significant in separating the oxidation subclasses. Using alteration filters to eliminate altered samples tightened the spread of points on the K_2O/SiO_2 variation diagrams into narrow bands for each alkalinity type. Using isotopic age dates to eliminate igneous rocks five million years older or younger than the mineralization was critical in several districts that had overlapping mineralization events of different alkalinities. The adages against 'mixing apples and oranges' and 'garbage in, garbage out' were heeded in this study with rewarding results.

Classification Efficiency of Neural Networks for Mineral Deposits

Effectiveness of Pattern Recognition by Neural Networks

Neural networks were very effective in classifying geochemical data into

the six petrochemical classes in this study. The LVQ networks were easier to use, faster, and more effective than the back propagation networks. The LVQ networks converged within ten minutes to correctly classify 100 percent of the igneous rocks and 99.6 percent of the mineralized samples. The back propagation networks required much longer training times of from one to eight hours and more experimentation to achieve the best configuration. The back-propagation networks were also not as effective as the LVQ networks and only achieved 99.2 percent accuracy on the fresh igneous samples and 93.3 percent on the mineralized rock chips. However, the back propagation test results yielded more useful information because the floating point outputs indicated the level of confidence for assigning each sample to the various classes.

The LVQ networks performed best when presented with more kinds of information. The poorest outcome on whole rock samples resulted from use of only the two parameters, SiO_2/K_2O and Fe_2O_3/FeO ratios, that were the chief classification criteria in defining the petrochemical class. The best results were when all the whole rock oxides, oxide ratios, some alteration indices, and magnetite and ilmenite concentrations from the modal mineralogy of the plutons were used. The neural networks were even able to correctly classify the samples when erroneous iron oxide data were included from those analyses that had combined Fe_2O_3 and FeO and assigned the total to one or the other category. The best results were obtained when samples with a zero in either Fe_2O_3 or FeO were omitted. The neural networks are obviously extracting useful classification

criteria from oxides or ratios in addition to the two ratios used to define the classes.

The LVQ networks also performed better with more processing elements in the hidden layer. Increasing the number of hidden PEs from 6 to 10 to 14 hastened the convergence time from 20,000 to 9,000 iterations and increased the accuracy from 92 percent to 100 percent.

Testing the networks that had been trained on data sets with 10, 20, 30 and 50 percent of the samples randomly removed showed little difference in the number of withheld test cases that were missed. Accuracy ranged from 82 to 94 percent when the networks that had been trained on the limited data sets were tested with the full data set. The networks missed from 6 to 18 percent of the test cases, with some of the best results from the most limited training sets. Which samples were removed was more important than how many were removed, up to a point. Some of the samples that defined the limits of the class were probably withheld in those trials that missed the most test cases.

Comparison of Neural Networks with Conventional Statistics

Neural networks were much more effective in classifying samples into the six petrochemical classes than discriminant analysis. The LVQ neural networks correctly classified 100 percent of the igneous samples and 99 percent of the mineralized samples; the back propagation networks correctly classified 99.2 percent of the igneous and 93.3 percent of the mineralized samples. Discriminant

analysis correctly classified only 88 percent of the igneous samples and 76 percent of the mineralized ones.

The better performance of neural networks compared to statistics was probably related to the distribution of the data in the igneous samples. Most whole rock oxides varied positively or negatively with SiO_2 and formed narrow bands on Harker variation diagrams. Mines were assigned to magma series classes based on their position on those graphs (Chapters 3 and 4). Because class boundaries were defined by the linked changes in two parameters, particularly the increase in K_2O with increasing SiO_2, means of any single parameter did not effectively distinguish between the classes. Even though the whole rock data generally had normal distributions, the means and standard deviations of oxides from different classes overlapped. The exceptions were the SiO_2/K_2O ratio, which represented the K_2O versus SiO_2 variation diagram that defined the alkalinity classes, and the Fe_2O_3/FeO ratio, which defined the oxidation state subclasses.

The poor performance of discriminant analysis on the mineralized samples was probably a result of the erratic data distribution partly caused by the nonstandard analyses, as samples were not analyzed for the same chemical elements in each class. Most of the samples contained zeros for more than ten of the 32 elements and the missing ones differed throughout the data set. The mineralized data was also not normally distributed, but had abrupt cutoffs on one side or the other, with very large numbers of samples in the zero or lowest bin,

and erratic groupings throughout the range. Discriminant analysis is based on the assumption that the samples have a normal distribution and that the examples are typical of the larger group. With an asymmetrical data distribution and missing chemical analyses, neither of these assumptions was correct for the mineralized data set. Therefore, means and standard deviations of this data were not as useful in distinguishing petrochemical classes as they are in populations that have a normal distribution and complete data sets.

Possible Applications of Techniques in this Study

Only compositional end results of the ore deposition process were studied in this dissertation on six types of deposits, in order to limit the scope of the study, yet allow a thorough evaluation. Structural and environmental features are also extremely important and they have been the object of many other studies. The trace elements, mineralogy, and production of the ore deposits were correlated with the whole rock geochemistry of fresh igneous rocks associated with the mineralization. The application of neural networks to classify geochemical data is a technique with great promise in economic geology.

Alteration Filters

The alteration filters used in this study, such as Figure 3-3, were very effective in eliminating scatter from the variation diagrams used to assign mining districts to petrochemical classes. The alteration indices, particularly the K

index, Na index, A/CNK ratio, and alteration index, would also be very effective exploration tools if they were plotted on maps to show areas of a pluton that were most affected by alteration. These spatial alteration patterns could be recognized by neural networks in areas where mineralization is not obvious. Neural networks could also be used to distinguish horizontal or vertical alteration zoning patterns that are characteristic of various ore deposit types or wall rock types.

Exploration Application of Petrochemical Classification

Because this study has demonstrated the correlation of petrochemical classes with six types of ore deposits, exploration could be based on either kind of information. If mineralization is present, the trace element geochemistry of rock chip samples could distinguish the type of ore deposit that is potentially present. As not all examples of each class produce ore deposits, standard economic evaluations would also be required. However, the correlation of prospects with petrochemical classes would indicate if further evaluation was warranted. Many companies have an abundance of information on prospects in their files that could be subjected to the type of analysis in this study to determine if the claims should continue to be held or if they should be dropped.

If only igneous rocks were present without obvious veins or mineralization, potential mineralization of the particular ore deposit type could be predicted by the petrochemical class. As not all igneous rocks of a particular class are

associated with ore deposits, structural studies and other standard exploration investigations should also be applied. However, the magma series classification is an inexpensive preliminary step that can eliminate prospects that do not fall into the targeted type of deposit. For example, even though alkali-calcic oxidized silver deposits have some gold and copper in the trace element analyses, they would not make good exploration targets for porphyry copper deposits or Carlin-type gold deposits. In addition, simply because one igneous complex of a particular age indicates alkali-calcic oxidized silver deposits, it does not preclude the existence of a different type of ore deposit associated with a considerably later or earlier igneous complex in the same area. Sampling all the igneous complexes for whole rock oxides, preparing a geologic sketch map, and understanding the age relationships in a prospective area are important in an exploration project and much cheaper than an improperly located drill hole.

Neural Networks

The success of neural networks in classifying geochemical data in this study indicates their usefulness in mineral exploration and in deciphering geological systems. Trace element data from exploration projects of unknown ore types can be tested on the networks trained in this study to determine the types of deposits that could be found. The networks trained in this study correctly classify unknowns if they are of the six classes in this study. If the unknowns are from classes unknown to the network, the network will classify the unknown into

the most similar class, an inherently flawed conclusion. However, this problem can be rectified by adding an Adaptive Resonance Theory (ART) neural network prefaced to the previously trained networks in order to detect novel classes. In order to correctly classify any unknown district without the ART, the network would have to be trained with analyses of samples from all of the classes. This training could be done in hierarchial steps, such as first determining peraluminous or metaluminous classes, then determining alkalinity classes, and then determining oxidation subclasses. Although some classes are not well documented with large numbers of analyses, data are available for most classes in Table 2-2. Collecting this type of data is an ongoing project, with more data accumulating for those types of deposits that are in economic demand.

Neural networks can be applied to geological patterns at many different scales. This study detected patterns in the broadest range of data that could be used to classify the type of ore deposit. Within each deposit type, more detailed representation of the areal distribution of the data would allow a neural network to find zoning patterns within the trace element data, alteration, fracture density, ore grade or type, or whole rock data. As long as there are numerically definable differences in the data, neural networks can be trained to detect those patterns. The challenge is to define training patterns that have predictive value in exploring for ore deposits. The petrochemical classification has this predictive power because it was empirically based on the correlation between ore deposit types and natural geological processes.

APPENDIX A: LOCATION AND DESCRIPTION OF SAMPLES COLLECTED BY MAGMACHEM EXPLORATION, INC., STAFF

88-1262 Alabaugh Creek, MT, Castle mining district, White Sulphur Springs 1x2° quadrangle, SW 1/4, SE 1/4, sec. 27, T.8N., R.9E., medium-grained hornblende (~4%) biotite (~3%) monzodiorite porphyry dike.

88-1263 Alabaugh Creek, MT, Castle mining district, White Sulphur Springs 1x2° quadrangle, SW 1/4, SE 1/4, sec. 27, T.8N., R.9E., medium-grained hornblende (~4%) biotite (~3%) monzodiorite porphyry dike, with trace pyrite.

88-1271 Castle mining district, at head of Robinson Creek, White Sulphur Springs 1x2° quadrangle, SW 1/4, SW 1/4, sec. 6, T.8N., R.9E., medium-grained biotite monzodiorite, weakly magnetic.

88-1560 Cherry Creek mining district, White Pine County Mineral Resource Map (1:250,000), T.24N., R.62E., section 36, medium-grained biotite granite porphyry (biotite - 14%), with biotites showing some bronziness and with minor iron staining around some of the biotites, K-feldspar up to 2 cm.

88-1561 Cherry Creek mining district, White Pine County Mineral Resource Map (1:250,000), T.24N., R.62E., section 36, same as 1560.

88-1577 Kinsley Range, Elko County (1:250,000), T.26N., R.68E., section 18; medium-grained biotite hornblende granite; (7% biotite, 1-2% hornblende, trace of sphene), mafics are black and fresh.

88-1578 Kinsley Range, Elko County (1:250,000), T.26N., R.68E., section 18; medium-grained biotite hornblende granite; (7% biotite, 1-2% hornblende, trace of sphene), mafics are black and fresh (same as 1577).

88-1579 Kinsley Range, Elko County (1:250,000), T.26N., R.68E., section 18; fine-grained biotite hornblende granite; (fine-grained phase of 1577 and 1578); biotite about 1%, about 0.4 cm; black and fresh.

88-0880 Linka mine, Lander County, Nevada geologic map (1:250,000), T.17N, R.46E., west border of sections 17 and 20; medium- to fine-grained biotite (~30%) monzodiorite, biotite is pretty fresh, (~10% quartz), has an unidentified mineral that fluoresces under ultraviolet lamp.

88-0881 Linka mine, Lander County, Nevada geologic map (1:250,000), T.17N, R.46E., west border of sections 17 and 20; biotite hornblende rhyodacite porphyry dike, presumable intruded Linka stock, but relationship to tungsten skarn is uncertain as it could be much younger, iron-magnesium minerals are moderately chloritized. Plagioclase is slightly cloudy.

88-0883 Linka mine, Lander County, Nevada geologic map (1:250,000), T.17N, R.46E., west border of sections 17 and 20; biotite monzodiorite similar to 88-0881 (medium- to fine-grained biotite (~30%) monzodiorite, biotite is pretty fresh, (~10% quartz), has an unidentified mineral that fluoresces under ultraviolet lamp),

88-0884 Linka mine, Lander County, Nevada geologic map (1:250,000), T.17N, R.46E., west border of sections 17 and 20; medium-grained hornblende (20-25%) quartz monzonite (with a trace of biotite and apatite). Hornblende is locally altered to iron oxide in cores. Sample is float collected at mill site foundation which is build on biotite monzodiorite.

88-1051 Swales Mountain, 3-5 Nevada map atlas, NW 1/4, SE 1/4, section 8, T.35N, R.53E.; fine-grained biotite granite (~2-3% biotite, black and fresh).

88-1052 Swales Mountain, 3-5 Nevada map atlas, NW 1/4, SE 1/4, section 8, T.35N, R.53E.; same as 88-1051 (fine-grained biotite granite (~2-3% biotite, black and fresh)).

88-1547 Taylor dike, White Pine County Mineral Resource Map, T.14N., R.65E.; drill core material of dikes (D-16 (173); fine-grained dacite porphyry; biotite (~1%, black and fresh).

88-1548 Taylor dike, White Pine County Mineral Resource Map, T.14N., R.65E.; (same as 88-1547) drill core material of dikes (D-16 (173); fine-grained dacite porphyry; biotite (~1%, black and fresh).

88-1549 Taylor dike, White Pine County Mineral Resource Map, T.14N., R.65E.; (same as 88-1547) drill core material of dikes (D-16 (173); fine-grained dacite porphyry; biotite (~1%, black and fresh).

88-1096 Elk Mountain, Jarbridge Mountain 1:100,000 map, SE 1/4, NW 1/4, Sec. 10, T.46N., R.61E.; fine-grained aplitic phase of granite found within

coarse-grained granite; some biotite showed minimum oxidation rings around the grains.

88-1097 Elk Mountain, Jarbridge Mountain 1:100,000 map, NE 1/4, SE 1/4, Sec. 10, T.46N., R.61E.; biotite-hornblende granite; sample has some thin outside weathered surfaces. K-feldspar crystals range in size up to 1 1/4 inches long; biotite and hornblende are fresh and black.

88-1098 Elk Mountain, Jarbridge Mountain 1:1,000 map, NE 1/4, SW 1/4, Sec. 10, T.46N., R.61E; coarse-grained biotite-hornblende granite with K-feldspar crystals up to 1 1/4 inches long; sample has slight FeO staining along cracks.

88-0290 Bald Mountain, White Pine County, Nevada; biotite granodiorite porphyry, medium to medium-coarse grained biotite granodiorite with trace hornblende; conspicuous orthoclase porphyrocrysts. Biotite has a slight bronzy tinge, but sample otherwise appears fairly fresh.

88-0291 Bald Mountain, White Pine County, Nevada; biotite-hornblende granodiorite porphyry as in #290, but biotites are black; this is the freshest sample of the three.

88-0292 Bald Mountain, White Pine County, Nevada; biotite rhyodacite porphyry dikes from Bald Mountain pluton; contains slightly bronzy biotite to 1/2 cm, K-spar, and resorbed quartz eyes set in greenish-gray aphanitic ground mass.

88-0281 Asa Moore Canyon, Osgood Mountains quadrangle, scale 1:100,000, Nevada, NW 1/4, NE 1/4, Sec. 17, T.39N., R.38E.; medium-fine-grained biotite hornblende granodiorite from Asa Moore pluton. Biotite is very weakly chloritized and very slightly decomposed.

88-0282 Asa Moore Canyon, Osgood Mountains quadrangle, scale 1:100,000, Nevada, SW 1/4, NW 1/4, Sec. 7, T.39N., R.38E.; fine-grained aplitic biotite granite from one foot wide dike cutting granodiorite of Asa Moore pluton; biotite is fresh. Dike strikes N.55°W. at 80°SW.

88-0283 Asa Moore Canyon, Osgood Mountains quadrangle, scale 1:100,000, Nevada, SW 1/4, NW 1/4, Sec. 7, T.39N., R.38E.; medium-fine-grained biotite-hornblende granodiorite from Asa Moore pluton.

88-0284 Asa Moore Canyon, Osgood Mountains quadrangle, scale 1:100,000, Nevada, SW 1/4, NW 1/4, Sec. 7, T.39N., R.38E.; very fine-grained aplite

dike (8 inches thick) cutting biotite hornblende granodiorite of Asa Moore pluton; contains trace of biotite.

1000 Santa Eulalia, Mexico, West Camp Drill Hole #1813, at 1750 feet, deep granodiorite (probably same as no. 5 in Megaw, 1990, p. 380).

1001 Santa Eulalia, Mexico, West Camp Drill Hole #1813 at 700 feet from collar, felsite (probably same as no. 1 in Megaw, 1990, p. 380).

1005 Santa Eulalia, Mexico, East Camp Drill Hole #1199 at 850 feet from collar, San Antonio felsite, phenocryst poor, remote from ore (probably same as no. 2 in Megaw, 1990, p. 380).

1006 Santa Eulalia, Mexico, San Antonio mine, 14 level, from core of major skarn ore zone , mineralized and altered (probably same as no. 3 in Megaw, 1990, p. 380).

R6-GD 1773-1780' Santa Eulalia, Mexico, Buena Tierra mine Drill Hole, granodiorite.

R6-829 Santa Eulalia, Mexico, dike margin.

R6-879 Santa Eulalia, Mexico, rholite, 'pretty fresh', minor MnO, hematite.

APPENDIX B: WHOLE ROCK DATA FROM IGNEOUS ROCKS ASSOCIATED WITH MINERALIZATION

MACo incl.	Alabaugh C	Alabaugh C	Robinson/C	Robinson/C	Ontario stoc	Ontario stoc	Ontario sto	Alta Stock	Alta Stock	Alta Stock	Alta Stock	Alta stock	Alta Stock	Alta Stock
COUNTY	Meagher	Meagher	Meagher	Meagher	Summit	Summit	Summit	Summit	Summit	Summit	Summit	Summit	Summit	Summit
STATE	MT	MT	MT	MT	UT	UT	UT	2	UT	UT	UT	UT	UT	UT
SAMPLE #	1262	1263	1271	XI (4)	PC-392	PC-393	3o	82-PC-17	82-PC-206	82-PC-272	82-PC-276	PC-392	PC-26	2
NAME	CASTLE	CASTLE	CASTLE	CASTLE	PARKCITY	PARKCITY	PARKCITY	PARKCITY	PARKCITY	PARKCITY	PARKCITY	PARKCITY	PARKCITY	PARKCITY
SOURCE:	MagmaChe	MagmaChe	MagmaChe	Weed & Pir	Bromfield et	Bromfield et	Villas & Nor	John, 1991	John, 1991	John, 1991	John, 1991	Bromfield et	Bromfield et	Calkins & B
Rock Type	monzodiorit	monzodiorit	biotite mon	diorite	porphyry st	porphyry st	----------	granodiorite	granodiorite	granodiorite	granodiorite	seriate porp	seriate porp	granodiorite
SiO2	66.15	66.16	56.07	56.8	64	65.1	60.8	62.90	63.50	63.90	67.20	61.80	67.20	65.27
TiO2	0.59	0.57	1.27	0.46	0.58	0.53	?	0.58	0.58	0.58	0.50	0.53	0.44	0.55
Al2O3	14.75	14.59	17.71	18.3	15.2	15	16.7	16.40	16.60	16.00	15.50	16.90	15.10	15.75
Fe2O3	1.47	1.58	3.34	1.64	2.4	2.2	3.96	2.48	2.53	2.30	1.56	2.40	2.30	2.31
FeO	1.7	1.55	2.9	5.58	2.5	2.4	1.2	2.43	2.13	2.15	1.71	2.40	1.80	1.85
MgO	2.07	2	2.97	3.63	2.3	2.2	1.81	2.25	1.81	2.19	1.61	2.20	1.80	1.62
MnO	0.05	0.05	0.07	-0.02	0.13	0.11	?	0.08	0.08	0.05	0.03	0.11	0.04	0.10
CaO	2.9	3.02	5.29	5.31	4.4	4.4	3.15	4.84	4.39	4.21	2.73	5.10	3.30	4.09
Na2O	4.31	4.34	4.59	4.35	3.5	3.4	5.39	3.66	3.88	3.70	3.38	3.90	3.00	3.92
K2O	3.73	3.65	3.04	3.28	3.6	3.3	3.6	2.99	3.14	3.08	4.22	3.10	3.50	3.25
P2O5	0.31	0.3	0.53	-0.5	0.27	0.24	?	0.32	0.32	0.29	0.26	0.46	0.40	0.25
LOI	0.5	0.7	0.2	0.55	0.71	0.61	1.17	0.23	0.31	0.67	0.58	1.12	0.86	0.74
TOTAL	98.53	98.51	97.98	99.93	100	100	97.8	99.16	99.27	99.12	99.28	100.00	100.00	99.91
Mining Dist.	Castle	Castle	Castle	Castle	Park City	Park City	Park City	Park City	Park City	Park City	Park City	Park City	Park City	Park City
Ba	2100	2100	1500	0	0	0	0	1300	1750	2000	1350	0	0	0
Rb	77	81	63	0	0	0	0	91	116	109	184	0	0	0
Sr	570	591	880	0	0	0	0	680	696	745	450	0	0	0
Y	0	0	14	0	0	0	0	20	20	25	25	20	0	0
Zr	160	170	280	0	0	0	0	177	10	1500	161	0	0	0
Nb	27	26	38	0	0	0	0	8	1	500	13	0	0	0
CLASS	MACo	MACo	MACo	MACo	MACo	MACo	MACo	MACo	MACo	MACo	MACo	MACo	MACo	MACo
A/CNK	0.898	0.879	0.865	0.898	0.860	0.873	0.902	0.907	0.933	0.936	1.026	0.886	1.024	0.904
A/NK	1.32	1.31	1.63	1.71	1.57	1.63	1.31	1.77	1.70	1.70	1.53	1.73	1.73	1.58
Na2O+K2	8.04	7.99	7.63	7.63	7.10	6.70	8.99	6.65	7.02	6.78	7.60	7.00	6.50	7.17
Na2O/K2O	1.16	1.19	1.51	1.33	0.97	1.03	1.50	1.22	1.24	1.20	0.80	1.26	0.86	1.21
NaO+K2O-	5.14	4.97	2.34	2.32	2.70	2.30	5.84	1.81	2.63	2.57	4.87	1.90	3.20	3.08
K2O-CaO	0.83	0.63	-2.25	-2.03	-0.80	-1.10	0.45	-1.85	-1.25	-1.13	1.49	-2.00	0.20	-0.84
K2O-MgO	1.66	1.65	0.07	-0.35	1.30	1.10	1.79	0.74	1.33	0.89	2.61	0.90	1.70	1.63
FeO/MgO*	1.46	1.49	1.99	1.94	2.03	1.99	2.63	2.07	2.43	1.93	1.93	2.07	2.15	2.43
Fe3+/Fe2+	0.86	1.02	1.15	0.29	0.96	0.92	3.30	1.02	1.19	1.07	0.91	1.00	1.28	1.25
LARSEN	20.81	20.68	13.47	13.27	18.23	18.40	18.91	16.87	18.11	17.98	22.28	16.40	20.80	19.30
ALKALI IN	-0.57	-0.62	2.77	2.50	-0.71	-1.52	2.37	-0.75	-0.60	-0.99	-1.40	0.01	-2.50	-1.11
ALT INDE	44.581	43.428	37.823	41.702	42.754	41.353	38.781	38.137	37.443	39.985	48.827	37.063	45.690	37.811
K INDEX	1.71	1.67	0.95	0.91	1.04	1.01	2.48	1.22	1.35	1.41	2.07	1.23	1.63	1.48
Na INDEX	2.0538	2.0679	2.3744	2.2238	1.8320	1.9030	2.3994	2.1311	2.1690	2.1371	1.8266	2.1443	1.8813	2.1100
Al2O3/Na2	3.422274	3.361751	3.858388	4.206897	4.342857	4.411765	3.09833	4.480874	4.278351	4.324324	4.585799	4.333333	5.033333	4.017857
SiO2/Al2O	4.4847	4.5346	3.1660	3.1038	4.2105	4.3400	3.6407	3.8354	3.8253	3.9938	4.3355	3.6568	4.4503	4.1441
Ti/Nb	131.11	131.54	200.53	2760.00	3480.00	3180.00	0.00	435.00	3480.00	6.96	230.77	3180.00	2640.00	3300.00
----------	----------	----------	----------	----------	----------	----------	----------	----------	----------	----------	----------	----------	----------	----------
use?	ok	ok	ok	no	ok	ok	no	ok	ok	ok	ok	ok	ok	ok
altered?							alt.KI							
why not use				differ. rx										

MACo incl.	Alta Stock	Alta Stock	Alta stock	Alta stock	Clayton Pea	Clayton Pea	Clayton Pe	Clayton Pea	Pine Creek	Pine Creek	Pine Creek	Valeo stock	Valeo stock	Flagstaff sto
COUNTY	Summit	Summit	Summit	Summit	Summit	Summit	Summit	Summit	Summit	Summit	Summit	Summit	Summit	Summit
STATE	UT	UT	UT	UT	UT	UT	UT	UT	UT	UT	UT	UT	UT	UT
SAMPLE #	3	4	5a	5b	3cp	5	PC-380	PC-25	PC-27	PC-202	3pc	PC-379	PC-1	PC-133
NAME	PARKCITY	PARKCITY	PARKCITY	PARKCITY	PARKCITY	PARKCITY	PARKCITY	PARKCITY	PARKCITY	PARKCITY	PARKCITY	PARKCITY	PARKCITY	PARKCITY
SOURCE:	Calkins & B	Calkins & B	Wilson, 196	Wilson, 196	Villas & Nor	Calkins & B	Bromfield et	Bromfield et	Bromfield et	Bromfield et	Villas & Nor	Bromfield et	Bromfield et	Bromfield et
Rock Type	granodiorite	granodiorite	----------	----------	----------	qtz. diorite	----------	----------	porphyry st	porphyry st	----------	porphyry st	porphyry st	porphyry st
SiO2	63.46	62.16	63.92	63.70	61.40	59.35	58.20	58.90	63.4	60.5	60.70	63.5	66.1	60
TiO2	0.62	0.53	0.61	0.53	?	0.87	0.94	0.95	0.55	0.48		0.48	0.42	0.8
Al2O3	15.93	17.17	16.13	15.89	17.90	16.36	16.80	15.90	16.3	16.5	17.50	16.2	16.1	16
Fe2O3	2.61	2.26	2.03	2.09	2.90	2.90	2.40	2.70	2.9	2.7	3.05	2	2.1	2.9
FeO	2.31	2.78	2.43	1.97	3.36	3.36	3.80	4.10	1.7	1.7	1.89	2.1	1.7	2.6
MgO	2.27	1.81	1.90	1.73	2.22	3.08	3.00	4.20	2.2	2.2	2.49	2	1.9	2.9
MnO	0.09	0.06	0.08	0.07	?	0.07	0.12	0.06	0.05	0.08	?	0.13	0.05	0.17
CaO	4.33	4.70	4.50	4.07	4.30	5.03	5.30	5.70	4.6	5.8	4.60	4.5	3.2	6
Na2O	3.66	3.96	3.96	3.85	4.48	3.73	3.60	2.90	3.6	4.1	4.46	4.2	3.4	3.9
K2O	3.49	3.58	3.24	3.19	2.40	3.85	4.00	3.20	2.3	2.2	2.54	3	2.7	2.5
P2O5	0.16	0.17	0.31	0.25	?	0.44	0.61	0.55	0.52	0.4	?	0.18	0.52	0.39
LOI	1.01	0.63	0.45	0.52	?	0.92	1.20	0.76	1.09	2.68	1.00	1.15	1.25	1.83
TOTAL	100.17	100.03	99.37	99.86	100.00	100.29	100.00	100.00	99	99	98.20	99	99	100
Mining Dist.	Park City	Park City	Park City	Park City	Park City	Park City	Park City	Park City	Park City	Park City	Park City	Park City	Park City	Park City
Ba	0	0	0	0	0	0	0	0	0	0	0	0	0	0
Rb	0	0	0	0	0	0	0	0	0	0	0	0	0	0
Sr	0	0	0	0	0	0	0	0	0	0	0	0	0	0
Y	0	0	0	0	0	0	0	0	0	0	0	0	0	0
Zr	0	0	0	0	0	0	0	0	0	0	0	0	0	0
Nb	0	0	0	0	0	0	0	0	0	0	0	0	0	0
CLASS	MACo	MACo	MACo	MACo	MACo	MACo	MACo	MACo	MCAo	MCAo	MCAo	MCAo	MCAo	MCAo
A/CNK	0.900	0.906	0.885	0.923	3.448	0.840	0.844	0.854	0.970	0.838	0.947	0.882	1.122	0.798
A/NK	1.62	1.65	1.61	1.62	6.16	1.59	1.64	1.93	1.94	1.81	1.73	1.59	1.89	1.75
Na2O+K2	7.15	7.54	7.20	7.04	6.88	7.58	7.60	6.10	5.90	6.30	7.00	7.20	6.10	6.40
Na2O/K2O	1.05	1.11	1.22	1.21	1.87	0.97	0.90	0.91	1.57	1.86	1.76	1.40	1.26	1.56
NaO+K2O-	2.82	2.84	2.70	2.97	2.58	2.55	2.30	0.40	1.30	0.50	2.40	2.70	2.90	0.40
K2O-CaO	-0.84	-1.12	-1.26	-0.88	-1.90	-1.18	-1.30	-2.50	-2.30	-3.60	-2.06	-1.50	-0.50	-3.50
K2O-MgO	1.22	1.77	1.34	1.46	0.18	0.77	1.00	-1.00	0.10	0.00	0.05	1.00	0.80	-0.40
FeO/MgO*	2.05	2.66	2.24	2.23	2.69	1.94	1.99	1.55	1.96	1.88	1.86	1.95	1.89	1.80
Fe3+/Fe2+	1.13	0.81	0.84	1.06	0.86	0.86	0.63	0.66	1.71	1.59	1.61	0.95	1.24	1.12
LARSEN	18.04	17.79	18.15	18.62	16.35	15.52	15.10	12.93	16.63	14.37	15.68	17.67	19.63	13.60
ALKALI IN	-0.46	0.42	-0.58	-0.66	0.04	1.50	1.95	0.19	-1.68	-0.21	0.42	-0.42	-2.49	0.08
ALT INDE	41.891	38.363	37.794	38.318	34.478	44.168	44.025	46.250	35.433	30.769	35.699	36.496	41.071	35.294
K INDEX	1.42	1.25	1.31	1.45	1.19	1.27	1.16	1.05	1.29	1.13	1.46	1.39	1.63	1.08
Na INDEX	1.9490	2.0117	2.1072	2.1303	5.3148	1.8088	1.7435	1.7599	2.5356	2.7013	2.7033	2.2823	2.3811	2.3577
Al2O3/Na2	4.352459	4.335859	4.073232	4.127273	13.70536	4.386059	4.666667	5.482759	4.527778	4.02439	3.923767	3.857143	4.735294	4.102564
SiO2/Al2O	3.9837	3.6203	3.9628	4.0088	1.0000	3.6278	3.4643	3.7044	3.8896	3.6667	3.4686	3.9198	4.1056	3.7500
Ti/Nb	3720.00	3180.00	3660.00	3180.00	0.00	5220.00	5640.00	5700.00	3300.00	2880.00	0.00	2880.00	2520.00	4800.00
use?	ok	ok	ok	ok	no	ok	ok	ok	no	no	no	no	no	no
altered?										alt.LOI				
why not use									older	older	older	older	older	older

MACo incl.	Flagstaff sto	Flagstaff st	Mayflower s	Mayflower s	Mayflower s	Packard Qu	Packard Qu	Packard Qu	Packard Qu	Packard Qu	Packard Qu	Packard Qu	Swansea Q	Copperopoli
COUNTY	Summit	Summit	Summit	Summit	Summit	Juab-Utah	Juab-Utah	Juab-Utah	Juab-Utah	Juab-Utah	Juab-Utah	Juab-Utah	Juab-Utah	Juab-Utah
STATE	UT	UT	UT	UT	UT	UT	UT	UT	UT	UT	UT	UT	UT	UT
SAMPLE #	PC-5	3f	2pc	PC-388	PC-69	1-D102203	2	3-D102204	4-D101864	5	6-D101871	7-D101872	10-D10225	1-M110-361
NAME	PARKCITY	PARKCITY	PARKCITY	PARKCITY	PARKCITY	TINTIC	TINTIC	TINTIC	TINTIC	TINTIC	TINTIC	TINTIC	TINTIC	TINTIC
SOURCE:	Bromfield et	Villas & Nor	Villas, 1975	Bromfield et	Bromfield et	Morris & Lo	Morris & Lo	Morris & Lo	Morris & Lo	Morris & Lo	Morris & Lo	Morris & Lo	Morris & Lo	Morris & Lo
Rock Type	porphyry st	----------	----------	porphyry st	porphyry st	lower vitrop	qtz latite	por. qtz.latit	por. qtz.latit	por. qtz.latit	por. qtz.latit	por. qtz.latit	qtz.monz.	latite
SiO2	61.9	59.50	61.11	62.3	59.3	67.68	71.1	70.87	69.76	70.82	69.27	69.33	70.08	60.2
TiO2	0.64	?	0.82	0.55	0.69	0.38	0.39	0.38	0.36	0.34	0.34	0.35	0.41	0.89
Al2O3	16.9	17.20	18.20	16.3	16.4	14.73	14.45	14.36	14.75	13.95	14.52	14.49	15.01	19
Fe2O3	2.7	2.66	?	2.2	3.7	1.71	2.02	1.91	2.16	1.82	1.64	1.63	1.66	2.5
FeO	2.2	2.54	3.93	2.1	1.9	0.59	0.61	0.49	0.22	1.46	0.52	0.53	0.57	1.2
MgO	2.6	2.93	3.04	2.6	2.5	0.67	0.48	0.46	0.5	0.43	0.59	0.59	0.69	1
MnO	0.1	?	0.10	0.11	0.05	0.06	0.05	0.03	0.04	0.02	0.06	0.06	0.07	0.08
CaO	4	3.09	5.10	3.7	5.4	2.5	2.01	1.62	2.2	1.94	2.08	2.05	1.12	4.7
Na2O	3.6	4.26	3.94	4.4	3.7	3.05	2.78	2.61	3.02	2.76	2.96	2.89	2.96	3.5
K2O	2.5	2.37	2.95	2.9	3.8	3.98	5.13	5.95	4.5	4.18	4.67	4.79	5.69	4.7
P2O5	0.45	?	?	0.14	0.35	0.13	0.14	0.18	0.11	0.14	0.1	0.1	0.12	0.35
LOI	1.85	2.79	<1.18	2.6	1.55	4.25	0.58	0.56	2.11	1.91	2.8	2.76	1.09	1.81
TOTAL	99	97.30	100.37	100	99	99.66	99.94	99.39	99.68	99.77	99.51	99.52	99.44	100.00
Mining Dist.	Park City	Park City	Park City	Park City	Park City	Tintic	Tintic	Tintic	Tintic	Tintic	Tintic	Tintic	Tintic	Tintic
Ba	0	0	0	0	0	2000	0	2000	3000	0	3000	3000	3000	2000
Rb	0	0	0	0	0	0	0	0	0	0	0	0	0	0
Sr	0	0	0	0	0	700	0	500	500	0	300	500	500	1000
Y	0	0	0	0	0	30	0	30	20	0	15	15	30	30
Zr	0	0	0	0	0	200	0	200	150	0	150	150	100	300
Nb	0	0	0	0	0	10	0	10	0	0	0	0	10	15
CLASS	MCAo	MCAo	MACo	MACo	MACo	MACo	MACo	MACo	MACo	MACo	MACo	MACo	MACo	MACo
A/CNK	1.061	1.131	0.959	0.952	0.818	1.060	1.047	1.048	1.064	1.106	1.058	1.059	1.147	0.978
A/NK	1.96	1.80	1.88	1.57	1.61	1.58	1.43	1.34	1.50	1.54	1.46	1.46	1.36	1.75
Na2O+K2	6.10	6.63	6.89	7.30	7.50	7.03	7.91	8.56	7.52	6.94	7.63	7.68	8.65	8.20
Na2O/K2O	1.44	1.80	1.34	1.52	0.97	0.77	0.54	0.44	0.67	0.66	0.63	0.60	0.52	0.74
NaO+K2O-	2.10	3.54	1.79	3.60	2.10	4.53	5.90	6.94	5.32	5.00	5.55	5.63	7.53	3.50
K2O-CaO	-1.50	-0.72	-2.15	-0.80	-1.60	1.48	3.12	4.33	2.30	2.24	2.59	2.74	4.57	0.00
K2O-MgO	-0.10	-0.56	-0.09	0.30	1.30	3.31	4.65	5.49	4.00	3.75	4.08	4.20	5.00	3.70
FeO/MgO*	1.78	1.68	1.29	1.57	2.09	3.18	5.06	4.80	4.33	7.20	3.38	3.38	2.99	3.45
Fe3+/Fe2+	1.23	1.05	0.00	1.05	1.95	2.90	3.31	3.90	9.82	1.25	3.15	3.08	2.91	2.08
LARSEN	16.53	16.18	15.18	17.37	15.67	23.37	26.34	27.49	25.05	25.42	25.09	25.26	27.24	19.07
ALKALI IN	-0.93	0.50	0.16	0.12	1.44	-2.15	-2.54	-1.80	-2.43	-3.41	-2.14	-2.11	-1.42	1.81
ALT INDE	40.157	41.897	39.854	40.441	40.909	45.588	53.942	60.244	48.924	49.517	51.068	52.132	60.994	41.007
K INDEX	1.40	1.70	1.10	1.71	1.37	1.66	1.89	2.36	1.84	1.46	2.02	2.04	2.93	1.13
Na INDEX	2.5015	2.9284	2.2949	2.4691	1.7918	1.8268	1.5889	1.4868	1.7354	1.7666	1.6917	1.6621	1.6674	1.7231
Al2O3/Na2	4.694444	4.037559	4.619289	3.704545	4.432432	4.829508	5.197842	5.501916	4.884106	5.054348	4.905405	5.013841	5.070946	5.428571
SiO2/Al2O	3.6627	3.4593	3.3577	3.8221	3.6159	4.5947	4.9204	4.9352	4.7295	5.0767	4.7707	4.7847	4.6689	3.1684
Ti/Nb	3840.00	0.00	4920.00	3300.00	4140.00	228.00	2340.00	228.00	2160.00	2040.00	2040.00	2100.00	246.00	356.00
use?	no	no	no	no	ok	no	no	no	no	no	no	no	no	no
altered?		alt.LOI		alt.LOI		alt.LOI		alt.KI	alt.LOI		alt.LOI	alt.LOI	alt.KI	
why not use	older	older				volc	volc	volc	volc	volc	volc	volc	volc	volc

MACo incl.	Copperopoli	Latite Ridge	Latite Ridge	Big Canyon	Gough sill	Gough sill	Gough sill	Latite brecc	Sunrise Pe	Pinyon Que	Pinyon Que	Tintic Delm	Silver City s	Silver City s
COUNTY	Juab-Utah	Juab-Utah	Juab-Utah	Juab-Utah	Juab-Utah	Juab-Utah	Juab-Utah	Juab-Utah	Juab-Utah	Juab-Utah	Juab-Utah	Juab-Utah	Juab-Utah	Juab-Utah
STATE	UT	UT	UT	UT	UT	UT	UT	UT	UT	UT	UT	UT	UT	UT
SAMPLE #	1-M110-362	3-M110-35	4-D102257	5-M110-359	6-M110-363	7-M110-364	8-D101873	9-D102260	10	1-M110-35	2-D102256	3-M110-365	4-D102261	5-D102259
NAME	TINTIC	TINTIC	TINTIC	TINTIC	TINTIC	TINTIC	TINTIC	TINTIC	TINTIC	TINTIC	TINTIC	TINTIC	TINTIC	TINTIC
SOURCE:	Morris & Lo	Morris & Lo	Morris & Lo	Morris & Lo	Morris & Lo	Morris & Lo	Morris & Lo	Morris & Lo	Morris & Lo	Morris & Lo	Morris & Lo	Morris & Lo	Morris & Lo	Morris & Lo
Rock Type	latite	latite	latite	latite	monz.por.	monz.por.	monz.por.	latite brecci	monzonite	latite	latite	latite	monz. & Q	monz. & Q
SiO2	61.9	63.70	64.09	57.70	61.00	60.30	59.90	59.23	58.22	59.6	58.64	59.7	52.84	60.9
TiO2	0.85	0.82	0.76	1.10	0.84	0.87	0.85	0.93	0.86	1.1	0.85	0.94	1	1.06
Al2O3	18.2	17.40	16.87	16.10	17.10	16.90	17.20	17.17	15.68	15.2	15.61	15.4	12.96	16.51
Fe2O3	3.8	4.20	3.30	4.80	5.90	5.10	6.00	3.31	3.41	6	5	4.6	4.2	6.69
FeO	0.6	0.36	0.54	3.40	0.12	0.68	0.20	1.28	3.17	1.6	1.88	2.5	3.78	0.42
MgO	0.74	0.82	0.87	2.80	1.00	1.70	1.50	1.08	2.75	2.8	2.95	3.1	7.36	0.78
MnO	0.11	0.18	0.11	0.08	0.20	0.08	0.06	0.07	0.14	0.12	0.11	0.12	0.13	0.1
CaO	4.4	0.83	1.97	5.70	3.70	4.50	3.90	3.08	4.03	5.7	5.88	5.9	8.14	4.02
Na2O	3.6	3.70	3.66	3.10	3.40	3.60	2.90	2.45	3.10	3.1	2.78	3.1	2.76	3.41
K2O	5	6.40	6.10	2.90	4.80	4.60	4.70	4.94	4.72	3	2.9	3	2.6	3.37
P2O5	0.35	0.30	0.26	0.44	0.42	0.45	0.47	0.32	0.39	0.42	0.29	0.35	0.42	0.29
LOI	1.31	2.42	1.32	1.52	1.52	1.22	3.32	5.65	3.37	1.18	2.74	1.84	3.55	2.42
TOTAL	101.00	101.00	99.77	101.00	100.00	100.00	101.00	99.51	99.84	100.00	99.57	101.00	99.69	99.92
Mining Dist.	Tintic	Tintic	Tintic	Tintic	Tintic	Tintic	Tintic	Tintic	Tintic	Tintic	Tintic	Tintic	Tintic	Tintic
Ba	2000	2000	2000	1500	2000	2000	2000	2000	1000	1500	1000	1500	1500	1000
Rb	0	0	0	0	0	0	0	0	0	0	0	0	0	0
Sr	1500	500	700	1000	1500	1500	1000	1000	1000	1000	1000	1000	1500	1000
Y	30	50	70	30	30	30	30	30	70	30	30	30	50	50
Zr	300	700	500	200	300	300	200	300	200	200	200	200	200	200
Nb	15	20	10	10	10	10	15	1	5	15	15	10	0	0
CLASS	MACo	MACo	MACo	MACo	MACo	MACo	MACo	MACo	MACo	MACo	MACo	MACo	MACo	MACo
A/CNK	0.940	1.196	1.040	0.864	0.975	0.884	1.013	1.145	0.893	0.811	0.847	0.806	0.584	0.995
A/NK	1.60	1.34	1.33	1.95	1.58	1.55	1.74	1.83	1.53	1.82	2.02	1.84	1.76	1.78
Na2O+K2	8.60	10.10	9.76	6.00	8.20	8.20	7.60	7.39	7.82	6.10	5.68	6.10	5.36	6.78
Na2O/K2O	0.72	0.58	0.60	1.07	0.71	0.78	0.62	0.50	0.66	1.03	0.96	1.03	1.06	1.01
NaO+K2O-	4.20	9.27	7.79	0.30	4.50	3.70	3.70	4.31	3.79	0.40	-0.20	0.20	-2.78	2.76
K2O-CaO	0.60	5.57	4.13	-2.80	1.10	0.10	0.80	1.86	0.69	-2.70	-2.98	-2.90	-5.54	-0.65
K2O-MgO	4.26	5.58	5.23	0.10	3.80	2.90	3.20	3.86	1.97	0.20	-0.05	-0.10	-4.76	2.59
FeO/MgO*	5.43	5.05	4.03	2.76	5.43	3.10	3.73	3.94	2.27	2.50	2.16	2.14	1.03	8.26
Fe3+/Fe2+	6.33	11.67	6.11	1.41	49.17	7.50	30.00	2.59	1.08	3.75	2.66	1.84	1.11	15.93
LARSEN	20.49	25.98	24.62	13.63	20.43	18.50	19.27	20.52	17.35	14.37	13.62	13.90	4.71	18.87
ALKALI IN	1.57	2.40	1.92	0.54	1.51	1.77	1.32	1.36	2.16	-0.07	-0.13	-0.11	1.70	0.13
ALT INDE	41.776	61.447	55.317	39.310	44.961	43.750	47.692	52.121	51.164	39.726	40.317	40.397	47.747	35.838
K INDEX	1.11	2.20	1.94	0.66	1.01	1.01	0.96	1.15	1.03	0.70	0.70	0.73	0.81	0.72
Na INDEX	1.6600	1.7745	1.6395	1.9332	1.6832	1.6669	1.6303	1.6405	1.5496	1.8445	1.8056	1.8395	1.6456	2.0071
Al2O3/Na2	5.055556	4.702703	4.60929	5.193548	5.029412	4.694444	5.931034	7.008163	5.058065	4.903226	5.615108	4.967742	4.695652	4.841642
SiO2/Al2O	3.4011	3.6609	3.7991	3.5839	3.5673	3.5680	3.4826	3.4496	3.7130	3.9211	3.7566	3.8766	4.0772	3.6887
Ti/Nb	340.00	246.00	456.00	660.00	504.00	522.00	340.00	5580.00	1032.00	440.00	340.00	564.00	6000.00	6360.00
use?	no	no	no	no	no	no	no	no	no	no	no	no	no	no
altered?		alt.A/CNK,KI,LOI					alt.LOI	alt.LOI	alt.LOI		alt.LOI		alt.LOI	alt.LOI
why not use	volc	volc	volc	volc	volc	volc	volc	volc		volc	volc	volc		

MACo incl.	Silver City s	Silver City s	Silver City s	Silver City s	Silver City s	Silver City s	Silver City s	Silver City s	Silver City s	Silver City s	Tintic	Tintic	rhyolite sout	Swansea m
COUNTY	Juab-Utah	Juab-Utah	Juab-Utah	Juab-Utah	Juab-Utah	Juab-Utah	Juab-Utah	Juab-Utah	Juab-Utah	Juab-Utah	Juab-Utah	Juab-Utah	Juab-Utah	Juab-Utah
STATE	UT	UT	UT	UT	UT	UT	UT	UT	UT	UT	UT	UT	UT	UT
SAMPLE #	6-D101859	7-D102253	8-D102250	9-D101867	10-D10226	11-D10224	12-D10226	13-D10225	15-D10225	16	17	18	A	B
NAME	TINTIC	TINTIC	TINTIC	TINTIC	TINTIC	TINTIC	TINTIC	TINTIC	TINTIC	TINTIC	TINTIC	TINTIC	TINTIC	TINTIC
SOURCE:	Morris & Lo	Morris & Lo	Morris & Lo	Morris & Lo	Morris & Lo	Morris & Lo	Morris & Lo	Morris & Lo	Morris & Lo	Tower and	MagmaChe	MagmaChe	Clarke, 191	Clarke, 191
Rock Type	monz. & Q	monz. & Q	monz. & Q	monz. & Q	monz. & Q	monz. & Q	monz. & Q	monz. & Q	monzonite	monzonite	?	?	porphyritic r	quartz porp
SiO2	53.24	57.67	64.04	59.83	58.95	58.29	62.29	62.99	61.35	59.76	60.6	61.3	69.13	71.56
TiO2	0.9	1.15	0.71	0.88	0.93	1.04	0.82	0.78	0.84	0.87	0	0	0.69	0.38
Al2O3	12.9	15.59	15.7	15.11	16.38	15	15.66	15.29	15.94	15.79	15.1	15.3	14.36	14.27
Fe2O3	4.51	5.11	3.13	4.47	5.39	4.08	3.75	3.95	3.55	3.77	4.1	3.5	2.52	0.89
FeO	3.05	1.98	1.85	2.3	1.26	2.97	2.07	1.61	2.43	3.3	2.3	2.4	0.57	0
MgO	6.66	3.46	2	3.37	2.92	4.19	2.27	2.15	2.22	2.16	2.5	2.5	0.7	0.42
MnO	0.11	0.09	0.09	0.12	0.13	0.11	0.1	0.05	0.1	0.12	0	0	0.1	-0.1
CaO	7.87	5.40	3.88	5.21	4.09	4.39	4.08	3.73	4.46	3.88	4.2	4	1.88	1.18
Na2O	2.67	3.47	3.76	3.4	3.53	4.06	3.43	3.47	3.52	3.01	3.7	3.7	3.58	3
K2O	2.63	3.09	3.43	3.14	3.05	3.18	3.77	3.86	3.89	4.4	3.7	3.8	5	4.37
P2O5	0.39	0.59	0.29	0.34	0.35	0.37	0.3	0.36	0.34	0.42	0	0	0.26	0.13
LOI	4.86	2.12	0.89	1.75	2.83	2.22	1.24	1.47	0.98	2.24	0	0	0.58	1.21
TOTAL	99.74	99.64	99.71	99.87	99.75	99.84	99.72	99.66	99.83	99.72	? 96.2	? 96.5	99.54	99.99
Mining Dist.	Tintic	Tintic	Tintic	Tintic	Tintic	Tintic	Tintic	Tintic	Tintic	Tintic	Tintic	Tintic	Tintic	Tintic
Ba	1000	1500	1000	1500	1000	1000	1000	1000	0	1000	0	0	0	0
Rb	0	0	0	0	0	0	0	0	0	0	0	0	0	0
Sr	1000	1000	1000	700	1000	1000	1000	1000	0	1000	0	0	0	0
Y	20	50	30	20	50	50	50	50	0	50	0	0	0	0
Zr	150	200	100	150	200	200	200	100	0	100	0	0	0	0
Nb	0	10	0	0	0	0	10	0	0	10	0	0	0	0
CLASS	MACo	MACo	MACo	MACo	MACo	MACo	MACo	MACo	MACo	MACo	MACo	MACo	MACo	MACo
A/CNK	0.598	0.825	0.925	0.817	0.989	0.828	0.912	0.916	0.879	0.940	0.851	0.874	0.974	1.207
A/NK	1.78	1.72	1.58	1.68	1.80	1.48	1.61	1.54	1.59	1.62	1.49	1.50	1.27	1.47
Na2O+K2	5.30	6.56	7.19	6.54	6.58	7.24	7.20	7.33	7.41	7.41	7.40	7.50	8.58	7.37
Na2O/K2O	1.02	1.12	1.10	1.08	1.16	1.28	0.91	0.90	0.90	0.68	1.00	0.97	0.72	0.69
NaO+K2O-	-2.57	1.16	3.31	1.33	2.49	2.85	3.12	3.60	2.95	3.53	3.20	3.50	6.70	6.19
K2O-CaO	-5.24	-2.31	-0.45	-2.07	-1.04	-1.21	-0.31	0.13	-0.57	0.52	-0.50	-0.20	3.12	3.19
K2O-MgO	-4.03	-0.37	1.43	-0.23	0.13	-1.01	1.50	1.71	1.67	2.24	1.20	1.30	4.30	3.95
FeO/MgO*	1.07	1.90	2.33	1.88	2.09	1.59	2.40	2.40	2.53	3.10	2.40	2.22	4.05	1.91
Fe3+/Fe2+	1.48	2.58	1.69	1.94	4.28	1.37	1.81	2.45	1.46	1.14	1.78	1.46	4.42	ERR
LARSEN	5.85	13.45	18.90	14.50	15.69	14.03	18.18	18.98	17.66	18.28	17.20	17.73	25.46	26.62
ALKALI IN	1.49	1.11	-0.63	0.28	0.65	1.56	0.03	-0.10	0.59	1.18	0.86	0.70	-1.14	-3.25
ALT INDE	46.848	42.477	41.546	43.056	43.929	46.587	44.576	45.496	43.364	48.773	43.972	45.000	51.075	53.400
K INDEX	0.80	0.84	1.08	0.86	0.93	1.04	0.99	1.07	0.95	0.91	0.97	1.05	1.97	3.93
Na INDEX	1.6130	1.9480	2.0211	1.9000	2.1461	2.1043	1.8221	1.8150	1.7838	1.6243	1.8506	1.8482	1.6903	1.8931
Al2O3/Na2	4.831461	4.492795	4.175532	4.444118	4.640227	3.694581	4.565598	4.40634	4.528409	5.245847	4.081081	4.135135	4.011173	4.756667
SiO2/Al2O	4.1271	3.6992	4.0790	3.9596	3.5989	3.8860	3.9777	4.1197	3.8488	3.7847	4.0132	4.0065	4.8141	5.0147
Ti/Nb	5400.00	690.00	4260.00	5280.00	5580.00	6240.00	492.00	4680.00	5040.00	522.00	0.00	0.00	4140.00	2280.00
use?	no	no	ok	ok	no	no	ok	ok	ok	ok	ok	ok	no	no
altered?	alt.LOI	alt.LOI			alt.LOI	alt.LOI								alt.A/CNK,
why not use													volc	

MACo incl.	Tintic Moun	Iron Duke	rhyolite por	quartz mon	TOMBSTO	TOMBSTO	TOMBSTO	TOMBSTO	Tombstone	Tombstone	Tombstone	Tombstone	Tombstone	Tombstone
COUNTY	Juab-Utah	Juab-Utah	Cochise	Cochise	Cochise	Cochise	Cochise	Cochise	Cochise	Cochise	Cochise	Cochise	Cochise	Cochise
STATE	UT	UT	AZ	AZ	AZ	AZ	AZ	AZ	AZ	AZ	AZ	AZ	AZ	AZ
SAMPLE #	C	D	M	N	A1, 1 p. 99	A2, 2 p. 99	JD-19	JD-20	T11	T12	T13	T21	T22	T23
NAME	TINTIC	TINTIC	TOMBSTO	TOMBSTO	TOMBSTO	TOMBSTO	TOMBSTO	TOMBSTO	TOMBSTO	TOMBSTO	TOMBSTO	TOMBSTO	TOMBSTO	TOMBSTO
SOURCE:	Clarke, 191	Clarke, 191	Clarke, 191	Clarke, 191	Gilluly, 195	Gilluly, 195	Dewhurst 7	Dewhurst 7	Lang, 1991	Lang, 1991	Lang, 1991	Lang, 1991	Lang, 1991	Lang, 1991
Rock Type	andesite	monzonite	U.S.rhyolite	Schiefflin gr	U.S.qtz latit	U.S.qtz latit	Schieffelin	Schieffelin	Bronco Vol	Bronco Vol	Bronco Vol	Schieffelin	Schieffelin	Schieffelin
SiO2	60.17	59.76	68.04	62.33	66.59	68.16	63.87	63.03	53.2	55.1	53.9	66.6	64.8	63.7
TiO2	0.87	0.75	0.42	0.63	0.38	0.43	0.83	0.87	1.3	0.7	1	0.66	0.7	0.61
Al2O3	15.77	15.77	15.82	16.92	16.77	16.07	16.20	15.93	18.5	16.2	15	15.7	15.4	15.6
Fe2O3	3.42	3.77	2.34	3.95	1.94	1.75	0	0	8.54	5.78	4	3.73	2.63	3.04
FeO	2.95	3.3	0.84	1.24	1.26	1.15	4.16	4.48	0.52	1.68	3.33	1.29	2.65	2.46
MgO	2.52	2.16	0.8	1.97	1.04	0.90	2.21	2.89	3.6	3.5	5.07	1.9	2.2	2.2
MnO	0.11	0.12	0.07	0.07	0.11	0.11	0	0	0.13	0.1	0.14	0.08	0.09	0.09
CaO	4.69	3.88	3.26	4.48	2.86	2.61	4.06	3.85	8.5	7	5.02	4.5	4.5	4.7
Na2O	2.96	3.01	3.93	3.62	3.66	3.79	3.44	3.78	3.1	2.8	4.2	3	2.9	2.9
K2O	4.16	4.4	3.32	3.36	3.77	3.64	3.37	3.42	1.1	1.2	2	3.3	3.2	3.3
P2O5	0.4	0.42	0.15	0.17	0.26	0.16	0	0	0.11	0.16	0.22	0.1	0.11	0.11
LOI	1.52	2.24	1.17	1.42	1.19	1.26	0	0	1.9	6.6	4.64	0.8	1.3	1.3
TOTAL	99.78	99.81	100.24	100.38	99.83	100.03	98.14	98.25	100.5	100.82	98.62	101.66	100.48	100
Mining Dist.	Tintic	Tintic	Tombstone	Tombstone	Tombstone	Tombstone	Tombstone	Tombstone	Tombstone	Tombstone	Tombstone	Tombstone	Tombstone	Tombstone
Ba	0	0	0	0	0	0	0	0	575.7	1069.1	1092.6	879.6	775.2	808.1
Rb	0	0	0	0	0	0	0	0	22.65	56.59	47.68	125.62	126.4	131.09
Sr	0	0	0	0	0	0	0	0	620.9	585	579.9	530	439.8	485.3
Y	0	0	0	0	0	0	0	0	22.29	14.16	13.6	22.02	21.85	27.66
Zr	0	0	0	0	0	0	0	0	99.63	144.29	127.59	200.56	187.18	221.77
Nb	0	0	0	0	0	0	0	0	4.29	7.65	1	10.67	9.35	9.95
CLASS	MACo	MACo	MACo	MACo	MACo	MACo	MACo	MACo	MACo	MACo	MACo	MACo	MACo	MACo
A/CNK	0.880	0.939	0.988	0.953	1.095	1.076	0.969	0.940	0.850	0.868	0.823	0.939	0.937	0.922
A/NK	1.68	1.62	1.57	1.76	1.66	1.58	1.74	1.60	2.94	2.74	1.65	1.84	1.87	1.87
Na2O+K2	7.12	7.41	7.25	6.98	7.43	7.43	6.81	7.20	4.20	4.00	6.20	6.30	6.10	6.20
Na2O/K2O	0.71	0.68	1.18	1.08	0.97	1.04	1.02	1.11	2.82	2.33	2.10	0.91	0.91	0.88
NaO+K2O-	2.43	3.53	3.99	2.50	4.57	4.82	2.75	3.35	-4.30	-3.00	1.18	1.80	1.60	1.50
K2O-CaO	-0.53	0.52	0.06	-1.12	0.91	1.03	-0.69	-0.43	-7.40	-5.80	-3.02	-1.20	-1.30	-1.40
K2O-MgO	1.64	2.24	2.52	1.39	2.73	2.74	1.16	0.53	-2.50	-2.30	-3.07	1.40	1.00	1.10
FeO/MgO*	2.39	3.10	3.68	2.43	2.89	3.03	1.88	1.55	2.28	1.97	1.37	2.45	2.28	2.36
Fe3+/Fe2+	1.16	1.14	2.79	3.19	1.54	1.52	0.00	0.00	16.42	3.44	1.20	2.89	0.99	1.24
LARSEN	17.01	18.28	21.94	17.69	22.07	22.85	18.39	17.69	6.73	9.07	9.88	19.10	18.10	17.63
ALKALI IN	0.74	1.18	-2.06	-0.21	-1.34	-1.93	-0.95	-0.25	0.41	-0.50	2.15	-2.48	-2.01	-1.50
ALT INDE	46.615	48.773	36.428	39.687	42.454	41.499	42.661	45.265	28.834	32.414	43.401	40.945	42.188	41.985
K INDEX	0.90	0.91	1.30	0.96	1.44	1.56	1.10	1.21	0.47	0.54	0.94	0.90	0.87	0.85
Na INDEX	1.5913	1.6231	2.1721	2.0300	2.0654	2.1169	1.9902	2.0455	3.6678	3.2016	2.9231	1.8485	1.8430	1.8012
Al2O3/Na2	5.327703	5.239203	4.025445	4.674033	4.581967	4.240106	4.709302	4.214286	5.967742	5.785714	3.571429	5.233333	5.310345	5.37931
SiO2/Al2O	3.8155	3.7895	4.3009	3.6838	3.9708	4.2414	3.9426	3.9567	2.8757	3.4012	3.5933	4.2420	4.2078	4.0833
Ti/Nb	5220.00	4500.00	2520.00	3780.00	2280.00	2580.00	4980.00	5220.00	1818.18	549.02	6000.00	371.13	449.20	367.84
use?	no	no	no	ok	no	no	ok	ok	no	no	no	ok	ok	ok
altered?	I	alt.LOI								alt.LOI	alt.LOI			
why not use	volc		volc		volc	volc			volc	volc	volc			

MACo incl.	Tombstone	Tombstone	Tombstone	Tombstone	Tombstone	Tombstone	Tombstone
COUNTY	Cochise	Cochise	Cochise	Cochise	Cochise	Cochise	Cochise
STATE	AZ	AZ	AZ	AZ	AZ	AZ	AZ
SAMPLE #	T24	T25	T2a2	T2a3	T2a5	T43	T44
NAME	TOMBSTO	TOMBSTO	TOMBSTO	TOMBSTO	TOMBSTO	TOMBSTO	TOMBSTO
SOURCE:	Lang, 1991	Lang, 1991	Lang, 1991	Lang, 1991	Lang, 1991	Lang, 1991	Lang, 1991
Rock Type	Schieffelin	Schieffelin	Uncle Sam	Uncle Sam	Uncle Sam	Tombstone	Tombstone
SiO2	63.2	62.9	72.4	72.3	71.5	78.1	78.9
TiO2	0.85	0.85	0.37	0.38	0.39	1.06	0.06
Al2O3	16.2	16.1	15.1	14.7	14.5	13.3	132
Fe2O3	5.91	6.35	2.12	2.9	0.97	0.62	0.63
FeO	0.39	0.26	0.78	0	1.55	0	0
MgO	2.5	2.6	0.93	0.92	0.87	0.24	0.23
MnO	0.1	0.11	0.09	0.1	0.1	0.08	0.06
CaO	5.4	5.5	2.8	2.7	2.5	0.6	0.15
Na2O	3.1	3	3.7	3.4	3.5	0.13	0.18
K2O	3	3	3.5	3.5	3.5	5	5.9
P2O5	0.11	0.11	0.06	0.05	0.04	0.02	0.02
LOI	0.4	0.5	0.8	1.1	1	3.2	2.6
TOTAL	101.16	101.28	102.65	102.05	100.42	101.35	101.93
Mining Dist.	Tombstone	Tombstone	Tombstone	Tombstone	Tombstone	Tombstone	Tombstone
Ba	779.9	917.7	1414.9	1001.9	1231.9	141.9	0
Rb	113.62	108.66	128.6	44.55	125.67	247.75	0
Sr	506.6	434.2	316.7	209.2	262.1	48.4	0
Y	23.07	22.77	25.54	23.68	26.02	18.31	0
Zr	203.5	253.01	227.35	238.88	208.08	41.91	0
Nb	9.81	9.29	11.4	12.28	11.41	19.05	0
CLASS	MACo	MACo	MACo	MACo	MACo	MCAo	MCAo
A/CNK	0.891	0.884	1.008	1.027	1.028	1.976	18.934
A/NK	1.94	1.97	1.53	1.57	1.52	2.36	19.71
Na2O+K2	6.10	6.00	7.20	6.90	7.00	5.13	6.08
Na2O/K2O	1.03	1.00	1.06	0.97	1.00	0.03	0.03
NaO+K2O-	0.70	0.50	4.40	4.20	4.50	4.53	5.93
K2O-CaO	-2.40	-2.50	0.70	0.80	1.00	4.40	5.75
K2O-MgO	0.50	0.40	2.57	2.58	2.63	4.76	5.67
FeO/MgO*	2.28	2.30	2.89	2.84	2.79	2.33	2.47
Fe3+/Fe2+	15.15	24.42	2.72	ERR	0.63	ERR	ERR
LARSEN	16.17	15.87	23.90	23.98	23.96	30.19	31.82
ALKALI IN	-1.41	-1.40	-3.73	-4.00	-3.60	-7.92	-7.27
ALT INDE	39.286	39.716	40.531	42.015	42.141	87.772	94.892
K INDEX	0.77	0.75	1.48	1.47	1.60	4.64	8.80
Na INDEX	1.9239	1.8842	2.0648	1.9987	2.0277	2.0016	18.9648
Al2O3/Na2	5.225806	5.366667	4.081081	4.323529	4.142857	102.3077	733.3333
SiO2/Al2O	3.9012	3.9068	4.7947	4.9184	4.9310	5.8722	0.5977
Ti/Nb	519.88	548.98	194.74	185.67	205.08	333.86	ERR
---	---	---	---	---	---	---	---
use?	ok	ok	no	no	no	no	no
altered?				alt.Al		alt.LOI	alt.LOI
why not use			volc	volc.	volc	younger vol	younger vol

MACow - in	Cherry Cree	Cherry Cree	Cherry Cree	Linka granit	Linka	Linka	Linka	KINSLEY	KINSLEY	KINSLEY	RAILROAD	RAILROAD	RAILROAD	RAILROAD
COUNTY	White Pine	White Pine	White Pine	Lander	Lander	Lander	Lander	Elko	Elko	Elko	ELKO	ELKO	ELKO	ELKO
STATE	NV	NV	NV	NV	NV	NV	NV	NV	NV	NV	NV	NV	NV	NV
SAMPLE #	88-1560	88-1561	I	R2 88-0880	R2 88-0881	R2 88-0883	R2 88-0884	88-1577	88-1578	88-1579	SR-344	SR-374A	SR-375	SR-376
ABBREV.	CherryCr	CherryCr	CherryCr	LINKA	LINKA	LINKA	LINKA	KINSLEGR	KINSLEGR	KINSLEGR	EL28	EL28	EL28	EL28
SOURCE:	MagmaChe	MagmaChe	Clarke, 191	MagmaChe	MagmaChe	MagmaChe	MagmaChe	MagmaChe	MagmaChe	MagmaChe	Smith and	Smith and	Smith and	Smith and
ROCK TYP	?	?	biotite quart	? Md	? Rd	? Md	? Om	GRANITE	GRANITE	APLITE	ash-flow tuff	vitrophyre	ash-flow tuff	ash-flow tuff
SiO2	69.82	69.92	67.6	57.14	63.82	55.3	64.21	66.53	65.99	76.60	63.68	70.06	68.84	69.86
TiO2	0.49	0.49	0.6	0.9	0.57	0.91	0.49	0.55	0.57	0.08	0.51	0.22	0.22	0.43
Al2O3	15.12	15.03	15.89	13.12	15.62	13.09	16.69	15.06	14.41	11.38	15.24	13.9	13.84	15.1
Fe2O3	1.71	1.22	1.77	4.97	1.59	5.2	1.93	1.75	1.85	0.63	3.35	1.23	1.17	2.27
FeO	1.4	1.85	1.82	1.38	2.29	0.92	0.85	1.85	2.10	0.25	0.23	0.62	0.63	0.32
MgO	0.75	0.62	0.96	3.52	2.56	3.5	1.85	1.64	1.69	0.01	1.48	0.44	0.58	0.49
MnO	0.06	0.05	-0.05	0.11	0.09	0.09	0.07	0.05	0.06	0.02	0.05	0.06	0.06	0.03
CaO	2.79	2.75	3.38	6.95	4.4	8.27	3.46	3.28	3.49	1.00	4.32	1.72	1.85	2.82
Na2O	3.23	3.25	3.39	2.61	4.29	2.77	4.48	3.29	3.18	2.99	3.05	2.89	1.89	3.3
K2O	3.9	3.93	3.39	3.32	3.05	3.07	4.04	3.94	3.84	4.68	2.7	4.47	4.78	3.67
P2O5	0.15	0.13	0.19	0.31	0.19	0.3	0.18	0.22	0.27	0.10	0.14	0.07	0.08	0.14
LOI	0.37	0.34	1.1	4.88	0.94	6.58	1.1	0.58	0.65	0.41	4.74	3.83	5.74	1.31
TOTAL	99.79	99.58	100.09	99.21	99.61	100	99.35	98.74	98.10	98.15	99.49	99.51	99.68	99.74
MINING DI	Cherry Cree	Cherry Cree	Cherry Cree	Linka	Linka	Linka	Linka	KINSLEY	KINSLEY	KINSLEY	RAILROAD	RAILROAD	RAILROAD	RAILROAD
Ba	1100	1000	1	1100	1100	1100	920	1300	1400	-20	763	790	1000	540
Rb	150	140	1	120	96	100	130	135	135	210	153	138	100	150
Sr	355	345	1	315	460	340	450	400	410	58	415	482	430	250
Y	17	15	0	8	5	8	11	17	20	5	18	16	19	12
Zr	180	175	0	170	130	180	130	200	200	95	260	160	5	13
Nb	31	25	1	21	22	23	25	23	28	20	59	53	21	15
CLASS	MACow	MACow	MACow	MACow	MACow	MACow	MACow	MACow	MACow	MACow	MACow	MACow	MACow	MACow
A/CNK	1.034	1.028	1.031	0.638	0.850	0.570	0.924	0.962	0.915	0.963	0.964	1.091	1.186	1.038
A/NK	1.58	1.56	1.72	1.66	1.51	1.66	1.42	1.55	1.53	1.14	1.92	1.45	1.67	1.60
Na2O+K2	7.13	7.18	6.78	5.93	7.34	5.84	8.52	7.23	7.02	7.67	5.75	7.36	6.67	6.97
Na2O/K2O	0.83	0.83	1.00	0.79	1.41	0.90	1.11	0.84	0.83	0.64	1.13	0.65	0.40	0.90
NaO+K2O-	4.34	4.43	3.40	-1.02	2.94	-2.43	5.06	3.95	3.53	6.67	1.43	5.64	4.82	4.15
K2O-CaO	1.11	1.18	0.01	-3.63	-1.35	-5.20	0.58	0.66	0.35	3.68	-1.62	2.75	2.93	0.85
K2O-MgO	3.15	3.31	2.43	-0.20	0.49	-0.43	2.19	2.30	2.15	4.67	1.22	4.03	4.20	3.18
FeO/MgO*	3.92	4.75	3.56	1.66	1.45	1.60	1.40	2.09	2.23	81.70	2.19	3.93	2.90	4.82
Fe3+/Fe2+	1.22	0.66	0.97	3.60	0.69	5.65	2.27	0.95	0.88	2.52	14.57	1.98	1.86	7.09
LARSEN	23.63	23.87	21.58	11.90	17.36	9.73	20.13	21.20	20.66	29.20	18.13	25.66	25.30	23.65
ALKALI IN	-2.84	-2.83	-2.37	0.67	-0.40	1.27	0.63	-1.52	-1.53	-4.83	-1.94	-2.70	-2.94	-3.02
ALT INDE	43.580	43.128	39.119	41.707	39.231	37.308	42.589	45.926	45.328	54.032	36.190	51.576	58.901	40.467
K INDEX	1.38	1.37	1.14	0.74	1.22	0.67	1.71	1.32	1.20	4.23	0.96	2.26	2.05	1.44
Na INDEX	1.8619	1.8550	2.0310	1.4244	2.2563	1.4726	2.0332	1.7966	1.7427	1.6018	2.0932	1.7378	1.5818	1.9371
Al2O3/Na2	4.681115	4.624615	4.687316	5.02682	3.641026	4.725632	3.725446	4.577508	4.531447	3.80602	4.996721	4.809689	7.322751	4.575758
SiO2/Al2O	4.6177	4.6520	4.2542	4.3552	4.0858	4.2246	3.8472	4.4177	4.5795	6.7311	4.1785	5.0403	4.9740	4.6265
Ti/Nb	94.84	117.60	3600.00	257.14	155.45	237.39	117.60	143.48	122.14	24.00	51.86	24.91	62.86	172.00
use?	ok	ok	ok	no	ok	NO	ok	ok	ok	no	no	no	no	no
altered?				alt.LOI		alt.LOI				alt.NAl,Al	alt.LOI	alt.LOI	alt.A/CNK,KI,LOI	
why not use											volc.	volc.	volc.	volc.

MACow - in	RAILROAD	RAILROAD	RAILROAD	RAILROAD	RAILROAD	RAILROAD	RAILROAD	RAILROAD	RAILROAD	RAILROAD	RAILROAD	Santa Eulali	Santa Eulali	Santa Eulali
COUNTY	ELKO	ELKO	ELKO	ELKO	ELKO	ELKO	ELKO	ELKO	ELKO	ELKO	ELKO	Chihuahua	Chihuahua	Chihuahua
STATE	NV	NV	NV	NV	NV	NV	NV	NV	NV	NV	NV	2	MEX	MEX
SAMPLE #	SR-333	654	672	662	665	657	659	845	SR-358	SR-359	SR-368	1000	1001	1005
ABBREV.	EL28	EL28	EL28	EL28	EL28	EL28	EL28	EL28	EL28	EL28	EL28	SNTEULAL	SNTEULAL	SNTEULAL
SOURCE:	Smith and	Smith and	Smith and	Smith and	Smith and	Smith and	Smith and	Smith and	Smith and	Smith and	Smith and	MagmaChe	MagmaChe	MagmaChe
ROCK TYP	ash-flow tuff	qtz monz st	qtz monz st	qtz monz st	rhy porph st	rhy porph di	rhy porph st	porph qtz m	pyrx and po	pyrx and po	biot and por	granodiorite	felsite	felsite
SiO2	63.83	70.52	69.23	69.72	72.26	66.14	77.33	65.94	62.51	62.36	65.55	60.9	75.6	76.1
TiO2	0.64	0.37	0.4	0.39	0.27	0.44	0.09	0.55	0.74	0.81	0.75	1.12	0.06	0.06
Al2O3	16.11	15.05	15.27	15.18	14.87	13.75	12.29	14.91	16.26	16.57	11.41	15.5	12.8	12.7
Fe2O3	3.84	0.86	1.04	0.61	0.24	4.26	0.4	1.57	2.36	3.13	6.22	6.27	1	0.46
FeO	0.59	1.04	1.8	2.05	0.5	0.09	0.12	2.34	2.21	1.91	0.09	0	0	0
MgO	1.53	0.67	0.95	0.86	0.3	0.15	0.02	1.73	1.95	1.87	1	2.12	0.08	0.07
MnO	0.04	0.04	0.07	0.05	0.02	0.02	0.01	0.11	0.08	0.07	0.04	0.12	0.12	0.11
CaO	3.42	2.78	2.95	2.95	1.59	0.38	0.44	2.62	4.81	5.15	3.19	4.11	0.9	0.88
Na2O	2.98	3.25	3.47	3.41	2.85	0.38	2.14	2.46	2.69	3.18	1.86	4.41	2.77	0.24
K2O	3	4.26	3.65	3.69	5.78	6.98	5.93	4.64	3.64	3.19	3.69	3.41	5.42	7.87
P2O5	0.21	0.13	0.14	0.14	0.09	0.18	0.02	0.16	0.24	0.26	0.19	0.32	0.02	0.01
LOI	3.52	0.81	0.79	0.79	0.87	1.35	0.86	2.5	1.96	1.12	5.56	1.47	1.23	1.77
TOTAL	99.71	99.75	99.73	99.80	99.62	99.61	99.65	99.48	99.65	99.62	99.55	99.9	100.1	100.3
MINING DI	RAILROAD	RAILROAD	RAILROAD	RAILROAD	RAILROAD	RAILROAD	RAILROAD	RAILROAD	RAILROAD	RAILROAD	RAILROAD	Santa Eulali	Santa Eulali	Santa Eulali
Ba	1	1	1	1	1	1	1	1	1	1	1	1	1	1
Rb	1	1	1	1	1	1	1	1	1	1	1	110	230	250
Sr	1	1	1	1	1	1	1	1	1	1	1	390	40	60
Y	0	0	0	0	0	0	0	0	0	0	0	40	20	50
Zr	0	0	0	0	0	0	0	0	0	0	0	370	10	100
Nb	1	1	1	1	1	1	1	1	1	1	1	30	1	40
CLASS	MACow	MACow	MACow	MACow	MACow	MACow	MACow	MACow	MACow	MACow	MACow	MACow	MACow	MACow
A/CNK	1.120	1.001	1.015	1.013	1.073	1.546	1.143	1.076	0.949	0.917	0.886	0.840	1.060	1.205
A/NK	1.97	1.51	1.58	1.58	1.36	1.68	1.23	1.64	1.94	1.91	1.62	1.41	1.23	1.42
Na2O+K2	5.98	7.51	7.12	7.10	8.63	7.36	8.07	7.10	6.33	6.37	5.55	7.82	8.19	8.11
Na2O/K2O	0.99	0.76	0.95	0.92	0.49	0.05	0.36	0.53	0.74	1.00	0.50	1.29	0.51	0.03
NaO+K2O-	2.56	4.73	4.17	4.15	7.04	6.98	7.63	4.48	1.52	1.22	2.36	3.71	7.29	7.23
K2O-CaO	-0.42	1.48	0.70	0.74	4.19	6.60	5.49	2.02	-1.17	-1.96	0.50	-0.70	4.52	6.99
K2O-MgO	1.47	3.59	2.70	2.83	5.48	6.83	5.91	2.91	1.69	1.32	2.69	1.29	5.34	7.80
FeO/MgO*	2.64	2.71	2.88	3.02	2.39	26.16	24.00	2.17	2.22	2.53	5.69	2.66	11.25	5.91
Fe3+/Fe2+	6.51	0.83	0.58	0.30	0.48	47.33	3.33	0.67	1.07	1.64	69.11	0.00	0.00	0.00
LARSEN	19.33	24.32	22.83	23.12	27.98	28.50	31.25	22.27	17.72	16.96	21.35	17.48	29.64	32.29
ALKALI IN	-1.76	-2.72	-2.63	-2.84	-2.25	-1.24	-4.70	-1.43	-0.92	-0.83	-2.83	1.17	-3.93	-4.20
ALT INDE	41.446	44.982	41.742	41.705	57.795	90.368	69.754	55.633	42.704	37.789	48.152	39.359	59.978	87.638
K INDEX	1.01	1.78	1.42	1.43	3.87	1.74	8.79	1.39	0.91	0.83	0.74	1.02	4.59	6.32
Na INDEX	2.1131	1.7640	1.9658	1.9370	1.5662	1.6009	1.5034	1.6064	1.6879	1.9137	1.3903	2.1338	1.5709	1.2357
Al2O3/Na2	5.40604	4.630769	4.400576	4.451613	5.217544	36.18421	5.742991	6.060976	6.04461	5.210692	6.134409	3.514739	4.620939	52.91667
SiO2/Al2O	3.9621	4.6857	4.5337	4.5929	4.8594	4.8102	6.2921	4.4225	3.8444	3.7634	5.7450	3.9290	5.9063	5.9921
Ti/Nb	3840.00	2220.00	2400.00	2340.00	1620.00	2640.00	540.00	3300.00	4440.00	4860.00	4500.00	224.00	360.00	9.00
use?	no	ok	ok	ok	no	no	no	no	ok	ok	no	ok	no	no
altered?	alt.LOI				alt.KI	alt.AI	alt.AI,NAI	alt.LOI			alt.LOI		alt.AI,NAI	alt.NAI
why not use	volc.													

MACow - in	Santa Eulali	Santa Eulali	Santa Eulali	Santa Eulali	SWALES	SWALES	TAYLOR D	TAYLOR DI	TAYLOR DI	Shell Creek	Shell Creek	TEMPIUTE	TEMPIUTE
COUNTY	Chihuahua	Chihuahua	Chihuahua	Chihuahua	Elko	Elko	White Pine	White Pine	White Pine	White Pine	White Pine	Lincoln	Lincoln
STATE	MEX	MEX	MEX	MEX	NV	NV	NV	NV	NV	NV	NV	NV	NV
SAMPLE #	1006	R6 1772-17	R6 829	R6 879	88-1051	88-1052	88-1547	88-1548	88-1549	H3186	H3187	117	118
ABBREV.	SNTEULAL	SNTEULAL	SNTEULAL	SNTEULAL	SWALSMT	SWALSMT	TAYLDKD	TAYLDKD	TAYLDKD	Shellcr	Shellcr	LI5	LI5
SOURCE:	MagmaChe	MagmaChe	MagmaChe	MagmaChe	MagmaChe	MagmaChe	MagmaChe	MagmaChe	MagmaChe	Drewes, 19	Drewes, 19	Lee, 1984	Lee, 1984
ROCK TYP	altered felsit	granodiorite	felsite dike	felsite (rhyol	PLUTON	PLUTON	dike	dike	dike	porph. rhy.	porph. rhy.	intrusions	intrusions
SiO2	79.7	58.4	74.4	77.2	72.23	72.9	71.28	72.07	72.22	65.54	76.26	70.1	68.3
TiO2	0.07	1.06	0.06	0.05	0.3	0.32	0.07	0.06	0.06	0.05	0.05	0	0
Al2O3	11.3	16.22	12.98	12.82	14.67	14.81	13.12	13.23	13.21	11.73	12.61	15.5	15.3
Fe2O3	1.12	5.36	0.64	1.08	1.1	1.51	0.51	0.62	0.53	0.4	0.25	1.6	1.6
FeO	0	0	0	0	1.2	1.05	0.25	0.2	0.3	0.59	0.44	0.6	0.96
MgO	0.27	2.24	0.23	0.22	0.66	0.72	0.74	0.87	0.78	0.45	0.22	0.35	0.57
MnO	0.05	0.1	0.04	0.07	0.03	0.06	0.08	0.06	0.07	0.19	0.05	0	0
CaO	1.29	3.62	1.64	0.3	1.93	2.14	1.29	0.73	0.85	6.83	0.71	2	2.6
Na2O	0.15	4.72	-0.01	0.08	3.45	3.55	0.75	0.86	0.86	2.47	3.03	3.8	3.7
K2O	0.9	2.68	8.9	7.46	4.39	4.29	4.92	4.88	4.94	4.19	4.79	4.6	4.1
P2O5	0.02	0.08	0.07	0.02	0.37	0.19	0.01	0.01	0.01	0.01	0.01	0	0
LOI	4.39	4.3	1.45	1.6	0.6	0.8	5.81	5.81	5.87	6.41	1.35	0	0
TOTAL	99.3	98.78	100.4	100.9	100.93	102.34	98.83	99.40	99.70	99.81	99.73	98.55	97.13
MINING DI	Santa Eulali	Santa Eulali	Santa Eulali	Santa Eulali	Swales Mtn	Swales Mtn	Taylor	Taylor	Taylor	Taylor	Taylor	Tempiute	Tempiute
Ba	1	948	398	36	1200	1200	80	20	90	300	150	1	1
Rb	70	98	321	345	120	110	345	335	340	1	1	1	1
Sr	-10	246	151	76	400	400	55	38	27	150	30	1	1
Y	10	38	35	53	7	11	49	45	62	70	15	0	0
Zr	90	368	107	109	140	130	91	90	88	30	30	0	0
Nb	70	19	53	52	31	29	52	51	53	15	30	1	1
CLASS	MACow	MACow	MACow	MACow	MACow	MACow	MACow	MACow	MACow	MACow	MACow	MACow	MACow
A/CNK	3.163	0.939	1.028	1.461	1.051	1.029	1.470	1.646	1.587	0.600	1.099	1.041	1.002
A/NK	9.24	1.52	1.35	1.56	1.41	1.41	2.00	1.97	1.95	1.36	1.24	1.38	1.45
Na2O+K2	1.05	7.40	8.89	7.54	7.84	7.84	5.67	5.74	5.80	6.66	7.82	8.40	7.80
Na2O/K2O	0.17	1.76	-0.00	0.01	0.79	0.83	0.15	0.18	0.17	0.59	0.63	0.83	0.90
NaO+K2O-	-0.24	3.78	7.25	7.24	5.91	5.70	4.38	5.01	4.95	-0.17	7.11	6.40	5.20
K2O-CaO	-0.39	-0.94	7.26	7.16	2.46	2.15	3.63	4.15	4.09	-2.64	4.08	2.60	1.50
K2O-MgO	0.63	0.44	8.67	7.24	3.73	3.57	4.18	4.01	4.16	3.74	4.57	4.25	3.53
FeO/MgO*	3.73	2.15	2.50	4.42	3.32	3.35	0.96	0.87	1.00	2.11	3.02	5.83	4.21
Fe3+/Fe2+	0.00	0.00	0.00	0.00	0.92	1.44	2.04	3.10	1.77	0.68	0.57	2.67	1.67
LARSEN	25.91	16.29	31.83	32.67	25.88	25.73	26.65	27.30	27.38	18.76	29.28	25.62	23.70
ALKALI IN	-12.60	1.68	-2.79	-5.18	-3.03	-3.28	-4.85	-5.07	-5.07	-1.72	-4.55	-1.68	-1.61
ALT INDE	44.828	37.104	84.851	95.285	48.418	46.822	73.506	78.338	76.985	33.286	57.257	46.047	42.571
K INDEX	0.57	1.14	4.12	6.10	2.06	1.88	3.21	4.44	4.04	0.91	5.85	2.17	1.67
Na INDEX	3.3293	2.7006	1.0267	1.4720	1.8371	1.8565	1.6229	1.8218	1.7612	1.1467	1.7314	1.8673	1.9043
Al2O3/Na2	75.33333	3.436441	-1298	160.25	4.252174	4.171831	17.49333	15.38372	15.36047	4.748988	4.161716	4.078947	4.135135
SiO2/Al2O	7.0531	3.6005	5.7319	6.0218	4.9237	4.9223	5.4329	5.4475	5.4671	5.5874	6.0476	4.5226	4.4641
Ti/Nb	6.00	334.74	6.79	5.77	58.06	66.21	8.08	7.06	6.79	20.00	10.00	0.00	0.00
use?	no	no	no	no	ok	ok	no	no	no	no	no	ok	ok
altered?	alt.Al,NAI,L	alt.LOI	alt.Al,KI,NA	alt.Al,NAI			alt.A/CNK,	alt.A/CNK,	alt.A/CNK/L	alt.LOI	alt.Al		
why not use										volc.	volc.		

MACr - Pot	Uncia stock	Oruro stock	San Jose d	Karikari plut	Karikari plut	Karikari plut	Karikari plut	Karikari plut	Karikari plut	Karikari plut	Karikari plut	Karikari plut	Karikari plut	Karikari plut
COUNTY	Llallagua ar	Oruro area	Oruro area	?	?	?	?	?	?	?	?	?	?	?
STATE	2	BOLIVIA	BOLIVIA	Bolivia	Bolivia	Bolivia	Bolivia	Bolivia	Bolivia	Bolivia	Bolivia	Bolivia	Bolivia	Bolivia
SAMPLE #	p. 245	?	90BSL010	Ka 11	Ka 12	Ka 21f	Ka 30	Ka 31	Ka 32	Ka 33	Ka 34	Ka 35	Me 1	Me 4
NAME	Llallaga	Oruro	Oruro	POTOSI	POTOSI	POTOSI	POTOSI	POTOSI	POTOSI	POTOSI	POTOSI	POTOSI	POTOSI	POTOSI
SOURCE:	Ahlfeld,193	Ahlfeld,193	USGS 199	Wolf, 1973	Wolf, 1973	Wolf, 1973	Wolf, 1973	Wolf, 1973	Wolf, 1973	Wolf, 1973	Wolf, 1973	Wolf, 1973	Wolf, 1973	Wolf, 1973
ROCK TYP	intrusive da	fresh dacite	?	qtz latite	qtz latite	qtz latite	qtz latite	qtz latite	qtz latite	qtz latite	qtz latite	qtz latite	qtz latite	qtz latite
SiO2	67.75	64.73	63.8	63.5	62.8	63.2	62.8	62.5	62.5	63.4	63.6	62.9	63.7	63.2
TiO2	0.24	0	0.65	0.65	1	0.55	0.6	0.6	0.7	0.7	0.55	0.6	0.6	0.6
Al2O3	18.45	14.04	13.8	18.4	18.6	17.4	18.8	18.1	18.2	17.6	18	18	18	17.4
Fe2O3	0.95	0.63	9.76	0.65	0.2	0.95	0.35	1.15	0.25	0.85	0.35	0.9	0.55	0.3
FeO	2.04	2.33	0	2.9	3.4	3.2	3.6	3.4	3.9	3.3	3.3	2.9	3.2	3.5
MgO	1.39	1.52	0.5	0.55	1	1.2	0.85	1.2	1	0.9	0.7	1.1	0.9	1.3
MnO	0	0.08	0	0.05	0.04	0.04	0.06	0.06	0.04	0.05	0.05	0.05	0.05	0.05
CaO	0.84	4.03	0.04	3.5	3.5	3.5	3.8	4.1	4.1	3.7	3.8	4	3.7	5.1
Na2O	2.46	4.63	0	2.9	3	2.6	2.6	2.9	2.8	3.1	2.7	3	2.2	2
K2O	5.67	2.43	2.77	5	5.2	5.2	5	5	4.9	5	5.5	5	4.9	4.5
P2O5	0	0.54	0.15	0.29	0.29	0.27	0.28	0.3	0.34	0.29	0.28	0.27	0.27	0.27
LOI	0.32	3.84	7.19	1.52	1.04	1.66	1.7	0.94	1.02	1.02	1.44	1.2	1.6	1.56
TOTAL	100.11	98.8	98.66	99.91	100.07	99.77	100.44	100.25	99.8	99.81	100.27	99.92	99.81	99.78
MINING DI	Llallagua	Oruro	Oruro	Potosi	Potosi	Potosi	Potosi	Potosi	Potosi	Potosi	Potosi	Potosi	Potosi	Potosi
Ba	0	0	0	1040	1040	850	1120	1130	1500	1250	985	1100	1200	650
Rb	0	0	0	300	310	310	230	230	350	250	220	210	1	1
Sr	0	0	0	0	0	0	0	0	0	0	0	0	0	0
Y	0	0	0	0	0	0	0	0	0	0	0	0	0	0
Zr	0	0	0	280	218	295	275	180	350	325	250	250	200	250
Nb	0	0	0	0	0	0	0	0	0	0	0	0	0	0
CLASS	MACr	MACr	MACr	MACr	MACr	MACr	MACr	MACr	MACr	MACr	MACr	MACr	MACr	MACr
A/CNK	1.573	0.798	4.483	1.110	1.097	1.068	1.131	1.025	1.046	1.019	1.039	1.020	1.148	0.996
A/NK	1.81	1.37	4.59	1.80	1.76	1.75	1.94	1.78	1.83	1.67	1.73	1.74	2.01	2.13
Na2O+K2	8.13	7.06	2.77	7.90	8.20	7.80	7.60	7.90	7.70	8.10	8.20	8.00	7.10	6.50
Na2O/K2O	0.43	1.91	0.00	0.58	0.58	0.50	0.52	0.58	0.57	0.62	0.49	0.60	0.45	0.44
NaO+K2O-	7.29	3.03	2.73	4.40	4.70	4.30	3.80	3.80	3.60	4.40	4.40	4.00	3.40	1.40
K2O-CaO	4.83	-1.60	2.73	1.50	1.70	1.70	1.20	0.90	0.80	1.30	1.70	1.00	1.20	-0.60
K2O-MgO	4.28	0.91	2.27	4.45	4.20	4.00	4.15	3.80	3.90	4.10	4.80	3.90	4.00	3.20
FeO/MgO*	2.08	1.91	17.57	6.34	3.58	3.38	4.61	3.70	4.13	4.52	5.16	3.37	4.11	2.90
Fe3+/Fe2+	0.47	0.27	ERR	0.22	0.06	0.30	0.10	0.34	0.06	0.26	0.11	0.31	0.17	0.09
LARSEN	26.02	18.46	23.50	22.12	21.63	21.57	21.28	20.53	20.63	21.53	22.20	20.87	21.53	19.17
ALKALI IN	-1.07	-1.02	-4.96	0.28	0.84	0.29	0.24	0.65	0.45	0.52	0.54	0.60	-0.60	-1.01
ALT INDE	68.147	31.324	98.792	46.444	48.819	51.200	47.755	46.970	46.094	46.457	48.819	46.565	49.573	44.961
K INDEX	2.55	1.24	0.37	1.21	1.30	1.19	1.10	1.07	1.06	1.16	1.20	1.18	1.08	0.88
Na INDEX	2.0068	2.7033	4.4826	1.6903	1.6741	1.5678	1.6509	1.6047	1.6179	1.6394	1.5295	1.6200	1.5973	1.4409
Al2O3/Na2	7.5	3.032397	ERR	6.344828	6.2	6.692308	7.230769	6.241379	6.5	5.677419	6.666667	6	8.181818	8.7
SiO2/Al2O	3.6721	4.6104	4.6232	3.4511	3.3763	3.6322	3.3404	3.4530	3.4341	3.6023	3.5333	3.4944	3.5389	3.6322
Ti/Nb	1440.00	ERR	ERR	ERR	ERR	ERR	ERR	ERR	ERR	ERR	ERR	ERR	ERR	ERR
use?	no	no	no	ok	ok	ok	no	ok	ok	ok	ok	ok	no	ok
altered?	alt KI,AI	alt.LOI	alt.AI,LOI				alt.A/CNK						alt.A/CNK	
why not use														

MACr - Pot	Karikari plut	Karikari plut	Karikari plut	Karikari plut	Karikari plut	Karikari plut	Karikari plut	Karikari plut	Karikari plut	Karikari plut	Karikari plut	Karikari plut	Karikari plut	Karikari plut
COUNTY	?	?	?	?	?	?	?	?	?	?	?	?	?	?
STATE	Bolivia	Bolivia	Bolivia	Bolivia	Bolivia	Bolivia	Bolivia	Bolivia	Bolivia	Bolivia	Bolivia	Bolivia	Bolivia	Bolivia
SAMPLE #	A41	A42	Ka01	Ka02	Ka03	Ka04	Ka07	Ka08	Ka09	Ka10	Ka14	Ka16	Ka18	Ka29
NAME	POTOSI	POTOSI	POTOSI	POTOSI	POTOSI	POTOSI	POTOSI	POTOSI	POTOSI	POTOSI	POTOSI	POTOSI	POTOSI	POTOSI
SOURCE:	Wolf, 1973	Wolf, 1973	Wolf, 1973	Wolf, 1973	Wolf, 1973	Wolf, 1973	Wolf, 1973	Wolf, 1973	Wolf, 1973	Wolf, 1973	Wolf, 1973	Wolf, 1973	Wolf, 1973	Wolf, 1973
ROCK TYP	qtz latite	qtz latite	qtz latite	qtz latite	qtz latite	qtz latite	qtz latite	qtz latite	qtz latite	qtz latite	qtz latite	qtz latite	qtz latite	qtz latite
SiO2	62.3	61.8	63.7	63.2	61.2	61.4	65.4	63.5	64.2	65.7	63.4	63.6	64.1	63.3
TiO2	0.7	0.7	0.55	0.6	0.6	0.6	0.45	0.5	0.45	0.4	0.6	0.6	0.6	0.55
Al2O3	18.5	17.8	17.8	17.8	18	18.2	17.5	18	17.4	16.6	18.4	17.8	17.2	18.7
Fe2O3	0.8	1	0.7	0.7	0.9	0.95	0.8	1.3	0.9	1.4	0.25	0.35	0.55	1.4
FeO	3.6	3.5	2.9	2.9	2.3	2.8	2.4	2.4	2.7	2.1	3.1	3.2	3.2	3.1
MgO	0.5	1	1	1.2	1.1	1.2	0.8	0.95	0.8	1.2	0.65	0.8	0.6	0.75
MnO	0.08	0.06	0.04	0.05	0.04	0.08	0.04	0.05	0.05	0.06	0.06	0.05	0.05	0.05
CaO	4.6	4.5	3.7	3.5	3.7	3.7	3.1	3.4	3.8	3	3.1	3.7	3.5	3.9
Na2O	2.6	2.4	2.9	2.8	3.8	3.1	3	3	3.2	2.4	3.4	2.9	2.8	2.7
K2O	4	4.7	4.8	5	4.3	5	5.3	5.2	5	5.2	4.9	5	5	4.9
P2O5	0.39	0.33	0.28	0.26	0.29	0.26	0.27	0.27	0.27	0.28	0.28	0.29	0.28	0.27
LOI	1.66	1.92	1.33	1.82	3.52	2.52	1.01	1.32	1.14	1.92	2.06	1.66	1.92	0.74
TOTAL	99.73	99.71	99.7	99.83	99.75	99.81	100.07	99.89	99.91	100.26	100.2	99.95	99.8	100.26
MINING DI	Potosi	Potosi	Potosi	Potosi	Potosi	Potosi	Potosi	Potosi	Potosi	Potosi	Potosi	Potosi	Potosi	Potosi
Ba	1200	1100	730	700	865	380	700	1115	830	1230	1030	760	1280	1160
Rb	170	270	260	0	220	0	0	270	310	250	270	230	340	310
Sr	0	0	167	0	185	0	0	145	143	172	225	203	190	163
Y	0	0	0	0	0	0	0	0	0	0	0	0	0	0
Zr	420	280	275	130	210	100	260	230	210	290	250	145	245	207
Nb	0	0	0	0	0	0	0	0	0	0	0	0	0	0
CLASS	MACr	MACr	MACr	MACr	MACr	MACr	MACr	MACr	MACr	MACr	MACr	MACr	MACr	MACr
A/CNK	1.088	1.032	1.065	1.085	1.019	1.054	1.071	1.073	0.988	1.103	1.111	1.051	1.048	1.109
A/NK	2.15	1.97	1.78	1.77	1.65	1.73	1.64	1.70	1.63	1.73	1.69	1.75	1.71	1.92
Na2O+K2	6.60	7.10	7.70	7.80	8.10	8.10	8.30	8.20	8.20	7.60	8.30	7.90	7.80	7.60
Na2O/K2O	0.65	0.51	0.60	0.56	0.88	0.62	0.57	0.58	0.64	0.46	0.69	0.58	0.56	0.55
NaO+K2O-	2.00	2.60	4.00	4.30	4.40	4.40	5.20	4.80	4.40	4.60	5.20	4.20	4.30	3.70
K2O-CaO	-0.60	0.20	1.10	1.50	0.60	1.30	2.20	1.80	1.20	2.20	1.80	1.30	1.50	1.00
K2O-MgO	3.50	3.70	3.80	3.80	3.20	3.80	4.50	4.25	4.20	4.00	4.25	4.20	4.40	4.15
FeO/MgO*	8.64	4.40	3.53	2.94	2.83	3.05	3.90	3.76	4.39	2.80	5.12	4.39	6.16	5.81
Fe3+/Fe2+	0.22	0.29	0.24	0.24	0.39	0.34	0.33	0.54	0.33	0.67	0.08	0.11	0.17	0.45
LARSEN	19.67	19.80	21.33	21.37	19.90	20.57	23.20	22.02	21.80	22.90	22.28	21.70	22.27	21.35
ALKALI IN	-0.58	0.11	0.00	0.29	1.33	1.26	-0.03	0.58	0.32	-0.84	0.72	0.24	-0.05	0.05
ALT INDE	38.462	45.238	46.774	49.600	41.860	47.692	50.000	49.004	45.313	54.237	46.058	46.774	47.059	46.122
K INDEX	0.80	0.91	1.20	1.28	1.35	1.26	1.46	1.31	1.23	1.38	1.39	1.21	1.17	1.01
Na INDEX	1.7385	1.5428	1.6688	1.6449	1.9032	1.6742	1.6375	1.6502	1.6280	1.5641	1.8052	1.6310	1.6083	1.6600
Al2O3/Na2	7.115385	7.416667	6.137931	6.357143	4.736842	5.870968	5.833333	6	5.4375	6.916667	5.411765	6.137931	6.142857	6.925926
SiO2/Al2O	3.3676	3.4719	3.5787	3.5506	3.4000	3.3736	3.7371	3.5278	3.6897	3.9578	3.4457	3.5730	3.7267	3.3850
Ti/Nb	ERR	ERR	ERR	ERR	ERR	ERR	ERR	ERR	ERR	ERR	ERR	ERR	ERR	ERR
use?	ok	ok	ok	ok	no	no	ok	ok	ok	ok	ok	ok	ok	ok
altered?					alt.LOI	alt.LOI								
why not use														

MACr - Pot	Karikari plut	Karikari plut	Karikari plut	Karikari plut	Karikari plut	Karikari plut	Karikari plut	Karikari plut	Karikari plut	Karikari plut	Karikari plut	Karikari plut	Karikari plut	Kumurana
COUNTY	?	?	?	?	?	?	?	?	?	?	?	?	?	?
STATE	Bolivia	Bolivia	Bolivia	Bolivia	Bolivia	Bolivia	Bolivia	Bolivia	Bolivia	Bolivia	Bolivia	Bolivia	Bolivia	Bolivia
SAMPLE #	A43	Ka28	Ka41a	Ka41b	Ka36	Ka13	Ka15a	Ka15b	Ka20	Ka22	Ka23	Ka40	Ka38	Ku33a
NAME	POTOSI	POTOSI	POTOSI	POTOSI	POTOSI	POTOSI	POTOSI	POTOSI	POTOSI	POTOSI	POTOSI	POTOSI	POTOSI	POTOSI
SOURCE:	Wolf, 1973	Wolf, 1973	Wolf, 1973	Wolf, 1973	Wolf, 1973	Wolf, 1973	Wolf, 1973	Wolf, 1973	Wolf, 1973	Wolf, 1973	Wolf, 1973	Wolf, 1973	Wolf, 1973	Wolf, 1973
ROCK TYP	qtz lat, Ulist	qtz lat, Ulist	qtz lat, Ulist	qtz lat, Ulist	qtz lat, Ulist	qtz lat, Ulist	qtz lat, Ulist	qtz lat, Ulist	qtz lat, Ulist	qtz lat, Ulist	qtz lat, Ulist	qtz lat, Ulist	qtz lat, Ulist	granodiorite
SiO2	62.1	61.2	62.6	62.6	59.9	62.6	60.4	60.4	62.4	61.9	62.4	62.2	62.2	58.2
TiO2	0.9	0.55	0.95	0.95	0.8	0.7	0.5	0.5	0.55	0.6	0.55	0.6	0.7	1.2
Al2O3	16	18.4	15.8	15.8	16.7	16	16.6	16.6	17.8	17.7	18.6	17.4	18.5	17.9
Fe2O3	3.1	1.2	2	2	2.6	1.2	2.1	2.1	0.8	0.5	0.8	0.9	0.6	5.5
FeO	2.7	2.5	2.7	2.7	2.3	2.8	1.1	1.1	3.1	2.5	2.5	2.1	2.3	0.65
MgO	2.1	1.1	1.4	1.5	1.4	0.9	0.95	0.95	0.6	0.8	1.3	0.95	1.6	2.6
MnO	0.08	0.06	0.08	0.08	0.07	0.05	0.07	0.07	0.05	0.04	0.07	0.05	0.04	0.08
CaO	3.4	3.8	3.8	3.6	2.9	3.7	3.5	3.4	3.9	4.1	4	3.6	4.2	4.9
Na2O	2.5	3.2	2.5	2.5	1.4	2.9	3.4	3.2	3.5	4	3.6	3.5	3.2	2.7
K2O	4.2	4.8	4.8	4.7	5.9	5	6.1	6.3	5.4	5.3	4.6	5	4.7	4.2
P2O5	0.45	0.27	0.33	0.33	0.32	0.25	0.3	0.3	0.32	0.26	0.29	0.27	0.28	0.55
LOI	2.22	1.78	2.89	2.89	4.6	3.72	4.68	4.68	1.86	2.04	1.42	3.33	1.72	1.35
TOTAL	99.75	99.76	99.85	99.65	99.89	99.82	99.7	99.6	100.28	99.74	100.13	99.9	100.4	99.83
MINING DI	Potosi	Potosi	Potosi	Potosi	Potosi	Potosi	Potosi	Potosi	Potosi	Potosi	Potosi	Potosi	Potosi	Potosi
Ba	1300	1055	750	0	1100	715	715	0	1230	1130	1200	500	950	1730
Rb	0	210	240	0	420	270	400	0	310	240	0	210	170	260
Sr	0	0	0	0	0	0	0	0	0	0	0	0	0	950
Y	0	0	0	0	0	0	0	0	0	0	0	0	0	0
Zr	220	200	200	0	170	220	90	0	200	220	230	140	200	170
Nb	0	0	0	0	0	0	0	0	0	0	0	0	0	0
CLASS	MACr	MACr	MACr	MACr	MACr	MACr	MACr	MACr	MACr	MACr	MACr	MACr	MACr	MACr
A/CNK	1.076	1.058	0.973	1.002	1.194	0.945	0.893	0.907	0.951	0.894	1.022	0.981	1.027	0.999
A/NK	1.85	1.76	1.70	1.71	1.92	1.57	1.36	1.37	1.53	1.44	1.70	1.56	1.78	1.99
Na2O+K2	6.70	8.00	7.30	7.20	7.30	7.90	9.50	9.50	8.90	9.30	8.20	8.50	7.90	6.90
Na2O/K2O	0.60	0.67	0.52	0.53	0.24	0.58	0.56	0.51	0.65	0.75	0.78	0.70	0.68	0.64
NaO+K2O-	3.30	4.20	3.50	3.60	4.40	4.20	6.00	6.10	5.00	5.20	4.20	4.90	3.70	2.00
K2O-CaO	0.80	1.00	1.00	1.10	3.00	1.30	2.60	2.90	1.50	1.20	0.60	1.40	0.50	-0.70
K2O-MgO	2.10	3.70	3.40	3.20	4.50	4.10	5.15	5.35	4.80	4.50	3.30	4.05	3.10	1.60
FeO/MgO*	2.61	3.25	3.21	3.00	3.31	4.31	3.15	3.15	6.37	3.69	2.48	3.06	1.78	2.15
Fe3+/Fe2+	1.15	0.48	0.74	0.74	1.13	0.43	1.91	1.91	0.26	0.20	0.32	0.43	0.26	8.46
LARSEN	19.40	20.30	20.47	20.47	21.57	21.27	21.78	22.08	21.70	21.03	20.10	21.18	19.63	16.10
ALKALI IN	-0.40	1.23	0.01	-0.09	1.02	0.61	3.03	3.03	1.69	2.27	0.99	1.36	0.76	1.25
ALT INDE	51.639	45.736	49.600	50.407	62.931	47.200	50.538	52.347	44.776	42.958	43.704	45.594	45.985	47.222
K INDEX	0.99	1.23	1.05	1.07	1.15	1.16	1.61	1.64	1.23	1.43	1.32	1.45	1.35	0.90
Na INDEX	1.6717	1.7245	1.4936	1.5338	1.4312	1.5247	1.4504	1.4154	1.5989	1.6487	1.8046	1.6808	1.7078	1.6415
Al2O3/Na2	6.4	5.75	6.32	6.32	11.92857	5.517241	4.882353	5.1875	5.085714	4.425	5.166667	4.971429	5.78125	6.62963
SiO2/Al2O	3.8813	3.3261	3.9620	3.9620	3.5868	3.9125	3.6386	3.6386	3.5056	3.4972	3.3548	3.5747	3.3622	3.2514
Ti/Nb	ERR	ERR	ERR	ERR	ERR	ERR	ERR	ERR	ERR	ERR	ERR	ERR	ERR	ERR
use?	ok	ok	no	no	no	no	no	no	ok	ok	ok	no	ok	ok
altered?			alt.LOI	alt.LOI	alt.LOI,Al,A	alt.LOI	alt.LOI,KI	alt.LOI,KI				alt.LOI		
why not use														

MACr - Pot	Kumurana	Kumurana	Kumurana	Kumurana	Kumurana	Kumurana	Kumurana	Kumurana	Kumurana
COUNTY	?	?	?	?	?	?	?	?	?
STATE	Bolivia	Bolivia	Bolivia	Bolivia	Bolivia	Bolivia	Bolivia	Bolivia	Bolivia
SAMPLE #	Ku33b	Ku33c	Ku64a	Ku64b	Ku64c	Ku23a	Ku23b	Ku107a	Ku107b
NAME	POTOSI	POTOSI	POTOSI	POTOSI	POTOSI	POTOSI	POTOSI	POTOSI	POTOSI
SOURCE:	Wolf, 1973	Wolf, 1973	Wolf, 1973	Wolf, 1973	Wolf, 1973	Wolf, 1973	Wolf, 1973	Wolf, 1973	Wolf, 1973
ROCK TYP	granodiorite	granodiorite	granodiorite	granodiorite	granodiorite	granodiorite	granodiorite	granodiorite	granodiorite
SiO2	58.2	59	62	62	61.1	60.4	60.4	57.5	57.7
TiO2	1.2	1.2	1	1	1	1.2	1.2	1.5	1.5
Al2O3	17.9	15.3	16.1	16.1	15	13.8	13.8	15.4	15.4
Fe2O3	5.5	3.3	4.4	4.4	2	1	1	2.4	2.4
FeO	0.65	5.1	1.1	1.1	5.5	5.3	5.3	0.2	6.2
MgO	3	3.3	1.7	2.4	2.9	3.6	3.6	3.1	3.3
MnO	0.08	0.09	0.07	0.07	0.07	0.17	0.17	0.23	0.23
CaO	5	4.6	3.9	3.7	3.9	3.9	3.8	3.4	3.2
Na2O	2.6	2.8	2.7	2.7	2.7	2.1	2.1	2.2	2.2
K2O	4.1	4.4	4.8	4.7	4.7	3.7	3.7	4.1	3.9
P2O5	0.55	0.48	0.47	0.47	0.4	0.61	0.61	0.62	0.62
LOI	1.35	0.72	1.55	1.55	0.94	3.4	3.4	3.21	3.21
TOTAL	100.13	100.29	99.79	100.19	100.21	99.78	99.68	100	99.83
MINING DI	Potosi	Potosi	Potosi	Potosi	Potosi	Potosi	Potosi	Potosi	Potosi
Ba	1530	1370	1730	1380	1270	700	0	1100	0
Rb	180	160	430	180	210	180	0	250	0
Sr	0	0	750	0	0	0	0	0	0
Y	0	0	0	0	0	0	0	0	0
Zr	160	210	230	230	160	140	0	180	0
Nb	0	0	0	0	0	0	0	0	0
CLASS	MACr	MACr	MACr	MACr	MACr	MACr	MACr	MACr	MACr
A/CNK	1.004	0.862	0.961	0.989	0.901	0.947	0.959	1.080	1.126
A/NK	2.05	1.63	1.67	1.69	1.57	1.85	1.85	1.91	1.96
Na2O+K2	6.70	7.20	7.50	7.40	7.40	5.80	5.80	6.30	6.10
Na2O/K2O	0.63	0.64	0.56	0.57	0.57	0.57	0.57	0.54	0.56
NaO+K2O-	1.70	2.60	3.60	3.70	3.50	1.90	2.00	2.90	2.90
K2O-CaO	-0.90	-0.20	0.90	1.00	0.80	-0.20	-0.10	0.70	0.70
K2O-MgO	1.10	1.10	3.10	2.30	1.80	0.10	0.10	1.00	0.60
FeO/MgO*	1.87	2.45	2.98	2.11	2.52	1.72	1.72	0.76	2.53
Fe3+/Fe2+	8.46	0.65	4.00	4.00	0.36	0.19	0.19	12.00	0.39
LARSEN	15.50	16.17	19.87	19.27	18.27	16.33	16.43	16.77	16.63
ALKALI IN	1.05	1.25	0.44	0.34	0.67	-0.67	-0.67	0.91	0.64
ALT INDE	48.299	50.993	49.618	52.593	53.521	54.887	55.303	56.250	57.143
K INDEX	0.92	0.83	1.03	1.12	0.92	0.93	0.94	1.63	0.81
Na INDEX	1.6379	1.4979	1.5235	1.5633	1.4756	1.5145	1.5265	1.6164	1.6898
Al2O3/Na2	6.884615	5.464286	5.962963	5.962963	5.555556	6.571429	6.571429	7	7
SiO2/Al2O	3.2514	3.8562	3.8509	3.8509	4.0733	4.3768	4.3768	3.7338	3.7468
Ti/Nb	ERR	ERR	ERR	ERR	ERR	ERR	ERR	ERR	ERR
use?	ok	ok	ok	ok	ok	no	no	no	no
altered?						alt.LOI	alt.LOI	alt.LOI,KI,A	alt.LOI,A/C
why not use									

MCAo incl.	CHRISTMA	CHRISTMA	CHRISTMA	CHRISTMA	CHRISTMA	CHRISTMA	CHRISTMA	CHRISTMA	Christmas p	Christmas	Christmas p	Christmas p	Christmas	Christmas p
COUNTY	Gila	Gila	Gila	Gila	Gila	Gila	Gila	Gila	Gila	Gila	Gila	Gila	Gila	Gila
STATE	AZ	AZ	AZ	AZ	AZ	AZ	AZ	AZ	AZ	AZ	AZ	AZ	AZ	AZ
SAMPLE #	54AB75	72AB74	AB64-73A	83AB75	D99-430	AB77-73	D256-148	38D	CHa1	CH-11	CH-12	CH-12A	CH-12B	CH-12C
NAME	CRISMASP	CRISMASP	CRISMASP	CRISMASP	CRISMASP	CRISMASP	CRISMASP	CRISMASP	CRISMASP	CRISMASP	CRISMASP	CRISMASP	CRISMASP	CRISMASP
SOURCE:	Koski, 1978	Koski, 1978	Koski, 1978	Koski, 1978	Koski, 1978	Koski, 1978	Koski, 1978	Koski, 1978	Lang, 1991	Lang, 1991	Lang, 1991	Lang, 1991	Lang, 1991	Lang, 1991
ROCK TYP	Hbl And Po	Hbl And Po	Hbl Rhyoda	Hbl Rhyoda	phases X-m	phases X-m	phases X-m	Gr. Basin S	Hornblende	MacDonald	MacDonald	MacDonald	MacDonald	MacDonald
SiO2	59.00	56.80	61.90	63.10	63.20	66.50	67.00	62.40	56.80	66.80	65.70	64.90	61.10	62.89
TiO2	0.72	0.95	0.74	0.69	0.80	0.36	0.34	0.49	0.95	0.60	0.57	0.60	0.71	0.73
Al2O3	16.70	17.20	15.80	16.00	16.50	15.10	16.30	16.00	17.20	15.60	15.70	15.90	16.00	16.17
Fe2O3	3.70	4.10	2.50	2.50	2.20	2.10	1.30	2.50	4.10	2.70	2.71	4.60	4.23	4.55
FeO	2.80	2.80	2.00	1.80	2.60	1.90	1.80	1.70	2.80	1.42	1.68	n.a.	n.a.	n.a.
MgO	2.30	2.40	2.60	2.30	3.60	2.30	2.40	2.70	2.40	2.20	2.30	2.40	2.30	2.33
MnO	0.11	0.10	0.06	0.06	0.04	0.00	0.22	0.00	0.10	0.06	0.06	0.06	0.07	0.07
CaO	6.50	6.60	4.20	4.00	3.40	3.60	3.50	3.30	6.60	4.40	4.50	4.50	3.92	4.16
Na2O	4.00	3.80	4.20	4.50	4.10	4.10	4.00	4.50	3.80	3.70	3.90	3.90	4.31	4.08
K2O	1.60	2.00	2.40	2.10	2.10	2.10	2.20	2.50	2.00	2.20	2.30	2.30	2.22	2.22
P2O5	0.28	0.40	0.17	0.17	0.22	0.26	0.22	0.27	0.40	0.06	0.07	0.05	0.23	0.15
LOI	2.19	2.32	2.97	2.46	2.57	1.57	2.14	2.39	0.19	2.50	1.50	1.50	1.99	2.03
TOTAL	99.90	99.47	99.54	99.68	101.33	99.89	101.42	98.75	97.34	102.24	101.00	100.71	97.15	99.45
MINING DI	Christmas	Christmas	Christmas	Christmas	Christmas	Christmas	Christmas	Christmas	Christmas	Christmas	Christmas	Christmas	Christmas	Christmas
Ba	0	0	0	0	0	0	0	0	0	764.50	703.60	781.40	0	0
Rb	0	0	0	0	0	0	0	0	0	50.42	48.04	49.14	0	0
Sr	0	0	0	0	0	0	0	0	0	670.00	648.50	735.90	0	0
Y	0	0	0	0	0	0	0	0	0	8.74	7.29	7.80	0	0
Zr	0	0	0	0	0	0	0	0	0	108.84	105.24	98.65	0	0
Nb	0	0	0	0	0	0	0	0	0	6.39	10.75	5.82	0	0
CLASS	MCAo	MCAo	MCAo	MCAo	MCAo	MCAo	MCAo	MCAo	MCAo	MCAo	MCAo	MCAo	MCAo	MCAo
A/CNK	0.829	0.841	0.921	0.943	1.084	0.969	1.062	0.992	0.841	0.946	0.918	0.929	0.962	0.968
A/NK	2.01	2.04	1.66	1.65	1.83	1.67	1.82	1.58	2.04	1.84	1.76	1.78	1.68	1.77
Na2O+K2	5.60	5.80	6.60	6.60	6.20	6.20	6.20	7.00	5.80	5.90	6.20	6.20	6.53	6.30
Na2O/K2O	2.50	1.90	1.75	2.14	1.95	1.95	1.82	1.80	1.90	1.68	1.70	1.70	1.94	1.84
NaO+K2O-	-0.90	-0.80	2.40	2.60	2.80	2.60	2.70	3.70	-0.80	1.50	1.70	1.70	2.61	2.14
K2O-CaO	-4.90	-4.60	-1.80	-1.90	-1.30	-1.50	-1.30	-0.80	-4.60	-2.20	-2.20	-2.20	-1.70	-1.94
K2O-MgO	-0.70	-0.40	-0.20	-0.20	-1.50	-0.20	-0.20	-0.20	-0.40	0.00	0.00	-0.10	-0.08	-0.11
FeO/MgO*	2.67	2.70	1.63	1.76	1.27	1.65	1.24	1.46	2.70	1.75	1.79	ERR	ERR	ERR
Fe3+/Fe2+	1.32	1.46	1.25	1.39	0.85	1.11	0.72	1.47	1.46	1.90	1.61	ERR	ERR	ERR
LARSEN	12.47	11.93	16.23	16.83	16.17	18.37	18.63	17.30	11.93	17.87	17.40	17.03	16.37	16.69
ALKALI IN	-0.35	0.67	-0.43	-0.87	-1.31	-2.54	-2.72	-0.21	0.67	-2.95	-2.24	-1.94	-0.20	-1.10
ALT INDE	27.083	29.730	37.313	34.109	43.182	36.364	38.017	40.000	29.730	35.200	35.385	35.878	35.451	35.575
K INDEX	0.63	0.63	1.09	1.11	1.23	1.15	1.33	1.34	0.63	0.96	0.99	1.00	1.14	1.05
Na INDEX	3.3285	2.7414	2.6705	3.0858	3.0367	2.9215	2.8806	2.7921	2.7414	2.6279	2.6133	2.6250	2.9030	2.8062
Al2O3/Na2	4.175	4.526316	3.761905	3.555556	4.02439	3.682927	4.075	3.555556	4.526316	4.216216	4.025641	4.076923	3.712297	3.963235
SiO2/Al2O	3.5329	3.3023	3.9177	3.9438	3.8303	4.4040	4.1104	3.9000	3.3023	4.2821	4.1847	4.0818	3.8188	3.8893
Ti/Nb	24000.00	22800.00	25200.00	27000.00	24600.00	24600.00	24000.00	27000.00	22800.00	3474.18	2176.74	4020.62	25860.00	24480.00
use?	no	no	no	no	no	ok	no	no	ok	no	ok	ok	ok	ok
altered?	alt.LOI	alt.LOI	alt.LOI	alt.LOI	alt.LOI		alt.LOI	alt.LOI		alt.LOI				
why not use														

MCAo incl.	Christmas p	Christmas	Christmas p	Christmas p	ELK MOUN	ELK MOUN	ELK MOUN	ELK MOUN	ELK MOUN	ELK MOUN	ELK MOUN	ELK MOUN	ELK MOUN	ELK MOUN
COUNTY	Gila	Gila	Gila	Gila	Elko	Elko	Elko	Elko	Elko	Elko	Elko	Elko	Elko	Elko
STATE	AZ	AZ	AZ	AZ	NV	NV	NV	NV	NV	NV	NV	NV	NV	NV
SAMPLE #	CH-13	CH-14	CH-31	CH-32	881096	881097	881098	C3D	C5	C10D	C11	C11I	C11K	C13
NAME	CRISMASP	CRISMASP	CRISMASP	CRISMASP	ELKMTNPL	ELKMTNPL	ELKMTNPL	ELKMTNPL	ELKMTNPL	ELKMTNPL	ELKMTNPL	ELKMTNPL	ELKMTNPL	ELKMTNPL
SOURCE:	Lang, 1991	Lang, 1991	Lang, 1991	Lang, 1991	MagmaChe	MagmaChe	MagmaChe	MagmaChe	MagmaChe	MagmaChe	MagmaChe	MagmaChe	MagmaChe	MagmaChe
ROCK TYP	MacDonald	Granite Bas	Christmas s	Christmas s	APLITE	GRANITE	GRANITE	PLUTON	PLUTON	PLUTON	PLUTON	PLUTON	PLUTON	PLUTON
SiO2	53.36	61.90	64.80	66.75	75.05	69.73	70.54	73.98	74.42	74.38	67.85	68.86	62.66	75.84
TiO2	0.13	0.53	0.59	0.35	0.09	0.38	0.36	0.11	0.07	0.07	0.38	0.44	0.24	0.08
Al2O3	16.27	16.95	15.60	15.70	12.42	14.73	15.2	12.46	12.31	12.94	14.58	14.64	19.05	13.38
Fe2O3	8.18	3.02	2.60	1.70	0.53	0.75	0.9	0.15	0.31	0.28	1.38	1.31	0.23	0.23
FeO	n.a.	1.84	1.42	1.85	0.2	1.2	1.05	0.19	0.4	0.37	1.74	1.74	0.1	0.31
MgO	4.69	2.43	2.10	2.35	0.13	1.23	0.99	0.77	0.73	0.76	1.5	1.63	0	0.69
MnO	0.11	0.18	0.05	0.00	-0.01	0.05	0.05	0.01	0.04	0.02	0.09	0.09	0.01	0.01
CaO	5.60	3.98	4.10	3.55	0.76	3.15	2.8	1	0.7	1.35	3.52	3.44	1.44	0.9
Na2O	3.47	4.34	3.90	4.05	3.11	4.34	4.13	2.68	3.71	4.8	3.76	3.76	4.99	3.68
K2O	1.84	2.31	2.30	2.15	5.05	3.29	3.79	5.14	4.89	4.23	2.57	2.41	10.22	5.52
P2O5	0.16	0.21	0.04	0.24	-0.03	0.26	0.24	0.02	0.07	0.04	0.17	0.19	0.11	0.24
LOI	4.19	1.63	1.80	0.73	0.2	0.6	0.3	2.2	1.8	1.1	2	1.4	2	0.3
TOTAL	99.25	99.32	99.30	99.42	97.54	99.71	100.35	98.71	99.45	100.34	99.54	99.91	101.66	101.18
MINING DI	Christmas	Christmas	Christmas	Christmas	ELK MOUN	ELK MOUN	ELK MOUN	ELK MOUN	ELK MOUN	ELK MOUN	ELK MOUN	ELK MOUN	ELK MOUN	ELK MOUN
Ba	0	0	861.20	0	90	670	980	1100	1020	1180	815	0	0	0
Rb	0	0	47.45	0	240	125	150	0	0	0	97.7	0	0	0
Sr	0	0	660.90	0	69	380	420	0	0	0	672.4	0	0	0
Y	0	0	6.78	0	-5	-5	-5	0	0	0	18.3	0	0	0
Zr	0	0	100.08	0	85	145	135	0	0	0	147.8	0	0	0
Nb	0	0	5.07	0	18	29	24	0	0	0	19	0	0	0
CLASS	MCAo	MCAo	MCAo	MCAo	MCAo	MCAo	MCAo	MCAo	MCAo	MCAo	MCAo	MCAo	MCAo	MCAo
A/CNK	0.909	1.003	0.952	1.015	1.037	0.896	0.950	1.055	0.970	0.866	0.948	0.972	0.869	0.978
A/NK	2.11	1.76	1.75	1.75	1.17	1.38	1.39	1.25	1.08	1.04	1.62	1.66	0.99	1.11
Na2O+K2	5.31	6.65	6.20	6.20	8.16	7.63	7.92	7.82	8.60	9.03	6.33	6.17	15.21	9.20
Na2O/K2O	1.89	1.88	1.70	1.88	0.62	1.32	1.09	0.52	0.76	1.13	1.46	1.56	0.49	0.67
NaO+K2O-	-0.29	2.67	2.10	2.65	7.40	4.48	5.12	6.82	7.90	7.68	2.81	2.73	13.77	8.30
K2O-CaO	-3.76	-1.67	-1.80	-1.40	4.29	0.14	0.99	4.14	4.19	2.88	-0.95	-1.03	8.78	4.62
K2O-MgO	-2.85	-0.12	0.20	-0.20	4.92	2.06	2.80	4.37	4.16	3.47	1.07	0.78	10.22	4.83
FeO/MgO*	ERR	1.88	1.79	1.44	5.21	1.52	1.88	0.42	0.93	0.82	1.99	1.79	ERR	0.75
Fe3+/Fe2+	ERR	1.64	1.83	0.92	2.65	0.63	0.86	0.79	0.78	0.76	0.79	0.75	2.30	0.74
LARSEN	9.34	16.53	17.70	18.50	29.18	22.15	23.51	28.03	28.27	26.91	20.17	20.29	29.67	29.21
ALKALI IN	1.46	-0.38	-1.91	-2.63	-3.76	-2.31	-2.32	-3.70	-3.08	-2.64	-2.91	-3.45	7.90	-3.01
ALT INDE	41.859	36.294	35.484	37.190	57.238	37.635	40.820	61.627	56.032	44.794	35.859	35.943	61.381	57.553
K INDEX	0.77	1.06	1.06	1.23	5.77	1.76	1.91	6.48	6.77	4.96	1.20	1.23	8.71	6.98
Na INDEX	2.7945	2.8820	2.6480	2.8991	1.6525	2.2147	2.0393	1.5766	1.7292	2.0006	2.4107	2.5318	1.3572	1.6445
Al2O3/Na2	4.688761	3.90553	4	3.876543	3.993569	3.394009	3.680387	4.649254	3.318059	2.695833	3.87766	3.893617	3.817635	3.63587
SiO2/Al2O	3.2797	3.6519	4.1538	4.2516	6.0427	4.7339	4.6408	5.9374	6.0455	5.7481	4.6536	4.7036	3.2892	5.6682
Ti/Nb	20820.00	26040.00	4615.38	24300.00	1036.67	897.93	1032.50	16080.00	22260.00	28800.00	1187.37	22560.00	29940.00	22080.00
use?	no	ok	ok	ok	no	ok	ok	no	no	no	no	no	no	no
altered?	alt.LOI				alt.KI			alt.KI,LOI	alt.KI	alt.KI	alt.NAI	alt.NAI	alt.AI,KI	alt.AI
why not use														

MCAo incl.	ELK MOUN	ELK MOUN	ELK MOUN	ELK MOUN	ELK MOUN	ELK MOUN	ELK MOUN	ELK MOUN	ELK MOUN	ELK MOUN	ELK MOUN	ELK MOUN	ELK MOUN	ELK MOUN
COUNTY	Elko	Elko	Elko	Elko	Elko	Elko	Elko	Elko	Elko	Elko	Elko	Elko	Elko	Elko
STATE	NV	NV	NV	NV	NV	NV	NV	NV	NV	NV	NV	NV	NV	NV
SAMPLE #	C14	C15	C15D	C16	C16D	C21	C21K	C22	C23	C23I	C24	C24I	C25	C26
NAME	ELKMTNPL	ELKMTNPL	ELKMTNPL	ELKMTNPL	ELKMTNPL	ELKMTNPL	ELKMTNPL	ELKMTNPL	ELKMTNPL	ELKMTNPL	ELKMTNPL	ELKMTNPL	ELKMTNPL	ELKMTNPL
SOURCE:	MagmaChe	MagmaChe	MagmaChe	MagmaChe	MagmaChe	MagmaChe	MagmaChe	MagmaChe	MagmaChe	MagmaChe	MagmaChe	MagmaChe	MagmaChe	MagmaChe
ROCK TYP	PLUTON	PLUTON	PLUTON	PLUTON	PLUTON	PLUTON	PLUTON	PLUTON	PLUTON	PLUTON	PLUTON	PLUTON	PLUTON	PLUTON
SiO2	75.59	66.32	74.05	67.66	77.07	66.32	61.81	69.12	67.64	68.11	66.63	66.37	67.04	68.95
TiO2	0.08	0.05	0.09	0.5	0.08	0.43	0.21	0.48	0.42	0.45	0.41	0.39	0.45	0.39
Al2O3	12.83	15.73	12.88	15.3	12.57	15.73	19.33	15.26	14.99	15.28	15.72	15.7	15.19	15.09
Fe2O3	0.24	1.38	0.24	1.5	0.19	1.29	0.12	1.26	1.16	1.36	1.28	1.25	1.25	1.24
FeO	0.32	1.85	0.34	2	0.27	1.71	0.05	1.7	1.56	1.56	1.58	1.57	1.66	1.65
MgO	0.69	1.75	0.58	1.79	0.61	1.73	0	1.72	1.49	1.58	1.49	1.47	1.58	1.53
MnO	0.05	0.1	0.06	0.12	0.02	0.09	0	0.1	0.09	0.11	0.09	0.09	0.1	0.11
CaO	0.83	3.72	0.99	3.73	0.98	3.36	0.84	3.17	3.23	3.18	3.26	3.38	3.25	3.34
Na2O	3.43	3.64	3.64	3.54	3.67	3.87	4.19	3.92	3.57	3.57	3.73	3.87	3.63	3.76
K2O	4.83	3.41	4.93	2.99	4.69	3.47	11.1	3.47	3.59	3.59	3.62	3.5	3.5	2.76
P2O5	0.03	0.19	0.04	0.22	0.02	0.27	0.07	0.19	0.2	0.13	0.17	0.24	0.2	0.17
LOI	0.8	1.2	1.1	1.2	0.4	0.8	1.5	0.4	0.8	2	1.5	1.5	0.8	0.8
TOTAL	99.72	99.79	98.94	100.55	100.57	99.07	98.82	100.79	98.74	100.92	99.48	99.33	98.65	99.79
MINING DI	ELK MOUN	ELK MOUN	ELK MOUN	ELK MOUN	ELK MOUN	ELK MOUN	ELK MOUN	ELK MOUN	ELK MOUN	ELK MOUN	ELK MOUN	ELK MOUN	ELK MOUN	ELK MOUN
Ba	0	1120	1050	770	0	1120	0	0	1660	0	1270	0	1270	570
Rb	231.5	0	0	82.4	0	126	0	0	126.7	0	0	0	119.2	106.8
Sr	9	0	0	608.7	0	648.7	0	0	657.8	0	0	0	650.2	607.5
Y	6.9	0	0	15.7	0	13.9	0	0	15.9	0	0	0	22.1	16
Zr	113.5	0	0	135.3	0	141.2	0	0	146.2	0	0	0	133.4	137
Nb	22.6	0	0	15.3	0	16.3	0	0	19.9	0	0	0	20	18.7
CLASS	MCAo	MCAo	MCAo	MCAo	MCAo	MCAo	MCAo	MCAo	MCAo	MCAo	MCAo	MCAo	MCAo	MCAo
A/CNK	1.035	0.955	0.980	0.965	0.974	0.968	0.944	0.954	0.958	0.982	0.982	0.962	0.968	0.989
A/NK	1.18	1.62	1.14	1.69	1.13	1.55	1.02	1.49	1.53	1.56	1.56	1.54	1.55	1.64
Na2O+K2	8.26	7.05	8.57	6.53	8.36	7.34	15.29	7.39	7.16	7.16	7.35	7.37	7.13	6.52
Na2O/K2O	0.71	1.07	0.74	1.18	0.78	1.12	0.38	1.13	0.99	0.99	1.03	1.11	1.04	1.36
NaO+K2O-	7.43	3.33	7.58	2.80	7.38	3.98	14.45	4.22	3.93	3.98	4.09	3.99	3.88	3.18
K2O-CaO	4.00	-0.31	3.94	-0.74	3.71	0.11	10.26	0.30	0.36	0.41	0.36	0.12	0.25	-0.58
K2O-MgO	4.14	1.66	4.35	1.20	4.08	1.74	11.10	1.75	2.10	2.01	2.13	2.03	1.92	1.23
FeO/MgO*	0.78	1.77	0.96	1.87	0.72	1.66	ERR	1.65	1.75	1.76	1.83	1.83	1.76	1.81
Fe3+/Fe2+	0.75	0.75	0.71	0.75	0.70	0.75	2.40	0.74	0.74	0.87	0.81	0.80	0.75	0.75
LARSEN	28.51	20.05	28.04	20.02	28.79	20.49	30.86	21.62	21.42	21.53	21.08	20.77	21.02	20.87
ALKALI IN	-3.86	-1.62	-2.98	-2.64	-4.31	-1.33	8.30	-2.32	-2.00	-2.18	-1.44	-1.32	-1.81	-3.13
ALT INDE	56.442	41.214	54.339	39.668	53.266	41.834	68.816	42.264	42.761	43.372	42.231	40.671	42.475	37.665
K INDEX	6.55	1.29	5.92	1.18	6.31	1.46	15.32	1.52	1.48	1.47	1.48	1.46	1.44	1.32
Na INDEX	1.7452	2.0228	1.7185	2.1485	1.7560	2.0831	1.3219	2.0841	1.9521	1.9764	2.0127	2.0677	2.0053	2.3509
Al2O3/Na2	3.740525	4.321429	3.538462	4.322034	3.425068	4.064599	4.613365	3.892857	4.19888	4.280112	4.214477	4.056848	4.184573	4.013298
SiO2/Al2O	5.8917	4.2161	5.7492	4.4222	6.1313	4.2161	3.1976	4.5295	4.5123	4.4575	4.2385	4.2274	4.4134	4.5693
Ti/Nb	910.62	21840.00	21840.00	1388.24	22020.00	1424.54	25140.00	23520.00	1076.38	21420.00	22380.00	23220.00	1089.00	1206.42
use?	no	ok	no	ok	no	ok	no	ok	ok	ok	ok	ok	ok	ok
altered?	alt.KI		alt.KI		alt.NAI,AI,KI		alt.AI,KI							
why not use														

MCAo incl.	ELK MOUN	ELK MOUN	ELK MOUN	ELK MOUN	ELK MOUN	ELK MOUN	ELK MOUN	ELK MOUN	ELK MOUN	ELK MOUN	ELK MOUN	ELK MOUN	ELK MOUN	ELK MOUN
COUNTY	Elko	Elko	Elko	Elko	Elko	Elko	Elko	Elko	Elko	Elko	Elko	Elko	Elko	Elko
STATE	NV	NV	NV	NV	NV	NV	NV	NV	NV	NV	NV	NV	NV	NV
SAMPLE #	C26I	C26D	C29	C32	C34	C34X	C38	C39	C41	C43D	C4	C47	C47D	C47P
NAME	ELKMTNPL	ELKMTNPL	ELKMTNPL	ELKMTNPL	ELKMTNPL	ELKMTNPL	ELKMTNPL	ELKMTNPL	ELKMTNPL	ELKMTNPL	ELKMTNPL	ELKMTNPL	ELKMTNPL	ELKMTNPL
SOURCE:	MagmaChe	MagmaChe	MagmaChe	MagmaChe	MagmaChe	MagmaChe	MagmaChe	MagmaChe	MagmaChe	MagmaChe	MagmaChe	MagmaChe	MagmaChe	MagmaChe
ROCK TYP	PLUTON	PLUTON	PLUTON	PLUTON	PLUTON	PLUTON	PLUTON	PLUTON	PLUTON	PLUTON	PLUTON	PLUTON	PLUTON	PLUTON
SiO2	67.83	73.82	66.13	69.62	64.78	47.37	66.53	73.69	65	67.96	74.15	68.83	73.1	78.26
TiO2	0.36	0.08	0.53	0.39	0.43	1.2	0.42	0.08	0.52	0.38	0.08	0.37	0.07	0.08
Al2O3	15.61	12.6	15.41	14.26	15.56	20.05	15.47	12.96	15.67	15.06	12.21	15.08	12.96	9.86
Fe2O3	1.16	0.22	1.63	1.18	1.27	4.72	0.76	0.1	1.51	1.04	0.21	0.98	0.18	0.17
FeO	1.65	0.29	2.18	1.58	1.69	7.14	1.03	0.12	2.01	1.39	0.28	1.31	0.26	0.22
MgO	1.68	0.5	1.7	1.38	1.31	3.56	1.25	0.57	1.64	1.22	0.45	0.95	0.43	0.45
MnO	0.1	0.02	0.11	0.1	0.09	0.46	0.08	0.01	0.1	0.09	0.02	0.08	0.03	0.01
CaO	3.23	0.95	3.79	3.05	3.39	4.66	3.78	1.07	3.91	2.96	0.75	2.76	1.16	0.66
Na2O	3.76	3.87	3.76	4.08	3.99	4.5	3.76	3.69	3.76	3.75	3.13	3.29	3.85	2.34
K2O	3.37	5.49	2.91	3.63	3.29	4.09	3.93	7.3	2.91	3.65	5.4	4.12	4.43	4.97
P2O5	0.18	0.02	0.23	0.21	0.22	1.18	0.17	0.04	0.22	0.14	0.02	0.17	0.03	0.04
LOI	1.5	0.8	1	0.8	2.7	0.8	2.8	0.8	1.2	1.2	1.4	1.2	1.2	0.8
TOTAL	100.43	98.66	99.38	100.28	98.72	99.63	99.98	100.43	98.45	98.84	98.1	99.14	97.7	97.86
MINING DI	ELK MOUN	ELK MOUN	ELK MOUN	ELK MOUN	ELK MOUN	ELK MOUN	ELK MOUN	ELK MOUN	ELK MOUN	ELK MOUN	ELK MOUN	ELK MOUN	ELK MOUN	ELK MOUN
Ba	0	0	509	0	1030	0	0.0	0	1200	0.0	0	1640	140	60
Rb	0	0	99	0	129.9	0	118.1	0	98.3	200.2	0	151.4	0	228.7
Sr	0	0	706.9	0	714.4	0	656.3	0	720	73.6	0	586.4	0	91.8
Y	0	0	22.9	0	23.7	0	20.1	0	24.3	0.0	0	10.8	0	5
Zr	0	0	152	0	149.6	0	112.9	0	146.5	35.3	0	116.8	0	43.6
Nb	0	0	16.3	0	23.7	0	25.1	0	21.2	10.9	0	17.3	0	11.9
CLASS	MCAo	MCAo	MCAo	MCAo	MCAo	MCAo	MCAo	MCAo	MCAo	MCAo	MCAo	MCAo	MCAo	MCAo
A/CNK	0.993	0.897	0.949	0.880	0.954	0.986	0.892	0.813	0.952	0.970	0.987	1.011	0.978	0.944
A/NK	1.59	1.02	1.65	1.34	1.54	1.69	1.48	0.93	1.68	1.49	1.11	1.53	1.16	1.07
Na2O+K2	7.13	9.36	6.67	7.71	7.28	8.59	7.69	10.99	6.67	7.40	8.53	7.41	8.28	7.31
Na2O/K2O	1.12	0.70	1.29	1.12	1.21	1.10	0.96	0.51	1.29	1.03	0.58	0.80	0.87	0.47
NaO+K2O-	3.90	8.41	2.88	4.66	3.89	3.93	3.91	9.92	2.76	4.44	7.78	4.65	7.12	6.65
K2O-CaO	0.14	4.54	-0.88	0.58	-0.10	-0.57	0.15	6.23	-1.00	0.69	4.65	1.36	3.27	4.31
K2O-MgO	1.69	4.99	1.21	2.25	1.98	0.53	2.68	6.73	1.27	2.43	4.95	3.17	4.00	4.52
FeO/MgO*	1.60	0.98	2.15	1.91	2.16	3.20	1.37	0.37	2.05	1.91	1.04	2.31	0.98	0.83
Fe3+/Fe2+	0.70	0.76	0.75	0.75	0.75	0.66	0.74	0.83	0.75	0.75	0.75	0.75	0.69	0.77
LARSEN	21.07	28.65	19.46	22.41	20.18	11.66	21.08	30.22	19.03	22.12	28.92	23.35	27.21	29.95
ALKALI IN	-2.10	-2.10	-1.93	-2.19	-0.82	6.97	-1.06	-0.42	-1.51	-1.88	-3.05	-2.19	-2.91	-5.80
ALT INDE	41.944	55.412	37.911	41.269	38.397	45.509	40.723	62.312	37.234	42.055	60.123	45.594	49.240	64.371
K INDEX	1.49	6.86	1.13	1.60	1.38	0.76	1.63	9.03	1.14	1.63	7.37	1.69	5.51	7.51
Na INDEX	2.1084	1.6014	2.2406	2.0039	2.1668	2.0865	1.8491	1.3185	2.2438	1.9977	1.5663	1.8099	1.8469	1.4148
Al2O3/Na2	4.151596	3.255814	4.098404	3.495098	3.899749	4.455556	4.114362	3.512195	4.167553	4.016	3.900958	4.583587	3.366234	4.213675
SiO2/Al2O	4.3453	5.8587	4.2914	4.8822	4.1632	2.3626	4.3006	5.6860	4.1481	4.5126	6.0729	4.5643	5.6404	7.9371
Ti/Nb	22560.00	23220.00	1384.05	24480.00	1010.13	27000.00	898.80	22140.00	1064.15	2064.22	18780.00	1141.04	23100.00	1179.83
use?	ok	no	ok	ok	no	no	no	no	ok	ok	no	ok	no	no
altered?		alt.KI			alt.LOI	alt.A/CNK	alt.LOI	alt.Al,KI			alt.Al,KI		alt.KI	alt.Al,NAl
why not use														

MCAo incl.	ELK MOUN	ELK MOUN	ELK MOUN	ELK MOUN	ELK MOUN	ELK MOUN	ELK MOUN	ELK MOUN	ELK MOUN	ELK MOUN	ELK MOUN	ELK MOUN	ELK MOUN	ELK MOUN
COUNTY	Elko	Elko	Elko	Elko	Elko	Elko	Elko	Elko	Elko	Elko	Elko	Elko	Elko	Elko
STATE	NV	NV	NV	NV	NV	NV	NV	NV	NV	NV	NV	NV	NV	NV
SAMPLE #	C50	C50I	C51	C51I	C51D	C52	C52I	C53D	C53	C55	C56	C56I	C57	C58
NAME	ELKMTNPL	ELKMTNPL	ELKMTNPL	ELKMTNPL	ELKMTNPL	ELKMTNPL	ELKMTNPL	ELKMTNPL	ELKMTNPL	ELKMTNPL	ELKMTNPL	ELKMTNPL	ELKMTNPL	ELKMTNPL
SOURCE:	MagmaChe	MagmaChe	MagmaChe	MagmaChe	MagmaChe	MagmaChe	MagmaChe	MagmaChe	MagmaChe	MagmaChe	MagmaChe	MagmaChe	MagmaChe	MagmaChe
ROCK TYP	PLUTON	PLUTON	PLUTON	PLUTON	PLUTON	PLUTON	PLUTON	PLUTON	PLUTON	PLUTON	PLUTON	PLUTON	PLUTON	PLUTON
SiO2	69.59	69.96	68.52	65.13	74.96	66.94	66.62	75.26	69.05	68.98	67.49	68.2	69.34	69.18
TiO2	0.37	0.36	0.39	0.42	0.07	0.38	0.45	0.07	0.35	0.34	0.33	0.32	0.41	0.41
Al2O3	14.29	14.48	14.52	17.87	12.7	15.69	15.54	13.05	14.82	14.97	14.76	14.83	14.32	15.09
Fe2O3	1.31	1.06	1.17	0.76	0.17	1.19	1.24	0.18	1.05	1.04	1.01	1.04	1.1	1.18
FeO	1.42	1.42	1.56	1	0.25	1.68	1.68	0.25	1.41	1.38	1.42	1.42	1.49	1.58
MgO	1.36	1.25	1.4	1.42	0.45	1.6	1.39	0.34	1.07	1.25	1.49	1.49	1.12	1.15
MnO	0.09	0.08	0.09	0.06	0.02	0.1	0.1	0.02	0.08	0.08	0.1	0.09	0.1	0.09
CaO	3.4	3.24	3.32	4.74	0.94	3.16	3.41	0.79	2.97	3.23	3.17	3.15	2.83	3.39
Na2O	3.45	3.45	3.75	3.76	3.77	3.77	3.77	3.45	4.52	3.61	3.63	3.63	3.32	3.63
K2O	2.7	2.97	2.58	2.83	5.17	3.59	3.07	5.01	2.77	3.24	3.35	3.44	4.01	3.19
P2O5	0.18	0.15	0.25	0.24	0.02	0.15	0.18	0.03	0.15	0.19	0.17	0.17	0.16	0.17
LOI	2.5	0.8	1.2	1.2	1.2	2	1.2	0.8	1.4	1.3	1.85	1.85	1.3	1.1
TOTAL	100.66	99.22	98.75	99.43	99.72	100.26	98.65	99.25	99.64	99.61	98.77	99.53	99.5	100.16
MINING DI	ELK MOUN	ELK MOUN	ELK MOUN	ELK MOUN	ELK MOUN	ELK MOUN	ELK MOUN	ELK MOUN	ELK MOUN	ELK MOUN	ELK MOUN	ELK MOUN	ELK MOUN	ELK MOUN
Ba	760	0	920	0	0.0	0	0	0	690	795	1100	0	1540	930
Rb	98.9	0	121.4	0	249.2	0	0	126.5	245.4	109.5	106.9	0	129.8	104.9
Sr	592.5	0	656	0	85.5	0	0	555.1	39	627.9	571.7	0	603.3	608.2
Y	12.4	0	13.7	0	0.0	0	0	12.6	0	12.8	13.2	0	15.5	10.5
Zr	109.5	0	127.9	0	17.9	0	0	140.1	34.6	127.5	132.4	0	138.3	138.8
Nb	17.1	0	20.2	0	7.1	0	0	16.3	12.7	18.1	18.9	0	22.4	16.9
CLASS	MCAo	MCAo	MCAo	MCAo	MCAo	MCAo	MCAo	MCAo	MCAo	MCAo	MCAo	MCAo	MCAo	MCAo
A/CNK	0.966	0.978	0.967	0.999	0.939	0.990	0.987	1.040	0.935	0.976	0.960	0.960	0.957	0.967
A/NK	1.66	1.63	1.62	1.93	1.08	1.55	1.63	1.17	1.42	1.58	1.54	1.53	1.46	1.60
Na2O+K2	6.15	6.42	6.33	6.59	8.94	7.36	6.84	8.46	7.29	6.85	6.98	7.07	7.33	6.82
Na2O/K2O	1.28	1.16	1.45	1.33	0.73	1.05	1.23	0.69	1.63	1.11	1.08	1.06	0.83	1.14
NaO+K2O-	2.75	3.18	3.01	1.85	8.00	4.20	3.43	7.67	4.32	3.62	3.81	3.92	4.50	3.43
K2O-CaO	-0.70	-0.27	-0.74	-1.91	4.23	0.43	-0.34	4.22	-0.20	0.01	0.18	0.29	1.18	-0.20
K2O-MgO	1.34	1.72	1.18	1.41	4.72	1.99	1.68	4.67	1.70	1.99	1.86	1.95	2.89	2.04
FeO/MgO*	1.91	1.90	1.87	1.19	0.90	1.72	2.01	1.21	2.20	1.85	1.56	1.58	2.21	2.30
Fe3+/Fe2+	0.92	0.75	0.75	0.76	0.68	0.71	0.74	0.72	0.74	0.75	0.71	0.73	0.74	0.75
LARSEN	21.14	21.80	20.70	18.38	28.77	21.14	20.48	28.97	21.75	21.75	21.19	21.53	23.17	21.71
ALKALI IN	-3.74	-3.61	-3.16	-1.64	-2.95	-1.54	-1.94	-3.54	-2.40	-2.81	-2.13	-2.30	-2.46	-2.91
ALT INDE	37.214	38.680	36.018	33.333	54.405	42.822	38.316	55.787	33.892	39.629	41.581	42.101	45.479	38.204
K INDEX	1.25	1.37	1.30	1.25	6.99	1.52	1.33	7.32	1.57	1.46	1.54	1.55	1.59	1.32
Na INDEX	2.2434	2.1400	2.4205	2.3275	1.6683	2.0398	2.2150	1.7284	2.5667	2.0902	2.0432	2.0156	1.7846	2.1047
Al2O3/Na2	4.142029	4.197101	3.872	4.75266	3.3687	4.161804	4.122016	3.782609	3.278761	4.146814	4.066116	4.085399	4.313253	4.157025
SiO2/Al2O	4.8698	4.8315	4.7190	3.6447	5.9024	4.2664	4.2870	5.7670	4.6592	4.6079	4.5725	4.5988	4.8422	4.5845
Ti/Nb	1210.53	20700.00	1113.86	22560.00	3185.92	22620.00	22620.00	1269.94	2135.43	1196.69	1152.38	21780.00	889.29	1288.76
use?	no	ok	ok	ok	no	ok	ok	no	ok	ok	ok	ok	ok	ok
altered?	alt.LOI				alt.KI			alt.KI						
why not use														

MCAo incl.	ELK MOUN	ELK MOUN	ELK MOUN	ELK MOUN	ELK MOUN	ELK MOUN	ELK MOUN	ELK MOUN	ELK MOUN	ELK MOUN	ELK MOUN	ELK MOUN	EUGENE	EUGENE	Eugene Mtn
COUNTY	Elko	Elko	Elko	Elko	Elko	Elko	Elko	Elko	Elko	Elko	Elko	Elko	Pershing	Pershing	Pershing
STATE	NV	NV	NV	NV	NV	NV	NV	NV	NV	NV	NV	NV	NV	NV	NV
SAMPLE #	C59	C62	C103	C105	C106	C107	C108	C109	C110	C111	C112	89	90	MC70-1	
NAME	ELKMTNPL	ELKMTNPL	ELKMTNPL	ELKMTNPL	ELKMTNPL	ELKMTNPL	ELKMTNPL	ELKMTNPL	ELKMTNPL	ELKMTNPL	ELKMTNPL	PR3	PR3	Eugene	
SOURCE:	MagmaChe	MagmaChe	MagmaChe	MagmaChe	MagmaChe	MagmaChe	MagmaChe	MagmaChe	MagmaChe	MagmaChe	MagmaChe	Lee, 1984	Lee, 1984	Johnson &	
ROCK TYP	PLUTON	PLUTON	PLUTON	PLUTON	PLUTON	PLUTON	PLUTON	PLUTON	PLUTON	PLUTON	PLUTON	plutons	plutons	granodiorite	
SiO2	69.24	69.03	65.31	66.05	66.72	67.41	66.42	66.53	68.09	67.94	67.68	67	66.7	69.86	
TiO2	0.4	0.37	0.55	0.42	0.42	0.47	0.44	0.42	0.38	0.43	0.36	0.35	0.45	0.36	
Al2O3	14.64	14.72	15.72	15.61	15.59	15.26	15.61	15.65	15.52	1513	14.82	15.1	16	15.40	
Fe2O3	1.14	1.08	1.47	1.32	1.22	1.63	0.82	1.03	1.18	1.27	1.28	1.5	1.5	1.72	
FeO	1.53	1.46	2.12	1.56	1.63	1.87	1.01	1.72	1.53	1.63	1.79	1.6	1.9	1.43	
MgO	1.13	1.19	1.58	1.34	1.43	1.83	1.25	1.37	1.61	1.52	1.57	1.5	1.8	1.14	
MnO	0.09	0.08	0.09	0.08	0.11	0.11	0.06	0.09	0.13	0.1	0.07	0.08	0.06	0.11	
CaO	3.12	3.2	3.96	3.43	3.26	3.62	4.01	3.74	3.28	3.21	3.41	3.3	4	3.57	
Na2O	3.42	3.56	3.81	3.91	3.71	3.61	3.7	3.65	3.79	3.69	3.92	3.6	3.6	2.63	
K2O	3.53	3.34	2.83	3.34	3.38	3.12	3.96	3.62	3.13	3.6	2.73	3.5	3	2.53	
P2O5	0.16	0.18	0.24	0.2	0.16	0.16	0.12	0.15	0.15	0.14	0.15	0.16	0.17	0.14	
LOI	1.2	1.3	1.4	1.5	1.4	1.1	1.2	1.4	1.6	1.1	1.3	0	0	0.93	
TOTAL	99.6	99.51	99.08	98.76	99.03	100.19	98.56	99.37	100.39	99.76	99.08	98.61	100.25	100.01	
MINING DI	ELK MOUN	ELK MOUN	ELK MOUN	ELK MOUN	ELK MOUN	ELK MOUN	ELK MOUN	ELK MOUN	ELK MOUN	ELK MOUN	ELK MOUN	ELK MOUN	Mill City	Mill City	Mill City
Ba	530	740	0	0	0	0	0	0	0	0	0	0	1003	1001	0
Rb	164.8	0	0	0	0	0	0	0	0	0	0	0	108	91	0
Sr	344.2	0	0	0	0	0	0	0	0	0	0	0	471	499	0
Y	6	0	0	0	0	0	0	0	0	0	0	0	17	18	0
Zr	76	0	0	0	0	0	0	0	0	0	0	0	84	130	0
Nb	12.7	0	0	0	0	0	0	0	0	0	0	0	16	30	0
CLASS	MCAo	MCAo	MCAo	MCAo	MCAo	MCAo	MCAo	MCAo	MCAo	MCAo	MCAo	MCAo	MCAo	MCAo	MCAo
A/CNK	0.967	0.961	0.950	0.957	0.992	0.959	0.883	0.935	0.995	95.615	0.949	0.960	0.972	1.134	
A/NK	1.55	1.55	1.68	1.55	1.60	1.64	1.50	1.58	1.61	151.65	1.57	1.55	1.74	2.18	
Na2O+K2	6.95	6.90	6.64	7.25	7.09	6.73	7.66	7.27	6.92	7.29	6.65	7.10	6.60	5.16	
Na2O/K2O	0.97	1.07	1.35	1.17	1.10	1.16	0.93	1.01	1.21	1.03	1.44	1.03	1.20	1.04	
NaO+K2O-	3.83	3.70	2.68	3.82	3.83	3.11	3.65	3.53	3.64	4.08	3.24	3.80	2.60	1.59	
K2O-CaO	0.41	0.14	-1.13	-0.09	0.12	-0.50	-0.05	-0.12	-0.15	0.39	-0.68	0.20	-1.00	-1.04	
K2O-MgO	2.40	2.15	1.25	2.00	1.95	1.29	2.71	2.25	1.52	2.08	1.16	2.00	1.20	1.39	
FeO/MgO*	2.26	2.04	2.18	2.05	1.91	1.82	1.40	1.93	1.61	1.82	1.87	1.97	1.81	2.61	
Fe3+/Fe2+	0.75	0.74	0.69	0.85	0.75	0.87	0.81	0.60	0.77	0.78	0.72	0.94	0.79	1.20	
LARSEN	22.36	21.96	19.06	20.59	20.93	20.14	20.84	20.69	20.94	21.52	20.31	21.03	19.43	21.11	
ALKALI IN	-2.81	-2.78	-1.66	-1.32	-1.73	-2.35	-1.05	-1.48	-2.41	-1.98	-2.53	-1.82	-2.21	-4.83	
ALT INDE	41.607	40.124	36.207	38.935	40.832	40.640	40.325	40.307	40.135	42.596	36.973	42.017	38.710	37.183	
K INDEX	1.42	1.44	1.11	1.39	1.42	1.23	1.55	1.35	1.45	1.47	1.29	1.38	1.16	0.96	
Na INDEX	1.9358	2.0274	2.2960	2.1281	2.0901	2.1157	1.8169	1.9429	2.2054	96.6404	2.3845	1.9884	2.1718	2.1740	
Al2O3/Na2	4.280702	4.134831	4.125984	3.992327	4.202156	4.227147	4.218919	4.287671	4.094987	410.0271	3.780612	4.194444	4.444444	5.856	
SiO2/Al2O	4.7295	4.6895	4.1546	4.2313	4.2797	4.4174	4.2550	4.2511	4.3872	0.0449	4.5668	4.4371	4.1688	4.5360	
Ti/Nb	1615.75	21360.00	22860.00	23460.00	22260.00	21660.00	22200.00	21900.00	22740.00	22140.00	23520.00	1350.00	720.00	ERR	
use?	ok	ok	ok	ok	ok	ok	ok	ok	ok	ok	ok	ok	ok	ok	
altered?															
why not use															

MCAo incl.	Eugene Mtn	Eugene Mt	Eugene Mtn	Eugene Mtn	Eugene Mtn	Eugene Mtn	Ithaca Peak	Ithaca Peak	Patagonia	Patagonia	Patagonia	Patagonia	Patagonia	Patagonia
COUNTY	Pershing	Pershing	Pershing	Pershing	Pershing	Pershing	Mohave	Mohave	Santa Cruz	Santa Cruz	Santa Cruz	Santa Cruz	Santa Cruz	Santa Cruz
STATE	NV	NV	NV	NV	NV	NV	AZ	AZ	AZ	AZ	AZ	AZ	AZ	AZ
SAMPLE #	SMC70-2	SMC72-1	SMC72-2	SMC73-2	SMC74-2	SMC75-1	MP-78	MP-80	2	7	13	15	26	27
NAME	Eugene	Eugene	Eugene	Eugene	Eugene	Eugene	MinPark	MinPark	RedMtn	RedMtn	RedMtn	RedMtn	RedMtn	RedMtn
SOURCE:	Johnson &	Johnson &	Johnson &	Johnson &	Johnson &	Johnson &	Wilkinson e	Wilkinson e	Graybeal, 1	Graybeal, 1	Graybeal, 1	Graybeal, 1	TableB-1,p	TableB-1,p
ROCK TYP	granodiorite	granodiorite	granodiorite	granodiorite	granodiorite	granodiorite	biot. qtz.mo	biot. qtz.mo	Patagonia	Patagonia	Patagonia	Patagonia	Patagonia	Patagonia a
SiO2	69.50	69.15	67.92	67.36	67.62	65.61	72.20	71.60	68.34	68.75	66.54	68.71	78.20	77.56
TiO2	0.38	0.30	0.31	0.37	0.40	0.48	0.04	0.11	0.40	0.44	0.48	0.44	n.a.	n.a.
Al2O3	15.40	15.41	16.19	16.25	16.03	17.08	14.70	15.50	15.43	15.30	15.77	14.81	12.00	12.17
Fe2O3	1.72	2.94	2.42	2.10	2.02	2.91	3.35	3.15	n.a.	n.a.	n.a.	n.a.	0.65	0.97
FeO	1.43	0.35	0.35	1.05	1.45	0.93	n.a.	n.a.	3.30	3.28	4.26	3.58	n.a.	n.a.
MgO	0.95	0.71	0.74	1.19	1.27	0.91	0.71	0.73	1.25	1.30	1.73	1.51	n.a.	n.a.
MnO	0.11	0.09	0.10	0.11	0.11	0.10	0.03	0.01	0.07	0.06	0.09	0.07	n.a.	n.a.
CaO	3.58	3.59	3.72	3.59	3.59	3.66	1.68	2.10	3.34	3.05	3.43	3.25	0.40	0.40
Na2O	3.04	3.44	3.14	2.83	3.49	3.78	3.37	3.10	4.08	3.82	4.00	3.73	2.30	2.40
K2O	2.49	2.62	2.66	2.69	2.89	2.59	3.73	2.89	3.79	4.00	3.70	3.90	6.80	6.70
P2O5	0.15	0.13	0.13	0.14	0.16	0.18	n.a.	n.a.	n.a.	n.a.	n.a.	n.a.	n.a.	n.a.
LOI	0.93	1.08	1.08	1.23	1.07	1.39	3.00	2.14	n.a.	n.a.	n.a.	n.a.	n.a.	n.a.
TOTAL	99.88	99.15	98.82	99.05	10.28	99.73	104.75	102.67	n.a.	n.a.	n.a.	n.a.	n.a.	n.a.
MINING DI	Mill City	Mill City	Mill City	Mill City	Mill City	Mill City	Mineral Par	Mineral Par	Red Mounta	Red Mount	Red Mounta	Red Mounta	Red Mount	Red Mounta
Ba	0	0	0	0	0	0	0	0	0	0	0	0	0	0
Rb	0	0	0	0	0	0	0	0	0	0	0	0	0	0
Sr	0	0	0	0	0	0	0	0	0	0	0	0	0	0
Y	0	0	0	0	0	0	0	0	0	0	0	0	0	0
Zr	0	0	0	0	0	0	0	0	0	0	0	0	0	0
Nb	0	0	0	0	0	0	0	0	0	0	0	0	0	0
CLASS	MCAo	MCAo	MCAo	MCAo	MCAo	MCAo	MCAo	MCAo	MCAo	MCAo	MCAo	MCAo	MCAo	MCAo
A/CNK	1.083	1.025	1.092	1.151	1.040	1.088	1.162	1.285	0.913	0.946	0.936	0.909	1.009	1.019
A/NK	2.00	1.81	2.01	2.15	1.81	1.89	1.53	1.88	1.43	1.44	1.49	1.43	1.08	1.08
Na2O+K2	5.53	6.06	5.80	5.52	6.38	6.37	7.10	5.99	7.87	7.82	7.70	7.63	9.10	9.10
Na2O/K2O	1.22	1.31	1.18	1.05	1.21	1.46	0.90	1.07	1.08	0.96	1.08	0.96	0.34	0.36
NaO+K2O-	1.95	2.47	2.08	1.93	2.79	2.71	5.42	3.89	4.53	4.77	4.27	4.38	8.70	8.70
K2O-CaO	-1.09	-0.97	-1.06	-0.90	-0.70	-1.07	2.05	0.79	0.45	0.95	0.27	0.65	6.40	6.30
K2O-MgO	1.54	1.91	1.92	1.50	1.62	1.68	3.02	2.16	2.54	2.70	1.97	2.39	ERR	ERR
FeO/MgO*	3.13	4.22	3.42	2.47	2.57	3.90	ERR	ERR	2.64	2.52	2.46	2.37	ERR	ERR
Fe3+/Fe2+	1.20	8.40	6.91	2.00	1.39	3.13	ERR	ERR	0.00	0.00	0.00	0.00	ERR	ERR
LARSEN	21.13	21.37	20.84	20.36	20.57	19.89	25.41	23.93	21.98	22.57	20.72	22.04	ERR	ERR
ALKALI IN	-4.32	-3.66	-3.47	-3.54	-2.77	-2.04	-3.76	-4.65	-1.55	-1.76	-1.05	-1.93	-3.99	-3.75
ALT INDE	34.195	32.143	33.138	37.670	37.011	31.993	46.786	41.043	40.449	43.550	42.224	43.664	ERR	ERR
K INDEX	0.99	1.03	1.05	1.03	1.12	1.01	ERR	ERR	1.37	1.44	1.23	1.34	ERR	ERR
Na INDEX	2.3040	2.3375	2.2723	2.2034	2.2474	2.5477	2.0654	2.3578	1.9891	1.9006	2.0174	1.8657	1.3474	1.3769
Al2O3/Na2	5.066	4.48	5.156	5.742	4.593	4.519	4.362018	5	3.781863	4.005236	3.9425	3.970509	5.217391	5.070833
SiO2/Al2O	4.5130	4.4873	4.1952	4.1452	4.2180	3.8413	4.9116	4.6194	4.4290	4.4935	4.2194	4.6394	6.5167	6.3730
Ti/Nb	ERR	ERR	ERR	ERR	ERR	ERR	20220.00	18600.00	24480.00	22920.00	24000.00	22380.00	13800.00	14400.00
use?	ok	ok	ok	no	OK	OK	no	no	ok	ok	ok	ok	no	no
altered?				alt.A/CNK			alt.LOI,KI	alt.LOI,KI					alt.	alt.
why not use													data lack	data lack

MCAo incl.	Patagonia	Patagonia	Patagonia	Patagonia	Patagonia	Patagonia	Patagonia	Patagonia	Patagonia	Ray plutons	Ray plutons	Ray plutons	Ray plutons	Ray plutons
COUNTY	Santa Cruz	Santa Cruz	Santa Cruz	Santa Cruz	Santa Cruz	Santa Cruz	Santa Cruz	Santa Cruz	Santa Cruz	Pinal	Pinal	Pinal	Pinal	Pinal
STATE	AZ	AZ	AZ	AZ	AZ	AZ	AZ	AZ	AZ	AZ	AZ	AZ	AZ	AZ
SAMPLE #	28	29	30	31	JD-4	JD-5	JD-6	JD-7	JD-8	D in Clarke	A in Clarke	C in Clarke	B in Clarke	D
NAME	RedMtn	RedMtn	RedMtn	RedMtn	RedMtn	RedMtn	RedMtn	RedMtn	RedMtn	RAY	RAY	RAY	RAY	RAY
SOURCE:	TableB-1,p	TableB-1,p	TableB-1,p	TableB-1,p	Dewhurst, 1	Dewhurst, 1	Dewhurst,	Dewhurst, 1	Dewhurst, 1	Ransome,	Ransome, 1	Ransome, 1	Ransome,	Ransome, 1
ROCK TYP	Patagonia a	Patagonia a	Patagonia a	Patagonia a	biotite gran	Syenodiorit	granodiorite	granodiorite	granodiorite	qtz diorite	Granite Mtn	Granodiorit	dior por	Qtz dior por
SiO2	77.65	77.40	77.79	77.53	63.32	56.10	65.94	67.49	66.73	60.42	70.52	64.84	65.30	68.26
TiO2	n.a.	n.a.	n.a.	n.a.	0.65	0.87	0.55	0.57	0.50	0.83	0.27	0.50	0.50	0.29
Al2O3	12.17	12.16	12.25	12.30	17.03	17.75	17.22	15.19	16.61	17.27	15.54	16.49	15.92	15.91
Fe2O3	0.97	0.95	0.89	0.92	n.a.	n.a.	n.a.	n.a.	n.a.	2.60	0.77	1.87	1.37	3.09
FeO	n.a.	n.a.	n.a.	n.a.	4.06	6.02	3.16	3.81	2.98	3.47	1.31	2.28	2.19	0.00
MgO	n.a.	n.a.	n.a.	n.a.	2.27	3.72	1.40	1.71	1.55	2.30	0.66	1.58	1.59	0.87
MnO	n.a.	n.a.	n.a.	n.a.	n.a.	n.a.	n.a.	n.a.	n.a.	0.13	0.02	0.06	0.05	0.00
CaO	0.45	0.47	0.42	0.45	3.49	6.77	3.26	2.44	2.82	6.36	2.49	4.54	3.89	2.11
Na2O	2.60	2.10	2.30	2.25	4.62	3.47	4.10	3.46	3.80	3.14	3.96	4.18	4.01	2.80
K2O	6.25	6.75	6.50	6.65	2.84	1.89	3.28	3.55	3.40	2.34	3.72	2.46	3.08	0.00
P2O5	n.a.	n.a.	n.a.	n.a.	n.a.	n.a.	n.a.	n.a.	n.a.	0.20	0.09	0.19	0.29	0.00
LOI	n.a.	n.a.	n.a.	n.a.	n.a.	n.a.	n.a.	n.a.	n.a.	0.85	1.27	1.20	1.71	6.67
TOTAL	n.a.	n.a.	n.a.	n.a.	98.28	96.59	98.91	98.22	98.39	100.46	100.62	100.19	99.90	100.00
MINING DI	Red Mounta	Red Mount	Red Mounta	Red Mounta	Red Mounta	Red Mounta	Red Mount	Red Mounta	Red Mounta	Mineral Cre	Mineral Cre	Mineral Cre	Mineral Cre	Mineral Cre
Ba	0	0	0	0	0	0	0	0	0	0	0	0	0	0
Rb	0	0	0	0	0	0	0	0	0	0	0	0	0	0
Sr	0	0	0	0	0	0	0	0	0	0	0	0	0	0
Y	0	0	0	0	0	0	0	0	0	0	0	0	0	0
Zr	0	0	0	0	0	0	0	0	0	0	0	0	0	0
Nb	0	0	0	0	0	0	0	0	0	0	0	0	0	0
CLASS	MCAo	MCAo	MCAo	MCAo	MCAo	MCAo	MCAo	MCAo	MCAo	MCAo	MCAo	MCAo	MCAo	MCAo
A/CNK	1.024	1.045	1.056	1.048	0.999	0.883	1.060	1.086	1.102	0.895	1.030	0.926	0.935	1.883
A/NK	1.10	1.13	1.13	1.13	1.59	2.29	1.67	1.59	1.67	2.24	1.47	1.73	1.60	3.45
Na2O+K2	8.85	8.85	8.80	8.90	7.46	5.36	7.38	7.01	7.20	5.48	7.68	6.64	7.09	2.80
Na2O/K2O	0.42	0.31	0.35	0.34	1.63	1.84	1.25	0.97	1.12	1.34	1.06	1.70	1.30	ERR
NaO+K2O-	8.40	8.38	8.38	8.45	3.97	-1.41	4.12	4.57	4.38	-0.88	5.19	2.10	3.20	0.69
K2O-CaO	5.80	6.28	6.08	6.20	-0.65	-4.88	0.02	1.11	0.58	-4.02	1.23	-2.08	-0.81	-2.11
K2O-MgO	ERR	ERR	ERR	ERR	0.57	-1.83	1.88	1.84	1.85	0.04	3.06	0.88	1.49	-0.87
FeO/MgO*	ERR	ERR	ERR	ERR	1.79	1.62	2.26	2.23	1.92	2.53	3.03	2.51	2.15	3.20
Fe3+/Fe2+	ERR	ERR	ERR	ERR	0.00	0.00	0.00	0.00	0.00	0.75	0.59	0.82	0.63	ERR
LARSEN	ERR	ERR	ERR	ERR	18.19	10.10	20.60	21.90	21.27	13.82	24.08	17.95	19.37	19.77
ALKALI IN	-4.04	-3.94	-4.14	-3.94	-0.10	0.49	-1.15	-2.10	-1.62	-1.00	-2.55	-1.48	-1.20	-6.59
ALT INDE	ERR	ERR	ERR	ERR	38.654	35.394	38.870	47.133	42.783	32.815	40.443	31.661	37.152	15.052
K INDEX	ERR	ERR	ERR	ERR	1.29	0.71	1.37	1.40	1.51	0.64	1.86	0.97	1.19	0.75
Na INDEX	1.4405	1.3562	1.4097	1.3863	2.6262	2.7195	2.3102	2.0605	2.2193	2.2372	2.0946	2.6248	2.2371	ERR
Al2O3/Na2	4.680769	5.790476	5.326087	5.466667	3.686147	5.115274	4.2	4.390173	4.371053	5.5	3.924242	3.944976	3.970075	5.682143
SiO2/Al2O	6.3804	6.3651	6.3502	6.3033	3.7181	3.1606	3.8293	4.4431	4.0175	3.4986	4.5380	3.9321	4.1018	4.2904
Ti/Nb	15600.00	12600.00	13800.00	13500.00	27720.00	20820.00	24600.00	20760.00	22800.00	18840.00	23760.00	25080.00	24060.00	16800.00
use?	no	no	no	no	ok	ok	ok	ok	ok	ok	ok	ok	ok	no
altered?	alt.NAI	alt.NAI	alt.NAI	alt.NAI										alt.LOI
why not use														

MCAo incl.	Ray plutons	Ray plutons	Ray plutons	Ray plutons	Ray plutons	Ray plutons	Ray plutons	Ray plutons	Ray plutons	Ray plutons	Ray plutons	Ray plutons	Ray plutons	Ray plutons
COUNTY	Pinal	Pinal	Pinal	Pinal	Pinal	Pinal	Pinal	Pinal	Pinal	Pinal	Pinal	Pinal	Pinal	Pinal
STATE	AZ	AZ	AZ	AZ	AZ	AZ	AZ	AZ	AZ	AZ	AZ	AZ	AZ	AZ
SAMPLE #	D	A	9	10	B	C	D	E	14	F	6	2	13	4
NAME	RAY	RAY	RAY	RAY	RAY	RAY	RAY	RAY	RAY	RAY	RAY	RAY	RAY	RAY
SOURCE:	Ransome, 1	Banks et al,	Banks et al,	Banks et al,	Banks et al,	Banks et al,	Banks et al,	Banks et al,	Banks et al,	Banks et al,	Creasey, 19	Creasey, 19	Creasey, 19	Creasey, 19
ROCK TYP	diorite porp	Rattler Grn	Rattler Grn	Rattler Grn	Rattler Grn	hrnblnd and	melanocrati	rhyodacite	Granite Mtn	Granite Mtn	Granite Mtn	Teapot Mtn.	Rattler Grn	Tortilla Qtz
SiO2	63.30	55.80	67.10	66.10	74.60	57.00	65.30	68.30	68.40	76.40	70.12	67.00	67.10	56.61
TiO2	0.50	0.87	0.45	0.41	0.12	0.59	0.50	0.29	0.38	0.11	0.31	0.35	0.45	0.54
Al2O3	15.92	18.70	16.20	16.40	13.90	16.30	15.90	15.90	15.90	13.10	15.53	15.45	16.43	17.38
Fe2O3	1.87	4.20	1.60	2.60	0.41	4.20	1.40	1.40	1.40	0.06	1.06	1.25	1.71	3.88
FeO	2.19	3.70	1.80	1.30	0.18	2.50	2.20	1.70	1.20	0.60	1.27	1.03	1.73	3.75
MgO	1.59	2.70	1.50	1.20	0.32	5.30	1.60	0.90	1.30	0.10	0.92	0.75	1.43	3.20
MnO	0.05	0.14	0.07	0.07	0.00	0.08	0.05	0.00	0.06	0.00	0.04	0.05	0.06	0.14
CaO	3.89	8.20	4.00	3.90	0.72	5.40	3.90	2.10	2.60	0.59	2.42	2.75	3.95	6.70
Na2O	4.01	3.30	3.80	3.30	2.50	3.50	4.00	2.70	4.20	3.30	3.88	2.80	3.68	3.23
K2O	3.08	1.20	2.50	2.60	6.30	2.10	3.10	2.80	3.00	5.20	3.32	4.10	2.55	2.08
P2O5	0.29	0.30	0.16	0.17	0.06	0.28	0.29	0.00	0.13	0.00	0.16	0.15	0.24	0.30
LOI	3.21	0.89	0.82	0.95	0.89	1.75	1.76	3.91	1.43	0.54	0.85	1.49	0.64	0.97
TOTAL	99.90	100.00	100.00	99.00	100.00	99.00	100.00	100.00	100.00	100.00	99.88	97.17	99.97	98.78
MINING DI	Mineral Cre	Mineral Cre	Mineral Cre	Mineral Cre	Mineral Cre	Mineral Cre	Mineral Cre	Mineral Cre	Mineral Cre	Mineral Cre	Mineral Cre	Mineral Cre	Mineral Cre	Mineral Cre
Ba	0	0	0	0	0	0	0	0	0	0	0	0	0	0
Rb	0	0	0	0	0	0	0	0	0	0	0	0	0	0
Sr	0	0	0	0	0	0	0	0	0	0	0	0	0	0
Y	0	0	0	0	0	0	0	0	0	0	0	0	0	0
Zr	0	0	0	0	0	0	0	0	0	0	0	0	0	0
Nb	0	0	0	0	0	0	0	0	0	0	0	0	0	0
CLASS	MCAo	MCAo	MCAo	MCAo	MCAo	MCAo	MCAo	MCAo	MCAo	MCAo	MCAo	MCAo	MCAo	MCAo
A/CNK	0.935	0.863	0.997	1.068	1.134	0.912	0.933	1.406	1.067	1.079	1.079	1.099	1.026	0.879
A/NK	1.60	2.78	1.81	1.99	1.27	2.03	1.60	2.13	1.56	1.18	1.56	1.71	1.86	2.30
Na2O+K2	7.09	4.50	6.30	5.90	8.80	5.60	7.10	5.50	7.20	8.50	7.20	6.90	6.23	5.31
Na2O/K2O	1.30	2.75	1.52	1.27	0.40	1.67	1.29	0.96	1.40	0.63	1.17	0.68	1.44	1.55
NaO+K2O-	3.20	-3.70	2.30	2.00	8.08	0.20	3.20	3.40	4.60	7.91	4.78	4.15	2.28	-1.39
K2O-CaO	-0.81	-7.00	-1.50	-1.30	5.58	-3.30	-0.80	0.70	0.40	4.61	0.90	1.35	-1.40	-4.62
K2O-MgO	1.49	-1.50	1.00	1.40	5.98	-3.20	1.50	1.90	1.70	5.10	2.40	3.35	1.12	-1.12
FeO/MgO*	2.44	2.77	2.16	3.03	1.72	1.18	2.16	3.29	1.89	6.54	2.42	2.87	2.29	2.26
Fe3+/Fe2+	0.85	1.14	0.89	2.00	2.28	1.68	0.64	0.82	1.17	0.10	0.83	1.21	0.99	1.03
LARSEN	18.70	8.90	19.37	19.53	30.13	10.40	19.37	22.57	21.90	29.98	23.35	22.93	19.54	11.05
ALKALI IN	-0.46	-0.26	-2.66	-2.69	-2.95	0.40	-1.19	-3.91	-2.24	-3.92	-2.88	-2.02	-2.73	0.25
ALT INDE	37.152	25.325	33.898	34.545	67.276	45.399	37.302	43.529	38.739	57.671	40.228	46.635	34.281	34.714
K INDEX	1.12	0.46	1.08	0.94	7.19	0.93	1.18	1.26	1.68	6.91	1.75	1.56	1.06	0.61
Na INDEX	2.2371	3.6131	2.5169	2.3374	1.5305	2.5787	2.2230	2.3707	2.4671	1.7131	2.2476	1.7815	2.4690	2.4318
Al2O3/Na2	3.970075	5.666667	4.263158	4.969697	5.56	4.657143	3.975	5.888889	3.785714	3.969697	4.002577	5.517857	4.464674	5.380805
SiO2/Al2O	3.9761	2.9840	4.1420	4.0305	5.3669	3.4969	4.1069	4.2956	4.3019	5.8321	4.5151	4.3366	4.0840	3.2572
Ti/Nb	24060.00	19800.00	22800.00	19800.00	15000.00	21000.00	24000.00	16200.00	25200.00	19800.00	23280.00	16800.00	22080.00	19380.00
use?	no	ok	ok	ok	no	no	ok	no	ok	no	no	ok	ok	ok
altered?	alt.LOI				alt.Al,KI			alt.LOI		alt.Al,KI	alt.NAI			
why not use						volc.								

MCAo incl.	Ray plutons	Ray plutons	Ray plutons	Ray plutons	Ray plutons	Ray plutons	Ray plutons	Ray plutons	Ray plutons	Ray plutons	Ray plutons	Ray plutons	Ray plutons	Ray plutons
COUNTY	Pinal	Pinal	Pinal	Pinal	Pinal	Pinal	Pinal	Pinal	Pinal	Pinal	Pinal	Pinal	Pinal	Pinal
STATE	AZ	AZ	AZ	AZ	AZ	AZ	AZ	AZ	AZ	AZ	AZ	AZ	AZ	AZ
SAMPLE #	R1a1	R1a2	R1a3	R1a4	R21	R22	R2a4	R25	R2a7	R31	R32	R33	R34	R41
NAME	RAY	RAY	RAY	RAY	RAY	RAY	RAY	RAY	RAY	RAY	RAY	RAY	RAY	RAY
SOURCE:	Lang, 1991	Lang, 1991	Lang, 1991	Lang, 1991	Lang, 1991	Lang, 1991	Lang, 1991	Lang, 1991	Lang, 1991	Lang, 1991	Lang, 1991	Lang, 1991	Lang, 1991	Lang, 1991
ROCK TYP	Rattler Grn	Rattler Grn	Rattler Grn	Rattler Grn	Teacup Grn	Teacup Grn	hrnblnd and	Teacup gra	rhyodac dik	Granite Mtn	Granite Mtn	Granite Mtn	aplite dike	Teapot Mtn
SiO2	67.60	67.40	59.50	58.90	68.90	78.10	50.23	71.81	75.10	71.80	72.30	71.50	77.70	64.22
TiO2	0.50	0.45	0.60	0.70	0.40	0.06	1.13	0.23	0.12	0.31	0.24	0.32	0.02	0.49
Al2O3	15.70	15.60	17.60	18.60	17.20	12.80	15.44	15.01	16.90	14.90	14.10	15.10	12.50	15.40
Fe2O3	2.30	1.86	3.03	3.92	2.69	0.38	7.97	1.05	0.76	1.14	1.02	1.28	0.40	2.31
FeO	1.42	1.33	2.65	2.20	1.42	0.00	0.00	0.77	0.39	1.30	0.78	0.91	0.00	1.29
MgO	1.70	1.60	2.10	1.70	1.30	0.03	8.43	0.58	0.35	0.94	0.63	0.81	0.04	1.28
MnO	0.06	0.06	0.12	0.17	0.11	0.02	0.12	0.06	0.03	0.05	0.04	0.04	0.01	0.12
CaO	4.00	4.00	7.20	8.10	5.20	1.30	7.39	2.44	3.80	2.50	2.10	2.70	0.40	3.56
Na2O	3.50	3.50	3.40	3.50	3.60	3.00	3.64	4.15	4.50	3.60	3.50	3.80	2.90	2.68
K2O	2.70	2.80	2.00	1.60	2.20	5.40	1.87	2.97	1.70	3.30	3.90	3.70	6.00	3.03
P2O5	0.05	0.04	0.06	0.08	0.05	0.02	0.28	0.06	0.55	0.04	0.05	0.04	0.02	0.11
LOI	0.60	0.50	0.80	0.30	0.40	0.20	3.20	0.57	0.40	0.40	0.40	0.40	0.20	5.04
TOTAL	100.13	99.36	99.06	99.77	103.47	101.30	99.76	99.78	104.60	100.28	99.04	100.60	100.20	99.56
MINING DI	Mineral Cre	Mineral Cre	Mineral Cre	Mineral Cre	Mineral Cre	Mineral Cre	Mineral Cre	Mineral Cre	Mineral Cre	Mineral Cre	Mineral Cre	Mineral Cre	Mineral Cre	Mineral Cre
Ba	0	0	0	0	643	1	1	779.20	827.50	789.50	545.40	836.30	152.20	326.50
Rb	0	0	0	0	65	1	1	88.62	29.27	107.08	92.45	100.06	144.27	106.91
Sr	0	0	0	0	662	1	1	452.10	654.80	508.10	374.50	540.70	99.70	259.20
Y	0	0	0	0	16	1	1	9.28	4.42	6.29	5.67	7.23	10.31	8.47
Zr	0	0	0	0	100	10	10	92.37	53.11	111.66	96.07	116.35	34.07	99.67
Nb	0	0	0	0	7	1	1	7.77	2.10	65.87	6.72	7.08	2.05	6.49
CLASS	MCAo	MCAo	MCAo	MCAo	MCAo	MCAo	MCAo	MCAo	MCAo	MCAo	MCAo	MCAo	MCAo	MCAo
A/CNK	0.983	0.970	0.843	0.836	0.967	0.972	0.719	1.036	1.045	1.060	1.021	0.994	1.041	1.086
A/NK	1.81	1.77	2.27	2.48	2.07	1.19	1.93	1.49	1.83	1.57	1.41	1.47	1.11	2.00
Na2O+K2	6.20	6.30	5.40	5.10	5.80	8.40	5.51	7.12	6.20	6.90	7.40	7.50	8.90	5.71
Na2O/K2O	1.30	1.25	1.70	2.19	1.64	0.56	1.95	1.40	2.65	1.09	0.90	1.03	0.48	0.88
NaO+K2O-	2.20	2.30	-1.80	-3.00	0.60	7.10	-1.88	4.68	2.40	4.40	5.30	4.80	8.50	2.15
K2O-CaO	-1.30	-1.20	-5.20	-6.50	-3.00	4.10	-5.52	0.53	-2.10	0.80	1.80	1.00	5.60	-0.53
K2O-MgO	1.00	1.20	-0.10	-0.10	0.90	5.37	-6.56	2.39	1.35	2.36	3.27	2.89	5.96	1.75
FeO/MgO*	2.05	1.88	2.56	3.37	2.95	11.40	0.85	2.96	3.07	2.47	2.70	2.55	9.00	2.63
Fe3+/Fe2+	1.62	1.40	1.14	1.78	1.89	ERR	ERR	1.36	1.95	0.88	1.31	1.41	ERR	1.79
LARSEN	19.53	19.67	12.53	11.43	18.67	30.10	2.79	23.89	22.58	23.79	25.27	24.02	31.46	19.60
ALKALI IN	-2.95	-2.77	-0.73	-0.81	-3.83	-4.65	2.82	-3.59	-5.74	-3.81	-3.50	-3.10	-4.00	-2.18
ALT INDE	36.975	36.975	27.891	22.148	28.455	55.807	48.289	35.010	19.807	41.006	44.719	40.963	64.668	40.853
K INDEX	1.05	1.13	0.60	0.49	0.79	5.13	0.96	1.85	1.34	1.62	2.11	1.75	11.76	1.01
Na INDEX	2.2792	2.2200	2.5430	3.0235	2.6037	1.5280	2.6654	2.4329	3.6922	2.1509	1.9181	2.0215	1.5241	1.9704
Al2O3/Na2	4.485714	4.457143	5.176471	5.314286	4.777778	4.266667	4.241758	3.616867	3.755556	4.138889	4.028571	3.973684	4.310345	5.746269
SiO2/Al2O	4.3057	4.3205	3.3807	3.1667	4.0058	6.1016	3.2532	4.7841	4.4438	4.8188	5.1277	4.7351	6.2160	4.1701
Ti/Nb	21000.00	21000.00	20400.00	21000.00	3004.17	18000.00	21840.00	3204.63	12857.14	327.92	3125.00	3220.34	8487.80	2477.66
use?	ok	ok	ok	ok	no	no	no	ok	no	ok	no	ok	no	no
altered?					alt.NAl	alt.Al,Kl	alt.LOI		alt.Al		alt.Al		alt.Al,Kl	alt.Al
why not use														

MCAo incl.	Ray plutons	SIERRITA	SIERRITA	SIERRITA	SIERRITA	SIERRITA	SIERRITA	SIERRITA	SIERRITA	SIERRITA	SIERRITA	SIERRITA	Sierrita	Sierrita
COUNTY	Pinal	Pima	Pima	Pima	Pima	Pima	Pima	Pima	Pima	Pima	Pima	Pima	Pima	Pima
STATE	AZ	AZ	AZ	AZ	AZ	AZ	AZ	AZ	AZ	AZ	AZ	AZ	AZ	AZ
SAMPLE #	R42	RS-MR-5	RSMR3-6	RSMR-8	RSMR3-2	RSMR3-5	RSMR3-8	QL-MR-7	TWB-PA	QL-85-1	RSMR-6	RSMR-4	32	33
NAME	RAY	SIERRITA	SIERRITA	SIERRITA	SIERRITA	SIERRITA	SIERRITA	SIERRITA	SIERRITA	SIERRITA	SIERRITA	SIERRITA	SIERRITA	SIERRITA
SOURCE:	Lang, 1991	Anthony ('8	Anthony '86	Anthony '86	Anthony '86	Anthony '86	Anthony '86	Anthony '86	Anthony '86	Anthony '86	Anthony '86	Anthony '86	?,Table B-1	?,Table B-1
ROCK TYP	Teapot Mtn	Granodiorit	Granodiorit	Granodiorit	Granodiorit	Granodiorit	Granodiorit	Late-stage	Late-stage	Late-stage	Aplites & rh	Aplites & rh	aplite	aplite
SiO2	68.58	65.70	68.90	67.70	68.30	67.20	69.80	68.90	69.40	69.60	76.70	69.60	77.40	77.30
TiO2	0.34	0.42	0.41	0.41	0.36	0.41	0.28	0.37	0.31	0.36	0.10	0.28	n.a.	n.a.
Al2O3	15.50	15.60	15.70	15.70	16.00	16.00	15.40	15.30	15.60	15.20	12.40	14.70	12.00	12.58
Fe2O3	1.71	3.37	3.17	3.13	2.92	2.87	2.27	2.89	1.89	1.76	0.67	1.87	0.95	0.90
FeO	0.51	n.a.	n.a.	n.a.	n.a.	n.a.	n.a.	n.a.	n.a.	n.a.	n.a.	n.a.	n.a.	n.a.
MgO	0.80	1.20	0.90	0.89	0.81	0.88	0.65	0.80	0.73	0.78	0.05	0.54	n.a.	n.a.
MnO	0.05	0.05	0.03	0.04	0.02	0.04	0.04	0.03	0.03	0.02	0	0.02	n.a.	n.a.
CaO	1.83	3.16	2.66	2.79	2.34	2.67	2.05	2.20	2.22	1.34	0.69	1.62	0.65	0.80
Na2O	2.88	3.89	4.10	4.20	4.04	4.12	3.98	3.99	4.20	3.90	2.92	3.64	2.30	2.57
K2O	4.21	3.71	3.92	3.53	3.72	3.81	3.95	4.29	4.24	5.59	5.51	5.28	6.25	6.08
P2O5	0.09	0	0	0	0	0	0	0	0.11	0.14	n.a.	n.a.	n.a.	n.a.
LOI	3.39	0	0	0	0	0	0	0	1.47	1.31	n.a.	n.a.	n.a.	n.a.
TOTAL	99.99	97.10	99.79	98.39	98.51	98.00	98.42	98.77	100.20	100.00	99.04	97.55	n.a.	n.a.
MINING DI	Mineral Cre	Sierrita	Sierrita	Sierrita	Sierrita	Sierrita	Sierrita	Sierrita	Sierrita	Sierrita	Sierrita	Sierrita	Sierrita	Sierrita
Ba	1197.70	878.59	1029.38	891.64	1154.19	1090.93	1138.03	1350.19	1097.37	1523.79	202.64	1501.84	0	0
Rb	126.78	146.45	164.70	142.30	163.05	149.50	163.75	160.70	154.70	247.70	190.40	211.70	0	0
Sr	353.10	448.37	507.21	528.35	468.75	511.48	420.16	479.11	481.80	391.17	63.17	350.03	0	0
Y	8.36	1.00	1.00	1.00	1.00	1.00	1.00	1.00	1.00	1.00	1.00	1.00	0	0
Zr	99.50	132.25	168.14	175.04	166.66	161.01	151.62	184.96	166.07	181.62	65.03	190.63	0	0
Nb	7.03	1.00	1.00	1.00	1.00	1.00	1.00	1.00	1.00	1.00	1.00	1.00	0	0
CLASS	MCAo	MCAo	MCAo	MCAo	MCAo	MCAo	MCAo	MCAo	MCAo	MCAo	MCAo	MCAo	MCAo	MCAo
A/CNK	1.226	0.964	0.991	0.992	1.071	1.014	1.057	1.005	1.003	1.019	1.030	1.002	1.021	1.024
A/NK	1.67	1.50	1.43	1.46	1.50	1.47	1.42	1.36	1.36	1.22	1.15	1.25	1.14	1.16
Na2O+K2	7.09	7.60	8.02	7.73	7.76	7.93	7.93	8.28	8.44	9.49	8.43	8.92	8.55	8.65
Na2O/K2O	0.68	1.05	1.05	1.19	1.09	1.08	1.01	0.93	0.99	0.70	0.53	0.69	0.37	0.42
NaO+K2O-	5.26	4.44	5.36	4.94	5.42	5.26	5.88	6.08	6.22	8.15	7.74	7.30	7.90	7.85
K2O-CaO	2.38	0.55	1.26	0.74	1.38	1.14	1.90	2.09	2.02	4.25	4.82	3.66	5.60	5.28
K2O-MgO	3.41	2.51	3.02	2.64	2.91	2.93	3.30	3.49	3.51	4.81	5.46	4.74	ERR	ERR
FeO/MgO*	2.56	2.53	3.17	3.17	3.24	2.94	3.14	3.25	2.33	2.03	12.06	3.12	ERR	ERR
Fe3+/Fe2+	3.35	1.00	ERR	ERR	ERR	ERR	1.09	ERR	ERR	ERR	ERR	ERR	ERR	ERR
LARSEN	24.44	21.25	23.33	22.42	23.34	22.66	24.52	24.26	24.42	26.67	30.34	26.32	ERR	ERR
ALKALI IN	-2.42	-0.84	-1.61	-1.45	-1.65	-1.07	-2.04	-1.35	-1.38	-0.40	-4.10	-0.97	-4.24	-4.11
ALT INDE	51.543	41.054	41.623	38.738	41.522	40.854	43.274	45.124	43.635	54.866	60.632	52.527	ERR	ERR
K INDEX	2.03	1.42	1.62	1.54	1.73	1.68	2.10	1.89	2.34	3.51	6.56	2.86	5.68	ERR
Na INDEX	1.9104	2.0126	2.0368	2.1821	2.1566	2.0956	2.0647	1.9349	1.9935	1.7163	1.5599	1.6915	1.3893	1.4469
Al2O3/Na2	5.381944	4.010283	3.829268	3.738095	3.960396	3.883495	3.869347	3.834586	3.714286	3.897436	4.246575	4.038462	5.217391	4.894942
SiO2/Al2O	4.4245	4.2115	4.3885	4.3121	4.2688	4.2000	4.5325	4.5033	4.4487	4.5789	6.1855	4.7347	6.4500	6.1447
Ti/Nb	2458.04	23340.00	24600.00	25200.00	24240.00	24720.00	23880.00	23940.00	25200.00	23400.00	17520.00	21840.00	13800.00	15420.00
use?	no	ok	ok	ok	ok	ok	ok	ok	no	no	no	no	no	no
altered?	alt.LOI								alt.KI	alt.KI	alt.Al,KI	alt.KI	alt.KI,NAI	alt.NAI
why not use														

MCAo incl.	Sierrita	Sierrita	Sierrita	Sierrita	Sierrita	Sierrita	Sierrita	Sierrita	Sierrita	Sierrita	Sierrita	Sierrita	Sierrita	Sierrita
COUNTY	Pima	Pima	Pima	Pima	Pima	Pima	Pima	Pima	Pima	Pima	Pima	Pima	Pima	Pima
STATE	AZ	AZ	AZ	AZ	AZ	AZ	AZ	AZ	AZ	AZ	AZ	AZ	AZ	AZ
SAMPLE #	34	35	36	37	38	39	40	RS-MR-5	RS-MR-8	RS-MR3-6	RS-MR3-5	RS-SM-1	RS-SM-10	RS-MR3-8
NAME	SIERRITA	SIERRITA	SIERRITA	SIERRITA	SIERRITA	SIERRITA	SIERRITA	SIERRITA	SIERRITA	SIERRITA	SIERRITA	SIERRITA	SIERRITA	SIERRITA
SOURCE:	?,Table B-1	Table B-1,p	Table B-1,p	Table B-1,p	Table B-1,p	Table B-1,p	Table B-1,p	Hess, 1986	Hess, 1986	Hess, 1986	Hess, 1986	Hess, 1986	Hess, 1986	Hess, 1986
ROCK TYP	aplite	aplite	aplite	aplite	aplite	pegmatite	aplite	Equigran. ri	Equigran. ri	Equigran. ri	Equigran. ri	Equigran. ri	Equigran. ri	Porphyry co
SiO2	77.40	77.57	77.80	77.60	77.23	77.49	77.40	67.66	68.80	69.97	68.57	68.12	70.25	70.93
TiO2	n.a.	n.a.	n.a.	n.a.	n.a.	n.a.	n.a.	0.43	0.42	0.40	0.42	0.47	0.33	0.28
Al2O3	11.91	12.17	12.25	12.25	12.43	12.43	12.25	16.07	15.96	15.33	16.33	16.04	15.84	15.65
Fe2O3	0.92	1.18	0.94	1.25	0.97	0.84	0.99	3.47	3.18	3.22	2.93	3.92	2.21	2.31
FeO	n.a.	n.a.	n.a.	n.a.	n.a.	n.a.	n.a.	n.a.	n.a.	n.a.	n.a.	n.a.	n.a.	n.a.
MgO	n.a.	n.a.	n.a.	n.a.	n.a.	n.a.	n.a.	1.24	0.90	0.90	0.90	1.45	0.78	0.66
MnO	n.a.	n.a.	n.a.	n.a.	n.a.	n.a.	n.a.	0.05	0.04	0.03	0.04	0.04	0.02	0.04
CaO	0.55	0.66	0.80	0.75	0.60	0.55	0.66	3.25	2.84	2.64	2.72	3.07	2.16	2.08
Na2O	2.25	2.57	2.25	2.47	2.38	2.40	2.70	4.01	4.27	3.96	4.20	3.99	4.03	4.04
K2O	6.60	6.10	6.10	6.20	6.70	6.60	6.05	3.82	3.59	3.55	3.89	2.90	4.38	4.01
P2O5	n.a.	n.a.	n.a.	n.a.	n.a.	n.a.	n.a.	n.a.	n.a.	n.a.	n.a.	n.a.	n.a.	n.a.
LOI	n.a.	n.a.	n.a.	n.a.	n.a.	n.a.	n.a.	n.a.	n.a.	n.a.	n.a.	n.a.	n.a.	n.a.
TOTAL	n.a.	n.a.	n.a.	n.a.	n.a.	n.a.	n.a.	97.10	98.39	98.48	98.00	96.61	100.36	98.42
MINING DI	Sierrita	Sierrita	Sierrita	Sierrita	Sierrita	Sierrita	Sierrita	Sierrita	Sierrita	Sierrita	Sierrita	Sierrita	Sierrita	Sierrita
Ba	0	0	0	0	0	0	0	0	0	0	0	0	0	0
Rb	0	0	0	0	0	0	0	0	0	0	0	0	0	0
Sr	0	0	0	0	0	0	0	0	0	0	0	0	0	0
Y	0	0	0	0	0	0	0	0	0	0	0	0	0	0
Zr	0	0	0	0	0	0	0	0	0	0	0	0	0	0
Nb	0	0	0	0	0	0	0	0	0	0	0	0	0	0
CLASS	MCAo	MCAo	MCAo	MCAo	MCAo	MCAo	MCAo	MCAo	MCAo	MCAo	MCAo	MCAo	MCAo	MCAo
A/CNK	1.004	1.010	1.040	1.008	1.012	1.026	1.003	0.964	0.992	1.010	1.015	1.048	1.034	1.058
A/NK	1.10	1.12	1.19	1.14	1.11	1.12	1.11	1.50	1.46	1.48	1.47	1.65	1.39	1.42
Na2O+K2	8.85	8.67	8.35	8.67	9.08	9.00	8.75	7.83	7.86	7.51	8.09	6.89	8.41	8.05
Na2O/K2O	0.34	0.42	0.37	0.40	0.36	0.36	0.45	1.05	1.19	1.12	1.08	1.38	0.92	1.01
NaO+K2O-	8.30	8.01	7.55	7.92	8.48	8.45	8.09	4.58	5.02	4.87	5.37	3.82	6.25	5.97
K2O-CaO	6.05	5.44	5.30	5.45	6.10	6.05	5.39	0.57	0.75	0.91	1.17	-0.17	2.22	1.93
K2O-MgO	ERR	ERR	ERR	ERR	ERR	ERR	ERR	2.58	2.69	2.65	2.99	1.45	3.60	3.35
FeO/MgO*	ERR	ERR	ERR	ERR	ERR	ERR	ERR	ERR	ERR	ERR	ERR	ERR	ERR	ERR
Fe3+/Fe2+	ERR	ERR	ERR	ERR	ERR	ERR	ERR	ERR	ERR	ERR	ERR	ERR	ERR	ERR
LARSEN	ERR	ERR	ERR	ERR	ERR	ERR	ERR	21.88	22.78	23.33	23.13	21.09	24.86	24.91
ALKALI IN	-3.94	-4.19	-4.59	-4.20	-3.65	-3.83	-4.04	-1.34	-1.73	-2.52	-1.42	-2.45	-1.72	-2.34
ALT INDE	ERR	ERR	ERR	ERR	ERR	ERR	ERR	41.071	38.707	40.271	40.905	38.124	45.463	43.281
K INDEX	ERR	ERR	ERR	ERR	ERR	ERR	ERR	1.42	1.54	1.52	1.68	1.26	2.21	2.09
Na INDEX	1.3447	1.4313	1.4089	1.4060	1.3676	1.3899	1.4496	2.0142	2.1811	2.1257	2.0949	2.4240	1.9542	2.0659
Al2O3/Na2	5.293333	4.735409	5.444444	4.959514	5.222689	5.179167	4.537037	4.007481	3:737705	3.871212	3.888095	4.02005	3.930521	3.873762
SiO2/Al2O	6.4987	6.3739	6.3510	6.3347	6.2132	6.2341	6.3184	4.2103	4.3108	4.5643	4.1990	4.2469	4.4350	4.5323
Ti/Nb	13500.00	15420.00	13500.00	14820.00	14280.00	14400.00	16200.00	24060.00	25620.00	23760.00	25200.00	23940.00	24180.00	24240.00
use?	no	no	no	no	no	no	no	ok	ok	ok	ok	ok	no	ok
altered?	alt.NAl	alt.NAl	alt.NAl	alt.NAl	alt.NAl	alt.NAl	alt.NAl						alt.Kl	
why not use														

MCAo incl.	Sierrita	Sierrita	Sierrita	Sierrita	SIERRITA	SIERRITA	SIERRITA	SIERRITA	SIERRITA	SIERRITA	SIERRITA	SIERRITA	SIERRITA	SIERRITA
COUNTY	Pima	Pima	Pima	Pima	Pima	Pima	Pima	Pima	Pima	Pima	Pima	Pima	Pima	Pima
STATE	AZ	AZ	AZ	AZ	AZ	AZ	AZ	AZ	AZ	AZ	AZ	AZ	AZ	AZ
SAMPLE #	RS-MR3-2	RS-MR-4	RS-MR-6	S27	D-MR2-2	D-MR2-3	KD-GR2-7	KDR-GR2-	KDGR-4	KD-GR2-5	6-81-2	KD-GR2-1	KDR-GR-7	KR-MR2-4
NAME	SIERRITA	SIERRITA	SIERRITA	SIERRITA	SIERRITA	SIERRITA	SIERRITA	SIERRITA	SIERRITA	SIERRITA	SIERRITA	SIERRITA	SIERRITA	SIERRITA
SOURCE:	Hess, 1986	Hess, 1986	Hess, 1986	Laine,p.72,	Anthony ('8	Anthony ('8	Anthony ('8	Anthony ('8	Anthony ('8	Anthony ('8	Anthony ('8	Anthony ('8	Anthony '86	Anthony '86
ROCK TYP	Porphyry co	aplite dike	aplite dike	qtz monz	diorite	diorite	andesite	andesite	andesite	andesite	andesite	andesite	Aplites & rh	Aplites & rh
SiO2	69.33	71.29	77.44	65.00	59.30	60.90	62.70	61.90	59.20	57.90	60.70	61.10	74.70	73.00
TiO2	0.37	0.29	0.10	0.50	0.68	0.66	0.55	0.59	0.48	0.42	0.42	0.50	0.09	0.27
Al2O3	16.24	15.10	12.52	15.83	16.80	17.00	16.90	17.00	15.90	16.20	16.00	16.70	13.70	14.50
Fe2O3	2.96	1.92	0.67	0.69	6.15	5.86	5.61	6.33	5.58	5.41	5.29	5.39	0.94	2.60
FeO	n.a.	n.a.	n.a.	2.26	0	0	0	0	0	0	0	0	0	0
MgO	0.82	0.56	0.05	0.93	2.10	2.00	2.50	2.30	2.20	1.50	2.00	0.93	0.17	0.65
MnO	0.02	0.02	0.01	0.03	0.09	0.09	0.09	0.11	0.08	0.08	0.08	0.04	0.03	0.08
CaO	2.38	1.66	0.70	2.52	4.90	4.87	2.88	3.31	3.69	4.81	3.91	2.25	0.70	2.28
Na2O	4.10	3.74	2.95	4.04	3.87	3.85	4.77	4.29	3.71	4.02	3.38	4.55	3.38	2.95
K2O	3.78	5.42	5.56	3.73	3.39	3.58	3.65	3.80	3.66	3.60	3.00	4.27	5.48	4.16
P2O5	n.a.	n.a.	n.a.	n.a.	0	0	0	0	0.29	0.28	0.15	0.30	0	0
LOI	n.a.	n.a.	n.a.	n.a.	0	0	0	0	5.08	4.93	4.15	3.23	0	0
TOTAL	98.51	97.35	99.05	96.51	97.28	98.81	99.65	99.63	99.87	99.15	99.08	99.26	99.19	100.49
MINING DI	Sierrita	Sierrita	Sierrita	Sierrita	Sierrita	Sierrita	Sierrita	Sierrita	Sierrita	Sierrita	Sierrita	Sierrita	Sierrita	Sierrita
Ba	0	0	0	0	978.59	1002.21	1016.56	1331.64	1145.64	1004.62	952.26	1016.64	789.29	1723.18
Rb	0	0	0	0	113.7	116.1	98.11	115.9	111.8	101.5	95.09	114.8	144.1	153.85
Sr	0	0	0	0	642.31	615.67	853.72	926.37	503.79	656.4	457.6	615.87	214.63	277.25
Y	0	0	0	0	0	0	0	0	0	0	0	0	0	0
Zr	0	0	0	0	236.36	221.13	178.26	205.23	170.35	169.27	161.95	171.53	95.62	140.07
Nb	0	0	0	0	0	0	0	0	0	0	0	0	0	0
CLASS	MCAo	MCAo	MCAo	MCAo	MACo	MACo	MACo	MACo	MACo	MACo	MACo	MACo	MACo	MACo
A/CNK	1.070	1.003	1.029	1.036	0.886	0.891	0.991	0.988	0.947	0.840	1.004	1.030	1.072	1.072
A/NK	1.50	1.25	1.15	1.48	1.67	1.66	1.43	1.52	1.58	1.54	1.81	1.38	1.19	1.55
Na2O+K2	7.88	9.16	8.51	7.77	7.26	7.43	8.42	8.09	7.37	7.62	6.38	8.82	8.86	7.11
Na2O/K2O	1.08	0.69	0.53	1.08	1.14	1.08	1.31	1.13	1.01	1.12	1.13	1.07	0.62	0.71
NaO+K2O-	5.50	7.50	7.81	5.25	2.36	2.56	5.54	4.78	3.68	2.81	2.47	6.57	8.16	4.83
K2O-CaO	1.40	3.76	4.86	1.21	-1.51	-1.29	0.77	0.49	-0.03	-1.21	-0.91	2.02	4.78	1.88
K2O-MgO	2.96	4.86	5.51	2.80	1.29	1.58	1.15	1.50	1.46	2.10	1.00	3.34	5.31	3.51
FeO/MgO*	ERR	ERR	ERR	3.10	2.64	2.64	2.02	2.48	2.28	3.25	2.38	5.22	4.98	3.60
Fe3+/Fe2+	ERR	ERR	ERR	0.31	ERR	ERR	ERR	ERR	ERR	ERR	ERR	ERR	ERR	ERR
LARSEN	23.69	26.96	30.62	21.95	16.16	17.01	19.17	18.82	17.50	16.59	17.32	21.46	29.51	25.56
ALKALI IN	-1.91	-1.36	-4.30	-0.41	1.20	0.78	1.10	1.06	1.35	2.08	-0.20	2.09	-2.93	-4.05
ALT INDE	41.516	52.548	60.583	41.533	38.499	39.021	44.565	44.526	44.193	36.612	40.683	43.333	58.068	47.908
K INDEX	1.72	2.87	6.57	1.61	0.90	0.93	1.38	1.15	1.10	0.94	0.97	1.37	5.84	1.68
Na INDEX	2.1544	1.6928	1.5601	2.1188	2.0272	1.9660	2.2978	2.1167	1.9603	1.9569	2.1306	2.0954	1.6886	1.7816
Al2O3/Na2	3.960976	4.037433	4.244068	3.918317	4.341085	4.415584	3.542977	3.962704	4.285714	4.029851	4.733728	3.67033	4.053254	4.915254
SiO2/Al2O	4.2691	4.7212	6.1853	4.1061	3.5298	3.5824	3.7101	3.6412	3.7233	3.5741	3.7938	3.6587	5.4526	5.0345
Ti/Nb	24600.00	22440.00	17700.00	24240.00	23220.00	23100.00	28620.00	25740.00	22260.00	24120.00	20280.00	27300.00	20280.00	17700.00
use?	ok	no	no	no	no	no	no	no	no	no	no	no	no	no
altered?		alt.KI	alt.Al,KI	alt.										alt.KI
why not use					K=older	K=older	K=older	K=older	K=older	K=older	K=older	K=older	K=older	K=older

MCAo incl.	SIERRITA	SIERRITA	Sierrita	Sierrita	Sierrita	Sierrita	Sierrita	Guichon Cr	Guichon Cr	Guichon Cr	Guichon Cr	Guichon Cr	Guichon Cr	Guichon Cr
COUNTY	Pima	Pima	Pima	Pima	Pima	Pima	Pima	?	?	?	?	?	?	?
STATE	AZ	AZ	AZ	AZ	AZ	AZ	AZ	BC	BC	BC	BC	BC	BC	BC
SAMPLE #	KR-3	KR-2	RS-MR2-2	RS-MR-5	S12	S19	S17	1	2	5	6	GB-3	GB-4	GB-7
NAME	SIERRITA	SIERRITA	SIERRITA	SIERRITA	SIERRITA	SIERRITA	SIERRITA	GUICHON	GUICHON	GUICHON	GUICHON	GUICHON	GUICHON	GUICHON
SOURCE:	Anthony '86	Anthony '86	Hess, 1986	Hess, 1986	Laine,p.106	Laine,p.106	Laine,p.106	Briskey & B	Briskey & B	Briskey & B	Briskey & B	Jones, 197	Jones, 197	Jones, 197
ROCK TYP	Aplites & rh	Aplites & rh	biotite qtz di	biotite qtz di	qtz diorite	qtz diorite	qtz diorite	Guichon gr	Guichon gr	Bethlehem	Bethlehem	Black Lake	hybrid phas	Chataway p
SiO2	75.60	76.30	60.96	61.63	56.00	54.00	58.00	61.44	62.37	62.91	64.33	55.31	46.06	64.98
TiO2	0.10	0.14	0.70	0.67	0.67	0.83	0.67	0.48	0.69	0.55	0.51	1.23	0.83	0.65
Al2O3	12.90	12.80	17.27	17.21	16.63	16.44	15.50	17.43	16.27	16.42	16.79	17.29	22.01	15.44
Fe2O3	0.77	0.88	6.32	5.93	4.14	2.76	3.45	1.46	2.39	3.26	2.37	3.57	3.03	2.04
FeO	0	0	0.00	0.00	5.22	5.19	4.88	4.19	2.56	3.06	1.54	4.44	4.04	2.25
MgO	0.17	0.25	2.16	2.02	3.48	4.31	2.82	2.48	2.34	1.10	1.37	3.91	4.79	2.22
MnO	0.19	0.09	0.09	0.09	0.06	0.09	0.09	0.09	0.08	0.06	0.08	0.20	0.25	0.15
CaO	0.98	0.78	5.04	4.93	6.02	5.88	4.90	5.27	4.88	6.09	4.73	7.37	11.79	4.71
Na2O	5.93	5.15	3.98	3.90	3.64	3.51	3.37	3.99	3.93	2.88	4.60	3.61	2.54	3.96
K2O	2.44	3.09	3.48	3.62	2.41	2.41	2.41	1.99	2.35	1.32	1.66	1.63	0.98	2.33
P2O5	0.03	0.04	n.a.	n.a.	n.a.	n.a.	n.a.	0.16	0.11	0.09	0.15	0.01	0.01	0.01
LOI	1.23	0.77	n.a.	n.a.	n.a.	n.a.	n.a.	1.01	1.18	2.08	1.01	1.39	3.32	1.16
TOTAL	100.34	100.29	97.28	98.81	98.66	96.21	96.67	99.99	99.15	99.82	99.14	99.96	99.65	99.90
MINING DI	Sierrita	Sierrita	Sierrita	Sierrita	Sierrita	Sierrita	Sierrita	Valley Copp	Valley Copp	Bethlehem	Bethlehem	Valley Copp	Valley Copp	Valley Copp
Ba	69.87	259.25	0	0	0	0	0	0	0	0	0	0	0	0
Rb	116.1	113.2	0	0	0	0	0	0	0	0	0	0	0	0
Sr	76.18	183.09	0	0	0	0	0	0	0	0	0	0	0	0
Y	0	0	0	0	0	0	0	0	0	0	0	0	0	0
Zr	85.96	85.5	0	0	0	0	0	0	0	0	0	0	0	0
Nb	0	0	0	0	0	0	0	0	0	0	0	0	0	0
CLASS	MACo	MACo	MACo	MACo	MACo	MACo	MACo	MCAo	MCAo	MCAo	MCAo	MCAo	MCAo	MCAo
A/CNK	0.909	0.966	0.885	0.891	0.850	0.861	0.907	0.951	0.909	0.951	0.934	0.818	0.824	0.876
A/NK	1.04	1.08	1.67	1.66	1.93	1.96	1.90	2.00	1.80	2.66	1.79	2.24	4.20	1.71
Na2O+K2	8.37	8.24	7.46	7.52	6.05	5.92	5.78	5.98	6.28	4.20	6.26	5.24	3.52	6.29
Na2O/K2O	2.43	1.67	1.14	1.08	1.51	1.46	1.40	2.01	1.67	2.18	2.77	2.21	2.59	1.70
NaO+K2O-	7.39	7.46	2.42	2.59	0.03	0.04	0.88	0.71	1.40	-1.89	1.53	-2.13	-8.27	1.58
K2O-CaO	1.46	2.31	-1.56	-1.31	-3.61	-3.47	-2.49	-3.28	-2.53	-4.77	-3.07	-5.74	-10.81	-2.38
K2O-MgO	2.27	2.84	1.32	1.60	-1.07	-1.90	-0.41	-0.49	0.01	0.22	0.29	-2.28	-3.81	0.11
FeO/MgO*	4.08	3.17	ERR	ERR	2.57	1.78	2.83	2.22	2.01	5.45	2.68	1.96	1.41	1.84
Fe3+/Fe2+	ERR	ERR	ERR	ERR	0.79	0.53	0.71	0.35	0.93	1.07	1.54	0.80	0.75	0.91
LARSEN	26.49	27.49	16.60	17.21	11.58	10.22	14.02	14.72	15.92	15.10	17.00	8.79	-0.25	17.06
ALKALI IN	-3.75	-4.14	0.78	0.59	1.22	1.83	0.20	-0.88	-0.92	-3.20	-1.67	0.66	2.39	-1.88
ALT INDE	27.416	36.030	38.472	38.977	37.878	41.713	38.741	32.556	34.741	21.247	24.515	33.535	28.706	34.418
K INDEX	5.10	5.40	0.90	0.93	0.64	0.75	0.67	0.79	0.90	0.44	0.91	0.61	0.45	0.97
Na INDEX	3.3395	2.6330	2.0291	1.9680	2.3602	2.3172	2.3056	2.9563	2.5811	3.1330	3.7047	3.0329	3.4157	2.5757
Al2O3/Na2	2.175379	2.485437	4.339196	4.412821	4.568681	4.683761	4.599407	4.368421	4.139949	5.701389	3.65	4.789474	8.665354	3.89899
SiO2/Al2O	5.8605	5.9609	3.5298	3.5811	3.3674	3.2847	3.7419	3.5250	3.8334	3.8313	3.8314	3.1990	2.0927	4.2085
Ti/Nb	35580.00	30900.00	23880.00	23400.00	21840.00	21060.00	20220.00	23940.00	23580.00	17280.00	27600.00	21660.00	15240.00	23760.00
use?	no	no	no	no	no	no	no	no	ok	no	ok	ok	no	ok
altered?	alt.	alt.KI	alt.KI					alt.		alt.Al			alt.LOI	
why not use	K=older	K=older	K=older	K=older	K=older	K=older	K=older							

MCAo incl.	Guichon Cr	Guichon Cr	Guichon Cr	Guichon Cr	Guichon Cr	Guichon Cr	Guichon Cr	Guichon Cr	Guichon Cr	Guichon Cr	Guichon Cr	Guichon Cr	Guichon Cr	Guichon Cr
COUNTY	?	?	?	?	?	?	?	?	?	?	?	?	?	?
STATE	BC	BC	BC	BC	BC	BC	BC	BC	BC	BC	BC	BC	BC	BC
SAMPLE #	GB-6	GB-2	GB-1	GB-5	BS-2	69-30/820	69-47/1364	12-2/2.584	5	6	16	17	30	24
NAME	GUICHON	GUICHON	GUICHON	GUICHON	GUICHON	GUICHON	GUICHON	GUICHON	GUICHON	GUICHON	GUICHON	GUICHON	GUICHON	GUICHON
SOURCE:	Jones, 197	Jones, 197	Jones, 197	Jones, 197	Jones, 197	Jones, 197	Jones, 197	Jones, 197	Briskey, 19	Briskey, 19	Briskey, 19	Briskey, 19	Briskey, 19	Briskey, 19
ROCK TYP	Guichon	Bethlehem	Sheena	Bethsaida p	Bethsaida p	Porph. phas	Tan felsite	aplite	Guichon	Guichon	Guichon	Guichon	Guichon	Guichon
SiO2	66.04	65.79	64.44	68.39	68.86	72.64	75.60	78.78	60.60	62.10	65.40	66.80	65.75	68.14
TiO2	0.53	0.45	0.68	0.40	0.29	0.14	0.04	0.04	0.51	0.59	0.31	0.31	0.49	0.30
Al2O3	15.88	16.91	17.23	15.79	15.94	14.88	14.23	12.01	16.30	16.70	16.80	16.70	16.47	16.71
Fe2O3	1.88	1.94	1.76	1.33	1.56	0.60	n.a.	n.a.	n.a.	n.a.	n.a.	n.a.	1.97	1.43
FeO	1.93	1.44	1.79	1.77	1.41	0.75	n.a.	n.a.	4.90	4.80	3.10	2.80	2.04	1.07
MgO	1.59	1.64	2.04	1.18	0.45	0.40	0.10	0.00	3.10	3.00	1.20	1.10	1.53	0.83
MnO	0.19	0.13	0.19	0.19	0.06	0.00	0.00	0.00	n.a.	n.a.	n.a.	n.a.	0.07	0.04
CaO	4.03	4.78	4.89	3.37	3.38	2.04	0.86	0.53	5.10	5.10	3.90	3.90	3.98	3.51
Na2O	4.05	4.54	4.33	4.42	5.11	4.60	4.00	3.20	4.10	4.30	4.70	4.80	4.09	4.85
K2O	2.67	1.33	1.31	1.72	1.63	1.96	4.03	4.52	2.18	1.72	1.32	1.71	1.99	2.00
P2O5	0.02	0.02	0.02	0.02	0.13	0.00	0.00	0.00	n.a.	n.a.	n.a.	n.a.	0.12	0.11
LOI	1.24	0.81	0.75	0.94	0.65	0.00	0.00	0.00	0.00	0.00	0.00	0.00	0.87	0.84
TOTAL	100.05	99.78	99.43	99.52	99.47	98.01	98.86	99.08	96.80	98.40	96.70	98.10	99.38	99.83
MINING DI	Valley Copp	Bethlehem	Valley Cu	Valley Cu	Valley Cu	Valley Cu	Valley Cu	Valley Cu	Valley Cu	Valley Cu	Valley Cu	Valley Cu	Valley Cu	Valley Cu
Ba	0	0	0	0	0	0	0	0	0	0	0	0	0	0
Rb	0	0	0	0	0	0	0	0	0	0	0	0	0	0
Sr	0	0	0	0	0	0	0	0	0	0	0	0	0	0
Y	0	0	0	0	0	0	0	0	0	0	0	0	0	0
Zr	0	0	0	0	0	0	0	0	0	0	0	0	0	0
Nb	0	0	0	0	0	0	0	0	0	0	0	0	0	0
CLASS	MCAo	MCAo	MCAo	MCAo	MCAo	MCAo	MCAo	MCAo	MCAo	MCAo	MCAo	MCAo	MCAo	MCAo
A/CNK	0.940	0.960	0.987	1.034	0.976	1.110	1.137	1.079	0.886	0.916	1.033	0.991	1.021	1.010
A/NK	1.66	1.90	2.02	1.73	1.57	1.53	1.30	1.18	1.79	1.87	1.83	1.71	1.85	1.65
Na2O+K2	6.72	5.87	5.64	6.14	6.74	6.56	8.03	7.72	6.28	6.02	6.02	6.51	6.08	6.85
Na2O/K2O	1.52	3.41	3.31	2.57	3.13	2.35	0.99	0.71	1.88	2.50	3.56	2.81	2.06	2.43
NaO+K2O-	2.69	1.09	0.75	2.77	3.36	4.52	7.17	7.19	1.18	0.92	2.12	2.61	2.10	3.34
K2O-CaO	-1.36	-3.45	-3.58	-1.65	-1.75	-0.08	3.17	3.99	-2.92	-3.38	-2.58	-2.19	-1.99	-1.51
K2O-MgO	1.08	-0.31	-0.73	0.54	1.18	1.56	3.93	4.52	-0.92	-1.28	0.12	0.61	0.46	1.17
FeO/MgO*	2.28	1.94	1.65	2.51	6.25	3.23	ERR	ERR	1.58	1.60	2.58	2.55	2.49	2.84
Fe3+/Fe2+	0.97	1.35	0.98	0.75	1.11	0.80	ERR	ERR	0.00	0.00	0.00	0.00	0.97	1.34
LARSEN	19.06	16.84	15.86	19.97	20.75	23.73	28.27	30.25	14.18	14.32	18.02	18.98	18.40	20.37
ALKALI IN	-1.85	-2.60	-2.33	-3.30	-2.88	-4.46	-4.09	-5.59	-0.26	-1.08	-2.31	-2.34	-2.38	-2.50
ALT INDE	34.522	24.166	26.651	27.128	19.678	26.222	45.940	54.788	36.464	33.428	22.662	24.414	30.371	25.290
K INDEX	1.09	0.94	0.93	1.16	1.16	2.09	ERR	ERR	0.94	0.91	1.03	1.14	0.98	1.31
Na INDEX	2.4565	4.3733	4.2926	3.6034	4.1110	3.4565	2.1291	1.7866	2.7666	3.4161	4.5933	3.7978	3.0759	3.4351
Al2O3/Na2	3.920988	3.72467	3.979215	3.572398	3.119374	3.234783	3.5575	3.753125	3.97561	3.883721	3.574468	3.479167	4.026895	3.445361
SiO2/Al2O	4.1587	3.8906	3.7400	4.3312	4.3199	4.8817	5.3127	6.5595	3.7178	3.7186	3.8929	4.0000	3.9921	4.0778
Ti/Nb	24300.00	27240.00	25980.00	26520.00	30660.00	27600.00	24000.00	19200.00	24600.00	25800.00	28200.00	28800.00	24540.00	29100.00
use?	ok	ok	ok	ok	ok	ok	ok	no	ok	ok	ok	ok	ok	ok
altered?								alt.Al						
why not use														

MCAo incl.	Guichon Cr	Guichon Cr	Guichon Cr	Guichon Cr	Guichon Cr	Guichon Cr	Guichon Cr	Guichon Cr	Guichon Cr	Guichon Cr	Guichon Cr	Guichon Cr	Guichon Cr	Guichon Cr
COUNTY	?	?	?	?	?	?	?	?	?	?	?	?	?	?
STATE	BC	BC	BC	BC	BC	BC	BC	BC	BC	BC	BC	BC	BC	BC
SAMPLE #	24b	15	37	38	39	6	32	33	34	35	46	47	48	45
NAME	GUICHON	GUICHON	GUICHON	GUICHON	GUICHON	GUICHON	GUICHON	GUICHON	GUICHON	GUICHON	GUICHON	GUICHON	GUICHON	GUICHON
SOURCE:	Briskey, 19	Briskey, 19	Briskey, 19	Briskey, 19	Briskey, 19	Briskey, 19	Briskey, 19	Briskey, 19	Briskey, 19	Briskey, 19	Briskey, 19	Briskey, 19	Briskey, 19	Briskey, 19
ROCK TYP	Guichon	Bethlehem	Bethlehem	Bethlehem	Bethlehem	leucocratic	Bethlehem	Bethlehem	Bethlehem	Bethlehem	granite post	granite post	granite post	granodior p
SiO2	70.20	66.90	67.80	68.10	68.60	62.80	65.60	68.50	66.60	66.20	76.90	73.40	76.00	70.80
TiO2	0.24	0.33	0.36	0.33	0.32	0.59	0.27	0.28	0.28	0.31	0.10	0.15	0.11	0.20
Al2O3	15.85	17.90	17.50	17.20	17.40	17.20	16.70	17.50	17.60	17.90	12.70	13.40	13.00	15.60
Fe2O3	1.08	n.a.	n.a.	n.a.	n.a.	n.a.	n.a.	n.a.	n.a.	n.a.	n.a.	n.a.	n.a.	n.a.
FeO	0.80	0.80	0.90	0.70	0.40	4.30	2.00	2.70	2.60	3.00	0.50	1.30	0.60	1.90
MgO	0.51	1.20	1.20	1.10	0.70	2.60	0.90	0.90	0.70	0.80	0.00	0.40	0.10	0.70
MnO	0.06	n.a.	n.a.	n.a.	n.a.	n.a.	n.a.	n.a.	n.a.	n.a.	n.a.	n.a.	n.a.	n.a.
CaO	2.48	5.20	5.00	5.00	4.70	5.40	3.00	4.00	4.10	4.40	0.50	1.20	0.70	2.80
Na2O	4.92	5.80	5.50	6.20	6.00	4.50	4.80	5.40	5.30	5.30	4.00	3.90	4.10	4.40
K2O	1.94	0.13	0.19	0.17	0.20	0.49	1.68	0.88	1.37	1.32	4.25	3.57	3.75	2.36
P2O5	tr	n.a.	n.a.	n.a.	n.a.	n.a.	n.a.	n.a.	n.a.	n.a.	n.a.	n.a.	n.a.	n.a.
LOI	0.92	0.00	0.00	0.00	0.00	0.00	0.00	0.00	0.00	0.00	0.00	0.00	0.00	0.00
TOTAL	99.00	98.30	98.50	98.80	98.30	97.90	95.40	100.20	98.60	99.20	99.00	97.30	98.40	98.80
MINING DI	Valley Cu	Valley Cu	Valley Cu	Valley Cu	Valley Cu	Valley Cu	Valley Cu	Valley Cu	Valley Cu	Valley Cu	Valley Cu	Valley Cu	Valley Cu	Valley Cu
Ba	0	0	0	0	0	0	0	0	0	0	0	0	0	0
Rb	0	0	0	0	0	0	0	0	0	0	0	0	0	0
Sr	0	0	0	0	0	0	0	0	0	0	0	0	0	0
Y	0	0	0	0	0	0	0	0	0	0	0	0	0	0
Zr	0	0	0	0	0	0	0	0	0	0	0	0	0	0
Nb	0	0	0	0	0	0	0	0	0	0	0	0	0	0
CLASS	MCAo	MCAo	MCAo	MCAo	MCAo	MCAo	MCAo	MCAo	MCAo	MCAo	MCAo	MCAo	MCAo	MCAo
A/CNK	1.077	0.935	0.953	0.882	0.933	0.968	1.100	1.022	0.996	0.985	1.049	1.074	1.075	1.047
A/NK	1.55	1.85	1.89	1.66	1.72	2.17	1.72	1.78	1.72	1.76	1.13	1.30	1.20	1.59
Na2O+K2	6.86	5.93	5.69	6.37	6.20	4.99	6.48	6.28	6.67	6.62	8.25	7.47	7.85	6.76
Na2O/K2O	2.54	44.62	28.95	36.47	30.00	9.18	2.86	6.14	3.87	4.02	0.94	1.09	1.09	1.86
NaO+K2O-	4.38	0.73	0.69	1.37	1.50	-0.41	3.48	2.28	2.57	2.22	7.75	6.27	7.15	3.96
K2O-CaO	-0.54	-5.07	-4.81	-4.83	-4.50	-4.91	-1.32	-3.12	-2.73	-3.08	3.75	2.37	3.05	-0.44
K2O-MgO	1.43	-1.07	-1.01	-0.93	-0.50	-2.11	0.78	-0.02	0.67	0.52	4.25	3.17	3.65	1.66
FeO/MgO*	3.47	0.67	0.75	0.64	0.57	1.65	2.22	3.00	3.71	3.75	ERR	3.25	6.00	2.71
Fe3+/Fe2+	1.35	0.00	0.00	0.00	0.00	0.00	0.00	0.00	0.00	0.00	0.00	0.00	0.00	0.00
LARSEN	22.35	16.03	16.59	16.77	17.67	13.42	19.65	18.81	18.77	18.19	29.38	26.44	28.28	22.46
ALKALI IN	-3.25	-2.96	-3.53	-2.96	-3.32	-2.37	-1.92	-3.20	-2.11	-2.01	-4.36	-3.83	-4.42	-3.58
ALT INDE	24.873	10.787	11.690	10.184	7.759	23.788	24.855	15.921	18.047	17.936	48.571	43.771	44.509	29.825
K INDEX	1.73	1.19	1.17	1.31	1.35	0.78	1.48	1.07	1.10	1.00	8.25	3.15	6.12	1.59
Na INDEX	3.6131	45.5499	29.9004	37.3530	30.9330	10.1516	3.9570	7.1583	4.8644	5.0005	1.9905	2.1665	2.1687	2.9114
Al2O3/Na2	3.221545	3.086207	3.181818	2.774194	2.9	3.822222	3.479167	3.240741	3.320755	3.377358	3.175	3.435897	3.170732	3.545455
SiO2/Al2O	4.4290	3.7374	3.8743	3.9593	3.9425	3.6512	3.9281	3.9143	3.7841	3.6983	6.0551	5.4776	5.8462	4.5385
Ti/Nb	29520.00	34800.00	33000.00	37200.00	36000.00	27000.00	28800.00	32400.00	31800.00	31800.00	24000.00	23400.00	24600.00	26400.00
use?	ok	no	no	no	no	no	ok	no	no	no	no	no	no	ok
altered?		alt.Al,NAl	alt.Al,NAl	alt.Al,NAl	alt.Al	alt.Al,NAl		alt.Al	alt.Al	alt.Al	alt.Kl	alt.Kl	alt.Kl	
why not use														

MCAo incl.	Guichon Cr	Guichon Cr	Guichon Cr	Guichon Cr	Guichon Cr
COUNTY	?	?	?	?	?
STATE	BC	BC	BC	BC	BC
SAMPLE #	74	75	76	78	79
NAME	GUICHON	GUICHON	GUICHON	GUICHON	GUICHON
SOURCE:	Briskey, 19	Briskey, 19	Briskey, 19	Briskey, 19	Briskey, 19
ROCK TYP	K-feld-poor	K-feld-poor	K-feld-poor	K-feld-rich a	K-feld-rich a
SiO2	77.60	78.60	79.00	77.50	77.20
TiO2	0.16	0.08	0.08	0.08	0.06
Al2O3	12.80	12.40	12.60	12.60	13.00
Fe2O3	n.a.	n.a.	n.a.	n.a.	n.a.
FeO	0.30	0.30	0.40	0.60	0.60
MgO	0.00	0.00	0.20	0.10	0.40
MnO	n.a.	n.a.	n.a.	n.a.	n.a.
CaO	2.30	1.00	2.20	0.70	0.50
Na2O	4.50	6.00	5.40	3.30	4.20
K2O	0.33	0.24	0.13	4.60	4.40
P2O5	n.a.	n.a.	n.a.	n.a.	n.a.
LOI	0.00	0.00	0.00	0.00	0.00
TOTAL	98.00	98.60	100.00	99.50	100.40
MINING DI	Valley Cu	Valley Cu	Valley Cu	Valley Cu	Valley Cu
Ba	0	0	0	0	0
Rb	0	0	0	0	0
Sr	0	0	0	0	0
Y	0	0	0	0	0
Zr	0	0	0	0	0
Nb	0	0	0	0	0
CLASS	MCAo	MCAo	MCAo	MCAo	MCAo
A/CNK	1.071	1.037	0.967	1.077	1.032
A/NK	1.65	1.22	1.40	1.21	1.11
Na2O+K2	4.83	6.24	5.53	7.90	8.60
Na2O/K2O	13.64	25.00	41.54	0.72	0.95
NaO+K2O-	2.53	5.24	3.33	7.20	8.10
K2O-CaO	-1.97	-0.76	-2.07	3.90	3.90
K2O-MgO	0.33	0.24	-0.07	4.50	4.00
FeO/MgO*	ERR	ERR	2.00	6.00	1.50
Fe3+/Fe2+	0.00	0.00	0.00	0.00	0.00
LARSEN	23.90	25.44	24.06	29.63	29.23
ALKALI IN	-8.04	-7.00	-7.86	-4.93	-4.12
ALT INDE	4.628	3.315	4.161	54.023	50.526
K INDEX	1.86	4.80	2.20	6.15	8.18
Na INDEX	14.7074	26.0374	42.5053	1.7947	1.9867
Al2O3/Na2	2.844444	2.066667	2.333333	3.818182	3.095238
SiO2/Al2O	6.0625	6.3387	6.2698	6.1508	5.9385
Ti/Nb	27000.00	36000.00	32400.00	19800.00	25200.00
---	---	---	---	---	---
use?	no	no	no	no	no
altered?	alt.Al,NAl	alt.Al,NAl,K	alt.Al,NAl	alt.NAl	alt.Kl
why not use					

MCAow in	Morenci	MORENCI	MORENCI	MORENCI	MORENCI	MORENCI	MORENCI	Hedley	HEDLEY B	HEDLEY B	HEDLEY B	HEDLEY B	HEDLEY B	HEDLEY B
COUNTY	Greenlee	Greenlee	Greenlee	Greenlee	Greenlee	Greenlee	Greenlee	?	Princeton M	Princeton M	Princeton M	Princeton M	Princeton M	Princeton M
STATE	AZ	AZ	AZ	AZ	AZ	AZ	AZ	BC	British Colu	British Colu	British Colu	British Colu	British Colu	British Colu
SAMPLE #	A	4A1	JD-42	JD-43	JD-44	M-36	M-37	Hed 113	50	51	52	60a	62	63
NAME	MORENCI	MORENCI	MORENCI	MORENCI	MORENCI	MORENCI	MORENCI	HEDLEY	HEDLEY	HEDLEY	HEDLEY	HEDLEY	HEDLEY	HEDLEY
SOURCE:	Clarke, 191	Lindgren'05	Dewhurst 7	Dewhurst 7	Dewhurst 7	Laine'74	Laine'74	Camsell, 19	Ray et al, 1	Ray et al, 1	Ray et al, 1	Ray et al, 1	Ray et al, 1	Ray et al, 1
ROCK TYP	porphyry, R	plutonic	diorite porp	old. gran. p	monzonite	qtz monz	qtz monz	Qtz dior Ste	?	?	?	?	?	?
SiO2	68.04	68.04	61.86	68.69	65.45	67.00	68.00	58.36	54.21	60.45	54.29	56.81	54.08	62.71
TiO2	0.41	0.41	0.58	0.26	0.51	0.67	0.33	0.54	0.79	0.46	0.83	0.6	0.68	0.36
Al2O3	17.2	17.20	19.60	17.36	17.45	16.44	15.31	18.38	19.2	17.12	19.53	17.5	18.35	18.24
Fe2O3	0.34	0.34	0.00	0.00	0.00	3.81	5.93	5.53	9.25	5.72	8.11	7.03	8.77	3.31
FeO	0.67	0.67	3.01	1.17	2.42	0.86	0.17	5.3	0	0	0	0	0	0
MgO	1.05	1.05	1.57	0.39	1.29	1.03	1.16	2.6	4.49	2.55	3.24	3.81	4.03	1.94
MnO	0.06	0.06	0.00	0.00	0.00	0.04	0.04	0.14	0.17	0.12	0.15	0.12	0.17	0.07
CaO	2.21	2.21	4.08	1.57	3.13	3.36	1.26	7.2	9.9	6.41	9.16	7.98	9.25	6.71
Na2O	5.33	5.33	4.74	4.39	4.95	5.26	5.12	3.15	2.69	3.48	3.12	3.03	2.91	3.68
K2O	2.65	2.65	1.23	3.94	2.46	2.29	1.93	1.98	0.83	1.67	0.93	1.64	1.11	2.03
P2O5	0.12	0.12	0	0	0	0	0	0.12	0	0	0	0	0	0
LOI	2.26	1.23	0.00	0.00	0.00	1.03	1.22	-3.87	0	0	0	0	0	0
TOTAL	100.34	99.31	96.67	97.77	96.66	101.79	100.47	99.43	101.53	97.98	99.36	98.52	99.35	99.05
MINING DI	Morenci	Morenci	Morenci	Morenci	Morenci	Morenci	Morenci	Hedley	Hedley	Hedley	Hedley	Hedley	Hedley	Hedley
Ba	0	0	0	0	0	0	0	0	0	0	0	0	0	0
Rb	0	0	0	0	0	0	0	0	0	0	0	0	0	0
Sr	0	0	0	0	0	0	0	0	0	0	0	0	0	0
Y	0	0	0	0	0	0	0	0	0	0	0	0	0	0
Zr	0	0	0	0	0	0	0	0	0	0	0	0	0	0
Nb	0	0	0	0	0	0	0	0	0	0	0	0	0	0
CLASS	MCAow	MCAow	MCAow	MCAow	MCAow	MCAow	MCAow	MCAow	MCAow	MCAow	MCAow	MCAow	MCAow	MCAow
A/CNK	1.098	1.098	1.183	1.209	1.057	0.953	1.195	0.899	0.822	0.891	0.856	0.822	0.803	0.891
A/NK	1.48	1.48	2.15	1.51	1.61	1.48	1.46	2.51	3.60	2.27	3.18	2.59	3.06	2.21
Na2O+K2	7.98	7.98	5.97	8.33	7.41	7.55	7.05	5.13	3.52	5.15	4.05	4.67	4.02	5.71
Na2O/K2O	2.01	2.01	3.85	1.11	2.01	2.30	2.65	1.59	3.24	2.08	3.35	1.85	2.62	1.81
NaO+K2O-	5.77	5.77	1.89	6.76	4.28	4.19	5.79	-2.07	-6.38	-1.26	-5.11	-3.31	-5.23	-1.00
K2O-CaO	0.44	0.44	-2.85	2.37	-0.67	-1.07	0.67	-5.22	-9.07	-4.74	-8.23	-6.34	-8.14	-4.68
K2O-MgO	1.60	1.60	-0.34	3.55	1.17	1.26	0.77	-0.62	-3.66	-0.88	-2.31	-2.17	-2.92	0.09
FeO/MgO*	0.93	0.93	1.92	3.00	1.88	4.16	4.75	3.95	1.85	2.02	2.25	1.66	1.96	1.54
Fe3+/Fe2+	0.51	0.51	0.00	0.00	0.00	4.43	34.88	1.04	ERR	ERR	ERR	ERR	ERR	ERR
LARSEN	22.07	22.07	16.20	24.88	19.86	20.23	22.18	11.63	4.51	12.86	6.63	8.79	5.86	14.28
ALKALI IN	-1.33	-1.33	-1.04	-1.22	-0.94	-1.37	-2.25	-0.58	-0.65	-1.34	-0.15	-0.46	-0.10	-1.62
ALT INDE	32.918	32.918	24.096	42.080	31.699	27.806	32.629	30.676	29.704	29.908	25.350	33.111	29.711	27.646
K INDEX	2.83	2.83	1.06	3.18	1.57	1.12	1.21	0.44	0.44	0.67	0.44	0.59	0.47	0.79
Na INDEX	3.1090	3.1090	5.0369	2.3234	3.0689	3.2495	3.8478	2.4899	4.0629	2.9749	4.2104	2.6692	3.4250	2.7035
Al2O3/Na2	3.227017	3.227017	4.135021	3.954442	3.525253	3.125475	2.990234	5.834921	7.137546	4.91954	6.259615	5.775578	6.305842	4.956522
SiO2/Al2O	3.9558	3.9558	3.1561	3.9568	3.7507	4.0754	4.4415	3.1752	2.8234	3.5310	2.7798	3.2463	2.9471	3.4380
Ti/Nb	31980.00	31980.00	28440.00	26340.00	29700.00	31560.00	30720.00	18900.00	16140.00	20880.00	18720.00	18180.00	17460.00	22080.00
use?	no	no	no	no	ok	ok	no	ok	ok	ok	ok	ok	ok	ok
altered?	alt.LOI	alt.KI	alt.A/CNK	alt.A/CNK,KI			alt.A/CNK							
why not use														

MCAow in	HEDLEY B	HEDLEY B	HEDLEY B	HEDLEY B	HEDLEY B	HEDLEY B	HEDLEY B	HEDLEY B	HEDLEY B	HEDLEY B	HEDLEY B	HEDLEY B	HEDLEY B	HEDLEY B
COUNTY	Princeton M	Princeton M	Princeton M	Princeton M	Princeton M	Princeton M	Princeton M	Princeton M	Princeton M	Princeton M	Princeton M	Princeton M	Princeton M	Princeton M
STATE	British Colu	British Colu	British Colu	British Colu	British Colu	British Colu	British Colu	British Colu	British Colu	British Colu	British Colu	British Colu	British Colu	British Colu
SAMPLE #	64	65	66	67	68	69	70	71	72	73a	60b	73b	130	131
NAME	HEDLEY	HEDLEY	HEDLEY	HEDLEY	HEDLEY	HEDLEY	HEDLEY	HEDLEY	HEDLEY	HEDLEY	HEDLEY	HEDLEY	HEDLEY	HEDLEY
SOURCE:	Ray et al, 1	Ray et al, 1	Ray et al, 1	Ray et al, 1	Ray et al, 1	Ray et al, 1	Ray et al, 1	Ray et al, 1	Ray et al, 1	Ray et al, 1	Ray et al, 1	Ray et al, 1	Ray et al, 1	Ray et al, 1
ROCK TYP	?	?	?	?	?	?	?	?	?	?	?	?	?	?
SiO2	52.94	59.48	53.27	50.82	59.46	54.27	49.17	55.92	54.85	57.68	57.24	55.38	54.01	54.6
TiO2	0.65	0.53	0.72	0.65	0.31	0.64	0.8	0.58	0.65	0.67	0.62	0.66	0.68	0.66
Al2O3	19.89	17.86	19.02	20.24	17.99	19.33	20.18	18.41	18.72	18.6	18.01	18.61	18.39	18.79
Fe2O3	7.93	6.41	8.75	8.39	5.83	7.66	9.07	7.27	8.08	7.91	7.13	8.05	8.74	8.32
FeO	0	0	0	0	0	0	0	0	0	0	0	0	0	0
MgO	4.04	2.51	3.93	4.18	2.88	3.27	5.09	3.13	3.54	3.1	3.86	3.06	4.44	4.18
MnO	0.15	0.11	0.16	0.17	0.13	0.17	0.16	0.14	0.15	0.15	0.13	0.15	0.15	0.13
CaO	10.15	6.66	9.12	10.3	7.24	9.19	11.46	8.14	8.73	8.23	8.04	8	8.93	8.14
Na2O	3.4	3.28	3.1	2.9	3.72	3.2	2.55	3.22	3.06	3.22	3.04	3.21	2.66	2.81
K2O	1.24	2	1.35	0.75	2.01	1.55	1.17	1.66	1.65	1.8	1.65	1.78	1.21	1.53
P2O5	0	0	0	0	0	0	0	0	0	0	0	0	0	0
LOI	0	0	0	0	0	0	0	0	0	0	0	0	0	0
TOTAL	100.39	98.84	99.42	98.4	99.57	99.28	99.65	98.47	99.43	101.36	99.72	98.9	99.21	99.16
MINING DI	Hedley	Hedley	Hedley	Hedley	Hedley	Hedley	Hedley	Hedley	Hedley	Hedley	Hedley	Hedley	Hedley	Hedley
Ba	0	0	0	0	0	0	0	0	0	0	0	0	0	0
Rb	0	0	0	0	0	0	0	0	0	0	0	0	0	0
Sr	0	0	0	0	0	0	0	0	0	0	0	0	0	0
Y	0	0	0	0	0	0	0	0	0	0	0	0	0	0
Zr	0	0	0	0	0	0	0	0	0	0	0	0	0	0
Nb	0	0	0	0	0	0	0	0	0	0	0	0	0	0
CLASS	MCAow	MCAow	MCAow	MCAow	MCAow	MCAow	MCAow	MCAow	MCAow	MCAow	MCAow	MCAow	MCAow	MCAow
A/CNK	0.782	0.907	0.821	0.831	0.837	0.816	0.766	0.840	0.824	0.836	0.840	0.854	0.838	0.890
A/NK	2.87	2.36	2.90	3.62	2.17	2.78	3.69	2.59	2.74	2.57	2.65	2.58	3.23	2.99
Na2O+K2	4.64	5.28	4.45	3.65	5.73	4.75	3.72	4.88	4.71	5.02	4.69	4.99	3.87	4.34
Na2O/K2O	2.74	1.64	2.30	3.87	1.85	2.06	2.18	1.94	1.85	1.79	1.84	1.80	2.20	1.84
NaO+K2O-	-5.51	-1.38	-4.67	-6.65	-1.51	-4.44	-7.74	-3.26	-4.02	-3.21	-3.35	-3.01	-5.06	-3.80
K2O-CaO	-8.91	-4.66	-7.77	-9.55	-5.23	-7.64	-10.29	-6.48	-7.08	-6.43	-6.39	-6.22	-7.72	-6.61
K2O-MgO	-2.80	-0.51	-2.58	-3.43	-0.87	-1.72	-3.92	-1.47	-1.89	-1.30	-2.21	-1.28	-3.23	-2.65
FeO/MgO*	1.77	2.30	2.00	1.81	1.82	2.11	1.60	2.09	2.05	2.30	1.66	2.37	1.77	1.79
Fe3+/Fe2+	ERR	ERR	ERR	ERR	ERR	ERR	ERR	ERR	ERR	ERR	ERR	ERR	ERR	ERR
LARSEN	4.70	12.66	6.06	3.21	11.71	7.18	1.01	9.03	7.66	9.70	8.83	9.18	5.84	7.41
ALKALI IN	0.95	-0.85	0.63	0.74	-0.39	0.56	1.43	0.08	0.31	-0.44	-0.60	0.39	-0.22	0.03
ALT INDE	28.040	31.211	30.171	27.192	30.852	28.007	30.883	29.659	30.565	29.969	33.213	30.156	32.773	34.274
K INDEX	0.50	0.63	0.49	0.44	0.69	0.50	0.45	0.55	0.52	0.53	0.59	0.53	0.49	0.55
Na INDEX	3.5242	2.5467	3.1170	4.6980	2.6879	2.8806	2.9457	2.7794	2.6783	2.6252	2.6826	2.6577	3.0360	2.7267
Al2O3/Na2	5.85	5.445122	6.135484	6.97931	4.836022	6.040625	7.913725	5.717391	6.117647	5.776398	5.924342	5.797508	6.913534	6.686833
SiO2/Al2O	2.6616	3.3303	2.8007	2.5109	3.3052	2.8076	2.4366	3.0375	2.9300	3.1011	3.1782	2.9758	2.9369	2.9058
Ti/Nb	20400.00	19680.00	18600.00	17400.00	22320.00	19200.00	15300.00	19320.00	18360.00	19320.00	18240.00	19260.00	15960.00	16860.00
use?	ok	ok	ok	ok	ok	ok	ok	ok	ok	ok	ok	ok	ok	ok
altered?														
why not use														

MCAow in	HEDLEY B	HEDLEY B	HEDLEY B	HEDLEY B	HEDLEY B	HEDLEY B	HEDLEY B	HEDLEY B	HEDLEY B	HEDLEY B	HEDLEY B	MCCOY	MCCOY	MCCOY
COUNTY	Princeton M	Princeton M	Princeton M	Princeton M	Princeton M	Princeton M	Princeton M	Princeton M	Princeton M	Princeton M	Princeton M	Lander	Lander	Lander
STATE	British Colu	British Colu	British Colu	British Colu	British Colu	British Colu	British Colu	British Colu	British Colu	British Colu	British Colu	NV	NV	NV
SAMPLE #	156	157	158	159	161	162	163	164	218	Hed 97	Hed 156	5080-II 16	5080-II 24	5100-II 1
NAME	HEDLEY	HEDLEY	HEDLEY	HEDLEY	HEDLEY	HEDLEY	HEDLEY	HEDLEY	HEDLEY	HEDLEY	HEDLEY	MCCOY	MCCOY	MCCOY
SOURCE:	Ray et al, 1	Ray et al, 1	Ray et al, 1	Ray et al, 1	Ray et al, 1	Ray et al, 1	Ray et al, 1	Ray et al, 1	Ray et al, 1	Camsell, 19	Camsell, 19	Brooks et al	Brooks et al	Brooks et al
ROCK TYP	?	?	?	?	?	?	?	?	?	granodiorite	gabbro	bio-hb grdr	FG Dike	bio-hb grdr
SiO2	54.83	55.56	53.33	55.61	54.12	53.36	54.13	56.38	54.31	62.08	51.08	65.2	66.8	66.06
TiO2	0.67	0.66	0.56	0.61	0.65	0.68	0.62	0.58	0.61	0.54	0.45	0.65	0.72	0.64
Al2O3	18.81	18.71	19.24	18.38	18.22	18.57	17.55	18.37	18.29	17.91	19.77	17.65	17.66	17.92
Fe2O3	7.98	7.53	8.19	7.35	8.32	7.31	6.64	6.29	6.01	1.08	trace	0	0	0
FeO	0	0	0	0	0	0	0	0	0	3.08	3.6	4.52	3.34	3.05
MgO	4.83	4.16	4.45	3.69	4.1	4.23	3.99	3.41	3.83	1.17	4.57	2.09	3.03	1.97
MnO	0.14	0.16	0.14	0.12	0.14	0.12	0.09	0.01	0.07	0.11	0.09	0.05	0.03	0.02
CaO	8	7.13	9.47	8.12	8.32	8.32	6.48	7.1	7.45	4.54	16.03	5.15	4.1	4.38
Na2O	3.2	3.28	2.77	2.91	2.72	2.77	4.79	4.06	3.34	5.12	2.56	3.11	1.45	2.96
K2O	0.64	1.37	1.17	1	1.01	1.1	2.13	1.01	2.08	2.96	0.28	2.82	3.26	3.01
P2O5	0	0	0	0	0	0	0	0	0	0.17	0.14	0.21	0.2	0.2
LOI	0	0	0	0	0	0	0	0	0	0	0	0	0	0
TOTAL	99.1	98.56	99.32	97.79	97.6	96.46	96.42	97.3	95.99	99.77	99.69	101.45	100.59	100.21
MINING DI	Hedley	Hedley	Hedley	Hedley	Hedley	Hedley	Hedley	Hedley	Hedley	Hedley	Hedley	McCoy	McCoy	McCoy
Ba	0	0	0	0	0	0	0	0	0	0	0	1001	923	1220
Rb	0	0	0	0	0	0	0	0	0	0	0	93	132	87
Sr	0	0	0	0	0	0	0	0	0	0	0	652	546	608
Y	0	0	0	0	0	0	0	0	0	0	0	19	19	20
Zr	0	0	0	0	0	0	0	0	0	0	0	185	199	191
Nb	0	0	0	0	0	0	0	0	0	0	0	13	13	13
CLASS	MCAow	MCAow	MCAow	MCAow	MCAow	MCAow	MCAow	MCAow	MCAow	MCAow	MCAow	MCAow	MCAow	MCAow
A/CNK	0.916	0.942	0.834	0.890	0.879	0.888	0.798	0.887	0.858	0.900	0.586	1.005	1.319	1.112
A/NK	3.16	2.72	3.30	3.13	3.27	3.23	1.72	2.36	2.36	1.54	4.38	2.16	2.98	2.20
Na2O+K2	3.84	4.65	3.94	3.91	3.73	3.87	6.92	5.07	5.42	8.08	2.84	5.93	4.71	5.97
Na2O/K2O	5.00	2.39	2.37	2.91	2.69	2.52	2.25	4.02	1.61	1.73	9.14	1.10	0.44	0.98
NaO+K2O-	-4.16	-2.48	-5.53	-4.21	-4.59	-4.45	0.44	-2.03	-2.03	3.54	-13.19	0.78	0.61	1.59
K2O-CaO	-7.36	-5.76	-8.30	-7.12	-7.31	-7.22	-4.35	-6.09	-5.37	-1.58	-15.75	-2.33	-0.84	-1.37
K2O-MgO	-4.19	-2.79	-3.28	-2.69	-3.09	-3.13	-1.86	-2.40	-1.75	1.79	-4.29	0.73	0.23	1.04
FeO/MgO*	1.49	1.63	1.66	1.79	1.83	1.56	1.50	1.66	1.41	3.46	0.79	2.16	1.10	1.55
Fe3+/Fe2+	ERR	ERR	ERR	ERR	ERR	ERR	ERR	ERR	ERR	0.35	0.00	0.00	0.00	0.00
LARSEN	6.09	8.60	5.03	7.73	6.63	6.34	9.70	9.29	8.90	17.94	-3.29	17.31	18.40	18.68
ALKALI IN	-0.56	-0.02	0.10	-0.78	-0.40	0.02	2.78	0.10	1.22	0.99	-0.16	-2.32	-4.14	-2.60
ALT INDE	32.813	34.693	31.467	29.835	31.641	32.460	35.193	28.370	35.389	29.949	20.691	37.282	53.125	40.422
K INDEX	0.57	0.63	0.50	0.52	0.50	0.54	0.88	0.66	0.72	1.08	0.38	0.83	1.04	1.07
Na INDEX	5.9162	3.3358	3.2013	3.7995	3.5722	3.4065	3.0468	4.9069	2.4636	2.6295	9.7293	2.1081	1.7636	2.0955
Al2O3/Na2	5.878125	5.704268	6.945848	6.316151	6.698529	6.703971	3.663883	4.524631	5.476048	3.498047	7.722656	5.675241	12.17931	6.054054
SiO2/Al2O	2.9149	2.9695	2.7718	3.0256	2.9704	2.8735	3.0843	3.0691	2.9694	3.4662	2.5837	3.6941	3.7826	3.6864
Ti/Nb	19200.00	19680.00	16620.00	17460.00	16320.00	16620.00	28740.00	24360.00	20040.00	30720.00	15360.00	1435.38	669.23	1366.15
use?	ok	ok	ok	ok	ok	ok	ok	ok	ok	ok	no	ok	ok	ok
altered?											alt.Al			
why not use														

MCAow in	MCCOY	MCCOY	MCCOY	MCCOY	MCCOY	El Teniente	El Teniente	El Salvador	El Salvador	El Salvador	El Salvador	El Salvador	El Salvador	El Salvador
COUNTY	Lander	Lander	Lander	Lander	Lander	?	?	Atacama de	Atacama de	Atacama de	Atacama de	?	?	?
STATE	NV	NV	NV	NV	NV	CHILE	CHILE	Chile	Chile	Chile	Chile	CHILE	CHILE	CHILE
SAMPLE #	5120-II 20	5300 17	122531	803447	122469	6	10	ES 3338	IL	6BL	24L	3-ES-2699	4-DDH 547-	5-ES-2691
NAME	MCCOY	MCCOY	MCCOY	MCCOY	MCCOY	TENIENTE	TENIENTE	ELSALVAD	ELSALVAD	ELSALVAD	ELSALVAD	SALVADO	SALVADO	SALVADO
SOURCE:	Brooks et al	Brooks et al	Brooks et al	Brooks et al	Brooks et al	Camus, 19	Camus, 19	Baldwin &	Baldwin &	Baldwin &	Baldwin &	Gustafson	Gustafson	Gustafson
ROCK TYP	bio-hb grdr	bio-hb grdr	bio-hb grdr	bio-hb grdr	alt'd grdr	qtz diorite, f	dacite, surf	L granodior	L granodior	L granodior	L granodior	X porphyry	K porphyry	L porphyry
SiO2	65.39	64.39	65.27	65.14	67.27	65.42	66.45	64.53	62.34	60.94	62.08	57.75	62.93	56.58
TiO2	0.71	0.42	0.46	0.44	0.35	0.34	0.29	0.7	0.67	0.64	0.74	0.99	0.62	0.73
Al2O3	17.48	15.6	15.27	15.09	15.18	16.64	15.22	15.99	16.65	16.81	18.26	16.44	14.66	17.41
Fe2O3	0	0	0	0	0	1.41	2.35	3.56	3.69	3.74	3.83	0.59	1	3.44
FeO	4.81	5.79	5.33	6	3.51	2.48	2.35	0	0	0	0	2.22	1	2.72
MgO	2.23	2.63	2.69	2.65	2.01	1.25	1.16	2.25	1.91	2.08	1.5	2.58	1.33	2.15
MnO	0.03	0.05	0.05	0.04	0.02	0.04	0.05	0.032	0.025	0.037	0.019	0.06	0.01	0.03
CaO	5.23	3.76	4.12	4.12	2.17	2.68	0.16	4.41	4.14	4.54	3.53	6.39	4.66	6.14
Na2O	3.01	2.93	3.08	3.24	1.62	4.97	1.93	5	4.77	5.25	5.41	4.04	6.73	4.65
K2O	2.25	4.18	3.47	3.22	7.49	2.28	4.78	2.7	2.17	2.54	1.93	2.28	1.45	1.57
P2O5	0.22	0.18	0.25	0.25	0.16	0.16	0.13	0.23	0.21	0.23	0.28	0.85	0.55	0.48
LOI	0	0	0	0	0	1.22	2.62	1.77	2.65	1.55	1.17	1.04	0.62	1.18
TOTAL	101.36	99.97	99.99	100.19	99.78	99.28	98.24	99.17	99.23	98.36	98.75	100.15	101.11	100.52
MINING DI	McCoy	McCoy	McCoy	McCoy	McCoy	El Teniente	El Teniente	El Salvador	El Salvador	El Salvador	El Salvador	El Salvador	El Salvador	El Salvador
Ba	795	0	0	0	0	0	0	565	541	589	598	0	0	0
Rb	102	0	0	0	0	0	0	74	56	58	34	0	0	0
Sr	646	0	0	0	0	0	0	696	602	676	690	0	0	0
Y	19	0	0	0	0	0	0	6	6	7	6	0	0	0
Zr	182	0	0	0	0	0	0	125	121	128	128	0	0	0
Nb	13	0	0	0	0	0	0	6	5	7	6	0	0	0
CLASS	MCAow	MCAow	MCAow	MCAow	MCAow	MCAow	MCAow	MCAow	MCAow	MCAow	MCAow	MCAow	MCAow	MCAow
A/CNK	1.033	0.963	0.935	0.924	1.029	1.071	1.759	0.833	0.938	0.855	1.048	0.792	0.694	0.848
A/NK	2.36	1.67	1.73	1.71	1.41	1.56	1.82	1.43	1.63	1.48	1.66	1.80	1.16	1.86
Na2O+K2	5.26	7.11	6.55	6.46	9.11	7.25	6.71	7.70	6.94	7.79	7.34	6.32	8.18	6.22
Na2O/K2O	1.34	0.70	0.89	1.01	0.22	2.18	0.40	1.85	2.20	2.07	2.80	1.77	4.64	2.96
NaO+K2O-	0.03	3.35	2.43	2.34	6.94	4.57	6.55	3.29	2.80	3.25	3.81	-0.07	3.52	0.08
K2O-CaO	-2.98	0.42	-0.65	-0.90	5.32	-0.40	4.62	-1.71	-1.97	-2.00	-1.60	-4.11	-3.21	-4.57
K2O-MgO	0.02	1.55	0.78	0.57	5.48	1.03	3.62	0.45	0.26	0.46	0.43	-0.30	0.12	-0.58
FeO/MgO*	2.16	2.20	1.98	2.26	1.75	3.00	3.85	1.42	1.74	1.62	2.30	1.07	1.43	2.71
Fe3+/Fe2+	0.00	0.00	0.00	0.00	0.00	0.57	1.00	ERR	ERR	ERR	ERR	0.27	1.00	1.26
LARSEN	16.59	19.25	18.42	18.16	25.73	20.16	25.61	17.55	16.90	16.23	17.59	12.56	16.44	12.14
ALKALI IN	-3.07	-0.84	-1.73	-1.77	0.09	-1.09	-2.01	-0.31	-0.25	1.12	0.25	0.84	0.77	1.17
ALT INDE	35.220	50.444	46.108	44.369	71.482	31.574	73.973	34.471	31.409	32.061	27.728	31.785	19.619	25.637
K INDEX	0.75	1.02	0.98	0.90	1.96	1.32	1.70	1.31	1.19	1.25	1.27	0.97	1.45	0.70
Na INDEX	2.3709	1.6636	1.8223	1.9304	1.2458	3.2512	2.1626	2.6852	3.1366	2.9219	3.8511	2.5639	5.3351	3.8095
Al2O3/Na2	5.807309	5.324232	4.957792	4.657407	9.37037	3.348089	7.88601	3.198	3.490566	3.201905	3.375231	4.069307	2.178306	3.744086
SiO2/Al2O	3.7408	4.1276	4.2744	4.3168	4.4315	3.9315	4.3660	4.0356	3.7441	3.6252	3.3998	3.5128	4.2926	3.2499
Ti/Nb	1389.23	17580.00	18480.00	19440.00	9720.00	29820.00	11580.00	5000.00	5724.00	4500.00	5410.00	24240.00	40380.00	27900.00
use?	ok	ok	ok	ok	alt.Al,KI	ok	no	ok	**no**	ok	ok	ok	no	ok
altered?							alt.KI,Al,A/CNK		**alt.LOI**				alt.Al	
why not use														

MCAow in	El Salvador	El Salvador	El Salvador	El Salvador	Dos Pobres	Dos Pobres	Dos Pobres	Dexing	Dexing	Dexing	Dexing	Ajo (Corneli	Ajo (Corneli	Ajo (Corneli
COUNTY	?	?	?	?	Graham	Graham	Graham	?	?	?	?	Pima	Pima	Pima
STATE	CHILE	CHILE	CHILE	CHILE	AZ	AZ	AZ	CHINA	CHINA	CHINA	CHINA	AZ	AZ	AZ
SAMPLE #	6-ES-2689	7-ES-2688	8-ES-2687	9-ES-2703	1	SF-32	SF-33	(4)	Tongchang	Fujiawu	Zhushahon	1	2	3
NAME	SALVADO	SALVADO	SALVADO	SALVADO	DOSPOBR	DOSPOBR	DOSPOBR	DEXING	DEXING	DEXING	DEXING	AJO	AJO	AJO
SOURCE:	Gustafson	Gustafson	Gustafson	Gustafson	Langton &	Lang, 1991	Lang, 1991	Chung-We	Yan & Hu,	Yan & Hu,	Yan & Hu,	Gilluly, 193	Gilluly, 193	Gilluly, 193
ROCK TYP	L porphyry	L porphyry	L porphyry	L porphyry	fresh porph	porphyry di	porphyry di	granodiorite	granodiorite	granodiorite	granodiorite	bt-qtz diorit	qtz dior	hb-bt qtz m
SiO2	64.31	64.53	65.09	62.46	64.42	67.4	65.8	63.38	62.94	65.56	62.04	60.59	62.27	65.29
TiO2	0.71	0.43	0.48	0.45	0.5	0.45	0.5	0.43	0.43	0.4	0.45	0.61	0.84	0.54
Al2O3	16.29	16.1	15.03	17.39	15.69	14.8	15.3	15.19	15.4	15.51	14.88	17.39	17.4	15.74
Fe2O3	2.63	1.23	2.05	2.42	5	1.82	1.84	1.69	2.33	1.81	1.49	1.6	2.35	2.05
FeO	1.77	1.37	1.27	1.64	0	2.07	1.97	2.78	2.74	2.4	2.4	1.98	2.79	2.03
MgO	1.6	1.34	1.31	1.48	0.97	1.79	2.07	2.29	2.42	1.61	2.23	2.38	2.86	1.84
MnO	0.03	0.01	0.02	trace	0	0.04	0.03	0.06	0.32	0.14	0.03	0.08	0.05	0.07
CaO	4.34	4.55	3.87	4.4	3.54	2.44	2.56	3.78	4.13	3.25	3.48	5.06	1.19	3.66
Na2O	4.79	3.99	3.56	4.29	2.56	3.69	3.82	3.86	3.77	3.92	2.5	4.09	4.1	3.77
K2O	1.79	2.3	2.68	3.58	4.04	3.41	2.93	3.23	3.18	3.24	4.45	1.63	2.76	4.11
P2O5	0.32	0.26	0.22	0.2	0.025	0.16	0.13	0.26	0.24	0.19	0.25	0.36	0.3	0.24
LOI	0.98	1.24	2.47	0.93	2.22	0.98	2.17	2.09	1.4	1.72	2.62	3.29	2.65	0.62
TOTAL	100.87	101.02	101.74	100.34	99.421	99.16	99.19	99.44	99.3	99.75	99.67	99.84	100.06	100.1
MINING DI	El Salvador	El Salvador	El Salvador	El Salvador	Dos Pobres	Dos Pobres	Dos Pobres	Dexing	Dexing	Dexing	Dexing	Ajo	Ajo	Ajo
Ba	0	0	0	0	0	0.11	0.07	0	1100	0	0	0	0	0
Rb	0	0	0	0	0	58.19	22.67	0	0	0	0	0	0	0
Sr	0	0	0	0	0	454.9	390.5	0	0	0	0	0	0	0
Y	0	0	0	0	0	3.28	6.45	0	0	0	0	0	0	0
Zr	0	0	0	0	0	79.04	88.41	0	0	0	0	0	0	0
Nb	0	0	0	0	0	4.81	5.32	0	0	0	0	0	0	0
CLASS	MCAow	MCAow	MCAow	MCAow	MCAow	MCAow	MCAow	MCAow	MCAow	MCAow	MCAow	MCAow	MCAow	MCAow
A/CNK	0.919	0.928	0.950	0.917	1.043	1.041	1.083	0.907	0.897	0.976	0.974	0.982	1.461	0.908
A/NK	1.66	1.78	1.71	1.59	1.83	1.51	1.62	1.54	1.60	1.56	1.66	2.05	1.79	1.48
Na2O+K2	6.58	6.29	6.24	7.87	6.60	7.10	6.75	7.09	6.95	7.16	6.95	5.72	6.86	7.88
Na2O/K2O	2.68	1.73	1.33	1.20	0.63	1.08	1.30	1.20	1.19	1.21	0.56	2.51	1.49	0.92
NaO+K2O-	2.24	1.74	2.37	3.47	3.06	4.66	4.19	3.31	2.82	3.91	3.47	0.66	5.67	4.22
K2O-CaO	-2.55	-2.25	-1.19	-0.82	0.50	0.97	0.37	-0.55	-0.95	-0.01	0.97	-3.43	1.57	0.45
K2O-MgO	0.19	0.96	1.37	2.10	3.07	1.62	0.86	0.94	0.76	1.63	2.22	-0.75	-0.10	2.27
FeO/MgO*	2.59	1.85	2.38	2.58	4.64	2.07	1.75	1.88	2.00	2.50	1.68	1.44	1.72	2.11
Fe3+/Fe2+	1.49	0.90	1.61	1.48	ERR	0.88	0.93	0.61	0.85	0.75	0.62	0.81	0.84	1.01
LARSEN	17.29	17.92	19.20	18.52	21.00	21.65	20.23	18.29	17.61	20.23	19.42	14.39	19.47	20.37
ALKALI IN	-1.34	-1.72	-1.97	0.63	-1.36	-1.97	-1.73	-0.49	-0.46	-1.23	-0.13	-0.82	-0.30	-0.41
ALT INDE	27.077	29.885	34.939	36.800	45.095	45.896	43.937	41.945	41.481	40.349	52.765	30.471	51.512	44.469
K INDEX	0.96	1.09	1.08	1.14	0.94	1.45	1.43	1.16	1.04	1.20	1.27	0.96	1.59	1.29
Na INDEX	3.5949	2.6629	2.2788	2.1157	1.6767	2.1233	2.3868	2.1024	2.0822	2.1863	1.5356	3.4909	2.9468	1.8256
Al2O3/Na2	3.400835	4.035088	4.22191	4.053613	6.128906	4.01084	4.005236	3.935233	4.084881	3.956633	5.952	4.251834	4.243902	4.175066
SiO2/Al2O	3.9478	4.0081	4.3307	3.5917	4.1058	4.5541	4.3007	4.1725	4.0870	4.2270	4.1694	3.4842	3.5787	4.1480
Ti/Nb	28740.00	23940.00	21360.00	25740.00	15360.00	4602.91	4308.27	23160.00	22620.00	23520.00	15000.00	24540.00	24600.00	22620.00
use?	ok	ok	no	ok	no	ok	ok	ok	ok	ok	no	no	no	no
altered?			alt.LOI		alt.LOI						alt.LOI	alt.LOI	alt.LOI	
why not use														mT=younge

MCAow in	Ajo (Corneli	Ajo (Corneli	Ajo (Corneli	Ajo (Corneli	Ajo (Corneli	Ajo (Corneli	Ajo (Corneli	Ajo (Corneli	Ajo (Corneli	Ajo (Corneli	Ajo (Corneli	Ajo (Corneli	Ajo (Corneli	Ajo (Corneli	Ajo (Corneli
COUNTY	Pima	Pima	Pima	Pima	Pima	Pima	Pima	Pima	Pima	Pima	Pima	Pima	Pima	Pima	Pima
STATE	AZ	AZ	AZ	AZ	AZ	AZ	AZ	AZ	AZ	AZ	AZ	AZ	AZ	AZ	AZ
SAMPLE #	4	JD-25	A-1	A-2	A-5	A-6	A-7	A-8	A-10	A-14	A-16	A-19	A-20	A-26	
NAME	AJO	AJO	AJO	AJO	AJO	AJO	AJO	AJO	AJO	AJO	AJO	AJO	AJO	AJO	
SOURCE:	Gilluly, 193	Dewhurst,	Laine, 1974	Laine, 1974	Laine, 1974	Laine, 1974	Laine, 1974	Laine, 1974	Laine, 1974	Laine, 1974	Laine, 1974	Laine, 1974	Laine, 1974	Laine, 1974	
ROCK TYP	hb-bt qtz m	qtz diorite	qtz monzon	qtz monzon	qtz monzon	qtz monzon	qtz monzon	qtz monzon	qtz monzon	qtz monzon	qtz monzon	qtz monzon	qtz monzon	qtz monzon	
SiO2	66.23	54.06	64	66	67	64	63	64	66	66	66	64	68	71	
TiO2	0.47	0.84	0.33	0.5	0.5	0.33	0.33	0.33	0.5	0.33	0.5	0.5	0.5	0.33	
Al2O3	15.71	15.42	15.12	15.5	15.5	16.06	15.12	15.5	14.74	15.69	15.5	15.12	15.12	15.5	
Fe2O3	2.2	0	2.38	2.07	1.38	2.07	2.76	0.59	0.69	0.69	0.69	2.76	0	0	
FeO	1.98	4.91	2.41	2.54	2.6	2.67	2.36	3.29	2.91	2.91	2.91	1.72	2.96	1.67	
MgO	1.58	4.08	2.16	1.99	1.99	1.99	1.82	1.82	1.82	1.82	1.82	2.16	1.99	1.14	
MnO	0.08	0	0.04	0.02	0.02	0.02	0.03	0.03	0.03	0.02	0.03	0.02	0.03	0.02	
CaO	3.78	5.88	3.36	2.94	2.38	2.8	3.36	3.08	2.52	2.1	1.82	2.38	1.96	0.97	
Na2O	3.89	3.75	4.04	3.24	3.64	3.77	4.04	4.04	4.04	3.91	3.51	3.1	3.37	4.18	
K2O	3.22	2.44	3.85	4.22	4.34	3.61	3.49	3.85	4.34	3.61	4.22	3.98	4.46	4.22	
P2O5	0.24	0	0	0	0	0	0	0	0	0	0	0	0	0	
LOI	0.67	0	0.33	0	1.64	0	1.15	0	0.59	0.89	0	0.18	0.41	0.27	
TOTAL	100.08	91.38	101.2	101.35	100.18	99.76	97.09	99.15	100.58	99.32	99.35	98.63	100.89	100.72	
MINING DI	Ajo	Ajo	Ajo	Ajo	Ajo	Ajo	Ajo	Ajo	Ajo	Ajo	Ajo	Ajo	Ajo	Ajo	
Ba	0	0	0	0	0	0	0	0	0	0	0	0	0	0	
Rb	0	0	0	0	0	0	0	0	0	0	0	0	0	0	
Sr	0	0	0	0	0	0	0	0	0	0	0	0	0	0	
Y	0	0	0	0	0	0	0	0	0	0	0	0	0	0	
Zr	0	0	0	0	0	0	0	0	0	0	0	0	0	0	
Nb	0	0	0	0	0	0	0	0	0	0	0	0	0	0	
CLASS	MCAow	MCAow	MCAow	MCAow	MCAow	MCAow	MCAow	MCAow	MCAow	MCAow	MCAow	MCAow	MCAow	MCAow	
A/CNK	0.936	0.790	0.892	1.015	1.031	1.055	0.913	0.943	0.924	1.107	1.134	1.099	1.084	1.172	
A/NK	1.59	1.75	1.40	1.56	1.45	1.59	1.45	1.43	1.30	1.52	1.50	1.61	1.46	1.35	
Na2O+K2	7.11	6.19	7.89	7.46	7.98	7.38	7.53	7.89	8.38	7.52	7.73	7.08	7.83	8.40	
Na2O/K2O	1.21	1.54	1.05	0.77	0.84	1.04	1.16	1.05	0.93	1.08	0.83	0.78	0.76	0.99	
NaO+K2O-	3.33	0.31	4.53	4.52	5.60	4.58	4.17	4.81	5.86	5.42	5.91	4.70	5.87	7.43	
K2O-CaO	-0.56	-3.44	0.49	1.28	1.96	0.81	0.13	0.77	1.82	1.51	2.40	1.60	2.50	3.25	
K2O-MgO	1.64	-1.64	1.69	2.23	2.35	1.62	1.67	2.03	2.52	1.79	2.40	1.82	2.47	3.08	
FeO/MgO*	2.51	1.20	2.11	2.21	1.93	2.28	2.66	2.10	1.94	1.94	1.94	1.95	1.49	1.46	
Fe3+/Fe2+	1.11	0.00	0.99	0.81	0.53	0.78	1.17	0.18	0.24	0.24	0.24	1.60	0.00	0.00	
LARSEN	19.94	10.50	19.66	21.29	22.30	20.15	19.31	20.28	22.00	21.69	22.58	20.77	23.18	25.78	
ALKALI IN	-1.53	2.08	0.08	-1.09	-0.94	-0.43	0.09	0.08	-0.17	-1.03	-0.82	-0.73	-1.47	-2.01	
ALT INDE	38.492	40.372	44.817	50.121	51.255	46.015	41.778	44.332	48.428	47.465	53.122	52.840	54.754	50.999	
K INDEX	1.12	0.95	1.27	1.29	1.60	1.28	1.14	1.41	1.69	1.66	1.78	1.40	2.00	3.61	
Na INDEX	2.1444	2.3266	1.9417	1.7832	1.8698	2.0995	2.0710	1.9925	1.8553	2.1900	1.9657	1.8782	1.8392	2.1627	
Al2O3/Na2	4.03856	4.112	3.742574	4.783951	4.258242	4.259947	3.742574	3.836634	3.648515	4.012788	4.415954	4.877419	4.486647	3.708134	
SiO2/Al2O	4.2158	3.5058	4.2328	4.2581	4.3226	3.9851	4.1667	4.1290	4.4776	4.2065	4.2581	4.2328	4.4974	4.5806	
Ti/Nb	23340.00	22500.00	24240.00	19440.00	21840.00	22620.00	24240.00	24240.00	24240.00	23460.00	21060.00	18600.00	20220.00	25080.00	
use?	ok	no	no	no	no	no	no	no	no	no	no	ok	no	no	
altered?		west of ore	alt.potassic	alt.potassic	alt.potassic	alt.potassic	alt.potassic	alt.potassic	alt.pot,phyl.	alt.pot.,phyl	alt.pot.,phyl.		alt.pot.,phyl	alt.Kl	
why not use		mT=younger													

MCAow in	Ajo (Corneli	Ajo (Corneli	Ajo (Corneli	Ajo (Corneli	Ajo (Corneli	COPPER C	COPPER C	COPPER C	COPPER C	COPPER C	COPPER C	COPPER C
COUNTY	Pima	Pima	Pima	Pima	Pima	Lander	Lander	Lander	Lander	Lander	Lander	Lander
STATE	AZ	AZ	AZ	AZ	AZ	NV	NV	NV	NV	NV	NV	NV
SAMPLE #	A-32	A-34	A-39	A-40	A-41	3	4	15-MB10	3-MB20	4-MB12	5-MB16	7-MB9
NAME	AJO	AJO	AJO	AJO	AJO	LA3	LA3	LA3	LA3	LA3	LA3	LA3
SOURCE:	Laine, 1974	Laine, 1974	Laine, 1974	Laine, 1974	Laine, 1974	Roberts, 19	Roberts, 19	Theodore,et	Theodore,et	Theodore,et	Theodore,et	Theodore,et
ROCK TYP	qtz monzon	qtz monzon	qtz monzon	qtz monzon	qtz monzon	granodiorite	granodior.p	intrusives	intrusives	intrusives	intrusives	intrusives
SiO2	71	65	66	65	65	68.33	64	62.5	64.5	66.3	65.6	68.4
TiO2	0.33	0.5	0.67	0.67	0.67	0.33	0.41	0.75	0.46	0.54	0.51	0.35
Al2O3	13.23	13.8	16.25	15.69	14.74	15.22	15.2	16.9	15.4	15.2	16.2	15.6
Fe2O3	0	1.38	4.14	3.45	3.45	0.28	1.4	1.6	1.3	0.62	0.81	0.73
FeO	2.57	2.34	1.74	1.8	1.54	2.28	2.4	3.4	2.7	2.8	2.9	1.7
MgO	1.82	1.65	1.82	1.82	1.21	1.86	2.7	2.9	2.9	3	1.8	1.5
MnO	0.02	0.02	0.04	0.04	0.04	0.06	0.08	0.09	0.06	0.05	0.08	0.03
CaO	3.92	3.64	3.08	2.8	2.66	3.2	3.8	4.8	4.7	4.5	3.8	3.6
Na2O	3.24	2.83	4.31	3.91	4.04	3.23	3.2	3.3	3.1	3	3.4	3.9
K2O	4.45	4.58	3.61	3.49	3.61	2.92	2.8	2.4	3.2	2.6	3.2	3
P2O5	0	0	0	0	0	0.1	0.16	0.18	0.11	0.1	0.17	0.08
LOI	0.7	0.93	0.8	1.34	0.64	0	0	2.00	1.39	1.09	0.75	1.84
TOTAL	103.2	97.36	102.11	99.31	97.4	100.09	100.00	100.00	100.00	100.00	99.00	100.00
MINING DI	Ajo	Ajo	Ajo	Ajo	Ajo	Copper Can	Copper Can	Copper Can	Copper Can	Copper Can	Copper Can	Copper Can
Ba	0	0	0	0	0	0	0	0.07	0.15	0.1	0.1	0.15
Rb	0	0	0	0	0	0	0	0	0	0	0	0
Sr	0	0	0	0	0	0	0	0.07	0.07	0.07	0.05	0.07
Y	0	0	0	0	0	0	0	0.002	0.001	0.0015	0.002	0.001
Zr	0	0	0	0	0	0	0	0	0	0	0	0
Nb	0	0	0	0	0	0	0	0	0	0	0	0
CLASS	MCAow	MCAow	MCAow	MCAow	MCAow	MCAow	MCAow	MCAow	MCAow	MCAow	MCAow	MCAow
A/CNK	0.765	0.849	0.978	1.024	0.957	1.064	0.998	1.007	0.899	0.953	1.013	0.961
A/NK	1.30	1.43	1.48	1.54	1.40	1.79	1.83	2.10	1.80	1.96	1.79	1.61
Na2O+K2	7.69	7.41	7.92	7.40	7.65	6.15	6.00	5.70	6.30	5.60	6.60	6.90
Na2O/K2O	0.73	0.62	1.19	1.12	1.12	1.11	1.14	1.38	0.97	1.15	1.06	1.30
NaO+K2O-	3.77	3.77	4.84	4.60	4.99	2.95	2.20	0.90	1.60	1.10	2.80	3.30
K2O-CaO	0.53	0.94	0.53	0.69	0.95	-0.28	-1.00	-2.40	-1.50	-1.90	-0.60	-0.60
K2O-MgO	2.63	2.93	1.79	1.67	2.40	1.06	0.10	-0.50	0.30	-0.40	1.40	1.50
FeO/MgO*	1.41	2.17	3.00	2.70	3.84	1.36	1.36	1.67	1.33	1.12	2.02	1.57
Fe3+/Fe2+	0.00	0.59	2.38	1.92	2.24	0.12	0.58	0.47	0.48	0.22	0.28	0.43
LARSEN	22.38	20.96	20.71	20.54	21.41	20.64	17.63	15.53	17.10	17.20	19.47	20.70
ALKALI IN	-2.72	-0.77	-0.63	-0.78	-0.53	-3.27	-1.81	-1.55	-1.69	-3.06	-1.80	-2.54
ALT INDE	46.687	49.055	42.356	44.176	41.840	42.640	44.000	39.552	43.885	42.748	40.984	37.500
K INDEX	1.47	1.25	1.14	1.20	1.21	1.40	1.17	0.89	1.07	1.07	1.13	1.41
Na INDEX	1.4929	1.4668	2.1718	2.1445	2.0757	2.1697	2.1413	2.3824	1.8676	2.1066	2.0758	2.2613
Al2O3/Na2	4.083333	4.876325	3.770302	4.012788	3.648515	4.712074	4.75	5.121212	4.967742	5.066667	4.764706	4
SiO2/Al2O	5.3666	4.7101	4.0615	4.1428	4.4098	4.4895	4.2105	3.6982	4.1883	4.3618	4.0494	4.3846
Ti/Nb	19440.00	16980.00	25860.00	23460.00	24240.00	19380.00	19200.00	19800.00	18600.00	18000.00	20400.00	23400.00
use?	no	no	no	no	ok	ok	ok	ok	ok	ok	ok	ok
altered?	alt.pot.,phyl	alt.pot.,phyl	alt.pot.,phyl	alt.pot.,phyl	alt.phyllic							
why not use					minor alt.							

MCAr incl.	Bald Mount	Bald Mount	Bald Mount	Bald Mount	Bald Mount	Bald Mount	Bald Mount	BLOODY R	BLOODY R	BLOODY R	ASA MOO	ASA MOO	ASA MOO	ASA MOO
COUNTY	White Pine	White Pine	White Pine	White Pine	White Pine	White Pine	White Pine	Humboldt	Humboldt	Humboldt	Humboldt	Humboldt	Humboldt	Humboldt
STATE	NV	NV	NV	NV	NV	NV	NV	NV	NV	NV	NV	NV	NV	NV
SAMPLE #	R2-88-292	R2-88-290	R2-88-291	1	4	7	8	2	77	78	281	282	283	284
NAME	BALD	BALDMTN	BALDMTN	BALDMTN	BALDMTN	BALDMTN	BALDMTN	HM1	HM1	HM1	ASAMOOR	ASAMOOR	ASAMOOR	ASAMOOR
SOURCE:	MagmaChe	MagmaChe	MagmaChe	MagmaChe	MagmaChe	MagmaChe	MagmaChe	Willden,196	Lee, 1984;	Lee, 1984;	MagmaChe	MagmaChe	MagmaChe	MagmaChe
ROCK TYP	dikes	pluton	pluton	pluton	pluton	dikes	pluton	stocks	stocks	stocks	granodiorite	aplite	granodiorite	aplite
SiO2	68.19	72.74	70.14	68.90	69.40	70.80	71.40	63.6	65.7	67.3	65.08	75.04	65.10	76.58
TiO2	0.42	0.27	0.49	0.47	0.37	0.28	0.26	0.5	0.46	0.46	0.58	0.13	0.58	0.08
Al2O3	14.64	13.79	14.22	14.40	14.60	14.80	12.70	17.3	15.8	16.4	16.67	13.34	16.43	12.96
Fe2O3	1.07	0.80	1.01	1.30	1.10	0.64	0.71	2.2	2.2	1.5	1.65	0.55	1.65	0.45
FeO	1.85	1.00	1.70	2.00	1.80	1.50	1.50	1.9	2	1.8	1.95	0.50	1.95	0.25
MgO	1.58	0.66	1.37	1.40	1.20	0.50	0.48	2.1	1.7	1.5	2.00	0.17	2.04	0.01
MnO	0.04	0.05	0.07	0.05	0.04	0.05	0.05	0.08	0.11	0.08	0.07	0.03	0.07	0.02
CaO	2.11	1.45	2.42	2.70	2.20	2.30	1.60	4.6	4.6	3.9	3.93	1.08	3.93	0.75
Na2O	3.66	3.42	3.10	3.50	3.30	3.50	3.70	4	3.9	3.8	4.53	4.19	4.44	3.74
K2O	4.44	4.64	4.01	3.60	4.00	4.80	4.10	2.2	2.6	3	2.34	4.00	2.28	4.69
P2O5	0.33	0.22	0.28	0.00	0.00	0.00	0.00	0.22	0.23	0.16	0.32	0.15	0.34	0.16
LOI	1.04	0.62	0.89				0.00	0	0	0	0.70	0.35	0.75	0.26
TOTAL	99.37	99.60	99.70	98.32	98.01	99.17	96.50	98.70	100.26	100.63	99.82	99.53	99.56	99.95
MINING DI	Alligator Ri	Alligator Ri	Alligator Ri	Alligator Ri	Alligator Ri	Alligator Ri	Alligator Ri	Basque	Basque	Basque	Basque	Basque	Basque	Basque
Ba	1400	510	740	0	0	0	0	0	1001	1081	1300	710	1200	230
Rb	150	180	145	0	0	0	0	0	82	92	55	105	48	130
Sr	1000	185	295	0	0	0	0	0	585	553	405	88	400	30
Y	12	15	13	0	0	0	0	0	15	14	0	0	0	0
Zr	72	110	165	0	0	0	0	0	90	120	140	90	125	90
Nb	22	19	18	0	0	0	0	0	15	14	14	16	15	15
CLASS	MCAr	MCAr	MCAr	MCAr	MCAr	MCAr	MCAr	MCAr	MCAr	MCAr	MCAr	MCAr	MCAr	MCAr
A/CNK	0.997	1.037	1.026	0.987	1.060	0.977	0.944	0.997	0.897	0.987	972.000	1.011	0.970	1.028
A/NK	1.35	1.29	1.50	1.49	1.49	1.35	1.21	1.93	1.71	1.73	1.67	1.19	1.68	1.15
Na2O+K2	8.10	8.06	7.11	7.10	7.30	8.30	7.80	6.20	6.50	6.80	6.87	8.19	6.72	8.43
Na2O/K2O	0.82	0.74	0.77	0.97	0.83	0.73	0.90	1.82	1.50	1.27	1.94	1.05	1.95	0.80
NaO+K2O-	5.99	6.61	4.69	4.40	5.10	6.00	6.20	1.60	1.90	2.90	2.94	7.11	2.79	7.68
K2O-CaO	2.33	3.19	1.59	0.90	1.80	2.50	2.50	-2.40	-2.00	-0.90	-1.59	2.92	-1.65	3.94
K2O-MgO	2.86	3.98	2.64	2.20	2.80	4.30	3.62	0.10	0.90	1.50	0.34	3.83	0.24	4.68
FeO/MgO*	1.78	2.61	1.90	2.26	2.33	4.15	4.46	1.85	2.34	2.10	1.72	5.85	1.68	65.50
Fe3+/Fe2+	0.58	0.80	0.59	0.65	0.61	0.43	0.47	1.16	1.10	0.83	0.85	1.10	0.85	1.80
LARSEN	23.48	26.78	23.60	22.47	23.73	25.60	25.82	16.70	18.20	20.03	18.10	27.76	18.01	29.46
ALKALI IN	-1.27	-3.00	-2.98	-2.53	-2.52	-2.04	-2.76	-1.46	-1.94	-2.24	-1.34	-3.72	-1.50	-4.06
ALT INDE	51.060	52.114	49.358	44.643	48.598	47.748	46.356	33.333	33.594	36.885	33.906	44.174	34.043	51.143
K INDEX	1.97	2.75	1.69	1.45	1.70	2.01	2.21	0.98	0.96	1.18	1.20	4.03	1.19	6.01
Na INDEX	1.8214	1.7737	1.7991	1.9597	1.8848	1.7057	1.8467	2.8155	2.3969	2.2540	2.9080	2.0580	2.9174	1.8252
Al2O3/Na2	4	4.032164	4.587097	4.114286	4.424242	4.228571	3.432432	4.325	4.051282	4.315789	3.68	3.184	3.7	3.465
SiO2/Al2O	4.6578	5.2748	4.9325	4.7847	4.7534	4.7838	5.6220	3.6763	4.1582	4.1037	3.9040	5.6252	3.9623	5.9090
Ti/Nb	998.18	1080.00	1033.33	ERR	ERR	ERR	ERR	ERR	1560.00	1628.57	248.57	48.75	232.00	32.00
use?	no	no	ok	ok	ok	no	ok	no	no	no	no	no	no	no
altered?		alt.KI						alt.A/CNK				alt. KI		alt.KI
why not use	volc.					volc.			? oxidation	? oxidation	? age		? age	

MCAr incl.	CARLIN IN	CARLIN IN	CARLIN IN	CARLIN IN	CARLIN IN	CARLIN IN	CARLIN IN	CARLIN IN	CARLIN IN	CARLIN IN	CARLIN IN	CARLIN IN	CARLIN IN	Goldstrike i
COUNTY	Eureka-Elko	Eureka-Elk	Eureka-Elko	Eureka-Elko	Eureka-Elko	Eureka-Elko	Eureka-Elk	Eureka-Elko	Eureka-Elko	Eureka-Elk	Eureka-Elko	Eureka-Elko	Eureka-Elk	Eureka
STATE	2	NV	NV	NV	NV	NV	NV	NV	NV	NV	NV	NV	NV	NV
SAMPLE #	L394	L374	L388	L383	L344	L335	L343	L356	L404	L340	1	2	4	R2-88-1004
NAME	EU3	EU3	EU3	EU3	EU3	EU3	EU3	EU3	EU3	EU3	EU3	EU3	EU3	AUSTRIKE
SOURCE:	Evans, 198	Evans, 198	Evans, 198	Evans, 198	Evans, 198	Evans, 198	Evans, 198	Evans, 198	Evans, 198	Evans, 198	Evans, 198	Evans, 198	Evans, 198	MagmaChe
ROCK TYP	Rhyodacite	Rhyodacite	Rhyodacite	Rhyodacite	Quartz Latit	Quartz Latit	Quartz Latit	Quartz Latit	Granodiorite	Granodiorite	N. Big 6	Au Strike	dike	Di intrusive
SiO2	59.6	63.4	63.8	59.8	69	75.2	67.3	69.8	61.9	62.1	57.8	59.4	70.4	57.34
TiO2	1.1	0.73	0.63	0.8	0.25	0	0.25	0.34	0.79	0.67	1	1.1	0.26	1.10
Al2O3	17.5	16.4	16.2	16.7	14.2	13.2	14.3	15.2	16.9	16.3	16.7	17.3	15.3	14.80
Fe2O3	3.1	4.5	3.9	3.9	1.1	0.32	1.5	0.9	1.1	3	1.2	3.2	1.7	2.14
FeO	3.1	1	0.76	2.6	1.1	0.2	0.76	0.36	4.2	2.8	5.5	2.1	0.8	5.00
MgO	2.3	0.85	1.3	2.2	1.5	0.2	1.1	0.72	1.9	2	5	2.9	0.86	4.90
MnO	0.09	0.05	0.06	0.1	0.05	0	0.03	0	0.12	0.05	0.09	0.02	0	0.10
CaO	5.3	4.2	4	5	1.8	0.85	2.3	2.4	5	4.4	4.4	4.5	1.4	6.97
Na2O	2.9	3.3	3.3	3.2	2.2	3.4	2	3	3.1	3.2	3	2.5	4	2.42
K2O	2.8	3.1	3.3	2.7	4.1	4.6	4.3	4.3	2.6	2.7	2.4	2.7	3.9	4.10
P2O5	0.32	0.1	0.24	0.34	0.11	0	0.08	0.13	0.28	0.31	0.24	0.31	0.1	0.61
LOI	0	0	0	0	0	0	0	0	0	0	0	0	0	0.70
TOTAL	100.00	100.00	100.00	100.00	100.00	100.00	100.00	100.00	100.00	100.00	100.00	100.90	100.30	100.18
MINING DI	Carlin	Carlin	Carlin	Carlin	Carlin	Carlin	Carlin	Carlin	Carlin	Carlin	Carlin	Carlin	Carlin	Gold Strike
Ba	1500	1500	1500	1500	1500	70	5000	2000	1000	1000	700	1000	1500	1100
Rb	0	0	0	0	0	0	0	0	0	0	0	0	0	110
Sr	700	1000	700	1000	200	50	1000	70	700	500	1000	1000	500	825
Y	30	20	15	20	15	15	15	20	20	20	30	30	10	18
Zr	150	0	150	150	100	50	70	150	150	100	150	200	150	245
Nb	15	0	0	10	15	30	10	10	7	10	10	10	7	24
CLASS	MCAr	MCAr	MCAr	MCAr	MCAr	MCAr	MCAr	MCAr	MCAr	MCAr	MCAr	MCAr	MCAr	MCAr
A/CNK	1.002	0.997	0.994	0.965	1.251	1.088	1.177	1.088	0.992	1.006	1.074	1.135	1.145	0.701
A/NK	2.24	1.87	1.80	2.04	1.76	1.25	1.80	1.58	2.13	1.99	2.21	2.46	1.42	1.76
Na2O+K2	5.70	6.40	6.60	5.90	6.30	8.00	6.30	7.30	5.70	5.90	5.40	5.20	7.90	6.52
Na2O/K2O	1.04	1.06	1.00	1.19	0.54	0.74	0.47	0.70	1.19	1.19	1.25	0.93	1.03	0.59
NaO+K2O-	0.40	2.20	2.60	0.90	4.50	7.15	4.00	4.90	0.70	1.50	1.00	0.70	6.50	-0.45
K2O-CaO	-2.50	-1.10	-0.70	-2.30	2.30	3.75	2.00	1.90	-2.40	-1.70	-2.00	-1.80	2.50	-2.87
K2O-MgO	0.50	2.25	2.00	0.50	2.60	4.40	3.20	3.58	0.70	0.70	-2.60	-0.20	3.04	-0.80
FeO/MgO*	2.56	5.94	3.28	2.78	1.39	2.44	1.92	1.63	2.73	2.75	1.32	1.72	2.71	1.41
Fe3+/Fe2+	1.00	4.50	5.13	1.50	1.00	1.60	1.97	2.50	0.26	1.07	0.22	1.52	2.13	0.43
LARSEN	15.07	19.18	19.27	15.43	23.80	28.62	23.33	24.45	16.33	17.00	12.27	15.10	25.11	11.34
ALKALI IN	-0.47	-1.18	-1.13	-0.35	-3.37	-3.97	-2.74	-2.67	-1.33	-1.20	-0.10	-0.90	-2.29	1.19
ALT INDE	38.346	34.498	38.655	37.405	58.333	53.039	55.670	48.177	35.714	38.211	50.000	44.444	46.850	48.940
K INDEX	0.71	0.78	0.96	0.73	2.01	6.13	1.68	2.25	0.75	0.80	0.95	0.85	2.35	0.82
Na INDEX	2.0378	2.0619	1.9941	2.1504	1.7880	1.8270	1.6425	1.7855	2.1848	2.1908	2.3237	2.0612	2.1706	1.2908
Al2O3/Na2	6.034483	4.969697	4.909091	5.21875	6.454545	3.882353	7.15	5.066667	5.451613	5.09375	5.566667	6.92	3.825	6.115702
SiO2/Al2O	3.4057	3.8659	3.9383	3.5808	4.8592	5.6970	4.7063	4.5921	3.6627	3.8098	3.4611	3.4335	4.6013	3.8743
Ti/Nb	1160.00	2828.57	1980.00	1920.00	880.00	680.00	1200.00	1800.00	2657.14	1920.00	1800.00	1500.00	3428.57	605.00
use?	no	no	no	no	no	no	no	no	ok	ok	no	ok	no	no
altered?					alt.A/CNK	alt.NAl	alt.A/CNK	alt.Kl			alt.A/CNK		alt.Kl	
why not use	volc.	volc.	volc.	volc.	volc.	volc.	volc.	volc.					volc.	older

MCAr incl.	Goldstrike i	Goldstrike i	Goldstrike i	Goldstrike i	Goldstrike i	Goldstrike i	Goldstrike i	Goldstrike i	Charleston	Charleston	Grassy Mou	NORTHUM	NORTHUM	NORTHUM
COUNTY	Eureka	Eureka	Eureka	Eureka	Eureka	Eureka	Eureka	Eureka	Elko	Elko	?	Nye	Nye	Nye
STATE	NV	NV	NV	NV	NV	NV	NV	NV	NV	NV	OR	NV	NV	NV
SAMPLE #	R2-88-1005	R2-88-1026	R2-88-1027	R2-88-1028	R2-88-1029	R2-88-1030	R2-88-1031	R2-88-1032	R2-88-0988	R2-88-0988	R2-88-MC-	113	114	Cret. dike
NAME	AUSTRIKE	AUSTRIKE	AUSTRIKE	AUSTRIKE	AUSTRIKE	AUSTRIKE	AUSTRIKE	AUSTRIKE	Charlstn	Charlstn	GRASSYM	NY18	NY18	NY18
SOURCE:	MagmaChe	MagmaChe	MagmaChe	MagmaChe	MagmaChe	MagmaChe	MagmaChe	MagmaChe	MagmaChe	MagmaChe	MagmaChe	Lee, 1984	Lee, 1984	McKee, 197
ROCK TYP	Di intrusive	MDi intrusiv	MDi intrusiv	Di intrusive	Di intrusive	Di intrusive	Di intrusive	Di intrusive	intrusive	intrusive	Grassy Mtn.	plutonic	plutonic	Cret. dike
SiO2	59.40	57.06	58.13	51.78	61.09	57.18	58.08	55.70	70.57	67.92	46.55	64.9	66	67.90
TiO2	1.40	1.23	1.12	1.45	1.01	1.01	1.15	0.95	0.21	0.43	1.45	0.47	0.44	0.42
Al2O3	17.20	16.95	16.71	17.06	16.59	19.79	18.03	15.57	15.06	17.25	15.88	16.2	16.1	15.80
Fe2O3	3.95	1.95	1.60	3.49	2.18	1.81	2.09	2.23	0.96	1.88	6.63	0.7	0.93	0.59
FeO	3.55	5.45	4.90	4.40	3.35	4.00	4.45	4.70	0.65	0.70	5.94	2.7	2.4	2.10
MgO	2.30	5.00	4.02	5.89	2.59	3.49	3.58	5.62	0.23	0.51	8.92	2.2	2.1	1.10
MnO	0.11	0.12	0.11	0.11	0.09	0.08	0.11	0.12	0.05	0.05	0.22	0.06	0.06	0.00
CaO	5.20	7.74	7.16	9.94	5.30	6.06	6.87	6.50	2.03	1.29	10.18	4	3.8	2.10
Na2O	3.20	2.82	2.87	3.00	2.93	2.92	3.04	3.15	3.57	2.27	2.31	4.2	4.3	3.90
K2O	3.00	2.54	2.08	1.83	2.66	2.48	2.17	3.00	2.96	3.08	0.64	2.2	2.3	3.70
P2O5	0.24	0.41	0.32	0.37	0.26	0.31	0.31	0.26	0.11	0.20	0.26	0.23	0.23	0.13
LOI	2.30	0.70	0.70	2.20	1.50	2.00	1.50	0.40	2.54	3.85	1.30	0	0	2.18
TOTAL	101.85	101.97	99.72	101.52	99.55	98.13	101.38	98.20	98.94	99.43	100.28	97.86	98.66	100.00
MINING DI	Gold Strike	Gold Strike	Gold Strike	Gold Strike	Gold Strike	Gold Strike	Gold Strike	Gold Strike	Charleston	Charleston	Grassy Mtn.	Northumber	Northumber	Northumber
Ba	950	970	820	700	920	810	800	770	1300	1500	360	1078	1021	0
Rb	78	78	55	18	89	84	66	88	84	85	<5	70	71	0
Sr	555	660	595	825	600	560	625	585	330	250	205	584	565	0
Y	24	17	13	32	19	23	10	7	<5	<5	6	15	15	0
Zr	195	215	170	91	175	195	195	145	145	200	105	82	92	0
Nb	24	29	27	16	28	23	25	20	19	13	18	15	18	0
CLASS	MCAr	MCAr	MCAr	MCAr	MCAr	MCAr	MCAr	MCAr	MCAr	MCAr	MCAr	MCAr	MCAr	MCAr
A/CNK	0.956	0.789	0.835	0.682	0.956	1.068	0.907	0.768	1.178	1.830	0.689	0.977	0.976	1.108
A/NK	2.02	2.29	2.39	2.46	2.15	2.64	2.45	1.85	1.66	2.44	3.53	1.74	1.68	1.51
Na2O+K2	6.20	5.36	4.95	4.83	5.59	5.40	5.21	6.15	6.53	5.35	2.95	6.40	6.60	7.60
Na2O/K2O	1.07	1.11	1.38	1.64	1.10	1.18	1.40	1.05	1.21	0.74	3.61	1.91	1.87	1.05
NaO+K2O-	1.00	-2.38	-2.21	-5.11	0.29	-0.66	-1.66	-0.35	4.50	4.06	-7.23	2.40	2.80	5.50
K2O-CaO	-2.20	-5.20	-5.08	-8.11	-2.64	-3.58	-4.70	-3.50	0.93	1.79	-9.54	-1.80	-1.50	1.60
K2O-MgO	0.70	-2.46	-1.94	-4.06	0.07	-1.01	-1.41	-2.62	2.73	2.57	-8.28	0.00	0.20	2.60
FeO/MgO*	3.09	1.44	1.58	1.28	2.05	1.61	1.77	1.19	6.58	4.69	1.33	1.51	1.54	2.39
Fe3+/Fe2+	1.11	0.36	0.33	0.79	0.65	0.45	0.47	0.47	1.48	2.69	1.12	0.26	0.39	0.28
LARSEN	15.30	8.82	10.28	3.26	15.13	11.99	11.08	9.45	24.22	23.92	-2.94	17.63	18.40	23.13
ALKALI IN	0.10	0.13	-0.67	1.57	-1.14	0.13	-0.40	1.43	-3.72	-3.92	1.63	-1.74	-1.95	-1.66
ALT INDE	38.686	41.657	37.818	37.367	38.947	39.933	36.718	47.181	36.291	50.210	43.356	34.921	35.200	44.444
K INDEX	0.69	0.69	0.66	0.61	0.77	0.76	0.67	0.89	1.91	1.59	0.54	1.17	1.24	1.84
Na INDEX	2.0227	1.8989	2.2145	2.3210	2.0571	2.2453	2.3084	1.8179	2.3842	2.5670	4.2987	2.8860	2.8458	2.1624
Al2O3/Na2	5.375	6.010638	5.8223	5.686667	5.662116	6.777397	5.930921	4.942857	4.218487	7.599119	6.874459	3.857143	3.744186	4.051282
SiO2/Al2O	3.4535	3.3664	3.4788	3.0352	3.6823	2.8893	3.2213	3.5774	4.6859	3.9374	2.9314	4.0062	4.0994	4.2975
Ti/Nb	800.00	583.45	637.78	1125.00	627.86	761.74	729.60	945.00	1127.37	1047.69	770.00	1680.00	1433.33	ERR
use?	no	no	no	no	no	no	no	no	no	no	no	ok	ok	no
altered?									alt.LOI	alt.LOI				alt.LOI
why not use	older	older	older	older	older	older	older	older			volc.			

MCAr incl.	OSGOOD	OSGOOD	OSGOOD	OSGOOD	OSGOOD	OSGOOD	OSGOOD	OSGOOD	OSGOOD	OSGOOD	Wenatchee	Wenatchee	Wenatchee	Wenatchee
COUNTY	Humboldt	Humboldt	Humboldt	Humboldt	Humboldt	Humboldt	Humboldt	Humboldt	Humboldt	Humboldt	Chelan	Chelan	Chelan	Chelan
STATE	NV	NV	NV	NV	NV	NV	NV	NV	NV	NV	WA	WA	WA	WA
SAMPLE #	MB-33B	MB-34	MB-32	MB-32A	A	B	1	2	3	4	C-2	C-3	308047	308048
NAME	HM13	HM13	HM13	HM13	HM13	HM13	HM13	HM13	HM13	HM13	WENA	WENA	WENA	WENA
SOURCE:	Silberman e	Silberman e	Silberman e	Silberman e	Hotz & Will	Hotz & Will	Hotz & Will	Hotz & Will	Hotz & Will	Hotz & Will	Coombs	Coombs	MagmaChe	MagmaChe
ROCK TYP	granodiorite	granodiorite	Andesite po	Andesite po	Andesite po	Andesite po	Andesite po	Andesite po	Andesite po	Andesite po	Perlite	Sperulitic br	No.2 Canyo	Rooster Co
SiO2	65.9	61.7	64.9	65.2	67.6	68.4	50.6	57.6	58	59.8	74.11	77.3	51.07	74.26
TiO2	0.53	0.7	0.63	0.58	0.42	0.4	1.9	1.9	1.2	1	0.11	0.12	0.75	0.18
Al2O3	16.8	17.8	16.9	17	16.8	16.8	16.3	15	17	16	11.2	12.39	19.24	13.21
Fe2O3	1.5	1	0.85	1.2	1.3	1.6	6.9	2	4.6	2.4	0.52	0.57	8.1	1.4
FeO	2	3.4	1.5	1.6	1.6	1.4	2.4	6.5	2.6	3.8	0.28	0.19	n.a.	n.a.
MgO	1.4	2.2	1.6	1.6	1	1.2	5.6	2.5	3.1	2.8	0.23	0.1	2.91	0.11
MnO	0.07	0.08	0.06	0.05	0.1	0.09	0.16	0.18	0.12	0.15	?	0	0	0
CaO	4.3	5.2	5.3	4.9	4	4	7.1	5.5	5.5	5	1.88	0.68	7.35	1.07
Na2O	3.6	3.6	3.5	3.3	3.5	3.5	4	3.5	3.9	3.4	3.17	3.14	3.73	3.83
K2O	2.8	2.8	3.3	2.7	2.8	2.8	2.1	2.7	2.8	3.2	1.04	4.36	1.12	3.51
P2O5	0.19	0.26	0.26	0.27	0.22	0.22	0.76	0.82	0.66	0.54	0.02	0.02	0	0
LOI	0	0	0	0	0	0	0	0	0	0	?	?	4.71	2.03
TOTAL	99.80	99.80	99.60	99.10	100.00	101.00	99.80	99.50	100.40	99.20	?	?	?	?
MINING DI	Potosi,Getc	Potosi,Getc	Potosi,Getc	Potosi,Getc	Potosi,Getc	Potosi,Getc	Potosi,Getc	Potosi,Getc	Potosi,Getc	Potosi,Getc	Wenatchee	Wenatchee	Wenatchee	Wenatchee
Ba	1500	1500	2000	1500	0.1	0.2	0	0	0	0	0	0	0	0
Rb	69	62	59	0	0	0	0	0	0	0	0	0	0	0
Sr	602	670	623	0	0.08	0.08	0	0	0	0	0	0	0	0
Y	20	20	20	15	0.002	0	0	0	0	0	0	0	0	0
Zr	100	70	100	100	0.007	0.007	0	0	0	0	0	0	0	0
Nb	10	10	10	7	0	0	0	0	0	0	0	0	0	0
CLASS	MCAr	MCAr	MCAr	MCAr	MCAr	MCAr	MCAr	MCAr	MCAr	MCAr	MCAr	MCAr	MCAr	MCAr
A/CNK	1.000	0.966	0.890	0.984	1.045	1.045	0.748	0.802	0.873	0.880	1.147	1.113	0.928	1.095
A/NK	1.87	1.99	1.81	2.03	1.91	1.91	1.84	1.73	1.80	1.76	1.77	1.25	2.62	1.31
Na2O+K2	6.40	6.40	6.80	6.00	6.30	6.30	6.10	6.20	6.70	6.60	4.21	7.50	4.85	7.34
Na2O/K2O	1.29	1.29	1.06	1.22	1.25	1.25	1.90	1.30	1.39	1.06	3.05	0.72	3.33	1.09
NaO+K2O-	2.10	1.20	1.50	1.10	2.30	2.30	-1.00	0.70	1.20	1.60	2.33	6.82	-2.50	6.27
K2O-CaO	-1.50	-2.40	-2.00	-2.20	-1.20	-1.20	-5.00	-2.80	-2.70	-1.80	-0.84	3.68	-6.23	2.44
K2O-MgO	1.40	0.60	1.70	1.10	1.80	1.60	-3.50	0.20	-0.30	0.40	0.81	4.26	-1.79	3.40
FeO/MgO*	2.39	1.95	1.42	1.68	2.77	2.37	1.54	3.32	2.17	2.13	3.25	7.03	ERR	ERR
Fe3+/Fe2+	0.75	0.29	0.57	0.75	0.81	1.14	2.88	0.31	1.77	0.63	1.86	3.00	ERR	ERR
LARSEN	19.07	15.97	18.03	17.93	20.33	20.40	6.27	13.90	13.53	15.33	23.63	29.35	7.88	27.08
ALKALI IN	-2.11	-0.55	-1.34	-2.25	-2.85	-3.14	3.28	0.77	1.12	0.35	-7.36	-5.26	1.85	-4.28
ALT INDE	34.711	36.232	35.766	34.400	33.628	34.783	40.957	36.620	38.562	41.667	20.095	53.865	26.671	42.488
K INDEX	1.02	0.91	1.11	1.00	1.08	1.10	0.74	0.63	0.80	0.86	1.69	5.50	ERR	ERR
Na INDEX	2.2861	2.2514	1.9504	2.2058	2.2946	2.2946	2.6528	2.0982	2.2659	1.9429	4.1947	1.8328	4.2581	2.1867
Al2O3/Na2	4.666667	4.944444	4.828571	5.151515	4.8	4.8	4.075	4.285714	4.358974	4.705882	3.533123	3.94586	5.158177	3.449086
SiO2/Al2O	3.9226	3.4663	3.8402	3.8353	4.0238	4.0714	3.1043	3.8400	3.4118	3.7375	6.6170	6.2389	2.6544	5.6215
Ti/Nb	2160.00	2160.00	2100.00	2828.57	ERR	ERR	ERR	ERR	ERR	ERR	ERR	ERR	ERR	ERR
use?	ok	ok	no	no	no	no	no	no	no	no	no	no	no	no
altered?											alt.A/CNK	alt.Al,NAl	alt.LOI	alt.LOI
why not use			volc.	volc.	volc.	volc.	volc.	volc.	volc.	volc.	volc.	volc.		

MCAr incl.	Wenatchee	Wenatchee	Wenatchee	Wenatchee	Yellow Pine
COUNTY	Chelan	Chelan	Chelan	Chelan	Valley
STATE	WA	WA	WA	WA	ID
SAMPLE #	308049	308050	308051	202991	Y-2;261378
NAME	WENA	WENA	WENA	WENA	YELL
SOURCE:	MagmaChe	MagmaChe	MagmaChe	MagmaChe	USGS, Silb
ROCK TYP	Wenathcee	Andesite W	Castle Rock	Andesite di	Yellow Pine
SiO2	76.31	70.89	66.76	68.6	66.9
TiO2	0.14	0.42	0.48	0	0.61
Al2O3	12.64	13.37	15.1	12.6	16.4
Fe2O3	1.05	2.96	3.58	3.76	1.709
FeO	n.a.	n.a.	n.a.	n.a.	1.61
MgO	0.07	1.15	1.4	1.85	0.96
MnO	0	0	0	0	0.04
CaO	0.85	3.77	2.5	5.36	3.15
Na2O	4	3.22	4.66	3.72	3.98
K2O	3.45	1.17	1.88	0.67	3.06
P2O5	0	0	0	0	0.31
LOI	1.15	2.85	3.07	?	0.54
TOTAL	?	?	?	?	98.73
MINING DI	Wenatchee	Wenatchee	Wenatchee	Wenatchee	Yellow Pine
Ba	0	0	0	0	0
Rb	0	0	0	0	0
Sr	0	0	0	0	0
Y	0	0	0	0	0
Zr	0	0	0	0	0
Nb	0	0	0	0	0
CLASS	MCAr	MCAr	MCAr	MCAr	MCAr
A/CNK	1.065	0.995	1.059	0.759	1.051
A/NK	1.22	2.04	1.56	1.84	1.66
Na2O+K2	7.45	4.39	6.54	4.39	7.04
Na2O/K2O	1.16	2.75	2.48	5.55	1.30
NaO+K2O-	6.60	0.62	4.04	-0.97	3.89
K2O-CaO	2.60	-2.60	-0.62	-4.69	-0.09
K2O-MgO	3.38	0.02	0.48	-1.18	2.10
FeO/MgO*	ERR	ERR	ERR	ERR	3.28
Fe3+/Fe2+	ERR	ERR	ERR	ERR	1.06
LARSEN	27.97	19.88	20.23	16.33	21.25
ALKALI IN	-4.94	-5.98	-2.29	-5.13	-1.85
ALT INDE	42.055	24.919	31.418	21.724	36.054
K INDEX	ERR	ERR	ERR	ERR	1.27
Na INDEX	2.2241	3.7474	3.5376	6.3108	2.3516
Al2O3/Na2	3.16	4.152174	3.240343	3.387097	4.120603
SiO2/Al2O	6.0372	5.3022	4.4212	5.4444	4.0793
Ti/Nb	ERR	ERR	ERR	ERR	ERR
use?	no	no	no	no	no
altered?		alt.Al,LOI	alt.LOI		
why not use	no oxid.data	volc.	volc.	volc.	? ages

APPENDIX C: VARIATION DIAGRAMS WITH AND WITHOUT ALTERED AND VOLCANIC SAMPLES

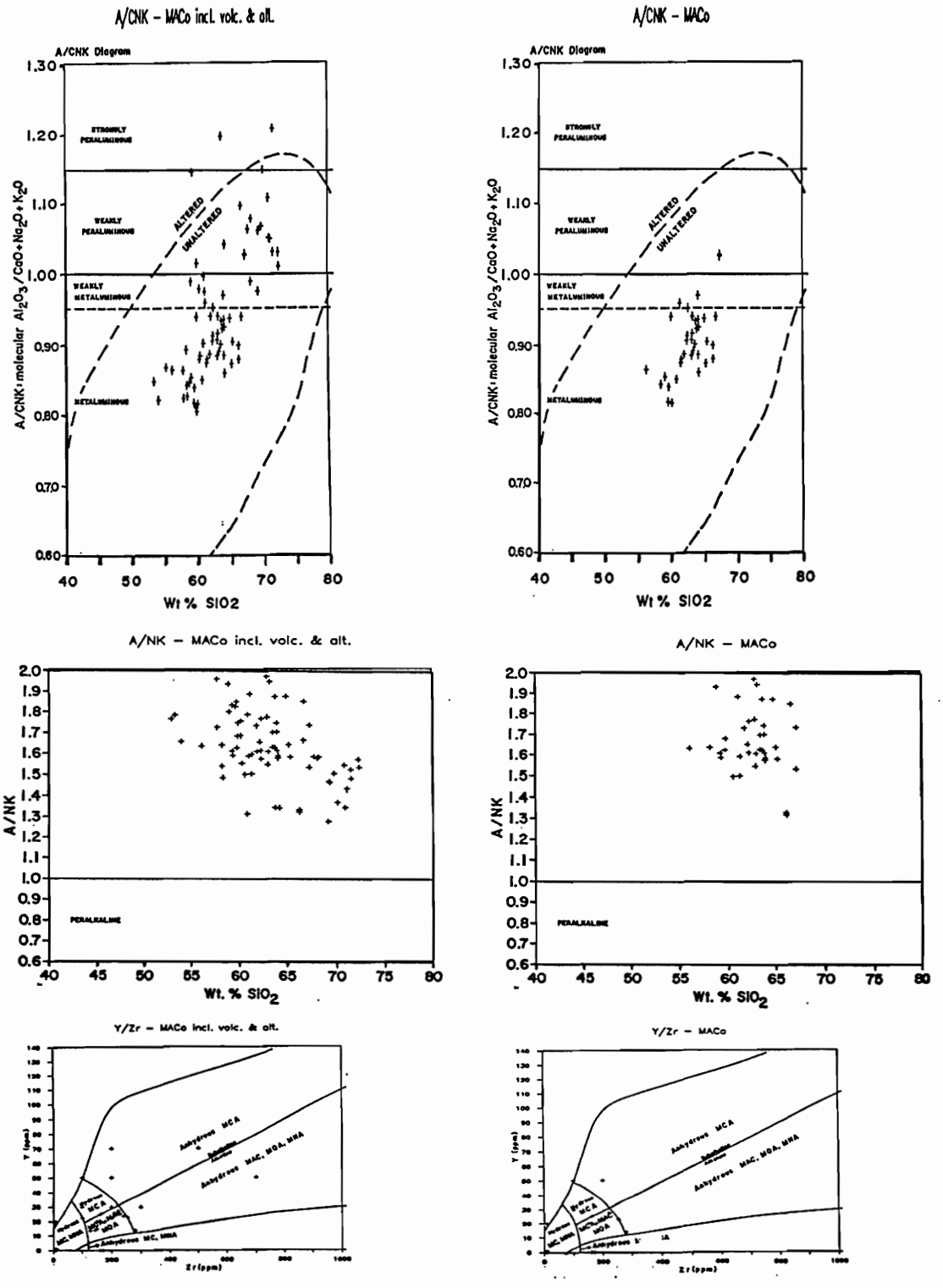

Figure C-1. A/CNK, A/NK, and Y/Zr diagrams of the metaluminous, alkali-calcic, oxidized class (left includes altered and volcanics; right is only unaltered).

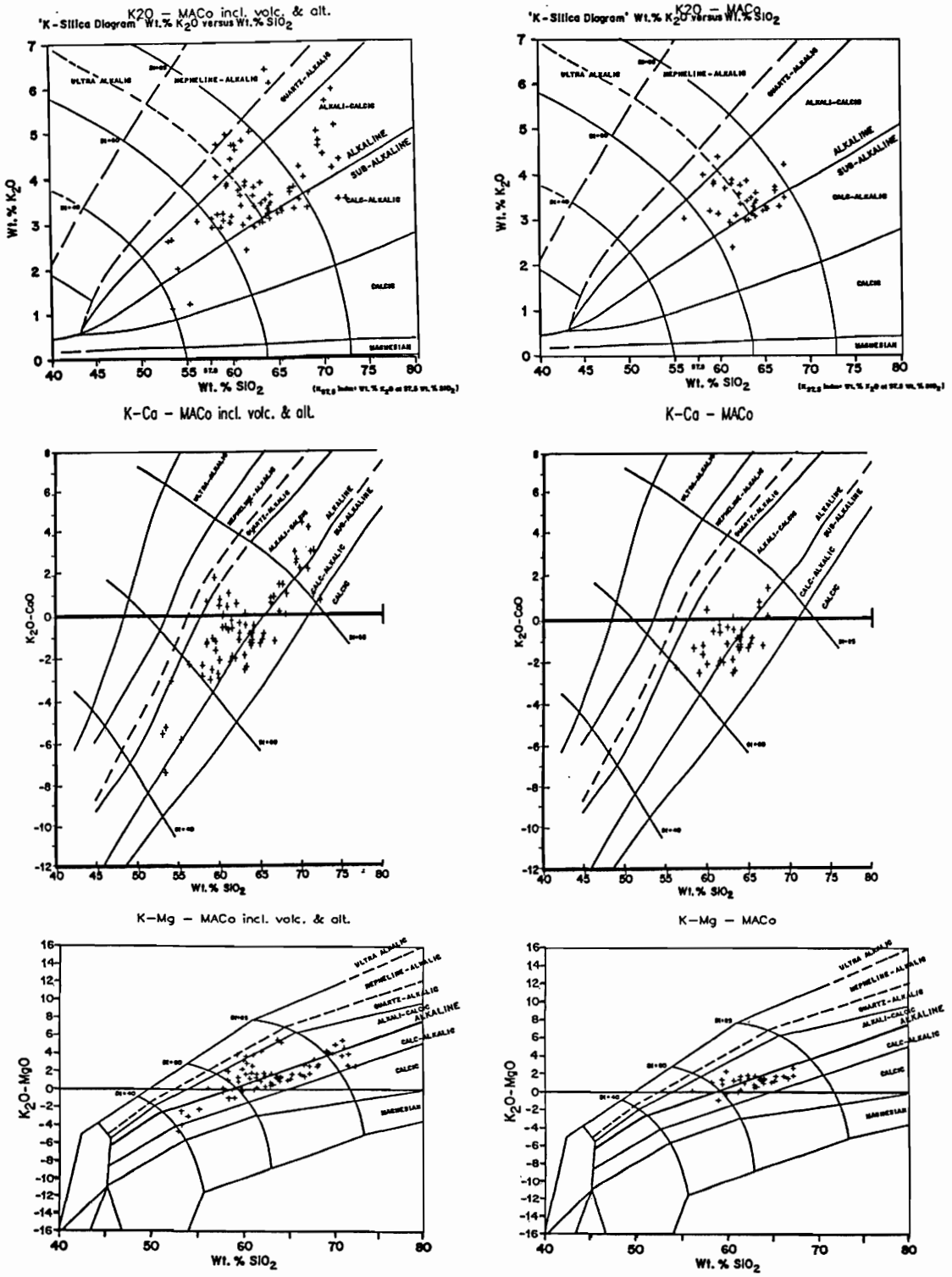

Figure C-2. Alkalinity diagrams of the metaluminous, alkali-calcic, oxidized class (left side includes altered and volcanics; right is only unaltered).

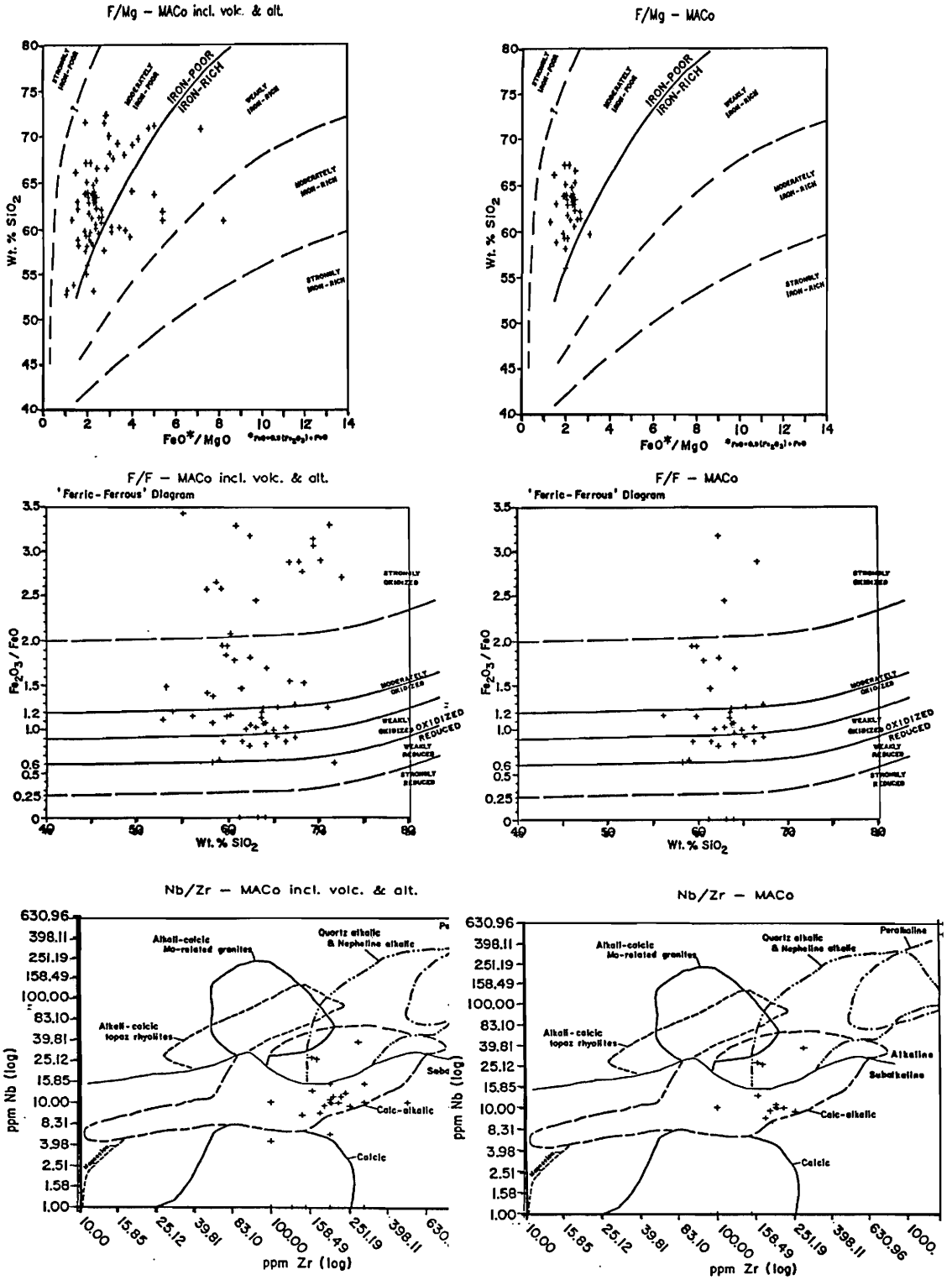

Figure C-3. Iron and Nb/Zr diagrams of the metaluminous, alkali-calcic, oxidized class (left side includes altered and volcanics; right is only unaltered).

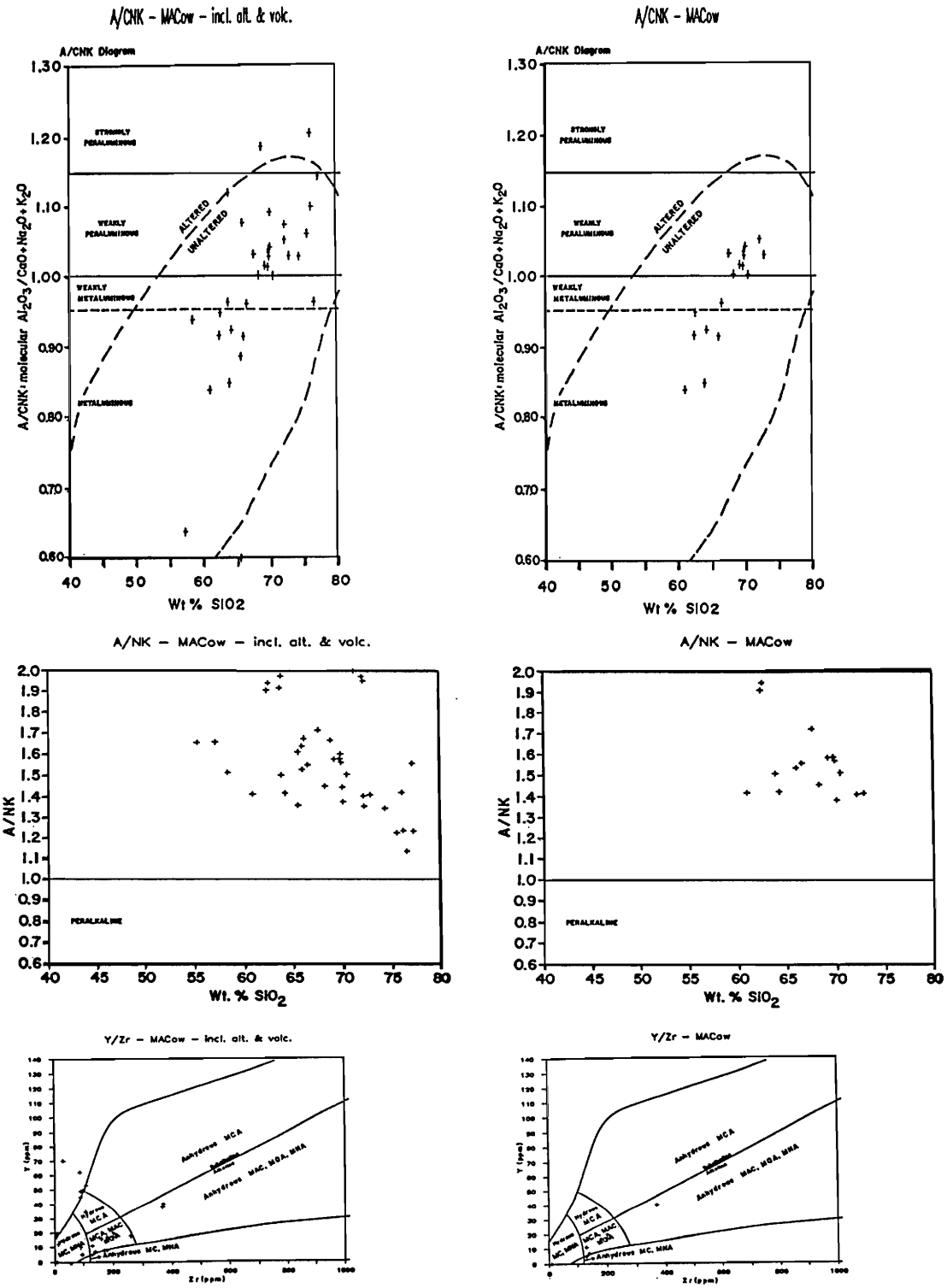

Figure C-4. A/CNK, A/NK, and Y/Zr diagrams of metaluminous, alkali-calcic, weakly oxidized (left includes altered and volcanics; right is only unaltered).

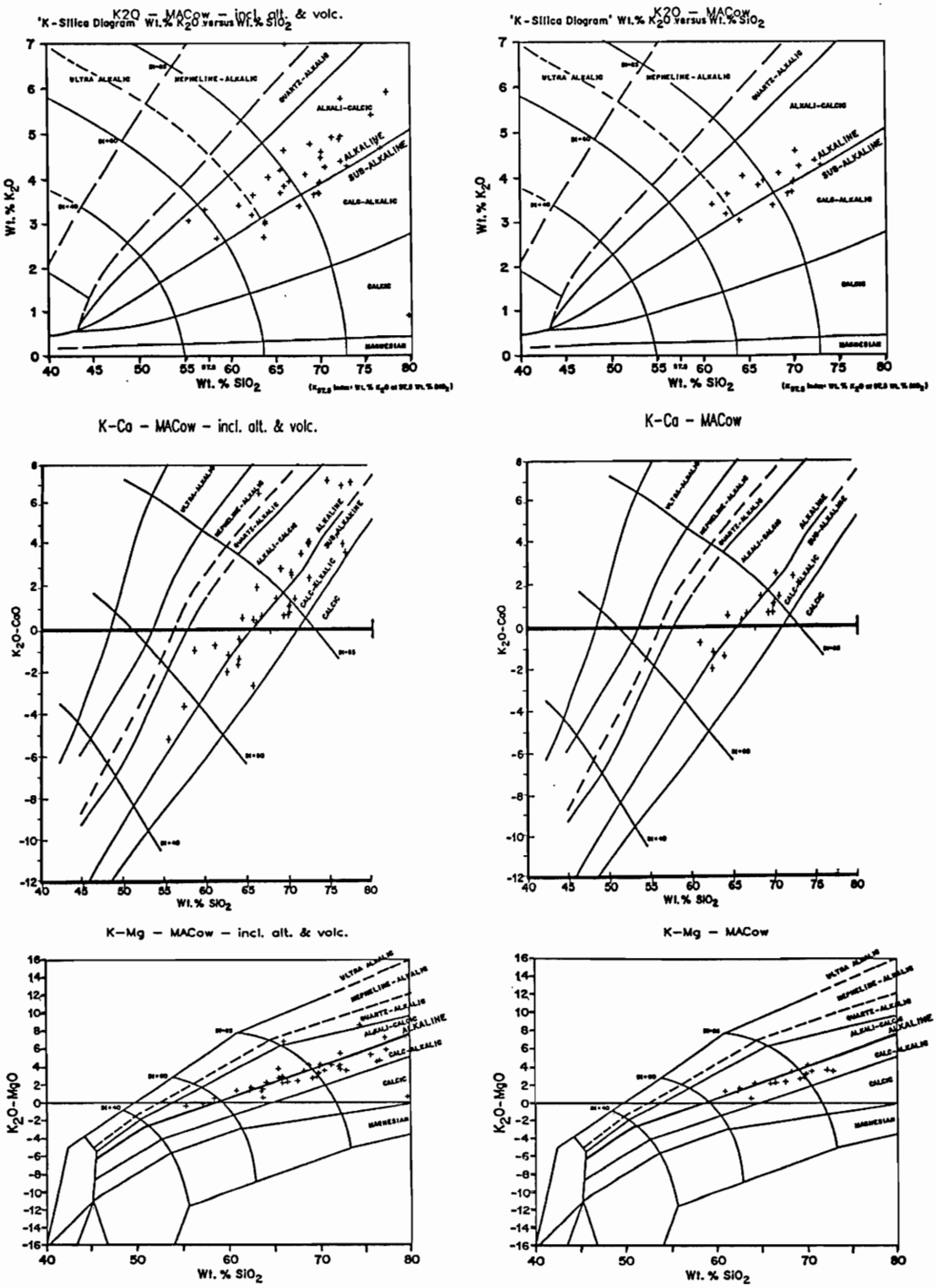

Figure C-5. Alkalinity diagrams of the metaluminous, alkali-calcic, weakly oxidized class (left side includes altered and volcanics; right is only unaltered).

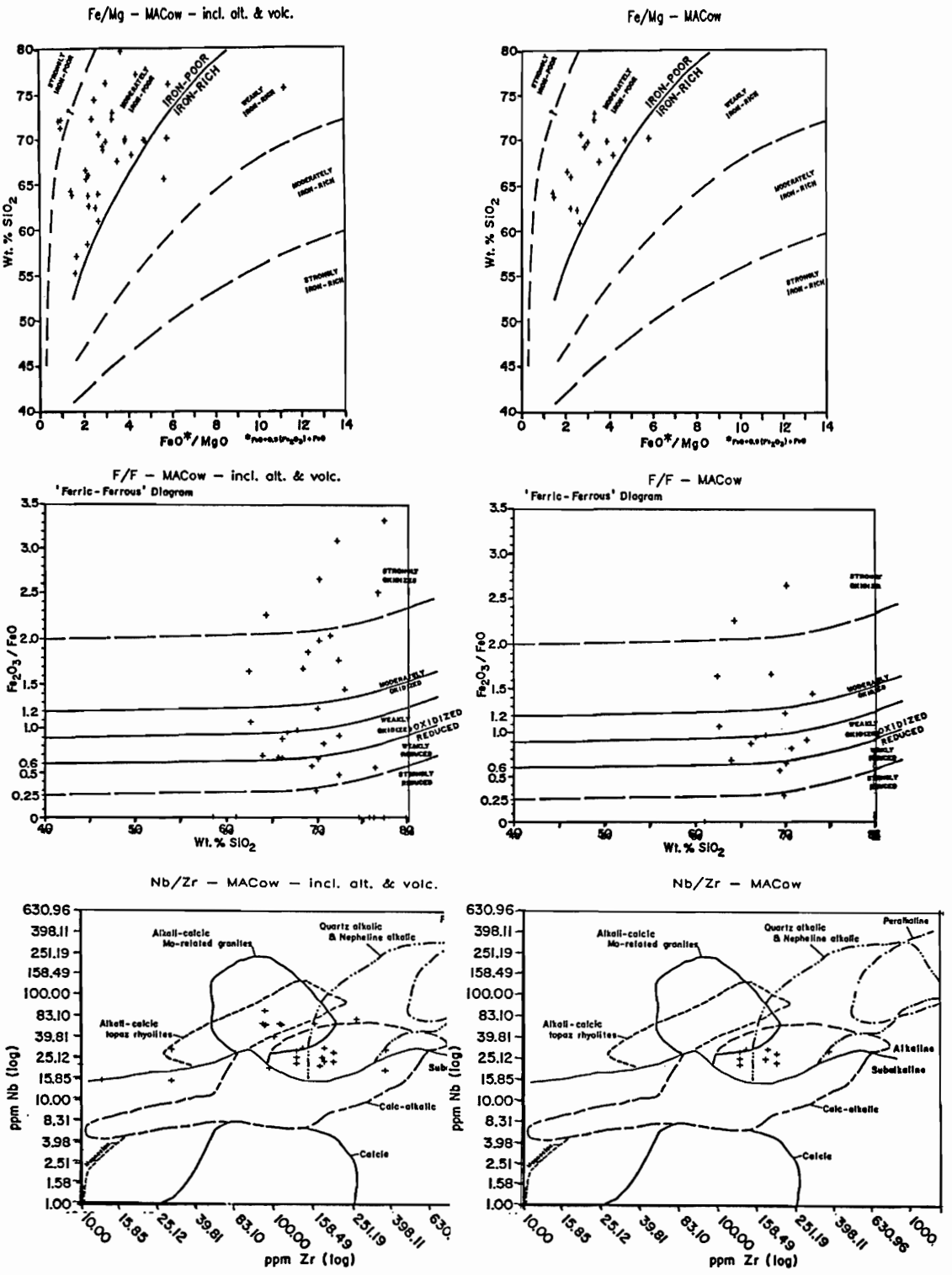

Figure C-6. Iron and Nb/Zr diagrams of metaluminous, alkali-calcic, weakly oxidized class (left includes altered and volcanics; right is only unaltered).

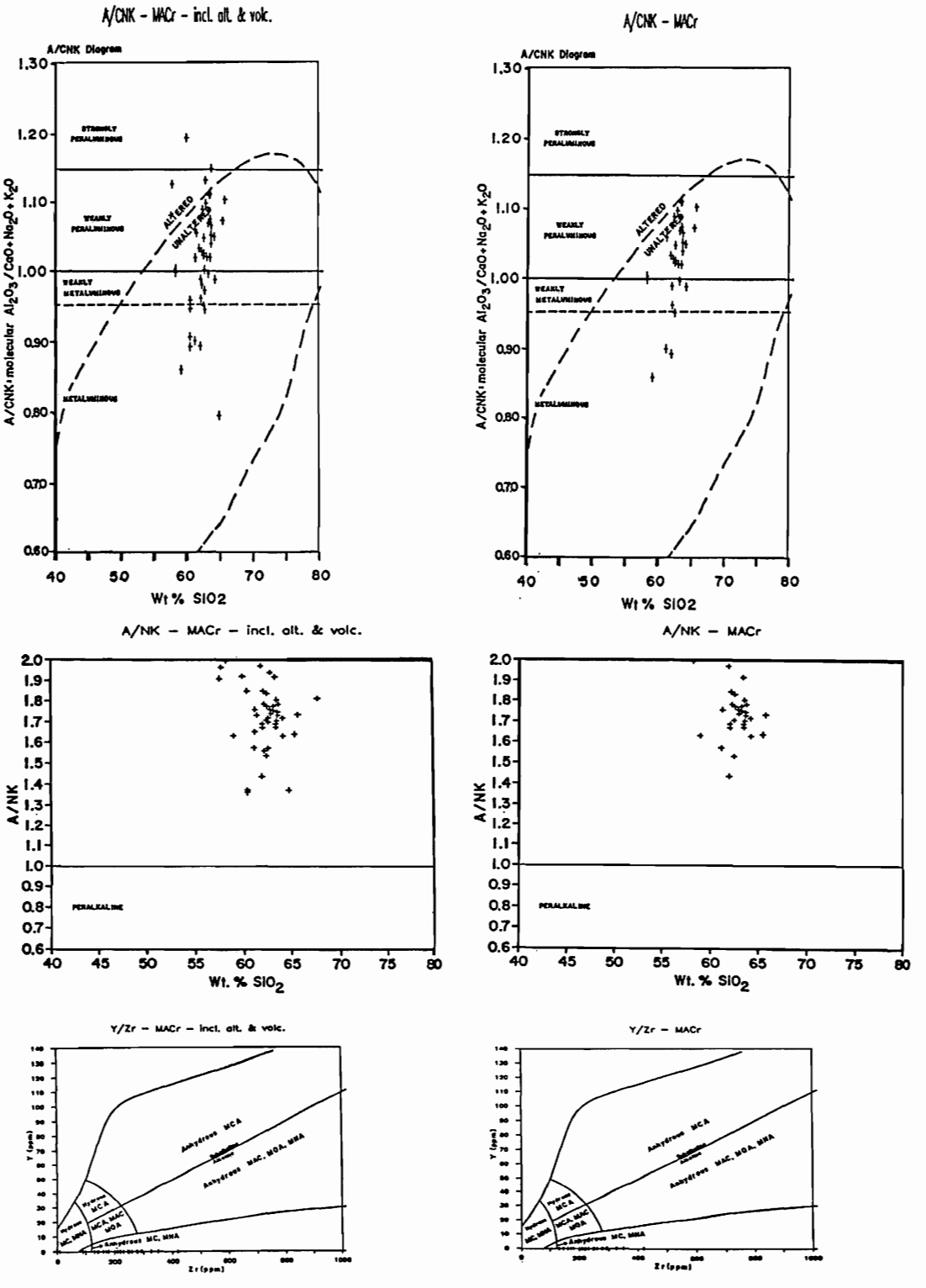

Figure C-7. A/CNK, A/NK, and Y/Zr diagrams of the metaluminous, alkali-calcic, reduced class.

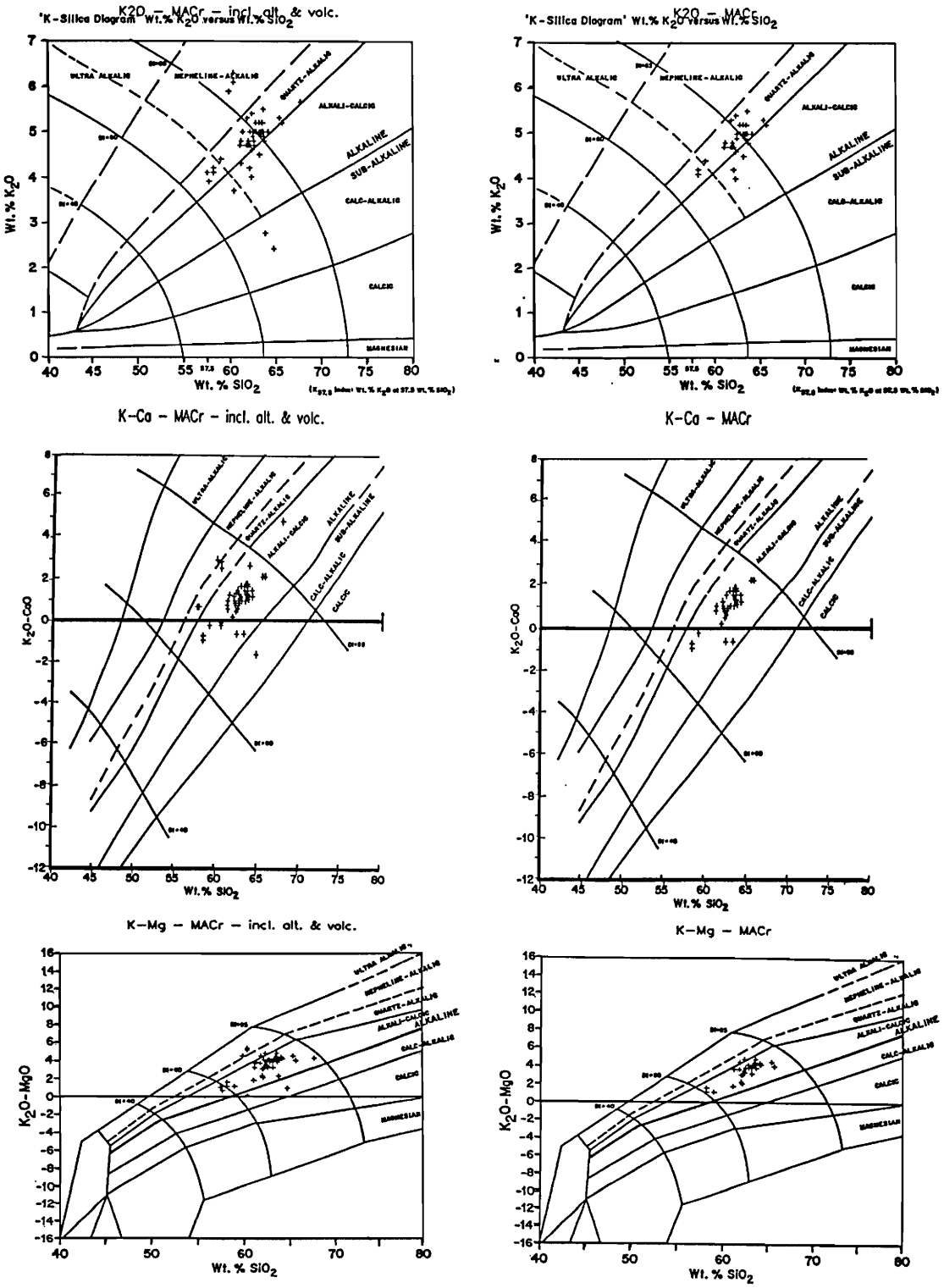

Figure C-8. Alkalinity variation diagrams of the metaluminous, alkali-calcic, reduced class (left includes altered and volcanics; right is only unaltered).

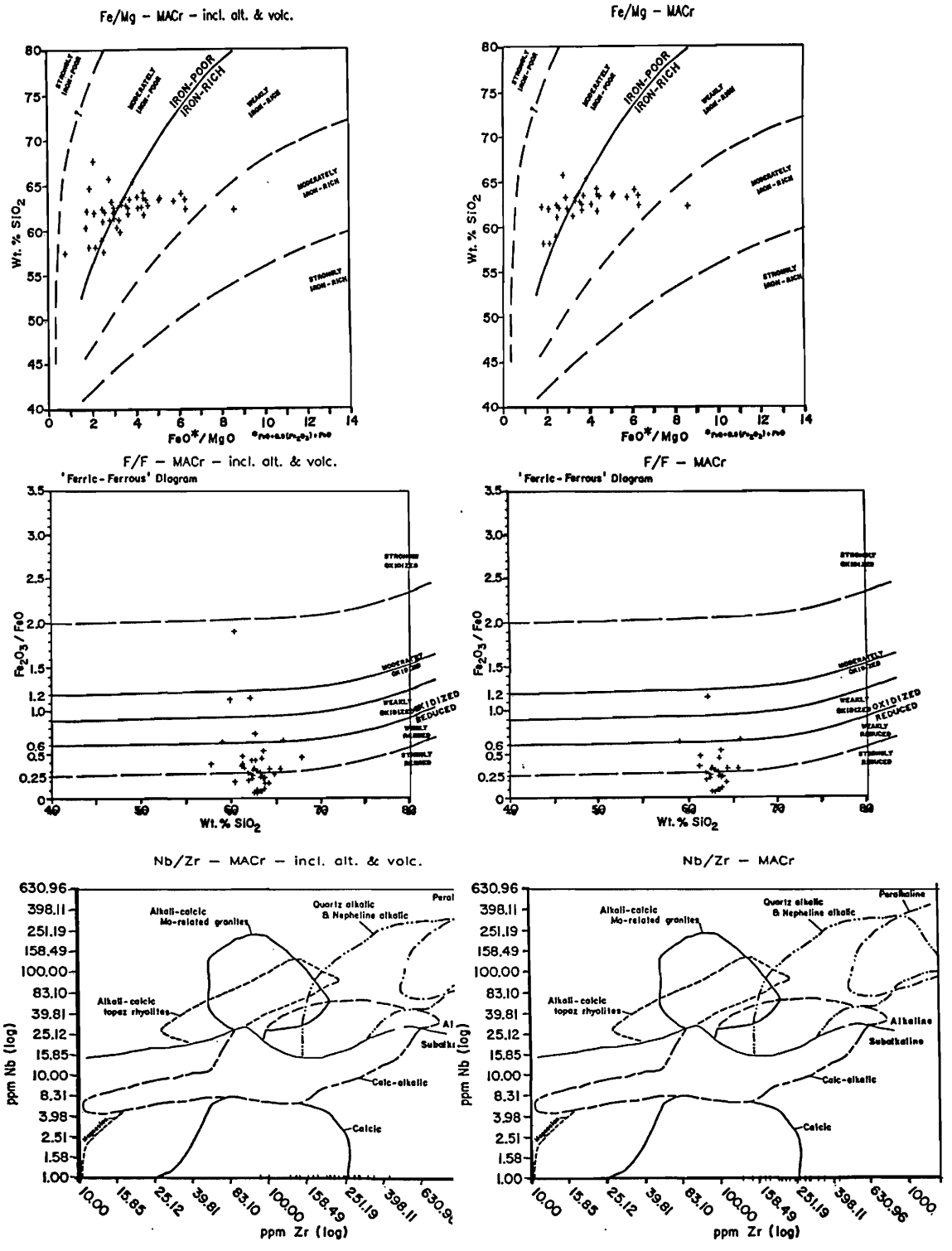

Figure C-9. Iron ratio variation diagrams of the metaluminous, alkali-calcic, reduced class (left includes altered and volcanics; right is only unaltered).

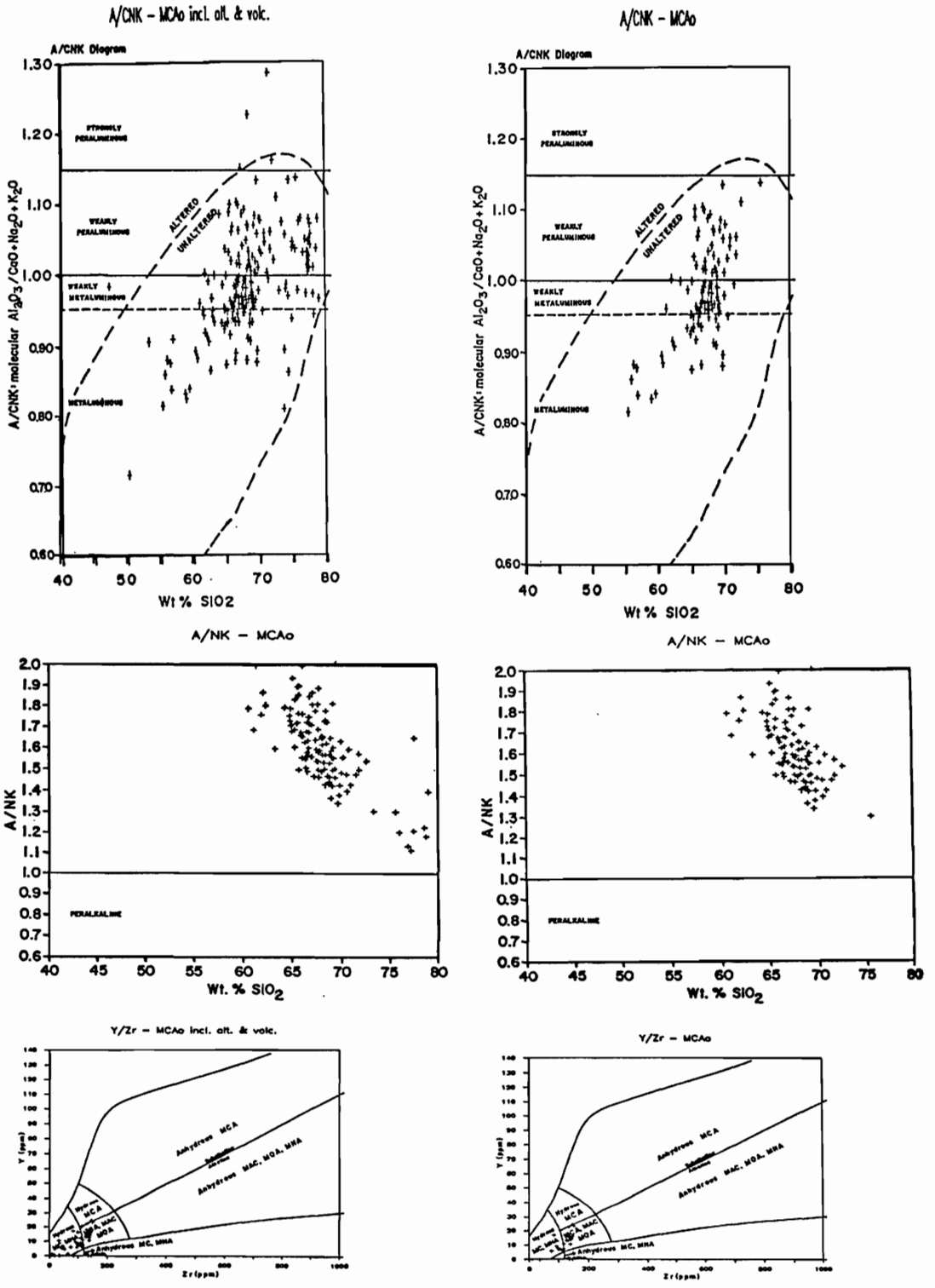

Figure C-10. A/CNK, A/NK, and Y/Zr diagrams of the metaluminous, calc-alkalic, oxidized class (left includes altered and volcanics; right is only unaltered).

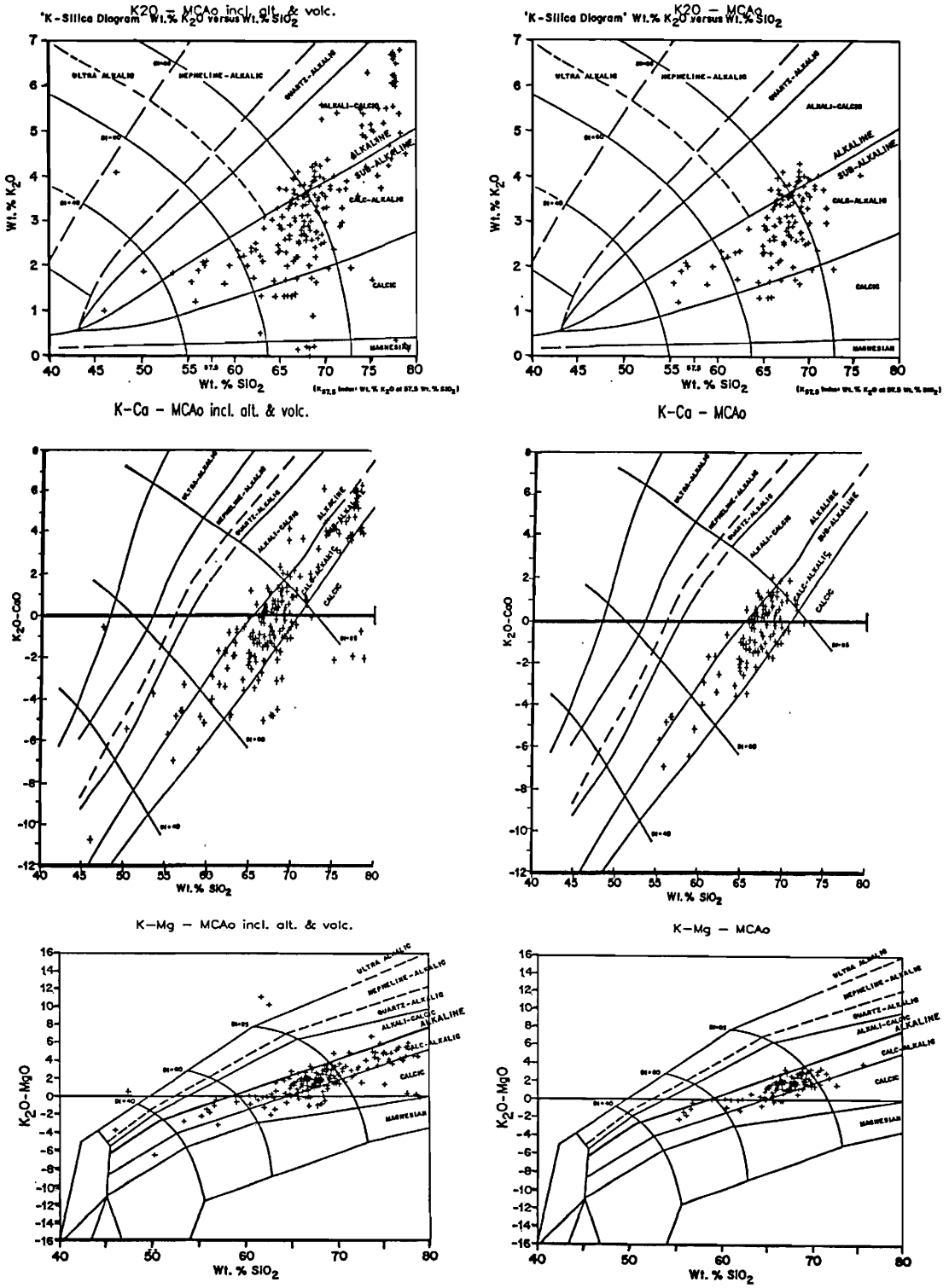

Figure C-11. Alkalinity variation diagrams of the metaluminous, calc-alkalic, oxidized class (left includes altered and volcanics; right is only unaltered).

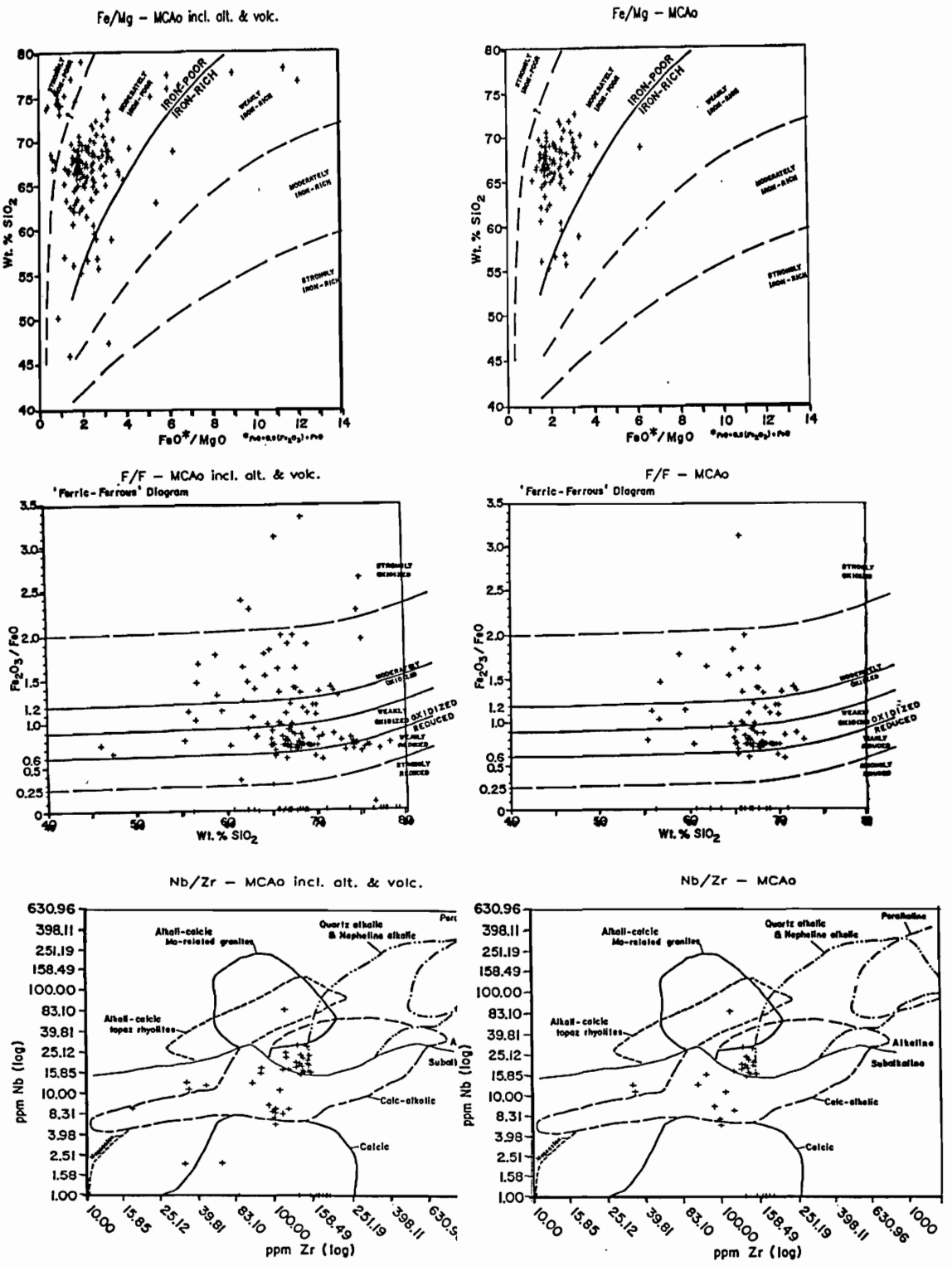

Figure C-12. Iron and Nb/Zr diagrams of the metaluminous, calc-alkalic, oxidized class (left includes altered and volcanics; right is only unaltered).

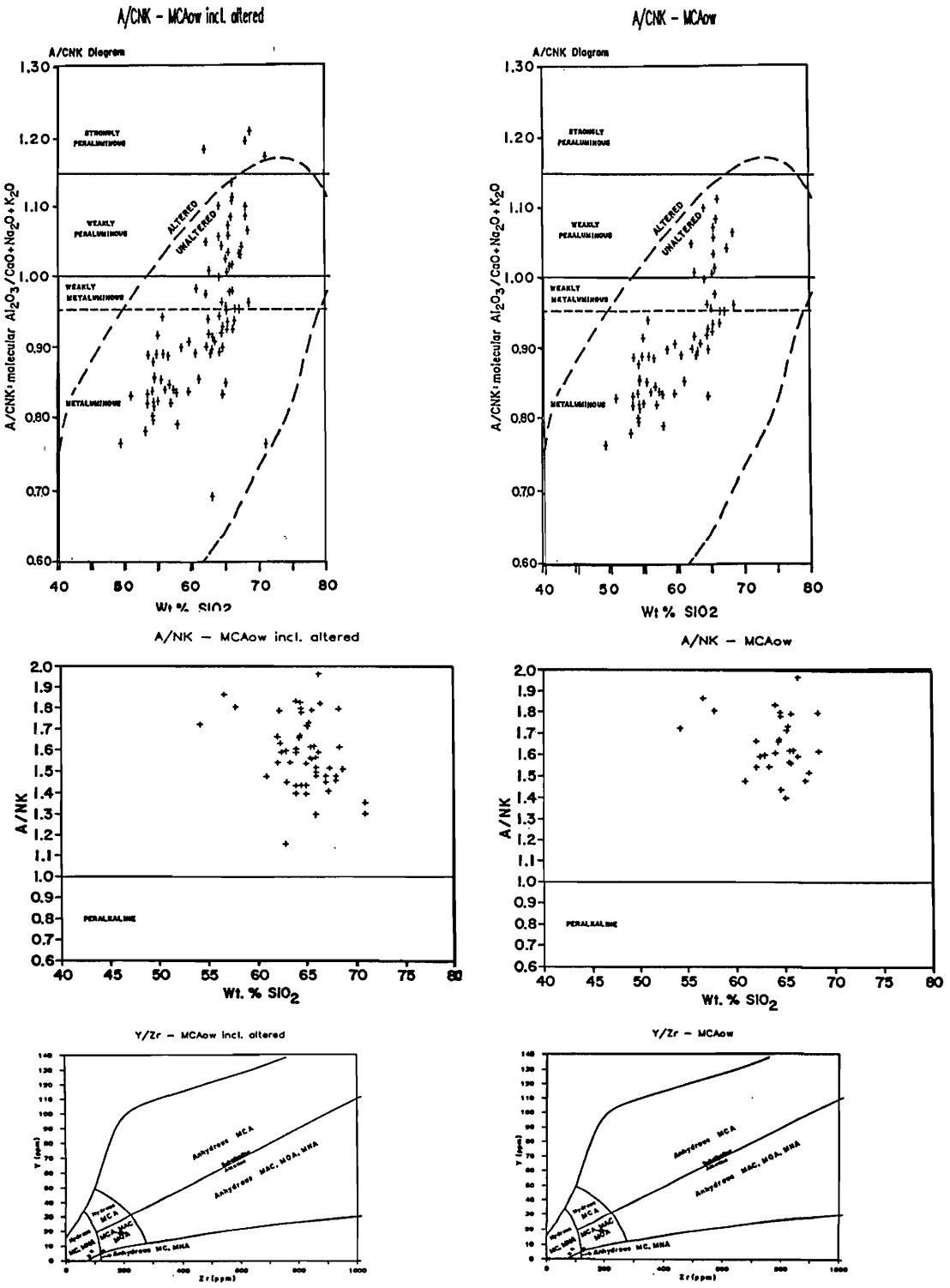

Figure C-13. A/CNK, A/NK, and Y/Zr diagrams of metaluminous, calc-alkalic, weakly oxidized (left includes altered and volcanics; right is only unaltered).

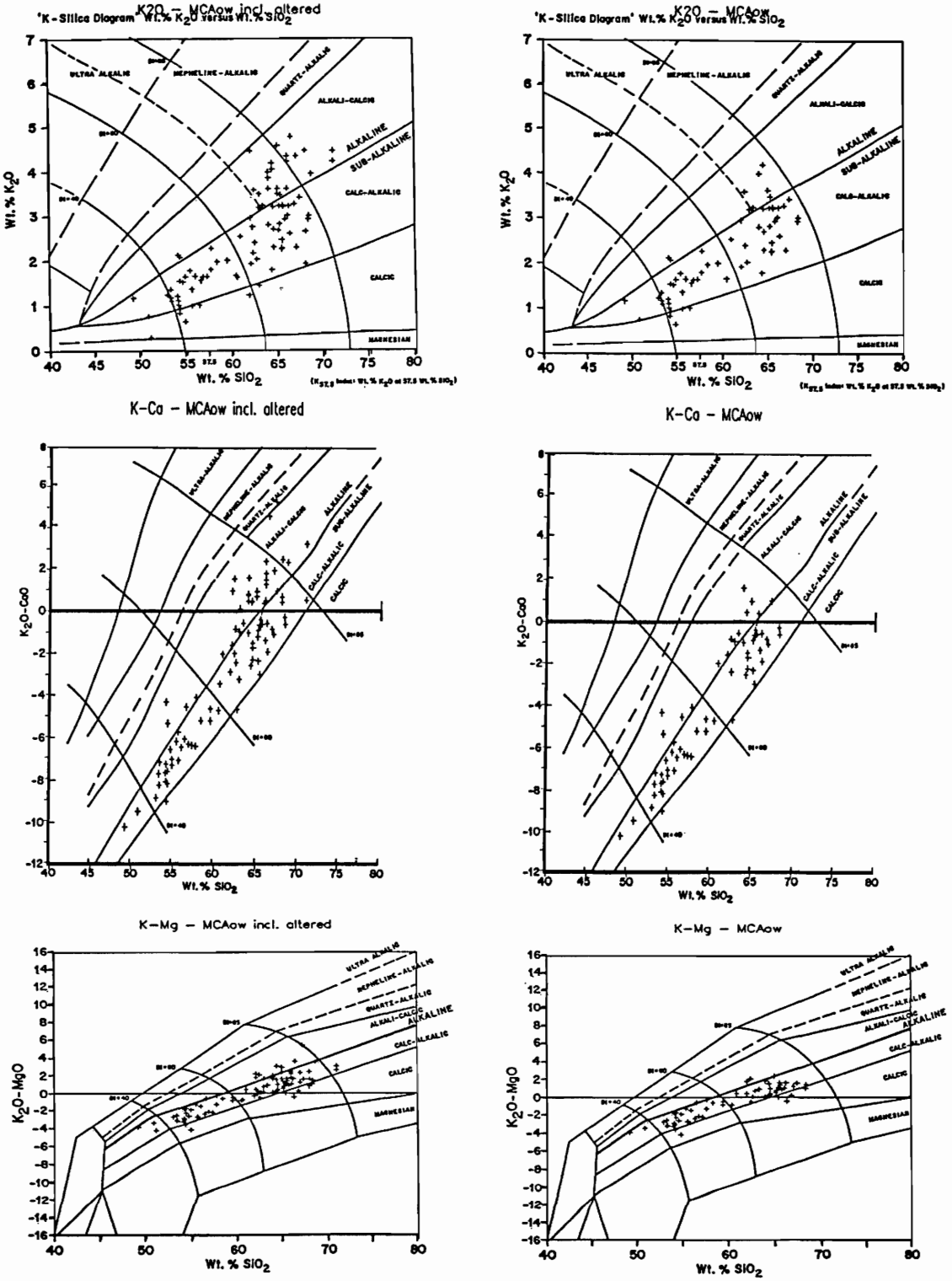

Figure C-14. Alkalinity variation diagrams of the metaluminous, calc-alkalic, weakly oxidized class (left includes altered and volcanics; right is only unaltered).

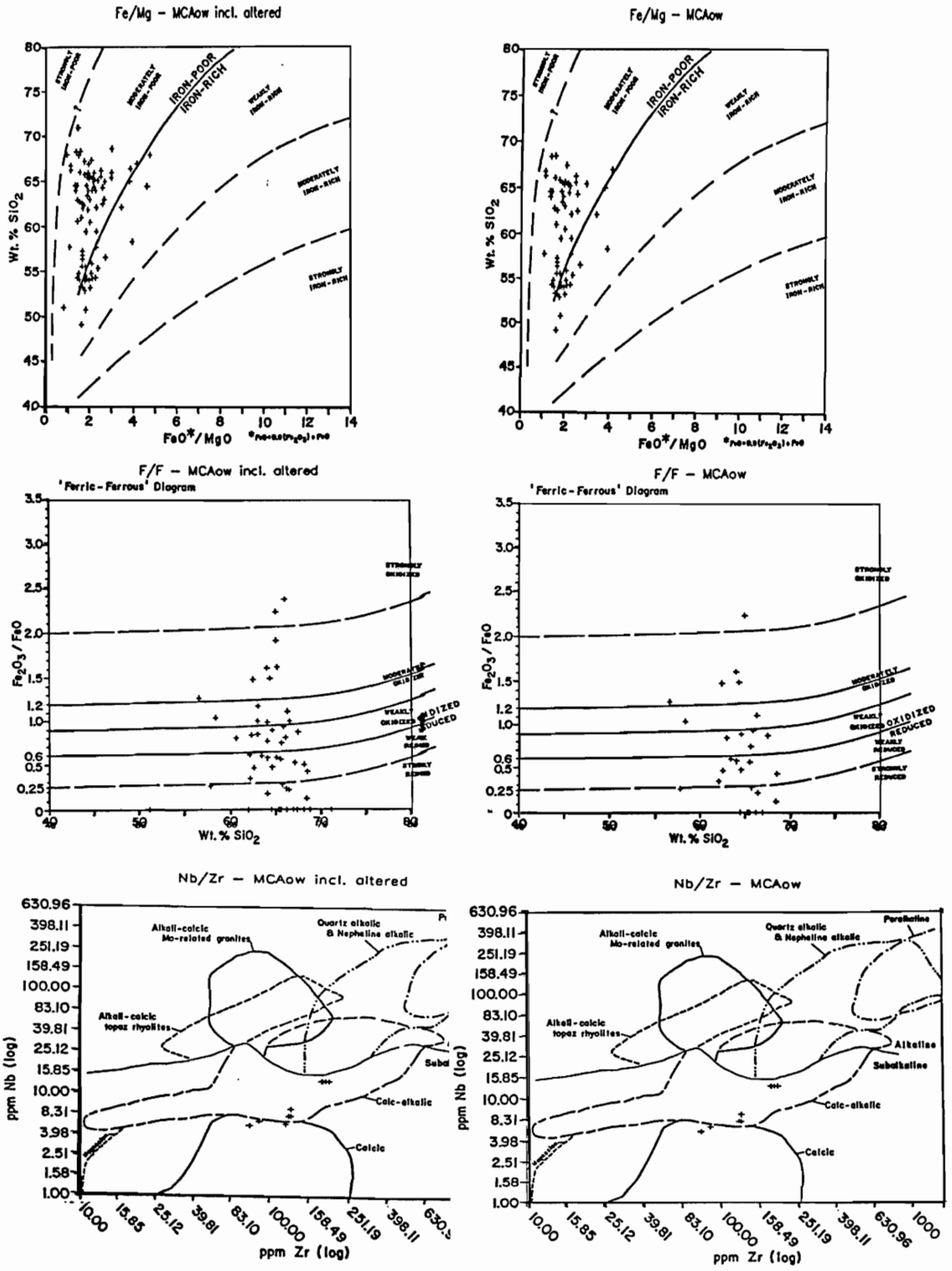

Figure C-15. Iron and Nb/Zr diagrams of the metaluminous, calc-alkalic, weakly oxidized class (left includes altered and volcanics; right is only unaltered).

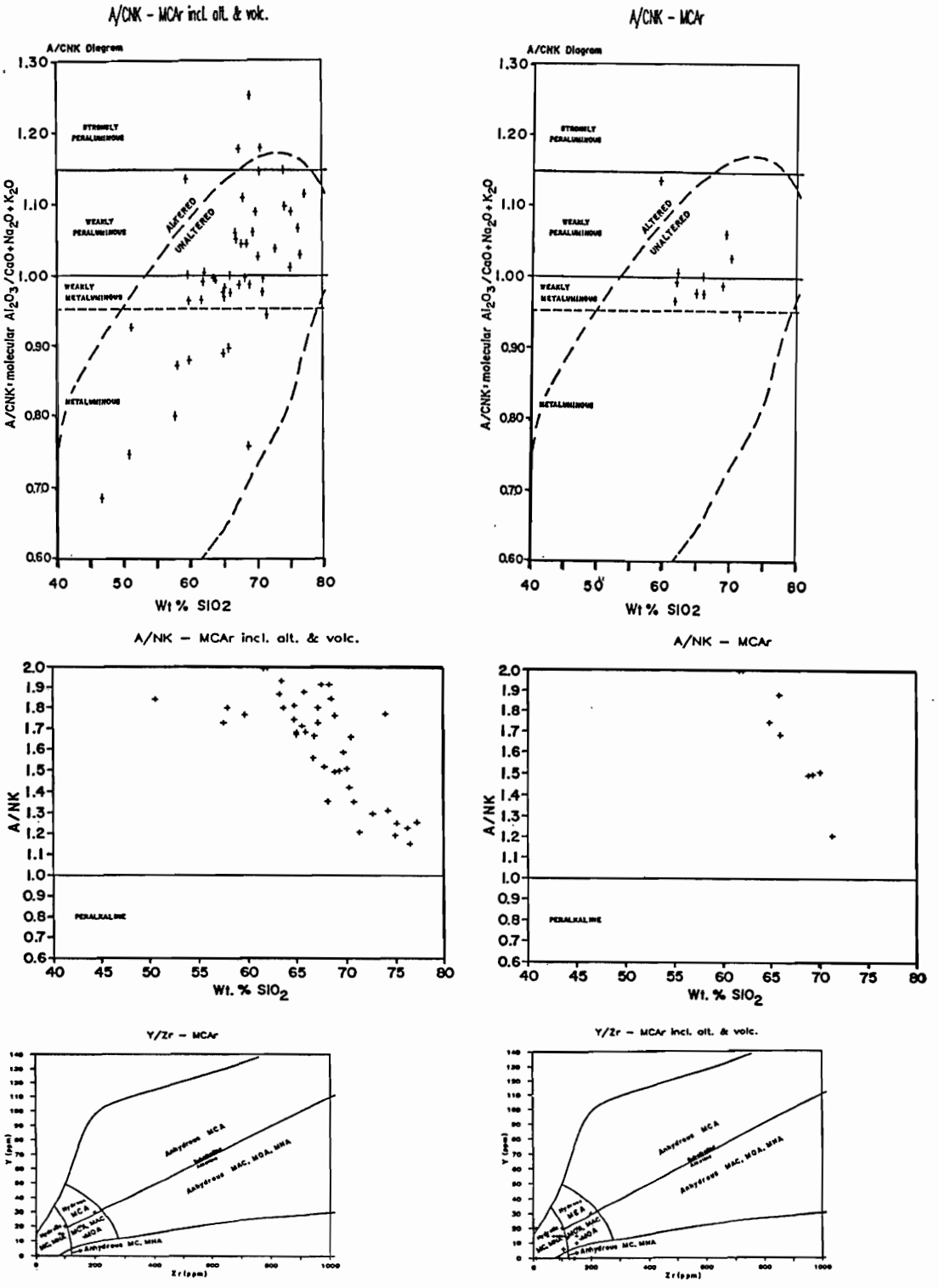

Figure C-16. A/CNK, A/NK, and Y/Zr diagrams of the metaluminous, calc-alkalic, reduced class (left includes altered and volcanics; right is only unaltered).

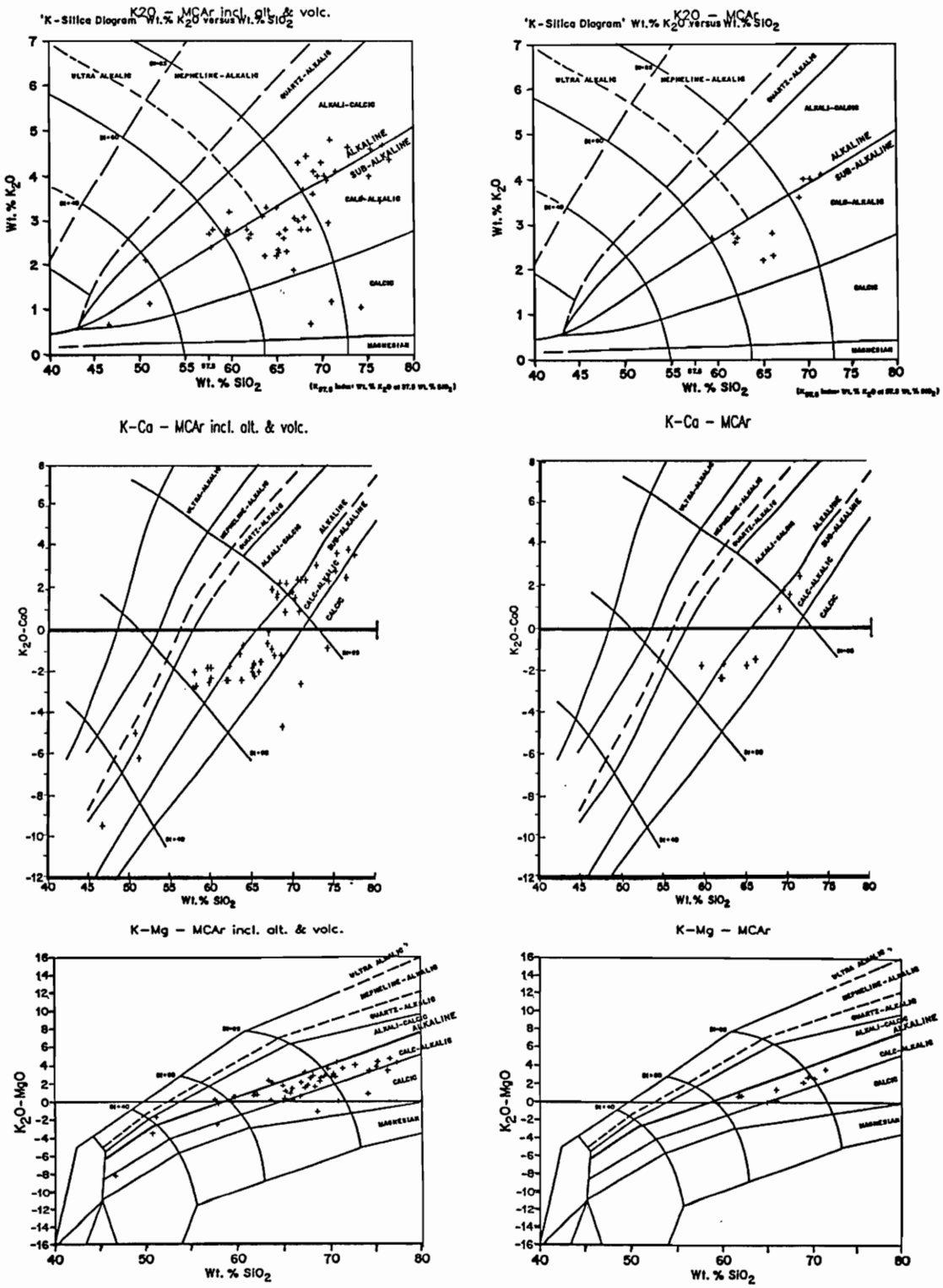

Figure C-17. Alkalinity variation diagrams of the metaluminous, calc-alkalic, reduced class (left includes altered and volcanics; right is only unaltered).

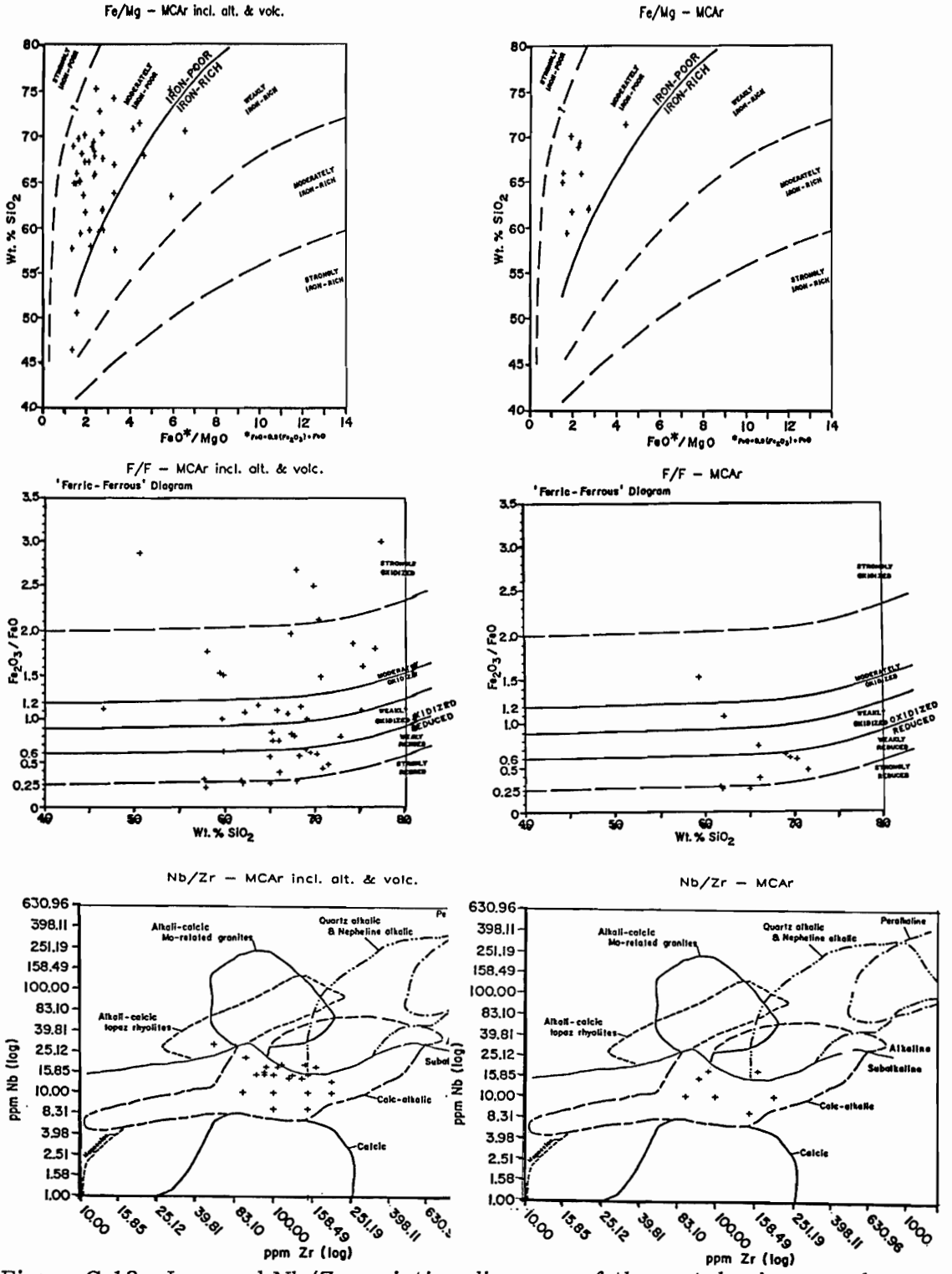

Figure C-18. Iron and Nb/Zr variation diagrams of the metaluminous, calc-alkalic, reduced class (left includes altered and volcanics; right is only unaltered).

APPENDIX D: MODAL MINERALOGY REPORTED IN LITERATURE

class	min.dist.	rock name	samp.#	ref.	qtz	orth	plag	bt	hbld	mt	ilm	ap	sphene/ti	zircon	pyrox	rutile	allanite
MACo	Park City	Alta non-porph tonalite	?	Belt, 1969	19.6	19.1	45.8	6.6	6	1.6	0	0.4	0.4	0.4	0	0	0
MACo	Park City	Alta equigran border phase	?	Belt, 1969	9.1	5.3	59.3	10.2	12.3	2.2	0	0.6	0.6	0.6	0	0	0
MACo	Park City	Alta stock	83-PC-276	John, 1991	21.5	22	44.6	9.9	0.8	0.6	0	0.05	0.5	0.05	0	0	0.05
MACo	Park City	Alta mafic-layer tonalite	?	Belt, 1969	12	12	27.4	17.5	21.5	5.6	0	1	1	1	0	0	0
MACo	Park City	Alta stock	83-PC-206	John, 1991	18.7	22	44.5	6.4	6	1.5	0	0.1	1	0.05	0	0	0.05
MACo	Park City	Clayton Peak hyper bt dior	?	Belt, 1969	3	15	45	12	0	3	0	0.05	0.05	0.05	5	0	0
MACo	Park City	Alta tonalite porph phase	?	Belt, 1969	21.2	18.5	48.6	6.3	3	1.1	0	0.3	0.3	0.3	0	0	0
MACo	Park City	Alta stock	82-PC-17	John, 1991	13.6	15.9	52.6	4.6	10.8	1.8	0	0.1	0.5	0.05	0	0	0
MACo	Park City	Alta stock	83-PC-272	John, 1991	20.8	16.8	46.9	7.5	6.4	1.5	0	0.05	0.3	0.05	0.05	0	0
MACo	Tombstone	Schieffelin granodior	T-23	Lang, 1991	12.7	26.5	42.8	5.8	0	3.8	0	0.05	0.2	0.05	8.2	0	0
MACo	Tombstone	Schieffelin granodior	T-25	Lang, 1991	11	17.2	56.4	7.6	0	3.2	0	0.4	0	0.05	4.2	0	0
MACo	Tombstone	Schieffelin granodior	T-24	Lang, 1991	14.2	28.2	43.2	3.4	0	3	0	0.05	0	0	8	0	0
MACo	Tombstone	Schieffelin granodior	T-21	Lang, 1991	17.6	24.4	45.8	4.6	5.8	1.6	0	0	0.05	0	0.2	0	0
MACo	Tombstone	Schieffelin granodior	T-22	Lang, 1991	15.1	207	47.9	5.1	5	1.8	0	0.05	0.05	0.05	0.05	0	0
MACow	Cherry Creek	Cherry Cr. bt qtz monz	ave	Morrabi	25	32	37	6	0	0.05	0	0.05	0.05	0	0	0	0
MACow	Cherry Creek	Cherry Cr qtz monz por	ave	Morrabi	25	30	30	2	0	0.05	0	0.05	0	0	0	0	0
MACow	Kinsley	Kinsley leucorhyolite	?	Steininger, 1966	41	46	9	1	1	2	0	0	0	0	0	0	0
MACow	Kinsley	Kinsley qtz monz dikes	?	Steininger, 1966	31	34	27	5	2	0.2	0	0.2	0.2	0.2	0	0	0
MACow	Kinsley	Kinsley qtz monz por	?	Steininger, 1966	24	44	25	1	5	0.2	0	0.2	0.2	0.2	0	0	0
MACow	Kinsley	Kinsley qtz monz mel dikes	?	Steininger, 1966	14	21	10	39	24	0.2	0	0.2	0.2	0.2	0	0	0
MACow	Kinsley	Kinsley mainstock	?	Steininger, 1966	15	40	36	3	5	0.2	0	0.2	0.2	0.2	0	0	0
MACr	Oruro	Oruro rhy por	est.	Campbell, 1942	25	40	20	15	0	0	0	0	0	0	0	0	0
MACr	Oruro	Oruro intrusives	?	Chace, 1948	20	25	40	15	0	0	0	0	0	0	0	0	0
MACr	Oruro	Oruro qtz monz por	est.	Campbell, 1942	20	30	35	15	0	0	0	0	0	0	0	0	0
MACr	Potosi	Kari Kari qtz lat W	Ka21f	Wolf, 1973	1.7	4.9	29.4	10.2	0	0	0	0	0	0	0	0	0
MACr	Potosi	Kari Kari qtz latite	8	Wolf, 1973	1.5	3.8	27.7	6.7	0	0	0.05	0.05	0	0.05	0	0.6	0
MACr	Potosi	Kari Kari qtz lat W	6W	Wolf, 1973	0.7	6.3	28.2	10.5	0	0	0.05	0.05	0	0.05	0	0.05	0
MACr	Potosi	Kumurana granodior	Ku107	Wolf, 1973	19.5	16.3	34.7	19.4	0	0	0	2	0	0	0	0	0
MACr	Potosi	Kari Kari qtz lat E	6E	Wolf, 1973	5.4	15.6	30.8	6.2	0	0	0.05	0.05	0	0.05	0	0.05	0
MACr	Potosi	Kumurana granodior	Ku23	Wolf, 1973	15	15.8	40.6	21.5	0	0	0	0	0	0	0	0	0
MACr	Potosi	Kari Kari qtz latite	5	Wolf, 1973	1.3	1	24.1	6.7	0	0	0.05	0.05	0.05	0.05	0	0	0
MACr	Potosi	Kari Kari qtz lat cen	Ka31	Wolf, 1973	0.4	4.3	30.2	6	0	0	0	0	0	0	0	0	0
MACr	Potosi	Kari Kari granodior	3	Wolf, 1973	17.3	16.6	37.6	20.4	3.3	0	0	0.05	0	0	0	0	0
MACr	Potosi	Kari Kari qtz lat W	Ka12	Wolf, 1973	0.7	6.3	28.3	10.6	0	0	0	0	0	0	0	0	0
MACr	Potosi	Kari Kari qtz lat cen	Ka30	Wolf, 1973	0.7	4.6	32.6	8.9	0	0	0	0	0	0	0	0	0
MACr	Potosi	Cerro Rico rhyodacite	10	Wolf, 1973	5.3	3	21.9	1.5	0	0	0	0.05	0	0.05	0	0	0
MCAo	Christmas	Christmas stock	CH-31	Lang, 1991	23	0	28.5	31.8	8.1	1.7	0	0.05	0.5	0.05	0	0	0.05
MCAo	Christmas	Christmas stock	CH-32	Lang, 1991	19.5	8.1	57.9	14.4	0	0.1	0	0.05	0	0.05	0	0	0
MCAo	Elk Mountain	Elk Mountain pluton	?	Coats, 1987	17.2	22	11.7	12	2	2	0	0.05	0.05	0.05	0	0	0
MCAo	Ray	rhyodac por	Kt	Cornwall & Krieger, 1975	0.5	10.2	54.3	0	31.1	3.9	0	0	0	0	0	0	0
MCAo	Ray	Teacup granodior	R26	Lang, 1991	25.2	19.6	46.8	7.3	0	0.3	0	0.2	0.3	0.05	0	0	0
MCAo	Ray	Teacup granodior	R25	Lang, 1991	39.5	13	42	4.5	0	0.2	0	0.05	0.05	0.05	0.8	0	0
MCAo	Ray	hrnblnd and dike alt.	R2a4	Lang, 1991	3.2	5.8	48.4	0	36.4	1	0	0.05	0	0	5.2	0	0
MCAo	Ray	Tortilla qtz dior	R11	Lang, 1991	3.9	4.8	61.9	11	0	3.4	0	2	0.05	0.05	13	0	0
MCAo	Ray	Teacup grandior alt.	R21	Lang, 1991	31.2	10 3	42.8	12.8	2.2	0.8	0	0.5	0.05	0.05	0	0	0
MCAo	Ray	Teapot Mtn por alt.	R42	Lang, 1991	18.9	0.7	66.4	6.3	7	0.7	0	0.05	0	0.05	0	0	0
MCAo	Ray	Rattler granodior	R1a4	Lang, 1991	13.6	12	56.7	0	13.3	3	0	0.4	0.8	0.05	0	0	0
MCAo	Ray	Granite Mtn por alt.	R33	Lang, 1991	36	14.9	40.5	8.3	0	0.3	0	0.05	0.05	0.05	0	0	0
MCAo	Ray	Rattler granodior	R1a3	Lang, 1991	10	10.2	59	13.6	3.2	2.2	0	0.05	0	0.05	0	0	0
MCAo	Ray	rhyodac dike	R2a7	Lang, 1991	42.7	7.4	37.1	8.8	0	0.5	0	0.05	0	0.05	0	0	0
MCAo	Ray	Rattler granodior	R1a2	Lang, 1991	39.9	0	48.5	6.4	3.7	1	0	0.1	0.5	0.05	0	0	0.05
MCAo	Ray	Teacup granodior	Ttc	Cornwall & Krieger, 1975	31.5	17.6	45.3	4.6	0.1	0.5	0	0.1	0.4	0.05	0	0	0.05
MCAo	Ray	Rattler granodior	R1a1	Lang, 1991	23.2	12.6	51.9	8.1	3	0.6	0	0.2	0.3	0.05	0	0	0.05

class	min.dist.	rock name	samp.#	ref.	qtz	orth	plag	bt	hbld	mt	ilm	ap	sphene/ti	zircon	pyrox	rutile	allanite
MCAo	Ray	Teapot Mtn por alt.	R41	Lang, 1991	14.3	8.7	67	9.7	0	0.3	0	0.05	0	0.05	0	0	0
MCAo	Ray	Tortilla qtz dior	R14	Lang, 1991	15.1	3.1	48	15.8	14.4	2.3	0	0.7	0.3	0.3	0	0	0
MCAo	Ray	rhyodac por	Tr2	Cornwall & Krieger, 1975	1.3	2.7	61	0	29.3	1.6	0	0.1	0	0	2.7	0	0
MCAo	Ray	Granite Mtn por alt.	R32	Lang, 1991	17.4	29.9	46	6.2	0	0.5	0	0.05	0.05	0.05	0	0	0
MCAo	Ray	rhyodacite plug	R51	Lang, 1991	17	51	29.7	1.5	0.3	0.05	0	0.05	0	0	0	0	0
MCAo	Ray	Tortilla qtz dior	R13	Lang, 1991	3.9	9.2	54.2	12.4	0	4.8	0	0.3	0.05	0	15.2	0	0
MCAo	Red Mountain	Patagonia granodior	2	Graybeal, 1972	22.9	21.7	42.1	2.7	2.8	1.2	0	0.05	0.1	0.05	0	0	0
MCAo	Red Mountain	Patagonia granodior por	5	Graybeal, 1972	20.4	20.6	39.7	6	6.5	3.8	0	0.05	0.05	0	0	0	0
MCAo	Red Mountain	Patagonia bt granodior	JD-4	Dewhurst, 1976, p. 51	20	20	35	25	3	0.05	0	0	0.05	0	0	0	0
MCAo	Red Mountain	Patagonia granodior	8	Graybeal, 1972	29	17.4	40	1.8	4.9	1.2	0	0.05	0.8	0.05	0	0	0
MCAo	Red Mountain	Patagonia granodior por	16	Graybeal, 1972	25.6	19.9	41.2	4.4	4.6	4.1	0	0.05	0	0	0	0	0
MCAo	Red Mountain	Patagonia granodior	7	Graybeal, 1972	24.2	21.9	43	4.3	3.9	0.9	0	0.05	0.05	0.05	0	0	0
MCAo	Red Mountain	Patagonia granodior por	14	Graybeal, 1972	22.2	18.8	38.1	9.4	7	2.2	0	0.05	0	0	0	0	0
MCAo	Red Mountain	Patagonia granodior	6	Graybeal, 1972	24	22.3	42	4	2.2	0.6	0	0.05	0.7	0.05	0	0	0
MCAo	Red Mountain	Patagonia granodior por	10	Graybeal, 1972	25	22.1	38.3	1.2	3	1	0	0.05	0.2	0	0	0	0
MCAo	Red Mountain	Patagonia granodior	4	Graybeal, 1972	27	20.8	38.2	6.9	0.05	1.4	0	0.05	0.05	0.05	0	0	0
MCAo	Red Mountain	Patagonia granodior por	17	Graybeal, 1972	30.8	22.3	40.3	1.6	2.6	1.7	0	0.05	0	0	0	0	0
MCAo	Red Mountain	Patagonia granodior	3	Graybeal, 1972	24.6	19.4	42.8	6.6	0.05	0.6	0	0.05	0.05	0.05	0	0	0
MCAo	Red Mountain	Patagonia granodior por	13	Graybeal, 1972	24	23.4	40.8	4.4	4.8	0.6	0	0.05	0.2	0	0	0	0
MCAo	Red Mountain	Patagonia granodior por	15	Graybeal, 1972	27.2	21.8	38.2	6	4.8	1.6	0	0.05		0	0	0	0
MCAo	Red Mountain	Patagonia granodior por	9	Graybeal, 1972	24.2	22	41.8	2	5.4	1.2	0	0.05	0.6	0	0	0	0
MCAo	Red Mountain	Patagonia granodior	1	Graybeal, 1972	18.9	17	53.5	3.3	2.4	0.6	0	0.05	0.4	0.05	0	0	0
MCAo	Sierrita	Ruby Star granodior	T-6	Cooper, 1960	24	19	48	5.5	2.3	0.6	0	0.1	0.5	0.05	0	0	0
MCAo	Sierrita	Ruby Star granodior	T-7	Cooper, 1960	23	19	47	6.3	2.4	0.8	0	0.3	0.4	0.05	0	0	0
MCAo	Sierrita	Ruby Star granodior	1	Manske, 1980	20.3	17.5	53.7	8	0	0.5	0	0	0	0	0	0	0
MCAo	Sierrita	Ruby Star granodior	2	Manske, 1980	44	6.4	46.7	1.7	3.7	0	0	0	1.2	0	0	0	0
MCAo	Sierrita	Ruby Star grndior alt.	RS-MR-5	Anthony, 1986	19.6	24.2	48	5.4	0.2	0.2	0	0.05	2	0.2	0	0	0
MCAo	Sierrita	Ruby Star grndior	RS-MR3-6	Anthony, 1986	22.6	21.4	49	6	0	0.8	0	0.05	0.2	0.05	0	0	0
MCAo	Sierrita	Ruby Star granodior	T-5	Cooper, 1960	23	22	50	3.3	0	0.8	0	0.3	0.3	0.05	0	0	0
MCAo	Sierrita	Ruby Star grndior	RS-MR-8	Anthony, 1986	15.2	9.8	65.6	6.2	1	1	0	0.2	0.6	0.2	0	0	0.05
MCAo	Sierrita	Ruby Star granodior	T-9	Cooper, 1960	37	10	43	5.1	0	0.5	0	0.2	0.8	0.05	0	0	0
MCAo	Sierrita	Ruby Star grndior	RS-MR3-5	Anthony, 1986	24.4	21	43.2	7.8	0.8	1.6	0	0.4	0.6	0.05	0	0	0.05
MCAo	Sierrita	Ruby Star aph qtz monz por	ave of 11	Smith, 1975	25.7	27	41.6	4.8	0	0	0	0.05	0	0.05	0	0	0
MCAo	Sierrita	Ruby Star grndior	RS-MR3-8	Anthony, 1986	27.8	20.4	45	5.2	0	0.4	0	0.2	0.6	0.05	0	0.05	0.05
MCAo	Sierrita	Ruby Star granodior	ave of 3	Lovering, 1970	25.1	20.6	45	5.9	2	0.8	0	0.02	0.4	0.2	0	0	0
MCAo	Sierrita	Ruby Star grndior alt.	QL-MR-7	Anthony, 1986	4	0	22	6	0	0.05	0	0.05	0.05	0.05	0	0	0
MCAo	Sierrita	Ruby Star granodior	1	Cooper, 1960	12	28	39	11	0	0	0	0	0.1	0.05	0	0	0
MCAo	Sierrita	Ruby Star grndior	RS-MR-6	Anthony, 1986	25.2	34.4	39.8	0.05	0	0.4	0	0.05	0	0.05	0	0.05	0
MCAo	Sierrita	Ruby Star granodior	T-10	Cooper, 1960	32	18	45	3.4	0	0.7	0	0.1	0.3	0	0	0	0
MCAo	Sierrita	Ruby Star grndior	RS-MR-4	Anthony, 1986	18.2	15	59.8	4.2	0	0.2	0	0.4	2.2	0.05	0	0.05	0.05
MCAo	Sierrita	Ruby Star aph qtz monz por	ave of 3	Lovering, 1970	27.4	35.4	33.5	2.8	0	0.8	0	0	0	0	0	0	0
MCAo	Sierrita	Ruby Star grndior por core	RS-M	Hess, 1986	4.6	46.8	38.4	9	0.05	0.05	0	0.8	0	0.4	0	0	0
MCAo	Sierrita	Ruby Star grndior S rim	RS-SM-1	Hess, 1986	26.2	17.8	445.4	8.8	0	1.4	0	0.05	0.4	0.05	0	0	0
MCAo	Sierrita	Ruby Star apl qtz monz	1	Lovering, 1970	26.4	30.1	38.3	3.7	0	1	0	0.05	0.1	0.05	0	0	0
MCAo	Sierrita	Ruby Star grndior S rim	RS-SM-10	Hess, 1986	15.8	22	53.2	7	0	0.4	0	0.2	0	0.05	0	0	0
MCAo	Valley Copper	Bethlehem dacite por	?	White et al. 1957	30	4	63	0.01	3	0.05	0	0.05	0.05	0	0	0	0
MCAo	Valley Copper	Valley granodior por	?	Osatenko & Jones,	23	13	63	1	0	0.05	0	0	0	0	0	0	0
MCAo	Valley Copper	Guichon qtz dior	?	White et al. 1957	20	15	50	5	10	0.05	0	0.05	0.05	0.05	0	0	0
MCAo	Valley Copper	Valley qtz dior por	?	Osatenko & Jones,	28	1	70	0	0	1	0	0	0	0	0	0	0
MCAo	Valley Copper	Bethsaida grandior	?	White et al. 1957	15	5	75	5	0.01	0	0	0	0	0	0	0	0
MCAo	Valley Copper	gran. W. of Iona	?	White et al. 1957	30	60	7	3	0	0.05	0	0	0.05	0	0	0	0
MCAo	Valley Copper	Bethlehem qtz dior	?	White et al. 1957	15	10	65	5	5	0.05	0	0	0.05	0	0	0	0
MCAo	Valley Copper	Valley aplite dikes	?	Osatenko & Jones,	44	45	10	1	0	0	0	0	0	0	0	0	0
MCAo	Valley Cu	Chataway variety	K63-204-IV	Northcote, 1969	22.12	11.65	52.89	6.43	4.98	1.81	0	0.07	0.05	0	0	0	0
MCAo	Valley Cu	Witches Brook phase	K64-17b	Northcote, 1969	41.53	25.44	30.26	2.02	0	0.75	0	0	0	0	0	0	0
MCAo	Valley Cu	Witches Brook phase	K63-222	Northcote, 1969	36.61	29.42	31	2.41	0	0.56	0	0	0	0	0	0	0
MCAo	Valley Cu	Guichon variety	K63-223-IIa	Northcote, 1969	18	16.03	47.79	5.06	10.68	0.24	0	0.02	0.4	0.03	1.74	0	0

class	min.dist.	rock name	samp.#	ref.	qtz	orth	plag	bt	hbld	mt	ilm	ap	sphene/ti	zircon	pyrox	rutile	allanite
MCAo	Valley Cu	Bethsaida phase	K64-64	Northcote, 1969	35.22	5.88	46.21	11.82	0.42	0.44	0	0.02	0	0	0	0	0
MCAo	Valley Cu	Guichon variety	K64-50aV	Northcote, 1969	18.75	11.42	52.32	5.92	9.68	2.38	0	0	0.03	0.03	0.47	0	0
MCAo	Valley Cu	Bethsaida phase	K63-115a	Northcote, 1969	16.38	13.93	62.16	4.49	0.55	2.05	0	0.21	0.2	0.05	0	0	0
MCAo	Valley Cu	Guichon variety	K63-136-I	Northcote, 1969	16.32	2.71	52.66	16.95	1.49	1.94	0	0	0	0	7.94	0	0
MCAo	Valley Cu	Bethsaida phase	K63-238a	Northcote, 1969	22.08	14.55	57.97	3.62	0.14	1.24	0	0.18	0.23	0	0	0	0
MCAo	Valley Cu	Chataway variety	K64-116a	Northcote, 1969	23.3	6.9	55.69	6.26	6.02	1.42	0	0.18	0.07	0.1	0	0	0
MCAo	Valley Cu	Bethsaida phase	K63-239	Northcote, 1969	45.71	5.28	37.62	10.17	0.81	0.25	0	0	0.1	0.05	0	0	0
MCAo	Valley Cu	Guichon variety	K63-223	Northcote, 1969	20.68	12.29	45.75	9.54	8.85	1.86	0	0.06	65	0.03	0.31	0	0
MCAo	Valley Cu	Bethsaida phase	K63-231	Northcote, 1969	30.14	10.76	52.07	4.82	0.29	1.26	0	0.3	0.33	0.03	0	0	0
MCAo	Valley Cu	Chataway variety	K63-185	Northcote, 1969	16.06	21.98	48.32	2.91	7.95	2.51	0	0.06	0.2	0	0	0	0
MCAo	Valley Cu	Bethsaida phase	K63-187	Northcote, 1969	26.81	12.95	56.67	2.71	0.18	0.56	0	0.07	0.05	0	0	0	0
MCAo	Valley Cu	Chataway variety	K63-34	Northcote, 1969	28.69	15.17	43.62	2.72	6.96	2.59	0	0	0.25	0	0	0	0
MCAo	Valley Cu	Guichon granodiorite	1	Wood, 1968	14.9	9.4	60.1	5	8.6	1	0	0.05	0.05	0.05	0.6	0.05	0
MCAo	Valley Cu	LeRoy granodiorite	K64-47a-III	Northcote, 1969	27.1	2.48	58.64	3.69	6.77	1.13	0	0.03	0.16	0	0	0	0
MCAo	Valley Cu	Guichon granodiorite	2	Briskey & Bellamy	17.2	9.6	48.7	7.9	5	1.7	0	0.3	0.3	0.3	0.6	0.3	0
MCAo	Valley Cu	LeRoy granodiorite	K63-37	Northcote, 1969	28.01	19.37	42.91	4.22	3.83	1.21	0	0.17	0.24	0.03	0	0	0
MCAo	Valley Cu	Bethlehem granodiorite	5	Wood, 1968	19	6.7	63.4	1.3	7.8	0.2	0	0.1	0.1	0.1	0	0.1	0
MCAo	Valley Cu	LeRoy granodiorite	K64-101	Northcote, 1969	25.59	14.86	45.8	5.95	5.62	1.69	0	0	0.49	0	0	0	0
MCAo	Valley Cu	Bethlehem granodiorite	6	Briskey & Bellamy	15.9	9.7	53.4	1.4	10	0.7	0	0.4	0.4	0.4	0	0.4	0
MCAo	Valley Cu	Gump Lake phase	K64-89	Northcote, 1969	32.64	11.98	48.72	4.81	0.49	1.26	0	0.05	0.05	0	0	0	0
MCAo	Valley Cu	Black Lake phase	GB-3	Jones, 1974	8	0.6	62	11.4	10.1	2.1	0	0.5	0.2	0.05	4.3	0	0
MCAo	Valley Cu	Bethlehem phase	K63-192	Northcote, 1969	19.7	10.82	58.95	0.51	7.05	2.94	0	0.02	0	0	0	0	0
MCAo	Valley Cu	Hybrid phase	GB-4	Jones, 1974	0.4	0	66.8	0	29.1	0.5	0	0	0	0	0	0	0
MCAo	Valley Cu	Bethlehem phase	K63-188a	Northcote, 1969	23.83	8.12	56.53	5.37	2.67	2.8	0	0.17	0.51	0	0	0	0
MCAo	Valley Cu	Chataway phase	GB-7	Jones, 1974	23.2	12.9	52.1	2	6.8	1.6	0	0	0.6	0	0	0	0
MCAo	Valley Cu	Bethlehem phase	K64-60a	Northcote, 1969	19.57	8.67	63.04	1.55	3.76	2.84	0	0.23	0.34	0	0	0	0
MCAo	Valley Cu	Guichon phase	GB-6	Jones, 1974	20.9	12.2	57.4	0.5	7.5	1	0	0	0.2	0	0	0	0
MCAo	Valley Cu	Bethlehem phase	K64-186a	Northcote, 1969	25.06	7.82	53.76	5.12	5.83	2.33	0	0.04	0	0.03	0	0	0
MCAo	Valley Cu	Bethlehem phase	GB-2	Jones, 1974	18.2	6.2	69.4	0.5	3.8	0.9	0	0.05	1.2	0.05	0	0	0
MCAo	Valley Cu	Witches Brook phase	K63-171	Northcote, 1969	25.74	10.44	52.11	5.18	3.78	1.99	0	0.03	0.31	0.05	0.03	0	0
MCAo	Valley Cu	Skeena phase	GB-1	Jones, 1974	19.3	4.9	65.5	3.2	5.2	1.5	0	0.3	0.05	0.01	0	0	0
MCAo	Valley Cu	Witches Brook phase	K64-111	Northcote, 1969	26.72	15.89	46.13	5.18	4.71	1.06	0	0	0.3	0	0	0	0
MCAo	Valley Cu	Bethsaida phase	GB-5	Jones, 1974	30.1	9.4	58.5	0.4	0.7	0.2	0	0.2	0.1	0	0	0	0
MCAo	Valley Cu	Witches Brook phase	K63-84	Northcote, 1969	29.09	18.87	40.79	5.04	5.57	1.1	0	0	0.23	0	0.3	0	0
MCAo	Valley Cu	Bethsaida phase	BS-2	Jones, 1974	28.5	9.6	58.1	1.8	0.05	1	0	0.05	0.05	0	0	0	0
MCAo	Valley Cu	Witches Brook phase	K64-17	Northcote, 1969	43.19	26.2	28.08	1.86	0	0.64	0	0	0	0	0.04	0	0
MCAo	Valley Cu	Witches Brook phase	K64-105-I	Northcote, 1969	27.92	20.05	39.76	3.34	5.33	1.38	0	0.03	2.13	0	0	0	0
MCAo	Valley Cu	Witches Brook phase	K64-102	Northcote, 1969	26.86	18.2	43.03	5.5	3.81	1.77	0	0.02	0.77	0	0	0	0
MCAo	Valley Cu	Guichon variety	K63-33b-I	Northcote, 1969	17.55	8.24	48.36	10.41	10.05	4.08	0	0	0.24	0	1.06	0	0
MCAo	Valley Cu	Witches Brook phase	K64-203	Northcote, 1969	27.84	12.14	50.93	5.99	2.23	0.65	0	0	0.18	0.03	0	0	0
MCAo	Valley Cu	Chataway variety	K64-48-I	Northcote, 1969	23.65	7.13	54.18	7.49	5.49	1.78	0	0.02	0.28	0	0	0	0
MCAo	Valley Cu	Witches Brook phase	K63-28a	Northcote, 1969	25.5	24.28	39.28	4.88	3.47	1.71	0	0	0.11	0.08	0.68	0	0
MCAo	Valley Cu	Chataway variety	K63-204-IV	Northcote, 1969	17.47	8.82	62.2	5.37	4.57	1.45	0	0.02	0.09	0	0	0	0
MCAo	Valley Cu	Guichon variety	K63-223-II	Northcote, 1969	19.8	14.32	45.98	8.09	8.47	1.59	0	0.08	0.47	0.03	1.17	0	0
MCAo	Valley Cu	LeRoy granodiorite	K63-202-V	Northcote, 1969	23.9	9.02	56.19	3.54	4.97	2.15	0	0.02	0.2	0	0	0	0
MCAo	Valley Cu	Guichon variety	K63-223-IIb	Northcote, 1969	18.55	15.47	47.96	4.22	11.36	1.51	0	0.02	0.45	0.2	0.26	0	0
MCAo	Valley Cu	Gump Lake phase	K64-98-I	Northcote, 1969	38.87	16.08	36.97	5.67	0.9	1.26	0	0.1	0	0.16	0	0	0
MCAo	Valley Cu	Gump Lake phase	K64-91	Northcote, 1969	29.11	11.02	49.95	6.67	0.95	2.62	0	0.18	0	0	0	0	0
MCAo	Valley Cu	Guichon hybrid	K64-10	Northcote, 1969	7.27	0.13	70.29	2.99	5.66	2.35	0	0.06	0.52	0.03	10.67	0	0
MCAo	Valley Cu	Bethlehem phase	K63-189a-II	Northcote, 1969	19.26	15.51	58.92	1.98	2.66	1.24	0	0	0.43	0	0	0	0
MCAo	Valley Cu	Bethlehem phase	K63-115	Northcote, 1969	18.26	12.7	58.42	1.88	5.85	2	0	0.14	0.65	0.1	0	0	0
MCAo	Valley Cu	Guichon hybrid	K64-10-I	Northcote, 1969	19.32	0.07	55.23	6.67	11.76	3.36	0	0.17	0	0	3.42	0	0
MCAo	Valley Cu	Guichon variety	K63-196	Northcote, 1969	11.7	0	58.93	13.22	4.61	4.02	0	0	0.79	0	6.73	0	0
MCAo	Valley Cu	Guichon hybrid	K63-13	Northcote, 1969	19.45	4.39	53.75	8.3	11.18	1.37	0	0.02	0.08	0.03	1.43	0	0
MCAo	Valley Cu	LeRoy granodiorite	K64-54	Northcote, 1969	25.61	17.53	43.69	5.8	4.77	2.46	0	0.02	0.11	0	0	0	0
MCAo	Valley Cu	Guichon hybrid	K64-156a	Northcote, 1969	20.2	10.09	49.86	6.49	0	2.47	0	0.07	0	0	10.83	0	0
MCAo	Valley Cu	Bethlehem phase	K64-61	Northcote, 1969	20.01	5.98	63.47	5.73	2.48	2.05	0	0.07	0.2	0	0	0	0

class	min.dist.	rock name	samp.#	ref.	qtz	orth	plag	bt	hbld	mt	ilm	ap	sphene/ti	zircon	pyrox	rutile	allanite
MCAo	Valley Cu	Guichon hybrid	K64-15	Northcote, 1969	23.27	2.49	51.4	10.5	9.55	1.98	0	0	0	0	0.82	0	0
MCAo	Valley Cu	Chataway variety	K63-44	Northcote, 1969	13.15	4.89	63.49	5.15	11.31	1.29	0	0.23	0.5	0	0	0	0
MCAo	Valley Cu	Guichon hybrid	K63-234a	Northcote, 1969	10.35	0.12	54.04	8.66	22.02	4.7	0	0.09	0	0	0.04	0	0
MCAo	Valley Cu	LeRoy granodiorite	K63-220	Northcote, 1969	17.75	9.32	57.23	1.81	12.39	1.39	0	0.02	0.09	0	0	0	0
MCAo	Valley Cu	Guichon hybrid	K64-15a	Northcote, 1969	25.12	4.95	48.55	7.66	12.1	1.34	0	0	0.09	0.12	0.08	0	0
MCAow	Dos Pobres	Dos Pobres por	SF-33	Lang, 1991	22.2	12	52.5	11.8	0	1.5	0	0.05	0	0.05	0	0	0
MCAow	Dos Pobres	Dos Pobres por	SF-32	Lang, 1991	17.9	18.5	45.8	15.4	0	2.1	0	0.2	0	0.05	0	0	0
MCAr	Osgood Mts	Osgood Mts granodior	75H53	Hotz & Willden, 1964	26	14	52	6	0.5	1	0.05	0	0	0	0	0	0
MCAr	Osgood Mts	Osgood Mts granodior	54W12	Hotz & Willden, 1964	25	7	56	8	3	0.5	0.05	0	0	0	0	0	0
MCAr	Osgood Mts	Osgood Mts granodior	H-1-55	Hotz & Willden, 1964	16	9	59	15	0.5	0	0.05	0	0	0	0	0	0
MCAr	Osgood Mts	Osgood Mts granodior	54W13	Hotz & Willden, 1964	23	11	55	7	2	1	0.05	0	0	0	0	0	0
MCAr	Osgood Mts	Osgood Mts granodior	H-2-55	Hotz & Willden, 1964	22	18	49	4	7	0	0.05	0	0	0	0	0	0
MCAr	Osgood Mts	Osgood Mts granodior	54W48	Hotz & Willden, 1964	24	11	51	12	5	1	0.05	0	0	0	0	0	0
MCAr	Osgood Mts	Osgood Mts granodior	54W16	Hotz & Willden, 1964	29	12	48	8	1	0.5	0.05	0	0	0	0	0	0
MCAr	Osgood Mts	Osgood Mts granodior	H-34-55	Hotz & Willden, 1964	21	12	54	12	1	0	0.05	0	0	0	0	0	0
MCAr	Osgood Mts	Osgood Mts granodior	H-5-55	Hotz & Willden, 1964	27	12	49	13	0.05	0	0.05	0	0	0	0	0	0
MCAr	Osgood Mts	Osgood Mts granodior	53W81	Hotz & Willden, 1964	25	16	49	6	1	1	0.05	0	0	0	0	0	0

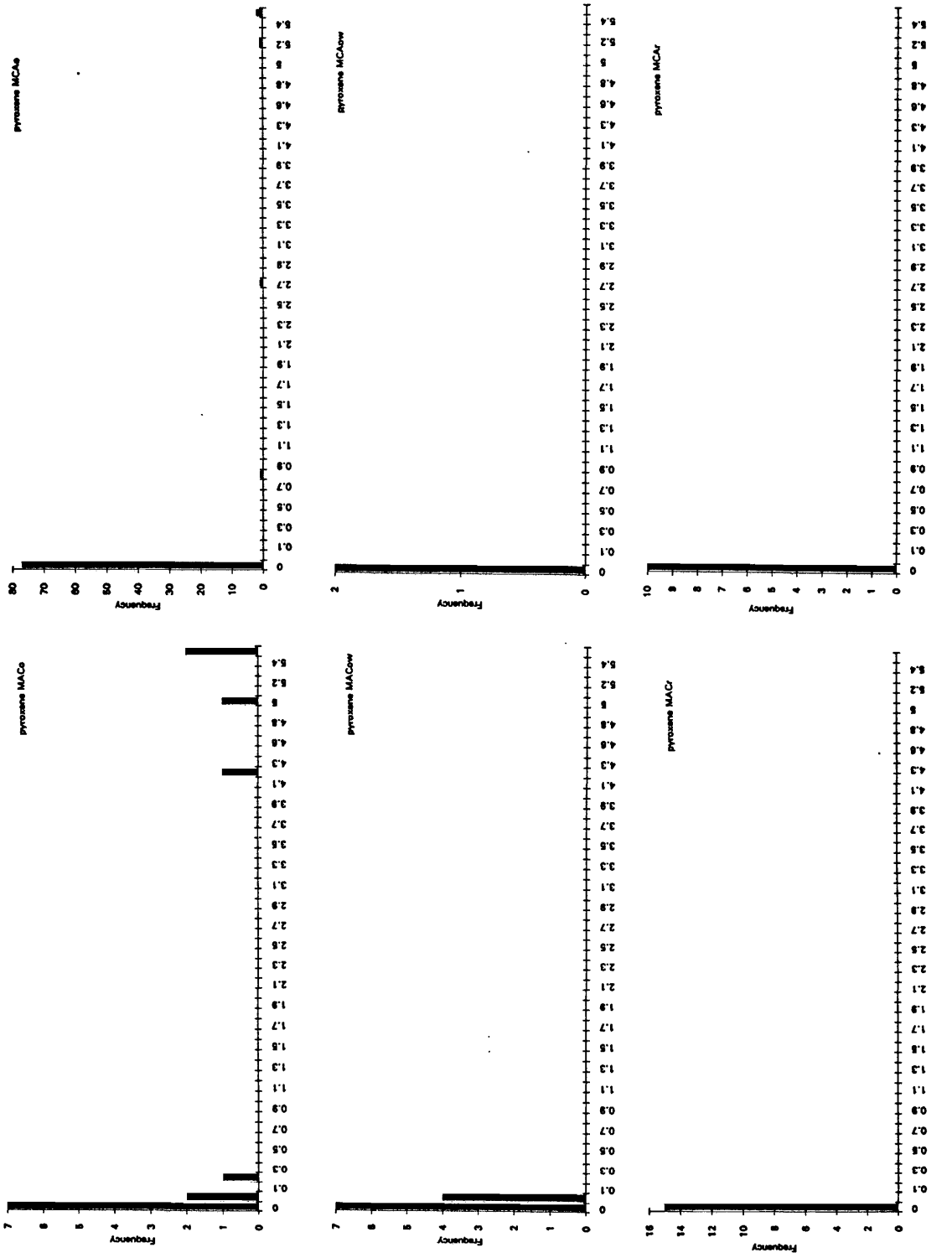

Figure D-1. Histograms of pyroxene in percent on the x-axis (MAC=alkali-calcic, MCA=calc-alkalic, o=oxidized, ow=weakly oxidized, and r=reduced).

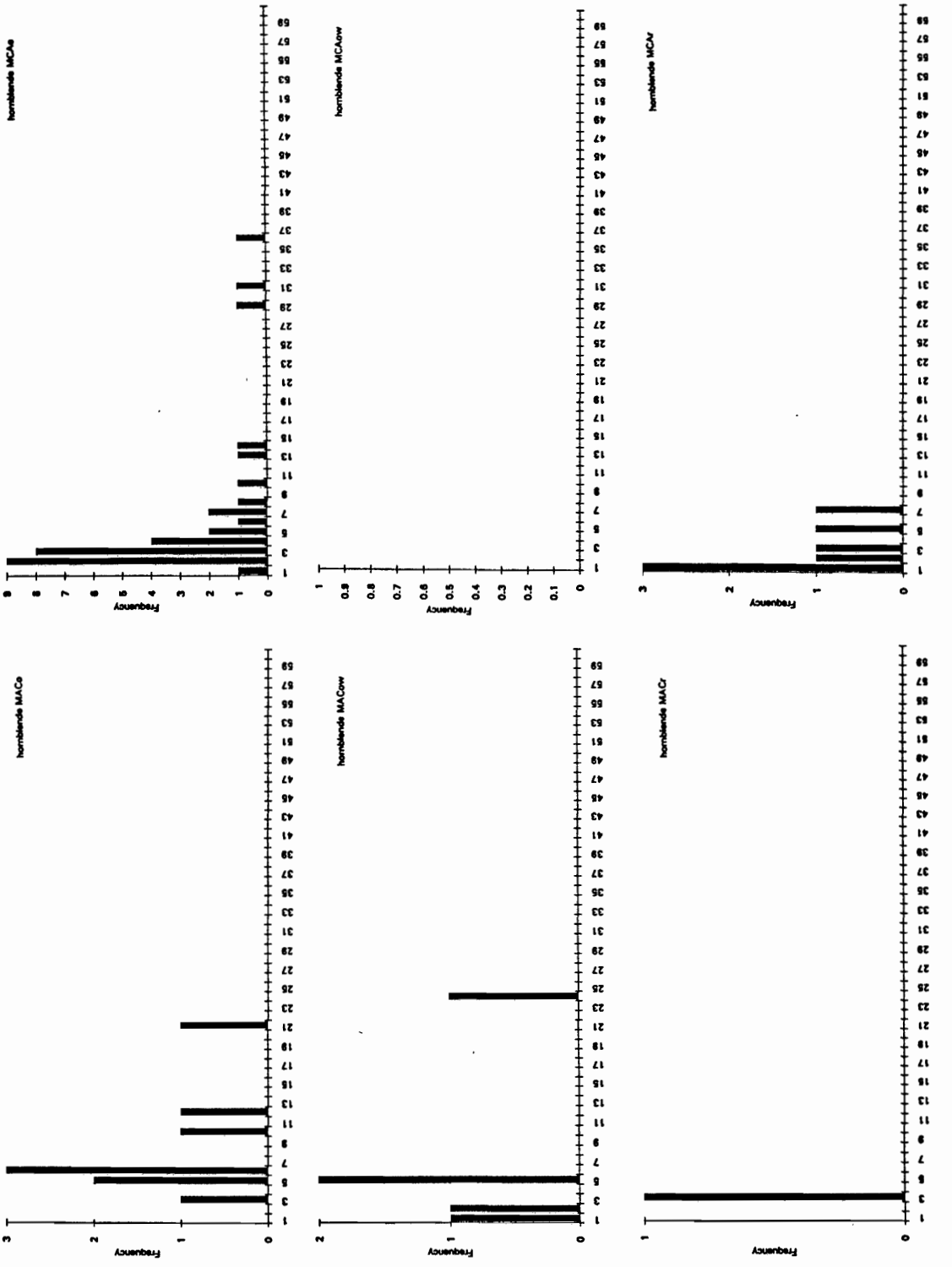

Figure D-2. Histograms of hornblende in percent on the x-axis (MAC=alkali-calcic, MCA=calc-alkalic, o=oxidized, ow=weakly oxidized, and r=reduced).

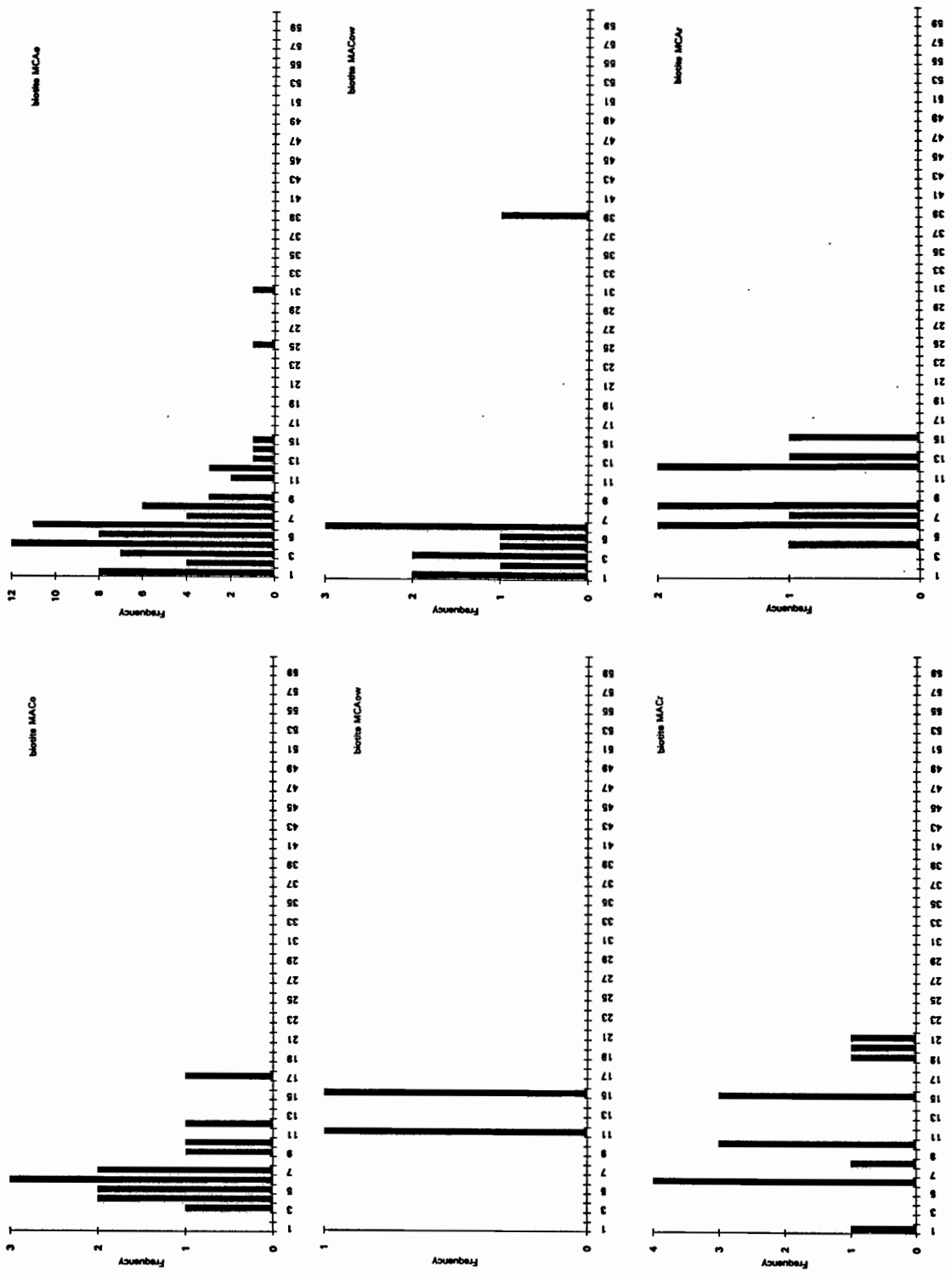

Figure D-3. Histograms of biotite in percent on the x-axis (MAC=alkali-calcic, MCA=calc-alkalic, o=oxidized, ow=weakly oxidized, and r=reduced).

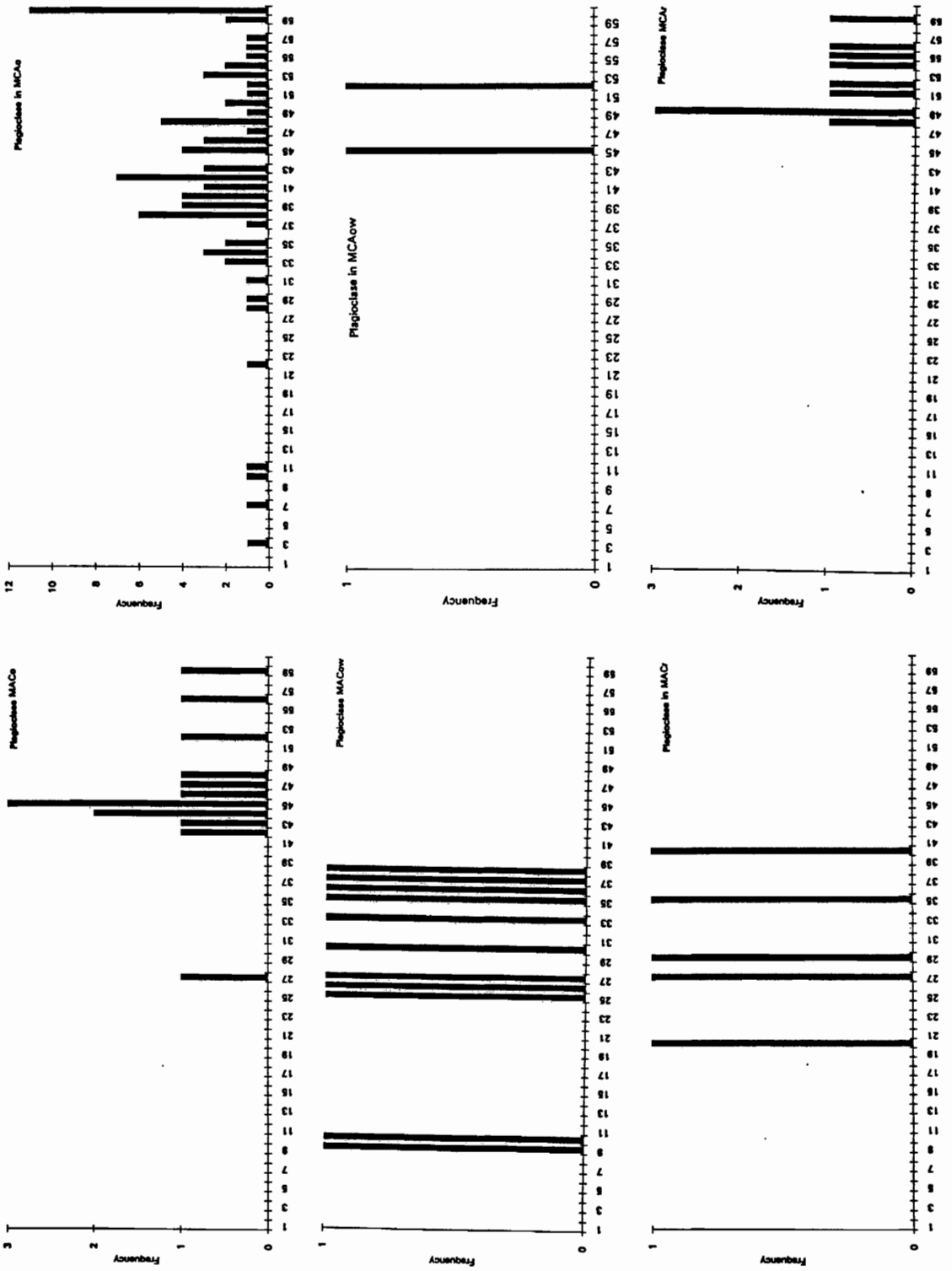

Figure D-4. Histograms of plagioclase in percent on the x-axis (MAC=alkali-calcic, MCA=calc-alkalic, o=oxidized, ow=weakly oxidized, and r=reduced).

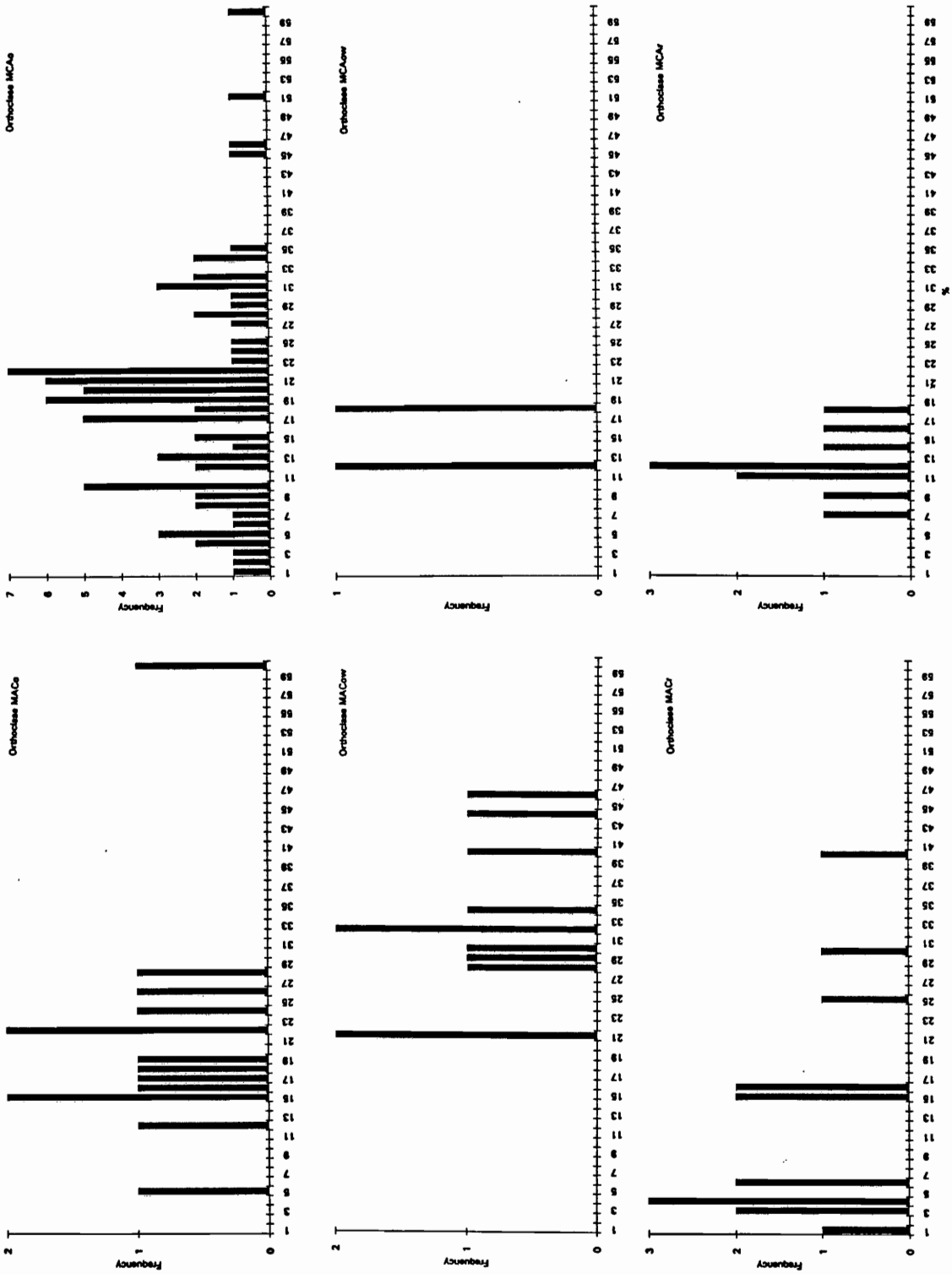

Figure D-5. Histograms of orthoclase in percent on the x-axis (MAC=alkali-calcic, MCA=calc-alkalic, o=oxidized, ow=weakly oxidized, and r=reduced).

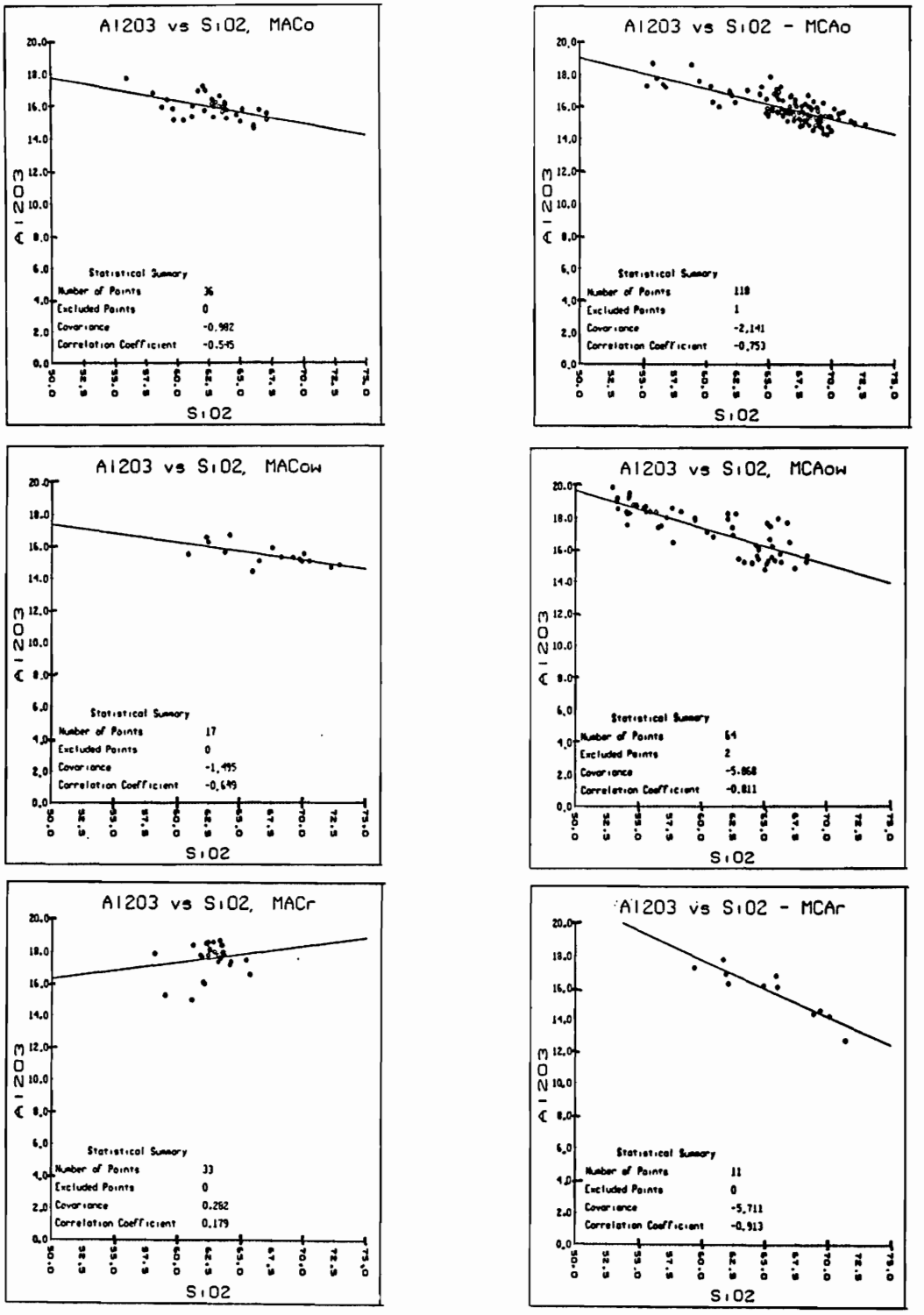

Figure D-6. Linear bands of magma series classes plotted on Al_2O_3 vs. SiO_2 variation diagrams (M= Metaluminous, AC= alkali-calcic, CA= calc-alkalic, o= oxidized, ow= weakly oxidized, r= reduced).

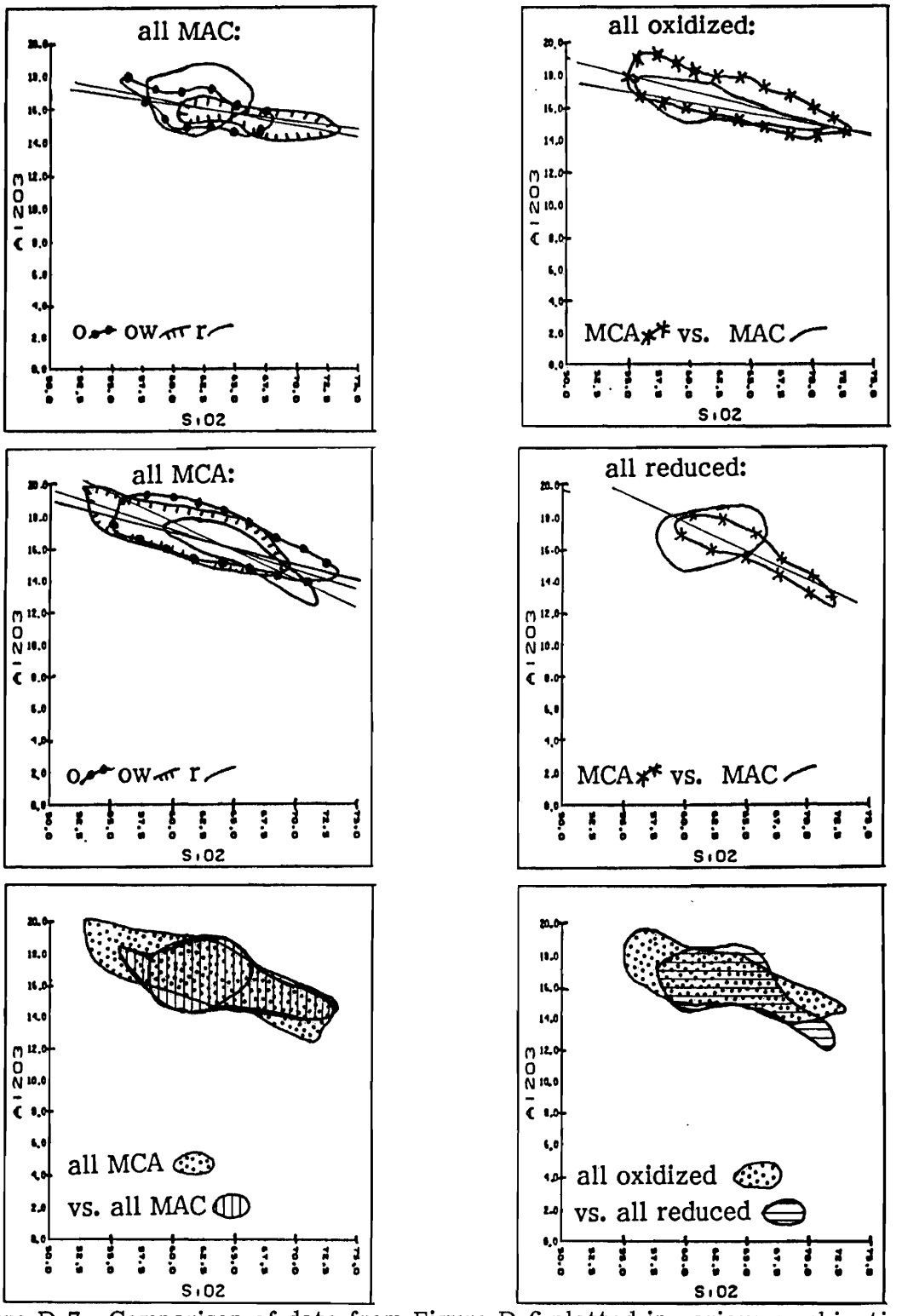

Figure D-7. Comparison of data from Figure D-6 plotted in various combinations on Al_2O_3 vs. SiO_2 variation diagrams (M= Metaluminous, AC= alkali-calcic, CA=calc-alkalic, o=oxidized, ow=weakly oxidized, r=reduced).

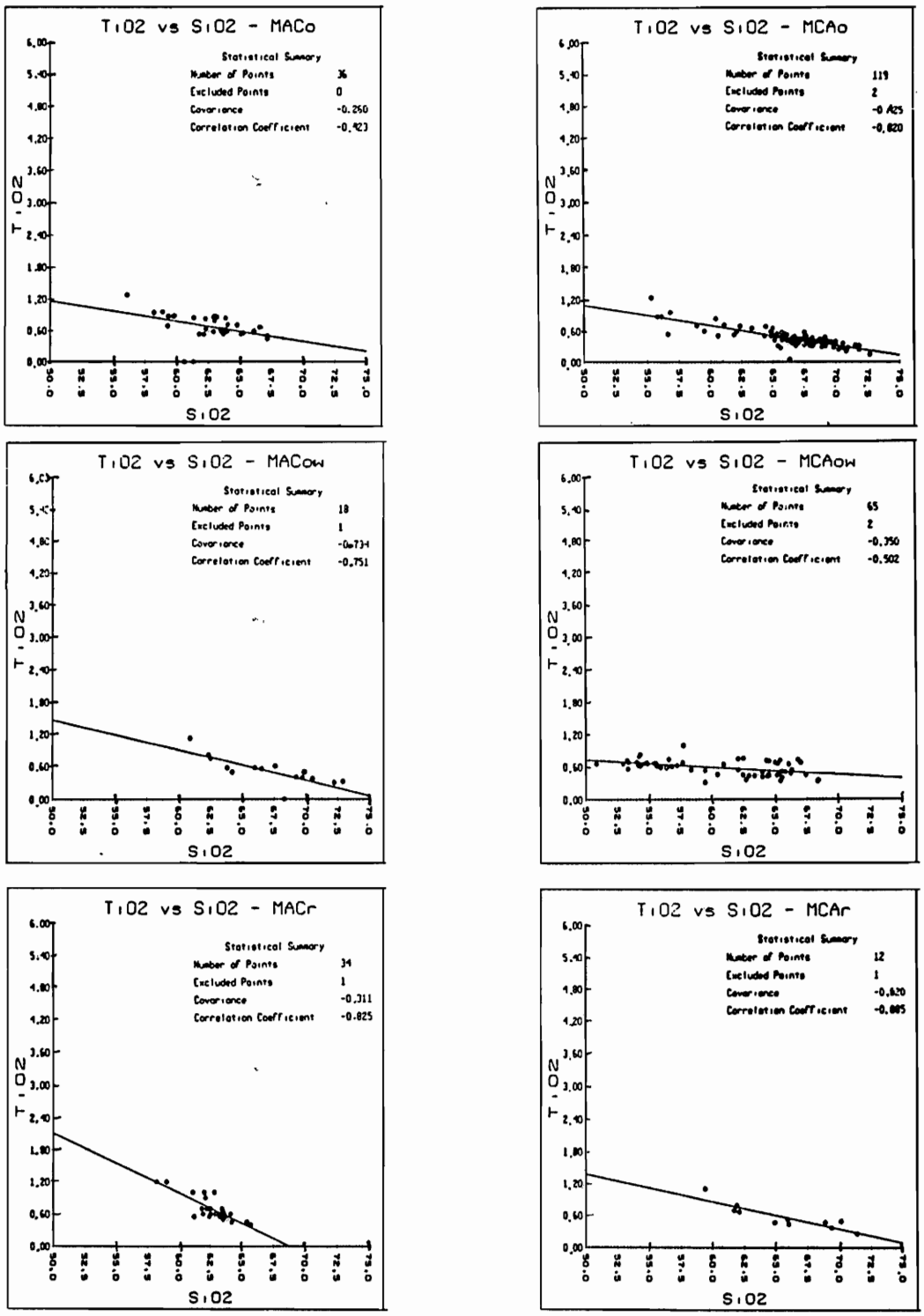

Figure D-8. Linear bands of petrochemical classes plotted on TiO_2 vs. SiO_2 variation diagrams showing no changes (M= Metaluminous, AC= alkali-calcic, CA= calc-alkalic, o= oxidized, ow= weakly oxidized, r=reduced).

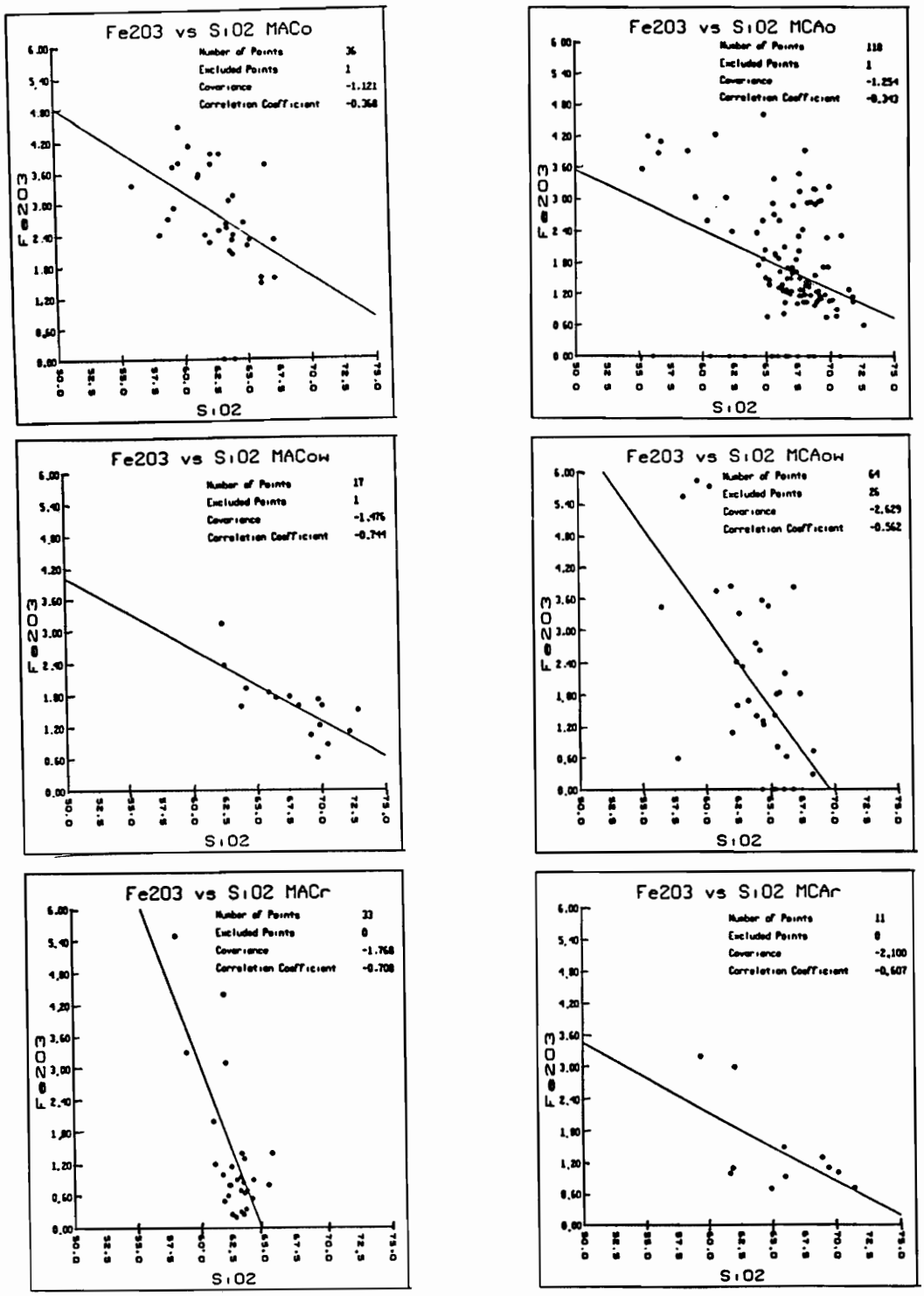

Figure D-9. Whole-rock chemistry of petrochemical classes plotted on Fe_2O_3 vs. SiO_2 variation diagrams (M= Metaluminous, AC= alkali-calcic, CA= calc-alkalic, o= oxidized, ow= weakly oxidized, r=reduced).

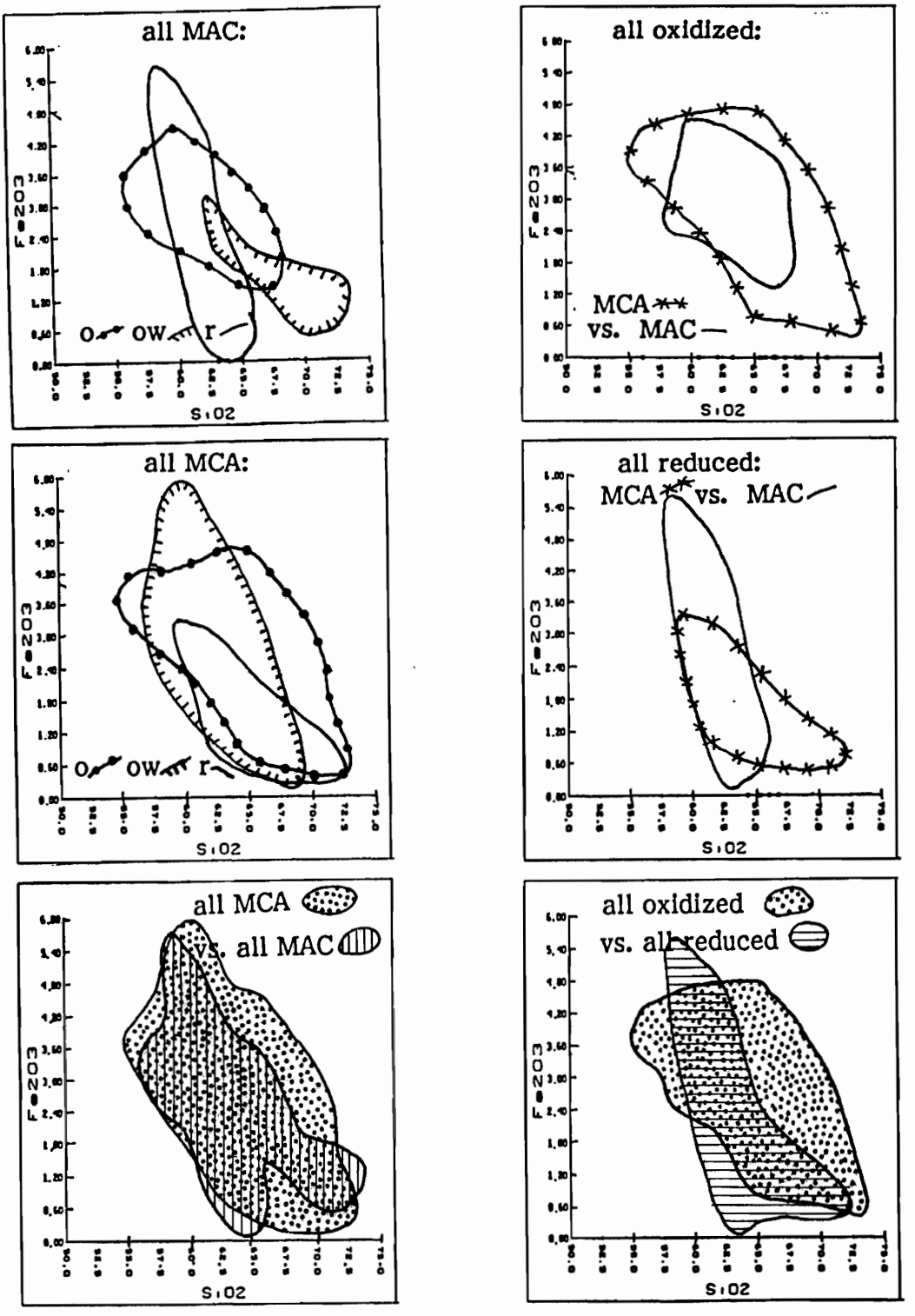

Figure D-10. Comparison of data from Figure D-9 plotted in various combinations on Fe_2O_3 vs. SiO_2 variation diagrams (M= Metaluminous, AC= alkali-calcic, CA=calc-alkalic, o=oxidized, ow=weakly oxidized, r=reduced).

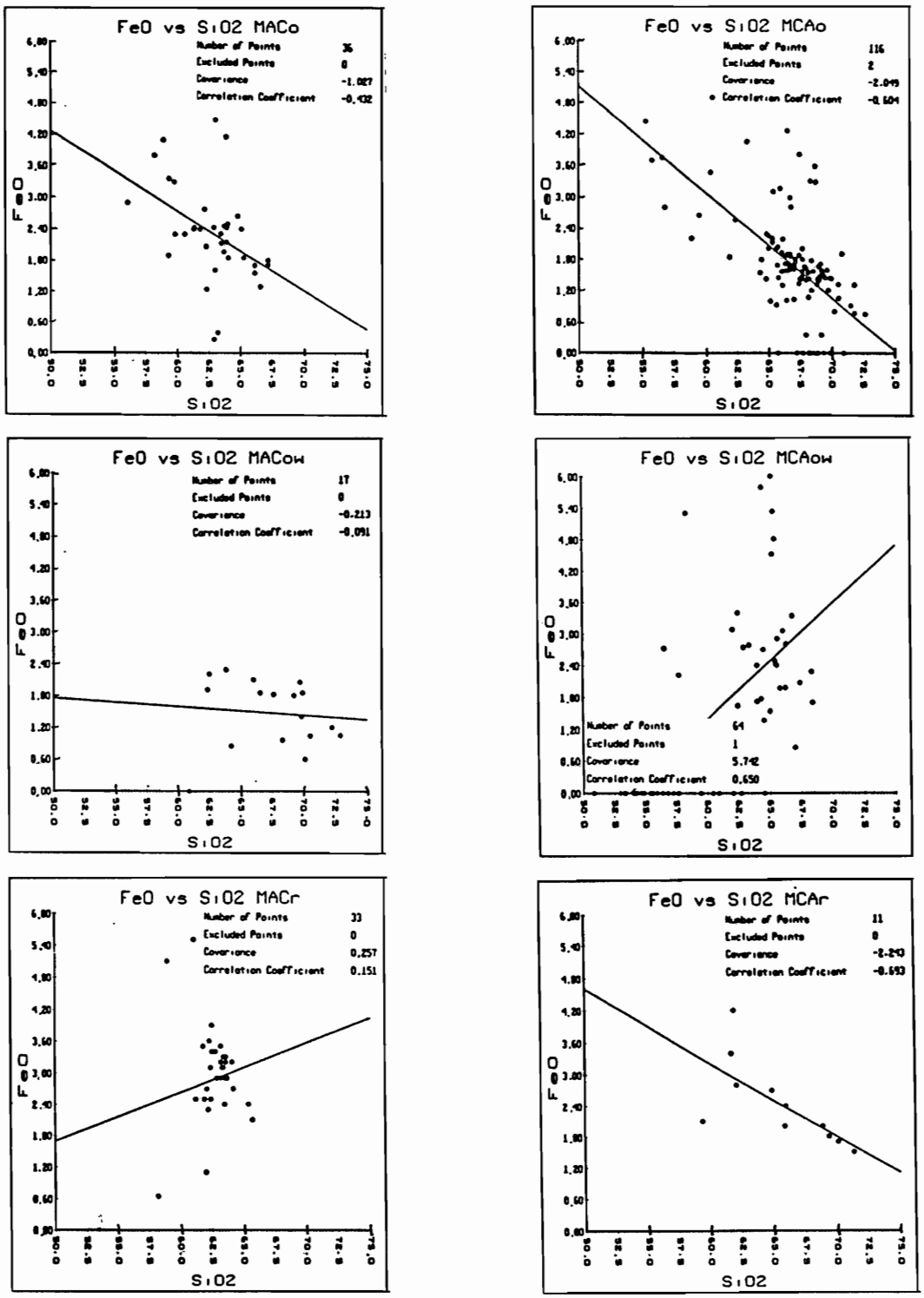

Figure D-11. Whole-rock chemistry of petrochemical classes plotted on FeO vs. SiO_2 variation diagrams (M= Metaluminous, AC= alkali-calcic, CA= calc-alkalic, o= oxidized, ow= weakly oxidized, r=reduced).

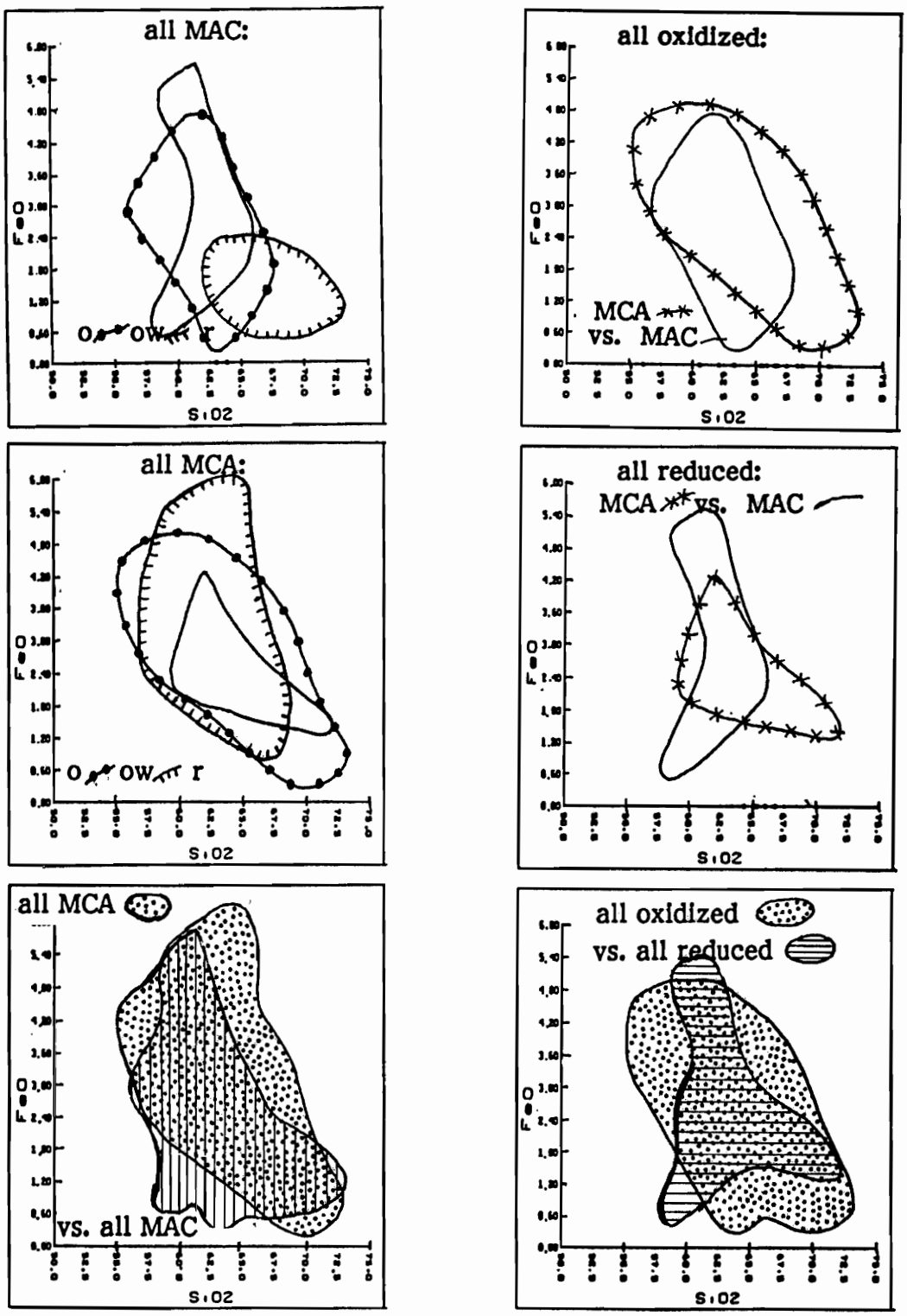

Figure D-12. Comparison of data from Figure D-11 plotted in various combinations on FeO vs. SiO_2 variation diagrams (M= Metaluminous, AC= alkali-calcic, CA=calc-alkalic, o=oxidized, ow=weakly oxidized, r=reduced).

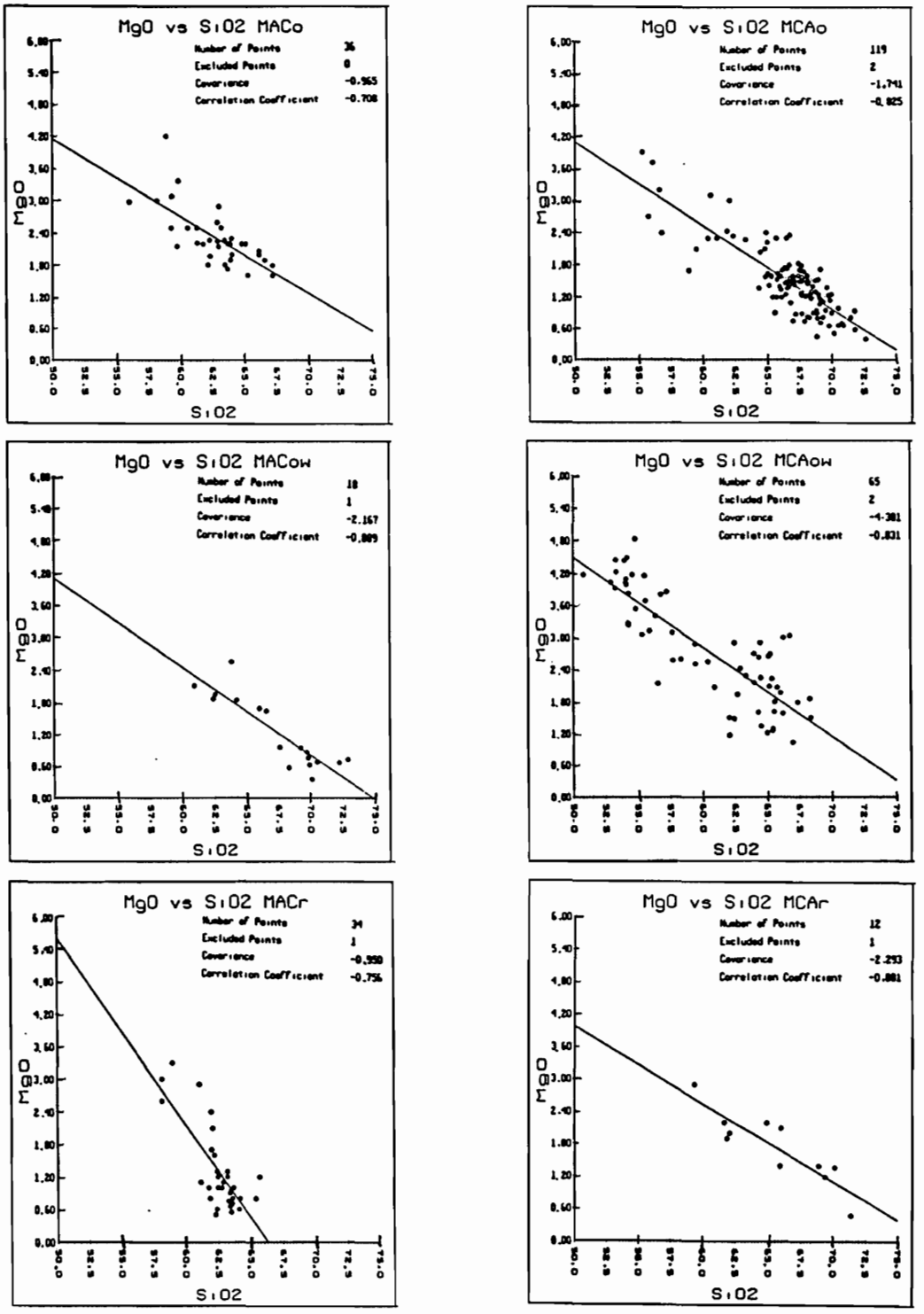

Figure D-13. Whole-rock chemistry of petrochemical classes plotted in lines on MgO vs. SiO_2 variation diagrams (M= Metaluminous, AC= alkali-calcic, CA= calc-alkalic, o= oxidized, ow= weakly oxidized, r=reduced).

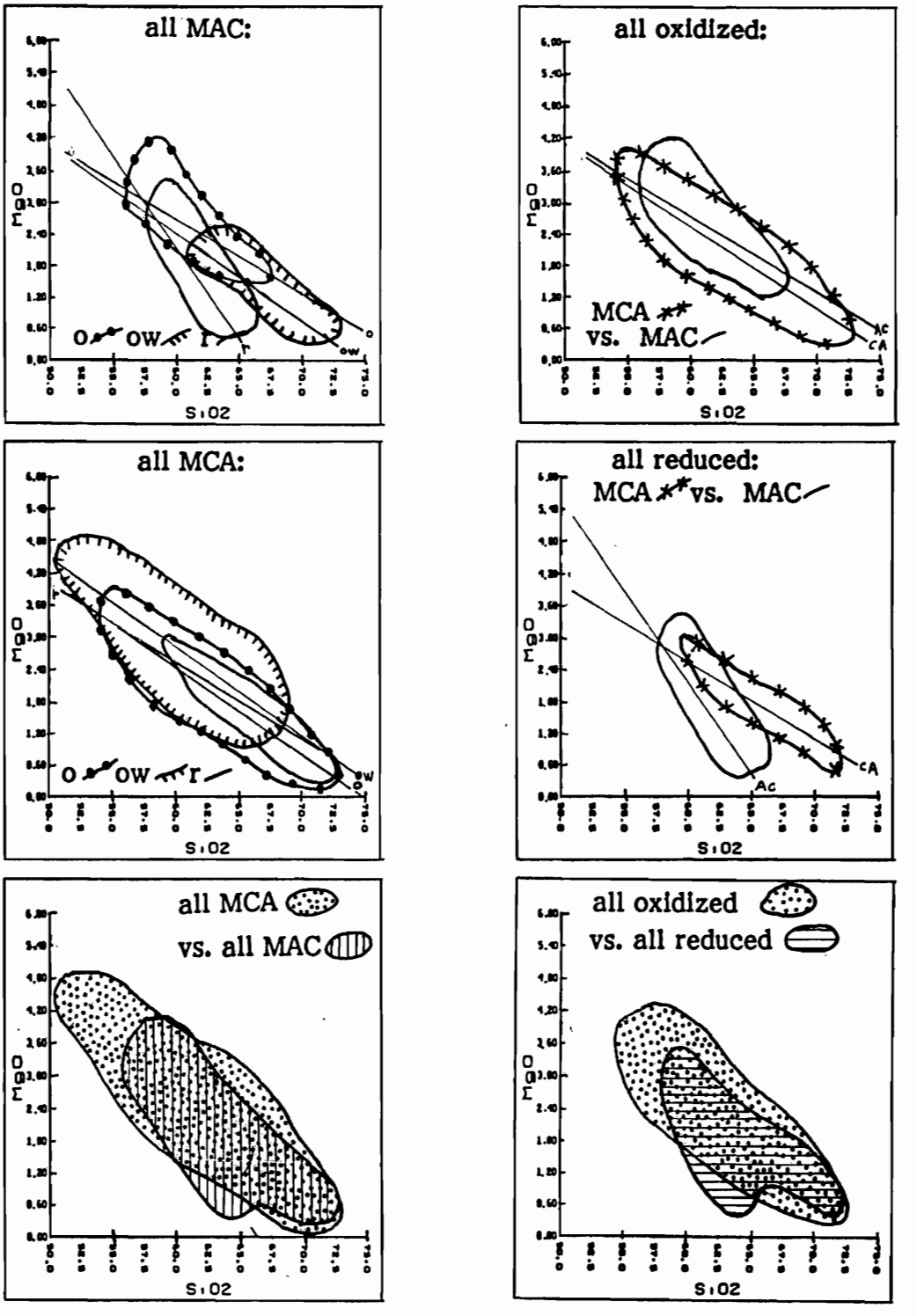

Figure D-14. Comparison of data from Figure D-13 plotted in various combinations on MgO vs. SiO_2 variation diagrams (M= Metaluminous, AC= alkali-calcic, CA=calc-alkalic, o=oxidized, ow=weakly oxidized, r=reduced).

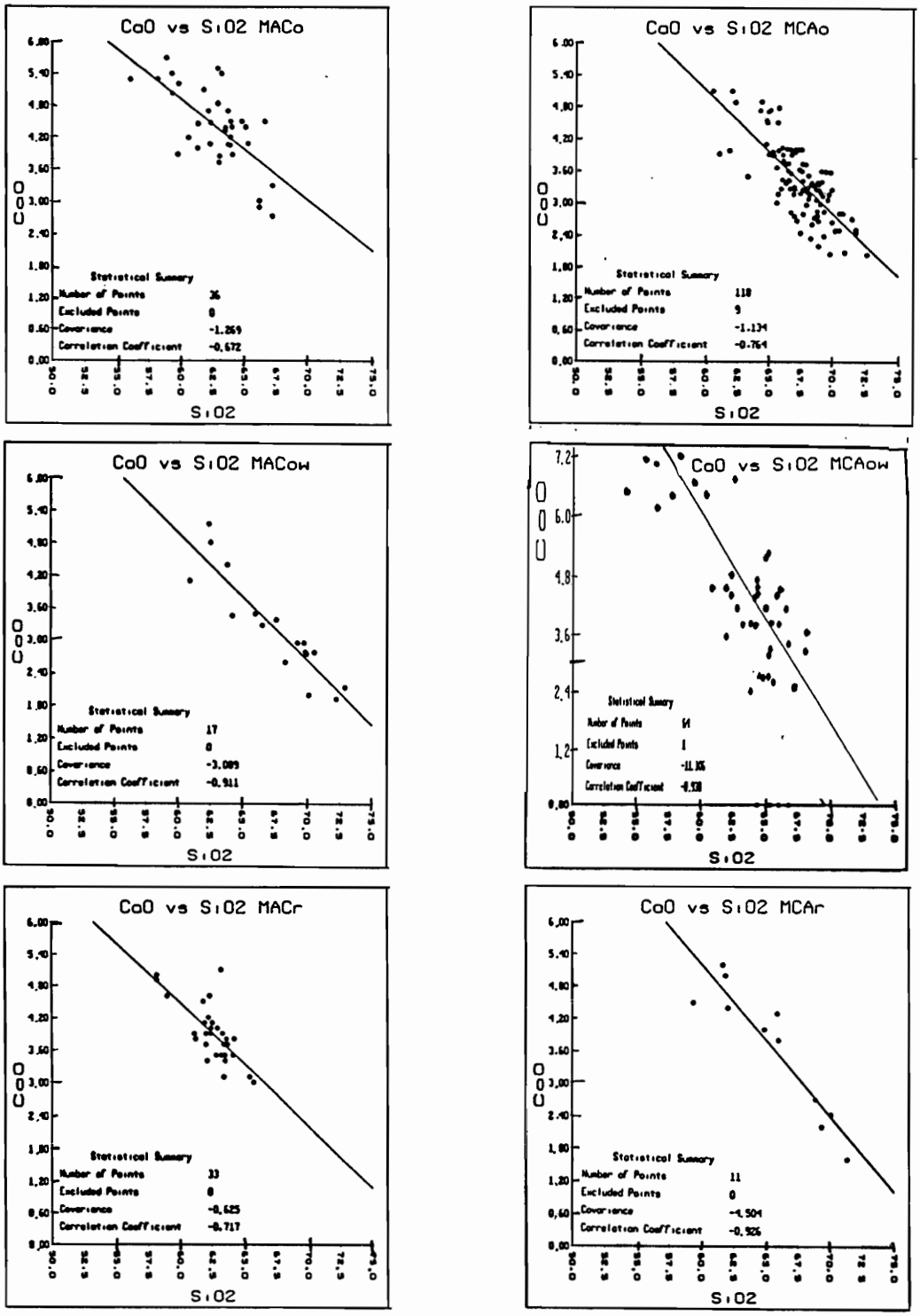

Figure D-15. Whole-rock chemistry of magma series classes plotted in linear bands on CaO vs. SiO_2 variation diagrams (M= Metaluminous, AC= alkali-calcic, CA= calc-alkalic, o= oxidized, ow= weakly oxidized, r=reduced).

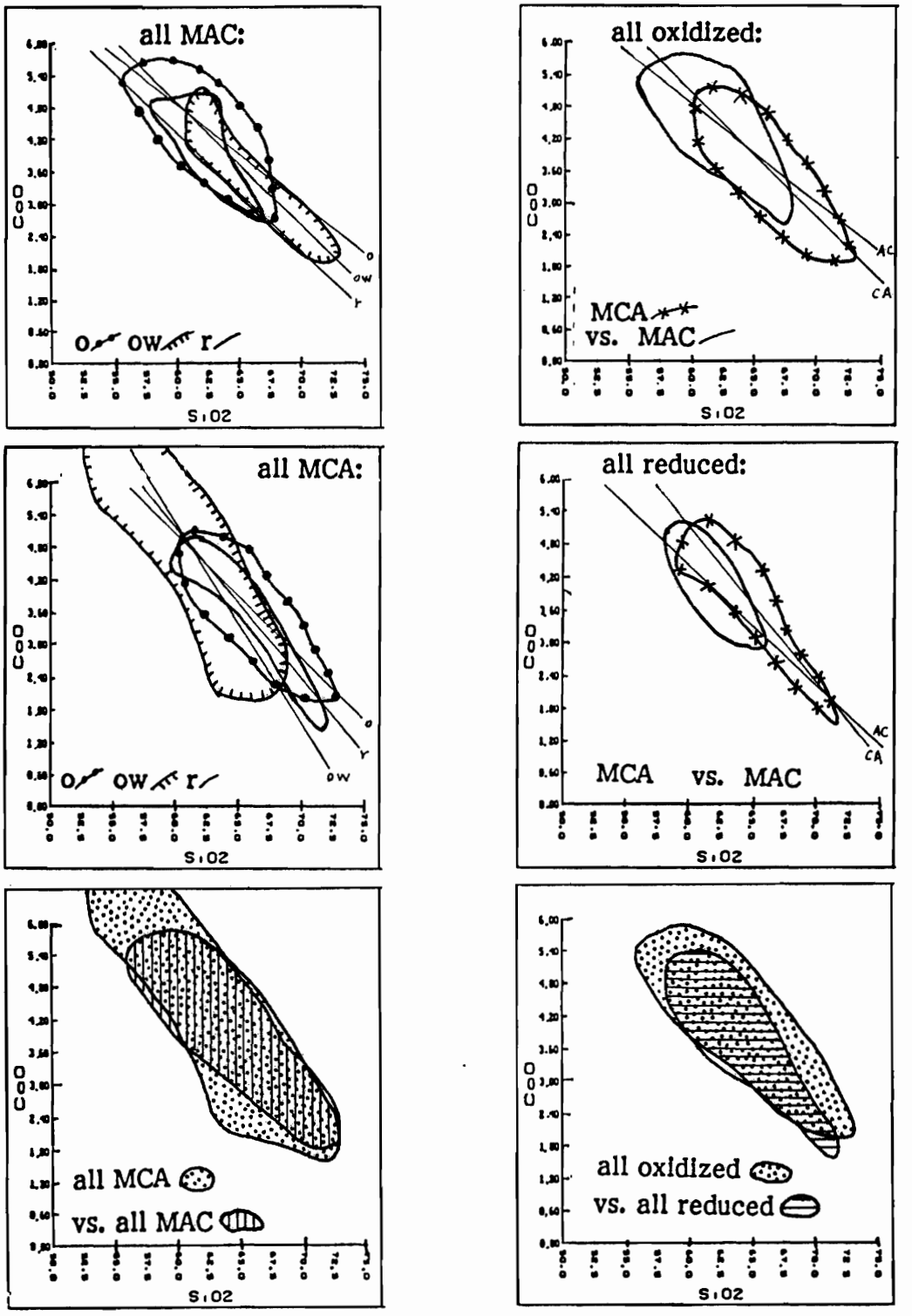

Figure D-16. Comparison of data from Figure 5-15 plotted in various combinations on CaO vs. SiO_2 variation diagrams (M= Metaluminous, AC= alkali-calcic, CA=calc-alkalic, o=oxidized, ow=weakly oxidized, r=reduced).

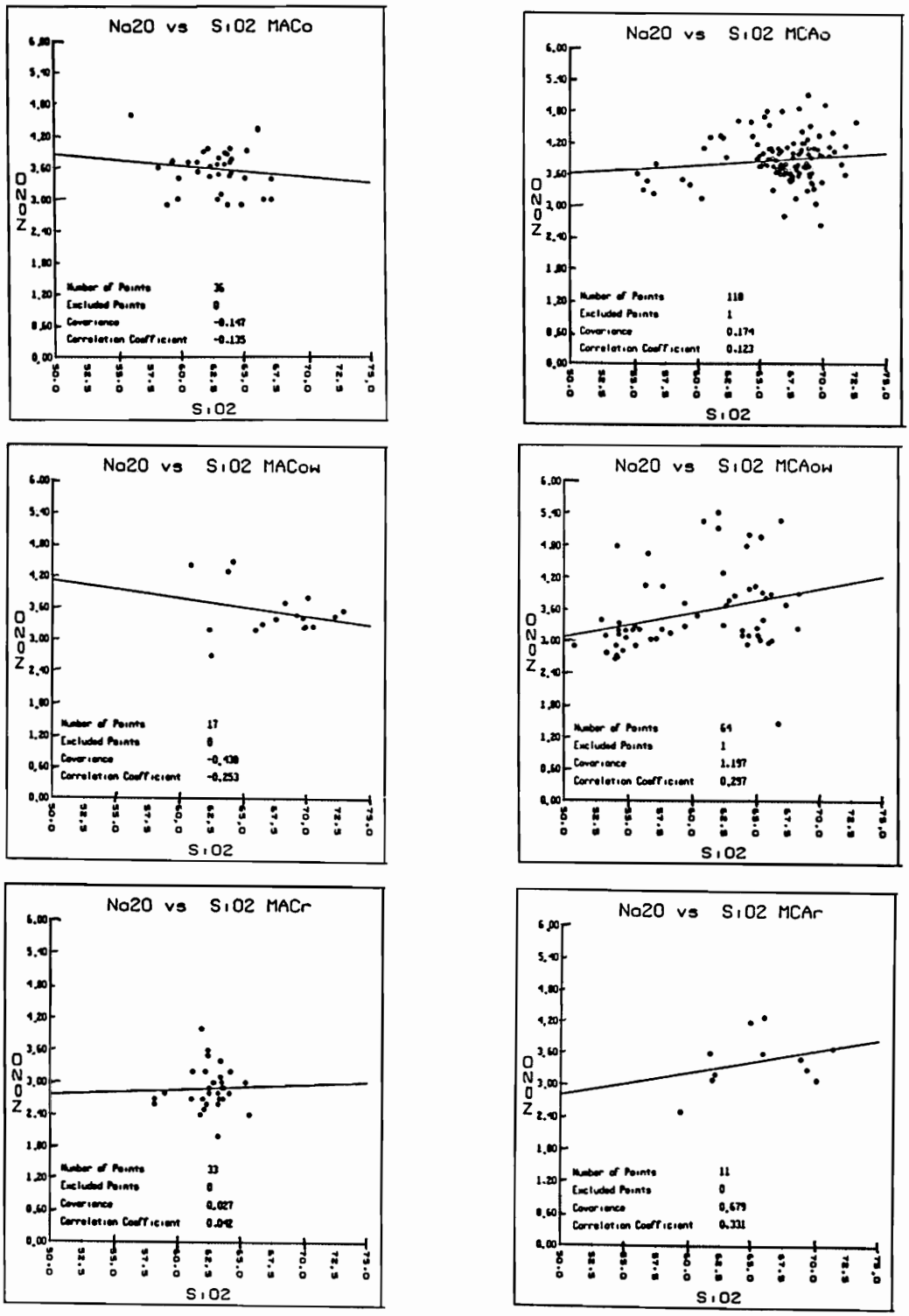

Figure D-17. Whole-rock chemistry of magma series classes plotted in fields on Na_2O vs. SiO_2 variation diagrams (M= Metaluminous, AC= alkali-calcic, CA= calc-alkalic, o= oxidized, ow= weakly oxidized, r=reduced).

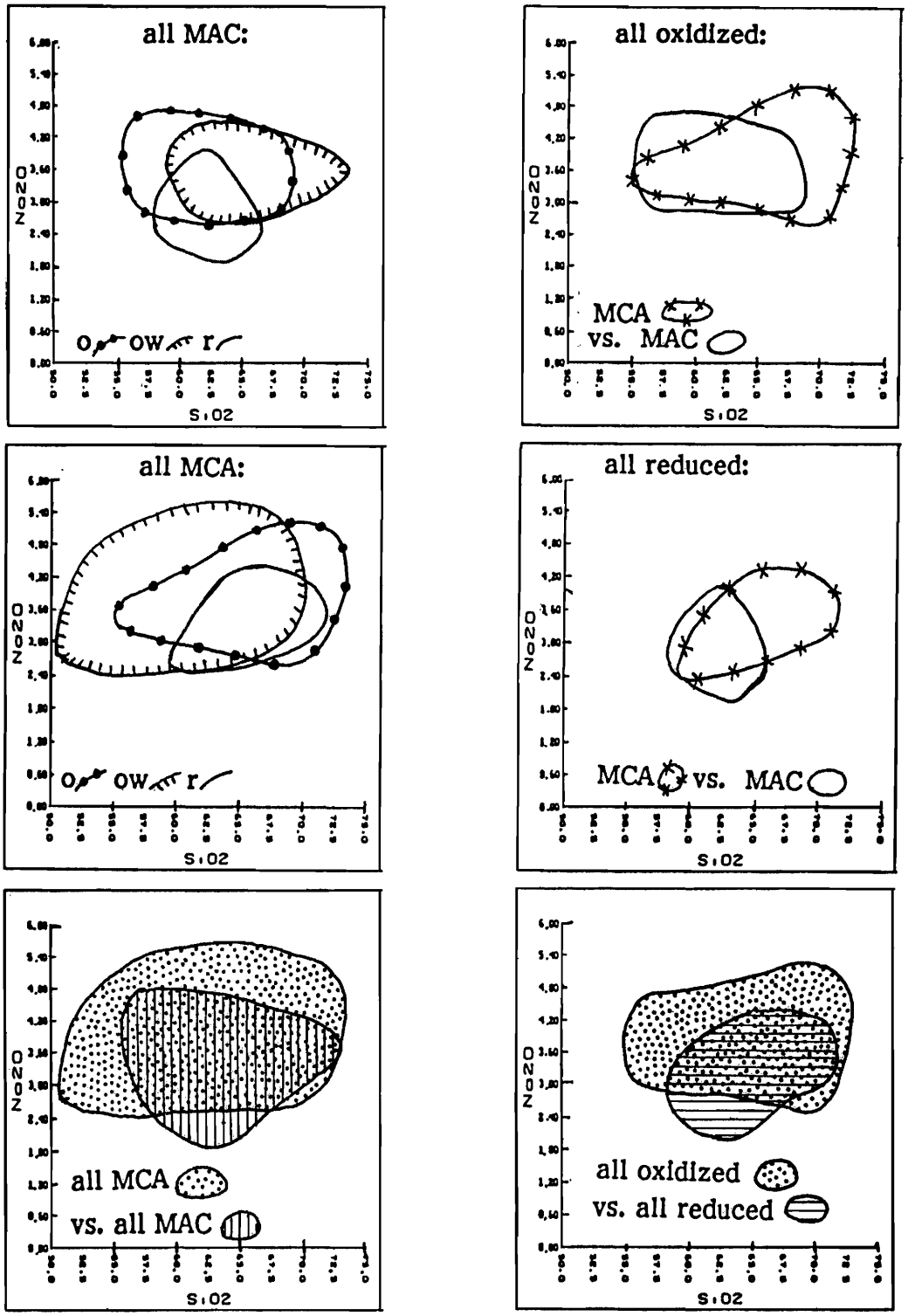

Figure D-17. Comparison of data from Figure D-16 plotted in various combinations on Na_2O vs. SiO_2 variation diagrams (M= Metaluminous, AC= alkali-calcic, CA=calc-alkalic, o=oxidized, ow=weakly oxidized, r=reduced).

APPENDIX E: PRODUCTION REPORTED IN LITERATURE

Appendix E: Production reported in Literature

ref. no.		ore deposit	kg ore	kg Au	kg Ag	kg Cu	kg Pb	kg Zn
MACo								
	1	Tintic, UT	16,654,327,000	83,599	8,379,982	113,065,576	1,027,879,788	187,766,326
	2	Castle Mountain, MT		0	66,802	0	12,657,031	66,502
	3	Park City, UT	13,291,023,545	30,236	7,388,959	49,770,816	1,150,999,388	596,060,247
	4	Tombstone, AZ	2,682,549,000	4,093	997,878	3,517,545	21,799,266	295,356
MACow								
	5	Cherry Creek, NV	283,244,494	1,009	48,207	65,022	376,699	2,310
	6	Kinsley, NV	0	3	73	14,365	9,519	0
	7	Linka, NV	4,539,000	0	0	0	0	0
	8	Railroad, NV	57,108,790	81	36,648	3,058,524	10,387,548	88,105
	9	Railroad, NV	39,888,732	15	11,881	1,291,050	1,966,020	168,516
	10	Taylor, NV	133,328,586	74	84,058	3,349	420,200	3,262
	11	Tem Piute, NV	150,854,573	0	5,169	1,767	20,249	19,570
	12	Santa Eulalia, MEX.	38,580,000,000	1,000,000	12,280,000	7,000,000	2,775,000,000	1,908,000,000
MACr								
	13	Llallagua, BOLIVIA	0	0	8,428,913	0	0	0
	14	Oruro, BOLIVIA	0	0	8,429,000	0	0	0
	15	San Jose m., Oruro	0	0	0	0	0	0
	16	Potosi, BOLIVIA	0	0	62,206,000	0	0	0
	17	Potosi, BOLIVIA	664,675,727	0	0	0	0	0
	18	Potosi, BOLIVIA	828,000,000,000	0	165,600,000	0	0	0
	19	Llallagua, BOLIVIA	80,000,000,000	0	240,000,000	0	0	0
MCAo								
	20	Christmas, AZ	19,226,296,200	1,462	56,794	141,131,697	0	0
	21	Elk Mountain, NV	363,120	0	0	0	0	0
	22	Mill City, NV	2,723,400,000	0	0	0	0	0
	23	Mineral Creek (Ray) AZ	297,310,854,600	1,795	272,459	2,533,153,350	5,491,266	129,105
	24	Wallapai -Mineral Park, AZ	87,983,976,000	4,697	358,773	301,760,061	36,283,488	57,298,611
	26	Pima, AZ	888,511,973,400	812	1,752,219	3,786,968,562	34,335,135	60,232,692
	27	Guichon Creek m. d., BC, total	384,170,000,000	0	0	1,616,040,000	0	0
	25	Red Mountain (Harshaw), AZ	736,225,800	56	80,930	1,431,027	37,063,101	47,248,353
	28	Bethlehem, BC, CANADA = GCB	105,870,000,000	0	0	502,000,000	0	0
	29	Highmont West, BC, CAN = GCB	14,200,000,000	0	0	21,300,000	0	0
	30	Highmont East, BC, CAN = GCB	20,500,000,000	0	0	53,300,000	0	0
	31	Highmont East, BC, total= GCB	34,700,000,000	0	0	74,600,000	0	0
	32	Lornex, BC, CAN = GCB	228,000,000,000	0	0	959,880,000	0	0
	33	Valley Copper, BC, CAN = GCB	15,600,000,000	0	0	79,560,000	0	0
	34	Bethlehem, BC, CANADA = GCB	37,670,000,000	0	0	400,000,000	0	0
	35	Krain, BC, CANADA = GCB	14,000,000,000	0	0	79,590,000	0	0
	36	Highmont West, BC, CAN = GCB	800,000,000	0	0	1,200,000	0	0
	37	Highmont East, BC, CAN = GCB	87,600,000,000	0	0	227,760,000	0	0
	38	J. A., BC, CAN = GCB	286,000,000,000	0	0	1,229,800,000	0	0
	39	Lornex, BC, CAN = GCB	350,000,000,000	0	0	1,309,000,000	0	0
	40	Valley Copper, BC, CAN = GCB	559,000,000,000	0	0	2,632,890,000	0	0
	41	Guichon Creek m. d., BC, CAN	1,335,070,000,000	0	0	5,880,240,000	0	0
	42	Guichon Creek, BC, CAN total	1,719,240,000,000	0	0	7,496,280,000	0	0
MCAow								
	43	Ajo, AZ	390,388,496,400	48,458	611,858	2,729,950,140	13,590	0
	44	Morenci, AZ	661,893,320,400	15,676	799,036	5,437,312,794	101,019	93,771
	45	Copper Canyon, NV	1,800,000,000	4,665	65,316	13,590,000	4,530,000	13,590,000
	46	El Salvador, CHILE	72,624,000,000	0	0	1,449,600,000	0	0
	47	El Teniente, CHILE	444,822,000,000	0	0	8,697,600,000	0	0
	48	Hedley, BC, CANADA	3,693,985,000	50,715	6,008	0	0	0
	49	Nickel Plate, Hedley, BC, CAN	3,010,083,240	15,470	0	0	0	0
	50	Copper Canyon, NV	597,243,436	1,501	26,854	4,359,193	2,853,378	1,475,240
	51	Dos Pobres, AZ	363,120,000,000	0	0	2,609,280,000	0	0
	52	Cu Canyon E & W orebodies	16,340,400,000	13,996	263,131	128,833,200	0	0
	53	Cu Canyon Tomboy-Minnie	3,540,420,000	10,917	33,964	0	0	0
	54	Cu Canyon NE extension	1,361,700,000	3,966	69,982	0	0	0
	55	Cu Canyon Fortitude	14,524,800,000	74,647	432,954	0	0	0
	56	Copper Canyon, NV, total	36,364,563,436	109,693	829,218	146,782,393	7,383,378	15,065,240
	57	Dexing, CHINA	1,361,700,000,000	9,797,445	1,166,363	5,526,600,000	0	0
	58	El Salvador, CHILE	317,730,000,000	0	0	2,609,280,000	0	0
	59	Hedley, BC, CANADA	6,445,380,000	33,125	0	0	0	0
MCAr								
	60	Bald Mountain area (Alligator)NV	817,020	4	529	13,590	0	0
	61	Vantage gold dep. (Alligator) NV	6,808,500,000	20,995	0	0	0	0
	64	Pinson, NV total	6,354,600,000	16,796	0	0	0	0
	62	Pinson, NV	3,631,200,000	14,929	0	0	0	0
	63	Pinson, NV	2,723,400,000	1,866	0	0	0	0
	65	MAG (Pinson) NV	3,903,540,000	10,699	0	0	0	0
	66	MAG (Pinson) NV	2,087,940,000	2,146	0	0	0	0
	67	Pinson, NV	2,945,811,000	12,011	0	0	0	0
	68	Northumberland, NV	15,432,600,000	23,794	0	0	0	0
	69	Gold Quarry/Maggie Creek, NV	485,067,497,400	311,870	0	0	0	0
	70	Carlin, NV	18,870,438,600	4,168	0	0	0	0
	71	Alligator Ridge, NV	5,265,240,000	2,104,155	0	0	0	0

ref. no.		ore deposit	kg Mo	kg W	kg Sn	kg V	kg Sb	kg Mn
MACo								
	1	Tintic, UT	0	0	0	0	0	0
	2	Castle Mountain, MT	0	0	0	0	0	0
	3	Park City, UT	0	0	0	0	0	0
	4	Tombstone, AZ	0	0	0	0	0	0
MACow								
	5	Cherry Creek, NV	0	215,820	0	0	0	0
	6	Kinsley, NV	0	0	0	0	0	0
	7	Linka, NV	0	0	0	0	0	0
	8	Railroad, NV	0	0	0	0	0	0
	9	Railroad, NV	0	0	0	0	0	0
	10	Taylor, NV	0	0	0	0	11,711	0
	11	Tem Piute, NV	0	2,063,513	0	0	0	0
	12	Santa Eulalia, MEX.	0	0	4,000,000	700,000,000	0	0
MACr								
	13	Llallagua, BOLIVIA	0	0	453,900,000	0	0	0
	14	Oruro, BOLIVIA	0	0	45,000,000	0	0	0
	15	San Jose m., Oruro	0	0	0	0	0	0
	16	Potosi, BOLIVIA	0	0	0	0	0	0
	17	Potosi, BOLIVIA	0	0	364,394,000	0	0	0
	18	Potosi, BOLIVIA	0	0	0	0	0	0
	19	Llallagua, BOLIVIA	0	0	0	0	0	0
MCAo								
	20	Christmas, AZ	0	0	0	0	0	0
	21	Elk Mountain, NV	725	1,439	0	0	0	0
	22	Mill City, NV	0	12,949,200	0	0	0	0
	23	Mineral Creek (Ray) AZ	3,610,863	0	0	0	0	0
	24	Wallapai -Mineral Park, AZ	24,090,540	0	0	0	0	0
	26	Pima, AZ	131,730,588	1,655	0	0	0	0
	27	Guichon Creek m. d., BC, total	373,641,000	0	0	0	0	0
	25	Red Mountain (Harshaw), AZ	0	0	0	0	0	4,555,821
	28	Bethlehem, BC, CANADA = GCB	0	0	0	0	0	0
	29	Highmont West, BC, CAN = GCB	6,816,000	0	0	0	0	0
	30	Highmont East, BC, CAN = GCB	4,305,000	0	0	0	0	0
	31	Highmont East, BC, total= GCB	11,121,000	0	0	0	0	0
	32	Lornex, BC, CAN = GCB	362,520,000	0	0	0	0	0
	33	Valley Copper, BC, CAN = GCB	0	0	0	0	0	0
	34	Bethlehem, BC, CANADA = GCB	0	0	0	0	0	0
	35	Krain, BC, CANADA = GCB	0	0	0	0	0	0
	36	Highmont West, BC, CAN = GCB	384,000	0	0	0	0	0
	37	Highmont East, BC, CAN = GCB	18,396,000	0	0	0	0	0
	38	J. A., BC, CAN = GCB	48,620,000	0	0	0	0	0
	39	Lornex, BC, CAN = GCB	45,150,000	0	0	0	0	0
	40	Valley Copper, BC, CAN = GCB	0	0	0	0	0	0
	41	Guichon Creek m. d., BC, CAN	112,550,000	0	0	0	0	0
	42	Guichon Creek, BC, CAN total	486,191,000	0	0	0	0	0
MCAow								
	43	Ajo, AZ	203,850	0	0	0	0	0
	44	Morenci, AZ	5,713,236	0	0	0	0	112,797
	45	Copper Canyon, NV	0	0	0	0	0	0
	46	El Salvador, CHILE	0	0	0	0	0	0
	47	El Teniente, CHILE	0	0	0	0	0	0
	48	Hedley, BC, CANADA	0	0	0	0	0	0
	49	Nickel Plate, Hedley, BC, CAN	0	0	0	0	0	0
	50	Copper Canyon, NV	0	0	0	0	0	0
	51	Dos Pobres, AZ	0	0	0	0	0	0
	52	Cu Canyon E & W orebodies	0	0	0	0	0	0
	53	Cu Canyon Tomboy-Minnie	0	0	0	0	0	0
	54	Cu Canyon NE extension	0	0	0	0	0	0
	55	Cu Canyon Fortitude	0	0	0	0	0	0
	56	Copper Canyon, NV, total	0	0	0	0	0	0
	57	Dexing, CHINA	0	0	0	0	0	0
	58	El Salvador, CHILE	0	0	0	0	0	0
	59	Hedley, BC, CANADA	0	0	0	0	0	0
MCAr								
	60	Bald Mountain area (Alligator)NV	0	0	0	0	0	0
	61	Vantage gold dep. (Alligator) NV	0	0	0	0	0	0
	64	Pinson, NV total	0	0	0	0	0	0
	62	Pinson, NV	0	0	0	0	0	0
	63	Pinson, NV	0	0	0	0	0	0
	65	MAG (Pinson) NV	0	0	0	0	0	0
	66	MAG (Pinson) NV	0	0	0	0	0	0
	67	Pinson, NV	0	0	0	0	0	0
	68	Northumberland, NV	0	0	0	0	0	0
	69	Gold Quarry/Maggie Creek, NV	0	0	0	0	0	0
	70	Carlin, NV	0	0	0	0	0	0
	71	Alligator Ridge, NV	0	0	0	0	0	0

ref. no.		% Au	% Ag	% Cu	% Pb	% Zn	% Mo	% W	% Sn	% V	% Sb	% Mn
MACo												
	1	0.0005	0.05	0.7	6.2	1.1	0	0	0	0	0	0
	2	0	0	0	0	0	0	0	0	0	0	0
	3	0.0002	0.06	0.4	8.7	4.5	0	0	0	0	0	0
	4	0.0002	0.04	0.1	0.8	0.01	0	0	0	0	0	0
MACow												
	5	0.0004	0.02	0.02	0.1	0.0008	0	0.08	0	0	0	0
	6	0	0	0	0	0	0	0	0	0	0	0
	7	0	0	0	0	0	0	0	0	0	0	0
	8	0.0001	0.06	5.4	18.2	0.2	0	0	0	0	0	0
	9	0.00004	0.03	3.2	4.9	0.4	0	0	0	0	0	0
	10	0.00006	0.06	0.003	0.3	0.002	0	0	0	0	0.009	0
	11	0	0.003	0.001	0.01	0.01	0	1.4	0	0	0	0
	12	0.003	0.03	0.02	7.2	4.9	0	0	0.01	1.8	0	0
MACr												
	13	0	0	0	0	0	0	0	0	0	0	0
	14	0	0	0	0	0	0	0	0	0	0	0
	15	0	0	0	0	0	0	0	0	0	0	0
	16	0	0	0	0	0	0	0	0	0	0	0
	17	0	0	0	0	0	0	0	54.8	0	0	0
	18	0	0.02	0	0	0	0	0	0	0	0	0
	19	0	0.3	0	0	0	0	0	0	0	0	0
MCAo												
	20	0.000008	0.0003	0.7	0	0	0	0	0	0	0	0
	21	0	0	0	0	0	0.2	0.4	0	0	0	0
	22	0	0	0	0	0	0	0.5	0	0	0	0
	23	0.000001	0.0001	0.9	0.002	0.00004	0.001	0	0	0	0	0
	24	0.000005	0.0004	0.3	0.04	0.07	0.03	0	0	0	0	0
	26	0.00000009	0.0002	0.4	0.004	0.007	0.01	0.0000002	0	0	0	0
	27	0	0	0.4	0	0	0.1	0	0	0	0	0
	25	0.000008	0.01	0.2	5.0	6.4	0	0	0	0	0	0.6
	28	0	0	0.5	0	0	0	0	0	0	0	0
	29	0	0	0.2	0	0	0.05	0	0	0	0	0
	30	0	0	0.3	0	0	0.02	0	0	0	0	0
	31	0	0	0.2	0	0	0.03	0	0	0	0	0
	32	0	0	0.4	0	0	0.2	0	0	0	0	0
	33	0	0	0.5	0	0	0	0	0	0	0	0
	34	0	0	1	0	0	0	0	0	0	0	0
	35	0	0	0.6	0	0	0	0	0	0	0	0
	36	0	0	0.2	0	0	0.05	0	0	0	0	0
	37	0	0	0.3	0	0	0.02	0	0	0	0	0
	38	0	0	0.4	0	0	0.02	0	0	0	0	0
	39	0	0	0.4	0	0	0.01	0	0	0	0	0
	40	0	0	0.5	0	0	0	0	0	0	0	0
	41	0	0	0.4	0	0	0.008	0	0	0	0	0
	42	0	0	0.4	0	0	0.03	0	0	0	0	0
MCAow												
	43	0.00001	0.0002	0.7	0.000003	0	0.00005	0	0	0	0	0
	44	0.000002	0.0001	0.8	0.00002	0.00001	0.0009	0	0	0	0	0.00002
	45	0.0003	0.004	0.8	0.3	0.8	0	0	0	0	0	0
	46	0	0	2.0	0	0	0	0	0	0	0	0
	47	0	0	2.0	0	0	0	0	0	0	0	0
	48	0.001	0.0002	0	0	0	0	0	0	0	0	0
	49	0.0005	0	0	0	0	0	0	0	0	0	0
	50	0.0003	0.004	0.7	0.5	0.2	0	0	0	0	0	0
	51	0	0	0.7	0	0	0	0	0	0	0	0
	52	0.00009	0.002	0.8	0	0	0	0	0	0	0	0
	53	0.0003	0.001	0	0	0	0	0	0	0	0	0
	54	0.0003	0.005	0	0	0	0	0	0	0	0	0
	55	0.0005	0.003	0	0	0	0	0	0	0	0	0
	56	0.0003	0.002	0.4	0.02	0.04	0	0	0	0	0	0
	57	0.0007	0.00009	0.4	0	0	0	0	0	0	0	0
	58	0	0	0.8	0	0	0	0	0	0	0	0
	59	0.0005	0	0	0	0	0	0	0	0	0	0
MCAr												
	60	0.0005	0.06	1.7	0	0	0	0	0	0	0	0
	61	0.0003	0	0	0	0	0	0	0	0	0	0
	64	0.0003	0	0	0	0	0	0	0	0	0	0
	62	0.0004	0	0	0	0	0	0	0	0	0	0
	63	0.00007	0	0	0	0	0	0	0	0	0	0
	65	0.0003	0	0	0	0	0	0	0	0	0	0
	66	0.0001	0	0	0	0	0	0	0	0	0	0
	67	0.0004	0	0	0	0	0	0	0	0	0	0
	68	0.0002	0	0	0	0	0	0	0	0	0	0
	69	0.00006	0	0	0	0	0	0	0	0	0	0
	70	0.00002	0	0	0	0	0	0	0	0	0	0
	71	0.0004	0	0	0	0	0	0	0	0	0	0

ref. no.		ore deposit	years	Ag/Au	Cu/(Pb+Zn)	base/prec.	Cu/Pb	Pb/Zn
MACo								
	1	Tintic, UT	1869-1976	100	0.09	157	0.1	5
	2	Castle Mountain, MT		0	0	190	0	190
	3	Park City, UT	1875-1964	244	0.03	242	0.04	2
	4	Tombstone, AZ	1879-1981	244	0.2	26	0.2	74
MACow								
	5	Cherry Creek, NV	1863-1968	48	0.2	9	0.2	163
	6	Kinsley, NV	-1966	0	2	316	1.5	0
	7	Linka, NV	1941-1977	0	0	0	0	0
	8	Railroad, NV	1869-1949	455	0.3	368	0.3	118
	9	Railroad, NV	1907-1956	772	0.6	288	0.7	12
	10	Taylor, NV	1875-1968	1136	0.008	5	0.008	129
	11	Tem Piute, NV	1869-1958	0	0.04	8	0.09	1
	12	Santa Eulalia, MEX.	1703-1986	12	0.001	353	0.003	1
MACr								
	13	Llallagua, BOLIVIA	-1946	0	0	0	0	0
	14	Oruro, BOLIVIA	1595-1944	0	0	0	0	0
	15	San Jose m., Oruro	1979 rate	0	0	0	0	0
	16	Potosi, BOLIVIA	1544-1948	0	0	0	0	0
	17	Potosi, BOLIVIA	1979-1980	0	0	0	0	0
	18	Potosi, BOLIVIA	reserves	0	0	0	0	0
	19	Llallagua, BOLIVIA	reserves	0	0	0	0	0
MCAo								
	20	Christmas, AZ	1915-1979	39	0	2423	0	0
	21	Elk Mountain, NV	1957-1958	0	0		0	0
	22	Mill City, NV	1925-1958	0	0	0	0	0
	23	Mineral Creek (Ray) AZ	1905-1981	152	451	9257	461	43
	24	Wallapai -Mineral Park, AZ	1901-1981	76	3	1088	8	0.6
	26	Pima, AZ	1880-1981	2158	40	2214	110	0.6
	27	Guichon Creek m. d., BC, total	1962-1984	0	0	0	0	0
	25	Red Mountain (Harshaw), AZ	1858-1965	1446	0.02	1059	0.04	0.8
	28	Bethlehem, BC, CANADA = GCB	1962-1984	0	0	0	0	0
	29	Highmont West, BC, CAN = GCB	1980-1984	0	0	0	0	0
	30	Highmont East, BC, CAN = GCB	1980-1984	0	0	0	0	0
	31	Highmont East, BC, total= GCB	1980-1984	0	0	0	0	0
	32	Lornex, BC, CAN = GCB	1972-1984	0	0	0	0	0
	33	Valley Copper, BC, CAN = GCB	1983-1984	0	0	0	0	0
	34	Bethlehem, BC, CANADA = GCB	reserves	0	0	0	0	0
	35	Krain, BC, CANADA = GCB	reserves	0	0	0	0	0
	36	Highmont West, BC, CAN = GCB	reserves 85	0	0	0	0	0
	37	Highmont East, BC, CAN = GCB	reserves 85	0	0	0	0	0
	38	J. A., BC, CAN = GCB	reserves 83	0	0	0	0	0
	39	Lornex, BC, CAN = GCB	reserves	0	0	0	0	0
	40	Valley Copper, BC, CAN = GCB	reserves	0	0	0	0	0
	41	Guichon Creek m. d., BC, CAN	reserves	0	0	0	0	0
	42	Guichon Creek, BC, CAN total	1962-84+reserve	0	0	0	0	0
MCAow								
	43	Ajo, AZ	1899-1979	13	200879	4134	200879	0
	44	Morenci, AZ	1873-1981	51	27914	6674	53825	1
	45	Copper Canyon, NV	1866-1967	14	0.8	453	3	0.3
	46	El Salvador, CHILE	Anaconda 12 yrs	0	0	0	0	0
	47	El Teniente, CHILE	-1974	0	0	0	0	0
	48	Hedley, BC, CANADA	1902-1955	0.1	0	0	0	0
	49	Nickel Plate, Hedley, BC, CAN	1920-1971	0	0	0	0	0
	50	Copper Canyon, NV	1871-1954	18	1	306	2	2
	51	Dos Pobres, AZ	reserves	0	0	0	0	0
	52	Cu Canyon E & W orebodies	reserves 67	18.8	0	465	0	0
	53	Cu Canyon Tomboy-Minnie	reserves 67	3	0	0	0	0
	54	Cu Canyon NE extension	reserves 67	18	0	0	0	0
	55	Cu Canyon Fortitude	reserves 67	6	0	0	0	0
	56	Copper Canyon, NV, total	reserves 67	8	7	180	20	0.5
	57	Dexing, CHINA	reserves 90	0.1	0	504	0	0
	58	El Salvador, CHILE	reserves 73	0	0	0	0	0
	59	Hedley, BC, CANADA	reserves, 1974	0	0	0	0	0
MCAr								
	60	Bald Mountain area (Alligator)NV	1869-1956	132	0	26	0	0
	61	Vantage gold dep. (Alligator) NV	1980-1990	0	0	0	0	0
	64	Pinson, NV total	- 1988	0	0	0	0	0
	62	Pinson, NV	- 1988	0	0	0	0	0
	63	Pinson, NV	- 1988	0	0	0	0	0
	65	MAG (Pinson) NV	reserves 1987	0	0	0	0	0
	66	MAG (Pinson) NV	reserves 1987	0	0	0	0	0
	67	Pinson, NV	reserves 82	0	0	0	0	0
	68	Northumberland, NV	reserves 81	0	0	0	0	0
	69	Gold Quarry/Maggie Creek, NV	reserves 89	0	0	0	0	0
	70	Carlin, NV	reserves 89	0	0	0	0	0
	71	Alligator Ridge, NV	reserves 90	0	0	0	0	0

APPENDIX F: MINERALOGY OF ORE SYSTEMS

1=rare,3=present,5=common 2=minor,trace;4=loc.abund 0=no mention of mineral mineral reference	MACo Tintic 1	MACo Tintic 2	MACo Tintic 3	MACo Tintic 4	MACo Tombstone 5	MACo Tombstone 6	MACo Tombstone 7	MACo Castle 8	MACo Park City 9	MACo Park City 10	MACo Park City 11
COMMON SULFIDES											
pyrite	3	0	5	3	5	5	3	5	3	5	2
chalcopyrite	3	0	1	2	1	5	3	5	0	3	1
galena	3	3	5	5	5	5	3	5	3	5	5
sphalerite	3	3	5	4	5	5	3	0	3	5	5
bornite	3	0	0	0	0	0	3	0	0	0	0
PRECIOUS METALS											
native silver	3	3	0	2	1	0	3	0	3	3	1
native gold	3	3	0	1	1	0	3	0	3	3	1
COPPER MINERALS											
native copper	3	0	0	4	1	0	3	0	0	0	0
COPPER SULFIDES											
chalcocite	3	0	0	2	1	0	3	0	0	3	1
covellite	3	0	0	4	2	0	3	0	0	0	0
COPPER SULFOSALTS											
enargite	3	0	0	3	0	0	0	0	0	3	0
tetrahedrite	3	0	1	2	4	5	3	0	3	3	5
tennantite	3	3	0	0	0	0	0	0	0	0	0
luzonite	3	0	0	0	0	0	0	0	0	0	0
famatinite	3	3	0	3	1	2	3	0	0	0	0
COPPER OXIDES											
tenorite	3	0	0	0	2	0	3	0	0	0	0
crednerite	3	0	0	0	0	0	0	0	0	0	0
copper pitch	0	0	0	4	0	0	0	0	0	0	0
cuprite	3	0	0	4	1	0	3	0	0	0	0
melaconite=tenorite	0	0	0	1	0	0	0	0	0	0	0
chalcotrichite (var. cuprite)	0	3	0	0	0	0	0	0	0	0	0
COPPER CARBONATES											
azurite	3	0	0	4	2	0	3	4	3	0	1
malachite	3	0	0	4	5	0	3	4	3	0	1
chrysocolla	0	0	0	2	2	0	3	4	3	0	1
rosasite	0	0	0	0	2	0	3	0	0	0	0
aurichalcite	3	0	1	1	2	0	3	0	0	0	0
COPPER SULFATES											
brochantite	0	0	0	3	1	0	3	0	0	0	0
chalcanthite	3	0	0	0	0	0	0	0	0	0	1
cyanotrichite	0	0	0	1	0	0	0	0	0	0	0
antlerite	3	0	0	0	0	0	0	0	0	0	0
cuprogoslarite	3	0	0	0	0	0	0	0	0	0	0
connellite	0	0	0	1	1	1	3	0	0	0	0
COPPER ARSENATES											
tyrolite	0	0	0	1	0	0	0	0	0	0	0
cornwallite (erinite)	0	0	0	1	0	0	0	0	0	0	0
chenevixite	3	0	0	1	0	0	0	0	0	0	0
olivenite	3	0	0	4	1	0	0	0	0	0	0
chalcophyllite	0	0	0	1	0	0	0	0	0	0	0
conichalcite	3	0	0	4	1	0	0	0	0	0	0
zeunerite	0	0	0	1	0	0	0	0	0	0	0
COPPER PHOSPHATES											
turquoise	0	0	0	0	1	0	0	0	0	0	0
LEAD MINERALS											
anglesite	3	0	2	3	2	0	3	5	3	0	4
cerussite	3	0	4	5	5	0	3	5	3	0	5
LEAD SULFOSALTS											
geocronite	0	0	0	2	0	0	0	0	0	0	0
bournonite	3	0	0	0	1	2	3	0	0	0	0
jamesonite	0	0	0	0	0	0	0	0	0	0	3
bindheimite	3	0	0	0	1	0	3	0	3	0	5
LEAD OXIDES											
minium	0	0	0	1	0	0	0	1	0	0	0
massicot	0	0	0	0	0	0	0	0	0	0	3
cotunnite	0	0	0	1	0	0	0	0	0	0	0
quenselite	3	0	0	0	0	0	0	0	0	0	0
lead oxychloride	0	0	0	1	0	0	0	0	0	0	0
phosgenite	0	0	0	1	0	0	0	0	0	0	0
LEAD SULFATES											
linarite	3	0	0	1	1	0	0	0	0	0	0
leadhillite	0	0	0	1	1	0	0	0	0	0	0

	Tintic	Tintic	Tintic	Tintic	Tombstone	Tombstone	Tombstone	Castle	Park City	Park City	Park City
beaverite	3	0	0	0	2	1	3	0	0	0	0
plumbojarosite	3	0	0	0	2	1	3	0	0	0	0
osarizawaite	0	0	0	0	1	0	0	0	0	0	0
LEAD ARSENATES											
mimetite	3	0	1	0	2	0	0	0	0	0	3
duftite	0	0	0	0	1	0	0	0	0	0	0
bayldonite	3	0	0	0	0	0	0	0	0	0	0
hidalgoite	0	0	0	0	1	0	0	0	0	0	0
LEAD PHOSPHATES											
corkite	0	0	0	0	1	0	0	0	0	0	0
pyromorphite	0	0	0	1	1	0	3	0	0	0	1
lead oxide phosphate	3	0	1	0	0	0	0	0	0	0	0
LEAD VANADATES ETC											
mottramite	0	0	0	0	5	0	3	0	0	0	0
vanadinite	0	0	0	0	1	0	3	0	0	0	0
descloizite	0	0	0	0	2	0	3	0	0	0	0
wulfenite	0	0	0	0	2	0	3	3	0	0	0
altaite	3	0	0	0	0	0	0	0	0	0	0
ZINC MINERALS											
wurtzite	3	0	0	0	0	0	0	0	0	0	0
ZINC OXIDES											
hetaerolite	3	0	0	0	1	1	3	0	0	0	0
chalcophanite	3	0	0	0	0	0	0	0	0	0	0
hydrohetaerolite	0	0	0	0	1	0	0	0	0	0	0
ZINC CARBONATES											
hydrozincite	0	0	0	3	1	0	3	0	0	0	0
smithsonite	3	0	4	4	1	0	3	0	0	0	0
ZINC SULFATES											
pisanite	3	0	0	0	0	0	0	0	0	0	0
ferrogoslarite	3	0	0	0	0	0	0	0	0	0	0
gunningite	3	0	0	0	0	0	0	0	0	0	0
ZINC OTHERS											
adamite	0	0	0	1	0	0	0	0	0	0	0
hemimorphite (calamine)	0	0	0	3	0	0	3	0	0	0	0
willemite	0	0	0	0	0	0	0	0	0	0	0
hemimorphite	0	0	0	0	0	0	3	0	0	0	0
SILVER MINERALS											
argentite	3	3	0	5	0	0	3	0	3	0	0
acanthite	3	3	0	0	1	0	0	0	0	0	0
stromeyerite	3	0	0	0	1	0	3	0	0	0	0
silver plumbate	3	0	0	0	0	0	0	0	0	0	0
argentojarosite	3	0	0	0	0	0	0	0	0	0	0
SILVER SULFOSALTS											
pyrargyrite (ruby silver)	3	0	0	0	0	0	0	0	3	0	0
polybasite	3	0	0	0	0	0	0	0	0	0	0
stephanite	0	0	0	1	0	0	0	0	0	0	0
proustite	3	3	0	1	0	0	0	0	0	0	0
freibergite	3	0	0	0	0	0	0	0	0	0	0
matildite	3	0	0	0	0	0	0	0	0	0	0
jalpaite	3	0	0	0	0	0	0	0	0	0	0
pearceite	3	0	0	1	0	0	0	0	0	0	0
SILVER HALIDES											
miersite	0	0	0	0	1	0	0	0	0	0	0
chlorargyrite (cerargyrite)	3	0	1	5	2	0	3	0	0	0	2
silver halides iodyrite, brom	0	0	0	0	1	0	3	0	0	0	0
bromargyrite (bromyrite)	0	0	0	0	2	0	3	0	0	0	0
chlorargyrite (embolite)	0	0	0	0	2	0	3	0	0	0	0
bromargyrite (bromyrite)	0	0	0	0	1	1	3	0	0	0	0
iodargyrite	0	0	0	0	1	0	0	0	0	0	0
SILVER TELLURIDES											
krennerite	3	0	0	0	1	0	0	0	0	0	0
sylvanite	3	0	0	0	0	0	0	0	0	0	0
hessite	3	3	0	0	1	1	3	0	0	0	0
calaverite	3	3	0	0	0	0	0	0	0	0	0
petzite	3	0	0	0	0	0	0	0	0	0	0
spangolite	0	0	0	1	0	0	0	0	0	0	0
IRON MINERALS											
COMMON IRON											
magnetite	0	0	0	0	5	0	3	0	0	0	3
hematite	0	0	1	3	5	0	3	1	3	5	3
limonite (goethite)	3	0	4	4	5	0	3	2	3	0	4
pentlandite	0	0	0	0	0	0	0	0	0	0	0
marcasite	3	0	0	1	0	0	0	0	0	0	0

	Tintic	Tintic	Tintic	Tintic	Tombstone	Tombstone	Tombstone	Castle	Park City	Park City	Park City
arsenopyrite	3	0	0	1	0	0	0	0	0	0	0
IRON SULFATES											
halotrichite	3	0	0	0	1	0	0	0	0	0	0
bilinite	3	0	0	0	0	0	0	0	0	0	0
melanterite	3	0	0	0	0	0	0	0	0	0	0
voltaite	3	0	0	0	0	0	0	0	0	0	0
szomolnokite	3	0	0	0	0	0	0	0	0	0	0
copiapite	3	0	0	0	0	0	0	0	0	0	0
siderotile	3	0	0	0	0	0	0	0	0	0	0
coquimbite	3	0	0	0	0	0	0	0	0	0	0
jarosite	3	0	3	3	5	0	3	0	0	0	0
kornelite	3	0	0	0	0	0	0	0	0	0	0
rhomboclase	3	0	0	0	0	0	0	0	0	0	0
melanterite	0	0	0	3	0	0	0	0	0	0	0
roemerite	3	0	0	0	0	0	0	0	0	0	0
IRON ARSENATES ETC											
pharmacosiderite	0	0	0	1	0	0	0	0	0	0	0
scorodite	3	0	0	3	0	0	0	0	0	0	0
tinticite	3	0	0	0	0	0	0	0	0	0	0
hisingerite	3	0	0	0	0	0	0	0	0	0	0
MOLYBDENUM MINERALS											
TUNGSTEN MINERALS											
scheelite	0	3	0	0	0	0	0	0	0	0	0
BISMUTH MINERALS											
native bismuth	0	0	0	1	0	0	0	0	0	0	0
bismuthinite	3	0	0	0	0	0	0	0	0	0	0
klaprothite	3	0	0	0	0	0	0	0	0	0	0
bismite	0	0	0	1	0	0	0	0	0	0	0
arsenobismite	0	0	0	1	0	0	0	0	0	0	0
mixite	0	0	0	1	1	0	0	0	0	0	0
tetradymite	3	0	0	0	0	0	0	0	0	0	0
ARSENIC MINERALS											
realgar	3	0	0	0	0	0	0	0	0	0	0
orpiment	3	0	0	0	0	0	0	0	0	0	0
claudetite 2	3	0	0	0	0	0	0	0	0	0	0
ANTIMONY MINERALS											
TIN MINERALS											
MANGANESE MINERALS											
alabandite	0	0	0	0	4	2	3	0	0	0	0
pyrolusite	3	0	0	2	5	0	3	5	0	0	4
manganese oxide	0	0	3	0	0	0	3	0	0	0	0
manjiroite	0	0	0	0	1	0	0	0	0	0	0
cryptomelane	0	0	0	0	2	0	0	0	0	0	0
manganite	0	0	0	1	2	0	3	0	0	0	0
hollandite	0	0	0	0	0	0	3	0	0	0	0
rhodochrosite	0	0	5	0	1	0	0	0	0	3	1
manganocalcite	3	0	0	0	0	0	0	0	0	0	0
COBALT MINERALS											
CADMIUM MINERALS											
greenockite	3	0	0	0	0	0	0	0	0	0	0
NICKEL MINERALS											
THALLIUM MINERALS											
MERCURY MINERALS											
TELLURIUM MINERALS											
tellurium	0	0	0	0	1	0	3	0	0	0	0
sonoraite	0	0	0	0	1	0	0	0	0	0	0
spiroffite	0	0	0	0	1	0	0	0	0	0	0
rodalquilarite	0	0	0	0	1	0	0	0	0	0	0
tlapallite	0	0	0	0	1	0	0	0	0	0	0
winstanleyite	0	0	0	0	1	0	0	0	0	0	0
xocomecatlite	0	0	0	0	1	0	0	0	0	0	0
schieffelinite	0	0	0	0	1	0	0	0	0	0	0
dugganite	0	0	0	0	1	0	0	0	0	0	0

	Tintic	Tintic	Tintic	Tintic	Tombstone	Tombstone	Tombstone	Castle	Park City	Park City	Park City
quetzalcoatlite	0	0	0	0	1	0	0	0	0	0	0
fairbankite	0	0	0	0	1	0	0	0	0	0	0
paratellurite	0	0	0	0	1	0	0	0	0	0	0
emmonsite	0	0	0	0	1	0	3	0	0	0	0
dunhamite	0	0	0	0	1	0	0	0	0	0	0
girdite	0	0	0	0	1	0	0	0	0	0	0
parakhinite	0	0	0	0	1	0	0	0	0	0	0
oboyerite	0	0	0	0	1	0	0	0	0	0	0
khinite	0	0	0	0	1	0	0	0	0	0	0
rickardite	0	0	0	0	1	0	0	0	0	0	0
empressite	0	0	0	0	1	0	0	0	0	0	0
frohbergite	0	0	0	0	1	0	0	0	0	0	0
MAGNESIUM MINERALS											
kieserite	3	0	0	0	0	0	0	0	0	0	0
epsomite	3	0	0	0	0	0	0	0	0	0	0

REFERENCES
'1=Morris & Lovering, 1979
3=Mafoud, 1971
4=Lindgren & Loughlin, 1919
5=Williams, 1980
6=Rasor, 1937
7=Butler, Wilson, Rasor, 1938
8=Weed & Pirsson, 1896
9,10=Barnes & Simos, 1968
11=Boutwell, 1912

1=rare,3=present,5=common 2=minor,trace;4=loc.abund 0=no mention of mineral	MACow Cherry C	MACow Kinsley	MACow Kinsley	MACow Linka	MACow Railroad	MACow Railroad	MACow Swales Mt	MACow Taylor, NV	MACow Taylor, NV	MACow Taylor, NV
mineral reference	12	13	14	15	16	17	18	19	20	21
COMMON SULFIDES										
pyrite	5	3	3	0	5	5	3	0	0	5
chalcopyrite	3	3	3	1	5	5	3	0	0	5
galena	5	3	3	0	5	5	0	3	0	5
sphalerite	5	0	0	0	0	5	0	3	0	5
bornite	3	3	0	0	5	1	1	0	0	0
PRECIOUS METALS										
native silver	1	0	3	0	0	1	0	0	3	0
electrum	0	0	0	0	0	0	0	0	0	0
native gold	1	0	3	0	0	0	0	1	0	0
COPPER MINERALS										
native copper	0	0	0	0	0	1	0	0	0	0
COPPER SULFIDES										
chalcocite	0	0	0	0	0	1	0	0	0	0
covellite	0	0	0	0	0	3	0	0	0	0
COPPER SULFOSALTS										
tetrahedrite	3	0	0	0	3	1	0	3	0	5
COPPER OXIDES										
tenorite	0	0	0	0	0	0	0	0	0	3
copper pitch	0	0	0	0	0	5	0	0	0	0
COPPER CARBONATES										
azurite	3	3	3	0	5	5	3	0	0	4
malachite	3	3	3	0	5	5	3	1	0	4
chrysocolla	0	3	3	0	5	5	0	1	0	3
COPPER SULFATES										
COPPER ARSENATES										
COPPER PHOSPHATES										
LEAD MINERALS										
anglesite	3	0	0	0	0	1	0	0	0	3
cerussite	3	0	3	0	5	5	0	3	0	4
LEAD SULFOSALTS										
bindheimite	0	0	0	0	0	0	0	0	0	5
LEAD OXIDES										
LEAD SULFATES										
LEAD ARSENATES										
duftite	0	0	0	0	0	5	0	0	0	0
LEAD PHOSPHATES										
LEAD VANADATES ETC										
ZINC MINERALS										
ZINC OXIDES										
ZINC CARBONATES										
smithsonite	0	0	0	0	0	0	0	0	0	5
ZINC SULFATES										
ZINC OTHERS										
hemimorphite (calamine)	0	0	0	0	0	1	0	0	0	0
willemite	0	0	0	0	0	1	0	0	0	3
hemimorphite	0	0	0	0	0	0	0	0	0	3
SILVER MINERALS										
argentite	3	0	0	0	0	0	0	0	3	0
SILVER SULFOSALTS										
pyrargyrite (ruby silver)	3	0	0	0	3	0	0	0	0	3
polybasite	3	0	0	0	0	0	0	0	0	0
stephanite	3	0	0	0	0	0	0	0	0	0
proustite	3	0	0	0	0	1	0	0	0	0
SILVER HALIDES										
chlorargyrite (cerargyrite)	3	0	0	0	1	0	0	3	3	4
silver halides iodyrite, brom	3	0	0	0	0	0	0	0	0	0
bromargyrite (bromyrite)	3	0	0	0	0	0	0	0	0	0
SILVER TELLURIDES										
IRON MINERALS										

	Cherry C	Kinsley	Kinsley	Linka	Railroad	Railroad	Swales Mt	Taylor, NV	Taylor, NV	Taylor, NV
COMMON IRON										
pyrrhotite	0	0	0	0	0	5	0	0	0	0
hematite	0	0	3	0	0	0	1	0	0	5
limonite (goethite)	3	3	3	0	0	0	0	0	0	5
pentlandite	0	0	0	0	0	1	0	0	0	0
marcasite	0	0	0	0	0	1	0	0	0	0
IRON SULFATES										
IRON ARSENATES ETC										
MOLYBDENUM MINERALS										
TUNGSTEN MINERALS										
scheelite	3	0	0	5	0	0	1	0	0	0
wolframite	1	0	0	0	0	0	0	0	0	0
BISMUTH MINERALS										
ARSENIC MINERALS										
ANTIMONY MINERALS										
stibnite	0	0	0	0	0	1	0	3	0	5
cervantite	0	0	0	0	0	0	0	3	0	5
antimony ochre	0	0	0	0	0	0	0	0	0	3
TIN MINERALS										
MANGANESE MINERALS										
manganese oxide	0	0	0	0	0	3	0	0	0	5
COBALT MINERALS										
CADMIUM MINERALS										
NICKEL MINERALS										
THALLIUM MINERALS										
MERCURY MINERALS										
TELLURIUM MINERALS										
MAGNESIUM MINERALS										

12=Schrader, 193
13=Hill, 1916
14=Steininger, 1966
15=Stewart et al., 1977
16=Lincoln, 1923
17=Ketner & Smith, 1963
18=Stager & Tingley, 1988
19=Hose et al., 1976
20=Havenstrite, 1991
21=Lovering & Heyl, 1974

1=rare,3=present,5=common 2=minor,trace;4=loc.abund 0=no mention of mineral mineral reference	MACr Potosi, Bol 22	MACr Potosi, Bol 23	MACr Potosi, Bol 24	MACr Llallagua 25	MACr Llallagua 26	MACr Llallagua 27	MACr Oruro, Bol 28	MACr San Jose O 29	MACr Oruro, Bol 30	MACr Oruro 31
COMMON SULFIDES										
pyrite	3	5	3	5	5	3	5	3	3	5
chalcopyrite	3	2	3	2	1	3	3	3	3	2
galena	0	2	0	1	0	0	5	3	3	2
sphalerite	3	5	3	5	2	3	3	3	3	2
PRECIOUS METALS										
COPPER MINERALS										
COPPER SULFIDES										
COPPER SULFOSALTS										
enargite	0	0	0	0	0	0	0	3	0	0
tetrahedrite	0	0	0	1	0	0	0	3	3	5
chalcostibite	0	0	0	0	0	0	0	0	3	0
COPPER OXIDES										
COPPER CARBONATES										
COPPER SULFATES										
COPPER ARSENATES										
COPPER PHOSPHATES										
LEAD MINERALS										
anglesite	0	0	0	0	0	0	0	0	3	0
cerussite	0	0	0	0	0	0	0	0	3	0
meneghinite	0	0	0	0	0	0	0	0	3	0
LEAD SULFOSALTS										
semseyite	0	0	0	0	0	0	0	0	3	0
bournonite	0	2	0	0	0	0	0	0	0	2
plagionite	0	0	0	0	0	0	0	0	3	0
jamesonite	0	2	0	1	0	0	3	3	3	1
cylindrite	0	0	0	0	0	0	3	0	0	0
andorite	0	5	0	1	0	0	3	3	3	5
plumosite	0	0	0	0	0	0	0	3	0	0
boulangerite	0	0	0	1	0	0	0	3	3	5
zinkenite	0	2	0	0	0	0	3	0	3	5
frankeite	0	0	0	5	2	0	3	0	3	1
LEAD OXIDES										
LEAD SULFATES										
LEAD ARSENATES										
LEAD PHOSPHATES										
LEAD VANADATES ETC										
ZINC MINERALS										
ZINC OXIDES										
ZINC CARBONATES										
ZINC SULFATES										
ZINC OTHERS										
SILVER MINERALS										
SILVER SULFOSALTS										
pyrargyrite (ruby silver)	0	5	0	0	0	0	0	0	3	0
stephanite	0	0	0	0	0	0	0	0	3	0
proustite	0	0	0	0	0	0	0	0	0	0
freibergite	0	0	0	0	0	0	0	3	0	0
miargyrite	0	0	0	0	0	0	0	0	3	0
matildite	0	2	0	0	0	0	0	0	0	0
freieslebenite	0	0	0	0	0	0	0	0	3	0
SILVER HALIDES										
chlorargyrite (cerargyrite)	0	0	0	0	0	0	0	0	3	0
SILVER TELLURIDES										
IRON MINERALS										
COMMON IRON										
pyrrhotite	0	0	0	5	5	5	5	0	0	0
hematite	0	0	0	0	0	0	0	0	3	0
limonite (goethite)	0	0	0	0	0	0	0	0	3	0
marcasite	0	0	0	5	0	0	3	0	3	1
arsenopyrite	3	5	3	5	2	0	5	0	3	1
IRON SULFATES										
IRON ARSENATES ETC										
MOLYBDENUM MINERALS										
TUNGSTEN MINERALS										
huebnerite	0	0	0	0	2	0	0	0	0	0
wolframite	3	2	0	2	5	0	0	0	3	0

	Potosi, Bol	Potosi, Bol	Potosi, Bol	Llallagua	Llallagua	Llallagua	Oruro, Bol	San Jose O	Oruro, Bol	Oruro
BISMUTH MINERALS										
native bismuth	0	0	0	0	2	0	0	0	0	0
bismuthinite	3	2	0	5	5	0	0	0	0	0
ARSENIC MINERALS										
ANTIMONY MINERALS										
stibnite	0	2	0	1	0	0	3	3	3	0
metastibnite	0	0	0	0	0	0	0	0	3	0
cervantite	0	0	0	0	0	0	0	0	3	0
TIN MINERALS										
cassiterite	5	5	5	5	5	5	5	3	3	5
stannite	3	5	3	2	5	3	5	3	3	5
MANGANESE MINERALS										
COBALT MINERALS										
CADMIUM MINERALS										
NICKEL MINERALS										
THALLIUM MINERALS										
MERCURY MINERALS										
TELLURIUM MINERALS										
MAGNESIUM MINERALS										

Sugaki et al 22,28=Sugaki et al. 1981
Grant etal 80 23,25,31=Turneaure, 1960
Grant etal 80 24,27=Grant et al., 1980
26=Ahlfield, 1931
29=USGS, 1992
30=Chace, 1948

1=rare,3=present,5=common 2=minor,trace;4=loc.abund 0=no mention of mineral	MCAo Christmas	MCAo Elk Mtn.	MCAo Mill City	MCAo Mill City	MCAo Min. Park	MCAo Min. Park	MCAo Red Mtn A	MCAo Ray, AZ	MCAo Pima	MCAo Pima	MCAo Valley Cu	MCAo Bethlehem
mineral	32	33	34	35	36	37	38	39	40	41	42	43
COMMON SULFIDES												
pyrite	5	5	5	3	5	5	5	5	5	5	1	5
chalcopyrite	5	5	5	0	5	5	5	5	5	5	5	5
galena	5	0	0	0	5	3	3	2	4	4	2	1
sphalerite	5	0	0	0	5	3	3	2	4	4	0	0
bornite	5	3	0	0	0	3	0	2	4	4	5	5
PRECIOUS METALS												
native silver	2	3	0	0	0	0	0	1	0	0	0	0
native gold	2	0	0	0	0	0	0	0	0	0	0	0
COPPER MINERALS												
native copper	3	3	0	0	0	3	0	3	0	0	3	0
COPPER SULFIDES												
chalcocite	4	0	0	0	5	5	5	5	4	0	2	2
covellite	3	0	0	0	0	3	0	0	0	0	1	0
cubanite	2	0	0	0	0	0	0	0	0	0	0	0
COPPER SULFOSALTS												
tetrahedrite	0	0	0	0	0	0	0	0	0	0	1	1
tennantite	0	0	0	0	0	0	0	0	0	3	0	0
COPPER OXIDES												
tenorite	3	0	0	0	0	0	3	0	0	0	0	0
cuprite	3	0	0	1	3	3	0	3	0	0	1	0
COPPER CARBONATES												
azurite	0	3	0	0	2	3	0	0	0	0	4	0
malachite	0	3	0	0	2	3	0	0	0	0	5	0
chrysocolla	3	3	0	0	0	0	0	5	0	0	5	0
COPPER SULFATES												
COPPER ARSENATES												
COPPER PHOSPHATES												
turquoise	0	0	0	0	5	0	0	0	0	0	0	0
LEAD MINERALS												
LEAD SULFOSALTS												
LEAD OXIDES												
LEAD SULFATES												
LEAD ARSENATES												
LEAD PHOSPHATES												
LEAD VANADATES ETC												
ZINC MINERALS												
ZINC OXIDES												
ZINC CARBONATES												
ZINC SULFATES												
ZINC OTHERS												
SILVER MINERALS												
argentite	0	3	0	0	0	0	0	0	0	0	0	0
SILVER SULFOSALTS												
SILVER HALIDES												
SILVER TELLURIDES												
IRON MINERALS												
COMMON IRON												
pyrrhotite	3	0	0	0	0	0	0	0	4	0	0	0
magnetite	3	0	0	0	0	0	0	0	0	3	0	2
hematite	3	0	0	0	0	0	5	0	0	3	5	5
limonite (goethite)	0	0	0	0	0	0	5	0	0	0	5	0
arsenopyrite	3	0	0	0	3	0	0	0	0	0	0	0
IRON SULFATES												
IRON ARSENATES ETC												
MOLYBDENUM MINERALS												
molybdenite	5	5	4	3	5	5	4	3	4	5	4	5
powellite	0	0	3	3	0	0	0	0	0	0	0	0
ferrimolybdite	0	0	0	0	5	3	0	0	0	0	0	0
TUNGSTEN MINERALS												
scheelite	0	5	0	5	0	0	0	0	0	0	0	0
wolframite	0	0	0	0	0	3	0	0	0	0	0	0
BISMUTH MINERALS												
bismuthinite	0	0	1	0	0	0	0	0	0	0	0	0
ARSENIC MINERALS												
ANTIMONY MINERALS												
stibnite	0	3	0	0	0	0	0	0	0	0	0	0
antimony ochre	3	0	0	0	0	0	0	0	0	0	0	0
TIN MINERALS												

	Christmas	Elk Mtn.	Mill City	Mill City	Min. Park	Min. Park	Red Mtn A	Ray, AZ	Pima	Pima	Valley Cu	Bethlehem
MANGANESE MINERALS												
manganese oxide	0	0	0	0	0	0	0	0	0	0	4	0
COBALT MINERALS												
CADMIUM MINERALS												
NICKEL MINERALS												
THALLIUM MINERALS												
MERCURY MINERALS												
TELLURIUM MINERALS												
MAGNESIUM MINERALS												

32=Koski & Cook, 1982
33=Lapointe et al., 1991
34=Stager & Tingley, 1988
35=Johnson & Keith, 1991
36=Eidel et al., 1968
37=MRDS
38=Quinlan, 1986
39=Metz & Rose, 1966
40=Barter & Kelley, 1982
41=Himes, 1973
42=White et al., 1957
43=Briskey & Bellamy, 1976

1=rare,3=present,5=common 2=minor,trace;4=loc.abund 0=no mention of mineral	MCAow Ajo, AZ	MCAow Ajo, AZ	MCAow Fortitude C	MCAow Fortitude C	MCAow Fortitude C	MCAow Copper Can	MCAow Copper Can	MCAow Dexing
mineral reference	44	45	46	47	48	49	50	51
COMMON SULFIDES								
pyrite	3	0	3	5	5	5	5	5
chalcopyrite	5	0	3	3	5	5	5	5
galena	0	1	3	3	2	3	3	0
sphalerite	1	0	3	3	2	3	3	0
bornite	5	0	0	0	0	0	0	0
PRECIOUS METALS								
native silver	0	0	0	0	1	0	0	1
electrum	0	0	3	0	3	0	0	0
native gold	0	1	0	3	1	0	4	1
COPPER MINERALS								
native copper	2	2	0	0	0	0	0	0
COPPER SULFIDES								
chalcocite	5	0	0	3	0	0	0	0
covellite	0	0	0	0	0	3	0	0
COPPER SULFOSALTS								
enargite	0	1	0	0	0	0	0	0
tetrahedrite	1	1	0	0	0	0	0	0
tennantite	3	4	0	0	0	0	0	0
famatinite	0	0	0	0	0	0	0	0
COPPER OXIDES								
tenorite	0	3	0	0	0	0	0	0
copper pitch	0	0	0	0	0	0	0	0
cuprite	0	3	0	0	3	0	0	0
atacamite	0	1	0	0	0	0	0	0
COPPER CARBONATES								
azurite	2	4	0	0	3	3	0	0
malachite	2	4	0	0	3	3	0	0
chrysocolla	3	5	0	0	3	3	0	0
aurichalcite	0	1	0	0	0	0	0	0
COPPER SULFATES								
brochantite	0	1	0	0	0	0	0	0
chalcanthite	0	0	0	0	0	0	0	0
langite	0	0	0	0	0	0	0	0
gerhardtite	0	0	0	0	0	0	0	0
COPPER ARSENATES								
olivenite	0	0	0	0	0	0	0	0
chalcophyllite	0	0	0	0	0	0	0	0
COPPER PHOSPHATES								
libethenite	0	0	0	0	0	0	0	0
turquoise	0	1	0	0	0	0	0	0
copper silicate, ajoite, papagoi	0	1	0	0	0	0	0	0
LEAD MINERALS								
cerussite	0	0	0	0	0	0	0	0
LEAD SULFOSALTS								
LEAD OXIDES								
coronadite	0	0	0	0	0	0	0	0
LEAD SULFATES								
LEAD ARSENATES								
LEAD PHOSPHATES								
LEAD VANADATES ETC								
ZINC MINERALS								
ZINC OXIDES								
ZINC CARBONATES								
smithsonite	0	0	0	0	0	0	0	0
ZINC SULFATES								
ZINC OTHERS								
hemimorphite (calamine)	0	0	0	0	0	0	0	0
willemite	0	0	0	0	0	3	0	0
SILVER MINERALS								

	Ajo, AZ	Ajo, AZ	Fortitude	Fortitude	Fortitude	Copper Can	Copper Can	Dexing
acanthite	0	0	0	3	0	0	0	0
SILVER SULFOSALTS								
matildite	0	0	0	0	0	0	0	3
SILVER HALIDES								
chlorargyrite (cerargyrite)	0	0	0	0	0	0	0	0
SILVER TELLURIDES								
spangolite	0	0	0	0	0	0	0	0
IRON MINERALS								
COMMON IRON								
pyrrhotite	0	0	3	5	5	5	5	0
magnetite	3	0	0	0	0	0	0	0
hematite	3	5	0	0	0	0	0	0
limonite (goethite)	0	1	0	0	0	0	0	0
marcasite	0	0	3	3	5	3	3	0
arsenopyrite	0	0	3	3	2	3	3	0
IRON SULFATES								
IRON ARSENATES ETC								
MOLYBDENUM MINERALS								
molybdenite	3	5	0	0	2	0	0	4
ferrimolybdite	0	0	0	0	0	0	0	0
TUNGSTEN MINERALS								
huebnerite	0	0	0	0	0	0	0	0
BISMUTH MINERALS								
native bismuth	0	0	1	0	3	0	0	0
joseite	0	0	3	0	3	0	0	0
hedleyite	0	0	3	0	3	0	0	0
ARSENIC MINERALS								
realgar	0	0	0	0	0	0	0	0
orpiment	0	0	0	0	0	0	0	0
ANTIMONY MINERALS								
stibnite	0	0	0	0	0	0	0	0
stibiconite	0	0	0	0	0	0	0	0
TIN MINERALS								
MANGANESE MINERALS								
manganese oxide	0	0	0	0	0	0	0	0
COBALT MINERALS								
erythrite	0	0	0	0	0	0	0	0
cobaltite	0	0	0	0	0	0	0	0
CADMIUM MINERALS								
NICKEL MINERALS								
millerite	0	0	0	0	0	0	0	3
siegenite	0	0	0	0	0	0	0	3
gersdorffite	0	0	0	0	0	0	0	0
THALLIUM MINERALS								
MERCURY MINERALS								
TELLURIUM MINERALS								
MAGNESIUM MINERALS								

44=Gilluly, 1937
45=Thomas & Gibbs, 1983
46=Myers, 1990
47=Wotruba et al., 1986, 1988
48,49=Sayers et al. 1968, 1969
50=Myers & Meinert, 1991
51=Yan & Hu, 1980
52=Chung Wen, 1981
53=Langton & Williams, 1982
54=Gustafson & Hunt, 1975
55=Swayne &Trask, 1960
56=Camus, 1975
57=Howell & Molloy, 1960
58,59=Ray et al. 1986
60=Billingsley & Hume, 1941
61=Stager, 1977
62=Schaller, 1934
63=Brooks et al. 1991
64=Kuyper, 1988
65=Moolick & Durek, 1966
66=Lindgren, 1902

1=rare,3=present,5=common 2=minor,trace;4=loc.abund 0=no mention of mineral mineral reference	MCAow Dexing 52	MCAow Dos Pobres 53	MCAow ElSalvador 54	MCAow ElSalvador 55	MCAow El Teniente 56	MCAow El Teniente 57	MCAow Hedley 58	MCAow NickelPlate 59
COMMON SULFIDES								
pyrite	5	1	3	5	5	5	5	3
chalcopyrite	5	5	3	5	5	5	5	3
galena	1	0	1	0	1	1	0	3
sphalerite	1	0	1	0	1	1	0	3
bornite	1	3	3	4	5	4	0	0
PRECIOUS METALS								
native silver	0	0	0	0	0	1	0	0
electrum	0	0	0	0	0	0	0	3
native gold	0	0	0	0	0	1	0	0
COPPER MINERALS								
native copper	0	0	0	0	1	4	0	0
COPPER SULFIDES								
chalcocite	0	0	0	0	5	5	0	0
covellite	0	0	0	0	1	1	0	0
COPPER SULFOSALTS								
enargite	4	0	3	1	1	1	0	0
tetrahedrite	2	0	0	0	3	0	0	0
tennantite	0	0	3	0	3	2	0	0
famatinite	0	0	0	1	2	0	0	0
COPPER OXIDES								
tenorite	0	0	0	0	1	2	0	0
copper pitch	0	0	0	0	0	0	0	0
cuprite	0	0	0	0	2	5	0	0
atacamite	0	0	0	0	0	0	0	0
COPPER CARBONATES								
azurite	0	0	0	0	2	4	0	0
malachite	0	0	0	0	2	4	0	0
chrysocolla	0	0	0	0	2	2	0	0
aurichalcite	0	0	0	0	0	0	0	0
COPPER SULFATES								
brochantite	0	0	0	0	2	1	0	0
chalcanthite	0	0	0	0	0	0	0	0
langite	0	0	0	0	1	0	0	0
gerhardtite	0	0	0	0	0	0	0	0
COPPER ARSENATES								
olivenite	0	0	0	0	1	0	0	0
chalcophyllite	0	0	0	0	1	4	0	0
COPPER PHOSPHATES								
libethenite	0	0	0	0	0	0	0	0
turquoise	0	0	0	0	0	0	0	0
copper silicate, ajoite, papagoi	0	0	0	0	0	0	0	0
LEAD MINERALS								
cerussite	0	0	0	0	0	0	0	0
LEAD SULFOSALTS								
LEAD OXIDES								
coronadite	0	0	0	0	0	0	0	0
LEAD SULFATES								
LEAD ARSENATES								
LEAD PHOSPHATES								
LEAD VANADATES ETC								
ZINC MINERALS								
ZINC OXIDES								
ZINC CARBONATES								
smithsonite	0	0	0	0	0	0	0	0
ZINC SULFATES								
ZINC OTHERS								
hemimorphite (calamine)	0	0	0	0	0	0	0	0
willemite	0	0	0	0	0	0	0	0
SILVER MINERALS								

	Dexing	Dos Pobres	ElSalvador	ElSalvador	El Teniente	El Teniente	Hedley	NickelPlate
acanthite	0	0	0	0	0	0	0	0
SILVER SULFOSALTS								
matildite	0	0	0	0	0	0	0	0
SILVER HALIDES								
chlorargyrite (cerargyrite)	0	0	0	0	0	0	0	0
SILVER TELLURIDES								
spangolite	0	0	0	0	0	0	0	0
IRON MINERALS								
COMMON IRON								
pyrrhotite	0	0	0	0	0	0	5	3
magnetite	1	0	0	0	1	1	0	3
hematite	2	0	0	0	2	5	3	0
limonite (goethite)	0	0	0	0	0	3	3	0
marcasite	0	0	0	0	0	0	0	3
arsenopyrite	0	0	0	0	0	0	5	3
IRON SULFATES								
IRON ARSENATES ETC								
MOLYBDENUM MINERALS								
molybdenite	4	0	0	4	3	4	0	3
ferrimolybdite	0	0	0	0	0	3	0	0
TUNGSTEN MINERALS								
huebnerite	0	0	0	0	0	1	0	0
BISMUTH MINERALS								
native bismuth	0	0	0	0	0	0	0	0
joseite	0	0	0	0	0	0	0	0
hedleyite	0	0	0	0	0	0	3	3
ARSENIC MINERALS								
realgar	0	0	0	0	0	0	0	0
orpiment	0	0	0	0	0	0	0	0
ANTIMONY MINERALS								
stibnite	0	0	0	0	0	1	0	0
stibiconite	0	0	0	0	0	0	0	0
TIN MINERALS								
MANGANESE MINERALS								
manganese oxide	0	0	0	0	0	0	0	0
COBALT MINERALS								
erythrite	0	0	0	0	0	0	0	3
cobaltite	0	0	0	0	0	0	0	3
CADMIUM MINERALS								
NICKEL MINERALS								
millerite	0	0	0	0	0	0	0	0
siegenite	0	0	0	0	0	0	0	0
gersdorffite	0	0	0	0	0	0	1	3
THALLIUM MINERALS								
MERCURY MINERALS								
TELLURIUM MINERALS								
MAGNESIUM MINERALS								

1=rare,3=present,5=common 2=minor,trace;4=loc.abund 0=no mention of mineral	MCAow Hedley	MCAow McCoy	MCAow McCoy	MCAow McCoy	MCAow McCoy	MCAow Morenci	MCAow Morenci
mineral reference	60	61	62	63	64	65	66
COMMON SULFIDES							
pyrite	0	3	3	5	5	5	0
chalcopyrite	5	0	3	5	5	5	5
galena	0	3	1	3	0	1	3
sphalerite	0	0	0	3	3	3	3
bornite	0	0	0	0	0	0	1
PRECIOUS METALS							
native silver	0	0	3	0	0	1	3
electrum	0	0	3	0	0	0	0
native gold	0	3	3	0	3	1	3
COPPER MINERALS							
native copper	0	0	0	0	0	3	3
COPPER SULFIDES							
chalcocite	0	0	0	0	2	5	5
covellite	0	0	0	0	0	3	1
COPPER SULFOSALTS							
enargite	0	0	0	0	0	0	0
tetrahedrite	0	0	0	0	0	0	0
tennantite	0	0	0	0	0	0	0
famatinite	0	0	0	0	0	0	0
COPPER OXIDES							
tenorite	0	0	0	0	0	2	0
copper pitch	0	0	0	0	0	0	3
cuprite	0	0	0	0	0	2	3
atacamite	0	0	0	0	0	0	0
COPPER CARBONATES							
azurite	0	3	3	0	3	2	3
malachite	0	3	3	0	3	3	3
chrysocolla	0	0	0	0	0	3	3
aurichalcite	0	0	0	0	0	0	0
COPPER SULFATES							
brochantite	0	0	0	0	0	2	5
chalcanthite	0	0	0	0	3	0	0
langite	0	0	0	0	0	0	0
gerhardtite	0	0	0	0	3	0	0
COPPER ARSENATES							
olivenite	0	0	0	0	0	0	0
chalcophyllite	0	0	0	0	0	0	0
COPPER PHOSPHATES							
libethenite	0	0	0	0	0	0	3
turquoise	0	0	0	0	0	3	0
copper silicate, ajoite, papagoi	0	0	0	0	0	0	0
LEAD MINERALS							
cerussite	0	3	3	0	0	0	0
LEAD SULFOSALTS							
LEAD OXIDES							
coronadite	0	0	0	0	0	0	3
LEAD SULFATES							
LEAD ARSENATES							
LEAD PHOSPHATES							
LEAD VANADATES ETC							
ZINC MINERALS							
ZINC OXIDES							
ZINC CARBONATES							
smithsonite	0	0	0	0	0	0	3
ZINC SULFATES							
ZINC OTHERS							
hemimorphite (calamine)	0	0	0	0	0	0	3
willemite	0	0	0	0	0	0	3
SILVER MINERALS							

	Hedley	McCoy	McCoy	McCoy	McCoy	Morenci	Morenci
acanthite	0	0	0	0	0	0	0
SILVER SULFOSALTS							
matildite	0	0	0	0	0	0	0
SILVER HALIDES							
chlorargyrite (cerargyrite)	0	3	3	0	0	0	0
SILVER TELLURIDES							
spangolite	0	0	0	0	0	0	3
IRON MINERALS							
COMMON IRON							
pyrrhotite	5	0	3	0	5	0	0
magnetite	0	0	0	0	3	0	3
hematite	0	0	0	0	0	3	3
limonite (goethite)	0	0	0	0	0	3	3
marcasite	0	0	0	0	0	0	0
arsenopyrite	5	0	0	0	0	5	3
IRON SULFATES							
IRON ARSENATES ETC							
MOLYBDENUM MINERALS							
molybdenite	0	0	0	0	0	5	3
ferrimolybdite	0	0	0	0	0	0	0
TUNGSTEN MINERALS							
huebnerite	0	0	0	0	0	0	0
BISMUTH MINERALS							
native bismuth	0	0	0	0	0	0	0
joseite	0	0	0	0	0	0	0
hedleyite	0	0	0	0	0	0	0
ARSENIC MINERALS							
realgar	0	0	0	0	0	3	3
orpiment	0	0	0	0	3	3	3
ANTIMONY MINERALS							
stibnite	0	0	0	0	0	0	0
stibiconite	0	0	0	0	0	3	0
TIN MINERALS							
MANGANESE MINERALS							
manganese oxide	0	0	0	0	0	0	3
COBALT MINERALS							
erythrite	0	0	0	0	0	0	0
cobaltite	0	0	0	0	0	0	0
CADMIUM MINERALS							
NICKEL MINERALS							
millerite	0	0	0	0	0	0	0
siegenite	0	0	0	0	0	0	0
gersdorffite	0	0	0	0	0	0	0
THALLIUM MINERALS							
MERCURY MINERALS							
TELLURIUM MINERALS							
MAGNESIUM MINERALS							

1=rare,3=present,5=common 2=minor,trace;4=loc.abund 0=no mention of mineral mineral reference	MCAr Alligator Rid 67	MCAr Gold Strike 68	MCAr Carlin 69	MCAr Carlin 70	MCAr Carlin 71	MCAr Potosi, NV 72	MCAr Potosi, NV 73	MCAr Getchell 74
COMMON SULFIDES								
pyrite	5	5	0	5	5	2	3	5
chalcopyrite	0	3	0	3	0	2	3	3
galena	0	0	0	3	1	1	3	3
sphalerite	0	1	0	3	1	0	3	3
PRECIOUS METALS								
native silver	0	0	0	0	0	0	0	0
electrum	0	0	0	0	0	0	0	0
native gold	3	0	0	3	3	0	0	3
COPPER MINERALS								
COPPER SULFIDES								
chalcocite	0	0	0	3	0	0	0	0
covellite	0	0	0	3	0	0	0	0
COPPER SULFOSALTS								
tetrahedrite	0	0	0	3	0	0	0	0
tennantite	0	0	0	3	3	0	0	0
famatinite	0	0	0	0	0	0	0	0
COPPER OXIDES								
COPPER CARBONATES								
azurite	0	0	0	0	0	0	0	0
malachite	0	3	0	0	0	0	0	0
COPPER SULFATES								
COPPER ARSENATES								
COPPER PHOSPHATES								
LEAD MINERALS								
LEAD SULFOSALTS								
jordanite	0	0	0	3	3	0	0	0
geocronite	0	0	0	0	0	0	0	0
gratonite	0	0	0	3	0	0	0	0
bournonite	0	0	0	0	0	0	0	0
plagionite	0	0	0	0	0	0	0	0
jamesonite	0	0	0	0	0	0	0	0
boulangerite	0	0	0	3	0	0	0	0
LEAD OXIDES								
LEAD SULFATES								
LEAD ARSENATES								
carminite	0	0	0	0	3	0	0	0
LEAD PHOSPHATES								
LEAD VANADATES ETC								
ZINC MINERALS								
ZINC OXIDES								
ZINC CARBONATES								
ZINC SULFATES								
ZINC OTHERS								
SILVER MINERALS								
argentite	0	0	0	0	0	0	0	0
SILVER SULFOSALTS								
laffittite	0	0	0	0	0	0	0	0
proustite	0	0	0	0	0	0	0	0
freibergite	0	0	0	0	0	0	0	0
jalpaite	0	0	0	0	0	0	0	0
SILVER HALIDES								
chlorargyrite (cerargyrite)	0	0	0	0	0	0	0	0
SILVER TELLURIDES								
IRON MINERALS								
COMMON IRON								
pyrrhotite	0	0	0	1	0	2	0	0
magnetite	0	0	0	0	0	0	0	0
limonite (goethite)	0	0	0	0	0	0	0	0

	Alligator Rid	Gold Strike	Carlin	Carlin	Carlin	Potosi, NV	Potosi, NV	Getchell
marcasite	0	0	0	0	0	0	0	0
arsenopyrite	0	0	0	0	0	0	0	0
IRON SULFATES								
IRON ARSENATES ETC								
scorodite	0	0	0	0	3	0	0	0
MOLYBDENUM MINERALS								
molybdenite	0	0	0	3	0	2	3	3
ilsemannite	0	0	0	0	0	0	0	0
ferrimolybdite	0	0	0	0	0	0	0	0
TUNGSTEN MINERALS								
scheelite	0	3	0	0	0	5	5	5
BISMUTH MINERALS								
bismuthinite	0	0	0	0	0	0	3	0
ARSENIC MINERALS								
elemental arsenic	0	0	0	3	3	0	0	0
realgar	0	0	3	3	5	0	0	3
orpiment	0	0	3	3	5	0	0	3
pararealgar	0	0	0	0	0	0	0	0
getchellite	0	0	0	3	0	0	0	0
arsenolite	0	0	0	0	3	0	0	0
weilite	0	0	0	0	0	0	0	0
picropharmacolite	0	0	0	0	0	0	0	0
ANTIMONY MINERALS								
stibnite	3	3	0	3	5	0	0	0
metastibnite	0	0	0	0	0	0	0	0
TIN MINERALS								
teallite	0	0	0	0	0	0	0	0
MANGANESE MINERALS								
COBALT MINERALS								
linnaeite	0	0	0	0	0	0	0	0
CADMIUM MINERALS								
NICKEL MINERALS								
THALLIUM MINERALS								
weissbergite	0	0	0	3	0	0	0	0
avicennite	0	0	3	3	0	0	0	0
ellisite	0	0	0	3	0	0	0	0
christite	0	0	0	3	0	0	0	0
galkhaite	0	0	0	3	0	0	0	0
lorandite	0	0	0	3	0	0	0	0
carlinite	0	0	3	3	0	0	0	0
MERCURY MINERALS								
cinnabar	0	0	0	3	5	0	0	0
schuetteite	0	0	0	0	3	0	0	0
coloradoite	0	0	0	0	0	0	0	0
TELLURIUM MINERALS								
MAGNESIUM MINERALS								

67=Ilchik, 1991,1990
68=Lowe et al.,1985
69=Radtke et al. 1978
70=Radtke 1985
71=Hausen & Key 1968
72=Bonham,1985
73=Hotz & Willden, 1964
74=Silberman et al., 1974
75=Kretschmer, 1984
76=Foster & Kretschmer 1991
77=Powers 1978
78=Tooker 1985
79=Stollberg & Dunning, 1985
80=Dunning 1988
81=Nanna et al., 1987
82=Joraleman 1951
83=Kokinos & Prenn, 1985
84=Kleinhampl & Ziony, 1984
85=Lowe et al., 1985

1=rare,3=present,5=common 2=minor,trace;4=loc.abund 0=no mention of mineral mineral reference	MCAr Preble 75	MCAr Mag-Pinson 76	MCAr Ogee-Pinson 77	MCAr Getchell 78	MCAr Getchell 79	MCAr Getchell 80	MCAr Getchell 81	MCAr Getchell 82
COMMON SULFIDES								
pyrite	4	5	3	3	3	3	3	3
chalcopyrite	2	3	0	0	4	3	3	0
galena	0	3	0	0	0	0	3	0
sphalerite	0	3	0	0	4	0	3	0
PRECIOUS METALS								
native silver	0	0	0	1	0	0	3	3
electrum	0	0	0	0	0	0	0	0
native gold	5	3	0	3	5	3	3	3
COPPER MINERALS								
COPPER SULFIDES								
chalcocite	0	0	0	0	0	0	3	0
covellite	0	3	0	0	0	0	3	0
COPPER SULFOSALTS								
tetrahedrite	0	0	0	0	0	0	0	0
tennantite	0	0	0	0	0	0	0	0
famatinite	0	3	0	0	0	0	0	0
COPPER OXIDES								
COPPER CARBONATES								
azurite	0	0	0	0	0	0	0	0
malachite	0	0	0	0	0	0	0	0
COPPER SULFATES								
COPPER ARSENATES								
COPPER PHOSPHATES								
LEAD MINERALS								
LEAD SULFOSALTS								
jordanite	0	0	0	0	0	0	0	0
geocronite	0	3	0	0	0	0	0	0
gratonite	0	0	0	0	0	0	0	0
bournonite	0	3	0	0	0	0	0	0
plagionite	0	0	0	0	0	0	0	0
jamesonite	0	0	0	0	0	0	3	0
boulangerite	0	0	0	0	0	0	0	0
LEAD OXIDES								
LEAD SULFATES								
LEAD ARSENATES								
carminite	0	0	0	0	0	0	0	0
LEAD PHOSPHATES								
LEAD VANADATES ETC								
ZINC MINERALS								
ZINC OXIDES								
ZINC CARBONATES								
ZINC SULFATES								
ZINC OTHERS								
SILVER MINERALS								
argentite	0	0	0	0	0	0	3	0
SILVER SULFOSALTS								
laffittite	0	0	0	0	1	3	3	0
proustite	0	0	0	0	0	0	0	0
freibergite	0	0	0	0	0	0	0	0
jalpaite	0	0	0	0	0	3	3	0
SILVER HALIDES								
chlorargyrite (cerargyrite)	0	0	0	0	0	0	0	0
SILVER TELLURIDES								
IRON MINERALS								
COMMON IRON								
pyrrhotite	0	0	0	0	0	0	0	2
magnetite	0	0	0	0	1	0	0	3
limonite (goethite)	3	0	0	0	0	0	0	0

	Preble	Mag-Pinson	Ogee-Pinson	Getchell	Getchell	Getchell	Getchell	Getchell
marcasite	0	3	3	3	3	3	0	3
arsenopyrite	0	3	0	3	3	3	3	3
IRON SULFATES								
IRON ARSENATES ETC								
scorodite	0	0	0	0	0	0	0	0
MOLYBDENUM MINERALS								
molybdenite	0	0	0	0	0	0	3	0
ilsemannite	0	0	0	1	1	3	0	3
ferrimolybdite	0	0	0	0	0	3	0	0
TUNGSTEN MINERALS								
scheelite	0	0	0	3	3	0	0	0
BISMUTH MINERALS								
bismuthinite	0	0	0	0	0	0	3	0
ARSENIC MINERALS								
elemental arsenic	0	0	0	0	0	0	3	0
realgar	0	3	0	5	3	3	3	0
orpiment	0	0	0	5	3	3	0	0
pararealgar	0	0	0	0	0	3	0	0
getchellite	0	0	0	1	1	3	0	0
arsenolite	0	0	0	0	0	3	0	0
weilite	0	0	0	0	0	3	0	0
picropharmacolite	0	0	0	0	1	3	0	0
ANTIMONY MINERALS								
stibnite	0	3	0	5	4	3	3	3
metastibnite	0	0	0	0	0	0	0	3
TIN MINERALS								
teallite	0	0	0	0	0	3	3	0
MANGANESE MINERALS								
COBALT MINERALS								
linnaeite	0	0	0	0	0	0	3	0
CADMIUM MINERALS								
NICKEL MINERALS								
THALLIUM MINERALS								
weissbergite	0	0	0	0	0	0	0	0
avicennite	0	0	0	0	0	0	0	0
ellisite	0	0	0	0	0	0	0	0
christite	0	0	0	0	0	0	0	0
galkhaite	0	0	0	1	1	3	3	0
lorandite	0	0	0	0	0	0	0	0
carlinite	0	0	0	0	0	0	3	0
MERCURY MINERALS								
cinnabar	0	3	0	1	4	3	3	3
schuetteite	0	0	0	0	0	0	0	0
coloradoite	0	0	0	0	0	3	3	0
TELLURIUM MINERALS								
MAGNESIUM MINERALS								

1=rare,3=present,5=common 2=minor,trace;4=loc.abund 0=no mention of mineral mineral reference	MCAr Northumber 83	MCAr Northumber 84	MCAr Northumber 85
COMMON SULFIDES			
pyrite	3	0	3
chalcopyrite	0	0	0
galena	0	0	0
sphalerite	0	0	0
PRECIOUS METALS			
native silver	0	0	0
electrum	0	0	0
native gold	3	3	3
COPPER MINERALS			
COPPER SULFIDES			
chalcocite	0	0	0
covellite	0	0	0
COPPER SULFOSALTS			
tetrahedrite	0	0	0
tennantite	0	0	0
famatinite	0	0	0
COPPER OXIDES			
COPPER CARBONATES			
azurite	3	3	0
malachite	3	3	0
COPPER SULFATES			
COPPER ARSENATES			
COPPER PHOSPHATES			
LEAD MINERALS			
LEAD SULFOSALTS			
jordanite	0	0	0
geocronite	0	0	0
gratonite	0	0	0
bournonite	0	0	0
plagionite	0	0	0
jamesonite	0	0	0
boulangerite	0	0	0
LEAD OXIDES			
LEAD SULFATES			
LEAD ARSENATES			
carminite	0	0	0
LEAD PHOSPHATES			
LEAD VANADATES ETC			
ZINC MINERALS			
ZINC OXIDES			
ZINC CARBONATES			
ZINC SULFATES			
ZINC OTHERS			
SILVER MINERALS			
argentite	0	0	0
SILVER SULFOSALTS			
laffittite	0	0	0
proustite	3	3	0
freibergite	3	0	0
jalpaite	0	0	0
SILVER HALIDES			
chlorargyrite (cerargyrite)	3	3	0
SILVER TELLURIDES			
IRON MINERALS			
COMMON IRON			
pyrrhotite	0	0	0
magnetite	0	0	0
limonite (goethite)	0	0	0

	Northumber	Northumber	Northumber
marcasite	0	0	0
arsenopyrite	3	0	3
IRON SULFATES			
IRON ARSENATES ETC			
scorodite	3	0	0
MOLYBDENUM MINERALS			
molybdenite	0	0	0
ilsemannite	0	0	0
ferrimolybdite	0	0	0
TUNGSTEN MINERALS			
scheelite	0	0	0
BISMUTH MINERALS			
bismuthinite	0	0	0
ARSENIC MINERALS			
elemental arsenic	0	0	0
realgar	0	0	3
orpiment	0	0	3
pararealgar	0	0	0
getchellite	0	0	0
arsenolite	0	0	0
weilite	0	0	0
picropharmacolite	0	0	0
ANTIMONY MINERALS			
stibnite	0	0	3
metastibnite	0	0	0
TIN MINERALS			
teallite	0	0	0
MANGANESE MINERALS			
COBALT MINERALS			
linnaeite	0	0	0
CADMIUM MINERALS			
NICKEL MINERALS			
THALLIUM MINERALS			
weissbergite	0	0	0
avicennite	0	0	0
ellisite	0	0	0
christite	0	0	0
galkhaite	0	0	0
lorandite	0	0	0
carlinite	0	0	0
MERCURY MINERALS			
cinnabar	0	0	3
schuetteite	0	0	0
coloradoite	0	0	0
TELLURIUM MINERALS			
MAGNESIUM MINERALS			

Mineral Names and Formulas

mineral name	formula
COMMON SULFIDES	
pyrite	FeS2
chalcopyrite	Cu2Fe2S4
galena	PbS
sphalerite	ZnS
bornite	Cu5FeS4
PRECIOUS METALS	
native silver	Ag
electrum	(Au,Ag)
native gold	Au
COPPER MINERALS	
native copper	Cu
COPPER SULFIDES	
chalcocite	Cu2S
neodigenite	blue chalcocite
covellite	CuS
cubanite	CuFe2S3
COPPER SULFOSALTS	
enargite	Cu3AsS4
tetrahedrite	(Cu,Fe)12Sb4S13
tennantite	(Cu,Fe)12As4S13
chalcostibite	CuSbS2
luzonite	Cu3(As,Sb)S4
famatinite	Cu3SbS4
COPPER OXIDES	
tenorite	CuO
crednerite	CuMnO2
copper pitch	CuO.SiO2.MnO2.H2O
cuprite	Cu2O
atacamite	Cu2Cl(OH)3
melaconite=tenorite	CuO
chalcotrichite (var. cuprite)	Cu2O
COPPER CARBONATES	
azurite	Cu3(CO3)2(OH)2
malachite	Cu2(CO3)(OH)2
chrysocolla	Cu,Al)2H2Si2O5(OH)4 . n H2O
rosasite	(Cu,Zn)2(CO3)(OH)2
aurichalcite	(Zn,Cu)5(CO3)2(OH)6
COPPER SULFATES	
brochantite	Cu4(SO4)(OH)6
chalcanthite	CuSO4 . 5H2O
antlerite	Cu3(SO4)(OH)4
cyanotrichite	Cu4Al2(SO4)(OH)12 . 2 H2O
langite	Cu4(SO4)(OH)6.2H2O
gerhardtite	Cu2(NO3)(OH)3
antlerite	Cu3SO4(OH)4
cuprogoslarite	(Zn,Cu)SO4 . 7 H2O
connellite	Cu19Cl4(SO4)(OH)32 . 3 H2O
COPPER ARSENATES	
tyrolite	CaCu5(AsO4)2(CO3)(OH)4 . 6 H2O
cornwallite (erinite)	Cu5(AsO4)2(OH)4 . H2O
chenevixite	Cu2Fe2(AsO4)2(OH)4 . H2O
olivenite	Cu2AsO4(OH)
chalcophyllite	Cu18Al2(AsO4)3(SO4)3(OH)27 . 33H2O
conichalcite	CaCu(AsO4)(OH)
zeunerite	Cu(UO2)2(AsO4)2 . 10-16 H2O
COPPER PHOSPHATES	
libethenite	Cu2(PO4)(OH)
turquoise	CuAl6(PO4)4(OH)8 . 5H2O
copper silicate, ajoite, papa	(K,Na)Cu7AlSi9O24(OH)6 . 3 H2O

mineral name	formula
LEAD MINERALS	
anglesite	PbSO4
cerussite	PbCO3
meneghinite	Pb13Cu7S24
LEAD SULFOSALTS	
jordanite	Pb14(As,Sb)6S23
geocronite	Pb14(Sb,As)6S23
gratonite	Pb9As4S15
semseyite	Pb9Sb8S21
bournonite	PbCuSbS3
plagionite	Pb5Sb8S17
jamesonite	Pb4FeSb6S14
cylindrite	Pb3Sn4FeSb2S14
andorite	PbAgSb3S6
plumosite	boulangerite or jamesonite
boulangerite	Pb5Sb4S11
zinkenite	Pb6Sb14S27
bindheimite	Pb2Sb2O6(O,OH)
frankeite	Pb5Sn3Sb2S14
LEAD OXIDES	
minium	Pb2+2Pb+4O4
massicot	PbO
cotunnite	PbCl2
quenselite	PbMnO2 . OH
coronadite	Pb(Mn+4,Mn+2)8O16
lead oxychloride	Pb O Cl
phosgenite	(Pb,Cl)2CO3
LEAD SULFATES	
linarite	PbCu(SO4)(OH)2
leadhillite	Pb4(SO4)(CO3)2(OH)2
beaverite	Pb(Cu,Fe,Al)3(SO4)2(OH)
plumbojarosite	PbFe6(SO4)4(OH)6
osarizawaite	PbCuAl2(SO4)2(OH)6
LEAD ARSENATES	
carminite	PbFe2+3(AsO4)2(OH)2
mimetite	Pb5(AsO4)3Cl
duftite	PbAsO
bayldonite	(Pb,Cu)3(AsO4)2(OH)2
hidalgoite	PbAl3(SO4)(AsO4)(OH)6
LEAD PHOSPHATES	
corkite	PbFe3'"(PO4)(SO4)(OH)6
pyromorphite	Pb5(PO4)3Cl
lead oxide phosphate	5PbO . Pb3(PO4)2
LEAD VANADATES ETC	
mottramite	PbCu(VO4)(OH)
vanadinite	Pb5(VO4)3Cl
descloizite	PbZn(VO4)(OH)
wulfenite	PbMoO4
altaite	PbTe

mineral name	formula
ZINC MINERALS	
wurtzite	(Zn,Fe)S
ZINC OXIDES	
hetaerolite	ZnMn2+3O4
chalcophanite	ZnMn3O7 . 2H2O
hydrohetaerolite	Zn2Mn4+3O8 . H2O
ZINC CARBONATES	
hydrozincite	Zn5(CO3)2(OH)6
smithsonite	ZnCO3
ZINC SULFATES	
pisanite	(Fe,Cu,Zn)SO4 . 7 H2O
ferrogoslarite	(Zn,Fe)SO4 . 7 H2O
gunningite	(Zn,Fe)SO4 . H2O
ZINC OTHERS	
adamite	Zn2(AsO4)(OH)
hemimorphite (calamine)	Zn4Si2O7(OH)2 . H2O
willemite	Zn2SiO4
hemimorphite	Zn4Si2O7(OH)2 . H2O
SILVER MINERALS	
argentite	Ag2S
acanthite	Ag2S
stromeyerite	AgCuS
silver plumbate	Ag5Pb2O6(?)
argentojarosite	AgFe3(SO4)2(OH)6
SILVER SULFOSALTS	
pyrargyrite (ruby silver)	Ag3SbS3
polybasite	(Ag,Cu)16Sb2S11
laffittite	AgHgAsS3
stephanite	Ag5SbS4
proustite	Ag3AsS3
freibergite	(Ag,Cu,Fe)12(Sb,As)4S13
miargyrite	AgSbS2
matildite	AgBiS2
freieslebenite	AgPbSbS3
jalpaite	Ag3CuS2
pearceite	(Ag,Cu)16As2S11
SILVER HALIDES	
miersite	(Ag,Cu)I
chlorargyrite (cerargyrite)	AgCl
silver halides iodyrite, brom	AgI, AgBr, AgCl
bromargyrite (bromyrite)	AgBr
chlorargyrite (embolite)	Ag(Cl,Br)
bromargyrite (bromyrite)	AgBr
iodargyrite	AgI
SILVER TELLURIDES	
krennerite	(Au,Ag)Te2
sylvanite	AgAuTe4
hessite	Ag2Te
calaverite	(Au,Ag)Te2
petzite	Ag3AuTe2
spangolite	Au6Al(SO4)(OH)12Cl . 3H2O

mineral name	formula
IRON MINERALS	
COMMON IRON	
pyrrhotite	Fe(1-x)S
magnetite	Fe+2Fe2+3O4
hematite	Fe2O3
limonite (goethite)	Fe+3O(OH)
pentlandite	(Fe,Ni)9S8
marcasite	FeS2
arsenopyrite	FeAsS
IRON SULFATES	
halotrichite	Fe"Al2(SO4)4 . 22 H2O
bilinite	Fe"Fe'"2(SO4)4 . 22H2O
melanterite	FeSO4 . 7 H2O
voltaite	K2Fe'"5Fe"4(SO4)12 . 18 H2O
szomolnokite	FeSO4 . H2O
copiapite	Fe",Mg)Fe'"4(SO4)6(OH)2 . 2 OH2O
siderotile	FeSO4 . 5 H2O
coquimbite	Fe2xAlx(SO4)3 . 9 H2O
jarosite	KFe3+3(SO4)2(OH)6
kornelite	Fe4(SO4)6 . 15 H2O
rhomboclase	HFe(SO4)2 . 4 H2O
melanterite	Fe+2SO4 . 7 H2O
roemerite	Fe"Fe2'"(SO4)4 . 14 H2O
IRON ARSENATES ETC	
pharmacosiderite	KFe4+3(AsO4)3(OH)4 . 6-7 H2O
scorodite	Fe+3AsO4 . 2H2O
tinticite	Fe'"2(PO4)2(OH)3 . 3 1/2 H2O
hisingerite	Fe'"2Si2O5(OH)4 . 2 H2O
MOLYBDENUM MINERALS	
molybdenite	MoS2
powellite	CaMoO4
ilsemannite	Mo3O8 . nH2O(?)
ferrimolybdite	Fe2+3(MoO4)3 . 8H2O(?)
TUNGSTEN MINERALS	
huebnerite	MnWO4
scheelite	CaWO4
wolframite	(Fe,Mn)WO4
BISMUTH MINERALS	
native bismuth	Bi
bismuthinite	Bi2S3
klaprothite	Cu3BiS3 3 CuBiS2
bismite	Bi2O3
arsenobismite	Bi2(AsO4)(OH)3
mixite	BiCu6(AsO4)3(OH)6 . 3 H2O
tetradymite	Bi2Te2S
joseite	Bi4Te2S
hedleyite	Bi7Te3
tetradymite	Bi2Te2S
ARSENIC MINERALS	
elemental arsenic	As
realgar	AsS
orpiment	As2S3
pararealgar	AsS
getchellite	AsSbS3
arsenolite	As2O3
claudetite 2	As2O3
weilite	CaHAsO4
pharmacolite	CaHAsO4 . 2H2O
guerinite	Ca5H2(AsO4)4 . 9 H2O
haidingerite	CaHAsO4 . H2O
picropharmacolite	H2Ca4Mg(AsO4)4 . 11H2O

mineral name	formula
ANTIMONY MINERALS	
stibnite	Sb2S3
metastibnite	Sb2S3
cervantite	Sb2O3.Sb2O5
stibiconite	Sb+3Sb2+5O6(OH)
antimony ochre	
TIN MINERALS	
cassiterite	SnO2
teallite	PbSnS2
stannite	Cu2FeSnS4
MANGANESE MINERALS	
alabandite	MnS
pyrolusite	MnO2
manganese oxide	Mn O
manjiroite	(Na,K)(Mn+4,Mn+2)8O16 . n H2O
cryptomelane	K(Mn+4,Mn+2)8O16
manganite	MnO(OH)
hollandite	Ba(Mn+4,Mn+2)8O16
rhodochrosite	MnCO3
manganocalcite	(Ca,Mn")CO3
COBALT MINERALS	
erythrite	Co3(AsO4)2 . 8H2O
linnaeite	CoCo2S4
cobaltite	CoAsS
CADMIUM MINERALS	
greenockite	CdS
NICKEL MINERALS	
millerite	NiS
siegenite	(Ni,Co)3S4
gersdorffite	NiAsS
THALLIUM MINERALS	
weissbergite	TlSbS2
avicennite	Tl2O3
ellisite	Tl3AsS3
christite	TlHgAsS3
galkhaite	(Cs,Tl)(Hg,Cu,Zn)6(As,Sb)4S12
lorandite	TlAsS2
carlinite	Tl2S
MERCURY MINERALS	
cinnabar	HgS
polhemusite	(Zn,Hg)S
schuetteite	Hg3(SO4)O2
coloradoite	HgTe

mineral name	formula
TELLURIUM MINERALS	
tellurium	Te
sonoraite	FeTeO3(OH) . H2O
spiroffite	(Mn,Zn)2Te3O8
rodalquilarite	H3Fe2(TeO3)4Cl
tlapallite	H6(Ca,Pb)2(Cu,Zn)3(SO4)(TeO3)4TeO
winstanleyite	TiTe3O8
xocomecatlite	Cu3(TeO4)(OH)4
schieffelinite	Pb(Te,S)O4 . H2O
dugganite	Pb3Zn3(TeO6)x(AsO4)2-x(OH)6-3x
quetzalcoatlite	Zn8Cu4(TeO3)3(OH)18
fairbankite	PbTeO3
paratellurite	TeO2
emmonsite	Fe2Te3O9 . 2 H2O
dunhamite	PbTeO3
girdite	H2Pb3(TeO3)TeO6
parakhinite	Cu3PbTeO4(OH)6
oboyerite	H6Pb6(TeO3)3(TeO6)2 . 2 H2O
khinite	Cu3PbTeO4(OH)6
rickardite	Cu7Te5
empressite	AgTe
frohbergite	FeTe2
MAGNESIUM MINERALS	
kieserite	MgSO4 . H2O
epsomite	MgSO4 . 7 H2O

mineral formulas from Fleischer, 1983

APPENDIX G: TRACE ELEMENT DATA ON MINERALIZED SAMPLES

Obtained from Stanley B. Keith, MagmaChem Exploration, Inc.

Key to Appendix G:

ore type	dist	mining district	ST	County	#smpl
MCA12A	ALLI	Alligator Ridge	NV	White Pine	12
MCA12C	BASQ	Basque (Shon, Sherman, Bloody Run)	NV	Humboldt	4
MCA12A	CARL	Carlin (Lynn)	NV	Eureka	35
MCA12B	CHIM	Chimney Creek North (Potosi, Getchell)	NV	Humboldt	242
MCA15D	GETC	Getchell (Potosi)	NV	Humboldt	91
MCA12A	GSTR	Goldstrike (Lynn, Gold Strike)	NV	Elko-Eureka	27
MCA12B	MAGG	Maggie Creek (Schroeder, Gold Quarry)	NV	Elko-Eureka	23
MCA12A	NUMB	Northumberland	NV	Nye	24
MCA15D	PINS	Pinson (Potosi)	NV	Humboldt	18
MCA15C	POTO	Potosi (Getchell)	NV	Humboldt	4
MCA15D	PREB	Preble (Golconda)	NV	Humboldt	16
MCA12B	RAIN	Rain (Carlin)	NV	Eureka-Elko	158
					654
MCA14B	AJO	Ajo (production)	AZ	Pima	8
MCA14A	CCAD	Copper Canyon (Galena Can.) (Battle Mtn.)	NV	Lander	121
MCA14E	CCAH	Cu Canyon Zn. H zone	NV	Lander	158
MCA14D	CCFT	Cu Canyon, Fortitude (Battle Mtn.)	NV	Lander	14
MCA14B	DEXI	Dexing	?	Jiangxi	3
MCA14B	DSPO	Dos Pobres	AZ	Graham	4
MCA14B	ELSA	El Salvador	?	?	5
MCA14B	ELTE	El Teniente	?	?	5
MCA14D	HEDL	Hedley (Nickel Plate Mine)	BC	?	4
MCA14D	MCCO	McCoy gold skarn	NV	Lander	19
MCA14B	MORE	Morenci	AZ	Greenlee	10
MCA14F	MORE	Morenci 14F zone	AZ	Greenlee	8
MCA14G	MORE	Morenci 14G zone	AZ	Greenlee	1
MCA14H	MORE	Morenci MCA14H zone	AZ	Greenlee	1
					361
MCA14C	BETH	Bethlehem	BC	?	3
MCA14C	CHRI	Christmas	AZ	Gila-Pinal	8
MCA16	ELKM	Elk Mountain	NV	Elko	7
MCA16	MILL	Mill City (Tungsten, Central)	NV	Pershing	21
MCA14F	MNCK	Mineral Creek 14F zone (Ray)	AZ	Pinal	12
MCA14C	MNCK	Mineral Creek (Ray)	AZ	Pinal	14
MCA14F	MNPK	Mineral Park (Wallapai m.d.)	AZ	Mohave	0
MCA14C	MNPK	Mineral Park (Wallapai m.d.)	AZ	Mohave	197
MCA14H	MNPK	Mineral Park (Wallapai m.d.)	AZ	Mohave	0
MCA14G	MNPK	Mineral Park (Wallapai m.d.)	AZ	Mohave	0
MCA14C	RMTN	Red Mountain	AZ	Santa Cruz	9
MCA14H	RMTN	Red Mountain MCA14H zone	AZ	Santa Cruz	1
MCA14C	SIES	Sierrita-Esperanza	AZ	Pima	12
MCA14G	TWIN	Twin Buttes-Mission 14G zone (Pima m.d.)	AZ	Pinal	3
MCA14C	TWIN	Twin Buttes-Mission (Pima m.d.)	AZ	Pima	3
MCA14C	VALC	Valley Copper	BC	?	3
					293
MAC28	LLA2	Llallagua	?	?	15
					15
MAC29	CHCR	Cherry Creek (Egan Canyon, Gold Canyon)	NV	White Pine	8
MAC29B	CHCB	Cherry Creek (polymetallic zone)	NV	White Pine	3
MAC29A	CHCA	Cherry Creek (proximal W zone)	NV	White Pine	5
MAC29A	KINS	Kinsley	NV	Elko	7
MAC29	KINS	Kinsley (Kingsley)	NV	Elko-White Pine	0
MAC29A	LINK	Linka	NV	Lander	6
MAC24	RAIL	Railroad (Bullion)	NV	Elko	27
MAC24	SNTE	Santa Eulalia	?	Chihuahua	5
MAC29B	SWAL	Swales Mountain	NV	Elko	7
MAC23	TAYL	Taylor	NV	White Pine	22
MAC29	TEMP	Tempiute	NV	Lincoln	17
MAC29C	TEMC	Tempiute (peripheral Ag zone)	NV	Lincoln	5
MAC29A	TEMA	Tempiute (proximal W zone)	NV	Lincoln	11
					123
MAC25	CSTL	Castle	MT	Meagher	7
MAC25	PARK	Park City	UT	Summit	43
MAC25	TINT	Tintic	UT	Juab-Utah	4
MAC25	TOMB	Tombstone	AZ	Cochise	5
					59
				total	1483

min.dist	sample no.	Ag	As	Au	Ba	Be	Bi	B	Cd	Co	Cr	Cu
CSTL	881264	13.4	1016	0.029	740	0	0.231	3	0.231	0.1	198	113
CSTL	881265	602	416	<0.0005	230	4	0.24	8	0.24	0.1	85	232
CSTL	881266	15.3	833	<0.0005	1200	3	0.24	21	0.24	7	91	474
CSTL	881267	18.6	3627	<0.0005	20	2	22.8	7	0.238	0.1	86	1301
CSTL	881268	166	3552	0.06	800	7	0.24	9	0.24	0.1	60	52.7
CSTL	881269	8.21	921	0.03	100	8	0.245	24	1.5	6	58	257
CSTL	881270	65.7	2472	<0.0005	150	2	4.52	4	8.4	4	95	348
PARK	79-11	1690	1750	1.39	2600	0.8	10	0	255	4	610	8500
PARK	79-13	925	2650	0.37	66	0.4	<5	0	1140	<2	50	6200
PARK	79-16	660	2400	0.81	29	0.3	106	0	58	<2	138	4500
PARK	79-4	640	3150	0.25	5	0.2	16	0	500	2	625	9300
PARK	79-8	1130	8900	0.75	15	<.2	<5	0	1500	<2	190	4600
PARK	8	47	0	0	0	0	0	0	0	0	0	495
PARK	9	65	0	0	0	0	0	0	0	0	0	133
TINT	58-10	405	1480	1	58	0.4	<2	51	37	20	106	5350
TINT	58-11	575	1360	1.33	37	0.4	9	43	48	19	87	4800
TINT	58-3	1140	285	0.58	24	<0.2	14	<5	6	<2	12	370
TINT	58-4	1250	25000	0.086	<2	<0.2	530	5	590	4	13	5600
TOMB	TE-1	1410	33	0.74	6	0.2	<5	0	54	3	21	355
TOMB	TE-10	765	560	2.9	23	0.3	12	0	11	5	415	35500
TOMB	TL-1	2.8	<10	0.002	29	1	<5	0	<1	18	138	176
TOMB	TL-13	450	150	0.94	41	0.6	<5	0	370	<2	30	1660
TOMB	TL-5	1560	455	12.5	71	0.9	17	0	1130	2	70	9500

min.dist	sample no.	Fe	F	Hg	Li	Mn	Mo	Nb	Ni	Pb	Rb	Sb
CSTL	881264	0	330	<0.926	7	271	31	0	7	27200	0	136
CSTL	881265	0	360	<0.962	3	213	48.9	0	14	>96000	0	402
CSTL	881266	0	530	<0.962	12	>20000	58.5	0	11	26500	0	81.8
CSTL	881267	0	700	<0.952	3	155	50.1	0	14	26400	0	914
CSTL	881268	0	450	<0.962	5	96	39.7	0	4	>96000	0	92.6
CSTL	881269	0	490	<0.98	3	5037	36.4	0	38	15100	0	26
CSTL	881270	0	620	<0.917	7	13262	37.2	0	18	26200	0	433
PARK	79-11	10700	0	0	0	2500	200	<2	34	58700	13	4100
PARK	79-13	5200	0	0	0	2100	15	<2	6	64800	<2	4300
PARK	79-16	154000	0	0	0	39	17	<2	10	68800	17	2850
PARK	79-4	22300	0	0	0	1180	<1	<2	21	58300	11	2350
PARK	79-8	16600	0	0	0	1970	<1	<2	10	67600	6	13200
PARK	8	0	0	0	0	14870	0	0	0	494	0	0
PARK	9	0	0	0	0	2150	0	0	0	253	0	0
TINT	58-10	80500	600	0	54	49	7	4	29	74800	<1	1770
TINT	58-11	85300	400	0	69	47	7	1	35	72900	<1	1770
TINT	58-3	2000	100	0	<10	13	<2	<1	<3	67400	<1	174
TINT	58-4	41100	100	0	<10	2	8	<1	6	17400	<1	11300
TOMB	TE-1	11900	0	0	0	<5	<1	<2	6	53300	5	1330
TOMB	TE-10	253000	0	0	0	97	30	<2	14	52700	12	58
TOMB	TL-1	100000	0	0	0	3950	230	3	6	200	<2	<5
TOMB	TL-13	7200	0	0	0	158000	<1	<2	9	7650	<2	970
TOMB	TL-5	75700	0	0	0	14900	3	<2	7	53900	42	635

min.dist	sample no.	Sn	Sr	Te	Ti	Tl	V	W	Y	Zn	Zr
CSTL	881264	<4.63	<5	<4.63	0	<4.63	49	6	0	1625	0
CSTL	881265	<4.8	0	<4.8	0	<4.8	26	12	0	3284	0
CSTL	881266	<4.8	0	<4.8	0	<4.8	169	34	0	26000	0
CSTL	881267	<4.76	0	<4.76	0	<4.76	228	34	0	1404	0
CSTL	881268	<4.80	0	<4.80	0	<4.80	28	12	0	411	0
CSTL	881269	<4.90	0	<4.90	0	<4.90	453	26	0	9662	0
CSTL	881270	<4.58	0	<4.58	0	<4.58	187	27	0	15600	<5
PARK	79-11	<5	146	0	20	4	12	27	4.2	9600	9
PARK	79-13	<5	55	0	26	6	3	<5	7.9	152000	9
PARK	79-16	<5	7	0	425	13	3	77	3.3	5250	5
PARK	79-4	<5	7	0	90	7	4	7	0.8	76800	7
PARK	79-8	<5	4	0	23	46	5	7	1.1	151000	9
PARK	8	0	0	0	0	0	0	0	0	1607	0
PARK	9	0	0	0	0	0	0	0	0	294	0
TINT	58-10	<5	580	0	1490	4	26	<5	5.9	1700	0
TINT	58-11	<5	180	0	1440	18	16	<5	7.3	2750	9
TINT	58-3	<5	545	0	93	<2	<3	<5	<2	86	7
TINT	58-4	6	108	0	14	14	<3	<5	<2	34900	5
TOMB	TE-1	<5	20	0	<10	4	<2	11	<.2	255	2
TOMB	TE-10	<5	79	0	235	<2	5	21	0.3	370	9
TOMB	TL-1	<5	565	0	2050	4	41	<5	9.9	415	9
TOMB	TL-13	96	118	0	86	8	4	<5	3.3	22900	0
TOMB	TL-5	<5	116	0	61	5	7	<5	2	93600	4

min.dist	sample no.	Ag	As	Au	Ba	Be	Bi	B	Cd	Co	Cr	Cu
CHCA	881552	3.34	18.6	0.008	140	4	<0.235	4	0.465	<1	8	16
CHCA	881553	13.6	52.2	0.011	2000	5	<0.242	8	4.22	<1	10	57.9
CHCA	881554	2.95	21.9	0.003	110	6	<0.246	10	0.698	2	12	7.84
CHCA	881555	35.6	14.5	0.013	<20	6	<0.235	9	0.485	<1	26	68.4
CHCA	881556	9.84	8.98	0.001	<20	6	<0.239	7	0.881	<1	47	16.7
CHCB	881557	1086	16.7	0.019	260	4	<0.246	3	11	<1	43	927
CHCB	881558	1200	22.6	0.058	<20	2	<0.246	<2	17.8	<1	36	1347
CHCB	881559	1143	23.7	0.033	<20	4	<0.246	5	16	<1	77	1614
KINS	881580	14.6	400	0.064	<20	3	1.49	8	3	<1	24	2012
KINS	881581	7.78	482	0.067	<20	3	3.26	9	10.6	7	25	24400
KINS	881582	46.5	1143	0.315	60	4	29.6	8	9.22	4	50	13200
KINS	881583	99.4	288	0.044	520	7	26.4	59	13.9	63	49	54600
KINS	881584	15.1	784	0.084	310	4	9.24	15	19.5	43	37	17100
KINS	881585	8.56	295	0.044	20	5	22.8	51	5.16	15	43	14400
KINS	881586	2.01	514	0.028	<20	2	0.543	7	5.99	2	17	851
LINK	880875	4.07	15.1	<0.0005	<20	3	15900	25	<1.96	14	80	257
LINK	880876	0.286	4.61	0.002	<20	3	10	38	0.503	10	43	11.5
LINK	880877	0.323	2.82	0.003	<20	6	45.9	7	0.445	20	86	12
LINK	880878	0.203	2.29	0.003	<20	2	65.7	35	0.589	10	48	12.5
LINK	880879	4.32	3.34	0.006	<20	3	606	23	1.57	21	71	62.3
LINK	880882	0.589	3.71	0.002	<20	<1	16.6	39	0.499	6	54	4.59
RAIL	10	7	<500	0	10000	70	10	15	0	15	10	7000
RAIL	12	20	<500	0	10000	70	200	10	0	20	10	10000
RAIL	13	10	700	0	15000	15	100	15	0	20	30	5000
RAIL	14	20	1000	0	1500	7	100	10	0	20	5	7000
RAIL	15	50	3000	0	3000	1	200	10	0	15	5	2000
RAIL	1532	100	500	0	2000	5	100	2000	0	100	0	>20000
RAIL	1533	300	<200	0	500	1	300	500	>500	30	<10	20000
RAIL	1534	300	300	0	500	30	>1000	500	100	5	15	>20000
RAIL	1535	500	700	0	3000	15	300	3000	500	10	0	>20000
RAIL	16	300	5000	0	1000	1	2000	10	0	10	10	1500
RAIL	17	30	1500	0	5000	20	5	10	0	15	15	50000
RAIL	21	2	500	0	7000	50	5	<10	0	50	5	20000
RAIL	22	30	1000	0	15000	10	150	10	0	30	50	20000
RAIL	24	5	<500	0	20000	5	<5	10	0	30	20	10000
RAIL	24	1	<500	0	7000	5	<5	20	0	20	10	10000
RAIL	27	100	2000	0	10000	10	200	<10	0	50	5	20000
RAIL	28	30	<500	0	7000	15	<5	<10	0	<10	<5	10000
RAIL	30	5	500	0	1000	5	20	10	0	20	10	7000
RAIL	33	15	500	0	1500	2	30	20	0	15	15	2000
RAIL	35	1	<500	0	10000	5	<5	15	0	70	20	10000
RAIL	41	7	1000	0	5000	2	7	<10	0	50	5	5000
RAIL	42	7	1000	0	1000	1	20	<10	0	10	10	2000
RAIL	45	20	500	0	5000	7	100	<10	0	50	<5	5000

min.dist	sample no.	Fe	F	Hg	Li	Mn	Mo	Nb	Ni	Pb	Rb	Sb
CHCA	881552	0	150	<0.094	31	484	0.349	0	<1	52.3	<5	94.2
CHCA	881553	0	100	<0.097	42	2114	0.386	0	<1	290	<5	134
CHCA	881554	0	120	<0.98	41	1215	0.244	0	8	32.6	7	60.6
CHCA	881555	0	340	<0.094	37	290	1.15	0	3	90	22	118
CHCA	881556	0	140	<0.096	3	117	3.58	0	<1	35.6	12	48.8
CHCB	881557	0	80	9.47	38	155	3.21	0	<1	911	<5	713
CHCB	881558	0	130	20.6	32	132	2.63	0	<1	1333	<5	992
CHCB	881559	0	90	19.2	38	158	2.59	0	17	1488	<5	919
KINS	881580	0	570	1.65	43	1279	6.47	0	1	103	17	13.3
KINS	881581	0	310	3.52	25	915	18.1	0	5	136	<5	30.8
KINS	881582	0	340	0.102	23	99	33.1	0	7	1094	22	286
KINS	881583	0	340	1.18	22	1177	16.9	0	28	131	<5	79.6
KINS	881584	0	340	0.288	15	6504	13.3	0	19	1360	<5	286
KINS	881585	0	290	<0.099	5	218	8.74	0	14	449	<5	45.5
KINS	881586	0	270	0.546	39	1387	21	0	4	49.5	<5	24.7
LINK	880875	0	560	0.827	20	5265	1655	0	26	964	1250	9.37
LINK	880876	0	440	0.466	23	6209	309	0	21	6.57	<5	2.46
LINK	880877	0	420	0.17	15	2341	267	0	49	8.55	21	1.42
LINK	880878	0	220	0.399	18	6510	675	0	28	12.1	<5	2.34
LINK	880879	0	280	<0.095	18	6936	825	0	29	269	35	1.23
LINK	880882	0	220	0.32	27	6165	147	0	9	52.3	<5	1.51
RAIL	10	0	0	0	0	10000	2	0	300	100	0	<50
RAIL	12	0	0	0	0	15000	150	0	500	1500	0	<50
RAIL	13	0	0	0	0	5000	20	0	200	1500	0	<50
RAIL	14	0	0	0	0	3000	150	0	20	7000	0	300
RAIL	15	0	0	0	0	3000	100	0	5	15000	0	100
RAIL	1532	200000	0	0	0	>5000	100	0	10	150	0	43
RAIL	1533	30000	0	0	0	>5000	100	0	5	>20000	0	22
RAIL	1534	150000	0	0	0	>5000	100	0	70	1500	0	<100
RAIL	1535	150000	0	0	0	1500	50	0	7	5000	0	71
RAIL	16	0	0	0	0	2000	200	0	5	20000	0	50
RAIL	17	0	0	0	0	2000	5	0	30	1000	0	50
RAIL	21	0	0	0	0	7000	10	0	50	200	0	<50
RAIL	22	0	0	0	0	3000	200	0	20	2000	0	700
RAIL	24	0	0	0	0	7000	15	0	200	100	0	<50
RAIL	24	0	0	0	0	5000	10	0	200	20	0	<50
RAIL	27	0	0	0	0	15000	2000	0	50	50000	0	700
RAIL	28	0	0	0	0	20000	500	0	30	100	0	<50
RAIL	30	0	0	0	0	2000	70	0	15	70	0	<50
RAIL	33	0	0	0	0	3000	50	0	10	1000	0	<50
RAIL	35	0	0	0	0	5000	10	0	200	20	0	<50
RAIL	41	0	0	0	0	10000	20	0	7	500	0	50
RAIL	42	0	0	0	0	3000	50	0	5	100	0	>100
RAIL	45	0	0	0	0	20000	70	0	15	10000	0	<50

min.dist	sample no.	Sn	Sr	Te	Ti	Tl	V	W	Y	Zn	Zr
CHCA	881552	<0.469	380	<0.469	0	<0.469	4	41	<5	52.5	3
CHCA	881553	<0.484	175	<0.484	0	<0.484	5	811	<5	466	3
CHCA	881554	<0.491	245	<0.491	0	<0.491	10	180	<5	53	4
CHCA	881555	<0.47	310	<0.47	0	<0.47	12	31	<5	103	7
CHCA	881556	<0.479	15	<0.479	0	<0.479	1	8	<5	199	5
CHCB	881557	<0.491	330	<0.491	0	<0.491	8	77	9	168	1
CHCB	881558	<0.492	450	<0.492	0	<0.492	6	44	22	251	7
CHCB	881559	1.2	375	<0.492	0	<0.492	4	47	26	838	6
KINS	881580	<0.478	115	0.481	0	<0.478	12	9	<5	120	4
KINS	881581	133	70	6.08	0	<4.80	7	22	8	334	3
KINS	881582	1.26	<5	3.7	0	<0.487	10	58	30	340	2
KINS	881583	134	66	10.8	0	<4.80	26	508	<5	631	8
KINS	881584	<0.495	<5	3.14	0	<0.495	28	302	0	742	5
KINS	881585	1.6	11	3.16	0	<0.495	44	506	6	325	9
KINS	881586	<0.474	72	<0.474	0	<0.474	6	9	<5	177	5
LINK	880875	11.7	50	58	0	<3.93	518	8000		101	<5
LINK	880876	10.1	31	2.89	0	0.553	386	2700	<5	49.1	0
LINK	880877	1.83	100	0.786	0	<0.472	75	781	<5	31.3	6
LINK	880878	12.6	23	3.16	0	<5	447	3210	<5	39.5	4
LINK	880879	3.96	49	3.3	0	<0.474	165	997	9	64.7	9
LINK	880882	13.1	<5	<0.468	0	<0.468	169	1460	<5	28.3	3
RAIL	10	15	70	0	300	0	10	<20	500	50000	0
RAIL	12	30	70	0	500	0	20	30	700	50000	0
RAIL	13	200	100	0	1000	0	70	100	1500	15000	0
RAIL	14	30	20	0	300	0	10	<20	150	10000	0
RAIL	15	150	30	0	700	0	15	30	20	50000	0
RAIL	1532	200	0	0	300	0	15	70	<10	2000	<10
RAIL	1533	150	0	0	70	0	<10	<50	<10	>10000	0
RAIL	1534	100	0	0	150	0	20	70	500	5000	0
RAIL	1535	0	0	0	200	0	10	0	30	>10000	0
RAIL	16	200	20	0	700	0	30	50	10	50000	50
RAIL	17	<10	20	0	700	0	15	<20	500	100000	0
RAIL	21	<10	100	0	500	0	20	<20	700	15000	0
RAIL	22	200	200	0	1000	0	70	150	70	50000	0
RAIL	24	<10	200	0	500	0	50	<20	100	5000	0
RAIL	24	<10	150	0	500	0	15	<20	100	7000	0
RAIL	27	200	100	0	500	0	20	<20	200	50000	0
RAIL	28	<10	100	0	300	0	20	<20	300	5000	0
RAIL	30	200	20	0	700	0	15	150	20	1500	0
RAIL	33	100	50	0	2000	0	50	50	10	2000	0
RAIL	35	<10	150	0	700	0	50	<20	100	2000	0
RAIL	41	20	100	0	700	0	15	<20	150	3000	0
RAIL	42	30	30	0	1000	0	20	<20	20	1500	0
RAIL	45	50	50	0	300	0	10	<20	150	20000	0

min.dist	sample no.	Ag	As	Au	Ba	Be	Bi	B	Cd	Co	Cr	Cu
RAIL	46	2	500	0	1000	2	10	10	0	20	10	3000
RAIL	626	20	<500	0	>10000	3	200	10	0	30	30	10000
RAIL	8	30	<500	0	1000	5	500	10	0	20	20	70000
RAIL	9	30	1500	0	2000	2	200	15	0	50	20	7000
SNTE	R6-807	26.37	60.4	0.01	39	<1	27	10	1280	160	61	1571
SNTE	R6-809	18.49	222	0.008	418	<1	23	20	423	17	210	462
SNTE	R6-830	400.34	946	0.038	296	1	665	20	527	39	74	10464
SNTE	R6-831	113.356	171	0.13	27	<1	174	<10	591	34	110	3198
SNTE	R6-853	25.342	>3000	0.11	967	<1	10	15	85	11	240	28
SWAL	881053	0.168	17.3	<0.05	0	0	<0.248	0	0	0	0	11.9
SWAL	881054	0	1740	0.046	260	<1	0	89	45	18	108	0
SWAL	881055	0.698	46.9	<0.049	1400	3	0.324	8	1	6	49	16.5
SWAL	881056	0	10600	<0.067	1700	2	0	66	109	5	60	0
SWAL	881057	0	692	<0.024	600	3	0	55	68	7	61	0
SWAL	881058	0	140	0.11	1200	2	0	112	47	8	67	0
SWAL	881059	4.07	108	<0.049	140	2	1.55	36	9	10	36	141
TAYL	10B	0	20	0.1	100	0	0	20	0	0	10	<5
TAYL	3A	150	20	0.1	100	0	0	100	11	0	0	50
TAYL	3B	10	0	0.05	0	0	0	0	5.2	0	0	7
TAYL	5A	50	<5	0.1	0	0	0	30	2.8	0	0	10
TAYL	6A	15	<5	0	50	<1	0	50	4.8	0	0	10
TAYL	75263	100	25	0.1	0	0	<.1	<2	34	1	34	105
TAYL	783	200	1000	0.3	1500	0	0	20	0	<5	0	500
TAYL	7A	7	20	0.05	100	<1	0	100	0.1	0	<10	7
TAYL	7B	7	20	0.05	100	<1	0	100	0.1	0	<10	7
TAYL	905	1500	1500	0	100	0	<10	0	500	0	10	10000
TAYL	906	300	0	0	150	0	0	50	0	0	20	150
TAYL	907	10	0	0	500	1	0	200	0	30	300	100
TAYL	9A	3	15	0.35	>5000	1.5	0	50	0.2	0	15	10
TAYL	9B	10	0	0.1	>5000	0	0	70	2.4	0	50	50
TAYL	9C	3	5	0.1	500	0	0	50	0.2	0	70	10
TAYL	D1-125-130	50	0	0	0	0.5	<1	0	0	2	81	0
TAYL	D1-50-55	50	0	0	0	0.5	<1	30	0	1	110	0
TAYL	D10-210-215	50	0	0	50	0.5	2600	0	0	1	16	0
TAYL	D9-60-65	50	0	0	50	0.5	<1	15	0	2	85	0
TAYL	D9-70-75	50	0	0	130	0.5	<1	<10	0	2	42	0
TAYL	J-33	590	627	0.3	22	0	2	2	347	108	47	4417
TAYL	J-34	5550	5841	3.4	815	0	3	5	1	2	162	11
TEMA	1452	0	5	0.05	0	10	0	20	50	20	0	200
TEMA	1453	0	800	0.05	1000	50	0	20	100	150	0	200
TEMA	1454	1	40	0.05	1000	7	10	100	0	0	0	100
TEMA	1455	2	5	0.05	150	30	10	50	0	50	0	2000
TEMA	1456	2	5	0.05	50	30	10	20	0	10	0	1000
TEMA	1457A	2	10	0.05	100	30	0	50	0	0	0	700

min.dist	sample no.	Fe	F	Hg	Li	Mn	Mo	Nb	Ni	Pb	Rb	Sb
RAIL	46	0	0	0	0	2000	70	0	10	15	0	<50
RAIL	626	0	0	0	0	3000	10	0	50	1000	0	<100
RAIL	8	0	0	0	0	5000	100	0	15	15000	0	<50
RAIL	9	0	0	0	0	3000	150	0	20	2000	0	200
SNTE	R6-807	130000	4700	0.205	3	7850	<1	3	<20	2500	13	17.5
SNTE	R6-809	57000	4500	0.09	2	4266	33	27	<20	2100	81	21.4
SNTE	R6-830	120000	>20000	0.22	3	5040	15	16	20	28000	<1	89.1
SNTE	R6-831	190000	6600	0.1	3	9161	19	3	<20	7100	<1	12.5
SNTE	R6-853	180000	8500	0.14	3	20000	2	<1	<20	1900	<1	149
SWAL	881053	0	0	0.161	0	0	1.81	0	0	43		1.18
SWAL	881054	0	500	0	6	408	0	0	66	0	<5	188
SWAL	881055	0	800	0.131	18	325	3.9	0	8	222	140	2.46
SWAL	881056	0	480	0	6	636	0	0	24	0	<5	241
SWAL	881057	0	3000	0	20	2165	0	0	56	0	<5	250
SWAL	881058	0	850	0	3	2297	0	0	25	0	<5	5
SWAL	881059	0	1150	0.118	11	4566	1.55	0	28	476	21	10.6
TAYL	10B	5000	200	0.2	0	100	0	0	<5	0	0	180
TAYL	3A	2000	300	6.5	0	150	0	0	0	200	0	180
TAYL	3B	0	0	0.62	0	1500	0	0	0	100	0	12
TAYL	5A	500	0	0.5	0	3000	0	0	0	50	0	26
TAYL	6A	2000	<100	1.2	0	50	0	0	0	10	0	12
TAYL	75263	0	570	11.4	0	0	22	0	14	550	0	290
TAYL	783	1000	0	0	0	300	0	<20	<5	200	0	>100
TAYL	7A	5000	500	1.1	0	50	0	0	0	30	0	12
TAYL	7B	5000	500	1.1	0	50	0	0	0	30	0	12
TAYL	905	5000	0	0	0	>5000	<5	<20	0	20000	0	10000
TAYL	906	2000	0	0	0	1000	<5	<20	<5	700	0	500
TAYL	907	7000	0	0	0	700	0	<20	70	70	0	<100
TAYL	9A	2000	100	3	0	0	0	0	10	<10	0	3200
TAYL	9B	2000	200	3.8	0	0	0	0	20	300	0	12000
TAYL	9C	3000	<100	1.3	0	10	0	0	20	0	0	3300
TAYL	D1-125-130	3000	395	0	5	1300	0	<5	11	0	8	0
TAYL	D1-50-55	2000	215	0	3	84	0	5	9	0	<5	0
TAYL	D10-210-215	6000	120	0	3	1588	0	<5	7	0	76	0
TAYL	D9-60-65	11500	>20000	0	4	295	0	<5	20	0	<5	0
TAYL	D9-70-75	9500	2770	0	5	209	0	<5	17	0	<5	0
TAYL	J-33	22600	0	22	0	227	13	0	50	17618	0	10222
TAYL	J-34	10700	0	5.5	0	208	7	0	7	33	0	287
TEMA	1452	200000	0	0	0	5000	0	20	0	10	0	2
TEMA	1453	200000	0	0	0	5000	300	0	70	50	0	2
TEMA	1454	150000	0	0	0	3000	30	20	0	100	0	2
TEMA	1455	200000	0	0	0	5000	0	20	20	20	0	2
TEMA	1456	200000	0	0	0	5000	0	20	20	20	0	2
TEMA	1457A	200000	0	0	0	5000	20	20	0	20	0	2

min.dist	sample no.	Sn	Sr	Te	Ti	Tl	V	W	Y	Zn	Zr
RAIL	46	500	30	0	1500	0	30	50	15	150	0
RAIL	626	200	700	0	700	0	70	<100	10	>10000	0
RAIL	8	150	50	0	700	0	20	100	<10	7000	0
RAIL	9	200	50	0	1000	0	30	150	70	7000	0
SNTE	R6-807	<1	47	<0.2	100	<0.5	1	29	<1	235500	5
SNTE	R6-809	34	262	0.2	200	0.5	2	5	17	68000	7
SNTE	R6-830	156	114	0.2	200	1	<1	37	<1	78500	9
SNTE	R6-831	109	29	0.4	<100	0.5	<1	170	<1	86500	1
SNTE	R6-853	<1	218	<0.2	200	1	19	7	<1	9600	8
SWAL	881053	0	0	<0.495	0	<0.495	0	0	0	270	0
SWAL	881054	22	<20	0	0	0	411	6	0	0	<5
SWAL	881055	9	235	<0.493	0	0.507	40	3	15	119	60
SWAL	881056	27	0	0	0	0	93	<6	0	0	<5
SWAL	881057	30	0	0	0	0	184	11	0	0	<5
SWAL	881058	26	10	0	0	0	167	<2	23	0	5
SWAL	881059	<5	445	0.712	0	0.817	48	<2	12	1243	7
TAYL	10B	0	700	0	500	0.2	20	0.5	20	25	0
TAYL	3A	0	0	0	500	2	20	1	<10	1000	0
TAYL	3B	0	500	0	70	0.2	<10	0.5	10	60	0
TAYL	5A	0	300	0	100	0.2	10	0.5	10	35	<10
TAYL	6A	0	0	0	200	0.3	<10	3	10	160	0
TAYL	75263	2	0	1.6	0	0.38	0	0	0	2100	0
TAYL	783	0	<100	0	150	0	<10	0	0	1500	<10
TAYL	7A	0	300	0	700	0.4	20	3.5	15	40	0
TAYL	7B	0	300	0	700	0.4	20	3.5	15	40	0
TAYL	905	20	300	0	100	0	<10	0	<10	10000	0
TAYL	906	0	200	0	500	0	50	0	<10	1000	50
TAYL	907	0	200	0	5000	0	200	0	30	0	0
TAYL	9A	0	500	0	300	0.6	20	1	10	20	0
TAYL	9B	0	300	0	200	2.4	10	0	10	190	0
TAYL	9C	0	500	0	500	0.2	20	0.5	15	50	0
TAYL	D1-125-130	<5	170	0.2	0	0	30	5	<5	0	0
TAYL	D1-50-55	<5	76	2.4	0	0	26	5	<5	0	0
TAYL	D10-210-215	<5	240	2.6	<100	0.5	14	4	<5	0	0
TAYL	D9-60-65	<5	71	1.8	<100	0.5	10	5	<5	0	0
TAYL	D9-70-75	<5	51	2.2	<100	1	9	4	<5	0	0
TAYL	J-33	0	32	0	100	0	156	48	0	3196	0
TAYL	J-34	0	88	0	100	0	265	1	0	23	0
TEMA	1452	0	0	0	100	0	150	10000	0	7000	0
TEMA	1453	20	100	0	100	0	20	100	50	10000	0
TEMA	1454	0	300	0	2000	0	20	50	20	700	0
TEMA	1455	30	0	0	200	0	200	10000	0	2000	0
TEMA	1456	300	0	0	200	0	100	10000	0	500	0
TEMA	1457A	300	100	0	500	0	100	5000	0	500	0

min.dist	sample no.	Ag	As	Au	Ba	Be	Bi	B	Cd	Co	Cr	Cu
TEMA	1458A	0	5	0.05	0	20	0	30	0	0	0	150
TEMA	1458B	0	5	0.05	100	10	0	10	0	0	50	100
TEMA	1459	3	5	0.05	20	20	1000	10	50	0	20	70
TEMA	1460	0	5	0.05	0	30	0	20	0	0	0	1000
TEMA	1461	0	5	0.05	150	5	0	500	0	0	0	50
TEMC	1462	500	300	0.05	0	0	0	10	150	0	0	5000
TEMC	1463	500	400	0.05	0	0	0	10	150	0	0	5000
TEMC	1464	500	220	0.05	20	0	0	20	200	0	0	1000
TEMC	1465	5000	400	0.05	20	0	0	20	200	0	0	1500
TEMC	1466	1500	180	0.05	20	0	0	50	200	0	0	200

min.dist	sample no.	Fe	F	Hg	Li	Mn	Mo	Nb	Ni	Pb	Rb	Sb
TEMA	1458A	200000	0	0	0	5000	0	20	0	10	0	2
TEMA	1458B	100000	0	0	0	5000	2000	20	20	20	0	2
TEMA	1459	100000	0	0	0	5000	100	20	50	700	0	2
TEMA	1460	200000	0	0	0	5000	20	20	0	10	0	2
TEMA	1461	100000	0	0	0	1000	20	50	0	100	0	2
TEMC	1462	5000	0	0	0	1000	0	0	0	20000	0	1000
TEMC	1463	2000	0	0	0	300	0	0	20	20000	0	1000
TEMC	1464	1000	0	0	0	300	10	0	20	10000	0	1000
TEMC	1465	20000	0	0	0	2000	20	0	50	15000	0	1000
TEMC	1466	20000	0	0	0	1500	0	0	50	7000	0	1000

min.dist	sample no.	Sn	Sr	Te	Ti	Tl	V	W	Y	Zn	Zr
TEMA	1458A	200	0	0	300	0	100	7000	0	500	0
TEMA	1458B	50	200	0	1000	0	200	1000	0	500	0
TEMA	1459	150	100	0	700	0	200	1000	50	5000	0
TEMA	1460	20	0	0	70	0	200	1000	0	500	0
TEMA	1461	0	100	0	1500	0	30	50	20	0	0
TEMC	1462	50	0	0	20	0	10	0	0	10000	0
TEMC	1463	0	0	0	50	0	20	0	0	10000	0
TEMC	1464	0	0	0	200	0	100	0	0	5000	0
TEMC	1465	0	0	0	500	0	50	0	0	5000	0
TEMC	1466	0	0	0	500	0	50	0	0	5000	0

min.dist	sample no.	Ag	As	Au	Ba	Be	Bi	B	Cd	Co	Cr	Cu
LLA2	LLallagua-7-4	50.6	<10	0.011	25	0.3	39	0	2250	12	75	995
LLA2	LLallagua-7-5	3.6	<10	0.006	43	0.5	280	0	4	<2	210	15
LLA2	LLallagua-7-6	1160	17900	0.46	34	0.9	485	0	63	12	126	15400
LLA2	LLallagua-7-8	1210	3200	2.7	2	<.2	1130	0	134	<2	116	14700
LLA2	LLallagua-7-9	112	420	0.66	18	12.1	400	0	340	66	62	1970
LLA2	LLallagua-7-12	3.3	<10	0.005	435	6	100	0	<1	3	156	53
LLA2	LLallagua-6-2	8.6	<10	0.039	3	<.2	21100	0	2	2	215	82
LLA2	LLallagua-6-4	0.4	110	0.003	67	1.7	110	0	<1	<2	176	86
LLA2	LLallagua-6-5	124	420	0.67	14	2.1	890	0	215	27	37	200
LLA2	LLallagua-6-6	<0.2	<10	0.002	26	0.4	66	0	<1	<2	188	73
LLA2	LLallagua-6-8	40.3	<10	0.002	<2	<.2	75800	0	4	14	116	1030
LLA2	LLallagua-6-9	138	<10	0.003	<2	<.2	71400	0	<1	13	69	820
LLA2	LLallagua-6-10	260	<10	0.54	12	0.5	3100	0	2050	26	93	605
LLA2	LLallagua-6-13	340	10100	0.9	6	0.4	340	0	85	65	188	13200
LLA2	LLallagua-6-15	58.6	183000	6.35	25	0.3	9300	0	33	4450	84	28

min.dist	sample no.	Fe	F	Hg	Li	Mn	Mo	Nb	Ni	Pb	Rb	Sb
LLA2	LLallagua-7-4	106000	0	0	0	1060	11	<2	4	11500	6	45
LLA2	LLallagua-7-5	4500	0	0	0	430	8	<2	10	154	31	10
LLA2	LLallagua-7-6	222000	0	0	0	55	83	<2	11	700	74	2250
LLA2	LLallagua-7-8	284000	0	0	0	40	31	<2	<2	45600	3	20600
LLA2	LLallagua-7-9	272000	0	0	0	895	31	<2	39	4900	<2	1390
LLA2	LLallagua-7-12	18900	0	0	0	196	11	7	9	80	194	65
LLA2	LLallagua-6-2	24400	0	0	0	415	8	<2	9	760	<2	205
LLA2	LLallagua-6-4	9400	0	0	0	32	30	5	<2	200	9	24
LLA2	LLallagua-6-5	327000	0	0	0	260	38	<2	13	6200	3	955
LLA2	LLallagua-6-6	2400	0	0	0	114	3	<2	7	94	4	<5
LLA2	LLallagua-6-8	5300	0	0	0	<5	<1	<2	9	2550	2	5950
LLA2	LLallagua-6-9	10400	0	0	0	1420	<1	<2	6	1930	6	4250
LLA2	LLallagua-6-10	293000	0	0	0	178	29	<2	700	3700	8	700
LLA2	LLallagua-6-13	285000	0	0	0	95	25	<2	220	136	7	340
LLA2	LLallagua-6-15	286000	0	0	0	37	28	<2	2250	585	12	1950

min.dist	sample no.	Sn	Sr	Te	Ti	Tl	V	W	Y	Zn	Zr
LLA2	LLallagua-7-4	1520	11	0	<10	8	<2	29	0.2	101000	1
LLA2	LLallagua-7-5	530	6	0	140	4	5	295	31.7	435	<2
LLA2	LLallagua-7-6	28900	36	0	345	4	17	138	0.4	1700	0
LLA2	LLallagua-7-8	<5	13	0	14	4	<2	8	<.2	28500	2
LLA2	LLallagua-7-9	2000	665	0	10	174	10	205	28.8	72900	5
LLA2	LLallagua-7-12	335	40	0	1210	24	45	32	11.8	1190	8
LLA2	LLallagua-6-2	860	4	0	<10	15	<2	130	0.4	61	<2
LLA2	LLallagua-6-4	355	13	0	250	49	<2	3150	1060	285	2
LLA2	LLallagua-6-5	750	37	0	<10	96	<2	49	7.2	8400	3
LLA2	LLallagua-6-6	124	9	0	172	<2	<2	345	4.4	82	3
LLA2	LLallagua-6-8	1780	<2	0	32	8	<2	116	2.2	2600	2
LLA2	LLallagua-6-9	1830	7	0	16	16	<2	7150	1	45	<2
LLA2	LLallagua-6-10	1510	16	0	18	370	3	172	2.6	11100	2
LLA2	LLallagua-6-13	17100	61	0	43	5	5	610	<.2	3050	3
LLA2	LLallagua-6-15	<5	36	0	<10	2	<2	225	3.4	2550	3

min.dist	sample no.	Ag	As	Au	Ba	Be	Bi	B	Cd	Co	Cr	Cu
BETH	117-B-	1.3	<10	0.01	350	1.5	<5	0	2	30	250	1440
BETH	117-B-7	0.9	<10	0.006	455	0.7	25	0	5	8	76	1000
BETH	118-9	2.1	<10	14	995	0.9	<5	<2	1	<2	190	3150
CHRI	100-6625	8.6	<10	0.27	23	0.7	27	172	12	86	93	8800
CHRI	100-6655	89.9	23	0.59	16	0.4	<2	120	12	89	24	4800
CHRI	100A	2.7	10	0.044	<2	0.3	<2	250	10	142	255	2350
CHRI	100B	124	<10	0.138	63	0.9	95	74	9	55	20	9600
CHRI	X-1	0.2	56	<0.001	6	0.9	<5	0	136	90	84	184
CHRI	X-2	<0.2	<10	0.012	345	1.4	13	0	<1	13	79	1290
CHRI	X-3	1	<10	<0.001	8	0.5	<5	0	9	65	25	194
CHRI	X-4	0.8	<10	0.026	645	1.1	<5	0	<1	20	79	1720
ELKM	881089	0.114	4.95	0.002	<20	<1	1.27	33	<0.241	12	77	20.9
ELKM	881090	1.48	646	0.006	120	2	0.944	40	3.74	29	48	764
ELKM	881091	0.108	15.7	0.002	90	<1	2.58	8	<0.242	18	65	50.3
ELKM	881092	0.121	23.1	<0.0005	110	3	1.16	32	<0.245	21	26	32.8
ELKM	881093	<0.015	1.56	0.001	<20	3	1.54	56	<0.246	28	45	13.8
ELKM	881094	0.414	16	0.001	560	8	2.35	64	0.456	42	43	212
ELKM	881095	0.061	1.61	<0.0005	1500	1	0.327	9	<0.243	<1	11	24.7
MILL	2657	30	10	0	0	1	150	10	0	10	30	300
MILL	2658	20	10	0	0	1.5	150	<10	0	20	10	500
MILL	2659	7	60	0	<20	1	150	<10	20	0	15	15
MILL	2662	50	220	0.05	20	5	200	10	70	7	30	1500
MNCK	prod	10.40069	0	0.066781	0	0	0	0	0	0	0	101350
MNCK	R-1	1.4	<10	<1	415	1.1	<5	22.4	2	<2	265	205
MNCK	R-10	1.9	26	<0.001	16	0.4	<5	0	<1	<2	172	595
MNCK	R-11	1	<10	<0.001	400	2	8	0	<1	58	60	2200
MNCK	R-12	0.6	<10	<0.001	590	2.2	<5	0	<1	90	29	480
MNCK	R-14	5.2	<10	0.062	12	0.4	<5	0	<1	2	87	95500
MNCK	R-2	<0.2	<10	39	550	1.4	<5	13.6	7	33	172	12600
MNCK	R-3	<0.2	<10	26	470	1.8	<5	43.5	3	35	154	13800
MNCK	R-4	0.9	<10	10	235	1.5	8	15.2	3	46	180	13400
MNCK	R-5	0.9	<10	2	820	2.3	16	<2	3	10	210	1600
MNCK	R-6	1.7	<10	6	320	2.7	<5	26.7	5	61	110	3200
MNCK	R-7	1.1	<10	2	940	1.8	<5	21.6	1	11	162	1690
MNCK	R-8	3	<10	14	480	1.7	<5	<2	5	32	184	7900
MNCK	R-9	0.7	<10	<1	845	2	10	11.5	2	3	154	96
RMTN	134-2837	8.3	18	0.037	19	0.7	22	220	16	192	176	6700
RMTN	134-2839	1.6	<10	0.006	765	1.6	<2	186	9	33	112	100
RMTN	134-2854	5	88	0.036	20	1.1	5	67	5	41	210	600
RMTN	134-3883	5	<10	0.045	320	1.3	<2	35	3	13	96	3050
RMTN	P56-669	12.2	55	1.3	655	1.2	22	22	3	27	210	10800
RMTN	RED-1	6.3	250	0.004	87	0.3	<5	0	2	<2	52	140
RMTN	RED-2	0.5	70	0.008	90	0.8	9	0	1	<2	104	230
RMTN	RED-3	4	18	0.004	240	0.7	<5	0	<1	2	60	235

min.dist	sample no.	Sn	Sr	Te	Ti	Tl	V	W	Y	Zn	Zr
BETH	117-B-	<5	790	0	1590	<2	75	8	5.8	49	36
BETH	117-B-7	<5	30	0	1280	<2	112	20	2.1	50	5
BETH	118-9	<5	615	0	1240	<2	49	8	2.2	42	6
CHRI	100-6625	<5	15	0	67	<2	9	29	<2	395	6
CHRI	100-6655	<5	50	0	61	<2	17	10	<2	310	5
CHRI	100A	<5	34	0	51	<2	12	69	<2	15	5
CHRI	100B	<5	57	0	350	<2	28	<5	4.3	575	9
CHRI	X-1	<5	57	0	3600	4	26	<5	6.7	43200	44
CHRI	X-2	<5	455	0	3200	<2	29	14	19	260	9
CHRI	X-3	<5	33	0	98	<2	6	<5	<.2	160	22
CHRI	X-4	<5	575	0	2650	<2	49	9	5.7	112	4
ELKM	881089	6.63	8	<0.482	0	<0.482	584	2560	12	28.5	50
ELKM	881090	3.46	14	<0.484	0	0.484	208	403	13	350	7
ELKM	881091	<0.484	27	<0.484	0	<0.484	56	2060	<5	43.1	90
ELKM	881092	1.1589	10	<0.489	0	<0.489	47	280	<5	58	9
ELKM	881093	1.38	18	<0.491	0	<0.491	137	864	7	35.8	3
ELKM	881094	0.645	18	<0.466	0	<0.466	85	417	<5	219	9
ELKM	881095	<0.486	195	<.0486	0	<0.486	38	22	<5	25.5	5
MILL	2657	0	150	0	700	0	700	5000	10	180	0
MILL	2658	0	200	0	1000	0	100	200	10	120	0
MILL	2659	20	500	0	500	0	700	100	10	550	0
MILL	2662	0	0	0	500	0	150	300	15	1500	0
MNCK	prod	0	0	0	0	0	0	0	0	0	0
MNCK	R-1	<5	205	0	1400	<2	61	19	<2	22	3
MNCK	R-10	<5	14	0	510	<2	54	13	0.7	82	7
MNCK	R-11	<5	138	0	10100	<2	235	7	28.9	136	6
MNCK	R-12	<5	245	0	26100	<2	290	8	42.2	144	1
MNCK	R-14	<5	82	0	168	<2	7	5	8.5	97	<2
MNCK	R-2	<5	230	0	10000	<2	240	10	51.6	196	0
MNCK	R-3	<5	116	0	8300	<2	250	43	71.8	210	5
MNCK	R-4	<5	52	0	6250	<2	245	28	55.5	250	3
MNCK	R-5	<5	108	0	3000	<2	61	38	7.7	53	3
MNCK	R-6	<5	215	0	10500	<2	420	11	27.3	130	6
MNCK	R-7	<5	345	0	1520	<2	53	23	3.5	60	9
MNCK	R-8	<5	230	0	15000	<2	290	38	27.3	210	4
MNCK	R-9	<5	280	0	2750	<2	30	33	25.2	41	8
RMTN	134-2837	<5	20	0	1950	<2	420	114	<2	225	1
RMTN	134-2839	<5	118	0	4000	<2	270	<5	2.1	158	8
RMTN	134-2854	<5	48	0	1460	<2	91	<5	3.4	40	8
RMTN	134-3883	<5	485	0	1690	<2	64	<5	4.7	80	7
RMTN	P56-669	<5	174	0	3950	<2	94	<5	4.5	77	0
RMTN	RED-1	<5	335	0	270	<2	28	14	<.2	184	1
RMTN	RED-2	<5	305	0	290	6	142	8	0.7	215	9
RMTN	RED-3	20	750	0	2150	5	102	29	1.9	136	20

min.dist	sample no.	Fe	F	Hg	Li	Mn	Mo	Nb	Ni	Pb	Rb	Sb
BETH	117-B-	33400	0	0	0	142	19	24	8	17	44	18
BETH	117-B-7	131000	0	0	0	210	42	11	4	28	176	<5
BETH	118-9	17400	0	<2	0	445	9	4	9	9	39	19
CHRI	100-6625	267800	800	0	<10	320	42	<1	3	24	9	<5
CHRI	100-6655	213300	1200	0	<10	220	7	<1	3	20	18	<5
CHRI	100A	239500	30800	0	24	200	27	<1	11	<10	<1	<5
CHRI	100B	90600	30900	0	<10	3000	260	<1	22	705	4	6
CHRI	X-1	93400	0	0	0	3850	<1	7	22	162	<2	<5
CHRI	X-2	27800	0	0	0	900	38	7	36	18	39	<5
CHRI	X-3	401000	0	0	0	1600	50	<2	9	32	8	<5
CHRI	X-4	26800	0	0	0	205	<1	<2	20	32	60	9
ELKM	881089	0	390	0.18	16	3070	205	0	14	5.65	<5	1.09
ELKM	881090	0	390	0.177	22	4048	268	0	25	6.52	8	16.3
ELKM	881091	0	500	<0.0	7	2791	654	0	28	3.06	<5	0.992
ELKM	881092	0	540	0.124	20	6849	22.8	0	12	3.92	<5	1.36
ELKM	881093	0	340	<0.098	27	4993	622	0	27	2.91	<5	0.321
ELKM	881094	0	250	0.256	11	10089	45.5	0	28	3.37	<5	2.64
ELKM	881095	0	910	<0.097	49	693	5.83	0	18	2.32	32-	0.336
MILL	2657	100000	0	0	0	5000	50	<20	15	70	0	10
MILL	2658	30000	0	0	0	2000	150	0	5	150	0	2
MILL	2659	30000	0	0	0	1500	15	0	5	300	0	4
MILL	2662	150000	0	0	0	5000	7	0	20	500	0	72
MNCK	prod	0	0	0	0	0	0	0	0	14	0	0
MNCK	R-1	31000	0	<2	0	70	134	9	6	40	55	<5
MNCK	R-10	165000	0	0	0	220	230	9	5	39	5	22
MNCK	R-11	121000	0	0	0	1520	21	42	23	13	178	<5
MNCK	R-12	130000	0	0	0	2300	16	62	32	53	75	<5
MNCK	R-14	6900	0	0	0	56	<1	<2	7	108	14	<5
MNCK	R-2	70300	0	<2	0	880	41	25	31	23	198	<5
MNCK	R-3	53600	0	7	0	645	67	30	46	39	210	<5
MNCK	R-4	68600	0	3	0	565	12	26	79	<2	205	<5
MNCK	R-5	37300	0	3	0	320	20	10	25	39	188	<5
MNCK	R-6	132000	0	<2	0	1780	18	56	49	<2	110	<5
MNCK	R-7	18800	0	3	0	290	265	7	19	8	162	<5
MNCK	R-8	101000	0	8	0	1770	29	36	66	<2	146	11
MNCK	R-9	19800	0	<2	0	515	12	7	6	11	154	10
RMTN	134-2837	300100	400	0	10	1010	11	64	90	26	71	<5
RMTN	134-2839	177500	1300	0	20	970	10	41	58	44	335	<5
RMTN	134-2854	120900	600	0	20	215	19	11	20	600	154	<5
RMTN	134-3883	25200	800	0	24	410	7	6	14	174	300	<5
RMTN	P56-669	53300	700	0	<10	230	9	16	18	285	144	5
RMTN	RED-1	124000	0	0	0	66	116	2	<2	985	15	18
RMTN	RED-2	171000	0	0	0	24	210	17	11	255	136	38
RMTN	RED-3	90800	0	0	0	44	42	16	<2	350	260	<5

min.dist	sample no.	Ag	As	Au	Ba	Be	Bi	B	Cd	Co	Cr	Cu
RMTN	RED-4	9.8	14	0.015	315	0.6	12	0	1	<2	77	225
SIES	E-1A	0.8	<10	3	1380	2.5	<5	7.9	2	4	198	1050
SIES	E-2	<0.2	<10	13	330	2.7	<5	23.6	2	5	160	1480
SIES	E-3	<0.2	<10	1	290	1.9	<5	12.6	1	5	114	1240
SIES	E-4	1.8	<10	4	240	3.9	<5	3.3	4	9	142	4050
SIES	E-5	1.5	<10	6	280	1.6	<5	19.9	4	<2	158	144
SIES	E-6	0.5	<10	<1	1600	3	<5	23.2	2	<2	168	600
SIES	ST-1	<0.2	49	4	1420	2.3	<5	22.8	1	3	168	990
SIES	ST-2	0.3	<10	4	380	2.3	19	12.7	4	4	128	2450
SIES	ST-3	<0.2	<10	3	640	3.2	<5	13.2	5	18	196	1890
SIES	ST-4	2.6	<10	9	1130	4.4	<5	6.3	5	15	116	4350
SIES	ST-5	<0.2	<10	1	905	2.6	<5	11.8	2	11	108	345
SIES	ST-6	1.1	<10	7	450	3.6	<5	2.4	1	8	144	1020
TWIN	M-1	138	<10	0.057	17	0.3	73	0	27	89	57	88800
TWIN	M-2	81.4	31	0.076	57	1.2	<5	0	29	54	17	92800
TWIN	M-3	22.9	<10	0.064	47	1.2	<5	0	10	49	93	77400
VALC	118-11	8.4	11	0.13	835	0.9	<5	0	2	8	285	18900
VALC	118-17	1.7	<10	0.005	1270	1.8	<5	0	<1	5	210	4000
VALC	118-5	3.9	<10	0.128	1040	0.9	<5	0	<1	8	140	7500

min.dist	sample no.	Fe	F	Hg	Li	Mn	Mo	Nb	Ni	Pb	Rb	Sb
RMTN	RED-4	100000	0	0	0	47	49	14	10	210	158	8
SIES	E-1A	15100	0	<2	0	555	805	3	9	36	310	<5
SIES	E-2	24000	0	<2	0	148	142	4	5	83	245	<5
SIES	E-3	12300	0	3	0	27	3	3	<2	72	315	<5
SIES	E-4	33000	0	2	0	470	81	12	18	47	325	17
SIES	E-5	21200	0	<2	0	56	29	8	4	38	340	<5
SIES	E-6	23100	0	2	0	166	22	7	6	63	235	13
SIES	ST-1	13600	0	<2	0	230	41	3	7	69	172	16
SIES	ST-2	18900	0	<2	0	225	22	2	8	35	220	<5
SIES	ST-3	57800	0	<2	0	1220	885	24	47	15	196	<5
SIES	ST-4	67900	0	<2	0	1000	1380	31	25	15	265	10
SIES	ST-5	22300	0	<2	0	675	5	15	6	46	240	<5
SIES	ST-6	37200	0	<2	0	475	12	16	12	27	275	<5
TWIN	M-1	229000	0	0	0	595	30	<2	20	24	12	<5
TWIN	M-2	230000	0	0	0	405	480	<2	27	19	86	<5
TWIN	M-3	159000	0	0	0	980	3200	<2	43	42	605	<5
VALC	118-11	28300	0	0	0	350	5	<2	8	108	71	11
VALC	118-17	14400	0	0	0	430	28	10	7	78	80	22
VALC	118-5	17500	0	0	0	330	4	<2	5	19	68	9

min.dist	sample no.	Sn	Sr	Te	Ti	Tl	V	W	Y	Zn	Zr
RMTN	RED-4	<5	300	0	875	6	77	14	0.8	114	8
SIES	E-1A	<5	355	0	1270	2	31	15	5.8	43	0
SIES	E-2	11	375	0	1390	<2	30	12	6.4	21	9
SIES	E-3	<5	65	0	700	<2	5	30	6.8	160	0
SIES	E-4	<5	425	0	2450	<2	93	16	12	84	5
SIES	E-5	<5	69	0	555	3	11	42	5.1	23	5
SIES	E-6	18	465	0	1740	<2	38	29	2.6	41	9
SIES	ST-1	<5	730	0	1650	<2	28	19	6.5	28	9
SIES	ST-2	<5	460	0	1410	<2	44	24	5.5	51	1
SIES	ST-3	<5	725	0	7600	<2	156	47	12.1	144	6
SIES	ST-4	<5	710	0	7500	<2	245	20	16.9	235	2
SIES	ST-5	<5	138	0	4000	<2	58	19	21.3	67	0
SIES	ST-6	<5	260	0	3600	<2	64	22	20.8	62	4
TWIN	M-1	<5	13	0	116	<2	<2	192	<.2	6000	6
TWIN	M-2	<5	45	0	330	<2	33	37	0.9	5050	8
TWIN	M-3	<5	245	0	5050	<2	150	45	9.6	1340	2
VALC	118-11	<5	245	0	1030	<2	67	15	2.2	375	5
VALC	118-17	<5	475	0	990	<2	30	11	2.5	74	9
VALC	118-5	<5	245	0	1160	<2	69	7	3.7	43	6

min.dist	sample no.	Ag	As	Au	Ba	Be	Bi	B	Cd	Co	Cr	Cu
CCAD	J-079	10	2000	1.3	700	0	20	0	0	0	20	30
CCAD	J-087	10	0	0.22	700	0	10	20	0	0	20	15
CCAD	J-088	10	2000	1.2	700	0	20	20	0	0	50	300
CCAD	J-096	0.5	300	0.04	500	0	0	20	0	0	30	50
CCAD	J-135	1	0	0.16	700	2	0	20	0	15	70	200
CCAD	J-137	0.5	0	0.16	700	0	0	70	0	0	100	10
CCAD	J-138	5	0	0.02	2000	0	0	30	0	7	300	30
CCAD	J-141	0	0	0.26	500	1	0	10	0	10	20	150
CCAD	J-145	0	0	0.18	500	0	0	10	0	0	50	100
CCAD	J-146	7	300	0.1	3000	0	20	50	0	0	150	30
CCAD	J-150	10	10000	0.46	500	0	30	20	500	5	70	2000
CCAD	J-177	2	0	0.02	1500	0	0	15	0	10	300	300
CCAD	J-178	200	3000	3	300	0	30	15	0	5	70	500
CCAD	J-180	2	0	0.04	1000	0	0	10	0	15	200	50
CCAD	J-181	0.5	0	0.06	1000	0	0	10	0	10	200	20
CCAD	J-182	100	2000	2	300	0	10	0	0	0	70	300
CCAD	J-183	5	0	0.02	2000	0	0	10	0	15	300	50
CCAD	J-184	15	5000	0.32	300	0	20	0	0	0	50	500
CCAD	J-185	15	1500	0.08	500	0	700	10	0	0	200	50
CCAD	J-186	20	5000	2	300	0	50	0	0	5	70	200
CCAD	J-187	50	5000	75	300	1	70	0	0	5	70	150
CCAD	J-188	3	1500	0.08	500	1	0	50	0	7	100	150
CCAD	J-189	2	0	0	700	0	0	20	0	7	70	30
CCAD	J-286	2	1000	0.14	700	1	0	20	50	0	150	150
CCAD	J-287	0.5	0	0.16	500	0	0	15	0	0	10	20
CCAD	J-291	0.7	1000	0.02	300	1	0	30	0	5	30	700
CCAD	J-305	0	0	0.06	700	0	0	30	0	0	100	100
CCAD	J-306	1	500	0.12	700	1	0	10	0	0	10	100
CCAD	J-307	10	1500	0.22	700	3	10	20	0	0	70	700
CCAD	J-310	1	0	0.06	2000	0	0	10	0	5	100	70
CCAD	J-315	100	700	1.3	700	0	0	50	0	0	200	200
CCAD	J-316	5	0	0.02	700	0	0	70	0	0	70	15
CCAD	J-318	1.5	200	0.06	700	0	0	100	0	0	70	30
CCAD	J-330	20	700	3.4	500	0	20	20	0	0	50	10
CCAD	J-336	50	5000	5	1000	1	100	30	0	0	50	200
CCAD	J-337	7	3000	1.3	500	0	20	20	0	0	30	150
CCAD	J-339	10	2000	0.26	500	0	20	30	0	0	50	100
CCAD	J-341	1	0	0.04	700	1	0	70	0	0	150	50
CCAD	J-343	3	0	0.1	1000	0	10	30	0	0	30	5
CCAD	J-344	30	3000	5.1	300	0	100	0	0	5	20	30
CCAD	J-346	3	0	0.16	700	0	0	20	0	0	20	10
CCAD	J-347	30	5000	0.6	1000	0	150	10	0	0	50	70
CCAD	J-349	3	0	0.1	1500	0	10	100	0	0	150	5
CCAD	J-350	5	200	0.44	1500	0	50	100	0	0	100	15

min.dist	sample no.	Fe	F	Hg	Li	Mn	Mo	Nb	Ni	Pb	Rb	Sb
CCAD	J-079	70000	0	0.05	0	20	0	10	0	150	0	0
CCAD	J-087	15000	0	0.14	0	50	0	0	0	100	0	0
CCAD	J-088	200000	0	0.13	0	20	0	0	0	500	0	0
CCAD	J-096	50000	0	0.04	0	30	0	0	7	70	0	0
CCAD	J-135	100000	0	0.06	0	150	0	0	0	50	0	0
CCAD	J-137	10000	0	0.04	0	50	0	10	0	0	0	0
CCAD	J-138	50000	0	0.08	0	1000	0	0	0	1000	0	0
CCAD	J-141	150000	0	0.05	0	100	0	0	0	0	0	0
CCAD	J-145	50000	0	0.06	0	200	0	0	0	10	0	0
CCAD	J-146	20000	0	0.05	0	70	0	10	0	500	0	0
CCAD	J-150	150000	0	0.05	0	30	0	0	0	50	0	0
CCAD	J-177	70000	0	0.13	0	1000	0	0	0	50	0	0
CCAD	J-178	200000	0	6.5	0	50	0	0	0	100	0	100
CCAD	J-180	70000	0	0.09	0	1000	0	0	50	1000	0	0
CCAD	J-181	50000	0	0.04	0	1000	0	0	30	50	0	0
CCAD	J-182	100000	0	2.8	0	100	0	0	20	500	0	0
CCAD	J-183	50000	0	0.03	0	500	0	0	50	150	0	0
CCAD	J-184	150000	0	2.2	0	100	0	0	30	70	0	0
CCAD	J-185	70000	0	0.26	0	50	10	0	0	5000	0	300
CCAD	J-186	150000	0	2.2	0	100	5	0	15	200	0	150
CCAD	J-187	100000	0	6.5	0	100	10	0	20	200	0	100
CCAD	J-188	50000	0	0.1	0	200	0	0	20	30	0	0
CCAD	J-189	30000	0	0.1	0	500	0	0	30	70	0	0
CCAD	J-286	150000	0	0.05	0	70	0	0	15	200	0	0
CCAD	J-287	2000	0	0.05	0	70	0	0	0	15	0	0
CCAD	J-291	70000	0	0.2	0	100	0	0	30	15	0	0
CCAD	J-305	30000	0	0.12	0	200	0	0	15	0	0	0
CCAD	J-306	50000	0	0.18	0	20	10	100	10	15	0	0
CCAD	J-307	100000	0	0.35	0	30	0	0	15	20	0	0
CCAD	J-310	30000	0	0.12	0	500	0	0	30	70	0	0
CCAD	J-315	200000	0	5.5	0	30	0	0	0	5000	0	300
CCAD	J-316	15000	0	0.26	0	70	0	0	0	200	0	0
CCAD	J-318	20000	0	0.15	0	50	0	0	0	100	0	0
CCAD	J-330	100000	0	0.18	0	70	0	15	5	300	0	0
CCAD	J-336	200000	0	0.3	0	50	7	10	20	1000	0	1000
CCAD	J-337	200000	0	0.15	0	30	0	10	0	500	0	0
CCAD	J-339	100000	0	0.3	0	50	0	10	0	500	0	100
CCAD	J-341	150000	0	0.18	0	150	0	10	10	700	0	0
CCAD	J-343	5000	0	0.26	0	100	15	10	5	100	0	0
CCAD	J-344	200000	0	0.22	0	50	0	10	10	200	0	0
CCAD	J-346	10000	0	0.35	0	150	0	10	0	20	0	0
CCAD	J-347	200000	0	0.15	0	30	0	0	5	1000	0	200
CCAD	J-349	15000	0	0.09	0	100	0	10	10	50	0	0
CCAD	J-350	70000	0	0.09	0	70	0	10	7	10	0	0

min.dist	sample no.	Sn	Sr	Te	Ti	Tl	V	W	Y	Zn	Zr
CCAD	J-079	20	0	0	5000	0	20	0	10	0	0
CCAD	J-087	10	0	0	5000	0	30	0	15	0	0
CCAD	J-088	20	0	0	2000	0	70	0	15	0	0
CCAD	J-096	10	0	0	2000	0	30	0	10	0	50
CCAD	J-135	0	0	0	3000	0	50	0	20	0	0
CCAD	J-137	10	0	0	5000	0	100	0	10	0	0
CCAD	J-138	0	0	0	10000	0	100	0	15	3000	0
CCAD	J-141	0	0	0	2000	0	20	0	10	0	0
CCAD	J-145	0	100	0	3000	0	50	0	15	0	0
CCAD	J-146	20	0	0	10000	0	150	0	0	0	0
CCAD	J-150	0	500	0	2000	0	70	0	30	1000	0
CCAD	J-177	0	300	0	7000	0	150	0	20	0	0
CCAD	J-178	0	0	0	500	0	50	0	0	500	0
CCAD	J-180	0	500	0	5000	0	100	0	15	0	0
CCAD	J-181	0	300	0	5000	0	100	0	15	200	0
CCAD	J-182	0	0	0	1500	0	70	0	10	300	0
CCAD	J-183	50	200	0	5000	0	150	0	15	500	50
CCAD	J-184	30	0	0	100	0	30	0	0	200	0
CCAD	J-185	0	300	0	1500	0	30	0	0	0	0
CCAD	J-186	0	0	0	700	0	30	0	0	700	0
CCAD	J-187	0	100	0	200	0	30	0	0	700	0
CCAD	J-188	0	0	0	3000	0	100	0	20	200	0
CCAD	J-189	10	0	0	3000	0	50	0	15	1000	0
CCAD	J-286	0	0	0	7000	0	100	0	30	1000	50
CCAD	J-287	0	0	0	2000	0	10	0	10	0	0
CCAD	J-291	0	0	0	3000	0	50	0	10	500	50
CCAD	J-305	0	0	0	7000	0	70	0	20	0	0
CCAD	J-306	0	0	0	300	0	10	0	15	0	0
CCAD	J-307	0	0	0	2000	0	50	0	30	200	0
CCAD	J-310	10	100	0	7000	0	100	0	15	1000	50
CCAD	J-315	20	0	0	3000	0	100	0	10	1000	50
CCAD	J-316	10	0	0	5000	0	70	0	10	0	0
CCAD	J-318	10	0	0	5000	0	70	0	15	0	0
CCAD	J-330	20	0	0	3000	0	70	0	0	0	0
CCAD	J-336	0	200	0	2000	0	70	0	30	200	0
CCAD	J-337	0	0	0	2000	0	30	0	15	0	0
CCAD	J-339	30	0	0	3000	0	50	0	15	0	0
CCAD	J-341	0	0	0	3000	0	100	0	10	700	0
CCAD	J-343	10	0	0	3000	0	300	0	15	0	0
CCAD	J-344	0	0	0	700	0	50	0	10	0	0
CCAD	J-346	0	0	0	2000	0	70	0	15	0	0
CCAD	J-347	20	0	0	2000	0	150	0	10	0	0
CCAD	J-349	30	0	0	10000	0	500	30	30	0	0
CCAD	J-350	30	0	0	10000	0	500	30	20	0	0

min.dist	sample no.	Ag	As	Au	Ba	Be	Bi	B	Cd	Co	Cr	Cu
CCAD	J-351	10	700	0.06	1000	0	50	10	0	0	15	20
CCAD	J-353	5	700	0.18	700	0	0	70	0	0	0	30
CCAD	J-355	200	10000	4.8	500	2	500	20	0	20	50	1000
CCAD	J-387	20	500	0.06	200	0	0	20	0	5	20	50
CCAD	J-388	2	300	0.02	700	1	0	50	20	30	50	30
CCAD	J-389	30	700	0	500	2	0	50	200	70	200	700
CCAD	J-390	2	200	0	500	0	0	20	0	0	30	50
CCAD	J-629	5	0	0.02	1000	1	10	20	0	0	30	70
CCAD	J-632	20	200	0.06	1000	0	15	0	0	0	20	100
CCAD	J-640	0.7	500	0.02	500	1	10	30	0	5	50	100
CCAD	J-641	2	2000	0.01	500	1	15	50	0	0	50	150
CCAD	J-654	3	300	0.26	700	1	30	20	0	0	70	500
CCAD	J-655	2	3000	0.06	1000	1	10	50	7	0	70	200
CCAD	J-660	10	500	0.26	500	1	100	15	0	10	70	200
CCAD	J-661	5	3000	0.24	700	1	50	15	0	0	100	500
CCAD	J-662	50	3000	0.78	700	0	100	10	0	7	50	50
CCAD	J-663	1.5	200	0.02	1000	0	10	30	0	0	70	30
CCAD	J-664	2	500	0.02	1000	0	10	50	0	0	100	700
CCAD	J-668	20	10000	3	700	0	150	70	0	0	200	200
CCAD	J-671	5	0	0	700	1	0	0	0	20	300	20
CCAD	J-672	1	0	0.04	1000	1	0	50	0	15	100	30
CCAD	J-674	5	200	0.02	700	1	10	20	0	0	70	50
CCAD	J-675	10	2000	0.78	500	1	100	10	0	0	100	200
CCAD	J-677	20	500	0.12	200	1.5	100	0	0	0	30	300
CCAD	J-678	0.5	0	0.32	700	1	0	0	0	0	0	15
CCAD	J-679	7	200	0.38	700	0	15	50	0	0	70	15
CCAD	J-680	3	0	0.12	700	0	10	50	0	0	100	10
CCAD	J-681	2	1500	0.06	700	1	50	10	0	0	70	100
CCAD	J-682	1.5	1000	0.24	500	0	0	50	0	0	150	100
CCAD	J-688	1	700	0.06	700	1	0	50	0	0	70	10
CCAD	J-689	2	0	0	1000	1	0	20	0	5	70	15
CCAD	J-691	7	300	0.26	700	0	15	30	0	0	70	15
CCAD	J-692	7	3000	1.4	500	0	20	10	0	0	30	30
CCAD	J-695	150	3000	2.1	300	1	15	20	0	10	30	200
CCAD	J-784	100	10000	10	1000	0	500	30	0	0	50	150
CCAD	J-785	5	200	0.12	700	0	0	70	0	0	50	5
CCAD	J-786	1.5	300	0.28	500	1.5	0	50	0	0	30	100
CCAD	J-788	5	700	0.62	500	1	0	30	0	0	50	20
CCAD	J-790	2	5000	0.1	5000	0	0	10	0	0	20	50
CCAD	J-793	10	200	0.2	300	0	0	10	0	0	5	15
CCAD	J-794	10	700	0.06	1500	0	0	70	0	0	500	70
CCAD	J-795	10	10000	2.5	700	0	50	30	0	0	50	150
CCAD	J-796	10	5000	0.68	200	0	10	0	0	10	10	100
CCAD	J-797	5	1500	0.02	500	0	10	20	0	10	10	70

min.dist	sample no.	Fe	F	Hg	Li	Mn	Mo	Nb	Ni	Pb	Rb	Sb
CCAD	J-351	30000	0	0.45	0	150	70	20	5	500	0	100
CCAD	J-353	150000	0	0.15	0	50	0	0	0	150	0	0
CCAD	J-355	200000	0	0.55	0	200	0	10	100	1500	0	0
CCAD	J-387	20000	0	0.4	0	500	0	10	10	1000	0	0
CCAD	J-388	50000	0	0.09	0	500	0	10	50	500	0	0
CCAD	J-389	150000	0	0.18	0	5000	0	30	150	5000	0	0
CCAD	J-390	30000	0	0.18	0	70	5	10	5	1000	0	0
CCAD	J-629	20000	0	3.5	0	50	0	10	5	200	0	0
CCAD	J-632	30000	0	0.28	0	150	0	0	10	500	0	0
CCAD	J-640	15000	0	0.45	0	100	0	10	5	100	0	0
CCAD	J-641	150000	0	0.18	0	70	0	10	5	100	0	0
CCAD	J-654	200000	0	0.05	0	30	0	10	50	15	0	0
CCAD	J-655	150000	0	0.06	0	100	0	10	20	20	0	0
CCAD	J-660	200000	0	0.07	0	100	0	10	50	50	0	0
CCAD	J-661	200000	0	0.07	0	50	0	10	20	200	0	0
CCAD	J-662	200000	0	0	0	20	0	10	10	1000	0	0
CCAD	J-663	30000	0	0	0	50	0	15	5	0	0	0
CCAD	J-664	70000	0	0.05	0	50	0	10	5	200	0	0
CCAD	J-668	150000	0	0.7	0	50	0	20	5	100	0	150
CCAD	J-671	70000	0	0.04	0	1000	0	10	100	15	0	0
CCAD	J-672	70000	0	0.05	0	300	0	10	50	15	0	0
CCAD	J-674	100000	0	0.05	0	150	0	10	20	300	0	0
CCAD	J-675	200000	0	0.14	0	50	0	0	15	1000	0	0
CCAD	J-677	150000	0	0.15	0	50	0	0	50	100	0	100
CCAD	J-678	70000	0	0.03	0	500	5	100	0	10	0	0
CCAD	J-679	10000	0	0.06	0	30	0	0	0	200	0	0
CCAD	J-680	10000	0	0.03	0	50	0	10	0	100	0	0
CCAD	J-681	100000	0	0.03	0	100	5	100	5	15	0	0
CCAD	J-682	150000	0	0	0	50	0	10	5	50	0	0
CCAD	J-688	150000	0	0.04	0	100	0	20	10	150	0	0
CCAD	J-689	50000	0	0.04	0	300	0	15	15	1000	0	0
CCAD	J-691	7000	0	0.05	0	100	0	10	0	150	0	0
CCAD	J-692	70000	0	0.4	0	50	0	0	0	500	0	100
CCAD	J-695	100000	0	0.14	0	200	0	10	10	200	0	0
CCAD	J-784	150000	0	0.3	0	50	0	10	5	700	0	700
CCAD	J-785	5000	0	0.15	0	70	0	15	0	200	0	0
CCAD	J-786	200000	0	0.12	0	100	0	15	10	1000	0	0
CCAD	J-788	150000	0	0.07	0	70	15	10	20	500	0	0
CCAD	J-790	50000	0	0.22	0	30	0	10	0	500	0	0
CCAD	J-793	30000	0	0.08	0	100	0	0	0	500	0	0
CCAD	J-794	100000	0	0.28	0	100	0	15	5	20000	0	300
CCAD	J-795	150000	0	0.3	0	150	0	10	10	1000	0	500
CCAD	J-796	200000	0	0.1	0	30	0	10	10	200	0	0
CCAD	J-797	150000	0	0.11	0	50	0	15	15	200	0	0

min.dist	sample no.	Sn	Sr	Te	Ti	Tl	V	W	Y	Zn	Zr
CCAD	J-351	15	0	0	3000	0	100	0	50	0	50
CCAD	J-353	0	0	0	2000	0	50	0	15	0	0
CCAD	J-355	0	200	0	1000	0	30	0	100	1000	0
CCAD	J-387	0	0	0	2000	0	30	0	20	500	0
CCAD	J-388	0	0	0	3000	0	50	0	30	700	0
CCAD	J-389	30	150	0	10000	0	200	100	50	5000	0
CCAD	J-390	10	100	0	2000	0	50	0	20	0	0
CCAD	J-629	0	0	0	3000	0	700	0	15	0	0
CCAD	J-632	0	0	0	1000	0	700	0	10	500	0
CCAD	J-640	0	0	0	3000	0	70	0	20	0	0
CCAD	J-641	0	0	0	2000	0	70	0	20	0	0
CCAD	J-654	0	0	0	1500	0	50	0	20	200	0
CCAD	J-655	0	0	0	5000	0	70	0	20	0	50
CCAD	J-660	0	0	0	2000	0	70	0	20	700	0
CCAD	J-661	0	0	0	3000	0	100	0	20	0	0
CCAD	J-662	0	0	0	2000	0	50	0	20	0.35	0
CCAD	J-663	0	0	0	5000	0	100	0	30	0.03	0
CCAD	J-664	0	0	0	2000	0	70	0	15	0	0
CCAD	J-668	0	0	0	7000	0	200	200	20	0	0
CCAD	J-671	0	300	0	7000	0	200	0	30	0	50
CCAD	J-672	0	0	0	5000	0	100	0	20	0	0
CCAD	J-674	0	0	0	2000	0	70	0	20	0	0
CCAD	J-675	0	0	0	1500	0	70	0	20	300	0
CCAD	J-677	0	0	0	300	0	20	0	20	300	5
CCAD	J-678	10	200	0	2000	0	0	0	30	0	0
CCAD	J-679	10	0	0	3000	0	50	0	20	0	0
CCAD	J-680	20	0	0	5000	0	100	0	20	0	0
CCAD	J-681	0	0	0	1000	0	50	0	15	0	0
CCAD	J-682	0	0	0	3000	0	150	0	20	0	50
CCAD	J-688	20	0	0	3000	0	70	0	20	0	50
CCAD	J-689	20	0	0	3000	0	50	0	20	0	0
CCAD	J-691	30	0	0	3000	0	70	50	15	0	0
CCAD	J-692	20	0	0	1000	0	30	0	0	0	50
CCAD	J-695	15	0	0	2000	0	20	0	15	200	0
CCAD	J-784	30	1000	0	3000	0	50	0	20	0	0
CCAD	J-785	10	0	0	5000	0	70	0	20	0	0
CCAD	J-786	0	0	0	5000	0	70	0	15	500	0
CCAD	J-788	0	0	0	3000	0	50	0	20	500	50
CCAD	J-790	10	150	0	1500	0	70	0	10	0	0
CCAD	J-793	0	0	0	500	0	20	0	0	0	0
CCAD	J-794	30	0	0	7000	0	200	50	20	5	0
CCAD	J-795	20	150	0	3000	0	50	0	20	0	0
CCAD	J-796	0	0	0	2000	0	10	0	50	0	0
CCAD	J-797	0	0	0	7000	0	100	0	15	0	0

min.dist	sample no.	Ag	As	Au	Ba	Be	Bi	B	Cd	Co	Cr	Cu
CCAD	J-798	2	300	0.44	500	1	130	100	0	30	10	150
CCAD	J-799	50	300	1.5	1000	0	0	50	0	0	50	70
CCAD	J-800	2	0	0.08	700	0	0	15	0	0	20	50
CCAD	J-803	30	200	1.1	700	0	15	50	0	0	20	50
CCAD	J-819	150	10000	31	150	0	150	10	0	5	20	1500
CCAD	J-820	20	2000	2.2	1000	0	15	50	0	0	70	30
CCAD	J-821	7	200	0.12	2000	0	0	70	0	0	500	200
CCAD	J-823	50	7000	17	500	0	100	10	0	0	70	150
CCAD	J-824	20	3000	10	300	0	200	10	0	0	70	200
CCAD	J-826	20	0	0.02	1000	0	0	0	0	15	700	70
CCAD	J-828	10	300	0.18	700	0	0	70	0	0	15	100
CCAD	J-934	7	0	0.02	500	0	0	30	0	0	30	20
CCAD	J-936	5	0	0.16	700	0	0	10	0	0	10	10
CCAD	J-937	50	700	0.62	1000	0	0	70	0	0	50	20
CCAD	J-938	7	200	0.04	700	0	0	100	0	0	70	30
CCAD	J-945	50	500	0.8	300	0	0	10	0	0	20	20
CCAD	J-948	30	10000	3.5	1000	0	0	70	0	0	150	150
CCAD	J-952	20	500	0.06	700	1	0	100	0	0	200	50
CCAD	J-954	20	500	0.26	5000	1	0	50	0	0	150	150
CCAD	J-956	10	0	0.02	500	0	0	30	0	5	70	10
CCAD	J-957	3	0	0	700	1	0	70	0	7	70	30
CCAD	J-958	2	0	0	1500	0	0	50	0	5	70	20
CCAD	J-960	10	0	0	700	1	0	50	20	10	150	20
CCAD	J-961	20	0	1.1	200	1	0	20	50	5	50	100
CCAD	J-962	150	500	1.9	200	0	0	20	0	5	50	30
CCAD	J-971	70	1500	17	100	0	0	0	70	15	30	500
CCAD	J-972	30	0	0.2	700	1.5	0	30	0	5	70	100
CCAD	J-974	5	0	0.08	500	1.5	0	30	30	7	70	150
CCAD	J-979	1.5	1500	0.02	1000	2	0	30	20	10	70	30
CCAD	J-981	2	0	0.5	150	0	0	0	20	10	30	30
CCAD	J-987	2	1500	0.3	700	0	0	30	70	5	200	100
CCAD	J-992	30	0	0	700	1.5	0	30	30	7	300	150
CCAD	J-994	0	0	0	300	1	0	15	300	10	30	100
CCAH	A-001	7	0	0.4	5000	0	10	10	0	0	100	1000
CCAH	A-002	5	0	0.04	1500	0	0	0	0	0	20	70
CCAH	A-003	10	500	0.4	3000	0	0	0	0	0	20	1000
CCAH	A-007	15	0	0.3	3000	1	20	10	0	0	70	7000
CCAH	A-008	150	10000	2	1500	1	50	20	0	0	100	20000
CCAH	A-019	5	0	0.1	3000	0	0	10	0	5	150	10000
CCAH	A-020	5	0	0.2	2000	1	0	10	0	0	70	10000
CCAH	A-021	2	0	0.04	5000	0	0	10	0	5	100	10000
CCAH	A-023	150	0	0.7	3000	1	0	0	0	0	70	1000
CCAH	A-104	10	300	0.08	3000	0	0	10	0	0	70	1500
CCAH	A-105	15	0	0.2	200	5	10	10	0	70	100	20000

min.dist	sample no.	Fe	F	Hg	Li	Mn	Mo	Nb	Ni	Pb	Rb	Sb
CCAD	J-798	150000	0	0.2	0	300	0	20	20	50	0	0
CCAD	J-799	30000	0	0.13	0	100	0	20	5	2000	0	0
CCAD	J-800	3000	0	0.08	0	100	0	0	5	20	0	0
CCAD	J-803	20000	0	0.15	0	70	0	20	0	500	0	0
CCAD	J-819	200000	0	0.5	0	20	0	0	10	1000	0	0
CCAD	J-820	200000	0	0.06	0	30	0	20	0	500	0	0
CCAD	J-821	50000	0	0.11	0	100	0	30	15	150	0	100
CCAD	J-823	200000	0	0.7	0	100	0	10	20	1500	0	300
CCAD	J-824	200000	0	0.1	0	50	0	20	5	300	0	200
CCAD	J-826	150000	0	0.05	0	1000	0	20	100	3000	0	0
CCAD	J-828	150000	0	0.1	0	70	0	20	10	10000	0	0
CCAD	J-934	5000	0	0.05	0	100	0	0	5	70	0	0
CCAD	J-936	15000	0	0.03	0	70	0	0	0	10	0	0
CCAD	J-937	50000	0	0.06	0	70	0	20	5	3000	0	0
CCAD	J-938	150000	0	0.05	0	20	5	10	5	500	0	0
CCAD	J-945	30000	0	0.1	0	150	0	0	5	100	0	0
CCAD	J-948	150000	0	0.04	0	50	0	20	10	5000	0	100
CCAD	J-952	50000	0	0.04	0	150	0	10	15	3000	0	0
CCAD	J-954	200000	0	0.05	0	100	0	10	10	5000	0	0
CCAD	J-956	50000	0	0	0	500	0	10	10	2000	0	0
CCAD	J-957	30000	0	0.07	0	500	0	10	20	1000	0	0
CCAD	J-958	30000	0	0.04	0	300	0	10	20	2000	0	0
CCAD	J-960	70000	0	0.08	0	500	0	10	50	1000	0	0
CCAD	J-961	100000	0	1.1	0	500	0	10	15	3000	0	0
CCAD	J-962	150000	0	0.22	0	150	5	10	15	20000	0	300
CCAD	J-971	200000	0	0	0	150	0	10	20	2000	0	700
CCAD	J-972	70000	0	0	0	200	0	10	7	20000	0	0
CCAD	J-974	150000	0	0	0	200	0	0	30	1500	0	0
CCAD	J-979	100000	0	0	0	150	0	0	15	700	0	0
CCAD	J-981	150000	0	0	0	150	20	0	30	150	0	0
CCAD	J-987	150000	0	0	0	150	0	0	30	3000	0	0
CCAD	J-992	150000	0	0	0	300	0	0	70	15000	0	0
CCAD	J-994	70000	0	0	0	700	0	0	15	7000	0	0
CCAH	A-001	20000	0	0.11	0	10	7	10	20	50	0	0
CCAH	A-002	3000	0	0.09	0	70	0	10	5	20	0	0
CCAH	A-003	5000	0	0.25	0	70	7	10	5	10	0	0
CCAH	A-007	20000	0	0.14	0	100	0	10	20	30	0	0
CCAH	A-008	200000	0	1.9	0	100	300	10	10	7000	0	0
CCAH	A-019	20000	0	0.03	0	100	5	10	70	50	0	0
CCAH	A-020	10000	0	0.04	0	70	5	10	20	30	0	0
CCAH	A-021	20000	0	0.04	0	100	0	0	20	150	0	0
CCAH	A-023	15000	0	0.02	0	100	5	10	30	20	0	0
CCAH	A-104	10000	0	0.08	0	100	30	10	10	500	0	0
CCAH	A-105	150000	0	0.1	0	2000	10	10	200	0	0	0

min.dist	sample no.	Sn	Sr	Te	Ti	Tl	V	W	Y	Zn	Zr
CCAD	J-798	20	100	0	10000	0	300	0	30	0	50
CCAD	J-799	50	0	0	5000	0	150	0	20	0	0
CCAD	J-800	0	0	0	500	0	100	0	0	0	0
CCAD	J-803	10	0	0	5000	0	100	0	10	0	0
CCAD	J-819	20	0	0	300	0	20	0	0	200	0
CCAD	J-820	30	0	0	10000	0	200	0	15	0	0
CCAD	J-821	10	0	0	10000	0	300	0	20	0	50
CCAD	J-823	100	0	0	2000	0	100	0	50	1000	0
CCAD	J-824	20	0	0	10000	0	50	0	50	200	0
CCAD	J-826	15	0	0	10000	0	300	0	20	0	0
CCAD	J-828	0	0	0	10000	0	500	0	50	500	0
CCAD	J-934	0	0	0	1500	0	100	0	0	0	0
CCAD	J-936	0	0	0	300	0	20	0	0	0	0
CCAD	J-937	50	100	0	7000	0	70	0	20	0	50
CCAD	J-938	0	0	0	2000	0	150	0	10	0	0
CCAD	J-945	10	0	0	1000	0	50	0	15	0	0
CCAD	J-948	30	100	0	10000	0	500	0	20	0	50
CCAD	J-952	10	0	0	5000	0	100	0	30	0	0
CCAD	J-954	20	0	0	2000	0	70	0	15	3000	0
CCAD	J-956	10	0	0	2000	0	50	0	20	200	0
CCAD	J-957	0	0	0	3000	0	70	0	20	700	0
CCAD	J-958	10	0	0	3000	0	100	0	20	500	0
CCAD	J-960	0	0	0	3000	0	100	0	30	700	50
CCAD	J-961	0	0	0	1000	0	20	0	50	2000	0
CCAD	J-962	0	0	0	1500	0	30	0	30	700	0
CCAD	J-971	0	0	0	700	0	20	0	15	10000	0
CCAD	J-972	15	0	0	7000	0	70	0	70	300	0
CCAD	J-974	0	0	0	3000	0	70	0	20	300	50
CCAD	J-979	10	0	0	3000	0	70	0	30	200	0
CCAD	J-981	0	0	0	1500	0	50	0	15	200	0
CCAD	J-987	15	0	0	5000	0	70	0	30	700	50
CCAD	J-992	30	0	0	5000	0	70	0	30	1500	0
CCAD	J-994	15	0	0	1500	0	30	0	15	10000	50
CCAH	A-001	0	200	0	3000	0	100	0	10	0	0
CCAH	A-002	0	200	0	1500	0	100	0	10	0	0
CCAH	A-003	0	200	0	3000	0	70	0	10	0	0
CCAH	A-007	0	200	0	3000	0	100	0	20	0	0
CCAH	A-008	50	500	0	1500	0	70	0	20	0	0
CCAH	A-019	0	200	0	7000	0	150	0	50	0	0
CCAH	A-020	0	200	0	2000	0	70	0	30	0	0
CCAH	A-021	0	200	0	2000	0	70	0	10	0	50
CCAH	A-023	0	500	0	2000	0	70	0	10	0	0
CCAH	A-104	0	200	0	2000	0	50	0	0	0	0
CCAH	A-105	30	200	0	2000	0	70	0	30	5000	0

min.dist	sample no.	Ag	As	Au	Ba	Be	Bi	B	Cd	Co	Cr	Cu
CCAH	H-356	10	5000	0.1	3000	2	10	15	0	7	30	20000
CCAH	Q-285	2	3000	1.1	300	1.5	20	15	0	0	70	500
CCAH	Q-286	7	700	0.4	2000	1	70	15	0	0	200	100
CCAH	Q-342	3	0	0.1	700	1	0	0	0	0	100	700
CCAH	Q-343	7	0	0.1	500	1	0	0	0	0	50	1000
CCAH	Q-344	7	0	0.1	1000	1	0	0	0	0	70	2000
CCAH	Q-345	20	0	0.2	700	1.5	0	0	0	0	30	5000
CCAH	Q-347	7	0	0.2	1500	1	0	0	0	5	70	2000
CCAH	Q-348	5	300	0.06	1500	1	0	10	0	5	50	2000
CCAH	Q-349	3	0	0.08	3000	1	0	10	0	0	70	700
CCAH	Q-350	3	0	0.1	1500	3	0	0	0	7	70	1500
CCAH	Q-351	7	0	0.04	3000	1.5	0	0	0	5	70	1500
CCAH	Q-352	3	0	0.04	1500	1.5	0	0	0	0	70	1000
CCAH	Q-354	2	2000	0	1500	1.5	0	30	0	0	70	1000
CCAH	Q-383	1	0	0.1	1000	1	0	0	0	5	100	2000
CCAH	Q-384	2	0	0.1	1500	1	0	0	0	0	50	2000
CCAH	Q-385	1.5	0	0.1	700	1.5	0	0	0	0	70	2000
CCAH	Q-390	0.5	0	0.08	1500	0	0	200	0	0	70	50
CCAH	Q-462	5	0	0.2	1000	1	10	0	0	0	150	3000
CCAH	Q-463	7	0	0.2	1000	1	10	10	0	10	150	1000
CCAH	Q-464	3	0	0.2	700	1	0	10	0	0	200	1000
CCAH	Q-465	10	0	0.1	1000	1.5	10	10	0	5	150	1500
CCAH	Q-466	1.5	0	0.3	500	1	0	10	0	0	200	700
CCAH	Q-467	10	3000	0.08	700	1	0	20	0	0	200	1500
CCAH	Q-468	10	0	0.3	1000	0	0	10	0	0	300	1000
CCAH	Q-469	1	1000	0.04	700	0	0	0	0	0	150	700
CCAH	Q-470	30	10000	1.3	500	0	200	10	0	0	300	700
CCAH	Q-471	1.5	0	0.2	700	1	0	10	0	5	150	700
CCAH	Q-472	7	0	0.2	300	1	0	15	0	0	200	2000
CCAH	Q-473	50	1500	2	150	0	100	10	0	0	150	1000
CCAH	Q-474	1.5	200	0.2	2000	1	20	20	0	0	500	200
CCAH	Q-475	7	0	0.6	1000	1	15	15	0	0	100	20000
CCAH	Q-476	0.7	0	0.08	700	0	0	10	0	0	200	5000
CCAH	Q-477	1	0	0.1	700	0	10	15	0	0	20	100
CCAH	Q-478	3	1000	0.2	1000	0	10	50	0	0	150	100
CCAH	Q-479	100	10000	4.2	1000	0	150	15	0	0	30	300
CCAH	Q-480	5	700	0.1	700	1.5	10	50	0	0	150	1000
CCAH	Q-481	1.5	500	0.1	1000	2	0	30	0	20	150	700
CCAH	Q-482	7	0	0.2	1000	1	10	15	0	0	100	200
CCAH	Q-483	5	200	0.3	700	1.5	10	20	0	0	150	200
CCAH	Q-551	3	700	0.1	500	0	10	1500	0	0	150	50
CCAH	Q-591	5	0	0.08	1500	1.5	10	20	0	0	50	200
CCAH	Q-598	0.5	700	0.08	1500	1	0	50	0	0	70	150
CCAH	Q-599	5	0	0.08	200	0	0	1500	0	0	70	15

min.dist	sample no.	Sn	Sr	Te	Ti	Tl	V	W	Y	Zn	Zr
CCAH	H-356	10	150	0	1500	0	100	0	20	0	0
CCAH	Q-285	30	0	0	3000	0	100	0	10	0	0
CCAH	Q-286	30	0	0	5000	0	150	0	10	0	0
CCAH	Q-342	0	150	0	2000	0	100	0	20	0	0
CCAH	Q-343	0	150	0	1000	0	50	0	10	0	0
CCAH	Q-344	0	300	0	1500	0	70	0	0	0	0
CCAH	Q-345	0	150	0	1500	0	50	0	0	0	0
CCAH	Q-347	0	300	0	2000	0	70	0	10	0	50
CCAH	Q-348	10	0	0	1000	0	50	0	0	0	0
CCAH	Q-349	10	150	0	2000	0	100	0	0	200	50
CCAH	Q-350	0	300	0	2000	0	70	0	15	500	0
CCAH	Q-351	0	200	0	1500	0	70	0	0	200	50
CCAH	Q-352	0	300	0	1500	0	70	0	0	0	0
CCAH	Q-354	30	0	0	2000	0	150	50	0	0	0
CCAH	Q-383	0	100	0	1500	0	100	0	0	0	0
CCAH	Q-384	0	0	0	1500	0	50	0	0	0	0
CCAH	Q-385	0	150	0	1000	0	70	0	0	0	0
CCAH	Q-390	15	0	0	1500	0	100	0	0	0	0
CCAH	Q-462	10	200	0	2000	0	200	0	20	0	0
CCAH	Q-463	20	200	0	2000	0	200	0	20	300	0
CCAH	Q-464	10	200	0	1500	0	200	0	20	0	0
CCAH	Q-465	10	300	0	2000	0	100	0	10	0	0
CCAH	Q-466	0	100	0	2000	0	100	0	30	0	0
CCAH	Q-467	30	500	0	1500	0	100	0	10	0	0
CCAH	Q-468	10	0	0	1500	0	100	0	20	0	0
CCAH	Q-469	0	100	0	1500	0	70	0	0	0	0
CCAH	Q-470	0	700	0	500	0	70	0	0	0	0
CCAH	Q-471	15	200	0	1500	0	100	0	20	0	0
CCAH	Q-472	10	150	0	1500	0	100	0	20	0	0
CCAH	Q-473	200	0	0	3000	0	200	0	50	0	0
CCAH	Q-474	30	0	0	2000	0	150	0	0	0	0
CCAH	Q-475	20	100	0	1500	0	10	0	20	0	0
CCAH	Q-476	10	100	0	1500	0	100	0	20	0	50
CCAH	Q-477	0	0	0	1000	0	70	0	10	0	0
CCAH	Q-478	0	0	0	2000	0	100	0	30	0	0
CCAH	Q-479	0	0	0	1000	0	70	0	10	0	0
CCAH	Q-480	30	0	0	1500	0	150	50	0	0	0
CCAH	Q-481	20	0	0	2000	0	150	0	0	0	0
CCAH	Q-482	10	200	0	1500	0	100	0	0	0	0
CCAH	Q-483	20	0	0	2000	0	100	0	0	0	0
CCAH	Q-551	15	0	0	3000	0	70	50	30	0	0
CCAH	Q-591	30	150	0	3000	0	150	0	10	0	0
CCAH	Q-598	20	0	0	1000	0	100	0	0	0	0
CCAH	Q-599	0	0	0	1000	0	50	0	20	0	0

min.dist	sample no.	Ag	As	Au	Ba	Be	Bi	B	Cd	Co	Cr	Cu
CCAH	Q-600	1.5	0	0.04	1000	1.5	0	50	0	0	100	70
CCAH	Q-606	1.5	0	0.08	1000	1	0	0	0	0	70	1000
CCAH	Q-607	30	2000	1.8	700	0	50	0	100	5	30	5000
CCAH	Q-609	3	0	0.2	1000	1	0	0	0	5	70	3000
CCAH	Q-610	5	0	0.08	1000	1	10	0	0	10	50	7000
CCAH	Q-611	1.5	0	0.08	1500	1	10	10	0	10	70	2000
CCAH	Q-613	0.5	500	0.04	500	20	0	0	50	50	20	3000
CCAH	Q-614	1.5	0	0.1	700	1	0	0	0	0	50	20000
CCAH	Q-615	100	700	0.02	1000	0	20	15	0	5	70	20000
CCAH	Q-616	1	1000	0.04	1000	7	0	10	20	20	150	5000
CCAH	Q-617	50	0	0.2	1000	0	10	10	0	5	50	20000
CCAH	Q-618	3	0	0.06	1500	0	0	0	0	0	100	700
CCAH	Q-620	7	5000	1.2	200	1	10	10	500	70	100	10000
CCAH	Q-621	5	0	0.1	500	0	0	15	0	0	100	100
CCAH	Q-624	2	0	0.1	2000	0	0	0	0	0	70	2000
CCAH	Q-636	20	10000	1.8	700	1	70	50	50	15	70	1500
CCAH	Q-637	5	0	0.1	1000	0	0	0	0	5	50	5000
CCAH	Q-638	20	500	0.1	1000	1	10	20	0	0	70	20000
CCAH	Q-641	7	0	0.08	1000	1	0	10	0	10	70	2000
CCAH	Q-676	3	0	0.1	1500	0	0	10	0	10	100	1000
CCAH	Q-680	10	0	0.1	1500	1	0	10	0	7	100	3000
CCAH	Q-683	20	0	0.1	1000	0	10	10	0	0	100	300
CCAH	Q-684	50	500	0.3	1500	1	150	20	0	70	70	20000
CCAH	Q-686	2	0	0.1	1500	1	10	10	0	0	100	500
CCAH	Q-687	2	0	0.1	100	1.5	10	10	0	5	100	2000
CCAH	Q-688	2	0	0.1	1500	1	0	10	0	10	100	2000
CCAH	Q-689	20	0	0.04	700	1	0	15	0	0	100	2000
CCAH	Q-690	0.5	200	0.08	300	0	0	10	0	0	30	1500
CCAH	Q-691	3	0	0.06	2000	0	0	10	0	0	100	10000
CCAH	Q-692	2	300	0.1	2000	1	10	10	0	5	100	5000
CCAH	Q-693	2	0	0.08	1000	1	0	0	0	5	100	2000
CCAH	Q-694	1.5	0	0.2	700	1	0	0	0	0	50	700
CCAH	Q-695	5	0	0.1	700	1	0	0	0	5	70	3000
CCAH	Q-696	2	0	0.06	700	1.5	0	0	0	5	70	1000
CCAH	Q-697	5	2000	0.06	200	0	0	10	0	5	50	200
CCAH	Q-698	3	2000	0.06	150	0	0	10	50	10	70	500
CCAH	Q-700	3	0	0.08	700	1	0	10	0	7	70	1000
CCAH	Q-701	2	0	0.08	500	1	0	10	0	0	100	1000
CCAH	Q-702	1.5	0	0.2	700	1.5	0	10	0	0	50	1000
CCAH	Q-703	100	1500	0.2	700	5	100	15	100	10	30	1000
CCAH	Q-704	7	700	1	500	2	20	20	70	10	50	1000
CCAH	Q-705	3	0	0.06	1500	1	0	10	0	5	70	700
CCAH	Q-706	20	5000	2	700	1.5	50	0	20	15	20	1000
CCAH	Q-707	2	0	0.1	700	1.5	0	10	0	5	70	700

min.dist	sample no.	Fe	F	Hg	Li	Mn	Mo	Nb	Ni	Pb	Rb	Sb
CCAH	Q-600	30000	0	0.4	0	70	10	10	5	10	0	0
CCAH	Q-606	20000	0	0	0	150	0	10	15	10	0	0
CCAH	Q-607	200000	0	0.11	0	100	20	0	15	10000	0	0
CCAH	Q-609	30000	0	0.05	0	100	5	10	20	20	0	0
CCAH	Q-610	30000	0	0.03	0	100	5	10	20	20	0	0
CCAH	Q-611	30000	0	0.04	0	150	5	15	50	30	0	0
CCAH	Q-613	200000	0	0	0	150	10	10	15	10	0	0
CCAH	Q-614	20000	0	0.03	0	150	0	10	15	20	0	0
CCAH	Q-615	5000	0	0.03	0	30	5	10	5	7000	0	0
CCAH	Q-616	150000	0	0.6	0	200	30	10	15	50	0	0
CCAH	Q-617	20000	0	0.26	0	100	0	10	15	20	0	0
CCAH	Q-618	20000	0	0.15	0	150	10	10	20	15	0	0
CCAH	Q-620	200000	0	0.2	0	50	50	10	500	1000	0	0
CCAH	Q-621	10000	0	0.05	0	50	5	15	5	20	0	0
CCAH	Q-624	15000	0	0.04	0	100	70	15	15	20	0	0
CCAH	Q-636	150000	0	0.07	0	20	150	10	10	2000	0	0
CCAH	Q-637	30000	0	0.04	0	150	0	10	30	100	0	0
CCAH	Q-638	20000	0	0.03	0	200	0	10	100	300	0	0
CCAH	Q-641	30000	0	0.03	0	150	0	10	15	15	0	0
CCAH	Q-676	20000	0	0.07	0	100	10	15	0	20	0	0
CCAH	Q-680	30000	0	0.04	0	150	5	0	50	15	0	0
CCAH	Q-683	15000	0	0.05	0	150	30	10	5	150	0	0
CCAH	Q-684	5000	0	0.05	0	70	70	10	200	1000	0	0
CCAH	Q-686	15000	0	0.04	0	100	30	10	10	30	0	0
CCAH	Q-687	30000	0	0.07	0	150	30	10	15	30	0	0
CCAH	Q-688	20000	0	0.03	0	100	20	10	30	70	0	0
CCAH	Q-689	3000	0	0.04	0	70	50	0	5	500	0	0
CCAH	Q-690	200000	0	0.04	0	700	10	0	5	0	0	0
CCAH	Q-691	20000	0	0.05	0	200	5	0	15	150	0	0
CCAH	Q-692	30000	0	0.04	0	200	200	0	20	150	0	0
CCAH	Q-693	20000	0	0.03	0	100	10	10	15	15	0	0
CCAH	Q-694	15000	0	0.07	0	70	20	0	20	0	0	0
CCAH	Q-695	15000	0	0	0	150	30	0	50	10	0	0
CCAH	Q-696	20000	0	0	0	100	150	0	20	20	0	0
CCAH	Q-697	50000	0	0.04	0	50	200	0	15	150	0	0
CCAH	Q-698	70000	0	0.08	0	50	300	0	20	500	0	0
CCAH	Q-700	20000	0	0.04	0	100	100	10	50	10	0	0
CCAH	Q-701	20000	0	0.03	0	100	50	10	20	10	0	0
CCAH	Q-702	15000	0	0.04	0	150	0	0	15	15	0	0
CCAH	Q-703	150000	0	0.13	0	50	2000	0	20	20000	0	0
CCAH	Q-704	50000	0	0.05	0	100	200	10	50	2000	0	0
CCAH	Q-705	10000	0	0.03	0	200	50	10	20	3000	0	0
CCAH	Q-706	200000	0	0.03	0	300	500	0	20	15000	0	0
CCAH	Q-707	15000	0	0	0	150	30	0	20	200	0	0

min.dist	sample no.	Sn	Sr	Te	Ti	Tl	V	W	Y	Zn	Zr
CCAH	Q-600	20	0	0	3000	0	100	0	10	0	0
CCAH	Q-606	0	200	0	2000	0	150	0	10	0	0
CCAH	Q-607	30	200	0	500	0	50	0	0	1500	0
CCAH	Q-609	0	300	0	2000	0	150	0	10	500	0
CCAH	Q-610	0	200	0	2000	0	150	0	10	700	0
CCAH	Q-611	10	200	0	2000	0	150	0	15	1000	0
CCAH	Q-613	0	0	0	500	0	70	0	10	5000	0
CCAH	Q-614	0	200	0	2000	0	150	0	20	0	0
CCAH	Q-615	20	150	0	2000	0	50	50	20	700	0
CCAH	Q-616	0	100	0	1500	0	150	0	15	700	0
CCAH	Q-617	0	200	0	1000	0	100	100	0	200	0
CCAH	Q-618	0	0	0	2000	0	150	0	15	200	50
CCAH	Q-620	0	150	0	1500	0	150	50	70	5000	0
CCAH	Q-621	15	0	0	3000	0	100	70	15	0	0
CCAH	Q-624	0	100	0	3000	0	150	0	20	0	0
CCAH	Q-636	0	500	0	1500	0	100	0	30	0	50
CCAH	Q-637	0	300	0	1500	0	100	0	10	300	0
CCAH	Q-638	10	0	0	2000	0	150	0	70	1000	0
CCAH	Q-641	0	300	0	2000	0	100	0	15	300	0
CCAH	Q-676	10	0	0	3000	0	100	100	15	0	0
CCAH	Q-680	0	200	0	1500	0	100	0	0	700	0
CCAH	Q-683	20	0	0	1500	0	100	0	0	0	0
CCAH	Q-684	20	0	0	1500	0	70	50	0	2000	0
CCAH	Q-686	20	100	0	1500	0	100	0	0	200	0
CCAH	Q-687	10	300	0	2000	0	100	0	20	300	0
CCAH	Q-688	10	200	0	1500	0	70	0	0	700	0
CCAH	Q-689	15	0	0	1500	0	70	0	0	0	0
CCAH	Q-690	0	0	0	500	0	50	0	0	0	0
CCAH	Q-691	10	200	0	1500	0	100	0	15	0	0
CCAH	Q-692	10	150	0	1500	0	150	0	10	300	0
CCAH	Q-693	0	300	0	1500	0	70	0	10	0	0
CCAH	Q-694	0	150	0	1000	0	50	0	0	300	0
CCAH	Q-695	0	200	0	1500	0	70	0	15	200	0
CCAH	Q-696	0	300	0	1500	0	70	0	0	200	0
CCAH	Q-697	0	0	0	700	0	50	0	0	0	0
CCAH	Q-698	0	100	0	1000	0	30	0	0	0	0
CCAH	Q-700	0	300	0	1500	0	70	0	0	500	0
CCAH	Q-701	0	200	0	1500	0	70	0	10	0	0
CCAH	Q-702	10	150	0	2000	0	70	0	10	0	0
CCAH	Q-703	100	1000	0	700	0	50	0	0	300	0
CCAH	Q-704	30	0	0	2000	0	70	0	0	700	0
CCAH	Q-705	20	0	0	1500	0	70	0	0	300	0
CCAH	Q-706	0	1500	0	200	0	50	0	0	2000	0
CCAH	Q-707	0	200	0	1500	0	50	0	10	500	0

min.dist	sample no.	Ag	As	Au	Ba	Be	Bi	B	Cd	Co	Cr	Cu
CCAH	Q-769	15	0	0.1	1000	1	0	10	0	10	150	1000
CCAH	Q-770	100	10000	0.1	700	1	20	20	0	0	200	1000
CCAH	Q-771	2	2000	0.4	100	0	20	0	0	0	100	1000
CCAH	Q-773	5	0	0.1	1000	1	0	0	0	5	150	2000
CCAH	Q-774	3	0	0.1	1000	0	0	0	0	5	20	2000
CCAH	Q-775	3	0	0.08	1000	0	0	10	0	0	300	2000
CCAH	Q-776	5	0	0.2	1000	1	0	10	0	5	100	1000
CCAH	Q-777	3	0	0.1	1000	1	0	0	0	0	100	5000
CCAH	Q-778	20	5000	0.2	700	1	20	10	150	0	100	700
CCAH	Q-779	3	0	0.1	1000	1.5	10	10	0	7	70	1000
CCAH	Q-780	3	0	0.1	1000	1	0	10	0	0	100	1000
CCAH	Q-781	20	700	0.08	1000	1	10	15	0	0	70	20000
CCAH	Q-784	15	10000	1.3	1000	1	150	10	0	0	100	2000
CCAH	Q-787	7	700	0.08	1000	1.5	10	20	0	0	100	1500
CCAH	Q-790	20	3000	1	300	1	0	10	0	0	200	3000
CCAH	Q-791	50	1500	1	200	0	15	10	0	0	100	700
CCAH	Q-794	0.5	0	0.1	2000	0	0	10	0	15	150	5000
CCAH	Q-795	7	0	0.04	1500	1.5	0	10	0	5	100	20000
CCAH	Q-796	3	0	0.1	1500	0	0	10	0	0	150	2000
CCAH	Q-798	30	200	0.06	500	1	15	20	0	0	100	200
CCAH	Q-799	30	3000	0.3	1000	1	15	20	0	0	100	1500
CCAH	Q-800	50	3000	0.08	1000	1	50	20	0	0	100	500
CCAH	Q-801	5	0	0.06	1000	1	0	0	0	10	150	2000
CCAH	Q-802	50	0	0.04	2000	1	0	15	0	0	30	20000
CCAH	Q-803	20	3000	0.3	300	1	30	20	0	7	30	5000
CCAH	Q-804	5	0	0.08	2000	0	0	0	0	0	70	10000
CCAH	Q-805	100	0	0.08	2000	1	0	20	0	0	70	20000
CCAH	Q-807	10	0	0.06	1000	1	0	15	0	5	70	200
CCAH	Q-808	7	0	0.04	1500	1	0	0	0	7	70	1500
CCAH	Q-809	5	0	0.2	1000	0	10	0	0	0	70	1500
CCAH	Q-810	3	0	0.06	1500	0	0	0	0	5	70	7000
CCAH	Q-811	50	0	0.06	1500	0	0	0	0	5	100	5000
CCAH	Q-812	2	0	0.08	1500	0	0	0	0	5	50	2000
CCAH	Q-813	7	0	0.1	1500	1	0	0	0	7	70	15000
CCAH	Q-814	1	0	0.1	1500	1	0	0	0	15	70	5000
CCAH	Q-815	2	0	0.06	1000	0	0	0	0	5	70	5000
CCAH	Q-816	3	0	0.08	1500	1.5	0	0	0	5	100	15000
CCAH	Q-817	1.5	0	0.08	1500	0	0	0	0	5	100	10000
CCAH	Q-818	2	0	0.06	1500	1	0	0	0	5	100	1000
CCAH	Q-870	30	2000	0.54	100	0	0	30	0	0	50	1000
CCAH	Q-871	3	700	0.06	2000	0	0	15	0	0	300	200
CCAH	Q-872	3	0	0.16	3000	0	0	10	0	15	70	2000
CCAH	Q-873	7	1500	1.26	300	0	0	0	0	5	300	2000
CCAH	Q-884	7	0	0.22	1000	1	0	15	0	0	70	500

min.dist	sample no.	Fe	F	Hg	Li	Mn	Mo	Nb	Ni	Pb	Rb	Sb
CCAH	Q-769	30000	0	0.05	0	150	30	10	30	15	0	0
CCAH	Q-770	200000	0	0.05	0	50	300	10	10	15000	0	0
CCAH	Q-771	10000	0	0	0	100	0	0	5	70	0	0
CCAH	Q-773	20000	0	0.03	0	100	30	10	30	15	0	0
CCAH	Q-774	30000	0	0.12	0	150	20	10	20	15	0	0
CCAH	Q-775	15000	0	0.04	0	150	20	10	5	20	0	0
CCAH	Q-776	20000	0	0.04	0	100	100	10	20	15	0	0
CCAH	Q-777	15000	0	0.04	0	70	20	10	20	10	0	0
CCAH	Q-778	150000	0	0.12	0	50	500	10	30	3000	0	150
CCAH	Q-779	20000	0	0.04	0	150	30	10	20	50	0	0
CCAH	Q-780	20000	0	0.07	0	70	30	10	30	10	0	0
CCAH	Q-781	15000	0	0.08	0	30	150	10	5	10	0	0
CCAH	Q-784	200000	0	0.04	0	30	1000	10	5	1500	0	0
CCAH	Q-787	50000	0	0.04	0	50	50	10	5	150	0	0
CCAH	Q-790	15000	0	1.1	0	50	20	20	0	70	0	0
CCAH	Q-791	50000	0	0.16	0	50	100	10	0	200	0	0
CCAH	Q-794	20000	0	0.04	0	150	0	15	10	15	0	0
CCAH	Q-795	20000	0	0.04	0	100	15	10	10	150	0	0
CCAH	Q-796	20000	0	0.04	0	100	0	10	10	70	0	0
CCAH	Q-798	20000	0	0.07	0	100	20	15	0	3000	0	0
CCAH	Q-799	150000	0	0.09	0	100	200	10	0	3000	0	0
CCAH	Q-800	50000	0	0.13	0	70	15	10	5	3000	0	0
CCAH	Q-801	20000	0	0	0	100	15	0	50	10	0	0
CCAH	Q-802	10000	0	0	0	50	30	0	10	100	0	0
CCAH	Q-803	100000	0	0	0	30	150	0	5	10000	0	0
CCAH	Q-804	10000	0	0	0	70	0	0	7	30	0	0
CCAH	Q-805	5000	0	0	0	100	50	0	5	70	0	0
CCAH	Q-807	10000	0	0	0	100	70	0	5	300	0	0
CCAH	Q-808	15000	0	0	0	100	5	0	20	20	0	0
CCAH	Q-809	10000	0	0	0	70	20	0	5	20	0	0
CCAH	Q-810	10000	0	0	0	100	7	0	30	15	0	0
CCAH	Q-811	20000	0	0	0	100	7	0	20	15	0	0
CCAH	Q-812	10000	0	0	0	100	0	0	20	20	0	0
CCAH	Q-813	15000	0	0	0	100	0	0	30	30	0	0
CCAH	Q-814	15000	0	0	0	100	20	10	50	10	0	0
CCAH	Q-815	7000	0	0	0	70	0	0	10	20	0	0
CCAH	Q-816	15000	0	0	0	150	5	10	20	15	0	0
CCAH	Q-817	15000	0	0	0	70	10	10	20	15	0	0
CCAH	Q-818	20000	0	0	0	150	20	0	50	10	0	0
CCAH	Q-870	70000	0	1.5	0	100	50	0	7	700	0	0
CCAH	Q-871	50000	0	0.22	0	10	5	0	7	150	0	150
CCAH	Q-872	20000	0	0.13	0	50	7	10	20	70	0	0
CCAH	Q-873	200000	0	0.26	0	10	15	30	0	20	0	0
CCAH	Q-884	15000	0	0.04	0	50	30	10	7	0	0	0

min.dist	sample no.	Sn	Sr	Te	Ti	Tl	V	W	Y	Zn	Zr
CCAH	Q-769	0	500	0	2000	0	150	0	15	300	0
CCAH	Q-770	30	500	0	1000	0	100	0	0	700	0
CCAH	Q-771	0	0	0	1000	0	20	0	30	0	0
CCAH	Q-773	0	300	0	2000	0	100	0	10	200	0
CCAH	Q-774	0	200	0	2000	0	150	0	10	0	0
CCAH	Q-775	0	0	0	2000	0	100	0	50	0	0
CCAH	Q-776	10	200	0	2000	0	100	0	10	500	0
CCAH	Q-777	0	70	0	1500	0	70	0	20	0	0
CCAH	Q-778	50	700	0	1500	0	70	0	0	1000	0
CCAH	Q-779	0	300	0	2000	0	70	0	0	500	0
CCAH	Q-780	0	300	0	1500	0	70	0	0	200	0
CCAH	Q-781	30	0	0	1500	0	100	50	10	0	0
CCAH	Q-784	20	500	0	1000	0	150	0	20	0	50
CCAH	Q-787	30	0	0	2000	0	150	50	15	0	0
CCAH	Q-790	50	0	0	3000	0	200	150	30	0	0
CCAH	Q-791	30	0	0	2000	0	50	50	50	0	50
CCAH	Q-794	15	200	0	2000	0	150	0	15	0	0
CCAH	Q-795	0	300	0	1500	0	100	0	100	0	0
CCAH	Q-796	20	200	0	2000	0	150	0	10	0	0
CCAH	Q-798	50	0	0	2000	0	100	50	10	0	0
CCAH	Q-799	50	100	0	2000	0	150	50	0	0	0
CCAH	Q-800	50	0	0	2000	0	100	70	0	0	0
CCAH	Q-801	0	500	0	2000	0	100	0	15	0	0
CCAH	Q-802	0	0	0	1000	0	150	0	10	0	0
CCAH	Q-803	20	300	0	700	0	50	0	0	0	50
CCAH	Q-804	0	150	0	1500	0	70	0	0	0	0
CCAH	Q-805	10	0	0	1500	0	100	0	10	0	50
CCAH	Q-807	20	0	0	3000	0	150	0	0	0	0
CCAH	Q-808	0	700	0	2000	0	100	0	20	0	0
CCAH	Q-809	10	0	0	1000	0	70	0	0	0	0
CCAH	Q-810	0	200	0	1500	0	70	0	15	0	50
CCAH	Q-811	0	300	0	1500	0	100	0	15	0	0
CCAH	Q-812	0	200	0	1500	0	50	0	10	0	0
CCAH	Q-813	0	300	0	1500	0	100	0	15	0	0
CCAH	Q-814	0	500	0	2000	0	70	0	30	200	0
CCAH	Q-815	0	300	0	1000	0	50	0	10	0	0
CCAH	Q-816	0	500	0	3000	0	100	0	20	0	0
CCAH	Q-817	0	500	0	1500	0	100	0	20	0	0
CCAH	Q-818	0	300	0	2000	0	100	0	10	200	50
CCAH	Q-870	15	0	0	3000	0	200	0	0	0	50
CCAH	Q-871	10	150	0	2000	0	150	0	0	0	0
CCAH	Q-872	10	0	0	5000	0	70	0	20	0	0
CCAH	Q-873	15	0	0	10000	0	300	70	70	0	0
CCAH	Q-884	10	0	0	5000	0	150	0	20	0	0

min.dist	sample no.	Ag	As	Au	Ba	Be	Bi	B	Cd	Co	Cr	Cu
CCAH	Q-891	7	1500	0.22	300	0	10	20	0	0	100	700
CCAH	Q-897	30	1500	1.8	70	0	20	0	0	0	70	1000
CCAH	Q-898	20	1000	0.5	700	1	10	20	0	0	200	30
CCAH	Q-899	7	0	0.06	2000	1.5	0	50	0	0	100	150
CCAH	Q-973	0.7	500	0.2	1500	1	0	70	0	0	150	200
CCAH	Q-974	3	300	0.14	5000	0	0	10	0	0	150	300
CCAH	Q-976	50	5000	0.28	1000	1	20	20	0	0	70	500
CCAH	Q-977	7	200	0.08	700	1.5	0	30	0	5	70	10000
CCAH	Q-978	7	0	0.06	1000	1.5	0	0	0	5	100	10000
CCAH	Q-979	3	0	0.08	700	0	0	0	0	10	70	10000
CCAH	Q-980	3	0	0.06	1000	1	0	15	0	15	70	1500
CCAH	Q-981	3	0	0.12	700	0	0	0	0	50	100	10000
CCAH	Q-982	5	0	0.16	1000	2	0	20	0	0	100	2000
CCAH	Q-983	7	0	0.28	700	0	0	0	0	7	100	10000
CCAH	Q-986	10	0	0.04	700	1.5	0	50	0	0	70	300
DEXI	DX-82-2A	1.2	196	0.23	590	1.3	305	50	3	18	106	4250
DEXI	DX-82-2B	4.4	22	0.33	172	0.9	5	31	<3	37	138	7000
DEXI	DX-82-4	5.5	250	0.73	640	1.1	24	86	<3	10	94	4200
DSPO	10	3.72	1.68	0.083	0	0	1.73	0	0.402	0	0	14900
DSPO	11	1.93	1.33	0.041	0	0	0.681	0	0.248	0	0	7703
DSPO	12	2.2	1.78	0.427	0	0	2.55	0	<.247	0	0	5070
DSPO	13	6.51	<0.991	0.636	0	0	2.39	0	<.248	0	0	9368
ELSA	ES-1-Y	1.7	<10	0.005	37	0.9	14	30	<3	21	57	340
ELSA	ES-2	2.7	<10	0.061	240	1.1	8	17	<3	22	55	3400
ELSA	ES-3	2.7	<10	0.041	215	1.6	<2	29	<3	34	120	2550
ELSA	ES-4	1.5	<10	0.031	81	1	<2	350	<3	54	192	550
ELSA	ES-6	1.4	<10	0.036	126	1.3	11	<5	<3	28	138	2700
ELTE	4-10	1.4	48	0.003	3	1	<2	13000	<3	29	150	925
ELTE	4-19	2.2	570	0.034	315	1.9	14	6250	<3	5	36	9100
ELTE	4-22	270	40000	4.8	<2	<0.2	92	116	144	38	26	5700
ELTE	4-23	122	3450	0.79	80	0.9	35	1390	19	26	205	15100
ELTE	4-30	11.9	140	0.034	126	1.4	20	6100	<3	10	280	8300
HEDL	D8457	2.12	38	0.046	930	0	9	0	0	16	92	84
HEDL	D8458	0.7	106	0.047	<20	0	3	0	0	3	65	92
HEDL	D8459	2.5	200	0.252	50	0	<2	0	0	45	30	14660
HEDL	D8460	4.3	1468	3.81	<20	0	28	0	0	43	51	239
MCCO	138311	16.3	97	0.86	7	0	6	2	7	56	22	3655
MCCO	138312	0.3	94	0.046	501	0	2	4	2	10	108	258
MCCO	138313	0.5	52	0.156	380	0	2	2	1	5	82	95
MCCO	138314	13.8	70	44.2	375	0	24	7	192	117	45	3385
MCCO	138315	56.4	1725	15.8	8	0	48	8	5	75	32	2469
MCCO	8951	1.66	33.3	0.059	0	0	0.462	0	1.81	0	0	62.9
MCCO	8952	0.748	67.7	0.125	0	0	0.705	0	11.5	0	0	191
MCCO	8953	0.854	17.5	<0.046	0	0	0.567	0	1.05	0	0	37.7

min.dist	sample no.	Fe	F	Hg	Li	Mn	Mo	Nb	Ni	Pb	Rb	Sb
CCAH	Q-891	100000	0	0.1	0	50	5	0	5	700	0	0
CCAH	Q-897	100000	0	0.14	0	30	0	0	0	70	0	0
CCAH	Q-898	50000	0	0.14	0	50	15	0	5	1000	0	0
CCAH	Q-899	30000	0	0.07	0	70	0	15	15	70	0	0
CCAH	Q-973	30000	0	0.16	0	15	15	15	5	0	0	0
CCAH	Q-974	15000	0	0.03	0	20	5	0	5	20	0	0
CCAH	Q-976	100000	0	0.8	0	30	70	0	0	15000	0	100
CCAH	Q-977	7000	0	0.75	0	200	15	10	15	300	0	0
CCAH	Q-978	10000	0	0.1	0	100	20	0	30	20	0	0
CCAH	Q-979	10000	0	0.05	0	100	30	0	30	0	0	0
CCAH	Q-980	7000	0	0.07	0	100	50	0	50	30	0	0
CCAH	Q-981	10000	0	0.06	0	100	20	0	100	0	0	0
CCAH	Q-982	20000	0	0.1	0	300	100	15	20	70	0	0
CCAH	Q-983	10000	0	0.07	0	70	0	0	30	0	0	0
CCAH	Q-986	7000	0	0.13	0	200	70	0	7	150	0	0
DEXI	DX-82-2A	28600	1000	0	97	295	310	9	22	28	136	54
DEXI	DX-82-2B	55400	400	0	<10	194	166	4	27	555	90	9
DEXI	DX-82-4	35500	800	0	23	580	11	6	0	855	164	12
DSPO	10	0	0	<.099	0	0	38.8	0	0	0.918	0	<.247
DSPO	11	0	0	<.098	0	0	14.5	0	0	1.67	0	<.245
DSPO	12	0	0	<.099	0	0	3.32	0	0	6.87	0	<.247
DSPO	13	0	0	<.099	0	0	4.41	0	0	4.17	0	<.248
ELSA	ES-1-Y	59100	500	0	27	225	18	21	5	12	72	<5
ELSA	ES-2	56200	700	0	31	425	25	29	13	15	89	<5
ELSA	ES-3	43800	200	0	12	152	13	6	11	10	70	<5
ELSA	ES-4	65100	500	0	24	180	13	10	12	<10	104	<5
ELSA	ES-6	32500	600	0	23	410	45	29	10	<10	58	<5
ELTE	4-10	41900	400	0	21	114	56	5	16	15	<1	<5
ELTE	4-19	39000	300	0	13	34	205	<1	12	775	178	21
ELTE	4-22	68800	100	0	37	615	16	<1	5	34	23	16600
ELTE	4-23	29800	100	0	50	325	15000	<1	13	24300	57	4150
ELTE	4-30	47400	300	0	15	128	2050	<1	28	37	88	<5
HEDL	D8457	0	0	<0.005	0	348	1	0	37	22	0	<5
HEDL	D8458	0	0	0.01	0	2102	4	0	5	<5	0	<5
HEDL	D8459	0	0	0.01	0	534	3	0	137	14	0	27
HEDL	D8460	0	0	0.005	0	2694	1	0	54	75	0	11
MCCO	138311	229000	25	0.08	0	955	3	0	6	93	0	2
MCCO	138312	138000	40	0.09	0	50	3	0	6	5	0	2
MCCO	138313	26800	21	0.02	0	460	14	0	9	10	0	2
MCCO	138314	21200	6	0.01	0	2781	5	0	29	33	0	2
MCCO	138315	402000	14	0.005	0	341	5	0	14	50	0	2
MCCO	8951	0	0	<.095	0	0	2.6	0	0	80.1	0	0.554
MCCO	8952	0	0	<.095	0	0	1.61	0	0	225	0	1.43
MCCO	8953	0	0	<.092	0	0	9.46	0	0	45.2	0	<.229

min.dist	sample no.	Sn	Sr	Te	Ti	Tl	V	W	Y	Zn	Zr
CCAH	Q-891	15	100	0	3000	0	200	50	15	0	0
CCAH	Q-897	100	0	0	3000	0	100	0	30	0	0
CCAH	Q-898	20	0	0	2000	0	100	0	0	0	50
CCAH	Q-899	0	0	0	5000	0	150	0	20	0	0
CCAH	Q-973	10	0	0	7000	0	200	50	20	0	0
CCAH	Q-974	0	200	0	3000	0	150	0	0	0	0
CCAH	Q-976	15	0	0	1500	0	50	0	0	0	0
CCAH	Q-977	15	0	0	1500	0	70	0	0	0	0
CCAH	Q-978	0	500	0	2000	0	100	0	15	0	0
CCAH	Q-979	0	200	0	1500	0	70	0	15	0	0
CCAH	Q-980	0	200	0	1500	0	70	0	15	0	0
CCAH	Q-981	0	300	0	1000	0	100	0	10	0	0
CCAH	Q-982	10	100	0	2000	0	150	0	10	0	0
CCAH	Q-983	0	300	0	1500	0	150	0	15	0	0
CCAH	Q-986	10	0	0	1500	0	100	0	0	0	0
DEXI	DX-82-2A	<5	55	0	1550	<2	83	<5	5.9	41	5
DEXI	DX-82-2B	<5	18	0	745	<2	58	<5	3.5	24	9
DEXI	DX-82-4	<5	81	0	1610	<2	73	<5	4	86	0
DSPO	10	0.932	0	<.495	0	<.495	0	0	0	38	0
DSPO	11	2	0	<.491	0	<.491	0	0	0	42.8	0
DSPO	12	1.13	0	<.493	0	<.493	0	0	0	62.5	0
DSPO	13	<.495	0	1.07	0	<.495	0	0	0	37.8	0
ELSA	ES-1-Y	<5	385	0	1750	<2	172	<5	4.9	8	<2
ELSA	ES-2	<5	560	0	3750	<2	270	<5	6.8	27	<2
ELSA	ES-3	<5	525	0	670	<2	78	<5	4.1	20	<2
ELSA	ES-4	<5	280	0	1140	<2	89	14	4	23	<2
ELSA	ES-6	<5	525	0	4500	<2	188	<5	9.2	60	1
ELTE	4-10	<5	210	0	750	<2	45	<5	5	40	<2
ELTE	4-19	<5	64	0	905	<2	64	18	5.8	275	<2
ELTE	4-22	<5	6	0	6	<2	<3	6	3.7	29700	<2
ELTE	4-23	<5	1140	0	610	<2	48	<5	2.6	3200	<2
ELTE	4-30	<5	35	0	1460	<2	156	67	<2	69	<2
HEDL	D8457	0	0	<0.5	0	<0.5	0	<10	0	74	0
HEDL	D8458	0	0	<0.5	0	<0.5	0	<10	0	6	0
HEDL	D8459	0	0	<0.5	0	<0.5	0	32	0	278	0
HEDL	D8460	0	0	0.9	0	<0.5	0	<10	0	67	0
MCCO	138311	0	45	0	300	0	0	2	0	782	0
MCCO	138312	0	24	0	100	0	0	5	0	81	0
MCCO	138313	0	33	0	900.0001	0	0	31	0	72	0
MCCO	138314	0	66	0	100	0	0	13	0	1943	0
MCCO	138315	0	12	0	100	0	0	10	0	687	0
MCCO	8951	0	0	<.474	0	<.474	0	0	0	187	0
MCCO	8952	0	0	<.476	0	<.476	0	0	0	301	0
MCCO	8953	0	0	<.458	0	<.458	0	0	0	103	0

min.dist	sample no.	Ag	As	Au	Ba	Be	Bi	B	Cd	Co	Cr	Cu
MCCO	8954	0.442	209	<0.049	0	0	1.46	0	6.02	0	0	314
MCCO	8955	0.552	11.7	<0.049	0	0	0.501	0	0.476	0	0	14.1
MCCO	8956	4.95	641	0.23	0	0	45.1	0	14.4	0	0	1922
MCCO	8957	0.372	26.3	<0.046	0	0	1.22	0	2.79	0	0	24.7
MCCO	8958	0.871	22.2	<0.047	0	0	0.241	0	3.94	0	0	29.3
MCCO	8959	10.6	123	0.3	0	0	9.79	0	5.34	0	0	2668
MCCO	8960	20.4	370	2.4	0	0	36.9	0	215	0	0	632
MCCO	8961	1.22	65.8	0.17	0	0	44.5	0	34.4	0	0	310
MCCO	8962	55.4	235	4.3	0	0	109	0	5.96	0	0	89
MCCO	8963	0.638	138	3.72	0	0	12.2	0	15.2	0	0	522
MCCO	8964	0.886	61.4	0.33	0	0	12.8	0	3.08	0	0	829
MORE	M-1	54.3	<10	425	<2	1.1	154	47.4	10	<2	132	325
MORE	M-2	2.6	<10	8	1930	1.4	7	7.2	2	11	118	5200
MORE	M-3	2.5	<10	9	1280	1.9	8	7.9	1	<2	102	5950
MORE	M-4	1.4	<10	10	325	2.5	16	11.1	1	31	134	5950
MORE	M-5	5.3	<10	17	<2	7.2	29	33.2	41	5	108	1920
MORE	M-6	1.8	<10	9	605	2	29	4.3	1	13	122	4050
MORE	M-7	0.2	<10	7	260	1.8	<5	25.3	1	5	162	685
MORE	M-8	3.7	<10	12	1280	1.9	<5	<2	4	11	158	5150
MORE	M-9	3.4	<10	18	166	5	<5	<2	5	56	114	9550
MORE	M-10	0.3	<10	8	1360	1.4	<5	<2	1	<2	104	3200

min.dist	sample no.	Fe	F	Hg	Li	Mn	Mo	Nb	Ni	Pb	Rb	Sb
MCCO	8954	0	0	<.097	0	0	1.61	0	0	255	0	4.61
MCCO	8955	0	0	<.098	0	0	2.38	0	0	37.4	0	<.245
MCCO	8956	0	0	0.213	0	0	4.97	0	0	901	0	31.4
MCCO	8957	0	0	<.092	0	0	3.88	0	0	22	0	0.419
MCCO	8958	0	0	<.095	0	0	0.557	0	0	55	0	0.322
MCCO	8959	0	0	<.095	0	0	5.82	0	0	60.2	0	<.236
MCCO	8960	0	0	7.09	0	0	12.1	0	0	607	0	14.9
MCCO	8961	0	0	0.234	0	0	0.79	0	0	17.7	0	1.34
MCCO	8962	0	0	0.33	0	0	2.6	0	0	3651	0	2.57
MCCO	8963	0	0	0.113	0	0	0.991	0	0	43.4	0	2.93
MCCO	8964	0	0	0.136	0	0	<.091	0	0	71.6	0	<.226
MORE	M-1	213000	0	4	0	10000	11	<2	9	3100	<2	<5
MORE	M-2	8900	0	<2	0	134	108	<2	9	53	196	<5
MORE	M-3	7900	0	<2	0	23	19	<2	6	29	116	<5
MORE	M-4	37900	0	<2	0	78	61	<2	10	21	122	<5
MORE	M-5	115000	0	<2	0	4150	7	6	16	<2	16	<5
MORE	M-6	18000	0	<2	0	71	8	<2	9	43	122	<5
MORE	M-7	36400	0	2	0	44	7	6	7	27	83	<5
MORE	M-8	16700	0	2	0	150	34	<2	11	87	158	<5
MORE	M-9	146000	0	2	0	815	39	56	9	<2	325	<5
MORE	M-10	7400	0	<2	0	74	54	2	6	168	134	<5

min.dist	sample no.	Sn	Sr	Te	Ti	Tl	V	W	Y	Zn	Zr
MCCO	8954	0	0	0.888	0	0.547	0	0	0	1571	0
MCCO	8955	0	0	<.49	0	<.49	0	0	0	60.1	0
MCCO	8956	0	0	11.4	0	1.18	0	0	0	5559	0
MCCO	8957	0	0	<.462	0	<.462	0	0	0	316	0
MCCO	8958	0	0	<.473	0	<.473	0	0	0	167	0
MCCO	8959	0	0	1.85	0	<.473	0	0	0	1378	0
MCCO	8960	0	0	6.58	0	21.8	0	0	0	10100	0
MCCO	8961	0	0	18.4	0	0.963	0	0	0	958	0
MCCO	8962	0	0	51.9	0	0.472	0	0	0	260	0
MCCO	8963	0	0	2.25	0	<.477	0	0	0	4222	0
MCCO	8964	0	0	<.453	0	0.812	0	0	0	14100	0
MORE	M-1	<5	6	0	34	8	7	42	<2	6050	0
MORE	M-2	<5	360	0	575	<2	22	<5	2.7	840	8
MORE	M-3	<5	330	0	345	<2	18	5	15.7	160	5
MORE	M-4	<5	134	0	1060	<2	41	7	3	505	4
MORE	M-5	<5	18	0	1630	<2	30	9	4.7	22600	4
MORE	M-6	<5	450	0	710	<2	19	11	5.3	186	8
MORE	M-7	<5	37	0	1220	<2	18	21	3.3	19	5
MORE	M-8	<5	435	0	1590	<2	23	15	6.8	710	8
MORE	M-9	<5	34	0	18600	<2	500	40	80.4	630	7
MORE	M-10	<5	915	0	565	<2	26	<5	<2	68	8

min.dist	sample no.	Ag	As	Au	Ba	Be	Bi	B	Cd	Co	Cr	Cu
ALLI	AR002A	0.5	320	0	2000	2	0	200	0.5	50	150	30
ALLI	AR003A	1.5	30	0.1	1000	0	0	50	0.1	0	<10 <5	
ALLI	AR003B	1	270	0.15	>5000	<1.0	0	100	0.2	0	0	5
ALLI	AR004A	2	55	0.25	>5000	1	0	50	0.3	0	0	5
ALLI	AR005A	2	65	0.3	>5000	1	0	100	0.1	0	20	10
ALLI	AR006A	2	120	0.9	700	0	0	150	0.5	0	20	10
ALLI	AR007A	0.7	350	0.1	2000	1.5	0	200	1.8	0	100	30
ALLI	AR009A	0.5	310	0	5000	2	0	200	2.2	15	70	20
ALLI	AR010A	0	780	0	500	3	0	500	0.7	15	150	30
ALLI	AR011A	5	600	1.2	300	1.5	0	200	0.2	0	100	20
ALLI	AR012A	7	1900	1	5000	3	0	500	1.1	10	100	30
ALLI	AR013A	5	80	0.25	500	1	0	100	0.2	0	10	5
BASQ	277	0.283	86.7	0.039	<20	<1	<.239	3	0.147	4	29	5.05
BASQ	278	0.432	503	0.269	140	4	0.451	22	0.242	50	398	52.1
BASQ	279	0.259	85.1	0.535	800	2	0.276	5	0.25	8	40	15.6
BASQ	280	3.33	182	14.4	370	2	<.241	5	0.163	15	62	15.9
CARL	01A	1	100	<0.3	4900	<1	0	20	0	<2	10	20
CARL	01B	0	740	9	200	0	0	70	0	<2	70	10
CARL	01C	0	30	2	700	1	0	15	0	20	200	15
CARL	01D	<0.7	840	5	200	<1	0	50	0	3	70	15
CARL	02A	1	280	0.15	165	1.5	0	50	0	2	30	30
CARL	02B	0	148	5	170	0	0	70	0	3	50	15
CARL	02C	0	15	0.1	1000	<1	0	10	0	10	70	15
CARL	02D	<0.7	760	12	190	<1	0	150	0	7	70	50
CARL	03A	1	370	0.03	205	1.5	0	30	0	3	20	20
CARL	03D	<0.7	154	6	180	<1	0	70	0	5	50	15
CARL	04A	1.5	235	<0.03	172	1.5	0	70	0	5	30	30
CARL	04D	<0.7	148	10	170	<1	0	70	0	3	50	15
CARL	05A	0.7	240	0.6	510	<1	0	<7	0	<2	100	7
CARL	05D	1.5	194	5	300	2	0	100	0	<2	70	50
CARL	06A	0.7	400	2.5	405	1.5	0	7	0	5	20	100
CARL	06D	0.7	1750	8	520	<1	0	10	0	2	10	50
CARL	07A	<0.7	185	0.6	255	<1	0	30	0	3	30	30
CARL	07D	1	385	23	500	<1	0	7	0	<2	10	70
CARL	08A	1.5	40	4.5	240	<1	0	30	0	<2	50	10
CARL	08D	<0.7	295	4	145	<1	0	70	0	5	70	20
CARL	09D	0.7	940	18	189	<1	0	70	0	5	100	50
CARL	10D	<0.7	760	6	180	<1	0	150	0	7	20	50
CARL	11D	<0.7	180	6	138	<1	0	20	0	7	30	30
CARL	12D	<0.7	610	34	255	<1	0	30	0	3	30	50
CARL	13D	<0.7	11100	69	800	<1	0	30	0	3	70	50
CARL	14D	0.7	24700	130	560	<1	0	30	0	2	100	70
CARL	75258	0.7	375	1.5	0	0	<.1	80	8.06	5	54	48
CARL	75259	0.5	440	10.6	0	0	<.1	75	2.1	6	56	53

min.dist	sample no.	Fe	F	Hg	Li	Mn	Mo	Nb	Ni	Pb	Rb	Sb
ALLI	AR002A	10000	600	0.4	0	100	0	0	50	10	0	10
ALLI	AR003A	2000	0	0.7	0	150	0	0	<5	0	0	12
ALLI	AR003B	15000	0	0.1	0	<10	0	0	<5	0	0	190
ALLI	AR004A	3000	100	0.06	0	<10	0	0	<5	10	0	80
ALLI	AR005A	5000	300	0	0	70	0	0	<5	0	0	18
ALLI	AR006A	7000	200	0.5	0	50	0	0	10	0	0	34
ALLI	AR007A	20000	300	1.1	0	20	30	0	20	0	0	92
ALLI	AR009A	15000	200	4	0	100	15	0	100	0	0	360
ALLI	AR010A	30000	700	0.7	0	300	50	0	20	30	0	50
ALLI	AR011A	50000	700	0.2	0	10	30	0	5	0	0	180
ALLI	AR012A	30000	2300	0.54	0	1000	7	<20	70	0	0	100
ALLI	AR013A	5000	200	0.26	0	10	0	0	20	0	0	56
BASQ	277	0	150	<.095	1	122	0.307	0	10	12.2	30	0.964
BASQ	278	0	670	2.07	65	1697	2.76	0	188	19.6	38	2.81
BASQ	279	0	180	1.58	10	183	0.515	0	18	4.83	49	1.47
BASQ	280	0	220	<.097	11	374	0.705	0	54	7.5	93	2.26
CARL	01A	0	0	6	0	3	<2	0	10	<7	0	55
CARL	01B	0	0	14	0	150	3	<7	15	<7	0	<40
CARL	01C	0	0	0	<100	1000	5	10	50	10	0	40
CARL	01D	0	0	23	0	200	<2	0	15	<7	0	140
CARL	02A	0	0	0.04	0	15	<2	0	20	10	0	330
CARL	02B	0	0	12	0	100	<2	<7	30	<7	0	<40
CARL	02C	0	0	1	<100	500	<2	10	10	<7	0	<40
CARL	02D	0	0	35	0	100	15	0	50	15	0	60
CARL	03A	0	0	14	0	10	<2	0	30	15	0	435
CARL	03D	0	0	48	0	150	<2	0	20	<7	0	<20
CARL	04A	0	0	7	0	50	<2	0	30	30	0	365
CARL	04D	0	0	28	0	100	<2	0	30	<7	0	<20
CARL	05A	0	0	13	0	2	15	0	10	30	0	930
CARL	05D	0	0	12	0	10	<2	0	20	<7	0	<20
CARL	06A	0	0	10	0	7	20	0	30	10	0	500
CARL	06D	0	0	20	0	7	5	0	30	<7	0	250
CARL	07A	0	0	11	0	500	7	0	20	20	0	245
CARL	07D	0	0	55	0	7	5	0	3	<7	0	40
CARL	08A	0	0	28	0	10	<2	0	5	<7	0	540
CARL	08D	0	0	15	0	150	15	0	50	10	0	25
CARL	09D	0	0	70	0	150	3	0	30	<7	0	45
CARL	10D	0	0	35	0	100	15	0	50	15	0	25
CARL	11D	0	0	25	0	150	70	0	70	10	0	30
CARL	12D	0	0	150	0	70	10	0	15	<7	0	76
CARL	13D	0	0	200	0	150	10	0	20	<7	0	115
CARL	14D	0	0	280	0	100	7	0	20	<7	0	100
CARL	75258	0	1570	13.9	0	190	35	0	58	170	0	78
CARL	75259	0	1430	19.4	0	145	19	0	55	15	0	75

min.dist	sample no.	Sn	Sr	Te	Ti	Tl	V	W	Y	Zn	Zr
ALLI	AR002A	0	200	0.04	5000	7.8	150	9	30	<5	0
ALLI	AR003A	0	0	0.01	200	0.4	10	1	<10	30	<10
ALLI	AR003B	0	300	0.02	50	3	100	0.5	0	15	0
ALLI	AR004A	0	500	0.025	100	0.4	10	1	<10	15	0
ALLI	AR005A	0	300	2.4	70	0.2	10	1	<10	15	0
ALLI	AR006A	0	200	0.005	700	0.6	70	2.5	15	40	0
ALLI	AR007A	0	500	0.095	2000	2	1000	6.5	30	160	0
ALLI	AR009A	0	200	0.045	2000	14	200	9	30	310	0
ALLI	AR010A	0	200	0.08	3000	2.8	100	7.5	30	100	0
ALLI	AR011A	0	700	0.215	2000	1.4	1000	7.5	30	20	0
ALLI	AR012A	0	700	0.12	5000	8	100	30	30	160	0
ALLI	AR013A	0	<100	0.06	200	0.9	10	1.5	20	35	0
BASQ	277	<5	57	<.477	0	0.51	35	6	<5	24.2	90
BASQ	278	7	305	<.491	0	0.838	266	9	25	69.4	20
BASQ	279	5	70	<.481	0	0.83	43	8	<5	18.3	42
BASQ	280	<5	94	<.483	0	<.483	95	8	9	48.3	15
CARL	01A	0	30	0	200	0	50	0	15	15	0
CARL	01B	0	500	0	3000	100	70	<20	30	6	50
CARL	01C	<7	1000	0	5000	0	150	10	30	70	50
CARL	01D	0	200	0	2000	200	30	20	30	38	0
CARL	02A	0	10	0	1500	0	500		10	63	0
CARL	02B	0	500	0	1500	<3	50	20	20	25	0
CARL	02C	<7	1000	0	7000	0	100	<10	30	95	0
CARL	02D	0	150	0	2000	70	200	<20	20	62	0
CARL	03A	0	10	0	1000	0	300	0	30	161	0
CARL	03D	0	500	0	2000	<3	50	25	30	51	50
CARL	04A	0	10	0	1500	0	700	0	30	120	0
CARL	04D	0	500	0	1500	<3	50	<20	20	25	0
CARL	05A	0	200	0	3000	0	200	0	15	52	50
CARL	05D	0	150	0	2000	<3	70	<20	50	53	50
CARL	06A	0	50	0	2000	0	150	0	15	66	50
CARL	06D	0	50	0	500	<3	30	<20	10	119	0
CARL	07A	0	15	0	1500	0	700	0	15	145	0
CARL	07D	0	10	0	200	<3	70	30	<7	6	0
CARL	08A	0	50	0	2000	0	100	0	10	28	0
CARL	08D	0	150	0	2000	70	200	30	20	<5	0
CARL	09D	0	150	0	2000	<3	100	35	20	25	50
CARL	10D	0	150	0	2000	70	200	<20	20	62	0
CARL	11D	0	100	0	1000	<3	100	<20	15	7	0
CARL	12D	0	100	0	1000	100	30	<20	10	22	0
CARL	13D	0	150	0	1500	150	70	20	20	<5	50
CARL	14D	0	200	0	1500	150	100	<20	20	9	50
CARL	75258	<1	0	0.38	0	12.4	0	0	0	830	0
CARL	75259	<1	0	0.44	0	41.4	0	0	0	320	0

min.dist	sample no.	Ag	As	Au	Ba	Be	Bi	B	Cd	Co	Cr	Cu
CARL	75261	0.3	390	8.4	0	0	<.1	80	2.32	7	41	51
CARL	84-11	0	4.71	0	1100	<1.0	0	0	<2	4	27	13
CARL	84-12	0	0	0	200	<1.0	0	0	<2	8	58	20
CARL	84-13c	0	46.8	0	250	<1.0	0	0	<2	7	49	13
CARL	84-13o	0	2.32	0.017123	1100	<1.0	0	0	<2	9	51	19
CARL	84-14	0	370	0	230	1	0	0	<2	11	76	23
CARL	84-16	0	195	0.017123	3800	<1.0	0	0	<2	10	200	140
GSTR	88-1001	0.166	1158	0.969	490	5	<0.236	8	<0.236	4	61	49.6
GSTR	88-1002	<0.015	7387	1.52	1100	5	<0.245	21	0.522	6	107	32.6
GSTR	88-1003	0.187	864	1.13	730	4	<0.235	7	<0.235	<1	61	18.6
GSTR	88-1006	0.165	1968	1.06	1100	<1	<0.244	87	<0.244	4	64	4.91
GSTR	88-1007	0.104	907	0.031	670	<1	<0.238	86	<0.238	6	24	3.79
GSTR	88-1008	0.456	1006	0.398	1700	2	<0.231	11	2.48	14	107	39.5
GSTR	88-1009	0.418	903	0.269	1100	3	<0.239	8	1.87	9	71	27.5
GSTR	88-1010	0.178	711	0.146	580	4	<0.242	17	1.2	3	160	63.5
GSTR	88-1011	0.235	429	0.286	940	4	<0.237	12	<0.237	<1	47	24.2
GSTR	88-1012	0.507	1618	0.126	>20000	5	<0.235	14	2.91	2	75	77.8
GSTR	88-1013	0.633	714	0.151	1200	5	<0.242	25	0.256	2	111	28.4
GSTR	88-1014	0.218	3063	0.088	880	5	<0.24	23	1.23	<1	162	69.2
GSTR	88-1015	0.314	30.7	0.001	960	4	<0.235	3	0.515	1	107	16.4
GSTR	88-1016	0.054	37.3	0.003	1300	3	<0.241	18	2.36	2	87	82.6
GSTR	88-1017	0.453	54.6	0.002	780	<1	<0.245	<2	1.12	3	139	74.1
GSTR	88-1018	0.294	17	0.002	680	<1	<0.239	<2	<0.239	2	170	37.8
GSTR	88-1019	0.121	185	0.01	1100	2	<0.234	9	1.88	12	168	152
GSTR	88-1020	0.064	130	0.009	940	4	<0.229	10	0.368	11	138	69.3
GSTR	88-1021	0.066	144	0.01	830	4	<0.241	13	0.425	8	75	163
GSTR	88-1022	0.073	140	0.019	450	4	<0.241	6	0.398	4	183	10.4
GSTR	88-1023	0.043	54.7	0.001	970	2	<0.235	26	0.281	4	89	21.7
GSTR	88-1033	0.557	275	1.77	30	2	<0.239	24	1.41	6	162	29.6
GSTR	88-1034	1.85	23900	45.5	200	3	<2.38	31	<2.38	9	102	78.6
GSTR	88-1035	6.59	96000	30.8	940	1	<2.40	12	<2.40	1	137	76.8
GSTR	88-1036	1.14	6817	77.7	2200	<1	<0.235	17	0.344	11	115	44.4
GSTR	88-1037	0.085	1894	1.53	<20	<1	6.15	3	<0.235	1	219	5.38
GSTR	88-1038	1.23	2062	23.6	1000	<1	<0.24	49	11.2	8	129	107
MAGG	133	1	1000	0	5000	<1	15	200	0	10	50	150
MAGG	1547A	<0.5	200	0	>5000	7	0	50	0	5	30	300
MAGG	1547B	0	60	0	>5000	<1	0	0	0	<5	<10	70
MAGG	1548B	0.7	300	0	200	<1	0	70	0	5	30	30
MAGG	1549	5	0	0	150	0	0	70	0	5	30	20
MAGG	1560	100	0	0	>5000	0	<10	20	0	<5	20	20
MAGG	1562	7	1500	10	100	5	15	100	300	100	50	100
MAGG	GQ1	2.2	0	0	0	<1	<2	15	11.7	16	414	112
MAGG	GQ2	<0.1	30	0.219	330	<1	<2	<10	<1	<1	163	4
MAGG	GQ3	<0.1	545	8.65	0	6	<2	<10	<1	<1	422	43

min.dist	sample no.	Fe	F	Hg	Li	Mn	Mo	Nb	Ni	Pb	Rb	Sb
CARL	75261	0	1580	17	0	130	13	0	75	14	0	13
CARL	84-11	0	0	0	9	0	5	<4	0	0	0	1.6
CARL	84-12	0	0	0	20	0	<2	0	0	0	0	0
CARL	84-13c	0	0	0	20	0	<2	9	0	0	0	2.26
CARL	84-13o	0	0	0	21	0	<2	9	0	0	0	25.2
CARL	84-14	0	0	0	31	0	<2	8	0	0	0	18.9
CARL	84-16	0	0	0	36	0	17	7	0	0	0	31.3
GSTR	88-1001	0	950	6.89	8	63	27.5	0	23	8.25	33	199
GSTR	88-1002	0	2100	44.8	10	64	49.7	0	23	15.5	<5	211
GSTR	88-1003	0	480	3.73	7	64	31	0	11	5.63	16	325
GSTR	88-1006	0	980	0.594	18	122	5.02	0	4	29.9	82	29.9
GSTR	88-1007	0	980	<0.095	9	425	1.55	0	4	9.31	135	7.16
GSTR	88-1008	0	1500	7.22	18	70	7.71	0	73	12.9	79	131
GSTR	88-1009	0	1100	7.65	19	63	13.3	0	57	12.3	<5	106
GSTR	88-1010	0	500	3.41	10	74	13.9	0	11	16.8	24	53.3
GSTR	88-1011	0	330	1.38	19	68	5.52	0	10	9.5	5	48.6
GSTR	88-1012	0	1300	1.22	4	64	14.1	0	8	12.4	34	158
GSTR	88-1013	0	820	0.88	12	76	5.49	0	7	11.6	53	61
GSTR	88-1014	0	650	0.225	7	95	16.6	0	17	12.5	29	187
GSTR	88-1015	0	700	9.81	3	30	28.2	0	20	5.37	17	13.3
GSTR	88-1016	0	1700	7.63	9	3	5.12	0	36	17.7	100	11.9
GSTR	88-1017	0	380	0.636	4	<1	31.2	0	59	7.86	29	28.8
GSTR	88-1018	0	610	12.6	4	<1	7.52	0	24	4.61	12	3.63
GSTR	88-1019	0	850	26.9	9	236	10.7	0	93	18.1	24	10.5
GSTR	88-1020	0	2300	3.17	9	435	4.47	0	59	8.19	64	5.03
GSTR	88-1021	0	850	48.6	11	313	4.73	0	66	13	46	6.19
GSTR	88-1022	0	1500	3132	8	311	13.2	0	23	4.17	<5	3.11
GSTR	88-1023	0	1200	9.13	11	91	3.09	0	16	4.03	91	2.03
GSTR	88-1033	0	1100	6.91	18	63	54.5	0	80	13	57	32.3
GSTR	88-1034	0	3000	219	22	65	5.57	0	29	23.3	<5	67.9
GSTR	88-1035	0	1000	121	19	45	0.991	0	17	3.99	<5	187
GSTR	88-1036	0	1650	175	29	838	8.12	0	38	10.4	<5	25.1
GSTR	88-1037	0	135	4	29	<1	13.5	0	8	3.08	<5	15.6
GSTR	88-1038	0	1850	230	22	<1	38.5	0	154	12.8	<5	191
MAGG	133	30000	0	0	0	500	15	0	100	70	0	200
MAGG	1547A	150000	0	0	0	5000	0	0	70	1500	0	10
MAGG	1547B	100000	0	0	0	150	10	0	7	1000	0	1
MAGG	1548B	7000	0	0	0	300	7	0	20	30	0	200
MAGG	1549	3000	0	0	0	150	<5	0	20	30	0	0
MAGG	1560	3000	0	0	0	70	5	<20	15	1500	0	700
MAGG	1562	20000	0	0	0	500	<5	0	500	100	0	1500
MAGG	GQ1	155000	2000	4900	26	195	8	94	142	207	4	2380
MAGG	GQ2	3000	153	400	24	37	2	41	4	136	<1	80.3
MAGG	GQ3	2000	1925	75	31	7	16	52	3	794	10	115

min.dist	sample no.	Sn	Sr	Te	Ti	Tl	V	W	Y	Zn	Zr
CARL	75261	<1	0	0.77	0	8.6	0	0	0	275	0
CARL	84-11	0	0	0	0	0	120	0	22	130	0
CARL	84-12	0	0	0	0	0	78	0	21	6	0
CARL	84-13c	0	0	0	0	0	47	0	23	38	0
CARL	84-13o	0	0	0	0	0	61	0	24	93	0
CARL	84-14	0	0	0	0	0	95	0	18	120	0
CARL	84-16	0	0	0	0	0	730	0	41	190	0
GSTR	88-1001	0.853	<5	<0.472	0	1.17	310	19	6	28.8	25
GSTR	88-1002	<0.49	11	<0.49	0	50.3	118	140	7	57.2	10
GSTR	88-1003	<0.471	<5	<0.471	0	4.6	109	10	<5	20.6	0
GSTR	88-1006	<0.488	120	<0.488	0	1.13	81	41	16	11.9	95
GSTR	88-1007	<0.475	130	<0.475	0	<0.475	64	9	18	45.9	5
GSTR	88-1008	0.609	79	<0.461	0	5.66	93	71	16	429	85
GSTR	88-1009	<0.478	24	<0.478	0	4.44	82	59	<5	276	30
GSTR	88-1010	<0.484	36	<0.484	0	<0.484	35	7	<5	16.1	3
GSTR	88-1011	<0.473	29	<0.473	0	<0.473	15	16	<5	7.21	7
GSTR	88-1012	<0.47	80	<0.47	0	3.65	114	15	11	13.5	90
GSTR	88-1013	<0.484	42	<0.484	0	2.08	135	7	7	8.34	80
GSTR	88-1014	<0.481	47	<0.481	0	3.25	342	25	8	23.9	75
GSTR	88-1015	<0.469	96	<0.469	0	<0.469	1487	4	40	66.5	25
GSTR	88-1016	<0.482	60	<0.482	0	<0.482	546	3	10	66	45
GSTR	88-1017	<0.49	23	<0.49	0	<0.49	2389	4	43	314	20
GSTR	88-1018	<0.477	100	<0.477	0	<0.477	1340	<2	8	41.6	15
GSTR	88-1019	<0.468	46	<0.468	0	<0.468	296	6	<5	233	5
GSTR	88-1020	<0.459	51	<0.459	0	<0.459	148	6	29	45.8	60
GSTR	88-1021	<0.483	39	<0.483	0	<0.483	96	4	5	67.8	65
GSTR	88-1022	<0.482	<5	<0.482	0	<0.482	50	<2	<5	25.6	10
GSTR	88-1023	<0.47	23	<0.47	0	<0.47	78	5	<5	27.9	5
GSTR	88-1033	<0.479	<5	<0.479	0	4.64	264	31	6	428	50
GSTR	88-1034	<4.76	<5	<4.76	0	216	116	130	50	305	85
GSTR	88-1035	<4.80	<5	<4.80	0	31.5	60	<42	135	<9.61	2
GSTR	88-1036	1.5	18	0.728	0	156	54	180	11	30.2	25
GSTR	88-1037	4.55	<5	2.21	0	4.68	6	6070	<5	15.4	7
GSTR	88-1038	0.858	<5	2.45	0	84.9	710	150	34	1214	10
MAGG	133	0	200	0	1500	0	500	0	30	700	0
MAGG	1547A	0	150	0	1000	0	300	70	50	1000	5
MAGG	1547B	0	3000	0	300	0	150	0	0	55	5
MAGG	1548B	0	0	0	2000	0	100	0	15	100	0
MAGG	1549	0	<100	0	1000	0	300	0	15	500	50
MAGG	1560	30	100	0	3000	0	200	0	<10	10	0
MAGG	1562	<10	0	0	1000	0	300	150	20	3000	0
MAGG	GQ1	<1	1380	<.2	800	2	507	<450	0	957	0
MAGG	GQ2	6	14	<.2	3100	0.3	32	7	0	3	0
MAGG	GQ3	<1	75	<.2	1500	0.4	1390	<20	0	128	0

min.dist	sample no.	Ag	As	Au	Ba	Be	Bi	B	Cd	Co	Cr	Cu
MAGG	J10	3.9	152	7.1	1310	0	2	0	1	21	168	776
MAGG	J11	0.9	327	0.8	298	0	2	0	7	15	77	137
MAGG	J12	7	217	0.55	1258	0	7	0	3	4	23	16
MAGG	J13	0.1	57	0.21	1153	0	2	0	3	6	76	20
MAGG	J16	1.8	55	3.6	543	0	4	0	4	9	166	14
MAGG	J17	3.5	370	2	192	0	3	0	12	5	165	35
MAGG	J18	1.3	354	3.4	1285	0	4	0	2	6	23	82
MAGG	J19	2.6	175	5.4	1696	0	2	0	1	4	134	49
MAGG	J20	3.6	153	0.36	1360	0	4	0	3	3	20	11
MAGG	J6	0.1	1655	0.04	161	0	2	0	2	7	104	38
MAGG	J7	0.1	2953	0.25	17	0	2	0	5	93	81	43
MAGG	J8	0.1	68	0.03	1011	0	2	0	5	2	5	4
MAGG	J9	0.4	270	0.75	1638	0	2	0	3	9	97	16
NUMB	001A	5	20	0.05	200	0	0	100	8.3	0	20	20
NUMB	001B	7	210	0.05	700	5	0	200	30	0	500	200
NUMB	002A	2	650	0	5000	3	0	500	66	30	500	100
NUMB	003A	0.5	520	0.35	150	0	0	30	0	0	50	50
NUMB	004A	0.5	1400	0.05	1500	1	0	70	0.1	<5	100	30
NUMB	005A	1.5	1400	0.15	2000	3	0	50	22	100	700	1000
NUMB	006A	0.5	680	0.05	1000	1	0	150	0.8	0	50	20
NUMB	007A	20	2	0.05	0	0.1	0	0	0	0	<20	0
NUMB	007B	0.5	1400	0.15	300	1.5	0	50	34	10	10	20
NUMB	008A	7	440	2.4	1500	1	0	50	6	0	0	20
NUMB	008B	3	2300	0.25	>5000	3	0	150	8.7	5	20	100
NUMB	012A	0.7	640	0.05	300	1	0	500	13	10	200	50
NUMB	013A	7	500	5.8	200	1	0	100	0	0	70	10
NUMB	014A	<0.5	10	0.05	1000	0	0	150	0	0	<10	<5
NUMB	014B	0	<5	0.05	1500	2	0	200	0	0	20	7
NUMB	015A	<0.5	0	0.1	2000	1	0	50	0.8	0	50	50
NUMB	018A	5	1500	0.1	700	2	0	1000	0	10	30	70
NUMB	019A	50	500	0.2	300	<1.0	0	70	0	0	0	10
NUMB	022A	3	1400	3.9	500	3	0	500	4.6	10	100	30
NUMB	023A	0.5	5	0.1	2000	1.5	0	50	0	7	20	50
NUMB	024A	3	2400	3.3	200	2	0	1000	2.5	10	100	20
NUMB	025A	50	70	0.05	200	1	0	30	0.7	0	0	30
NUMB	026A	15	650	0.15	1500	1.5	0	500	0	7	70	50
NUMB	027A	100	5500	4.6	300	<1.0	0	50	8.3	0	<10	50
PINS	202008	0.181	1033	0.324	706	3.33	<0.241	0	4.03	8.39	81.4	192
PINS	202009	1.11	1295	2.33	1648	5.85	<0.234	0	8.03	9.62	75.5	300
PINS	202010	0.06	1058	0.461	168	<0.5	<0.233	0	0.508	19.7	62.1	58.8
PINS	202011	0.034	169	0.006	194	<0.49	<0.231	0	0.792	4.46	26.9	16.1
PINS	202012	0.572	116	0.225	4223	1.96	<0.243	0	1.34	7.39	186	55.5
PINS	202013	0.209	1960	0.168	3909	6.13	<0.242	0	11.8	168	88.2	49.7
PINS	2644	2	1800	8.6	500	2	0	100	0	20	20	150

min.dist	sample no.	Fe	F	Hg	Li	Mn	Mo	Nb	Ni	Pb	Rb	Sb
MAGG	J10	8700	0	1.2	0	30	7	0	9	66	0	183
MAGG	J11	17100	0	19	0	265	5	0	72	12	0	124
MAGG	J12	17100	0	6.4	0	117	10	0	187	1448	0	717
MAGG	J13	75300	0	0.13	0	162	9	0	14	19	0	3
MAGG	J16	4100	0	0.6	0	0	4	0	21	8	0	41
MAGG	J17	13400	0	0.85	0	0	7	0	107	11	0	532
MAGG	J18	14100	0	1	0	0	7	0	50	15	0	318
MAGG	J19	14500	0	0.45	0	0	17	0	10	48	0	211
MAGG	J20	13100	0	3.6	0	0	9	0	13	1271	0	556
MAGG	J6	59900	0	4.8	0	72	30	0	26	22	0	130
MAGG	J7	113000	0	9.3	0	45	15	0	336	31	0	776
MAGG	J8	5200	0	0.15	0	623	1	0	13	32	0	39
MAGG	J9	18200	0	0.17	0	1069	5	0	86	8	0	466
NUMB	001A	2000	0	0.8	0	100	7	0	20	0	0	0
NUMB	001B	20000	2000	2.6	0	50	100	0	200	50	0	150
NUMB	002A	5000	1200	0.6	0	700	50	0	200	0	0	40
NUMB	003A	2000	0	0.8	0	10	7	0	0	0	0	24
NUMB	004A	15000	0	130	0	20	20	0	20	0	0	340
NUMB	005A	100000	500	50	0	1000	50	0	700	0	0	760
NUMB	006A	10000	600	40	0	30	20	0	20	0	0	62
NUMB	007A	0	0	0	0	<5	300	0	0.01	15	0	0.24
NUMB	007B	20000	1200	9	0	200	15	0	100	<10	0	280
NUMB	008A	7000	500	6.4	0	20	0	0	10	0	0	46
NUMB	008B	50000	500	18	0	50	10	0	100	0	0	310
NUMB	012A	30000	1400	3	0	<10	10	0	50	0	0	16
NUMB	013A	5000	200	4.2	0	50	20	0	5	0	0	60
NUMB	014A	7000	600	0.06	0	200	0	0	10	0	0	0
NUMB	014B	10000	1300	<.02	0	200	0	0	50	0	0	<2
NUMB	015A	10000	200	0.04	0	500	0	0	30	0	0	<2
NUMB	018A	15000	400	0.5	0	500	<5	0	20	0	0	34
NUMB	019A	3000	100	5	0	<10	0	0	0	0	0	48
NUMB	022A	50000	900	4.7	0	200	10	0	100	0	0	76
NUMB	023A	10000	300	0.1	0	500	10	0	20	0	0	<2
NUMB	024A	20000	900	8	0	500	5	0	50	20	0	58
NUMB	025A	3000	300	0.06	0	500	0	0	5	50	0	32
NUMB	026A	10000	200	0.06	0	700	<5	0	20	10	0	22
NUMB	027A	20000	0	7	0	200	10	0	5	20	0	260
PINS	202008	90100	599	1.61	0	2736	32.8	0	56.8	10	0	130
PINS	202009	88500	3820	54	0	>5140	137	0	132	7.53	0	4676
PINS	202010	42700	175	9.25	0	602	7.4	0	55.4	9.12	0	27.9
PINS	202011	6240	330	3.01	0	154	1.33	0	14.1	4.92	0	5.33
PINS	202012	13900	1549	1.63	0	42.9	3.03	0	157	16.8	0	15.7
PINS	202013	62600	1313	2.18	0	1136	38.7	0	508	59.1	0	233
PINS	2644	100000	0	0	0	300	100	0	50	10	0	150

min.dist	sample no.	Sn	Sr	Te	Ti	Tl	V	W	Y	Zn	Zr
MAGG	J10	0	49	0	100	0	68	11	0	28	0
MAGG	J11	0	29	0	100	0	143	49	0	253	0
MAGG	J12	0	20	0	100	0	652	96	0	102	0
MAGG	J13	0	29	0	100	0	30	1	0	221	0
MAGG	J16	0	7	0	100	0	42	13	0	75	0
MAGG	J17	0	13	0	100	0	147	43	0	452	0
MAGG	J18	0	18	0	100	0	79	45	0	319	0
MAGG	J19	0	32	0	100	0	81	19	0	49	0
MAGG	J20	0	24	0	100	0	515	106	0	78	0
MAGG	J6	0	23	0	100	0	81	6	0	117	0
MAGG	J7	0	27	0	100	0	137	257	0	860	0
MAGG	J8	0	109	0	100	0	12	10	0	190	0
MAGG	J9	0	25	0	100	0	86	87	0	357	0
NUMB	001A	0	0	0.055	500	1.6	1000	2.5	10	230	0
NUMB	001B	0	0	0.6	2000	3.7	10000	0	200	2000	0
NUMB	002A	0	0	0.045	7000	15.5	500	4	30	3200	0
NUMB	003A	0	0	0.01	20	1.8	50	1	15	15	0
NUMB	004A	0	0	0.04	10000	33	200	4.5	15	25	0
NUMB	005A	0	0	0.15	150	43	300	4	70	1700	0
NUMB	006A	0	0	0.6	2000	33	700	16	10	210	50
NUMB	007A	0	0	0.7	1000	50	0.5	0	0	0	0
NUMB	007B	0	0	0.4	1000	70	100	19	20	1200	0
NUMB	008A	0	0	0.19	200	5.6	70	3	15	100	0
NUMB	008B	0	0	0.2	700	48	200	3	30	710	0
NUMB	012A	0	0	0.055	5000	0.6	1000	47	70	240	0
NUMB	013A	0	0	0.19	500	5	70	4.5	15	15	0
NUMB	014A	0	0	0.01	1000	0.2	20	2	20	15	0
NUMB	014B	0	0	0.005	1500	0.6	50	1.5	20	90	0
NUMB	015A	0	0	0.03	1500	0.4	100	0	30	30	0
NUMB	018A	0	0	0.055	2000	2.2	70	5.5	15	10	0
NUMB	019A	0	0	0.09	200	5	70	1.4	10	<5	5
NUMB	022A	0	0	0.11	2000	3.9	500	60	30	250	50
NUMB	023A	0	0	0.035	2000	0.4	50	6	20	15	0
NUMB	024A	0	0	0.07	3000	26	500	70	30	200	0
NUMB	025A	0	0	0.07	500	0.6	20	1	15	25	0
NUMB	026A	0	0	0.13	1000	1.4	100	9	10	10	0
NUMB	027A	0	0	0.8	70	7.2	30	4.5	<10	450	0
PINS	202008	0	161	1.89	1581	3.02	373	140	38.1	129	0
PINS	202009	0	140	24.3	1372	88.8	647	590	60.1	97.2	0
PINS	202010	0	64.9	<0.466	2042	4.61	37.9	130	46.2	312	0
PINS	202011	0	164	<0.462	591	0.504	19.5	8	13.6	101	0
PINS	202012	0	154	<0.486	1246	1.89	152	55	33.2	479	0
PINS	202013	0	238	<0.484	2639	15.2	1087	780	44.5	1784	0
PINS	2644	0	200	0	1000	0	500	150	50	200	0

min.dist	sample no.	Ag	As	Au	Ba	Be	Bi	B	Cd	Co	Cr	Cu
PINS	2985	0	1100	1	2000	1.5	0	100	0	5	50	50
PINS	2A	0.5	2000	0.25	1500	2	0	50	0	0	70	100
PINS	2B	1.5	1500	4.8	1000	<1	0	100	0	0	50	50
PINS	30	0.1	1735	5	145	0	2	7	1	2	122	26
PINS	301	0.7	1000	1	500	1	0	70	0	7	15	50
PINS	302	0.5	2000	2.9	500	1.5	0	100	0	0	30	30
PINS	303	1	<200	1.5	500	1	0	100	0	0	70	20
PINS	304	0.7	0	0.15	2000	3	0	100	0	5	100	100
PINS	305	0.5	1000	4	1000	2	0	300	0	7	70	100
PINS	306	0	300	0.7	200	<1	0	70	0	7	0	15
PINS	31	0.1	1450	3.6	106	0	2	17	1	6	21	45
POTO	2611	0	40	<0.05	0	2	70	100	0	50	0	1000
POTO	2613	0	15	0	20	1.5	20	30	0	10	0	1000
POTO	2616	0	5	0	150	2	0	20	0	30	50	1000
POTO	2617	0	15	0	500	2	300	20	0	10	10	500
PREB	1A	5	1500	0.85	5000	7	0	1000	1.3	20	700	500
PREB	202001	0.353	715	0.655	624	<0.49	<0.242	0	3.51	7.4	40.3	37.5
PREB	202002	0.311	262	0.023	1034	<0.49	<0.237	0	2.18	6.43	121	109
PREB	202003	0.309	258	0.01	1344	1.77	<0.245	0	2.07	14.7	86.2	226
PREB	202004	0.78	290	2.58	1850	1.33	<0.235	0	2.15	11.1	129	105
PREB	202005	1.56	637	9.95	1041	0.5	<0.238	0	2.73	2.71	118	63.8
PREB	202006	0.56	226	1.26	1402	0.604	<0.248	0	5.25	9.45	148	90.8
PREB	202007	0.413	145	0.311	2762	1.1	<0.249	0	0.455	4.8	100	24.7
PREB	2A	0.5	700	0.1	5000	10	0	700	0.1	15	700	50
PREB	2B	0.7	700	0.1	3000	5	0	300	0.1	10	500	30
PREB	301	3	1000	1.8	5000	5	0	500	0	0	700	100
PREB	302	2	2000	0.3	1000	3	0	70	1.9	10	100	20
PREB	303	1	0	0.05	1500	<1	0	70	0.2	0	0	7
PREB	310	1	700	0.05	500	1	1	100	3.2	30	10	15
PREB	487	1	650	1.5	3000	2	0	200	0	50	70	150
PREB	6A	2	500	2.3	2000	1.5	0	150	0	0	20	30
RAIN	N11750	0.4	580	0.03	10000	<0.5	9	0	2	44	195	6
RAIN	N11751	0.2	300	0.005	0	0	0	0	0	0	0	0
RAIN	N11753	0.2	1000	0.085	10000	<0.5	12	0	2.5	60	97	16
RAIN	N11755	0.4	370	0.005	10000	<0.5	5	0	<0.5	9	120	44
RAIN	N11756	0.2	230	0.005	0	0	0	0	0	0	0	0
RAIN	N11757	0.4	178	0.005	2040	<0.5	<2	0	<0.5	4	135	32
RAIN	N11758	0.2	370	0.005	2420	<0.5	<2	0	<0.5	4	140	32
RAIN	N11760	0.2	183	0.005	2510	<0.5	<2	0	<0.5	5	120	49
RAIN	N11768	0.2	680	0.85	0	0	0	0	0	0	0	0
RAIN	N11769	0.2	116	0.1	0	0	0	0	0	0	0	0
RAIN	N11770	0.2	83	0.005	655	<0.5	<2	0	<0.5	4	335	11
RAIN	N11772	0.2	330	0.005	2610	<0.5	<2	0	<0.5	5	275	25
RAIN	N11774	0.2	310	0.005	0	0	0	0	0	0	0	0

min.dist	sample no.	Fe	F	Hg	Li	Mn	Mo	Nb	Ni	Pb	Rb	Sb
PINS	2985	50000	0	0	0	20	50	0	20	10	0	<100
PINS	2A	100000	<100	14	0	100	70	0	15	0	0	150
PINS	2B	20000	300	30	0	70	15	0	10	0	0	0
PINS	30	24200	0	32	0	336	12	0	16	2	0	5252
PINS	301	20000	200	8.4	0	700	100	0	150	70	0	0
PINS	302	30000	100	80	0	700	10	0	20	0	0	100
PINS	303	10000	700	15	0	0	5	0	<5	0	0	0
PINS	304	30000	900	1.6	0	300	0	<20	50	10	0	0
PINS	305	30000	900	40	0	10	20	0	50	10	0	0
PINS	306	10000	300	2.4	0	10	5	0	10	0	0	0
PINS	31	30100	0	25	0	689	30	0	37	2	0	73
POTO	2611	20000	0	0	0	<5000	300	0	10	1000	0	6
POTO	2613	<20000	0	0	0	<5000	1000	0	5	50	0	<2
POTO	2616	15000	0	0	0	<5000	100	0	50	30	0	0
POTO	2617	20000	0	0	0	<5000	100	0	15	1000	0	0
PREB	1A	30000	2400	17	0	70	30	0	70	10	0	58
PREB	202001	52200	5313	4.24	0	281	25.5	0	77.7	6.56	0	65.3
PREB	202002	51700	578	1.08	0	159	56.5	0	49.9	10.7	0	20.9
PREB	202003	43500	1117	1.88	0	99.5	13.4	0	93.8	30.1	0	23.3
PREB	202004	21900	1166	29.3	0	29	11.7	0	39.6	15.8	0	19.1
PREB	202005	32800	925	76	0	24.1	23	0	45.5	28.4	0	59.4
PREB	202006	22400	635	29.1	0	63.5	9.31	0	42.8	18.3	0	32.2
PREB	202007	15900	784	5.46	0	27.3	3	0	19.5	11.6	0	14.3
PREB	2A	50000	1800	0.12	0	300	10	<20	50	0	0	22
PREB	2B	30000	700	0.04	0	200	<5	0	30	0	0	10
PREB	301	30000	1400	65	0	70	30	0	20	100	0	110
PREB	302	50000	100	8	0	500	15	0	100	20	0	650
PREB	303	2000	0	0.32	0	30	0	20	0	50	0	190
PREB	310	50000	300	1.5	0	1000	15	0	100	0	0	20
PREB	487	50000	0	0	0	50	20	<20	100	50	0	43
PREB	6A	10000	400	34	0	<10	0	20	5	50	0	10
RAIN	N11750	0	0	0.84	0	62	7	0	5	22	0	39
RAIN	N11751	0	0	0.69	0	0	0	0	0	0	0	8
RAIN	N11753	0	0	4.05	0	14	10	0	8	73	0	2
RAIN	N11755	0	0	1.55	0	46	2	0	1	7	0	2
RAIN	N11756	0	0	0.89	0	0	0	0	0	0	0	14
RAIN	N11757	0	0	1.02	0	60	5	0	<1	25	0	15
RAIN	N11758	0	0	5	0	31	3	0	7	3	0	74
RAIN	N11760	0	0	3.65	0	42	2	0	8	4	0	37
RAIN	N11768	0	0	1.28	0	0	0	0	0	0	0	82
RAIN	N11769	0	0	5	0	0	0	0	0	0	0	14
RAIN	N11770	0	0	0.14	0	54	5	0	4	7	0	5
RAIN	N11772	0	0	0.73	0	74	3	0	12	<1	0	21
RAIN	N11774	0	0	0.4	0	0	0	0	0	0	0	4

min.dist	sample no.	Sn	Sr	Te	Ti	Tl	V	W	Y	Zn	Zr
PINS	2985	0	200	0	1500	0	200	100	20	500	0
PINS	2A	0	0	0.06	700	12	500	100	50	130	0
PINS	2B	0	0	1.2	700	7.4	500	200	20	75	0
PINS	30	0	24	0	100	0	93	0	0	68	0
PINS	301	0	0	0.6	300	2.2	150	200	15	80	<10
PINS	302	0	0	0.4	700	30	200	100	10	40	0
PINS	303	0	0	0.035	2000	0.6	200	200	50	15	0
PINS	304	0	300	0.025	5000	0.8	500	0	70	75	0
PINS	305	0	150	0.025	3000	4.2	200	100	50	70	0
PINS	306	0	<100	0.01	300	2.8	70	50	20	30	0
PINS	31	0	20	0	100	0	218	0	0	114	0
POTO	2611	30	0	0	1000	0	500	300	30	400	5
POTO	2613	150	0	0	700	0	1000	5000	0	85	0
POTO	2616	30	0	0	2000	0	500	300	30	200	0
POTO	2617	70	150	0	1500	0	500	500	10	250	0
PREB	1A	0	1000	0.015	10000	12	500	14	50	<200	50
PREB	202001	0	173	<0.484	923	13.1	169	5	18	129	0
PREB	202002	0	148	<0.474	1398	3.43	215	<4	11	151	0
PREB	202003	0	162	<0.49	2225	1.59	40	24	28.4	187	0
PREB	202004	0	111	<0.469	1392	4.05	21.7	8	21.6	55.8	0
PREB	202005	0	370	<0.476	508	2.07	37.3	41	9.56	82.7	0
PREB	202006	0	206	<0.496	1082	0.757	26.9	6	15.7	67.7	0
PREB	202007	0	77.9	<0.498	1372	0.762	19.4	7	15.2	41.9	0
PREB	2A	0	0	0.02	10000	2.6	500	31	30	200	50
PREB	2B	0	<100	0.005	5000	1.6	500	17.5	20	200	0
PREB	301	0	700	0.045	7000	8.2	500	0	20	0	0
PREB	302	0	200	0.03	500	6.8	100	38	15	1000	0
PREB	303	0	0	0.03	5000	4.4	100	0	15030	0	50
PREB	310	0	0	0.005	500	30	50	0	0	500	0
PREB	487	0	500	0	3000	0	500	<50	30	60	0
PREB	6A	0	0	0.14	7000	3.6	200	0	20	0	50
RAIN	N11750	0	420	0	0	0	22	40	0	16	0
RAIN	N11751	0	0	0	0	0	0	0	0	0	0
RAIN	N11753	0	740	0	0	0	102	30	0	46	0
RAIN	N11755	0	215	0	0	0	245	15	0	11	0
RAIN	N11756	0	0	0	0	0	0	0	0	0	0
RAIN	N11757	0	116	0	0	0	160	<10	0	18	0
RAIN	N11758	0	122	0	0	0	198	<10	0	37	0
RAIN	N11760	0	250	0	0	0	210	<10	0	16	0
RAIN	N11768	0	0	0	0	0	0	0	0	0	0
RAIN	N11769	0	0	0	0	0	0	0	0	0	0
RAIN	N11770	0	182	0	0	0	165	<10	0	51	0
RAIN	N11772	0	510	0	0	0	93	<10	0	16	0
RAIN	N11774	0	0	0	0	0	0	0	0	0	0

min.dist	sample no.	Ag	As	Au	Ba	Be	Bi	B	Cd	Co	Cr	Cu
RAIN	N11775	0.2	1000	0.01	10000	<0.5	<2	0	0.5	17	820	6
RAIN	N11776	0.2	1000	2.21	0	0	0	0	0	0	0	0
RAIN	N11777	0.2	520	3.96	0	0	0	0	0	0	0	0
RAIN	N11778	0.2	410	0.03	2120	<0.5	<2	0	<0.5	6	155	42
RAIN	N11779	0.2	510	0.03	0	0	0	0	0	0	0	0
RAIN	N11780	0.2	158	0.005	0	0	0	0	0	0	0	0
RAIN	N11800	0.2	1000	0.005	0	0	0	0	0	0	0	0
RAIN	N11801	0.2	37	0.005	0	0	0	0	0	0	0	0
RAIN	N11802	0.2	44	0.015	0	0	0	0	0	0	0	0
RAIN	N11803	0.2	430	0.68	10000	<0.5	<2	0	<0.5	13	415	15
RAIN	N11804	0.2	1000	0.105	10000	<0.5	<2	0	<0.5	15	210	16
RAIN	N11805	0.2	1000	0.065	0	0	0	0	0	0	0	0
RAIN	N11806	0.2	1000	0.015	0	0	0	0	0	0	0	0
RAIN	N11807	0.2	790	0.01	0	0	0	0	0	0	0	0
RAIN	N11808	0.2	1000	0.015	10000	<0.5	<2	0	<0.5	8	320	8
RAIN	N11809	0.2	990	0.015	0	0	0	0	0	0	0	0
RAIN	N11810	0.2	980	0.005	0	0	0	0	0	0	0	0
RAIN	N11812	0.2	138	0.005	2880	<0.5	<2	0	<0.5	9	120	32
RAIN	N11815	0.2	59	0.005	4950	<0.5	<2	0	<0.5	5	275	6
RAIN	N11817	0.2	77	0.015	1930	<0.5	<2	0	<0.5	4	340	8
RAIN	N11819	0.2	690	2.44	0	0	0	0	0	0	0	0
RAIN	N11820	0.2	1000	0.245	10000	<0.5	7	0	4.5	33	195	12
RAIN	N11821	0.2	1000	1.96	0	0	0	0	0	0	0	0
RAIN	N11822	0.2	1000	0.35	10000	<0.05	7	0	3	64	75	6
RAIN	N11823	0.2	1000	1	0	0	0	0	0	0	0	0
RAIN	N11824	0.2	480	0.015	0	0	0	0	0	0	0	0
RAIN	N11825	0.2	1000	1.6	10000	<0.5	10	0	2	57	63	2
RAIN	N11826	0.2	198	0.03	1900	<0.5	<2	0	<0.5	4	155	49
RAIN	N11827	0.2	176	0.01	0	0	0	0	0	0	0	0
RAIN	N11828	0.4	118	0.005	0	0	0	0	0	0	0	0
RAIN	N11829	0.2	260	0.005	0	0	0	0	0	0	0	0
RAIN	N11830	0.2	79	0.005	1740	<0.5	<2	0	<0.5	3	140	21
RAIN	N11831	0.2	230	0.005	2020	0.5	<2	0	<0.5	7	140	15
RAIN	N11832	0.2	470	0.005	2190	0.5	<2	0	<0.5	7	155	65
RAIN	N11833	0.2	590	0.015	6840	2.5	<2	0	<0.5	17	120	225
RAIN	N14432	0.2	1000	0.005	4770	<0.5	<2	0	<0.5	7	200	12
RAIN	N14433	0.2	38	0.005	2180	<0.5	<2	0	<0.5	<1	27	12
RAIN	N14434	0.2	590	0.005	0	0	0	0	0	0	0	0
RAIN	N14435	0.2	320	0.005	1980	<0.5	<2	0	1.5	7	255	17
RAIN	N14436	0.2	93	0.005	1970	<0.5	<2	0	<0.5	8	275	0.25
RAIN	N14437	0.2	430	0.005	0	0	0	0	0	0	0	0
RAIN	N14438	0.2	310	0.005	1610	<0.5	<2	0	<0.5	10	225	21
RAIN	N14439	0.2	78	0.005	0	0	0	0	0	0	0	0
RAIN	N14441	0.2	160	0.005	0	0	0	0	0	0	0	0

min.dist	sample no.	Fe	F	Hg	Li	Mn	Mo	Nb	Ni	Pb	Rb	Sb
RAIN	N11775	0	0	1.53	0	67	10	0	7	13	0	100
RAIN	N11776	0	0	3.35	0	0	0	0	0	0	0	17
RAIN	N11777	0	0	5	0	0	0	0	0	0	0	110
RAIN	N11778	0	0	1.44	0	20	5	0	4	3	0	7
RAIN	N11779	0	0	3.2	0	0	0	0	0	0	0	4
RAIN	N11780	0	0	3.35	0	0	0	0	0	0	0	6
RAIN	N11800	0	0	1.97	0	0	0	0	0	0	0	6
RAIN	N11801	0	0	5	0	0	0	0	0	0	0	2
RAIN	N11802	0	0	5	0	0	0	0	0	0	0	2
RAIN	N11803	0	0	2.05	0	40	3	0	15	6	0	68
RAIN	N11804	0	0	4.1	0	43	7	0	3	6	0	60
RAIN	N11805	0	0	0.62	0	0	0	0	0	0	0	26
RAIN	N11806	0	0	0.8	0	0	0	0	0	0	0	28
RAIN	N11807	0	0	0.45	0	0	0	0	0	0	0	6
RAIN	N11808	0	0	1.22	0	130	7	0	3	27	0	19
RAIN	N11809	0	0	0.17	0	0	0	0	0	0	0	21
RAIN	N11810	0	0	2.1	0	0	0	0	0	0	0	22
RAIN	N11812	0	0	3.8	0	16	<1	0	13	<1	0	2
RAIN	N11815	0	0	1.33	0	59	4	0	2	<1	0	40
RAIN	N11817	0	0	0.4	0	90	3	0	1	3	0	24
RAIN	N11819	0	0	5	0	0	0	0	0	0	0	1660
RAIN	N11820	0	0	1.59	0	84	7	0	16	13	0	72
RAIN	N11821	0	0	5	0	0	0	0	0	0	0	36
RAIN	N11822	0	0	5	0	33	9	0	5	22	0	120
RAIN	N11823	0	0	5	0	0	0	0	0	0	0	110
RAIN	N11824	0	0	5	0	0	0	0	0	0	0	21
RAIN	N11825	0	0	5	0	20	10	0	9	21	0	2
RAIN	N11826	0	0	5	0	33	2	0	<1	6	0	24
RAIN	N11827	0	0	3.2	0	0	0	0	0	0	0	9
RAIN	N11828	0	0	0.8	0	0	0	0	0	0	0	6
RAIN	N11829	0	0	0.89	0	0	0	0	0	0	0	4
RAIN	N11830	0	0	0.71	0	13	3	0	<1	2	0	5
RAIN	N11831	0	0	0.36	0	17	5	0	14	9	0	4
RAIN	N11832	0	0	0.51	0	24	6	0	4	7	0	7
RAIN	N11833	0	0	4.05	0	26	11	0	27	10	0	4
RAIN	N14432	0	0	0.76	0	120	5	0	57	2	0	2
RAIN	N14433	0	0	5	0	375	2	0	<1	<1	0	2
RAIN	N14434	0	0	0.34	0	0	0	0	0	0	0	15
RAIN	N14435	0	0	0.21	0	92	7	0	21	<1	0	11
RAIN	N14436	0	0	0.33	0	102	2	0	10	<1	0	9
RAIN	N14437	0	0	0.15	0	0	0	0	0	0	0	12
RAIN	N14438	0	0	0.29	0	93	8	0	29	<1	0	10
RAIN	N14439	0	0	0.72	0	0	0	0	0	0	0	11
RAIN	N14441	0	0	0.65	0	0	0	0	0	0	0	8

min.dist	sample no.	Sn	Sr	Te	Ti	Tl	V	W	Y	Zn	Zr
RAIN	N11775	0	132	0	0	0	29	15	0	4	0
RAIN	N11776	0	0	0	0	0	0	0	0	0	0
RAIN	N11777	0	0	0	0	0	0	0	0	0	0
RAIN	N11778	0	330	0	0	0	198	35	0	10	0
RAIN	N11779	0	0	0	0	0	0	0	0	0	0
RAIN	N11780	0	0	0	0	0	0	0	0	0	0
RAIN	N11800	0	0	0	0	0	0	0	0	0	0
RAIN	N11801	0	0	0	0	0	0	0	0	0	0
RAIN	N11802	0	0	0	0	0	0	0	0	0	0
RAIN	N11803	0	540	0	0	0	101	30	0	10	0
RAIN	N11804	0	730	0	0	0	315	40	0	9	0
RAIN	N11805	0	0	0	0	0	0	0	0	0	0
RAIN	N11806	0	0	0	0	0	0	0	0	0	0
RAIN	N11807	0	0	0	0	0	0	0	0	0	0
RAIN	N11808	0	2470	0	0	0	275	15	0	7	0
RAIN	N11809	0	0	0	0	0	0	0	0	0	0
RAIN	N11810	0	0	0	0	0	0	0	0	0	0
RAIN	N11812	0	240	0	0	0	164	<10	0	33	0
RAIN	N11815	0	135	0	0	0	54	10	0	2	0
RAIN	N11817	0	172	0	0	0	34	<10	0	<1	0
RAIN	N11819	0	0	0	0	0	0	0	0	0	0
RAIN	N11820	0	375	0	0	0	88	15	0	32	0
RAIN	N11821	0	0	0	0	0	0	0	0	0	0
RAIN	N11822	0	370	0	0	0	65	15	0	6	0
RAIN	N11823	0	0	0	0	0	0	0	0	0	0
RAIN	N11824	0	0	0	0	0	0	0	0	0	0
RAIN	N11825	0	175	0	0	0	5	25	0	14	0
RAIN	N11826	0	177	0	0	0	138	<10	0	4	0
RAIN	N11827	0	0	0	0	0	0	0	0	0	0
RAIN	N11828	0	0	0	0	0	0	0	0	0	0
RAIN	N11829	0	0	0	0	0	0	0	0	0	0
RAIN	N11830	0	85	0	0	0	116	<10	0	6	0
RAIN	N11831	0	105	0	0	0	210	10	0	44	0
RAIN	N11832	0	210	0	0	0	300	30	0	15	0
RAIN	N11833	0	425	0	0	0	180	40	0	61	0
RAIN	N14432	0	535	0	0	0	81	<10	0	71	0
RAIN	N14433	0	174	0	0	0	6	<10	0	17	0
RAIN	N14434	0	0	0	0	0	0	0	0	0	0
RAIN	N14435	0	530	0	0	0	95	15	0	45	0
RAIN	N14436	0	108	0	0	0	92	<10	0	10	0
RAIN	N14437	0	0	0	0	0	0	0	0	0	0
RAIN	N14438	0	115	0	0	0	98	15	0	52	0
RAIN	N14439	0	0	0	0	0	0	0	0	0	0
RAIN	N14441	0	0	0	0	0	0	0	0	0	0

min.dist	sample no.	Ag	As	Au	Ba	Be	Bi	B	Cd	Co	Cr	Cu
RAIN	N14442	0.2	325	0.005	0	0	0	0	0	0	0	0
RAIN	N14443	0.2	197	0.01	1630	1	<2	0	<0.5	8	135	36
RAIN	N14444	0.2	295	0.005	0	0	0	0	0	0	0	0
RAIN	N14445	0.2	137	0.005	1	250	<1	0	<2	<0.5	1.6	0.11
CHIM	01	6.5	960	2.12	80	0	0	0	0	0	0	20
CHIM	02	2.05	500	1.88	3000	0	0	0	0	0	0	20
CHIM	03	5.82	1300	3.83	50	0	0	0	0	0	0	20
CHIM	04	8.21	10000	6.67	60	0	0	0	0	0	0	125
CHIM	05	4.1	2800	0.445	1800	0	0	0	0	0	0	15
CHIM	06	6.5	860	1.67	150	0	0	0	0	0	0	30
CHIM	07	4.1	360	0.993	2400	0	0	0	0	0	0	10
CHIM	08	15.41	320	12.6	120	0	0	0	0	0	0	40
CHIM	09	0.17	110	1.02	1400	0	0	0	0	0	0	20
CHIM	10	1.71	210	2.43	2100	0	0	0	0	0	0	5
CHIM	202014	5.62	845	0.577	113	<0.49	0.46	0	11.3	1.86	108	7.21
CHIM	202015	1.09	422	0.668	140	1.98	<0.23	0	41	23.9	238	114
CHIM	202016	3.9	2765	7.38	149	<0.49	<0.231	0	29	1.96	142	11.4
CHIM	202017	0.971	265	0.615	226	<0.49	<0.241	0	6.86	7.71	52.9	4.33
CHIM	202018	8.84	1032	27.1	205	<0.49	<0.229	0	2.16	0.95	88.5	3.52
CHIM	202019	25.9	13200	2	141	<0.5	<0.231	0	25.2	3.63	74.2	30.2
CHIM	202020	6.97	7021	33.4	81.6	<0.5	<0.245	0	12.8	<0.98	57	15.3
CHIM	202021	9.73	496	4.51	160	<0.5	<0.244	0	2.2	1.31	202	5.82
CHIM	202022	2.3	217	11.9	49	<0.49	<0.249	0	0.701	<0.996	169	3.17
GETC	10A	0	145000	6.2	0	0	0	0	0	0	0	0
GETC	11B-D	0.05	3000	0	10000	<1	<10	15	0	<10	5	3
GETC	11B-E	0.05	1600	0	10000	<1	<10	20	0	10	10	15
GETC	11B-H	0.3	300	0	2000	2	<10	100	0	<10	<5	50
GETC	15A	0.1	300	0	500	<1	<10	<10	0	<10	15	10
GETC	198-B	0.1	2000	0	700	15	<10	0	0	20	<10	70
GETC	198-D	0.1	20	0	500	1	<10	0	0	10	<10	100
GETC	1B	0.5	600	0	1500	<1	<10	70	0	<10	50	70
GETC	205	5	20	0	500	<1	<10	0	0	<10	20	30
GETC	205-a	2	150	0	500	<1	<10	0	0	<10	<10	100
GETC	206	0.1	30	0	700	<1	<10	0	0	<10	50	70
GETC	211	0.1	60	0	700	1	<10	0	0	15	<10	70
GETC	211-A	15	200	0	100	<1	<10	0	0	<10	<10	200
GETC	212	0.1	3000	0	1000	<1	<10	20	0	<10	70	100
GETC	212-A	1	60	0	700	<1	<10	300	0	<10	100	10
GETC	214	0.1	30	0	1000	1	<10	50	0	10	70	100
GETC	214-A	2	700	0	700	1	<10	100	0	<10	70	70
GETC	214-b	2	80	0	1000	1	<10	100	0	<10	70	15
GETC	214-c	1	1000	0	200	<1	<10	50	0	<10	20	50
GETC	216AA	0.1	60	0	10000	2	<10	300	0	<10	200	200
GETC	216BB	0.1	75	0	2000	<1	<10	10	0	<10	20	15

min.dist	sample no.	Fe	F	Hg	Li	Mn	Mo	Nb	Ni	Pb	Rb	Sb
RAIN	N14442	0	0	0.67	0	0	0	0	0	0	0	8
RAIN	N14443	0	0	0.61	0	24	3	0	34	3	0	9
RAIN	N14444	0	0	0.65	0	0	0	0	0	0	0	6
RAIN	N14445	0	0	1.01	0	1650	3	0	5	2950	0	4
CHIM	01	0	1000	10	0	0	0	0	0	1400	0	150
CHIM	02	0	360	3.3	0	0	0	0	0	965	0	180
CHIM	03	0	2200	9.5	0	0	0	0	0	1100	0	230
CHIM	04	0	598	10	0	0	0	0	0	25000	0	1100
CHIM	05	0	405	6.3	0	0	0	0	0	1400	0	65
CHIM	06	0	1100	11	0	0	0	0	0	725	0	310
CHIM	07	0	523	3.3	0	0	0	0	0	655	0	59
CHIM	08	0	3300	30	0	0	0	0	0	650	0	390
CHIM	09	0	697	4.3	0	0	0	0	0	245	0	77
CHIM	10	0	2100	1.4	0	0	0	0	0	30	0	12
CHIM	202014	6242	463	98.6	0	40.4	1.26	0	6.38	2622	0	1781
CHIM	202015	195000	908	82.8	0	126	4.87	0	97.2	3449	0	1804
CHIM	202016	4678	241	138	0	43.8	2.76	0	7.15	1567	0	2435
CHIM	202017	11100	2754	18.5	0	1378	5.43	0	12.4	211	0	13.1
CHIM	202018	1679	59.8	44	0	13.7	0.225	0	1.53	1530	0	191
CHIM	202019	12100	339	103	0	583	2.59	0	8.93	8233	0	129
CHIM	202020	9450	349	28	0	66.2	1.51	0	5.14	1477	0	205
CHIM	202021	2579	3200	113	0	24.8	2.78	0	3.21	1882	0	1127
CHIM	202022	2131	93.1	66.6	0	17.7	0.779	0	2.31	253	0	415
GETC	10A	0	0	112.5	0	0	0	0	0	0	0	1700
GETC	11B-D	15000	0	2	0	1000	<2	0	<5	<10	0	<50
GETC	11B-E	200000	0	<2	0	>10000	15	0	200	<10	0	<50
GETC	11B-H	100000	0	<2	0	5000	5	0	7	15	0	<50
GETC	15A	30000	0	7	0	10	5	0	<10	30	0	<50
GETC	198-B	50000	0	0	0	1500	10	0	50	10	0	<50
GETC	198-D	50000	0	0	0	700	2	0	10	<10	0	<50
GETC	1B	150000	0	9	0	30	100	0	7	10	0	150
GETC	205	30000	0	0	0	200	<2	0	20	50	0	<50
GETC	205-a	50000	0	0	0	200	5	0	50	200	0	<50
GETC	206	7000	0	0	0	1000	<2	0	5	700	0	<50
GETC	211	20000	0	0	0	50	<2	0	10	70	0	<50
GETC	211-A	30000	0	0	0	70	2	0	<5	2000	0	<50
GETC	212	50000	0	3	0	30	10	0	100	50	0	0
GETC	212-A	5000	0	15	0	10	2	0	7	20	0	0
GETC	214	15000	0	<2	0	50	21	0	70	50	0	0
GETC	214-A	15000	0	3	0	20	10	0	20	70	0	0
GETC	214-b	10000	0	3	0	50	7	0	10	10	0	0
GETC	214-c	30000	0	10	0	30	7	0	30	30	0	0
GETC	216AA	20000	0	25	0	300	7	0	10	<10	0	<50
GETC	216BB	3000	0	3	0	50	<2	0	5	<10	0	<50

min.dist	sample no.	Sn	Sr	Te	Ti	Tl	V	W	Y	Zn	Zr
RAIN	N14442	0	0	0	0	0	0	0	0	0	0
RAIN	N14443	0	139	0	0	0	235	15	0	69	0
RAIN	N14444	0	0	0	0	0	0	0	0	0	0
RAIN	N14445	0	141	0	0	0	110	20	0	10	0
CHIM	01	0	0	0	0	0.25	0	0	0	490	0
CHIM	02	0	0	0	0	0.25	0	0	0	950	0
CHIM	03	0	0	0	0	0.25	0	0	0	965	0
CHIM	04	0	0	0	0	0.5	0	0	0	12500	0
CHIM	05	0	0	0	0	0.25	0	0	0	1100	0
CHIM	06	0	0	0	0	0.25	0	0	0	220	0
CHIM	07	0	0	0	0	0.25	0	0	0	1100	0
CHIM	08	0	0	0	0	0.25	0	0	0	385	0
CHIM	09	0	0	0	0	0.25	0	0	0	190	0
CHIM	10	0	0	0	0	0.25	0	0	0	130	0
CHIM	202014	0	246	24	471	<0.49	25.6	130	8.46	228	0
CHIM	202015	0	185	34.8	737	<0.46	203	880	30.3	7040	0
CHIM	202016	0	490	32.4	354	0.86	33.8	140	7.43	155	0
CHIM	202017	0	42.8	<0.486	1297	4.81	18.1	8	15.2	318	0
CHIM	202018	0	70.8	8.22	283	<0.457	3.02	25	<1.96	130	0
CHIM	202019	0	536	14.1	175	<0.463	9.89	67	14.6	1941	0
CHIM	202020	0	143	12.2	336	1.04	6.72	90	9.72	595	0
CHIM	202021	0	38.4	29	298	<0.487	8.59	22	3.37	79.8	0
CHIM	202022	0	12.6	7.96	185	<0.498	2.77	<4	2.01	28.6	0
GETC	10A	0	0	0	0	69	0	0	0	0	0
GETC	11B-D	0	1000	0	300	0	<10	<50	10	<200	<10
GETC	11B-E	0	2000	0	700	0	20	<50	30	200	<10
GETC	11B-H	0	70	0	1500	0	150	<50	20	200	0
GETC	15A	0	300	0	70	0	100	300	<10	<200	<10
GETC	198-B	0	100	0	5000	0	150	70	15	<200	50
GETC	198-D	0	200	0	10000	0	100	<50	50	<200	50
GETC	1B	0	200	0	500	0	500	200	<10	<200	0
GETC	205	0	<20	0	150	0	15	<50	<10	500	0
GETC	205-a	0	<20	0	100	0	70	<50	<10	1000	0
GETC	206	0	20	0	700	0	70	<50	15	500	0
GETC	211	0	<20	0	100	0	30	<50	<10	1000	0
GETC	211-A	0	<20	0	15	0	20	<50	<10	7000	0
GETC	212	0	20	0	700	0	300	50	20	1000	0
GETC	212-A	0	70	0	5000	0	500	<50	20	<200	0
GETC	214	0	300	0	1000	0	200	<50	150	200	0
GETC	214-A	0	100	0	1500	0	500	50		<200	50
GETC	214-b	0	150	0	2000	0	200	<50	20	<200	50
GETC	214-c	0	<20	0	300	0	150	100	10	300	0
GETC	216AA	0	150	0	5000	0	150	100	20	<200	0
GETC	216BB	0	200	0	150	0	20	<50	<10	<200	0

min.dist	sample no.	Ag	As	Au	Ba	Be	Bi	B	Cd	Co	Cr	Cu
GETC	216CC	0.1	40	0	3000	1	<10	200	0	<10	100	30
GETC	216DD	1	500	0	2000	1	<10	30	0	<10	30	100
GETC	216EE	0.1	200	0	2000	1	<10	20	0	<10	70	70
GETC	216F	1	20	0	1500	1	<10	700	0	<10	200	70
GETC	216FF	0.1	80	0	10000	<1	<10	100	0	<10	70	30
GETC	216G	0.1	500	0	500	1	<10	10	0	<10	100	100
GETC	216GG	0.1	200	0	500	7	<10	30	0	<10	10	70
GETC	216H	1	300	0	1000	1	<10	200	0	<10	200	500
GETC	216HH	0.1	500	0	2000	10	<10	<10	0	10	10	50
GETC	216I	3	50	0	500	<1	<10	20	0	<10	20	30
GETC	216II	10	60	0	5000	1	<10	20	0	<10	10	30
GETC	216J	2	1000	0	15000	<1	<10	200	0	<10	100	150
GETC	216JJ	2	500	0	0	5	<10	200	0	<10	70	100
GETC	216K	0.1	700	0	1000	1	<10	50	0	10	70	100
GETC	216KK	0.1	700	0	5000	7	<10	20	0	<10	<10	15
GETC	216L	0.1	150	0	1500	<1	<10	300	0	<10	150	100
GETC	216N	15	200	0	1500	<1	<10	30	0	<10	30	30
GETC	216O	7	40	0	500	1	<10	30	0	<10	30	20
GETC	216Q	0.1	100	0	1500	2	<10	100	0	15	70	50
GETC	216R	2	40	0	1000	<1	<10	20	0	<10	15	15
GETC	216S	10	1000	0	1500	<1	<10	10	0	<10	10	30
GETC	216T	1	500	0	1000	<1	<10	50	0	<10	30	20
GETC	216U	0.1	2000	0	2000	1	<10	150	0	<10	150	50
GETC	216V	0.1	100	0	10000	2	<10	700	0	<10	150	30
GETC	216W	1	300	0	10000	1	<10	100	0	<10	70	150
GETC	216X	0.1	150	0	5000	2	<10	200	0	<10	100	30
GETC	216Y	1	40	0	5000	<1	<10	20	0	<10	20	50
GETC	216Z	0.1	500	0	10000	1	<10	500	0	<10	200	2000
GETC	218A	0.1	100	0	300	2	<10	<10	0	15	10	500
GETC	218E	2	2000	0	300	<1	<10	<10	0	15	20	200
GETC	231	1	160	0	1500	1	<10	100	0	<10	100	70
GETC	232	0.1	160	0	10000	<1	<10	15	0	<10	30	50
GETC	234-A	1	150	0	5000	2	<10	150	0	10	100	100
GETC	234-B	2	600	0	1500	2	<10	100	0	10	70	500
GETC	235	0.1	500	0	1500	7	<10	2000	0	<10	<10	300
GETC	236	0.1	30	0	1500	<1	<10	10	0	<10	<10	70
GETC	237	0.1	80	0	1500	5	<10	10	0	10	10	100
GETC	239	0.1	600	0	700	2	<10	50	0	20	50	500
GETC	243	0.05	2000	0	10000	15	<10	10	0	<10	20	500
GETC	245	2	2000	0	5000	5	<10	1000	0	<10	50	70
GETC	246	1	1000	0	300	10	<10	50	0	20	70	200
GETC	247	1	250	0	1000	1	<10	30	0	<10	10	20
GETC	248	2	40	0	1000	1	<10	20	0	10	30	70
GETC	249	0.1	40	0	700	1	<10	10	0	<10	30	20

min.dist	sample no.	Fe	F	Hg	Li	Mn	Mo	Nb	Ni	Pb	Rb	Sb
GETC	216CC	20000	0	5	0	30	5	0	5	<10	0	<50
GETC	216DD	20000	0	5	0	30	7	0	30	200	0	<50
GETC	216EE	30000	0	9	0	30	2	0	20	50	0	<50
GETC	216F	10000	0	<2	0	70	7	0	30	50	0	<50
GETC	216FF	15000	0	5	0	20	5	0	15	10	0	<50
GETC	216G	30000	0	9	0	50	20	0	30	20	0	<50
GETC	216GG	50000	0	6	0	50	2	0	70	<10	0	<50
GETC	216H	20000	0	6	0	30	20	0	50	10	0	<50
GETC	216HH	30000	0	5	0	30	10	0	50	<10	0	<50
GETC	216I	3000	0	12	0	30	<2	0	5	10	0	<50
GETC	216II	5000	0	30	0	15	<2	0	10	5000	0	1500
GETC	216J	30000	0	5	0	20	50	0	10	50	0	<50
GETC	216JJ	30000	0	10	0	50	10	0	30	700	0	100
GETC	216K	30000	0	9	0	70	15	0	70	<10	0	<50
GETC	216KK	15000	0	<2	0	20	<2	0	15	30	0	<50
GETC	216L	15000	0	5	0	20	7	0	20	10	0	<50
GETC	216N	5000	0	6	0	30	2	0	7	10	0	<50
GETC	216O	7000	0	3	0	200	<2	0	10	<10	0	<50
GETC	216Q	20000	0	<2	0	300	2	0	20	30	0	<50
GETC	216R	20000	0	8	0	20	5	0	5	10	0	<50
GETC	216S	30000	0	30	0	30	10	0	20	20	0	<50
GETC	216T	30000	0	14	0	50	5	0	10	50	0	<50
GETC	216U	70000	0	15	0	30	7	0	20	10	0	<50
GETC	216V	30000	0	7	0	50	5	0	20	<10	0	<50
GETC	216W	30000	0	28	0	20	10	0	10	10	0	<50
GETC	216X	20000	0	80	0	10	7	0	5	<10	0	<50
GETC	216Y	3000	0	12	0	30	<2	0	<10	<10	0	<50
GETC	216Z	50000	0	14	0	50	10	0	20	<10	0	<50
GETC	218A	20000	0	<2	0	150	<2	0	30	<10	0	<50
GETC	218E	30000	0	6	0	500	2	0	30	<10	0	<50
GETC	231	30000	0	4	0	50	5	0	30	30	0	<50
GETC	232	10000	0	23	0	10	<2	0	20	10	0	<50
GETC	234-A	7000	0	<2	0	15	<2	0	50	20	0	<50
GETC	234-B	30000	0	<2	0	20	5	0	150	70	0	<50
GETC	235	30000	0	<2	0	100	10	0	100	30	0	<50
GETC	236	20000	0	<2	0	50	<2	0	50	15	0	<50
GETC	237	30000	0	<2	0	300	10	0	70	<10	0	<50
GETC	239	50000	0	<2	0	30	10	0	150	30	0	<50
GETC	243	70000	0	<2	0	100	15	0	200	<10	0	<50
GETC	245	30000	0	2	0	1500	2	0	100	<10	0	0
GETC	246	70000	0	8	0	70	10	0	200	70	0	0
GETC	247	15000	0	<2	0	100	15	0	20	<10	0	0
GETC	248	20000	0	<2	0	1500	<2	0	150	15	0	0
GETC	249	10000	0	<2	0	300	<2	0	50	<10	0	0

min.dist	sample no.	Sn	Sr	Te	Ti	Tl	V	W	Y	Zn	Zr
GETC	216CC	0	150	0	3000	0	100	50	10	<200	50
GETC	216DD	0	100	0	300	0	150	200	10	300	0
GETC	216EE	0	100	0	700	0	150	<50	10	300	0
GETC	216F	0	100	0	3000	0	500	<50	10	<200	0
GETC	216FF	0	200	0	3000	0	150	150	<10	300	50
GETC	216G	0	100	0	300	0	150	50	<10	<200	0
GETC	216GG	0	20	0	200	0	200	<50	<10	1000	0
GETC	216H	0	150	0	700	0	500	70	20	<200	50
GETC	216HH	0	150	0	500	0	150	50	30	<200	0
GETC	216I	0	300	0	200	0	70	<50	<10	<200	0
GETC	216II	0	2000	0	100	0	50	100	50	500	0
GETC	216J	0	100	0	700	0	200	100	10	<200	0
GETC	216JJ	0	2000	0	700	0	500	200	50	<200	0
GETC	216K	0	50	0	700	0	200	100	<10	200	0
GETC	216KK	0	300	0	150	0	50	50	10	300	0
GETC	216L	0	100	0	2000	0	300	70	<10	<200	50
GETC	216N	0	300	0	150	0	100	<50	10	<200	0
GETC	216O	0	150	0	700	0	70	<50	<10	<200	0
GETC	216Q	0	300	0	3000	0	100	<50	15	<200	50
GETC	216R	0	50	0	700	0	70	200	15	<200	0
GETC	216S	0	100	0	200	0	200	150	<10	200	0
GETC	216T	0	200	0	700	0	150	500	20	200	0
GETC	216U	0	700	0	500	0	150	1000	<10	<200	0
GETC	216V	0	700	0	3000	0	200	100	20	<200	0
GETC	216W	0	1500	0	2000	0	200	150	<10	<200	50
GETC	216X	0	100	0	2000	0	100	50	10	<200	50
GETC	216Y	0	300	0	200	0	30	<50	<10	<200	50
GETC	216Z	0	700	0	3000	0	200	150	20	<200	0
GETC	218A	0	30	0	200	0	70	<50	20	<200	0
GETC	218E	0	50	0	150	0	200	150	10	<200	0
GETC	231	0	300	0	2000	0	300	<50	20	200	0
GETC	232	0	300	0	700	0	300	<50	20	200	0
GETC	234-A	0	300	0	1500	0	300	<50	15	700	0
GETC	234-B	0	100	0	700	0	1000	70	20	700	50
GETC	235	0	50	0	300	0	150	70	10	500	0
GETC	236	0	<20	0	200	0	70	<50	<10	1000	0
GETC	237	0	50	0	300	0	150	<50	20	1000	0
GETC	239	0	150	0	300	0	300	50	50	1000	0
GETC	243	0	50	0	200	0	200	<50	30	3000	0
GETC	245	0	200	0	1500	0	200	150	70	1000	0
GETC	246	0	50	0	700	0	500	100	50	2000	0
GETC	247	0	150	0	2000	0	100	<50	10	<200	0
GETC	248	0	200	0	1000	0	200	<50	20	1000	0
GETC	249	0	300	0	300	0	100	<50	<10	700	0

min.dist	sample no.	Ag	As	Au	Ba	Be	Bi	B	Cd	Co	Cr	Cu
GETC	250	0.1	30	0	700	<1	<10	10	0	<10	15	10
GETC	251	0.1	500	0	2000	2	<10	200	0	15	30	100
GETC	252	2	700	0	500	1	<10	500	0	<10	70	70
GETC	253	0.1	500	0	1000	1	<10	100	0	10	30	50
GETC	2664	5	10000	4.7	100	1	0	100	0	5	20	50
GETC	2B	0.5	400	0	3000	<1	<10	100	0	<10	30	7
GETC	302	20	4200	0.6	1000	1.5	2	300	0.2	0	10	100
GETC	306	20	210	0.1	300	<1	1	70	0.7	0	0	100
GETC	3B	1	3000	0	1000	<1	<10	<10	0	<10	30	15
GETC	4A	0	5000	7.8	0	0	0	0	0	0	0	0
GETC	5B-A	0.05	400	0	10000	<1	<10	20	0	<10	50	300
GETC	6B	0.05	600	0	700	<1	<10	15	0	<10	5	10
GETC	7B-D	0.05	300	0	2000	5	<10	<10	0	20	70	300
GETC	8A	0	3900	9.3	0	0	0	0	0	0	0	0
GETC	8B	0.5	1600	0	700	5	<10	30	0	100	15	300
GETC	915	0.1	2000	0	2000	<1	<10	20	0	15	50	70
GETC	9A	0	36000	0.08	0	0	0	0	0	0	0	0
GETC	9B	0.05	400	0	5000	2	<10	0	0	<10	100	150
GETC	GMS5-11	5	0	0	1000	1	<10	0	0	<10	70	50
GETC	GMS5-12	2	0	0	700	1	<10	0	0	10	30	70
GETC	GMS5-2	10	0	0	1000	1	<10	0	0	<10	50	50
GETC	GMS5-3	5	0	0	1000	1	<10	0	0	15	70	150
GETC	GMS5-4	7	0	0	1000	1	<10	0	0	<10	30	70
GETC	GMS5-6	5	0	0	1000	1	<10	0	0	15	50	70
GETC	GMS5-8	7	0	0	1000	1	<10	0	0	<10	30	50
GETC	GMS5-9	5	0	0	700	1	<10	0	0	10	50	70

min.dist	sample no.	Fe	F	Hg	Li	Mn	Mo	Nb	Ni	Pb	Rb	Sb
GETC	250	5000	0	<2	0	500	<2	0	20	<10	0	0
GETC	251	30000	0	<2	0	200	5	0	50	50	0	0
GETC	252	20000	0	3	0	30	7	0	30	15	0	0
GETC	253	30000	0	<2	0	100	5	0	30	20	0	0
GETC	2664	15000	0	0	0	10	10	0	20	15	0	3000
GETC	2B	30000	0	5	0	10	2	0	<5	<10	0	<50
GETC	302	20000	200	4.4	0	300	0	0	0	10	0	50
GETC	306	7000	100	300	0	<10	10	0	5	20	0	130
GETC	3B	100000	0	26	0	20	5	0	5	10	0	<50
GETC	4A	0	0	19.5	0	0	0	0	0		0	10
GETC	5B-A	100000	0	<2	0	70	150	0	150	15	0	200
GETC	6B	70000	0	<2	0	70	10	0	70	<10	0	<50
GETC	7B-D	150000	0	2	0	150	20	0	300	20	0	<50
GETC	8A	0	0	101.8	0	0	0	0			0	50
GETC	8B	200000	0	<2	0	5000	30	0	500	50	0	150
GETC	915	100000	0	13	0	100	15	0	30	20	0	<50
GETC	9A	0	0	110.6	0	0	0	0	0		0	680
GETC	9B	>200000	0	14	0	200	50	0	20	30	0	<50
GETC	GMS5-11	0	0	0	0	100	100	0	15	<10	0	700
GETC	GMS5-12	0	0	0	0	200	200	0	20	<10	0	300
GETC	GMS5-2	0	0	0	0	100	50	0	15	<10	0	700
GETC	GMS5-3	0	0	0	0	200	200	0	30	<10	0	500
GETC	GMS5-4	0	0	0	0	100	100	0	15	<10	0	700
GETC	GMS5-6	0	0	0	0	200	200	0	30	<10	0	700
GETC	GMS5-8	0	0	0	0	50	100	0	15	<10	0	1000
GETC	GMS5-9	0	0	0	0	200	150	0	30	<10	0	300

min.dist	sample no.	Sn	Sr	Te	Ti	Tl	V	W	Y	Zn	Zr
GETC	250	0	300	0	200	0	70	<50	<10	<200	0
GETC	251	0	50	0	1000	0	150	100	50	200	0
GETC	252	0	100	0	1500	0	300	50	20	200	50
GETC	253	0	100	0	1500	0	100	150	20	200	0
GETC	2664	0	0	0	1000	0	50	<50	10	50	0
GETC	2B	0	500	0	1000	0	200	300	<10	<200	0
GETC	302	0	<100	0.3	1000	3.3	50	0	0	0	0
GETC	306	0	0	0.23	300	4.4	50	0	0	0	<10
GETC	3B	0	50	0	300	0	200	500	<10	<200	<10
GETC	4A	0	0	0	0	0	0	0	0	0	0
GETC	5B-A	0	5000	0	3000	0	1000	<50	<10	700	0
GETC	6B	0	50	0	300	0	200	<50	<10	700	0
GETC	7B-D	0	700	0	1500	0	1000	<50	70	2000	0
GETC	8A	0	0	0	0	80	0	0	0	0	0
GETC	8B	0	200	0	500	0	700	200	30	1500	0
GETC	915	0	700	0	700	0	1000	3000	<10	<200	0
GETC	9A	0	0	0	0	50	0	0	0	0	0
GETC	9B	0	5000	0	300	0	700	100	15	<200	0
GETC	GMS5-11	0	100	0	2000	0	100	150	10	<200	0
GETC	GMS5-12	0	50	0	1500	0	100	70	10	<200	0
GETC	GMS5-2	0	100	0	2000	0	100	100	10	<200	0
GETC	GMS5-3	0	100	0	2000	0	100	150	10	<200	0
GETC	GMS5-4	0	70	0	2000	0	100	100	10	<200	0
GETC	GMS5-6	0	50	0	2000	0	100	150	10	<200	0
GETC	GMS5-8	0	70	0	2000	0	1400	150	10	<200	0
GETC	GMS5-9	0	50	0	1500	0	100	100	10	<200	0

APPENDIX H: HISTOGRAMS SHOWING TRACE ELEMENTS OF MINERALIZED SAMPLES.

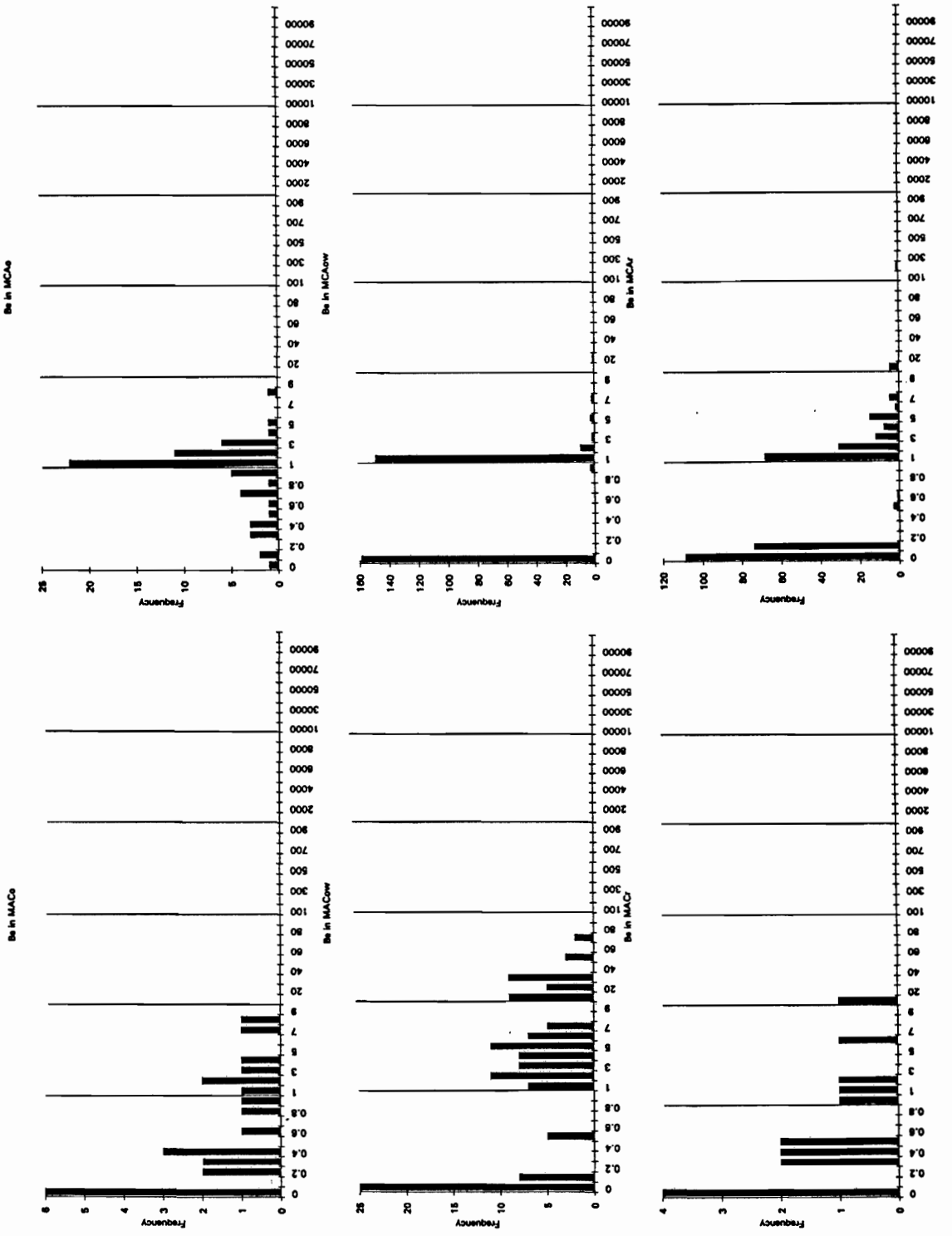

Figure H-1. Stepped histograms of beryllium in ppm (MAC=alkali-calcic, MCA=calc-alkalic; o=oxidized, ow=weakly oxidized, r=reduced).

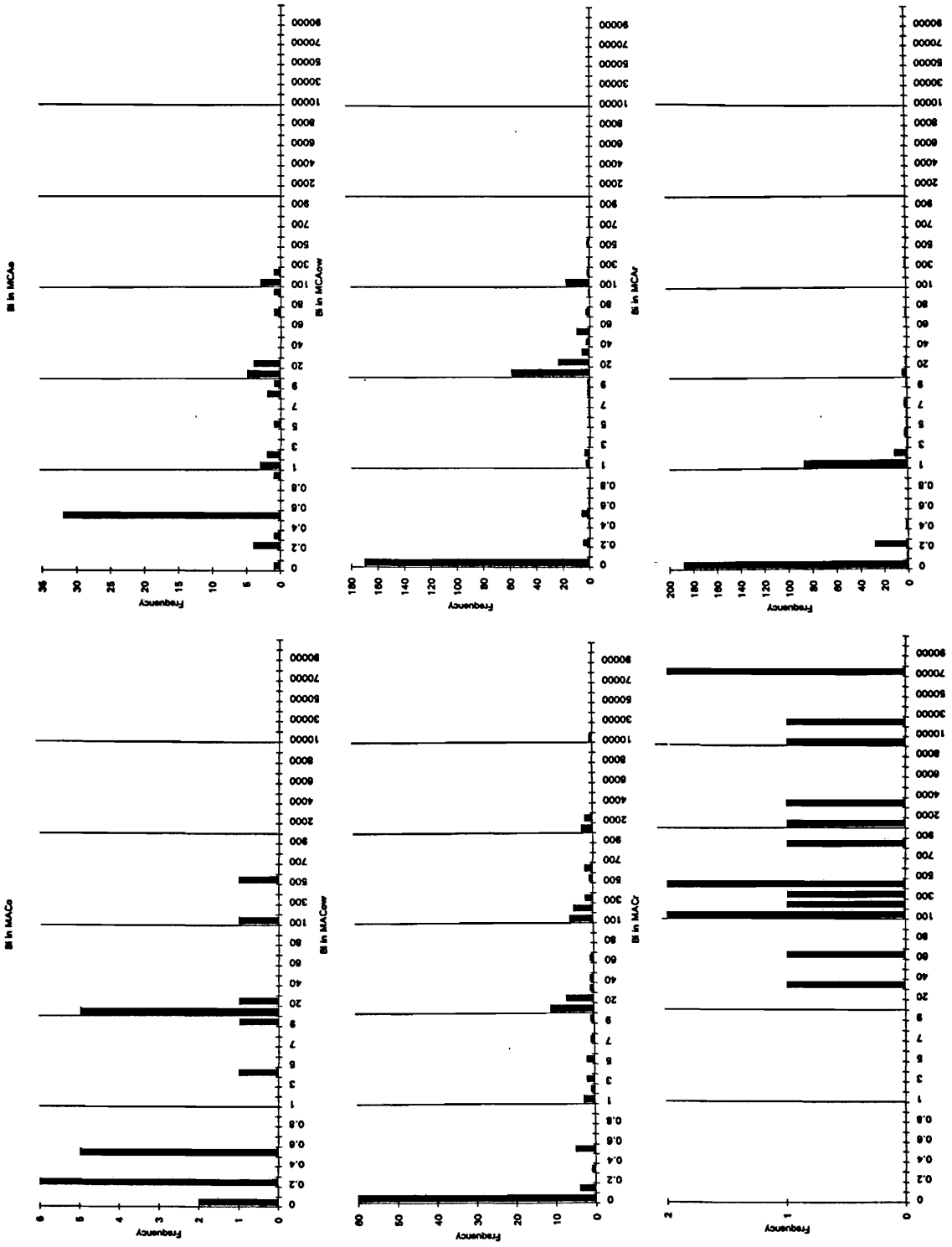

Figure H-2. Stepped histograms of bismuth in ppm (MAC=alkali-calcic, MCA=calc-alkalic; o=oxidized, ow=weakly oxidized, r=reduced).

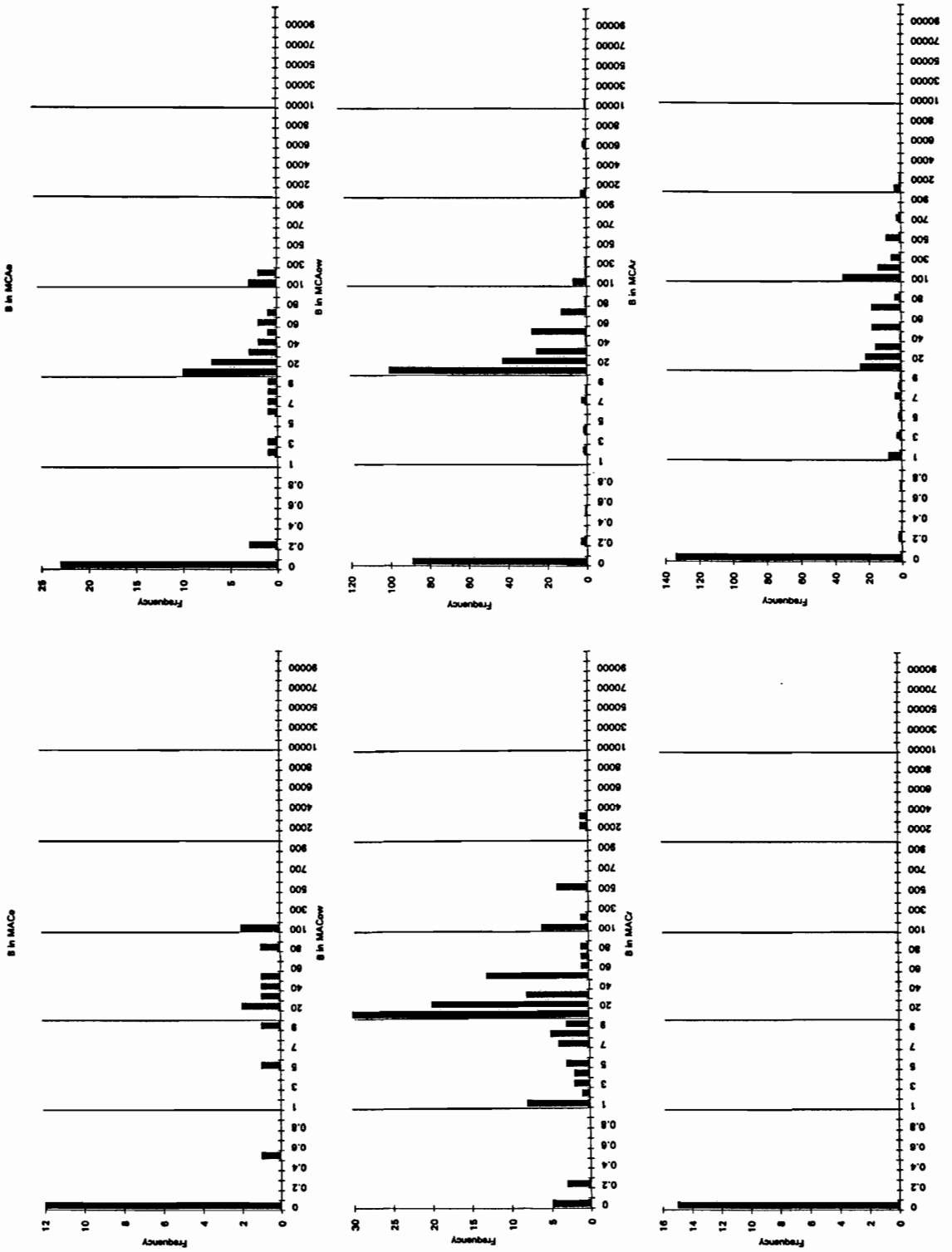

Figure H-3. Stepped histograms of boron in ppm (MAC=alkali-calcic, MCA=calc-alkalic; o=oxidized, ow=weakly oxidized, r=reduced).

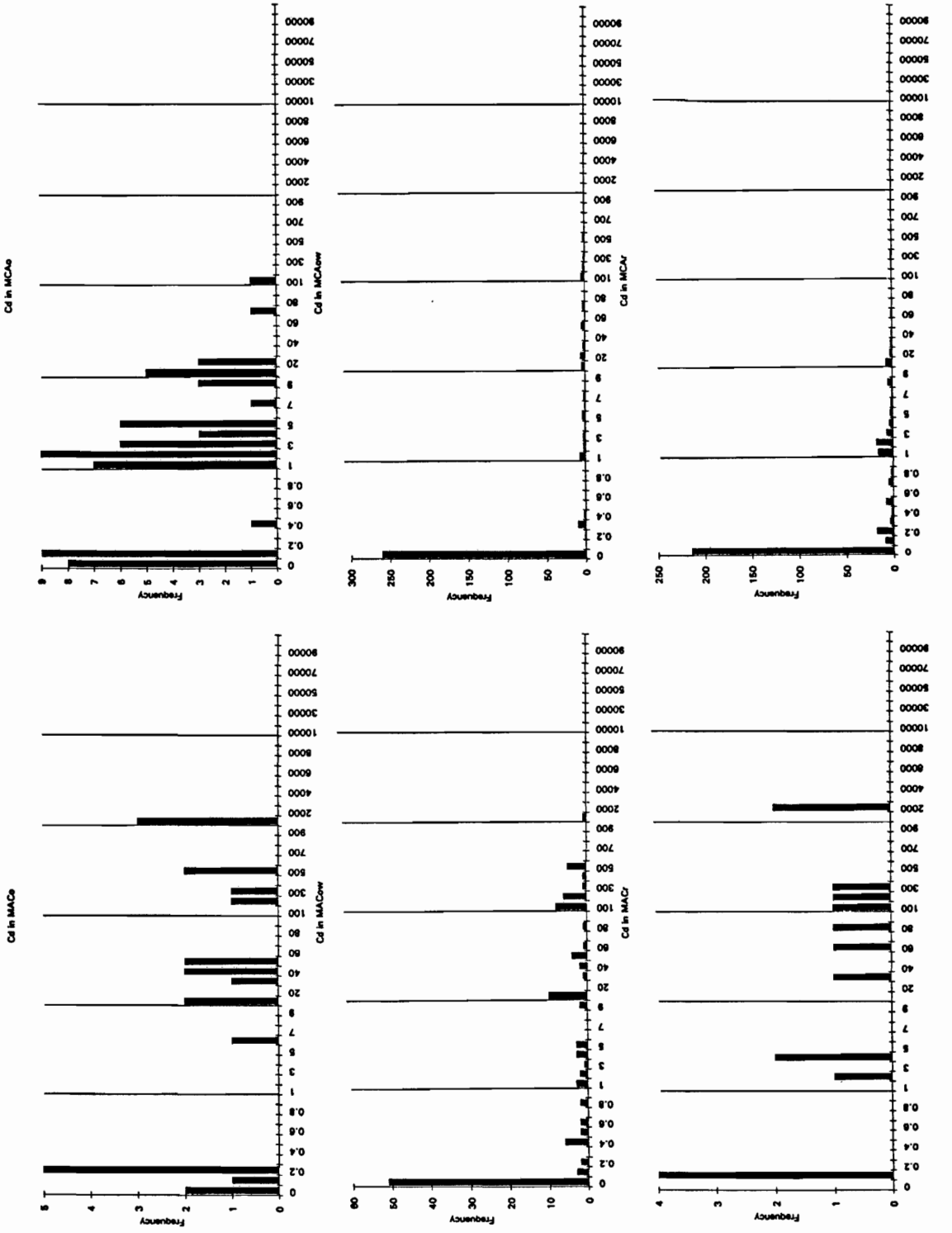

Figure H-4. Stepped histograms of cadmium in ppm (MAC=alkali-calcic, MCA=calc-alkalic; o=oxidized, ow=weakly oxidized, r=reduced).

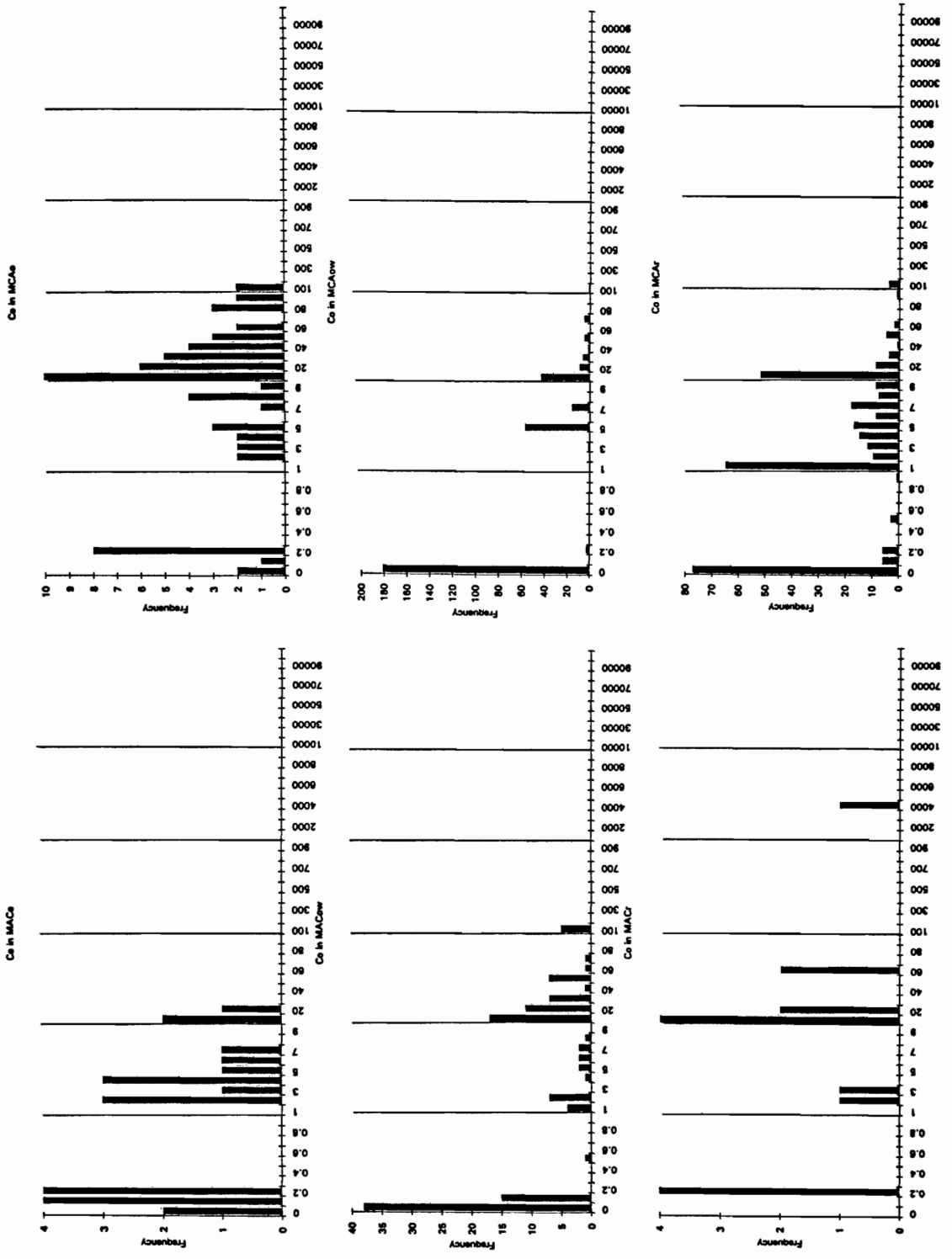

Figure H-5. Stepped histograms of cobalt in ppm (MAC=alkali-calcic, MCA=calc-alkalic; o=oxidized, ow=weakly oxidized, r=reduced).

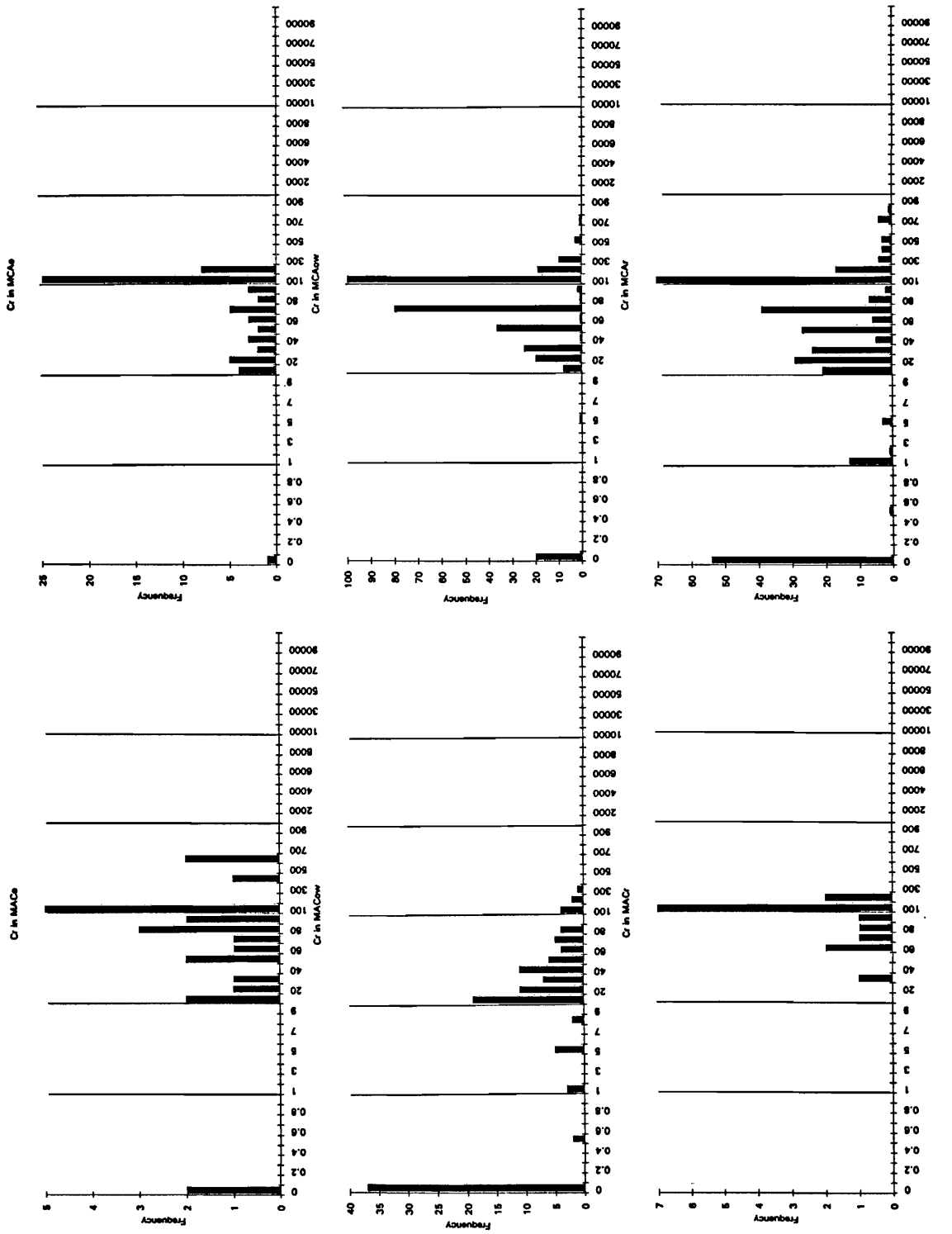

Figure H-6. Stepped histograms of chromium in ppm (MAC=alkali-calcic, MCA=calc-alkalic; o=oxidized, ow=weakly oxidized, r=reduced).

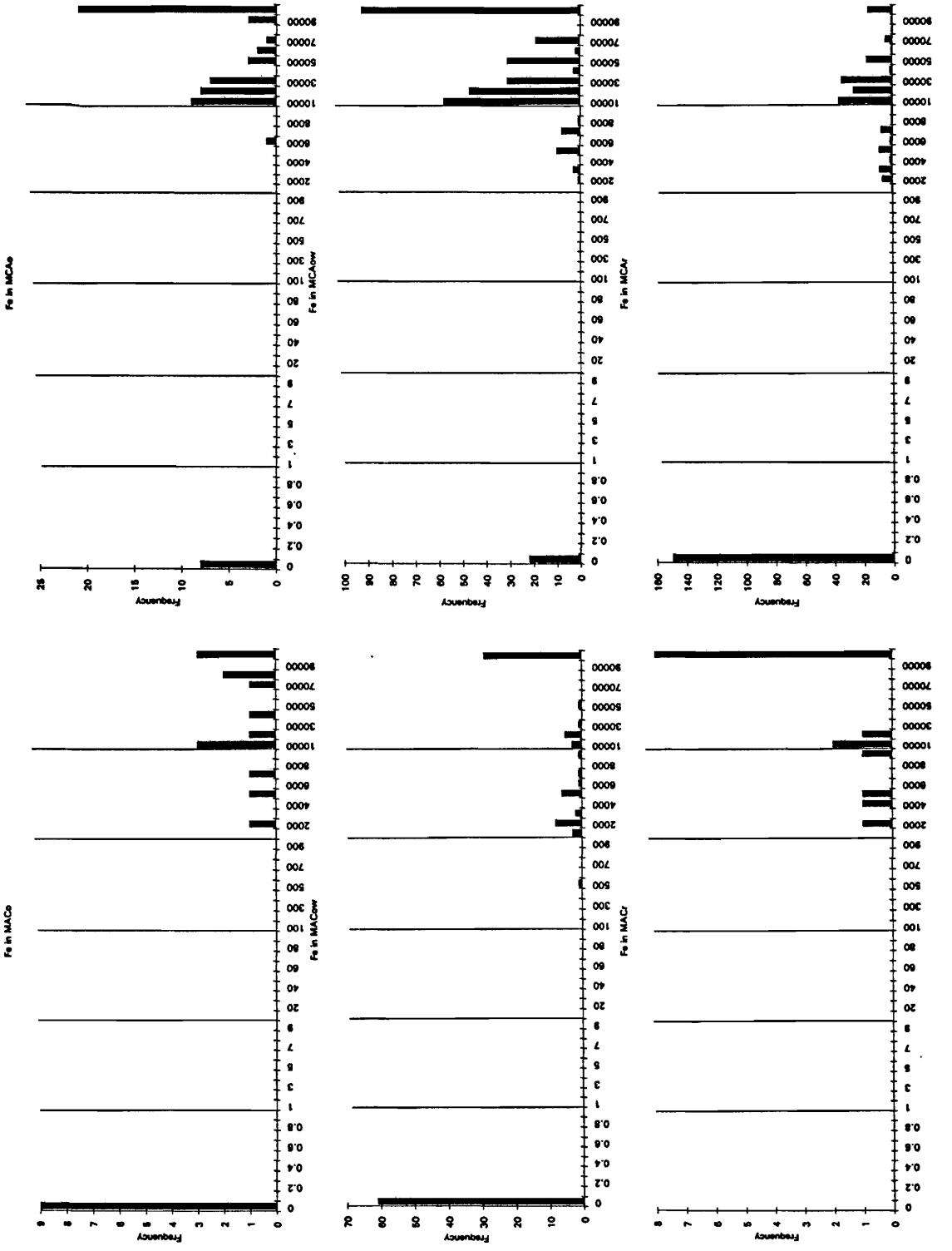

Figure H-7. Stepped histograms of iron in ppm (MAC=alkali-calcic, MCA=calc-alkalic; o=oxidized, ow=weakly oxidized, r=reduced).

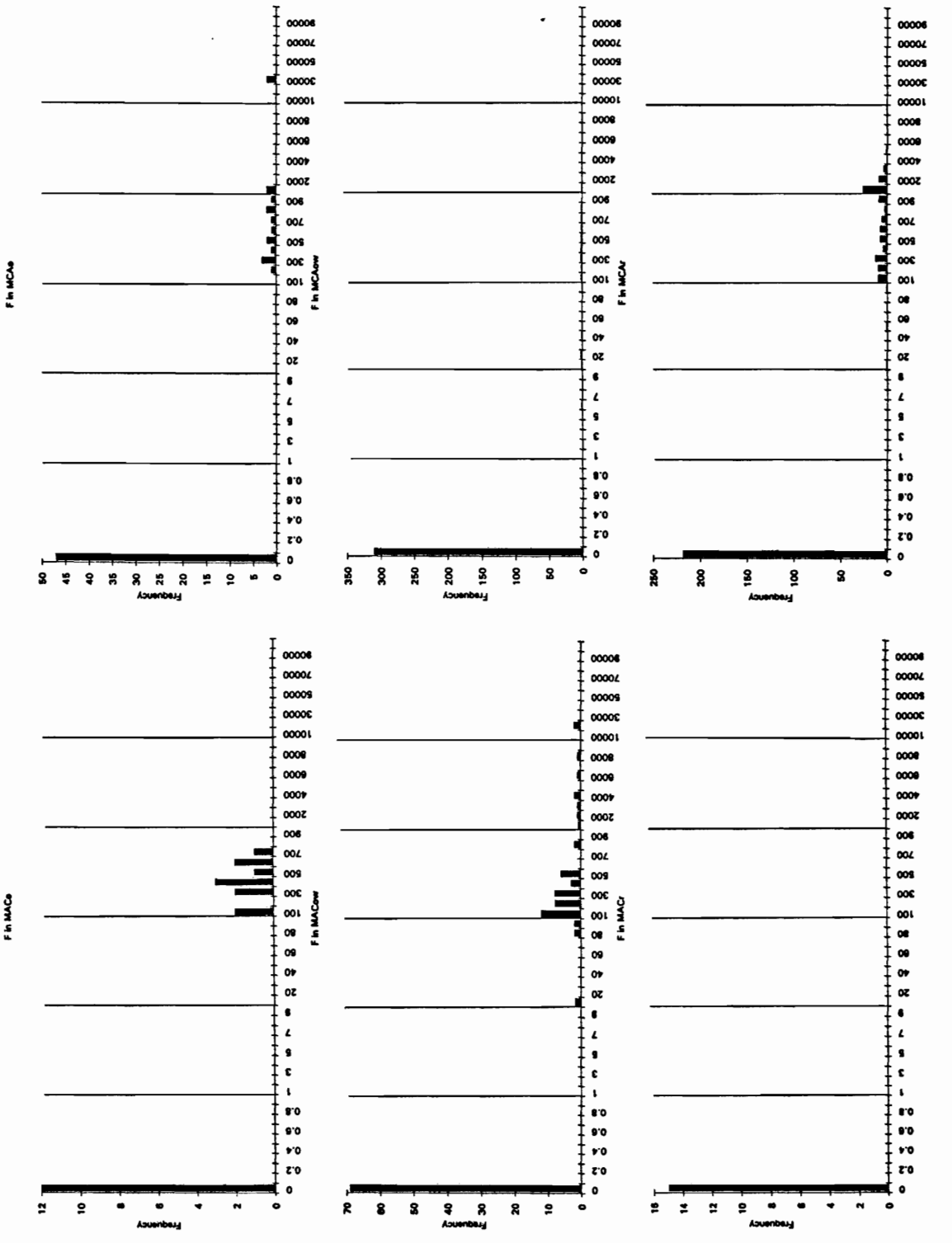

Figure H-8. Stepped histograms of fluorine in ppm (MAC=alkali-calcic, MCA=calc-alkalic; o=oxidized, ow=weakly oxidized, r=reduced).

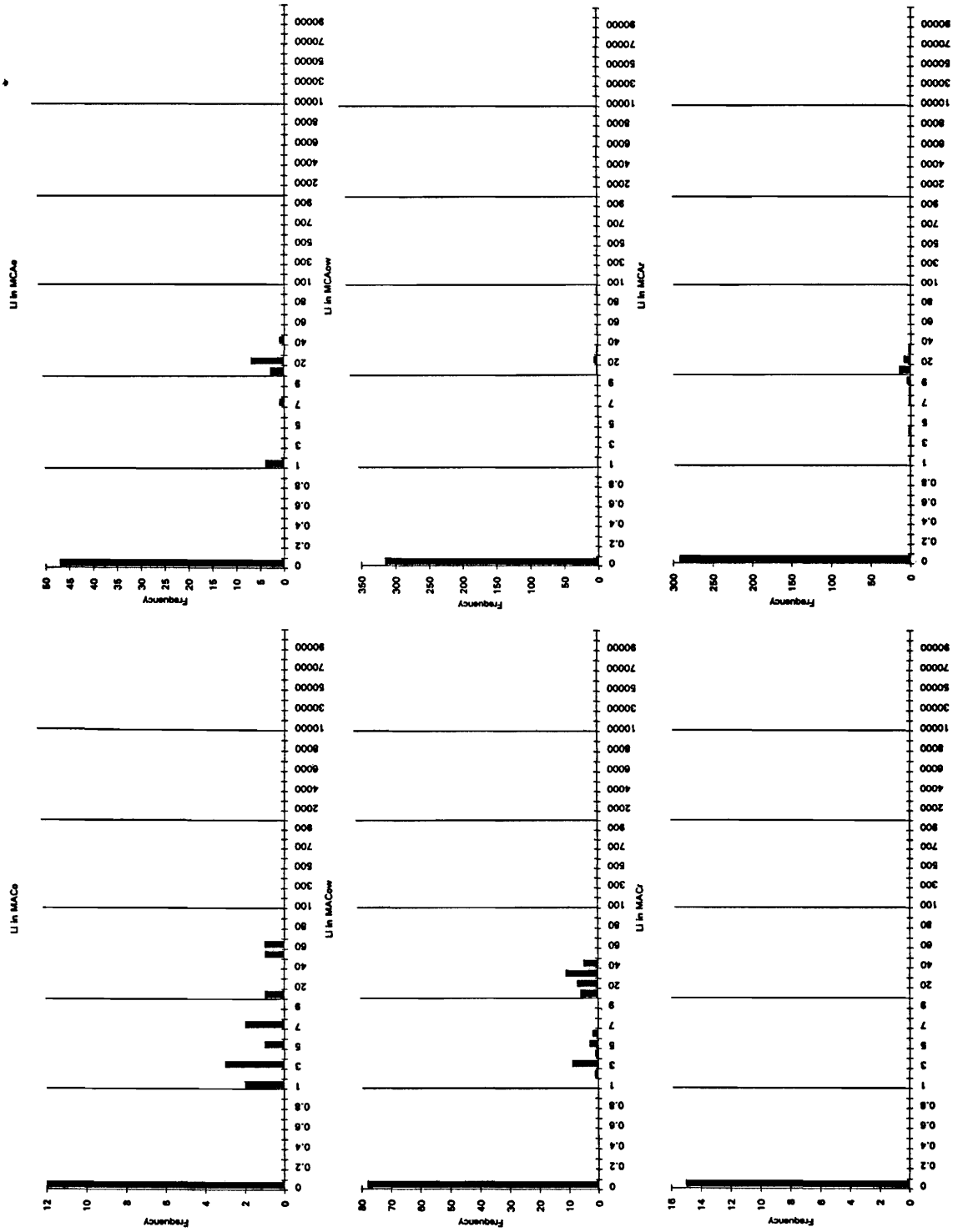

Figure H-9. Stepped histograms of lithium in ppm (MAC=alkali-calcic, MCA=calc-alkalic; o=oxidized, ow=weakly oxidized, r=reduced).

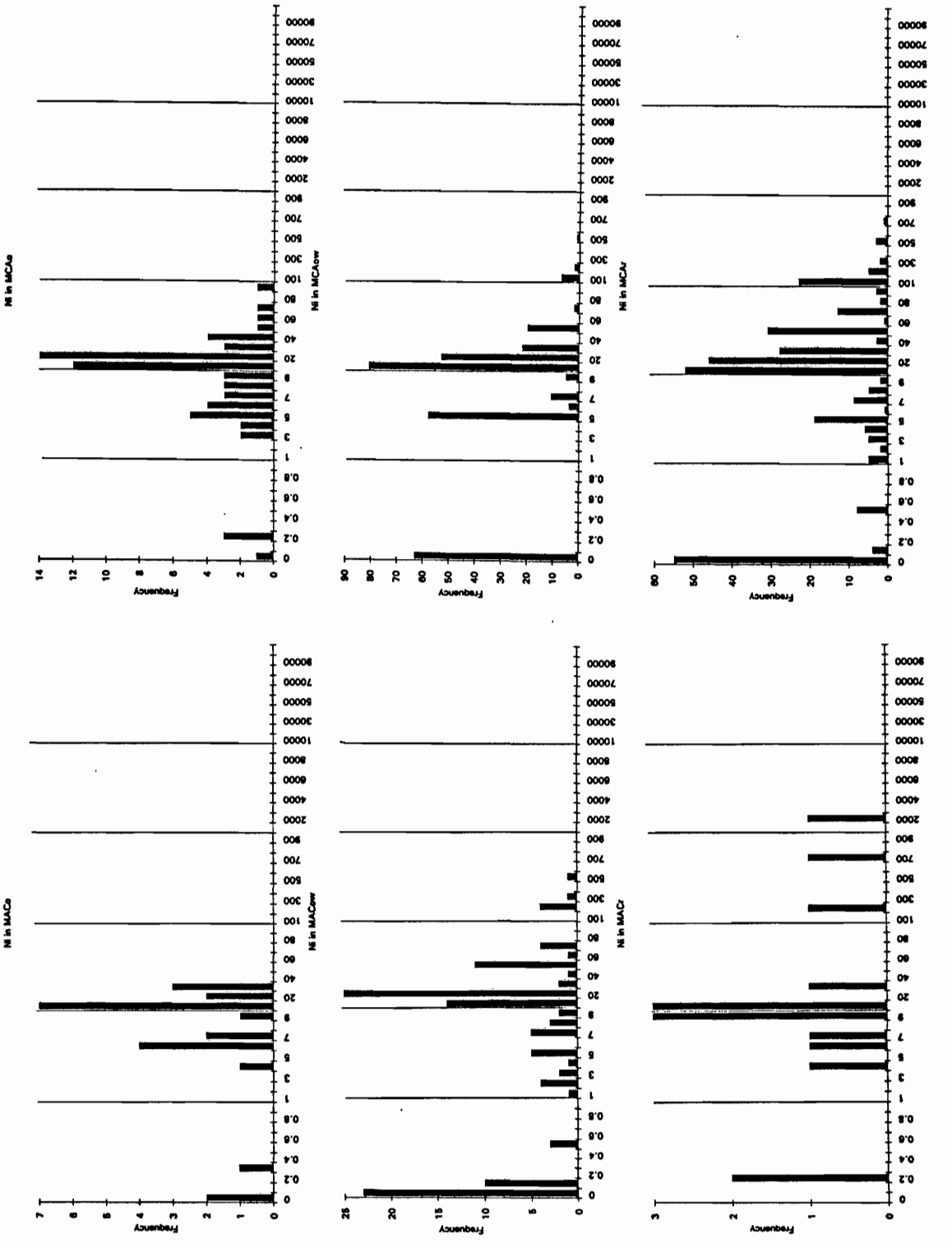

Figure H-10. Stepped histograms of nickel in ppm (MAC=alkali-calcic, MCA=calc-alkalic; o=oxidized, ow=weakly oxidized, r=reduced).

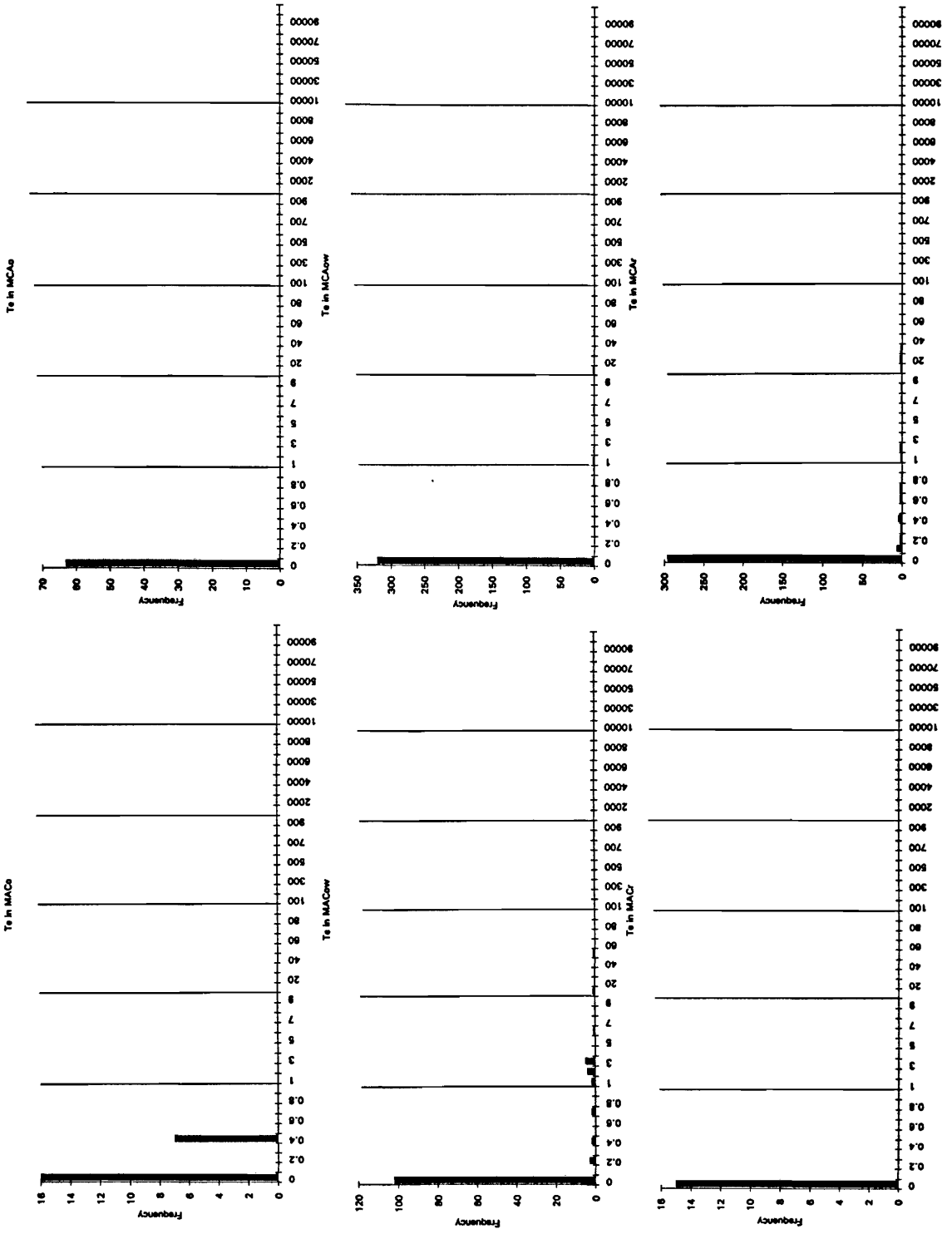

Figure H-11. Stepped histograms of tellurium in ppm (MAC=alkali-calcic, MCA=calc-alkalic; o=oxidized, ow=weakly oxidized, r=reduced).

APPENDIX I: HISTOGRAMS OF STATISTICS ON MINERALIZED SAMPLES.

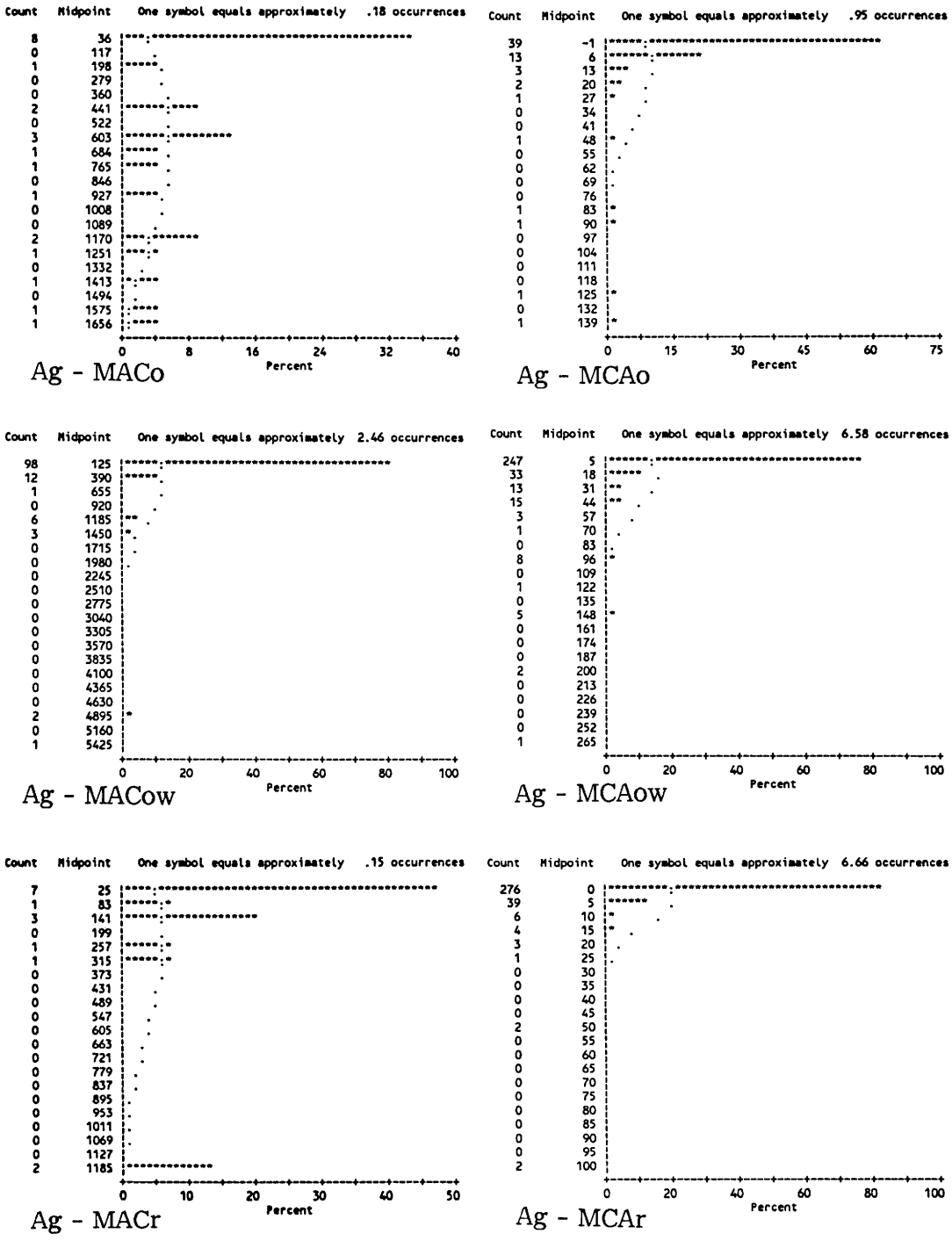

Figure I-1. Histograms of silver concentrations in ppm (MAC=alkali-calcic, MCA=calc-alkalic, o=oxidized, ow=weakly oxidized, r=reduced).

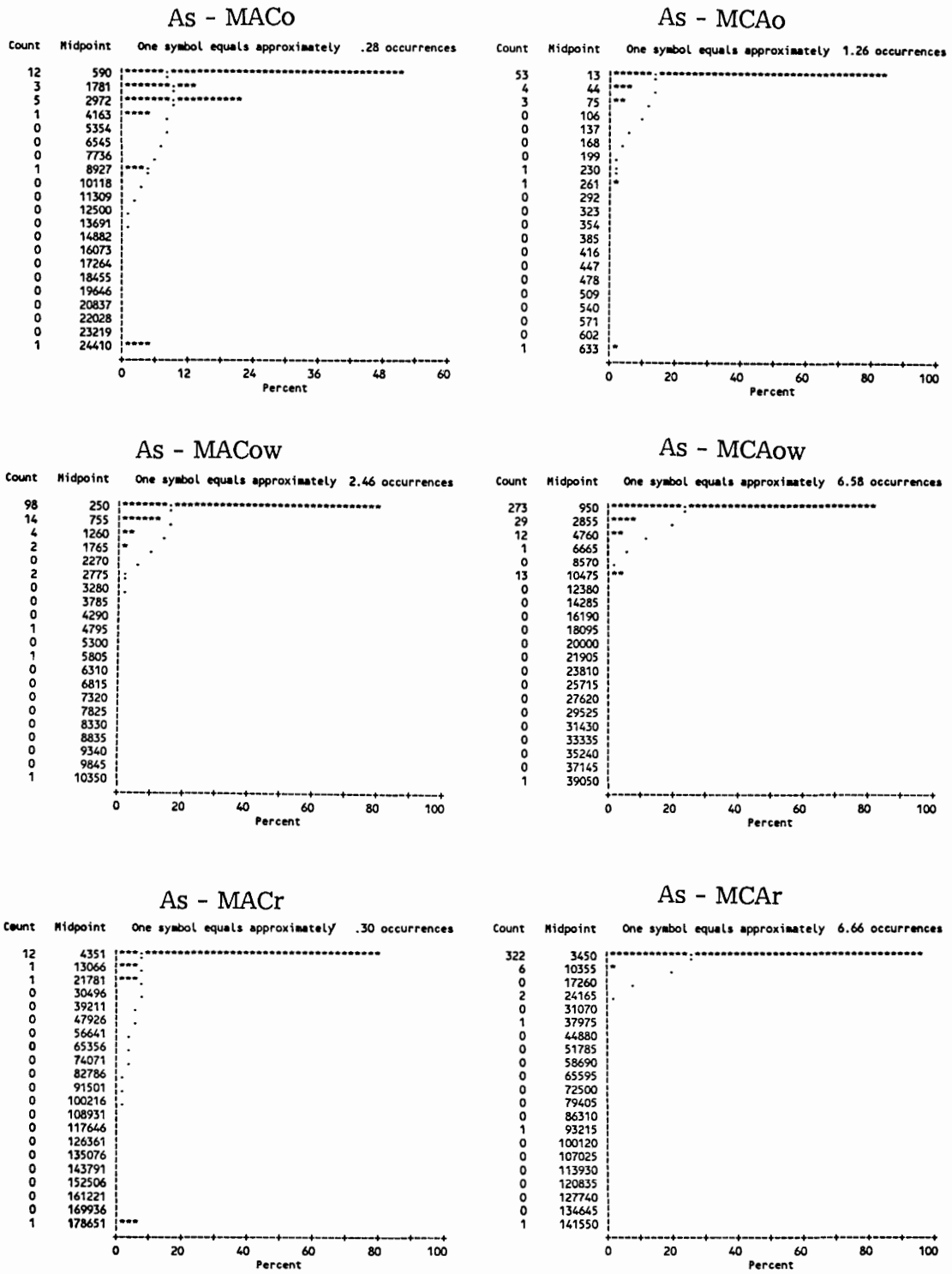

Figure I-2. Histograms of arsenic concentrations in ppm (MAC=alkali-calcic, MCA=calc-alkalic, o=oxidized, ow=weakly oxidized, r=reduced).

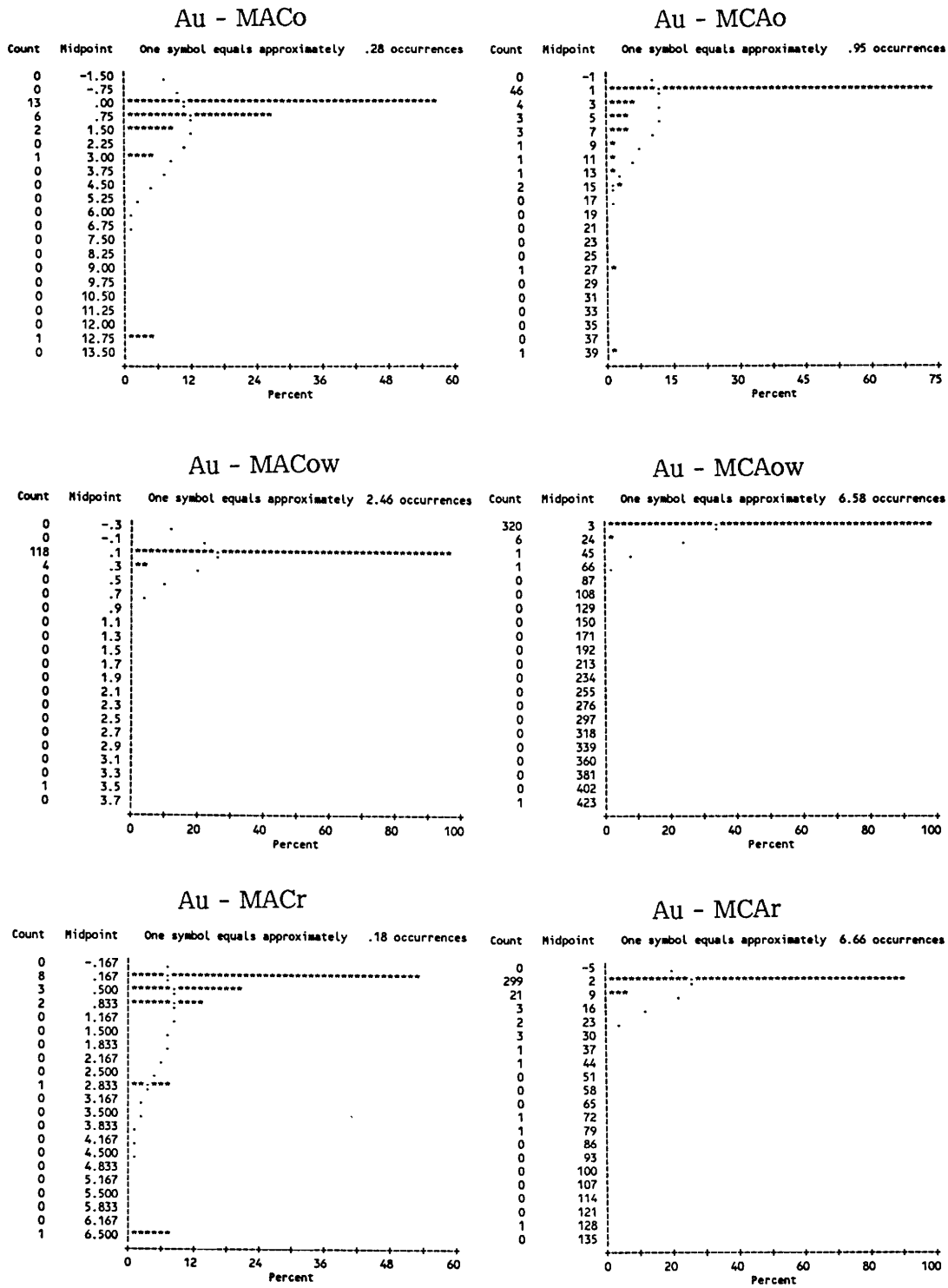

Figure I-3. Histograms of gold concentrations in ppm (MAC=metaluminous alkali-calcic, MCA=calc-alkalic, o=oxidized, ow=weakly oxidized, r=reduced).

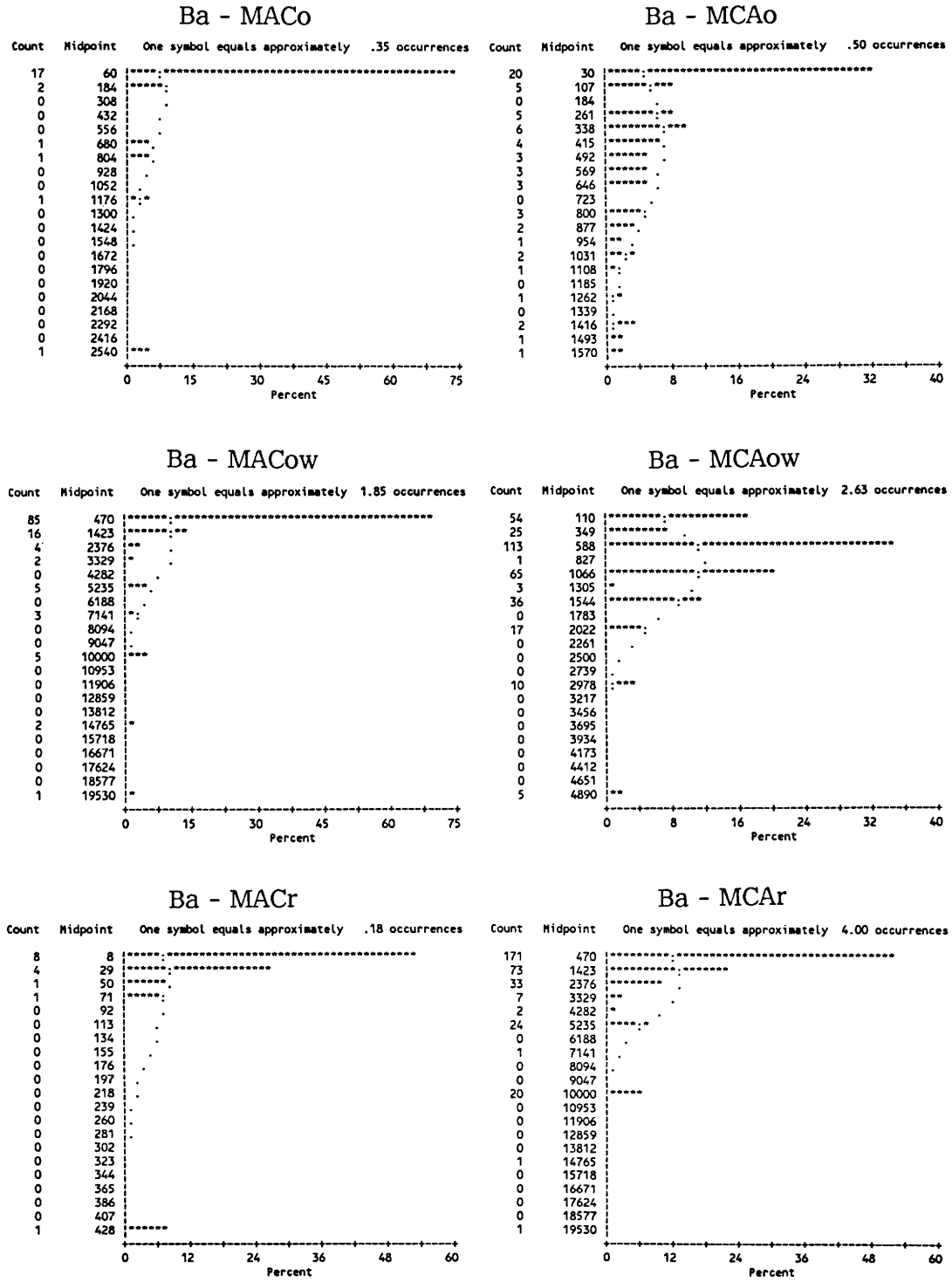

Figure I-4. Histograms of barium concentrations in ppm (MAC=alkali-calcic, MCA=calc-alkalic, o=oxidized, ow=weakly oxidized, r=reduced).

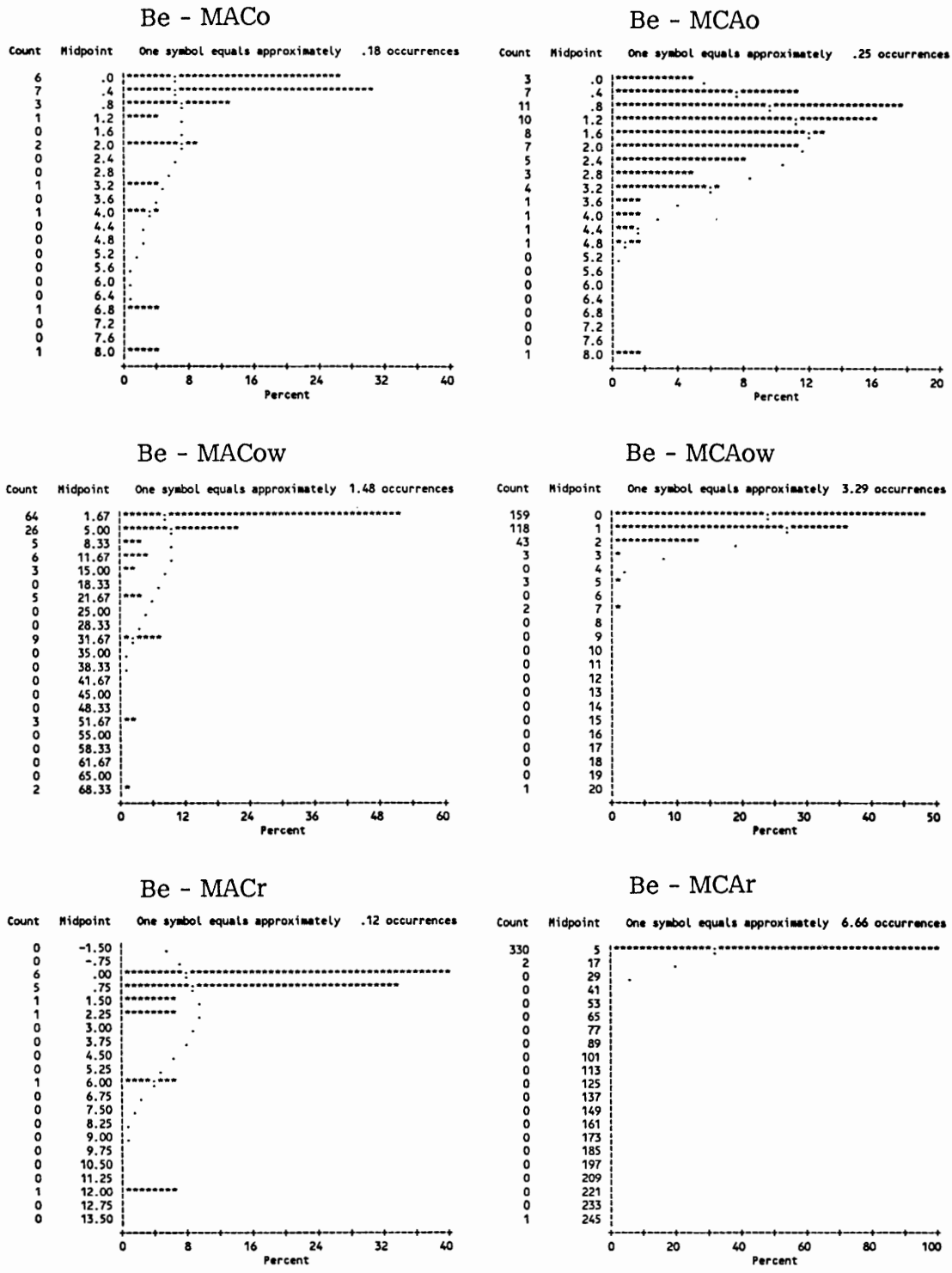

Figure I-5. Histograms of beryllium concentrations in ppm (MAC=alkali-calcic, MCA=calc-alkalic, o=oxidized, ow=weakly oxidized, r=reduced).

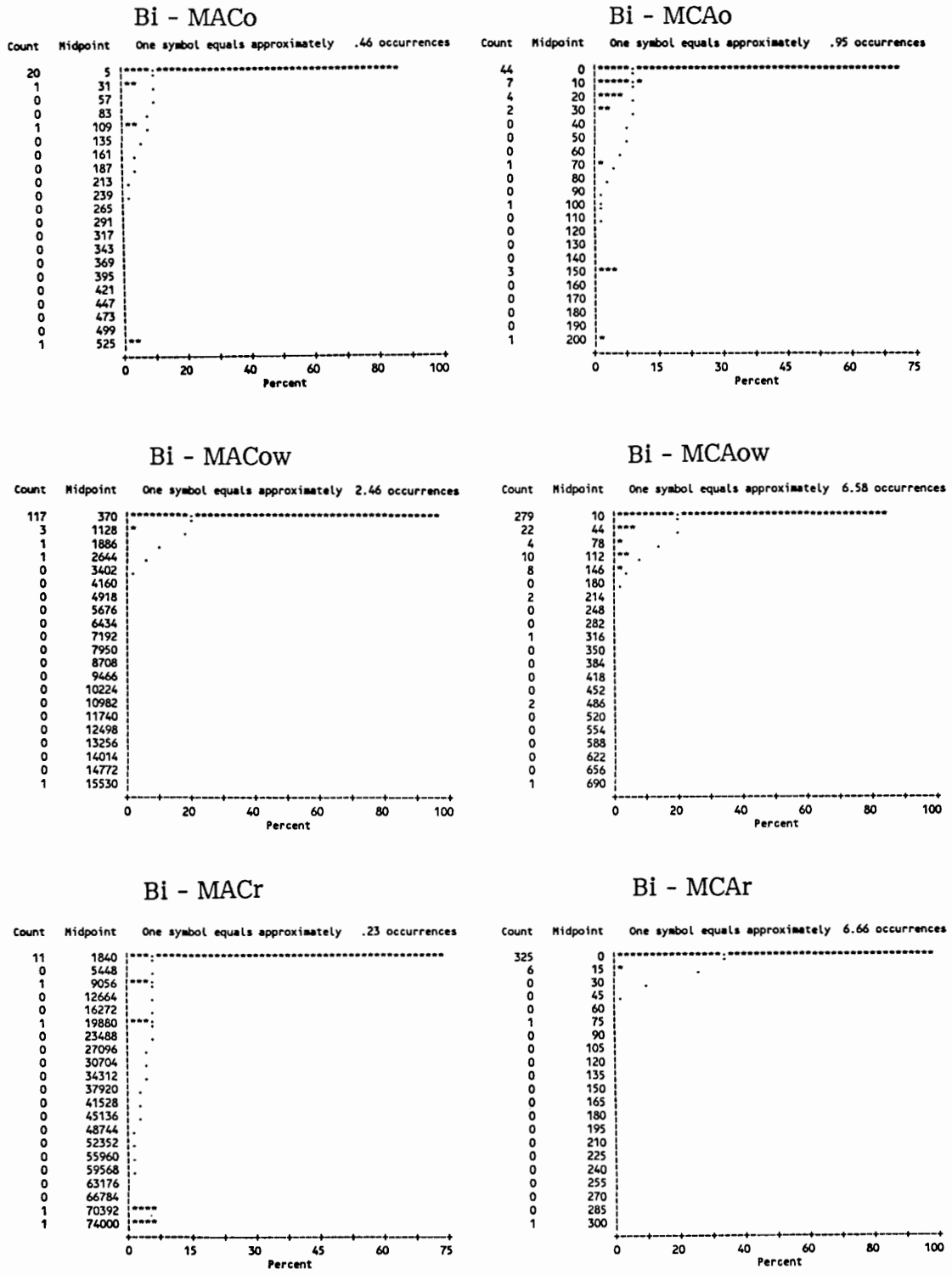

Figure I-6. Histograms of bismuth concentrations in ppm (MAC=alkali-calcic, MCA=calc-alkalic, o=oxidized, ow=weakly oxidized, r=reduced).

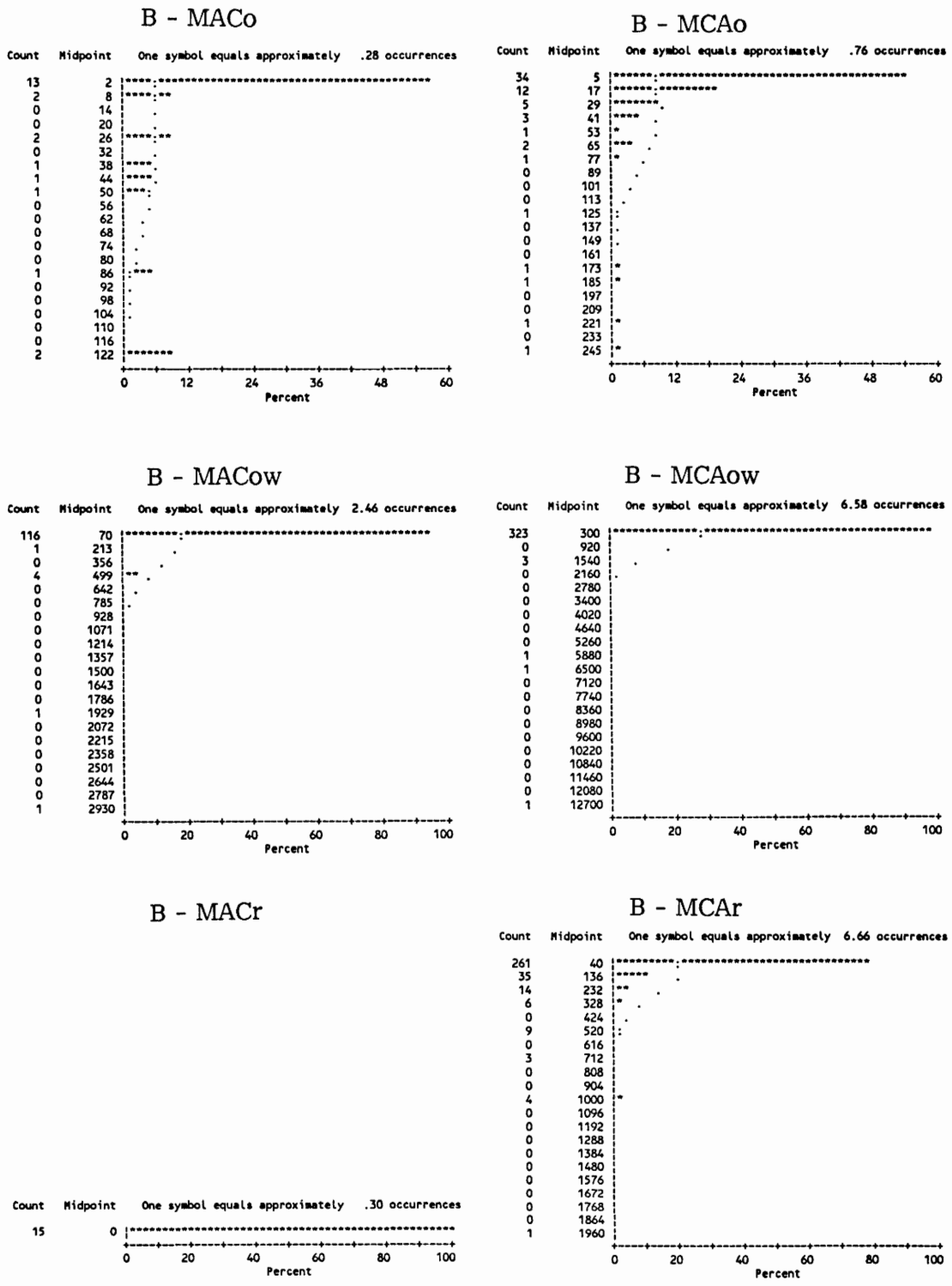

Figure I-7. Histograms of boron concentrations in ppm (MAC=alkali-calcic, MCA=calc-alkalic, o=oxidized, ow=weakly oxidized, r=reduced).

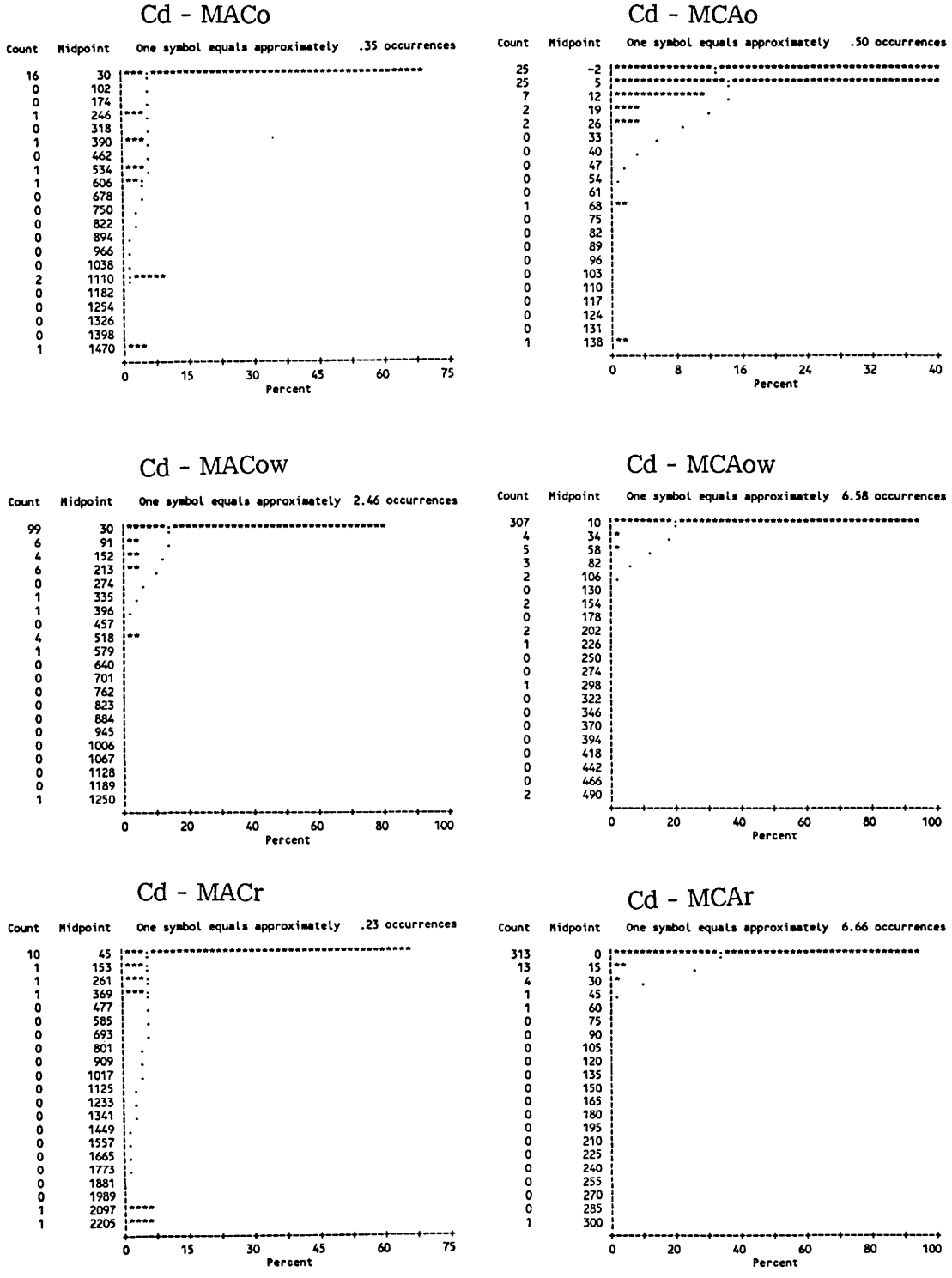

Figure I-8. Histograms of cadmium concentrations in ppm (MAC=alkali-calcic, MCA=calc-alkalic, o=oxidized, ow=weakly oxidized, r=reduced).

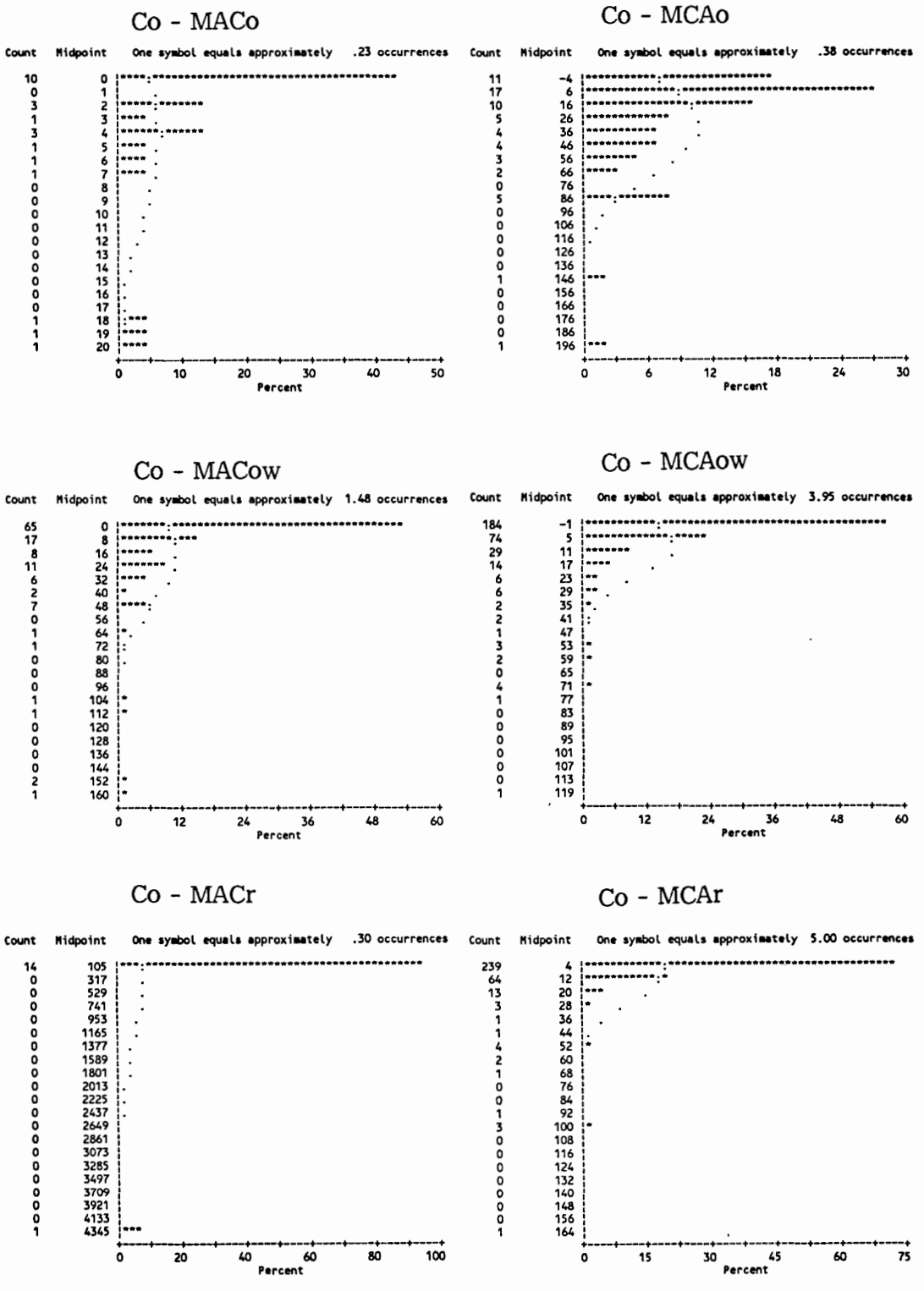

Figure I-9. Histograms of cobalt concentrations in ppm (MAC=alkali-calcic, MCA=calc-alkalic, o=oxidized, ow=weakly oxidized, r=reduced).

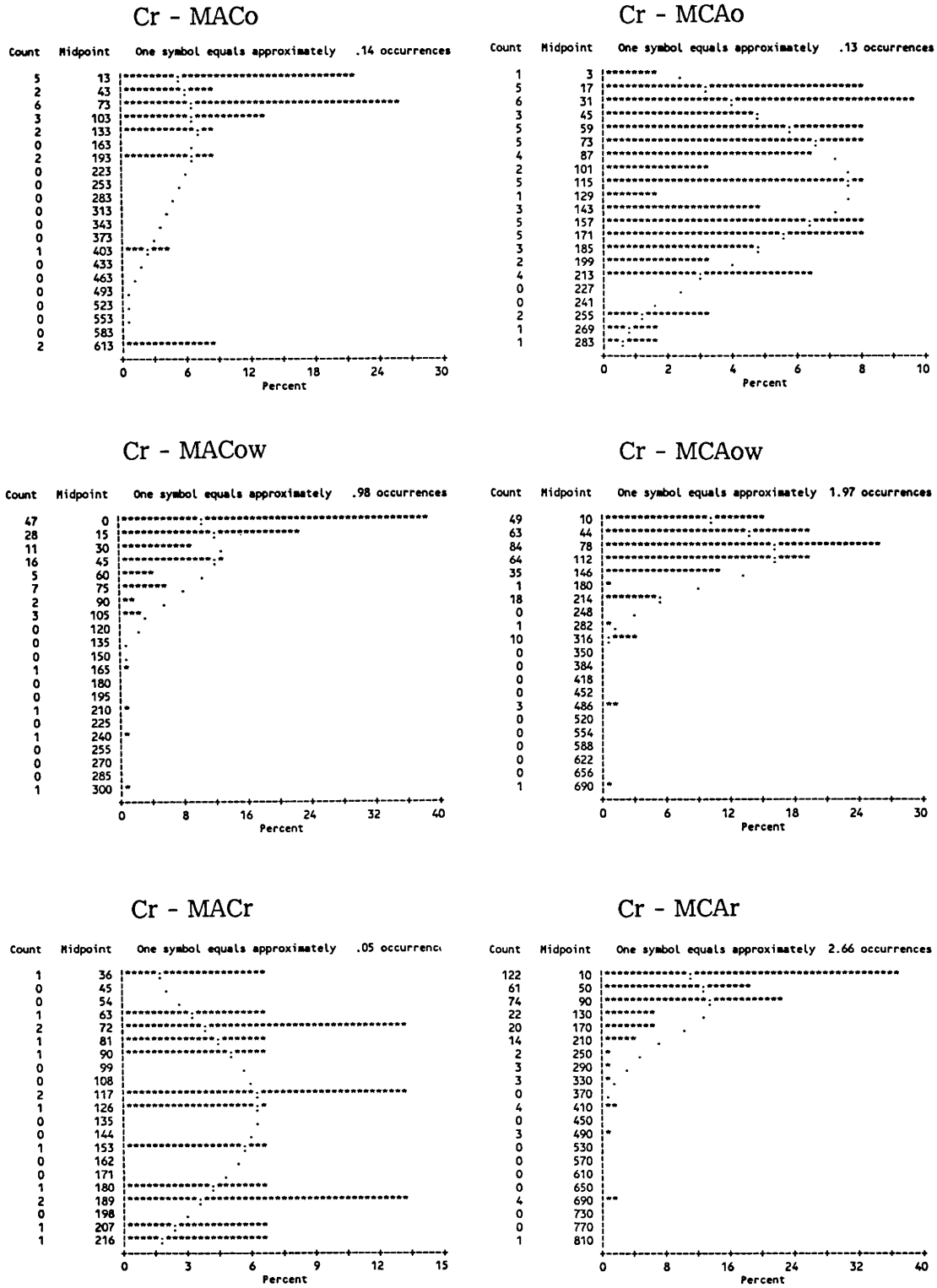

Figure I-10. Histograms of chromium concentrations in ppm (MAC=alkali-calcic, MCA=calc-alkalic, o=oxidized, ow=weakly oxidized, r=reduced).

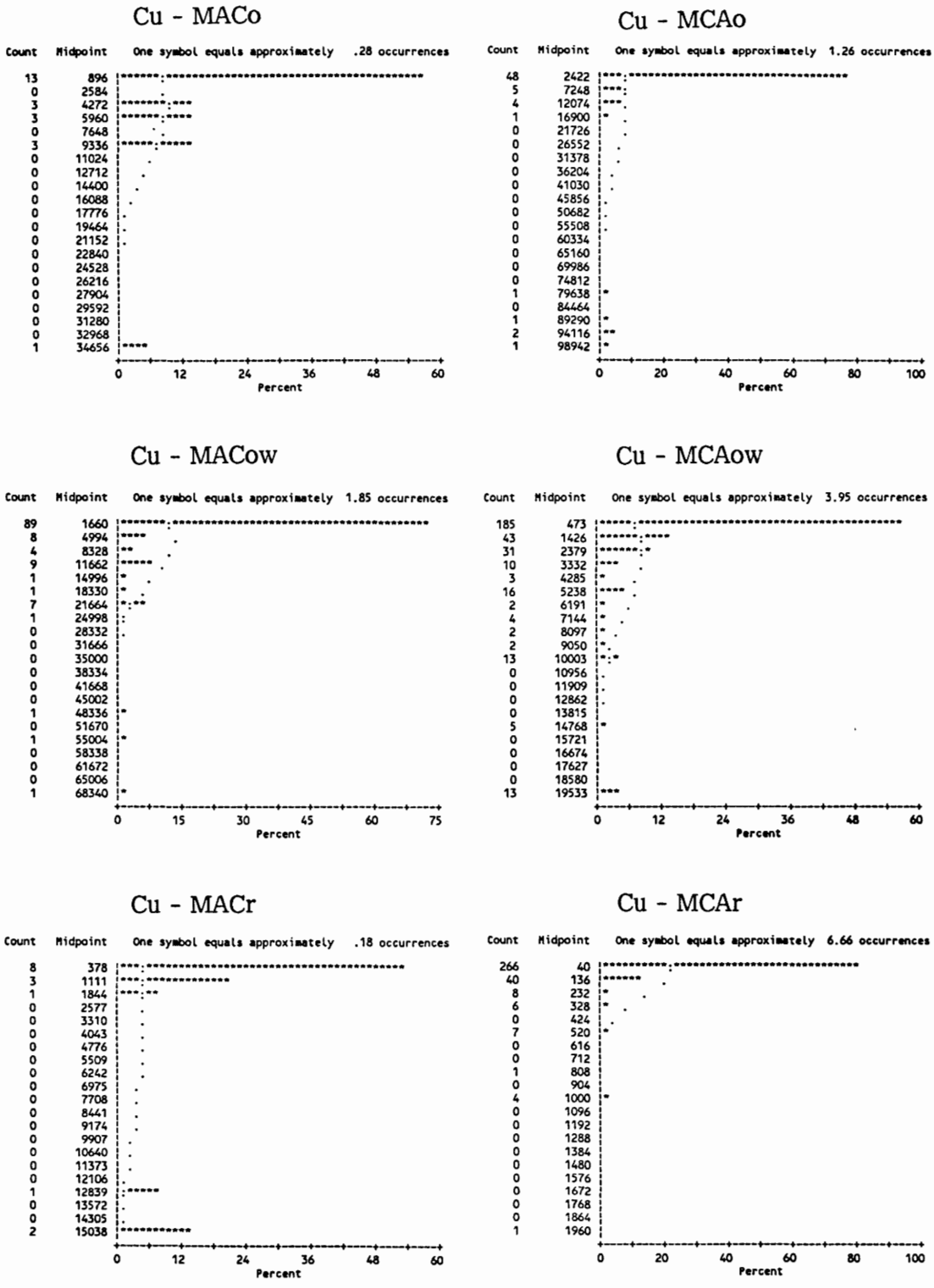

Figure I-11. Histograms of copper concentrations in ppm (MAC=alkali-calcic, MCA=calc-alkalic, o=oxidized, ow=weakly oxidized, r=reduced).

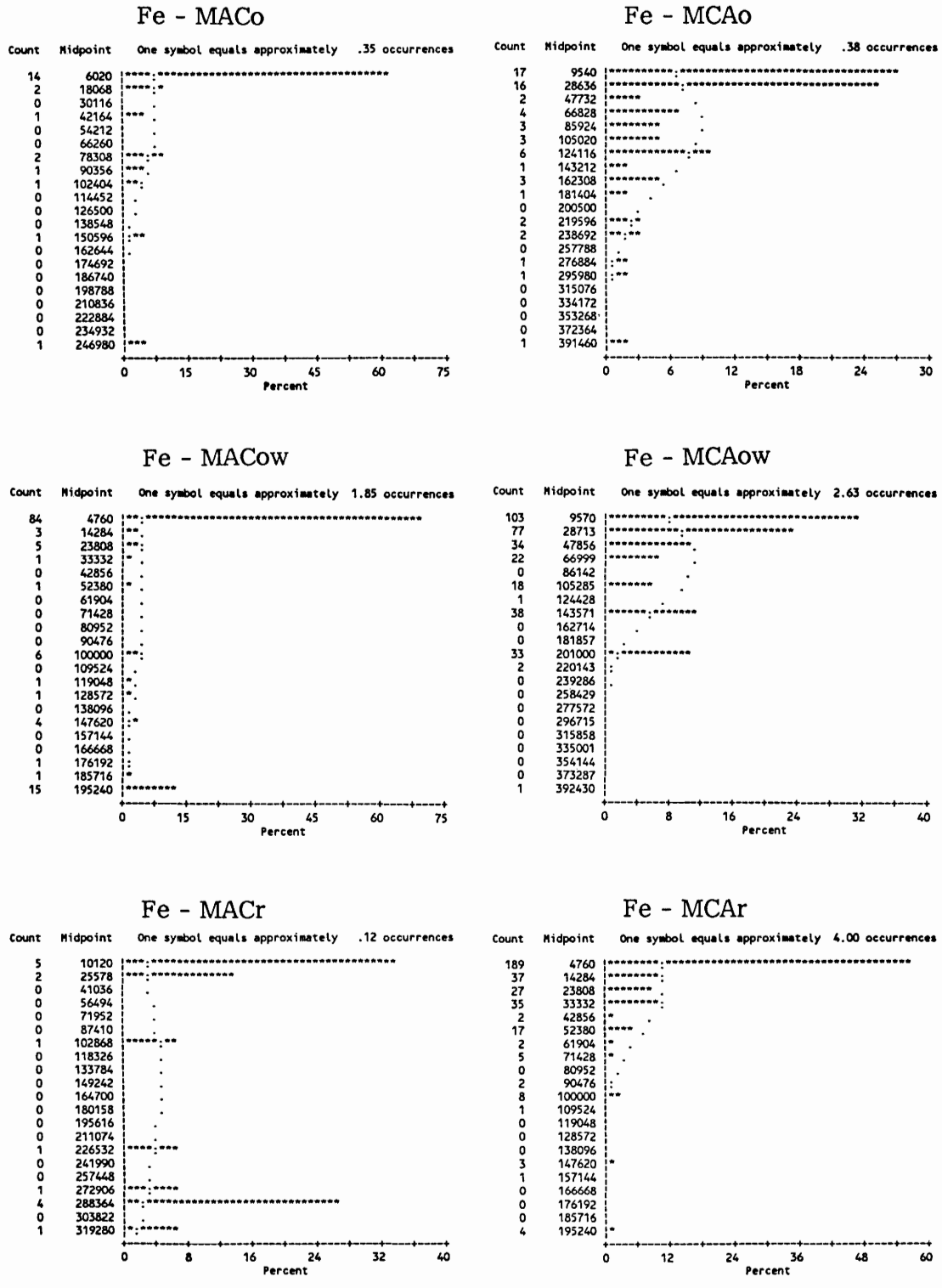

Figure I-12. Histograms of iron concentrations in ppm (MAC=alkali-calcic, MCA=calc-alkalic, o=oxidized, ow=weakly oxidized, r=reduced).

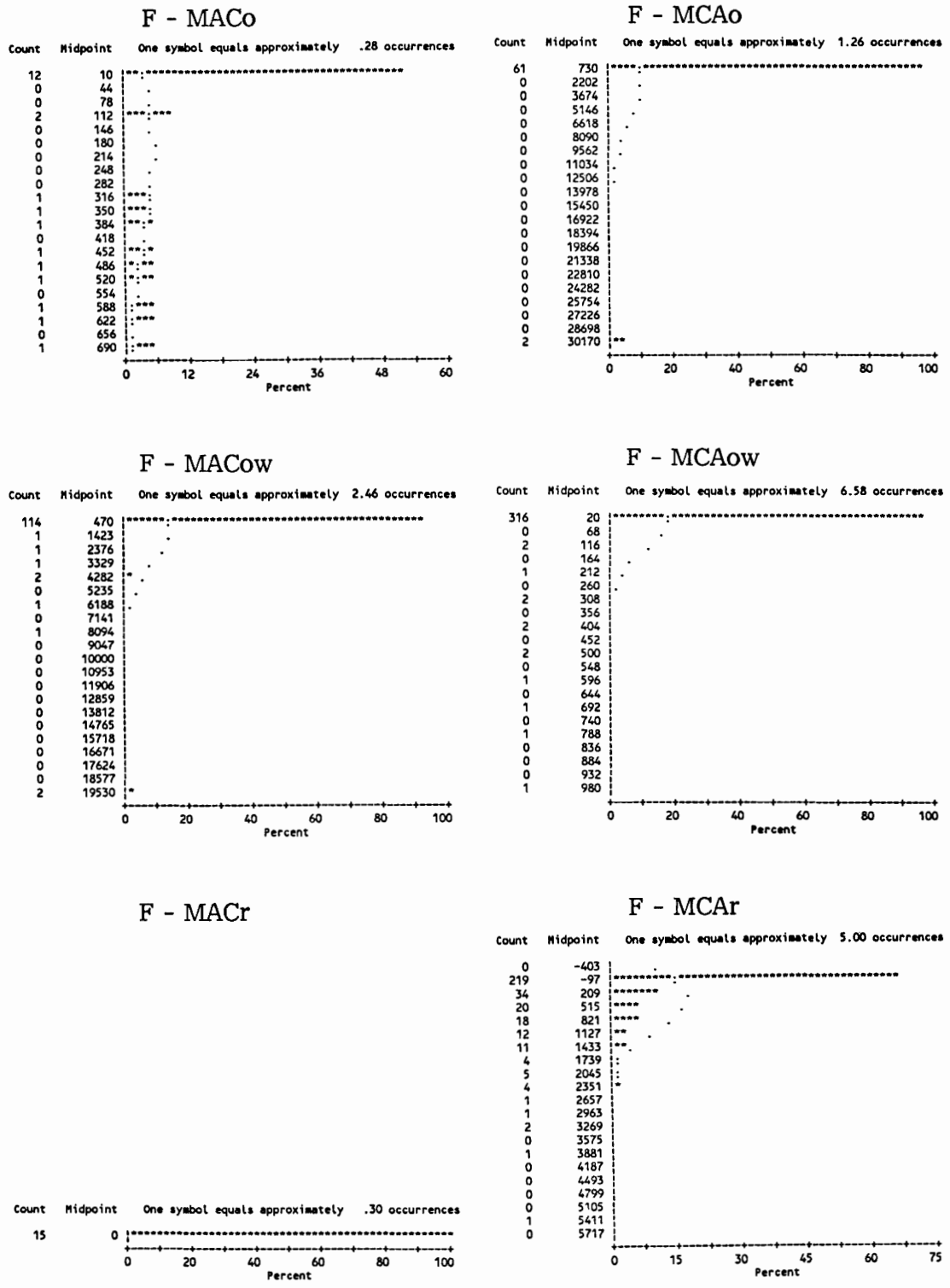

Figure I-13. Histograms of fluorine concentrations in ppm (MAC=alkali-calcic, MCA=calc-alkalic, o=oxidized, ow=weakly oxidized, r=reduced).

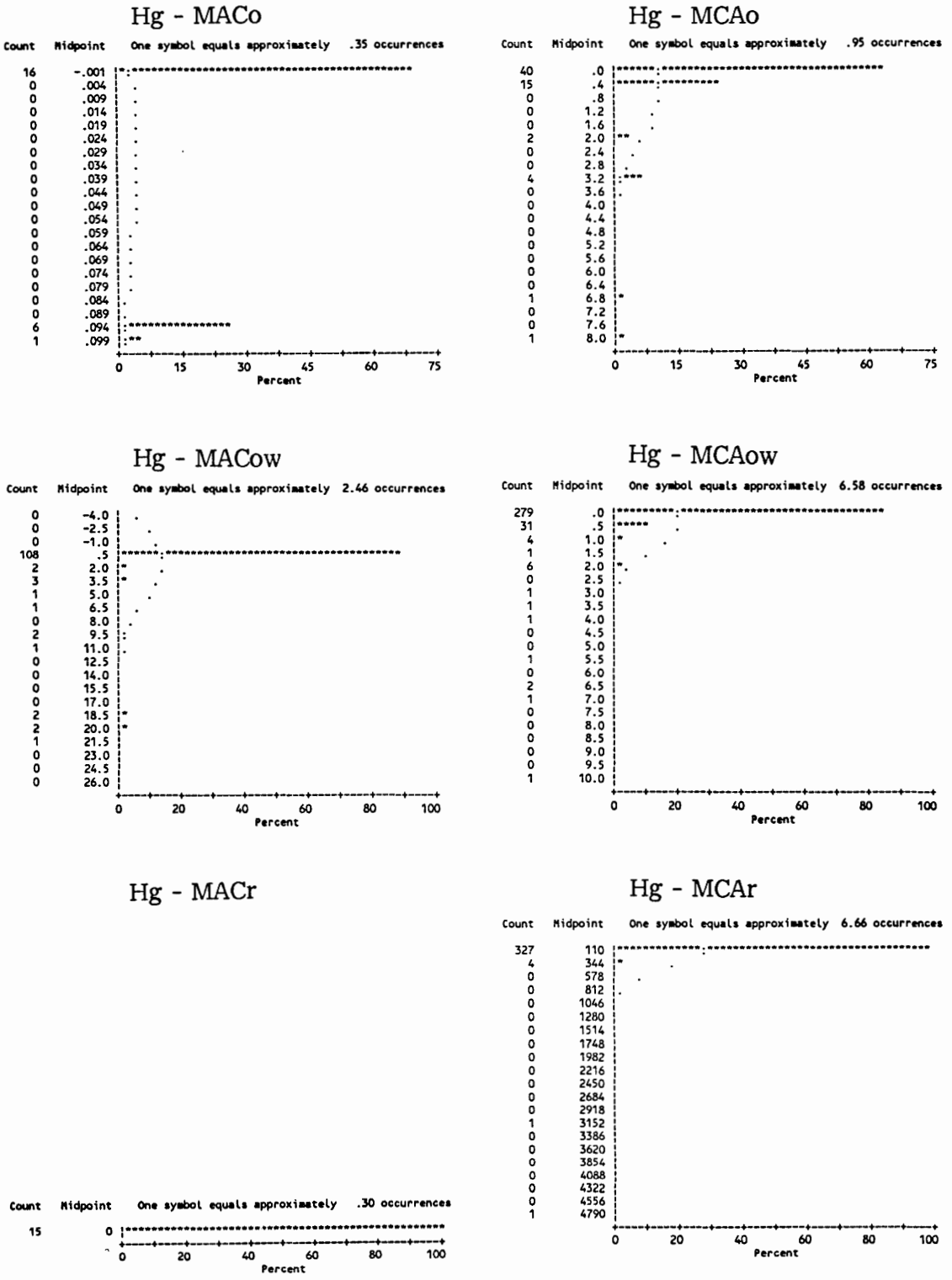

Figure I-14. Histograms of mercury concentrations in ppm (MAC=alkali-calcic, MCA=calc-alkalic, o=oxidized, ow=weakly oxidized, r=reduced).

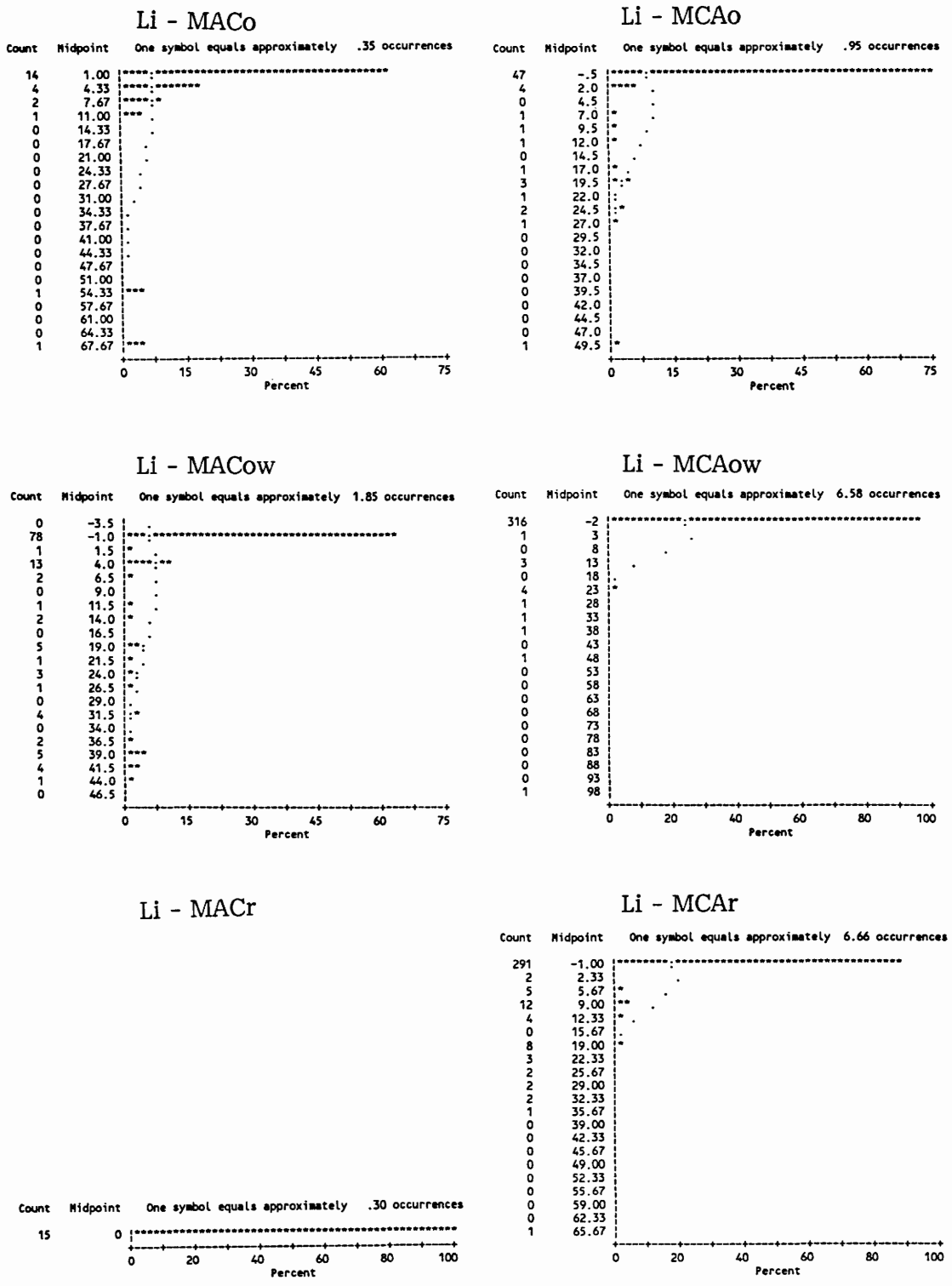

Figure I-15. Histograms of lithium concentrations in ppm (MAC=alkali-calcic, MCA=calc-alkalic, o=oxidized, ow=weakly oxidized, r=reduced).

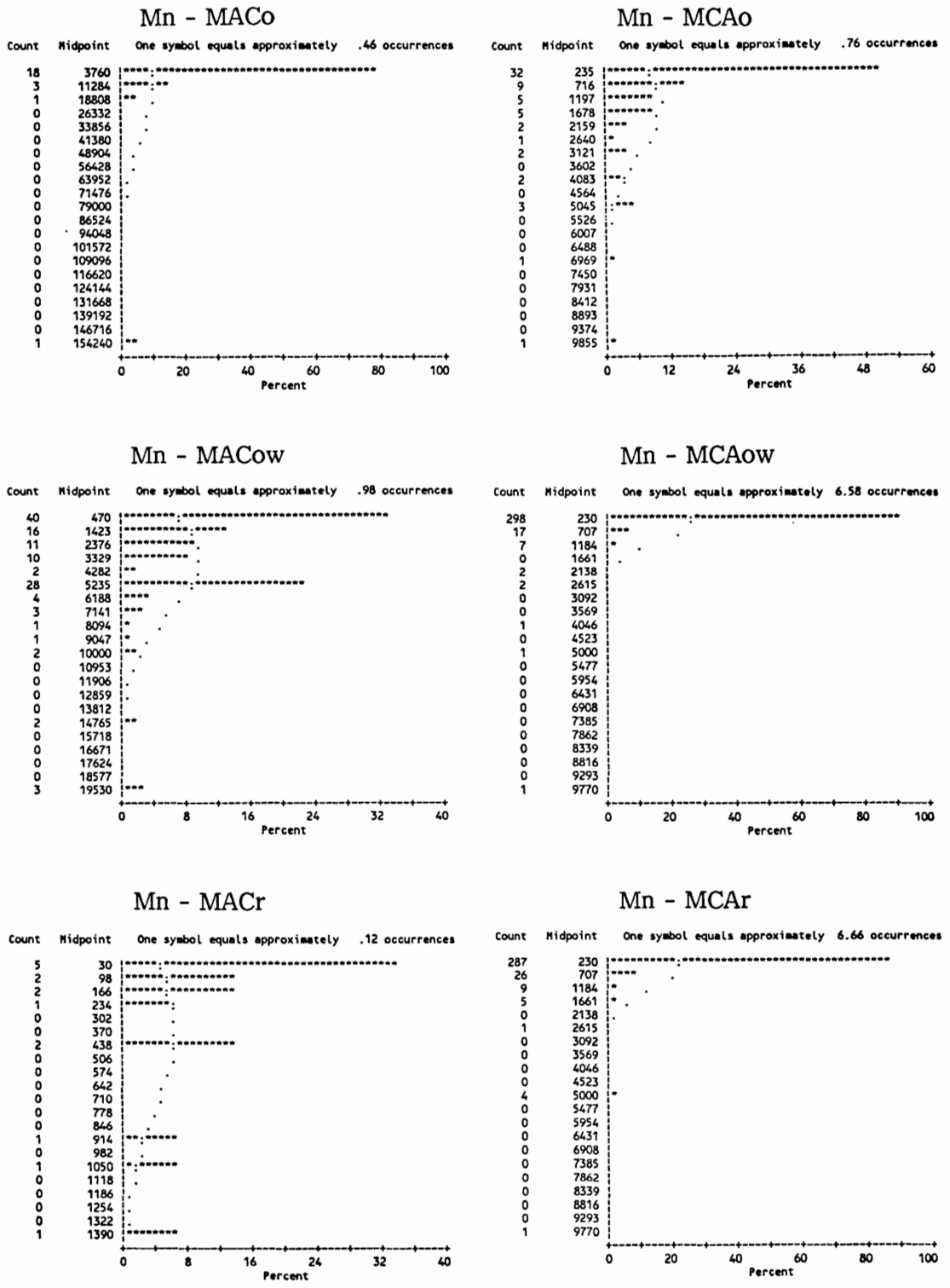

Figure I-16. Histograms of manganese concentrations in ppm (MAC=alkali-calcic, MCA=calc-alkalic, o=oxidized, ow=weakly oxidized, r=reduced).

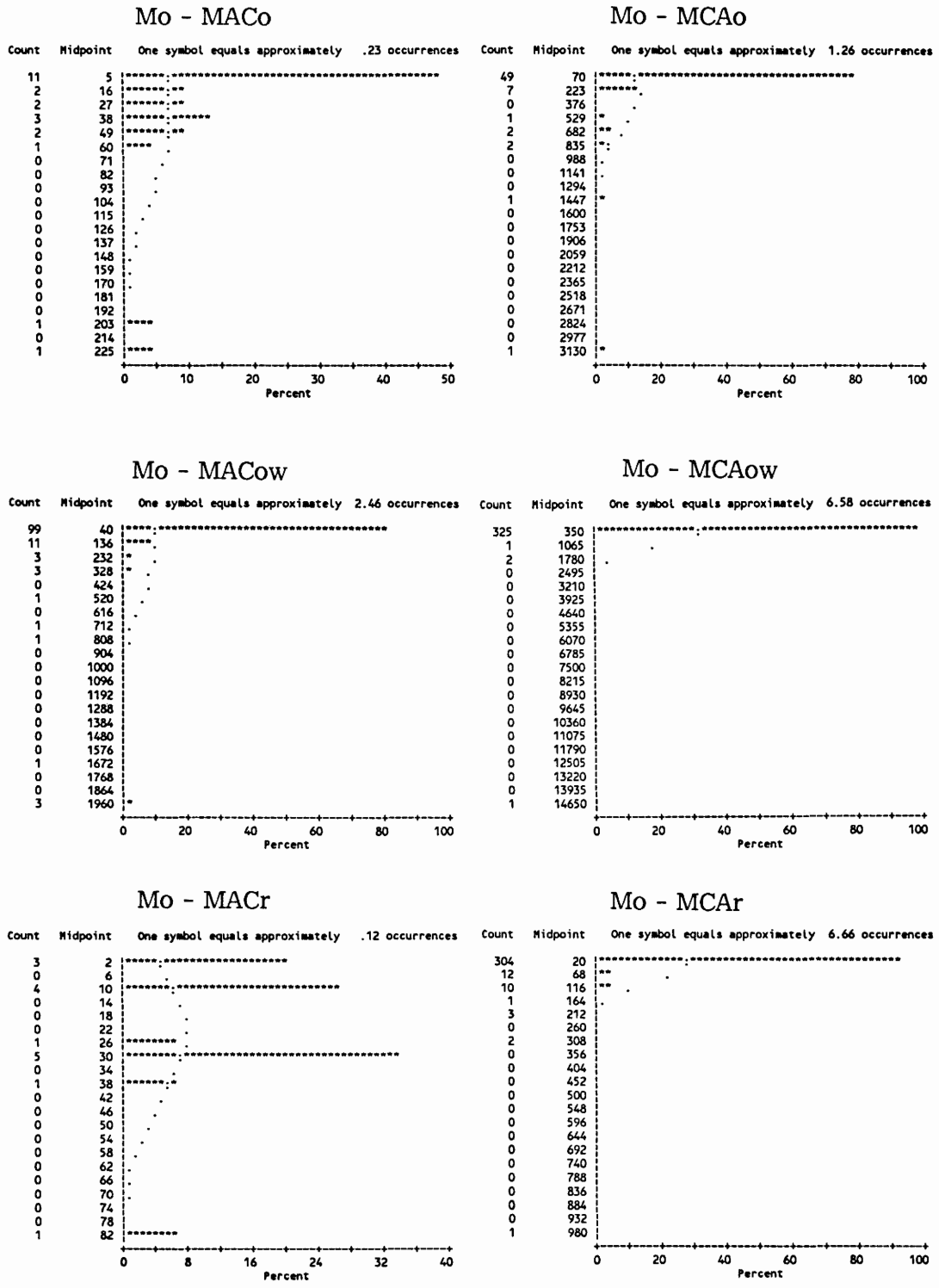

Figure I-17. Histograms of molybdenum concentrations in ppm (MAC=alkali-calcic, MCA=calc-alkalic, o=oxidized, ow=weakly oxidized, r=reduced).

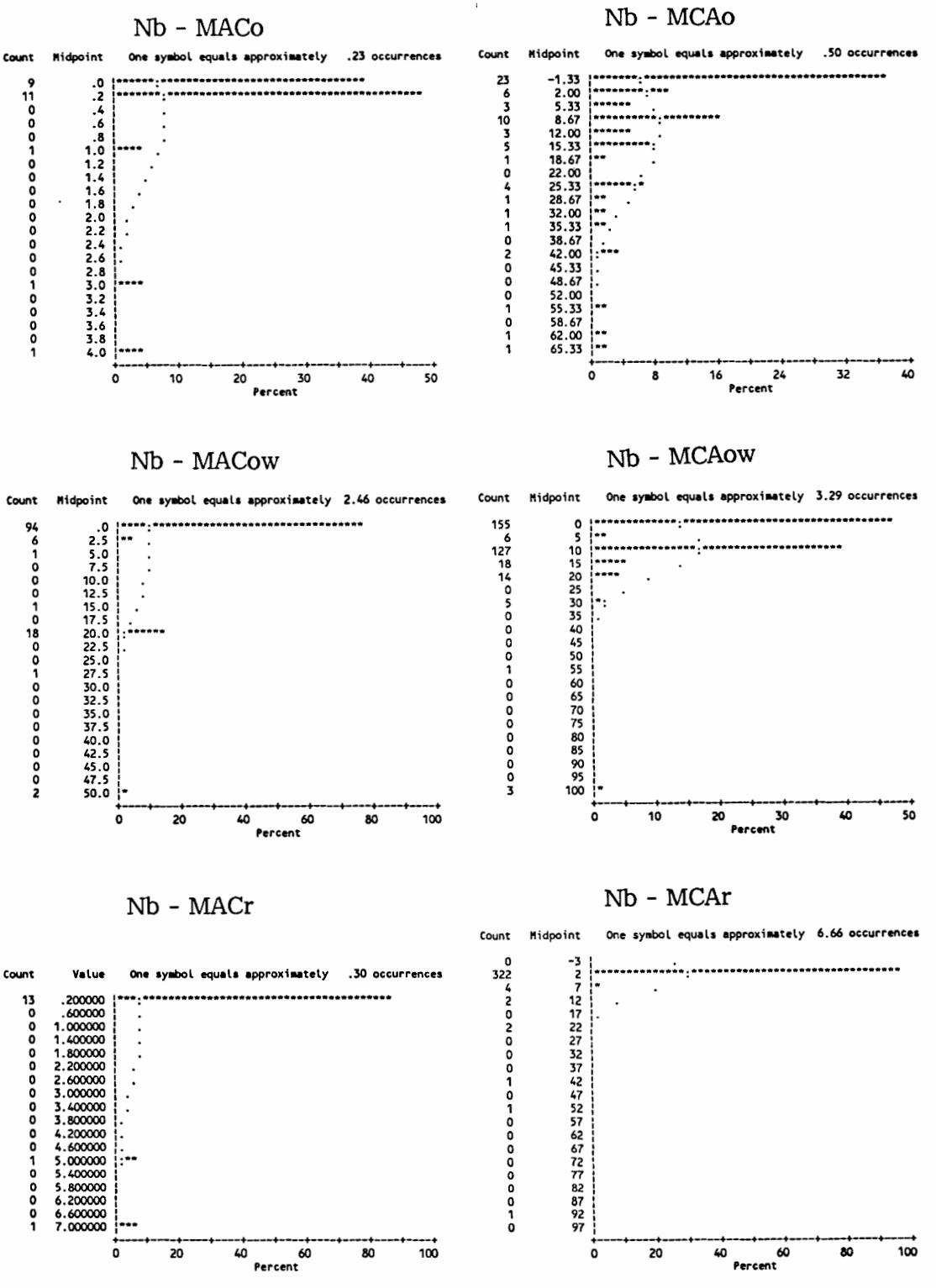

Figure I-18. Histograms of niobium concentrations in ppm (MAC=alkali-calcic, MCA=calc-alkalic, o=oxidized, ow=weakly oxidized, r=reduced).

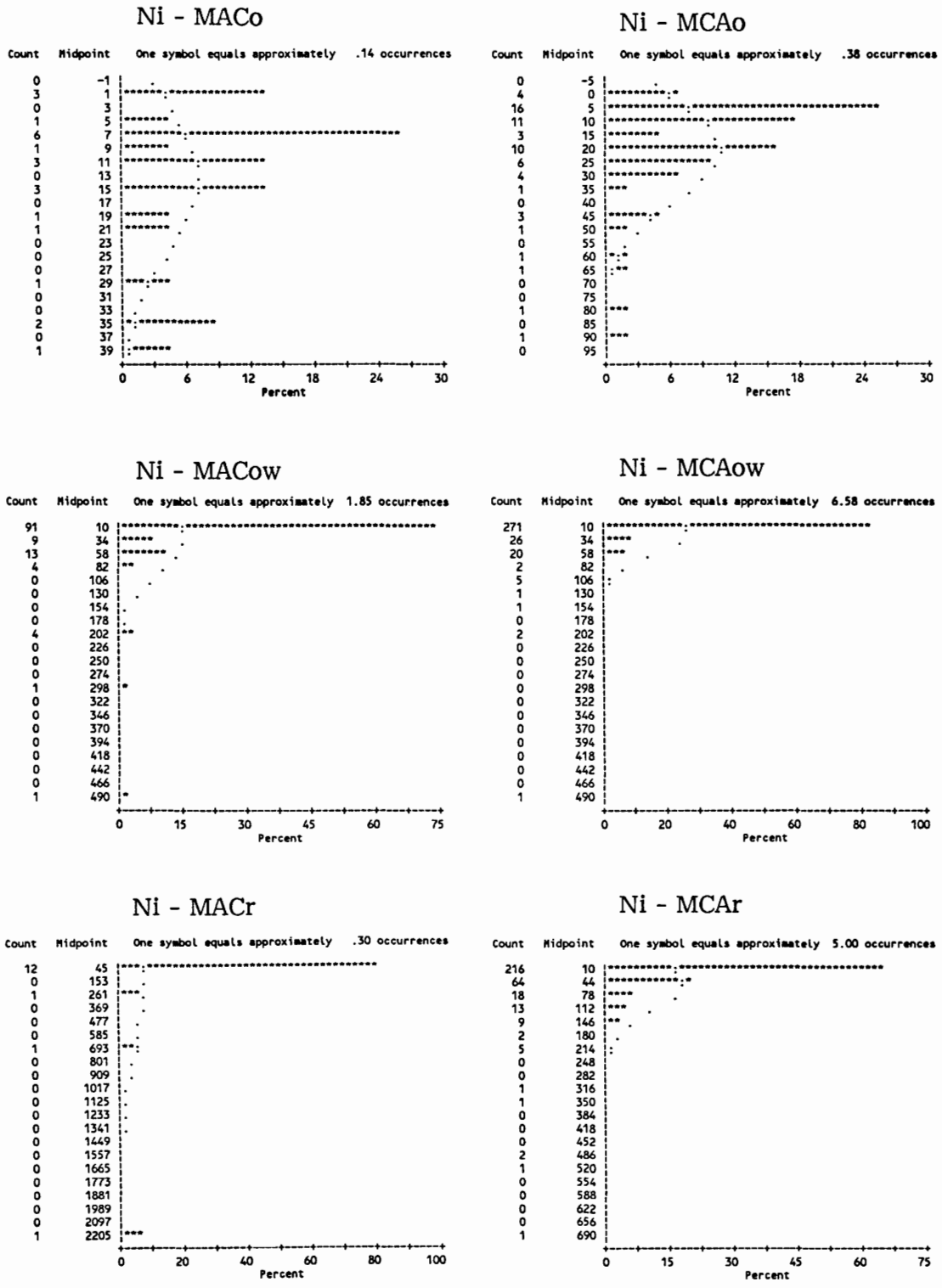

Figure I-19. Histograms of nickel concentrations in ppm (MAC=alkali-calcic, MCA=calc-alkalic, o=oxidized, ow=weakly oxidized, r=reduced).

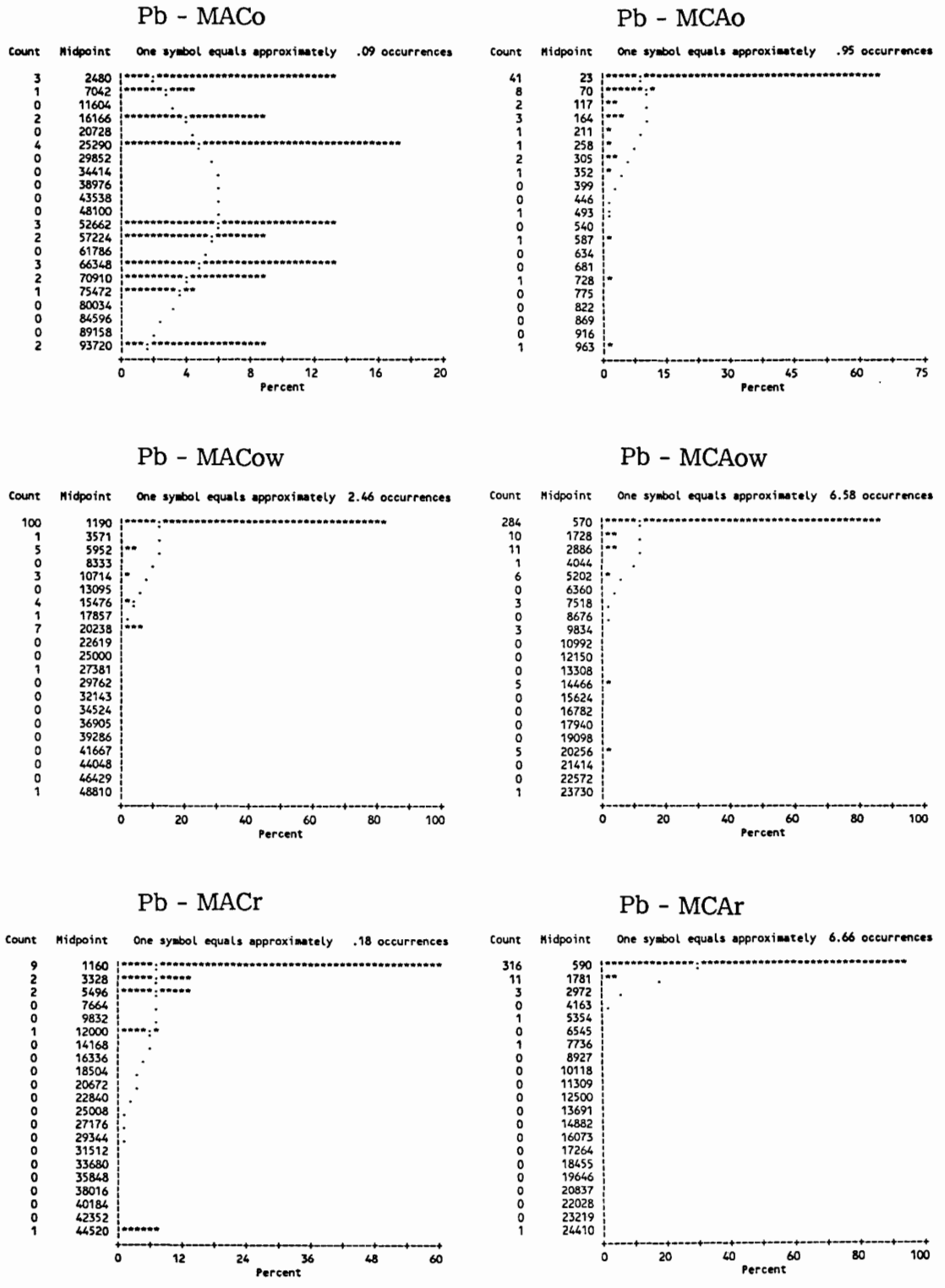

Figure I-20. Histograms of lead concentrations in ppm (MAC=alkali-calcic, MCA=calc-alkalic, o=oxidized, ow=weakly oxidized, r=reduced).

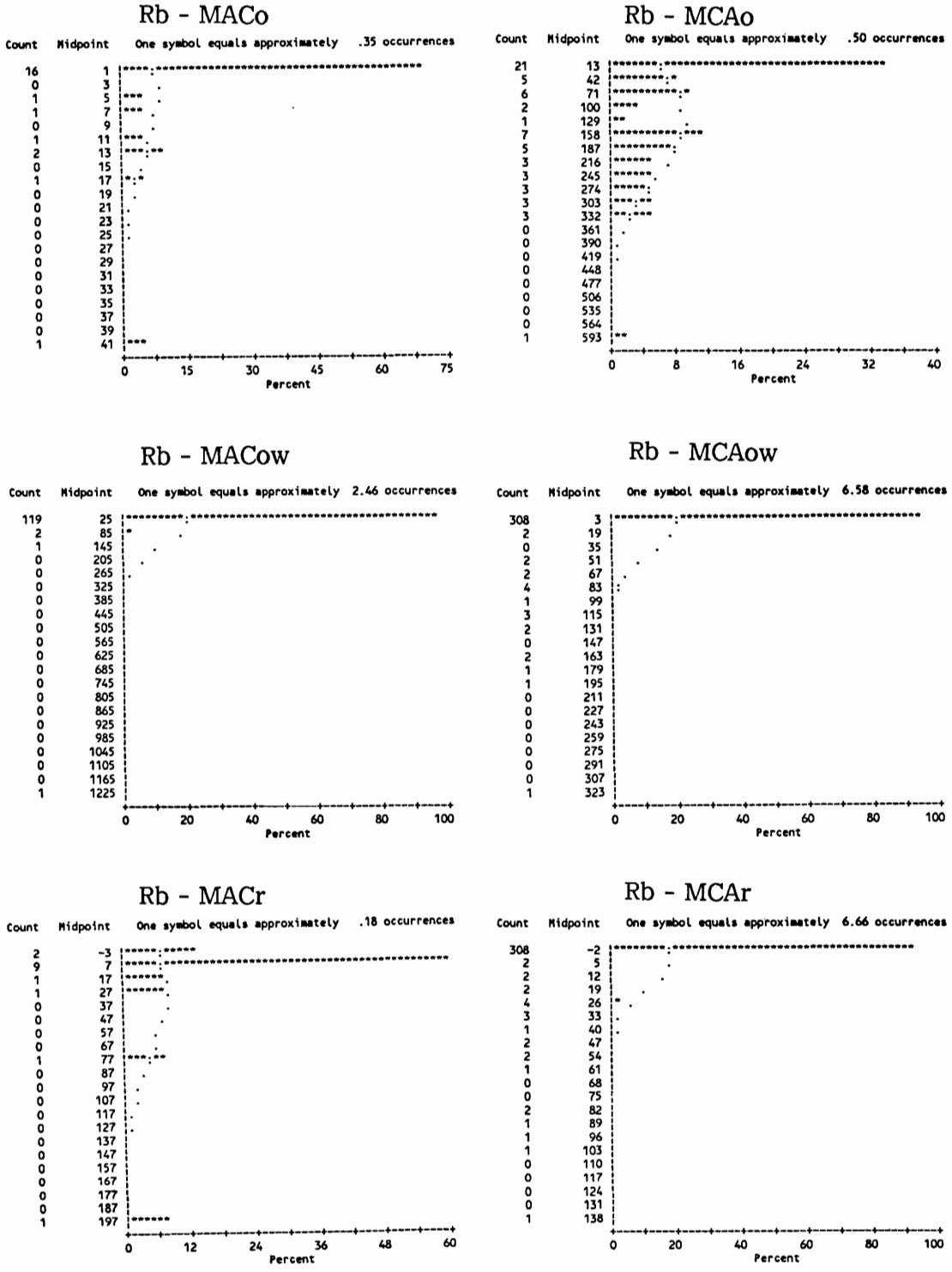

Figure I-21. Histograms of rubidium concentrations in ppm (MAC=alkali-calcic, MCA=calc-alkalic, o=oxidized, ow=weakly oxidized, r=reduced).

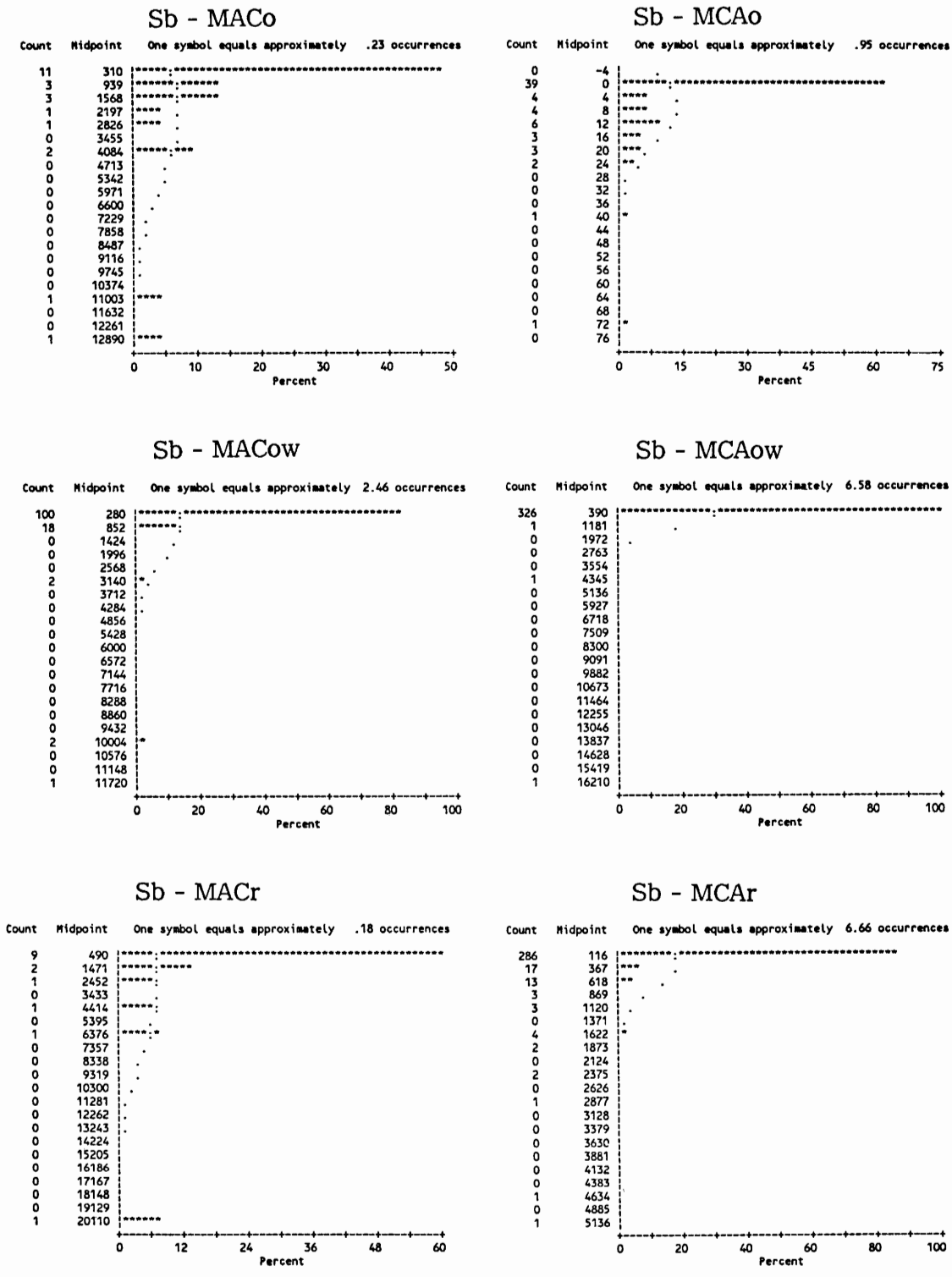

Figure I-22. Histograms of antimony concentrations in ppm (MAC=alkali-calcic, MCA=calc-alkalic, o=oxidized, ow=weakly oxidized, r=reduced).

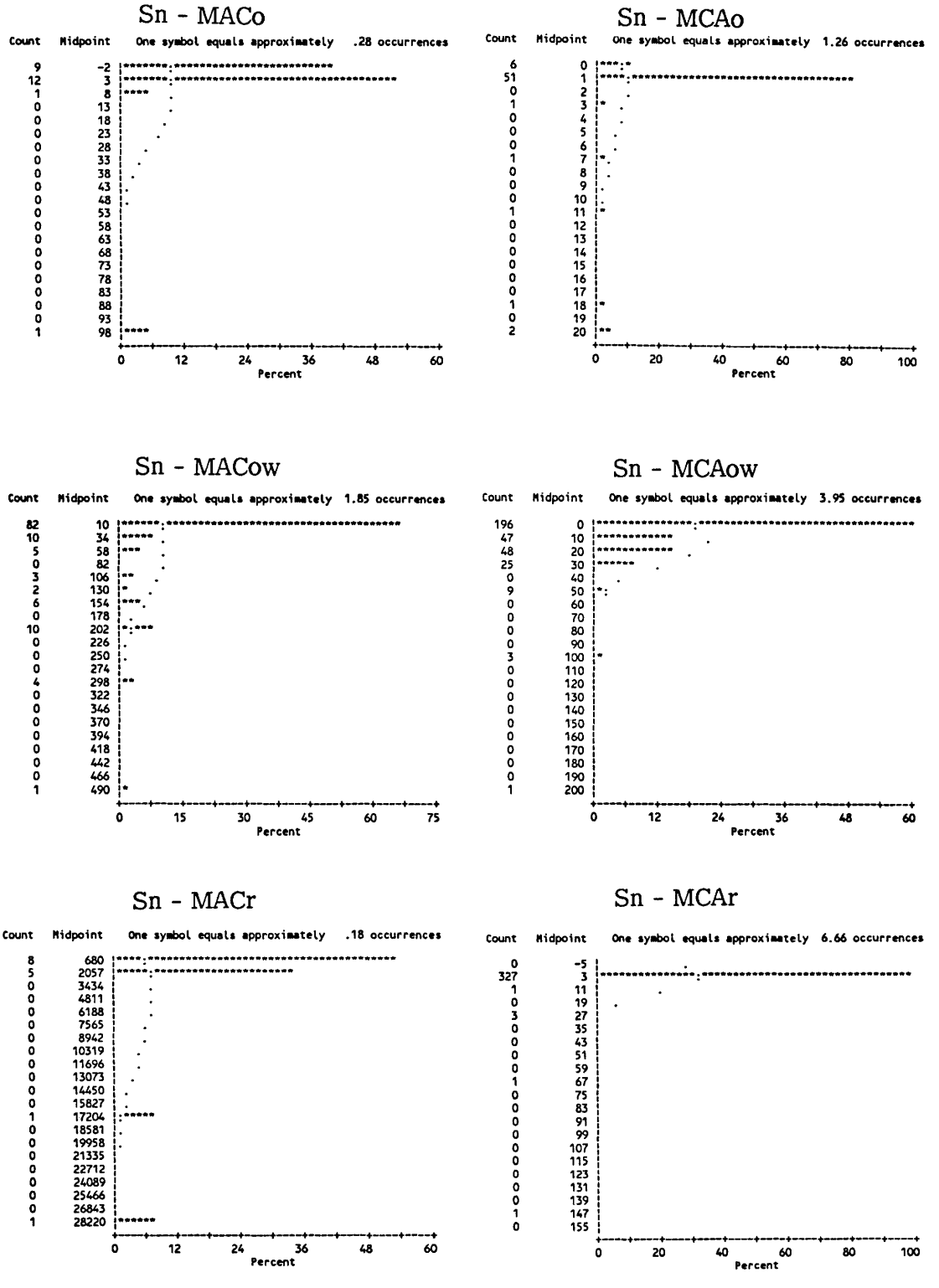

Figure I-23. Histograms of tin concentrations in ppm (MAC=alkali-calcic, MCA=calc-alkalic, o=oxidized, ow=weakly oxidized, r=reduced).

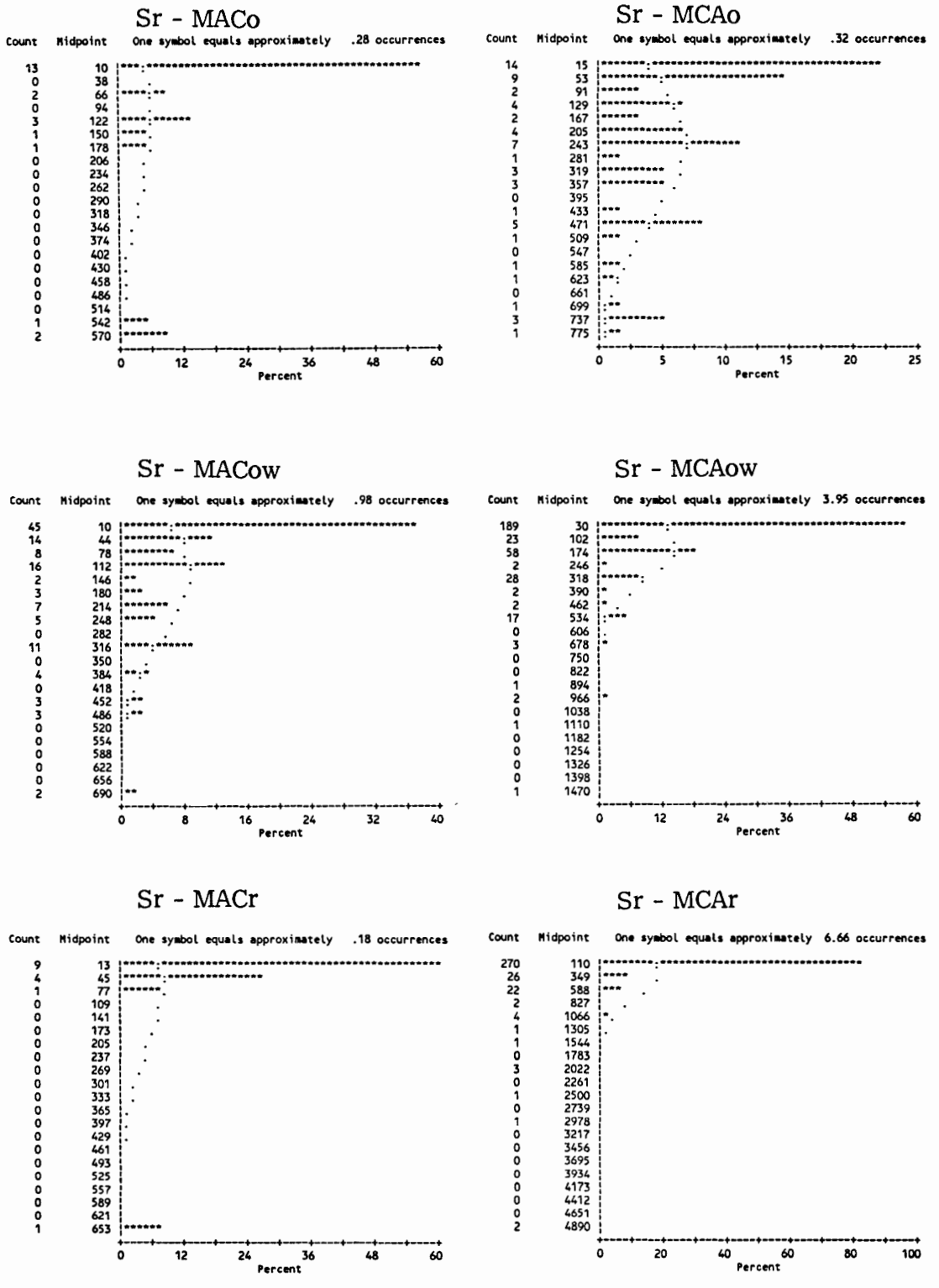

Figure I-24. Histograms of strontium concentrations in ppm (MAC=alkali-calcic, MCA=calc-alkalic, o=oxidized, ow=weakly oxidized, r=reduced).

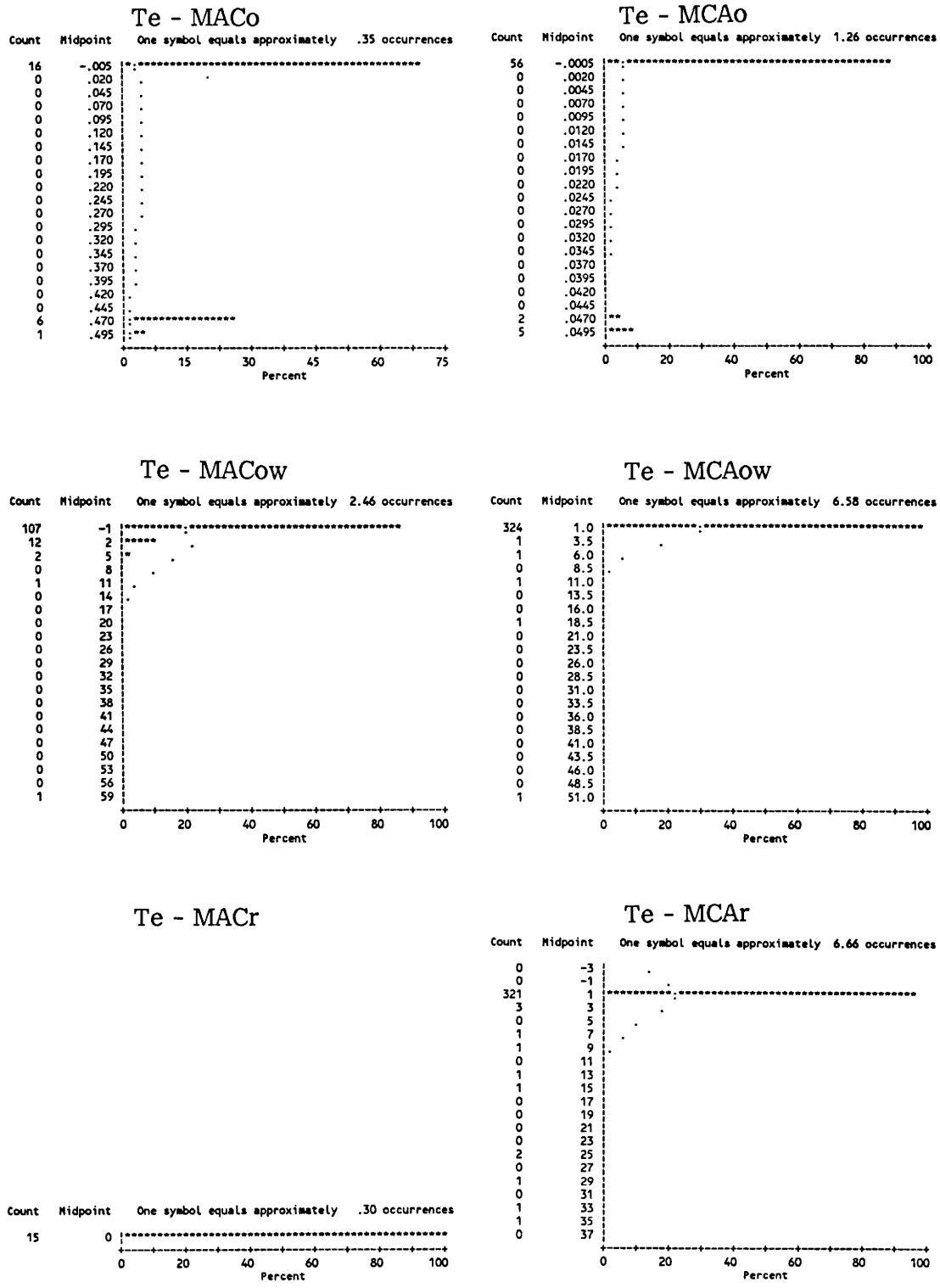

Figure I-25. Histograms of tellurium concentrations in ppm (MAC=alkali-calcic, MCA=calc-alkalic, o=oxidized, ow=weakly oxidized, r=reduced).

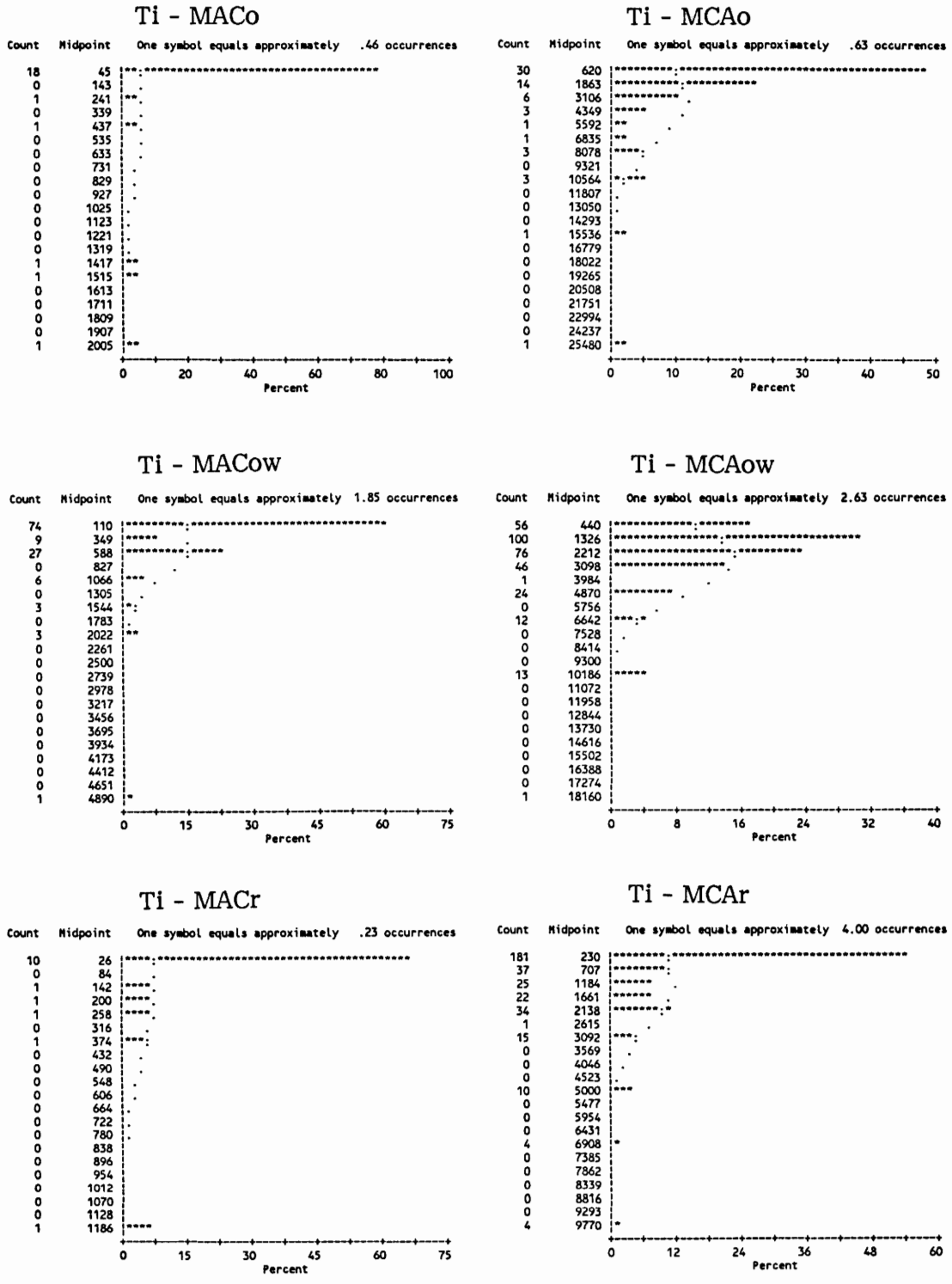

Figure I-26. Histograms of titanium concentrations in ppm (MAC=alkali-calcic, MCA=calc-alkalic, o=oxidized, ow=weakly oxidized, r=reduced).

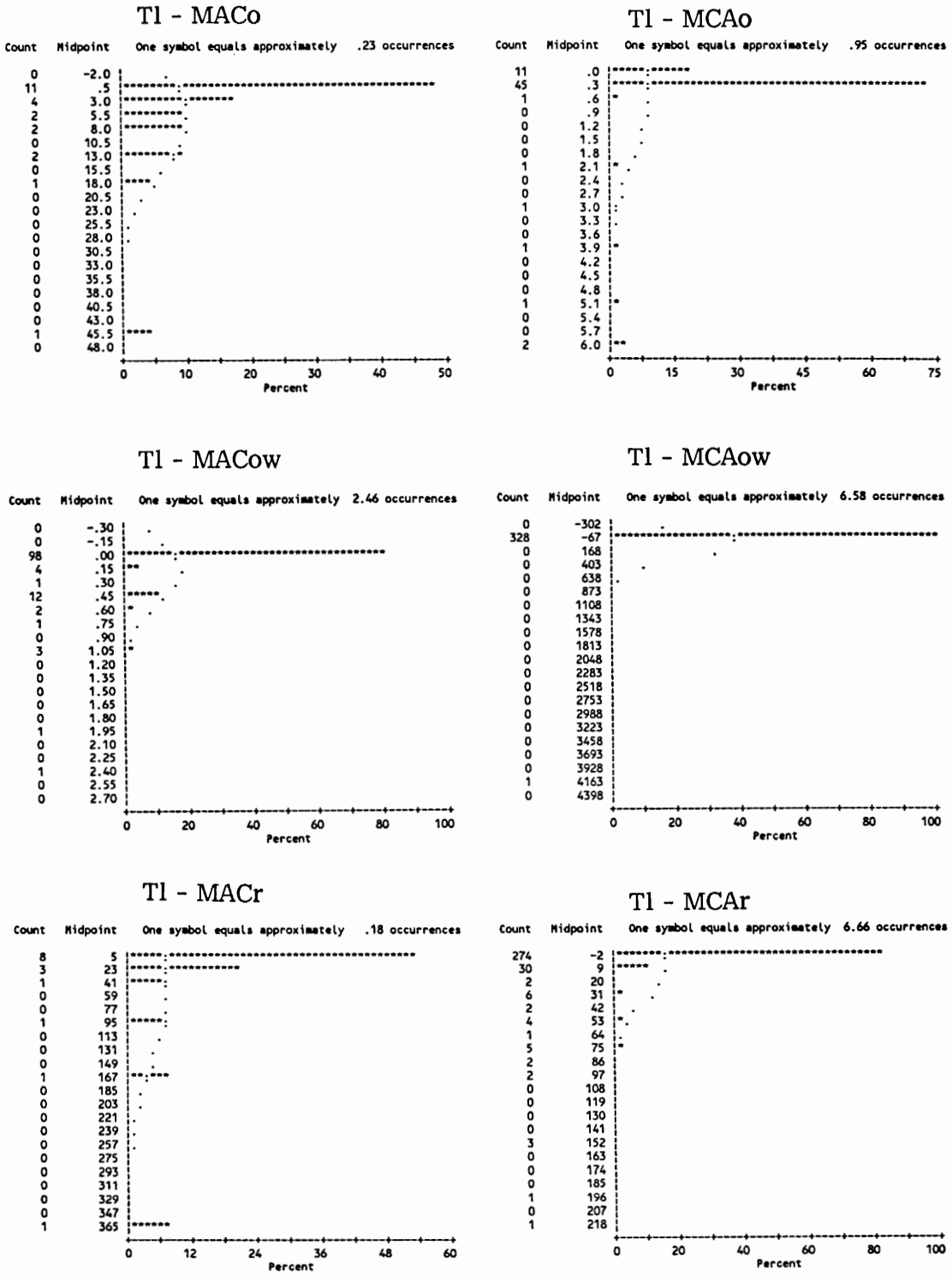

Figure I-27. Histograms of thallium concentrations in ppm (MAC=alkali-calcic, MCA=calc-alkalic, o=oxidized, ow=weakly oxidized, r=reduced).

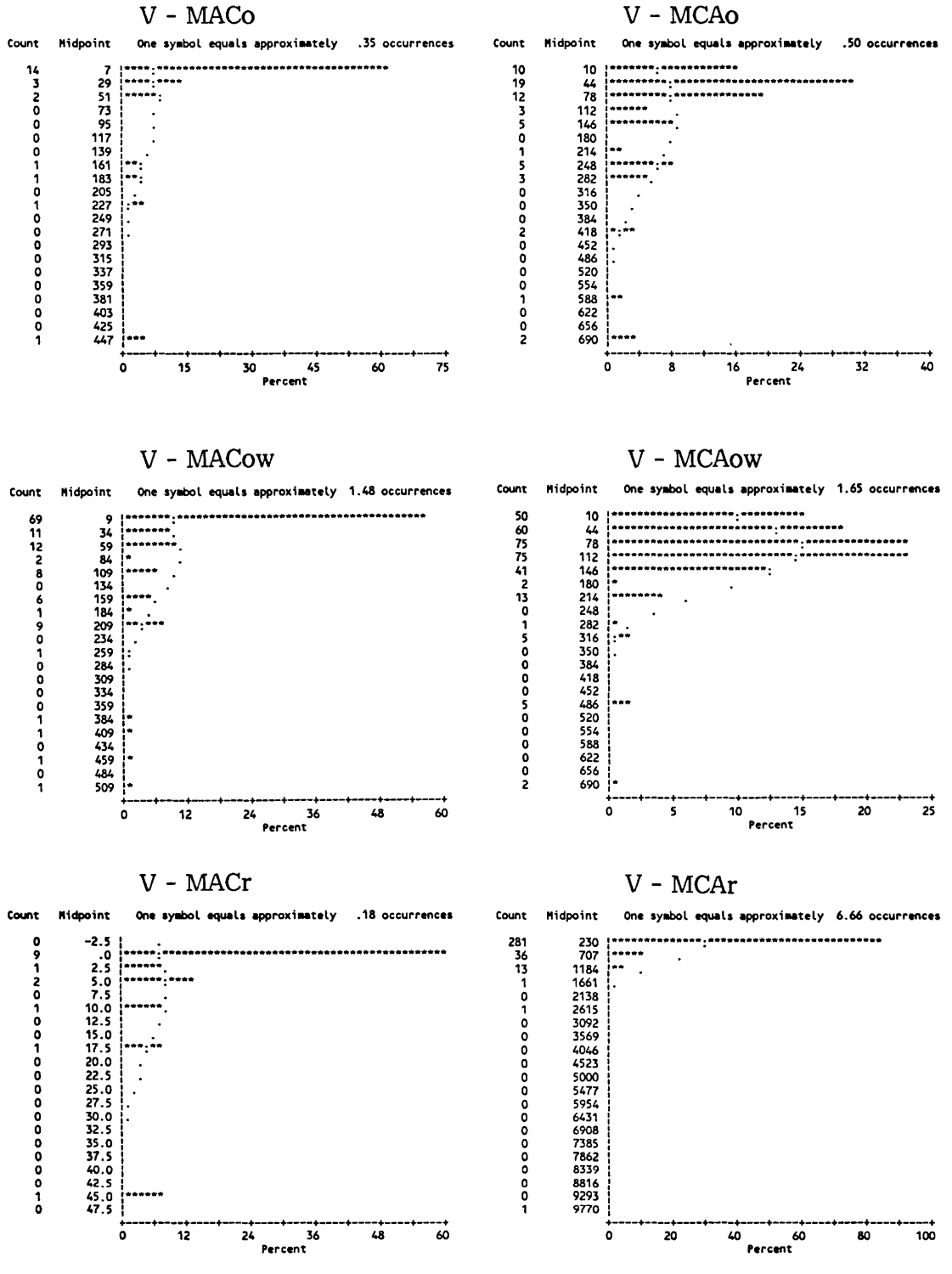

Figure I-28. Histograms of vanadium concentrations in ppm (MAC=alkali-calcic, MCA=calc-alkalic, o=oxidized, ow=weakly oxidized, r=reduced).

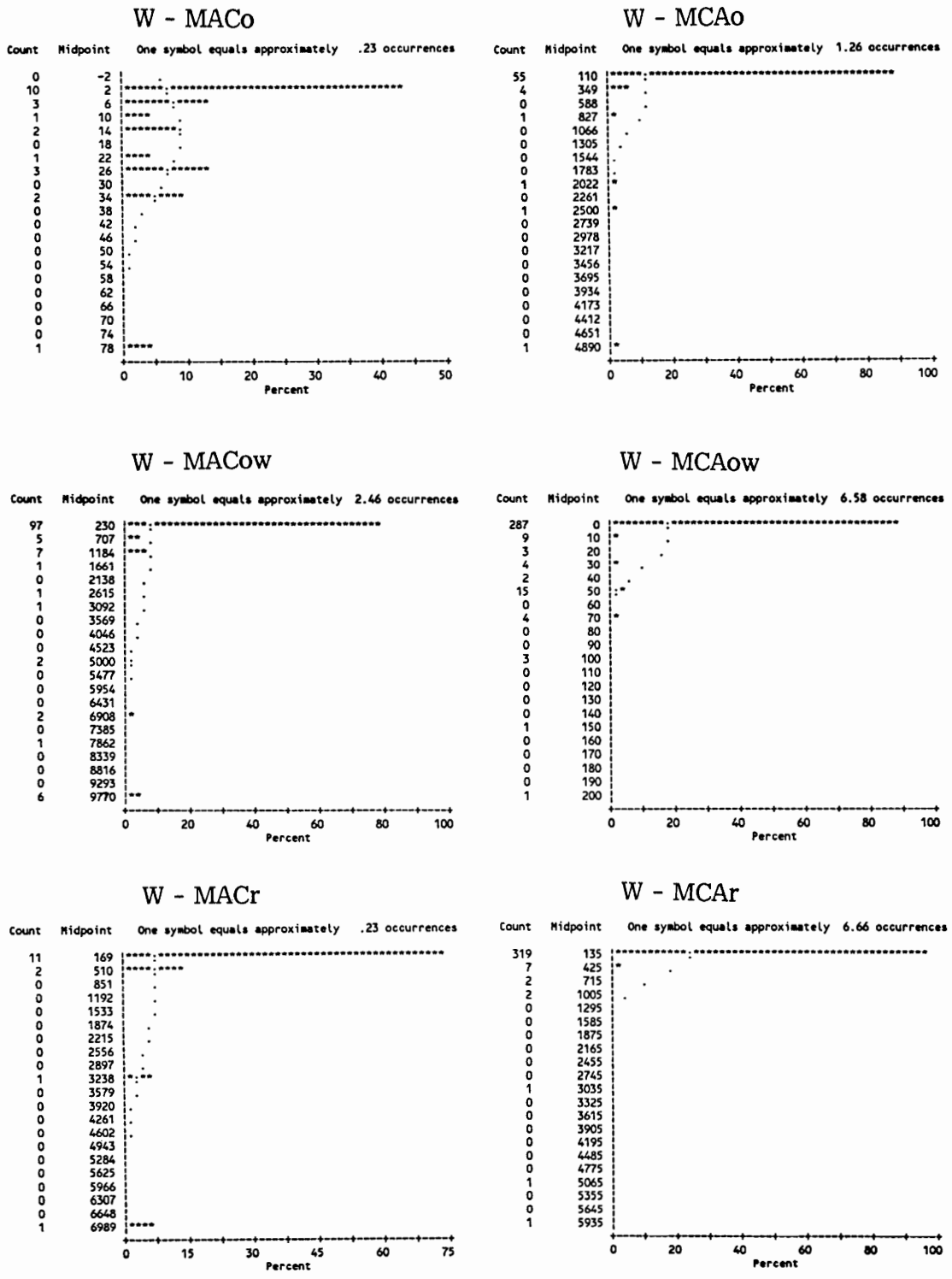

Figure I-29. Histograms of tungsten concentrations in ppm (MAC=alkali-calcic, MCA=calc-alkalic, o=oxidized, ow=weakly oxidized, r=reduced).

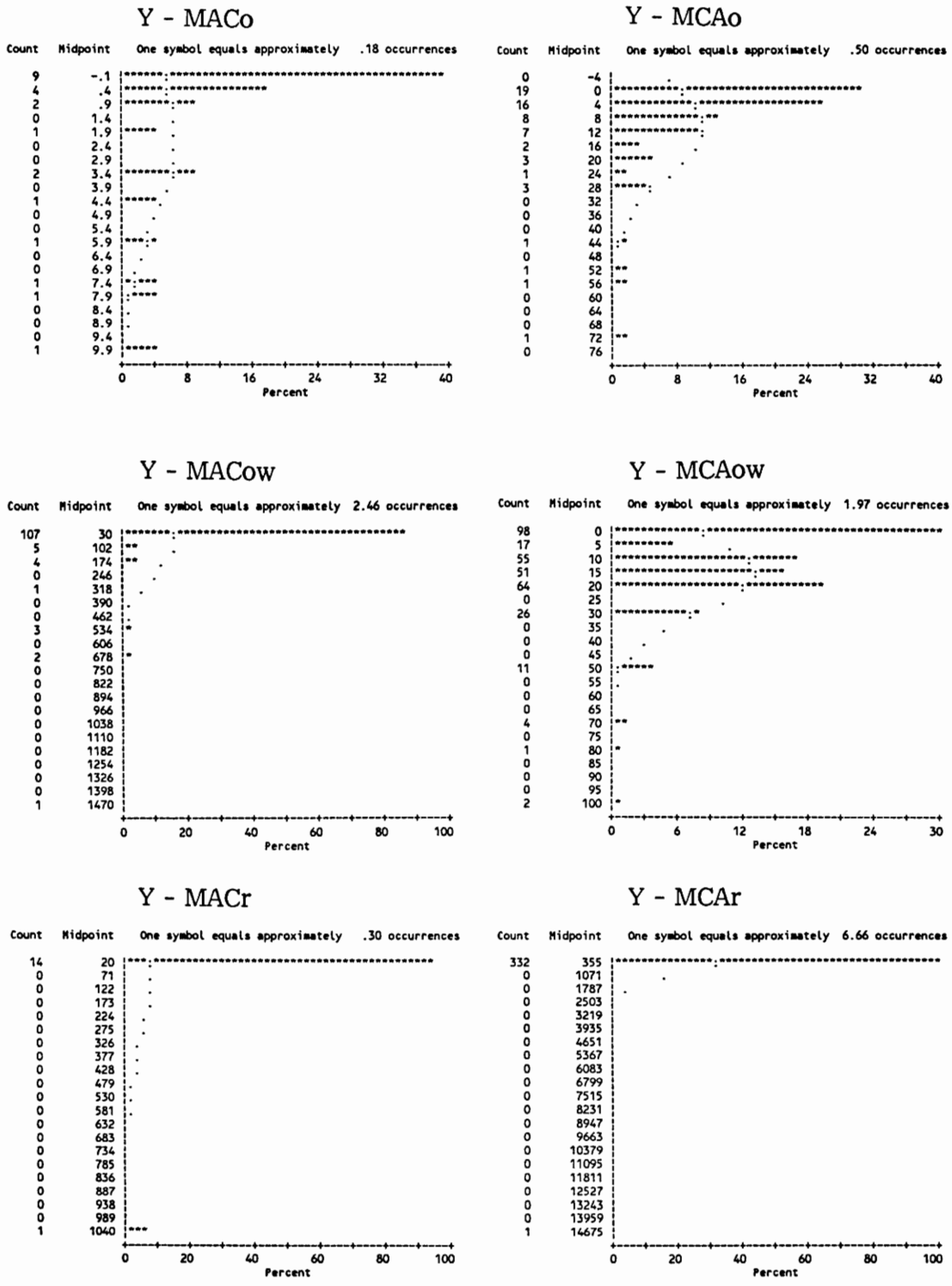

Figure I-30. Histograms of yttrium concentrations in ppm (MAC=alkali-calcic, MCA=calc-alkalic, o=oxidized, ow=weakly oxidized, r=reduced).

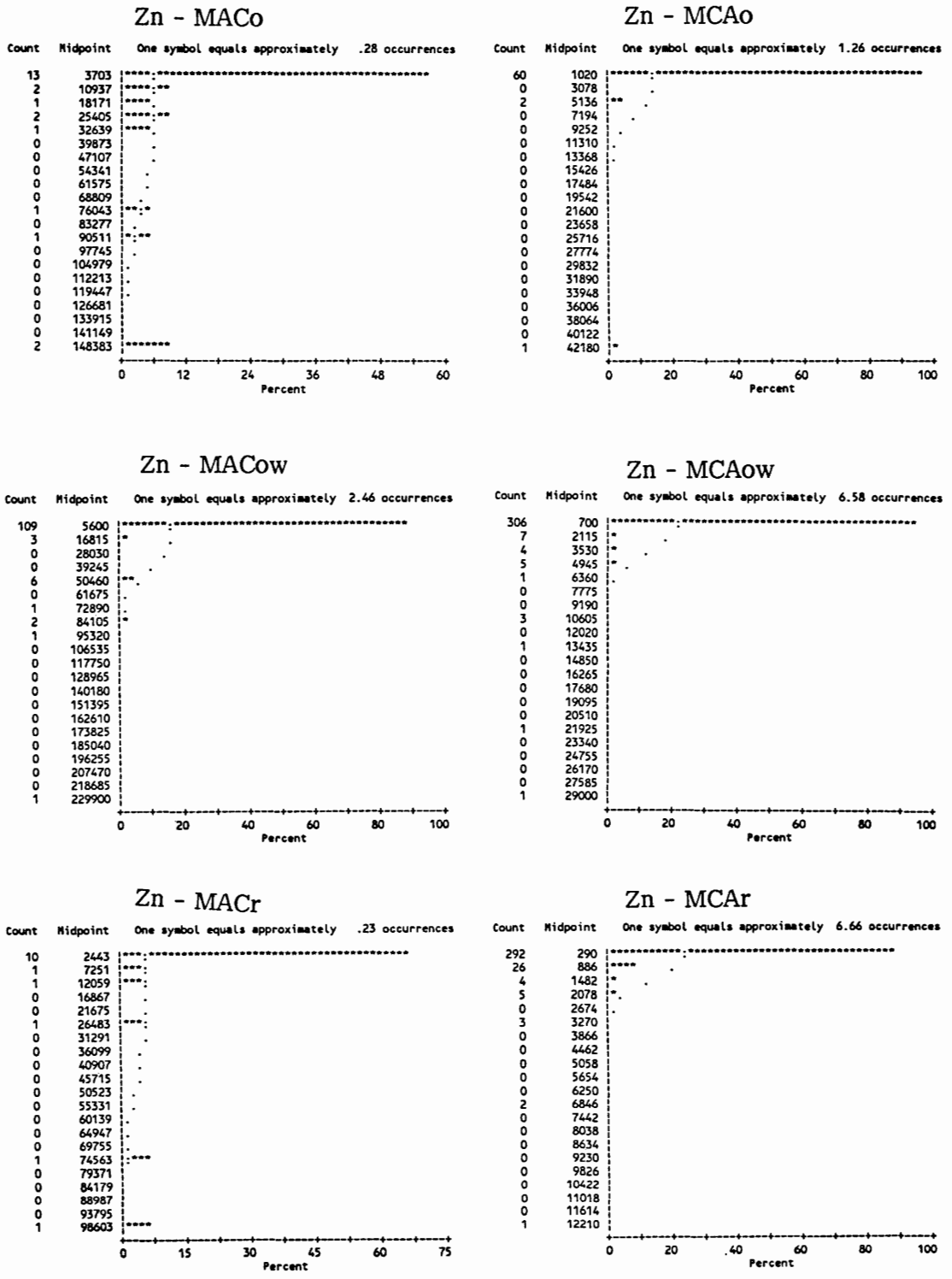

Figure I-31. Histograms of zinc concentrations in ppm (MAC=alkali-calcic, MCA=calc-alkalic, o=oxidized, ow=weakly oxidized, r=reduced).

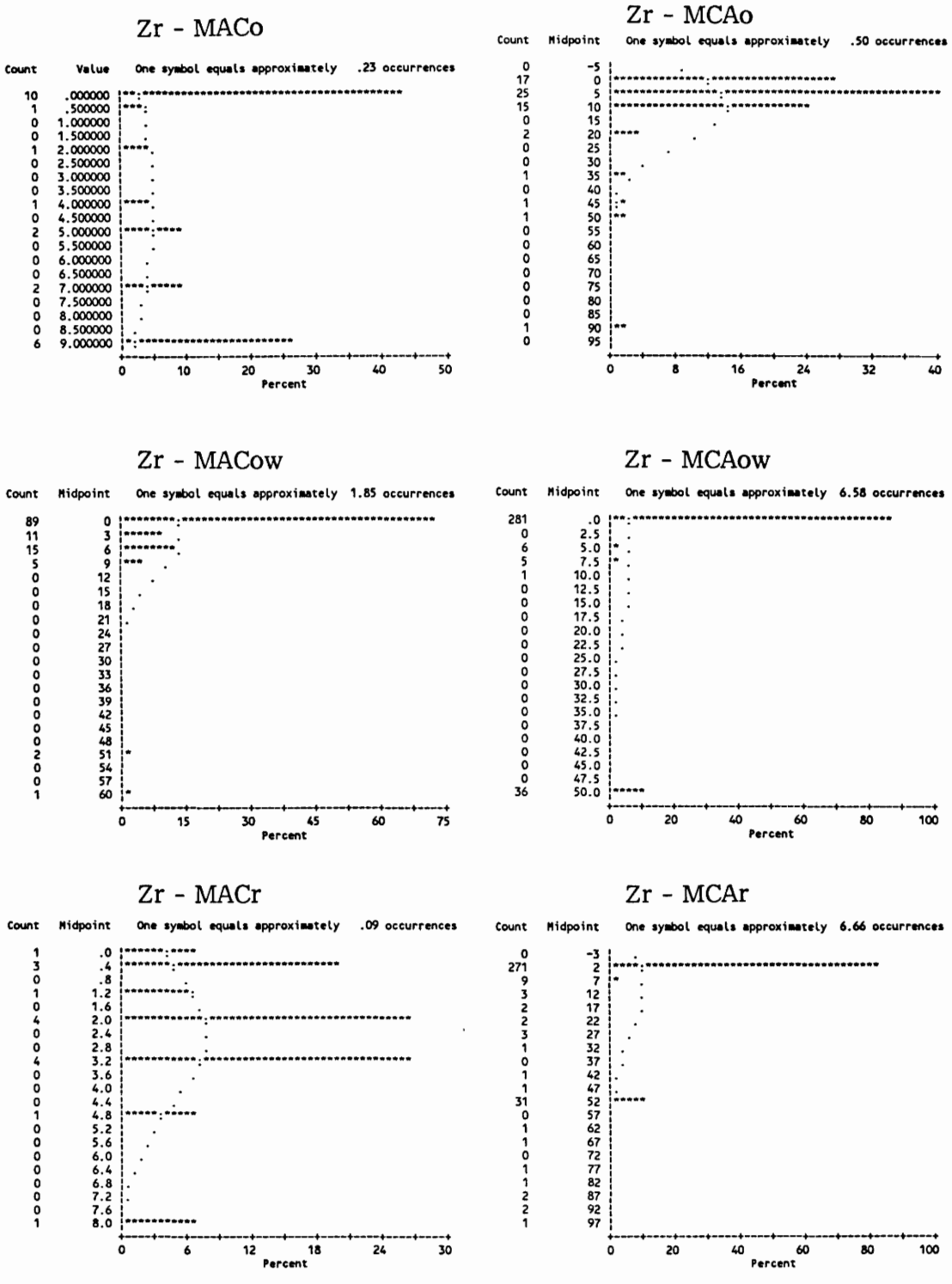

Figure I-32. Histograms of zirconium concentrations in ppm (MAC=alkali-calcic, MCA=calc-alkalic, o=oxidized, ow=weakly oxidized, r=reduced).

REFERENCES

Ague, J. J., and Brimhall, G. H., 1988, Magmatic arc asymmetry and distribution of anomalous plutonic belts in the batholiths of California: effects of assimilation, crustal thickness, and depth of crystallization: Geological Society of America Bulletin 100, p. 912-927.

Ague, J. J., and Brimhall, G. H., 1988, Regional variations in bulk chemistry, mineralogy, and the compositions of magmatic and accessory minerals in the batholiths of California: Geological Society of America Bulletin 100, p. 891-911.

Ahlfeld, F., 1931, The tin ores of Uncia-Llallagua, Bolivia: Economic Geology, v. 26, no. 3, p. 241-257.

Anthony, E. Y., 1986, Geochemical evidence for crustal melting in the origin of the igneous suite at the Sierrita porphyry copper deposit, southeastern Arizona: Tucson, University of Arizona, Ph.D. Dissertation, 85 p.

Antoniuk, T., and Crombie, D. R., 1982, The Pinson Mine; a Carlin type gold deposit: Canadian Mining Journal, v. 103, no. 4, p. 61-65.

Argall, G. O., Jr., 1981, Huge Chinese porphyry; Dexing operations and plans: World Mining, v. 34, no. 1, p. 24-28.

Armstrong, R. L., 1963, Age of intrusive rocks in the eastern Great Basin (abstract): American Geophysical Union Transactions, v. 44, p. 107.

Armstrong, R. L., 1964, Geochronology and geology of the eastern Great Basin in Nevada and Utah: Yale University, Ph.D. dissertation.

Armstrong, R. L., 1970b, K-Ar dating using neutron activation for Ar analysis - comparison with isotope dilution Ar analysis: Geochimica et Cosmochimica Acta, v. 34, no. 2, p. 233-236.

Arndt, N. T., and Nisbet, E. G., 1982, Komatiites: London, George Allen and Unwin, Ltd., 526 p.

Bacon, W. R., 1978, Lode gold deposits in western Canada: CIM Bulletin, v. 71 (795), p. 96-104.

Bagby, W. C., and Cline, J. S., 1991, Constraints on the pressure of formation of the Getchell gold deposit, Humboldt County, Nevada, as interpreted from

secondary-fluid-inclusion data, in Raines, G. L., Lisle, R. E., Schafer, R. W., and Wilkinson, W. H., editors, Geology and ore deposits of the Great Basin, symposium proceedings: Reno, Geological Society of Nevada, p. 793-804.

Bakken, B. M., 1991, Gold mineralization, wall-rock alteration, and the geochemical evolution of the hydrothermal system in the Main ore body, Carlin mine, Nevada, in Raines, G. L., Lisle, R. E., Schafer, R. W., and Wilkinson, W. H., editors, Geology and ore deposits of the Great Basin, symposium proceedings: Reno, Geological Society of Nevada, p. 233-234.

Bakken, B. M., and Einaudi, M. T., 1986, Spatial and temporal relations between wall rock alteration and gold mineralization, Main pit, Carlin Gold Mine, Nevada, U.S.A., in Macdonald, A. J., editor, Proceedings of Gold '86, an International Symposium on the Geology of Gold: Toronto, Canada, p. 388-403.

Baldwin, J. A., and Pearce, J. A., 1982, Discrimination of productive and nonproductive porphyritic intrusions in the Chilean Andes: Economic Geology, v. 77, p. 664-674.

Baldwin, J. L., Bateman, R. M., and Weatley, C. L., 1990, Application of a neural network to the problem of mineral identification from well logs: The Log Analyst, v. 31, no. 5, p. 279-293.

Baldwin, J. L., Otte, D. N., and Wheatley, C. L., 1989, Computer emulation of human mental processes; application of neural network simulators to problems in well log interpretation, in Tomich, J. F. O., Formation evaluation and reservoir geology: SPE (Society of Petroleum Engineers of AIME [American Institute of Mining, Metallurgical, and Petroleum Engineers]), v. 64, p. 481-493.

Banks, N. G., and Stuckless, J. S., 1973, Chronology of intrusion and ore deposition at Ray, Arizona: part II, fission-track ages: Economic Geology, v. 68, p. 657-664.

Banks, N. G., Cornwall, H. R., Silberman, M. L., Creasey, S. C., and Marvin, R., 1972, Chronology of intrusion and ore deposition at Ray, Arizona, part 1; K-Ar ages: Economic Geology, v. 67, p. 964-878.

Barnes, M. P., and Simos, J. G., 1968, Ore deposits of the Park City district with a contribution on the Mayflower lode, in Ore deposits of the United States, 1933-1967 (Graton-Sales Volume): New York, American Institute

of Mining, Metallurgical and Petroleum Engineers, v. 2, p. 1102-1126.

Barter, C. F., and Kelly, J. L., 1982, Geology of the Twin Buttes mineral deposit; Pima mining district, Pima County, Arizona, in Titley, S. R., editor, Advances in geology of porphyry copper deposits; southwestern North America: Tucson, University of Arizona Press, p. 407-432.

Baum, E., and Haussler, D., 1989, What size net gives valid generalization? in Touretzky, D., editor, Advances in neural information processing systems I: Morgan Kaufmann Publishers, p. 81-90.

Belt, C. B., Jr., 1969, Preliminary geochemical study of the Alta and Clayton Peak intrusives, in Jensen, M. L., editor, Guidebook of Northern Utah: Utah Geological and Mineralogical Survey Bulletin 82, p. 111-123.

Benediktsson, J., Swain, P., and Ersoy, O., 1990, Neural network approaches versus statistical methods in classification of multisource remote sensing data: IEEE Transactions on Geoscience and Remote Sensing, v. 28, p. 540-552.

Berger, B. R., and Taylor, B. E., 1974, Pre-Cenozoic age for "basin-range" faulting, Osgood Mountains, north-central Nevada (abstract): Geological Society of America Abstracts, Cordilleran Section, Las Vegas, Nevada.

Billingsley, P., and Hume, C. B., 1941, The ore deposits of Nickel Plate Mountain, Hedley, B.C.: Canadian Institute of Mining and Metallurgy Bulletin, v. 44, p. 524-590.

Blake, D. W., Wotruba, P. R., and Theodore, T. G., 1984, Zonation in the skarn environment at the Minnie-Tomboy gold deposits, Lander County, Nevada, in Wilkins, J., Jr., editor, Gold and silver deposits of the Basin and Range Province, western U.S.A.: Tucson, Arizona Geological Society Digest, v. 15, p. 67-72.

Blake, J. W., 1964, Geology of the Bald Mountain intrusive, Ruby Mountains, Nevada: Brigham Young University Geology Studies, v. 11, p. 3-35.

Bodnar, R. J., and Beane, R. E., 1980, Temporal and spatial variations in hydrothermal fluid characteristics during vein filling in preore cover overlying deeply buried porphyry copper-type mineralization at Red Mountain, Arizona: Economic Geology, v. 75, no. 6, p. 876-893.

Bonham, H. F., Jr., 1985, Characteristics of bulk-minable gold-silver deposits in

Cordilleran and island-arc settings, in Tooker, E. W., editor, Geologic characteristics of sediment- and volcanic-hosted disseminated gold deposits; search for an occurrence model: U. S. Geological Survey Bulletin 1646, p. 71-77.

Boutwell, J. M., and Woolsey, L. H., 1912, Geology and ore deposits of the Park City district, Utah: U. S. Geological Survey Professional Paper 77, 231 p.

Bowen, N. L., 1928, The evolution of igneous rocks: Dover, 334 p.

Brabec, D., and White, W. H., 1971, Distribution of copper and zinc in rocks of the Guichon Creek batholith, British Columbia, in Geochemical exploration (International Geochemical Exploration Symposium, 3rd, Proceedings: Canadian Institute of Mining and Metallurgy, Special Volume no. 11, p. 291-297.

Brimhall, G. H., and Crerar, D. A., 1989, Ore fluids: magmatic to supergene, Chapter 8, in Carmichael, L.S.E., and Eugster, H.P., editors, Thermodynamic modeling of geological materials: minerals, fluids and melts: Mineralogical Society of America, Reviews in Mineralogy, Volume 17, p. 235-282.

Briskey, J. A., Jr., 1980, Geology, petrology, and geochemistry of the Jersey, East Jersey, Huestis, and Iona porphyry copper-molybdenum deposits, Highland Valley, British Columbia: Corvallis, Oregon State University, Ph.D. Dissertation, 399 p.

Briskey, J. A., Jr., and Bellamy, J. R., 1976, Bethlehem Copper's Jersey, East Jersey, Huestis and Iona deposits, in Sutherland Brown, A., editor, Porphyry deposits of the Canadian Cordillera: Canadian Institute of Mining and Metallurgy, Special Volume 15, p. 105-119.

Bromfield, C. S., Erickson, A. J. J., Haddadin, M. A., and Mehnert, H. H., 1977, Potassium-argon ages of intrusion, extrusion, and associated ore deposits, Park City mining district, Utah: Economic Geology, v. 72, no. 5, p. 837-848.

Brooks, J. W., Meinert, L. D., Kuyper, B. A., and Lane, M. L., 1991, Petrology and geochemistry of the McCoy gold skarn, Lander County, Nevada, in Raines, G. L., Lisle, R. E., Schafer, R. W., and Wilkinson, W. H., editors, Geology and ore deposits of the Great Basin, Symposium proceedings: Reno, Geological Society of Nevada, p. 419-442.

Buseck, P. R., 1967, Contact metasomatism and ore deposition: Tem Piute, Nevada: Economic Geology, v. 62, p. 331-353.

Butler, B. S., Wilson, E. D., and Rasor, C. A., 1938, Geology and ore deposits of the Tombstone district, Arizona: Arizona Bureau of Mines Bulletin 143, 114 p.

Calkins, F. S., and Butler, B. S., 1943, Geology and ore deposits of the Cottonwood-American Fork area, Utah: U. S. Geological Survey Professional Paper 201, 152 p.

Campbell, D. F., 1942, The Oruro silver-tin district, Bolivia: Economic Geology, v. 37, no. 2, p. 87-115.

Camsell, C., 1910, Geology and ore deposits of Hedley mining district, B. C.: Geological Survey of Canada, Memoir 2.

Camus, F., 1975, Geology of the El Teniente orebody with emphasis on wall-rock alteration: Economic Geology, v. 70, no. 8, p. 1341-1372.

Carpenter, G., and Grossberg, S., 1987, ART2: self-organization of stable category recognition codes for analog input patterns: Applied Optics, v. 26, p. 4919-4930.

Caudill, M., and Butler, C., 1990, Naturally intelligent systems: Cambridge, Massachusetts, A Bradford Book, The MIT Press, 304 p.

Chace, F. M., 1948, Tin-silver veins of Oruro, Bolivia: Economic Geology, v. 43, no. 5, p. 333-383, 435-469.

Chappell, B. W., and White, A. J. R., 1974, Two contrasting granite types: Pacific Geology, v. 8, p. 173-174.

Chung-Wen, Yu, 1981, Mechanisms of ore formation and primary dispersion at the Dexing porphyry copper deposit, Jiangxi, and their implications in geochemical exploration: Journal of Geochemical Exploration, v. 15, p. 115-137.

Clarke, F. W., 1915, Analyses of rocks and minerals from the Laboratory of the United States Geological Survey, 1880-1914: U. S. Geological Survey Bulletin 591, 376 p.

Coats, R. R., 1987, Geology of Elko County, Nevada: Nevada Bureau of Mines and

Geology Bulletin 101, 112 p.

Coats, R. R., Marvin, R. F., and Stern, T. W., 1965, Reconnaissance of mineral ages of plutons in Elko County, Nevada, and vicinity: U. S. Geological Survey Professional Paper 525-D, p. D11-D15.

Coats, R. R., Marvin, R. F., and Stern, T. W., 1965, Reconnaissance of mineral ages of plutons in Elko County, Nevada, and vicinity: U. S. Geological Survey Professional Paper 525-D, p. D11-D15.

Cooper, J. R., 1960, Some geologic features of the Pima mining district, Pima County, Arizona: U. S. Geological Survey Bulletin 1112-C, p. 63-103.

Cooper, J. R., 1973, Geologic map of the Twin Buttes quadrangle, southwest of Tucson, Pima County, Arizona: U. S. Geological Survey Miscellaneous Investigations Map I-745.

Corn, R. M., 1975, Alteration-mineral zoning, Red Mountain, Arizona: Economic Geology, v. 70, p. 1437-1447.

Cornwall, H. R., 1982, Petrology and chemistry of igneous rocks, Ray porphyry copper district, Pinal County, Arizona, in Titley, S. R., editor, Advances in geology of the porphyry copper deposits, southwestern North America: Tucson, University of Arizona Press, p. 259-273.

Cornwall, H. R., Banks, N. G., and Phillips, C. H., 1971, Geologic map of the Sonora quadrangle, Pinal and Gila Counties, Arizona: U. S. Geological Survey Geologic Quadrangle Map GQ-1021, scale 1:24,000.

Cox, D. P., and Ohta, E., 1984, Maps showing rock types, hydrothermal alterations and distribution of fluid inclusions in the Cornelia pluton, Ajo mining district, Pima County, Arizona: U. S. Geological Survey Open-file report 84-388, 12 p.

Cox, D. P., Czamanske, G. K., and Bain, J. H. C., 1981, Mineral-rich fluid inclusions in the root zone of a porphyry copper system, Ajo, Arizona (abstract): Geological Society of America Abstracts with Programs, v. 13, p. 433.

Creasey, 1983, Geologic map of the Teapot Mountain quadrangle, Pinal County, Arizona: U. S. Geological Survey Geologic Quadrangle GQ-1559, scale 1:24,000.

Creasey, S. C., 1984, The Schultze Granite, the Tea Cup Granodiorite, and the Granite Basin Porphyry; a geochemical comparison of mineralized and unmineralized stocks in southern Arizona: U. S. Geological Survey Professional Paper 1303, 41 p.

Creasey, S. C., and Kistler, R. W., 1962, Age of some copper-bearing porphyries and other igneous rocks in southeastern Arizona, in Geological Survey Research 1962: U. S. Geological Survey Professional Paper 450-D, p. 1-5.

Crittenden, M. D., Jr., Stuckless, J. S., Kistler, R. N., and Stern, T. W., 1973, Radiometric dating of intrusive rocks in the Cottonwood area, Utah: U. S. Geological Survey Journal of Research, v. 1, p. 173-178.

Cybenko, G., 1989, Approximations by superpositions of a sigmoidal function: Math. of Control, Signals and Systems, v. 2, p. 303-314.

Damon, P. E., and Mauger, R. L., 1966, Epeirogeny-orogeny viewed from the Basin and Range Province of Arizona and Sonora: American Institute of Mining, Metallurgical, and Petroleum Engineers Transactions, v. 235, p. 99-112.

Damon, P. E., and others, 1970, New K-Ar dates for the southern Basin and Range Province, in Annual progress reports to Research Division: U. S. Atomic Energy Commission, June, 1970, p. 38.

Damon, P. E., compiler, 1965, Correlation and chronology of ore deposits and volcanic rocks: University of Arizona Geochronology Laboratory, Annual Progress Report, COO-689-50.

Damon, P. E., compiler, 1966, Correlation and chronology of ore deposits and volcanic rocks: University of Arizona Geochronology Laboratory, Annual Progress Report, COO-689-50.

Damon, P. E., Mauger, R. L., and Bikerman, M., 1964, K-Ar dating of Laramide plutonic and volcanic rocks within the Basin and Range Province of Arizona and Sonora: International Geological Congress, 22nd, New Delhi, India, Proceedings of Section 3, p. 45-55.

Date, J., Watanabe, Y., and Saeki, Y, 1983, Zonal alteration around the Fukazawa Kuroko deposits, Akita Prefecture, Northern Japan: Economic Geology Monograph 5, p. 365-386.

Dayhoff, J., 1990, Neural network architectures, an introduction: New York, Van Nostrand Reinhold, 259 p.

de Beaumont, L. E., 1852, Notice sur les Systemes des Montagnes: Paris, 3 volumes.

Dewhurst, J., 1976, Chemical ratios of Laramide igneous rocks and their relation to a paleosubduction zone under Arizona: Tucson, University of Arizona, unpublished M. S. thesis, 128 p.

Dickinson, W. R., 1975, Potash-depth (K-h) relations in continental margin and intra-oceanic magmatic arcs: Geology, v. 3, p. 53-56.

Dickinson, W. R., and Hatherton, T., 1967, Andesitic volcanism and seismicity around the Pacific: Science, v. 157, p. 801-803.

Dickson, F. W., and Rytuba, J. J., 1988, Transport and deposition of gold and associated substances at the Carlin gold deposit, Nevada, in Schafer, R. W., Cooper, J. J., and Vikre, P. G., 1988, Bulk mineable precious metal deposits of the western United States, symposium proceedings: Reno, Geological Society of Nevada, p. 728.

DiSieno, D., 1988, Adding a conscience to competitive learning: 2nd Ann. International Conference on Neural Networks, IEEE, Proceedings, v. 1, p. 117-124.

Dixon, D. W., 1966, Geology of the New Cornelia mine, Ajo, Arizona, in Titley, S. R., and Hicks, C. L., editors, Geology of the porphyry copper deposits, southwestern North America: Tucson, The University of Arizona Press, p. 123-132.

Dolmage, V., and Brown, C. E., 1945, Contact metamorphism at Nickel Plate Mountain, Hedley, B.C.: Canadian Institute of Mining and Metallurgy, Bulletin, v. 48.

Drewes, H., 1967, Geology of the Connors Pass quadrangle, Schell Creek Range, east central Nevada: U. S. Geological Survey Professional Paper 557, 93 p.

Drewes, H., 1972, Cenozoic rocks of the Santa Rita Mountains, southeast of Tucson, Arizona: U. S. Geological Survey Professional Paper 746.

Dunning, G. E., 1988, Calcium arsenate minerals new to the Getchell Mine, Nevada: The Mineralogical Record, v. 19, no. 4, p. 253-257.

Dysart, P. S., and Pulli, J. J., 1990, Regional seismic event classification at the

NORESS array; seismological measurements and the use of trained neural networks, in Ringdal, Frode, Regional seismic arrays and nuclear test ban verification: Bulletin of the Seismological Society of America, v. 80, no. 6, Part B, p. 1910-1933.

Eidel, J. J., Frost, J. E., and Clippinger, D. M., 1968, Copper-molybdenum mineralization at Mineral Park, Mohave County, Arizona, in Ridge, J. D., editor, Ore deposits of the United States, 1933-1967: New York, American Institute of Mining, Metallurgical and Petroleum Engineers, Graton-Sales Volume, v. 2, p. 1258-1281.

Ekburg, C. E., Rota, J. C., and Arkell, B. W., 1991, Geology and mineral deposits of the Maggie Creek subdistrict, Carlin Trend, Eureka County, Nevada, in Raines, G. L., Lisle, R. E., Schafer, R. W., and Wilkinson, W. H., editors, Geology and ore deposits of the Great Basin, symposium proceedings: Reno, Geological Society of Nevada, p. 625-633.

Erickson, R. L., Marranzino, A. P., Oda, U., and Janes, W. W., 1964, Geochemical exploration near the Getchell mine, Humboldt County, Nevada: U. S. Geological Survey Bulletin 1198-A, 26 p.

Evans, J. G., 1980, Geology of the Rodeo Creek NE and Welches Canyon quadrangles, Eureka County, Nevada: U. S. Geological Survey Bulletin 1473, 81 p.

Evans, J. G., and Ketner, K. B., 1971, Geologic map of the Swales Mountain quadrangle and part of the Adobe Summit quadrangle, Elko County, Nevada: U. S. Geological Survey Miscellaneous Geologic Investigations Map I-667, scale 1:24,000.

Evernden, J. F., Kriz, S. J., and Cherroni, M. C., 1977, Potassium-argon ages of some Bolivian rocks: Economic Geology, v. 72, no. 6, p. 1042-1061.

Flaherty, M. J., and King, G. C., 1991, A geologic overview of the Carlin Trend Subdistricts, in Buffa, R. H., and Coyner, A. R., editors, Geology and ore deposits of the Great Basin, field trip guidebook compendium, volume 2: Reno, Geological Society of Nevada, p. 844-849.

Foster, J. M., and Kretschmer, E. L., 1991, Geology of the Mag deposit, Pinson mine, Humboldt County, Nevada, in Raines, G. L., Lisle, R. E., Schafer, R. W., and Wilkinson, W. H., editors, Geology and ore deposits of the Great Basin, symposium proceedings: Reno, Geological Society of Nevada, p. 845-856.

Francis, P. W., Baker, M. C. W., and Halls, C., 1981, The Kari Kari caldera, Bolivia, and the Cerro Rico Stock: Journal of Volcanology and Geothermal Research, v. 10, p. 113-124.

Francis, P. W., Halls, C., and Baker, M. C. W., 1983, Relationships between mineralization and silicic volcanism in the central Andes: Journal of Volcanology and Geothermal Research, v. 18, p. 165-190.

Freeman, J. A., and Skapura, D. M., 1992, Neural networks: algorithms, applications, and programming techniques: Reading, MA, Addison-Wesley Publishing Company, 401 p.

Gans, P. B., Mahood, G. A., and Schermer, E., 1989, Synextentional magmatism in the Basin and Range province; A case study from the eastern Great Basin: Geological Society of America Special Paper 233, 53 p.

Garbrecht, D. A., Jones, S. K., and Slothower, G. E., 1991, Geology of the Alligator Ridge deposits, White Pine County, Nevada, in Buffa, R. H., and Coyner, A. R., editors, Field Trip Guidebook Compendium, Volume 1, Geology and Ore Deposits of the Great Basin: Reno, Geological Society of Nevada, p. 109-112.

Gillerman, V. S., 1984, Superimposed magmatism, limestone replacement ores, and tungsten and copper skarns of the Railroad mining districts, Elko County, Nevada: Geological Society of America, Abstracts with Programs, v. 16, no. 6, p. 519.

Gilluly, J., 1937, Geology and ore deposits of the Ajo quadrangle, Arizona: Arizona Bureau of Mines Bulletin 141, 83 p.

Gilluly, J., 1946, The Ajo mining district, Arizona: U. S. Geological Survey Professional Paper 209, 112 p.

Gilluly, J., 1956, General geology of central Cochise County, Arizona: U. S. Geological Survey Professional Paper 281, 169 p.

Goldstein, I. J., 1973, Gold mineralization at the Northumberland gold mine, Nye Co., Nevada (abstract): Geological Society of America Abstracts with Programs, v. 5, no. 1, p. 48.

Granger, A. E., Bell, M. M., Simmons, G. C., and Lee, F., 1957, Geology and mineral resources of Elko County, Nevada: Nevada Bureau of Mines Bulletin 54, 190 p.

Grant, J. N., Halls, C., Sheppard, S. M. F., and Avila, W., 1980, Evolution of the porphyry tin deposits of Bolivia: Mining Geology, Special Issue 8, p. 151-173.

Grant, J. N., Halls, C., Avila, W., and Avila, G., 1977, Igneous geology and the evolution of hydrothermal systems in the sub-volcanic tin deposits of Bolivia: Geological Society of London Special Publication 7, p. 117-127.

Grant, J. N., Halls, C., Avila, W., and Snelling, N. J., 1979, K-Ar ages of igneous rocks and mineralization in part of the Bolivian tin belt: Economic Geology, v. 74, p. 838-851.

Grauch, V. J. S., and Bankey, V., 1991, Preliminary results of aeromagnetic studies of the Getchell disseminated gold deposit trend, Osgood Mountains, north-central Nevada in Raines, G. L., Lisle, R. E., Schafer, R. W., and Wilkinson, W. H., editors, Geology and ore deposits of the Great Basin, symposium proceedings: Reno, Geological Society of Nevada, p. 781-791.

Graybeal, F. T., 1972, The partition of trace elements among coexisting minerals in some Laramide intrusive rocks in Arizona: Tucson, University of Arizona, Ph.D. dissertation, 220 p.

Graybeal, F. T., 1973, Copper, manganese, and zinc in coexisting mafic minerals from Laramide intrusive rocks in Arizona: Economic Geology, v. 68, p. 785-798.

Gustafson, L. B., and Hunt, J. P., 1975, Porphyry copper deposit at El Salvador, Chile: Economic Geology, v. 75, no. 5, p. 857-912.

Hagstrum, J. T., Cox, D. P., and Miller, R. J., 1987, Structural reinterpretation of the Ajo mining district, Pima County, Arizona, based on paleomagnetic and geochronologic studies: Economic Geology, v. 82, p. 1348-1361.

Hannah, J. L., Macbeth, A., and Stein, H. J., 1991, Field relations between Tertiary magmatism and Tintic-type ore deposits, East Tintic Mountains, Utah, in Raines, G. L., Lisle, R. E., Schafer, R. W., and Wilkinson, W. H., editors, Geology and ore deposits of the Great Basin, symposium proceedings: Reno, Geological Society of Nevada, p. 485-489.

Hardie, B. S., 1966, Carlin gold mine, Lynn district, Nevada: Nevada Bureau of Mines Report 13, p. 73-83.

Harvey, B. A., 1991, Structural overview of the Carlin Trend, Nevada, in Buffa,

R. H., and Coyner, A. R., editors, Geology and ore deposits of the Great Basin, field trip guidebook compendium, volume 2: Reno, Geological Society of Nevada, p. 834-837.

Hausen, D. M., and Kerr, P. F., 1968, Fine gold occurrence at Carlin, Nevada, in Ridge, J. D., editor, Ore deposits of the United States, 1933-1967 (Graton-Sales volume): New York, American Institute of Mining, Metallurgical, and Petroleum Engineers, v. 1, p. 908-940.

Havenstrite, S. R., 1983, Geology and ore deposits of the Taylor mining district, White Pine County, Nevada, in Kral, V. E., Hall, J. A., Blakestad, R. B., Bonham, H. F., Jr., Hartley, G. B., Jr., McClelland, G. E., McGlasson, J. A., Mousette Jones, P., editors, Papers given at the precious metals symposium: Nevada Bureau of Mines and Geology Report 36, p. 14-26.

Hecht-Nielsen, R., 1987, Kolmogorov's mapping and neural network existence theorem, 1st International Conference on Neural Networks, IEEE, Proceedings, p. 11-14.

Hecht-Nielsen, R., 1990, Neurocomputing: Addison-Wesley Publishing Company.

Hess, N. J., 1986, Petrology and crystal chemistry of the Ruby Star Granodiorite, Pima County, Arizona: Tucson, University of Arizona, unpublished Master's Thesis, 71 p.

Hewitt, W. P., 1943, Geology and mineralization of the San Antonio mine, Santa Eulalia district, Chihuahua, Mexico: Geological Society of America Bulletin, v. 54, p. 173-204.

Hill, J. M., 1916, Notes on some mining districts in eastern Nevada: U. S. Geological Survey Bulletin 648.

Hillman, B. A., 1970, Hydrothermal activity as related to ore deposition at the Sierrita porphyry copper-molybdenum deposit, southwestern Arizona: University of Cincinnati, unpublished Master's Thesis, 69 p.

Himes, M. D., 1973, Mineralization and alteration at Pima Mine: a complex porphyry copper deposit: Society of Mining Engineers, AIME Transactions, v. 254, p. 166-174.

Hobbs, S. W., 1948, Geology of the northern part of the Osgood Mountains, Humboldt County, Nevada: New Haven, Connecticut, Yale University, Ph. D. dissertation, 97 p.

Hollister, V. F., 1973, Regional characteristics of porphyry copper deposits of South America: Mining Engineer, August 1973, p. 51-56.

Hose, R. K., and Blake, M. C., Jr., 1976, Geology, in Hose, R. K., and Blake, M. C., Jr., and Smith, R. M., Geology and mineral resources of White Pine County, Nevada: Nevada Bureau of Mines and Geology Bulletin 85, 105 p.

Hose, R. K., Blake, M. C., Jr., and Smith, R. M., 1976, Geology and mineral resources of White Pine County, Nevada: Nevada Bureau of Mines and Geology Bulletin 85.

Hotz, P. E., and Willden, R., 1964, Geology and mineral deposits of the Osgood Mountains quadrangle, Humboldt County, Nevada: U. S. Geological Survey Professional Paper 431, 128 p.

Howell, F. H., and Molloy, J. S., 1960, Geology of the Braden orebody, Chile, South America: Economic Geology, v. 55, no. 5, p. 863-905.

Hutton, J., 1788, Theory of the Earth: Transactions of the Royal Society of Edinburgh, v. 1, p. 209-304.

Hutton, J., 1795, Theory of the Earth with proofs and illustrations, v. I, v. II: Edinburgh.

Ilchik, R. P., 1990, Geology and geochemistry of the Vantage gold deposits, Alligator Ridge-Bald Mountain Mining District, Nevada: Economic Geology, v. 85, no. 1, p. 50-75.

Ilchik, R. P., 1991, Geology of the Vantage gold deposits, Alligator Ridge, Nevada, in Raines, G. L., Lisle, R. E., Schafer, R. W., and Wilkinson, W. H., editors, Geology and ore deposits of the Great Basin, symposium proceedings: Reno, Nevada, Geological Society of Nevada, p. 645-663.

Ishihara, S., 1977, The magnetite-series and ilmenite-series granitic rocks: Mining Geology, v. 27, p. 293-305.

Ishihara, S., 1981, The granitoid series and mineralization: Economic Geology, 75th Anniversary Volume, p. 458-484.

Ishikawa, Y., Sawaguchi, T., Iwaya, S., Horiuchi, M., 1976, Delineation of prospecting targets for Kuroko deposits based on modes of volcanism of underlying dacite and alteration haloes: Mining Geology, v. 26, p. 106-117 (in Japanese, with English abstract).

John, D. A., 1989, Geologic setting, depths of emplacement, and regional distribution of fluid inclusions in intrusions of the central Wasatch Mountains, Utah: Economic Geology, v. 84, no. 2, p. 386-409.

John, D. A., 1991, Evolution of hydrothermal fluids in the Alta stock, central Wasatch Mountains, Utah: U. S. Geological Survey Bulletin 1977, 51 p.

Johnson, M. G., 1977, Geology and mineral deposits of Pershing County, Nevada: Nevada Bureau of Mines and Geology Bulletin 89, 115 p.

Johnson, V. Y., and Keith, J. D., 1991, Petrology and geochemistry of the Springer scheelite skarn deposit, Mill City, Nevada, in Raines, G. L., Lisle, R. E., Schafer, R. W., and Wilkinson, W. H., editors, Geology and ore deposits of the Great Basin, Symposium Proceedings: Reno, Geological Society of Nevada, p. 553-578.

Jones, M. B., 1974, Hydrothermal alteration and mineralization of the Valley Copper deposit, Highland Valley, British Columbia: Corvallis, Oregon State University, Ph.D. dissertation, 262 p.

Jones, M. B., Field, C. W., and Schmuck, R. A., 1972, K-Ar dates from the Valley Copper and Lornex deposits, Guichon Creek batholith, Highland Valley district: Corvallis, Oregon State University, Department of Geology, unpublished paper.

Joralemon, P., 1951, The occurrence of gold at the Getchell mine, Nevada: Economic Geology, v. 46, p. 267-310.

Kay, M., and Crawford, J. P., 1964, Paleozoic facies from the miogeosynclinal to the eugeosynclinal belt in thrust slices, central Nevada: Geological Society of America Bulletin, v. 75, no. 5, p. 425-454.

Keith, S. B., 1978a, Origins of Arizona copper deposits: hypotheses: Fieldnotes: State of Arizona Bureau of Geology and Mineral Technology, v. 8, no. 1-2, p.8-9, 12, 17.

Keith, S. B., 1978b, Paleosubduction geometries inferred from Cretaceous and Tertiary magmatic patterns in southwestern North America: Geology, v. 6, p. 516-521.

Keith, S. B., 1979, Spatial, temporal, chemical and structural evolution of the southeast Arizona-southwest New Mexico porphyry copper cluster: Society of Economic Geologists Field Conference, Tucson, Arizona, April

1979, p. 36-46.

Keith, S. B., 1982, Paleoconvergence rates determined from K_2O/SiO_2 ratios in magmatic rocks and their application to Cretaceous and Tertiary tectonic patterns in southwestern North America: Geological Society of America Bulletin, v. 93, p. 524-532.

Keith, S. B., 1986, Petrochemical variations in Laramide magmatism and their relationship to Laramide tectonic and metallogenic evolution in Arizona and adjacent regions, in Beatty, B., and Wilkinson, P. A. K., editors, Frontiers in geology and ore deposits of Arizona and the Southwest: Tucson, Arizona Geological Society Digest, v. 16, p. 89-101.

Keith, S. B., 1987, Space, time, geotectonics, magmatism, and metallogeny (abstract): Geological Society of America Abstracts with Programs, v. 19, no. 6, p. 393.

Keith, S. B., 1991, Mid-crustal formation fluids: a solution to the debate on crust vs. mantle as sources of metal for Cordilleran metal deposits: unpublished preprint, Northwest Mining Association, Left Lateral Leaps, 16 p.

Keith, S. B., and Reynolds, S. J, 1980, Geochemistry of Cordilleran metamorphic core complexes, in Coney, P. J., Reynolds, S. J. Cordilleran metamorphic core complexes and their uranium favorability; final report: U. S. Department of Energy, Grand Junction, CO, Open-file report GJBX-258-80, p. 247-310.

Keith, S. B., and Swan, M. M., 1987, Oxidation state of magma series in the Southwestern U.S.; implications for geographic distribution of base, precious, and lithophile metal metallogeny: Geological Society of America, Abstracts with Programs, v. 19, no. 7, p. 723-724.

Keith, S. B., and Wilt, J. C., 1985, Late Cretaceous and Cenozoic orogenesis of Arizona and adjacent regions; a strato-tectonic approach, in Flores, R. M., Kaplan, S. S., editors, Cenozoic paleogeography of the west-central United States: Society of Economic Paleontologists and Mineralogists, Rocky Mountain Section, p. 403-437.

Keith, S. B., and Wilt, J. C., 1986, Laramide Orogeny in Arizona and adjacent regions; a strato-tectonic synthesis, in Beatty, B., and Wilkinson, P. A. K., editors, Frontiers in geology and ore deposits of Arizona and the Southwest: Tucson, Arizona Geological Society Digest, v. 16, p. 502-554.

Keith, S. B., Gest, D. E., DeWitt, E., Toll, N. W., and Everson, B. A., 1983, Metallic mineral districts and production in Arizona: Arizona Bureau of Geology and Mineral Technology, Bulletin 194, 58 p.

Keith, S. B., Laux, D. P., Maughan, J., Schwab, K., Ruff, S., Swan, M. M., Abbott, E., and Friberg, S., 1991, Magma series and metallogeny: a case study from Nevada and environs, in Buffa, R. H., and Coyner, A. R., editors, Geology and ore deposits of the Great Basin, Field Trip Guidebook Compendium, Volume 1: Reno, Geological Society of Nevada, p. 404-493.

Keith, S. B., Maughan, J. R., and Laux, D. P., 1988, Use of metal chemistry and petrochemistry to screen epithermal Hg-Sb-As occurrences for gold metallization, in Buffa, R., Cuffney, B., and Seedorff, E., editors, Hot-spring gold deposits of northwestern Nevada and southeastern Oregon: Geological Society of Nevada, Special Publication 7, p. 43-59.

Ketner, K. B., and Smith, J. F., Jr., 1963, Geology of the Railroad mining district, Elko County, Nevada: U. S. Geological Survey Bulletin 1162-B, 27 p.

Ketner, K. B., Evans, J. G., and Hessin, T. D., 1968, Geochemical anomalies in the Swales Mountain area, Elko County, Nevada: U. S. Geological Survey Circular 588, 13 p.

Kistner, D. J., 1984, Fracture study of a volcanic lithocap, Red Mountain porphyry copper prospect, Santa Cruz County, Arizona: Tucson, University of Arizona, unpublished Master's Thesis, 75 p.

Kleinhampl, F. J., and Ziony, J. I., 1984, Mineral resources of northern Nye County, Nevada: Nevada Bureau of Mines and Geology Bulletin 99B, 243 p.

Klessig, P. J., 1984, History and geology of the Alligator Ridge gold mine, White Pine County, Nevada, in Wilkins, J., Jr., editor, Gold and silver deposits of the Basin and Range Province, western U.S.A.: Tucson, Arizona Geological Society Digest, v. 15, p. 77-88.

Kohonen, T., 1988, Self-organization and associative memory, 2nd ed.: New York, Springer-Verlag.

Kohonen,T., Barna, G., and Chrisley, R., 1988, Statistical pattern recognition with neural networks: benchmarking studies: 2nd International Conference on Neural Networks, IEEE, Proceedings, p. 61-68.

Kokinos, M., and Prenn, N., 1985, The Northumberland Mine, Nye County, Nevada: The Mineralogical Record, v. 16, no. 1 (Nevada special issue), p. 37-41.

Koski, R. A., 1978, Geology and porphyry copper-type alteration-mineralization of igneous rocks at the Christmas mine, Gila County, Arizona: Stanford University, Ph.D. dissertation, 196 p.

Koski, R. A., and Cook, D. S., 1982, Geology of the Christmas porphyry copper deposit; Gila County, Arizona, in Titley, Spencer R., Advances in geology of porphyry copper deposits; southwestern North America: Tucson, University of Arizona Press, p. 353-374.

Kral, V. E., 1951, Mineral resources of Nye County, Nevada: University of Nevada Bulletin, v. 45 (50), no. 3, 223 p.

Kretschmer, E. L., 1984, Geology of the Pinson and Preble gold deposits, Humboldt County, Nevada, in Wilkins, J., Jr., editor, Gold and silver deposits of the Basin and Range Province, western U.S.A.: Tucson, Arizona Geological Society Digest, v. 15, p. 59-66.

Kretschmer, E. L., 1986, Geology of the Pinyon mine, Humboldt County, Nevada, in Tingley, J. V., and Bonham, H. F., Jr., editors, Sediment-hosted precious-metal deposits of northern Nevada: Nevada Bureau of Mines and Geology Report 40, p. 52-55.

Kuehn, C. A., 1989, Studies of disseminated gold deposits near Carlin, Nevada: Evidence for deep geologic settings of ore formation: Pennsylvania State University, Ph.D. dissertation, 350 p.

Kung, S., and Hwang, J., 1988, An algebraic projection analysis for optimal hidden units size and learning rates in back-propagation learning: 1st International Conference on Neural Networks, IEEE, Proceedings, p. 363-370.

Kuyper, B. A., 1988, Geology of the McCoy gold deposit, Lander County, Nevada, in Schafer, R. W., Cooper, J. J., and Vikre, P. G., editors, Bulk mineable precious metal deposits of the western United States: Reno, Geological Society of Nevada, p. 173-186.

Laine, R. P., 1974, Geological-geochemical relationships between porphyry copper and porphyry molybdenum ore deposits: Tucson, University of Arizona, Ph.D. Dissertation, 326 p.

Lang, J. R., 1991, Isotopic and geochemical characteristics of Laramide igneous rocks in Arizona: Tucson, University of Arizona, Ph.D. Dissertation, 201 p.

Lang, J. R., and Eastoe, C. J., 1988, Relationships between a porphyry Cu-Mo deposit, base and precious metal veins and Laramide intrusions, Mineral Park, Arizona: Economic Geology, v. 83, no. 3, p. 551-567.

Langton, J. M., 1973, Ore genesis in the Morenci-Metcalf district: American Institute of Mining, Metallurgical, and Petroleum Engineers Transactions, v. 254, no. 3, p. 247-257.

Langton, J. M., and Williams, S. A., 1982, Structural, petrological and mineralogical controls for the Dos Pobres orebody, Lone Star mining district, Graham County, Arizona, in Titley, S. R., editor, Advances in geology of the porphyry copper deposits, southwestern North America: Tucson, University of Arizona Press, p. 335-352.

Lapointe, D. D., Tingley, J. V., and Jones, R. B., 1991, Mineral resources of Elko County, Nevada: Nevada Bureau of Mines and Geology Bulletin 106, 236 p.

Larsen, E. S., Jr., and Cross, W., 1956, Geology and petrology of the San Juan region, southwestern Colorado: U. S. Geological Survey Professional Paper 258, 303 p.

Laughlin, A. W., Lovering, T. S., and Mauger, R. L., 1969, Age of some Tertiary igneous rocks from the East Tintic district, Utah: Economic Geology, v. 64,. no. 8, p. 915-918.

Lee, D. E., 1984, Analytical data for a suite of granitoid rocks from the Basin and Range Province: U. S. Geological Survey Bulletin 1602, 54 p.

Lewis, P. R., 1991, Carlin mine geology, in Buffa, R. H., and Coyner, A. R., editors, Geology and ore deposits of the Great Basin, field trip guidebook compendium, volume 2: Reno, Geological Society of Nevada, p. 854-858.

Lincoln, F. C., 1923, Mining districts and mineral resources of Nevada: Reno, Nevada Newsletter Publishing Company, p. 53-54.

Lindgren, W., 1902, Copper deposits at Clifton, Arizona: U. S. Geological Survey Bulletin 213, p. 133-140.

Lindgren, W., 1905, The copper deposits of the Clifton-Morenci district, Arizona: U. S. Geological Survey Professional Paper 43, 375 p.

Lindgren, W., 1933, Differentiation and ore deposition, Cordilleran region of the United States, in Ore deposits of the western United States (Lindgren volume): New York, AIME (American Institute of Mining, Metallurgical and Petroleum Engineers), p. 152-180.

Lindgren, W., and Loughlin, G. F., 1919, Geology and ore deposits of the Tintic mining district, Utah: U. S. Geological Survey Professional Paper 107, 282 p.

Lippmann, R., 1987, An introduction to computing with neural nets, in Vemuri, V., editor, Artificial Neural Networks: Theoretical Concepts: IEEE ASSP, April, 4-22, Computer Press of the IEEE, p. 36-54.

Lovering, T. G., and Heyl, A. V., 1974, Jasperoid as a guide to mineralization in the Taylor mining district and vicinity near Ely, Nevada: Economic Geology, v. 69, no. 1, p. 46-58.

Lovering, T. G., Cooper, J. R., Drewes, H. D., and Cone, G. C., 1970, Copper in biotite from igneous rocks in southern Arizona as an ore indicator: U. S. Geological Survey Professional Paper 700-B, p. B1-B8.

Lowe, N. T., Raney, R. G., and Norberg, J. R., 1985, Principal deposits of strategic and critical minerals in Nevada: U. S. Bureau of Mines Information Circular 9035.

Mahfoud, R. F., 1971, Paragenesis and mineralogy of the Burgin Mine, East Tintic District, Utah County, Utah: Brigham Young University Geology Studies, v. 18, no. 3, p. 49-104.

Manske, S. L., 1980, Fracturing events in the Ruby Star Granodiorite adjacent to the Esperanza porphyry copper deposit, Pima County, Arizona: Tucson, University of Arizona, unpublished Master's thesis, 102 p.

Maren, A., Harston, C., and Pap, R., 1990, Handbook of neural computing applications: Academic Press Inc.

Marvin, R. F., and Cole, J. C., 1978, Radiometric ages; compilation A, U. S. Geological Survey: Isochron/West, no. 22, p.3-14.

Marvin, R. F., Stern, T. W., Creasey, S. C., and Mehnert, H. H., 1973, Radiometric ages of igneous rocks from Pima, Santa Cruz, and Cochise Counties, southeastern Arizona: U. S. Geological Survey Bulletin 1379, 27 p.

Mauger, R. L., 1966, A petrographic and geochemical study of Silver Bell and Pima mining districts, Pima County, Arizona: Tucson, University of Arizona, Ph.D. Dissertation, 140 p.

McClernan, H. G., 1980, Metallogenic map of the White Sulphur Springs quadrangle, central Montana: Montana Bureau of Mines and Geology, Geologic Map 7, 31 p., 2 map sheets.

McCormack, M., 1990, Seismic trace editing and first break picking using neural networks: 60th Annual International Meeting, Society of Exploration Geophysics, Expanded Abstracts, p. 321-324.

McDowell, F. W., 1966, Potassium-argon dating of Cordilleran intrusives: New York, Columbia University, Ph. D. Dissertation.

McDowell, F. W., 1971, K-Ar ages of igneous rocks from the western United States: Isochron/West, no. 2, p. 1-2.

McFarlane, D. N., 1987, Maggie Creek deposit, in Bulk mineable precious metal deposits of the western United States, Guidebook for field trips: Reno, Geological Society of Nevada, p. 274-275.

McKee, E. H., 1968, Geologic map of the Spencer Hot Springs quadrangle, Lander County, Nevada: U. S. Geological Survey Geologic Quadrangle map GQ-770.

McKee, E. H., 1972, Preliminary geologic map of the Wildcat Peak quadrangle and the western part of the Dianas Punch Bowl quadrangle, Nevada: U. S. Geological Survey Miscellaneous Field Studies Map MF-337, scale 1:62,500.

McKee, E. H., 1976, Geology of the northern part of the Toquima Range, Lander, Eureka, and Nye Counties, Nevada: U. S. Geological Survey Professional Paper 931, 49 p.

McKee, E. H., and Koski, R. A., 1981, K-Ar ages for igneous rocks and vein minerals from the Christmas mine area, Arizona: Isochron/West, v. 32, p. 7-11.

McKee, E. H., Silberman, M. L., Marvin, R. F., and Obradovich, J. D., 1971, a summary of radiometric ages of Tertiary volcanic rocks in Nevada and eastern California -- part 1, central Nevada: Isochron/West, no. 2, p. 21-42.

McMillan, W. J., 1976, Geology and genesis of the Highland Valley ore deposits and the Guichon Creek batholith, in Porphyry deposits of the Canadian Cordillera: Canadian Institute of Mining and Metallurgy, Special volume 15, p. 85-104.

McMillan, W. J., 1982, The behavior of U, Th, and other trace elements during evolution of the Guichon Creek batholith, British Columbia, in Maurice, Y. T., editor, Uranium in granites; proceedings of a workshop: Geological Survey of Canada Paper 81-23, p. 49-53.

McMillan, W. J., 1985, Geology and ore deposits of the Highland Valley camp: Ministry of Energy, Mines and Petroleum Resources, Mineral Resources Division, Victoria, British Columbia, Canada Field Guide and Reference Manual Series, v. 1, 121 p.

Megaw, P. K. M., 1990, Geology and geochemistry of the Santa Eulalia mining district, Chihuahua, Mexico: Tucson, University of Arizona, Ph.D. Dissertation, 549 p.

Metz, R. A., and Rose, A. W., 1966, Geology of Ray copper deposit, Ray, Arizona, in Titley, S. R., and Hicks, C. L., editors, Geology of the porphyry copper deposits, southwestern North America: Tucson, University of Arizona Press, p. 176-188.

Miyashiro, A., 1974, Volcanic rock series in island arcs and active continental margins: American Journal of Science, v. 274, p. 321-355.

Moolick, R. T., and Durek, J. J., 1966, The Morenci district, in Titley, S. R., and Hicks, C. L., editors, Geology of the porphyry copper deposits, southwestern North America: Tucson, University of Arizona Press, p. 221-231.

Morabbi, M., 1980, The geology and ore deposits of Cherry Creek pluton, White Pine County, Nevada: Idaho State University, unpublished Master's thesis.

Morris, H. T., 1964, Geology of the Eureka quadrangle, Utah and Juab counties, Utah: U. S. Geological Survey Bulletin 1142-K, p. K1-K29.

Morris, H. T., and Lovering, T. S., 1979, General geology and mines of the East Tintic mining district, Utah and Juab counties, Utah: U. S. Geological Survey Professional Paper 1024, 203 p.

Morris, H. T., and Mogensen, A. P., 1978, Tintic mining district, Juab and Utah

counties, Utah, in Shawe, D. R., editor, Guidebook to mineral deposits of the Central Great Basin: Nevada Bureau of Mines Report, v. 32, p. 69-74.

Motter, J. W., and Chapman, P. E., 1984, Sediment-hosted precious metal deposits; Northumberland gold deposit, Nye County, Nevada, in Johnson, J. L., Steininger, R. C., editors, Exploration for ore deposits of the North American Cordillera; field trip guidebook: Reno, Nevada, Association of Exploration Geochemists, p. 9-25; also in Lintz, J., Jr., editor, Western geological excursions; volume 3: MacKay School of Mines, Department of Geological Sciences, Reno, NV, p. 181-199..

Myers, G. L., 1990, Alteration zonation of the Fortitude gold skarn deposit, Lander County, NV: Mining Engineering, v. 42, no. 4, p. 360-368.

Myers, G. L., and Meinert, L. D., 1991, Alteration, mineralization, and gold distribution in the Fortitude gold skarn, in Raines, G. L., Lisle, R. E., Schafer, R. W., and Wilkinson, W. H., editors, Geology and ore deposits of the Great Basin, Symposium Proceedings: Reno, Geological Society of Nevada, p. 407-417.

Myers, G. L., and Meinert, L. D., 1991, Alteration, mineralization, and gold distribution in the Fortitude gold skarn, in Raines, G. L., Lisle, R. E., Schafer, R. W., and Wilkinson, W. H., editors, Geology and ore deposits of the Great Basin, Symposium Proceedings: Reno, Geological Society of Nevada, volume I, p. 407-417.

Naillon, M., and Theeton, J., 1989, Neural approach for TV image compression using a Hopfield type network in Touretzky, D., Ed., Advances in neural information processing systems I: Morgan Kaufmann Publishers, 264-271.

Nanna, D., Baumann, M., Berentsen, E., and Steinman, G., 1987, Getchell deposit, in Johnson, J. L., editor, Bulk mineable precious metal deposit of the western United States: Reno, Geological Society of Nevada, 1987 Symposium, p. 353-356.

NeuralWare, 1991, Neural Computing, NeuralWorks Professional II/PLUS and NeuralWorks Explorer: NeuralWare, Inc., Technical Publications Group, Pittsburgh, PA.

Newell, R. A., 1974, Exploration geology and geochemistry of the Tombstone-Charleston area, Cochise County, Arizona: Stanford University, Ph.D. Dissertation, 205 p.

Newell, R. A., 1978, Tectonics of Tombstone Hills, in Keith, S. B., and Wilt, J. C., Second day road log from Douglas to Tucson via Bisbee, Tombstone, Charleston, Fort Huachuca and Sonoita: New Mexico Geological Society, Twenty-ninth field conference, Land of Cochise, southeastern Arizona p. 46-47.

Nilsson, N, 1965, Learning machines: foundations of training pattern classifying systems: McGraw-Hill Book Company.

Nockolds, S. R., 1954, Average chemical compositions of some igneous rocks: Geological Society of America Bulletin, v. 65, p. 1007-1032.

Nockolds, S. R., and Allen, R., 1954, The geochemistry of some igneous rock series: part II: Geochimica et Cosmochimica Acta, v. 5, p. 245-285.

Northcote, K. E., 1969, Geology and geochronology of the Guichon Creek batholith: British Columbia, Department of Mines and Petroleum Resources, Bulletin no. 56, 73 p.

Olade, M. A., 1976, Geochemical evolution of copper-bearing granitic rocks of Guichon Creek batholith, British Columbia, Canada: Canadian Journal of Earth Sciences, v. 13, no. 2, p. 199-209.

Osatenko, M. J., and Jones, M. G., 1976, Valley Copper, in Porphyry deposits of the Canadian Cordillera: Canadian Institute of Mining and Metallurgy, Special Volume 15, p. 130-143.

Osterberg, M. W., 1990, Geology and geochemistry of the Chimney Creek gold deposit, Humboldt County, Nevada: Tucson, University of Arizona, Ph. D. Dissertation, 173 p.

Osterberg, M. W., and Guilbert, J. M., 1991, Geology, wall-rock alteration, and new exploration techniques at the Chimney Creek sediment-hosted gold deposit, Humboldt County, Nevada, in Raines, G. L., Lisle, R. E., Schafer, R. W., and Wilkinson, W. H., editors, Geology and ore deposits of the Great Basin, symposium proceedings: Reno, Geological Society of Nevada, p. 805-819.

Ott, L. E., 1983, Geology ad ore localization at the Northumberland gold mine, Nye County, Nevada: Butte, Montana, Montana College of Mineral Science and Technology, unpublished Master's Thesis.

Pao, Y., 1989, Adaptive pattern recognition and neural networks: Addison-Wesley

Publishing Company.

Parker, D. B., 1982, Learning logic: Invention Report S81-64, File 1, Office of Technology Licensing, Stanford University.

Parker, D. B., 1985, Learning logic: Technical Report TR-47, Center for Computational Research in Economics and Management Science, Massachusetts Institute of Technology, Cambridge, MA, April, 1985.

Peacock, M. A., 1931, Classification of igneous rock series: Journal of Geology, v. 39, p. 54-67.

Petersen, E. U., and Haileab, B., 1993, Application of artificial neural networks (ANN's) to geological problems: Geological Society of America, Abstracts with Programs, Boston, p. A-248.

Posepny, F., 1895, The genesis of ore-deposits, a treatise: American Institute of Mining Engineers, New York, 265 p., reprinted from Transactions of the American Institute of Mining Engineers, v. 23 and 24.

Poulton, M., and Zaverton, K., 1992, Comparison of neural network paradigms for classification of TM images: 23rd Application of Computers and Operations Research in the Minerals Industry, April 7-11, Tucson, AZ, p. 37-46.

Poulton, M. M., 1990, Neural network pattern recognition of electromagnetic ellipticity images: Tucson, University of Arizona, Ph. D. Dissertation, 142 p.

Poulton, M. M., Glass, C. E., and Sternberg, B. K., 1989, Recognizing EM ellipticity patterns with neural networks: Society of Exploration Geophysicists, 59th Annual International Meeting; Expanded abstracts with Biographies: 1989 Technical Program, SEG Abstracts, v. 59, v. 1, p. 208-212.

Poulton, M. M., Sternberg, B. K., and Glass, C. E., 1990, Continuous-output neural networks for EM ellipticity pattern recognition: Digest - International Geoscience and Remote Sensing Symposium (IGARSS), v. 2, published by IEEE, IEEE Service Center, Piscataway, NJ, USA, p. 1297-1300.

Poulton, M., Sternberg, B., and Glass, C., 1992, Neural network pattern recognition of subsurface EM images: Journal of Applied Geophysics, v. 29, p. 21-36.

Powers, S. L., 1978, Jasperoid and disseminated gold of the Agee-Pinson mine, Humboldt County, Nevada: Reno, University of Nevada, unpublished Master's thesis.

Quinlan, J. L., 1986, Geology and silicate alteration zoning at the Red Mountain porphyry copper deposit, Santa Cruz County, Arizona, in Beatty, B., and Wilkinson, P. A. K., editors, Frontiers in geology and ore deposits of Arizona and the southwest: Tucson, Arizona Geological Society Digest, v. 16, p. 294-305.

Quirt, S., Clark, A. H., Farrar, E., and Sillitoe, R. H., 1971, Potassium-argon ages of porphyry copper deposits in northern and central Chile (abstract): Economic Geology, v. 66, p. 980.

Radtke, A. S., 1985, Geology of the Carlin gold deposit, Nevada: U. S. Geological Survey Professional Paper 1267, 124 p.

Radtke, A. S., and Scheiner, B. J., 1970, Studies of hydrothermal gold deposition (I). Carlin gold deposit, Nevada: the role of carbonaceous materials in gold deposition: Economic Geology, v. 65, no. 2, p. 87-102.

Radtke, A. S., Rye, R. O., and Dickson, F. W., 1980, Geology and stable isotope studies of the Carlin gold deposit, Nevada: Economic Geology, v. 75, no. 5, p. 641-672.

Ransome, F. L., 1919, The copper deposits of Ray and Miami, Arizona: U. S. Geological Survey Professional Paper 115, 192 p.

Rasor, C. A., 1937, Mineralogy and petrography of the Tombstone mining district, Arizona: Tucson, University of Arizona, Ph.D. dissertation.

Ray, G. E., Dawson, G. L., and Simpson, R., 1987, Geology, geochemistry and metallogenic zoning in the Hedley gold-skarn camp (92H/08; 82E/05): British Columbia Ministry of Energy, Mines and Petroleum Resources, Geological Fieldwork, Paper 1988-1, p. 59-75.

Ray, G. E., Dawson, G. L., and Simpson, R., 1986, The geology and controls of skarn mineralization in the Hedley gold camp, southern British Columbia (92H/8, 82E/5): British Columbia Ministry of Energy, Mines and Petroleum Resources, Geological Fieldwork, Paper 1987-1, p. 65-79.

Redwood, S. D., and Macintyre, R. M., 1989, K-Ar dating of Miocene magmatism and related epithermal mineralization of the northeastern Altiplano of

Bolivia: Economic Geology, v. 84, p. 618-630.

Reynolds, S. J., and Keith, S. B., 1982, Geochemistry & mineral potential of peraluminous granitoids: Fieldnotes from the State of Arizona, Bureau of Geology and Mineral Technology, v. 12, no. 4, p. 4-6.

Reynolds, S. J., and Keith, S. B., 1983, A geochemical classification of peraluminous granitoids: The Geological Society of America, Abstracts with Programs, v. 15, no. 5, p. 421.

Reynolds, S. J., Florence, F. P., Welty, J. W., Roddy, M. S., Currier, D. A., Anderson, A. V., and Keith, S. B., 1986, Compilation of radiometric age determinations in Arizona: Arizona Bureau of Geology and Mineral Technology, Bulletin 197, 258 p.

Reynolds, S. J., Keith, S. B., and DeWitt, E., 1982, Late Cretaceous-early Tertiary peraluminous granitoids of Arizona - California and their related mineral deposits: The Geological Society of America, Abstracts with Programs, v. 14, no. 4, p. 227.

Reynolds, S. J., Keith, S. B., and DuBois, J. F., 1980, Locations, lithologic descriptions, petrographic information and analytical data for geochemical samples, in Coney, P. J., Reynolds, S. J., editors, Cordilleran metamorphic core complexes and their uranium favorability; final report: U. S. Department of Energy, Grand Junction, CO, Open-file report GJBX-258-80, p. 599-623.

Rice, H. M. A., 1947, Geology and mineral deposits of the Princeton map-area, B.C.: Geological Survey of Canada, Memoir 243.

Roberts, R. J., 1964, Stratigraphy and structure of the Antler Peak quadrangle, Humboldt and Lander Counties, Nevada: U. S. Geological Survey Professional Paper 459-A, 93 p.

Roberts, R., J., and Arnold, D. C., 1965, Ore deposits of the Antler Peak quadrangle, Humboldt and Lander Counties, Nevada: U. S. Geological Survey Professional Paper 459-B, 94 p.

Roberts, R. J., Radtke, A. S., and Coats, R. R., 1971, Gold-bearing deposits in north-central Nevada and southwestern Idaho: Economic Geology, v. 66, no. 1, p. 14-33.

Roddick, J. C., Farrar, E., and Procyshyn, E. L., 1972, Potassium-argon ages of

igneous rocks from the area near Hedley, southern B. C.: Canadian Journal of Earth Sciences, v. 9, p. 1632-1639.

Rumelhart, D., Hinton, G, and McClelland, J., 1986, A general framework for parallel distributed processing, in Rumelhart, D., and McClelland, J., editors, Parallel distributed processing, Vol 1: M.I.T. Press, p. 45-76.

Sayers, R. W., Tippett, M. C., and Fields, E. D., 1968, Duval's new copper mines show complex geologic history: Mining Engineering, v. 20, no. 3, p. 55-62.

Sayers, R. W., Tippett, M. C., and Fields, E. D., 1969, Ore deposits at Copper Canyon and Copper Basin, Lander County, Nevada: Society of Mining Engineers AIME Transactions, v. 244, no. 3, p. 320-331.

Sayyah, T. A., 1978, Geochronology studies of the Kinsley stock, Nevada, and Raft River Range, Utah (abstract): Utah Geological Survey Bulletin 86, p. 141-142.

Schrader, F. C., 1931, Spruce Mountain district, Elko County, and Cherry Creek, Egan Canyon district, White Pine County: University of Nevada Bulletin, v. 25, no. 7, 39 p.

Schrader, F. C., 1934, The McCoy mining district and gold veins in Horse Canyon, Lander County, Nevada: U. S. Geological Survey Circular 10, 13 p.

Schwab, K. J., 1990, Possible relations among magma oxidation state, element partitioning, and gold and copper mineralization: Tempe, Arizona State University, unpublished M.S. thesis, 190 p.

Schwab, K. J., and Keith, S. B., 1989, Influences of magma oxidation state on biotite and amphibole compositions and possible relations to metallogeny: Geological Society of America, Abstracts with Programs, v. 21, no. 6, p. 118-119.

Shafiqullah, M., and Langlois, J. D., 1978, The Pima mining district, Arizona - a geochronologic update, in Callender, J. W., Wilt, J. C., Clemons, R. E., and James, H. L., editors, Land of Cochise, southeastern Arizona: New Mexico Geological Society, 29th field conference guidebook, p. 321-327.

Shand, S. J., 1927, The eruptive rocks: New York, John Wiley.

Silberman, M. L., and McKee, E. H., 1971, Potassium-argon ages of plutons in north-central Nevada: Isochron/West, v. 71, p. 15-32.

Silberman, M. L., Berger, B. R., and Koski, R. A., 1974, K-Ar relations of granodiorite emplacement and tungsten and gold mineralization near the Getchell mine, Humboldt County, Nevada: Economic Geology,. v. 69, p. 646-656.

Sillitoe, R. H., Halls, C., and Grant, J. N., 1975, Porphyry tin deposits in Bolivia: Economic Geology, v. 70, p. 913-927.

Simpson, R., and Ray, G. E., 1986, Nickel Plate gold mine: CIM Bulletin (1974), v. 79 (891), p. 36.

Smith, D. L., 1983, Guidebook of the fold and thrust belt, west-central Montana: Montana Bureau of Mines and Geology, Special Publication 86, p. 14.

Smith, J. F., Jr., and Ketner, K. B., 1976, Geology of the Carlin-Pinon Range area, Nevada, in Smith, J. F., Jr., Ketner, K. B., and Mabey, D. R., Stratigraphy of post-Paleozoic rocks and summary of resources in the Carlin-Pinon Range area, Nevada: U. S. Geological Survey Professional Paper 867-B, 48 p.

Smith, J. F., Jr., and Ketner, K. B., 1977, Tectonic events since Early Paleozoic in the Carlin-Pinon Range area, Nevada: U. S. Geological Survey Professional Paper 867-C, 18 p.

Smith, J. G., McKee, E. H., Tatlock, D. B., and Marvin, R. F., 1971, Mesozoic granitic rocks in northwestern Nevada -- a link between the Sierra Nevada and Idaho batholiths: Geological Society of America Bulletin, v. 82, p. 2933-2944.

Smith, R. M., 1976, Mineral resources of Elko County, Nevada: U. S. Geological Survey open-file report 76-56.

Smith, R. M., 1976, Mineral resources of White Pine County, Nevada, Part II, in Hose, R. K., and Blake, M. C., Jr., and Smith, R. M., Geology and mineral resources of White Pine County, Nevada: Nevada Bureau of Mines and Geology Bulletin 85, 105 p.

Smith, V. L., 1975, Hypogene alteration at the Esperanza mine, Pima County, Arizona: Tucson, University of Arizona, unpublished Master's Thesis, 161 p.

Soulie, F., Gallinari, P., Le, C., and Thiria, S. 1987, Evaluation of neural network architectures on test learning tasks: 1st International Conference on

Neural Networks, IEEE, p. 653-660.

Specht, D., 1990, Probabilistic neural networks: Neural Networks, v. 3, p. 109-118.

Spurr, J. E., 1923, The ore magmas: New York.

Stager, H. K., 1977, Mineral deposits (Part II), in Stewart, J. H., McKee, E. H., and Stager, H. K., Geology and mineral deposits of Lander County, Nevada: Nevada Bureau of Mines and Geology Bulletin 88, 105 p.

Stager, H. K., and Tingley, J. V., 1988, Tungsten deposits in Nevada: Nevada Bureau of Mines and Geology Bulletin 105.

Steininger, R., 1966, Geology of the Kingsley mining district, Elko County, Nevada: Brigham Young University Geology Studies, v. 13, p. 69-88.

Stewart, J. H., and McKee, E. H., 1977, Geology (Part I), in Stewart, J. H., McKee, E. H., and Stager, H. K., 1977, Geology and mineral deposits of Lander County, Nevada: Nevada Bureau of Mines and Geology Bulletin 88, 106 p.

Stewart, J. H., McKee, E. H., and Stager, H. K., 1977, Geology and mineral deposits of Lander County, Nevada: Nevada Bureau of Mines and Geology Bulletin 88, 106 p.

Stolburg, C. S., and Dunning, G. E., 1985, The Getchell Mine, Humboldt County, Nevada: The Mineralogical Record, v. 16, no. 1 (Nevada special issue), p. 15-23.

Sugaki, A., Ueno, H., Shimada, M., Kitakaze, A., Hayashi, K., Shima, H., Sansines, O. V., Saavedra, A. M., 1981, Geological study on polymetallic hydrothermal deposits in the Oruro district, Bolivia: The Science Reports of the Tohoku University, Third series (Mineralogy, petrology and economic geology), v. 15, no. 3, p. 1-52.

Sugaki, A., Ueno, H., Shimada, N., Kusachi, I., Kitakaze, A., Hayashi, K., Kojima, S., and Sanjines V., O., 1983, Geological study on the polymetallic ore deposits in the Potosi district, Bolivia: The Science Reports of the Tohoku University, Third series (Mineralogy, petrology and economic geology), v. 15, no. 3, p. 409-460.

Suttill, K. R., 1988, Cerro Rico de Potosi: Engineering and Mining Journal, March

1988, p. 50-53.

Swan, M. M., Keith, S. B., and Parr, M. G., 1985, Magma series and their relationship to greenstone gold metallogeny in the Lake Superior region., in Blackburn, C. E., editor, Technical sessions and abstracts for the 31st annual institute on Lake Superior geology: Proceedings, Annual Institute on Lake Superior Geology, v. 31, p. 91-92.

Swayne, W. H., and Trask, F., 1960, Geology of El Salvador: Mining Engineering, v. 12, no. 4, p. 345-348.

Takahashi, M., Aramaki, S., and Ishihara, S., 1980, Magnetite-series/ilmenite-series vs. I-type/S-type granitoids: Mining Geology, Special Issue, no. 8, p. 13-28.

Tapper, C. J., 1986, Geology and genesis of the Alligator Ridge Mine, White Pine County, Nevada, in Tingley, J. V., and Bonham, H. F., Jr., editors, Sediment-hosted precious-metal deposits of Nevada: Nevada Bureau of Mines Report 40, p. 85-103.

Taylor, B. E., 1976, Origin and significance of C-O-H fluids in the formation of Ca-Fe-Si skarn, Osgood Mountains, Humboldt County, Nevada: Stanford University, unpublished Ph.D. dissertation, 285 p.

Theodore, T. G., and Blake, D. W., 1975, Geology and geochemistry of the Copper Canyon porphyry copper deposit and surrounding area, Lander County, Nevada: U. S. Geological Survey Professional Paper 798-B.

Theodore, T. G., Howe, S. S., and Blake, D. W., 1990, The Tomboy-Minnie gold deposits at Copper Canyon, Lander County, Nevada, in Tooker, E. W., James, L. P., Theodore, T. G., Howe, S. S., and Blake, D. W., editors, Gold in porphyry copper systems: U. S. Geological Survey Bulletin 1857-E, p. E43-E55.

Theodore, T. G., Silberman, M. L., and Blake, D. W., 1973, Geochemistry and potassium-argon ages of plutonic rocks in the Battle Mountain mining district, Lander County, Nevada: U. S. Geological Society Professional Paper 798-A, 24 p.

Thomas, W. J., and Gibbs, R. B., 1983, Famous mineral localities; the New Cornelia Mine, Ajo, Arizona: The Mineralogical Record, v. 14, no. 5, p. 283-298.

Thomas, W. J., and Gibbs, R. B., 1983, Famous mineral localities: The New Cornelia mine, Ajo, Arizona: Mineralogical Record, v. 14, no. 5, p. 283-298.

Thompson, R. N., and others, 1984, An assessment of the relative roles of crust and mantle in magma genesis, an elemental approach: Royal Society of London Philosophical Transactions, Series A., v. 310, p. 549-590.

Thornton, C. P., and Tuttle, O. F., 1060, Chemistry of igneous rocks: I. Differentiation Index: American Journal of Science, v. 258, p. 664-684.

Tingley, J. V., 1975, K-Ar dates on granodiorite and related scheelite-bearing quartz veins at Tungsten, Pershing County, Nevada: Isochron/West, no. 12, p. 3-4.

Tingley, J. V., 1984, A mineral inventory of the Caliente resource area, Caliente district, Lincoln County, Nevada: Nevada Bureau of Mines and Geology, open-file report 84-1.

Titley, S. R., 1982, Some features of tectonic history and ore genesis in the Pima mining district, in Titley, S. R., editor, Advances in geology of porphyry copper deposits; southwestern North America: Tucson, University of Arizona Press, p. 387-406.

Titley, S. R., and Beane, R. E., 1981, Porphyry copper deposits; part I, geologic settings, petrology, and tectogenesis: Economic Geology, 75th Anniversary volume, p. 214-269.

Tooker, E. W., 1985, Discussion of the disseminated-gold-ore-occurrence model, in Tooker, E. W., editor, Geologic characteristics of sediment- and volcanic-hosted disseminated gold deposits; search for an occurrence model: U. S. Geological Survey Bulletin 1646, p. 107-150.

Tower, G. W., and Smith, G. O., 1899, Geology and mining industry of the Tintic district, Utah: U. S. Geological Survey Annual Report, v. 19, part 3, p. 601-767.

Tschanz, C. M., and Pampeyan, E. H., 1970, Geology and mineral deposits of Lincoln County, Nevada: Nevada Bureau of Mines and Geology Bulletin 73, 188 p.

Turneaure, F. S., 1935, The tin deposits of Llallagua, Bolivia: Economic Geology, v. 30, p. 14-60, 170-190.

Turneaure, F. S., 1960, A comparative study of major ore deposits of central Bolivia: Economic Geology, v. 55, no. 2, p. 217-254, no. 3, p. 574-606.

U. S. Geological Survey and Servicio Geologico de Bolivia, 1992, Geology and mineral resources of the Altiplano and Cordillera Occidental, Bolivia: U. S. Geological Survey Bulletin 1975, 365 p.

Villas, R. N., 1975, Fracture analysis, hydrodynamic properties and mineral abundance in the altered igneous wall rocks of the Mayflower mine, Park City district, Utah: University of Utah, Ph.D. Dissertation, 271 p.

Villas, R. N., and Norton, D., 1977, Irreversible mass transfer between circulating hydrothermal fluids and the Mayflower stock: Economic Geology, v. 72, no. 8, p. 1471-1504.

Wadsworth, W. B., 1968, The Cornelia pluton, Ajo, Arizona: Economic Geology, v. 63, p. 101-115.

Wager, L. R., and Brown, G. M., 1967, Layered igneous rocks: San Francisco, Freeman; Layered igneous complexes: Edinburgh, Oliver and Boyd, 588 p.

Waldner, M. W., Smith, G. D., and Willis, R. D., 1976, Lornex, in Sutherland Brown, A., editor, Porphyry deposits of the Canadian Cordillera: Canadian Institute of Mining and Metallurgy, Special Volume 15, p. 120-129.

Wasserman, P. D., 1989, Neural computing, theory and practice: New York, Van Nostrand Reinhold, 230 p.

Weed, W. H., and Pirsson, L. V., 1896, Geology of the Castle Mountain mining district, Montana: U. S. Geological Survey Bulletin 139, 165 p.

Werbos, P., 1974, Beyond regression: new tools for prediction and analysis in the behavioral sciences, Ph.D. Dissertation, Harvard University.

West, R. J., and Aiken, D. M., 1982, Geology of the Sierrita Esperanza deposit; Pima mining district, Pima County, Arizona, in Titley, S. R., editor, Advances in geology of porphyry copper deposits; southwestern North America: Tucson, University of Arizona Press, p. 433-465.

Westra, G., and Keith, S. B., 1981, Classification and genesis of stockwork molybdenum deposits: Economic Geology, v. 76, no. 4, p. 844-873.

Westra, G., and Keith, S. B., 1982, Classification and genesis of stockwork

molybdenum deposits: reply: Economic Geology, v. 77, no. 5, p. 1252-1263.

White, W. H., Thompson, R. M., and McTaggart, K. C., 1957, The geology and mineral deposits of Highland Valley, B. C.: Canadian Mining and Metallurgy Bulletin, no. 544, p. 487-503.

Wiener, J., Rogers, J. A., Rogers, J. R., and Moll, R., 1991, Predicting carbonate permeabilities from wireline logs using a back propagation network: 61st Annual International Meeting, Society of Exploration Geophysics, Expanded Abstracts, p. 285-288.

Wilkinson, W. H., Jr., Vega, L. A., and Titley, S. R., 1982, Geology and ore deposits at Mineral Park, Mohave County, Arizona, in Titley, S. R., editor, Advances in geology of porphyry copper deposits, southwestern North America: Tucson, University of Arizona Press, p. 523-541.

Willden, R., 1964, Geology and mineral deposits of Humboldt County, Nevada: Nevada Bureau of Mines and Geology, Bulletin 59, 154 p.

Williams, S. A., 1980, The Tombstone District, Cochise County, Arizona: The Mineralogical Record, v. 11, no. 4 (Arizona-II), p. 251-256.

Wilson, J. C., 1961, Geology of the Alta stock, Utah: California Institute of Technology, Ph.D. Dissertation, 236 p.

Wilt, J. C., and Keith, S. B., 1980, Molybdenum in Arizona: Fieldnotes from the State of Arizona, Bureau of Geology and Mineral Technology, v. 10, no. 3, p. 1-3, 7-9, 12.

Wilt, J. C., and Keith, S. B., 1987, Correlation of magma alkalinity with metal contents in Tertiary and Cretaceous ore deposits, S. CA, AZ, and NM: Geological Society of America, Abstracts with Programs, v, 19, no. 7. p. 893.

Winters, A. S., 1968, Geology and ore deposits of the Castle Mountain mining district, Meagher County, Montana: State of Montana, Bureau of Mines and Geology, Bulletin 64, 64 p., maps.

Wolf, Manfred, 1973, Zum magmatismus der Cordillera de Potosie in Bolivien: Freiberger Forschungshefte, Reihe C. No. 275, 174 p.

Wood, J. A., 1968, Exploration opportunities in British Columbia: Mining Congress

Journal, v. 54, no. 6, p. 57-60.

Wotruba, P. R., Benson, R. G., and Schmidt, K. W., 1986, Battle Mountain describes the geology of its Fortitude gold-silver deposit at Copper Canyon: Mining Engineering, v. 38, no. 7, p. 495-499.

Wotruba, P. R., Benson, R. G., and Schmidt, K. W., 1988, Geology of the Fortitude gold-silver skarn deposit, Copper Canyon, Lander County, Nevada, in Schafer, R. W., Cooper, J. J., and Vikre, P. G., editors, Bulk mineable precious metal deposits of the Western United States; Symposium proceedings: Reno, Geological Society of Nevada, p. 159-171.

Wotruba, P. R., Benson, R. G., and Schmidt, K. W., 1986, Battle Mountain describes the geology of its Fortitude gold-silver deposit at Copper Canyon: Mining Engineering, v. 38, no. 7, p. 495-499.

Yan, Mei-Zhong, and Hu, Kui, 1980, Geological characteristics of the Dexing porphyry copper deposits, Jingxi, China: Mining Geology, Special Issue, no. 8, p. 197-203.